WESTINGHOUSE NON-PROPRIETARY CLASS 3

WCAP-9812

INVESTIGATION OF FEEDWATER LINE CRACKING IN PRESSURIZED WATER REACTOR PLANTS

DECEMBER 1980

WORKED PERFORMED BY
WESTINGHOUSE NUCLEAR TECHNOLOGY DIVISION

FOR

FEEDWATER CRACKING UTILITY OWNERS GROUP
WORK PERFORMED UNDER S.O. MUAN 1000 - 8000

APPROVED: D. H. White

D. H. White, Manager
Applied Mechanics
Westinghouse Nuclear Technology Division

APPROVED: T. E. Campbell

T. E. Campbell, Manager
Structural Mechanics Department
Westinghouse Nuclear Technology Division

8101200423

TABLE OF CONTENTS

SECTION	TITLE	TAB NUMBER
1.0	Introduction	1
2.0	Summary	2
3.0	Conclusions	3
4.0	Recommendations	4
5.0	Metallurgical Investigation	5
6.0	Chemistry Evaluation	6
7.0	Piping Design Verification Analysis	7
8.0	On-Site Feedwater Test Programs	8
9.0	Plant Operating History	9
10.0	Flow Model Tests	10
11.0	Stress Analysis and Structural Evaluation	11
12.0	Fatigue Crack Growth Consideration	12
[		] a,b,c,e

ACKNOWLEDGEMENTS

The following people contributed to the completion of this program either in writing of this report, technical consultation or effort at the sites during repair. Without their devoted efforts this effort could not have been accomplished.

Westinghouse NTD

C. Antoniak
A. J. Ayoob
W. H. Bamford - F.H.
T. J. Batt
D. A. Bierman
R. Biford
M. Bowler
R. E. Boylstein
R. Burkhart
T. E. Campbell
R. W. Carlson
W. Ciaramitaro
B. J. Coslow
J. Craig
G. R. Ellis
D. Engle
D. T. Entemann
F. R. Falise - F.H.
M. J. Fisher
C. W. Gay
J. M. Gilkison
R. Gopal
J. M. Hall
R. Harrell - Purchasing
C. Hirst
J. L. Houtman
M. H. Hu - F.H.
D. Jack
F. Klanica
A. W. Klein - F.H.

NTD (Continued)

J. Kormuth - F.H.
R. Krevosh
D. L. Lapay
S. Y. Lee
G. P. Lilly - F.H.
F. Loceff
R. Mach
T. R. Mager - F.H.
M. S. Mahlab
R. W. Manz
W. A. Massie
E. P. Morgan - F.H.
W. E. Moore
J. Parello
J. Petsche
R. Quaglia - F.H.
G. V. Rao - F.H.
D. Scherf
E. W. Smith
J. Smith
R. Soles
N. G. Sowko
R. Steer
R. Stivason
S. Swamy - F.H.
A. L. Thurman
J. Tomasic
T. A. Vukson
D. H. White

Westinghouse NSD

J. D. Campbell
S. Caslake
R. Cook
F. Goldbach
J. Gumbert
V. Nayyar
F. Noon
R. Powell
D. Peterson
W. Sharp
B. Simpson

Westinghouse NFD

A. Bigi
R. Gardner
B. Kleckner
D. McCarthy
J. McEvoy
M. Rinker
W. Ripple
W. Santacasa

Westinghouse ARD

D. C. Meess
E. H. Novendstern
D. K. Schmidt
C. R. Smith

ACKNOWLEDGEMENTS (CONTINUED)

Utility/Site Personnel

E. Bialkin - AEP
R. Bischoff - D. C. Cook
R. L. Cole - CWEC
A. E. Curtis - RGE
C. Edgar - RGE
B. Flannagan - H. B. Robinson
J. Gallagher - Salem
S. Grant - CPL
R. F. Hering - AEP
J. Hock - AEP
R. B. Jenkins - Consumers Power
R. Kinney - D. C. Cook
M. Kupinski - NUSC
S. Labruna - Salem
J. Markowsky - AEP
E. A. Merrick - TVA
D. A. Patience - AEP
R. Rothgeb - Millstone
R. F. Saunders - VEP
G. J. Schnabel - PSE
A. Tetzlaff - D. C. Cook
N. R. Tonet - Duquesne Light Co.
T. Turner - D. C. Cook
J. C. Winslow - CPL

SECTION 1.0

INTRODUCTION

1.0 INTRODUCTION

In May 1979, through wall cracks were detected in the pipe elbows of steam generators 1 and 4 of D. C. Cook Unit 2 plant which had been in operation approximately one (1) year (see Figure 1-1). Subsequent inspection of the remaining elbows in Units 1 and 2 revealed cracking in the same vicinity but limited to partial wall penetration. Unit 1 had been in operation approximately four (4) years. After removal of the elbows, liquid penetrant inspection of the steam generator nozzles revealed minor pitting and cracking in all eight (8) steam generators.

On June 11, 1979, Westinghouse assisted American Electric Power (AEP) in presenting this issue to the Nuclear Regulatory Commission (NRC) and defining the action plan developed to return the plant to power. In summary, this action plan consisted of:

1. Installation of new pipe elbows with improved counterbore geometry to reduce stress concentration.

2. Repair of steam generator nozzles to remove areas of pitting and cracking.

3. Installation of instrumentation to obtain data for evaluation of the operational variables.

It was acknowledged at this time that the cause of cracking was not known. Therefore, the plan of repair and instrumentation was accepted by the NRC until the next planned outage in October 1979, when another inspection could be performed. During this time theoretical and experimental analyses were to be performed to evaluate the cause of cracking and identify appropriate corrective measures.

As a result of the D. C. Cook cracking, the NRC Office of Inspection and Enforcement issued its Bulletin 79-13[1] requiring all Pressurized Water Reactor (PWR)

---

(1) U.S. Nuclear Regulatory Commission, Office Of Inspection and Enforcement, "Cracking in Feedwater System Piping," I.E. Bulletin No. 79-13, 6/25/79.

plants to perform inspection of their feedwater lines. This resulted in other plants detecting cracks in the same general areas, (See Figure 1-1) along with those which did not have any detectable indications. A summary of all the domestic and foreign plants inspection to date is presented in Table 1.1.

In order to provide a uniform and systematic approach to the assessment of this problem, a utilities Feedwater Line Cracking Owners Group was formed with Westinghouse Electric Corporation serving as its technical agent. It was recognized at this time that a combination of conditions were most likely contributing to the cracking, but, the dominant factor or factors were not obvious. Metallurgical analyses indicated that cracking was most likely the result of corrosion fatigue. Therefore, the specific tasks of the Owners Group Program were established to evaluate the thermal, hydraulic, structural and environmental conditions which could individually or collectively contribute to this mechanism of crack initiation and growth.

Table 1.2 shows the Utility members and the organization structure established for the Owners Group. The following is a summary of the major tasks which formed the initial program scope.

Task E1 - Piping System Analysis
Task E2 - Waterhammer Loading
Task E3 - Thermal and Hydraulics - Flow Model Test
Task E4 - Stress and Fatigue Analysis - 3D Finite Element
Task E5 - Plant Chemistry
Task E6 - Mechanical and System Modifications
Task E7 - Field Instrumentation
Task E8 - Licensing Support

As the program progressed, revisions to the base scope were incorporated to accommodate NRC actions, and knowledge gained from results of the tasks being performed. Early in the program pipe vibration and local geometrical discontinuities combined with excess oxygen in the feedwater systems, were considered prime candidates to produce the corrosion fatigue observed. However, though present, these conditions by themselves could not be sufficiently correlated to confirm this premise. This knowledge emphasized the need to have a more detailed under-

standing of other cyclic loading conditions which could produce fatigue damage. Task E3 thus became a major part of the overall program which dealt with evaluation of the thermal/hydraulic conditions at the feedwater pipe to steam generator nozzle entrance. Thermal stratification and striping were identified as the two principal conditions of concern. Field instrumentation coupled with a full scale flow model testing provided the data base for this evaluation. This ultimately was shown to be the dominant loading factors.

A key milestone for Task E6 was to have a mechanical and/or system modification concept developed by September, 1979. This was necessitated since[ ] next planned outage was in October 1979, at which time reinspection of their feedwater lines would be performed. Should cracking be detected again additional mechanical and/or system modifications would be required by the NRC to return the plant to operation. In compliance with this action a[ ]concept was developed and presented to the Owners Group on September 5, 1979. In addition, various system modification concepts were discussed[ ] as well as other techniques which would protect against, or minimize, the effects of thermal stratification and striping. Following this meeting,[ ]requested Westinghouse to develop the[ ]concept for their specific application. a,c

[ ] a,c

In summary, the objective of this program was to provide a uniform and systematic approach for all utilities in evaluating the cause(s) of feedwater line cracking, and to identify the mechanical and/or system modification options available to minimize or eliminate its continuance. No attempt was made to provide final design

details of each modification option. This is a plant specific decision which has to be made with consideration given to safety, methods of operation, accessibility, cost and schedule impacts.

Presented in this report are the detailed results of each task performed as part of the Owners Group Program. Sections 2, 3, and 4 provide a summary of results, a discussion of the conclusions reached, and finally the recommended actions or modifications considered available to minimize or eliminate the continuance of feedwater line cracking. The remaining sections provide the detailed results of each task.

TABLE 1.1

PLANT INSPECTION SUMMARY

I. Domestic Plants With Cracking

D. C. Cook 1 & 2	Surr 1 & 2
H. B. Robinson 2	Pt. Beach 1 & 2
Beaver Valley 1	Kewaunee
Salem 1	Yankee Rowe
Ginna	Palisades*
San Onofre	Millstone 2*
Zion 1 & 2	Turkey Pt. 4

II. Domestic Plants Without Cracking

Farley	N. Anna 1 & 2
Turkey Pt. 3	Conn. Yankee (Haddam Neck)
Indian Pt. 2 & 3	Prairie Island 1
Salem 2	Trojan

III. Foreign Plants Without Cracking**

Ringhals 2	Zorita
Trino	Doel 1 & 2
Mihama 1, 2, & 3	Beznau 1 & 2
Takahama 1 & 2	Genkai 1
Ikata 1	Fessenheime 2
Tihange	Bugey 2

* Combustion Engineering

** Inspections to date reveal no plants with cracking.

TABLE 1.2

FEEDWATER LINE CRACKING OWNERS GROUP ORGANIZATION

I. Initial Members

Utility	Plant
American Electric Power	D. C. Cook
Carolina Power & Light	H. B. Robinson
Duquesne Light Company	Beaver Valley
Public Service Electric & Gas	Salem
Rochester Gas & Electric	Ginna
Southern California Edison	San Onofre
Virginia Electric & Power	Surry

II. Added Members

Commonwealth Edison	Zion
Consumers Power	Palisades*
Northeast Utilities	Millstone*
Tennessee Valley Authority	Sequoyah

III. Organization

R. F. Hering, Executive Head	American Electric Power
G. J. Schnabel, Technical Advisory Committee, Chairman	Public Service Electric & Gas
R. L. Cole	Commonwealth Edison
A. E. Curtis	Rochester Gas & Electric
R. B. Jenkins	Consumers Power
M. Kupinski	Northeast Utilities
D. A. Patience	American Electric Power
R. F. Saunders	Virginia Electric & Power
N. R. Tonet	Duquesne Light Company
J. C. Winslow	Carolina Power & Light
E. A. Merrick	Tennessee Valley Authority

* Combustion Engineering Plants

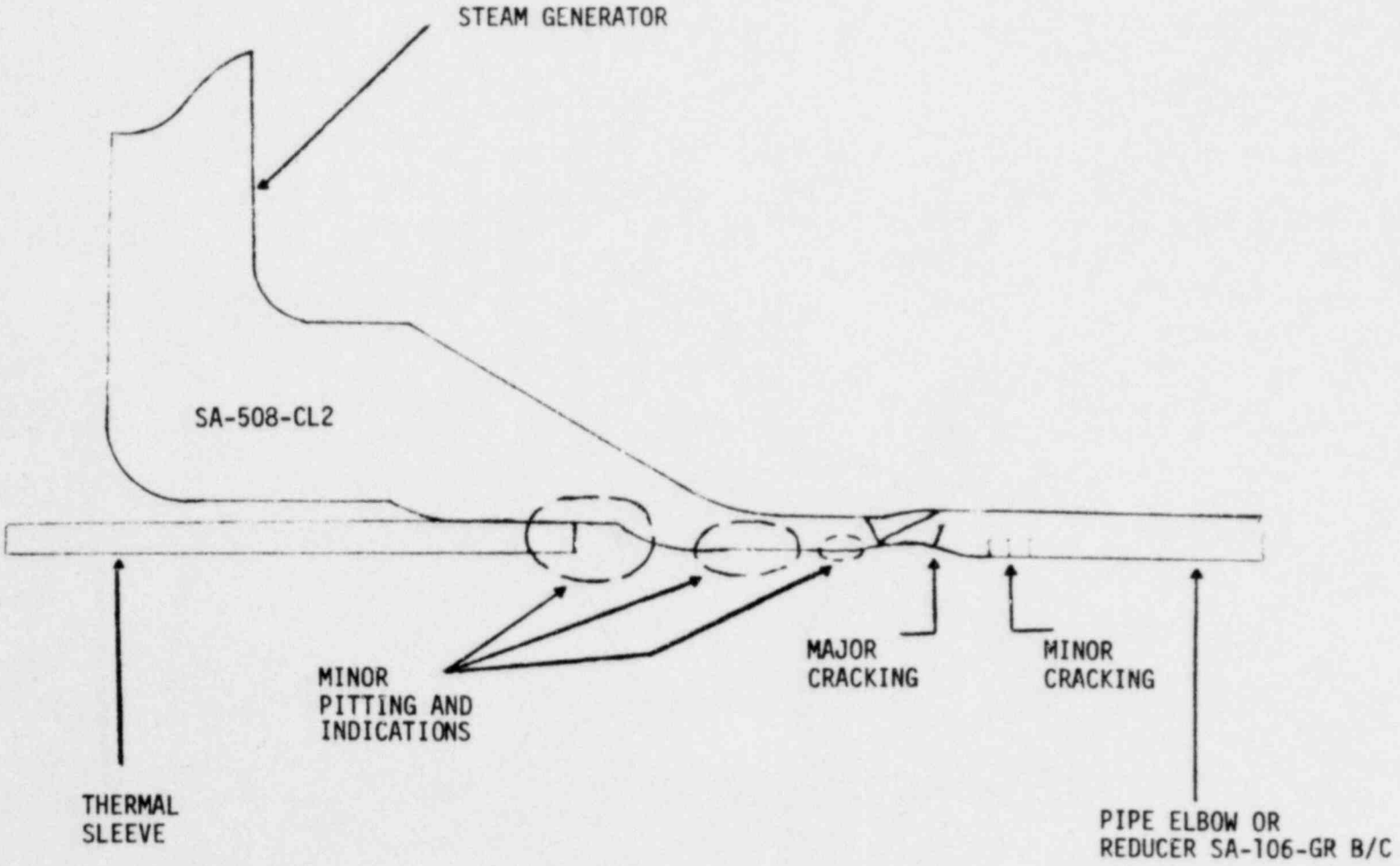

FIGURE 1-1: GENERAL DESCRIPTION OF PITTING AND CRACKING AT PIPE TO NOZZLE JUNCTION.

SECTION 2.0

SUMMARY

2.1 REPORT FORMAT

As discussed in Section 1.0, eight (8) major tasks were included in the initial feedwater cracking study program scope. These tasks, along with those efforts that were necessary to provide a uniform and systematic approach to the cracking investigations, form the basis of this report.

This report is formatted to provide easy reference to the detailed results of each of the major investigations performed under the scope of the feedwater cracking study. Sections 5 through 14 are self-contained reports describing the particular study, the results obtained, and the observations and conclusions that were drawn.

In this section, the results and observations of each study are briefly summarized. These summaries, along with the detailed results of each study, form the basis for the conclusions and recommendations which follow (Sections 3 and 4, respectively).

2.2 METALLURGICAL INVESTIGATIONS (SECTION 5)

The metallurgical investigation centered around the examination of cut-out ring sections containing the cracks from feedwater lines of several plants. The examinations included:

- --ID surface examination of the cracked regions of the elbows/reducers;
- --Metallographic examination of the sections containing some of the deepest cracks;
- --Microstructural characterization studies of the material by light optic and thin foil electron microscopy techniques;
- --Fractographic examinations of fracture faces of the crack;
- --Chemical evaluations of the base metal and of the deposits within the cracks.
- --Mechanical Properties

The results of these examinations led to the following observations:

--Cracking and pitting were essentially restricted to elbow/reducer counterbore regions;

--Crack depth varied significantly around the pipe circumference;

--Cracks were circumferential and growing radially from the I.D. to O.D. surface;

--Beach marks were discovered indicating the changing state of stress and environment during the life of the crack;

--Fatigue striations were also discovered in several cases, indicating the presence of a cyclic axial stress;

--Scanning electron fractography and Edax analysis of crack faces indicated presence of significant amount of corrosion deposits.

These observations suggest that the observed cracking was most likely a result of corrosion fatigue.

2.3 CHEMISTRY EVALUATION

Chemistry data were assimilated from existing Westinghouse records and from plant documentation in order to determine if any correlation existed between feedwater chemistry and the observed cracking. The extent of oxygen exposure and condenser in-leakage were the chemistry parameters considered. [

b

]. Though these parameters by themselves could not be directly correlated to predict the cracking observed, their contribution in the presence of high cyclic thermal stresses is considered significant.

2.4 PIPING DESIGN VERIFICATION ANALYSIS (SECTION 7)

Stress analyses were performed for the feedwater piping system for several plants to determine if the normally expected loads were sufficient to cause the observed cracking. The loads considered were normal operating thermal, deadweight and pressure loads, normal operating vibrations, waterhammer, and cold feedwater injection. Stresses obtained from these analyses were all below allowable limits and were not of sufficient magnitude to cause the observed cracking.

2.5 ON-SITE FEEDWATER TEST PROGRAMS (SECTION 8)

On-site testing of the feedwater systems at five plants was performed to investigate the normal operating behavior of the portion of the feedwater line in containment. The systems were instrumented to measure vibration during steady-state and transient conditions, thermal movement, pressure, flow, and internal and external wall temperatures of the piping within a few feet of attachment to the steam generator nozzles. Results of the first two tests did not indicate any abnormal vibration or dynamic transient conditions occurred which would significantly contribute to the cracking.
The results did indicate the presence of thermal stratification produced by the injection of cold auxiliary and main feedwater. Subsequent testing was performed to further quantify this phenomena with respect to plant operation and the cracking observed.

Results of the on-site testing indicate that stratification produces temperature differences between the top and bottom of the pipe as large as [ ] during hot standby conditions and cold feedwater injections. Furthermore, thermal stratification produces several different profiles of temperature across the pipe cross-section. These profiles are related to feed flow rate and suggest the presence of a hot-cold water interface. A significant amount of temperature cycling was seen to occur in all of the plant tested despite minor differences in feedring technique. A qualitative assessment of the potential for severity of thermal

b

hydraulic conditions at each plant test is summarized below:

PLANT RANKING IN TERMS OF POTENTIAL SEVERITY OF THERMAL-HYDRAULIC CONDITIONS AS OBTAINED FROM ON-SITE TEST RESULTS

(1 = Most severe)
(5 = Least severe)

PLANT	POTENTIAL FOR SEVERE THERMAL CYCLING	POTENTIAL FOR LONG HOT-COLD INTERFACE DURATION
[ ]	1	1
	4	2
	2	3
	3	4
	5	5

(a) Based on Line 14

2.6 PLANT OPERATING HISTORY (SECTION 9)

A survey was conducted to obtain data on the operational characteristics (procedures and history) of plants both with and without cracking. The objective of this effort was to evaluate the data to determine if a correlation existed to explain why certain plants produced more extensive cracking than others, why some produced cracking in a shorter period of time, and finally why some produced no identifiable cracking at all. Questionnaires and telephone contacts were made with eighteen(18) plants of which seven (7)

responded. Data was not received from any non-cracking plants. [ ] a,c

2.7 FLOW MODEL TESTS (SECTION 10)

Thermal stratification and striping were postulated as mechanisms which could promote fatigue cracking. On site instrumentation results revealed the presence of stratification. However, this instrumentation was not sufficient to quantify the amplitude and frequency of striping. Therefore, a [ ] flow model test program was conducted too: a,c

1. [
2.] a,c

3. Determine if thermal oscillations occur at the stratified interface.

4. [ ] a,c

5. Determine the temperature profile of the feed line during stratification conditions.

a,c The flow model is a [ ] feed line nozzle assembly [ ] for [ ] investigation and temperature measurement. It is a two temperature [ ] test operation. The inlet fluid was [ ] The tank representing the secondary side of the steam generator was initially filled with hot water at about [ ]. Test were conducted at [ ]

Temperature profiles and oscillations obtained have been scaled to steam generator conditions for thermal stress and fatigue evaluations.

The evaluation of the data obtained produced the following observations:

a,c 1. Thermal and fluid flow stratification exists in the feed line [ ] The hot-cold interface is subject to flow and thermal oscillations resulting in temperature fluctations.

a,c 2. Flow leakage can occur [ ].

a,c 3. During fluid flow stratifieation [ ]

Results of the flow model tests were used to establish the thermal boundary conditions for the three dimensional analysis of stratification stresses as well as providing oscillation data for evaluating high cycle fatigue.

2.8 STRESS ANALYSIS AND STRUCTURAL EVALUATION (SECTION 11)

The results of the 3D stress analysis performed to determine the contribution of thermally stratified flow conditions to the feedwater line cracking are presented in Section 11.

Two piping configurations were considered in the analysis; a 90 degree elbow welded to the nozzle, and a straight pipe welded to the nozzle. Generic stratified temperature profiles were developed for each configuration, based on field data and temperature measurements made during the flow test described in Section 10.

The on-site data described in Section 8 were used to determine the stratified load conditions along with their number of occurrences for the [ ] plants; [D.C. Cook, H.B. Robinson, R.E. Ginna, Salem and Millstone]. The stress conditions produced by the generic profiles were scaled to obtain the plant specific load conditions which were then used in the maximum range of stress intensity and fatigue evaluations for each plant. a,c

The stresses due to striping, produced by local temperature oscillations at the hot-cold fluid interface were determined [ ]. The fatigue damage due to striping was evaluated for each plant based on [ ] each generic temperature profile as obtained from field data. a,b,c

The peak axial stresses in the pipe/nozzle weld region resulting from the generic stratification profiles are summarized in the following Table. The associated maximum striping stress ranges are also included. The values given in this Table are for both the straight pipe and elbow configurations.

[redacted]

a, b, c

The following tables summarize the results of the fatigue evaluations due to stratification and striping for the five plants for which on site operating data had been obtained. The uncertainty in the number of stratification cycles and the duration of each stratified flow condition is reflected in the following tables by the lower and upper limits of the fatigue usage factors.

SUMMARY OF FATIGUE USAGE PRODUCED BY THERMAL STRATIFICATION

[ ] a,b,c

SUMMARY OF FATIGUE USAGE PRODUCED BY THERMAL STRIPING

[ ] a,b,c

Fatigue damage greater than one is predicted [ ] at locations which correlate well with the observed cracks. Thus, thermal stratification and the associated striping are considered prime contributions to the feedwater line cracking. a c

2.9 FATIGUE CRACK GROWTH CONSIDERATIONS(SECTION 12)

Fatigue crack growth analyses were performed for five of the operating plants. These five plants had both on-site tests (Section 8) and stress and fatigue analyses (Section 11) performed, the results of which were used as input for the fatigue crack growth analyses. Effects of water chemistry were also considered.

In general, the fatigue crack growth analyses results indicate that the crack growth behavior predicted for the five plants was in good qualitative agreement with the observed growth. [

a,c

]

The results of the fatigue crack growth analyses indicate that the major cause for the growth of the crack is the thermal stratification cycles. In addition to this, thermal striping at the stratified interface were found to have little influence on the crack growth even though there was some impact on the crack initiation predictions. Another concern was the water chemistry, which was found to be generally higher in dissolved oxygen than the specifications. Although this higher oxygen level would be expected to result in a worsening of the crack propagation, it cannot in itself be considered the primary cause of the extreme propagation.

2.10 PLANT COMPARISON (SECTION 13)

The major parameters and data involved in the feedwater cracking study were assembled into a format amenable to indicating trends or correlations of the parameters with respect to observed cracking or no cracking. The plant comparison study resulted in several tables which indicate that [

a,c

] The study also suggests that an

[

] can increase life but would not generally be sufficient to

prevent cracking in lines subjected to long term thermal stratification and striping.

2.11 MECHANICAL AND SYSTEM MODIFICATION (SECTION 14)

The following mechanical and system modifications were identified as means by which the effects of thermal stratification and striping could be eliminated or minimized. When combined with other corrective measures (i.e., reduced oxygen exposure, local geometry effects, etc.) they form the basic options available to each utility if additional repairs become necessary.

a,e,c

[

]

SECTION 3.0

CONCLUSIONS

3.0 CONCLUSIONS

Results of the Feedwater Line Program indicate the primary cause of cracking to be a fatigue loading mechanism induced by thermal stratification and striping during cold, low flow, feedwater injections. Significant secondary influences are attributed to [ ] large temperature differences (stratification) exist during heatup, hot standby. and low power operations. Another influential factor is the [ ]. [ ] The mode of failure is concluded to be a corrosion-fatigue mechanism. b a,c

The program results did not provide a conclusive understanding of why cracking was less severe in some plants, or why some cracked in a shorter period of time. Likewise, no specific conclusions could be drawn to explain why some had no evidence of cracking. However, based upon the result of this evaluation and the analysis of the field data, the severity of the observed cracking can be correlated to (1) high fatigue usage factor as a result of duration and number of cycles of induced thermal stratification and striping, piping and counterbore geometry, (2) [ ] and (3) [ ] From the results contained herein, it is expected that all plants will experience thermal stratification/striping during periods of cold feedwater injection. Therefore, the explanation of these circumstances lies primarily with the other contributing factors mentioned above, which may vary from plant to plant. Table 3.1 provides a summary of the overall conclusions developed. b

TABLE 3.1

CONCLUSIONS

PRIMARY CORRELATION

- THERMAL STRATIFICATION AND STRIPING DURING LOW FLOW RATE FEEDWATER INJECTION

SECONDARY CORRELATION

a,c [ ]

NO APPARENT CORRELATION

a,c [ ]

SECTION 4.0

RECOMMENDATIONS

4.0 RECOMMENDATIONS

Based on the results of the investigations presented herein, it is recommended that provisions be made to eliminate or minimize the effects of thermal stratification and striping in the feedwater lines. Further, steps should be taken [ ] Where impracticable, measures should be taken to protect the feedwater pipe to nozzle area from the effects of these conditions. b

Various mechanical and system modifications, shown in Table 4.1, have been identified which address the mechanism of thermal stratification. These have been categorized with respect to the role they play in eliminating stratification (and subsequent striping), protecting against it, or reducing its effects. [ ] No attempt was made to provide final design details for each of these options at this time. It is recognized that various techniques may be available to achieve any one of the modifications. [ ] Incorporation of any of these is a plant specific decision which must be made with consideration given to safety, method of operation, accessibility, cost and schedule impact. When selected, detailed design and analyses will be performed to qualify the modification to all required service conditions. a, c, e

TABLE 4.1

MODIFICATION SUMMARY

	SOLUTION FOR CONDITIONS	PROTECTION AGAINST CONDITION
a,c	[ ]	[ ]

	IMPROVE CONDITIONS	REDUCE EFFECTS
a,c	[ ]	[ ]

SECTION 5.0

METALLURGICAL INVESTIGATIONS

by

G. V. Rao

T. R. Mager

5.1 INTRODUCTION

This section summarizes the findings of metallurgical investigations into the cracking behavior of the steam generator feedwater lines. The results reported here are primarily based on the examinations of the feedwater line cracking incidents[1 to 8] at some ten different plants.* The feedwater piping is attached to the steam generator nozzles either through elbows or through reducers at the nozzle-to-pipe joints, depending on the plant and the loop being considered. The nozzles were made out of either schedule 60 ASTM A105 steel or schedule 60 ASTM SA508 grade steel while the elbows/reducers were generally made out of A106C steel. The cracks which were initially detected** by double wall radiography during service are located primarily in the elbows or reducers at the nozzle-to-elbow/reducer joints. Figure 1 illustrates schematically the typical cracking locations at the pipe-to-nozzle joints.

The metallurgical investigations were centered around cut out ring sections containing the cracks from the feedwater lines. The examinations included the following major tasks.

- ID surface examination of the cracked regions of the elbows/reducers
- Metallographic examination of the sections containing some of the deepest cracks
- Microstructural characterization studies of the material by light optic and thin foil electron microscopy techniques

---

[ ] a,c

** The cracking incident was first noted by the detection of leaks in the feedwater lines of loops 1 and 4 of the D.C. Cook 2 plant in May 1979.

- Fractographic examinations of fracture faces of the cracks

- Chemical evaluations of the base metal and of the deposits within the cracks

- Mechanical property tests

The purpose of the investigations were to determine the causes of cracking and to gather data in developing corrective actions.

5.2 EXAMINATIONS AND TESTS

5.2.1 ID SURFACE EXAMINATIONS

The inside diameter surface of the ring sections of the feedwater line elbows/reducers were carefully examined for cracks, pits and other effects due to surface finish, stress and corrosion. Longitudinal strips about 3/8" wide were then cut dry from the ring sections at various selected regions (corresponding to the significant cracking locations) around the circumference for microscopic examinations.

Typical ID surface topographies of the cracked regions at various locations around the circumference are illustrated by the light micrographs shown in figure 2. The angular locations of the strips shown here are measured clockwise from the top of the pipe (zero degree location) as viewed from the nozzle into the elbow/reducer.

5.2.2 METALLOGRAPHY

Studies on the distribution of cracks, microstructure studies by light microscopy, and fine microstructure studies by thin foil transmission electron microscopy are discussed in paragraphs 5.2.3 through 5.2.5, below.

5.2.3 MORPHOLOGY AND DISTRIBUTION OF CRACKS

The longitudinal strip sections from various cracked regions around the circumference of the reducer/elbows were rough ground on radial planes and were examined for the depth and the severity of cracking. The results[ ] summarized in table I illustrates typically the type of data collected. Mapings of the depth and location of cracks around the circumference of the pipes for various plants are shown in figure 3. a,c,e

The severly cracked sections were polished and metallographically examined under unetched and etched (2 percent Nital etch) conditions to study the morphology and distribution of cracks. Typical results are illustrated in figures 4 through 10. Figures 4 through 6 illustrate the distribution of cracks on radial planes. The details of the morphology of cracks are illustrated by the two typicals cases shown in figures 7 and 8 respectively.

5.2.4 MICROSTRUCTURAL STUDIES BY LIGHT MICROSCOPY

Light microscopy was conducted on material sections taken from severely cracked regions of the reducer/elbow material. The evaluations included morphology and distribution studies of the ferrite and pearlite phases and ASTM grain size determinations. The study was conducted primarily on the unaffected base material where most cracking was observed, although investigations on weld and heat affected zone regions were also conducted in some cases[ ] Measurements on the ASTM grain size were performed using the Heyn intercept method. a,c,e

Figures 9 and 10 illustrate typical optical micrographs of the unaffected base metal (A106B material) showing the distribution of the ferrite and pearlite phases. The microstructures generally showed even distribution of ferrite and pearlite phases with some banding of pearlite along the major working direction. Accicular ferrite is occasionally seen in some cases[ ]a,c,e ASTM grain size measurements showed that the grain sizes

generally were within ASTM grain size numbers of 9 and 10. The role of the various microstructural features on the observed mechanical properties and crack morphology are discussed in a later paragraph.

5.2.5 FINE STRUCTURE STUDIES BY THIN FOIL TRANSMISSION ELECTRON MICROSCOPY

Fine structure characterization studies of the ferrite and pearlite phases were conducted by thin foil transmission electron microscopy of the base metal. A Phillips-200 Electron Microscope with a 100 kv electron beam was employed for the study. Evidence for any precipitation or dislocation substructure that could have contributed to preferential corrosive attack through ferrite hardening was considered while examining the ferrite substructure. Pearlite phase was examined at different grain orientations to enable an accurate assessment of interlamellae spacing.

Figures 11 and 12 illustrate typically the two types of fine structures observed in the ferrite phase.

The electron micrographs showed that the ferrite phase is generally free of any appreciable dislocation substructure, although there are some clear exceptions to this observation. For example, a,c,e [ ] heavy dislocation-cell structure characteristics of work hardening and/or inadequate normalizing treatment, is present. In addition, in some cases appreciable amounts of fine precipitation contributing to the ferrite hardening was also evident. The fine structures of pearlite phase, typically illustrated in figure 13 demonstrated that the pearlite lamellaer spacing is rather fine in most cases. Exception to this general observation is the a,c,e case [ ] where the cementite phase in pearlite is often found in degenerated condition and is present primarily in the form of clusters of dispersed particles. The interlamellae spacings estimates from the thin foil transmission electron micrographs ranged from 6 to 8 micro inches.

5.2.6 FRACTOGRAPHY

Approximately half inch long sections containing some of the deepest cracks were cut dry from the longitudinal strips taken from the deepest cracked locations around the elbows/reducers. The deepest cracks were carefully opened dry, in the laboratory so as not to contaminate the cracks or remove any deposits. The crack surfaces were then examined in the as-received condition by light and scanning electron microscopy. The deposits on the crack surface were analyzed by energy dispersive x-rays as described in paragraph 5.2.7. The deposits and oxide were then removed by electrolytic means (endoxing) to facilitate further fractographic examinations by light optic, scanning electron and replica transmission electron microscopy techniques.

5.2.7 LIGHT OPTIC AND SCANNING ELECTRON MICROSCOPY FRACTOGRAPHY

The fracture faces were first examined in the as-received condition by a low power light microscope and scanning electron microscope. Following the removal of the deposits and oxide, a detailed examination of the topographic features of the fracture faces was conducted both at low magnifications by light microscopy and at higher magnifications by scanning electron microscopy. The appearance of the crack surfaces in the electrolytically cleaned condition is typically illustrated by the optical micrograph of the [ ] fracture shown in figure 14 and. Typical SEM fractographs of the fracture surface are illustrated in figures 15 and 16. The fractographs showed the appearance of "beach marks" and severe corrosion and pitting on the fracture surfaces. a,c,e

5.2.8 REPLICATION ELECTRON MICROSCOPY

Transmission electron replica examinations were carried out to establish whether metal fatigue played a role in the fracture process. Two-stage, platinum shadowed, cellulose-acetate carbon replicas were prepared from cleaned fracture surfaces and were examined for fatigue striations with a 100kv transmission electron microscope. The examinations were centered around crack-tip regions and other regions of the fracture surface where surface effects due to corrosion/oxidation were minimal and visibility of striations if present, is enhanced.

Close similarities between the fatigue striation spacings and pearlite lamaelle spacing in the material warranted extensive examinations of replica specimens (as many as 40 replicas per fracture surface, in some cases) to arrive at definitive conclusions. The similarities were so close that a definitive conclusion on the fatigue striations was difficult to reach in some cases. The definitive evidence of fatigue striations found [ ] however, clearly demonstrated the dominant role of fatigue in the fracture process. Figures 17 and 18 typically illustrate the electron fractographs of containing fatigue striations.

a,c,e

5.2.9 CHEMICAL ANALYSIS

5.2.10 BASE METAL CHEMISTRY

Base metal samples from cracked elbow/reducer regions were analyzed for complete chemistry to verify if the materials met the ASTM A106 Grade C chemical requirements. The listing of base metal compositions shown in table II suggests that the materials generally met the chemical requirements.

5.2.11 CORROSION DEPOSITS ON THE CRACK SURFACE

The corrosion deposits on the crack surfaces and at the crack-tips were analyzed by both the energy-dispersive x-ray technique and direct-imaging mass spectroscopy (DIMA) Typical EDAX Spectra are illustrated in figures 19 and 20. The results of DIMA analysis are listed in table III.

The analysis indicated that in addition to iron oxide, the corrosion deposits generally contained small amounts of chlorine, potassium, phosphorous, aluminum, sodium and copper, although some plants showed higher concentrations of some elements than others.

5.2.12 MECHANICAL PROPERTY TESTS

Mechanical property evaluations were conducted on specimens taken from the cracked regions of the elbow/reducer material. The tests included hardness measurements, tensile tests and charpy impact tests.

5.2.13 HARDNESS SURVEY

Microhardness measurements were conducted on pearlite and ferrite grains of polished and etched sections from base material. Microhardness traverses were also made across weld-base metal regions of elbows/reducers to detect any abnormalities. Table IV illustrates typical microhardness values in ferrite and pearlite phases[ ] while table V illustrates the results of ahardness survey made on a polished and etched section through the nozzle-weld-reducer regions[ ]. a,c,e

5.2.14 TENSILE TESTS

Tensile tests were conducted employing bar specimens in the axial and circumferential orientations. The specimens were 0.36 inch in diameter at the reduced section and 1.4 inches in gage length. A total of four specimens were tested for each orientation, two at room temperature and two at 440°F, the approximate service temperature of the elbow/reducer. The results of the tensile tests for several of the plants are tabulated in table VI. Following the testing of specimens from several plants, it has been noticed that some variations in yield strength values with circumferential location existed in some elbow/reducer materials. A systematic study of the affect of circumferential orientation on the yield strength though desirable, could not be conducted for all the plants at this stage, due to lace of material.

However, tests were conducted on specimens taken from top and bottom (0° and 180° locations) locations of the reducers/elbows from two different plants and the results are illustrated in table VII. The

a,c,e results shown here for [ ] feedwater line materials indicate that the 440°F yield strength changes significantly from top to bottom location of the [ ] pipe while the change is not appreciable in the case of Palisades feedwater pipe material.

5.2.15 CHARPY IMPACT TESTS

Charpy impact specimens were machined from reducer/elbow material, both in the axial and circumferential orientations. Ten specimens for each orientation were tested at temperatures ranging from 0°F to 440°F, in order to determine the FATT (Fracture Appearance Transition Temperature).

A listing of the fracture appearance transition temperatures for materials from various plants, obtained from the charpy impact curves, are
a,c,e presented in table VIII. The values ranged from 0°F to 70°F with the exception of [ ] which showed a FATT of 120°F, but well below the operating temperature of 440°F.

5.3 DISCUSSION

Visual and microscopic examinations of the inside surfaces and of the radial sections near the nozzle-to-pipe joint revealed cracks and pits. Figures 2 and 4 through 8. The examinations showed that the cracking and pitting were essentially restricted to elbow/reducer counterbore regions and that the cracks tended to initiate from machining, grooves or grinding marks below the "knee" of the reduced section. The depth of the cracks varied significantly around the circumference (figures 3 a,b,c,d and e, table I). The cracks were circumferential, growing in the radial direction, always from the ID surface to the OD surface.

Metallographic examinations of the sections containing the cracks revealed that the general character of the cracks varied between two
a,c,e distinctly different types of cracking behavior, namely single, straight types of cracks with little branching and relatively lower amounts of oxidation/corrosion as was shown by the [ ]

Cracks and, branched multiple type of cracks with large amounts of wide spread corrosion as was shown for example, by the [ ] a,c,e cracks (figures 7 and 8). Nevertheless, the cracks ran along the circumference of the pipe and grew radially inward from ID to OD surface. The cracks were transgranular in most cases and they disregarded the banded nature of the microstructure.

The general microstructures of the elbow/reducer materials as revealed by light microscopy showed typical pro-entechoid ferrite-pearlite grain distribution with fine grain size and some banding of pearlite along the major working direction. The ferrite grains were equiaxed in most cases although some acicular ferrite was noted in one or two instances. Thin foil transmission electron microscopy studies of the fine structure in the elbow/reducer materials showed that the ferrite phase is generally free of any appreciable dislocation substructure. Exception to this observation are the cases of [ ] a,c,e where heavy dislocation cell structure characteristic of work hardened and/or inadequately normalized condition. In addition, appreciable amounts of fine precipitation contributing to the ferrite hardening was also present in some instances. The fine structure in pearlite phase (figure 13) demonstrated that the pearlite lameallar spacing is rather fine in these materials. Exception to this general observation is the case of [ ] a,c,e pipe where the cementite phase in pearlite is degenerated and is present as clusters of dispersed particles . The lamaellar spacings estimated from thin foil TEM micrographs ranged from 6 to 8 micro inches.

An examination of the chemical composition and strength properties of the elbow/reducer materials listed in tables II and VI demonstrate the material confirmed to the ASTM A106 Gr. C specifications. No appreciable microstructural abnormalities contributing to the cracking were found in the material. The fracture appearance transition temperatures (table VIII) ranged from 0°F to 70°F (with the exception of San Onofre which showed a FATT of 120°F, but well below the operating temperature of 440°F). The materials can be considered as notch insensitive, having Charpy impact values well above 100 ft/lbs (usually

180 ft/lbs) at room temperature and operating temperature. A review of the strength values at service temperatures (440°F) suggests two notable observations. The drop in the yield strength values with increase in test temperature (from room temperature to service temperature) appears to vary appreciably from one plant to the other. This can be clearly seen in table IX. Also there appear to be significant differences in the yield strength values from top to bottom location of the pipe material, in few instances. (Table VII). The significance of these two observations on the cracking behavior is not clearly known. Also listed in Table IX is the normalized crack depth i.e. maximum crack depth to counter bore thickness ratio, for various plants.

Light microscope fractography as shown typically in figure 14, indicated that crack propogation was intermittant, as demonstrated by the "beach marks" (crack arrest lines). Because of the occasional blunting of the crack tips by heavy oxide formation and side growth of oxide along the crack path crack progression was determined to be a process of arrest and growth as marked by the "beach marks."

Typical fracture topography of one of the main cracks at various depth locations is shown in figures 15 and 16. The extent of ID surface pitting as well as general corrosion and cavitation is clearly indicated here by the topography of the fracture surfaces, after the removal of the oxide. Figure 16 also illustrates the branching nature of the crack. Energy dispersive x-ray analysis (EDAX) of the base metal and of the deposits on the fracture surface generally showed evidence of a number of detrimental (corrosive) elements. These included, in addition to iron oxide, chlorine, phosphorous, copper, aluminum, sulphur, silicon sodium and potassium, some of which can play a very aggressive role in corrosion process. Some of the above elements were found to be predominant in certain plants than others. For example, chlorine was present in large quantities in the case of [ ] while copper was found to be prevelant in the case of [ ]. Copper

deposited from an aquous solution is detrimental because it supplies electrons, and thus acts in a manner similar to oxygen in water. Furthermore, after copper is deposited on steel, it creates a galvanic couple in which steel is anodic and therefore is preferentially attacked.

Replication transmission electron microscopy examinations of the crack-tip regions clearly showed evidence of fatigue striations in the case of [ ]. Although the presence of beach marks could not be confirmed beyond doubt in other cracks, it is believed that the similarity of pearlite lamaelle spacing with striations and the presence of extensive corrosion may have precluded this confirmation in these plants. [a,c,e]

The relatively straight nature of crack growth in the radial direction suggests that axial stresses in the pipe played a significant role in the progression of the crack. The presence of beach marks indicated that the state of stress or of environment had changed during the life of crack. Corrosion products and pitting seen in the crack and on the OD surface of the pipe suggested that crack initiation was the result of an aquous attach on the metal at preferred stress concentration sites such as sharp changes in the cross section or machining grooves. The clear evidence of fatigue striations seen in several cases demonstrates the cyclic stress axial to the pipe played a significant role in the cracking process. Oxide formation could also have contributed to crack growth by the effect of volume expansion exerting tensile stresses at the crack tip, since iron oxide (Fe_3O_4) is more voluminous than parent metal.

The chemistry and mechanical properties of the materials confirmed to the ASTM specification. No appreciable microstructural abnormalities contributing to cracking were found. These observations clearly suggest that the observed cracking in the feedwater piping is most likely the result of corrosion fatigue. A geometrical discontinuity at the "knee" of the counter bore region and machining and grinding marks on the ID surface in the presence of general corrosion and pitting appears to have contributed to the crack initiation.

5.4 REFERENCES

1. "Metallurgical Investigation of Cracks in the Steam Generator Feedwater Line at the H. B. Robinson Station of the Carolina Power and Light Company," A. Madeyski, G. V. Rao and T. R. Mager, Westinghouse Class 3 Report, WCAP-9616.

2. "Metallurgical Investigation of Cracking in the Steam Generator Feedwater Pipes of D. C. Cook Station Units 1 and 2," A. Madeyski, G. V. Rao and T. R. Mager, Westinghouse Class 3 Report, WCAP-9581.

3. "Metallurgical Investigation of the Steam Generator Feedwater Piping Cracks at the Robert Emmet Ginna Nuclear Power Generating Station," L. Albertin, G. V. Rao, and T. R. Mager, Westinghouse Class 3 Report, WCAP-9563.

4. "Metallurgical Investigation of Cracks in the Steam Generator Feedwater Lines of Surry Station No. 1," L. Albertine, G. V. Rao and T. R. Mager, Westinghouse Report, WCAP-9638.

5. "Metallurgical Investigation of Cracks in the Steam Generator Feedwater Pipe of the Palisades Nuclear Generating Station," A. Madeyski, G. Rao, T. R. Mager, Westinghouse Class Report, WCAP-9669.

6. Metallurgical Investigation of Cracks in the Steam Generator Feedwater Piping of Salem Station Unit 1," L. Albertine, G. Rao and T. R. Mager, Westinghouse Report, WCAP-9591.

7. "Metallurgical Investigation of Cracks in the Steam Generator Feedwater LIne of the Wisconsin Public Service Corporation's Kewaunee Station," A. Madeyski, G. V. Rao and T. R. Mager, Westinghouse Report, WCAP-9673.

8. "Metallurgical Investigation of Cracks in the Steam Generator Feedwater Lines of San Onofre Station, Unit 1," J. F. Enrietto, A. Madeyski and G. V. Rao, Westinghouse Class 3 Report, WCAP-9544.

9. "Millstone Unit 2, Steam Generator 2, Feedwater Pipe Failure Analysis," Nuclear Power System Report, No. N-TP-MCM-001, Combustion Engineering Incorporated, March 1980.

TABLE I

a,c,e

CRACKS IN LONGITUDINAL SECTIONS TAKEN AT VARIOUS LOCATIONS AROUND THE CIRCUMFERENCE OF [redacted] UNIT 1 LOOP 2 ELBOW

Circumferential Location (deg)	Number of Major Cracks	Approximate Depth of the Largest Crack (in.)
25	2	0.025
55	9	0.015
60	6	0.020
70	15	0.050
115	12	0.060
160	9	0.040
215	11	0.050
260	8	0.065
305	7	0.030
350	2	0.025

TABLE II

CHEMISTRY OF THE ELBOW/REDUCER MATERIALS

Materials	Elements					
	C	Mn	Si	S	P	
ASTM A106 Grade C	0.35 Max.	0.29-1.06	0.10 Min.	0.058 Max.	0.048 Max.	a,c,e
[	0.205	0.99	0.18	0.022	0.011	
	0.25	0.72	0.21	0.009	0.007	
	0.26	0.84	0.14	0.018	0.007	
	0.25	1.03	0.17	0.013	0.006	
	0.26	0.89	0.19	0.018	0.010	
	0.28	0.86	0.22	0.030	0.011	
	0.22	0.75	0.23	0.024	0.016	
	0.27	0.88	0.21	0.021	0.014	
	0.23	1.09	0.37	0.015	0.015	
]	0.199	0.89	0.248	0.009	0.016	

TABLE III

RESULTS OF DIMA ANALYSIS

a,c,e

Utility Plant Location: [ ]
Loop: 3
Crack Location: Elbow, Nozzle Side End
Secondary Beam Current[a] (amperes)

Ion	Crack Plus Matrix Ic	Matrix Im	Ion Yield[b] I_o	Ic-Im[c] I_o	Continuity Within[d] Crack
Na	0.3	0.48	2400	--	D
Al	150.3	130.0	200	10000	
Si	5.0	43.0	44	--	--
K	0.18	0.08	2100	5	
Ca	0.0	0.0	400	0	
Ti	0.1	0.05	44	2159	
Cr	1.4	1.0	60	667	CD
Mn	21.0	18.0	94	3191	CD
FE	200.0	180.0	34	58824	C
Ni+Fe	0.06	0.04	NA	P	
O+S	0.3	0.25	NA	P	
O^-	42.0	31.0	10	9000	C
OH^-	0.08	0.05	NA	P	C
C^-	0.6	0.6	26	0	C
CL^-	0.42	0.02	11	3636	D
PO_2	0.21	0.18	NA	P	

a. A secondary beam current of 10^{14} ampere is employed as a unit value to reduce intensities to a common reference level.
b. Relative ion yield values are from published tables. NA = value not available.
c. Values shown are based on 10^{-5} to provide an easier concept of comparative magnitude. These values are approximately proportional to the relative concentrations of ions in the crack. A dash in this column indicates that the matrix concentration was higher than the crack concentration.
P = present, not quantified.
d. C = continuous distribution, D = discontinuous distribution, CD = continous discrete particles.

TABLE IV

AVERAGE MICROHARDNESS VALUES IN FERRITE AND PEARLITE PHASE

a,c,e

Vickers Indenter 10 Gram Load - 50X Objective
Sample No. 4C-DC
Mount No. 26080

Ferrite Filar Units		Pearlite Filar Units	
1.	58	1.	45
2.	59.5	2.	50
3.	57	3.	46
4.	59.5	4.	43.5
5.	59	5.	46.5
6.	59.5	6.	49
7.	57	7.	46.5
8.	59.5	8.	44.5
9.	57	9.	44
10.	59	10.	44
Avg.	58.5	Avg.	47.9
DPH	153	DPH	248

TABLE V

a.c.e | HARDNESS SURVEY FROM NOZZLE THROUGH WELD INTO REDUCER [ ]

Location Inches	Knoop Hardness 1000 gm Load	Material
0.00	162	Nozzle
0.05	172	Nozzle
0.10	207	Nozzle HAZ
0.15	243	Nozzle HAZ
0.20	222	Weld
0.25	204	Weld
0.30	226	Weld
0.35	225	Weld
0.40	212	Weld
0.45	208	Weld
0.50	215	Weld
0.55	243	Weld
0.60	209	Weld
0.65	219	Reducer HAZ
0.70	197	Reducer
0.75	195	Reducer
0.80	197	Reducer

TABLE VI

SUMMARY OF MECHANICAL PROPERTIES *

FEEDWATER LINE ELBOW/REDUCER MATERIAL

0533B

a,c,e

Plant/Unit	Test Temperature °F	0.2% Yield Strength (PSI)	Ultimate Strength (PSI)	% Elongation In./In.	Reduction In Area (%)
[	RT	42,270	67,475	40.00	70.15
	440	28,985	63,095	31.05	68.35
	RT	39,175	72,225	33.55	62.70
	440	34,025	66,850	25.45	55.90
	RT	63,200	79,725	20.35	62.05
	440	61,700	85,175	15.15	47.15
	RT	41,160	65,910	36.85	71.150
	440	31,565	62,375	32.40	69.50
	RT	43,025	72,650	34.55	64.45
	440	26,900	66,750	30.00	60.90
	RT	37,425	66,350	36.3	65.70
	440	23,500	50,125	31.4	64.85
	RT	38,700	69,050	35.35	65.80
	440	27,500	63,600	31.65	64.35
	RT	33,900	66,350	33.8	64.50
	440	31,550	66,225	29.0	64.10
	RT	30,500	62,900	38.0	70.90
	450	28,200	57,250	35.5	70.20

*Average values based on two tests.

**Gage diameter 0.36" for [ ]. All other plants gage diameter 0.252".

TABLE VII

MECHANICAL PROPERTIES*

FEEDWATER PIPE MATERIAL, TOP AND BOTTOM LOCATIONS

a,c,e

a,c,e

Plant/Unit	Location In The Pipe	Test Temp. (^{o}F)	Specimen Orientation	Yield 0.2% (PSI)	Ultimate Strength (PSI)	Elongation (%) In. Per In.	Reduction In Area (%)
	Top(2)	RT	Axial	47,645	69,660	32.7	67.15
	Location	440	Axial	41,880	65,280	28.05	65.1
	Bottom(2)	RT	Axial	39,445	66,750	37.95	67.9
	Location	440	Axial	27,250	59,130	32.7	68.0
	Top(1)	RT	Axial	43,500	70.04	35.2	67.25
	Location	440	Axial	30,950	63.20	30.35	64.45
	Bottom(2)	RT	Axial	40,960	68.82	39.10	68.75
	Location	440	Axial	29,615	62.68	32.25	65.85

(*) All the values listed here are the average from two tests.
(1) specimen diameter 0.504" (2) specimen diameter 0.36"

0533B

TABLE VIII

FRACTURE APPEARANCE TRANSITION
TEMPERATURE DATA

Plant	Fatt	
[	70°F	a,c,e
	25°F	
	40°F	
	25°F	
	120°F	
	0°F	
	5°F	
	20°F	
	20°F	
	45°F	
	20°F	
]	52°F	

TABLE IX

SUMMARY LISTING OF YIELD DROP WITH TEMPERATURE AND NORMALIZED CRACK DEPTH

FEEDWATER ELBOW/REDUCER MATERIAL

	RT Yield Strength (KSI)	440°F Yield Strength (KSI)	Maximum Crack Depth (a) Inches	Counter Bore Thickness (t) Inches	Normalized Crack Depth (a/t)
a,c,e	44.27	28.985	0.531	0.531	1.0
	37.425	23.500	0.750	1.210	0.62
	43.025	26.900	0.400	1.062	0.377
	46.965	35.135	0.170	0.710	0.24
	41.150	31.550	0.080	0.578	0.138
	38.700	27.500	0.120	0.875	0.137
	39.175	34.025	0.107	0.843	0.127
	63.200	61.700	0.050	0.578	0.086
	33.900	33.537	0.050	0.625	0.08
	43.510	30.950	0.088	1.187	0.074
	30.50	28.20	0.028	---	---

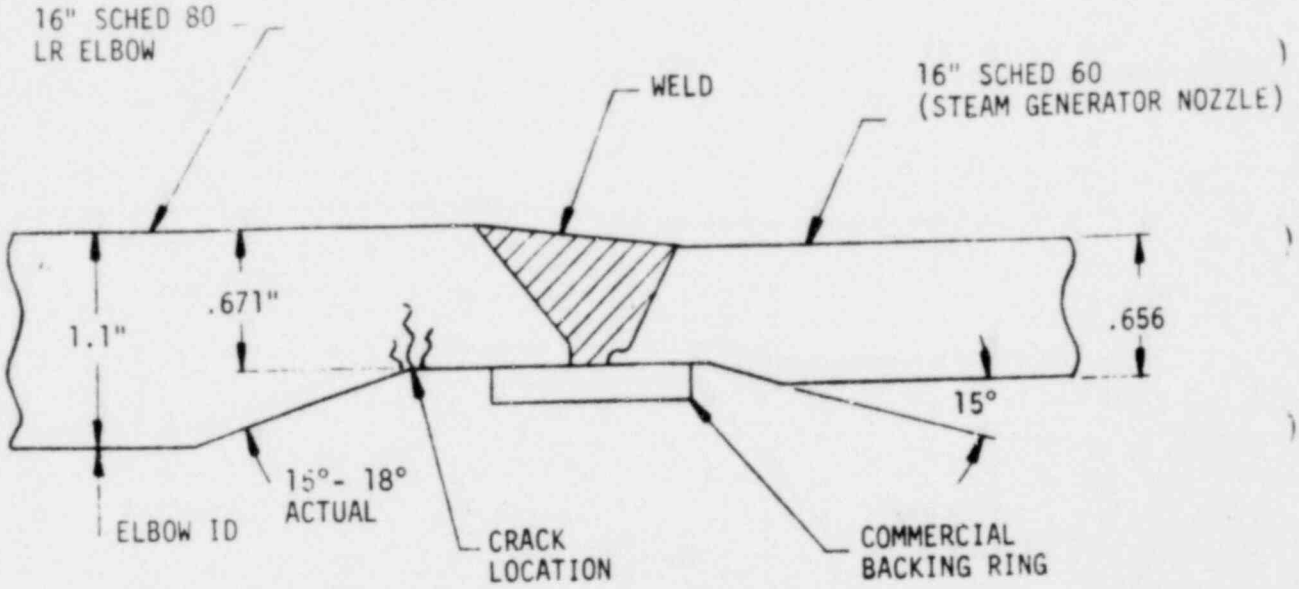

Figure 1.a. Schematic Diagram of the Crack Location in the Feed Water Pipe Elbow Next to the Steam Generator Nozzle Weld (D.C. Cook 2 loop 3) (Not to Scale)

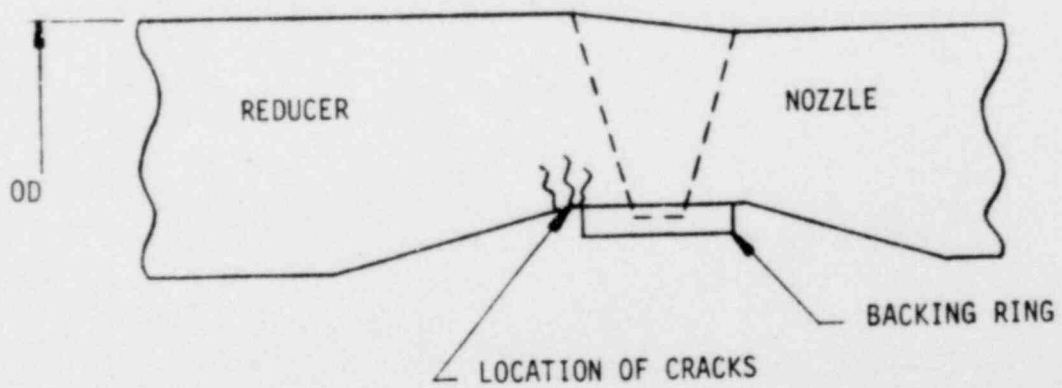

Figure 1.b. Reducer Crack Location Schematic Diagram and Crack Depth Man Around the Circumference (Based on UT Indications) (Sketch not to Scale) a.c.e

[ ]

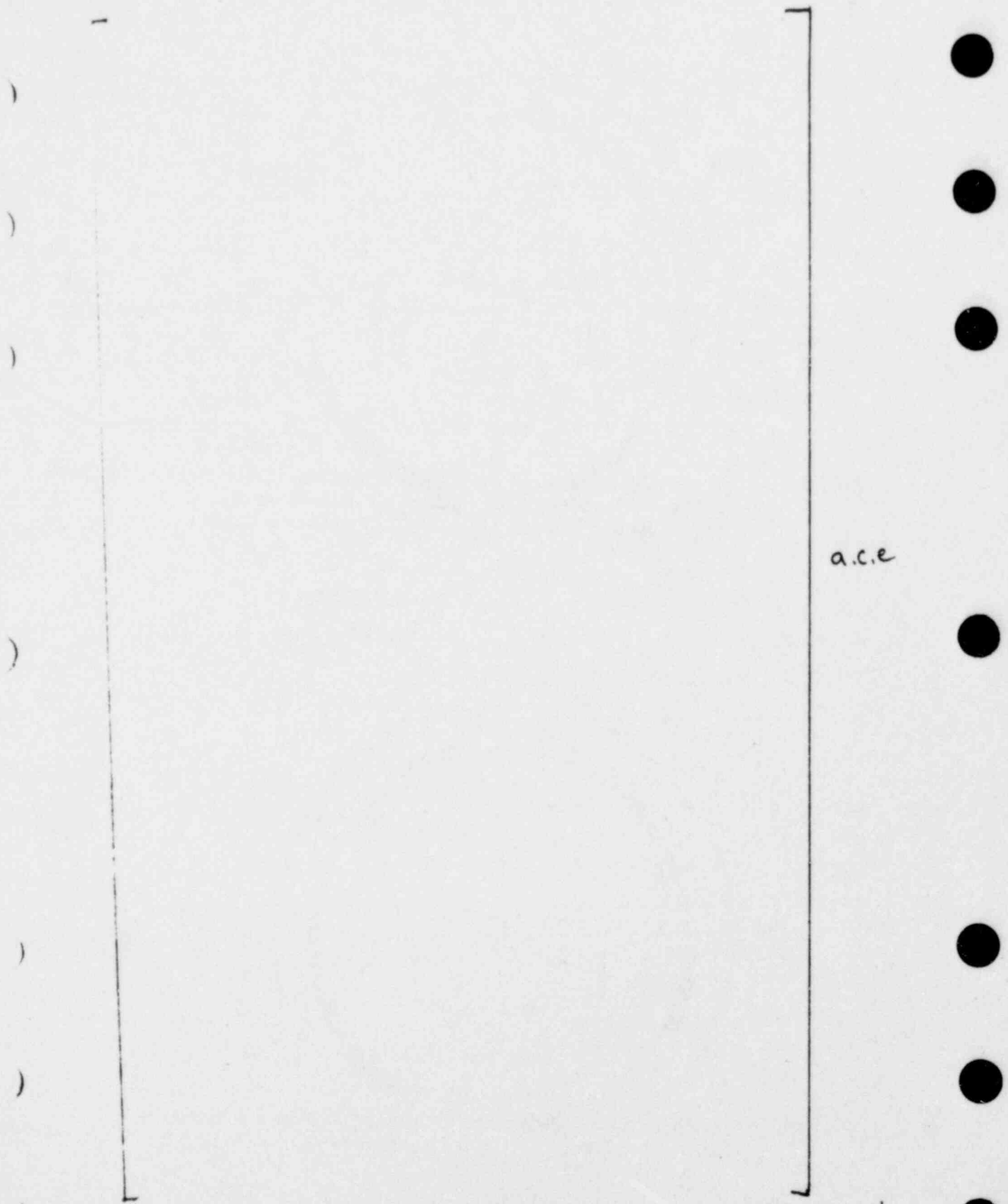

a,c,e

Figure 2.a. ID surface appearance of the safe end and of the pipe at various angular locations. Mag. 1x [ ]

a,c,e

Figure 2.b. ID surface appearance at the 180° location after the oxide was removed with the Endex treatment. Mag. 2x

[ ] a,c,e

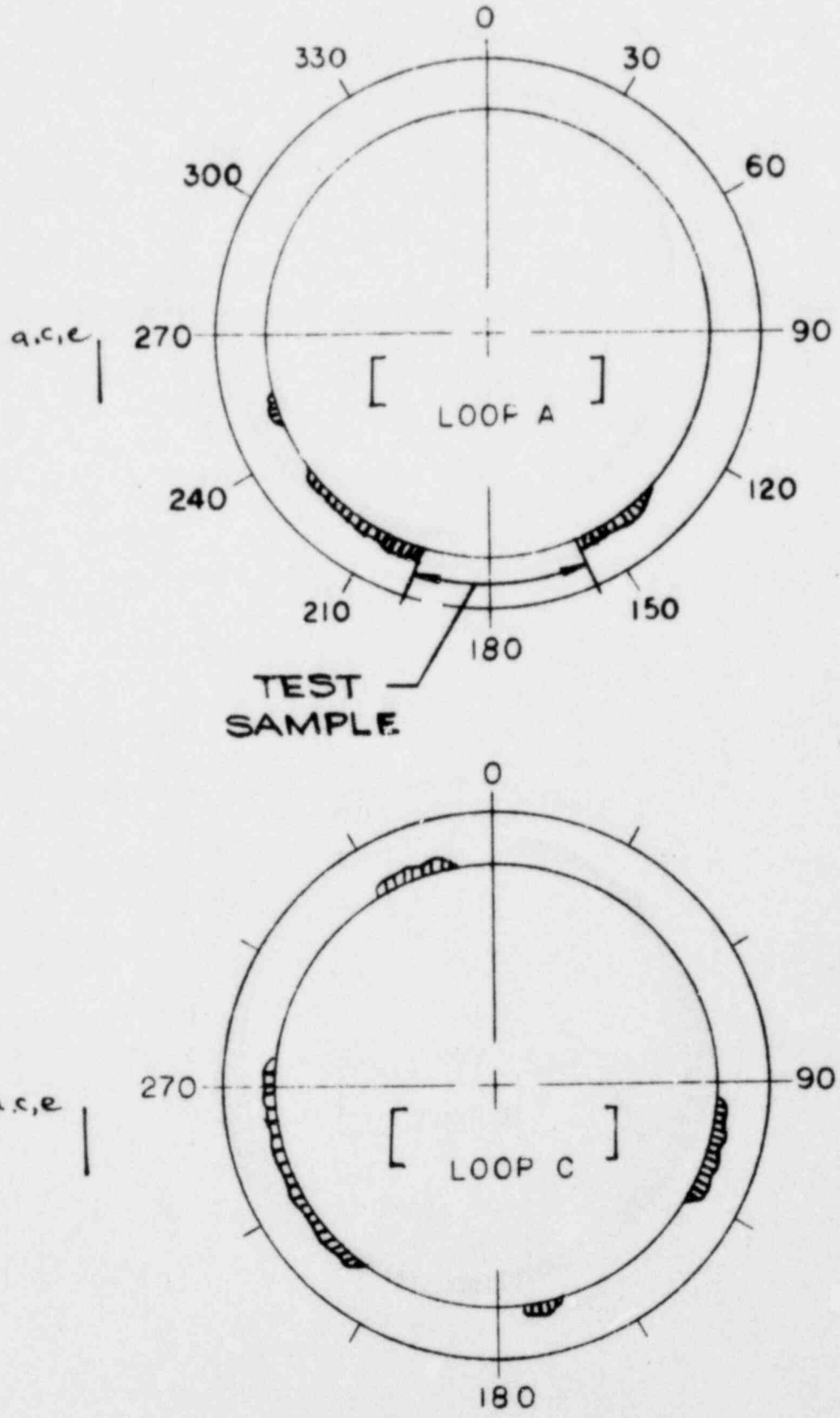

FIGURE 3(a) DEPTH AND LOCATION OF FEEDWATER PIPING CRACKS

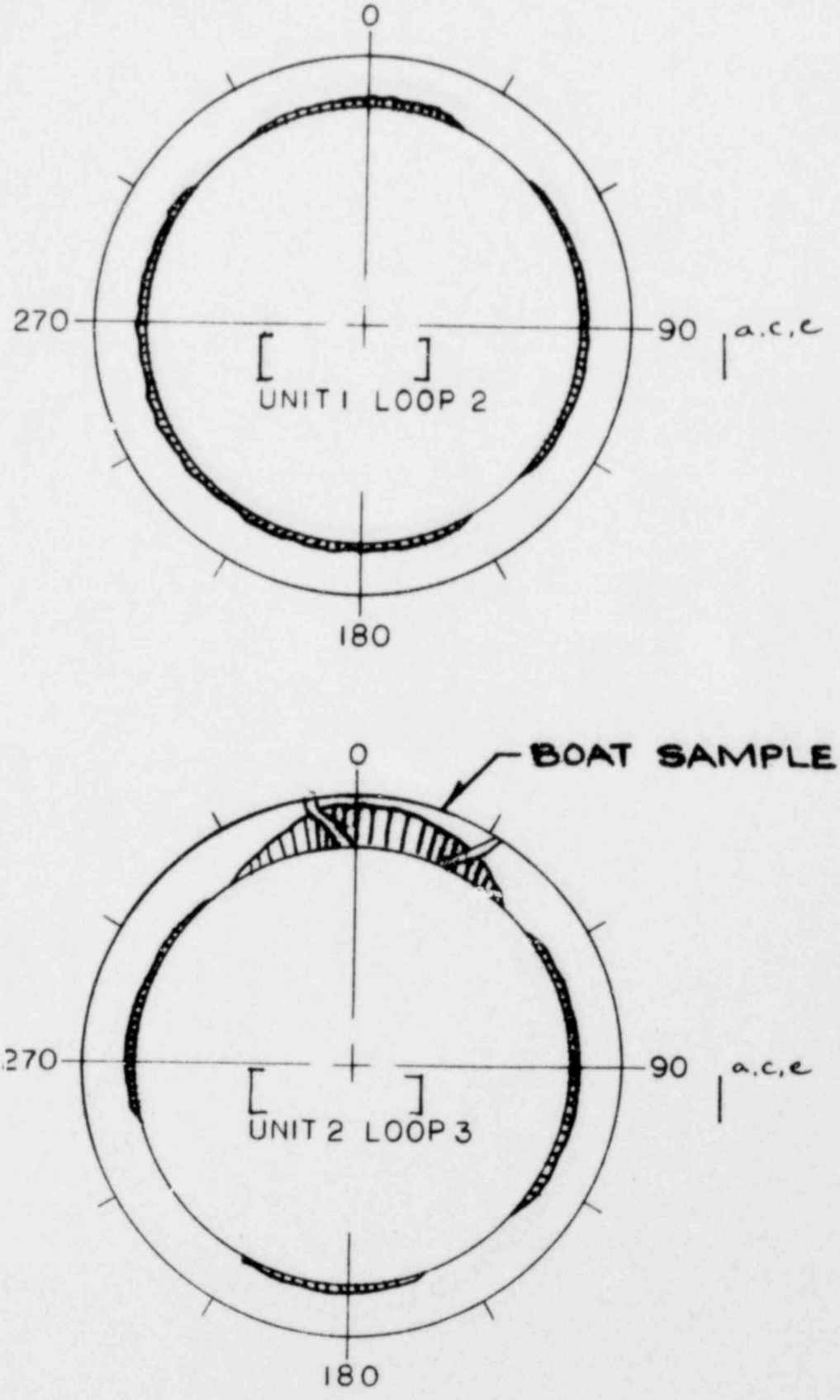

FIGURE 3(b) DEPTH AND LOCATION OF FEEDWATER PIPING CRACKS

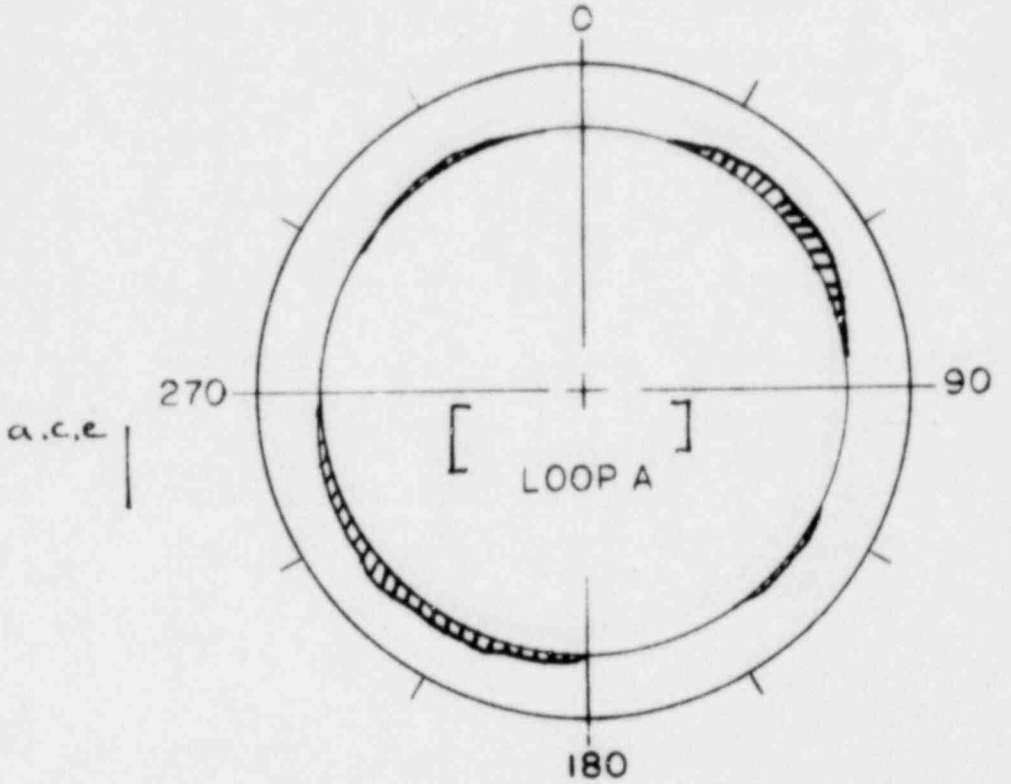

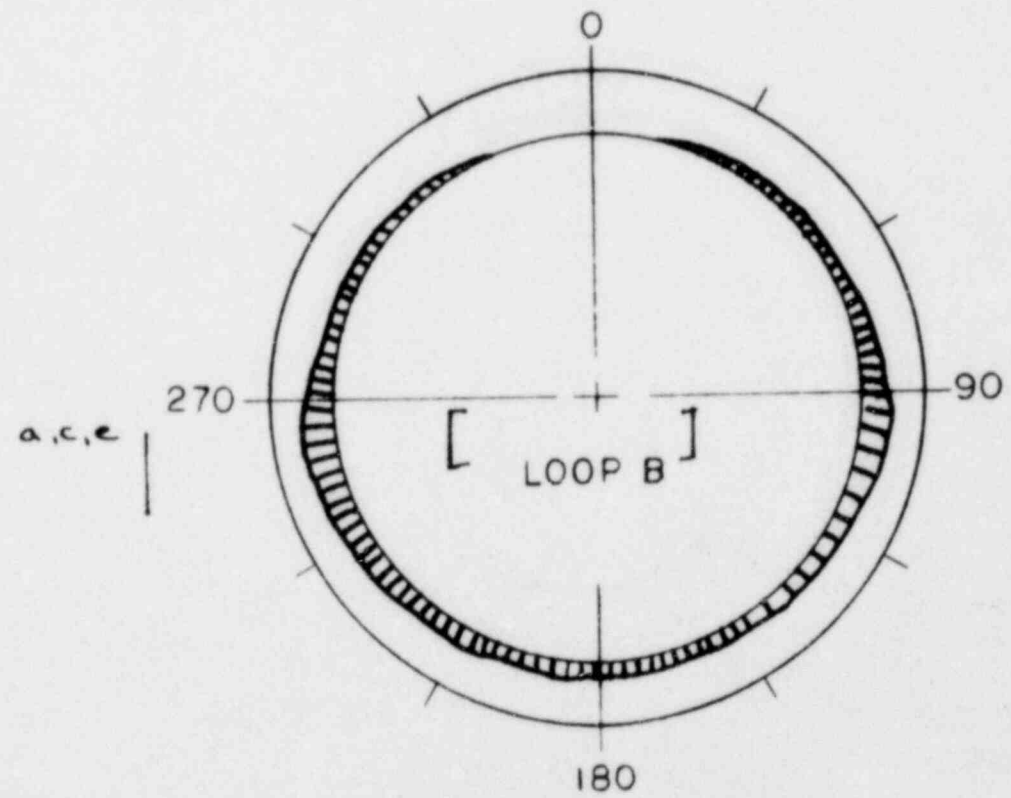

FIGURE 3(C) DEPTH AND LOCATION OF FEEDWATER PIPING CRACKS

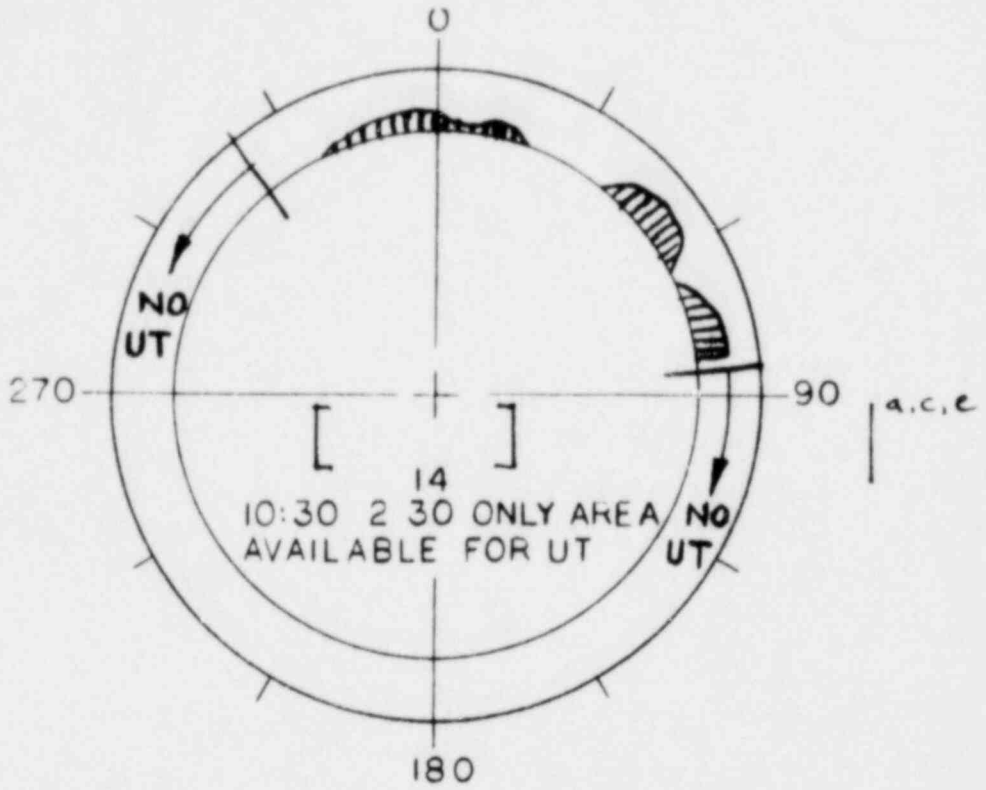

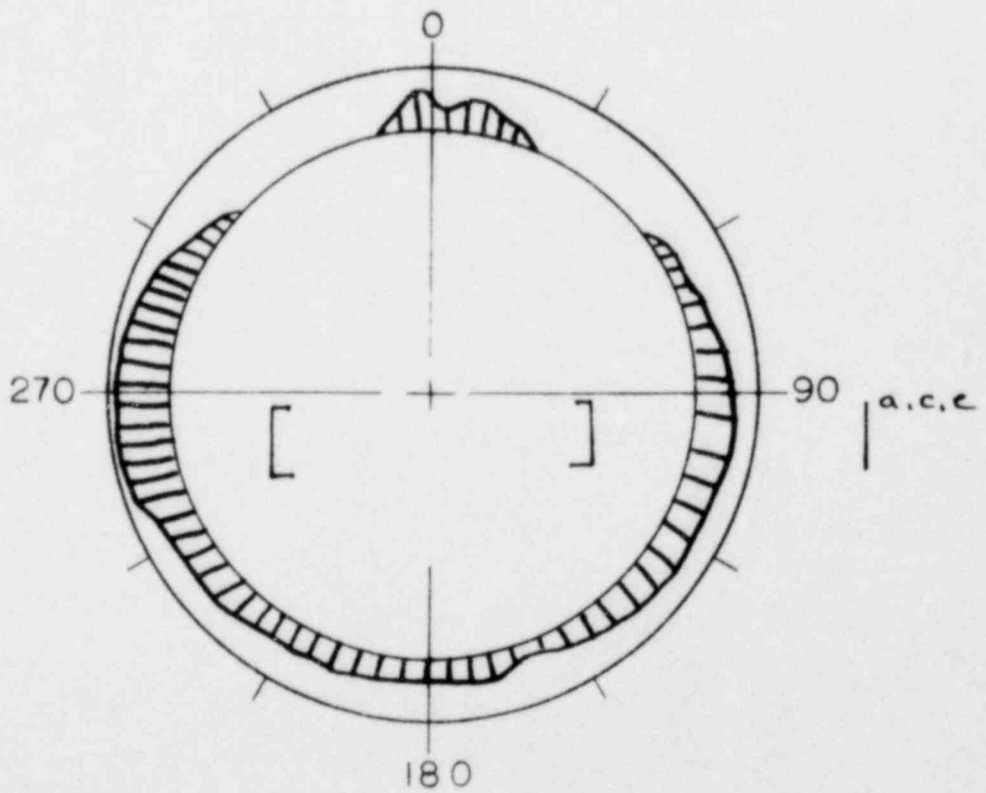

FIGURE 3(d) DEPTH AND LOCATION OF FEEDWATER PIPING CRACKS

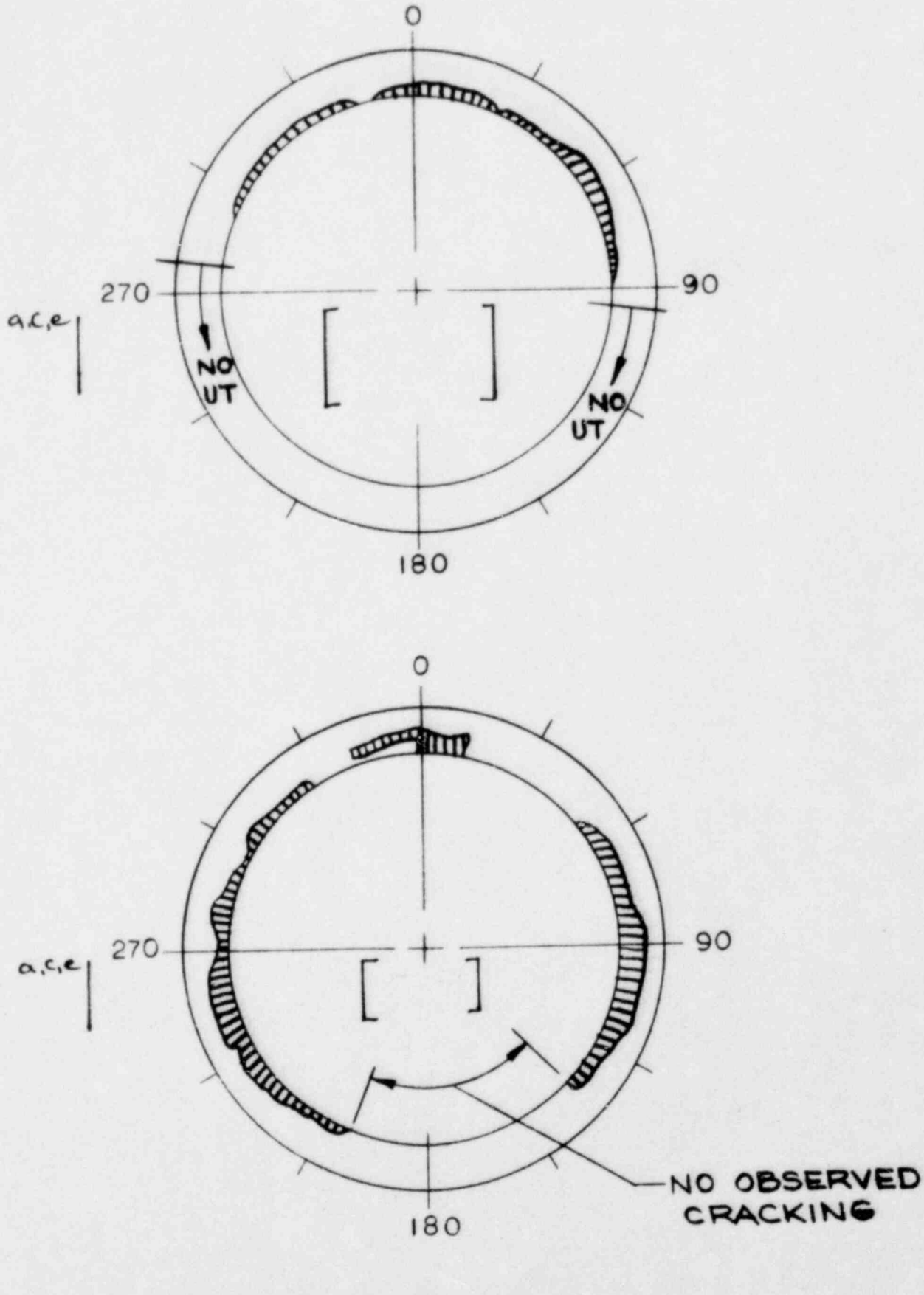

FIGURE 3(e) DEPTH AND LOCATION OF FEEDWATER PIPING CRACKS

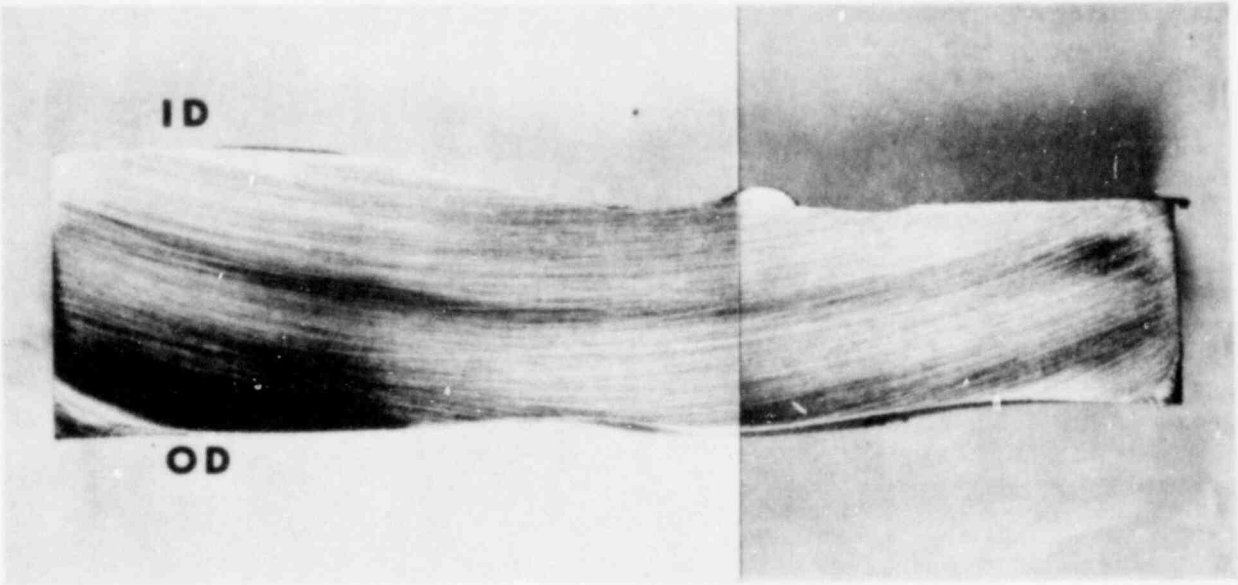

0° location

60° location

Figure 4 . Longitudinal sections of the "safe end" and of the pipe rough ground. Circumferential locations at 0° and 60° from the top of the pipe as attached to the steam generator nozzle. Note the absence of the cracks at the top. Mag. 1.5x.

POOR ORIGINAL

POOR ORIGINAL

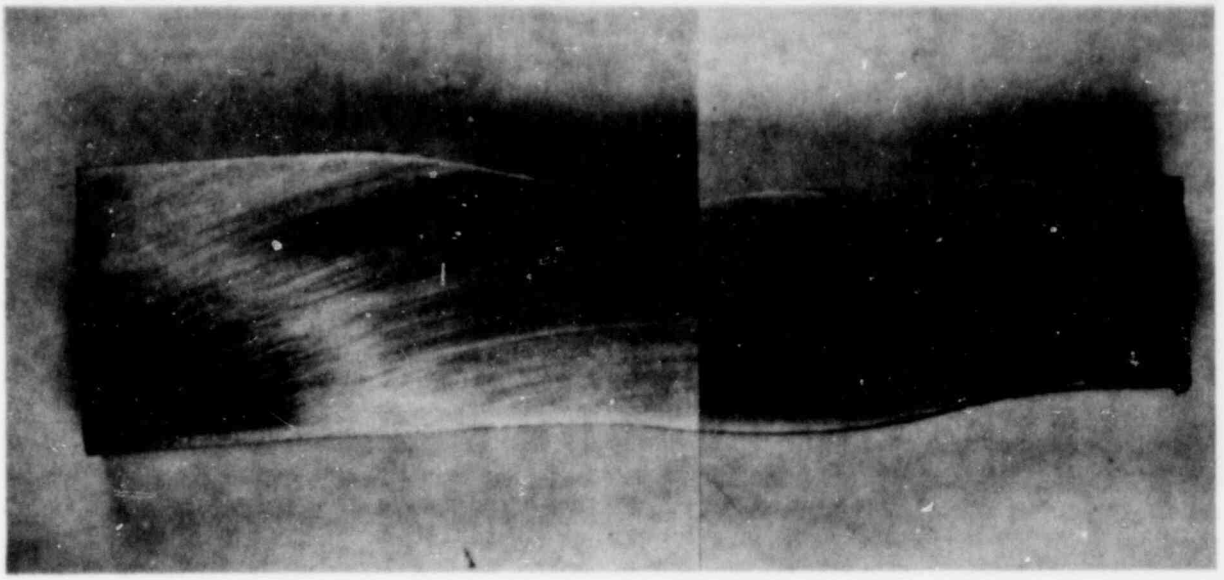

90°

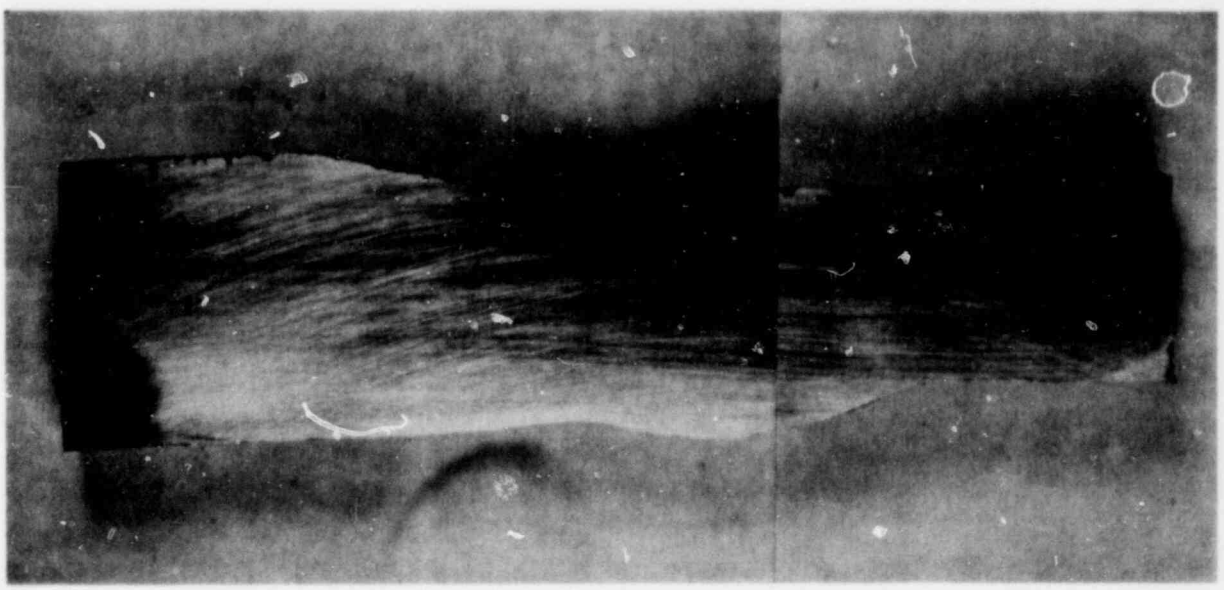

180°

Figure 5 . Longitudinal sections through the "safe end" and the pipe, rough ground. Circumferential locations at 90° and 180° from the top. The internal diate location (120°) section is shown at a higher magnification in figures 2-7 and 2-8. Note the extensive cracking at the bottom of the piping (180°). Mag. 1.5x

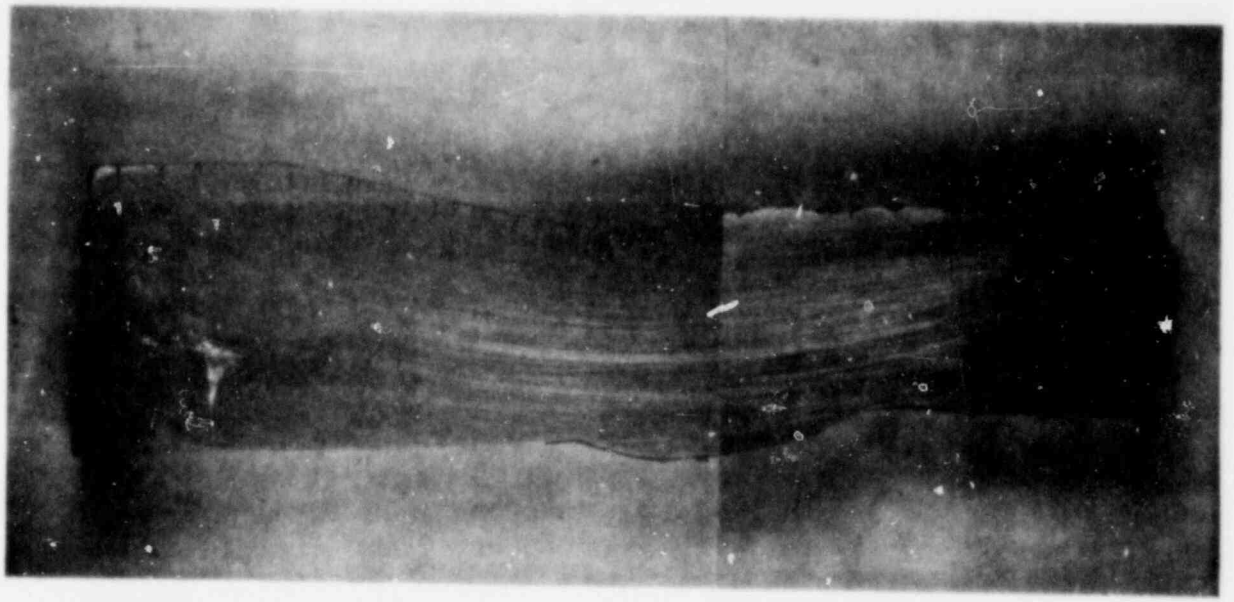

240°

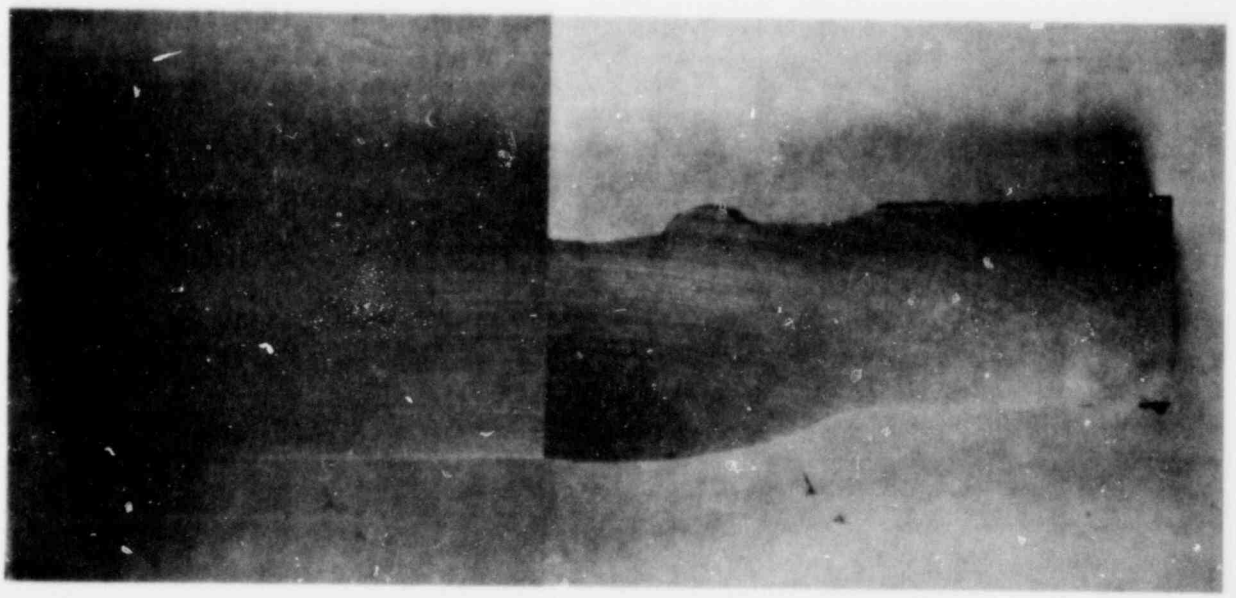

300°

Figure 6 Longitudinal sections through the "safe end" and the pipe, rough ground. Circumferential location at 240° and 300° from the top of the pipe. Mag. 1.5x.

POOR ORIGINAL

POOR ORIGINAL

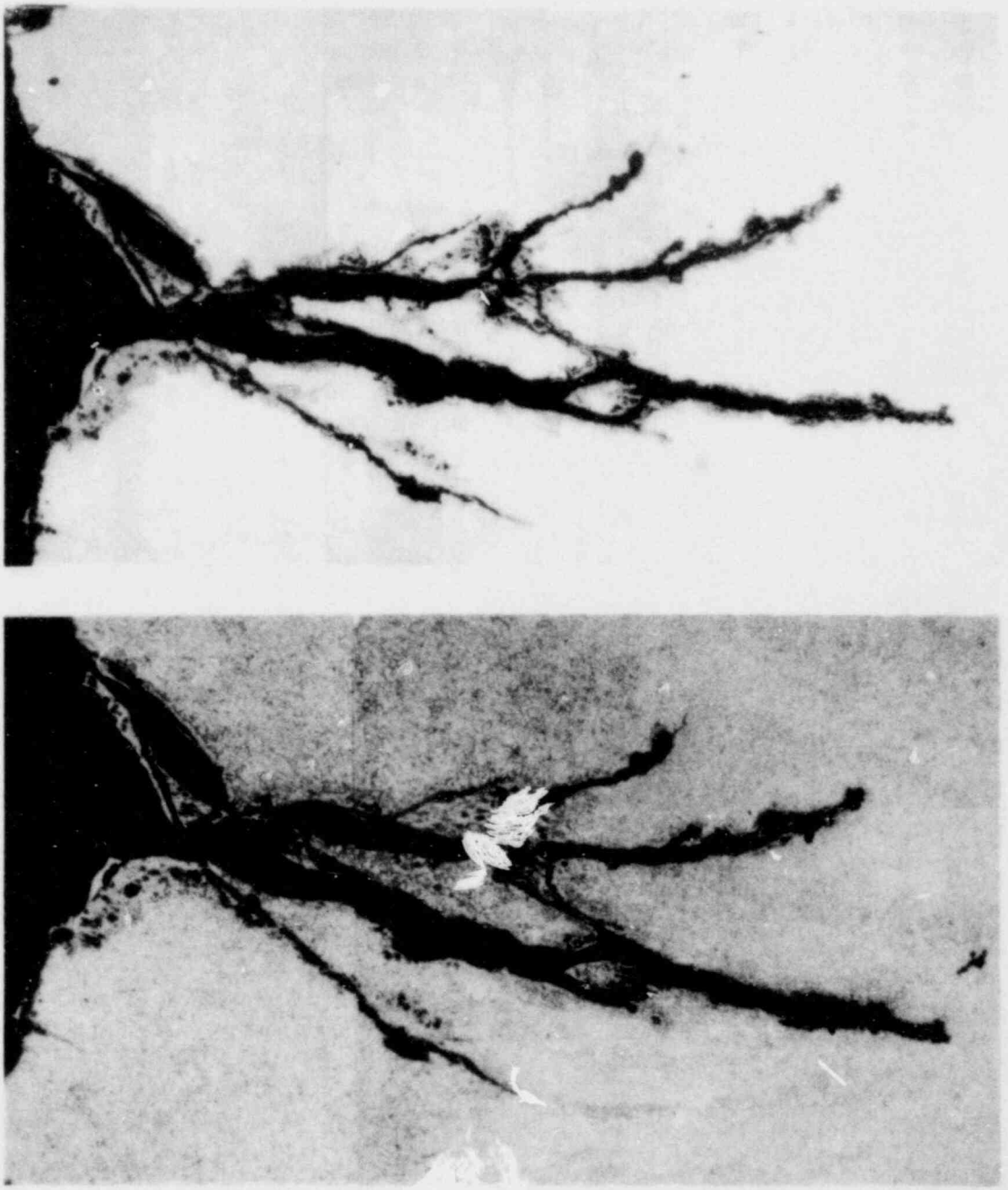

Figure 7. Loop B reducer crack at the weld. Longitudinal section 15" from the top (4 o'clock), re-polished and re-etched with Nital. Mag. 50X.

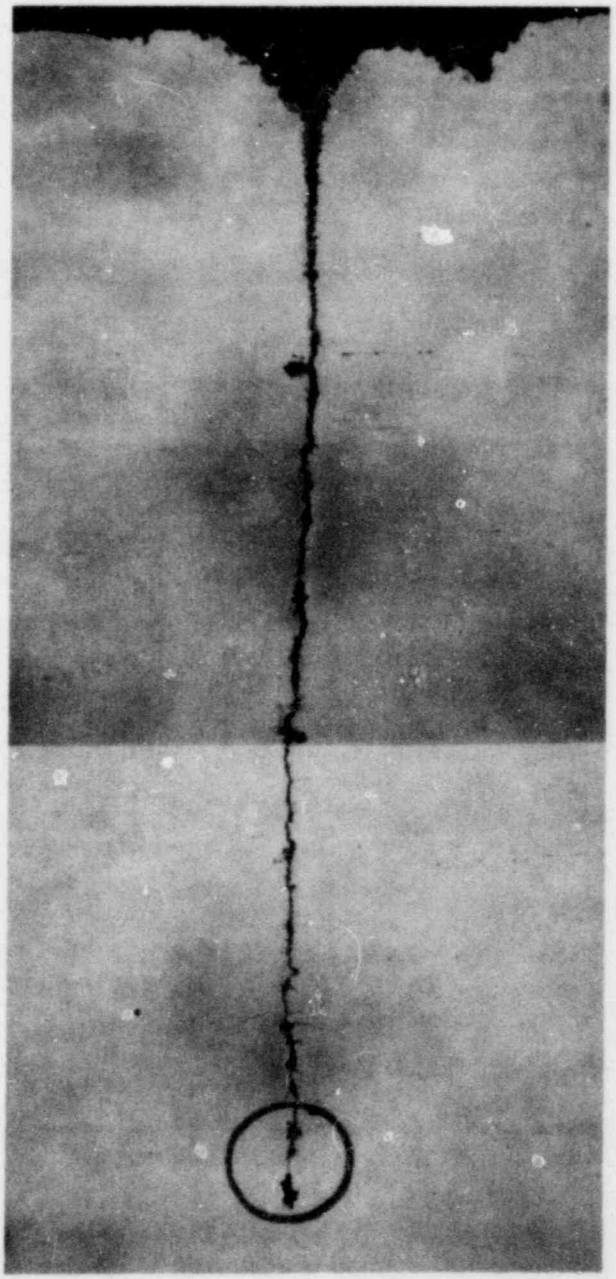

a. Main Crack (50X)

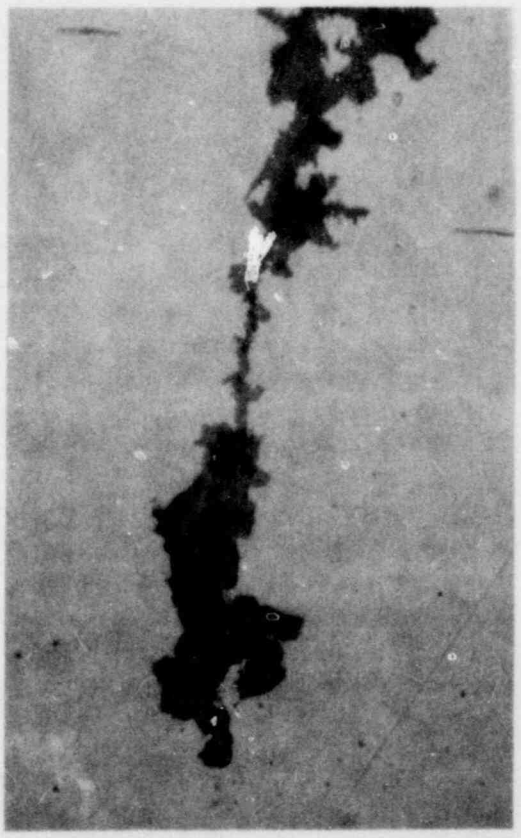

b. Crack Tip of Main Crack (500X)

POOR ORIGINAL

Figure 8. Largest crack found in Loop 1 reducer.

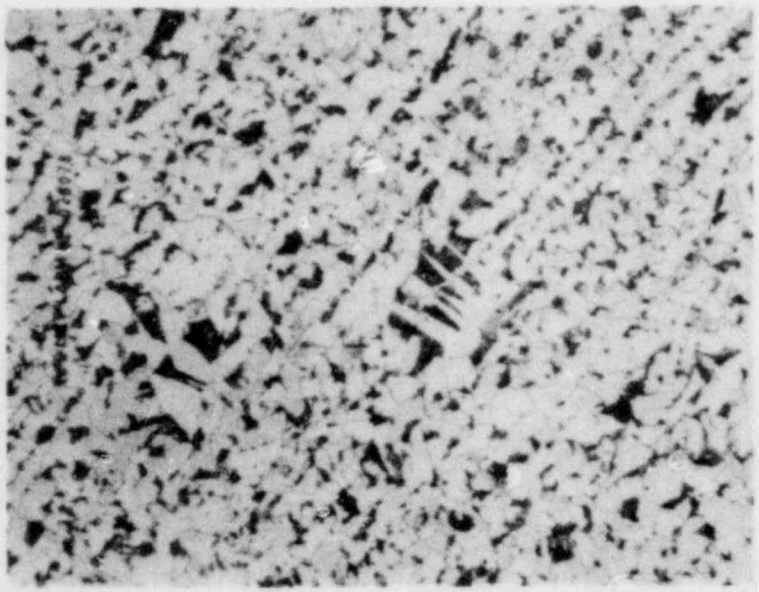

(a) 200X

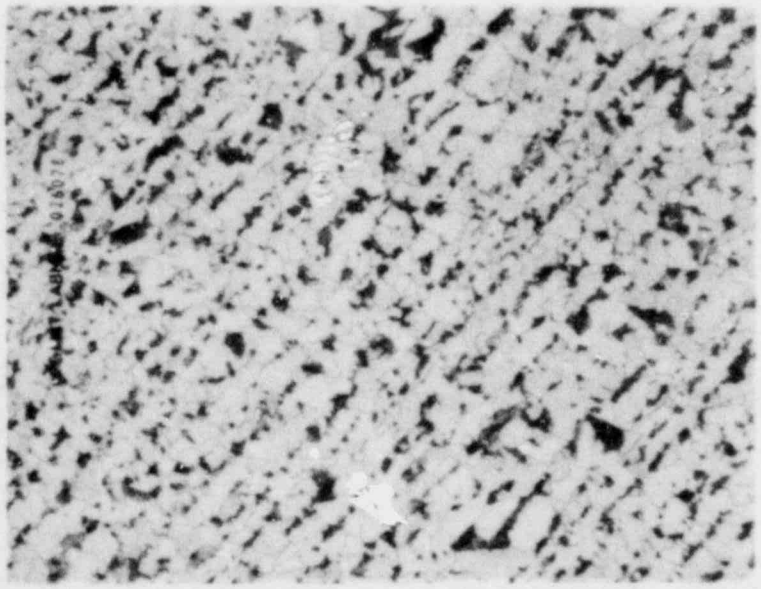

(b) 200X

Figure 9. Optical micrographs illustrating the grain size and distribution of ferrite and pearlite phases. 3% Nital Etch.

POOR ORIGINAL

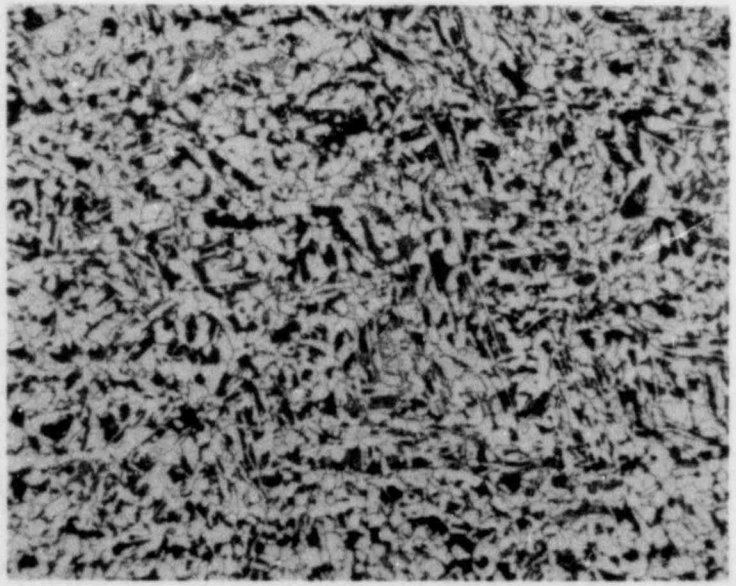

(100X)

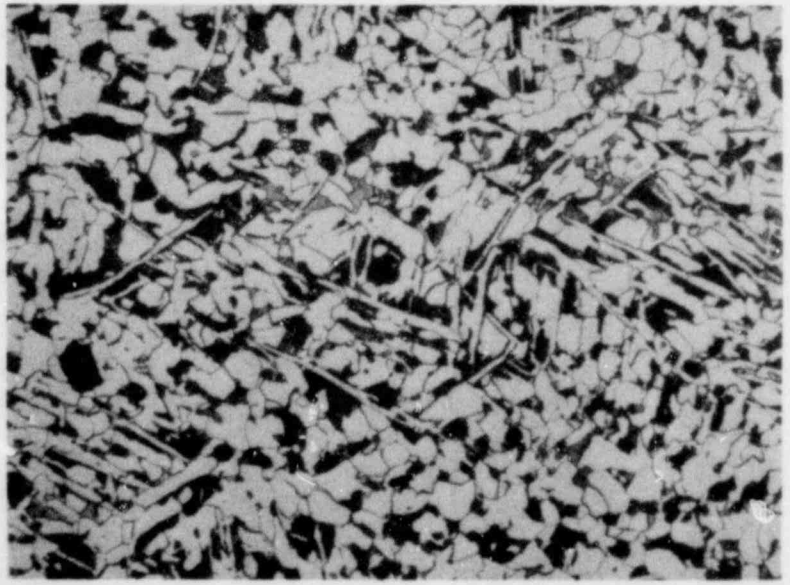

(200X)

POOR ORIGINAL

Figure 10. Light micrographs showing grain size and distribution of ferrite and pearlite phases in the feedwater pipe reducer (2 percent Nital Etch).

POOR ORIGINAL

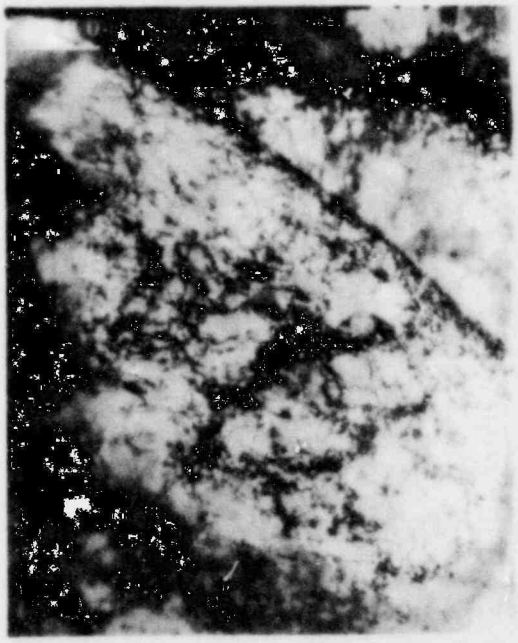

(a) 28,000X

(b) 37,000X

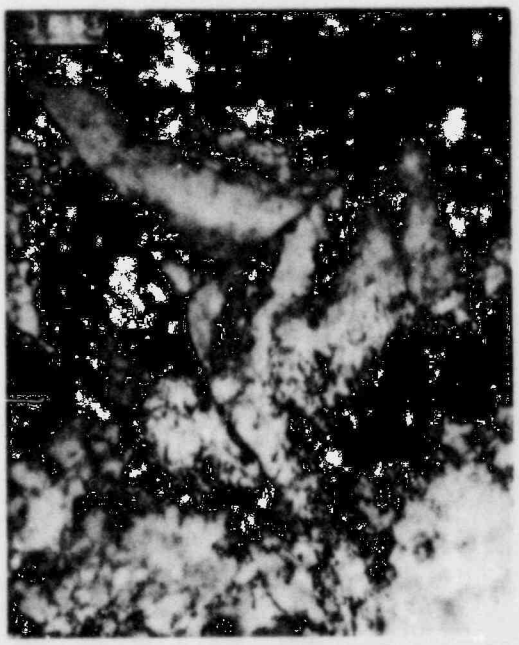

(c) 37,000X

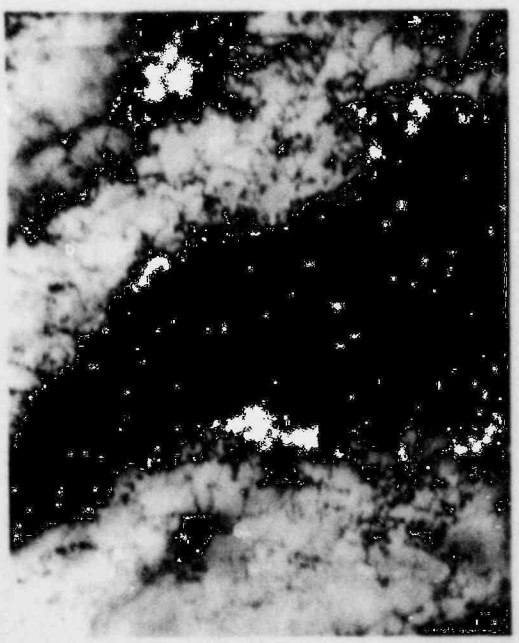

(d) 37,000X

Figure 11. Thin foil Transmission Electron Micrographs illustrating dislocation substructure within ferrite grains.

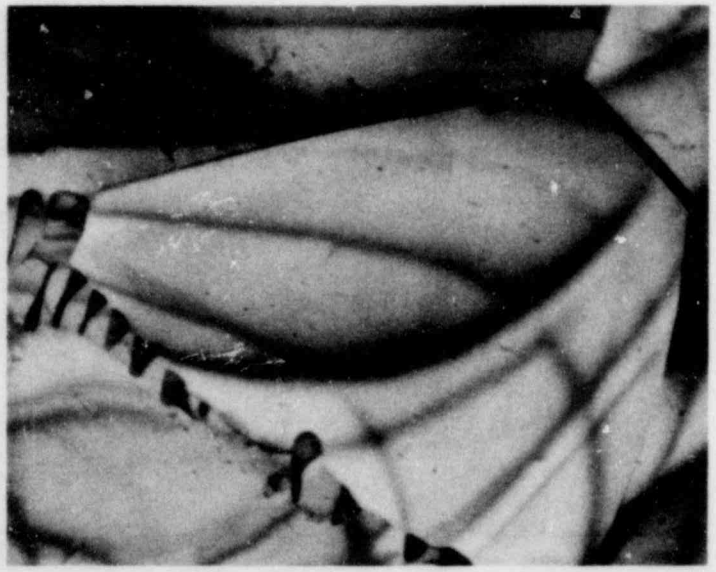

(12,000X)

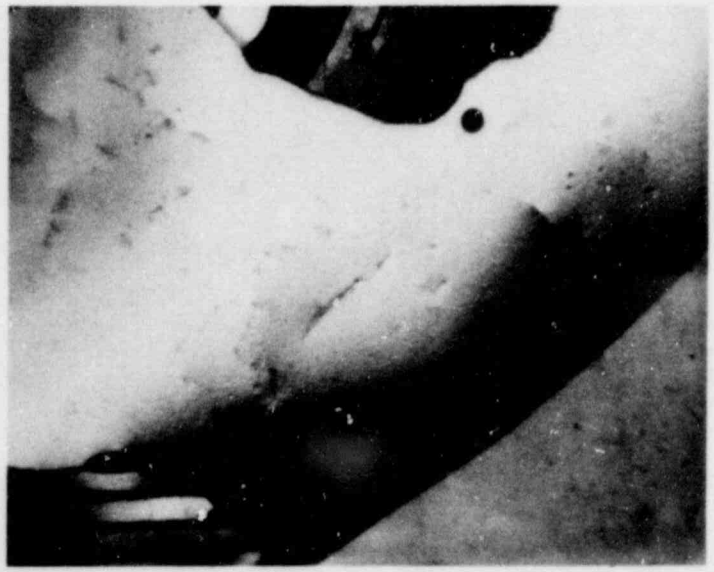

(12,000X)

Figure 12. Thin foil Transmission Electron Micrographs showing the reducer material's ferrite phase substructure.

POOR ORIGINAL

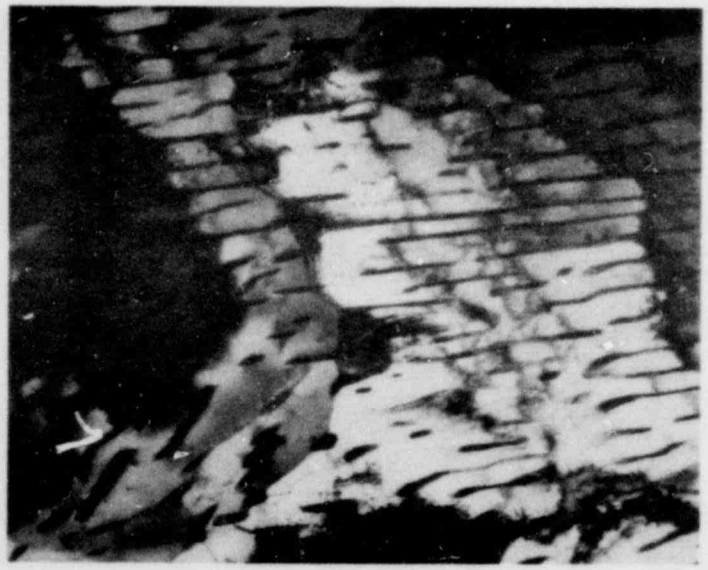

(12,000X)

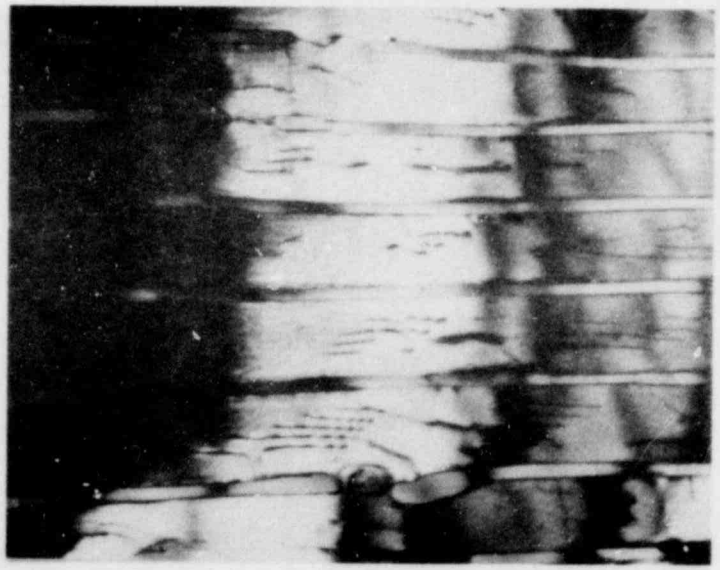

(27,200X)

POOR ORIGINAL

Figure 13. Thin foil Transmission Electron Micrographs showing the reducer material's pearlite phase Lamellae structure.

POOR ORIGINAL

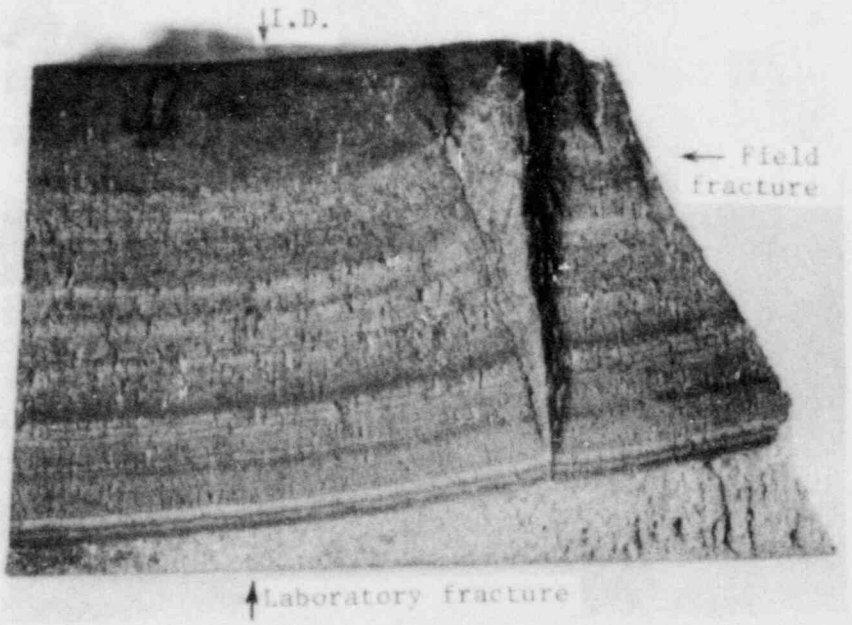

5.2X

Figure 14. Crack fracture surface showing beach marks and bands with slightly different fracture macrotopographies between the beach marks. The oxide was removed before the photograph was taken.

POOR ORIGINAL

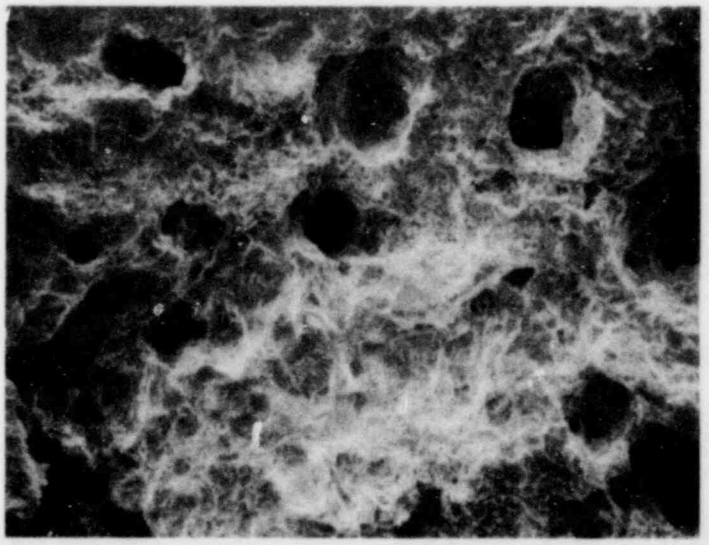

AREA B 200X

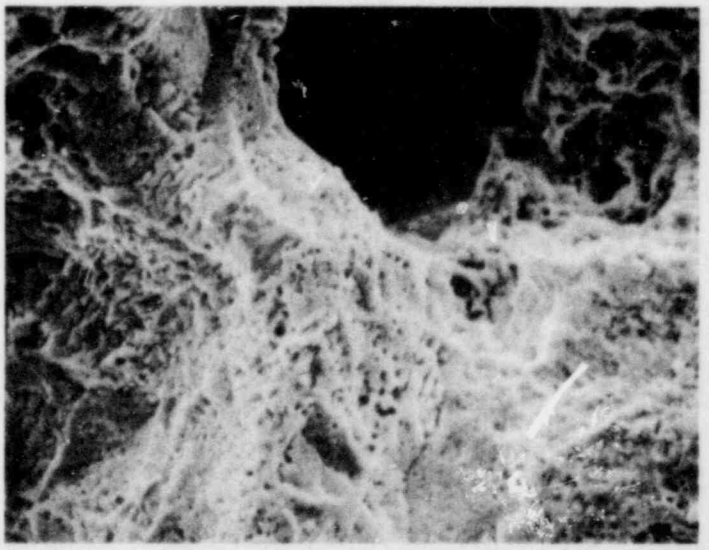

AREA B 1000X

Figure 15. Scanning electron fractograph from various locations of the fracture surface. (Note the severe corrosion pitting of the fracture surface.)

POOR ORIGINAL

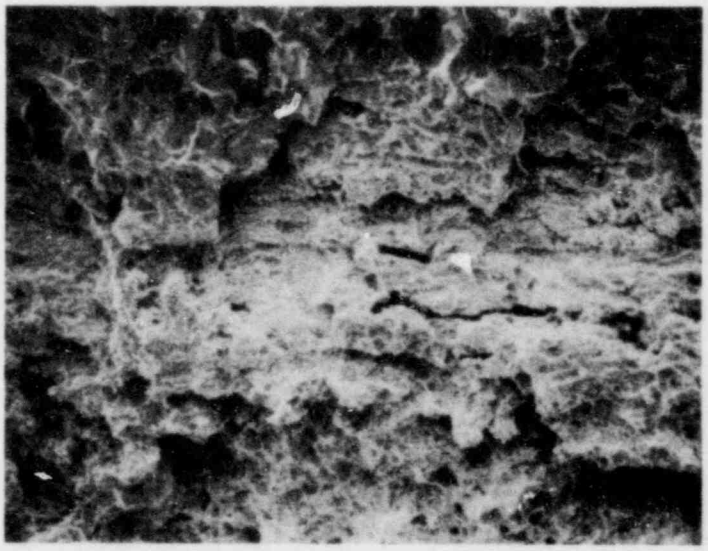

AREA C 200X

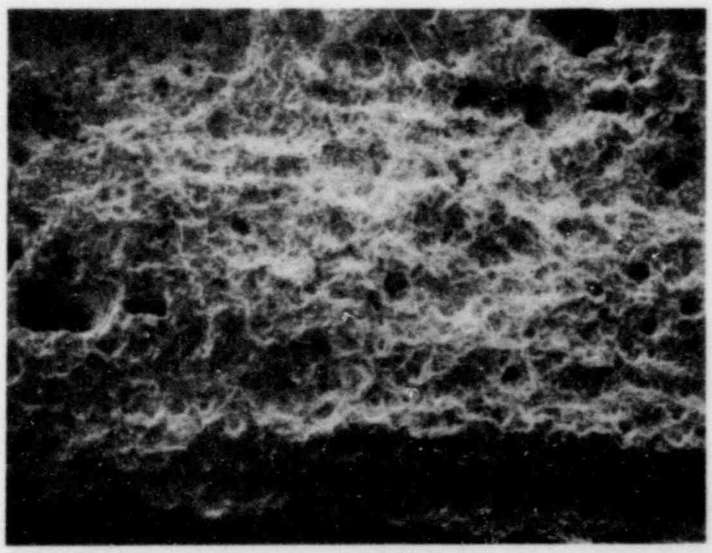

AREA A 200X

Figure 16. SEM fractographs of the fracture surface.

POOR ORIGINAL

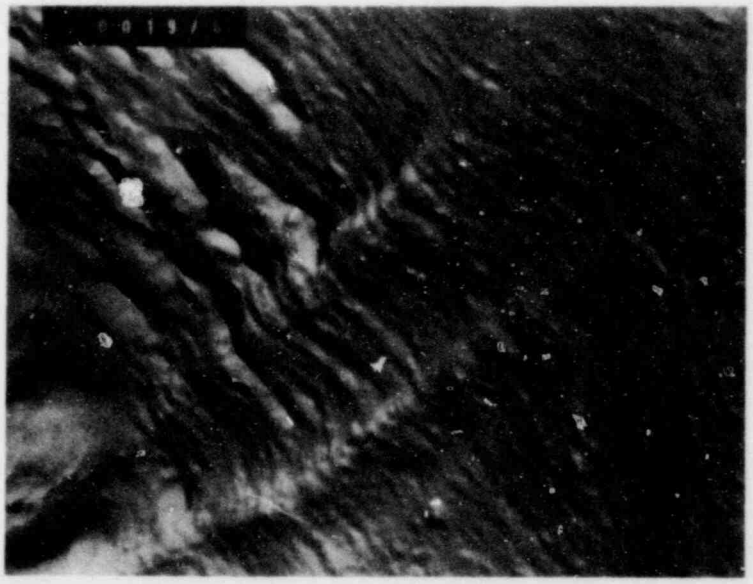

27100X

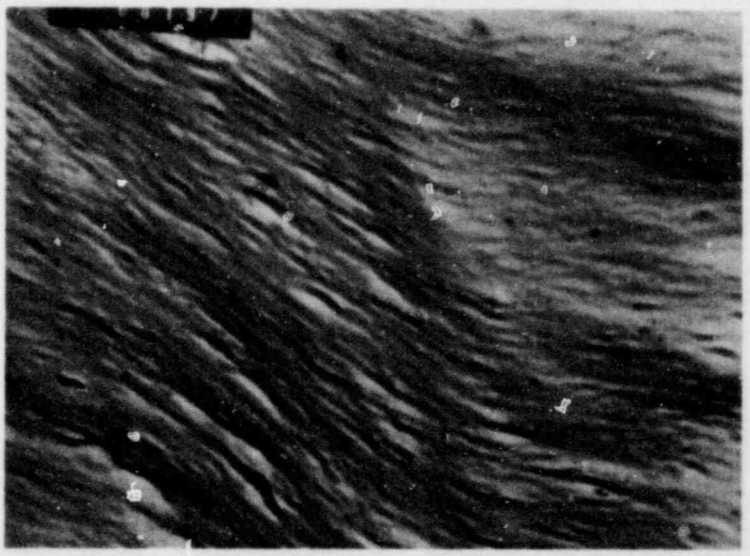

27100X

Figure 17. TEM fractographs of the main crack tip showing what are believed to be fatigue striations. Replica Grid F.

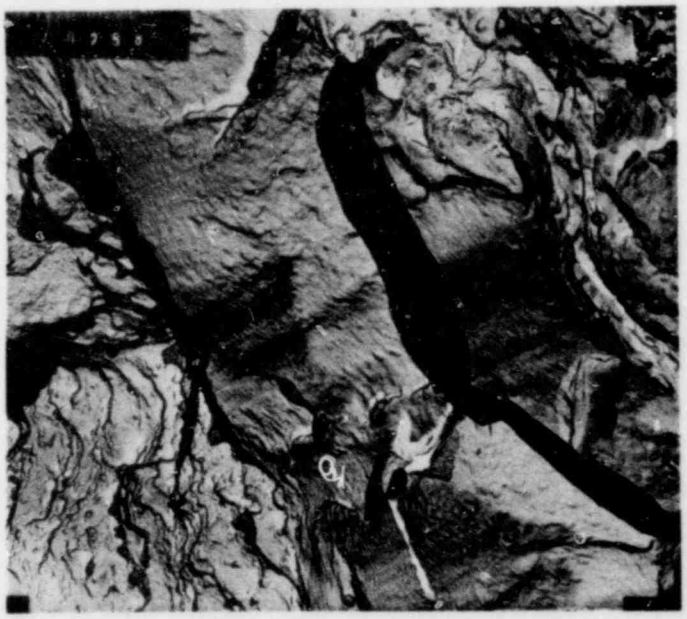

Grid A. Mag. 16500X

Grid A. Mag. 16500X

Figure 18. Loop A. Transmission Electron Microscope (TEM) fractographs showing probable fatigue striations.

POOR ORIGINAL

POOR ORIGINAL

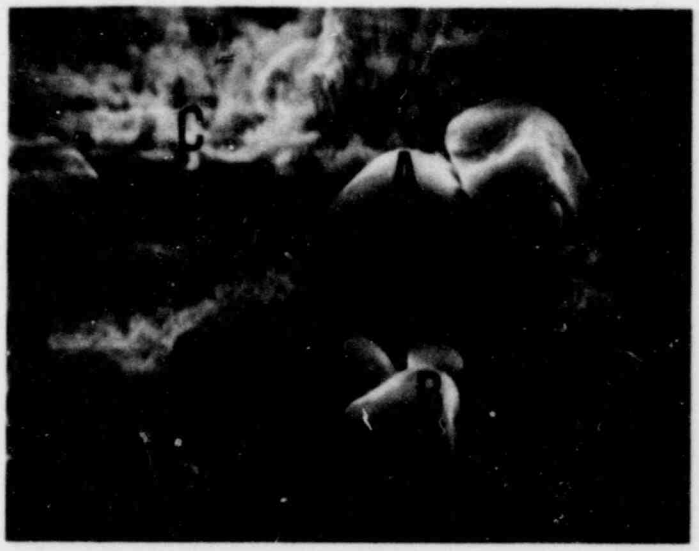

a) Crack deposits selected for EDAX analysis

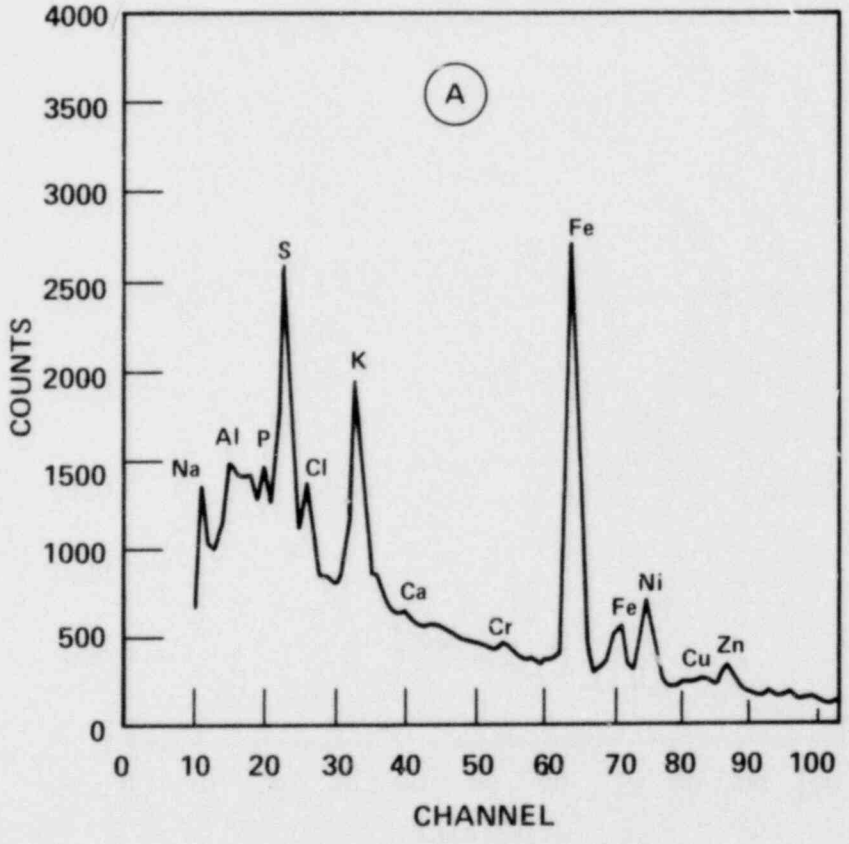

NOTE: Areas A, B and C were analyzed using the energy-dispersive X-ray analysis method -- results for area A are shown above.

b) Results from Region A in a).

Figure 19. EDAX analysis of the crack deposits.

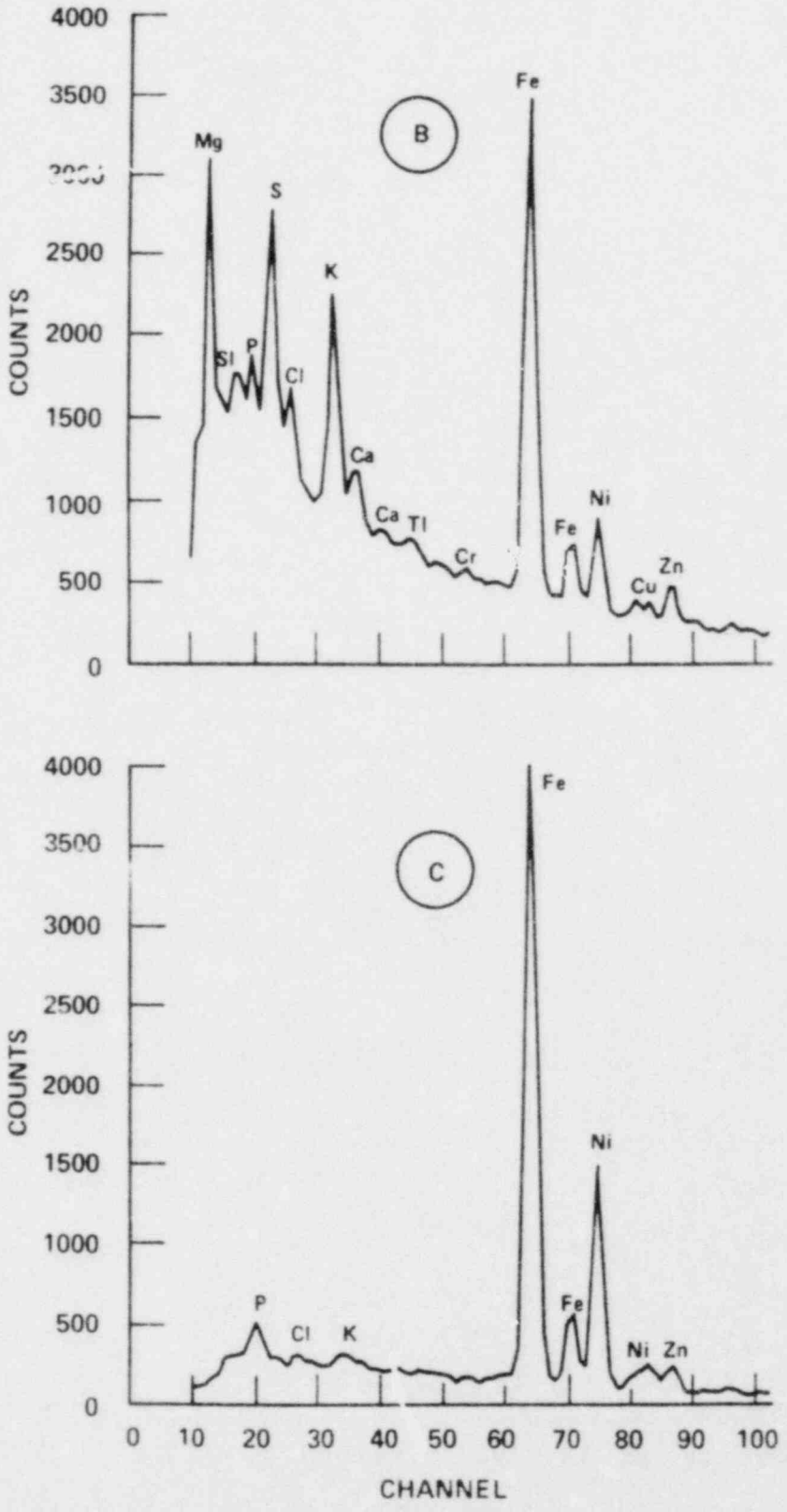

Figure 20. EDAX analysis results for Areas B and C from Figure 19. [a,c,e]

SECTION 6.0

CHEMISTRY EVALUATION

by

J. Kormuth

6.1 INTRODUCTION TO EVALUATION OF CHEMISTRY DATA

Early examination of feedwater piping that had experienced cracking identified the presence of pitting. Some of the cracks were identified in pitted areas, suggesting a possible relationship between the pipe cracking and the pitting corrosion. Historically, fossil boiler experience has shown that pitting of carbon steel will occur if oxygen is not completely removed from boiler feedwater. Additionally, the presence of ions such as chloride would promote the action within the corrosion cell by providing increased electrolyte and, thus, would be expected to enhance the corrosion mechanism. The above understanding of typical carbon steel feedwater line corrosion suggested that the approach to be taken in evaluating the feedwater chemistry should place emphasis on the identification of feedwater line oxygen exposure. It has been recognized that excessive oxygen contamination in feedwater lines may occur during (1) normal power operation, (2) operation of the auxiliary feedwater system, and (3) cold, wet layup. The first two modes of operation listed were considered to present the greater potential for a corrosive condition than the third listed, thus, the initial data review was planned accordingly. Preliminary review of feedwater oxygen contamination at power operation and during auxiliary feed identified a number of plant occurrences with significant oxygen exposure.

6.1.1 EXPANDED PROGRAM FOR DATA EVALUATION

The early investigations identified the need for a more complete accumulation of plant chemistry data (condensate and feedwater dissolved oxygen concentrations) in order that a more thorough and detailed evaluation of the data could be completed. The plan for the detailed data evaluation encompassed several parts. For those plants of interest, the chemistry data already available at Westinghouse was assimilated and requests for data were made of the plants where data was not available. It was judged that a meaningful assessment of such a large volume of

data would require computer assistance. The intention was to reduce the condensate and dissolved oxygen data from the copies of the plant logs so that the data could be stored by the computer. An existing chemistry computer program, which has been used for steam generator blowdown data, had portions of the program rewritten to have it accept the condensate/feedwater oxygen data. The computer output included a tabulation of the data, time plots of the data and a bar chart characterization of various numerical ranges in which the data might fall. Using the computer output, evaluations of plant oxygen exposure at power operation were completed to determine if any correlation existed with either the incidence or severity of feedwater pipe cracking.

6.2 METHOD OF CHEMISTRY DATA EVALUATION

The method chosen for comparison of the plants' pipe cracking experiences and exposure to oxygen contamination in the feedwater was to first group the plants into categories according to the severity of cracking. Those groups included plants with cracking 50% thru wall or greater, 0.1 inch or less, and those with no cracking indications. Using the data reduced by the computer, the plants were similarly categorized according to the extent of oxygen exposure. In defining the terms of the oxygen exposure for comparative purposes, concentration limits were selected relative to what the operating experience seemed to be in conjunction with the duration of the exposure. The comparative limits for the hotwell are shown in Table 6.2-1. The same type of arrangement was established for feedwater oxygen exposure. Those comparative limits are presented in Table 6.2-2.

6.2.1 RESULTS OF DATA EVALUATION

Data from thirteen units were evaluated and the plants thus categorized according to the respective oxygen exposure that was apparent from review of the data. It was noted that of the thirteen, five of the plants had experienced only their initial fuel cycle of operation. An

overall plant comparison was constructed using data from the thirteen plants, comparing cracking severity with dissolved oxygen concentrations in the condensate and feedwater. That comparison is shown in Table 6.2-3. A similar plant comparison was derived using only the data from the five units which operated for a single fuel cycle. That comparison is presented in Table 6.2-5. The comparison shown in Table 6.2-3 identifies [ ] as the three plants with very severe cracking experience. The oxygen exposure at [ ] was rated high while at [ ], it was moderate to light. There were two units, [ ] which had oxygen exposure comparable to [ ]. However, in both cases the severity of cracking was much less. The [ ] units were grouped by the criteria of cracking severity with plants which had generally experienced oxygen exposure that was moderate to light. Three plants [ ] were shown to have had oxygen exposure that was moderate to high, but none had indications of cracking. The evaluation showed no consistent pattern between the determined condensate or feedwater oxygen values and the identified cracking. A similar inconsistency was apparent for the single cycle plants. The data evaluation did reveal clearly, however, that when an absolute judgement was made of the oxygen exposure at the thirteen plants, nearly every one of the units had been operated with condensate and feedwater oxygen concentrations that were considered excessive by accepted standards of good operating practice.(1)

a,c,e

6.3 PLANT OPERATING AND DESIGN SURVEYS

A survey of seventeen units was conducted to glean information for a comprehensive overview of plant design and operating characteristics pertaining to the use of auxiliary feedwater. The information sought was to learn the source of the auxiliary feedwater, the quality of the deaeration of makeup to the condensate tank or any other tank which held the stored auxiliary feedwater, the tank protection provided to prevent

(1) Consensus On Operating Practices for the Control of Feedwater and Boiler Water Quality in Modern Industrial Boilers, ASME Research Committee on Water in Thermal Power Systems, F. J. Pocock, Chairman, 1979.

the stored water from becoming contaminated by air and the dissolved oxygen concentration normally determined for the stored water. The results of the survey are shown in Table 6.3-1. The survey revealed that the plants are designed such that the auxiliary feedwater nearly always comes from the condensate storage tank or an auxiliary feedwater storage tank. It was learned that with about half the plants the stored auxiliary feedwater is deaerated before storage. However, in nearly every case where the water was deaerated it became aerated in time because of ineffective tank protection or simply a lack of protection. The auxiliary feedwater was generally shown to have been in the ppm range of dissolved oxygen when used.

6.4 CONDENSER LEAKAGE AND PIPE CRACKING

In response to the Feedwater Pipe Cracking Owners Grop request for an evaluation of the role condenser leakage might have played in the feedwater pipe cracking occurrences, a further chemistry data review was completed. As an initial approximation of such a relationship, a correlation was sought between pipe cracking and the extent of condenser inleakage experience. Such an evaluation is necessarily complicated by the differences in chemical characteristics of the circulating water. In an attempt to reduce the impact of that complication on the evaluation, the plants reviewed were divided into the two categories, sea or brackish water cooled and fresh water cooled.

An exact quantification of the condenser inleakage experienced from startup at a given plant for the several plants evaluated would require a major data gathering effort. A reasonable approximation of condenser inleakage can be inferred, however, from an integration of a major cooling water contaminant such as chloride ion. The availablity of a steam generator blowdown chloride exposure survey for a number of plants with data up to mid-1977 made it possible to expedite the subject evaluation and was used for that purpose. The cumulative chloride exposures were given in the survey as chloride ppm/days. Thus, if the data showed 0.5 ppm chloride in the steam generator blowdown for five days, the total chloride exposure would be 2.5 ppm/days.

A comparison of the chloride exposures of seven plants cooled with fresh water or cooling towers was made relative to their respective experiences with feedwater pipe cracks. These data are shown in Table 6.4-1. The cumulative chloride exposures were separated into high and low exposure categories using 50 ppm days as an arbitrary differentiating value. [ ]had less than 50 ppm/days; however, two of the three experienced pipe cracks. [ ]had more than 50 ppm/days exposure. Among these four plants[ ]had pipe cracks. a,c,e

Data from the plants cooled with sea or brackish water are presented in Tabel 6.4-2. The cumulative chloride exposure data was similarly divided into high and low exposure categories using 500 ppm days as the arbitrary point of division. [ ]both experienced less than 500 ppm/days chloride exposure and neither plant has been shown to have feedwater line cracks. Four other plants,[ ], exceeded 500 ppm/days chloride exposure. Of the four in that group, the two[ ]Units have not experienced cracks. a,c,e

6.5 CONCLUSION OF THE CHEMISTRY DATA EVALUATION

A number of conclusions have been drawn after completion of the chemistry data evaluation. The first three conclusions pertain to the evaluation of condensate/feedwater dissolved oxygen data with the plants at power.

Conclusions

1. Neither incidence of feedwater line cracking nor severity of cracking can be shown to have an obvious correlation with oxygen exposure during operation.

2. Oxygen evaluation has revealed inadequate control of oxygen on the steam side. Corrective action to reduce oxygen exposure in steam side is indicated. Control condensate dissolved oxygen to 5 - 7 ppb. Control feedwater dissolved oxygen to <5 ppb, residual of hydrazine to 10 ppb or greater.

One conclusion was made following the survey of the design and operation of the auxiliary feedwater systems.

4. Essentially every plant contacted in the survey was shown to have exposed the feedwater inlet nozzles to excessive (>1 ppm) dissolved oxygen contamination during auxiliary feedwater flow to the steam generators. The relative, cumulative oxygen exposure for the individual plants was not determined.

A final conclusion was derived upon completion of the condenser inleakage evaluation.

5. The incidence of feedwater line cracking cannot be shown to have an obvious correlation with condenser inleakage, considering plants cooled by both fresh water and sea or brackish water.

TABLE 6.2-1

DEFINITION OF TERMS

Term	Concentration	Total Exposure		
High Hotwell	[ ]	Extended Periods	Months/Calender Year	a,c,e
Moderate Hotwell	[ ]	Shorter Periods	Weeks/Calender Year	
Light Hotwell	[ ]	Rare Periods	<5% Calendar Year	

TABLE 6.2-2

DEFINITION OF TERMS

Term	Concentration	Total Exposure	
High Feedwater	[ ]	Extended Periods	Months/Calendar Year
Moderate Feedwater		Shorter Periods	Weeks/Calendar Year
Light Feedwater		Rare Periods	<5% Calendar Year

TABLE 6.2-3

PLANT OVERALL COMPARISON

Cracking Severity			Dissolved Oxygen Exposure During Operation		
50% Thru Wall or Greater	0.1 inch or less	No Indications	Hotwell	Feedwater	
[			High	High	a,c,e
			Moderate	Moderate	
			Moderate	Light	
			High	High	
			High	High	
			Moderate	Moderate	
			No Data	Light	
			Light	Light	
			Moderate	Moderate	
			Moderate	Moderate	
			Moderate	Moderate	
			High	Moderate	
		]	Moderate	Moderate	

TABLE 6.2-4

FIRST CYCLE PLANT COMPARISON

Cracking Severity			Dissolved Oxygen Exposure During Operation	
50% Thru Wall or Greater	0.1 inch or less	No Indications	Hotwell	Feedwater
a,c,e [		]	High	High
			Moderate	Moderate
			High	High
			Moderate	Moderate
			Moderate	Moderate

TABLE 6.3-1

AUXILIARY FEEDWATER SURVEY

Plant	Source	Make-up	Tank Protection	Tank D. O.
a,c,e	Auxiliary Feedwater Storage Tank	Not Deaerated	None	Usually <100 ppb
	Auxiliary Feedwater Storage Tank	10 - 30 ppb	None	Not Analyzed
	Condensate Storage Tank	Not Deaerated	Bladder	5 - 8 ppm
	Condensate Storage Tank	Not Deaerated	Bladder	5 - 8 ppm
	Condensate Storage Tank	--	Diaphragm	1 - 3 ppm
	Condensate Storage Tank	Not Deaerated	None	--
	Condensate Storage Tank	<5 ppb	None	<100 ppb
	Condensate Storage Tank	Deaerated	--	<100 ppb
	Condensate Storage Tank	--	Diaphragm	100 - 200 ppb
	Condensate Storage Tank	10 ppb	None	100 ppb
	Auxiliary Feedwater Storage Tank	<100 ppb	Diaphragm	1 - 1.5 ppm
	Demineralized Water Storage Tank	--	None	1 ppm
	Condensate Storage Tank	50 ppb	None	Not Analyzed
	Condensate Storage Tank	Deaerated	Floating Roof	60 - 80 ppb
	Condensate Storage Tank	10 - 20 ppb	Floating Roof	1 - 3 ppm
	Auxiliary Feedwater Storage Tank	150 - 400 ppb	None	Not Analyzed
	Condensate Storage Tank	Not Deaerated	None	Not Analyzed

TABLE 6.4-1

COMPARISON CONDENSER LEAKAGE WITH
OCCURRENCE OF FEEDWATER PIPE CRACKS

Fresh Water Cooled Plants

Cumulative Chloride Exposure

Plant	<50 ppm days	> 50 ppm days	Piping Cracks
a,c,e	40		Yes
		268	No
	3		Yes
	22		No
		895	Yes
		66	Yes
		380	Yes

TABLE 6.4-2

COMPARISON CONDENSER LEAKAGE WITH
OCCURRENCE OF FEEDWATER PIPE CRACKS

Seawater or Brackish Water Cooled

Cumulative Chloride Exposure

Plant	<50 ppm days	> 50 ppm days	Piping Cracks	
[ ]	361		No	a,c,e
	13		No	
		16,300	Yes	
		2,938	Yes	
		1,301	No	
		905	No	

SECTION 7.0

PIPING DESIGN VERIFICATION ANALYSIS

by

G. R. Ellis

ACKNOWLEDGMENTS

Thanks are expressed to the following people who performed analysis as part of the input to this report:

Structural Analysis: W. A. Massie, R. M. Manz, E. W. Smith, M. J. Fisher

Water Hammer Analysis: C. W. Gay, R. Carlson

2D Finite Element Analysis: T. J. Batt

7.1 INTRODUCTION

Stress analysis was performed for the feedwater line configuration for several plants to determine if the normally expected loads would have caused the observed cracking. The analysis was broken into two parts. The first was the structural analysis of the feedwater piping from the steam generator to the contained penetration for the following loads:

1. Normal operating loads (thermal, deadweight, pressure)
2. Frequency/normal operation vibration
3. Water hammer

The second was a 2-D detailed finite element analysis of the feedwater nozzle to piping junction for the hot standby condition, which is the worst expected thermal transient.

7.2 STRUCTURAL ANALYSIS

The structural analysis was performed using a 3-D finite element model of the feedwater line with anchors included at the steam generator (SG) and the containment penetration. Figures 7.1 through 7.19 show the layout and support locations for the lines considered in this analysis. It can be seen that the layout for each line is fairly simple with no intermediate tees on valves. All lines are modeled from the containment anchor to the centerline of the steam generator where an anchor is assumed and the vertical and horizontal growth of the steam generator is applied. Also, Section 14 shows detailed sketches of the feedwater piping layout to the first vertical elbow.

The Westinghouse piping analysis code, WESTDYN, was used for the analysis. The code employs lumped parameter finite element models of the piping systems for both static and modal dynamic analysis. The methods used to obtain the solution consist of the transfer matrix method for determining stiffness and the modal response method for determining frequencies and mode shapes.

7.2.1 NORMAL OPERATING LOADS

The loads considered in this evaluation consisted of thermal expansion, deadweight and pressure. Two thermal conditions were run. The first was run with the steam generator at ↶ 550°F and the feedwater line at ↶ 450°F representing normal operation. The second was run with the steam generator at ↶ 550°F and the feedwater line cold representing the hot shutdown condition. The vertical and horizontal growth of the steam generator were applied at the feedwater nozzle.

The criteria for evaluating piping stresses was as follows:

$$\frac{P\ D_o}{4\ tm} + .75\ i\ \left(\frac{M_A}{Z}\right) + i\ \left(\frac{M_c}{Z}\right) \leq S_h + S_A$$

where

P = internal design pressure, psig

D_o = outside diameter of pipe, inches

t_m = nominal wall thickness of component, inches

M_A = resultant normal loading on cross section due to weight and other sustained loads, inch pounds

M_c = range of resultant moments on the cross section due to thermal expansion, inch pounds

Z = section modules of pipe, inches

i = stress intensification factor

S_h = allowable stress at design temperature, psi

S_A = allowable stress range for thermal expansion stress, psi

$S_h + S_A$ = 22,500 psi for 106 Gr B material
= 26,250 psi for 106 Gr C material

Table 7.1 summarizes the stresses at the feedwater nozzle to pipe junction for the plants that were analyzed. Included in these stresses are the maximum load from the two thermal conditions analyzed.

7.2.2 FREQUENCY/NORMAL OPERATION VIBRATION

The analysis of frequency/normal operational vibration is not part of the original design for the feedwater piping, but the question arose as to whether normal operating steam generator vibration could be amplified in the feedwater piping and cause high stresses and the observed cracking. The analysis was performed in two phases. First, frequencies were calculated for the feedwater piping using the piping models developed for the normal operating load evaluation. Frequencies were calculated both with and without the effect of snubber stiffness since snubbers could be inactive for the low magnitude of vibration expected during normal plant operation. For each of the plants considered (i.e. the same plants included in the normal operating load evaluation) several frequencies existed in the range of 1.0 to 10.0 Hz. A recent report on nuclear power plant vibration[1] indicated that during normal operation, a steam generator might have a vibration with a ten mill amplitude and with a frequency in the two to ten Hz range. This is the same range observed for the feedwater lines considered.

The second phase of this analysis was designed to determine if a "typical" feedwater line could be excited to the point of causing the observed cracking. The [ ] layout was chosen for this analysis because its frequencies and stresses were typical of those lines evaluated. Also, [ ] experienced the most severe cracking, and if normal operation vibration was significant, it would have the largest effect for this plant. A time history analysis was run using the

a,c,e

Westinghouse computer codes FIXFM3 and WESDYN2 with a sinusoidal input at the steam generator nozzle of ± 10 mills along the axis of the inlet leg of the feedwater line. Input frequencies of 8.0, 6.0, 4.0 and 2.0 Hz were used. The line snubbers were assumed to have a ± 1/16" free deadband. Additional analyses were run where the input frequency was identical to the 2.93 Hz fundamental frequency of the line and a 10 Hz input with the snubbers fully active (no dead band). The maximum stress results from this analysis was 200 psi. This is caused by system response to the input motion which shows some small amplification.

7.2.3 WATER HAMMER

The effect of water hammer loads were analyzed to provide input to the crack growth evaluation, which will be discussed in Section 12. Four types of water hammer loads were considered for the analysis as follows:

1. Feedwater line break - check valve slam
2. Excessive feedwater flow
3. Bubble collapse - slugging
4. Bubble collapse - snapping

The loads expected for 2 and 4 above are very small and will have a negligible effect on crack growth. The loads due to bubble collapse - slugging (3 above) have been experienced by several plants in the past and have been found to have a severe effect on the feedwater piping. However, the recent adoption of administrative controls such as those outlined in Westinghouse technical bulletins[3] or the installation of J tubes in the feedring have eliminated this problem. The water hammer load evaluated here is the result of a pipe break and subsequent check valve slam. The assumption is made that a feedwater pipe ruptures either upstream or downstream of the check valve in one of the loops. The result would be flow reversals in the unbroken loops and check valve slams. A positive pressure wave would be generated and propagated toward the steam generators. Figure 7.20 shows this forcing function as a function of time and distance from the steam generator.

The time history structural analysis was performed using the standard model developed for the system vibration analysis described in Section 7.2.2. Again, the [ ] layout was taken as "typical". The time history resultant moment and the corresponding time history pressures at the feedwater nozzle to pipe junction are shown in Figure 7.21. The effect these loads have on crack growth will be described in the fracture mechanics evaluation, Section 12. The stress resulting from this loading at the nozzle to pipe junction is 38.7 ksi versus an allowable of 60 ksi using Appendix F of the ASME Section III code. This is also the maximum in the line.

a.c.e

7.3 2-D FINITE ELEMENT ANALYSIS

The purpose of this analysis was to investigate a possible cause of the observed cracking which has occurred in the vicinity of the steam generator feedwater nozzle. The loading condition analyzed is the thermal transient caused by the injection of 60°F auxiliary feedwater through the nozzle which was initially at a uniform 547°F. This condition occurs as a normal function during hot shutdown.

It should be noted that subsequent testing and analysis have shown the assumptions in this section to be unconservative. The description of this analysis is included here to give a base line reference of the expected stresses on a design basis and for comparison of the results obtained from testing described elsewhere in this report.

To perform the analysis, a 2-D axisymmetric finite element model was constructed, for use with the WECAN computer code. This model was intended to predict accurate stresses in the region near (and to both sides of) the safe end girth butt weld, and to account for gross effects of the regions further than several inches (axially) from the weld. For this reason, the element mesh was more refined in the weld region than elsewhere. The annulus between the nozzle and the thermal sleeve is assumed to be stagnant water, with an equivalent conductivity input to account for heat transfer across the gap.

Two types of elements were used to generate the 2-D finite element models. First, the models for [ ] were developed using constant strain elements. When the analysis is performed using this type of element, the surface stresses are calculated by extrapolating from the centroids of the three elements nearest the surface. In addition, a local stress concentration factor of 1.7 must be applied to the surface stress intensity to account for the effect of the "notch" at the counterbore. The models generated for [ ] used isoparametric elements which give a much better representation of the stresses. As a result, the use of a stress concentration factor was not necessary. Figures 7.22 through 7.25 show the models used for each of the element types.

The thermal transient definition is illustrated by Figure 7.26. After the initiation of auxiliary feedwater injection, the flow rate is less than 200 gallons per minute. With this low flow rate, the convection film coefficient for the inside surface of the pipe and nozzle was calculated to be 193 btu/hr-ft^2-fo(2). It was assumed to take 9 seconds for the bulk fluid temperature to change from 547° to 60° in the nozzle, since mixing occurs as the auxiliary feedwater moves up the many feet of piping. When injection is terminated, it was conservatively assumed that the 547° water in the steam generator immediately comes back into the nozzle (in 1 sec. time), with the film coefficient remaining at 193 btu/hr-ft^2-^{o}F. It was also assumed that the feedwater completely fills the pipe and nozzle, and that for any given cross section, the fluid temperature is a function of time only. On the inside surface of the steam generator, the conditions remain constant in time, at 547°F and 83 btu/hr-ft^2-^{o}F. The WECAN analysis was run in two stages. First, the fluid temperatures and film coefficients were applied as a function of time in order to calculate temperatures throughout the metal, which were written to tape. In the second stage, these temperatures were applied to the model in order to calculate stresses as a function of time, and to determine the times at which the highest stresses occur.

A summary of the stress intensities and stress intensity ranges is vided in Table 7.2 for the geometries considered. All stresses are a maximum with respect to time and are located at the counterbore "notch", which is the highest stressed part of the model.

7.4 SUMMARY

Results of structural evaluation show that all thermal, deadweight and pressure stresses are below the allowable. The frequency evaluation shows that the fundamental modes of the feedwater pipe is in the range of expected Steam Generator frequencies. However, the normal operating vibration has been found to be too small to cause signficant feedwater piping response.

The stresses obtained from the 2-D finite element analysis are also not of sufficient magnitude to have caused the observed cracking. Also, the design transients given in the Steam Generator E-Spec has shown acceptable values of usage factors for the feedwater nozzle. Correspondingly, analysis of the nozzle to piping junction will have an acceptable value of usage factor since the thermal transient stresses are lower at this junction than in the nozzle.

The results of the above analysis show that the normally expected operation of the feedwater system did not cause the observed cracking.

7.5 REFERENCES

1. Ayoob, A. J., "Vibration of Nuclear Power Plant Primary Coolant System Piping During Normal Operation," ASME Paper 79-DET-28.

2. Bertech, O., "51 Series Steam Generator Feedwater Nozzle Analysis," W. Tampa Division, 10/69, Section 3.11.

3. NSD-TB-75-7 Rev. 1, "Water Hammer in Steam Generator Feedwater Lines", March 9, 1977.

TABLE 7.1

STRESSES AT THE FEEDWATER NOZZLE TO PIPE
JUNCTION FOR NORMAL OPERATING LOADS

PLANT	STRESS (KSI)	ALLOWABLE (KSI)
a,c,e.	11.3	22.5
	12.1	22.5
	7.7	22.5
	16.3	22.5
	10.0	22.5
	12.4	26.2
	5.1	22.5

TABLE 7.2

STRESS RESULTS FROM 2-D FINITE ELEMENT ANALYSIS
AT THE PIPE SIDE COUNTERBORE

a,c,e

STRESS (ksi)(1)	[			]
σ_y max	30.5	30.6	55.3	56.5
σ_z max	19.4	20.4	36.6	26.5
σ_y min	-22.1	-22.4	-34.4	-39.5
σ_z min	-15.0	-15.3	-26.2	-21.2
Peak Stress Intensity Range	89.4	90.1	89.7	96.0

(1) σ_x = Radial σ_y = Axial σ_z = Loop

a,c,e

(2) [ ]

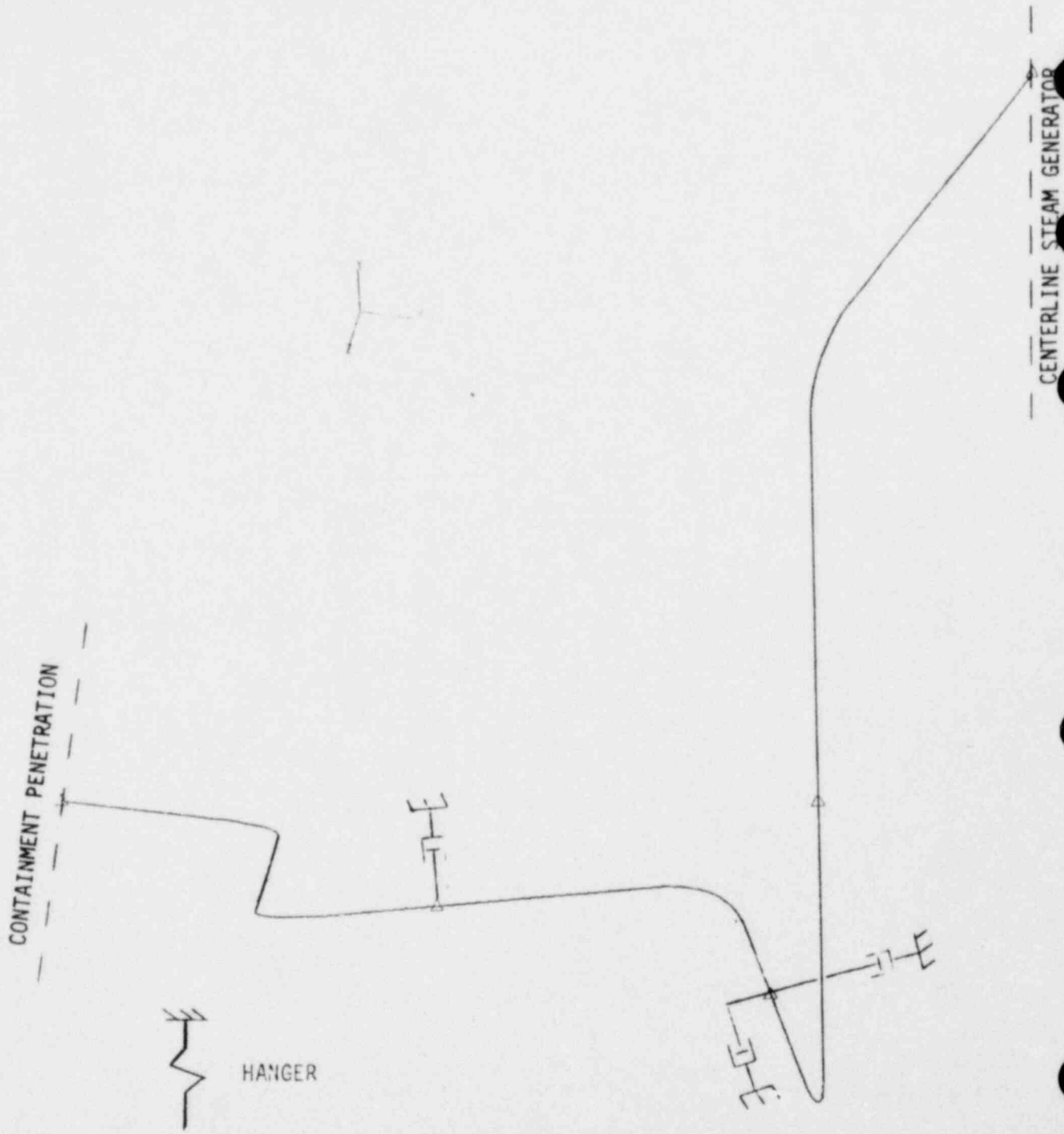

FIGURE 7.1: [ ] UNITS 1&2 FEEDWATER LAYOUT

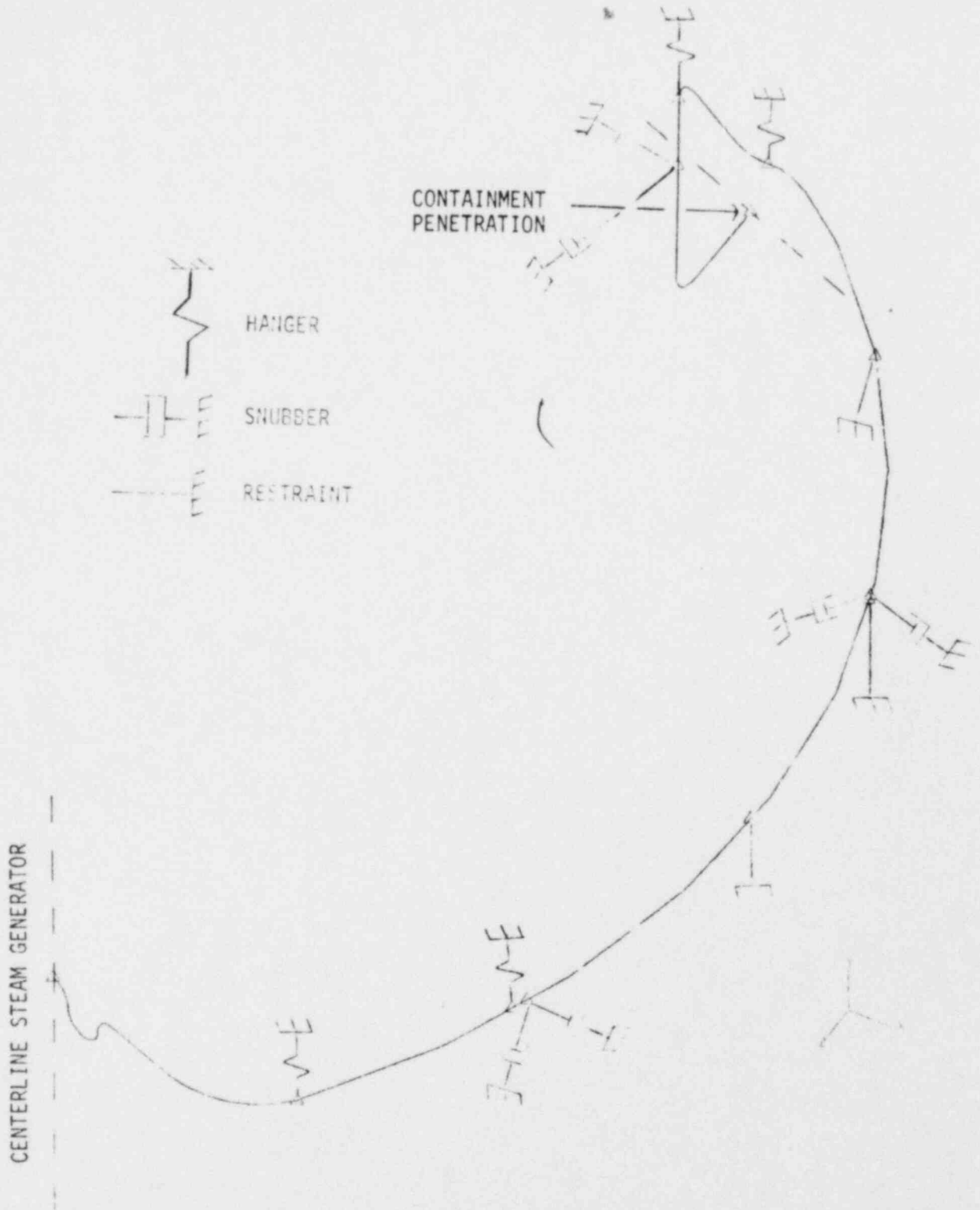

FIGURE 7.2: [ ] FEEDWATER LAYOUT LOOP A [a,c,e

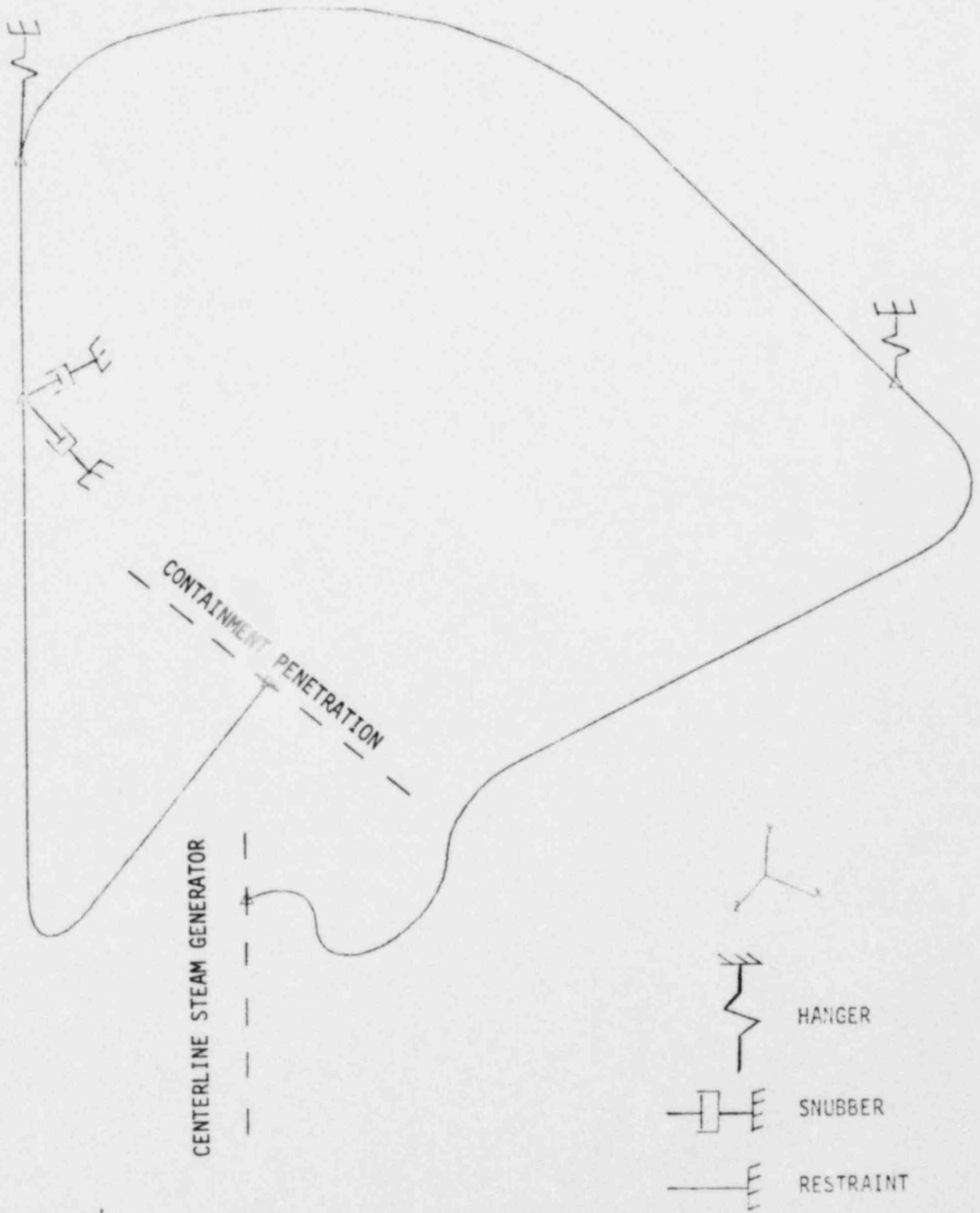

a,c,e

FIGURE 7.3: [ ] FEEDWATER LAYOUT LOOP B

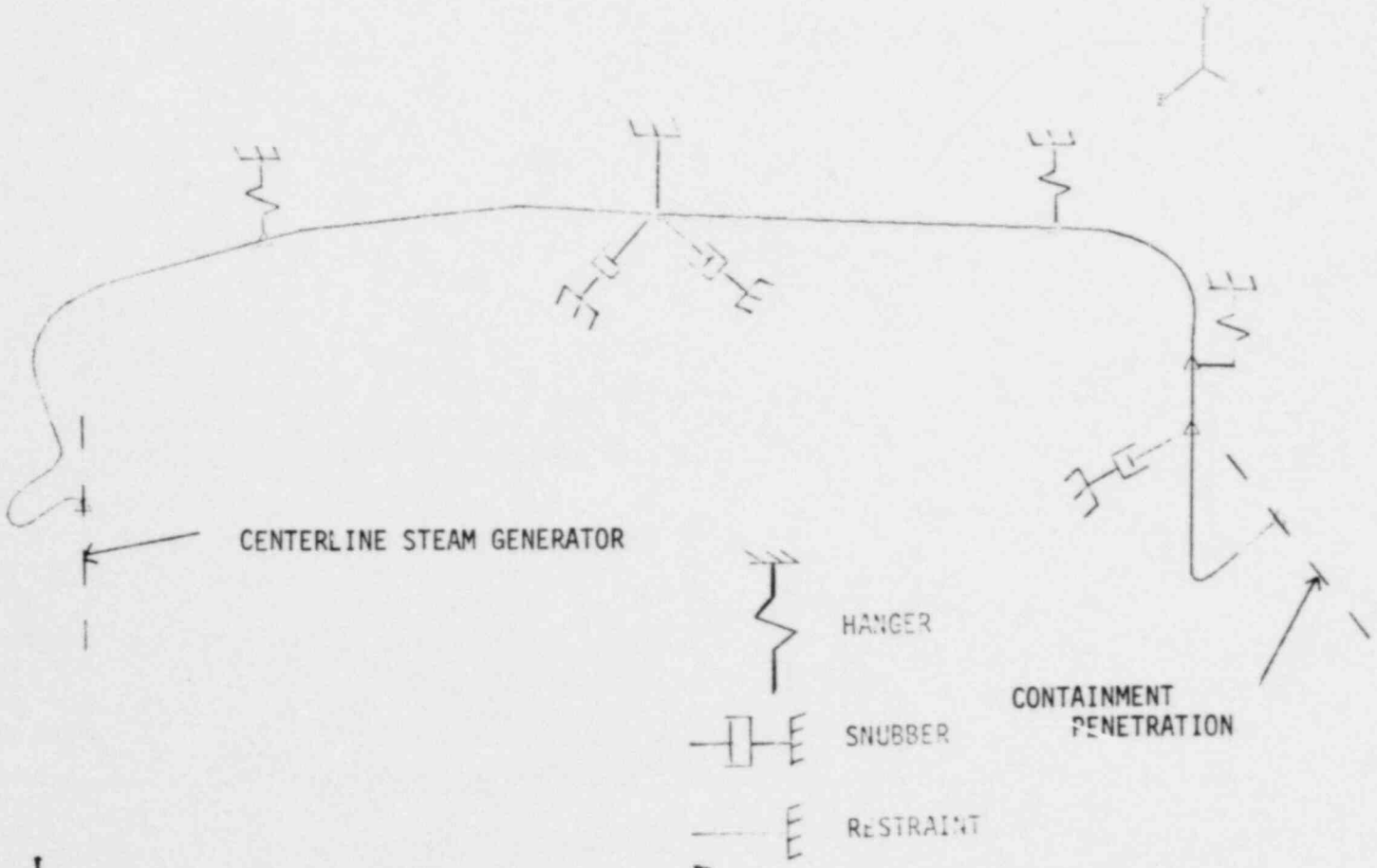

a,c,e

FIGURE 7.4: [ ] FEEDWATER LAYOUT LOOP C

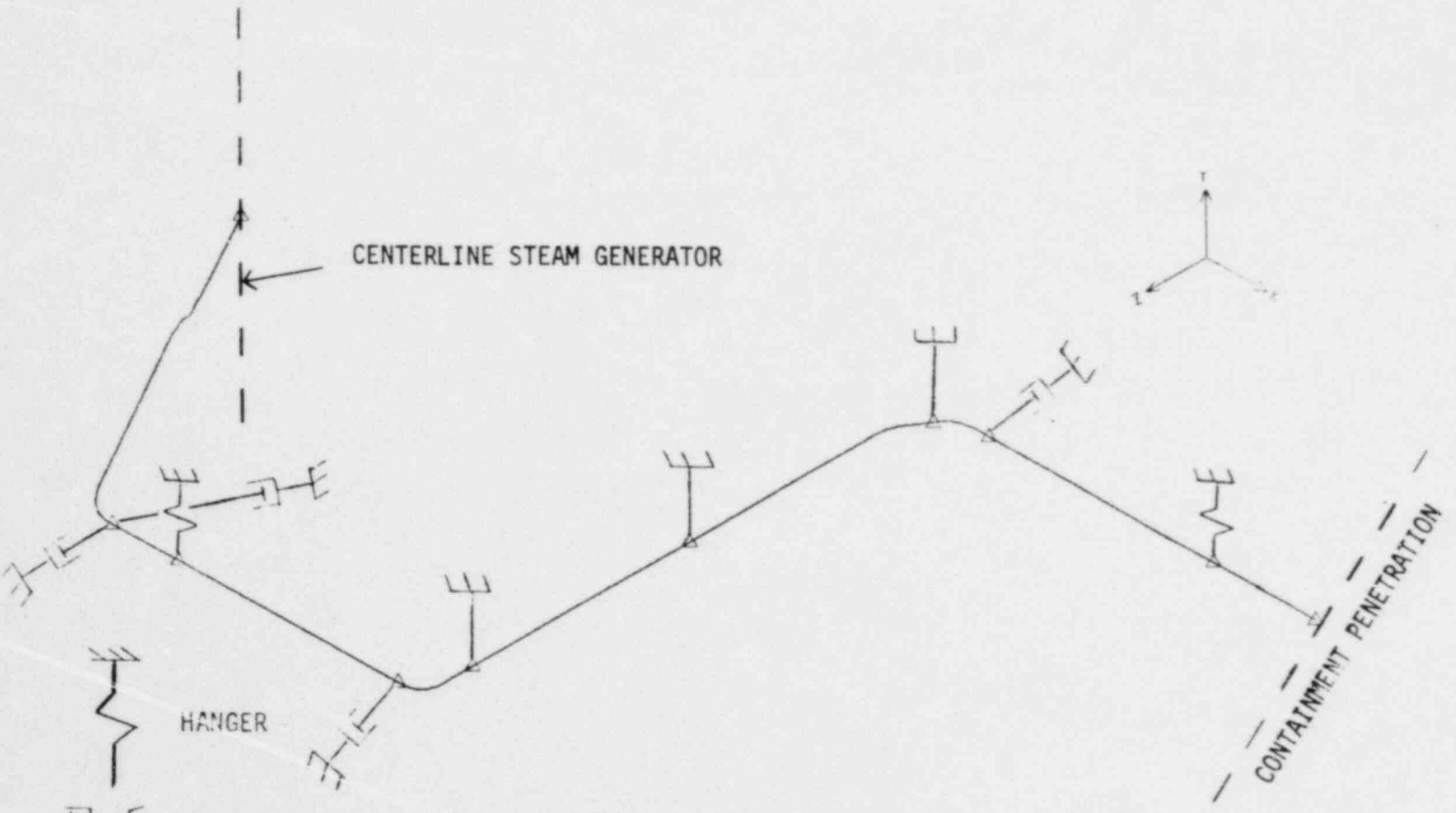

a.c.e

FIGURE 7.5: [ ] FEEDWATER LAYOUT LOOP A

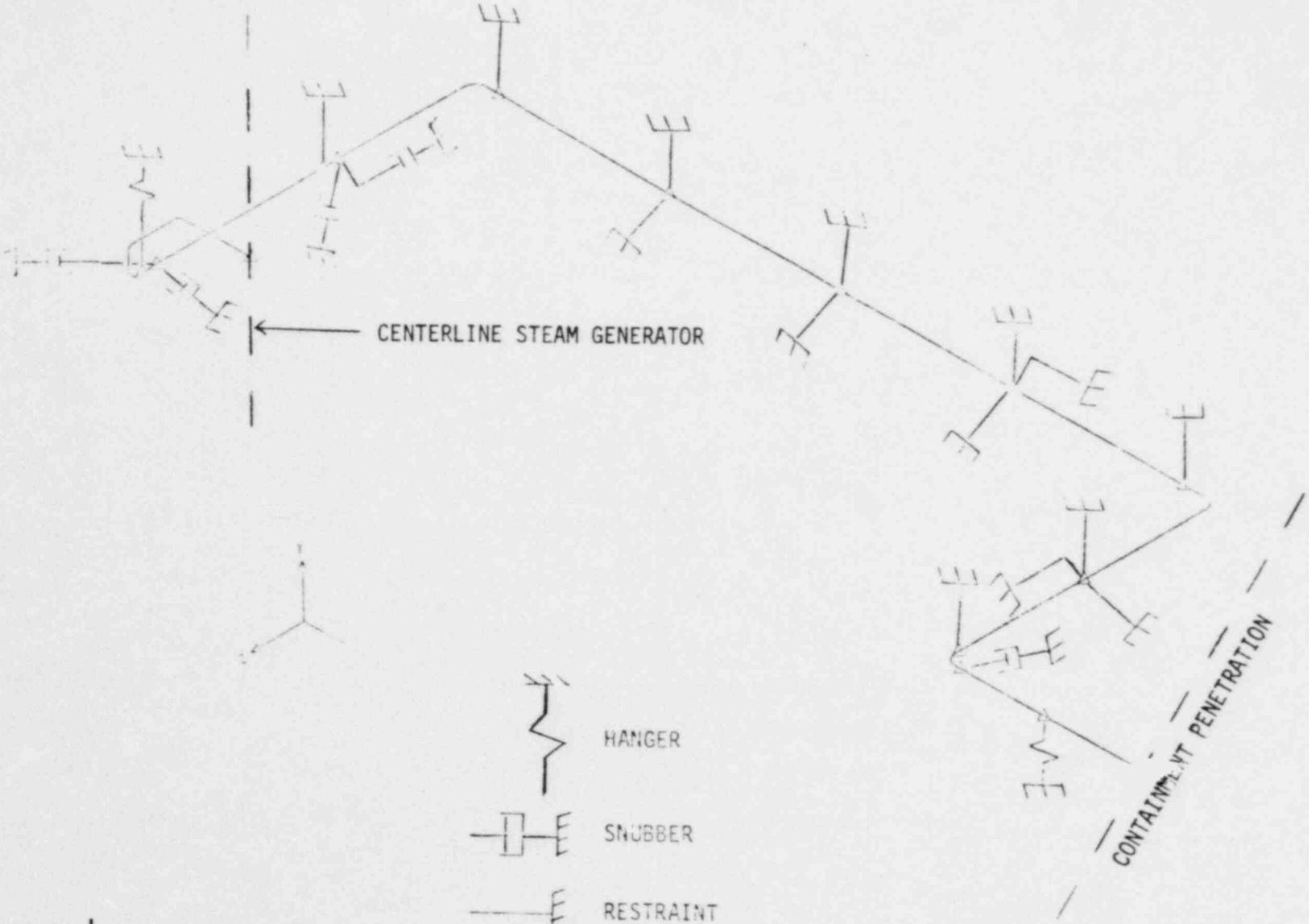

a,c,e

FIGURE 7.6: [ ] FEEDWATER LAYOUT LOOP B

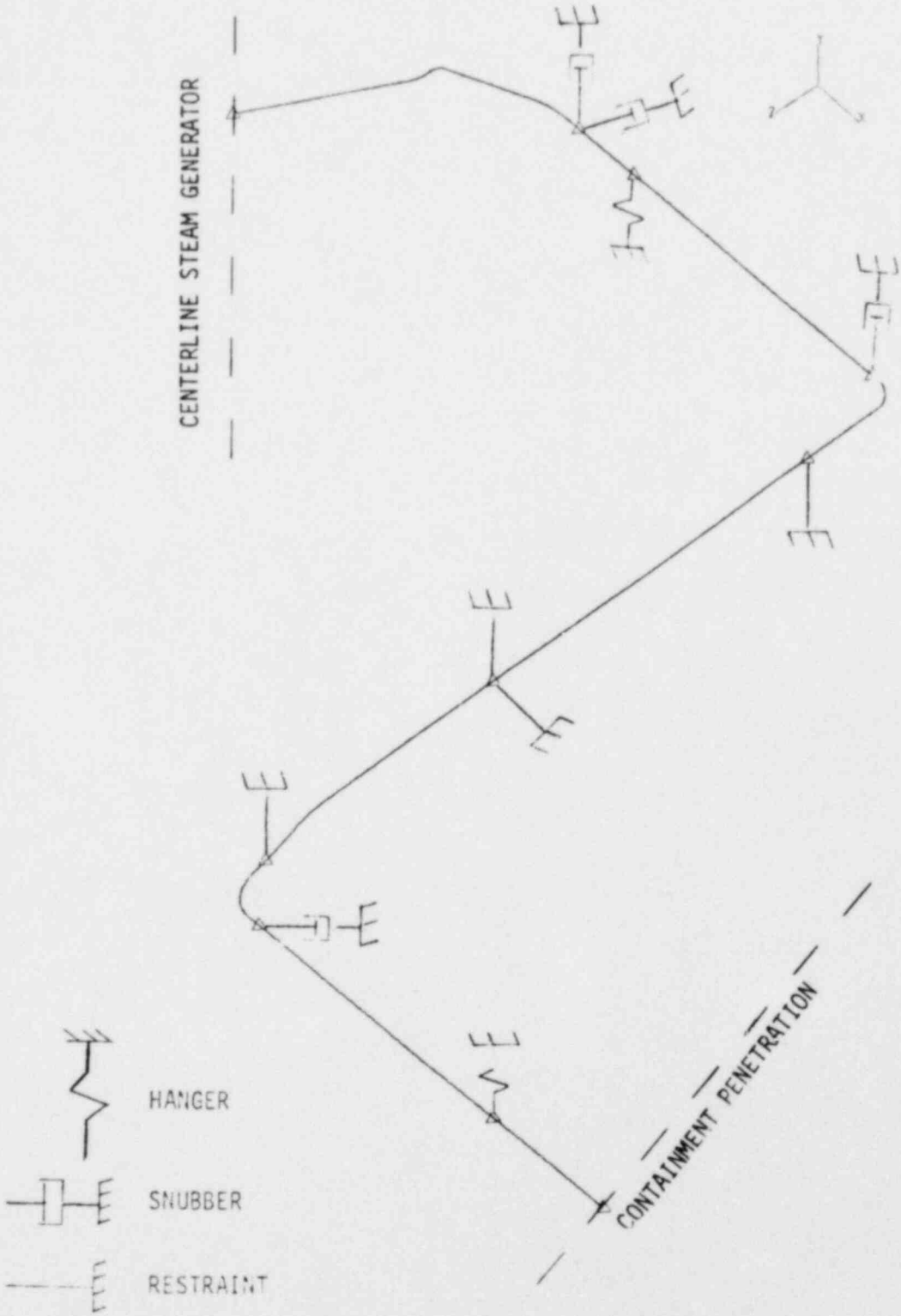

a,c,e

FIGURE 7.7: [ ] FEEDWATER LOOP C

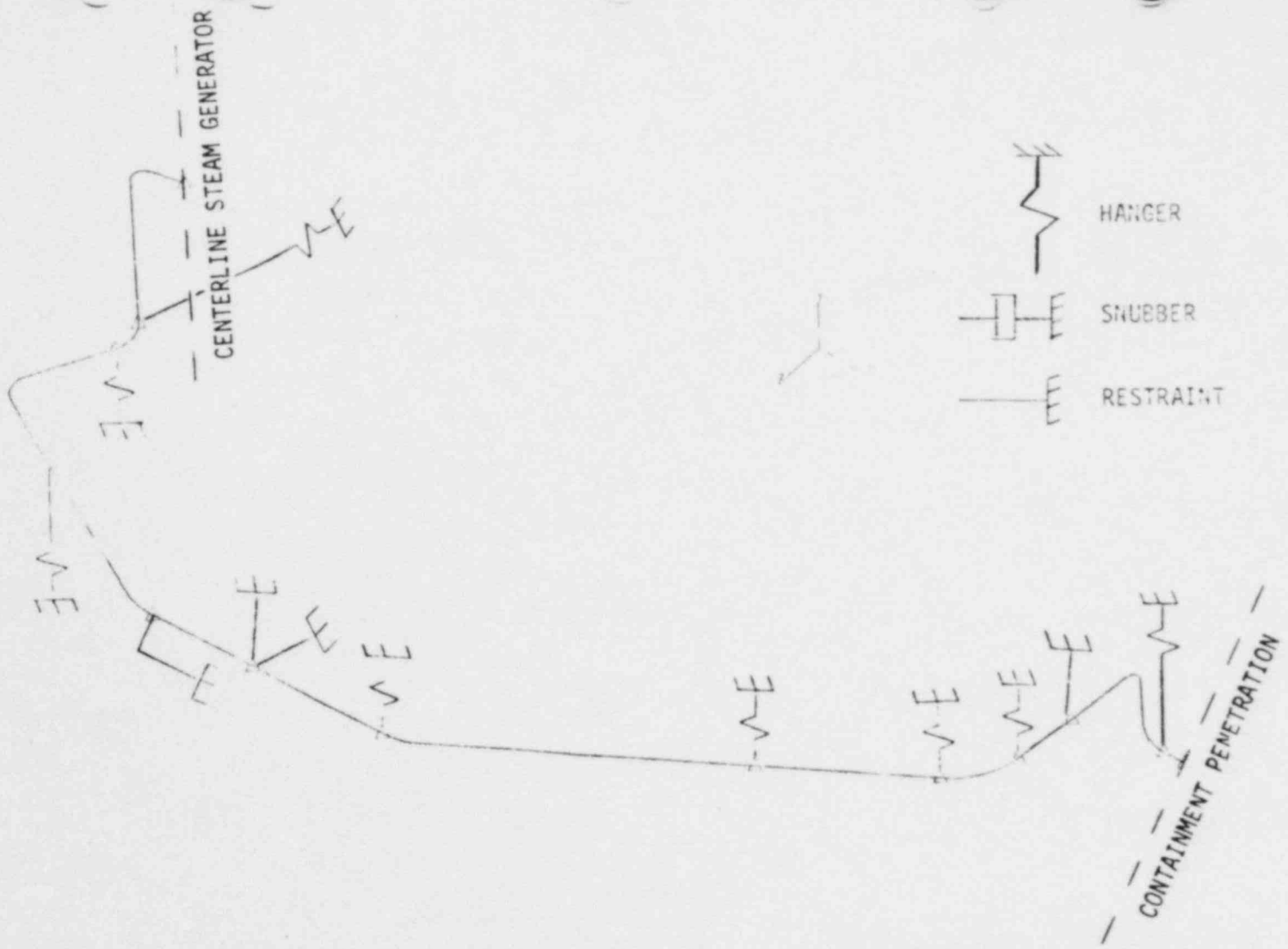

a,c,e

FIGURE 7.8: [ ] FEEDWATER LAYOUT LOOP A

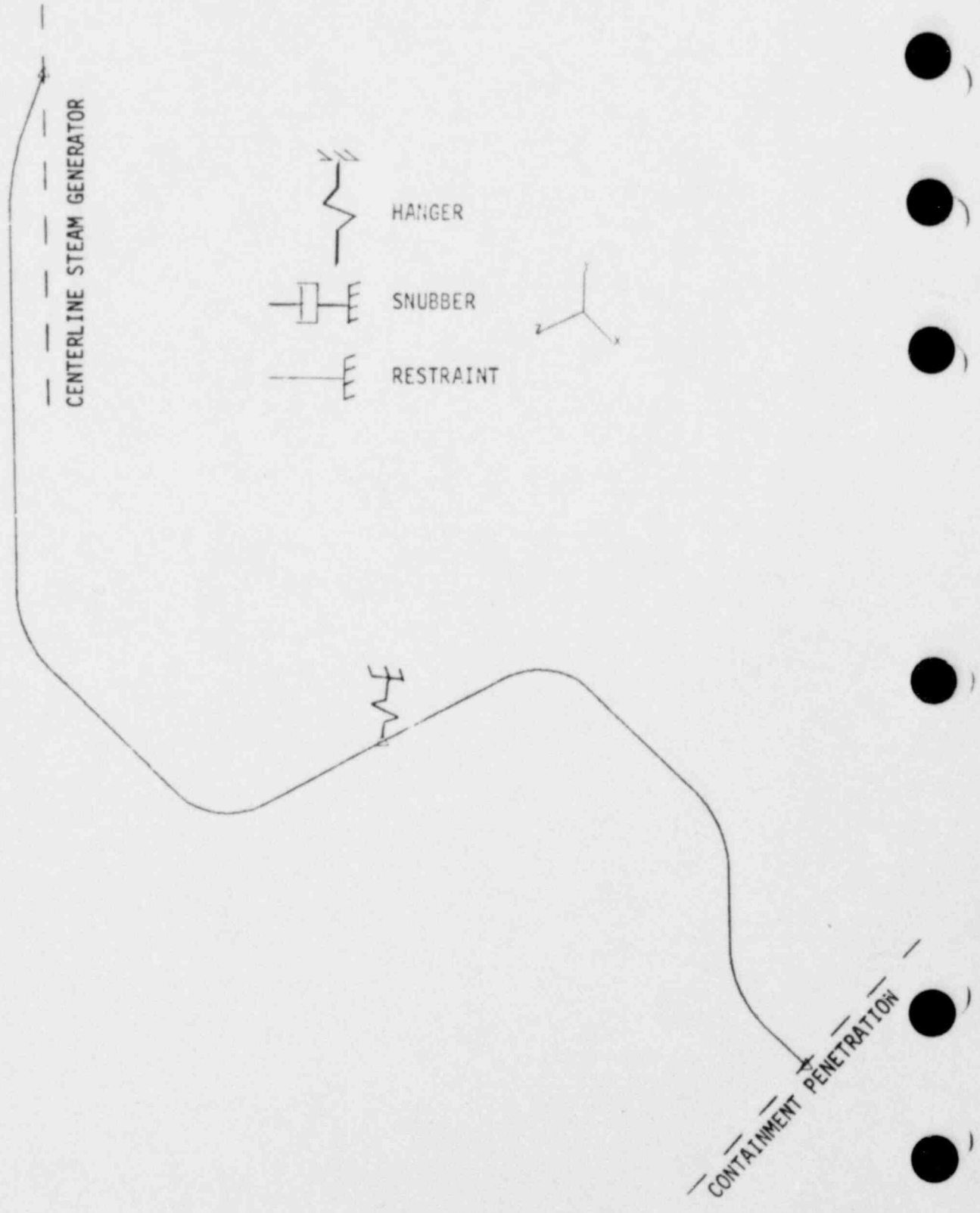

a,c,e

FIGURE 7.9: [ ] FEEDWATER LAYOUT LOOP B

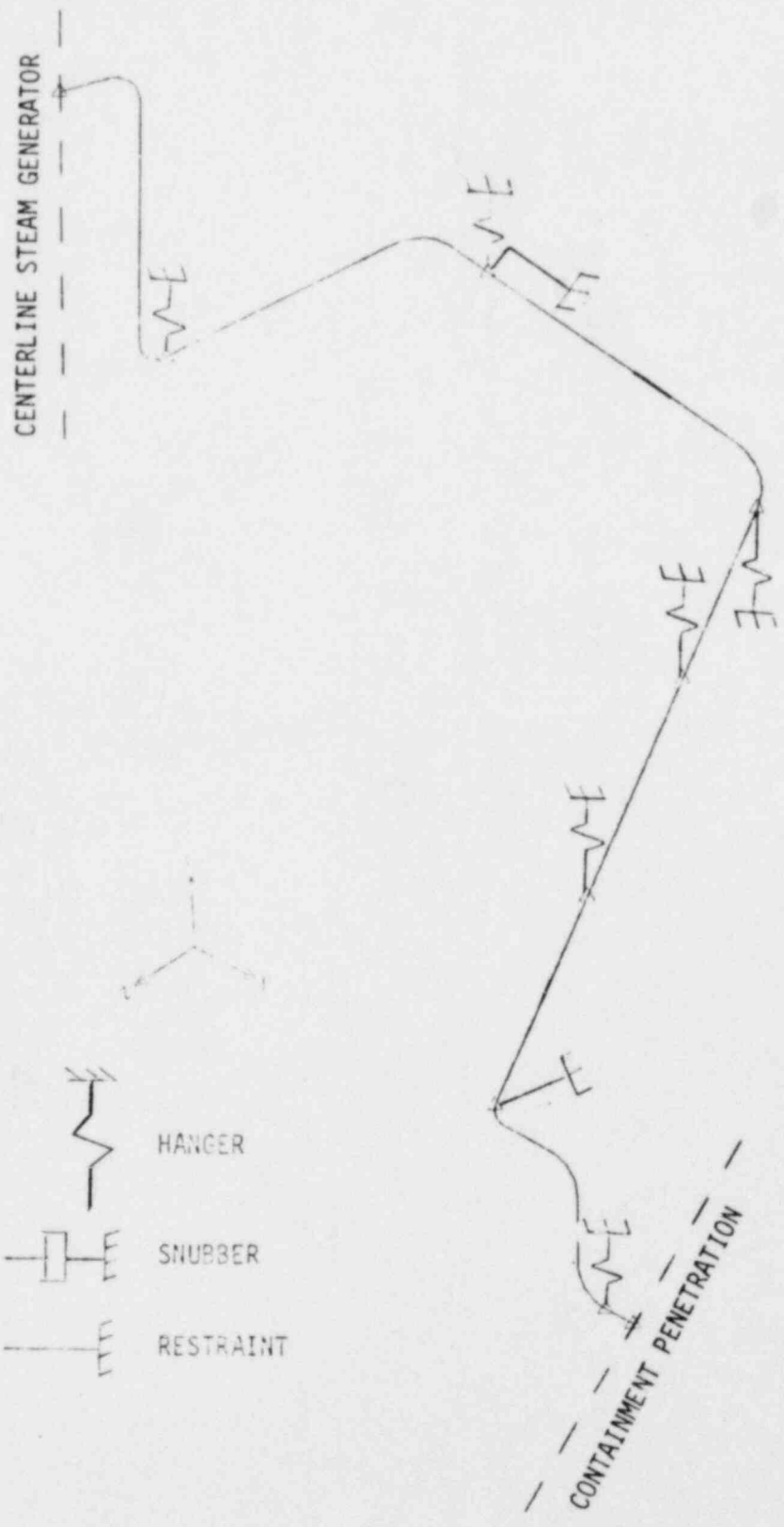

FIGURE 7.10: [ ] FEEDWATER LOOP C | a.c.e

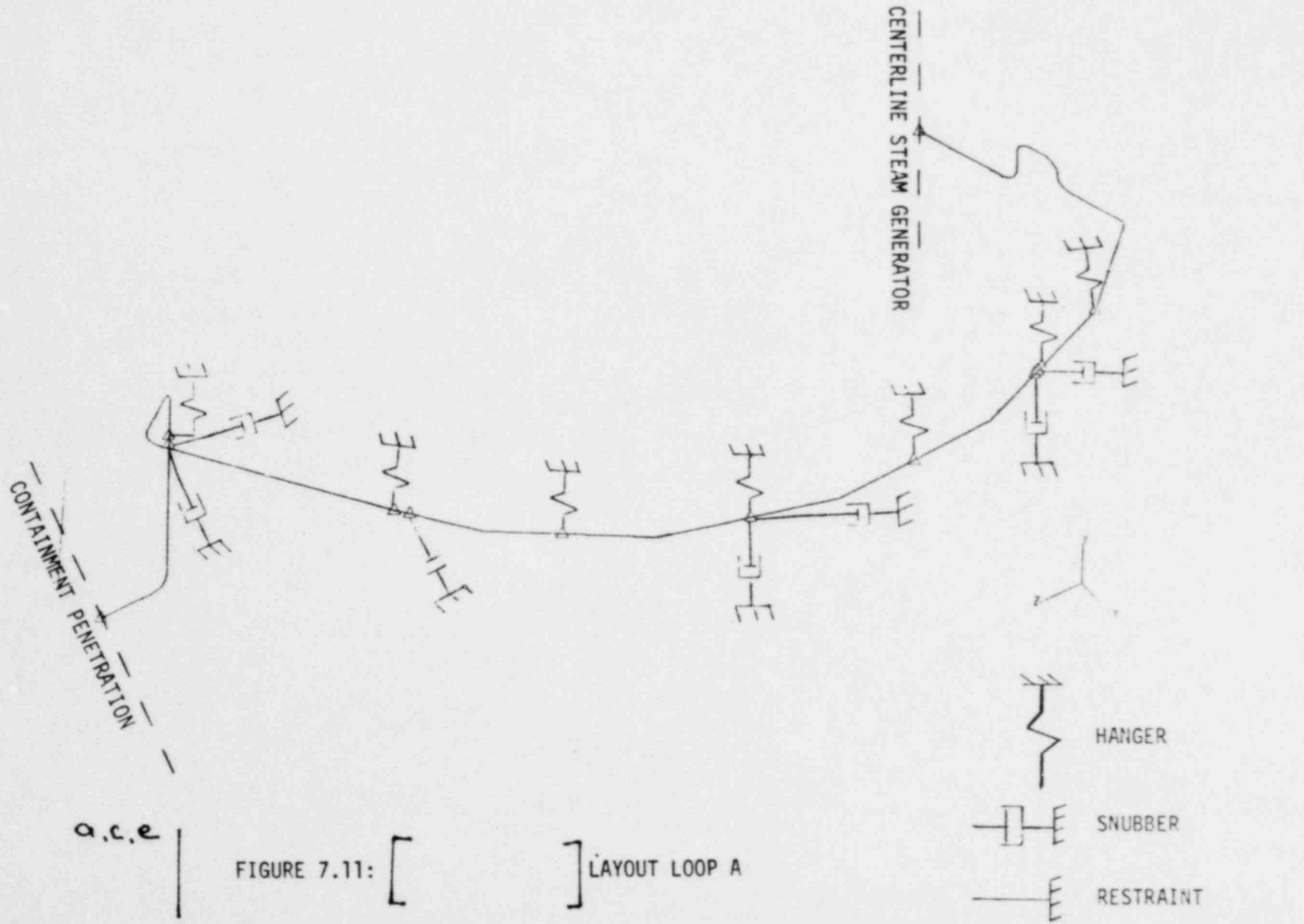

FIGURE 7.11: [ ] LAYOUT LOOP A

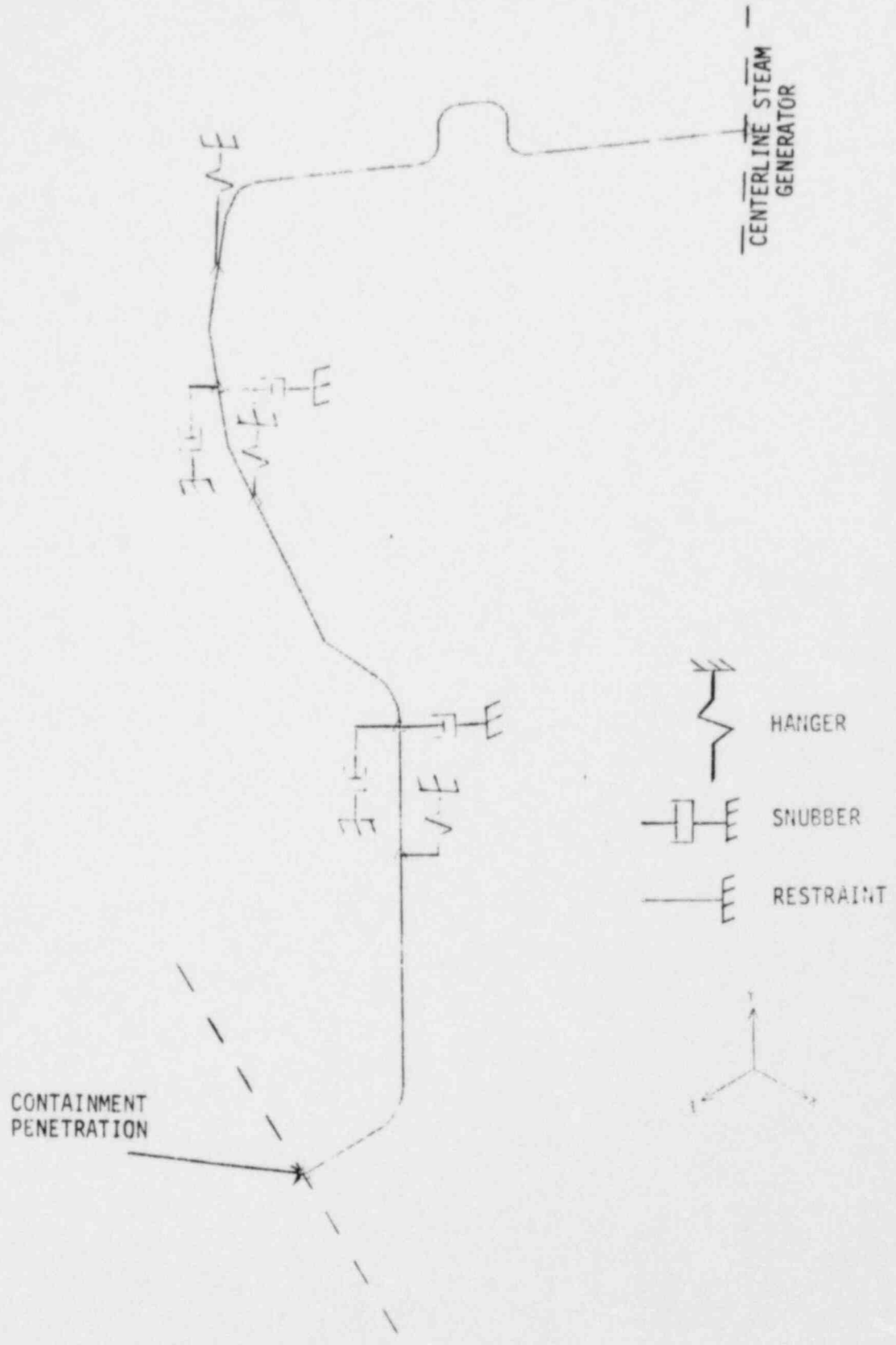

FIGURE 7.12: [ ] LAYOUT LOOP B a,c,e

a,c,e | FIGURE 7.13: [ ] LAYOUT LOOP C

FIGURE 7.14: [ ] LAYOUT LOOP 1 [a,c,e]

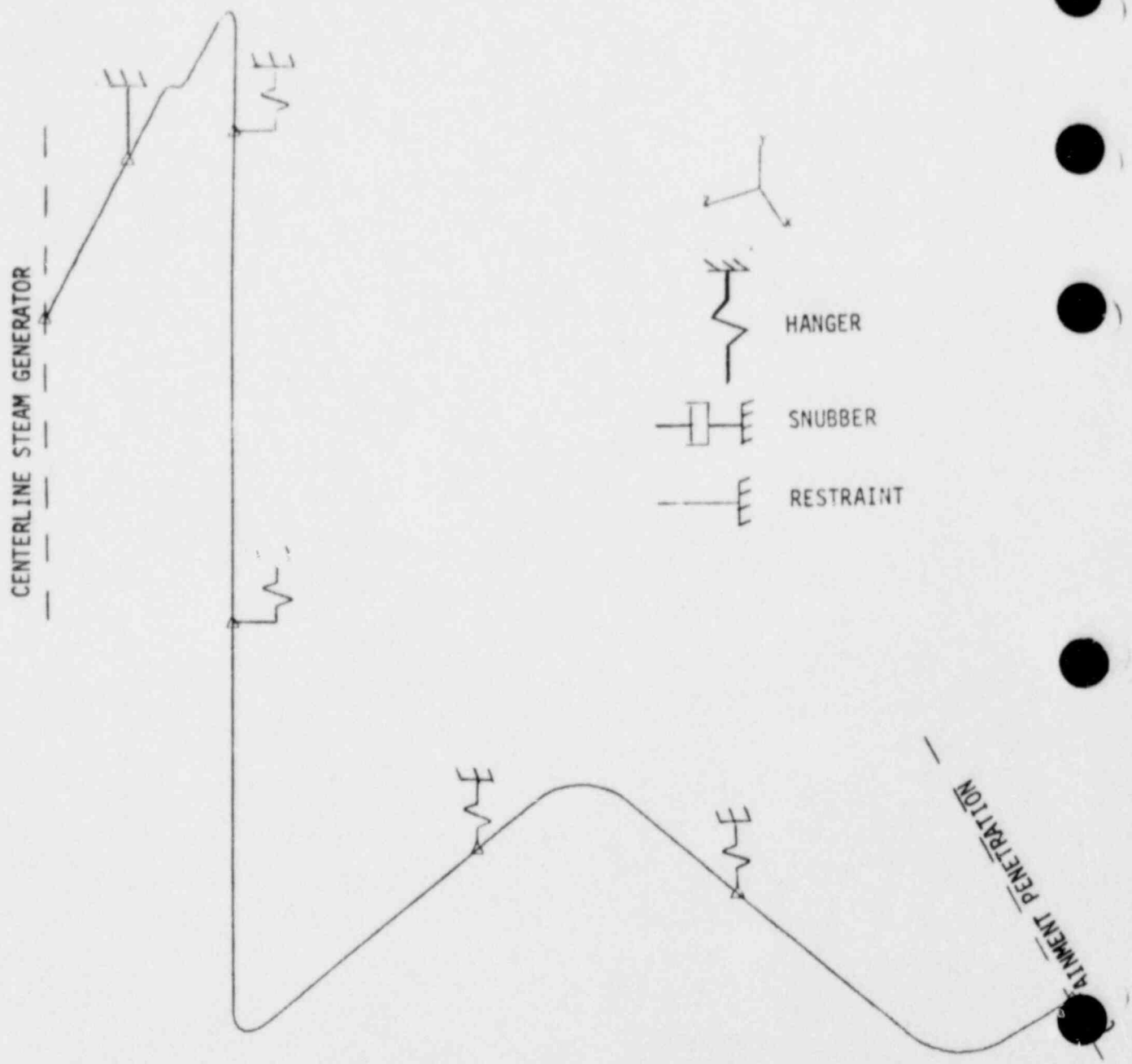

a,c,e | FIGURE 7.15: [ ] LAYOUT LOOP 2

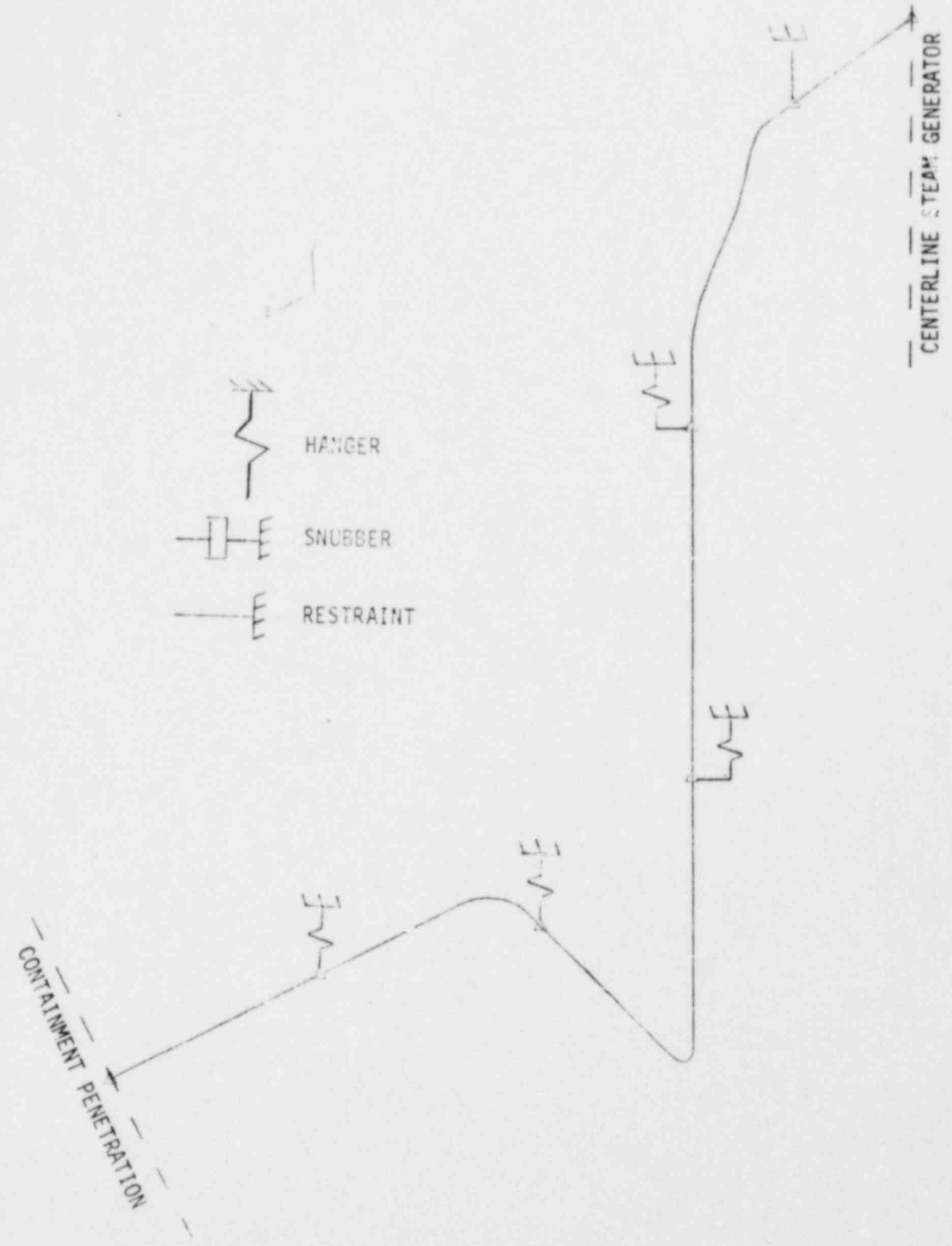

FIGURE 7.16: [ ] LAYOUT LOOP 3 | a,c,e

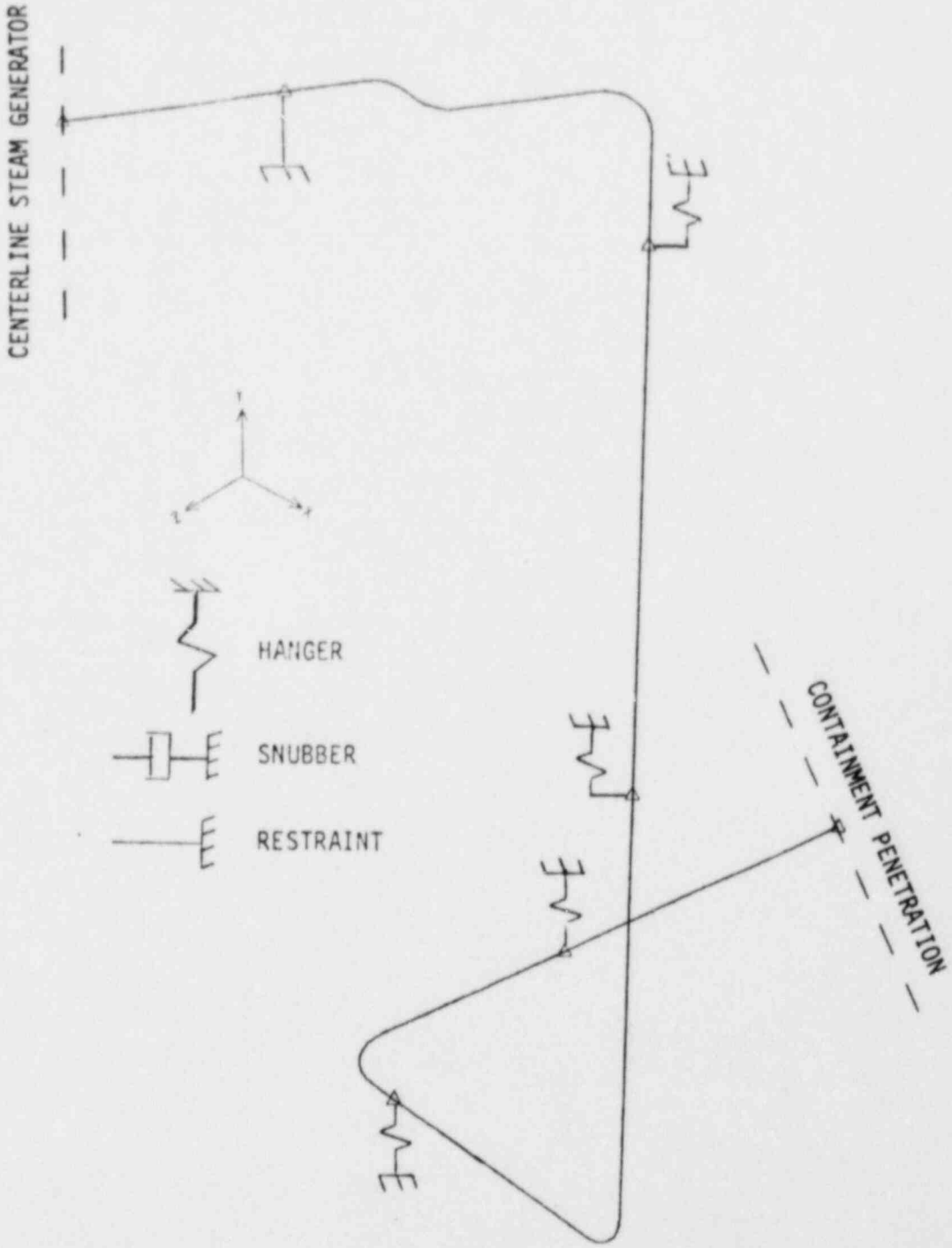

a,c,e FIGURE 7.17: [ ] LAYOUT LOOP 4

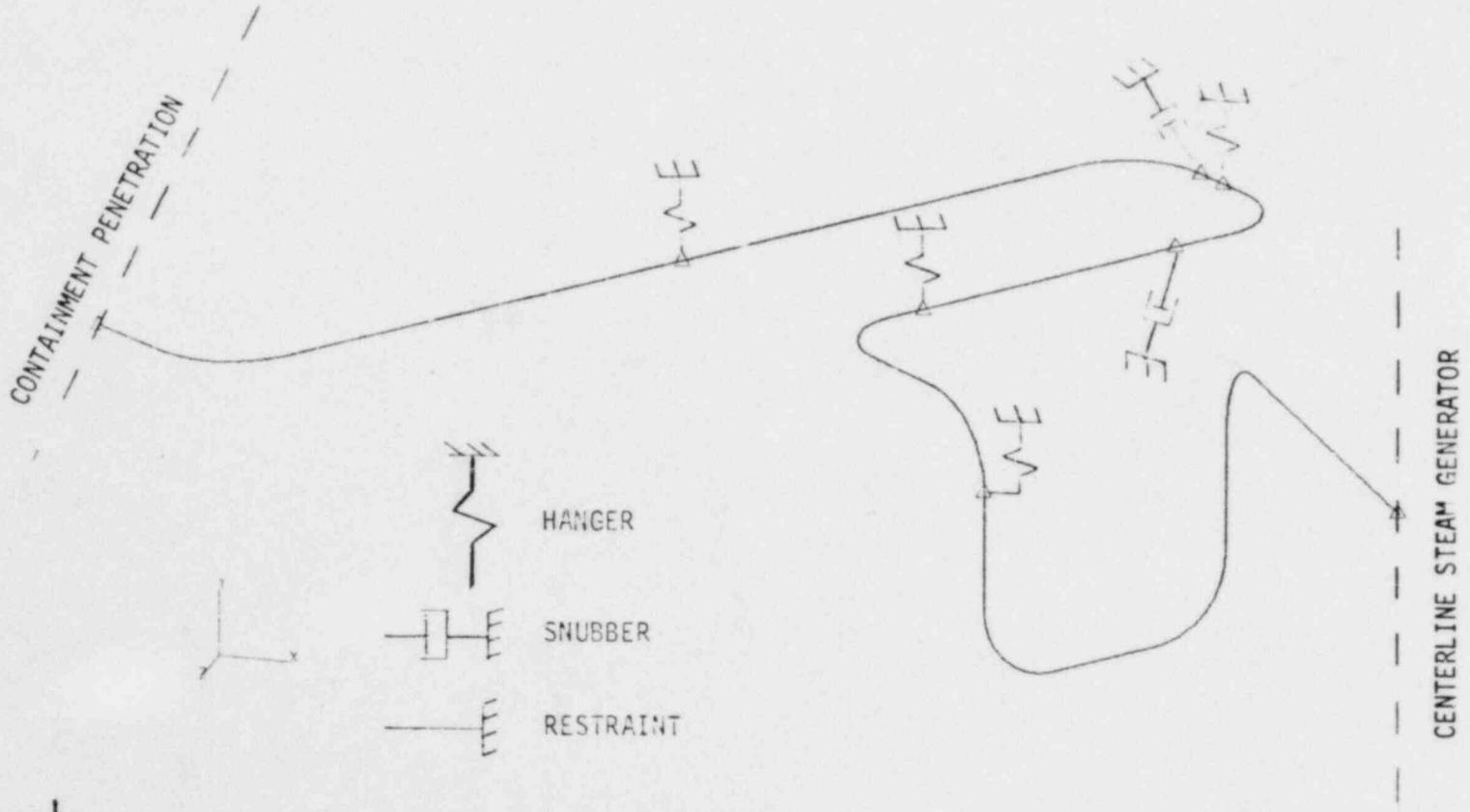

a,c,e

FIGURE 7.18: [ ] FEEDWATER LAYOUT LOOP 1A

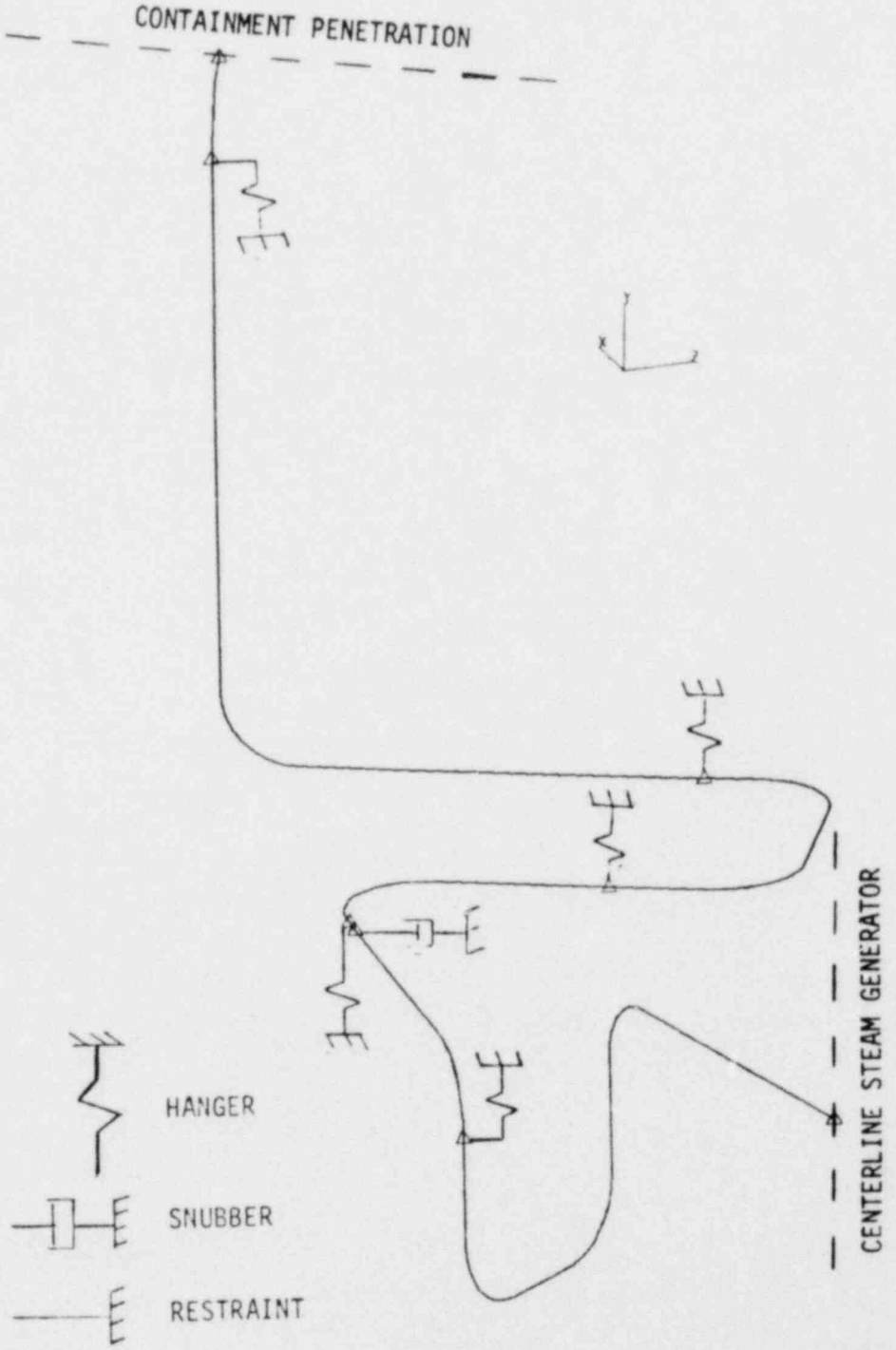

a,c,e

FIGURE 7.19: [ ] FEEDWATER LAYOUT LOOP 1B

FIGURE 7.20. CHECK VALVE SLAM FORCING FUNCTION

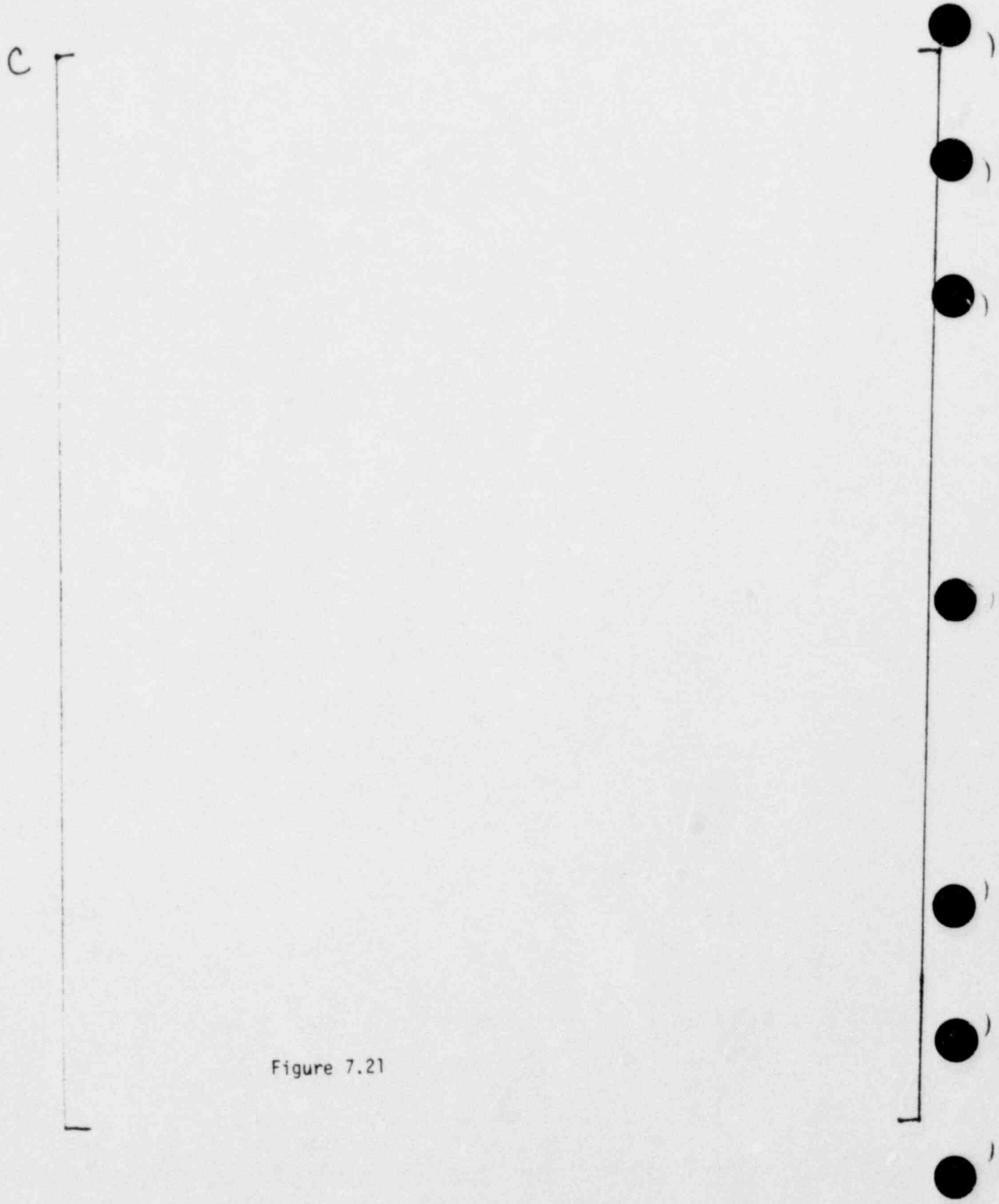

Figure 7.21

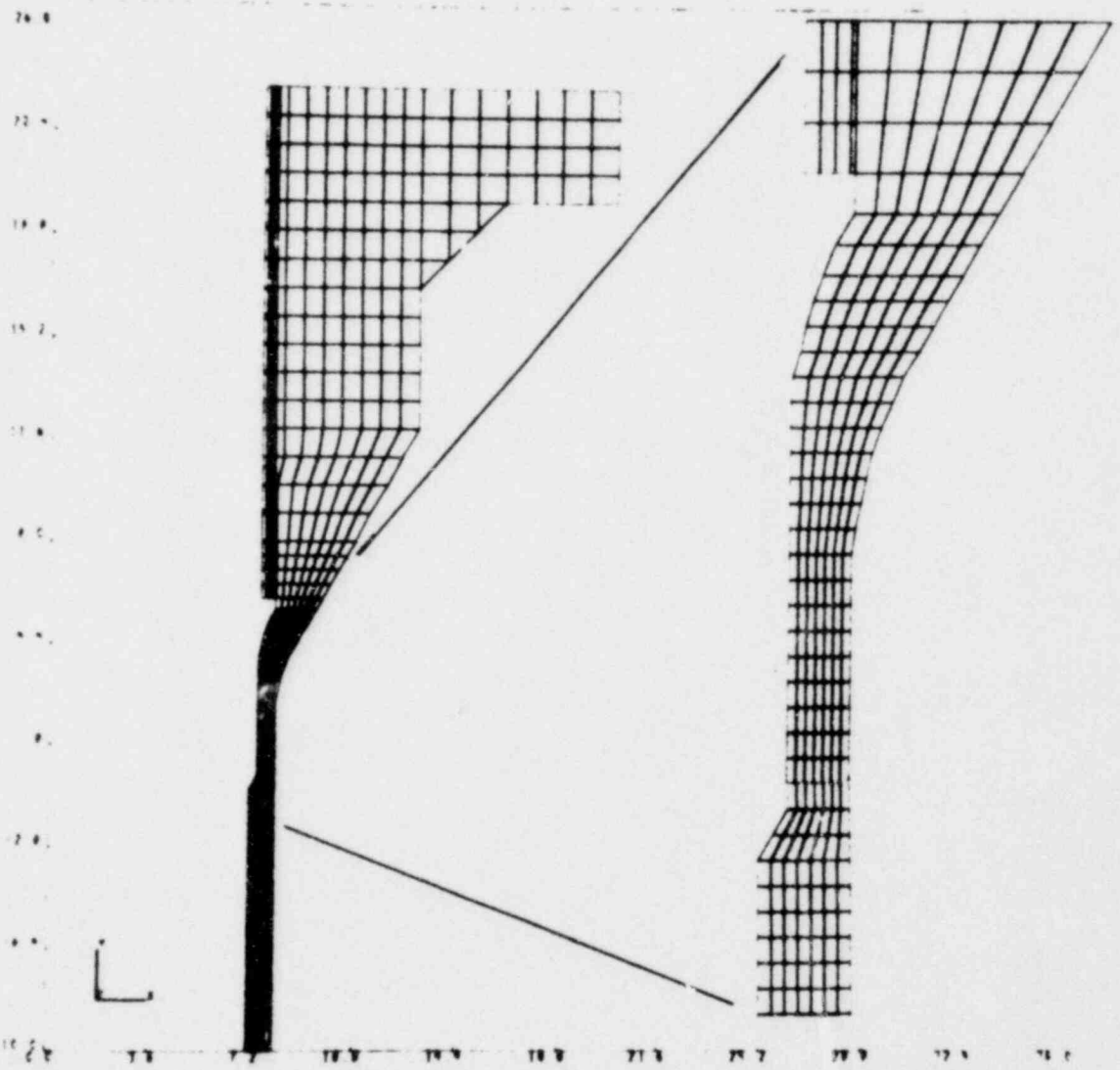

Figure 7.22 2D Finite Element Model for [ ] Feedwater Nozzle. a,c,e

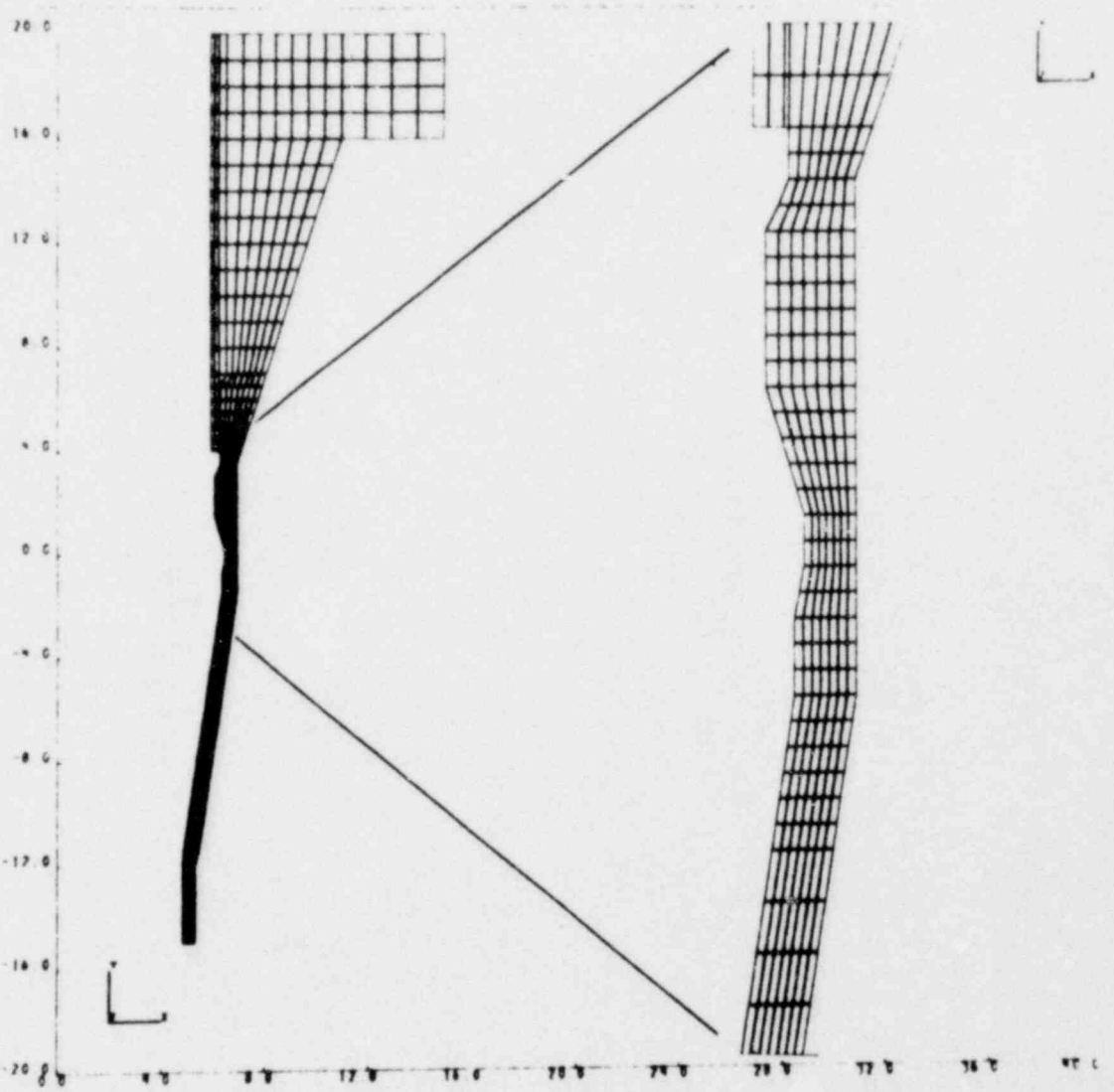

a.c.e | Figure 7.23 2D Finite Element Model for [ ] Feedwater Nozzle.

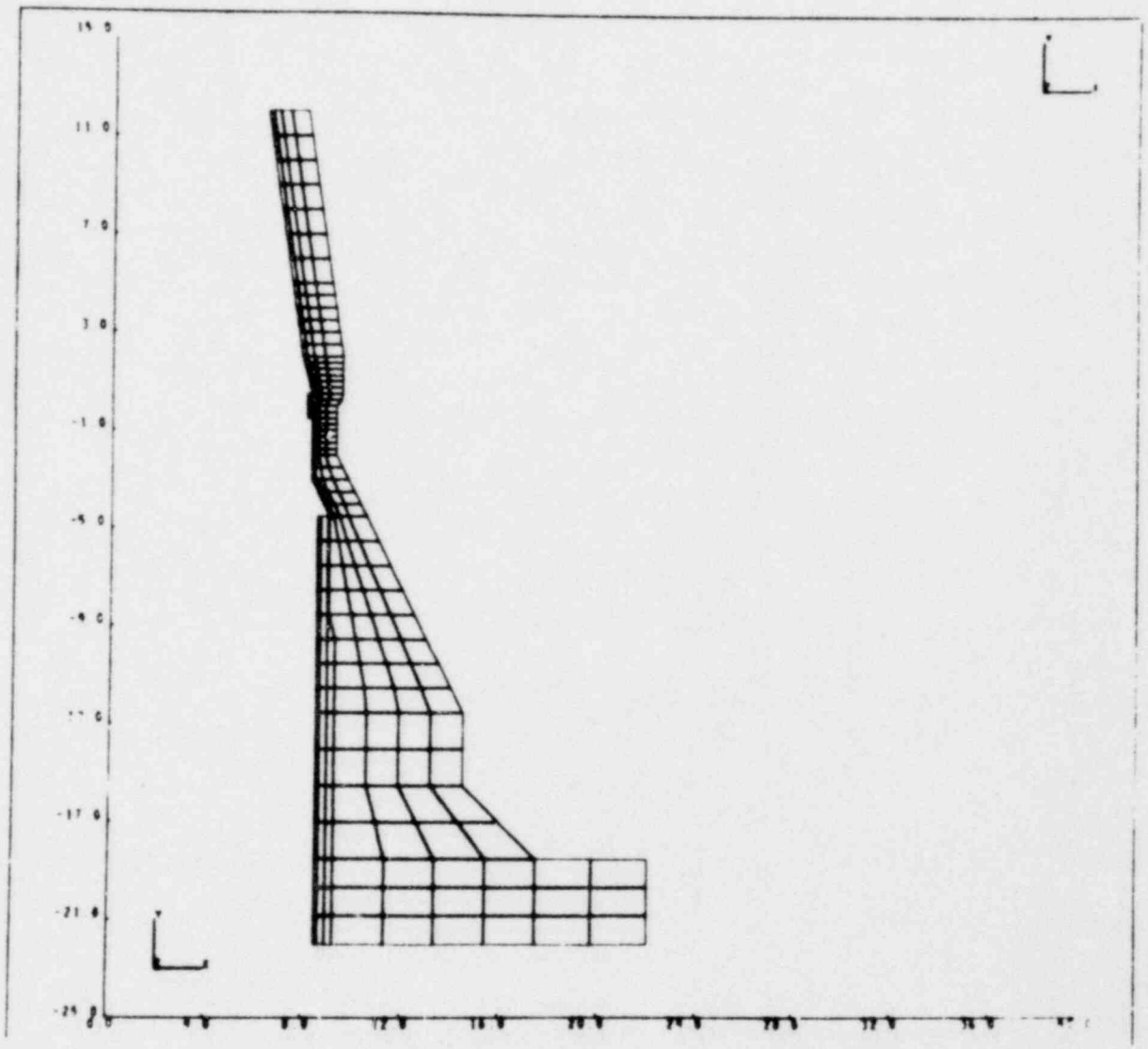

Figure 7.24 2D Finite Element Model for [ ] Feedwater Nozzle. a.c.e

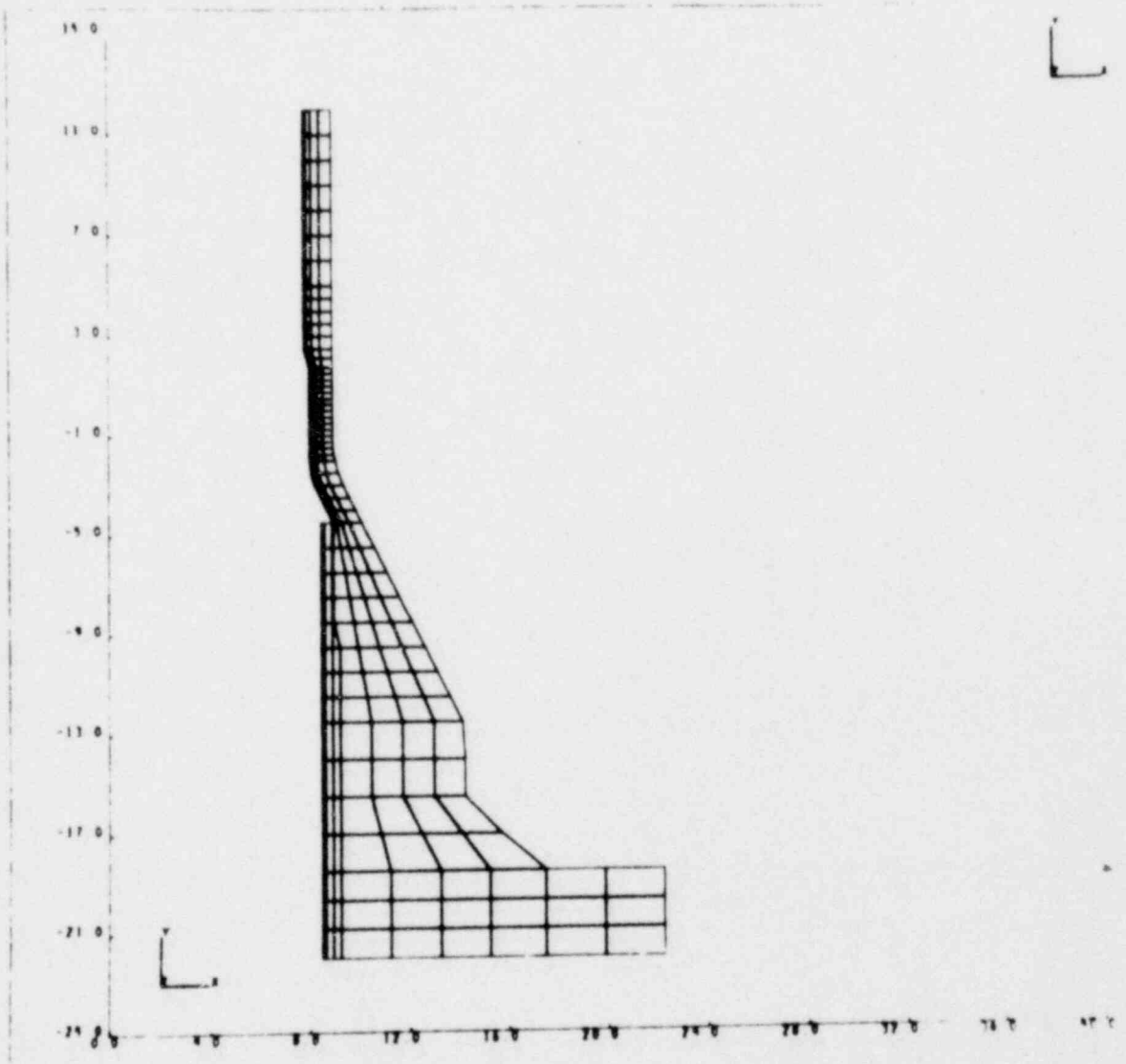

a,c,e

Figure 7.25 2D Finite Element Model for [ ] Feedwater Nozzle.

FIGURE 7.26

HOT STANDBY

THERMAL TRANSIENT DEFINITION

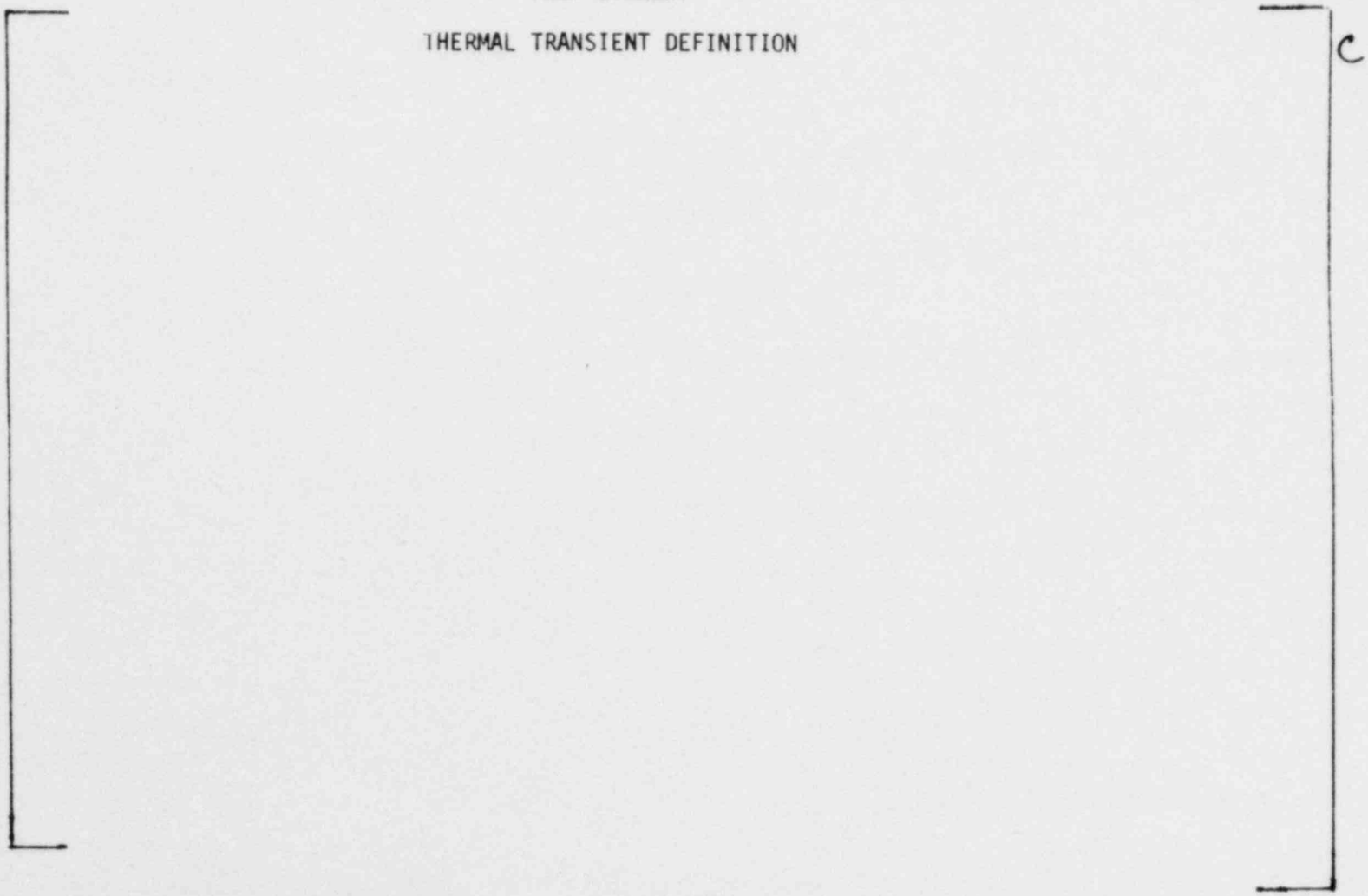

SECTION 8.0

ON-SITE FEEDWATER TEST PROGRAMS

BY

A. J. AYOOB

ACKNOWLEDGEMENTS

The author wishes to acknowledge the work of all the following people who were instrumental in the performance of the on-site test programs and the data reduction effort.

Westinghouse NTD

B. J. Coslow
W. E. Moore
F. Klanica
D. Scherf
S. Y. Lee
D. L. LaPay
N. G. Sowko
M. Bowler
D. Y. Jack
R. Steer
F. Loceff
W. Ciaramitaro
R. Soles
J. Craig
R. Burkhart
C. Antoniak
R. Stivason
R. Krevosh
R. Mach
J. Tomasic
D. Engle
J. Smith
R. Biford
R. Gopal
R. Harrell (Purchasing)

Westinghouse NSD

D. Peterson
R. Cook
J. Gumbert
F. Goldbach
V. Nayyar
R. Powell
B. Simpson

Westinghouse NFD

J. McEvoy
R. Gardner
D. McCarthy
A. Bigi
W. Santacasa
W. Ripple
B. Kleckner

Utility/Site Personnel

J. Gallagher - Salem
S. Labruna - Salem
R. Rothgeb - Millstone
B. Flannagan - H. B. Robinson
S. Grant - CPL
R. Bischoff - D. C. Cook
T. Turner - D. C. Cook
A. Tetzlaff - D. C. Cook

R. Kinney - D. C. Cook
J. Hoch - AEP
E. Bialkin - AEP
J. Markowsky - AEP
C. Edgar - RGE

8.1 INTRODUCTION

The discovery of the cracking in the feedwater lines[ ]a,c,e and the results of the subsequent metallurgical evaluation led to the development of an on-site test program to investigate the possible causes of the cracking. At that time, sufficient information was not available to identify to the characteristics of the feedwater system which should be investigated. The preliminary metallurgical observation[ ]a,c,e (refer to Section 5.0) suggested that some unexpected dynamic events may be ocurring, such as waterhammer or large magnitude flow induced vibration. Because of this, the initial instrumentation plans emphasized investigation of piping vibration. Thermal hydraulic conditions were also monitored but, at the time, were not considered to be cyclic enough to produce[ ]a,c,e. As the test programs commenced, (the chronological order is given in Table 8.1), the data obtained enabled the thermal hydraulic condition to be singled out as the most likely contributor to the cause of the cracking. Subsequent test programs emphasized obtaining data to further characterize the thermal-hydraulic conditions.

The following sections present a discussion of instrumentation, data collection, data reduction, and results obtained for the test programs conducted by Westinghouse for the utility members of the Feedwater Pipe Cracking Owner's Group.

8.2 TEST OBJECTIVES

The objectives of the on-site test programs remained relatively unchanged from the beginning of the test programs despite specific differences in the number, location, and type of instrumentation.

The objectives of the test programs were threefold:

1. To determine differences between actual and design conditions of the feedwater piping;

2. To characterize any unusual or unexpected conditions that may be existing during the normal operating sequence from cold shutdown to 100 percent power; and

3. To characterize the similarities or differences in operation and behavior of the feedwater lines between the various plants tested.

As testing progressed, more specific objectives were established to further characterize the thermal-hydraulic conditions which were found to exist. These objectives were:

c,e [ ]

It was anticipated that achievement of the objectives would provide the following:

1. Data to be used as input for the feedwater line stress and fatigue analyses to predict the crack phenomena;

2. Data to be used to correlate the plant specific feedwater activity with the observed cracking; and

3. Data to assist in the development of off-site test or analytical programs to study, in more detail, the phenomena observed from the site testing.

8.3 INSTRUMENTATION

Each instrumentation package used for the performance of the on-site tests generally consisted of transducers*, signal conditioners, amplifiers,

*Herein the term "transducer" will be used to refer to any measurement device including strain gages, accelerometers, pressure and flow rate cells, LVDT's, and thermocouples.

recording equipment, calibration equipment, and playback equipment. The number and location of transducers varied between plants. A summary of the plant specific instrumentation is given in Table 8.2.

Each monitoring package was tailored to the technical needs and licensing concerns that existed prior to testing. Each plant specific test procedure contained the list of test equipment used during the performance of each plants' test program in addition to specific installation procedures.

A summary of the type, performance characteristics, and installation of transducers used in the testing is given in Table 8.3. Table 8.4 contains a summary of typical data acquisition equipment. Figures 8-1 thru 8-6 depict the signal paths and associated instruments used for the measurement of temperature, strain, acceleration, pressure, displacement, and flow.

8.4 TEST PERFORMANCE

As stated in section 8.2 one of the objectives of the feedwater testing was to determine or characterize the conditions that the feedwater piping experiences during a "normal" plant start up. Therefore, transducer installation was carried out during the scheduled plant outage and was concurrent with or followed the cracked pipe replacement. Data acquisition occurred from the cold shutdown condition and continued on thru 100 percent power for nearly all of the plants tested.

The majority of the testing was passive; that is, data were collected at intervals determined by normal plant condition or feedwater activity. In some cases, certain operator actions, such as feedwater initiation or flow rate changes, were initiated to gain more information about the feedwater thermal hydraulic characteristics and related plant operation.

Communication with the plant operator during testing enabled data to be collected for nearly all typical plant conditions and in some cases during unexpected conditions (such as low power trips etc).

Data collection included recording on 14 channel FM tape recorders during specific data collection periods and continuous sampling and recording on a digital data logger.

In general all data related to dynamic events was recorded on FM magnetic tape. These included acceleration, strain, pressure, displacement, and internal temperature data. Data related to slowly varying conditions such as external temperature, flow rate, and mean internal temperatures, were sampled and recorded using the data logger.

The data were recorded on the data logger almost continuously from cold shutdown to 100 percent power. The sampling and recording rate varied from 10 seconds to 15 minutes. The shorter sample rates were used during periods of high feedwater activity and were sufficiently fast enough to characterize mean internal temperatures, flow rate, and external temperatures. This provision of continuous sampling and recording provided the data necessary for correlation of thermal hydraulic conditions and plant operating characteristics. Table 8.5 presents a summary of the plant conditions during which data were collected.

8.5 DATA REDUCTION METHODS

Due to the number of test programs and the long data sampling periods, a large amount of data to be evaluated soon became available. Therefore, it was necessary to develop standard procedures for data reduction and evaluation.

8.5.1 REDUCTION OF DYNAMIC DATA

The data recorded on FM tape included measurements of acceleration pressure, internal temperature, displacement and strain. Following the data collection phase of the testing, the FM tapes were played back on paper chart recorders (visicorder or oscillograph), in order to quickly survey the data and determine if any unusual conditions existed. Maximum values of each parameter were tabulated and further data analysis to

determine frequency content was identified when necessary. Power spectral density of acceleration, strain, pressure and internal temperatures were calculated on a selected basis to assist in the interpretation of the dynamic data. Results of the reduction and evaluation of dynamic data are presented in section 8.6.

8.5.2 TEMPERATURE AND FLOW

[redacted] a,c,e

**In all test cases, each thermocouple location was denoted by both a thermocouple location designation and a data logger channel number. Both designations will be used when appropriate.

8.6 PLANT SPECIFIC TEST RESULTS

This section presents the plant specific test results as obtained from the reduction of the test data using the methods described in Section 8.5. Due to the extremely large amount of data collected during the tests, only that reduced data pertinent to the observations contained herein are presented. Complete documentation of plant specific test results is contained in the Westinghouse Structural Mechanics Department documentation file (MUAN-7000).

For each plant, the test results are presented to characterize the dynamic response of the piping during steady-state and transient conditions; thermal-hydraulic response of the piping during steady-state stratified conditions and during transient flow conditions; and the long-term stratification, temperature profiles and temperature cycling.

In each case, the correlation of the results with plant conditions or operations is presented when available. Sketches of the transducer locations and designations as used in the presented results precede the results for each plant.*

a.c.e

8.6.1 [ ] (FIRST TEST)

As listed in Table 8.1, the first test at [ ] was not performed by Westinghouse. Therefore, the raw test data was not in a format compatible with Westinghouse developed computerized data reduction methods. However, the data was reduced manually to a format consistent with the other site test data.

a.c.e

The locations of the transducers during the first [ ] test are shown in Figures 8-9 and 8-10. Thermal-hydraulic data and measured strain are shown in Figures 8-11 through 8-17.

*Complete documentation of transducer locations is contained in the plant specific test procedure.

Figures 8-11 (line 3) and 8-12 (line 1) depict temperature at each measurement location versus time during startup. These plots illustrate the existence of long term temperature stratification and the thermal cycling that can be experienced by the feedline during a normal start-up. Since the interval of time between temperature samples (as represented by the dots on the curve) is relatively long, it is doubtful that the curves represent the majority of the cycling that occurred. This will be clarified by the results of the second test at [ ]. (Section 8.6.6) a,c,e

Table 8.6 summarizes the plant conditions and events which occurred during the test period. Figures 8-13 (line 3) and 8-14 (line 1) are plots of selected temperatures for a portion of event number 30. During this event, the feedwater flow was cycled at several flow rates, three of which are shown on the figures. The large rapid response of the two internal thermocouples (36 RB and 45 WG at the bottom of the figures) suggests the presence of [ ]. (Note that a decreasing temperature is represented by a movement upward on the curve. An increasing temperature is represented by movement downward. Absolute temperatures can only be approximated due to instrument zero drifts.) Also note during the event that the presence of the rapid temperature oscillations (water temperature 45 WG) at the onset of the transient suggests the presence of striping. The striping phenomena is shown to exist from the flow model tests and is discussed further in Section 10.0. Comparing the large variations of sidewall temperature to the smaller variations at the top of the pipe suggests that the flow rate was not of sufficient magnitude or duration to "wash out" the pipe. a,b,c

Figures 8-15, 8-16 and 8-17 depict event 31 which represents a portion of time from initial criticality (boron dilution) to low power escalation (less than 10 percent power). [ ] a,b,c

"wash-out" of the pipe and the corresponding temperature drop of the outside wall. Figure 8-17 illustrates the flow rate changes during event 31 (for line 3) along with the strain readings that were obtained. Comparing Figures 8-15 and 8-17, a close correlation of temperature change and strain oscillation is noted. However, the magnitude of the actual stress induced in the piping during these events is not directly obtainable from the strain readings without considering the boundary conditions of the elbow as imposed by the connecting piping*.

a,c,e Temperature profiles across the pipe cross section and along the feedwater pipe for [ ] are shown in Figures 8-18 and 8-19, respectively. The profiles of Figure 8-18 became the basis for initial stress analyses and have remained relatively the same throughout the feedwater crack studies. The profiles of Figure 8-19 indicate that large ΔT_{t-b} can exist as far as 2 feet from the steam generator nozzle.

a,c,e Dynamic acceleration and pressure data collected during the [ ] testing did not indicate any unusual or large steady-state or transient events.

a,c,e 8.6.2 [ ]

a,c,e The feedwater tests conducted at the [ ] site were the first tests conducted by Westinghouse. The benefit of the data from the test at [ ] was not yet available, and therefore a complete instrumentation package was included for the [ ] testing. As summarized in Table 8.2, the instrumentation package provided for the measurement of both thermal hydraulic data and dynamic data. The transducer locations for the [ ] test are shown in Figures 8-20, 8-21 and 8-22.

b,c [

]

(Footnote continued, next page)

Footnote continued:

[redacted] b,c

a,c,e The data acquisition and recording techniques described in Section 8.4 were employed at the [ ] testing and all subsequent tests performed by Westinghouse. Consequently, the standardized data reduction methods described in Section 8.5 were able to be employed.

a,c,e The plant conditions monitored during the testing at H. B. Robinson was similar to those at [ ]. Of these events, the period from initial criticality through low power (less than 20 percent) contains representative thermal hydraulic and dynamic activity. Figure 8-23 depicts the strain, acceleration, displacement, pressure, and internal temperature response of line 1 (loop C) during a portion of this event. a,c,e The similarity of this event to the event 31 at [ ] (Figures 8-15, 8-16, 8-17) is evident in the temperature and strain response. It is noted, however, that the change in temperature on the inside wall of a,c,e the [ ] feedwater pipe is nearly 100°F less than the change of the outer wall temperature at [ ]. This is due in part to the [

a,b]. Examining the temperature response of 1T1 and 1T2 during this "top wash transient" one can again find the evidence of rapid internal temperature oscillations that suggest the presence of striping.

Dynamic response of the piping is evident in the acceleration, pressure, strain, and displacement traces during the event shown in Figure 8-23. The rapid transient spikes are associated with pump and valve operations and switching. The strain and displacement response of the piping is still small during these events.The steady-state and transient accelerations and pressures are relatively small for this type of event.

a,c,e The evidence of long term stratification and temperature cycling at [ ] is shown in Figures 8-24a through 8-24i (Line B) and 8-25a thru 8-25i (Line C). These plots depict the temperature variations of the inner and outer walls of feedwater pipes B and C as they occurred during plant startup. In general, at primary coolant temperaa,b,c tures of [ ] Top and bottom pipe wall temperature remain relatively

steady throughout the startup whereas side wall temperature tends to vary significantly.* This may correlate with the fact that there is less operator controlled variation of feedwater flow when the main feedwater system is used. Flow rates tend to remain relatively constant and the hot/cold interface appears positioned near the[ ] a,c,e

Typical temperature profiles obtained from the[ ]data are shown in Figures 8-26a, 8-26b and 8-27. Figure 8-26 shows the temperature profiles which exist from top to bottom of the pipe at various times during startup. Typical profiles of temperature along the feedwater pipe are shown in Figure 8-27. Again, large ΔT_{t-b} can exist a few feet from the nozzle. a,c,e

The[ ]testing confirmed the significance of the thermal-hydraulic characteristics of the feedwater piping. The similarities and differences between[ ]thermal-hydraulic feedwater behavior suggested that there may exist a strong correlation between this behavior and the observed cracking phenomena. a,c,e

8.6.3 [ ] a,c,e

The feedwater tests at[ ]site comprised measurement of internal and external wall temperature of feedwater lines 1A and 1B.

The thermocouple locations and designations are shown in Figures 8-28 and 8-29.

Location of the internal thermocouples was chosen to assist in better definition of the[ ] c,e

*Minor discrepancies that exist in these temperature plots are due to some initial wiring errors at the beginning of testing. All errors were corrected after 7/19/79.

a,c

Playback of the FM recordings of internal temperature did not reveal any significant differences between [ ] Intermittent evidence of striping existed but was not persistent.

Long term stratification at the [ ] site is evident in Figures 8-30a through 8-30g for Line 1A and Figures 8-31a thru 8-31g for line 1B. Internal temperatures are seen to vary by as much as 100° during "steady" stratification conditions.

Typical profiles of temperature from the bottom to top of the feedwater pipe (Line 1B is typical) are shown on Figures 8-32a and 8-32b. Again these are very similar to the original profiles established from the first [ ] test. The profile of temperature along the pipe (Line 1B) is shown in Figure 8-33 for two typical steady conditions.

a,c

8.6.4 [ ]

The tests performed at [ ] were the first feedwater tests performed for a plant with a primary system not supplied by Westinghouse. The feedwater line at [ ] is characterized as a "straight configuration", i.e., a relatively long horizontal run of straight pipe is present between the steam generator nozzle and the first vertical elbow. A sketch of the piping layout is shown in Figure 8-34. Also shown are the locations and designations of the transducers used during the [ ] tests. Because of licensing concerns at the time, the feedwater line was instrumented with both thermocouples and strain gages and accelerometers.*

a,c

Maximum steady-state values of acceleration and strain are given in Table 8.7. These are consistent with measurements at other plants tested.

a,c

Long term temperature stratification at [ ] is depicted in Figures 8-35a through 8-35i. These plots of outer wall temperature

reveal very little temperature cycling. This is in part due to the relatively short outage. During this outage, there were no long term hold points at full temperature and the power escalation from 0-30 percent was rapid. Therefore, relatively little temperature cycling was experienced during this test period. Plots of the temperature profile across the pipe cross section are shown in Figures 8-36a and 8-36b. Again, these bear close similarity to the profiles obtained from the other plants tested.

Examination of the profiles of temperature along the pipe as shown on Figure 8-37 reveal that significant ΔT_{t-b}'s can exist as far as [ ] from the nozzle. | c,e

8.6.5 [ ] | a,c

The feedwater testing at [ ] included both internal and external thermocouples and dynamic pressure and flow rate measurements. Locations of thermocouples are shown in Figures 8-38a (line 13) and 8-38b (line 14).

Playback of the dynamic pressures during steady-state and transient conditions did not reveal that any unusually large dynamic pressure transients occurred. Steady-state pressures were of the same magnitude as observed at [ ] | a,c

Plots of temperature versus time during startup are shown in Figures 8-39a through 8-39e (line 13) and 8-40a through 8-40m (line 14). The most significant characteristic of the feedwater temperature activity at [ ] is the ability to [ ]. This type of feeding (as opposed to [ ] feeding) causes the temperatures of the pipe to be uniform but to alternate from hot to cold. Figure 8-39c illustrates this type of operation. All previous tests seem to indicate that feedwater operation is of | a,c | c,e

*Due to the difficult pipe replacement job, [ ] requested startup without repairing the pipe and to repair at the next scheduled outage. Start-up approved on the condition that on-line vibration monitoring of pipe be performed in addition to acoustic leak detection. | a,c

a,c | the [ ] technique with [ ] when necessary. [ ] appears to use both methods as is evidenced by the plots of Figures 8-40e through 8-40h.

a,c | The temperature profiles along the pipe cross section obtained from the [ ] data are shown in Figures 8-41a and 8-41b.

The profiles of temperature along the feedwater pipe outer wall are shown in Figures 8-42a (line 13) and 8-42b (line 14). The configuration of the piping is slightly different than at the other plants tested. However, large ΔT_{t-b} can still exist a significant distance away from the nozzle.

a,c | 8.6.6 [ ] (SECOND TEST)

a,c,e | The second test of the feedwater piping at [ ] was performed to evaluate the effect of the [ ] modification that was made to line 24. Both the modified line (line 24) and an [ ] line (line 21) were instrumented with external thermocouples, strain gages, and flow meters. The location of the thermocouples and strain gages are shown in Figure 8-43a (line 21) and 8-43b (line 24).

The strain gages were installed in an attempt to measure strain due to thermal stratification. However, as discussed in Section 8.6.1, the temperature conditions imposed on the feedwater lines are too severe to allow confident evaluation of stress conditions in the piping. Standard strain gage temperature compensation techniques are not sufficient.

Temperature plots of the outer wall of the feedwater piping are shown in Figures 8-44a through 8-44j. Examination of line 21 reveals that significantly more temperature cycling occurred during this startup than was indicated in the first test even though the startups were of similar duration.*

b,c | *This is probably due to the smaller [ ] used during this test than in the first test.

At first examination line 24 which incorporates the [ ] does not appear to experience significantly different temperature characteristics than line 21. However, the average top to bottom temperature difference (ΔT_{t-b}) of line 24 is somewhat less than 21; specifically, | a,c,e

(ΔT_{t-b}) line 21 = [ ] versus (ΔT_{t-b}) line 24 = [ ] | a,b,c

Selection of three typical transient conditions further reveals the benefit of the [ ]. Figures 8-45 through 8-47 show the comparison of the temperature responses of lines 21 and 24 under similar flow conditions. In Figure 8-45 three flow rates are shown and it is noted that the response of line 24 is somewhat slower than line 21, as expected. Further, the top to bottom profile of temperature for line 24 seems less sharp than line 21. In Figure 8-46, a significant difference in the time response of line 24 and line 21 is noted. In addition, the minimum temperature reached by the top wall of the pipe is significantly increased in line 24 as compared to line 21. Further, the high flow rate had to be maintained nearly twice as long in order for line 24 to reach its minimum temperature. | a,c,e

The previous two transient conditions were imposed by the operator at the request of the test coordinator. The results of the true test of [ ] effectiveness are shown in Figure 8-47. In this case, the plant is in the | a,c,e

[ ]. | b,c

This causes the "top wash" conditions described in previous sections. The comparisons of line 24 and line 21 indicate much less severe top wall temperature changes occur on the [ ] line than on the [ ] line. Further, the profile of temperature from the top to bottom of the pipe appears less severe. Further evaluation of thermal sleeve using these test results is presented in the stress and fatigue analysis section (Section 11.0). | a,c,e

The temperature profiles from the top to bottom of the line 21 are shown in Figures 8-48a and 8-48b. Again it is seen that the profiles for

line 21 are similar to the profiles from the other plants. For the thermal sleeved line (line 24) however, the profiles are somewhat smoother, as seen in Figures 8-49a and 8-49b. The [ ] Profiles of temperature along the piping is shown in Figures 8-50 and 8-51.

b,c

8.7 SUMMARY AND OBSERVATIONS

The results of feedwater test programs presented in the previous section suggest that thermal hydraulic conditions of the near nozzle feedwater piping that exist during a typical plant startup contain the possible link to the observed cracking. Both the similarity of the conditions and the dissimilarities in temperature cycling and plant operation seemed sufficient to provide correlation of the plant specific thermal hydraulic characteristics with plant specific cracking. The following sections summarize the more significant thermal hydraulic conditions.

8.7.1 THERMAL STRATIFICATION/PLANT OPERATION

The plots of temperature versus time for each plant tested, as presented in Section 8.6, provide adequate data for extraction of the general relationship between thermal stratification and plant operation. Two plant operational characteristics; that is overall [ ] and [ ] are significant with respect to thermal stratification.

b,c

These characteristics are discussed in more detail in the following paragraphs.

a,b,c [ ]

*The generalizations presented in this section resulted from the author's observation while performing the testing on site. Detailed analysis of actual plant operating history could provide much deeper insights.

[ ] a,b,c

auxiliary feeding. The significant effect of this startup phase on thermal stratification is shown in Figures 8-30e, 8-39l, and 8-44j. This stratification is characterized by the feedwater pipe temperature that is all cold (at T_{FS}) except for the top which cycles between T_{FS} and T_{PR}.* This cycling can be as much as 450°F and a significant number of cycles can occur.

b,c

[

]

*The profiles corresponding to this condition involves cycling from profile 1 to profile 4. As discussed in Section 11.0, this can be a particularly severe temperature condition.

[ ] a,b,c

Concerning establishment of the minimum flow rate necessary to fully "wash out" the pipe with cold water, data from the plant tests suggest that a flow rate above approximately [ ] will cause the outer wall at the top of the 16" pipe to decrease in temperature. [data from the site tests is insufficient at this time to establish a minimum flow rate which would guarantee "wash out" for the majority of] This could be determined on a plant specific basis with a simple monitoring program if the need arises. b,c e

8.7.2 TEMPERATURE PROFILES - CYCLING AND INTERFACE DURATION

As discussed in previous sections, the cyclic behavior of the temperature profiles across the pipe cross section is considered a significant characteristic of the thermal hydraulic condition. The typical profiles exhibited at each plant were presented in Section 8.6. These were classified into one of the [ ] types. Associated with each profile type, the approximate location of the hot-cold water interface can be established based on the [ ]. This approximate [interface location can then be specified as the fractional diametral distance from the bottom of the pipe (the pipe diameter was normalized to 1.0). The interface location along with the total duration of this interface, and ΔT_{t-b} can then be used to assist in the determination of the effects of striping.] b,c

a,b,c

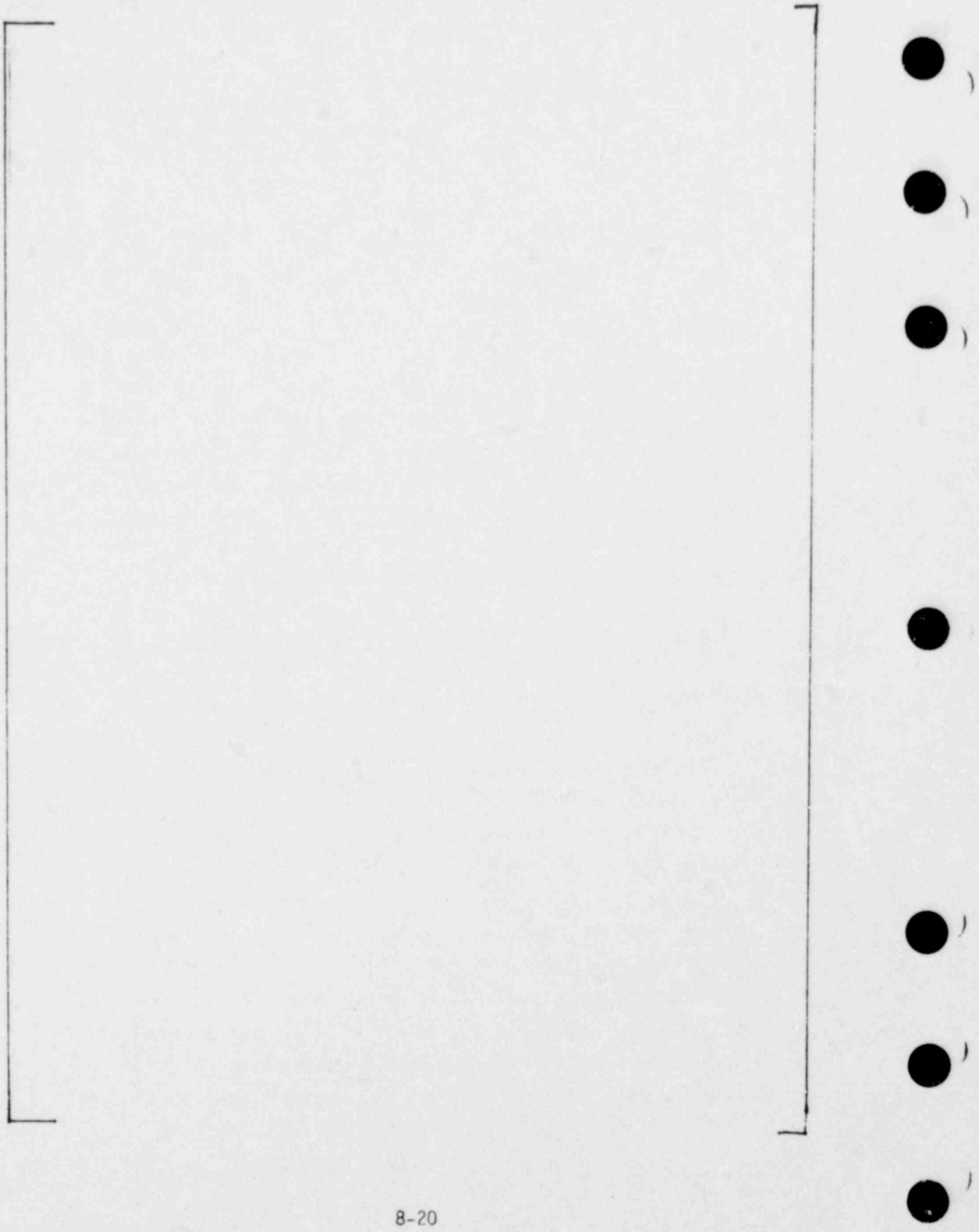

[ ] a,b,c

8.7.3 PIPING VIBRATION AND DYNAMIC RESPONSE

[ ] a,b,c

TABLE 8.1

SUMMARY OF ON-SITE FEEDWATER LINE TEST PROGRAMS

PLANT SITE	UTILITY/OWNER/SERVICE CORP	TEST PERIOD* FROM	TEST PERIOD* TO	APPROXIMATE NUMBER OF TEST DAYS	REMARKS
[ ]	[ ]	6/28/79	7/4/79	7	Test performed by [ ]
		7/16/79	7/25/79	5	--
		8/1/79	8/6/79	5	--
		8/26/79	8/28/79	2	Short outage, no pipe repair
		11/13/79	12/27/79	7	Long outage
		1/12/80	1/20/80	8	Test conducted to determine effectiveness of fixes.
		--	--	--	Testing has not yet commenced.
		--	--	--	No test performed.

a.c

TABLE 8.1 (cont.)

SUMMARY OF ON-SITE FEEDWATER LINE TEST PROGRAMS

PLANT SITE	UTILITY/OWNER/SERVICE CORP	TEST PERIOD* FROM	TEST PERIOD* TO	APPROXIMATE NUMBER OF TEST DAYS	REMARKS
[ ]	[ ]	--	--	--	No test performed.
[ ]	[ ]	--	--	--	No test performed.
[ ]	[ ]	--	--	--	No test perfomed.

a,c

*Test period includes only the time from beginning to end of data collection.

TABLE 8.2

SUMMARY OF PLANT SPECIFIC INSTRUMENTATION USED DURING
THE FEEDWATER TEST PROGRAMS

a,c

*Also included acoustic leak detection

TABLE 8.3

PERFORMANCE AND INSTALLATION SPECIFICATIONS OF TYPICAL
TRANSDUCERS USED DURING FEEDWATER TESTING

TABLE 8.3 (cont.)

PERFORMANCE AND INSTALLATION SPECIFICATIONS OF TYPICAL
TRANSDUCERS USED DURING FEEDWATER TESTING

C

[

]

TABLE 8.4

TYPICAL DATA ACQUISTION RECORDING AND SIGNAL CONDITIONING
EQUIPMENT USED DURING FEEDWATER TESTING

[redacted]

This is only a partial list of major equipment. Peripheral equipment for calibration, set-up and trouble shooting was always a part of the instrumentation package.

TABLE 8.5

SUMMARY OF TYPICAL TEST DATA COLLECTION PERIODS

b,c

[redacted]

TABLE 8.6

DESCRIPTION OF TEST EVENTS CONDUCTED AT [ ] (1st TEST) [a,c]

[b,c]

TABLE 8.6 (cont.)

a,c

DESCRIPTION OF TEST EVENTS CONDUCTED AT [ ] (1st TEST)

EVENT	APPROXIMATE FEEDWATER FLOW (lbs/hr)	EVENT DESCRIPTION

b,c

TABLE 8.6 (cont.)

DESCRIPTION OF TEST EVENTS CONDUCTED AT [ ] (1st TEST) [a,c]

EVENT	APPROXIMATE FEEDWATER FLOW (lbs/hr)	EVENT DESCRIPTION [b,c]
[		]

TABLE 8.7

MAXIMUM MEASURED STEADY STATE DYNAMIC STRAINS AND ACCELERATION OF THE FEEDWATER PIPING AT [ ]

a,c [ ]

a,b,c [ ]

TABLE 8.8

NORMALIZED NUMBER OF PROFILE (ALL TYPES)
OCCURRENCES WITHIN EACH ΔT RANGE

a,b,c

[redacted]

*Line 24 had the thermal sleeve. The profiles are smoother than the profiles without sleeve.

TABLE 8.9

NORMALIZED DURATION OF HOT-COLD INTERFACE

a,b,c

[ ]

TABLE 8.10

PLANT RANKING IN TERMS OF SEVERITY OF
THERMAL-HYDRAULIC CONDITIONS

(1 = MOST SEVERE)
(5 = LEAST SEVERE)

PLANT	POTENTIAL FOR SEVERE THERMAL CYCLING	POTENTIAL FOR LONG HOT-COLD INTERFACE DURATION
[redacted]		

a,b,c

(a) Based on line 14

b, c

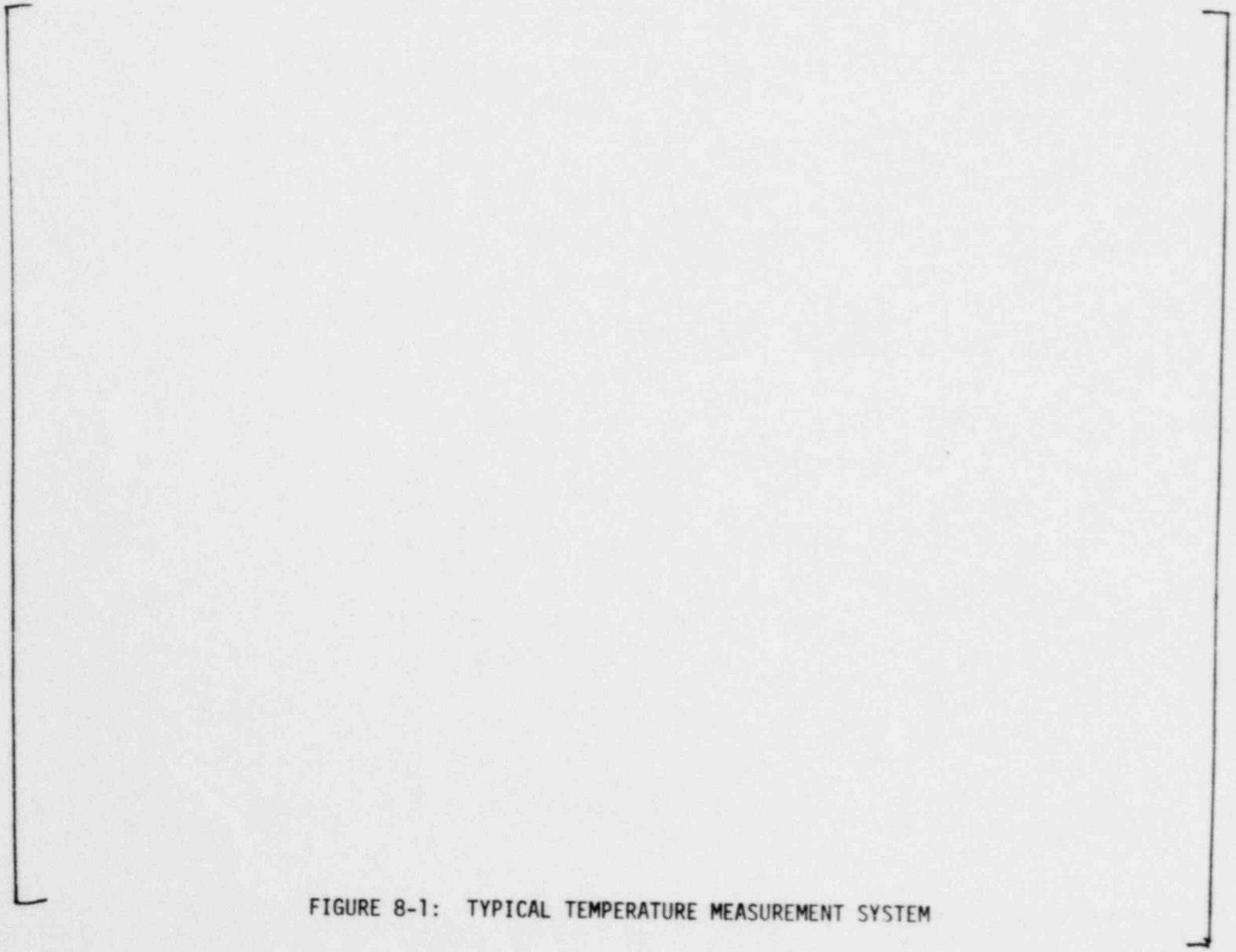

FIGURE 8-1: TYPICAL TEMPERATURE MEASUREMENT SYSTEM

b,c

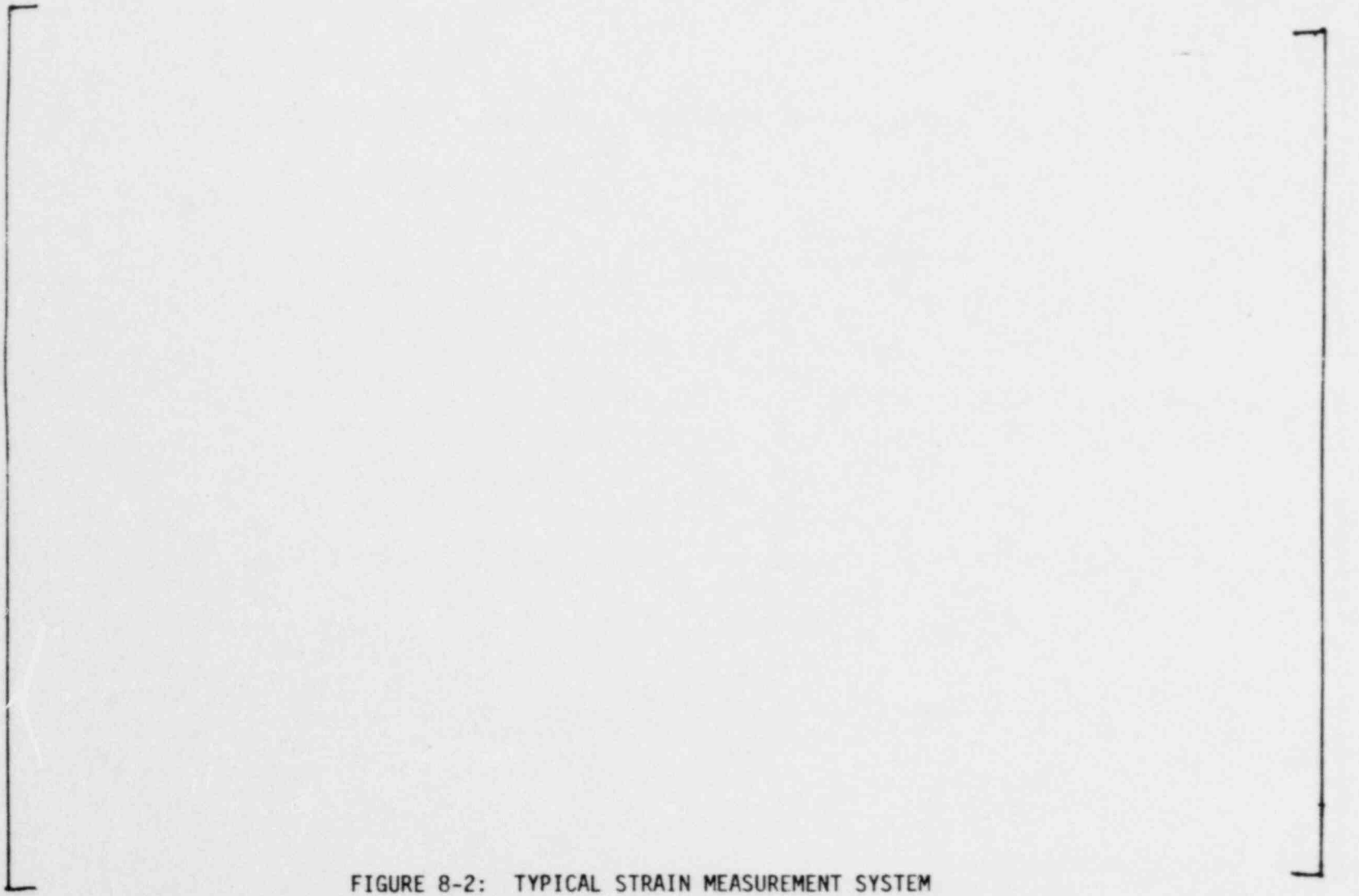

FIGURE 8-2: TYPICAL STRAIN MEASUREMENT SYSTEM

b, c

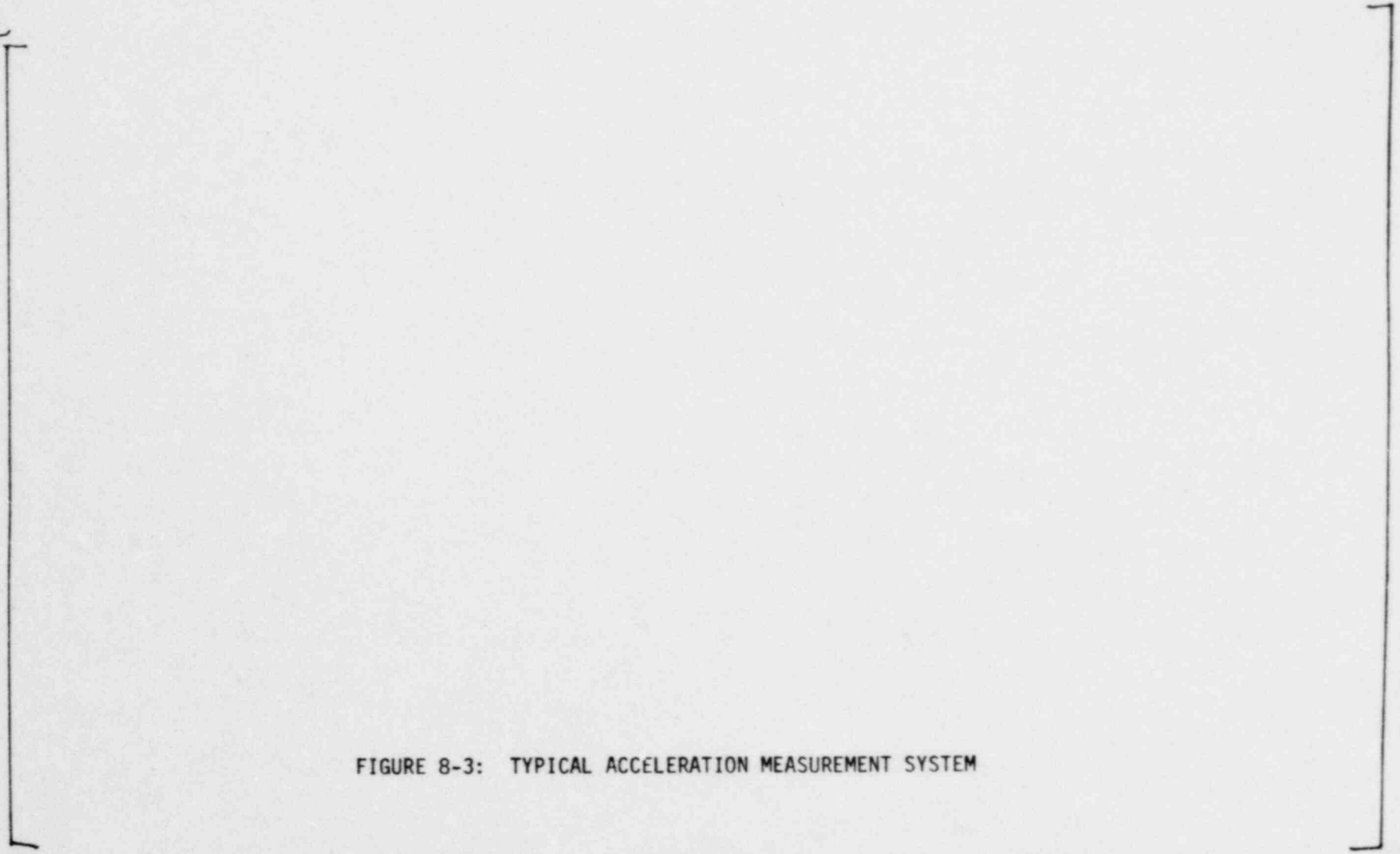

FIGURE 8-3: TYPICAL ACCELERATION MEASUREMENT SYSTEM

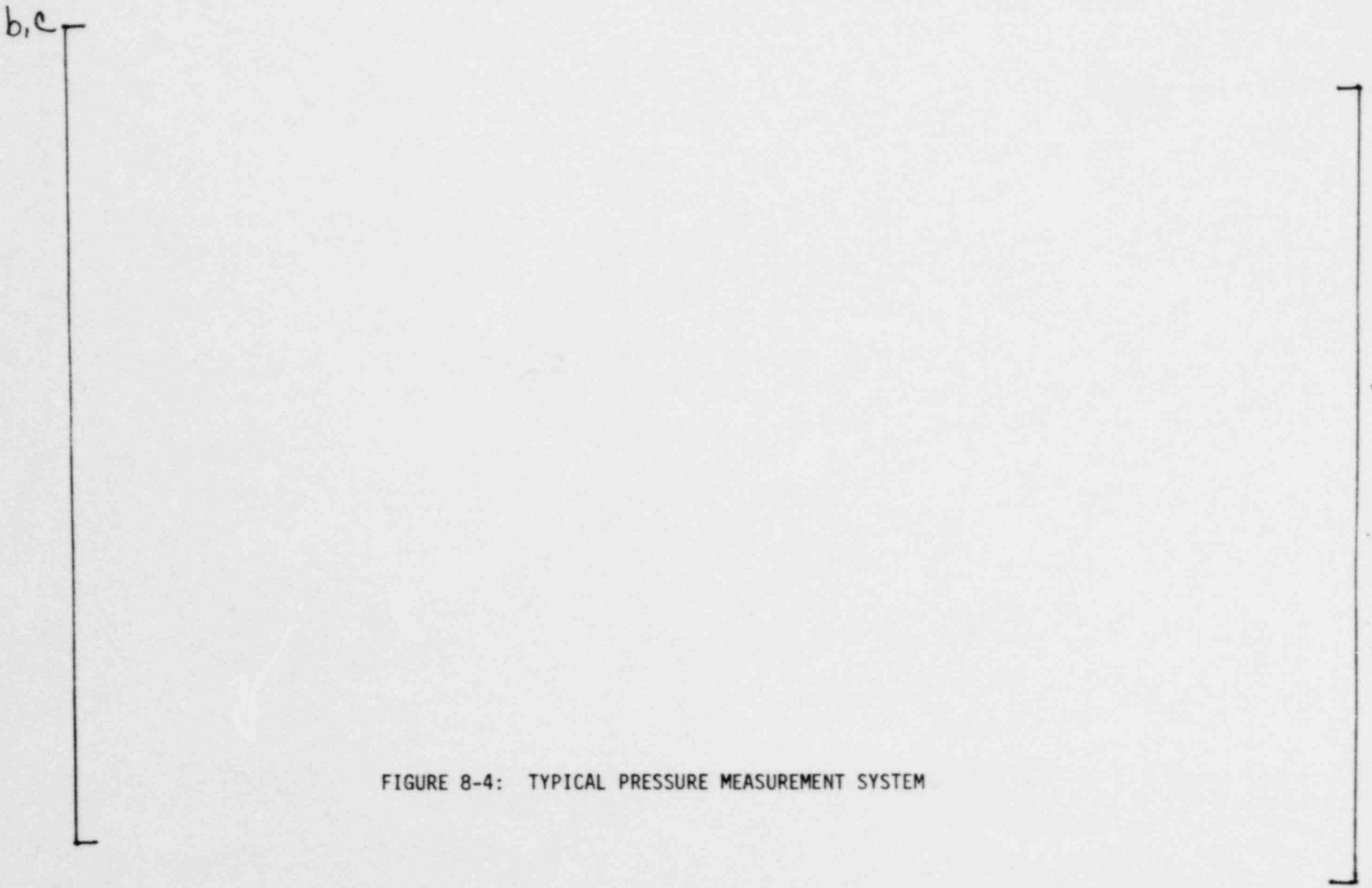

FIGURE 8-4: TYPICAL PRESSURE MEASUREMENT SYSTEM

b,c

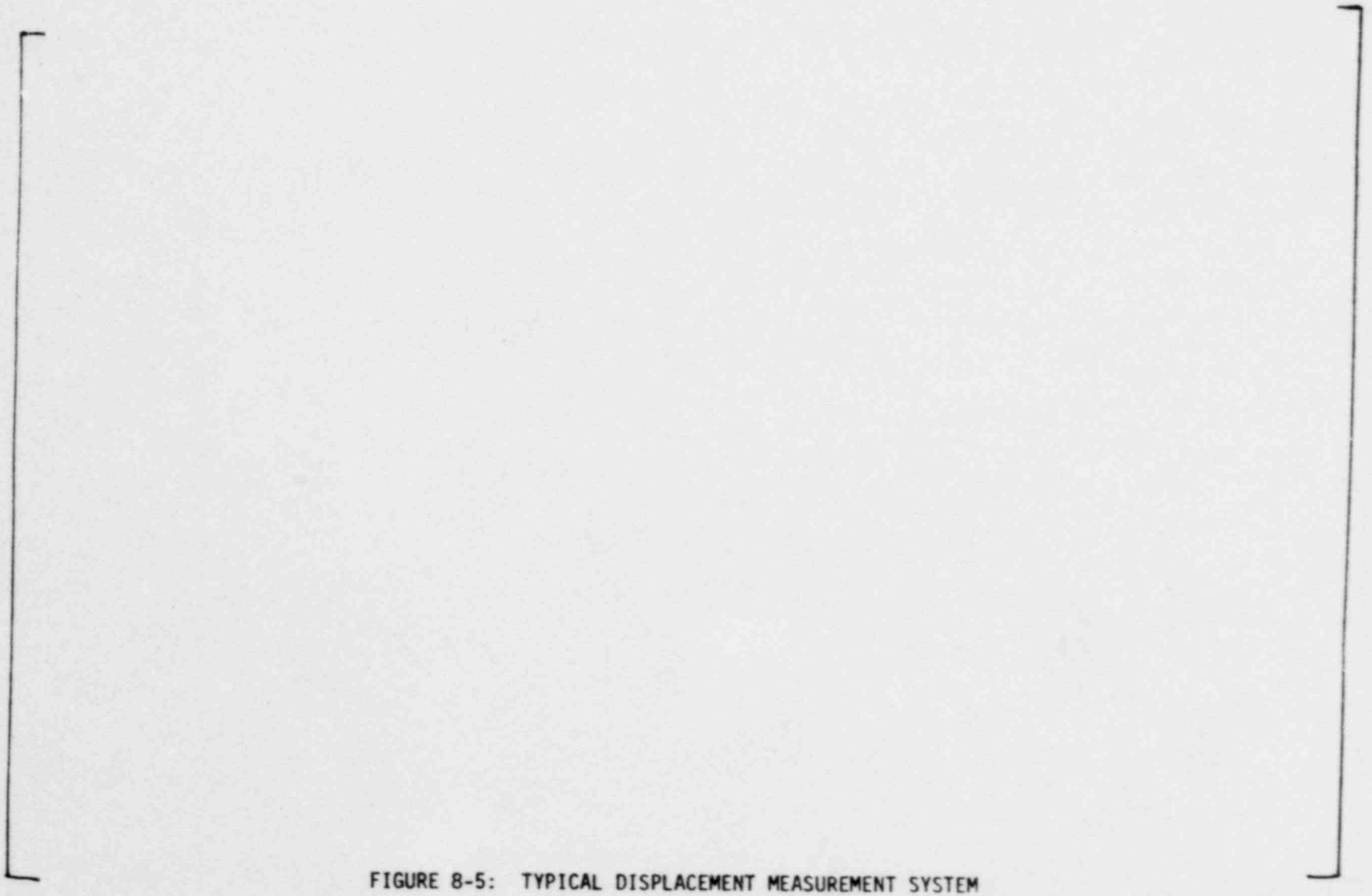

FIGURE 8-5: TYPICAL DISPLACEMENT MEASUREMENT SYSTEM

FIGURE 8-6: TYPICAL FLOW MEASUREMENT SYSTEM

FIGURE 8-7: FORMAT FOR TEMPERATURE VERSUS TIME PLOTS

a,b,c

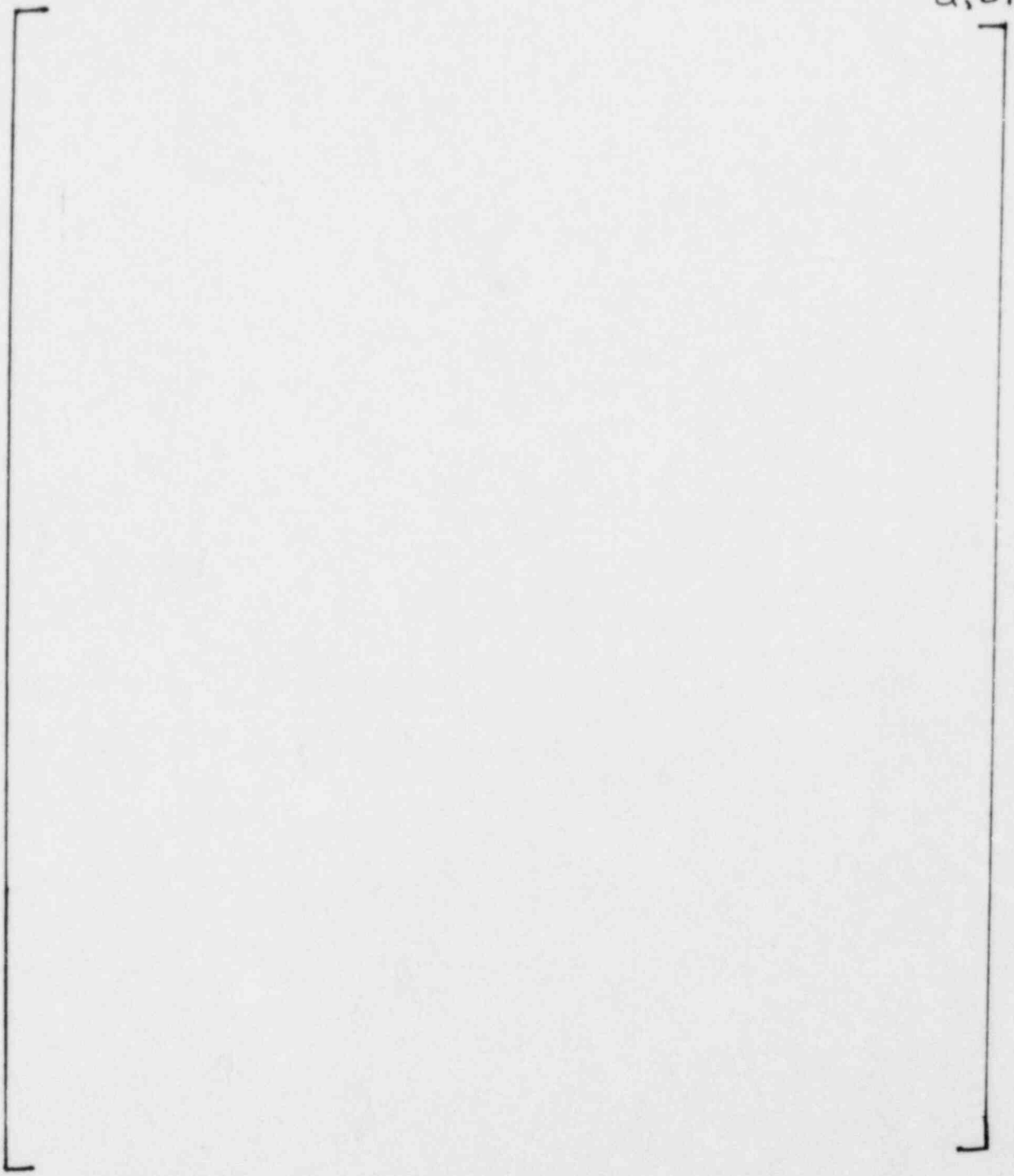

FIGURE 8-8: FORMAT FOR PLOTS OF TEMPERATURE PROFILE ACROSS THE PIPE CROSS-SECTION

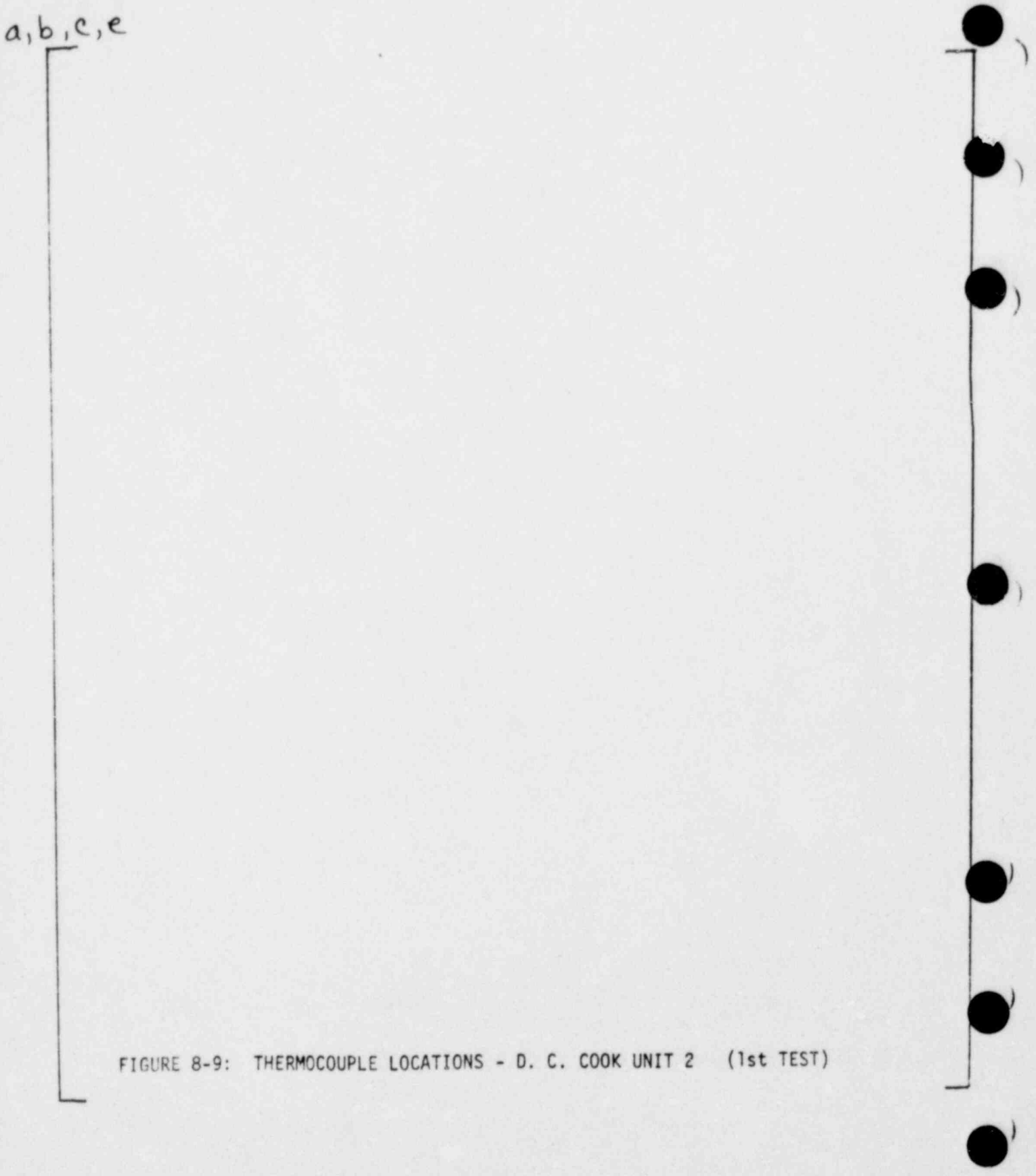

FIGURE 8-9: THERMOCOUPLE LOCATIONS - D. C. COOK UNIT 2 (1st TEST)

a,b,c,e

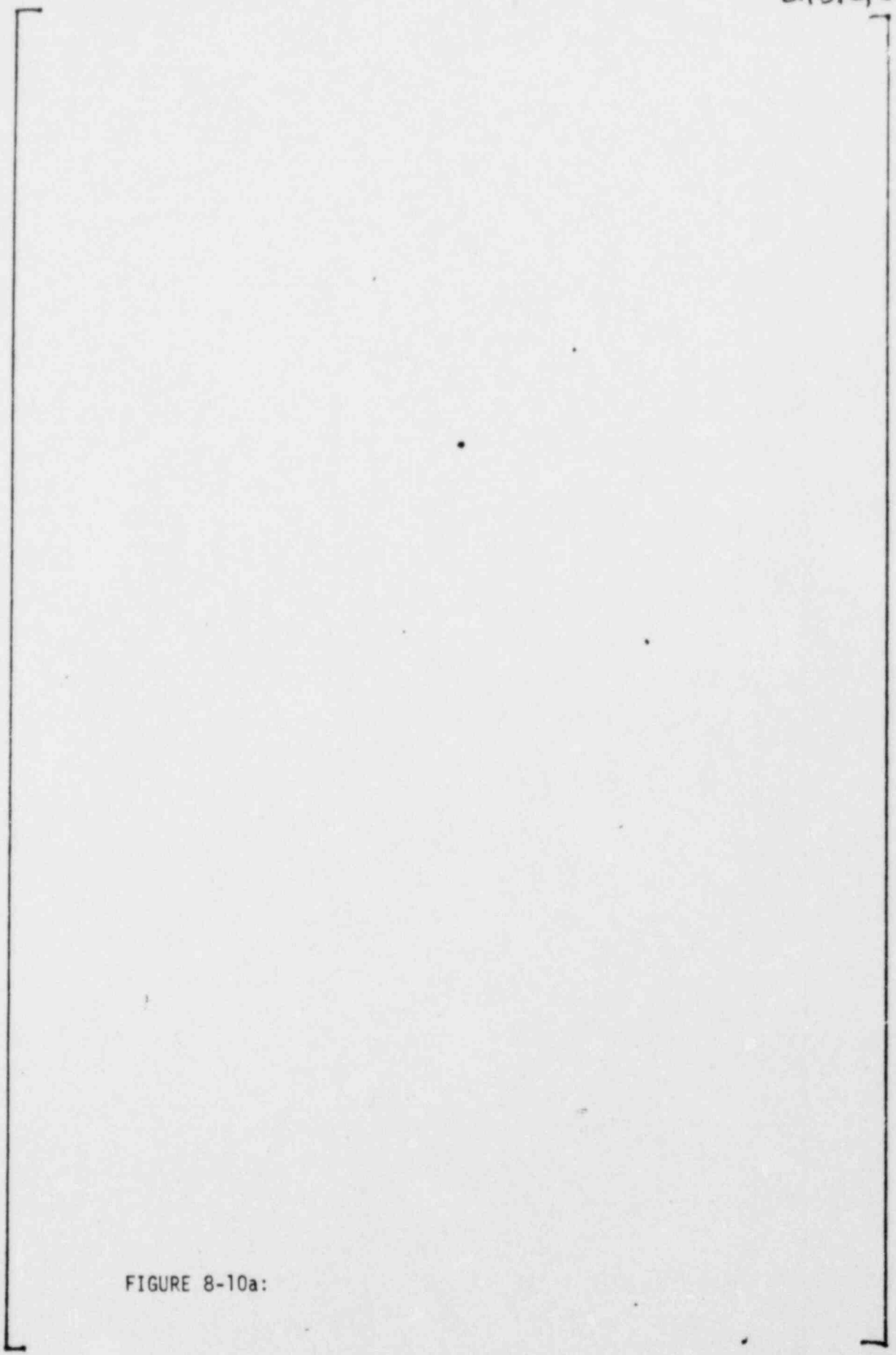

FIGURE 8-10a:

a,b,c,e

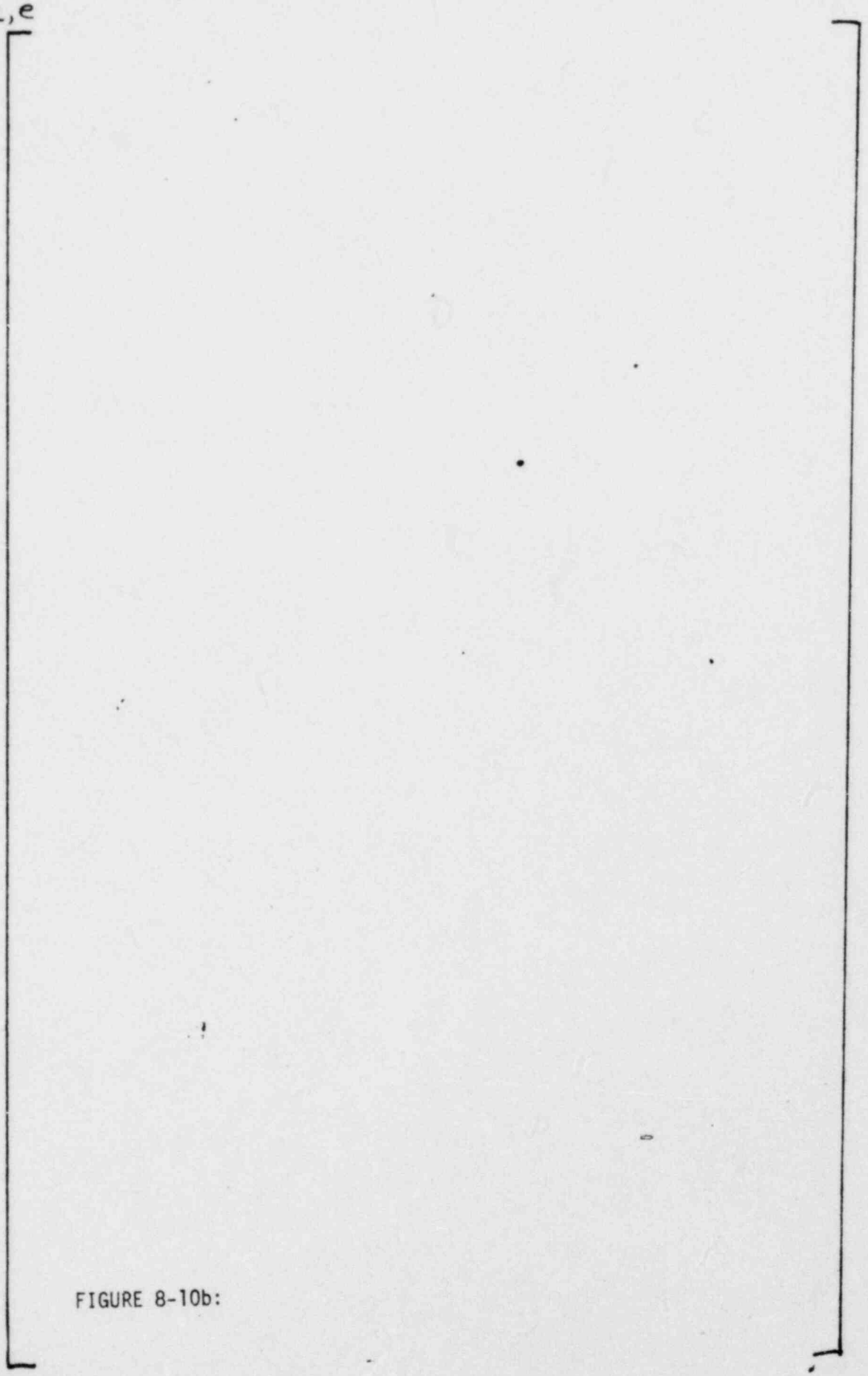

FIGURE 8-10b:

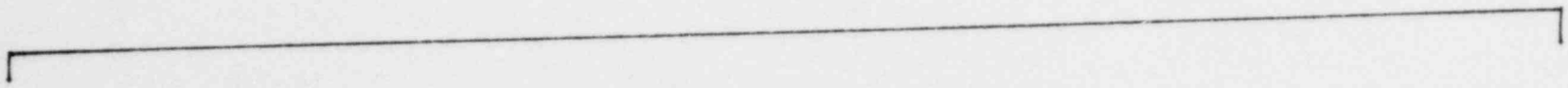

a, b, c, e

16,292-1

Figure 8-11.

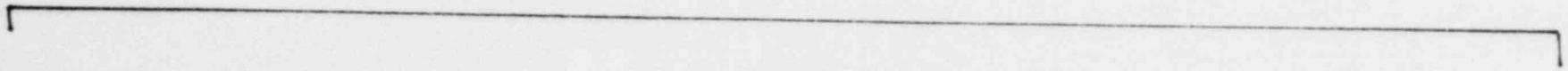

a.b.c.c

16,292-2

Figure 8-12

a, b, c, e

16,292-3

Figure 8-13.

a,b,c,e

16,292-4

Figure 8-14.

a,b,c,e

16,292-5

Figure 8-15.

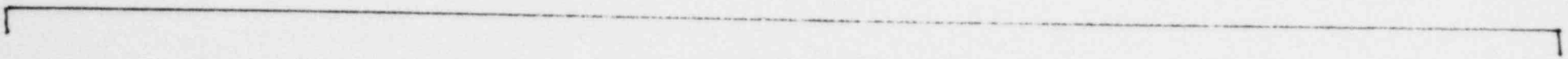

a,b,c,e

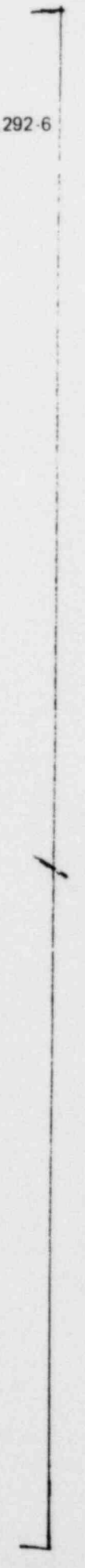

Figure 8-16.

a,b,c,e

16,292-7

Figure 8-17.

a,b,c,e

FIGURE 8-18:

a,b,c,e

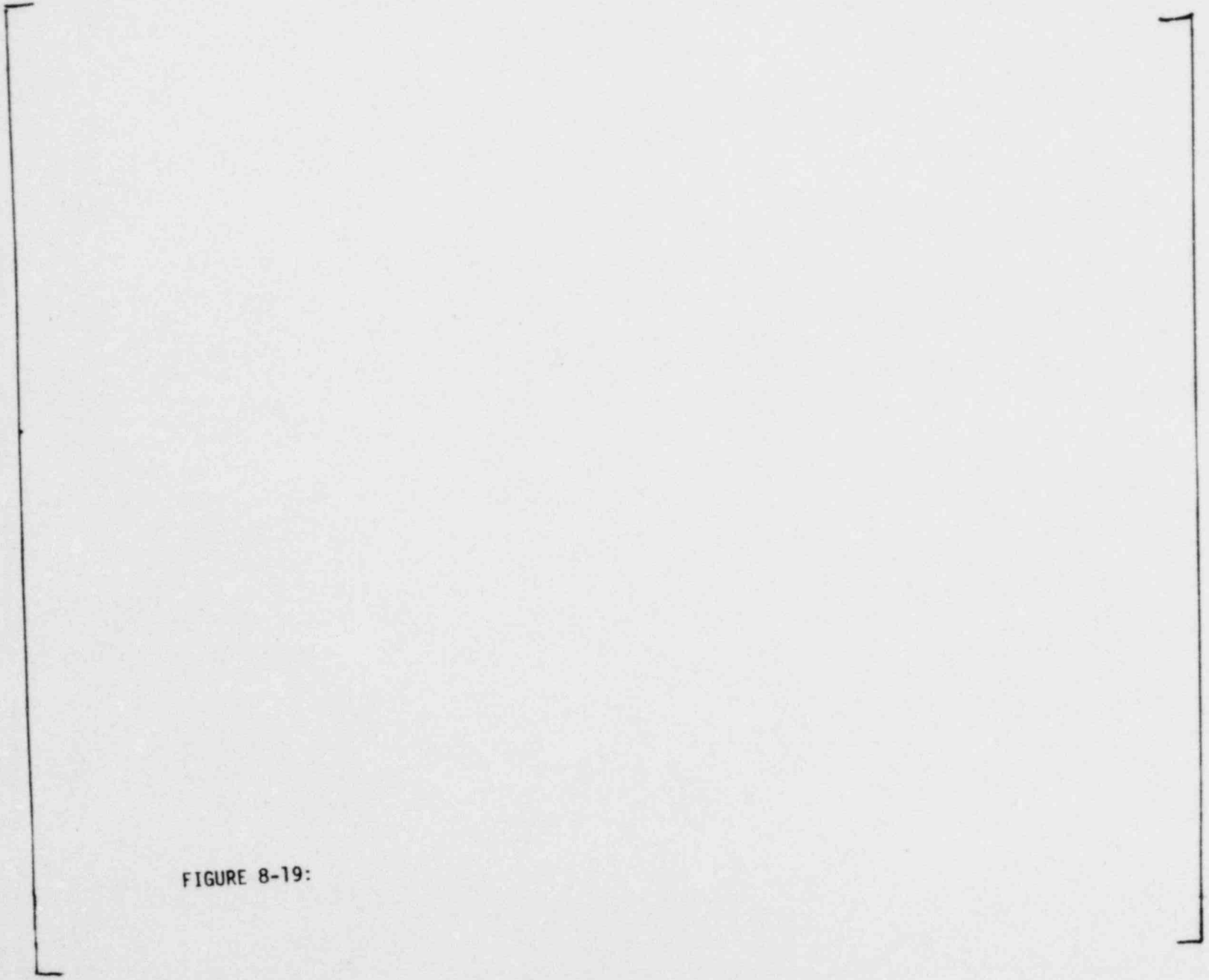

FIGURE 8-19:

FIGURE 8-20:

a,b,c,e

a,b,c,e

FIGURE 8-21:

a,b,c,e

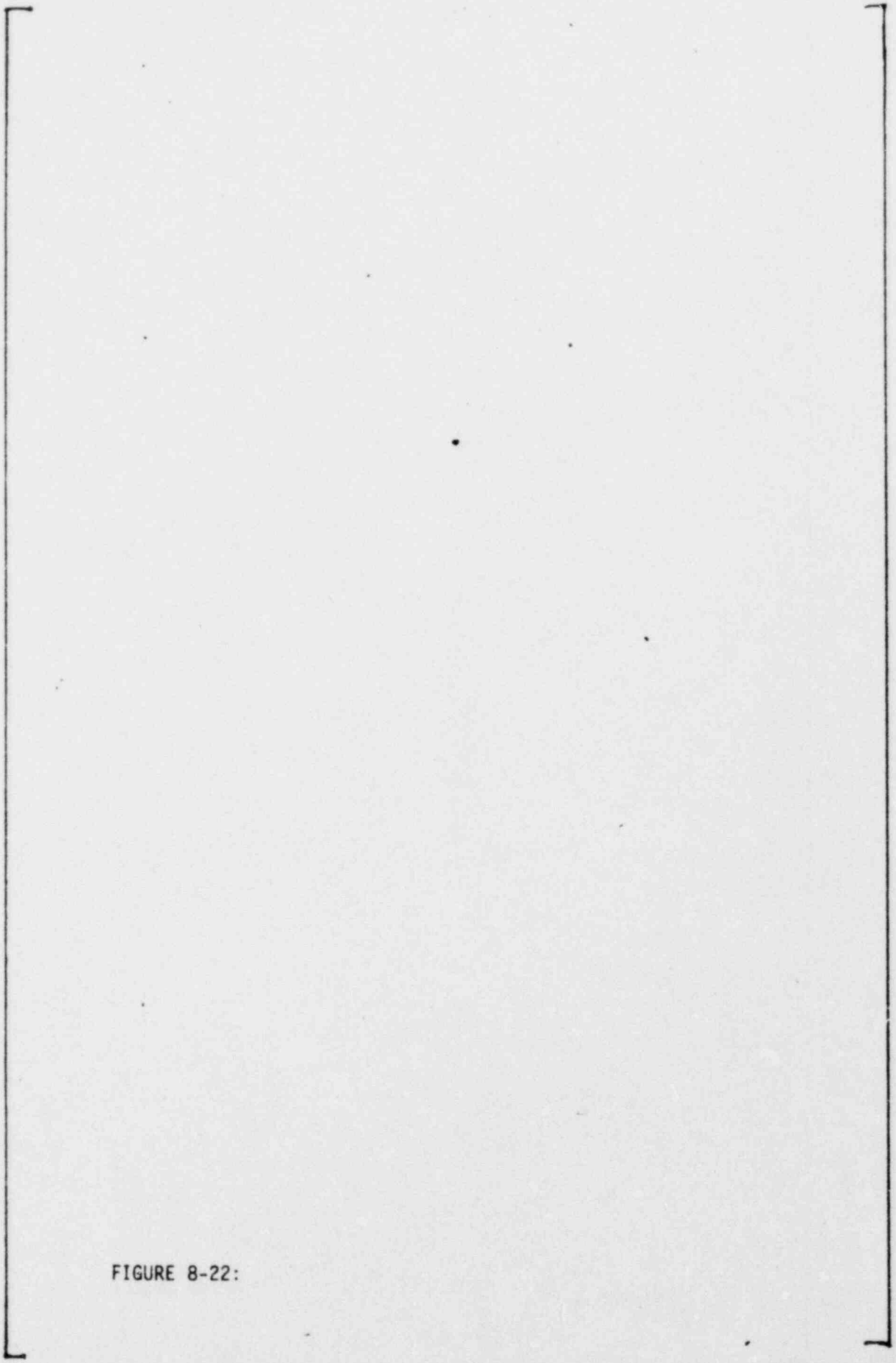

FIGURE 8-22:

a,b,c,e

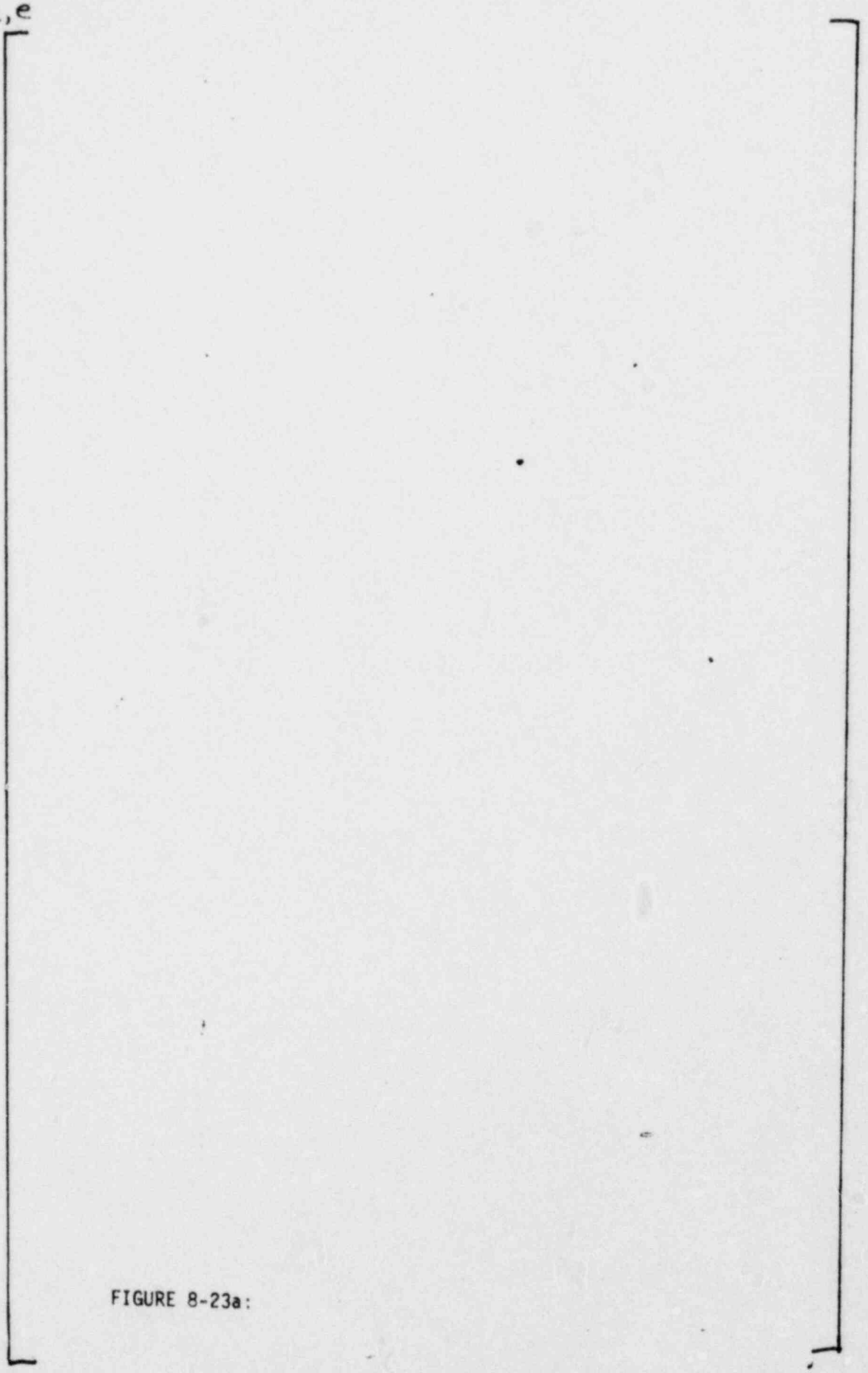

FIGURE 8-23a:

a,b,c,e

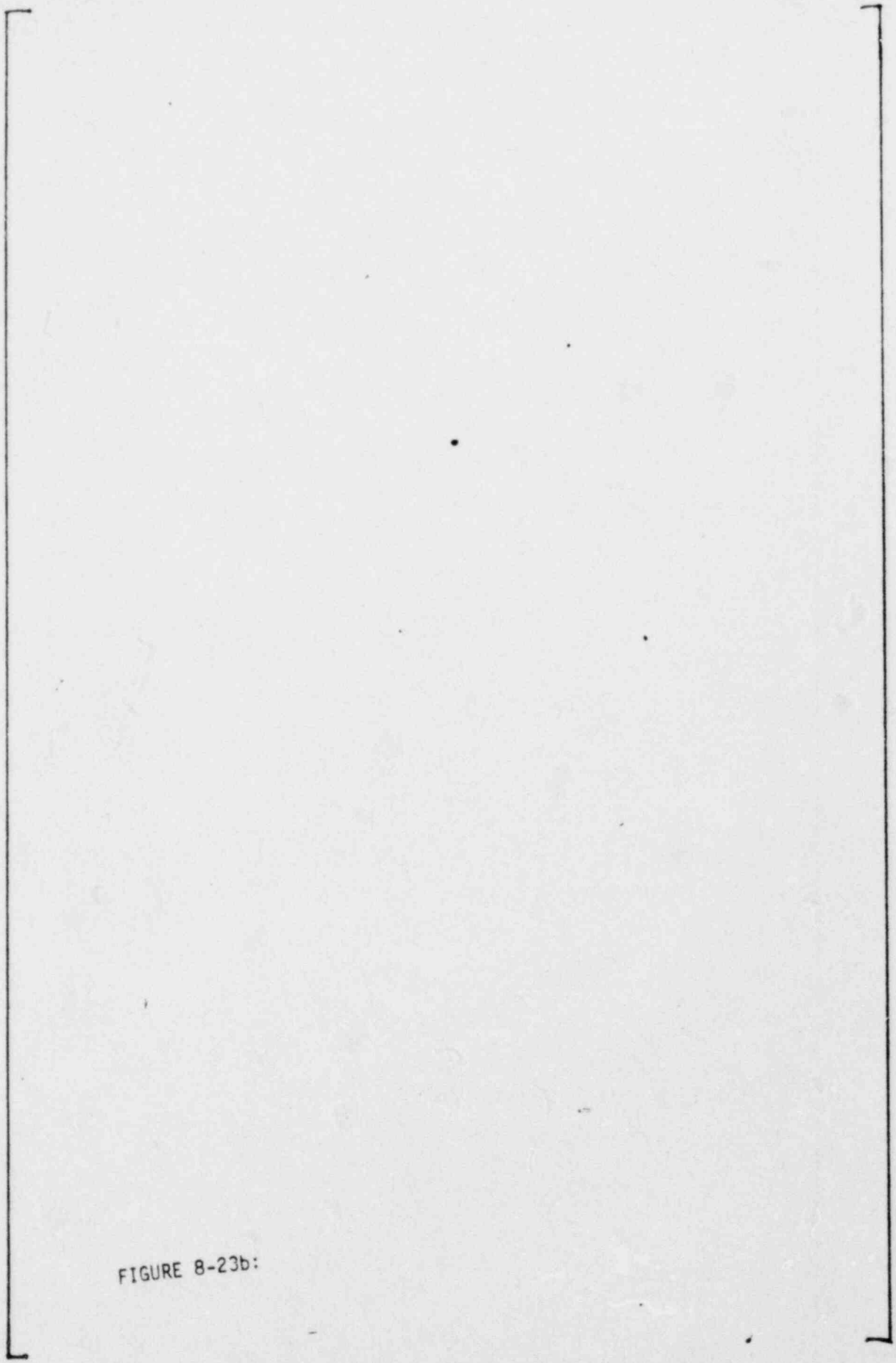

FIGURE 8-23b:

a,b,c,e

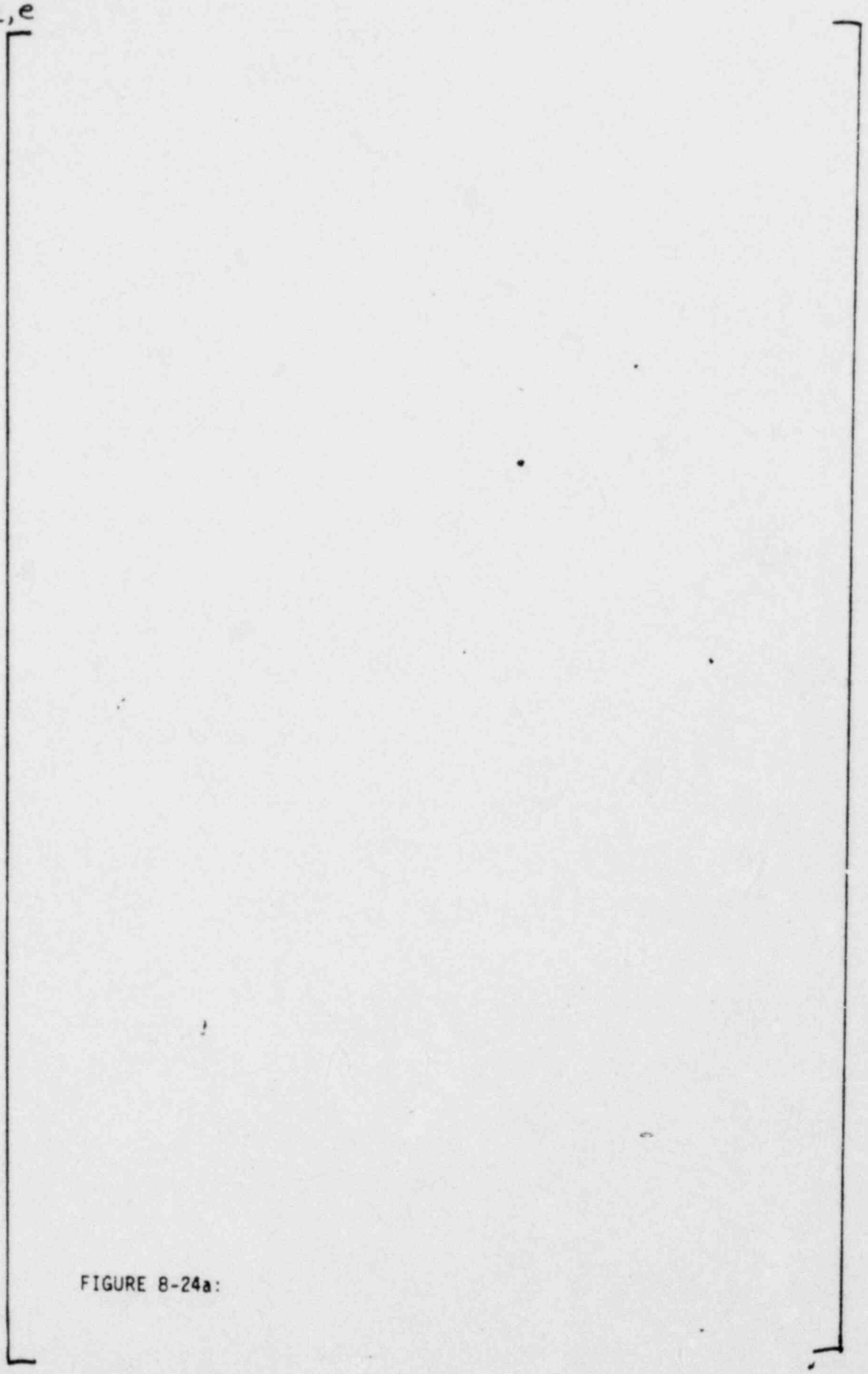

FIGURE 8-24a:

a,b,c,e

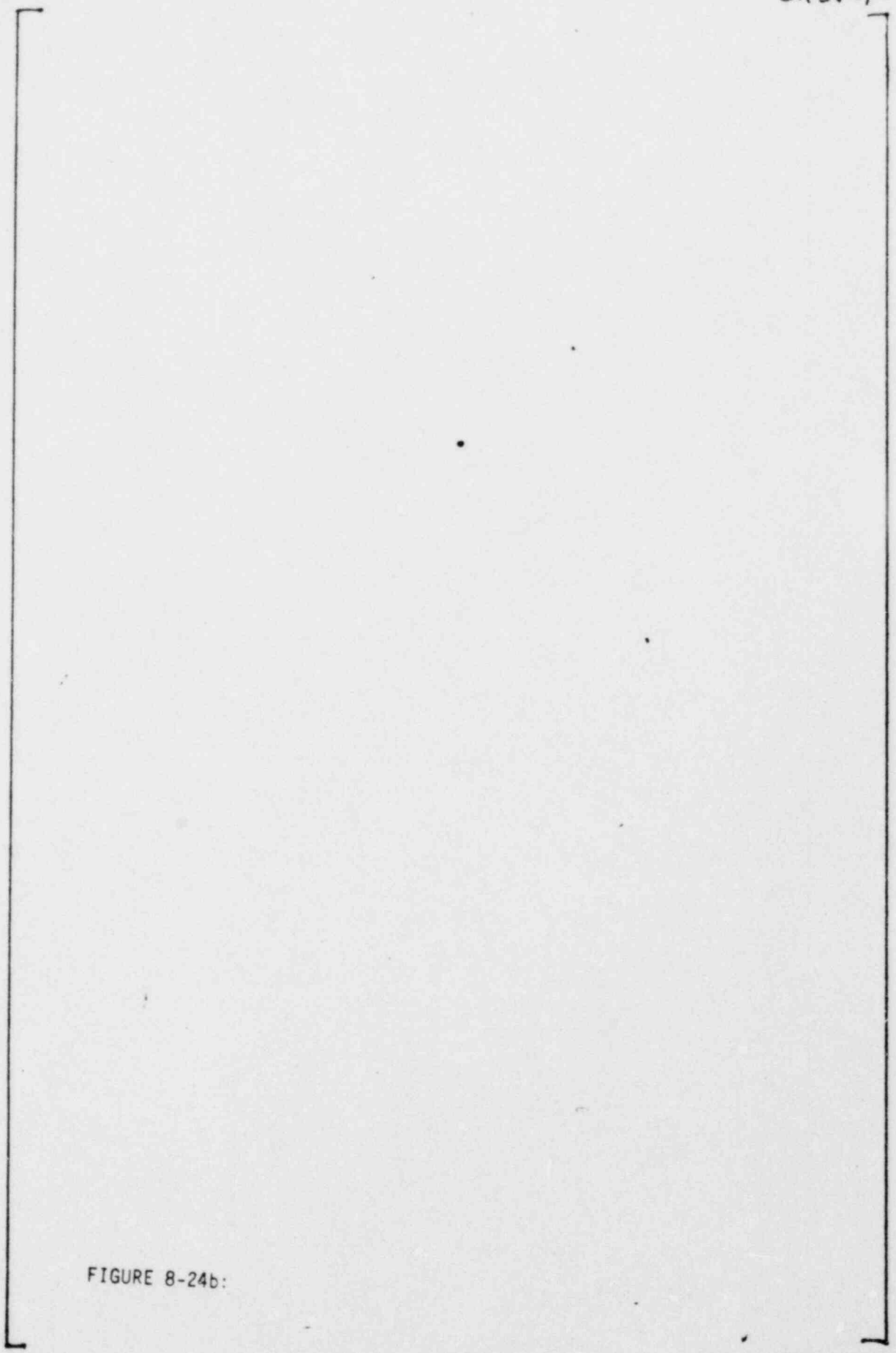

FIGURE 8-24b:

a,b,c,e

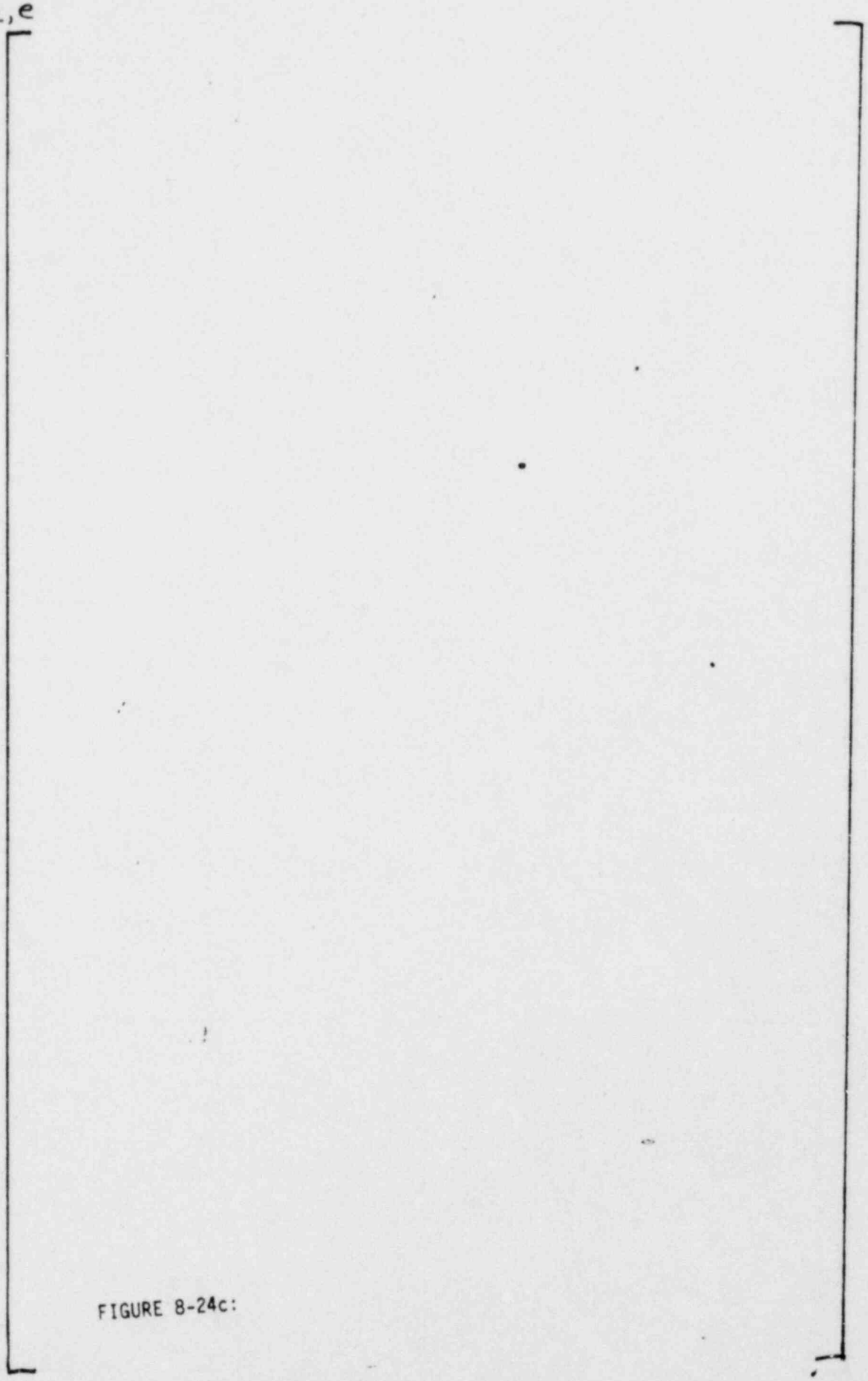

FIGURE 8-24c:

a,b,c,e

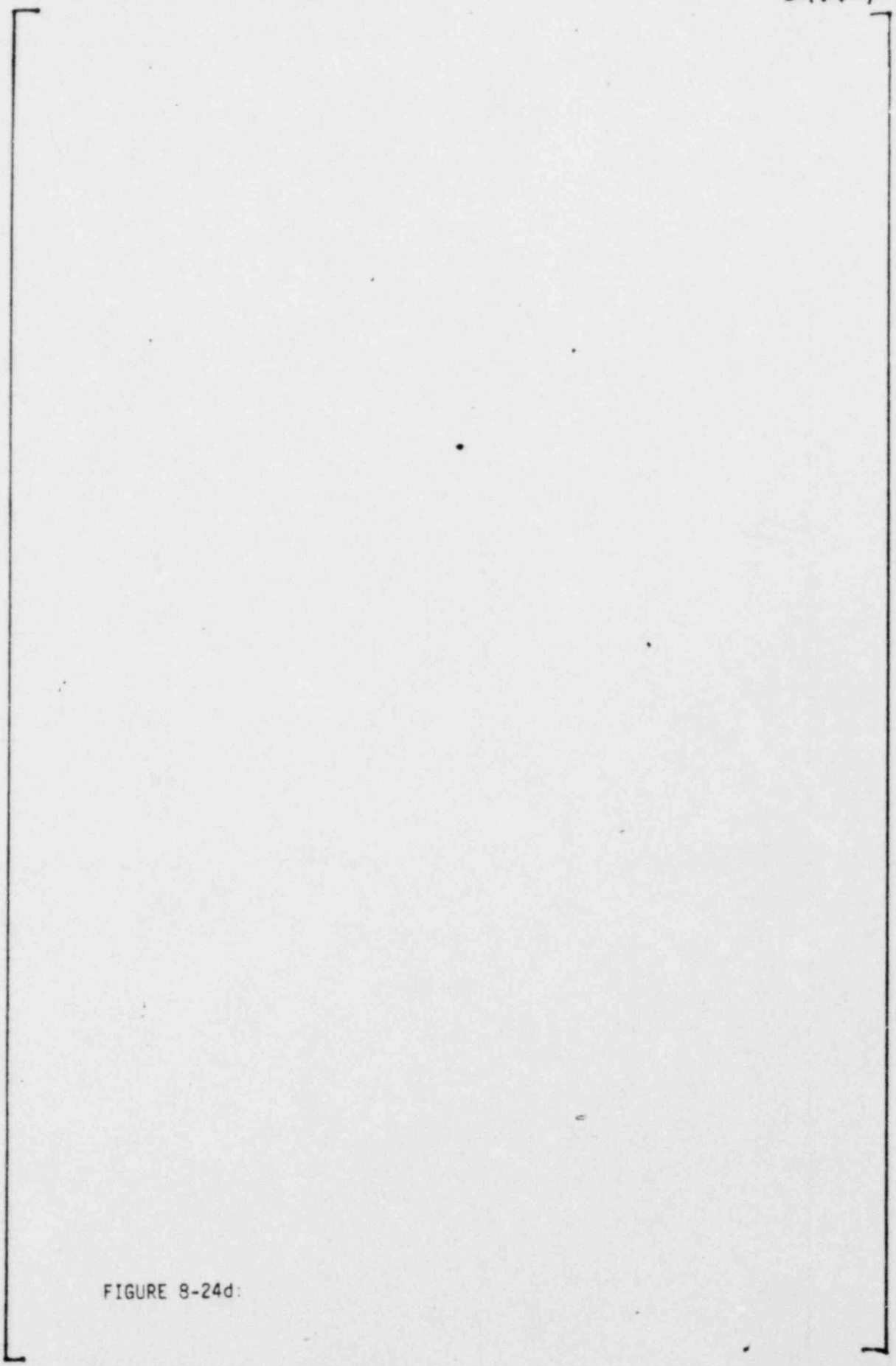

FIGURE 8-24d:

a,b,c,e

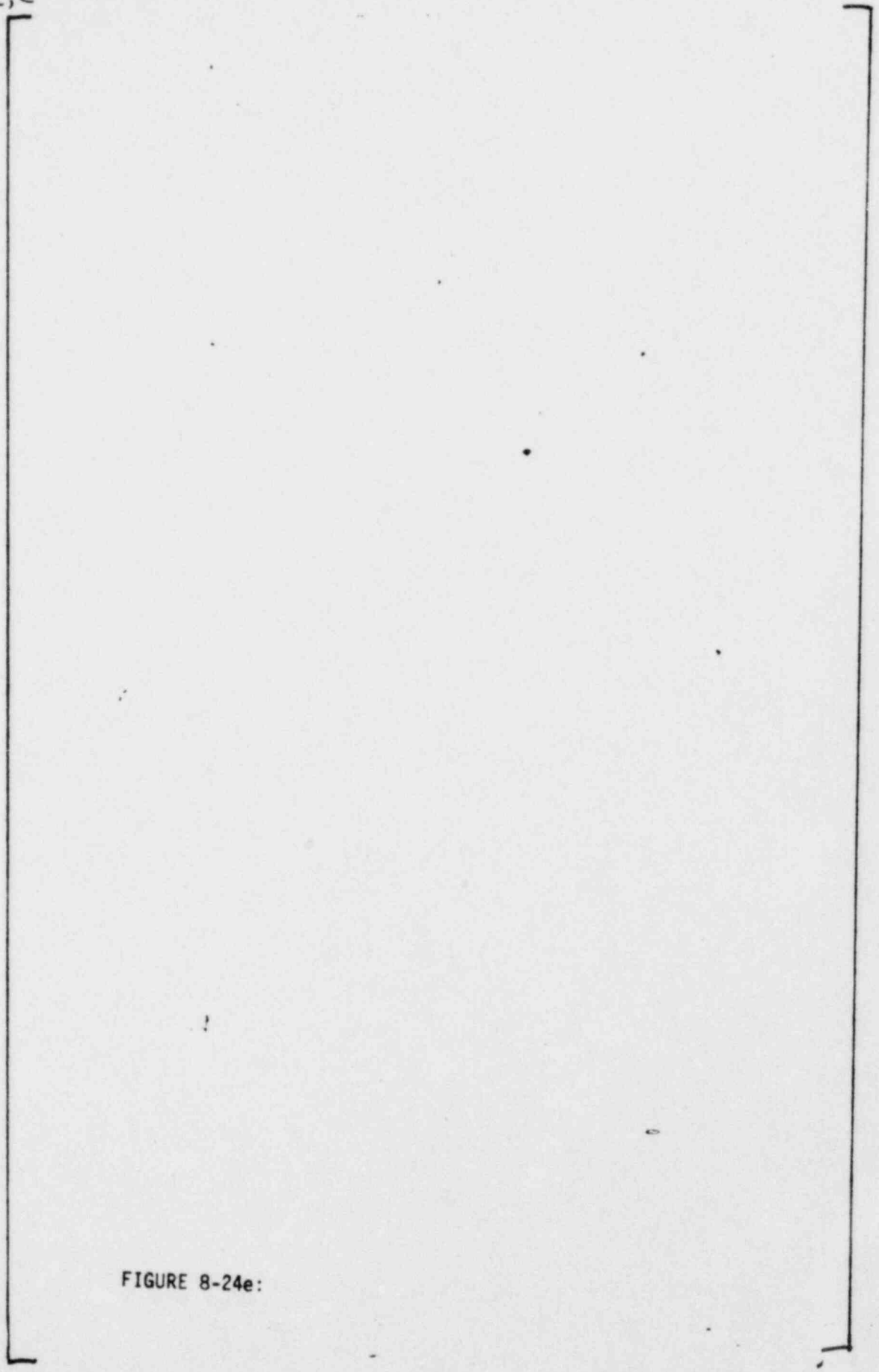

FIGURE 8-24e:

a,b,c,e

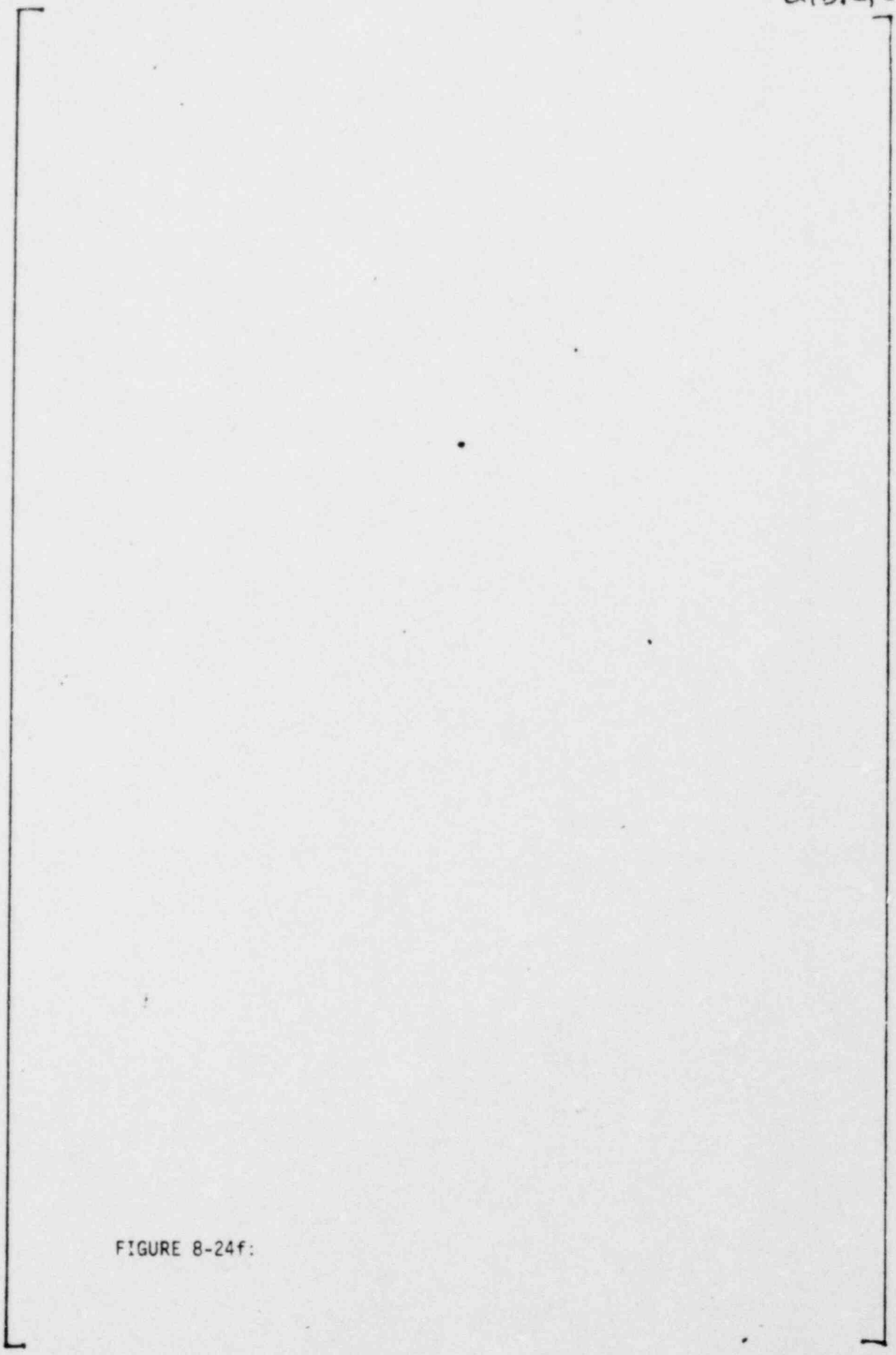

FIGURE 8-24f:

a,b,c,e

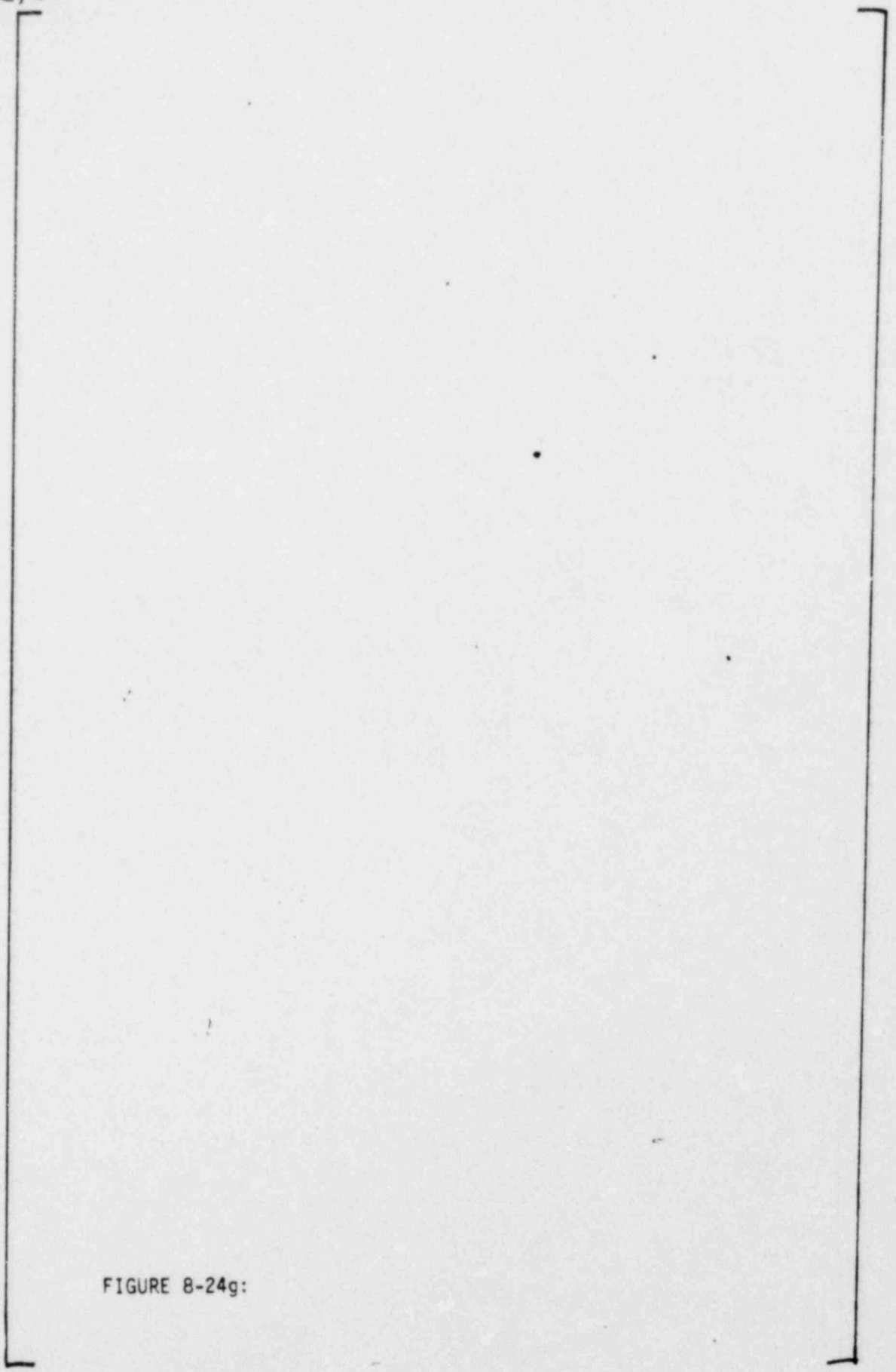

FIGURE 8-24g:

a,b,c,e

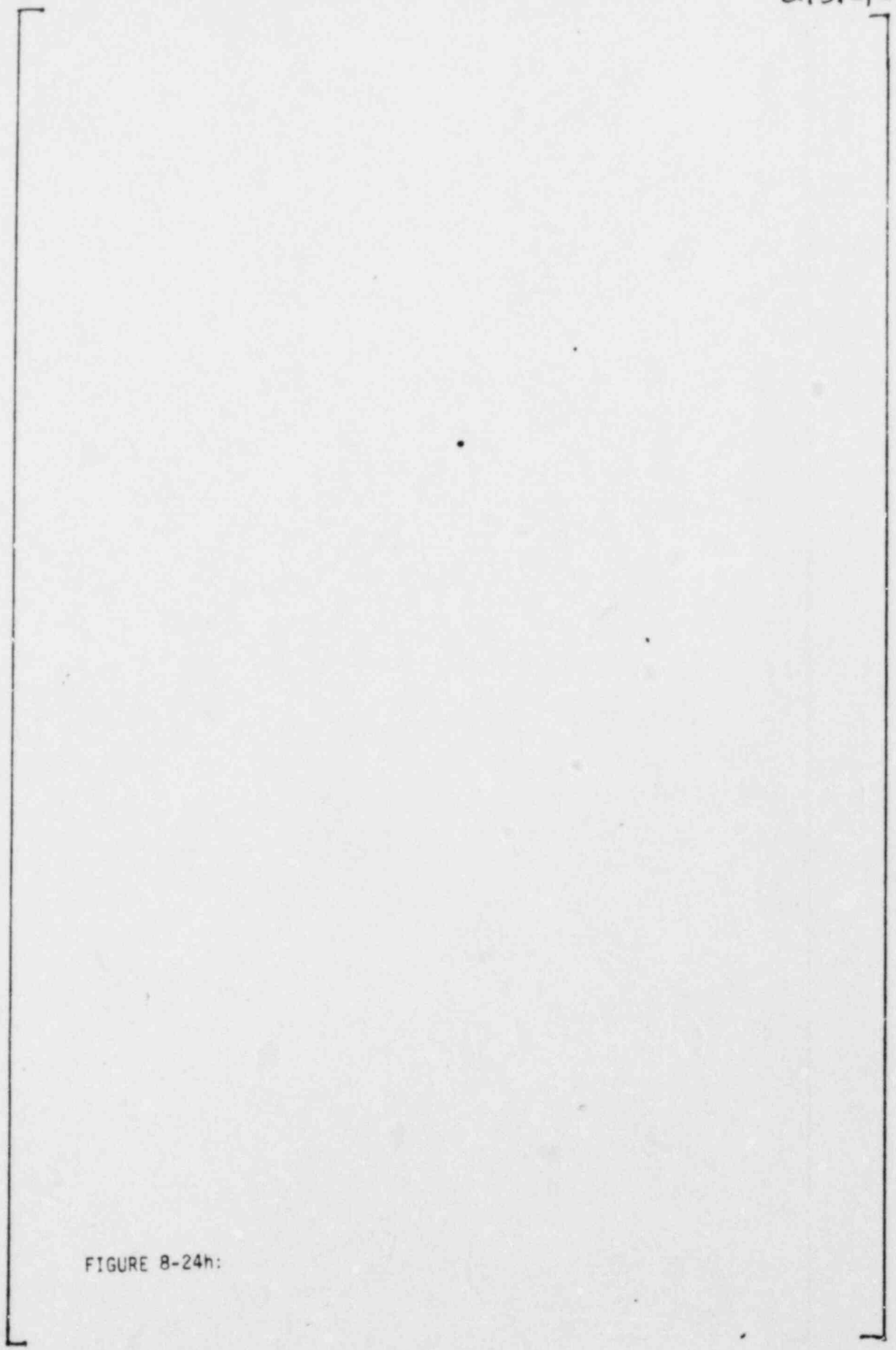

FIGURE 8-24h:

a,b,c,e

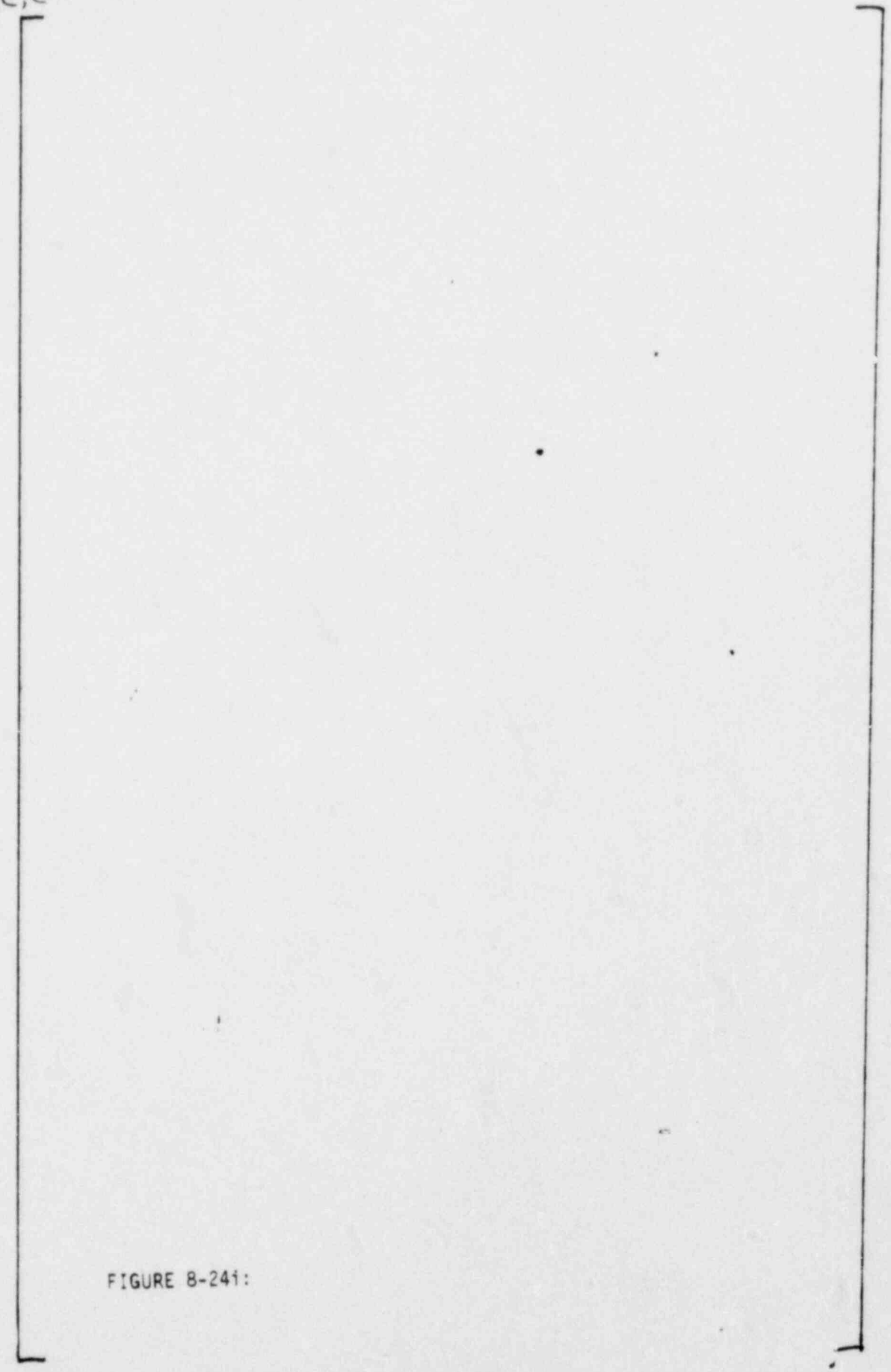

FIGURE 8-24i:

a,b,c,e

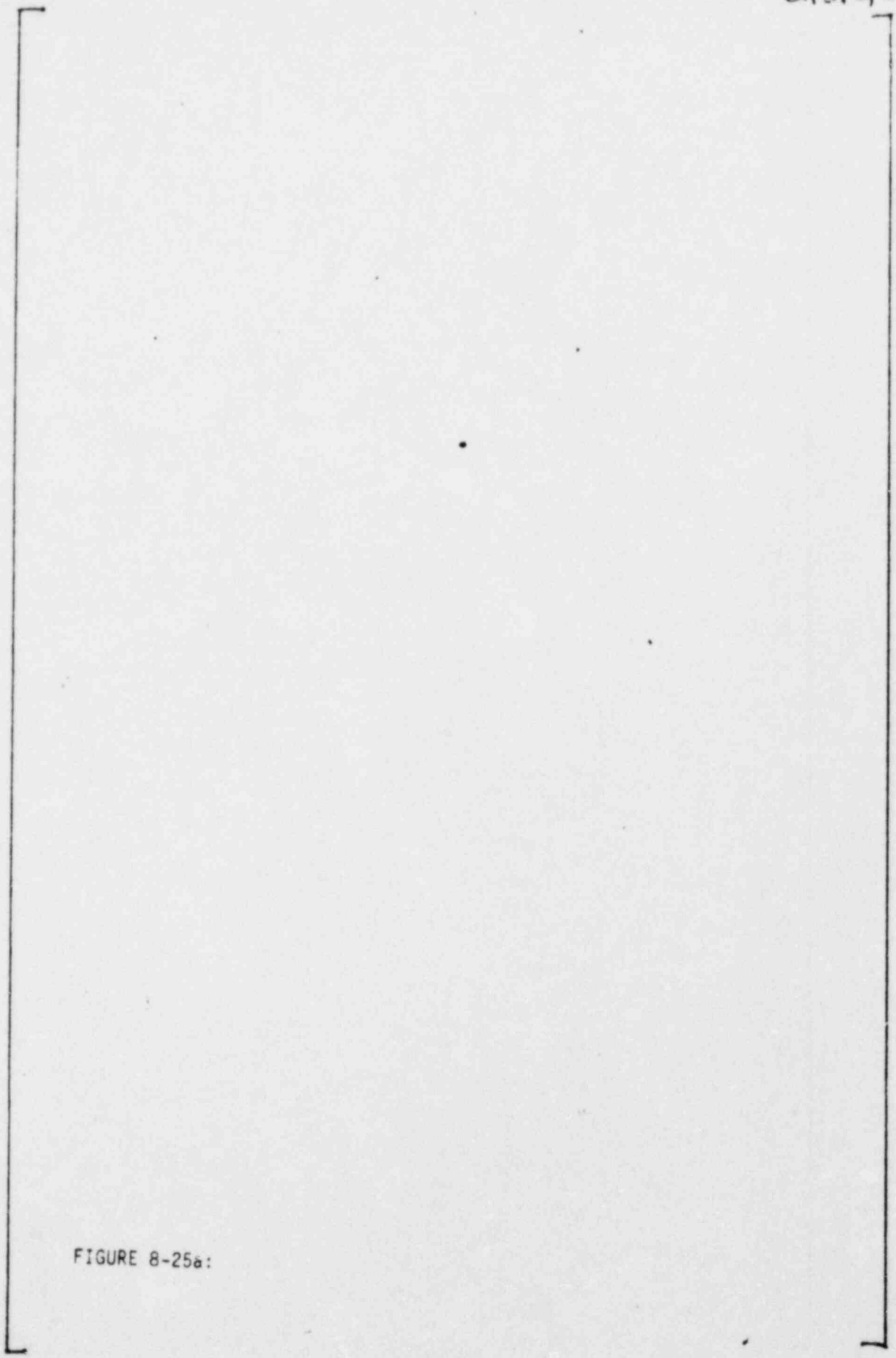

FIGURE 8-25a:

a,b,c,e

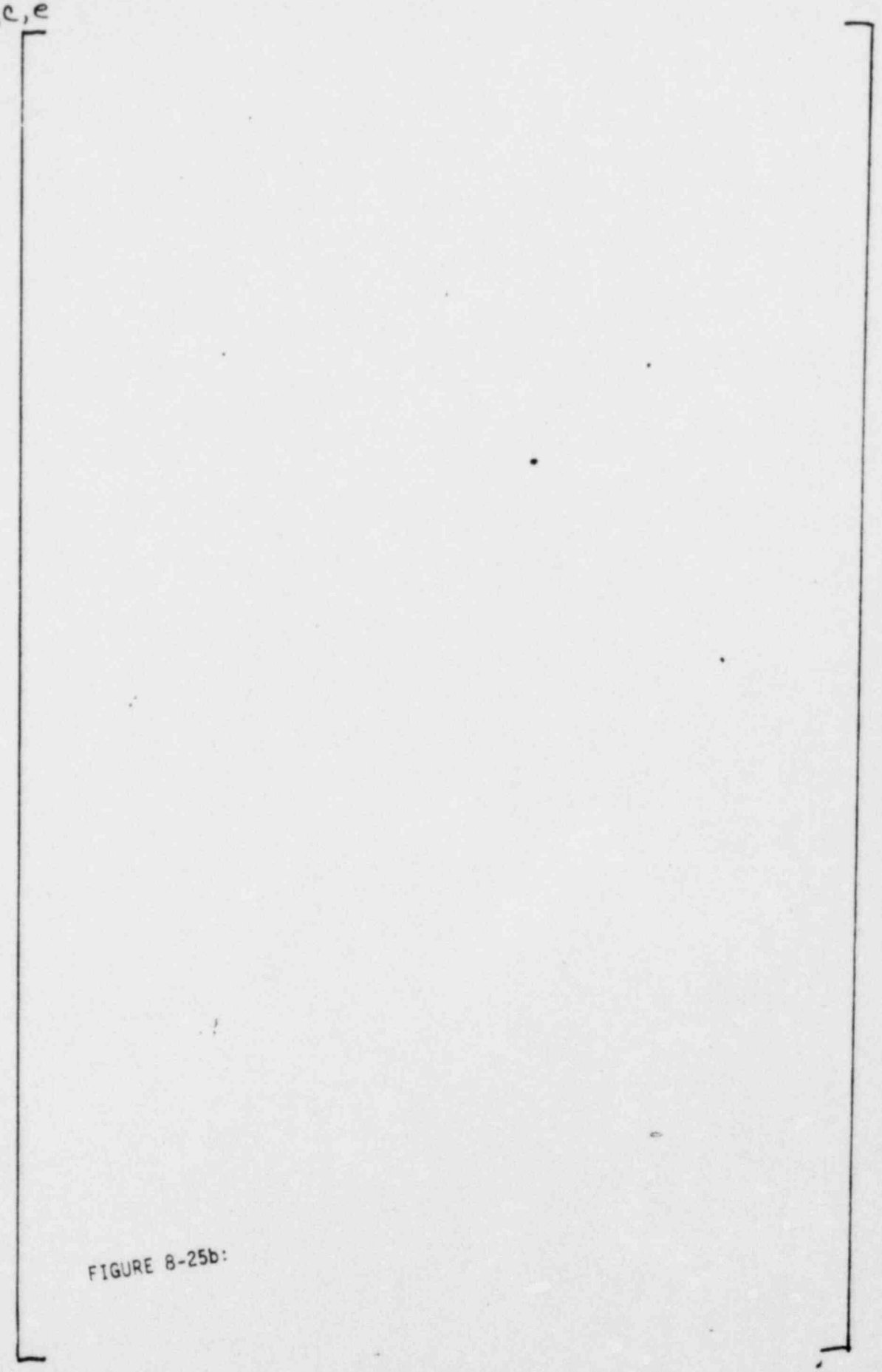

FIGURE 8-25b:

a,b,c,e

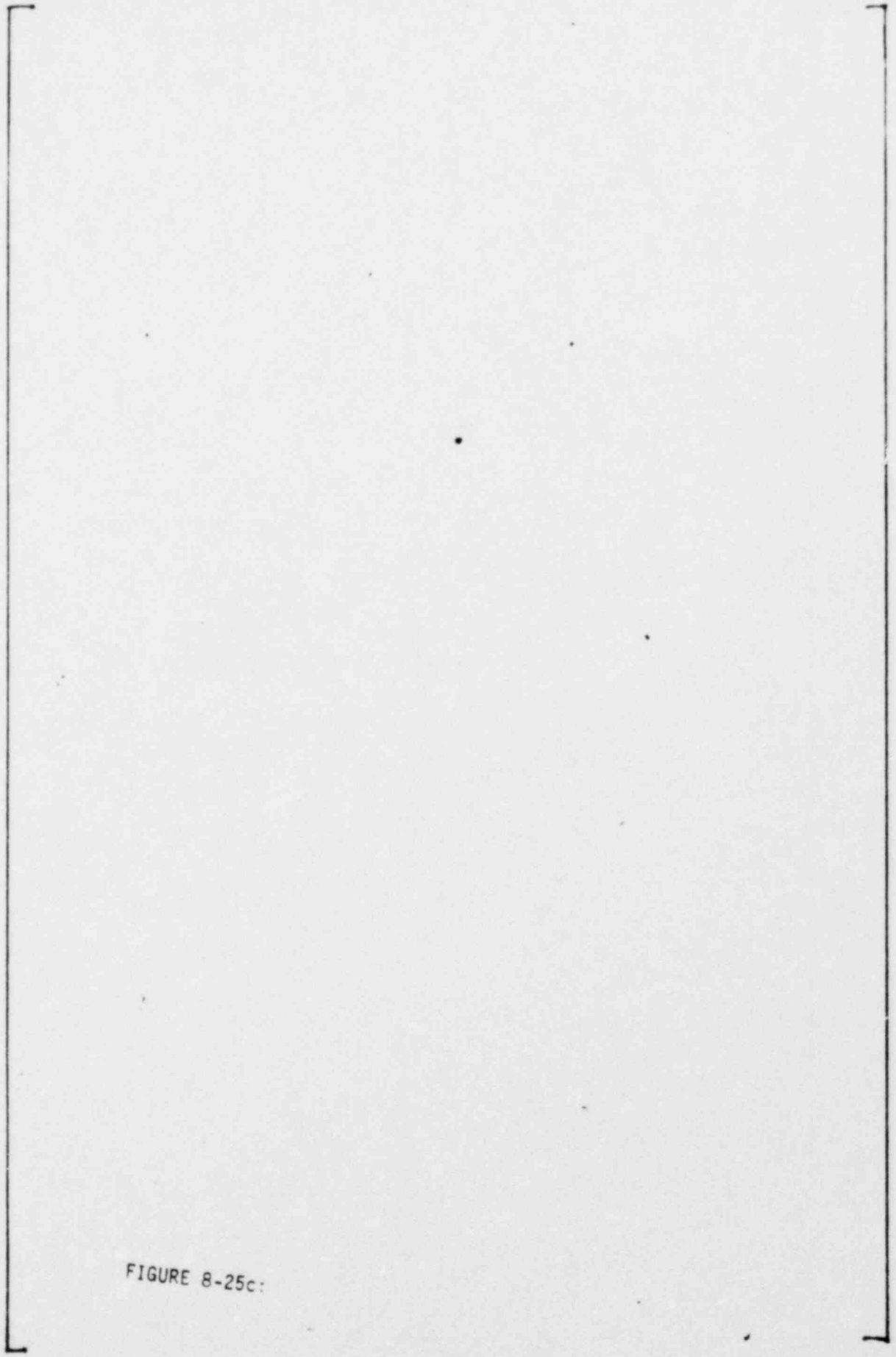

FIGURE 8-25c:

a,b,c,e

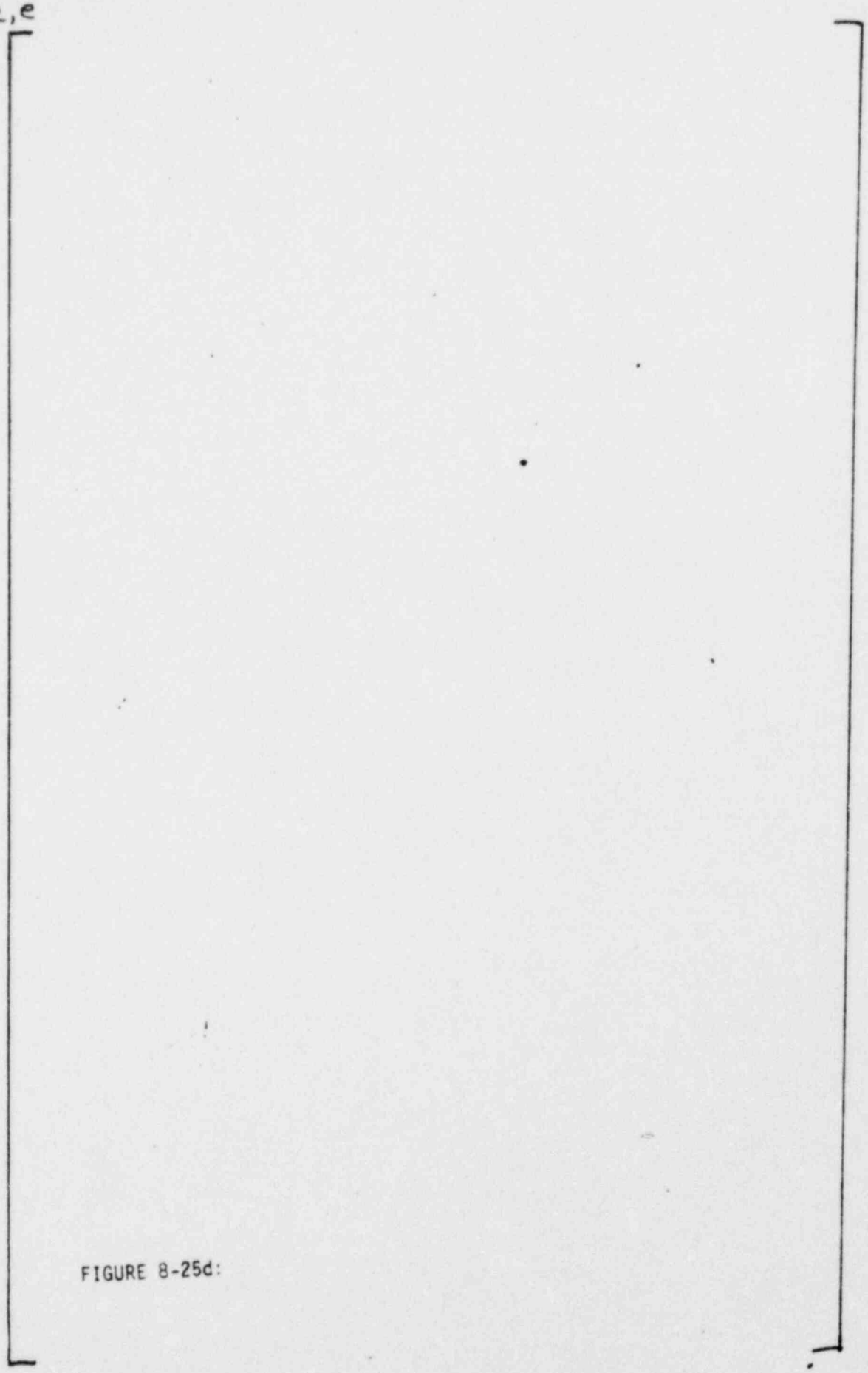

FIGURE 8-25d:

a,b,c,e

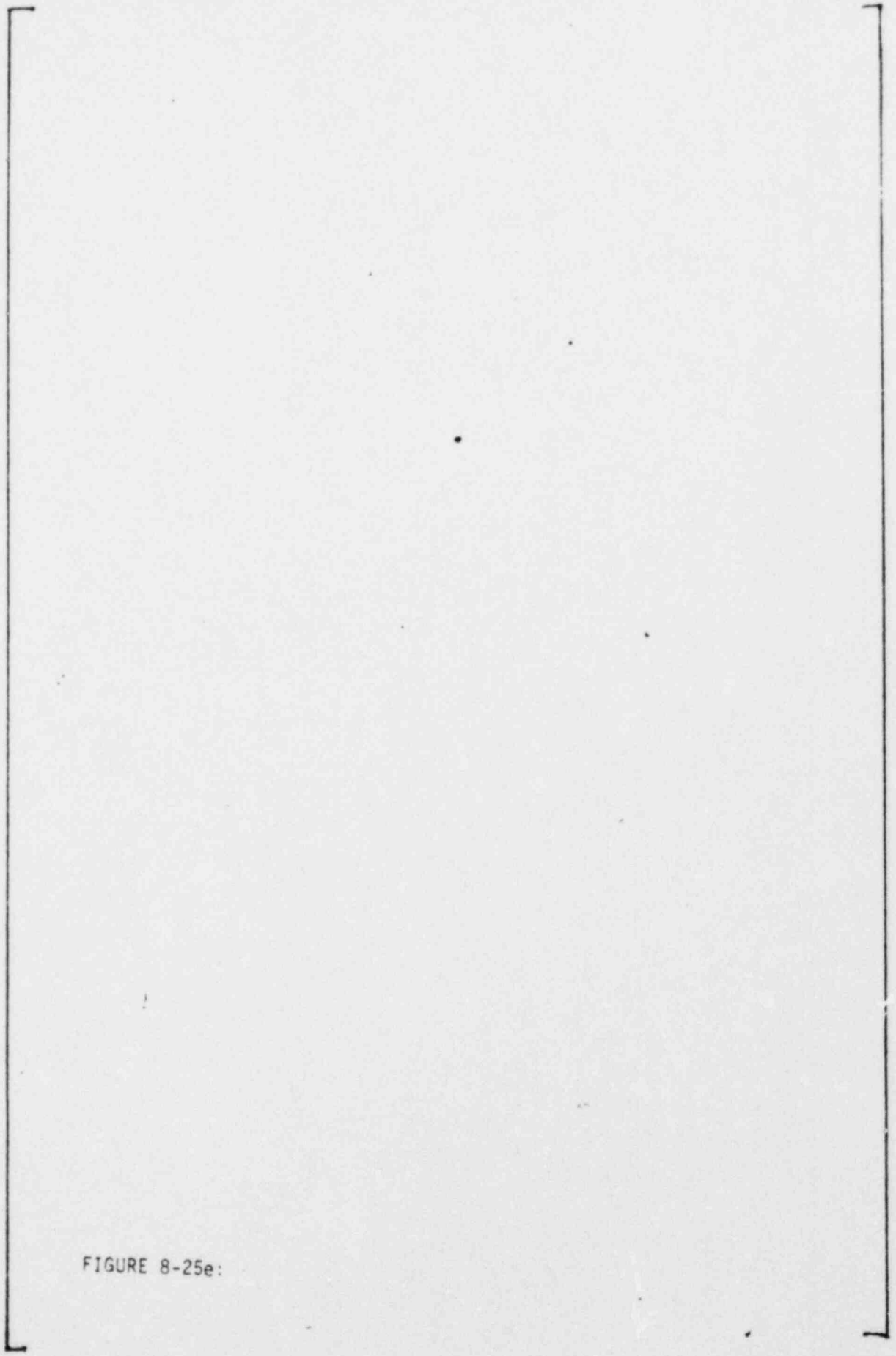

FIGURE 8-25e:

a,b,c,e

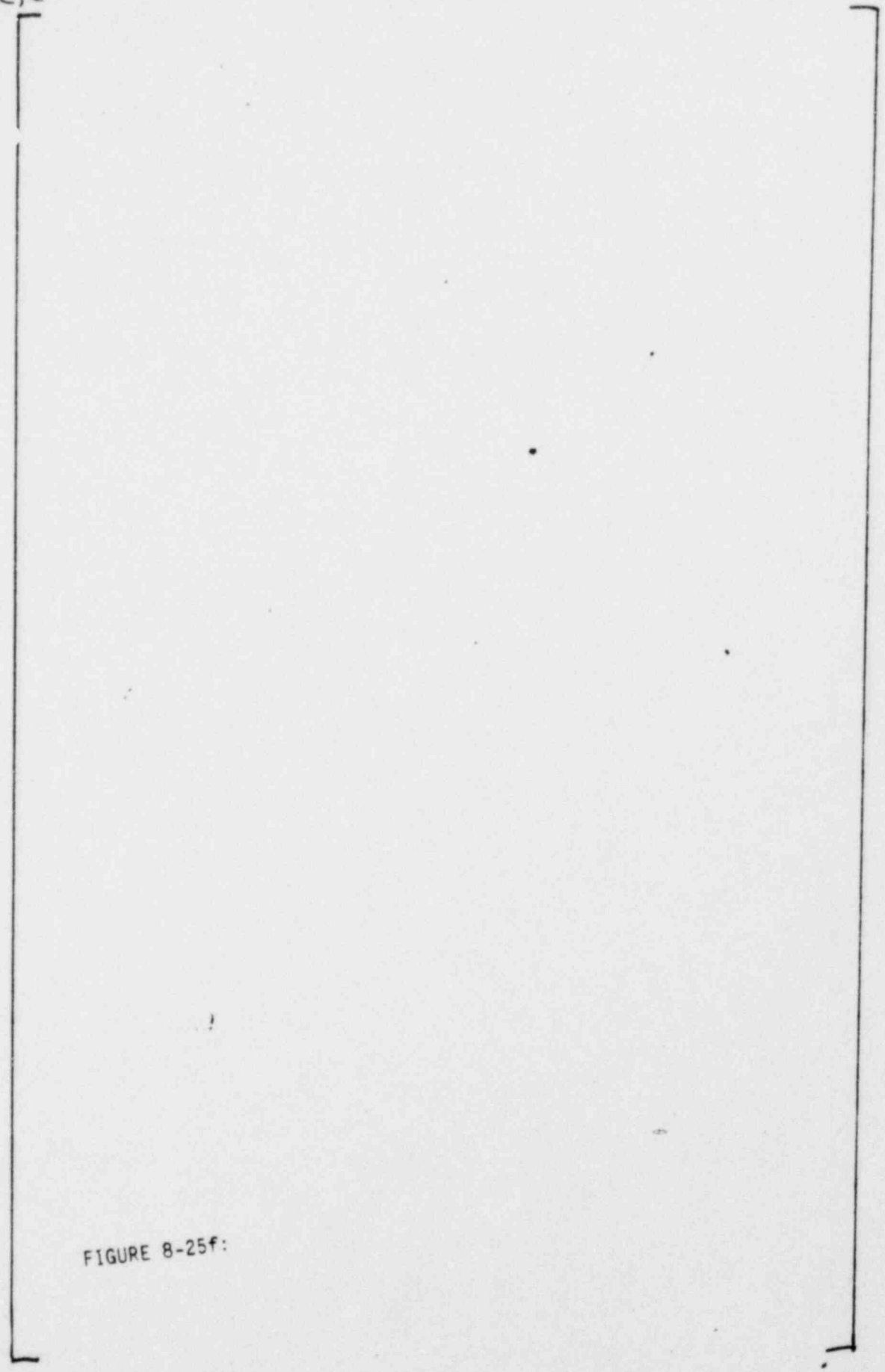

FIGURE 8-25f:

a,b,c,e

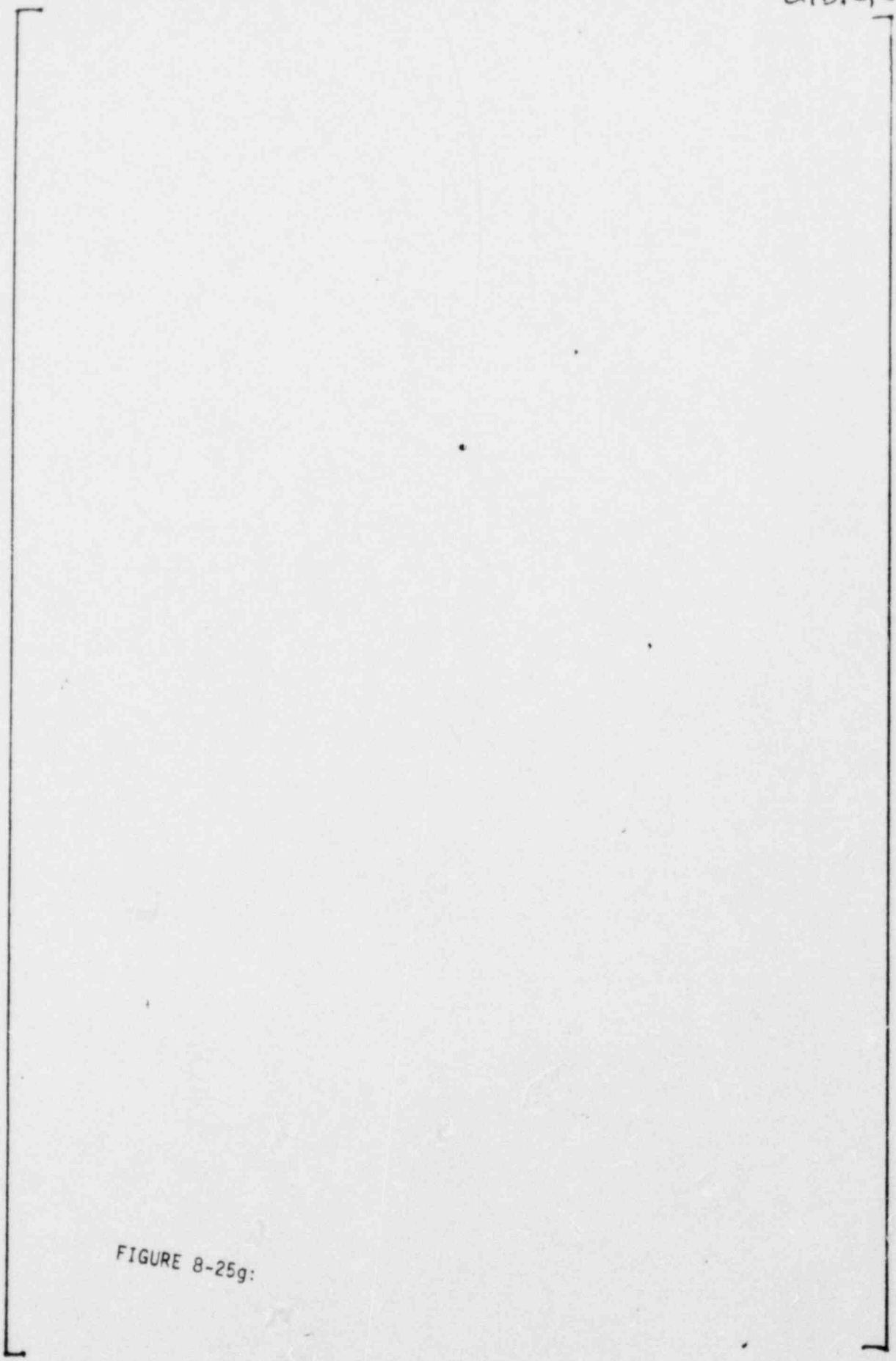

FIGURE 8-25g:

a,b,c,e

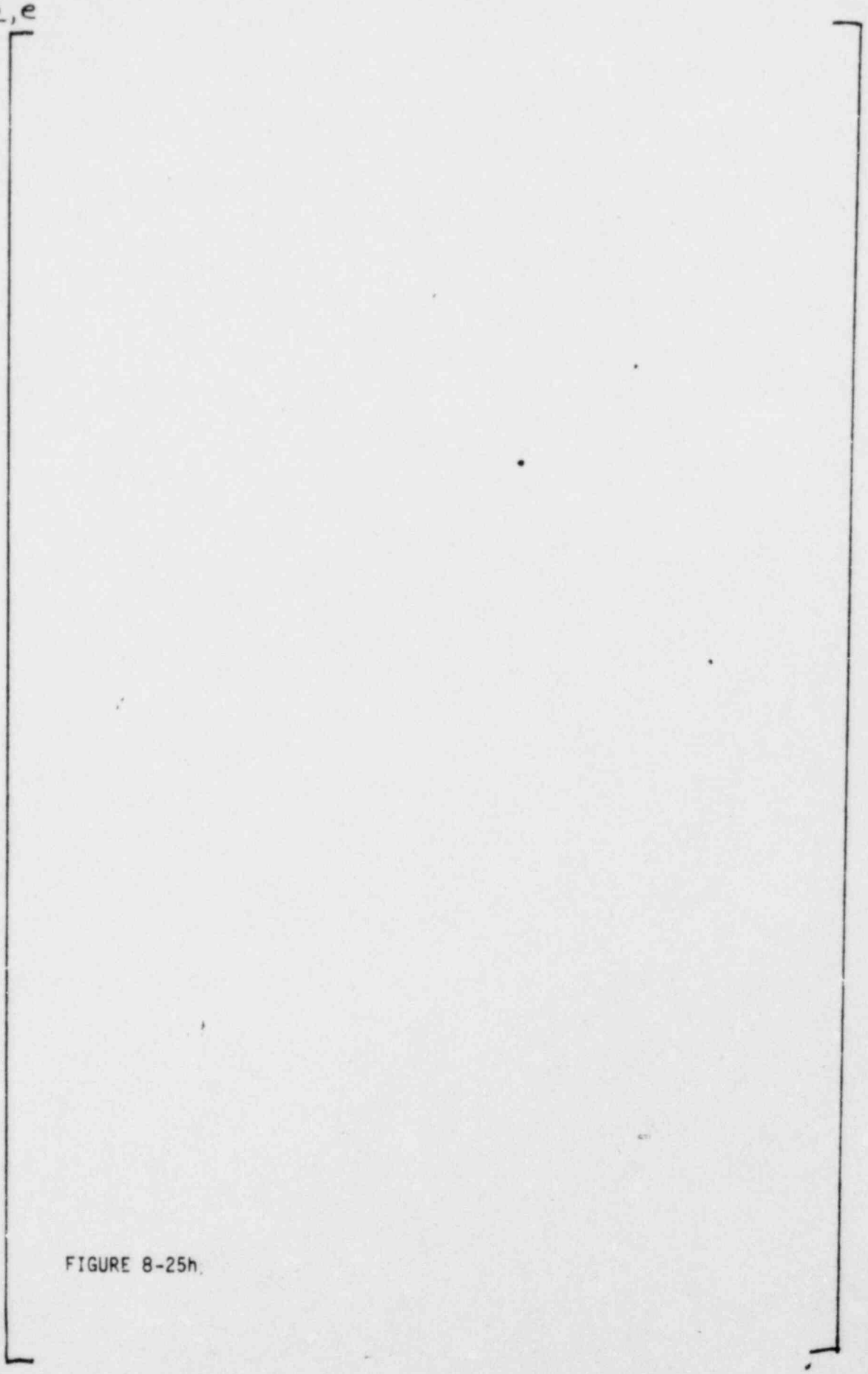

FIGURE 8-25h

a,b,c,e

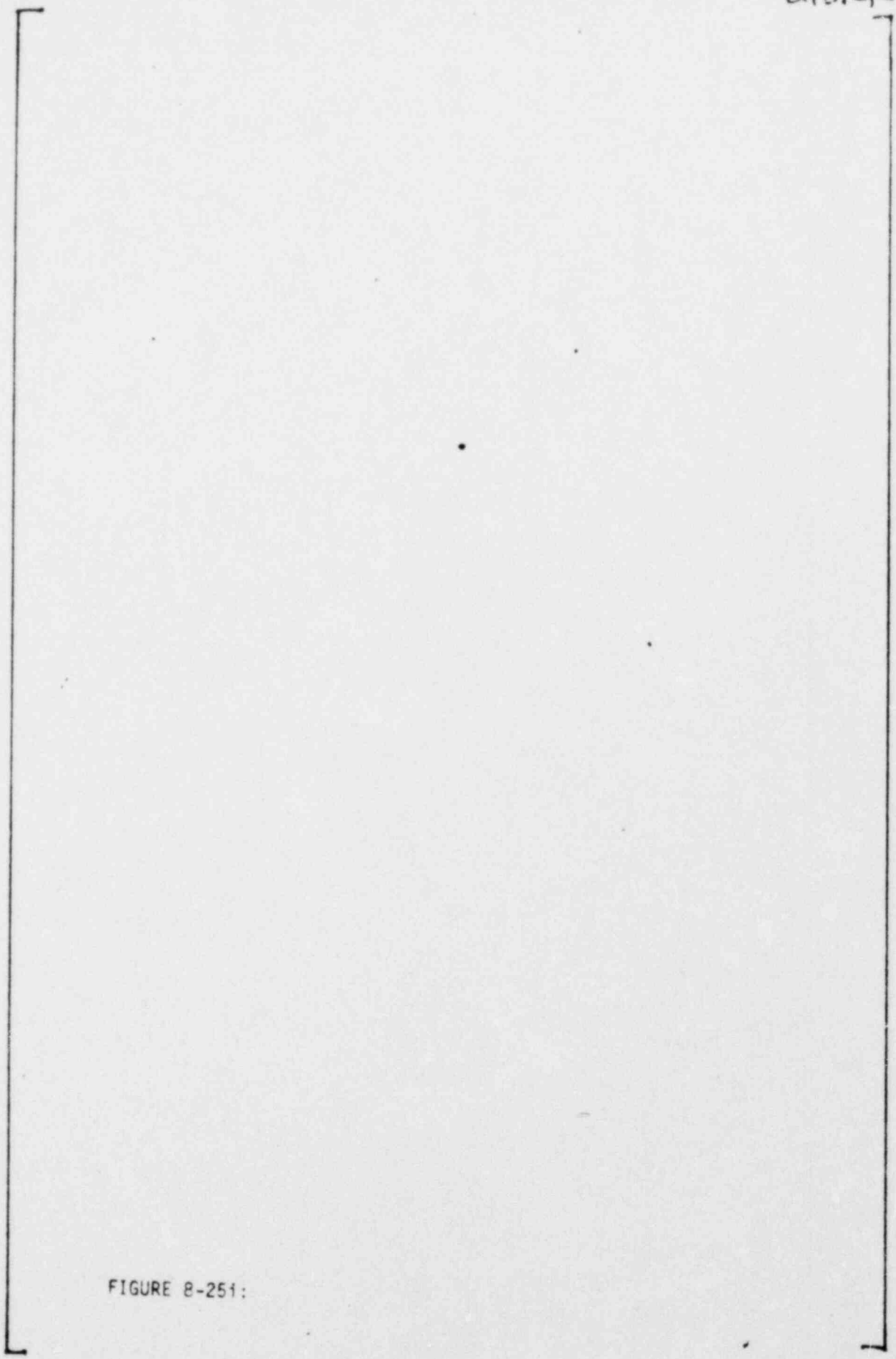

FIGURE 8-251:

a,b,c,e

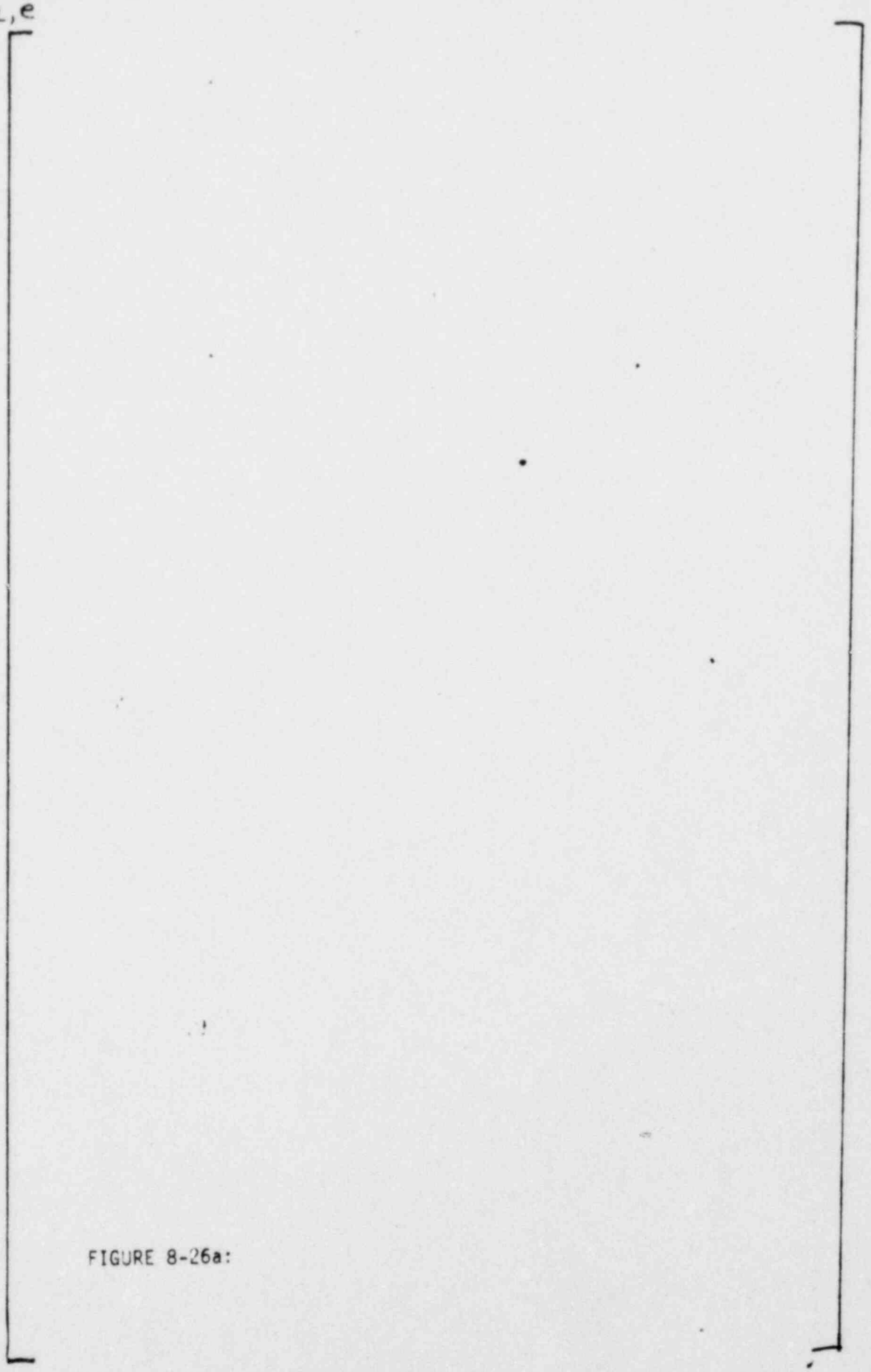

FIGURE 8-26a:

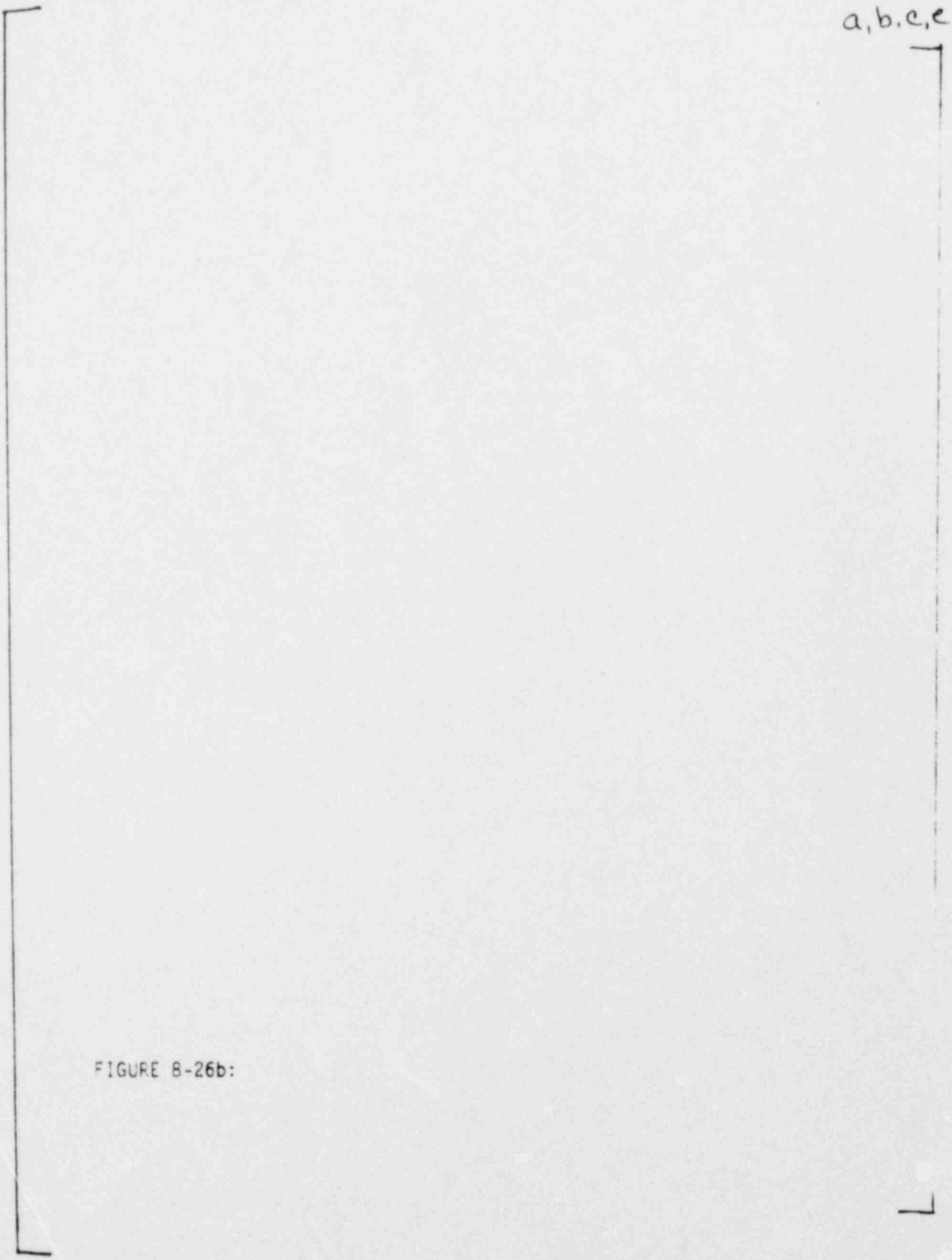

FIGURE 8-26b:

[a,b,c,e

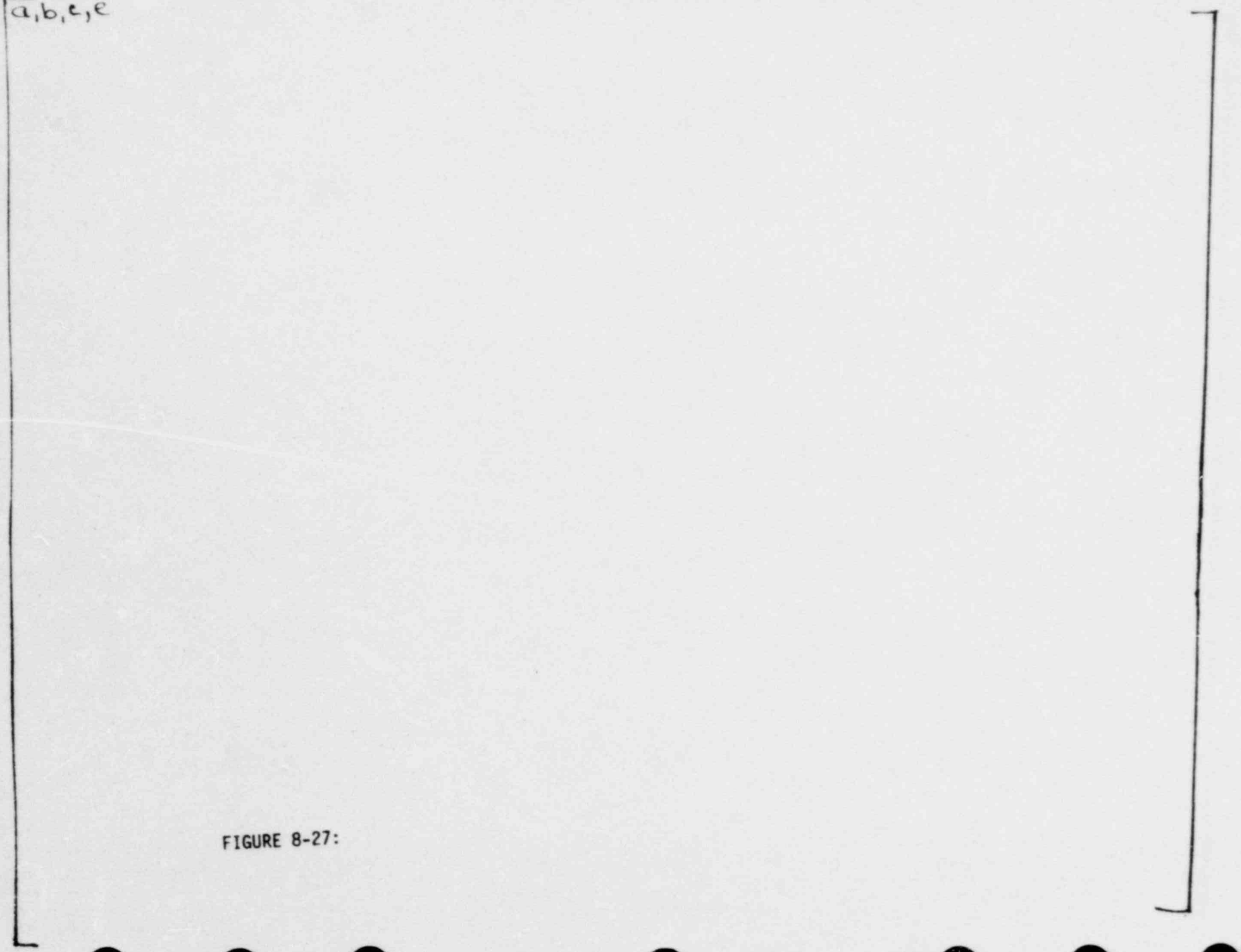

FIGURE 8-27:

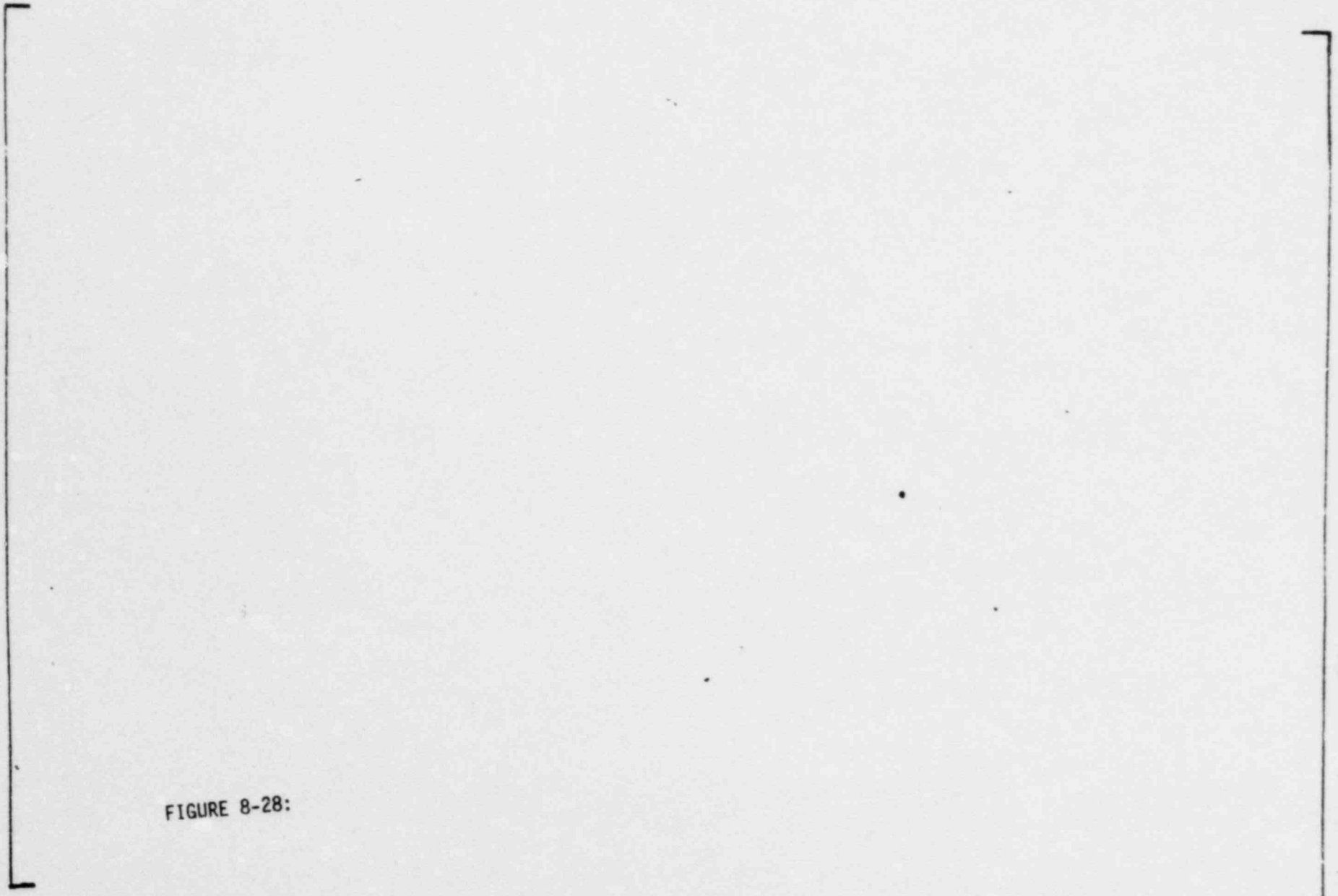

FIGURE 8-28:

a,b,c,e

a,b,c,e

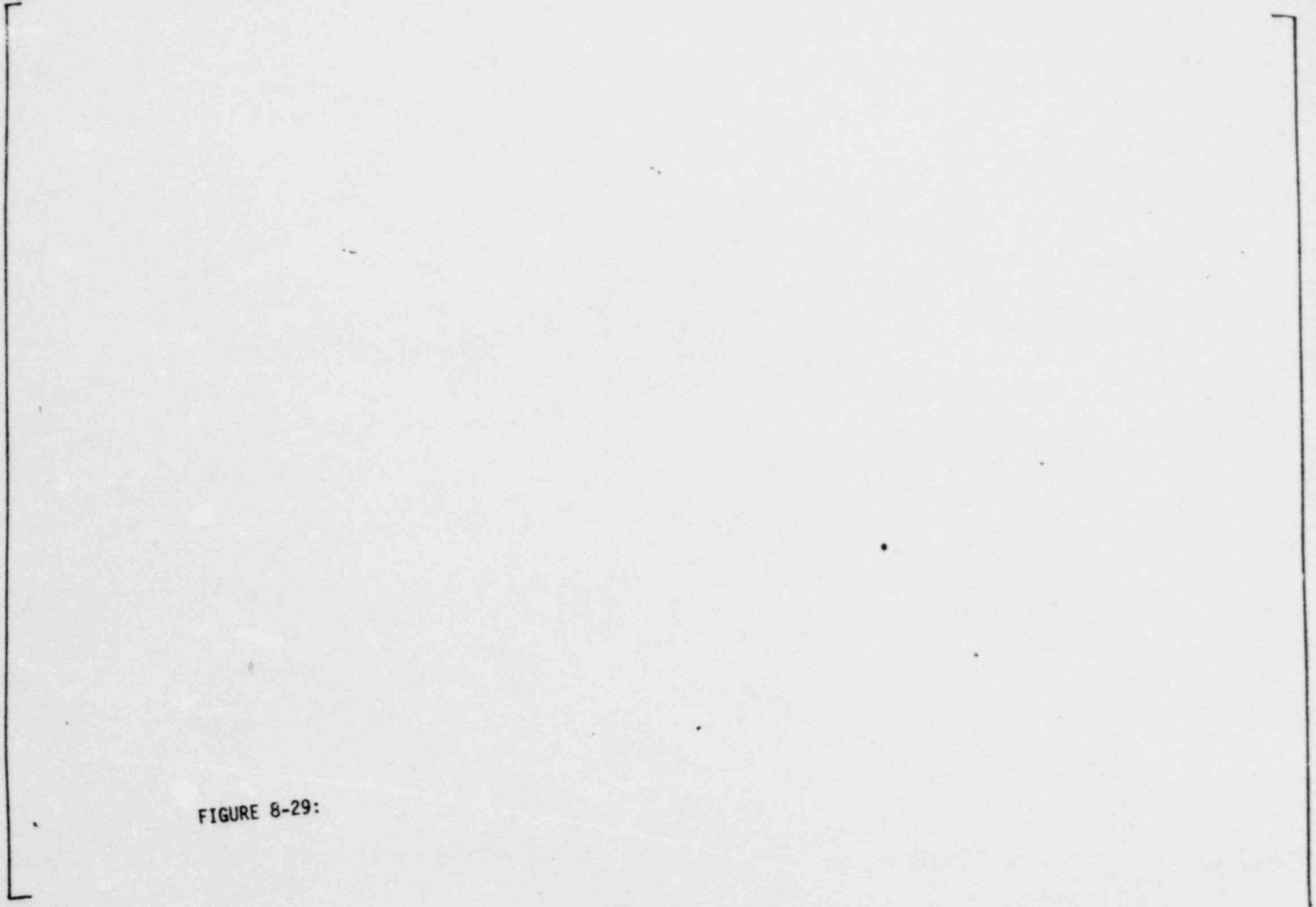

FIGURE 8-29:

a,b,c,e

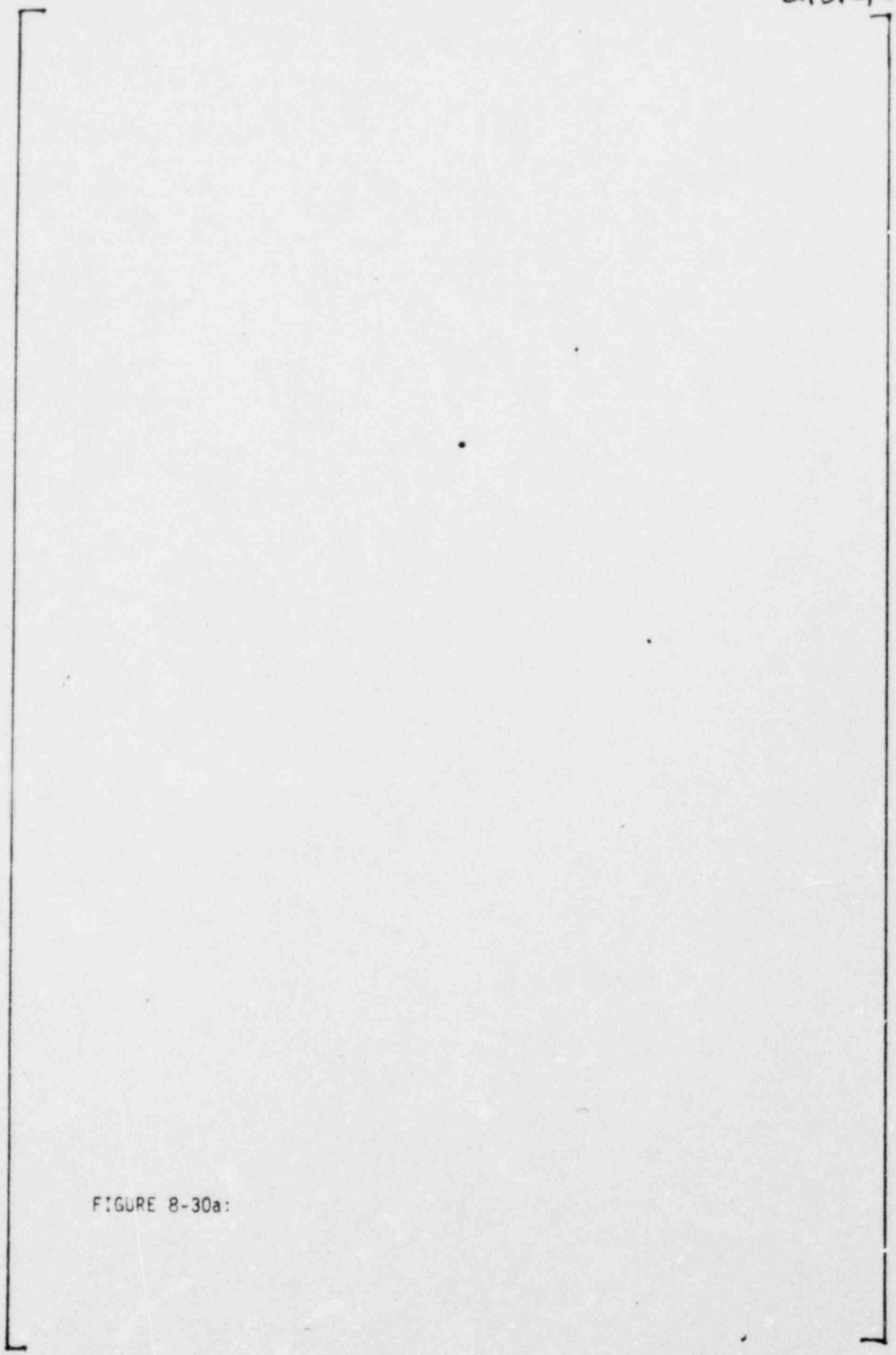

FIGURE 8-30a:

a,b,c,e

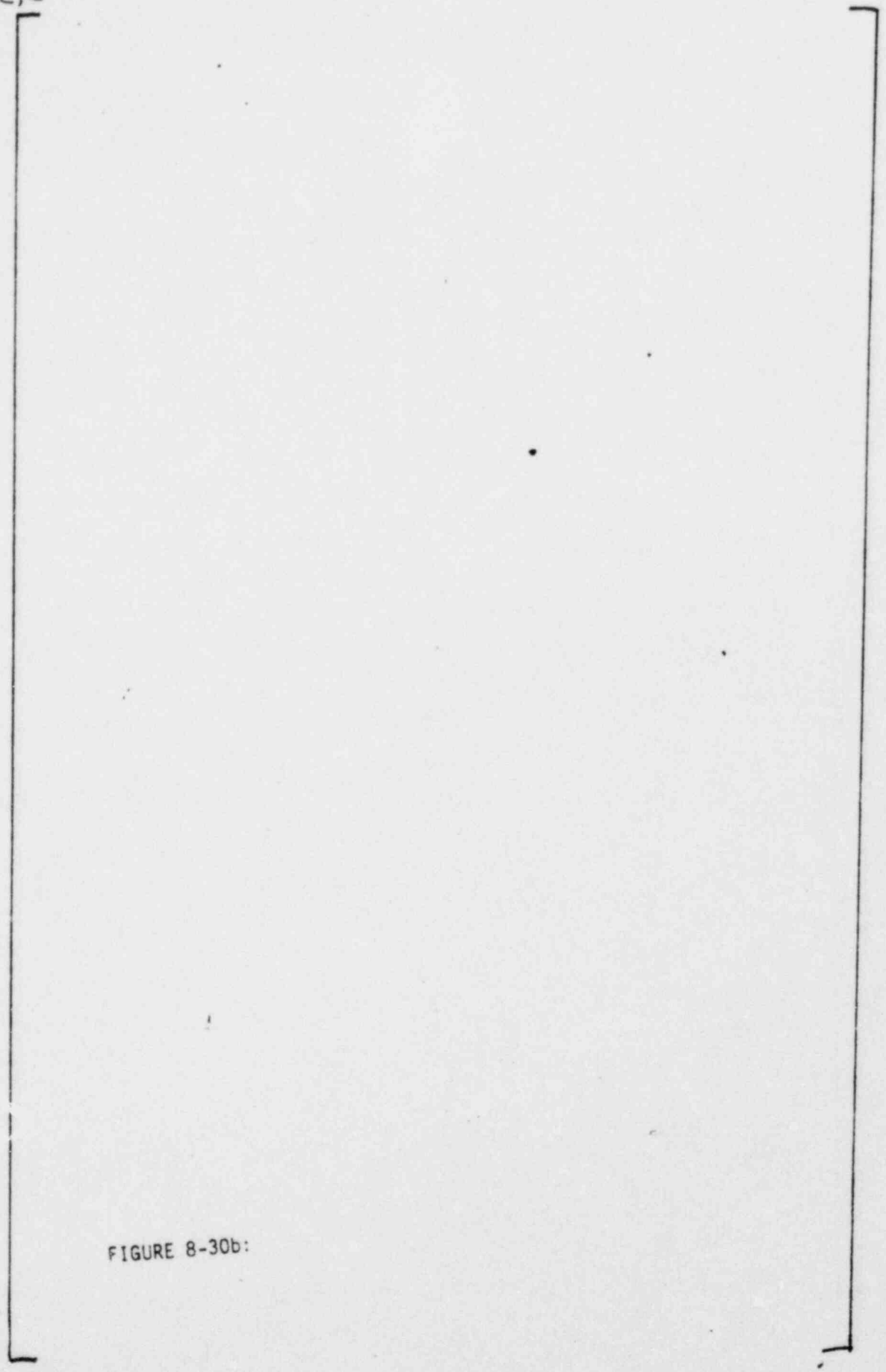

FIGURE 8-30b:

a,b,c,e

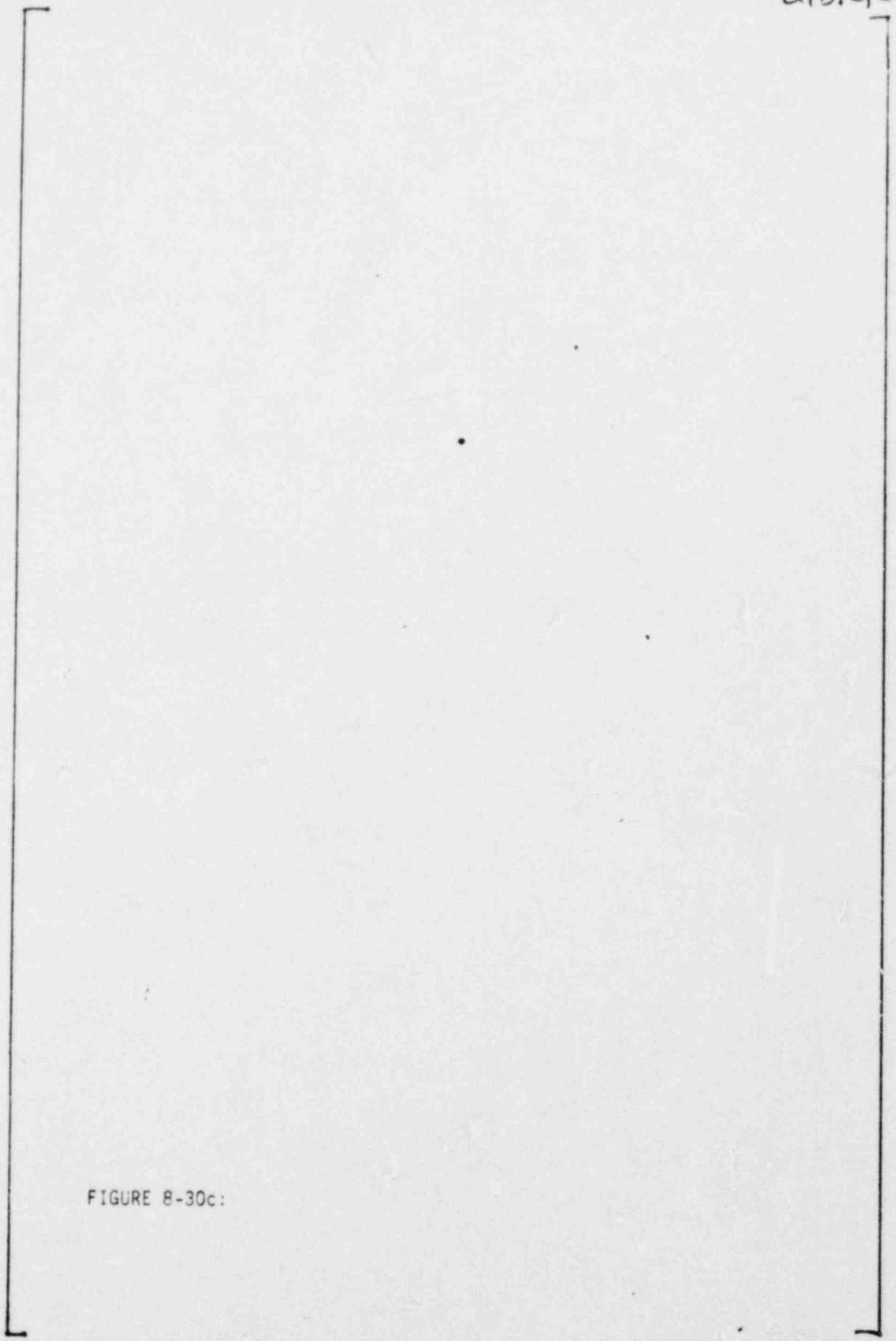

FIGURE 8-30c:

a,b,c,e

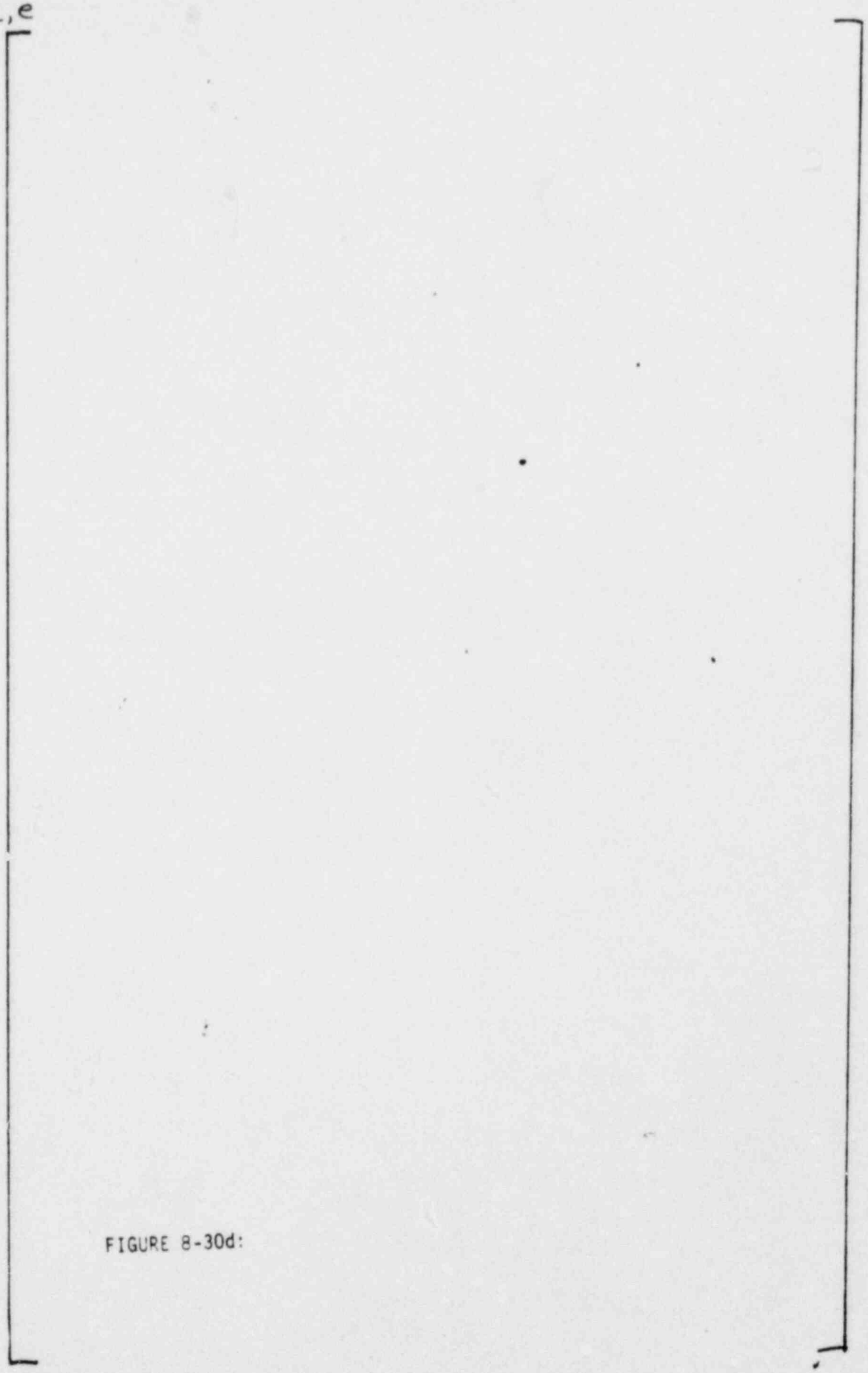

FIGURE 8-30d:

a,b,c,e

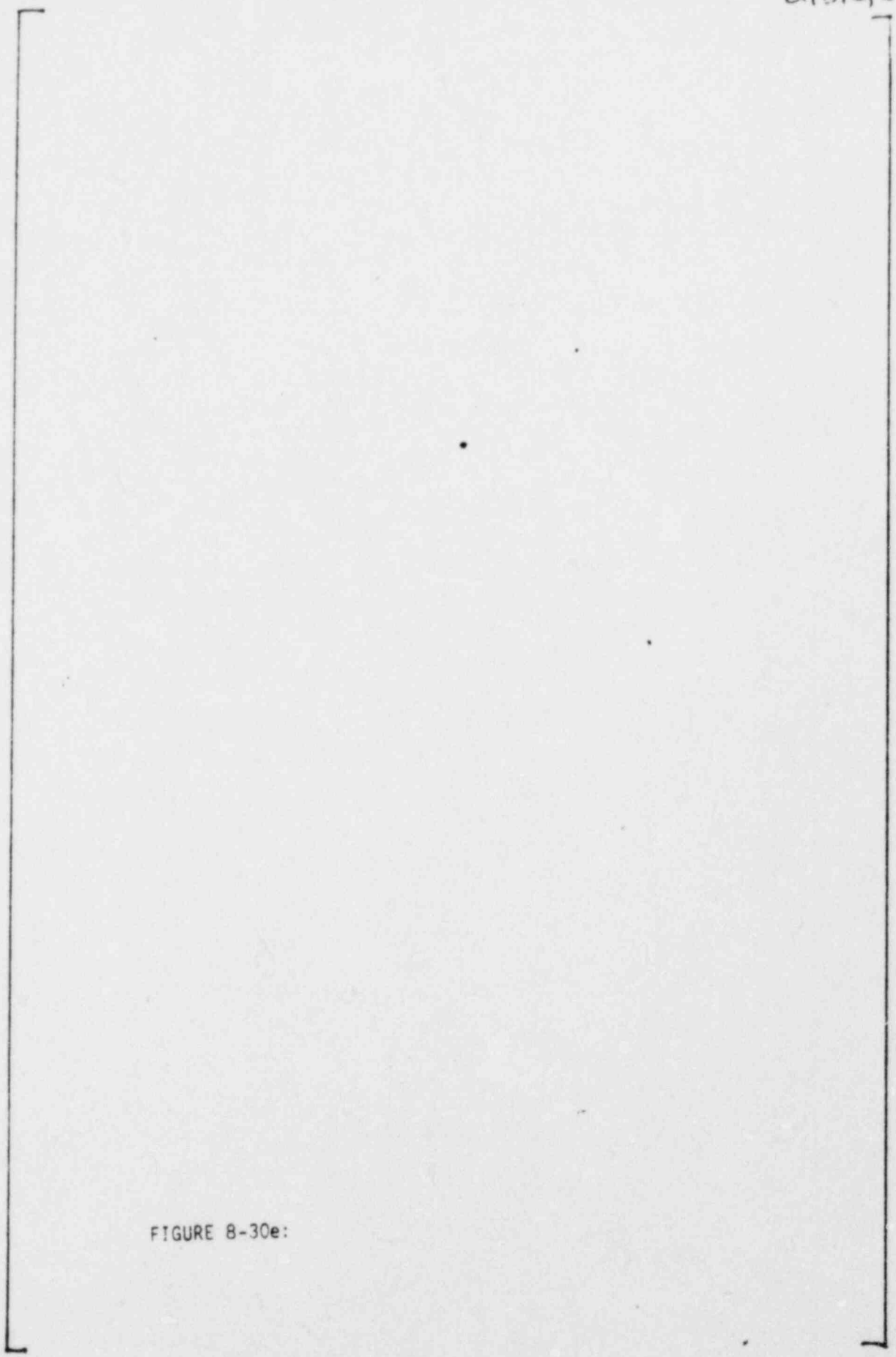

FIGURE 8-30e:

a,b,c,e

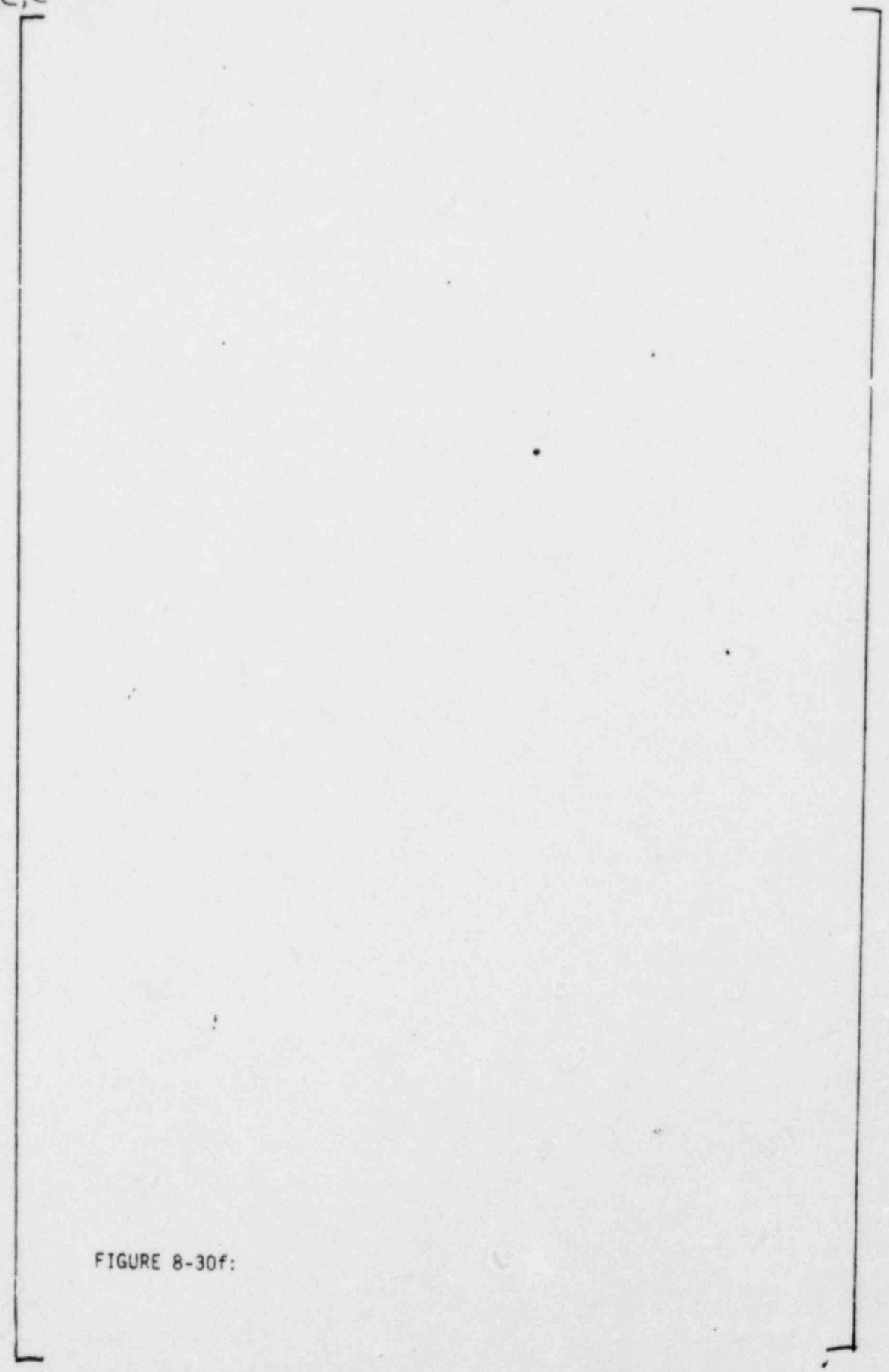

FIGURE 8-30f:

a,b,c,e

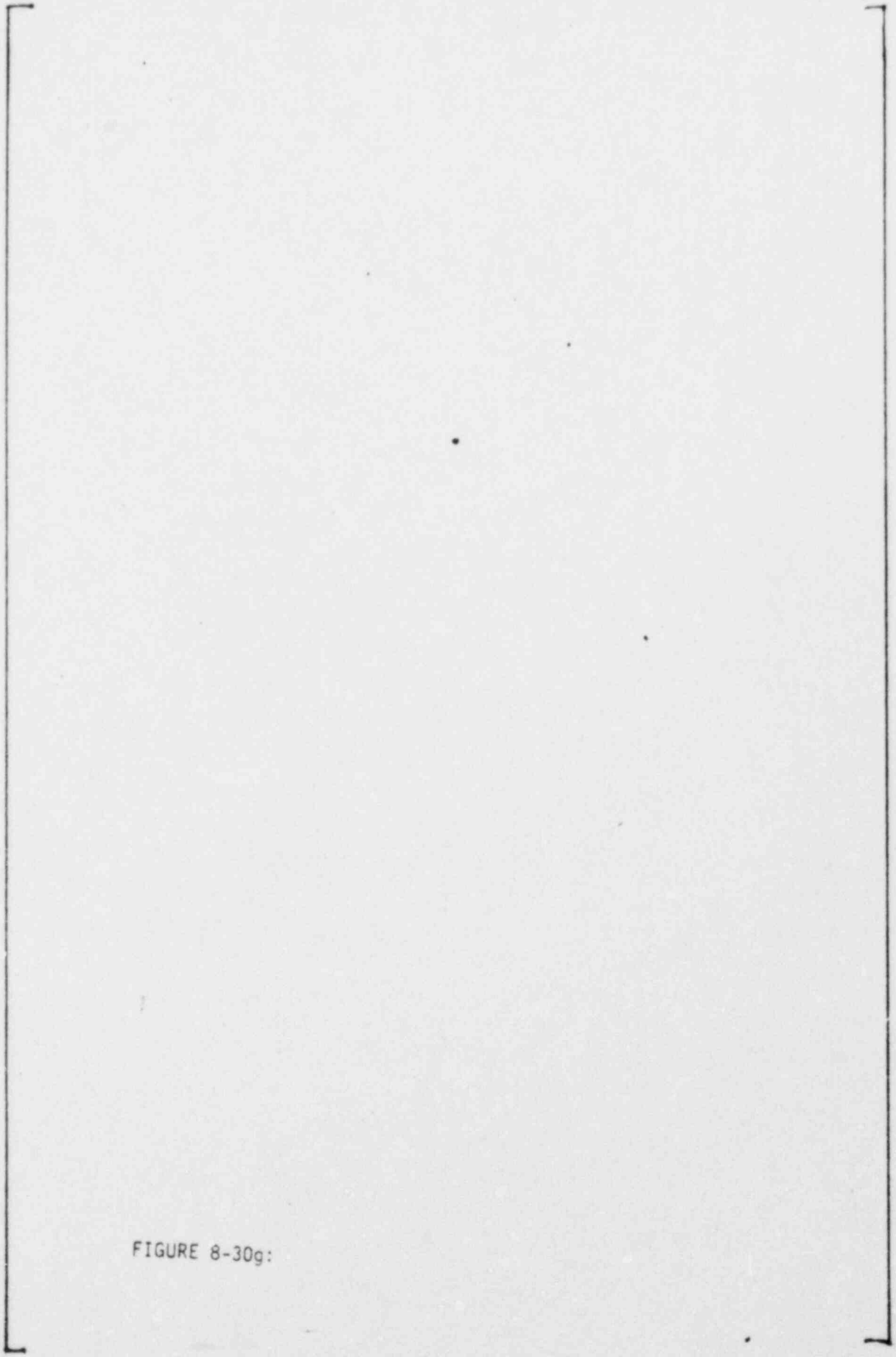

FIGURE 8-30g:

a,b,c,e

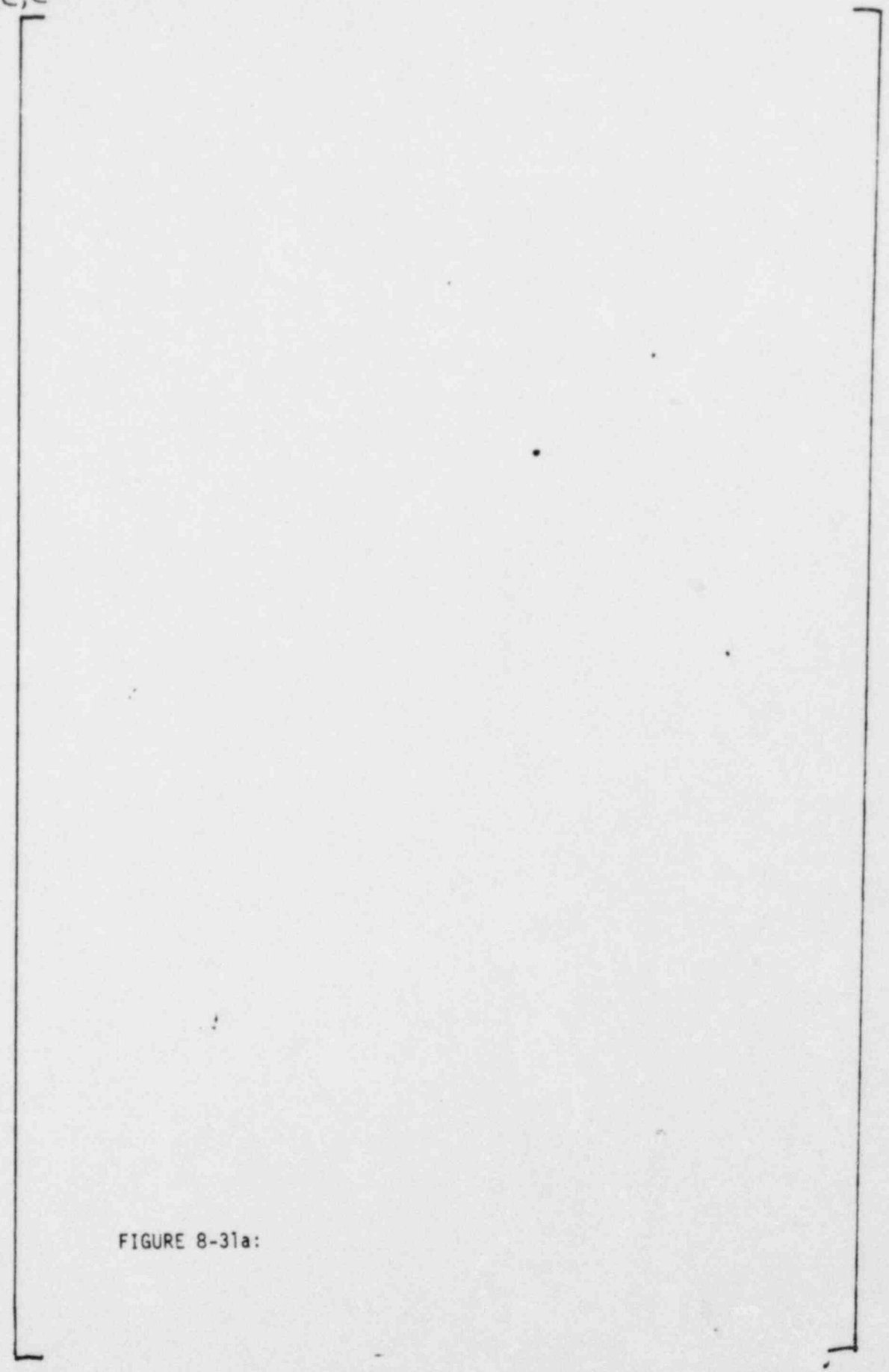

FIGURE 8-31a:

a,b,c,e

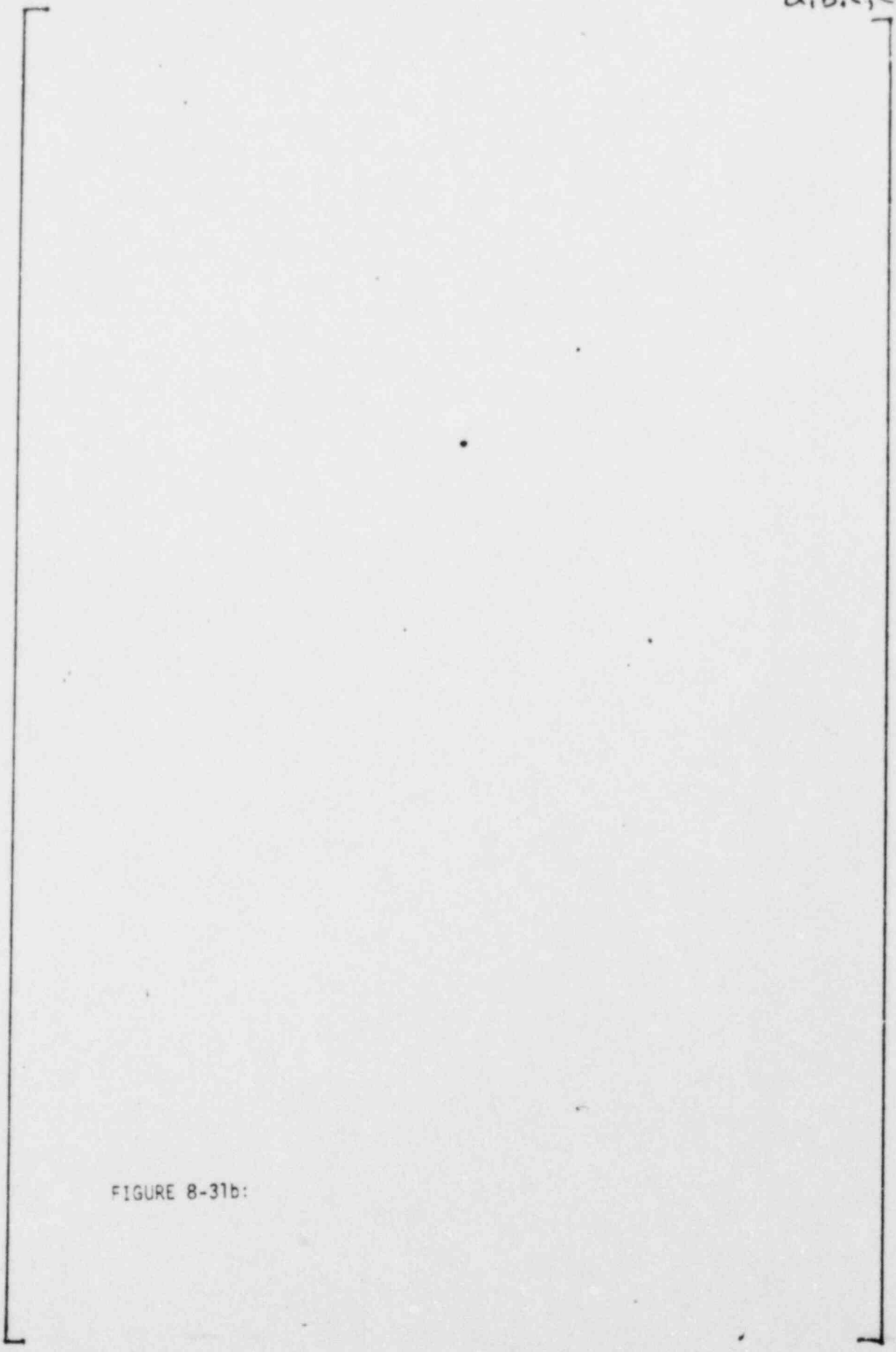

FIGURE 8-31b:

a,b,c,e

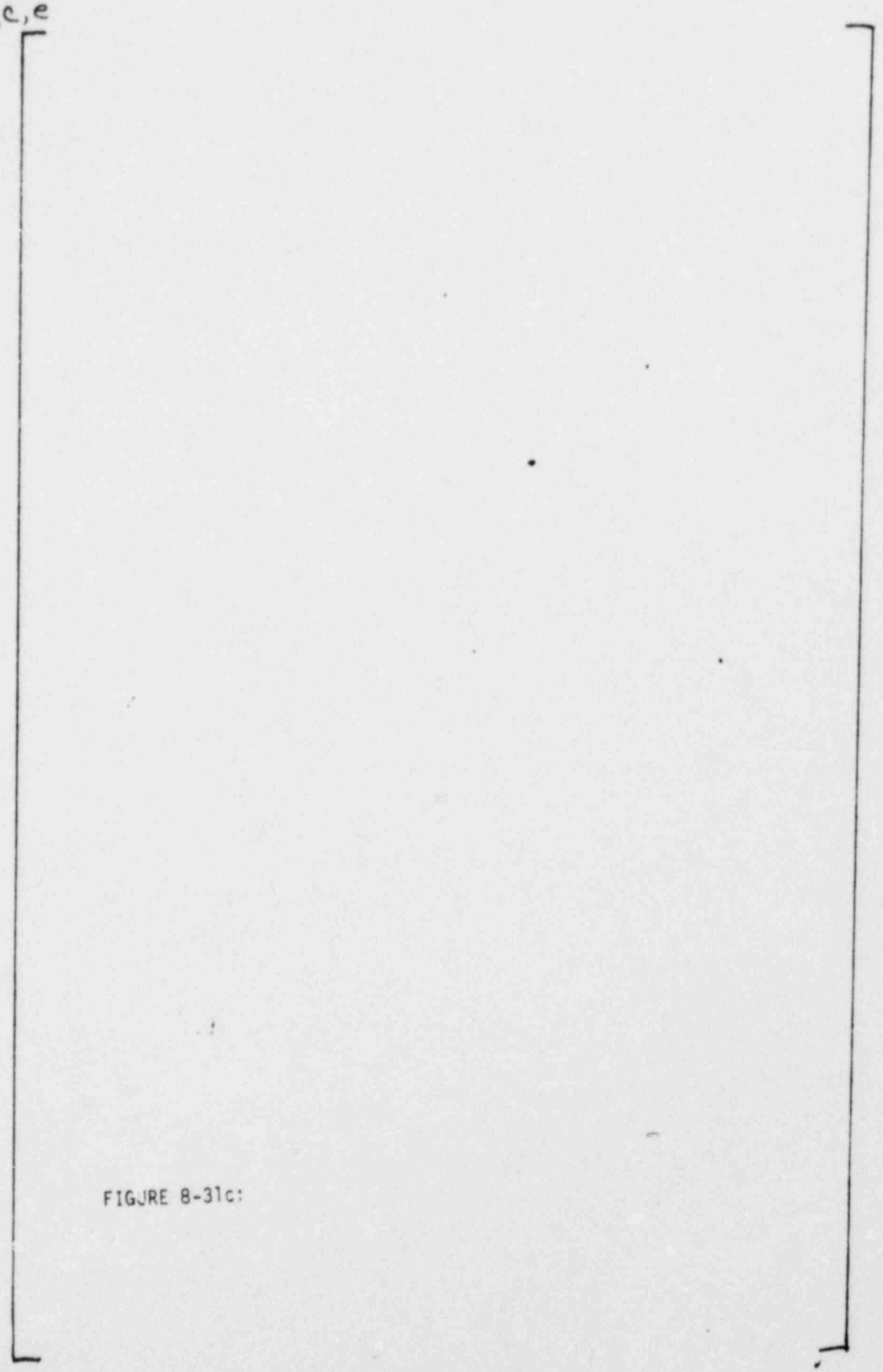

FIGURE 8-31c:

a,b,c,e

FIGURE 8-31d:

a, b, c, e

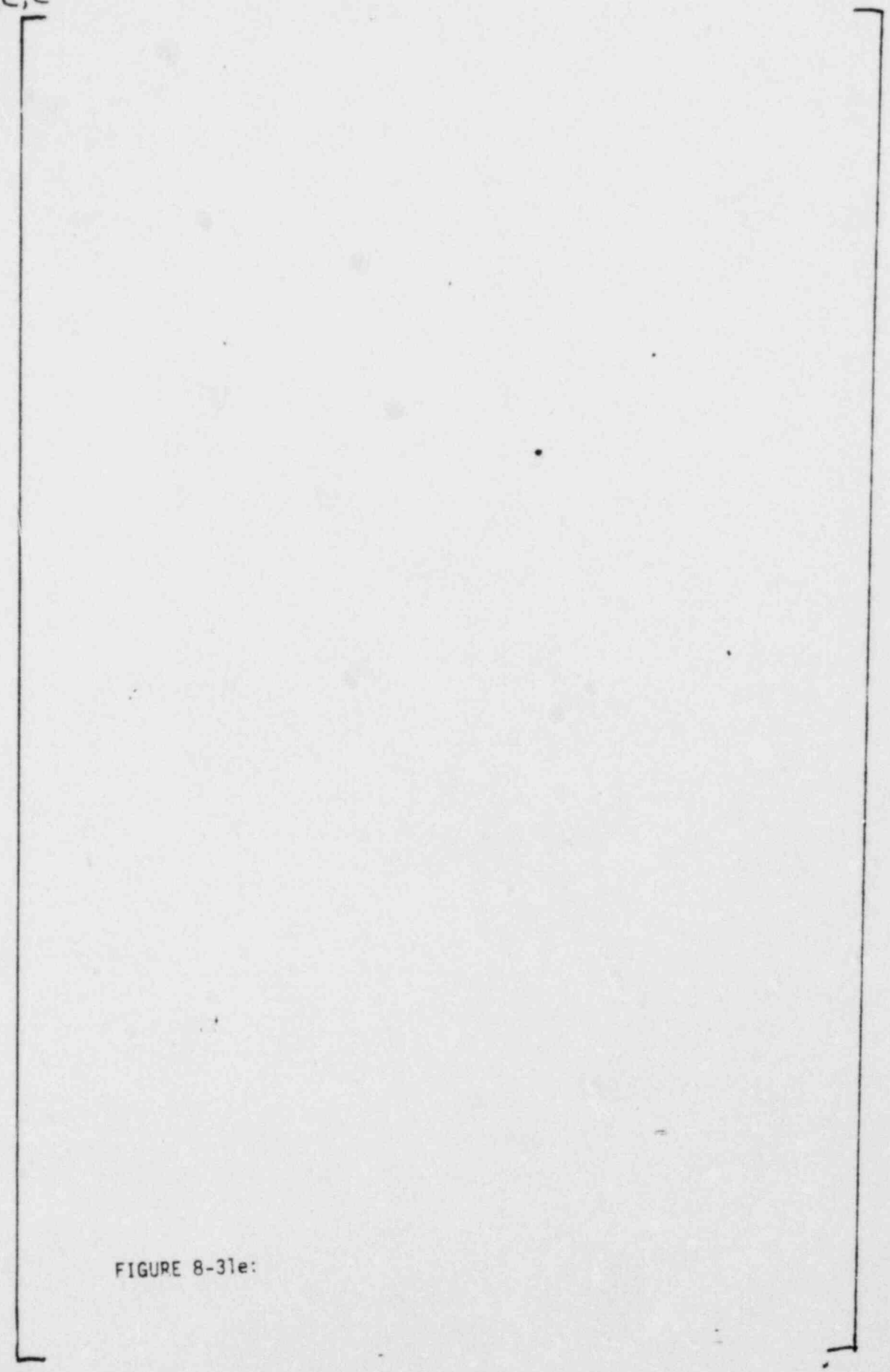

FIGURE 8-31e:

a,b,c,e

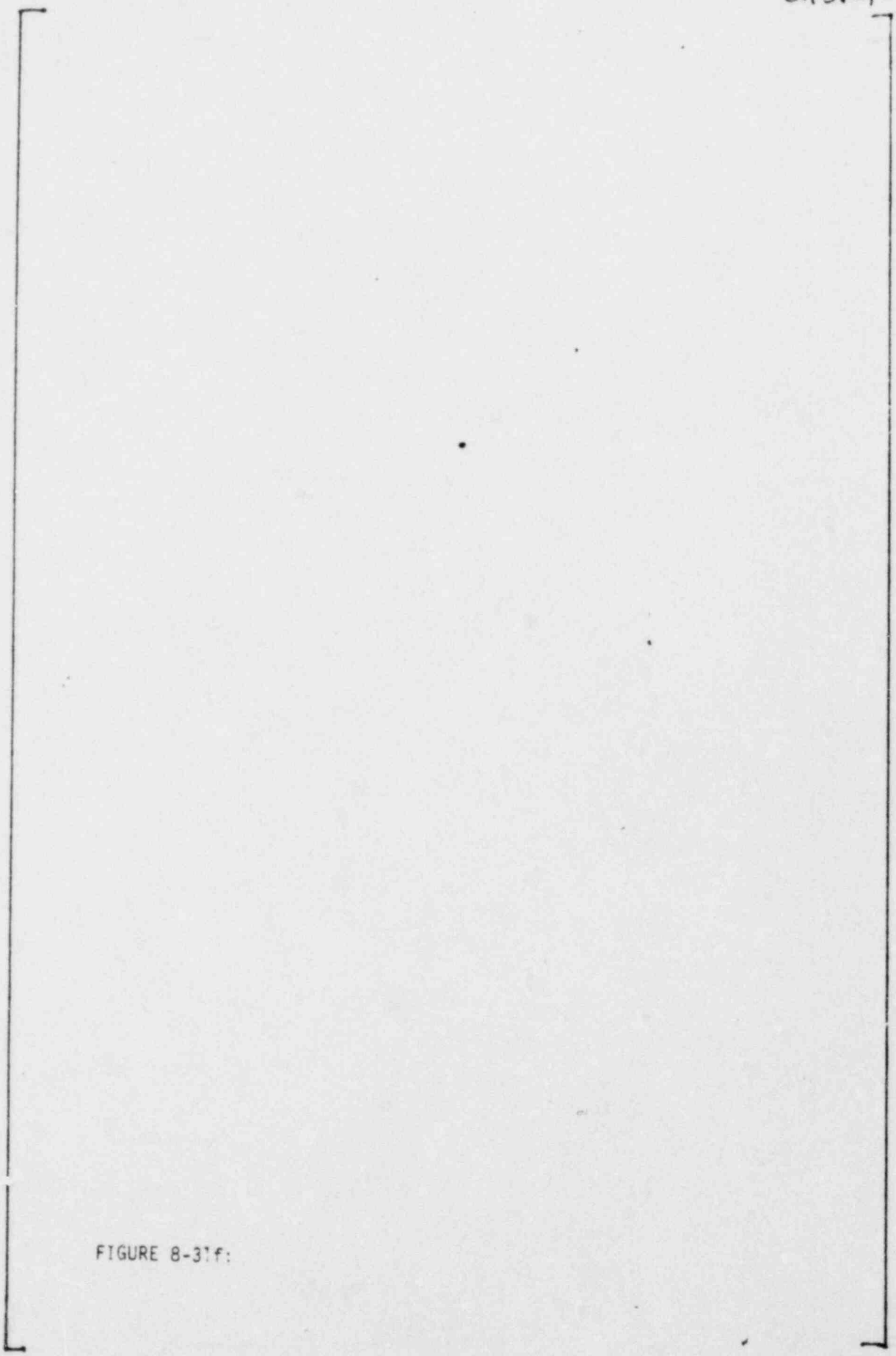

FIGURE 8-31f:

a,b,c,e

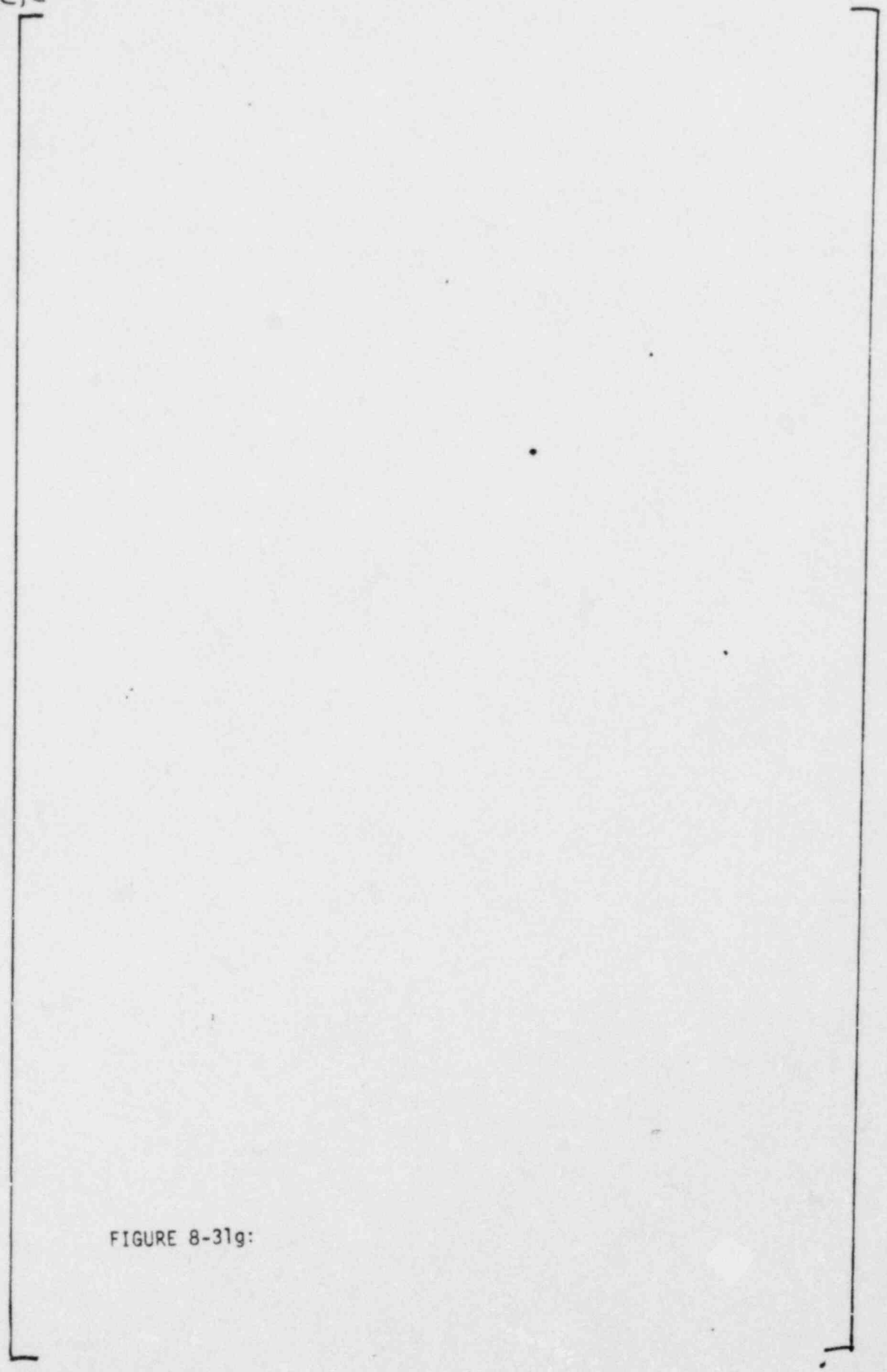

FIGURE 8-31g:

a,b,c,e

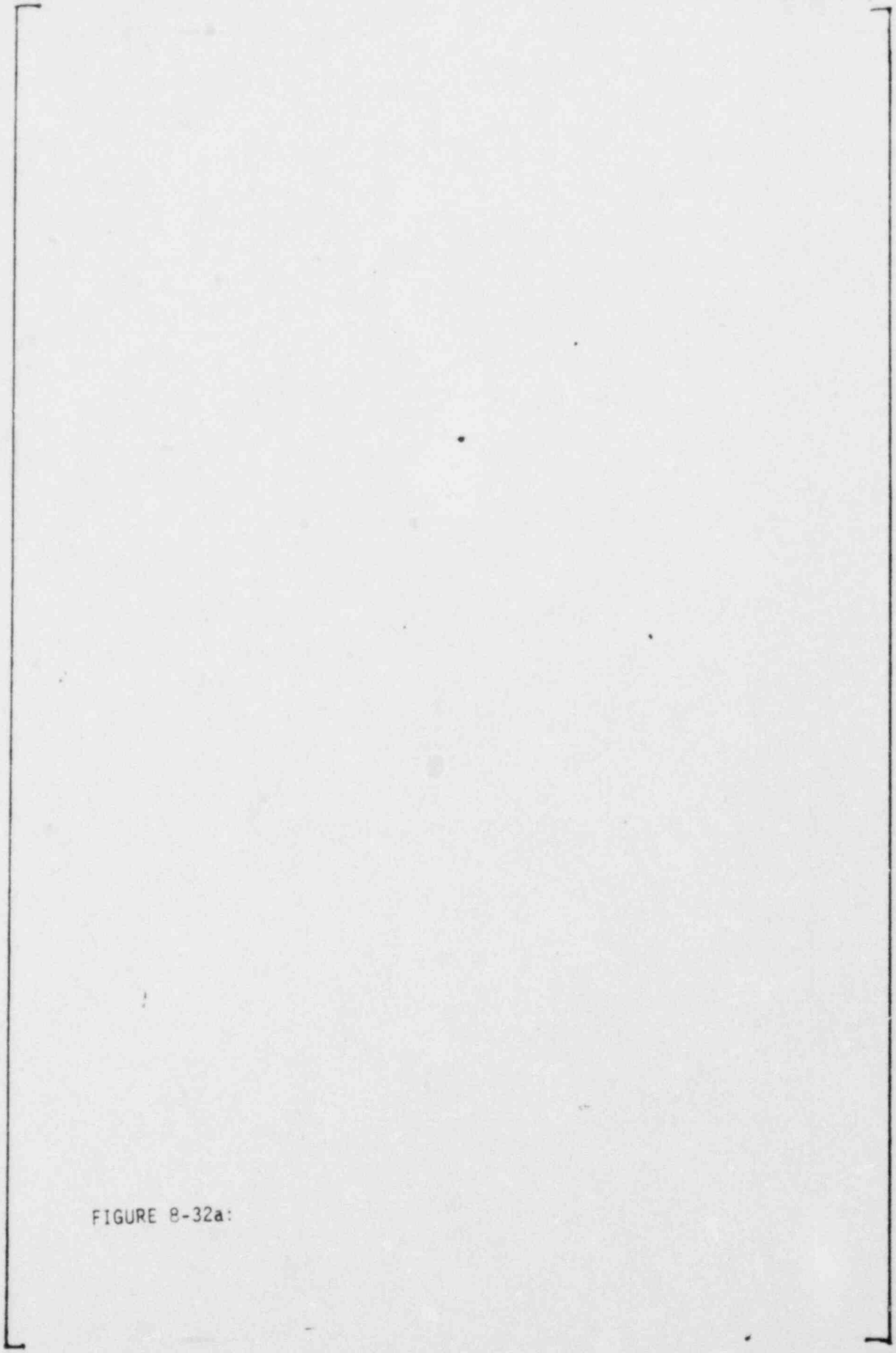

FIGURE 8-32a:

a,b,c,e

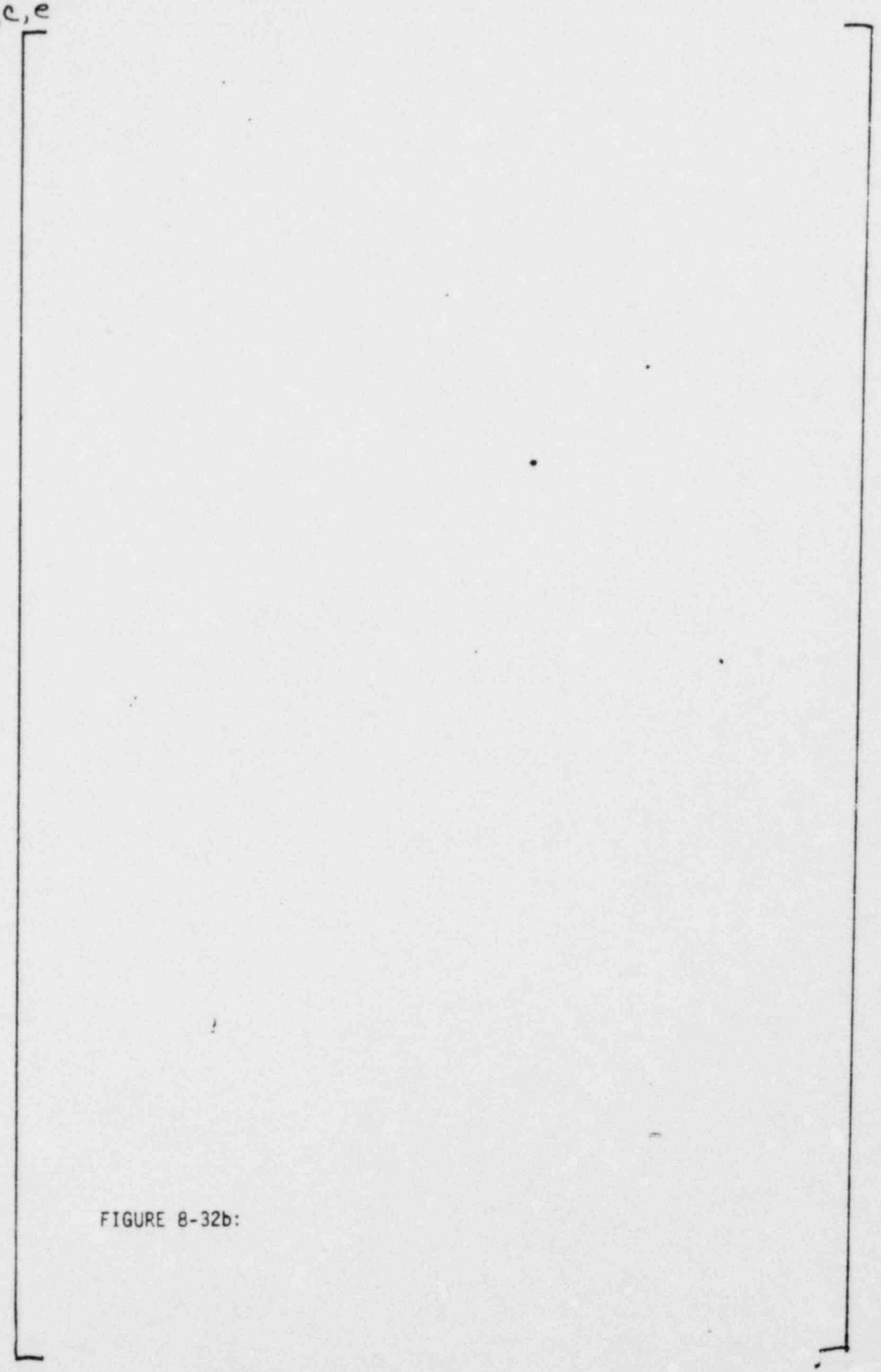

FIGURE 8-32b:

FIGURE 8-33:

a,b,c,e

a,b,c,e

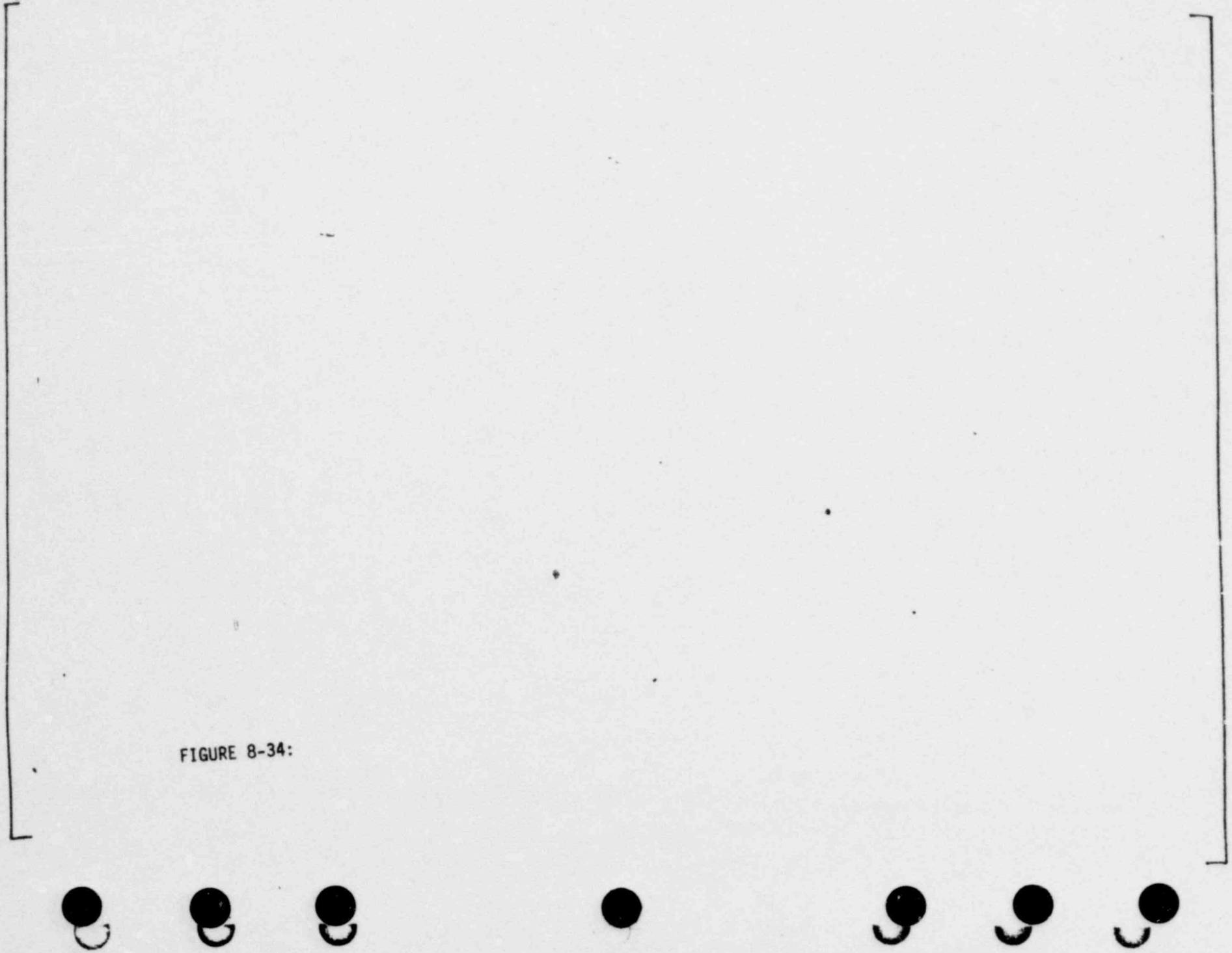

FIGURE 8-34:

a,b,c,e

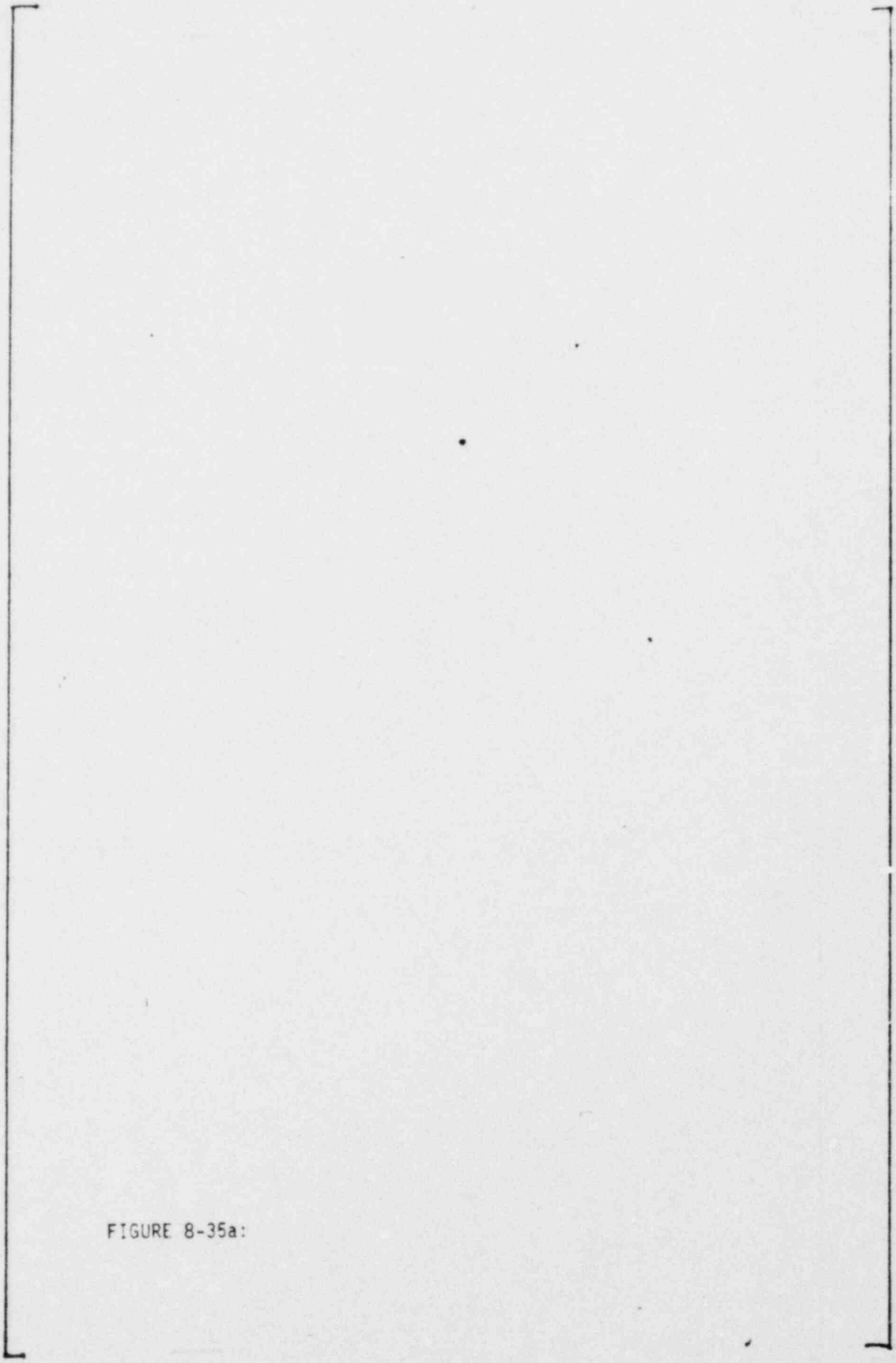

FIGURE 8-35a:

a,b,c,e

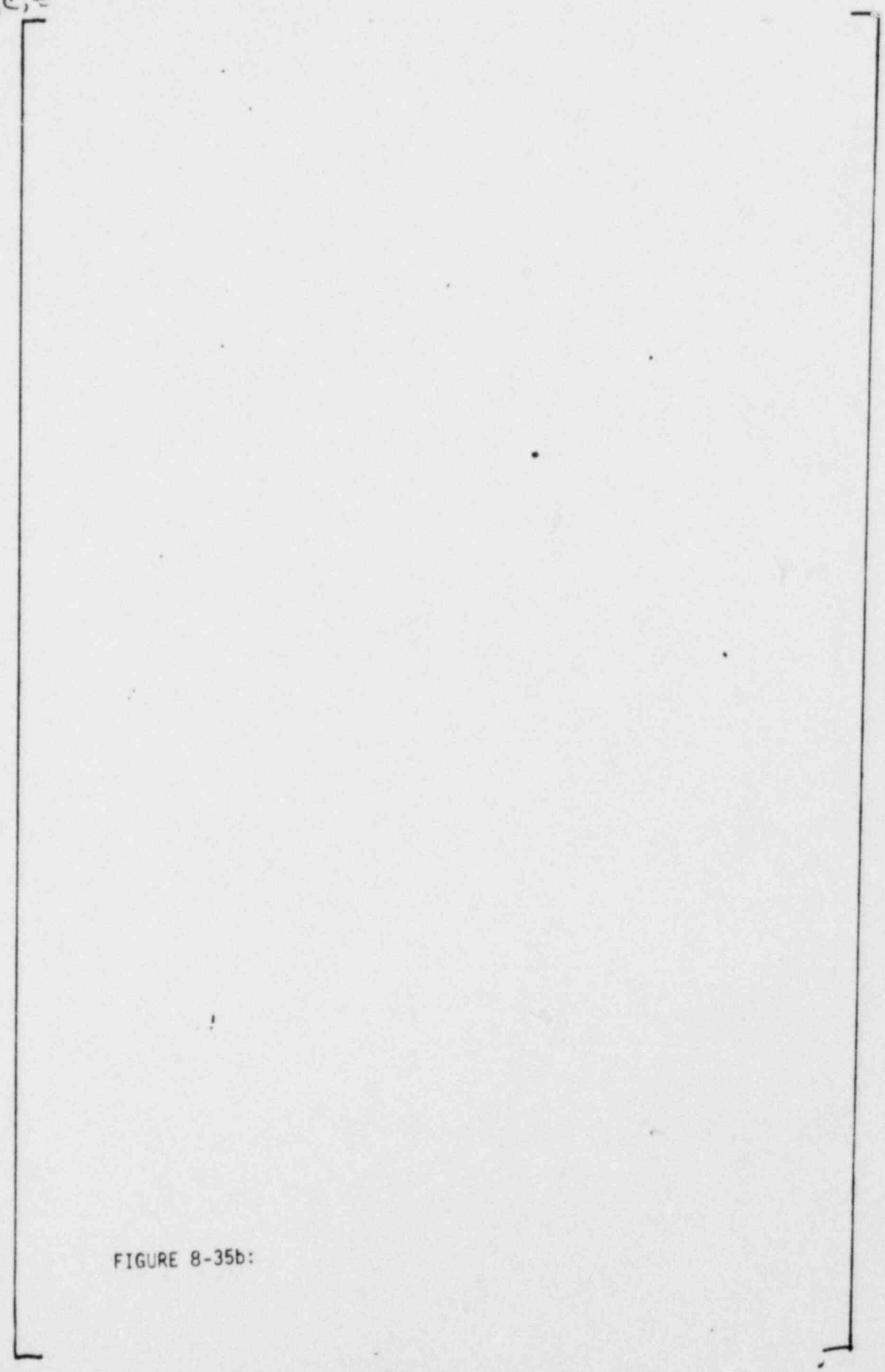

FIGURE 8-35b:

a,b,c,e

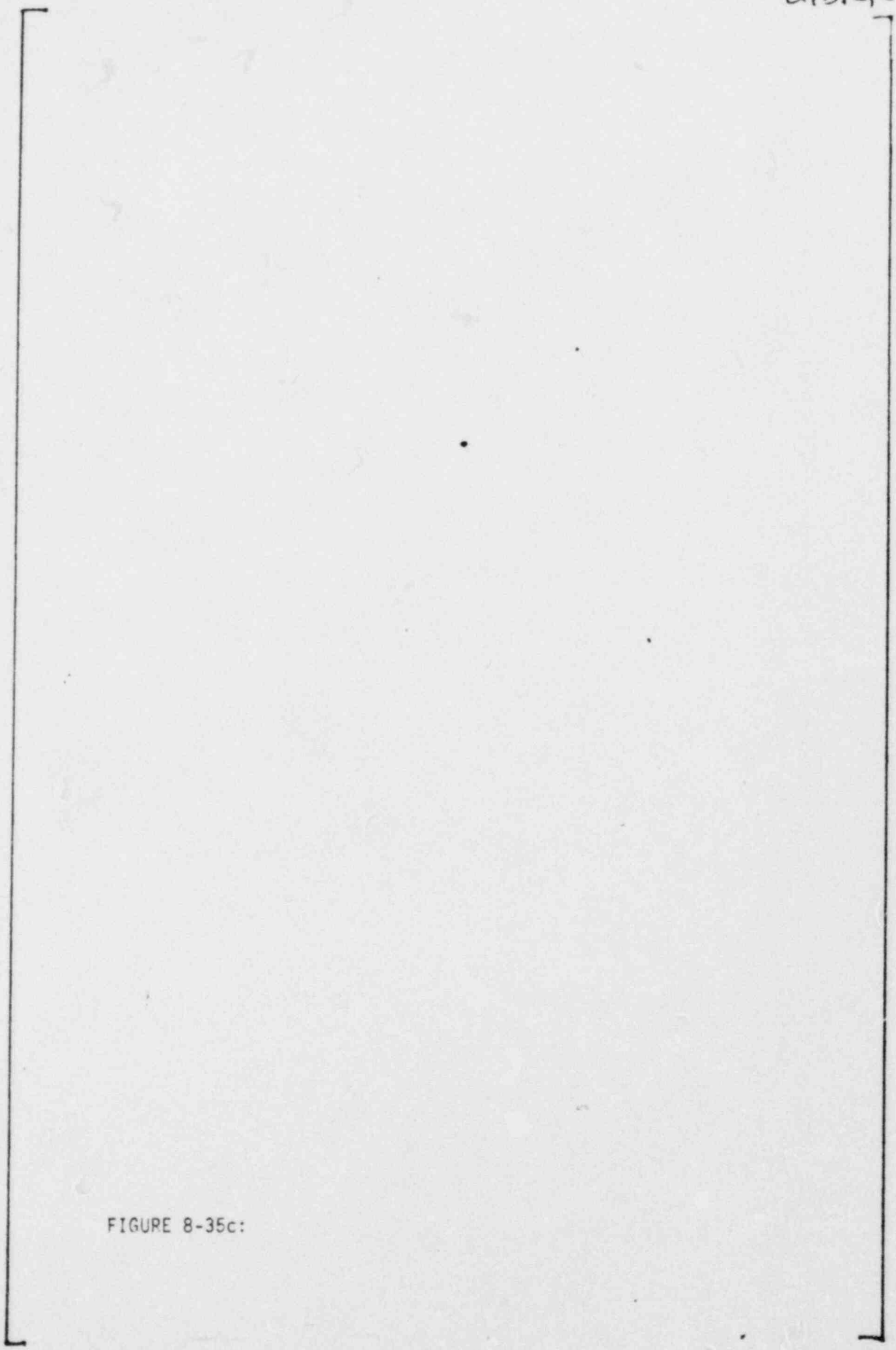

FIGURE 8-35c:

a,b,c,e

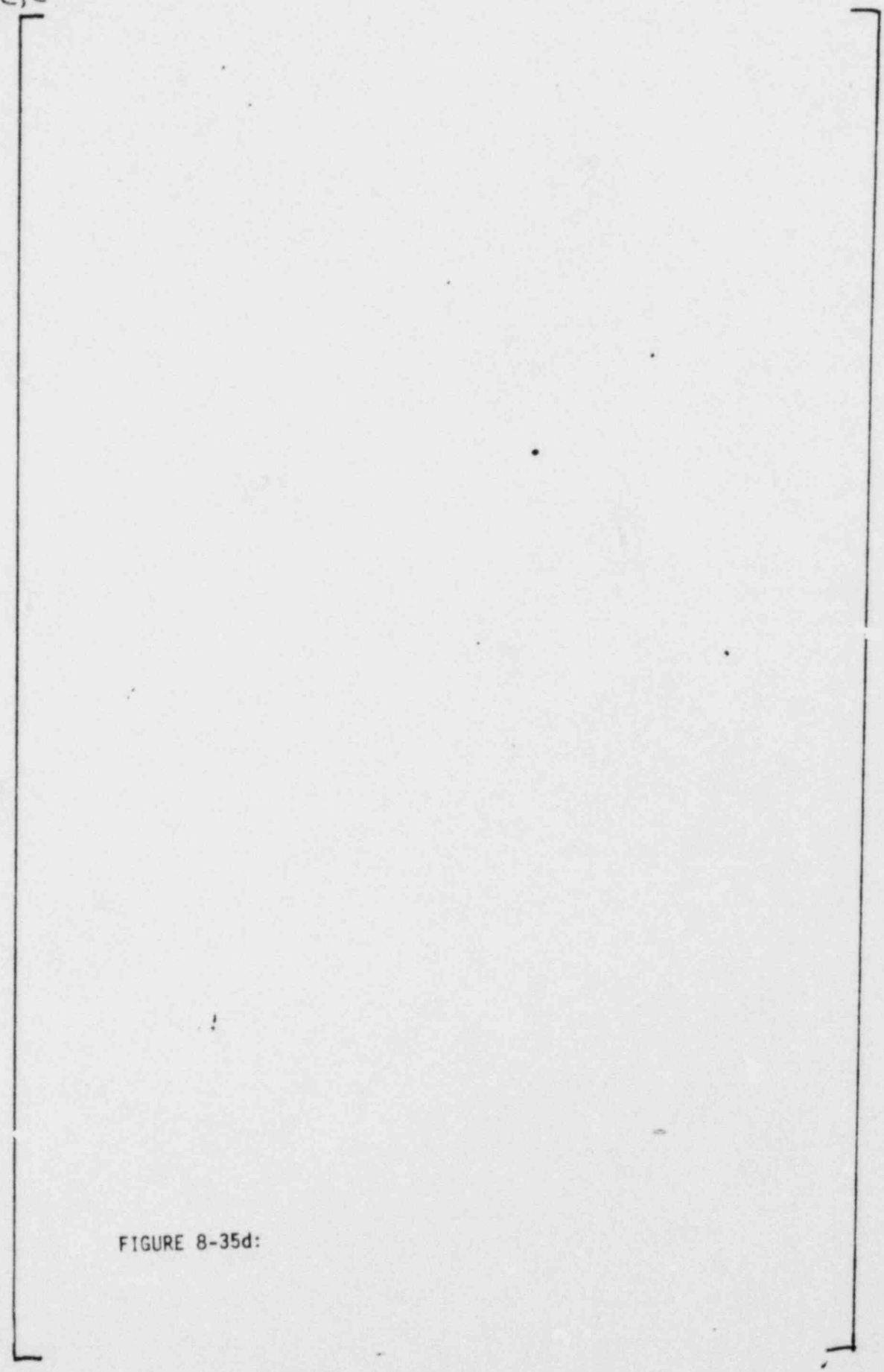

FIGURE 8-35d:

a,b,c,e

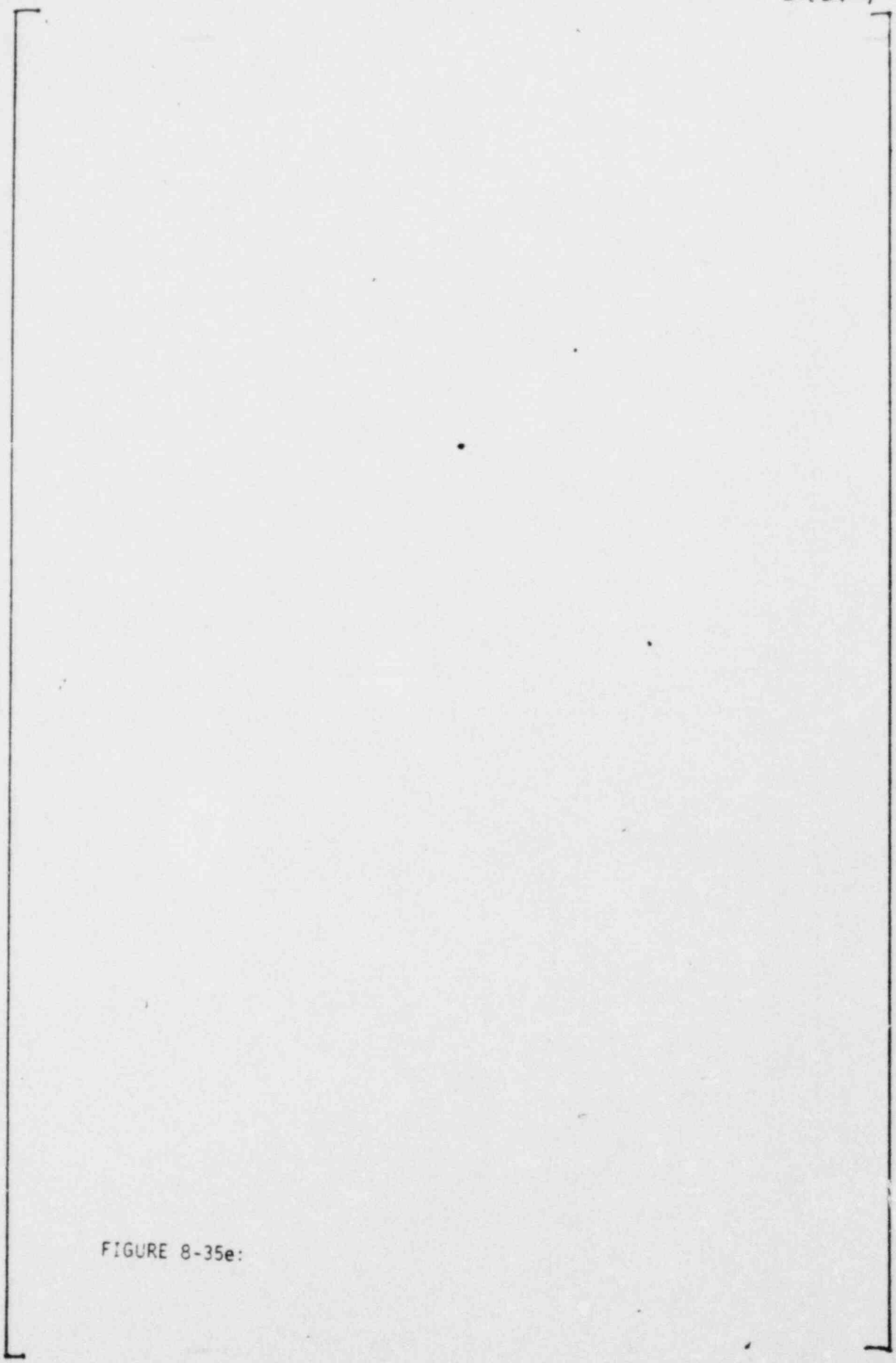

FIGURE 8-35e:

a,b,c,e

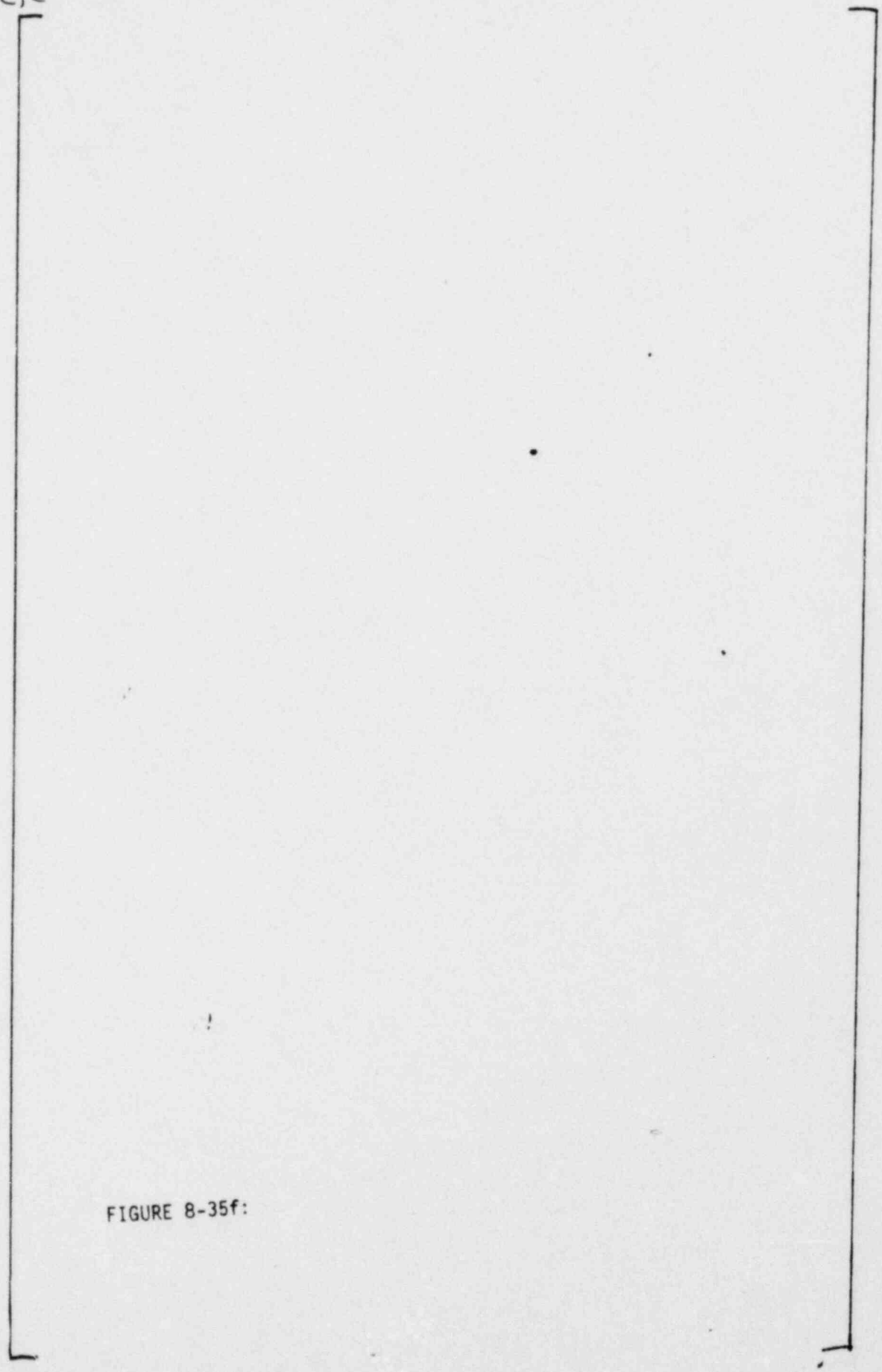

FIGURE 8-35f:

a,b,c,e

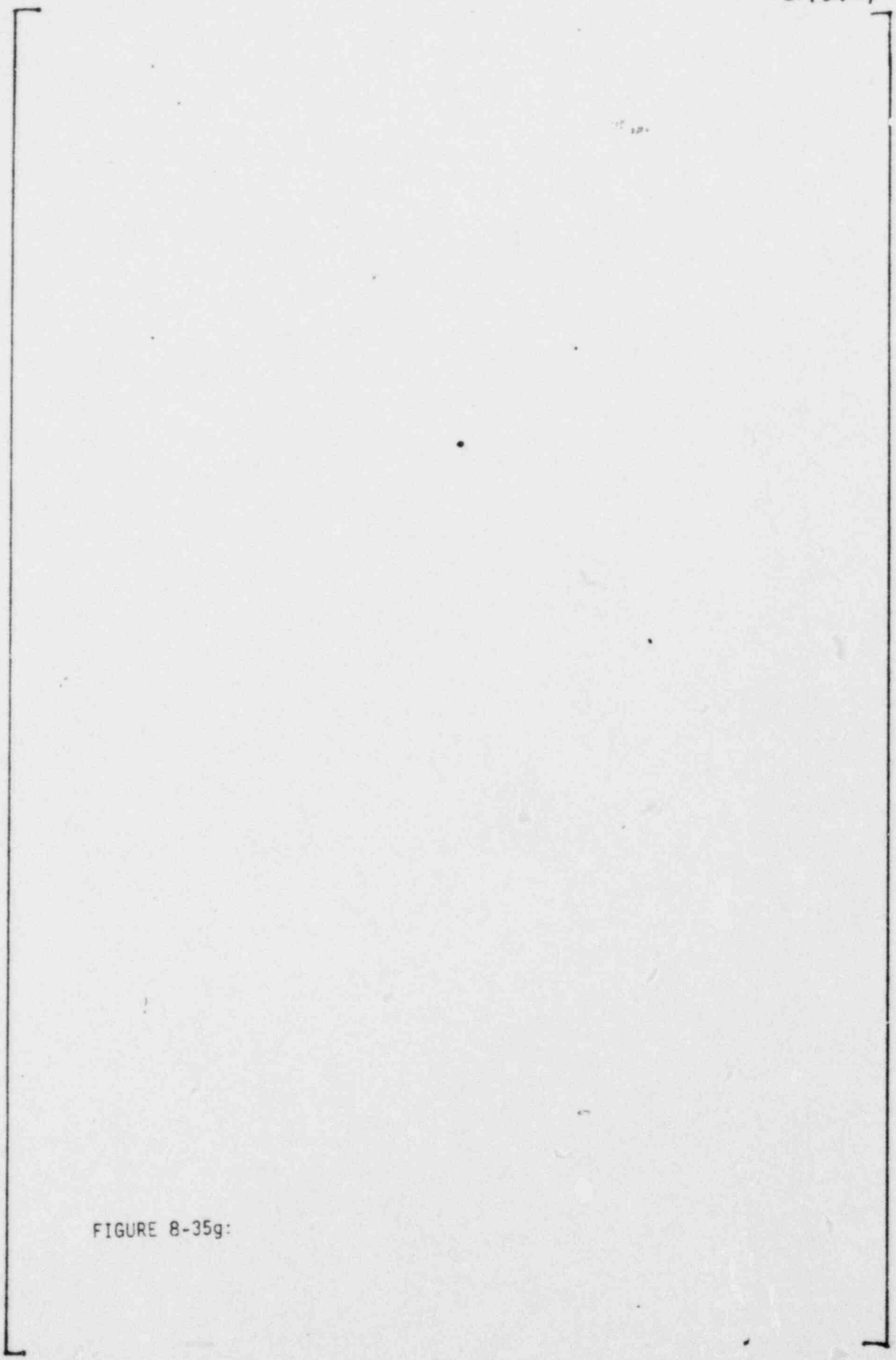

FIGURE 8-35g:

a,b,c,e

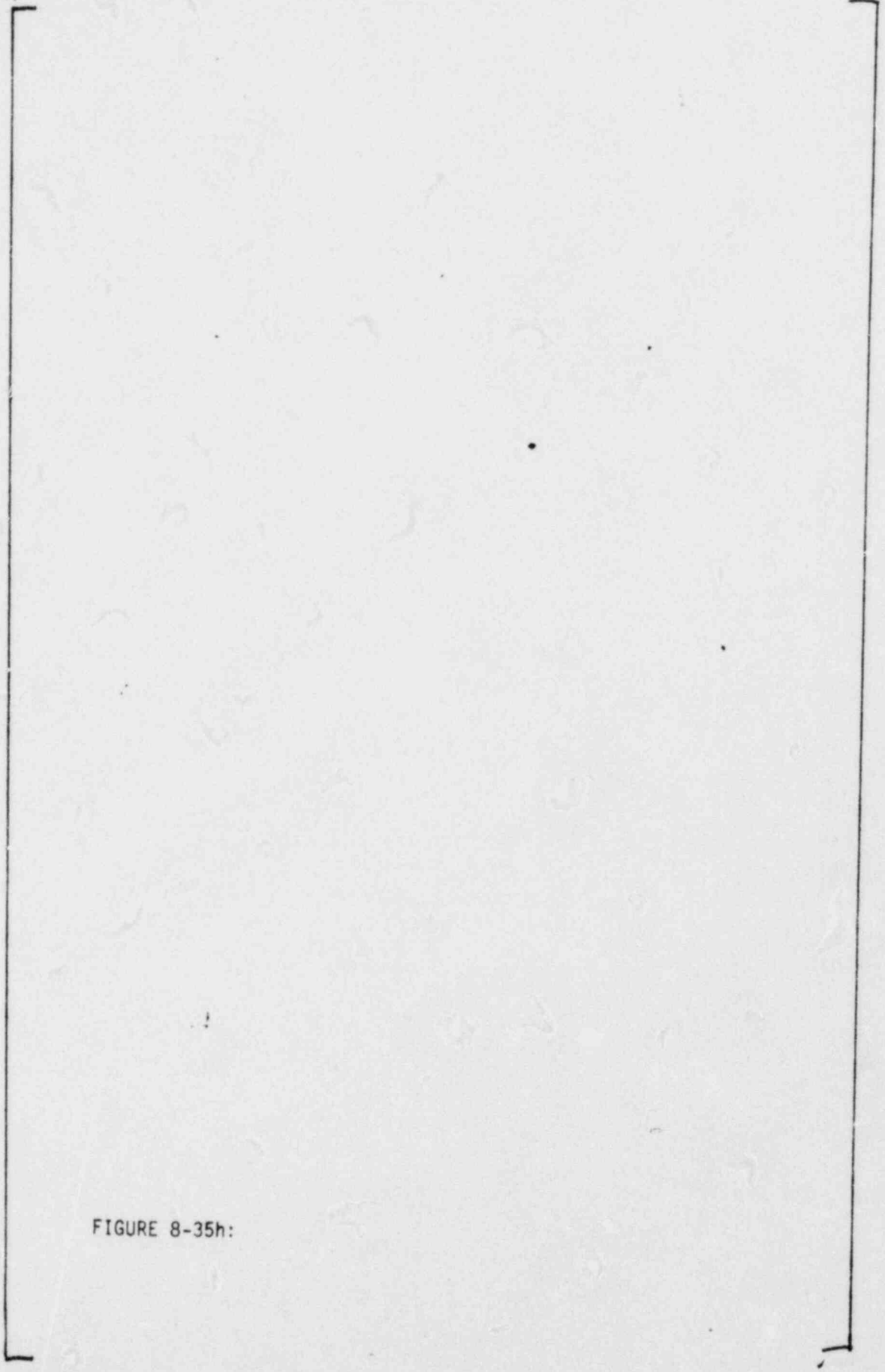

FIGURE 8-35h:

a,b,c,e

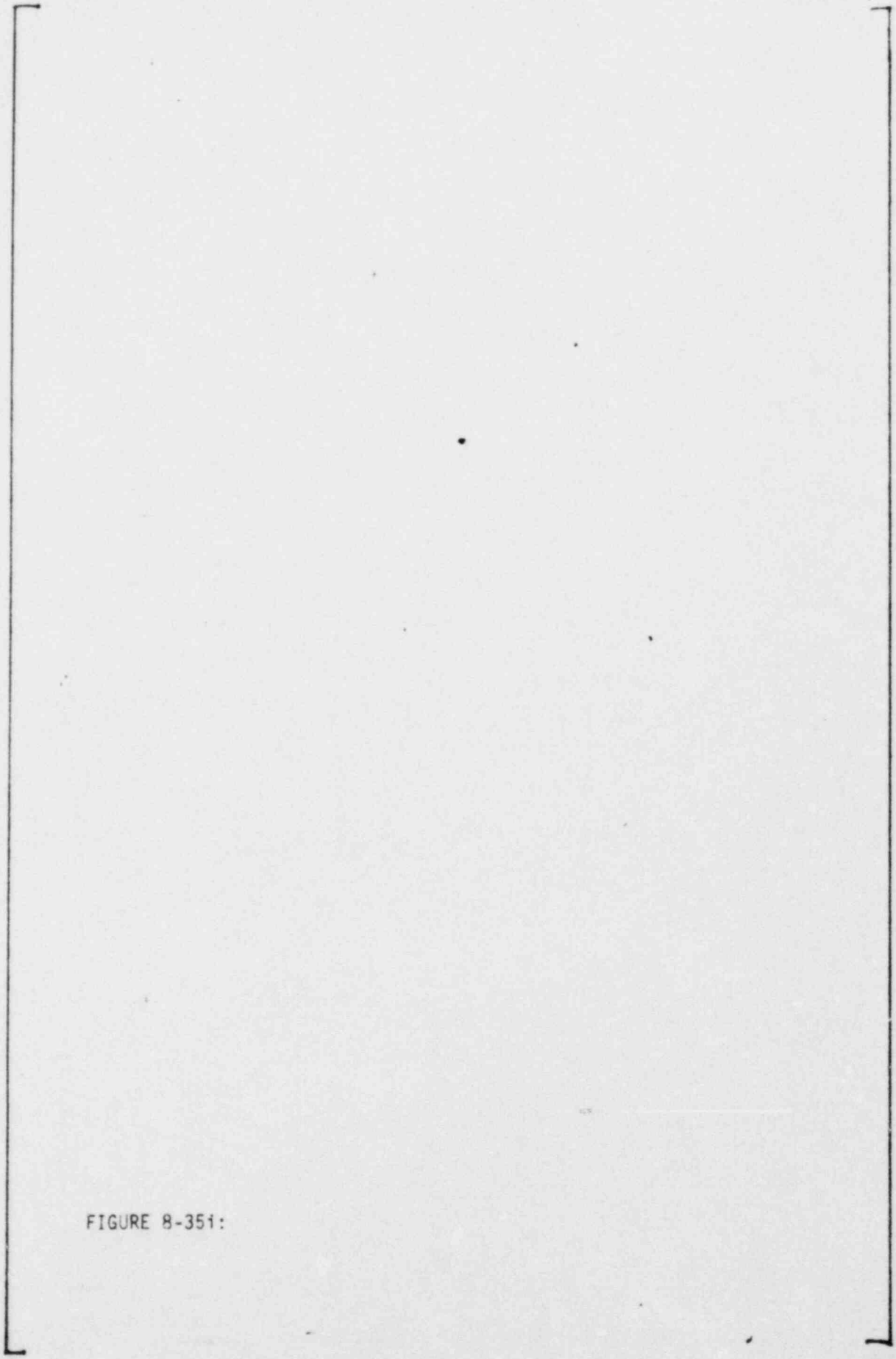

FIGURE 8-351:

a,b,c,e

[

]

FIGURE 8-36a:

a,b,c,e

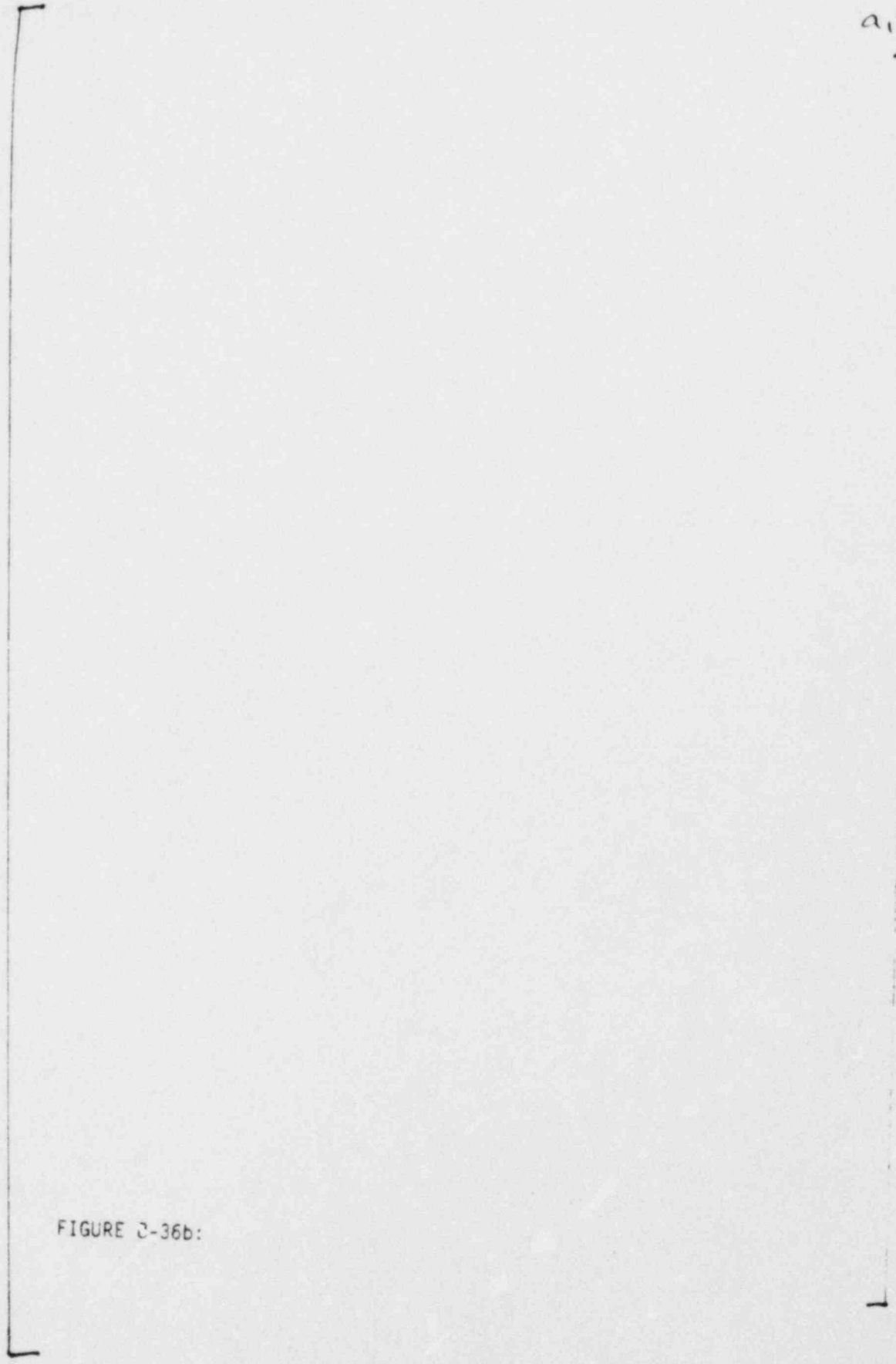

FIGURE 3-36b:

a,b,c,e

FIGURE 8-37:

FIGURE 8-38a:

a,b,c,e

a,b,c,e

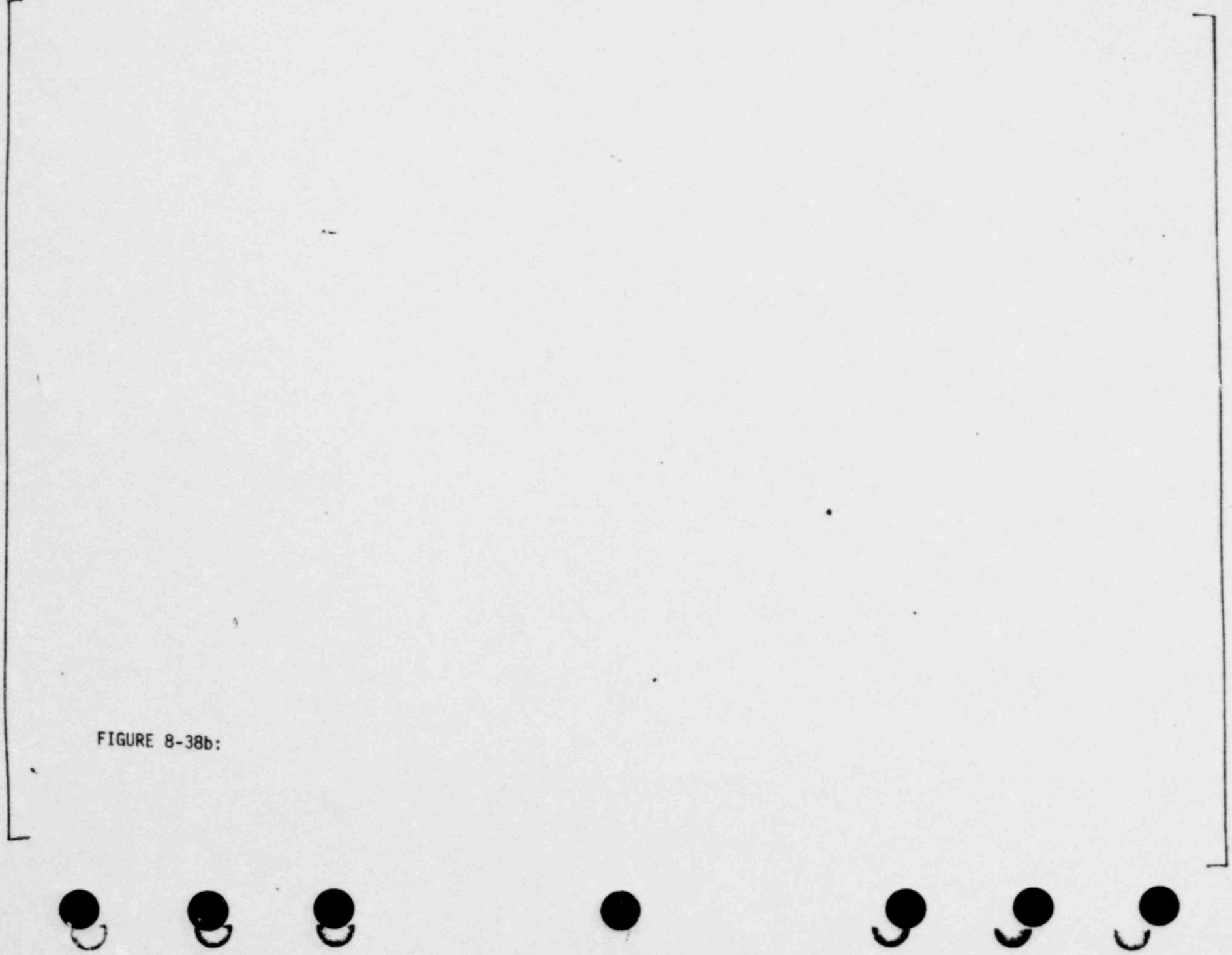

FIGURE 8-38b:

FIGURE 8-39a:

a,b,c,e

a,b,c,e

FIGURE 8-39b:

FIGURE 8-39c:

a,b,c,e

a,b,c,e

FIGURE 8-39d:

FIGURE 8-39e:

a,b,c,e

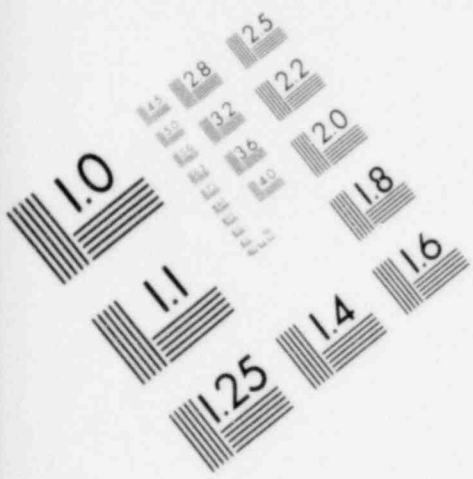

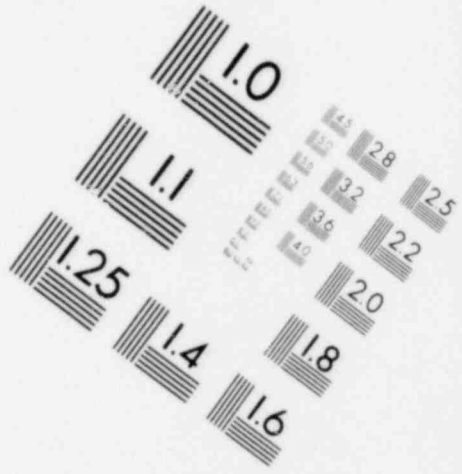

IMAGE EVALUATION TEST TARGET (MT-3)

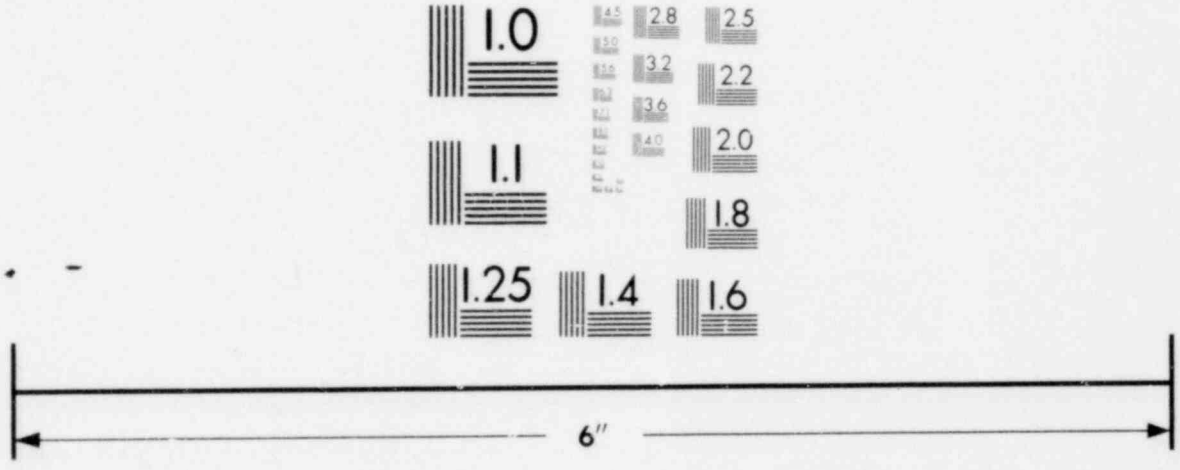

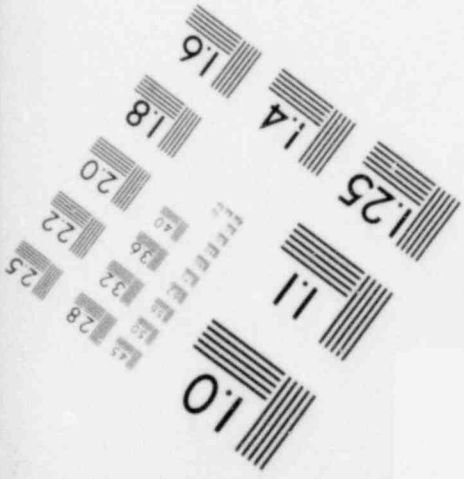

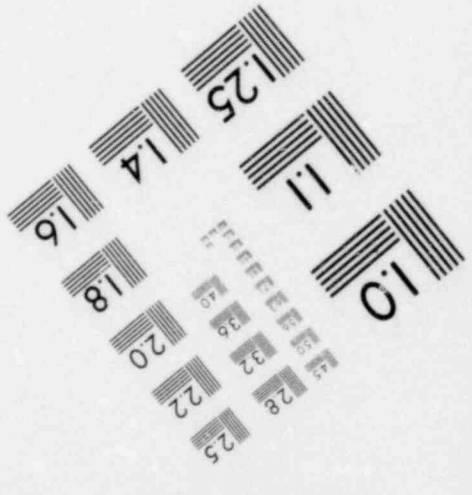

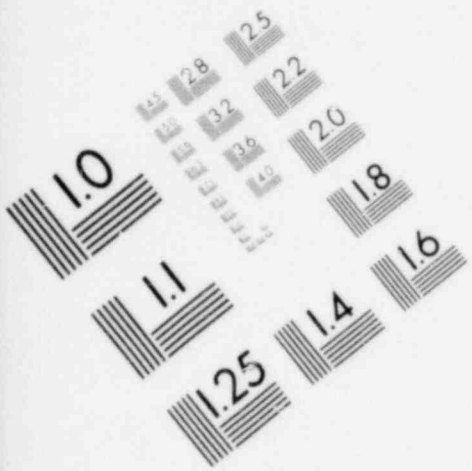

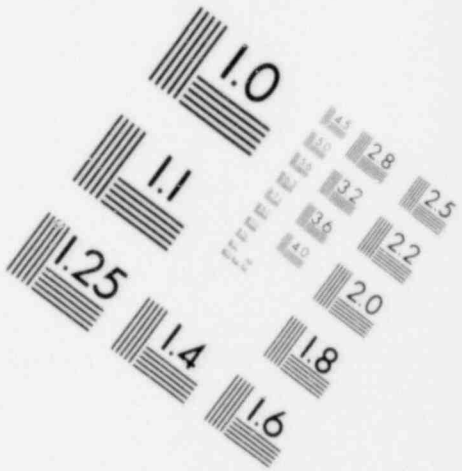

IMAGE EVALUATION TEST TARGET (MT-3)

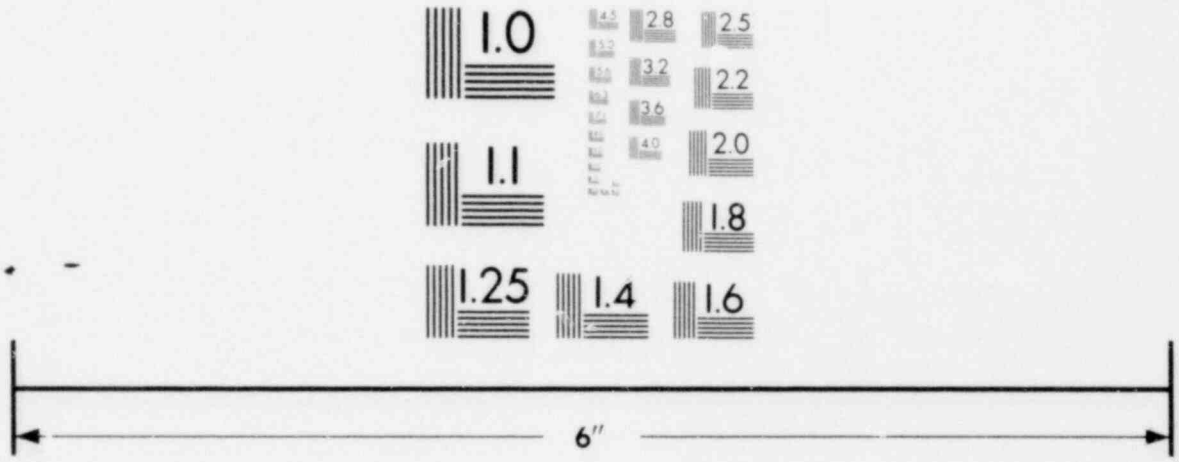

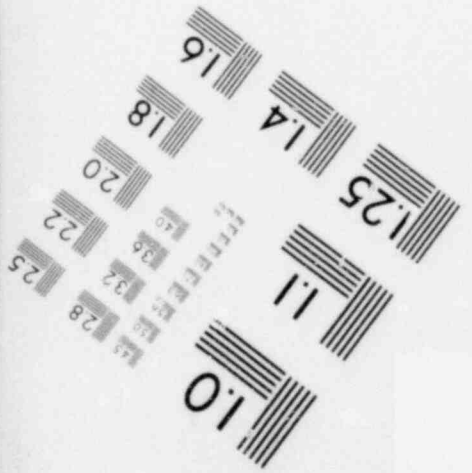

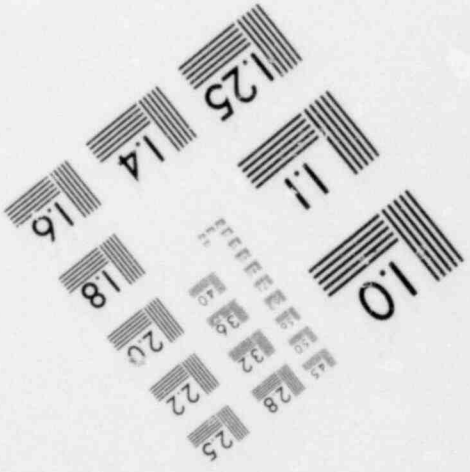

a,b,c,e

FIGURE 8-39f:

FIGURE 8-39g:

a,b,c,e

a,b,c,e

FIGURE 8-39h:

FIGURE 8-39i:

a,b,c,e

a,b,c,e

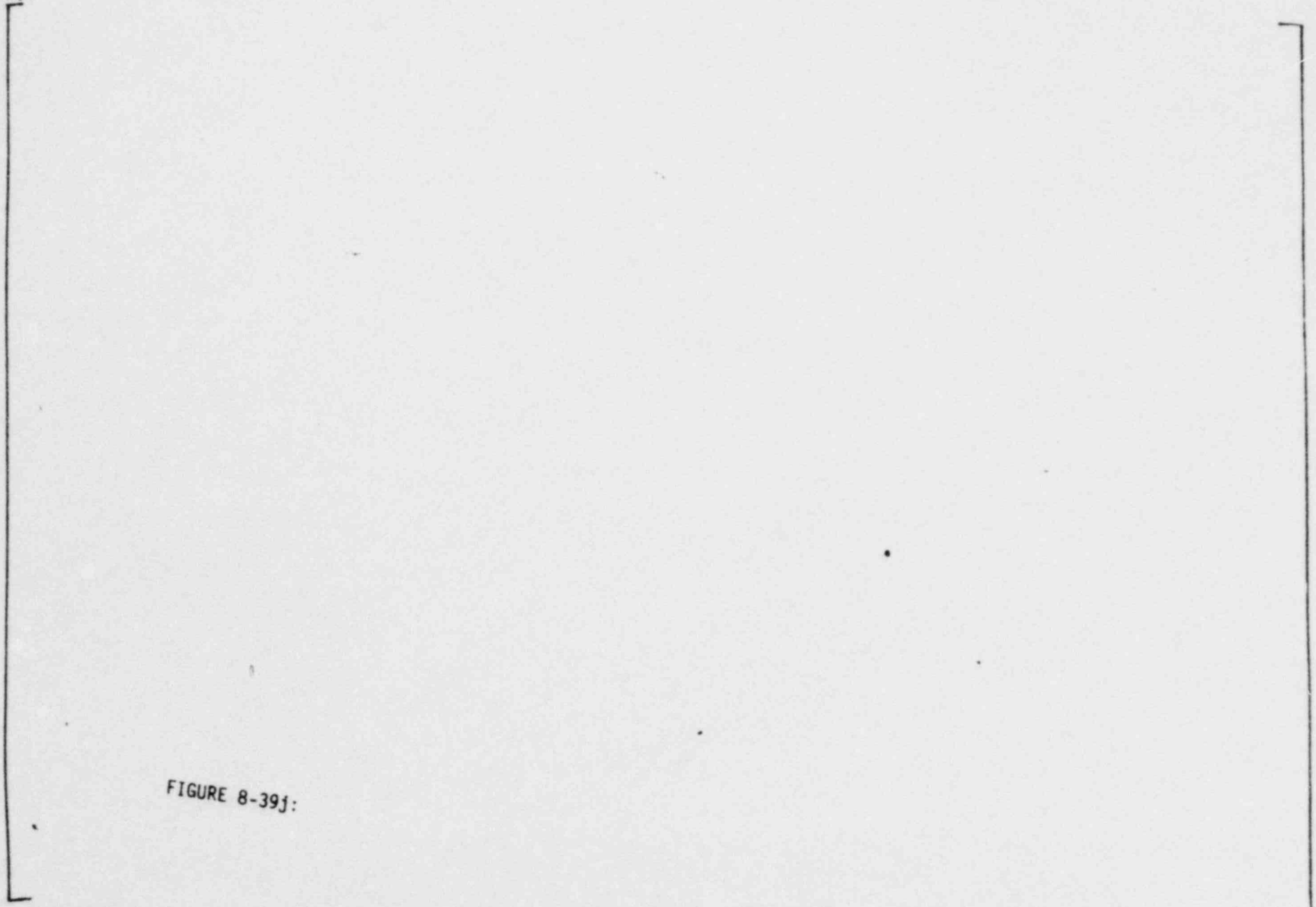

FIGURE 8-39j:

FIGURE 8-39k:

a,b,c,e

a,b,c,e

FIGURE 8-391:

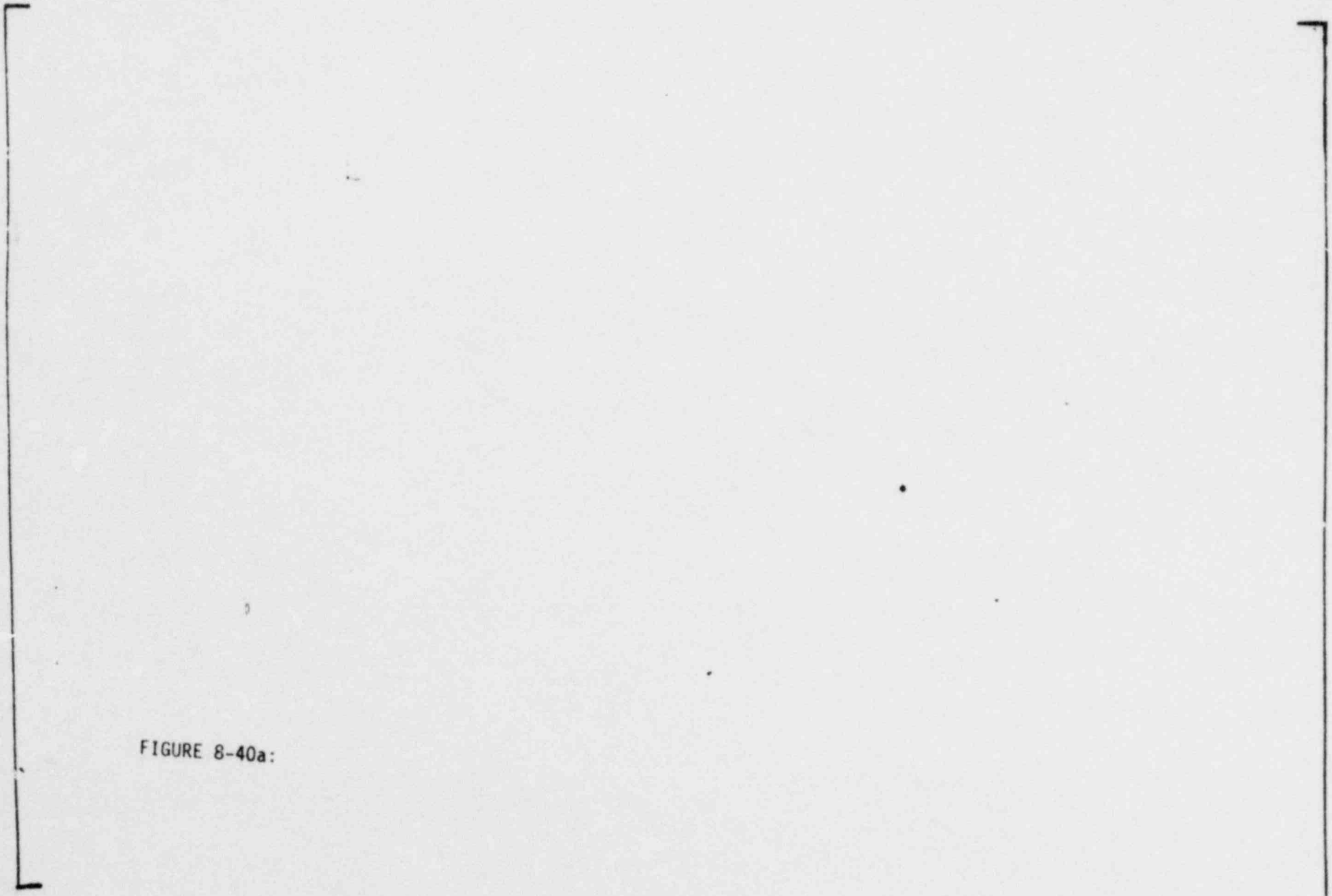

FIGURE 8-40a:

a,b,c,e

a,b,c,e

FIGURE 8-40b:

FIGURE 8-40c:

a,b,c,e

a,b,c,e

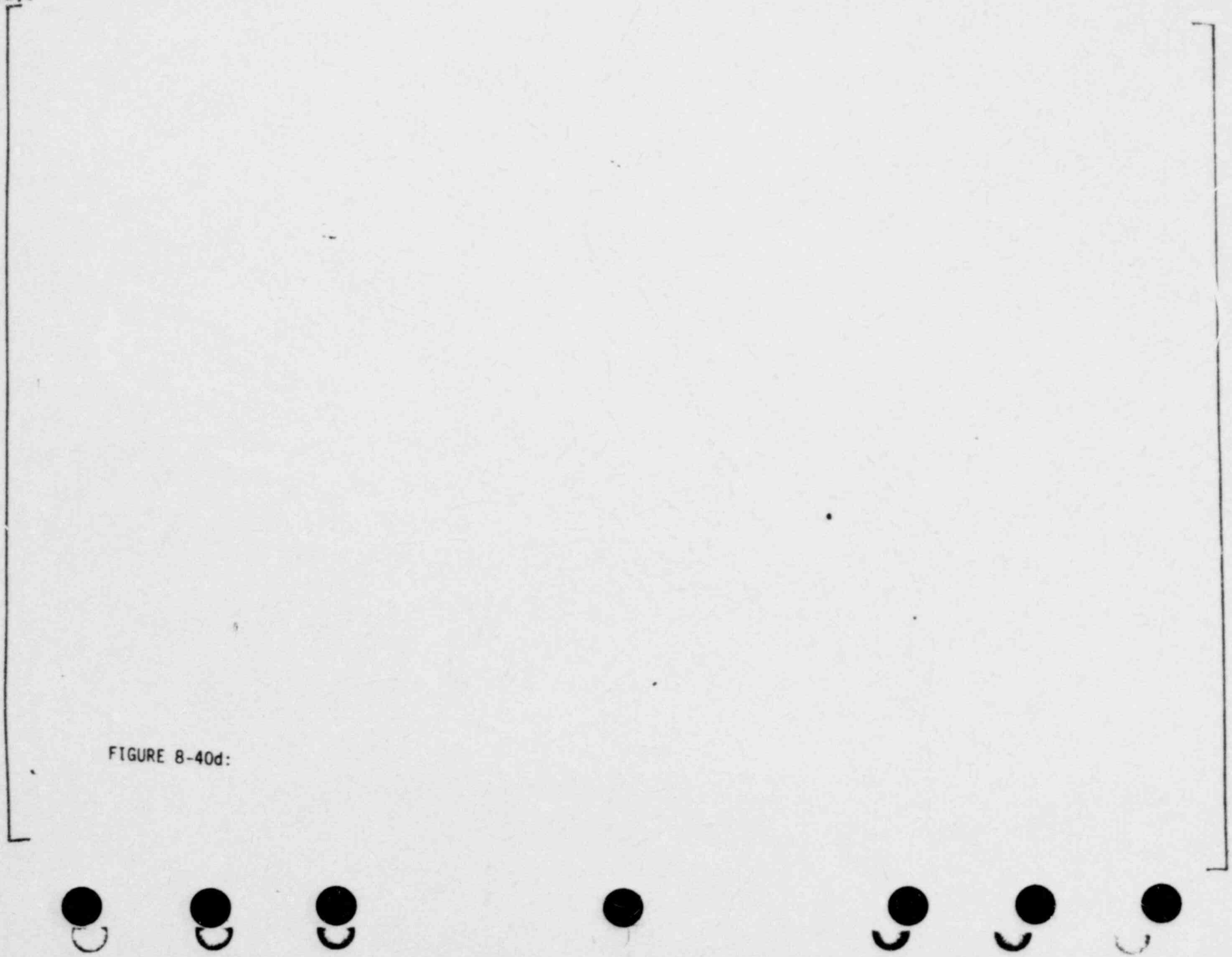

FIGURE 8-40d:

FIGURE 8-40e:

a,b,c,e

a,b,c,e

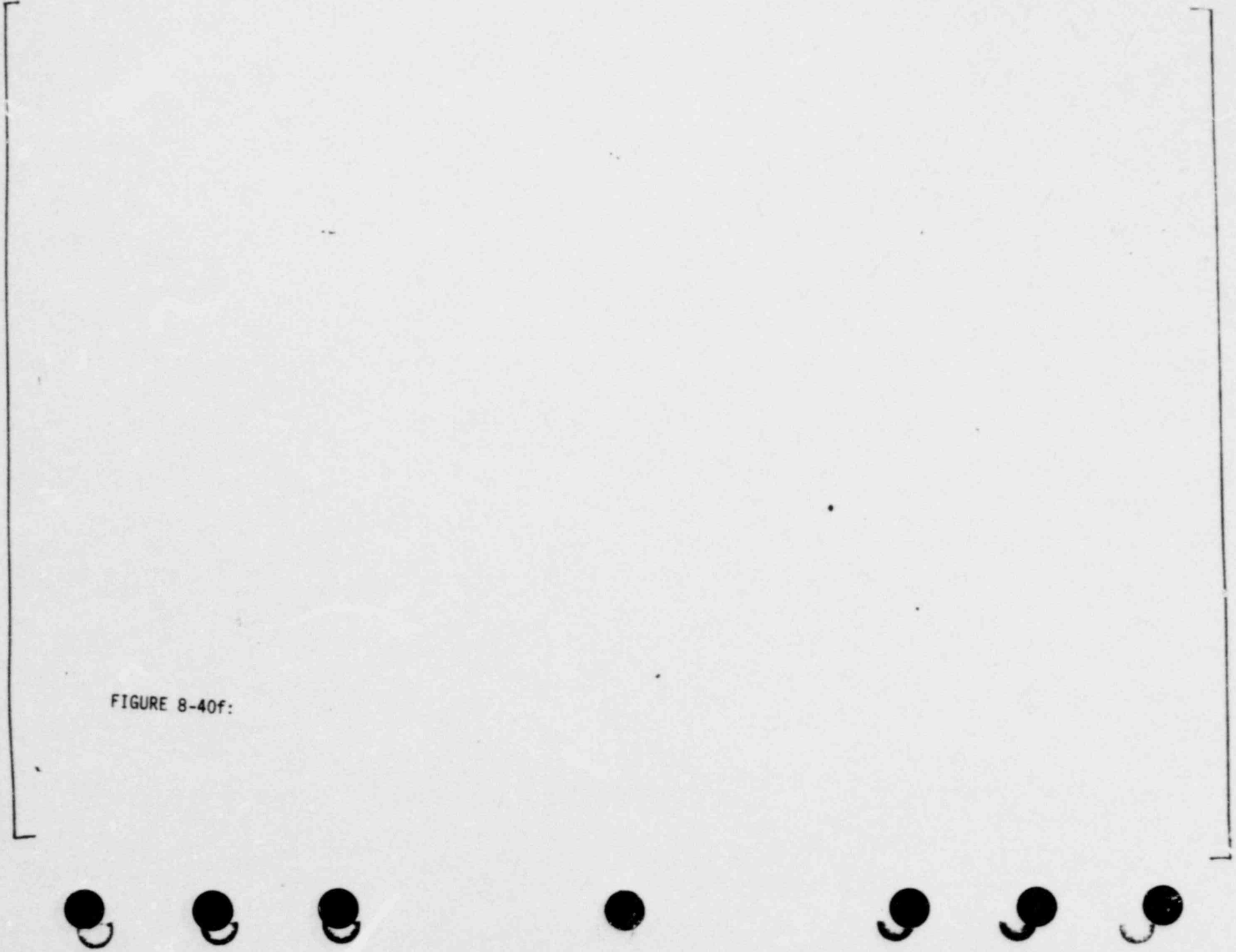

FIGURE 8-40f:

FIGURE 8-40g:

a,b,c,e

a,b,c,e

FIGURE 8-40h:

FIGURE 8-401

a,b,c,e

a,b,c,e

FIGURE 8-40j:

FIGURE 8-40k:

a,b,c,e

a,b,c,e

[

]

FIGURE 8-401:

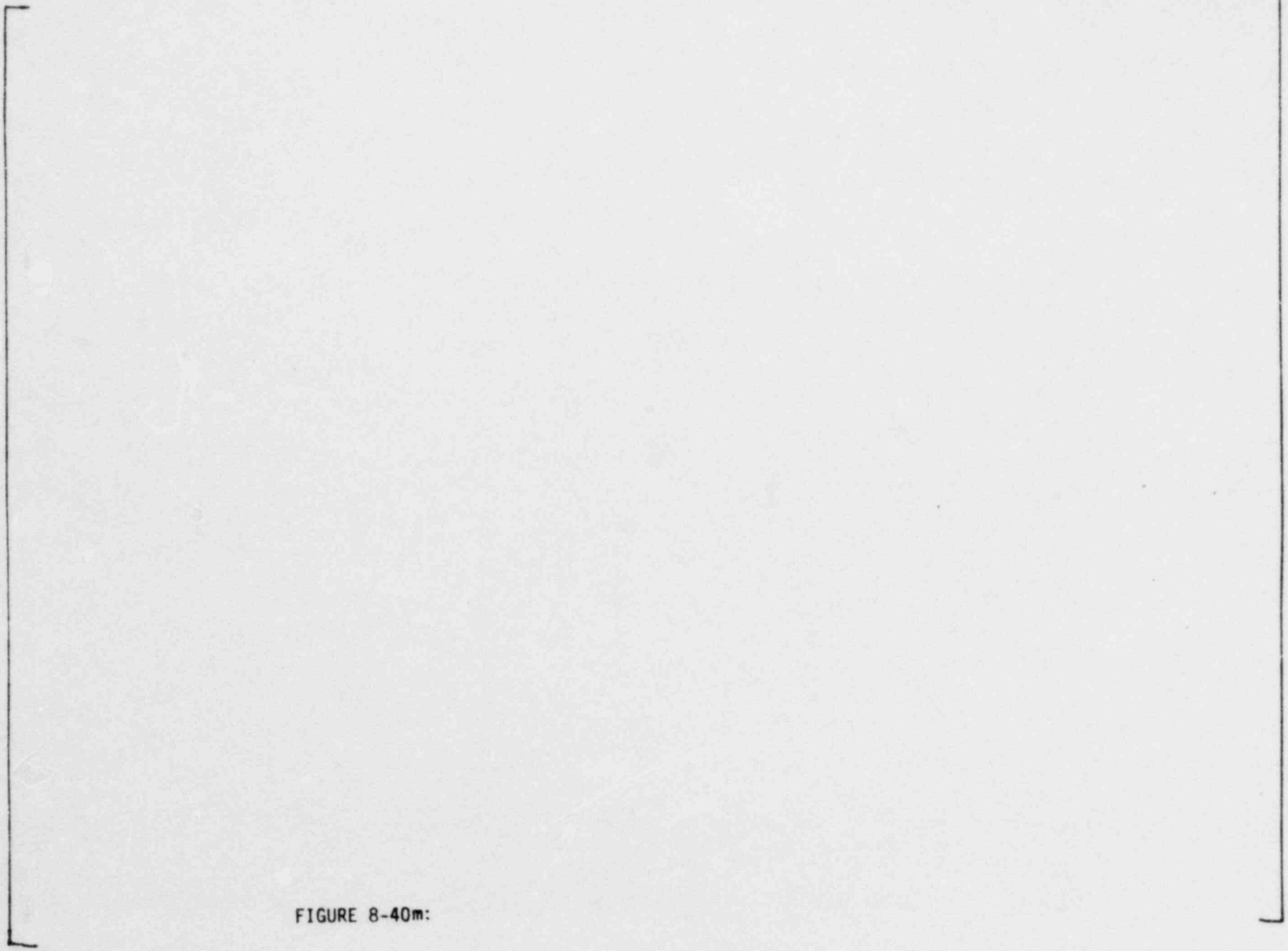

FIGURE 8-40m:

a,b,c,e

a,b,c,e

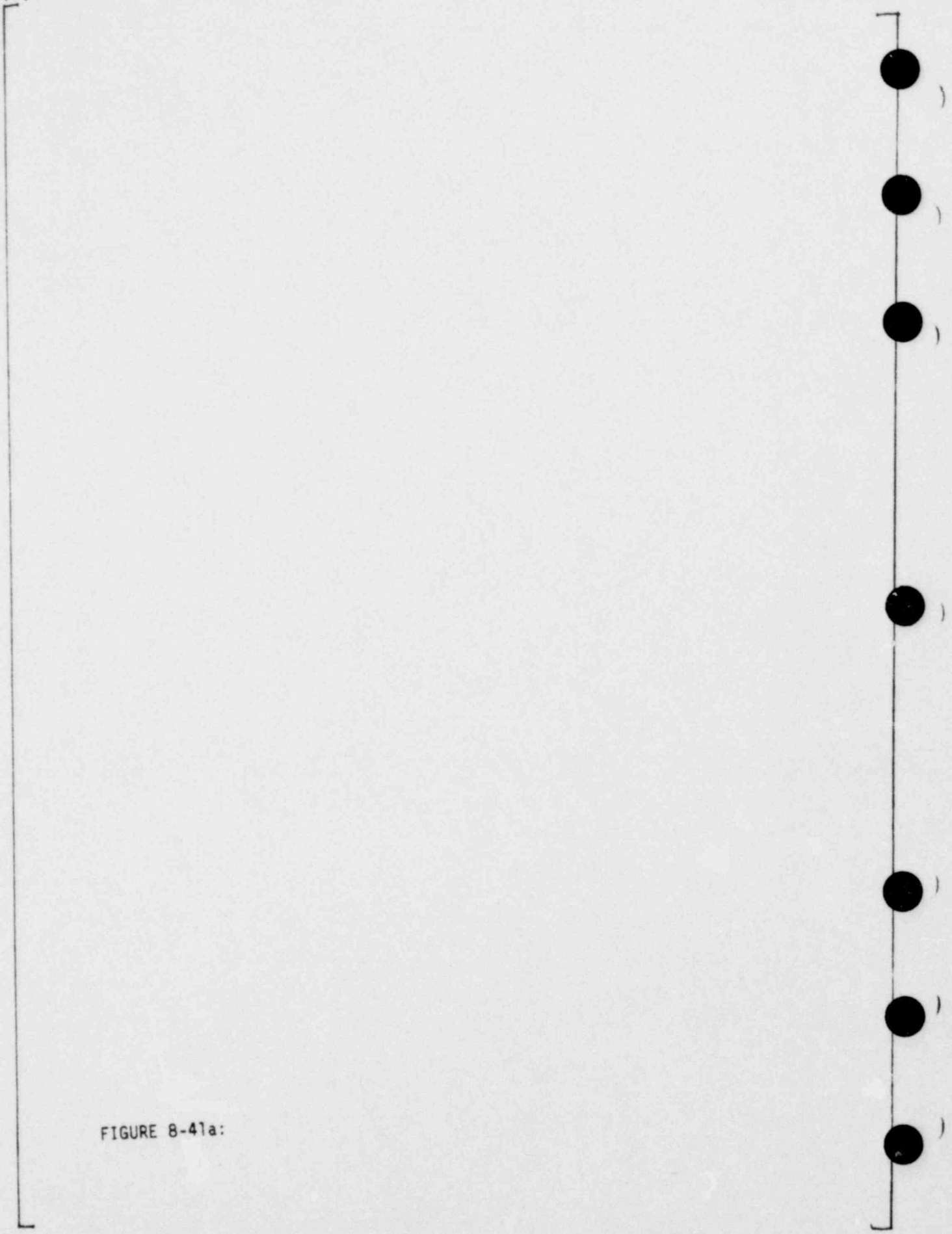

FIGURE 8-41a:

a,b,c,e

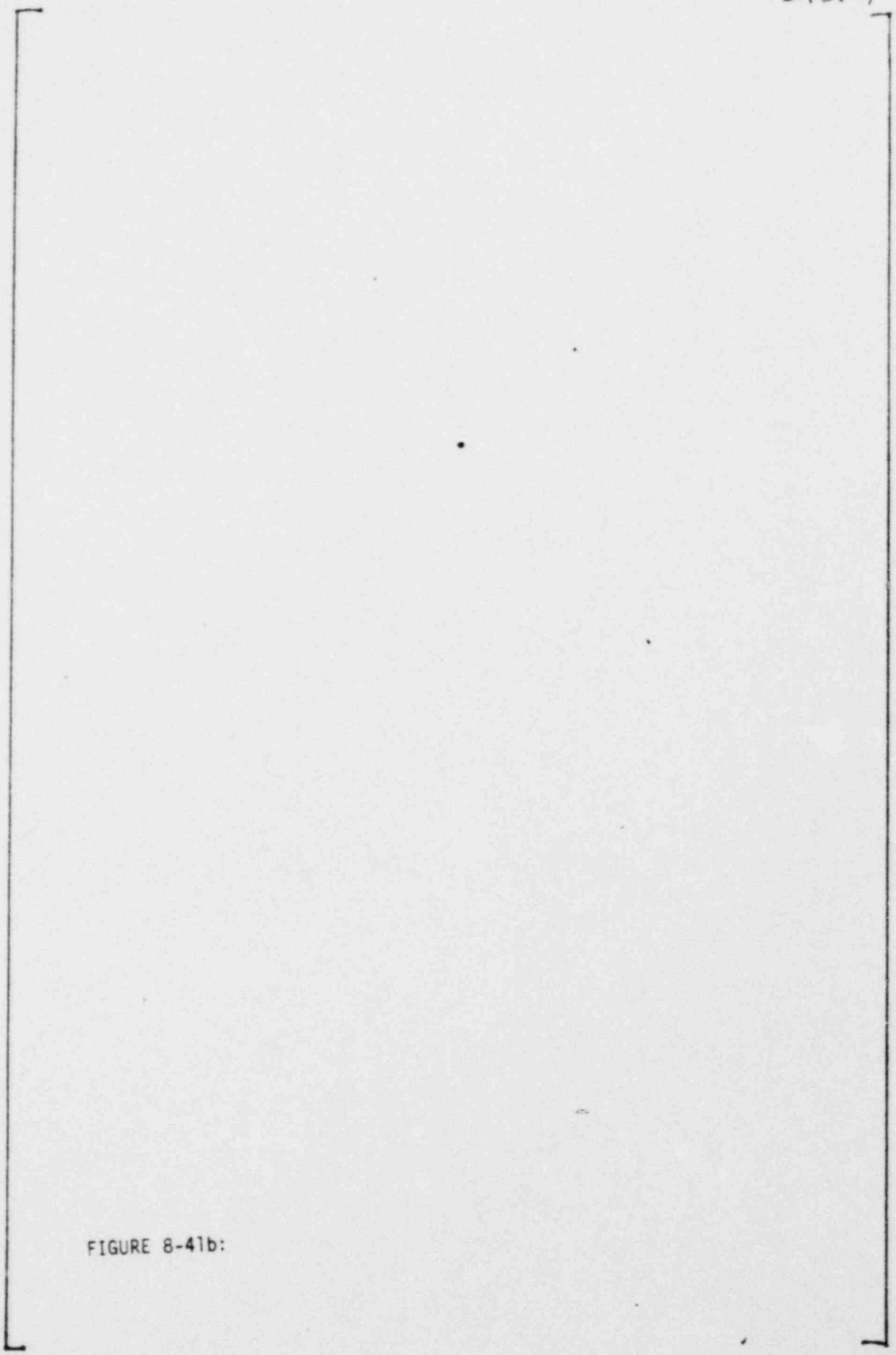

FIGURE 8-41b:

a,b,c,e

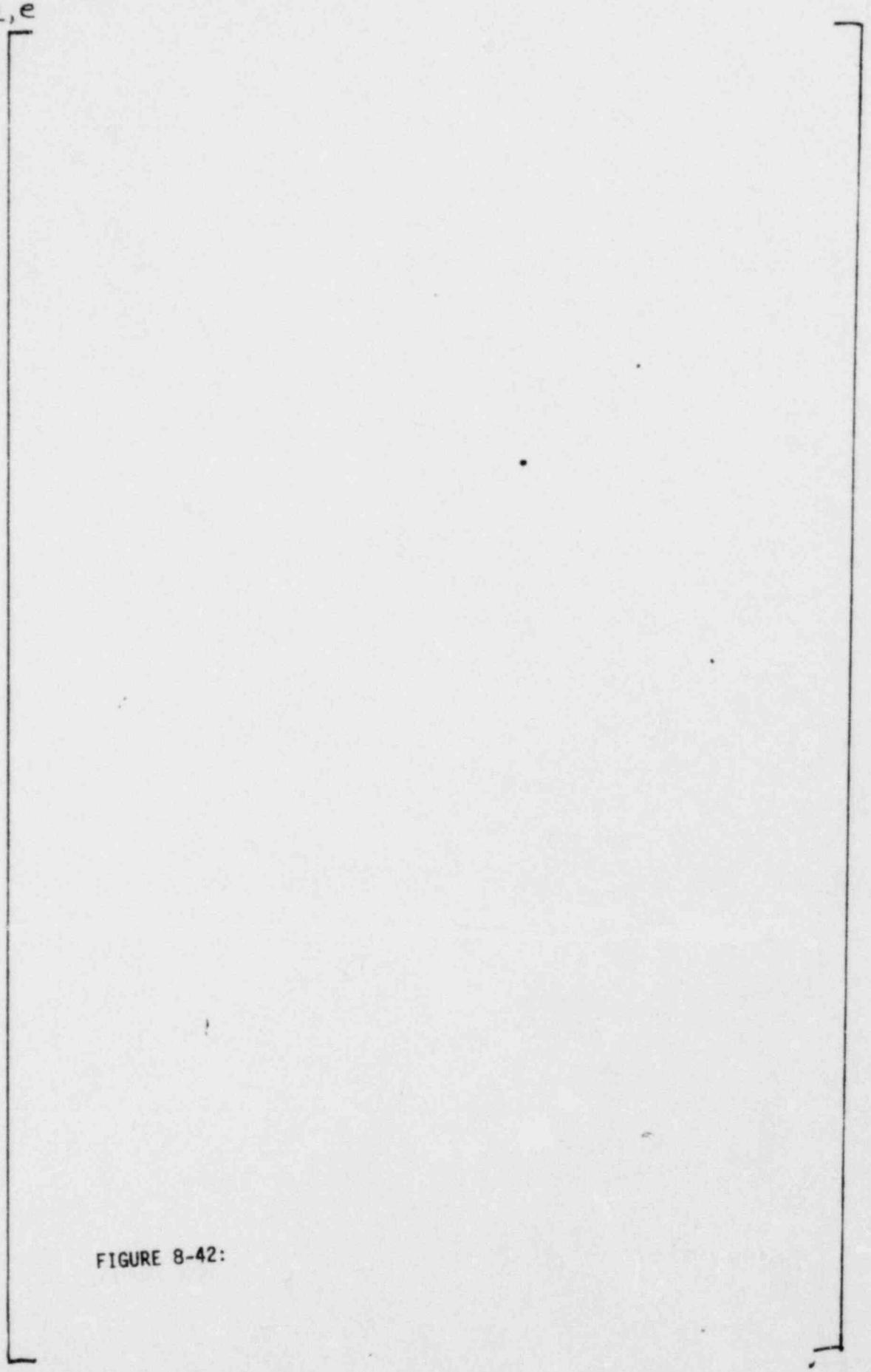

FIGURE 8-42:

FIGURE 8-43a:

a,b,c,e

a,b,c,e

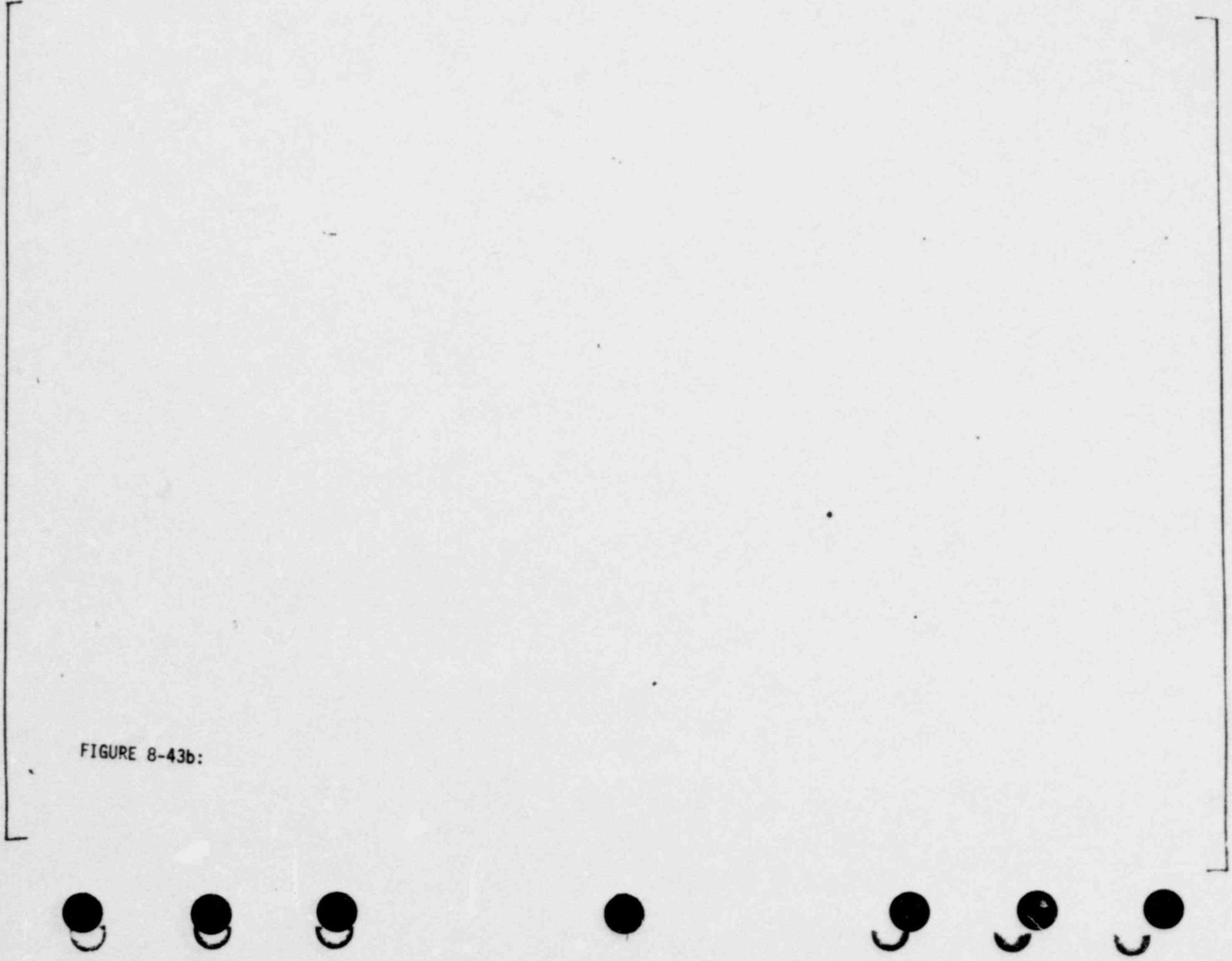

FIGURE 8-43b:

FIGURE 8-44a:

a,b,c,e

a,b,c,e

FIGURE 8-44b:

FIGURE 8-44c:

a,b,c,e

a,b,c,e

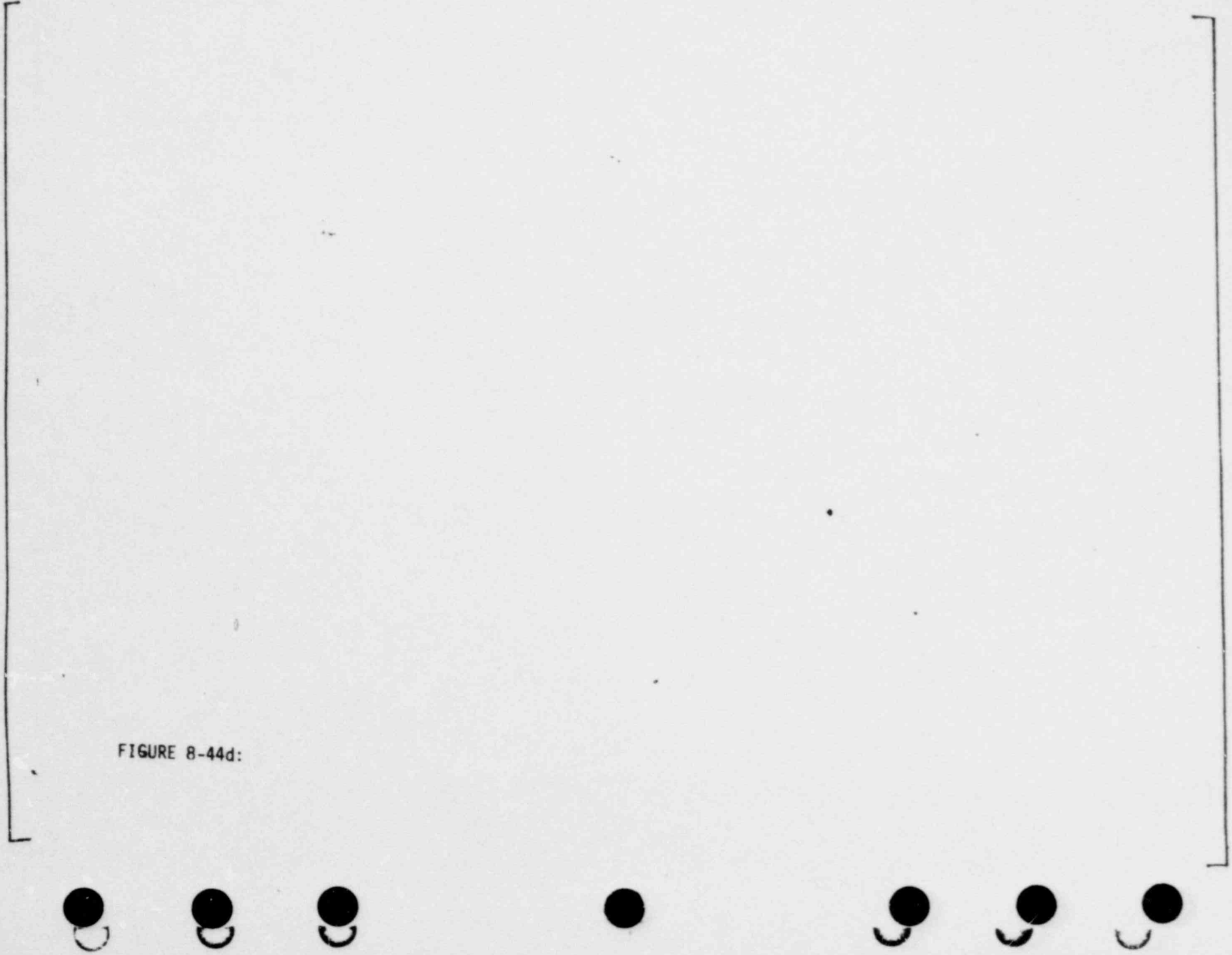

FIGURE 8-44d:

FIGURE 8-44e:

a,b,c,e

a,b,c,e

FIGURE 8-44f:

FIGURE 8-44g:

a,b,c,e

a,b,c,e

FIGURE 8-44h:

FIGURE 8-441:

a,b,c,e

1,b,c,e

FIGURE 8-44j:

FIGURE 8-45:

a,b,c,e

a,b,c,e

FIGURE 8-46:

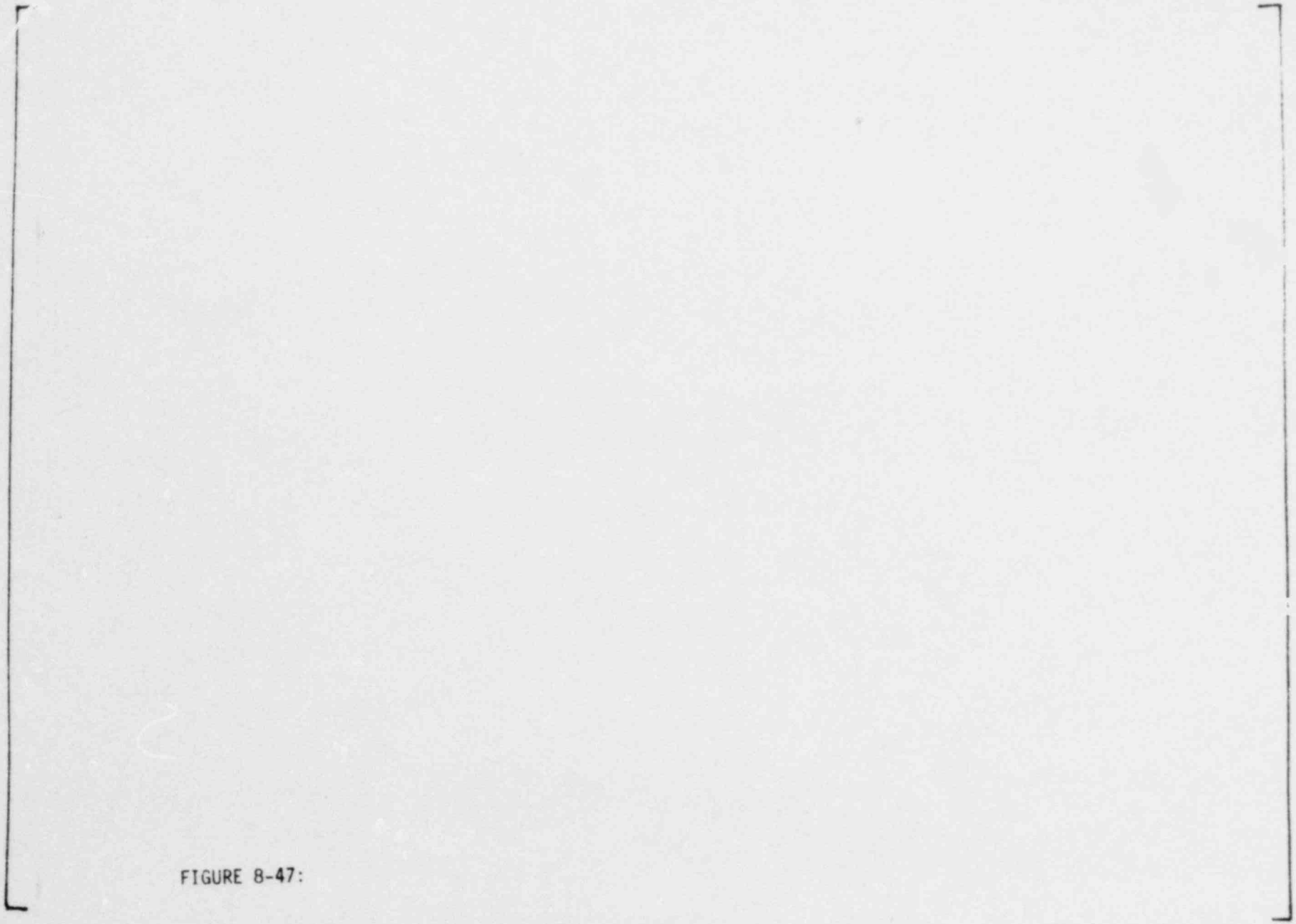

FIGURE 8-47:

a,b,c,e

a,b,c,e

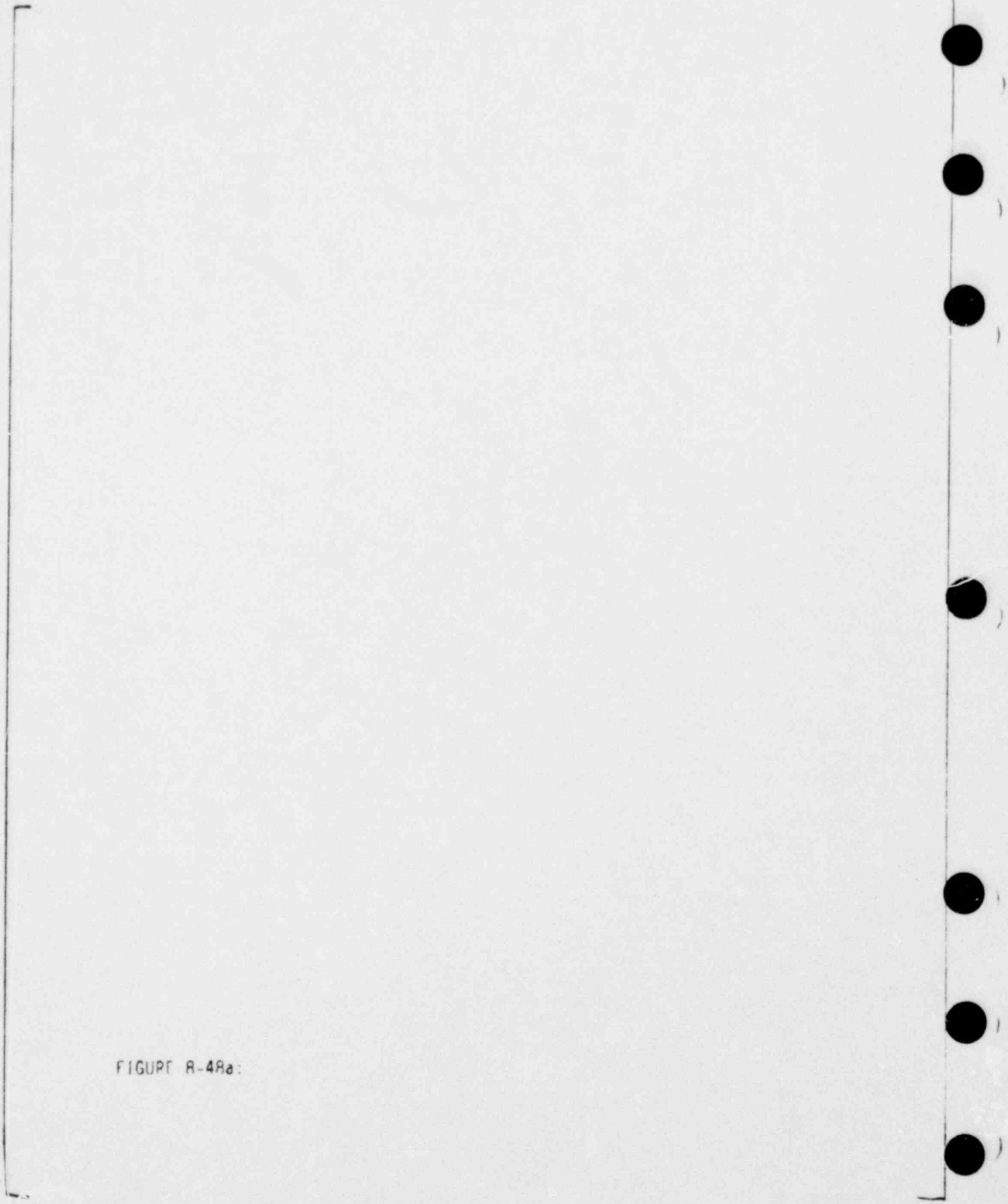

FIGURE 8-48a:

a,b,c,e

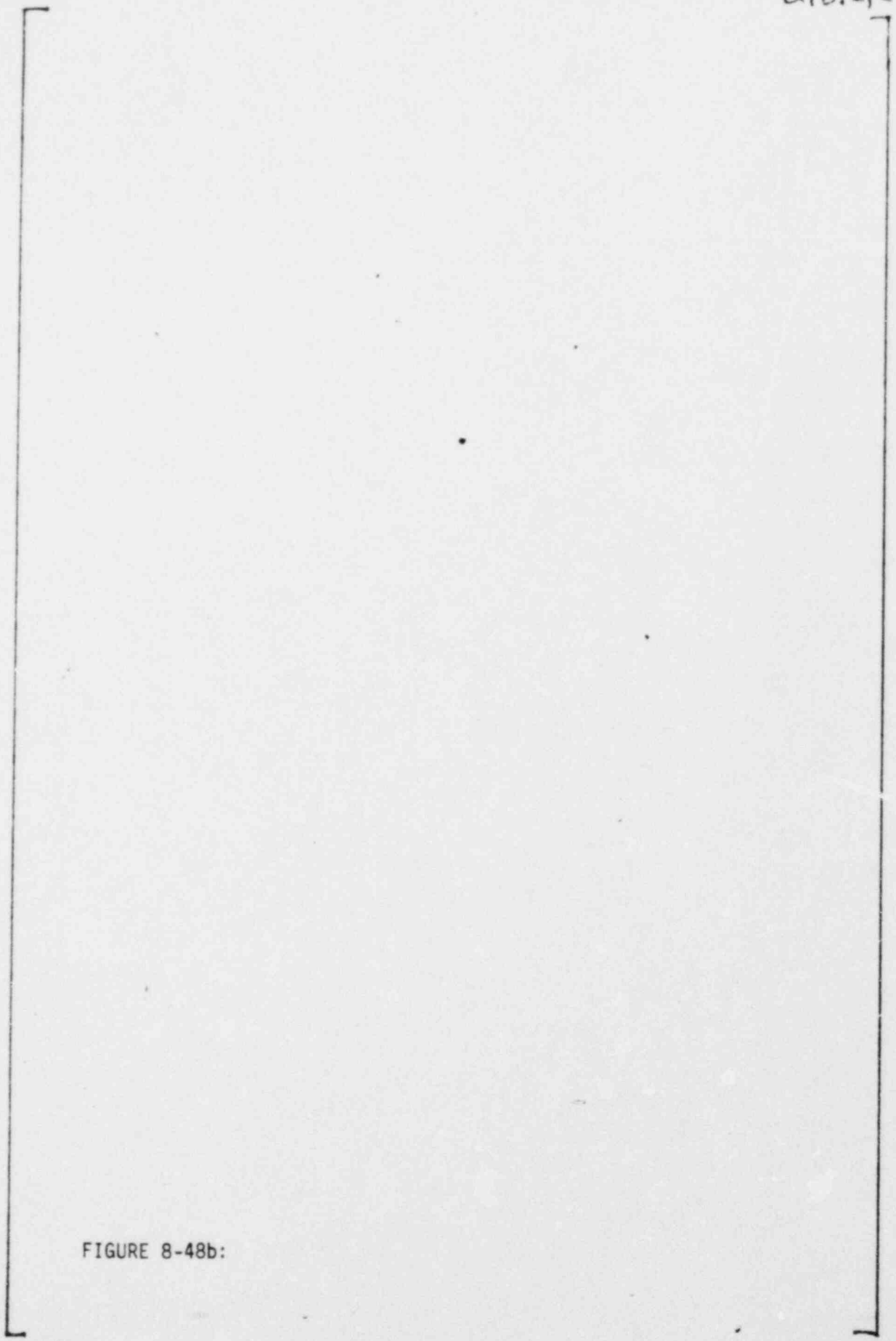

FIGURE 8-48b:

a, b, c, e

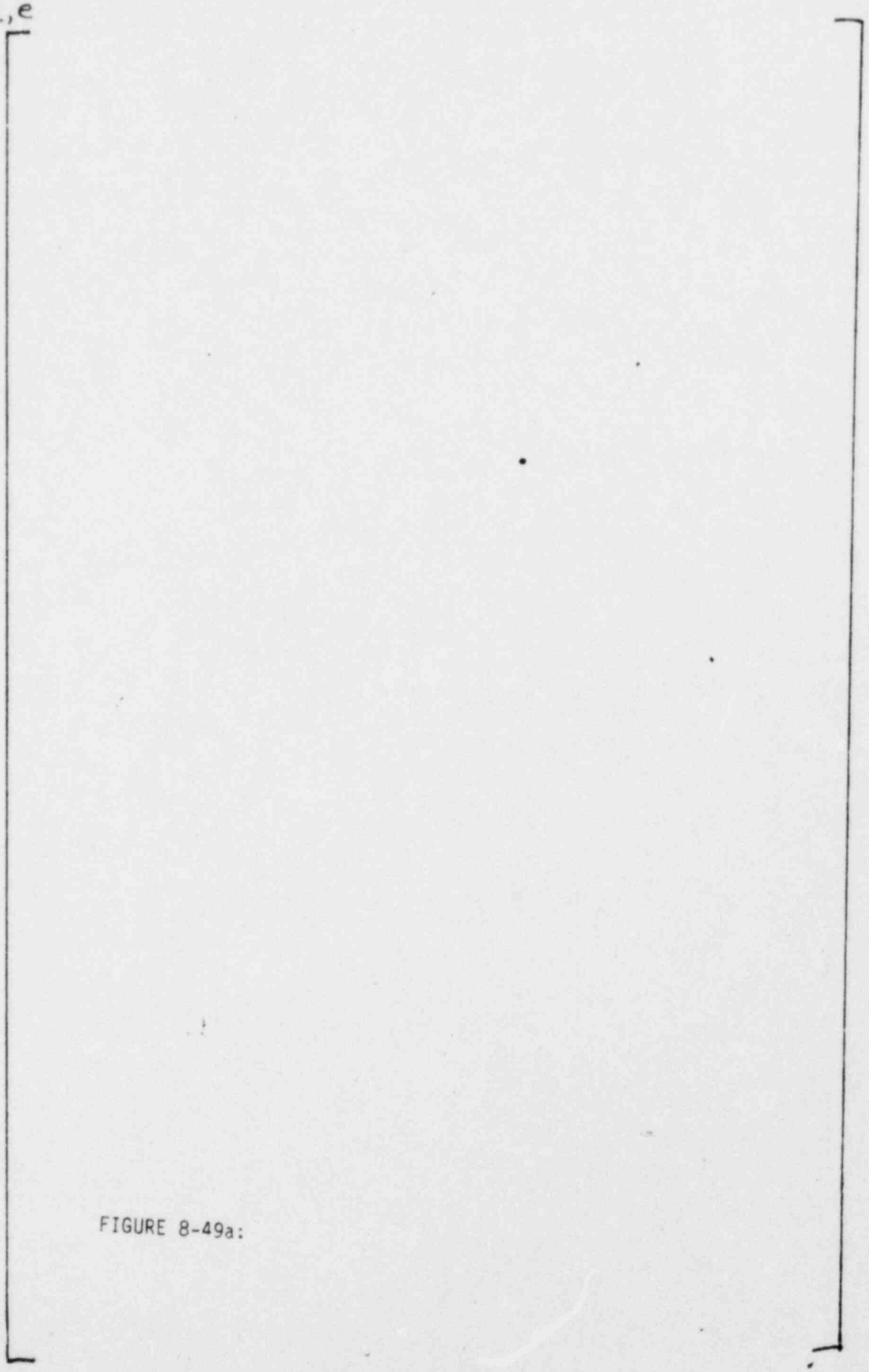

FIGURE 8-49a:

a,b,c,e

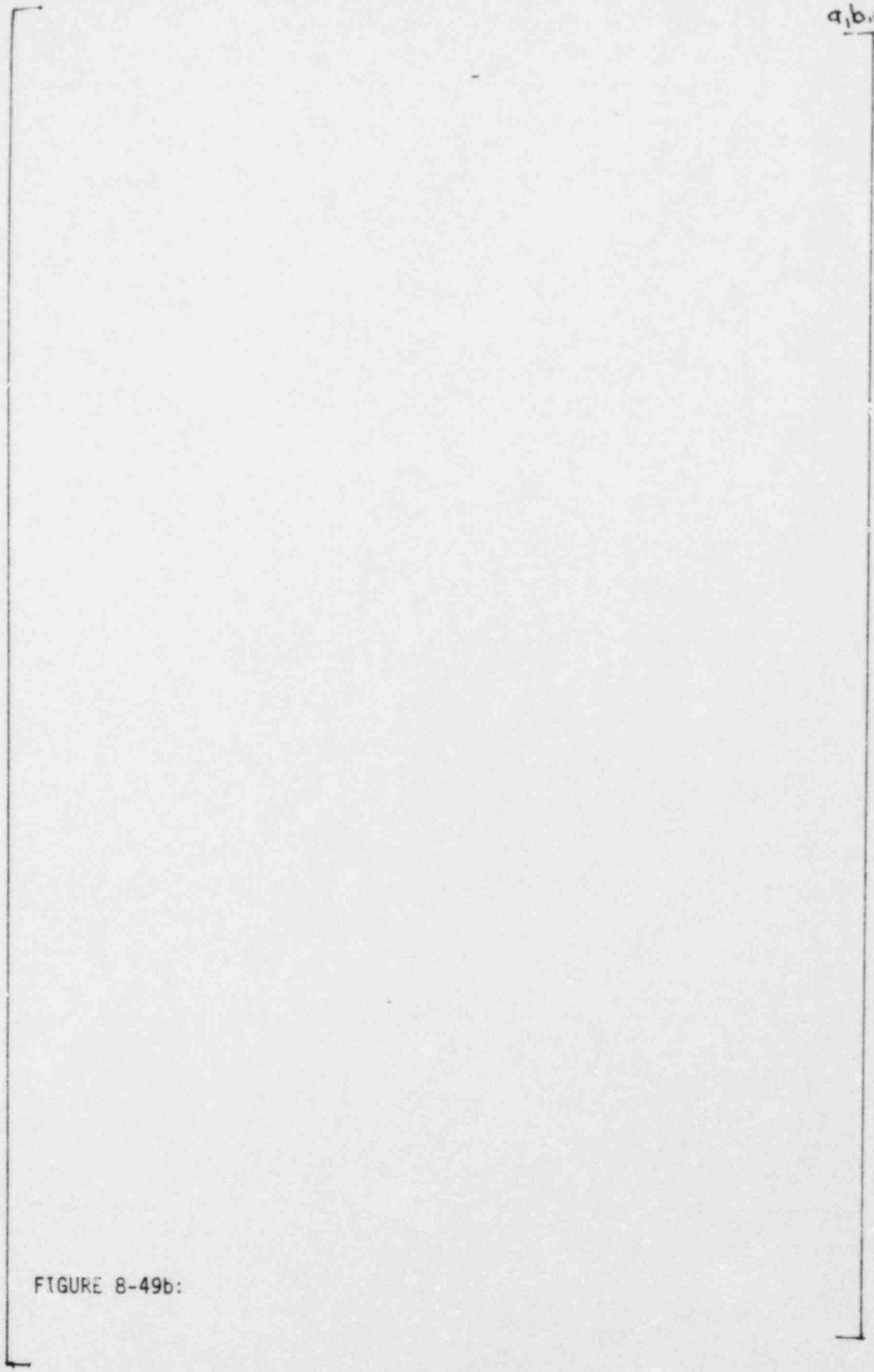

FIGURE 8-49b:

a,b,c,e

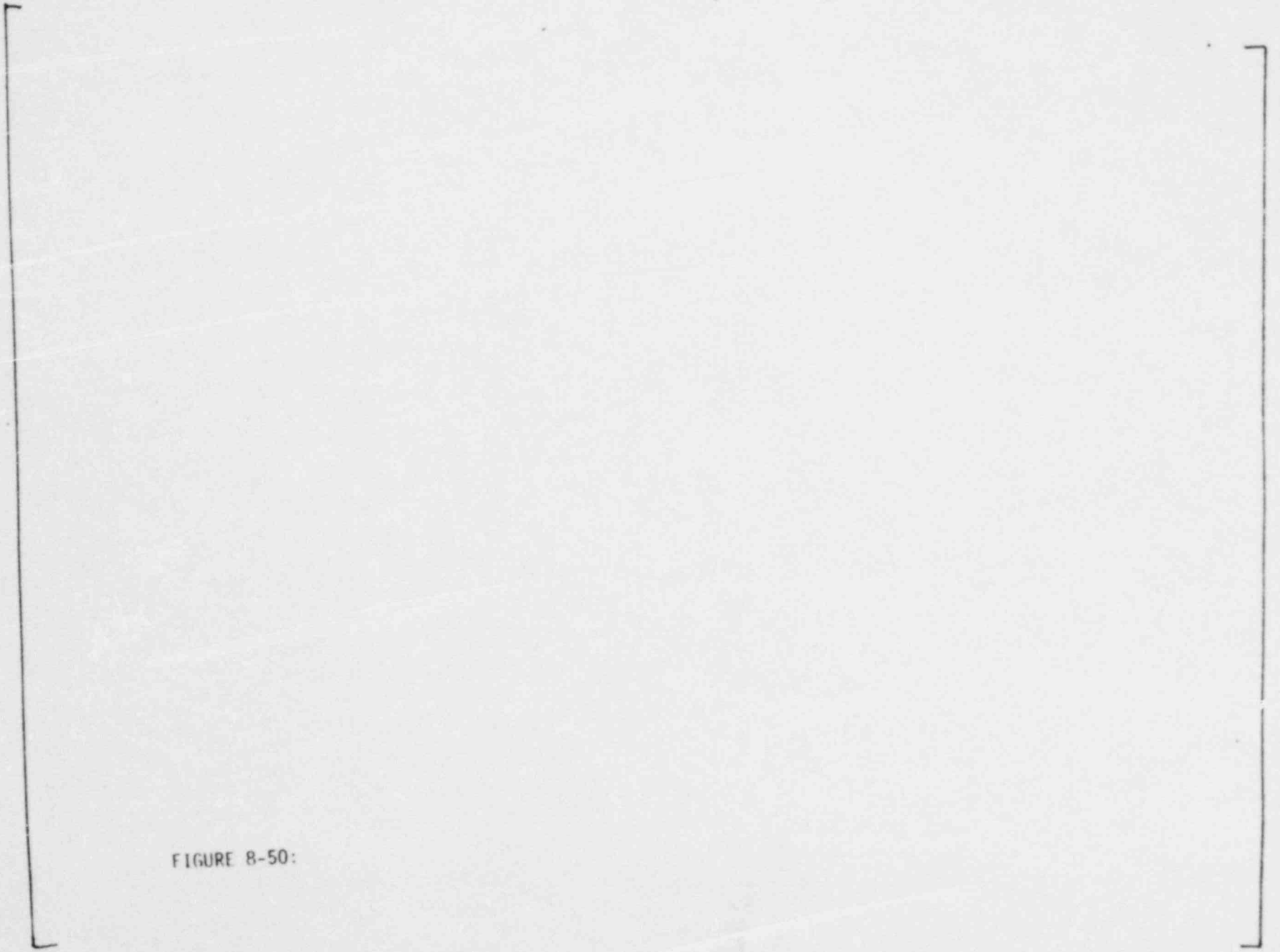

FIGURE 8-50:

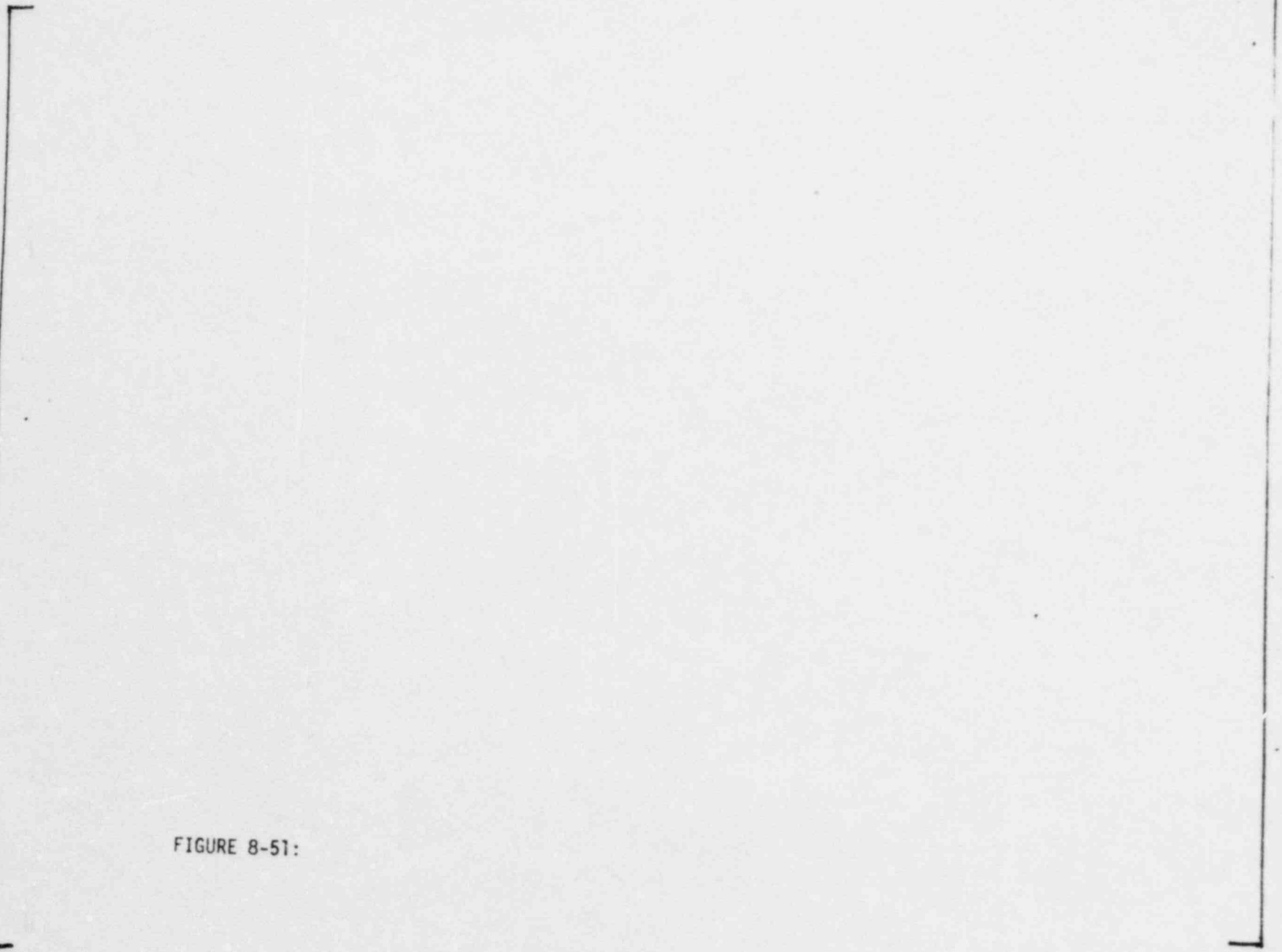

FIGURE 8-51:

a,b,e,e

APPENDIX 8A

FEEDWATER PROFILE SUMMARIES

This appendix contains plant specific profile data obtained from the site feedwater temperature data. The tabulated data cover the following sites tested to date:

PLANT	ACRONYM	LINE #	# PAGES
[		21	57
		24**	56
		1A	14
		1B	16
		2	5
		B Part I	5
		Part II	4
		C Part I	6
		Part II	5
		13	31 + 21
		14	43

a,c

*The data are for the test performed by W in 12/79 and 1/80.

[ ] a,b,c

The tables list the following information:

b,c

1. [redacted]
2. [redacted]
3. [redacted]
4. [redacted]
5. [redacted]
6. [redacted]
7. [redacted]
8. [redacted]

a,b,c

[redacted]

c

[redacted]

a,b,c

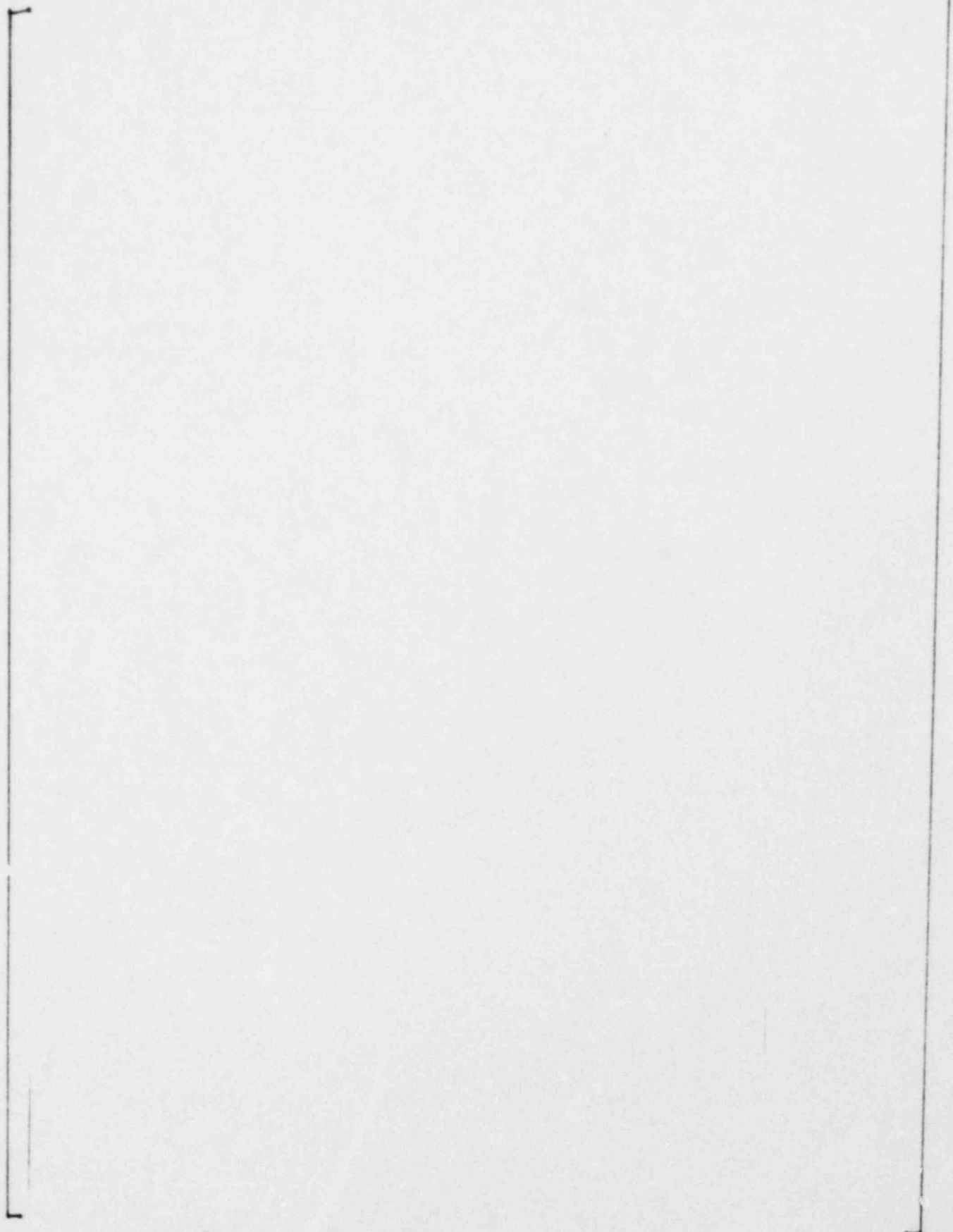

FIGURE 8A-1: [ ] TYPES USED IN THE CLASSIFICATION OF PLANT SPECIFIC PROFILES

[ ]a,b,c

a,b,c,e

a,b,c,e

[

a,b,c,e

[

]

a,b,c,e

[redacted]

a,b,c,e

a,b,c,e

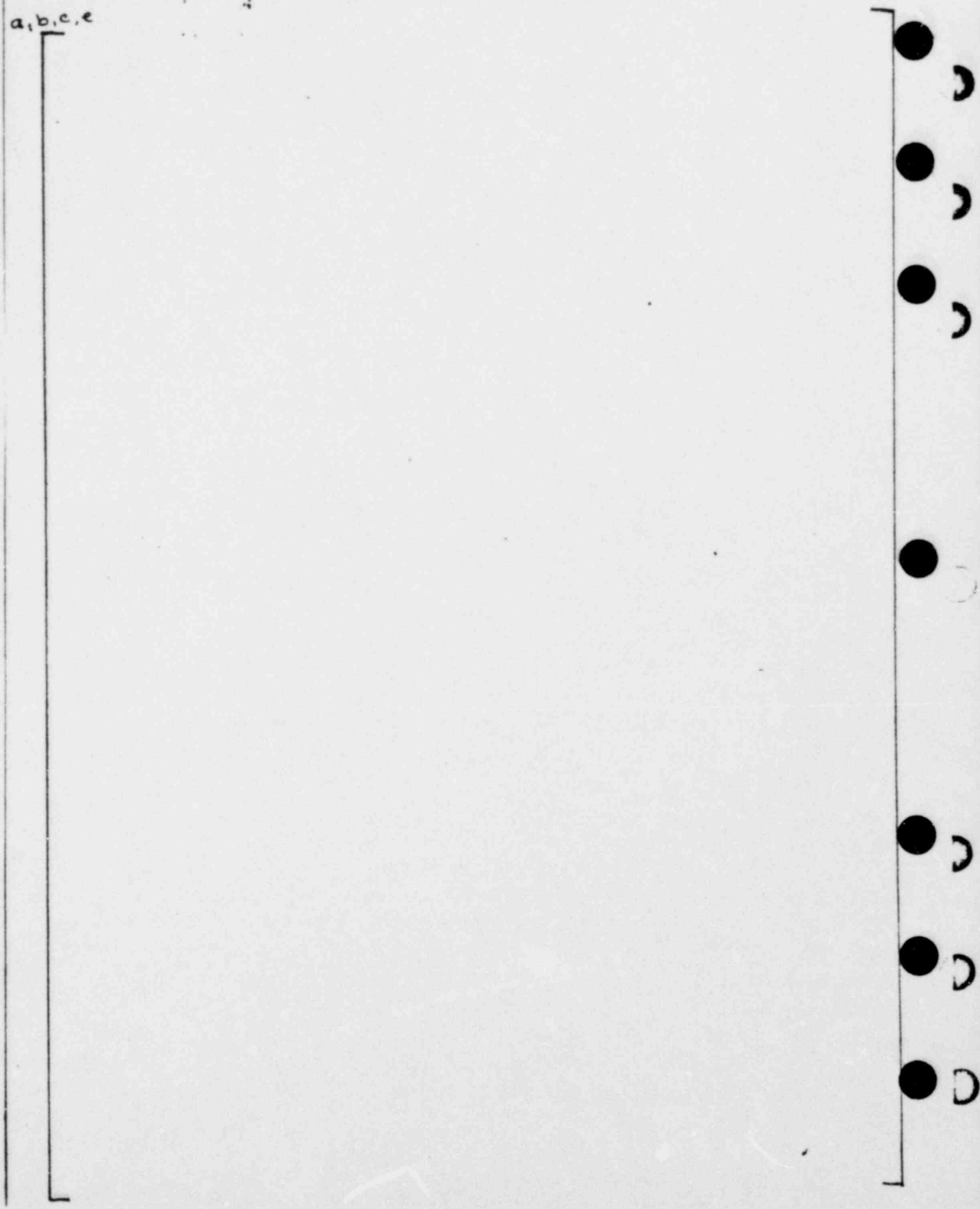

a,b,c,e

a,b,c,e

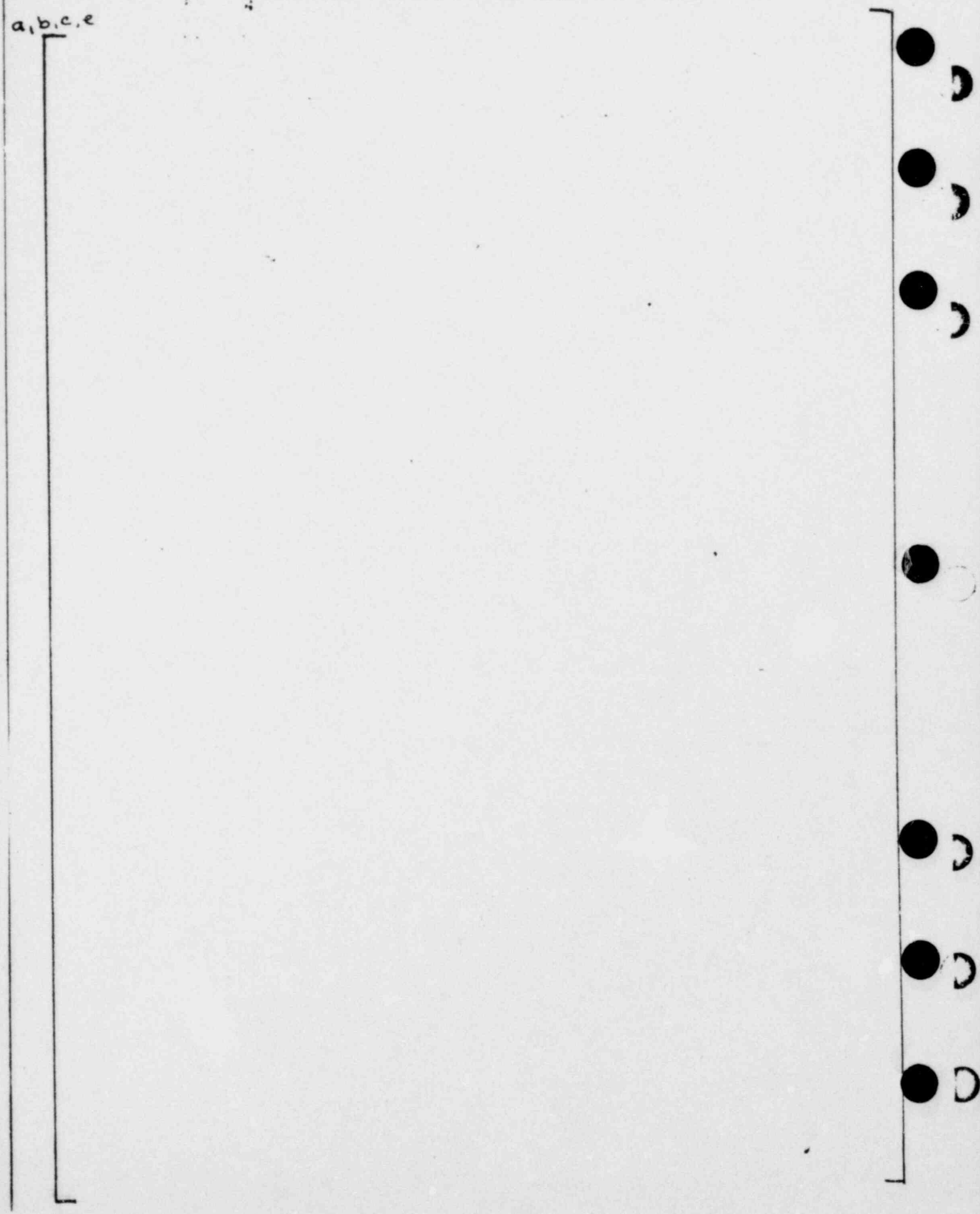

a,b,c,e

a,b,c,e

[redacted]

a,b,c,e

a,b,c,e

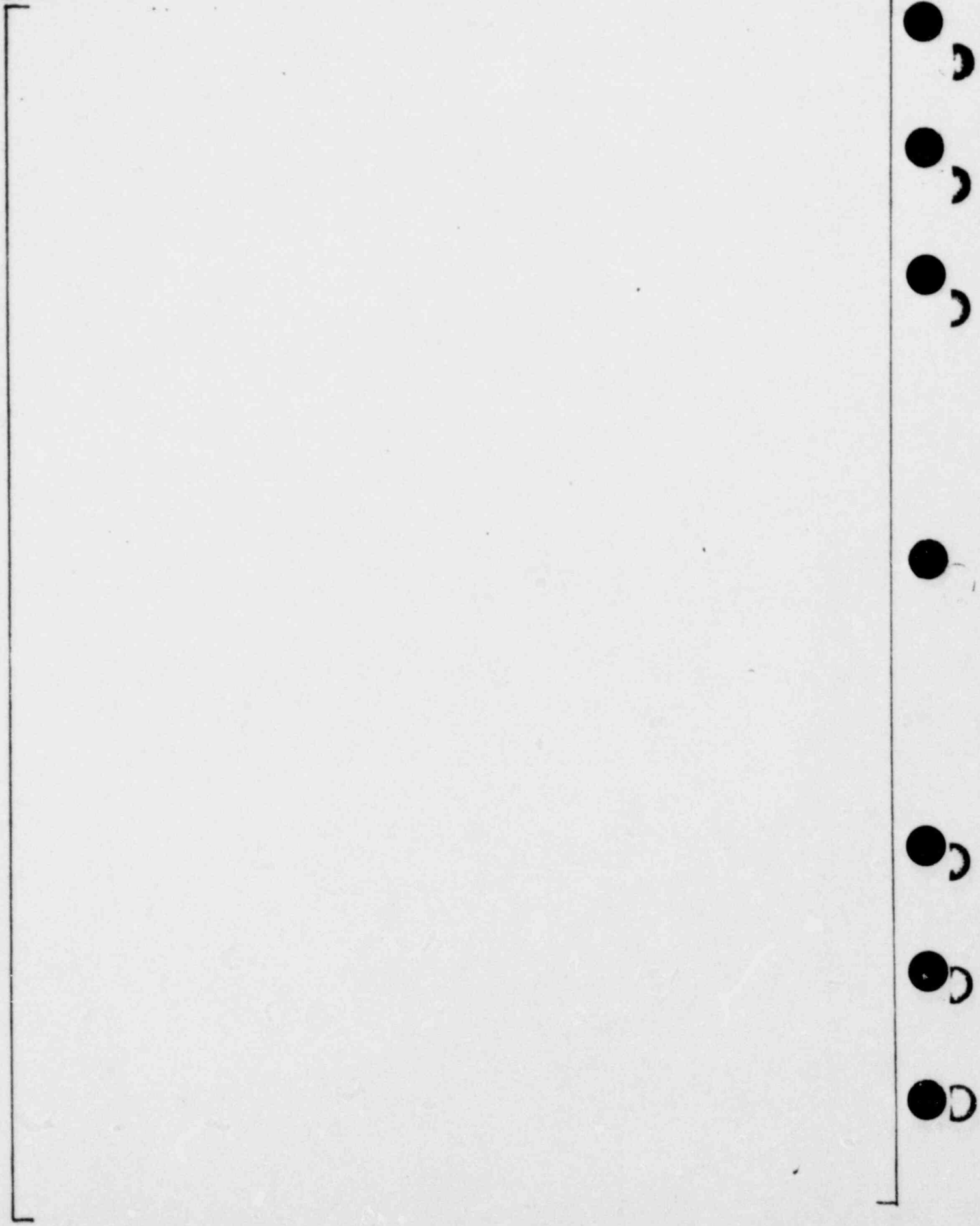

a,b,c,e

a,b,c,e

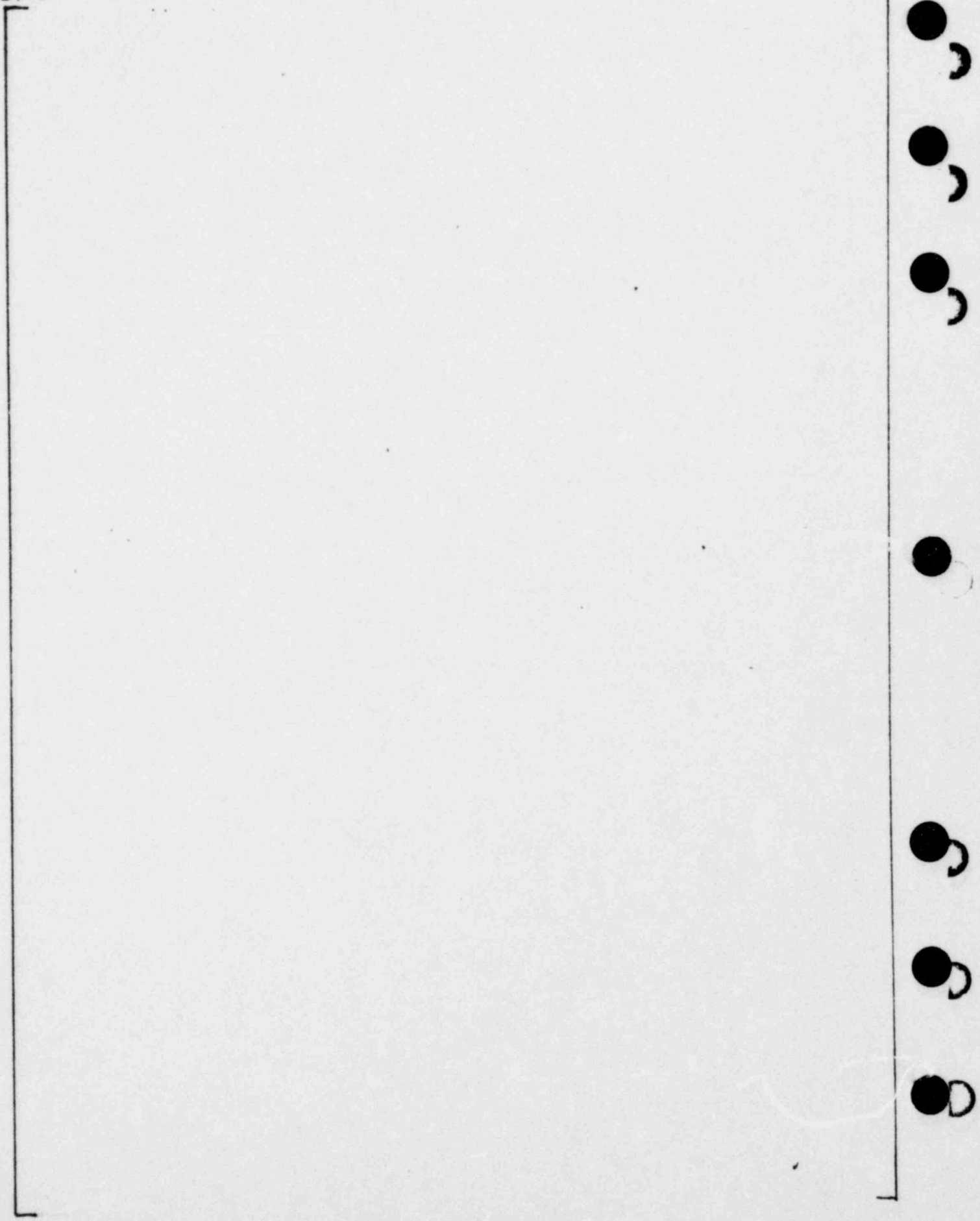

a,b,c,e

a,b,c,e

[redacted]

a,b,c,e

a,b,c,e

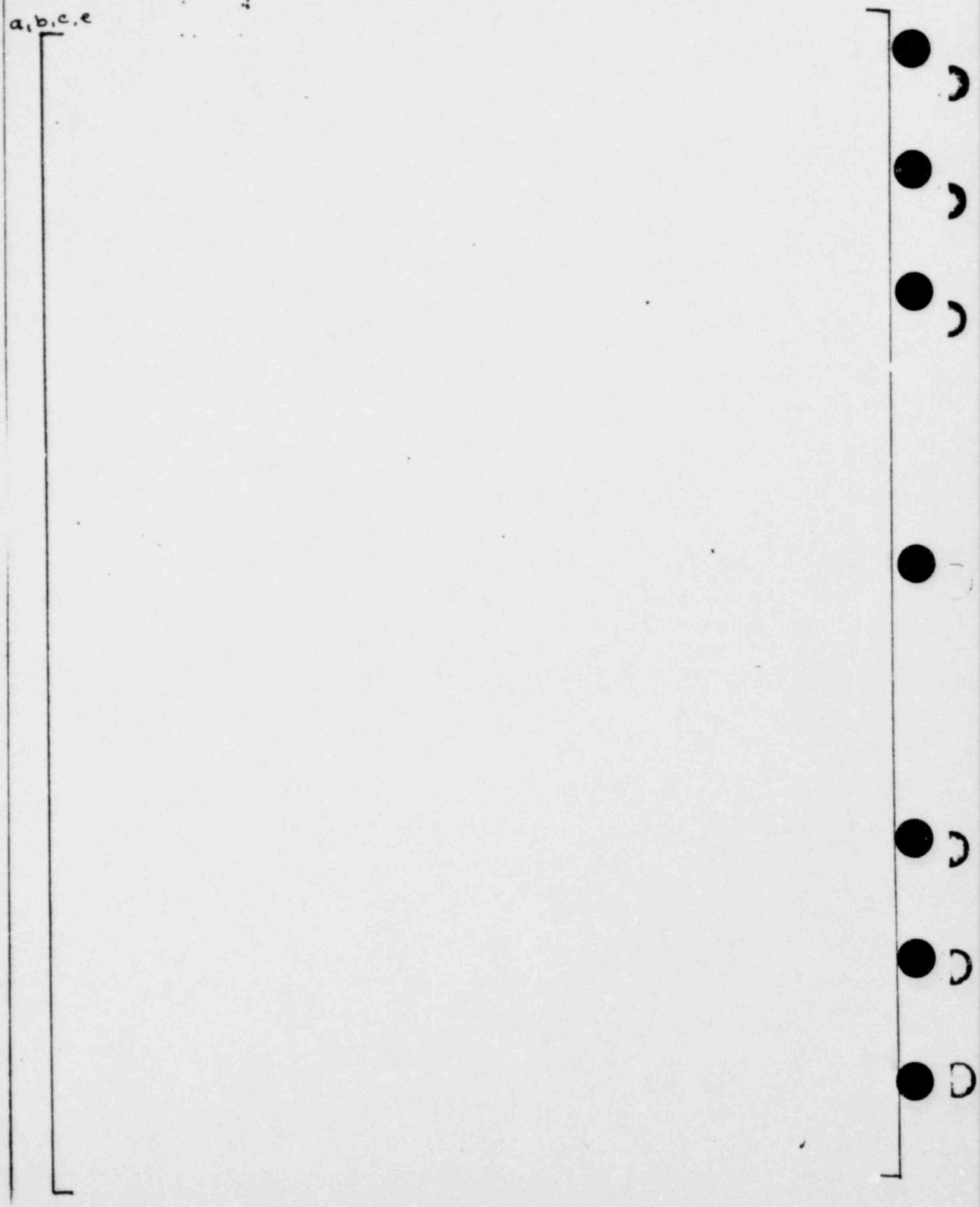

a,b,c,e

a,b,c,e

[redacted]

a,b,c,e

[

]

a,b,c,e

a,b,c,e

[

]

a,b,c,e

[

a,b,c,e

a,b,c,e

a,b,c,e

a,b,c,e

[redacted]

a,b,c,e

a,b,c,e

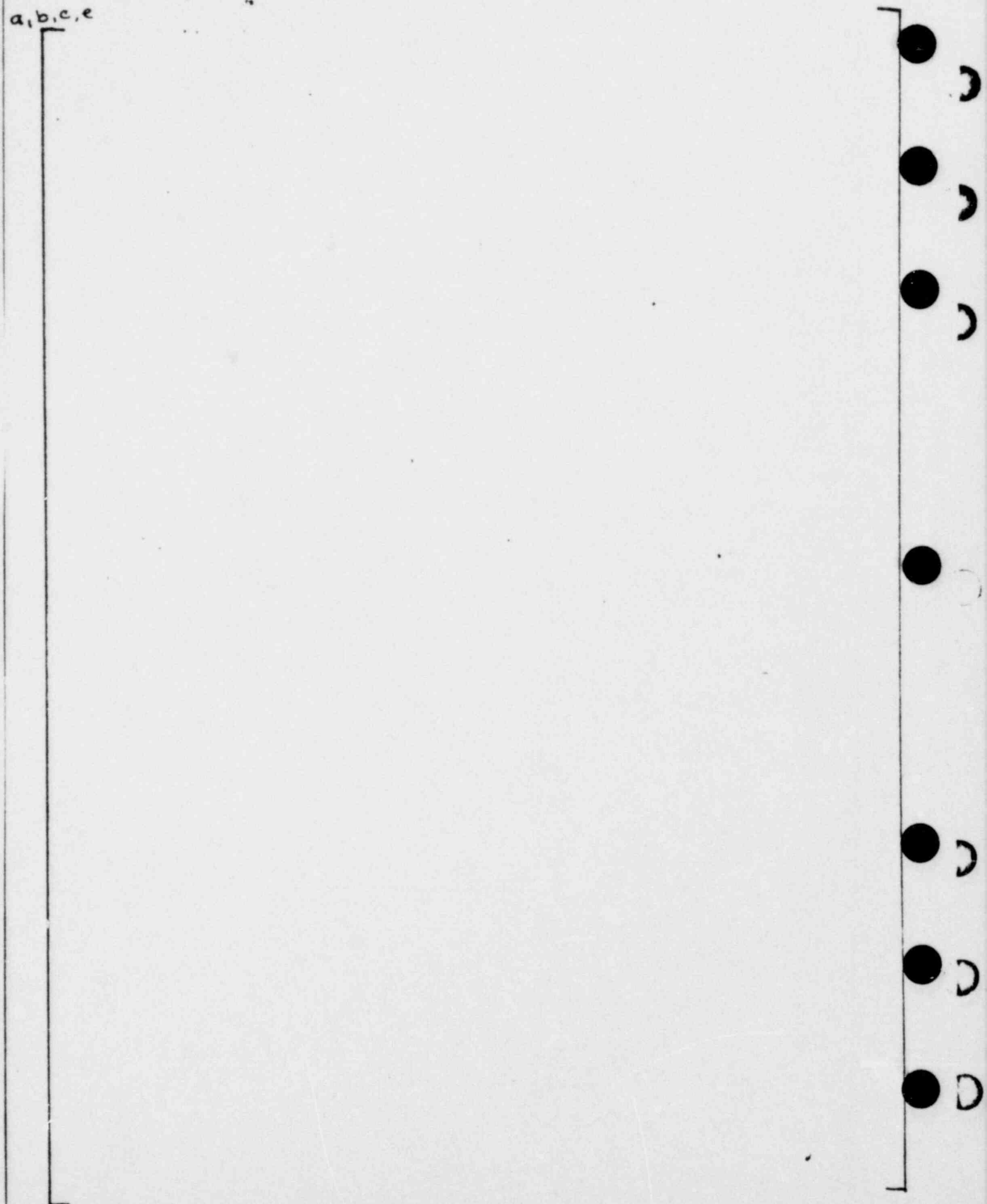

a,b,c,e

a,b,c,e

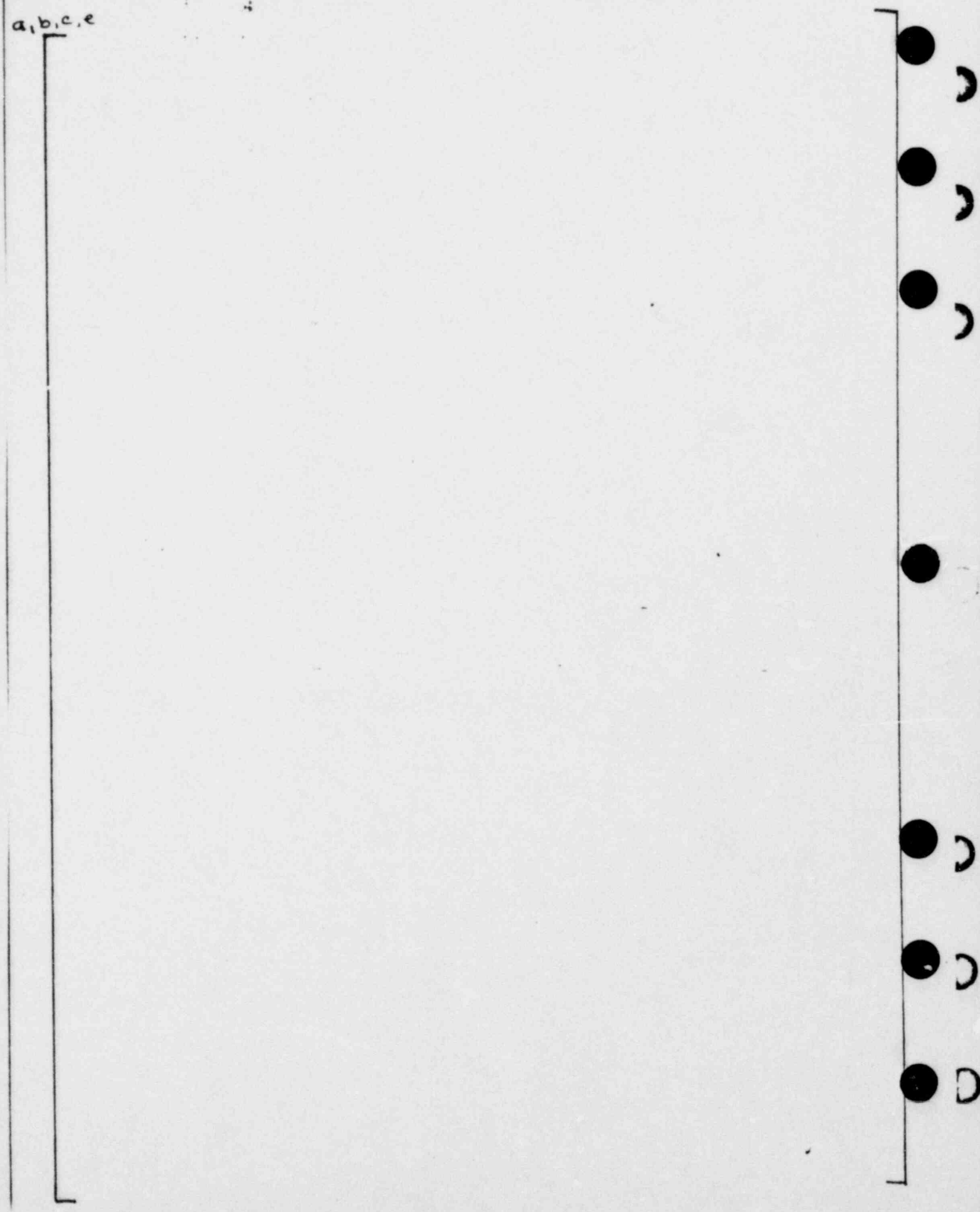

a,b,c,e

a,b,c,e

a,b,c,e

a,b,c,e

[redacted]

a,b,c,e

[

]

a,b,c,e

[redacted]

a,b,c,e

[redacted]

a,b,c,e

[redacted]

a,b,c,e

[
]

a,b,c,e

[redacted]

a,b,c,e

a,b,c,e

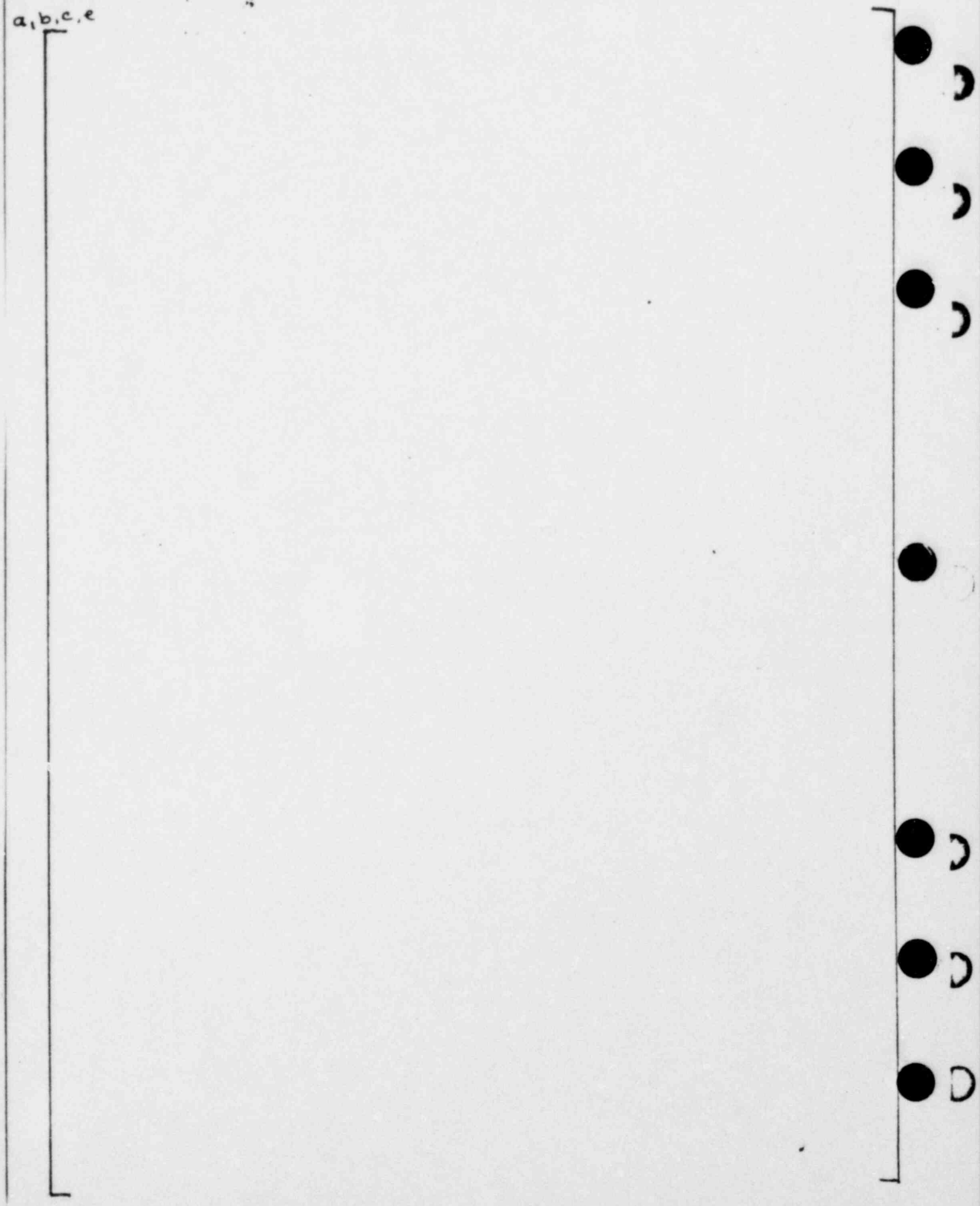

a,b,c,e

a,b,c,e

[redacted]

a,b,c,e

a,b,c,e

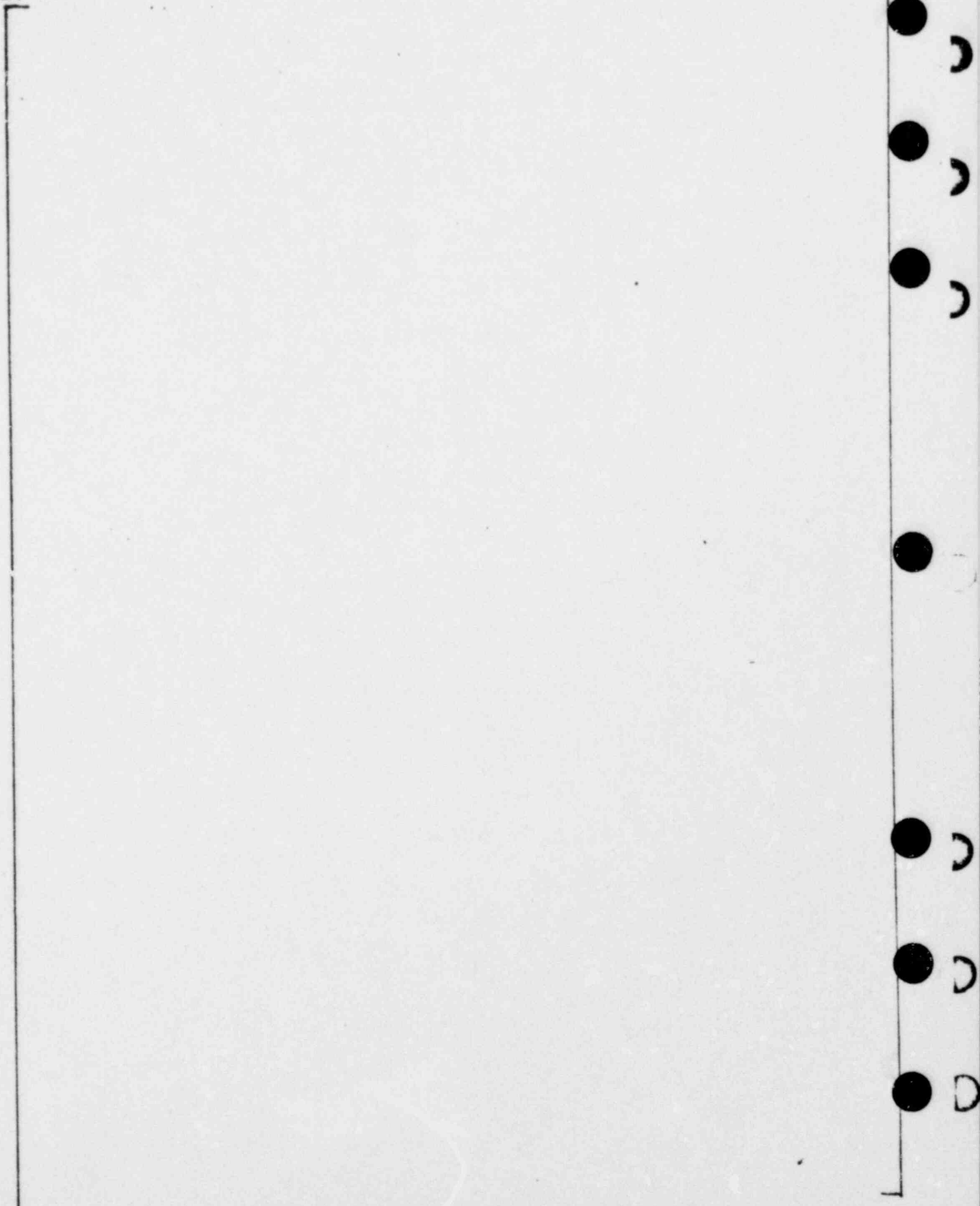

a,b,c,e

a,b,c,e

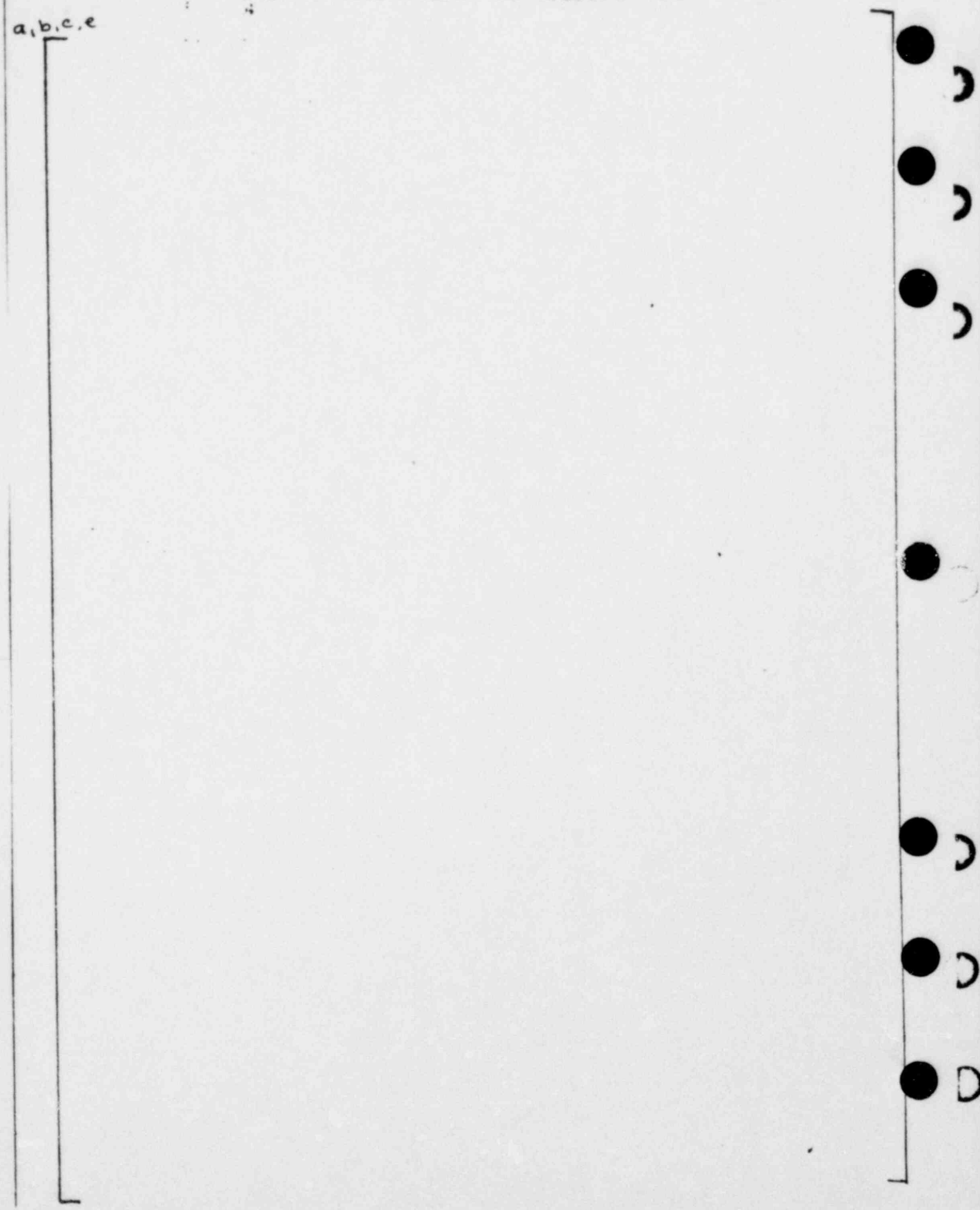

a,b,c,e

[
]

a,b,c,e

a,b,c,e

a,b,c,e

[redacted]

a,b,c,e

a,b,c,e

[redacted]

a,b,c,e

a,b,c,e

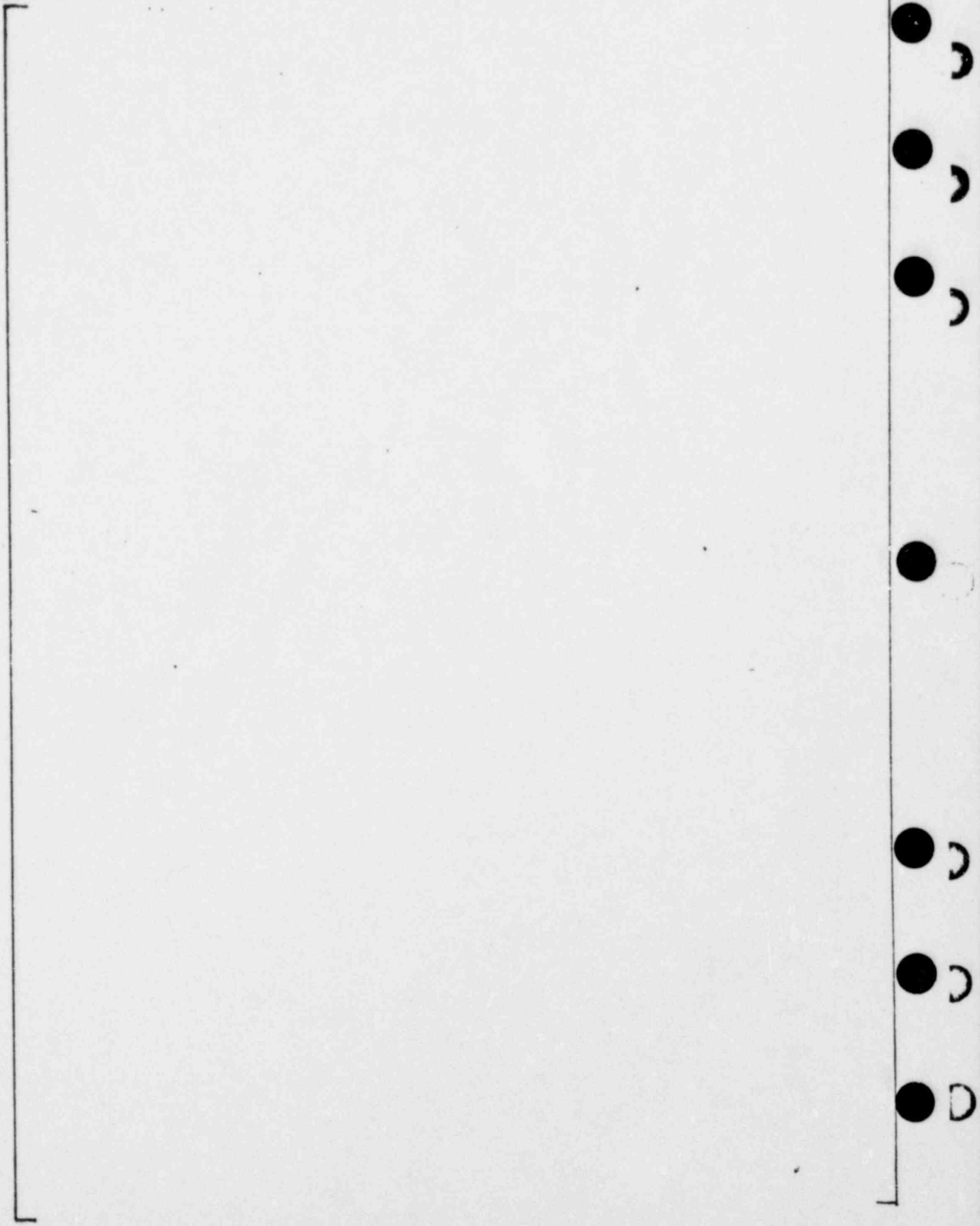

a,b,c,e

a,b,c,e

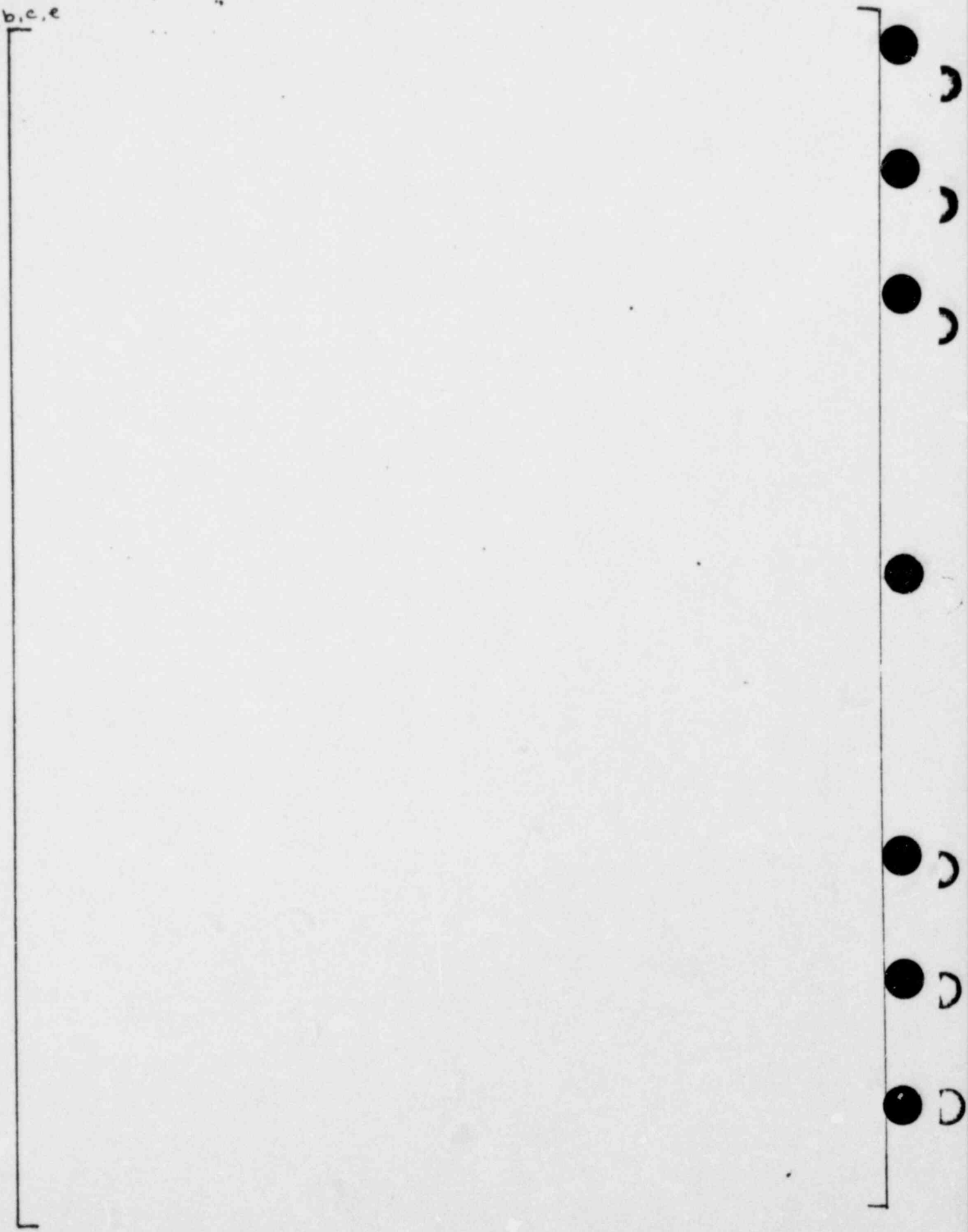

a,b,c,e

a,b,c,e

[redacted]

a,b,c,e

a,b,c,e

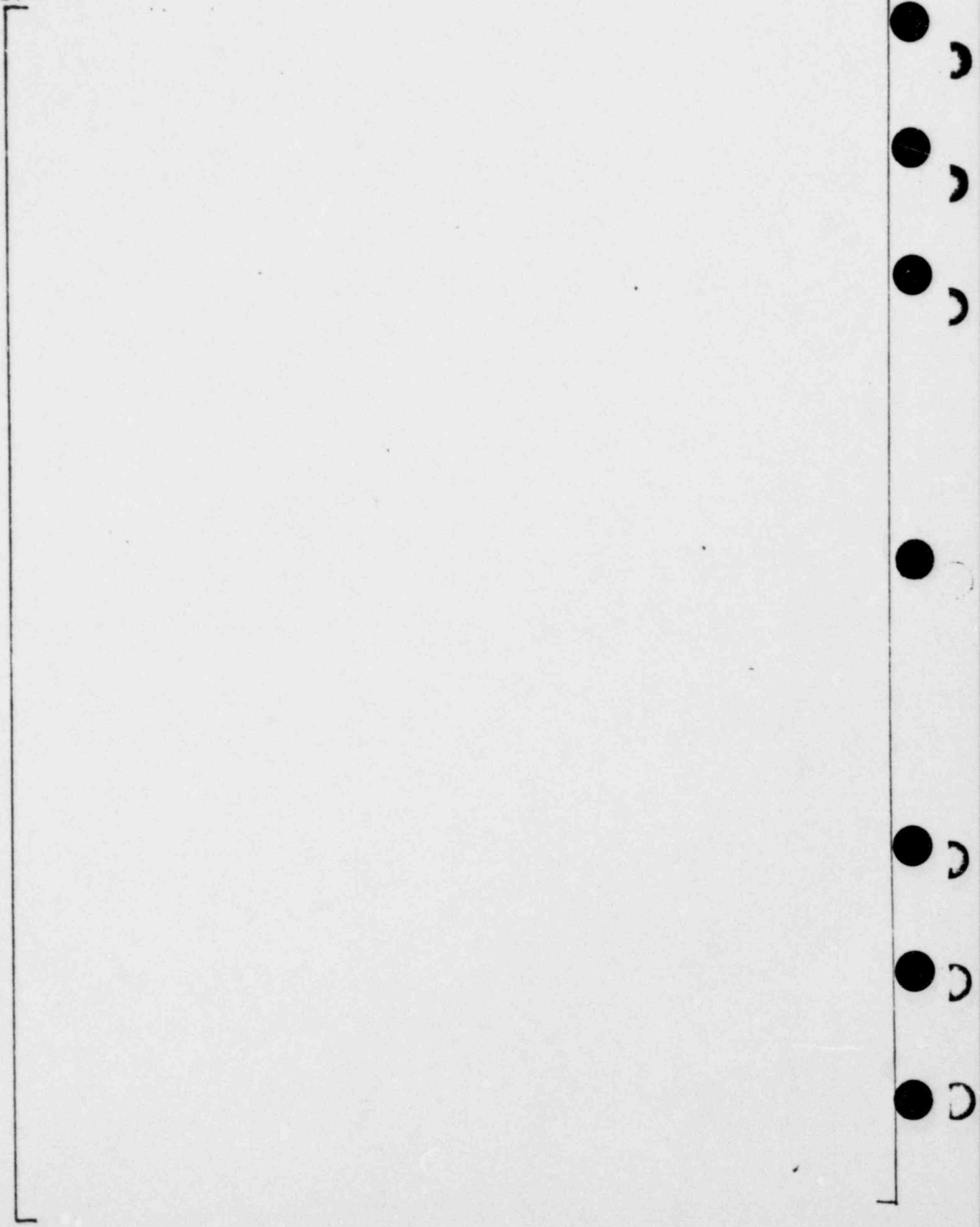

a,b,c,e

a,b,c,e

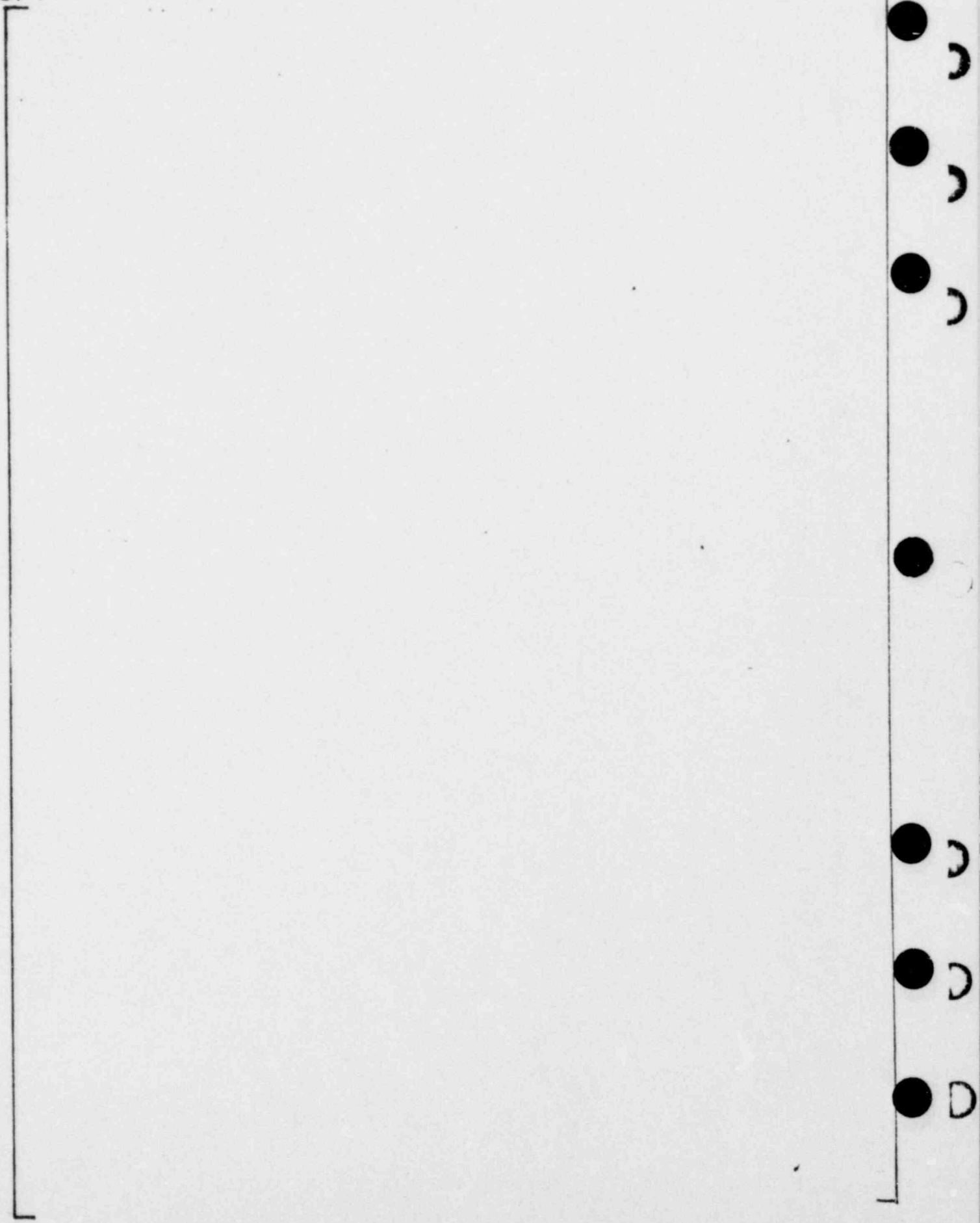

a,b,c,e

[

]

a,b,c,e

[redacted]

a,b,c,e

a,b,c,e

[

a,b,c,e

a,b,c,e

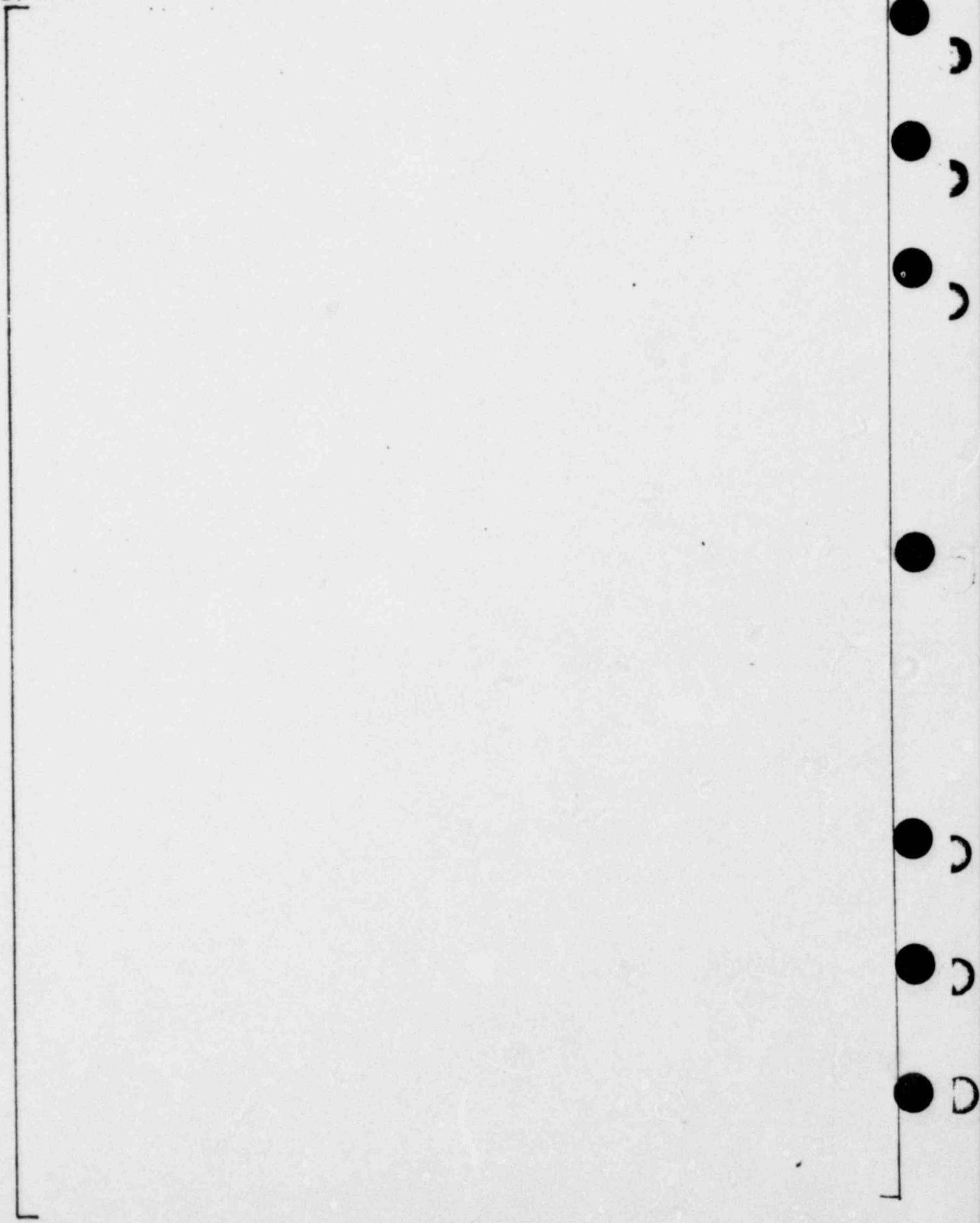

a,b,c,e

a,b,c,e

[redacted]

a,b,c,e

[

]

a,b,c,e

a,b,c,e

a,b,c,e

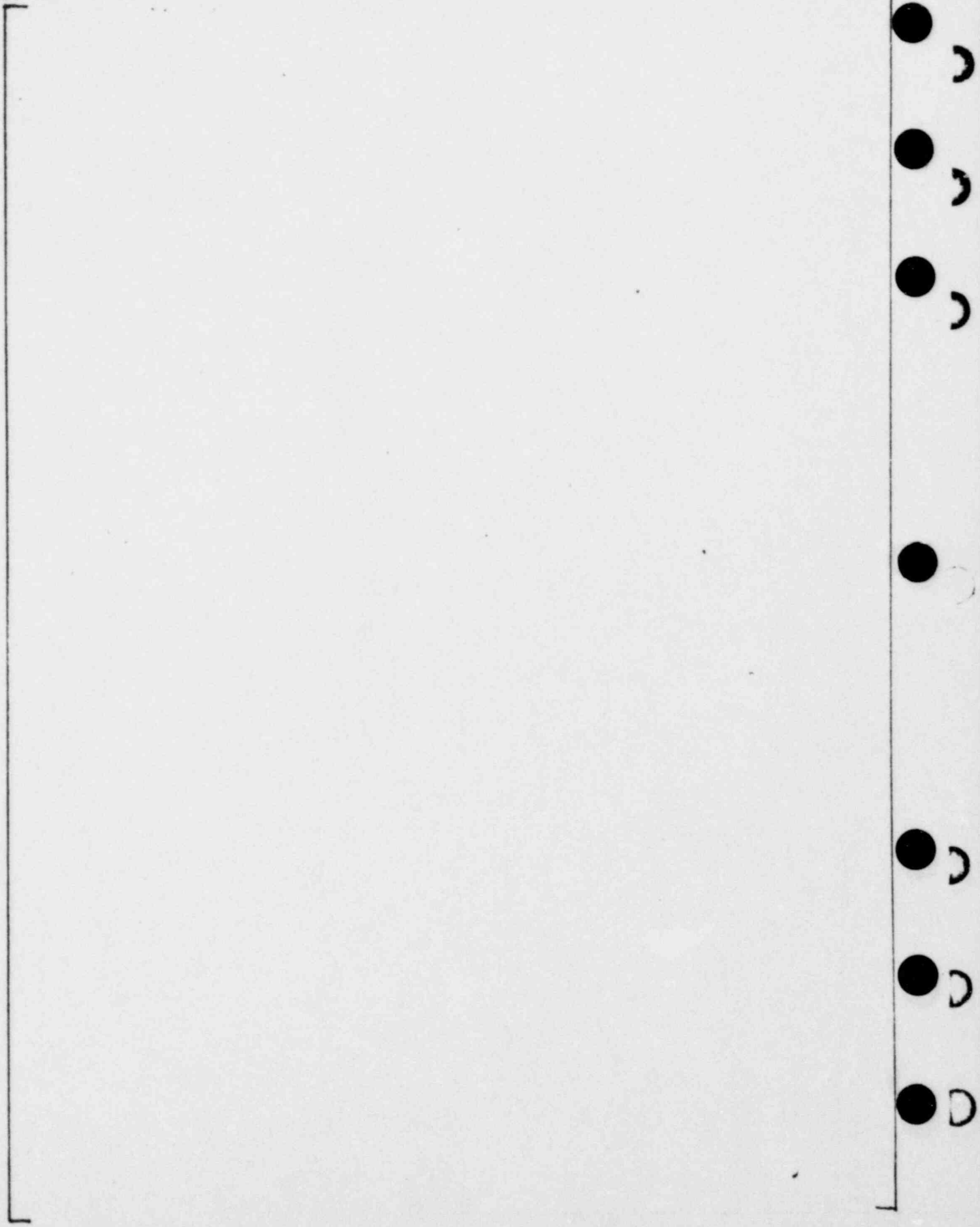

a,b,c,e

a,b,c,e

[redacted]

a,b,c,e

a,b,c,e

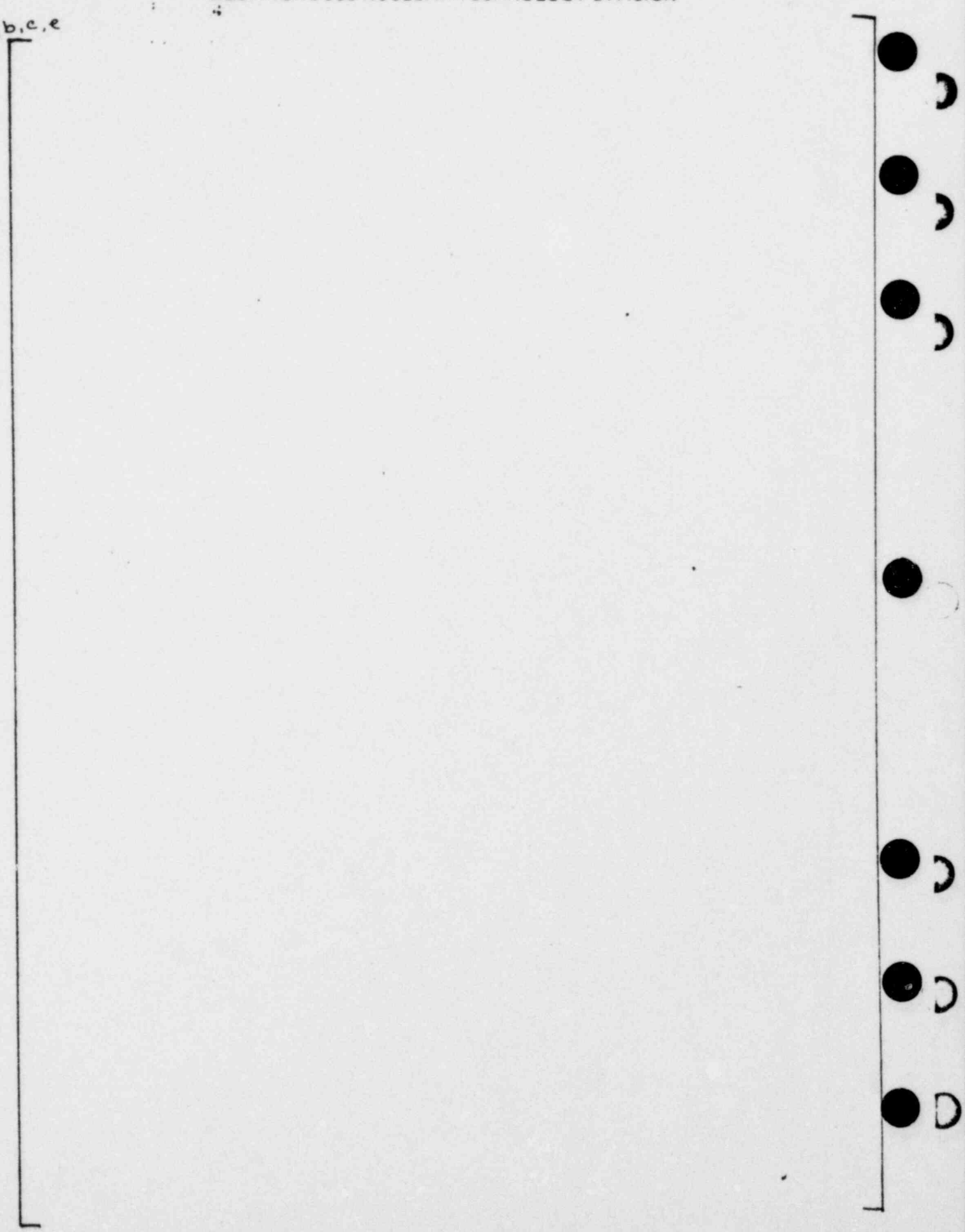

a,b,c,e

a,b,c,e

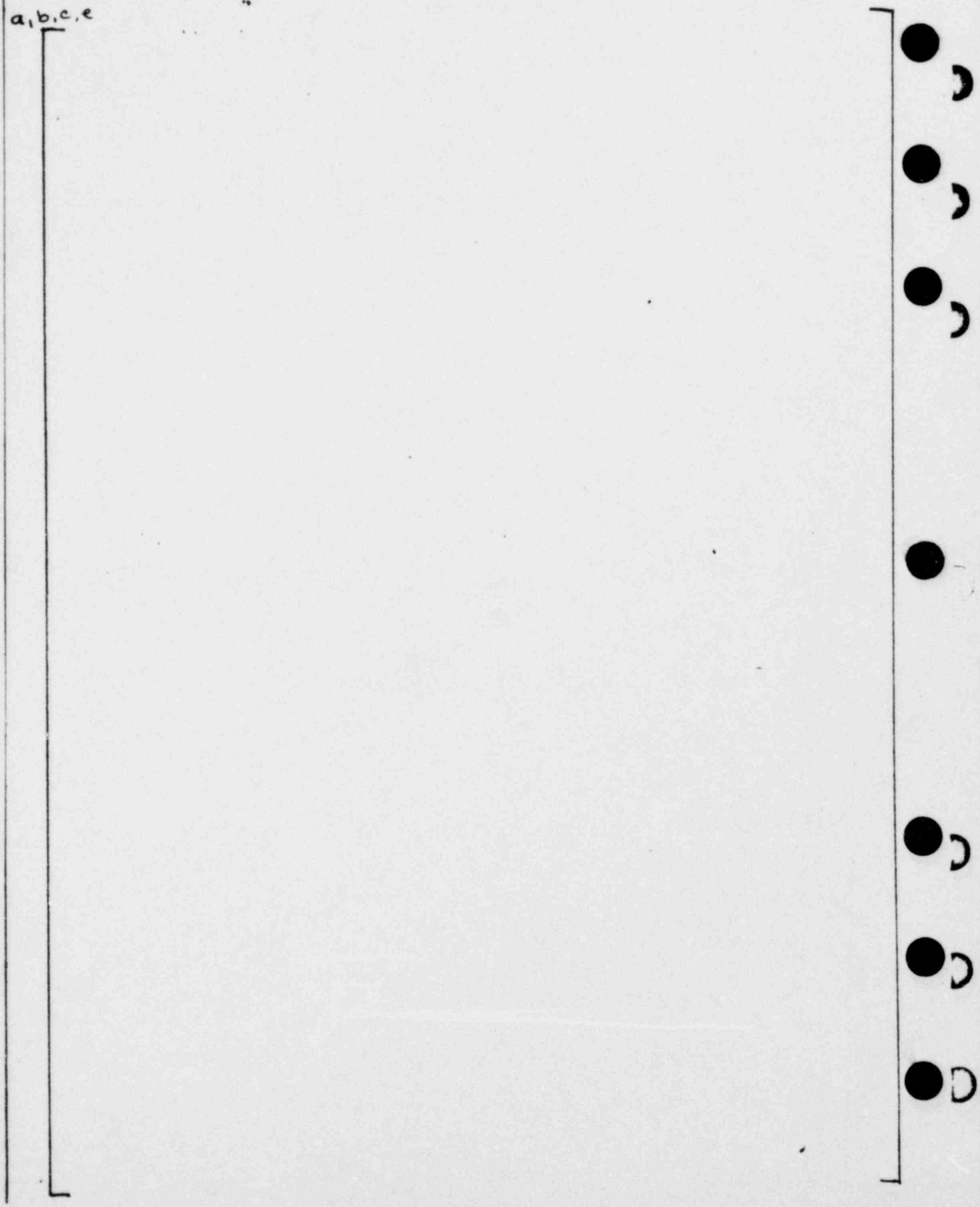

a,b,c,e

[

]

a,b,c,e

[
]

a,b,c,e

[

]

a,b,c,e

[
]

a,b,c,e

a,b,c,e

[redacted]

a,b,c,e

a,b,c,e

[redacted]

a,b,c,e

a,b,c,e

[redacted]

a,b,c,e

a,b,c,e

[

]

a,b,c,e

a,b,c,e

[redacted]

a,b,c,e

a,b,c,e

[

a,b,c,e

[

]

a, b, c, e

[redacted]

a,b,c,e

a,b,c,e

[redacted]

a,b,c,e

a,b,c,e

[
]

a,b,c,e

a,b,c,e

[redacted]

a,b,c,e

a,b,c,e

[redacted]

a,b,c,e

[ ]a,c,e

LINE 1A
LINE 1B

a,b,c,e

[

]

a,b,c,e

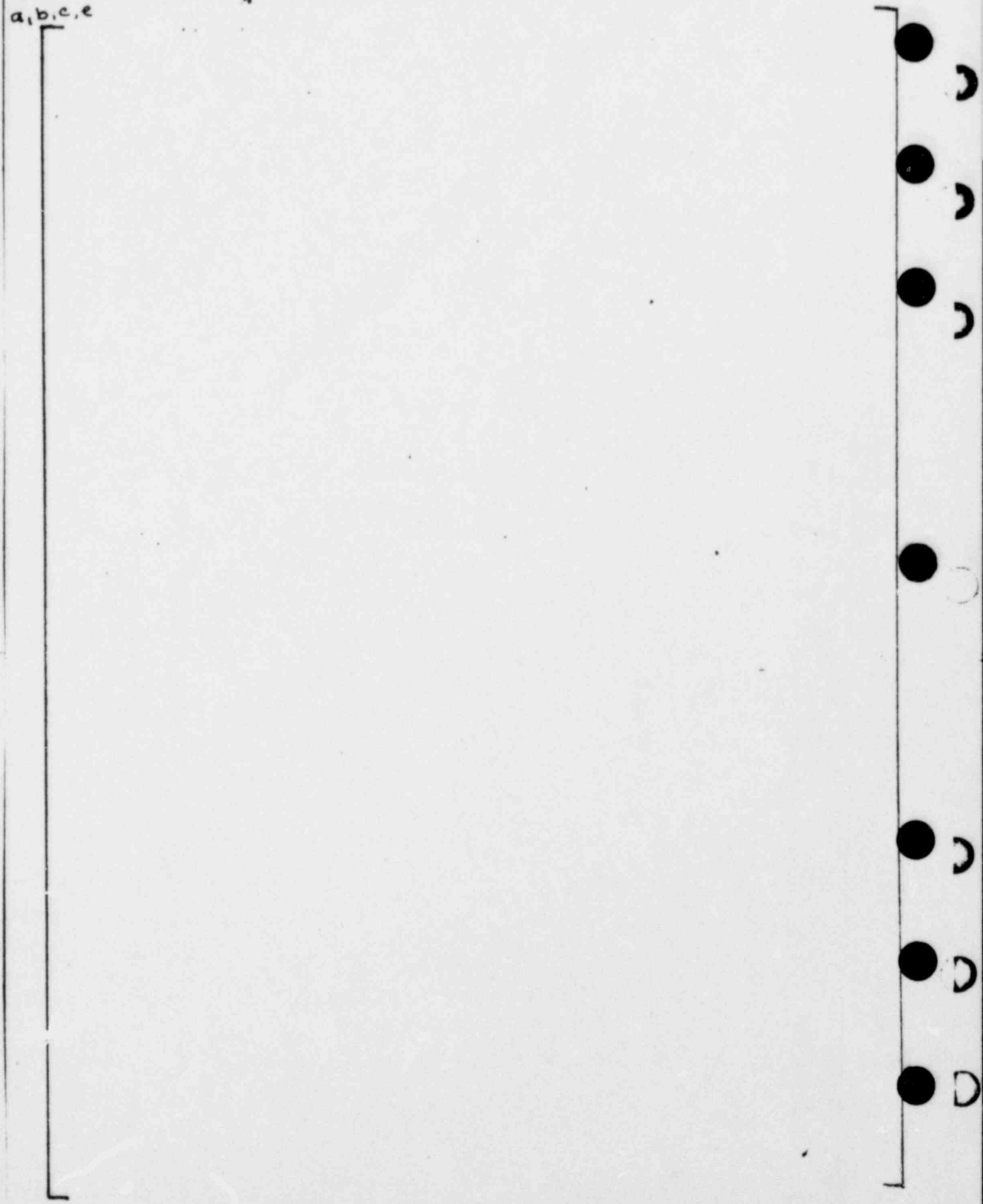

a,b,c,e

a,b,c,e

[
]

a,b,c,e

a,b,c,e

a,b,c,e

a,b,c,e

[
]

a,b,c,e

[
]

a,b,c,e

[redacted]

a,b.c,e

a,b,c,e

[redacted]

a,b,c,e

a,b,c,e

[

a,b,c,e

a,b,c,e

[
]

a,b,c,e

a,b,c,e

[redacted]

a,b,c,e

[

]

a,b,c,e

a,b,c,e

a,b,c,e

[redacted]

a,b,c,e

a,b,c,e

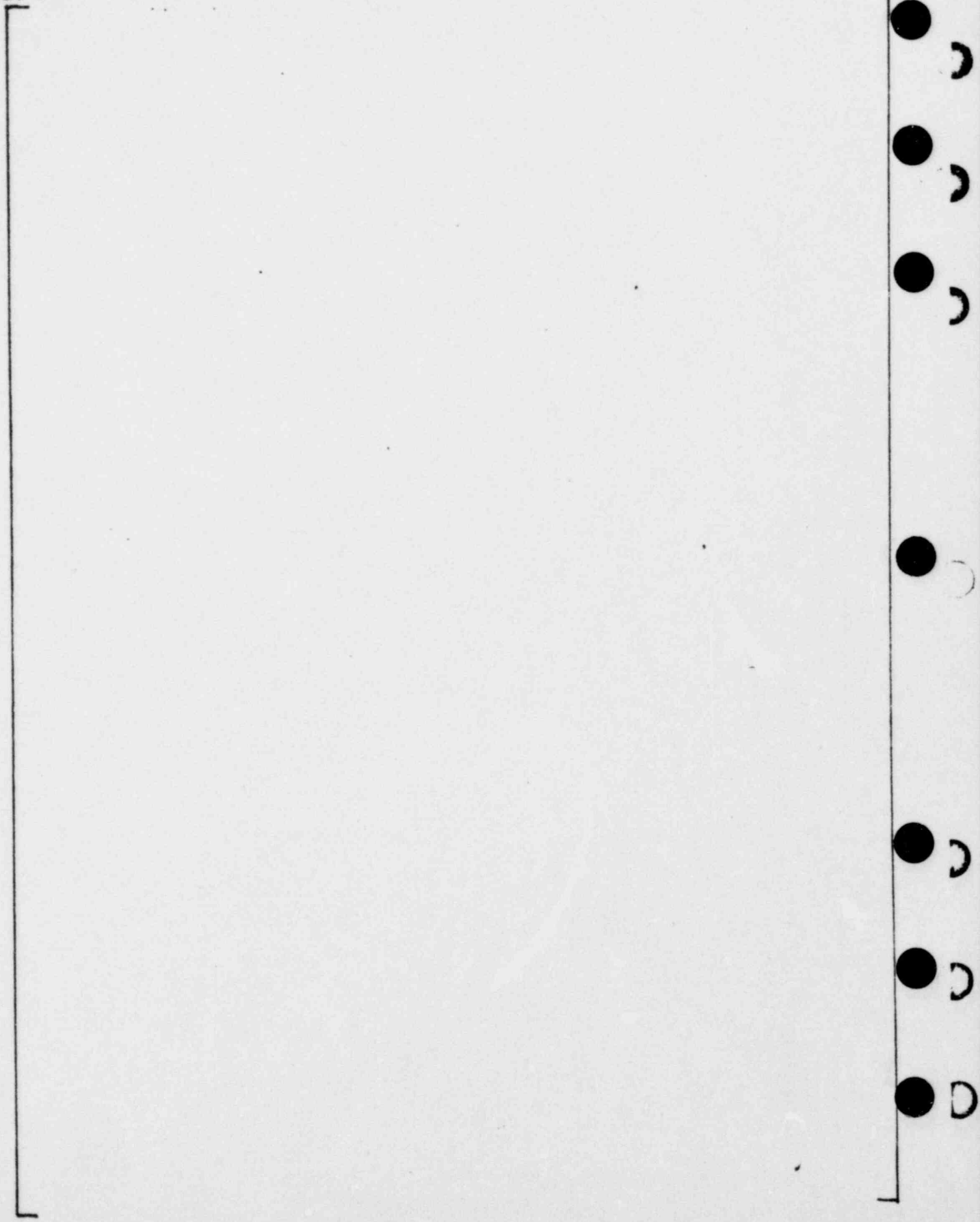

a,b,c,e

a,b,c,e

[redacted]

a,b,c,e

a,b,c,e

[redacted]

a,b,c,e

a,b,c,e

[redacted]

[ ]a,c,e

LINE 2

a,b,c,e

a,b,c,e

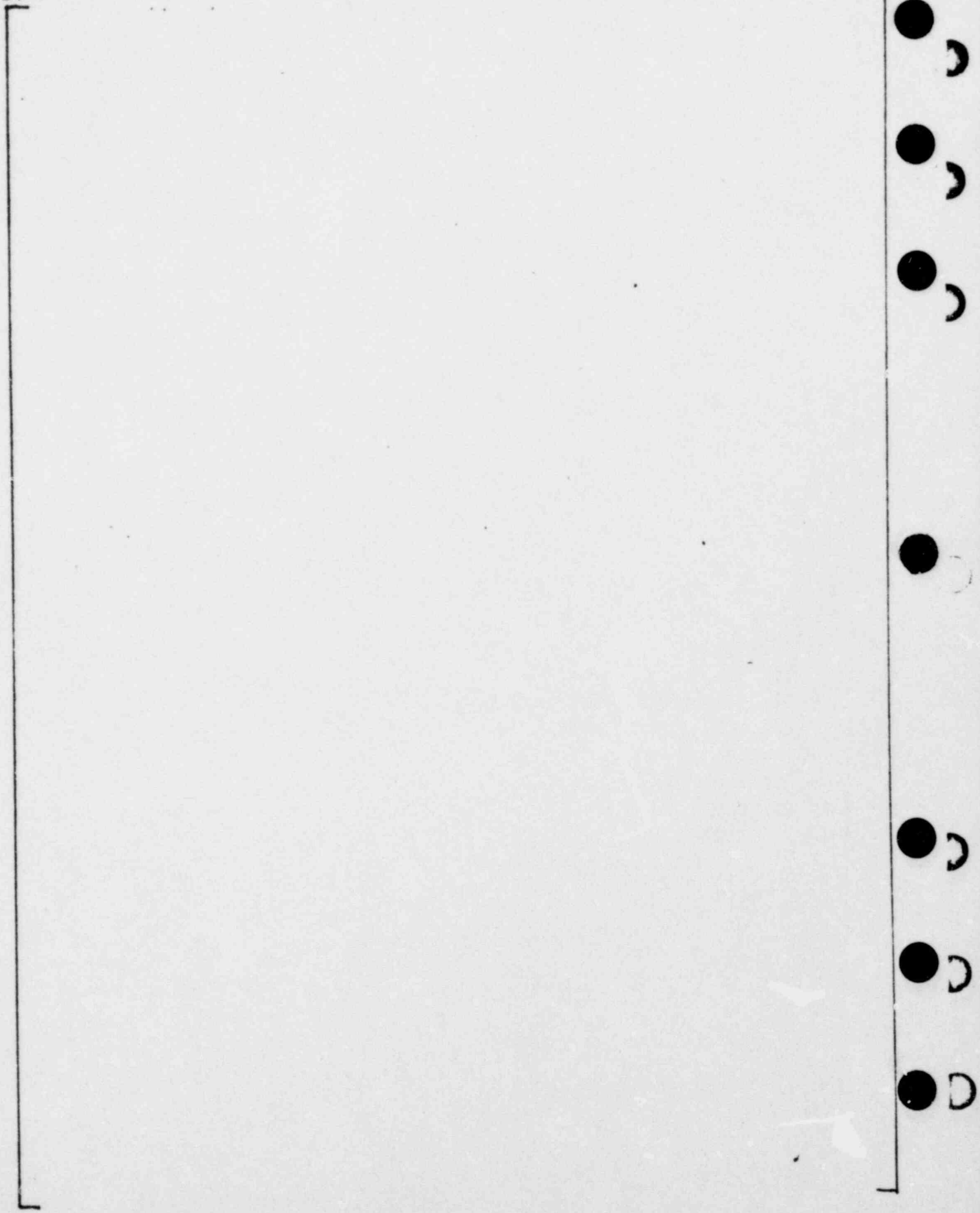

a,b,c,e

[

]

a,b,c,e

[redacted]

a,b,c,e

[ ]^{a,c,e}

LINE C
LINE B

a,b,c,e

a,b,c,e

[

]

a,b,c,e

[

]

a,b,c,e

[redacted]

a,b,c,e

[

]

a,b,c,e

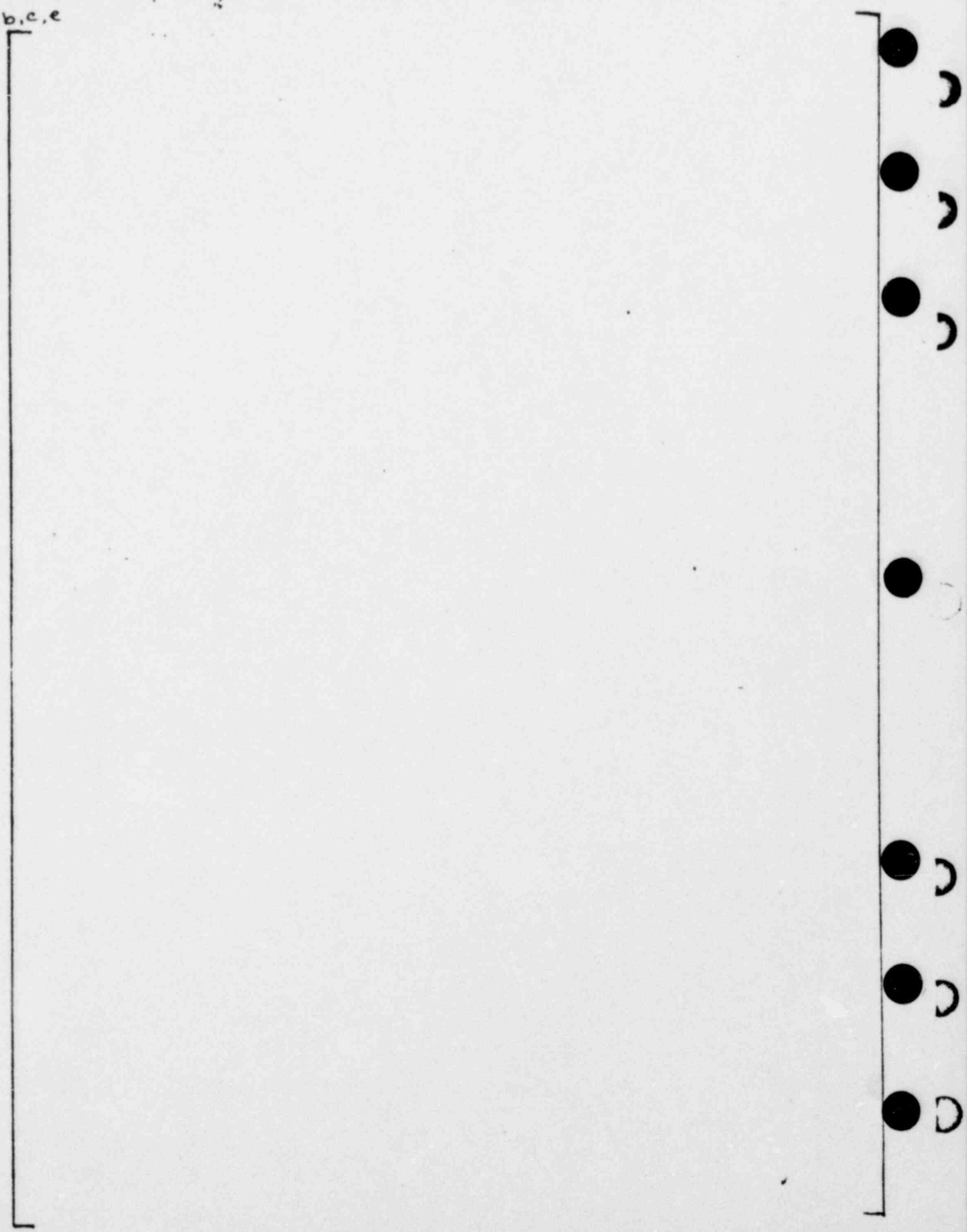

a,b,c,e

a,b,c,e

[redacted]

a,b,c,e

a,b,c,e

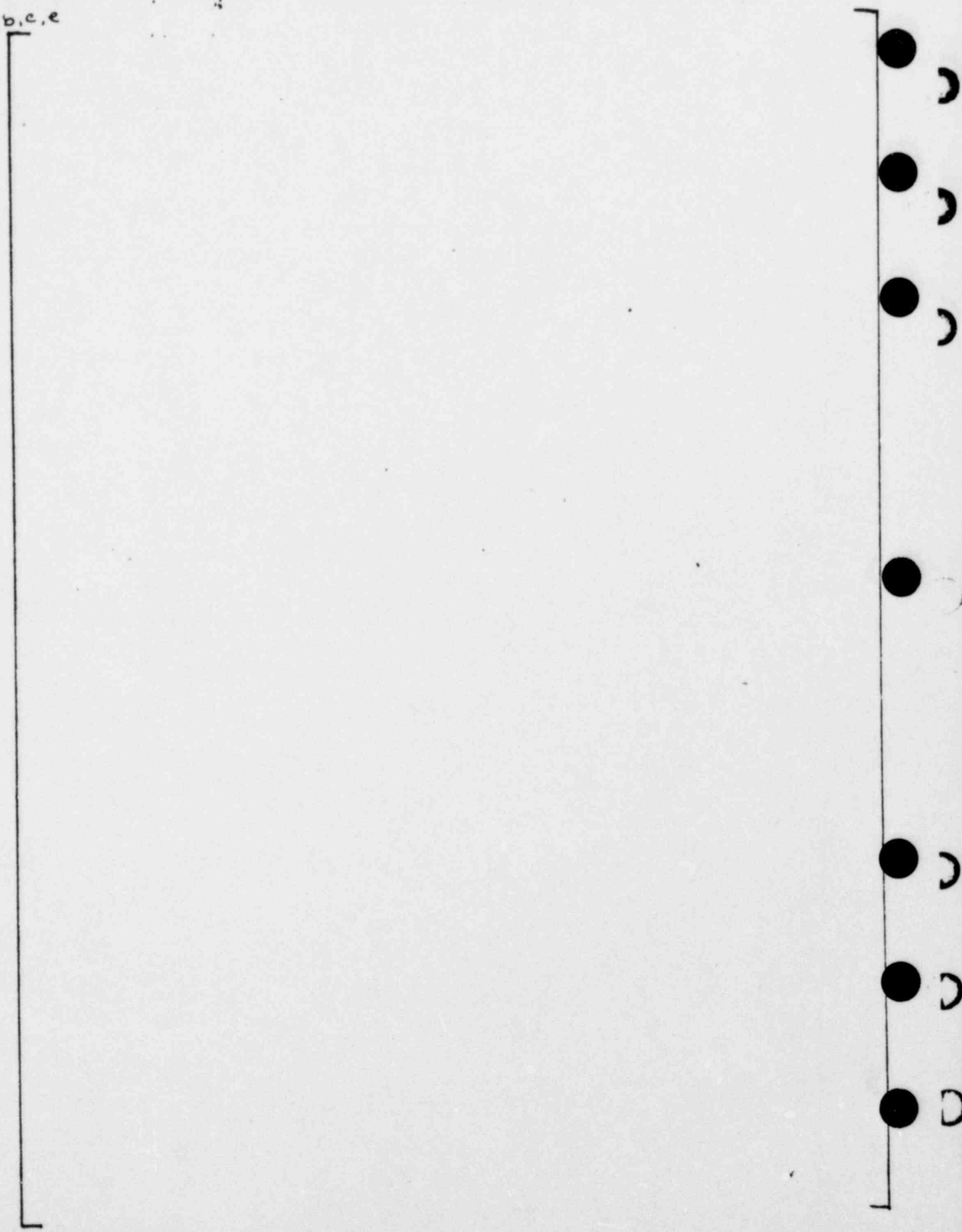

a,b,c,e

[

]

a,b,c,e

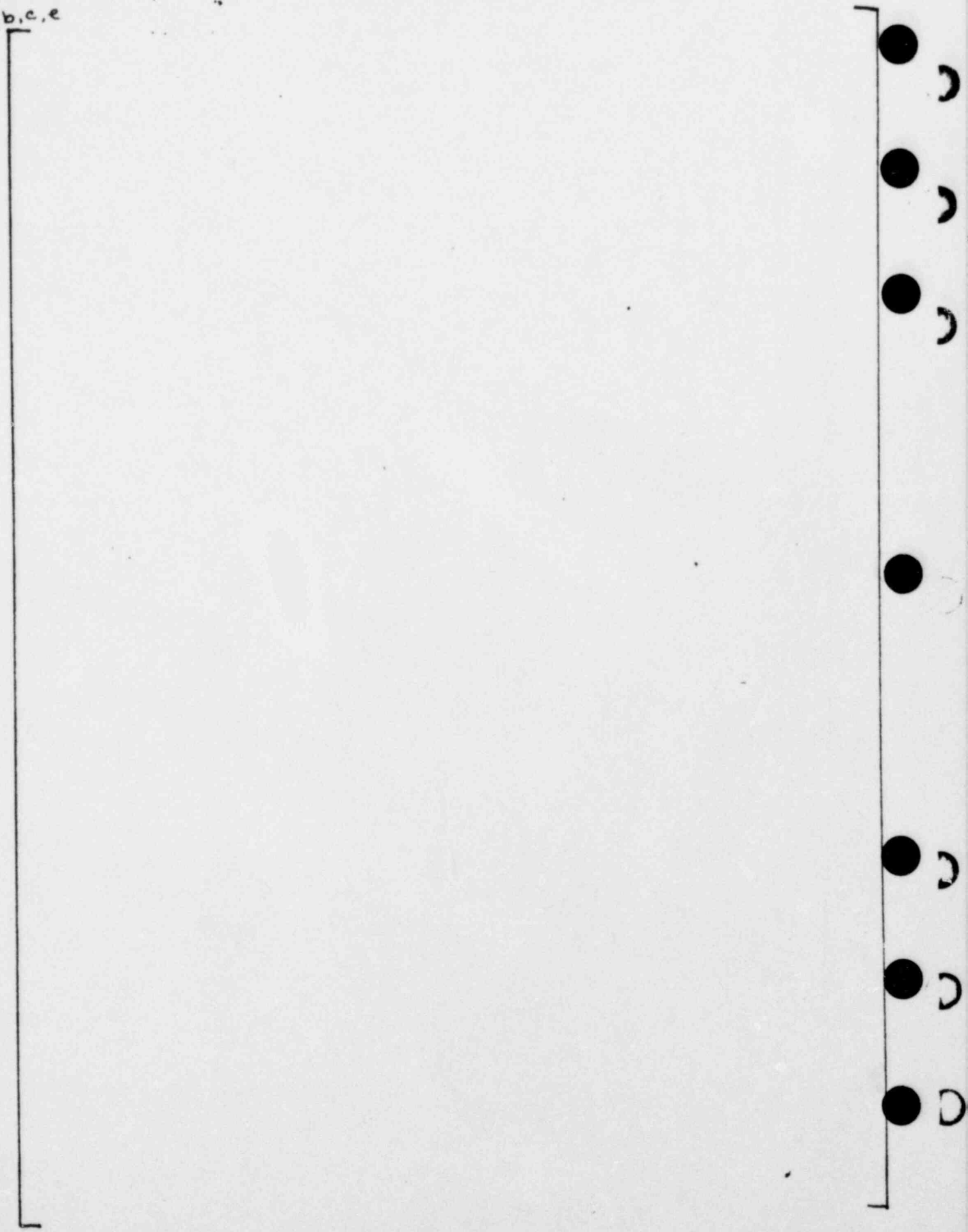

a,b,c,e

a,b,c,e

[redacted]

a,b,c,e

a,b,c,e

[
]

a,b,c,e

a,b,c,e

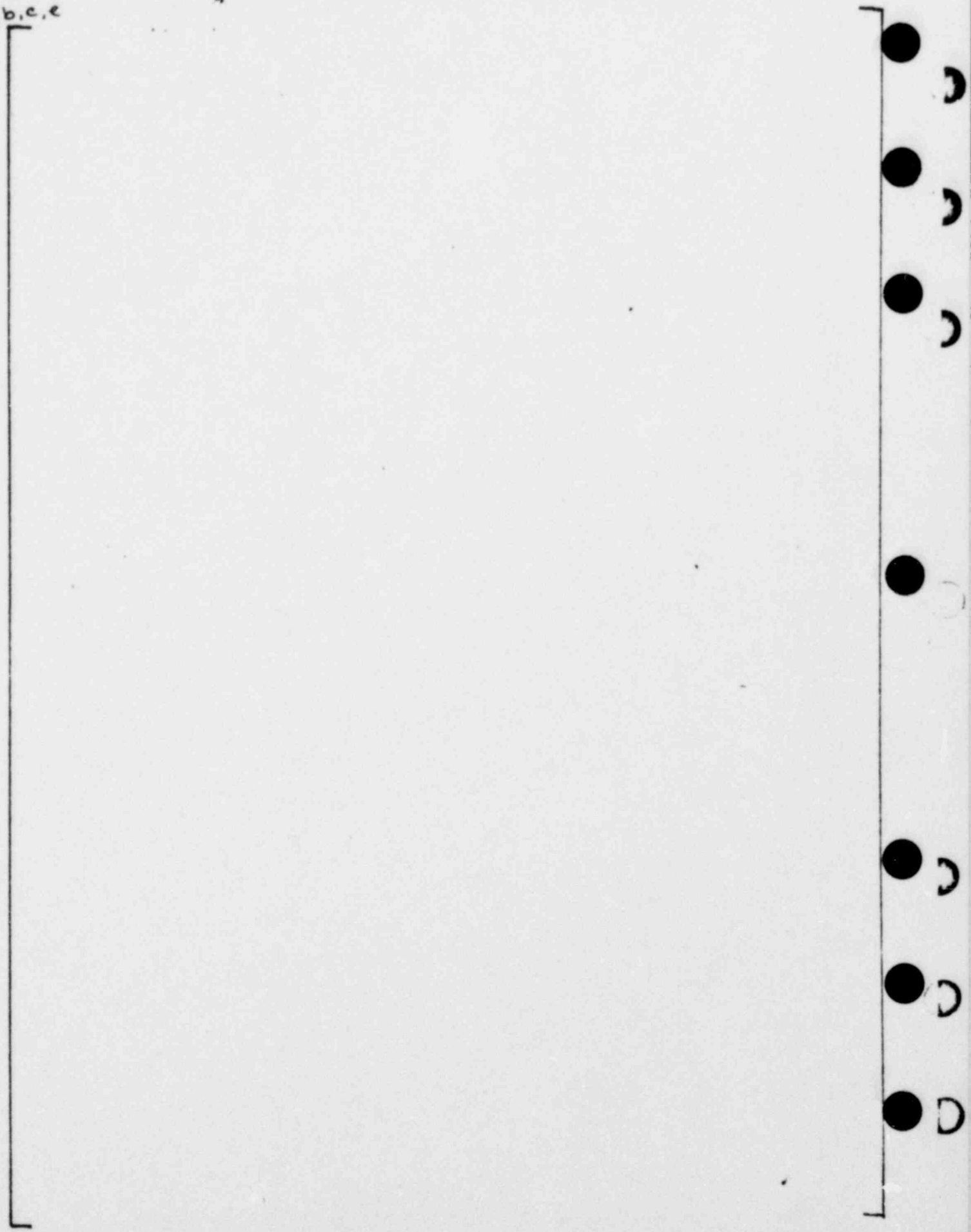

a,b.c,e

a,b,c,e

[redacted]

[ ]a,c,e

LINE 13
LINE 14

a,b,c,e

a,b,c,e

[redacted]

a,b,c,e

[

]

a,b,c,e

[redacted]

a,b.c,e

a,b,c,e

[redacted]

a,b,c,e

a,b,c,e

[redacted]

a,b,c,e

[
]

a,b,c,e

[redacted]

a,b,c,e

a,b,c,e

[
]

a,b,c,e

a,b,c,e

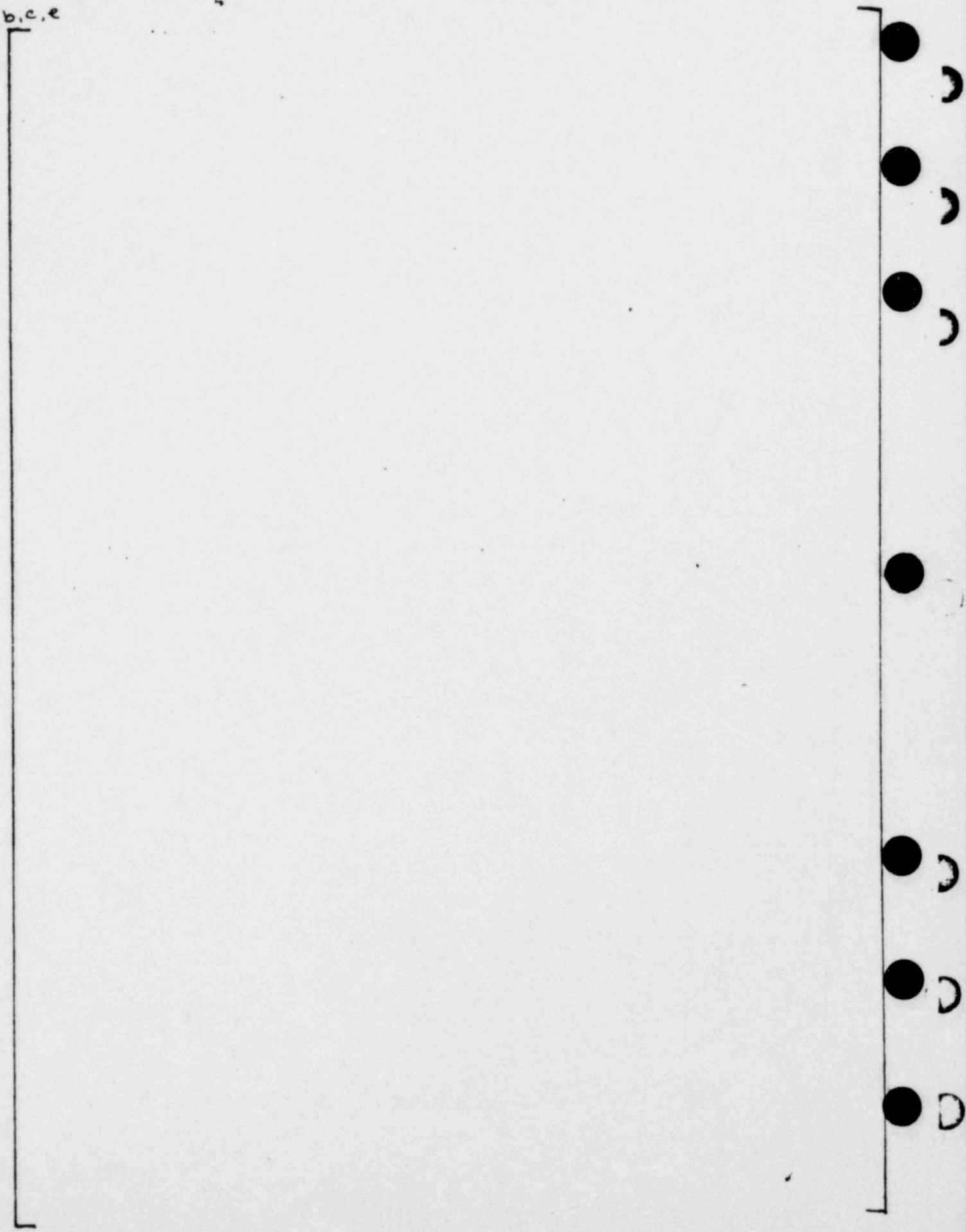

a,b,c,e

a,b,c,e

[redacted]

a,b,c,e

a,b,c,e

[redacted]

a,b,c,e

a,b,c,e

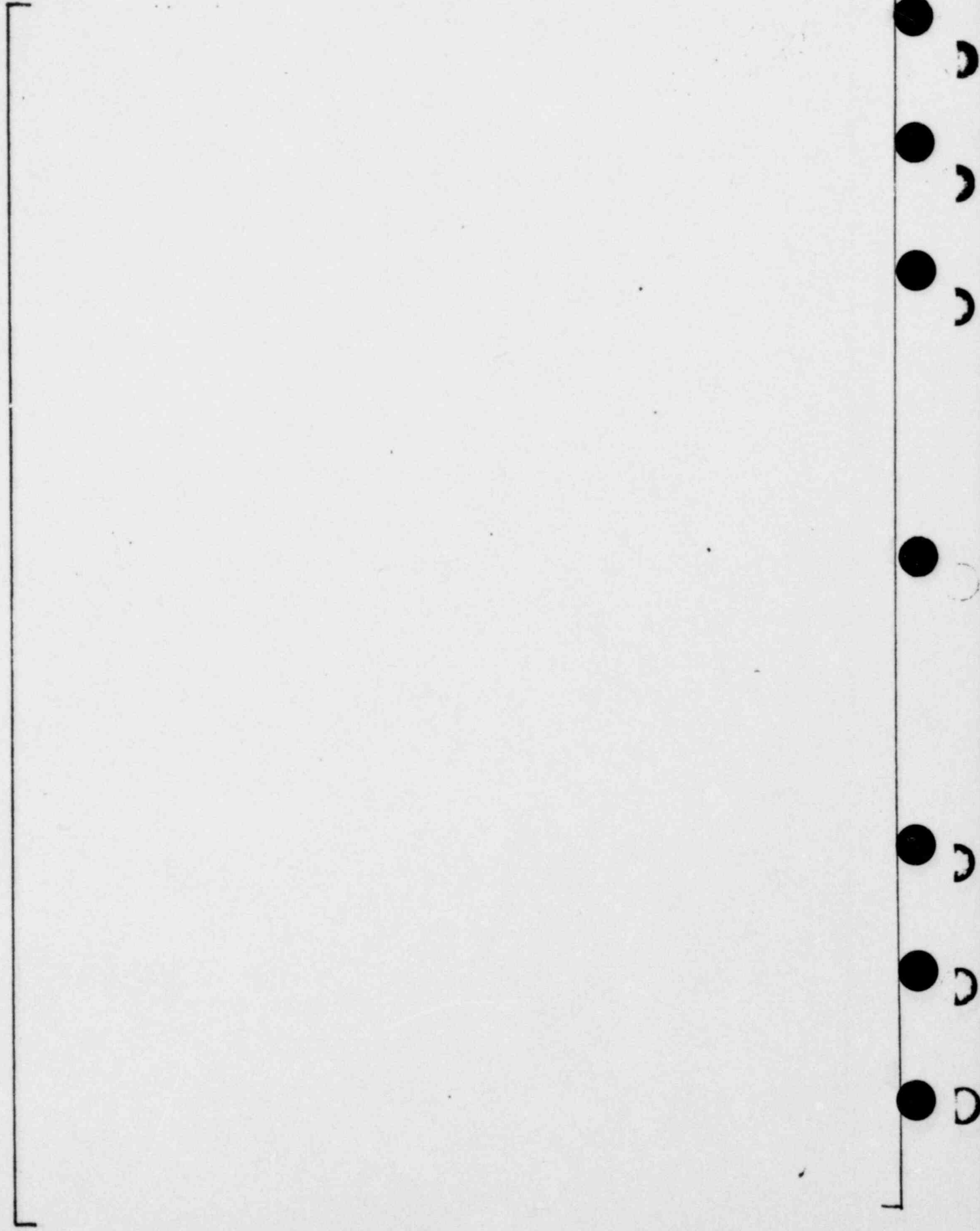

a,b,c,e

a,b,c,e

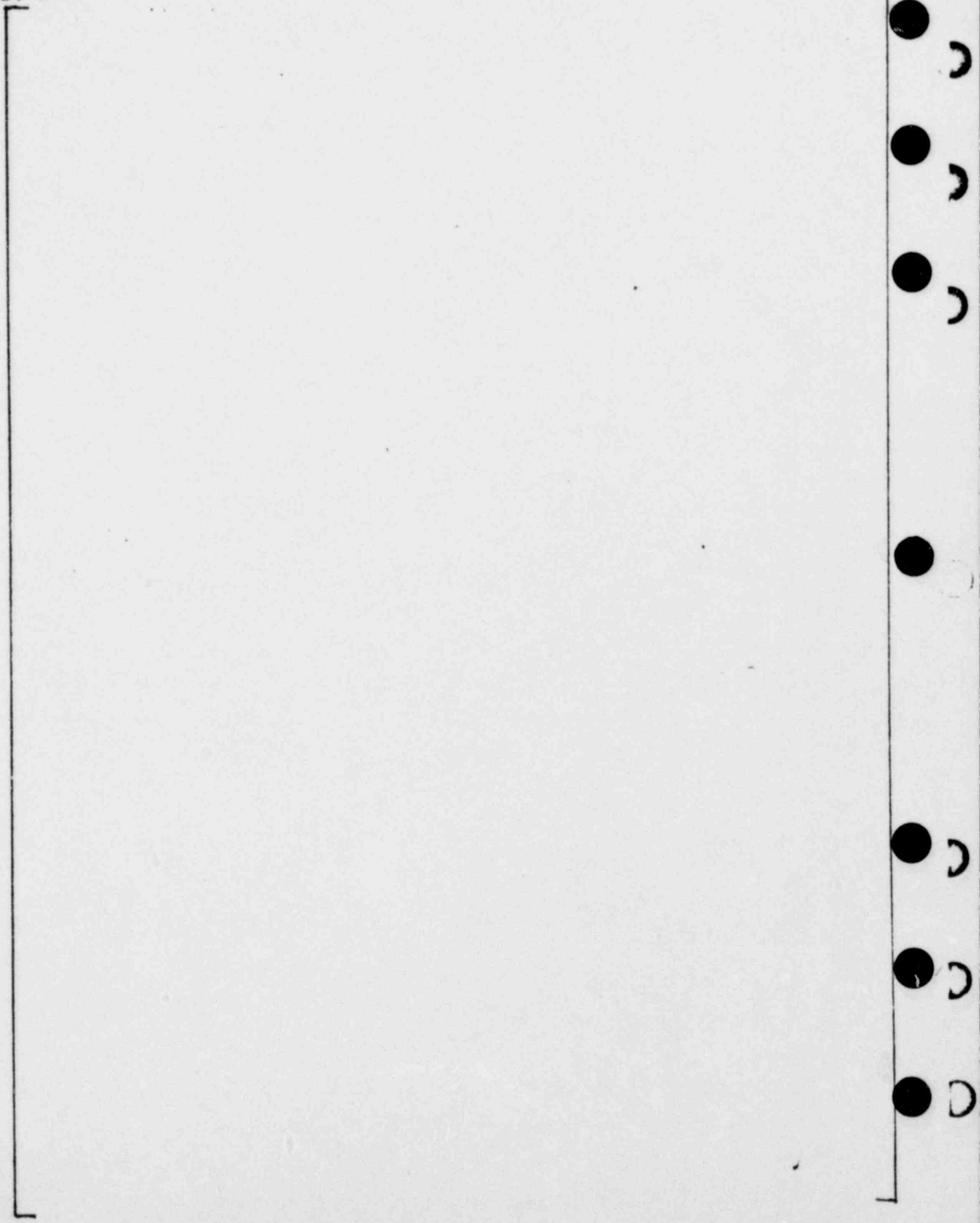

a,b,c,e

a,b,c,e

[redacted]

a,b,c,e

a,b,c,e

[

a,b,c,e

a,b,c,e

[redacted]

a,b,c,e

[

]

a,b,c,e

[redacted]

a,b,c,e

a,b,c,e

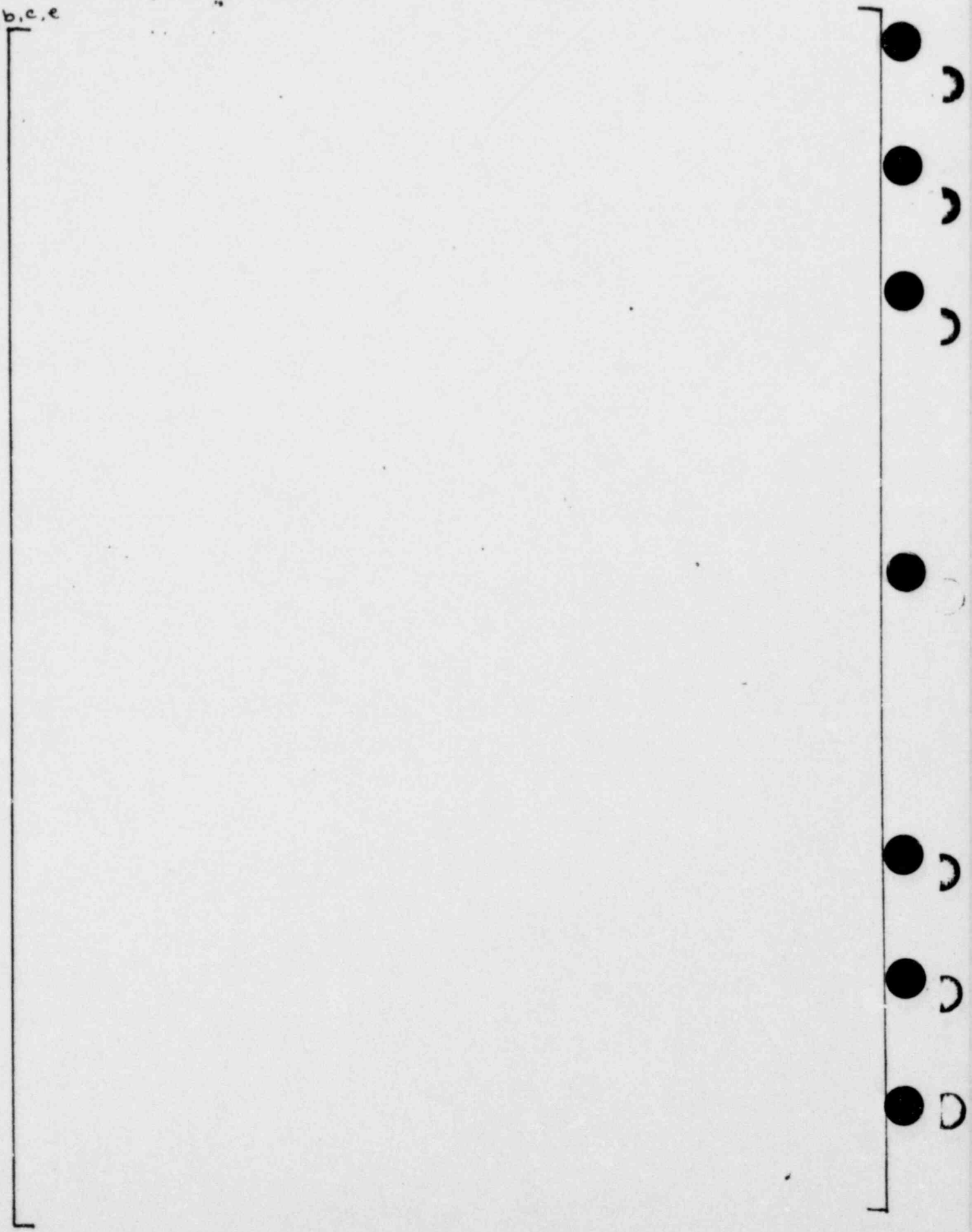

a,b,c,e

[

]

a,b,c,e

[redacted]

a,b,c,e

[redacted]

a,b,c,e

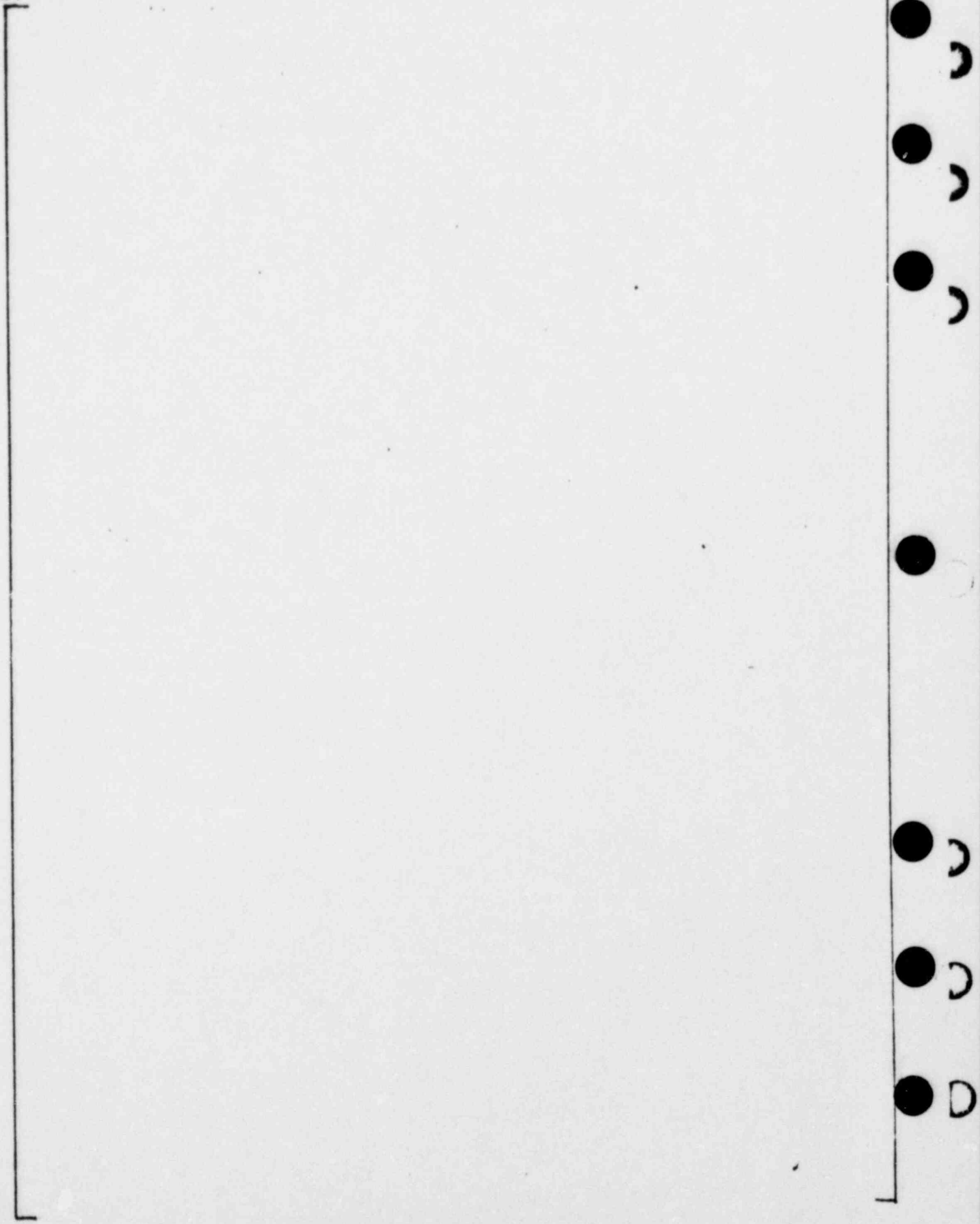

a,b,c,e

[

]

a,b,c,e

[redacted]

a,b,c,e

[

]

a,b,c,e

a,b,c,e

a,b,c,e

a,b,c,e

a,b,c,e

[redacted]

a,b,c,e

a,b,c,e

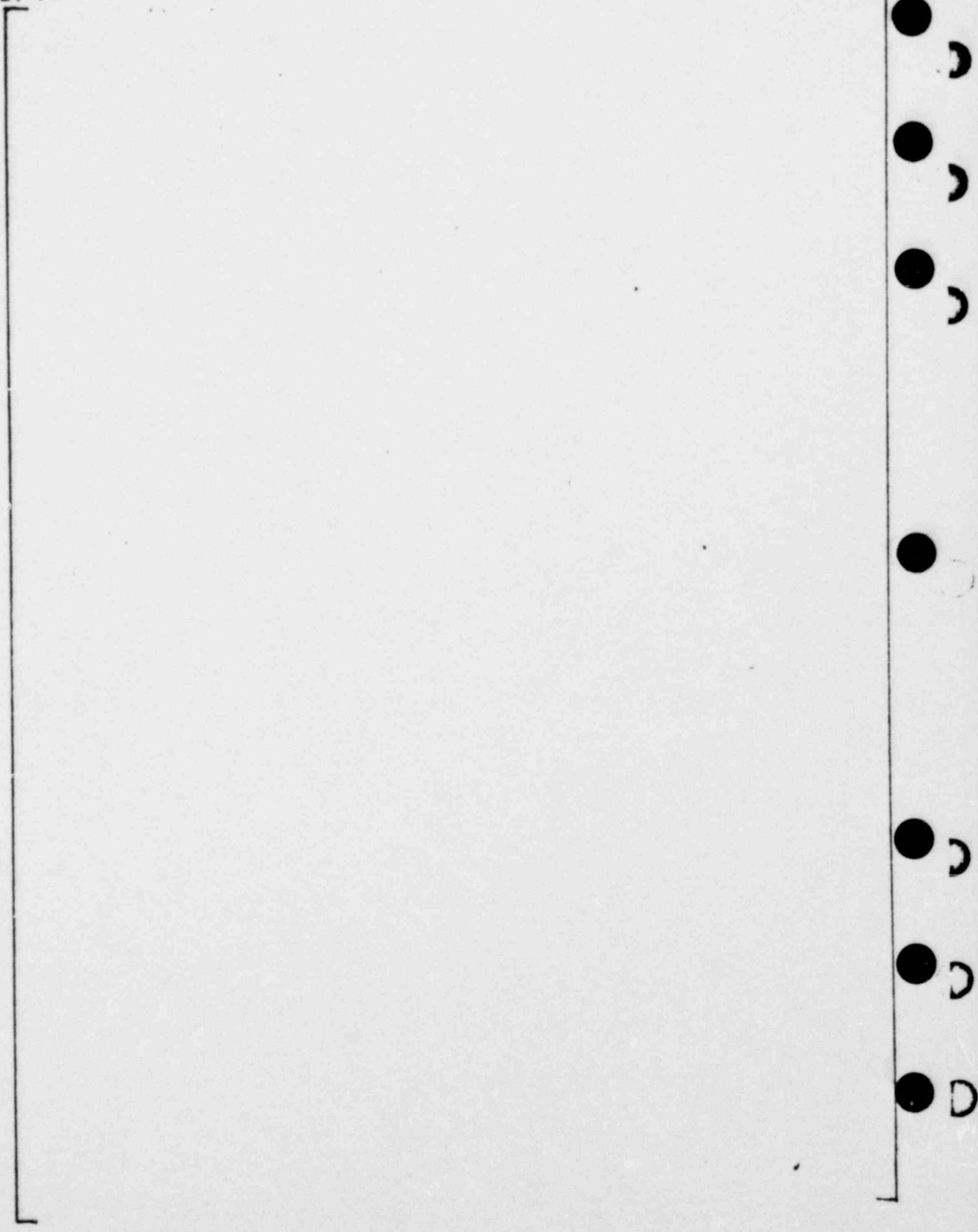

a,b,c,e

a,b,c,e

[redacted]

a,b,c,e

a,b,c,e

[redacted]

a,b,c,e

a,b,c,e

[redacted]

a,b,c,e

[redacted]

a,b,c,e

a,b,c,e

[

]

a,b,c,e

[

]

a,b,c,e

[redacted]

a,b,c,e

a,b,c,e

a,b,c,e

a,b,c,e

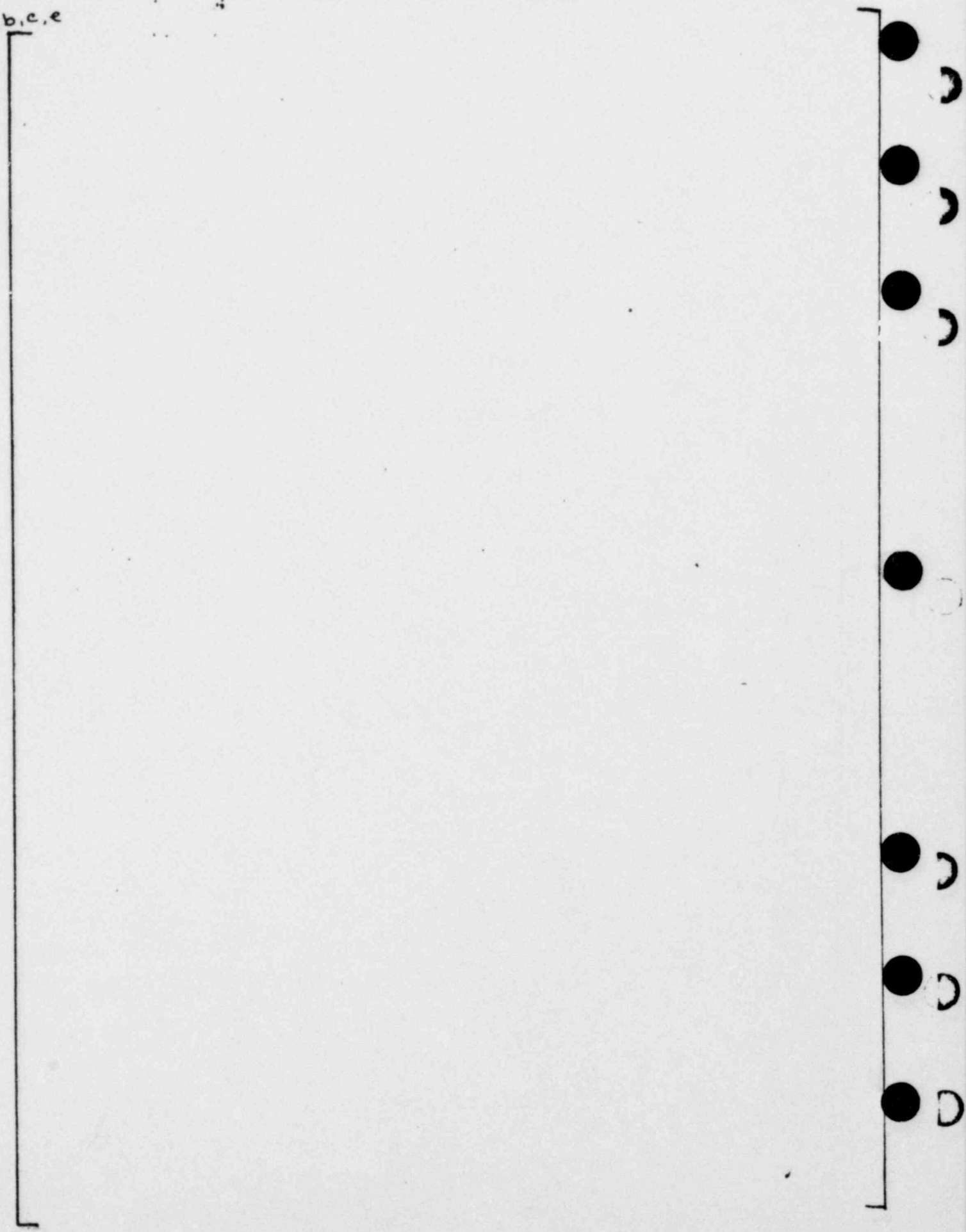

a,b,c,e

[

]

a,b,c,e

[

a,b,c,e

a,b,c,e

[redacted]

a,b,c,e

a,b,c,e

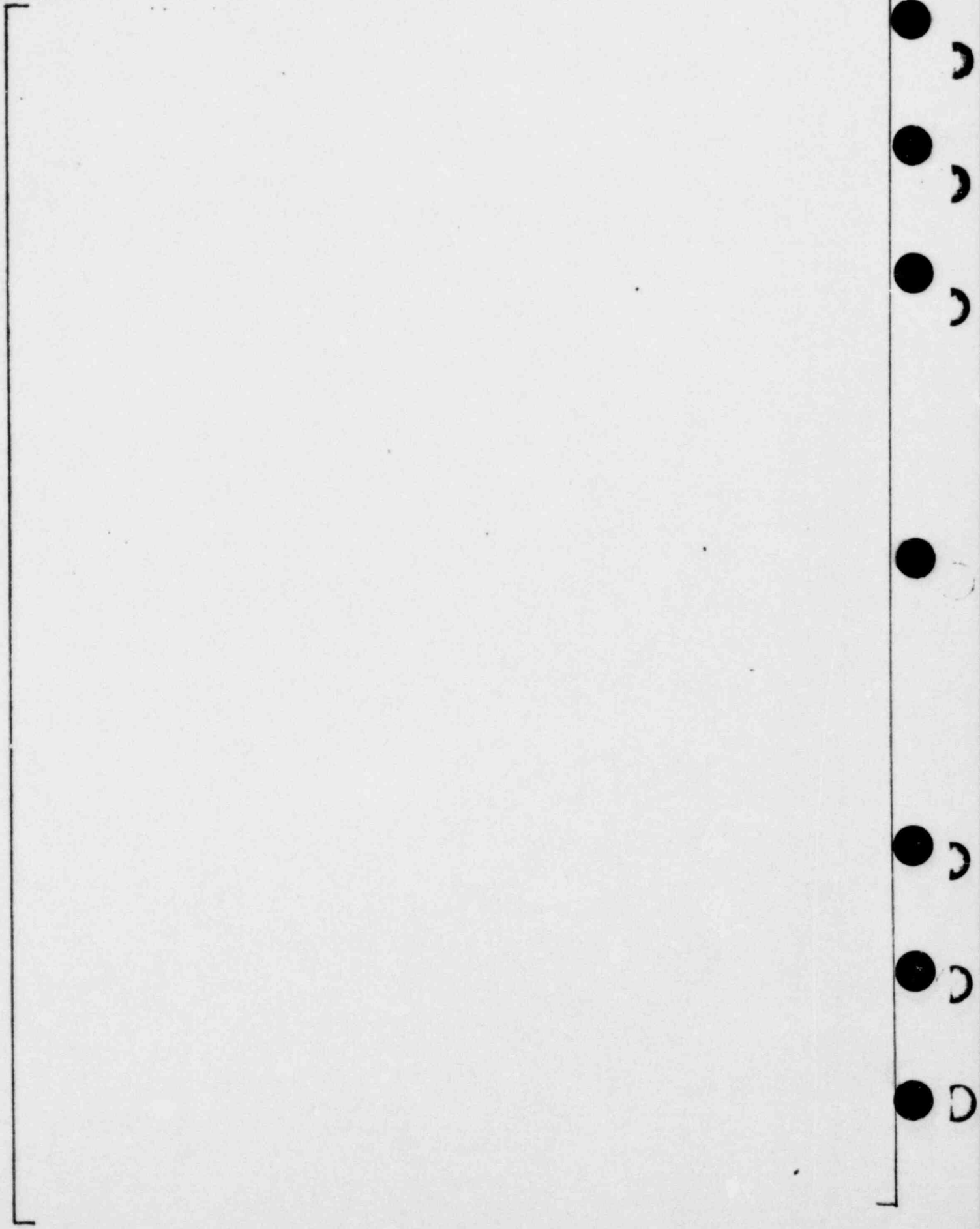

a,b,c,e

a,b,c,e

[

a,b,c,e

a,b,c,e

[redacted]

a,b,c,e

[

]

a,b,c,e

[redacted]

a,b,c,e

SECTION 9.0

PLANT OPERATING HISTORY

By

R. W. Carlson

9.1 INTRODUCTION

A survey of operating plants was conducted to obtain information on operating procedures and operating histories. The original objective was to uncover, if possible, the factors responsible for feedpipe cracking. As the effort proceeded, the emphasis changed to obtaining information on the thermal and hydraulic phenomena of feedpipe stratification and striping.

9.2 PROCEDURES

The desired information was solicited from utilities by means of a questionaire and telephone discussions. A comprehensive questionaire focusing on plant operating procedure and history was prepared. A blank copy is included in Appendix 9A. At the same time, the Westinghouse Nuclear Service Division generated a list giving the individual to be contacted at each plant. These individuals were telephoned to acquaint them with the program and to advise them about the questionaire. The questionaire was actually mailed in August and September, 1980.

Feedback from some utilities indicated that the questionaire was too extensive, requiring too much time and manpower to complete. As a consequence, a simpler, single sheet questionaire was prepared, a blank copy of which is included as Appendix 9B. The objective of this version was to solicit information specifically on conditions leading to stratification. This modified form was mailed following telephone contacts in November, 1979. Generally, it was mailed only to the plants that had not responded to the original questionaire.

As the feedpipe cracking program progressed, it became apparent that striping, as well as stratification, was probably a significant factor contributing to cracking. The revised questionaire provided information on this phenomenon also.

For purposes of this survey, one stratification cycle corresponds to the establishment of the condition where hot and cold feedwater co-exist in the horizontal feedpipe section at the main feedwater nozzle, separated by an approximately horizontal plane interface. Striping time refers to the time during which the stratification condition persists.

The revised questionaire, Appendix 9B, requests data on those operations where stratification and striping are most likely to occur. Those include hot standby, heatup and cooldown, and loading and unloading at low power (<5%). In all these cases, heated feedwater from the feedwater heaters is unavailable since the T/G set is not synchronized. As a consequence, cold feedwater is supplied to the steam generator as required to maintain waterlevel, either by the auxiliary or main feedwater system. Generally, the flowrates are low enough to permit stratification and striping.

Stratification and striping can also occur following a plant trip if the auxiliary feedwater system is actuated by a steam generator low-low level trip. The initial flowrate per loop will usually be high enough to prevent stratification and striping, but the flow is normally throttled back to a lower value where stratification and striping can occur.

9.3 SURVEY RESPONSE

The survey effort is documented in table 1. For each plant the following information is given: 1) the contact person, 2) when the original questionaire was mailed and when a response was received, if any, 3) when the revised questionaire was mailed and when a response was received, and 4) the present status.

The original questionaire was mailed in August and September, 1980, to eighteen plants and two Westinghouse representatives. Of the eighteen plants, eight are members of the Owner's Group and eleven had detected cracking. Five plants responded with at least some data and one responded negatively.

In November, 1979, the revised questionaire was mailed to eleven plants and one Westinghouse representative. Generally, it was mailed to plants that had not responded to the original questionaire. In addition, the revised questionaire was provided to the representatives from Consumers Power Co., Palisades plant, and Northeast Utilities , Millstone 2 plant, at an Owner's Group meeting. Three more responses were received after the revised questionaire was distributed.

In summary, nine plants res onded to one or the other questionaire. Seven provided useful data one provided insufficient data, and one declined to provide any da a.

In most cases where usefui data was provided, it was necessary to contact the utility to obtain additional information and to ask questions about the data provided. The additional data obtained by this means have not been documented by the utilities concerned.

9.4 SURVEY RESULTS

The results of the operating history survey are summarized in table 2. Included are the values up to the date of the survey of the number of stratification cycles and striping time. The detail data for the seven plants are presented in tables 3 through 9 as indicated in table 2.

It will be noted from table 2 that all the plants from which information was obtained did experience feedpipe cracking. It is not possible, therefore, to compare plants with and without cracks.

The number of stratification cycles and the striping time varied widely among the plants from which data was obtained. The stratification cycles ranged from[ ]a factor of approximately[ ]. The smallest and largest striping times were[ ] respectively. In this case, the factor is approximately[ ]. As a

a.c

a,c | generalization, there is some indication that plants with [

]

REQU

OPERATING

TABLE 1

EST FOR INFORMATION
ON
PROCEDURES AND EXPERIENCE

a,c

OPERA

TABLE 1 (Continued)

REQUEST FOR INFORMATION
ON
TING PROCEDURES AND EXPERIENCE

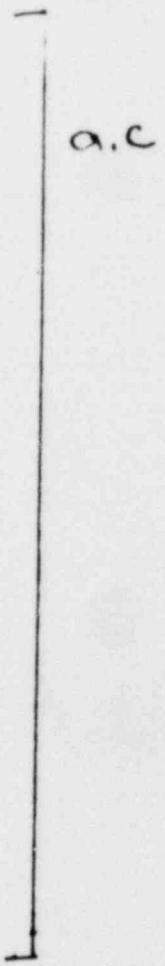

RE

OPERATIN

TABLE 1 (Continued)

QUEST FOR INFORMATION
ON
G PROCEDURES AND EXPERIENCE

a,c

TABLE 2

BER OF STRATIFICATION CYCLES

a,c

TABLE 3

PLANT OPERATING DATA

(Covering Period From First Commercial Operation to Present)

Plant: _____ a,c

Commercial Operation Date: 12/22/72

	Operations			
	Hot Standby	Unit Loading/ Unloading at Low Power <7-8%	Heatup/ Cooldown	Reactor Trip
1) No. of occurrences	[redacted]			
2) Avg. duration per occurrence, hours				
3) Total duration, hours				
4) Main FW System, if applicable				
a) Intermittent or continuous				
b) FW temperature, °F				
c) Flowrate, gpm per SG				
d) No. of flow initiations per hour				
5) Aux. FW System, if applicable				
a) Intermittent or continuous				
b) FW temperature, °F				
c) Flowrate, gpm per SG				
d) No. of flow initiations per day				
6) No. of stratification cycles				
7) Total no. of stratifiation cycles				

a,c

a,c

TABLE 4

PLANT OPERATING DATA

(Covering Period From First Commercial Operation to Present)

a,c

Plant:_____

Commercial Operation Date: 7/61

	Operations			
	Hot Standby	Unit Loading/ Unloading at Low Power <5%	Heatup/ Cooldown	Reactor Trip
1) No. of occurrences				
2) Avg. duration per occurrence				
3) Total duration, days				
4) Main FW System, if applicable				
a) Intermittent or continuous				
b) FW temperature, °F				
c) Flowrate, gpm per SG				
d) No. of flow initiations per day				
5) Aux. FW System, if applicable				
a) Intermittent or continuous				
b) FW temperature, °F				
c) Flowrate, gpm per SG				
d) No. of flow initiations per day				
6) No. of stratification cycles				
7) Total no. of stratification cycles				

a,c

TABLE 5

PLANT OPERATING DATA

(Covering Period From First Commercial Operation to Present)

Plant: _____ a,c

Commercial Operation Date: 10/1/76

Operations

	Hot Shutdown	Unit Loading 0 to 20 25% Power	Heatup/ Cooldown	Reactor Trip
1) No. of occurrences	[			] a,c
2) Avg. duration per occurence, hours				
3) Total duration, hours				
4) Main FW System, if applicable				
a) Intermittent or continuous				
b) FW temperature, °F				
c) Flowrate, gpm per SG				
d) No. of flow initiations per hour				
5) Aux. FW System, if applicable				
a) Intermittent or continuous				
b) FW temperature, °F				
c) Flowrate, gpm per SG				
d) No. of flow initiations per day				
6) No. of stratification cycles				
7) Total no. of stratification cycles				

TABLE 6

H. B. ROBINSON 2
COMMERCIAL OPERATIONS DATE: 3/7/71

Hot Shutdown Periods

a,c

Year	Number of times MFS was in use with continuous low flow rate (<200 gpm/SG)	Total time AFS was in use with intermittent 300-600 gpm/SG flowrate
3/1971 to 1973	[	[
1974		
1975		
1976		
1977		
1978		
1979		
No. of cycles		
Total no. of cycles	]	]

a,c

(1) Estimated, based on average for 1974 through 1976.

(2) Based on intermittent aux. feed at the rate of [ ].

TABLE 7 (SHEET 1)

PLANT OPERATING DATA

(Covering Period From First Commercial Operation to Present)

Plant: [ ]

Commercial Operation Date: 12/2/69

(First 1-1/2 years operation) to 5/28/71

	Operations				
	Hot Shutdown	Unit Loading/ Unloading at Low Power, <5%	Heatup/ Cooldown	Reactor Trip (at Power Trips)	
1) No. of occurrences	[			]	a,c
2) Avg. duration per occurrence, hours					
3) Total duration, hours					
4) Main FW System, if applicable					
a) Intermittent or continuous					
b) FW temperature, °F					
c) Flowrate, gpm per SG					
d) No. of flow initiations per day					
5) Aux. FW System, if applicable					
a) Intermittent or continuous					
b) FW temperature, °F					
c) Flowrate, gpm per SG					
d) No. of flow initiations per hour					
6) No. of stratification cycles					
7) Total no. of stratification cycles				]	

TABLE 7 (SHEET 2)

PLANT OPERATING DATA

(Covering Period From First Commercial Operation to Present)

a,c

Plant: _____

Commercial Operation Date: 12/2/69

(After 1-1/2 years operation)
from 5/30/71 to 8/5/79

	Operations			
	Hot Shutdown	Unit Loading/ Unloading at Low Power, <5%	Heatup/ Cooldown	React. Trip (at Power Trips)
1) No. of occurrences				
2) Avg. duration per occurrence, hours				
3) Total duration, hours				
4) Main FW System, if applicable				
a) Intermittent or continuous				
b) FW temperature, °F				
c) Flowrate, gpm per SG				
d) No. of flow initiations per day				
5) Aux. FW System, if applicable				
a) Intermittent or continuous				
b) FW temperature, °F				
c) Flowrate, gpm per SG				
d) No. of flow initiations per day				
6) No. of stratification cycles				
7) Total no. of stratification cycles				

a,c

TABLE 8

PLANT OPERATING DATA

(Covering Period From First Commercial Operation to Present)

Plant: _____

Commercial Operation Date: 12/31/71

a,c

	Operations			
	Hot Standby	Unit Loading/ Unloading at Low Power, <5%	Heatup/ Cooldown	Reactor Trip (From > 15% Power)
1. No. of occurrences	[			]
2) Avg. duration per occurrence, hours				
3) Total duration, hours				
4) Main FW System, if applicable				
a) Intermittent or continuous				
b) FW temperature, °F				
c) Flowrate, gpm per SG				
d) No. of flow initiations per day				
5) Aux. FW System, if applicable				
a) Intermittent or continuous				
b) FW temperature, °F				
c) Flowrate, gpm per SG				
d) No. of flow initiations per day				
6) No. of stratification cycles cycles				
7) Total no. of stratification cycles				]

a,c

(a) Zero when power ≥1% because then FW is supplied by main FW System. (100 gpm/SG ~1% power)

TABLE 9

PLANT OPERATING DATA

(Covering Period From First Commercial Operation to Present)

Plant: [redacted]

a,c

Commercial Operation Date: 12/26/75

	Operations			
	Hot Shutdown	Unit Loading/ Unloading at Low Power, <5%	Heatup/ Cooldown <200°F	Reactor Trip
1) No. of occurrences	[redacted]			
2) Avg. duration per occurrence, days				
3) Total duration, days				
4) Main FW System, if applicable				
a) Intermittent or continuous				
a,c b) FW temperature, °F				
c) Flowrate, gpm per SG				
d) No. of flow initiations per day				
5) Aux. FW System, if applicable				
a) Intermittent or continuous				
b) FW temperature, °F				
c) Flowrate, gpm per SG				
d) No. of flow initiations per day				
6) No. of stratification cycles				
7) Total no. of stratification cycles				
(1)				[redacted]
(2)				

Appendix 9A

Feedline Cracking Analysis
Plant Operating Information

The attached outline indicates the information desired for the analyses of feedline cracking. The information will be combined on a plant-by-plant basis with crack data and test data, if available, in an effort to isolate the factors responsible for the cracking. Basically, information is needed on those plant operations which influence the fluid and pipe wall conditions in the steam generator - feedpipe weld region. We realize that a large amount of information is being requested and that it may be necessary to compromise on a reduced scope.

Specifically, information needed is in one of two categories. The first relates to the operating procedures and system conditions that determine the fluid conditions in the nozzle - feedpipe region. We believe that feedwater temperature cycling may be an important factor. Since this is most likely to occur at power levels of 20% or less, the auxiliary feedwater system and how it interacts with the steam generator are of primary interest.

Section I lists the operational modes that are of particular interest. Section II outlines the information desired for each of the operational modes. In other words, there will be a separate Section II for each of the operational modes listed in Section I.

The second area is design information on the steam generator and the balance of plant systems. Only plants which have feedring type steam generators are of concern at this time. Of interest would be whether or not the feedrings are fitted with "J" tubes, details of the feedring - feedpipe geometry, the elevation of the ring relative to the narrow range level taps, etc. The design of the auxiliary feedwater system will also be needed. The information needed is outlined in Section III. Some of it, information concerning the steam generator, for example, Section IIIA, will be collected by Westinghouse.

Operating Information

I. Operating Modes of Interest

A. Steady State

1) Hot functional tests

2) Low power (20%) operation

3) Hot shutdown

B. Normal Transients

1) Heatup and cooldown

2) Unit loading and unloading

3) Feedwater cycling at hot shutdown

9A-3

C. Upset Transients

1) Loss of main feedwater with offsite power available

2) Reactor trip

Plant:_____ Unit:_____

II. Operating Mode:_____

A. Number of occurrences and duration of each occurrence (or percent of total operating time) since unit operation began.

B. Steam generator conditions

1) Feedring

a) Was feedring uncovered? How long?

b) Usual water level

2) Steam flowrate

3) Pressure

C. Conditions in SG nozzle - pipe weld region

1) Continuous or slug flow

2) Flowrate

3) Feedwater temperature

4) Pressure fluctuations (small amplitudes are of interest).

SG 1	2	3	4

D. Main Feedwater System

1) Flowrate

2) Usual minimum flowrate or power level

3) Continuous or slug flow

4) Minimum flowrate or power level with continuous flow

5) Feedwater temperature

6) Manual or automatic control

E. Auxiliary Feedwater System

1) Flowrate

2) Continuous or slug flow

3) Feedwater temperature

4) Manual or automatic control

5) No. of times activated.

F. What is procedure for switching from Main to Aux. Feedwater System and vice versa? When is the switch made?

SG			
1	2	3	4

G. Systems in use which connect to the SG nozzles other than the Main Feedwater System and Auxiliary Feedwater System.

H. Primary Coolant System

1) RC pump running?

2) Pressure

3 T_{hot}/T_{cold}

I. Miscellaneous information

1) Feedwater flowrate and temperature vs power level

SG			
1	2	3	4

Plant:_____ Unit:_____

III. Plant Design Information

A. Steam Generator (This information should be available within Westinghouse from NED and NSD)

1) No. of loops _____

2) Steam generator model _____

3) Feedring-thermal sleeve design

a) Feedring ID/OD _____

b) Thermal sleeve ID/OD _____

c) Feedring - thermal sleeve offset _____

d) Feedring length around centerline _____

e) Distance from nozzle weld prep to "T" centerline _____

f) Thermal sleeve - nozzle radial gap _____

g) Feedring/thermal sleeve materials _____

h) "J" tubes or feedring holes? _____

1) Number _____

2) ID _____

3) No. on hot leg side/cold leg side _____

i) Feedring/thermal sleeve materials _____

4) SG nozzle - pipe junction design (sketch would be helpful)

   a) Nozzle pipe schedule _____

   b) Feed pipe schedule _____

   c) Nozzle counterbore ID, if applicable _____

   d) Pipe counterbore ID, if applicable _____

   f) Nozzle/pipe materials _____

5) Narrow range level taps

   a) Span _____

   b) Elevation of feedring centerline _____

   c) Normal water level _____

B. Main Feedwater Piping and Valves

1) Feedpipe section from SG nozzle to first elbow.

a) Distance from SG nozzle to elbow face

b) Pipe dia. and schedule

c) Material

2) Elbow

a) Radius

b) Pipe dia. and schedule

c) Inclination

d) Material

3) Pipe length upstream of elbow

a) Length

b) Pipe dia. and schedule

c) Inclination

d) Material

4) Valves

a) Which, if any, valves are known to leak

b) Leakage rate

SG			
1	2	3	4

C. Auxiliary Feedwater System (A system flow diagram would be useful)

1) Location of aux. feedwater injection point, distance from SG nozzle

2) Valves

a) Which, if any, valves are known to leak

b) Leakage rate

3) Aux. feedwater temperature (does it vary with season of the year?)

	SG		
1	2	3	4

Appendix 9B

Attachment

Feedline Cracking Analysis
Modified Request for Plant Operating Information

Feedback regarding the original questionnaire titled "Feedline Cracking Analysis, Plant Operating Information" indicates that it was too extensive, requiring too much effort on the part of the utilities to complete. Consequently, the following form was devised which focuses on the specific information needed now for completion of the analyses of feedwater temperature stratification.

Stratification refers to the condition in the horizontal feedpipe section connecting to the steam generator where the feedwater is thermally stratified, cold water on the bottom and hot water on top. Such a condition can occur, for example, when the plant is in a hot standby condition and cold aux feedwater added periodically at a low flowrate to restore steam generator level.

It has been shown by stress analysis that stratification can result in significant pipe wall stresses. Combining these results with estimated numbers of stratification cycles leads to usage factors in some cases in excess of one. There is, therefore, evidence that the stresses resulting from stratification are at least a factor contributing to feedline cracking.

Plant Operating Data

(Covering Period from First Commercial Operation to Present)

Plant: _____

Commercial Operation Date: _____

	Operations			
	Hot Standby	Unit Loading/ Unloading at Low Power, <5%(4)	Heatup/ Cooldown	Reactor Trip
1) No. of occurrences				
2) Avg. duration per occurrence, days				
3) Total duration, days				
4) Main FW System, if applicable(1)				
a) Slug or continuous				
b) FW temperature, ^{o}F				
c) Flowrate, gpm per SG				
d) No. of flow initiations per day(2)				
5) Aux. FW System, if applicable(1)				
a) Slug or continuous				
b) FW temperature, ^{o}F				
c) Flowrate, gpm per SG				
d) No. of flow initiations per day(2)				
6) No. of stratification cycles(3)				
7) Total no. of stratification cycles				

Footnotes:

(1) Feedwater will usually be provided by either the main or aux feedwater system, but not both.

(2) Applies to slug flow.

(3) If flow is continuous, no. of cycles will be the same as the number of occurrences. If slug flow, no. of cycles will be equal to Total duration in days/No. of flow initiations per day.

(4) The number of trips while loading should be included. The unloading refers to planned unloadings, not reactor trips.

WESTINGHOUSE NON-PROPRIETARY CLASS 3

WCAP-9812

INVESTIGATION OF FEEDWATER LINE CRACKING IN PRESSURIZED WATER REACTOR PLANTS

DECEMBER 1980

WORKED PERFORMED BY
WESTINGHOUSE NUCLEAR TECHNOLOGY DIVISION

FOR

FEEDWATER CRACKING UTILITY OWNERS GROUP
WORK PERFORMED UNDER S.O. MUAN 1000 - 8000

APPROVED: D. H. White

D. H. White, Manager
Applied Mechanics
Westinghouse Nuclear Technology Division

APPROVED: T. E. Campbell

T. E. Campbell, Manager
Structural Mechanics Department
Westinghouse Nuclear Technology Division

TABLE OF CONTENTS

SECTION	TITLE	TAB NUMBER
1.0	Introduction	1
2.0	Summary	2
3.0	Conclusions	3
4.0	Recommendations	4
5.0	Metallurgical Investigation	5
6.0	Chemistry Evaluation	6
7.0	Piping Design Verification Analysis	7
8.0	On-Site Feedwater Test Programs	8
9.0	Plant Operating History	9
10.0	Flow Model Tests	10
11.0	Stress Analysis and Structural Evaluation	11
12.0	Fatigue Crack Growth Consideration	12
[		] a,b,c,e

SECTION 10.0

FLOW MODEL TESTS

BY

M. H. Hu
D. C. Meess
D. L. LaPay

ACKNOWLEDGMENT

We wish to express our sincere thanks to the following persons who have made valuable contributions as consultants, designers, and/or expediters:

E. H. Novendstern
J. L. Houtman
G. P. Lilly
R. Quaglia
J. Parello
F. R. Falise
D. H. White
F. Loceff
C. R. Smith
D. K. Smith

10.1 INTRODUCTION AND OBJECTIVES

10.1.1 BACKGROUND

As discussed in Section 1.0, cracks were observed in the feedline adjacent to the feedwater welds for the feedring-type steam generators. The problem occurred in various PWR plants despite differences in geometry. In addition, cracking was observed in plants with a feedring with bottom hole discharge and with top discharge through J-tubes.

Metallurgical investigations have pointed out that the major characteristics of the cracking indicate corrosion fatigue. It was also speculated that both high cycle fatigue and low cycle fatigue were involved.

Thermocouple data of the on-site testing, as discussed in Section 8, has confirmed the existence of persistent thermal stratification during operations of low feedwater flow, [

a,b

].

According to the on-site testing, no thermal oscillations except those due to transient variation of feedwater flow were detected. Thus, the potential fatigue mechanism of high cycle fatigue was yet to be verified by other means.

It was postulated at this time that a potential mechanism for producing high frequency thermal oscillations (striping) exists due to mixing of hot and cold fluid or turbulence in the hot/cold stratification as a result of the strong buoyancy forces occurring during low flow rate feedwater conditions. Because of the difficulty in measuring this type of local phenomenon in the field, the flow test presented in this section was proposed and conducted.

10.1.2 TEST OBJECTIVES

The flow model tests were performed to achieve the following specific objectives:

1. To determine if reverse flow leakage occurs through the annulus formed by the feedwater nozzle and the thermal sleeve.

2. To determine if reversal flow of hot water occurs from the feedring (downstream) to the feedline (upstream).

3. To determine if thermal oscillations occur at the stratified interface.

4. To determine if thermal oscillations occur as a result of mixing of hot and cold water.

5. To determine the temperature profile of the feedline during stratification conditions.

Thus, the flow model tests were aimed mainly at investigating the thermal-hydraulic mechanisms which contribute to fatigue damage. Results of the flow model tests are used to establish the thermal boundary conditions for the three dimensional analysis of stratification stresses as well as providing oscillation data for evaluating hig cycle fatigue.

10.2 TEST SECTION AND INSTRUMENTATION

10.2.1 CONFIGURATION OF FEEDLINE SYSTEM

A survey of various PWR plants has indicated that the configurations of the feedline system can, in general, be classified according to the types of feedlines and discharges. The type of the feedline will affect the inlet conditions of thermal and fluid flow to the feedwater nozzle,

including its upstream geometry such as the counterbore where cracks occurred. Differences in the type of discharge can also affect the upstream conditions in different ways. Thus, four configurations were selected to be incorporated in the test program as shown in Table 10.1.

10.2.2 FUNCTIONAL REQUIREMENTS

The functional requirements of the flow model test were established as given in Table 10.2. [

a,c

]

The range of flow rates is sufficient to obtain the full range of stratified flows from a shallow stratified cold layer up to the fully cold pipe. It was shown by the on-site testing that the feedwater pipe was filled with cold feedwater [ ] It is believed that the feedline and the nozzle will be free from any thermal and fluid flow oscillations once the line is filled with the cold water.

a,c

The temperature of the vessel hot water is limited to [

a,c

].

10.2.3 MODELING CRITERIA

In order to investigate thermal and fluid flow stratification and fluid mixing, dynamic similitude must exist. [

a,c

]

a,c [ ]

[ ]. The flow patterns would be similar provided that heat transfer process is similar too. [

a,c]. It is necessary to evaluate the flow regimes in order to select an appropriate dimensionless parameter [ ] to be used as a design criterion.

10.2.3.1 Basic Parameters and Dynamic Similitude

Table 10.3 lists the values of some basic parameters for the steam generator and the test model. [

a,c]

a,c [ ]

[

a,c

]

a,c [ ]

10.2.3.2 Selection of Geometric Scale

a,c [ ]

10.2.3.3 Design of Discharge Pipe

a,c [ ]

10.2.4 TEST SECTION DESCRIPTION

The test program consists of two series of tests, each of which has a different piping geometry upstream of the feedwater nozzle. The horizontal feedline configuration has a long horizontal run of piping connected directly to the feedwater nozzle, as shown in Figures 10-8 and 10-9. Piping for the elbow feedline configuration has a long radius 90° vertical elbow directly upstream of the nozzle, as shown in Figures 10-9 to 10-12.

10.2.4.1 Horizontal Feedline Model

[ ] a,c

a,c [ ]

10.2.4.2 Elbow Feedline Model

The elbow feedline test model is shown in Figures 10-10 to 10-13. It consists of the same reservoir, stand, and feedwater ring/thermal sleeve section described earlier. The straight nozzle/pipe section is replaced by a nozzle/elbow section.

a,c [ ]

10.2.5 THERMOCOUPLE INSTALLATIONS

Type J iron-constantine grounded junction sheathed thermocouples are installed in the piping, test sections and reservoir to measure temperatures and fluctuations. Table 10.5 lists the different thermocouples used at each measurement location and the parameter being measured.

The locations of the thermocouples used to measure [ ] and reservoir drain water temperatures are shown in Figure 10-14. Both are attached to the copper piping with standard compression type fittings and adjusted so that the tip of the thermocouple is in the center of the pipe.

Figure 10-15 illustrates the locations of the thermocouples on the reservoir. All four of these thermocouples are attached with compression fittings. The insertion of each thermocouple beyond the inside surface of the reservoir wall is also indicated on the figure.

Figures 10-16 through 10-22 document the locations of [ ] thermocouples installed in the straight nozzle/feedwater pipe test section and in the thermal liner/feedwater ring section. A list of these thermocouples is provided in Table 10.6 and indicates the thermocouple position identification number, the method of attachment and the insertion of the thermocouple [ ]

a,c

The thermocouple locations in the elbow nozzle/feedwater pipe test section are almost identical to the above positions. Figures 10-18 through 10-24 and Table 10.7 document these thermocouple positions.

10.2.6 DYE INJECTION LOCATIONS

The feedwater nozzle and the thermal liner/feedwater ring section have numerous penetrations for dye injection. Qualitative data regarding flow stratification, mixing and recirculation is obtained from flow visualization tests using colored dye. Two dye injection systems provide red or blue dye at an adjustable pressure to each individual dye injection penetration on the test section. [ ]

a,c [

]

The dye injection locations for elbow nozzle tests are nearly the same as for straight nozzle tests and are shown in Figures 10-27 and 10-28 and listed in Table 10.9. Dye injection points on the elbow tests section are also shown pictorially in Figure 10-29.

10.3 TEST FACILITY AND OPERATION

10.3.1 FEEDWATER NOZZLE TEST FACILITY

The Steam Generator Feedwater Nozzle/Piping Test Facility is located in the Hydraulic Testing Area at the Westinghouse Advanced Reactors Division (WARD), Waltz Mills, Pennsylvania. A schematic of this faciity with the test section and piping is shown in Figure 10-14. The test arrangement is shown pictorially in Figures 10-30 and 10-31.

[ ] a,c

a,c

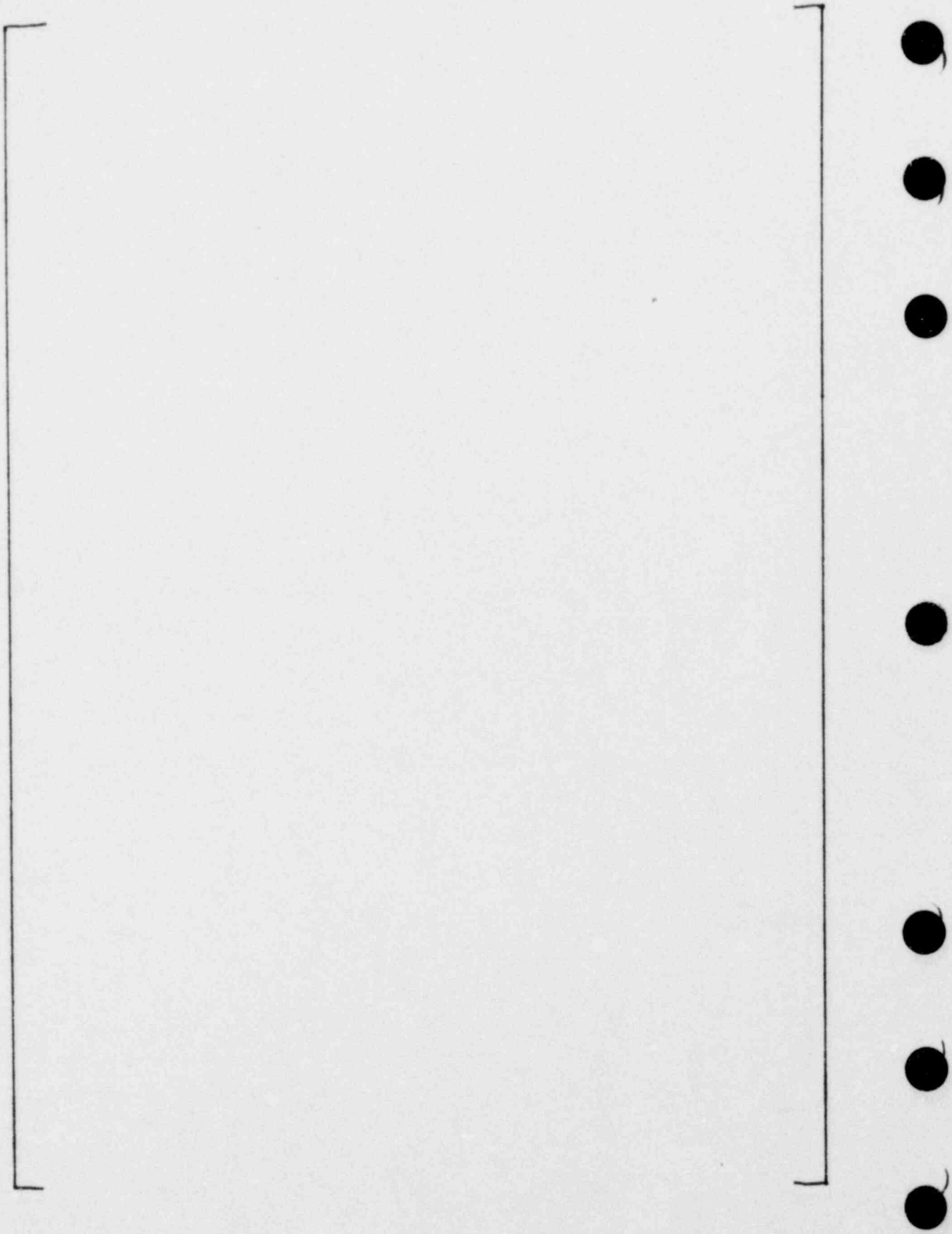

[ ] a,c

10.3.2 THERMAL MIXING HYDRAULIC LOOP (TMHL)

The Thermal Mixing Hydraulic Loop (TMHL), shown schematically in Figure 10-33 and pictorially in Figure 10-34, supplies the hot city water to initially fill the test section. The Thermal Mixing Hydraulic Loop is an open recirculation water loop [ ] a,c

10.3.3 MULTI-PURPOSE HYDRAULIC LOOP (MPHL)

[ ] a,c

a,c [ ]

a,c [ ]

a,c [ ]

10.3.4 TEST OPERATION

A detailed test plan and procedure was written to encompass all straight and elbow piping tests. A summary of typical test facility and loop operations follows.

10.3.4.1 Instrumentation Preparation

Power to all electrical equipment and instruments is turned on in advance of the test to insure that all signals had stabilized. The thermocouples of interest for each test are connected through a multi-channel reference junction and individual amplifiers to one of the three FM magnetic tape recorders. The output of the electronic manometer,

a,c which measures the differential pressure [ ], is connected to one channel of each tape machine. An event

marker (D.C. voltage signal) is connected to another channel of each recorder to provide a common reference signal on all tapes simultaneously. The gains and filters of all amplifiers are adjusted and set as specified in Section 10.4, "Data Acquisition Systems." The outputs of five thermocouples are monitored on a visicorder, as well as being recorded on magnetic tape, during the tests. All signal paths are recorded and documented on data forms.

Known calibration signals of 0.0000 volts D.C. and 1.000 volts A.C. RMS at a 50 Hz frequency are recorded on each tape channel, near the end of each tape. These signals are provided to assist in adjusting the instrumentation used to monitor these tapes during data reduction and analysis. Written tape logs with the chronology of events on each tape are maintained.

10.3.4.2 [ ] a,c

[ ] a,c

10.3.4.3 Hot Water Production

Hot [ ] city water that will fill the test reservoir is produced in the Thermal Mixing Hydraulic Loop (TMHL). A loop schematic is shown in Figure 10-33. The 3000-gallon storage tank is filled with city water a,c

and steam circulated through a large heat transfer coil inside the tank to heat the water. A 2000 GPM pump is also used to mix the water in the storage tank by circulating the water through the loop bypass valves. This hot water is also circulated through the reservoir fill line and back to the TMHL storage tank to prevent heat losses to the cold piping and subsequent lowering of the hot water temperature when later initiating the fill.

10.3.4.4 Reservoir Fill and Circulation

After the circulating hot water reaches [ ] as indicated by a mercury thermometer, the reservoir is filled to a level of [ ] inches from the top. The [ ] recirculation pump shown in Figure 10-14 is activated to pump water from the reservoir bottom to the upstream side of the test section. This flow of hot water is used to maintain a more a,c uniform test section temperature throughout the nozzle and reservoir than would have existed in a stagnant test section. This flow continues until prior to the start of a test. If additional heat is required to increase the water temperature, a [ ] immersion heater in the bottom of the reservoir is activated.

a,c 10.3.4.5 [ ]

To start the test sequence, all three FM magnetic tape recorders and the visicorder are activated to record the temperature of the hot and cold circulating solutions. [ ]

a,c temperatures are measured by thermocouples in the reservoir [ ]. These data are obtained from a DVM and recorded on a data sheet and on the tape voice tracks.

The reservoir heater and recirculation pump are shut down and the connecting valves closed. The water in the reservoir is now stagnant. [

a,c] recirculation is terminated by closing the appropriate valve. [ ]

slowly opened until the correct test flowrate is obtained, as indicated by the ΔP indicator. The automatic level control system opens the drain valve as required to maintain a level [ ] inches down from the reservoir top. This water flows by gravity into a [ ] storage tank. a,c

After the correct flowrate is achieved, the event marker is activated to denote the location of this event on the magnetic tapes, and the nominal flowrate is recorded by voice on all three recorders. The differential pressure [ ], as indicated by the gage and electronic manometer, are recorded on a data sheet. [ ] a,c

During various selected tests, flow visualization tests are performed. Different colors of dye are injected at various locations in the feedwater nozzle and thermal sleeve/feedwater ring during the test to observe flow patterns. The results were recorded on 16mm color motion picture film.

In the middle of the test run, the flowrate (ΔP across flow orifice) is recorded again [ ] Just prior to the end of the test, the flowrate is recorded for a third time [ ]. a,c

The test is terminated [ ], isolating the electronic manometer measuring the differential pressure across the flow orifice and stopping all tape recorders and the visicorder. The test section and reservoir are then drained in preparation for the next test. a,c

10.3.4.6 Draining Test Section

During the test, the [ ] storage tank shown in Figure 10-14 was filled with drain water from the reservoir. [ ] is pumped into a larger 7000-gallon storage pool. The remaining water in a,c

the reservoir and test section is then gravity-drained into the 900-gallon storage tank and transferred to the large storage pool.[

a,c |]

10.4 DATA ACQUISITION SYSTEMS (DAS)

10.4.1 TEST DATA ACQUISITION SYSTEM

The data acquisition system used for all tests is shown in Figure 10-37. All instruments are listed in Table 10.10 with the operational range and overall accuracy of each. The DAS consists of three basic parts, (1) temperature measurement system, (2) flow rate measurement system and (3) event marker system.

10.4.1.1 Temperature Measurement System

All Type-J iron-constantine thermocouples in the test article, piping and reservoir are routed to a thermocouple patch panel (Figure 10-37) where selective thermocouples may be plugged into the female jack panel. Forty female jacks in this panel are connected to a calibrated 50-channel ice-point reference junction which supplies a zero millivolt signal at a thermocouple temperature of 32°F. This reference junction is located adjacent to the reservoir. Signal cables connect the reference junction channels to the Hydraulic Facility Control Room where the signal amplifiers and recorders are located. These signal cables are connected to amplifiers which boost the small thermocouple signals by a gain of 300. Integral within these amplifiers is a set of filters which eliminates any stray signals above one of the selective frequencies. Initial tests were performed with all filters set to 100 Hz. The filters were subsequently adjusted to 10 Hz for test 6A and all remaining tests.

The output of the reference calibration thermocouple in the side of the reservoir, which measures the initial hot water temperature and the test section temperature during isothermal calibrations, is not amplified but

measured directly with a digital voltmeter as shown in Figure 10-37.

[ ] a,c

All amplified thermocouple signals are patched into one of the three 14-channel FM magnetic tape recorders as shown in Figure 10-37. Tape recorders R-1 and R-2 are the Honeywell Model 101. Machine R-3 is a Sangamo Saber III. All machines were set up to record and replay at 3-3/4 IPS with a IRIG Intermediate band configuration, which has a center frequency of 6.75 kHz and a data bandwidth of 0 to 1.25 kHz. The inputs and outputs were adjusted for a $\pm$ 1 volt RMS full scale signal.

Five thermocouples of interest were recorded on visicorder charts in addition to magnetic tape for each test. As shown in Figure 10-37, the amplifier outputs for there thermocouple signals are connected to both tape recorder and visicorder channels in parallel.

10.4.1.2 Flow Rate Measurement System

[ ] flowrate is measured by monitoring the differential pressure across one of four different sized orifice flow meter sections listed in Table 10.10. This ΔP is visually monitored by both an accurate ΔDP indicator (gage) and an electronic manometer (ΔP cell) connected in parallel. The electronic manometer has full scale ranges of 10 PSI and 1 PSI, and yields a 1 volt D.C. signal at the full scale on each range position. The relationship between output voltage and ΔP is linear from 0 PSI/0 volts through the full scale of each range. The analog output is recorded on one channel of each tape recorder to record any flow fluctuations during the test. The differential pressure is converted to GPM by utilizing a theoretical orifice calibration curve calculated according to ASME guidelines. a,c

10.4.1.3 Event Marker System

An event marker is connected to one channel of each tape recorder to provide a common reference signal on each tape at significant test events. The marker voltage is stepped from 0 to ~0.7 volts when activated.

10.4.2 MAGNETIC TAPE REPLAY SYSTEM

Various magnetic tapes are replayed into a visicorder as indicated in Figure 10-38 to verify that the thermocouple signals are recorded properly and that the entire DAS is functioning as designed. Also, the data can be quickly reviewed following each test, prior to processing the magnetic tape.

10.4.3 CALIBRATION SIGNAL SYSTEM

Precision measured calibration signals of 0.000 volts D.C. and 1.000 volts AC RMS at 50 Hz are recorded on each channel of every magnetic tape for use during data reduction. The systems used to accomplish this, shown in Figure 10-39, consist of a signal generator, counter, digital voltmeter and the DAS from the tape input patch panel through the tape machines.

For zero calibration, the first seven inputs of the first tape recorder are connected together and shorted at the DVM. After 20 feet of tape is recorded, the same is performed with the last seven tape channels.

A 1 volt RMS 50 Hz signal is obtained from the signal generator. The frequency is measured by the counter and the voltage by an A.C. DVM. This signal is recorded on the first tape recorder, seven channels at a time, just as with the zero signal. The above zero and 1 volt RMS 50 Hz signals are recorded as described above on each of the other tape machines in turn.

10.4.4 [ ] MEASUREMENT | a,c

[ ] a,c

10.5 DATA REDUCTION METHODS

Thermocouples and flow measurements from the flow model tests were recorded on fourteen channel tapes by three FM recorders. Before this data could be used by the Westinghouse Monroeville Nuclear Center (MNC) CDC-7600 computers, it was necessary to convert it to a format compatible with the CDC-7600 system. Several processes were involved in the data reduction of the flow model test data. These included digitization of the FM tapes, 16-bit to 60-bit computer word conversion, calibration and amplification adjustments, voltage-to-temperature conversions and generation of thermocouple flow plots.

10.5.1 DATA DIGITIZATION

The first step in the data reduction process was digitization of the test data recorded on the fourteen channel FM tapes. This function was performed by the MNC Analog-Hybrid Laboratory. For the straight pipe flow model tests, and the elbow flow model tests, data was digitized at 100 samples/second at 7-1/2 ips. This resulted in an effective sampling rate of 50 samples/second at 3-3/4 ips. The digitized data for each FM tape was written in units of voltages on a separate nine-track magnetic tape that is read into the CDC-7600 computers. In addition to digitizing the data, the analog-hybrid laboratory generated pen plots of the data recorded on each channel of the FM tapes.

10.5.2 CONVERSION OF BIT STRUCTURE

The next step in reducing the flow model test data involved changing the bit-structure of the data written on the nine-track magnetic tapes. More specifically, it was necessary to convert the 16-bit computer words for the MNC CDC-7600 computers. The Configuration Control computer code named CONBITS was used for this conversion. The computer code generated printed data lists and new permanent files of the converted 60-bit word data for specified straight pipe and elbow flow model tests.

10.5.3 DATA CALIBRATION AND AMPLIFICATION

The remaining portion of the flow model test data reduction was performed. As a first step, the zero volt calibration signals recorded on each of the FM tapes were plotted. Then the test data were adjusted slightly upwards or downwards to account for any differences between the zero volt signal produced by the FM recorder used to record the data and the signal ready by the FM recorder used to digitize the data. Since an accurate representation of the 50 Hz rms calibration signal could not be obtained with the sampling rates used to digitize the flow model test data, the pen plots generated by the analog laboratory were used to obtain the calibration multipliers. [ ] The calibration

a,c,e

multipliers are used to adjust the test data to account for any differences in the signal amplifications of the FM recorders used to record and digitize the test data. In addition to calibration considerations, an amplification (or gain) factor was associated with each thermcouple signal.

10.5.4 CONVERSION OF VOLTAGE TO TEMPERATURE

After the test data was adjusted for the calibration-amplification considerations it was necessary to convert the thermocouple voltages to the corresponding temperatures in degrees Fahrenheit. This was accomplished by first obtaining the correct voltage-to-temperature conversion chart for the Type J thermocouples used in the flow model test. Then, temperatures were plotted versus millivolts for the temperature range measured by the thermocouples during the flow model testing [ ] a,c.

10.5.5 TIME HISTORY PLOTS OF TEMPERATURE

Plots of the flow and thermocouple data were generated for the straight-pipe and elbow flow model tests. These plots were compared to plots generated by the analog laboratory for selected test cases and in all cases, the digitized and analog data plots were in agreement.

10.6 TEST RUNS PERFORMED

Test was planned to perform over a range of feedwater flow for both the horizontal and the elbow feedline configuration. For each feedline configuration, the test was grouped into two parts. The first part emphasizes the visual observations using dye injection although thermocouple data collection was also made. The second part is for thermocouple data acquisition without dye injection.

Table 10.11 lists the specifications of each of 27 test runs performed. The first 16 runs utilized the horizontal feedline-nozzle assembly and

the remaining 11 runs were performed with the elbow feedline-nozzle assembly. All test runs had been made according to the test procedure described in Section 10.3.

The last test run was to simulate the case with the annulus between the nozzle and the thermal sleeve sealed from the end of the test vessel (i.e. test tank).

10.7 TEST RESULTS AND DATA ANALYSIS

10.7.1 OBSERVATION OF FLOW PATTERNS

Test Run Nos. 1-6 are of J-tube discharge without holes in the flanges (or end cap) for the horizontal feedline. The cold stratified layer built up by pushing the existing hot water out of the feedline and the feedring via the J-tubes. During the build-up the interface was smooth at low feedwater flow [ ] and wavy at moderate and high flow [

a,c

] Test Run Nos. 7B and 7C were made to sustain stratification. The configuration of No. 7C was used throughout the rest of tests for the J-tube discharge with 2" holes in the lower portion of the flange (Figure 10-7).

Test Run Nos. 6A, 7, 7A, 10 and 11 are of the bottom discharge type for the horizontal feedline configuration. [

a,c

]

10.7.1.1 General Feedline Flow

The feedline flow is stratified and countercurrent; the cold feedwater flows in the bottom portion of the pipe and into the test section tank

(i.e. steam generator) via the feedring, and the hot water flows in the upper portion of the pipe and advances from the feedring into the feedline. This is illustrated in Figures 10-41 - 10-44. The cold layer is in the turbulent flow regime and the hot layer is in the laminar regime or may be stagnant.

Figure 10-41 shows the flow [ ] for the J-tube discharge [ ] the interface is essentially stable, [ ]. Figure 10-42 shows the flow at moderate and high flow rate for the same discharge arrangement as Figure 10-41, [ ]. Shown in Figure 10-43 is the flow conditions of Test Run No. 7C, which is the J-tube discharge [ ]. a,c

Test Run Nos. 7, 7A, 8 and 9 are of the bottom discharge for the horizontal feedline, [ ]. The flow stratification is persistent [ ] charge. Shown in Figure 10-44 is the general flow pattern; the hot layer flow is relatively high if there is the hot water communication between the vessel and the feedring. If there is no communication, such as Run No. 7 the hot layer is very slow or almost stagnant]. a,c

The above observations are general and applicable to the rest of test runs for the elbow feedline configuration (see Table 10.11).

10.7.1.2 Annular Gap Flow

In general, flow patterns in the annular gap are very complicated; the following is just a brief description.

Figure 10-45 is a schematic of flow pattern of the annular gap during the J-tube discharge at [ ]. This illustrates the gap flow under the conditions when the feedline is almost filled with a,c

cold water. [

a,c

] For Test Run No. 5, an eccentric gap was introduced by pushing the thermal sleeve into bottom contact with the nozzle. Figure 10-46 illustrates this eccentric gap flow; it was a forward leakage of the cold water. [

a,c

]

a,c

a,c

], Figure 10-48 illustrates the annular gap flow pattern, [

a,c

].

These general descriptions of the annular gap flow are applicable to the elbow feedline configuration.

10.7.1.3 Flow Patterns of Discharge Pipe

During the bottom hole discharge, the cold water was released through those holes [

a,c

]. Figure 10-51 shows that all of the bottom holes are discharging the cold water [

] [ ]

[ ] a,c

10.7.2 THERMAL AND FLOW OSCILLATIONS

Tables 10.12 and 10.13 list temperature oscillation data, which includes the amplitude, period and density of maximum temperature oscillation. The density is defined as the average cycles occurring in 100 seconds. In addition, the table contains the dominant temperature oscillation amplitude and period, and the ratios between the temperature oscillation amplitude and the potential (i.e. maximum possible) temperature difference. The potential temperature difference is that between the hot and the cold water sources.

For the horizontal configuration the amplitude may reach 35 percent of the potential temperature difference, and the period for the dominant amplitude ranges from 2 to 10 seconds. For the elbow configuration the amplitude may reach the potential difference (i.e. 100 percent), and the dominant period is about 1 to 10 seconds.

Figures 10-55 - 10-58 show the typical temperature oscillation profiles for the horizontal and elbow feedlines, respectively.

It is in order to mention that these tables were prepared only for general understanding and comparison between the horizontal and the elbow feedline configurations.

For the evaluation of thermal fatigue, a Fourier analysis will be used for detailed analysis of thermal striping effects in Section 11.

10.7.2.1 Amplitude of Temperature Oscillation

Figures 10-59 and 10-60 show the envelope of the relative oscillation amplitude for the horizontal feedline configuration. The bottom discharge seemed to give higher oscillation amplitude than the J-tube through the entire range. And the difference between them is very large at high cold layer depth.

Figures 10-61 and 10-62 present the envelope of the relative oscillation amplitude for the elbow configuration. The bottom discharge gave greater thermal oscillation at lower cold layer depth. Both the J-tube and the bottom discharge gave equivalent thermal oscillation at higher cold layer depth.

10.7.2.2 Scale Factors for Oscillation

Under the consideration of dynamic similitude, the oscillation amplitude can be scaled as follows:

$$(\Delta T)_{SG} = S_p (\Delta T)_M \qquad (10.1)$$

$$S_p = (\Delta T_p)_{SG} / (\Delta T_p)_M \qquad (10.2)$$

Where

S_p = amplitude scale factor

ΔT = peak to peak amplitude of temperature oscillation

ΔT_p = potential difference in temperature

[ ] a,c

Tables 10.14 and 10.15 list the values of various scale factors for the horizontal and the elbow feedline, respectively.

10.7.3 FLUID MIXING AND THERMAL STRIPING

As confirmed by the flow model tests and the on-site testing, thermal and fluid flow stratification can take place in the feedline and the interface between the hot and the cold layer is subject to oscillations. This oscillatory interface results in the pipe wall being subjected to a fluid flow with an oscillating bulk fluid temperature. In addition, the pipe wall is exposed to an oscillating velocity because the stratified flow is countercurrent and at different speeds; the hot layer being either laminar or stagnant and the cold layer being turbulent.

Mixing of fluid flow can also occur when a hot stream meets a cold one, such as those observed within the annulus or those within the engaging zone between the nozzle and the sleeve. Because the mixing processes of these types are oscillatory in nature, the bulk fluid temperature is thus oscillating.

a,c [ ]

The oscillatory thermal response which a solid surface such as the pipe wall experiences as a result of any bulk fluid thermal oscillations have been termed "thermal striping". The degree of thermal striping is related to the bulk fluid oscillation amplitude and heat transfer coefficient; the higher the amplitude and/or the coefficient, the higher the severity of thermal striping on the wall.

10.7.4 TEMPERATURE PROFILES

In order to calculate thermal stresses of the feedline and nozzle it is necessary to study the heat conduction within the pipe wall since the

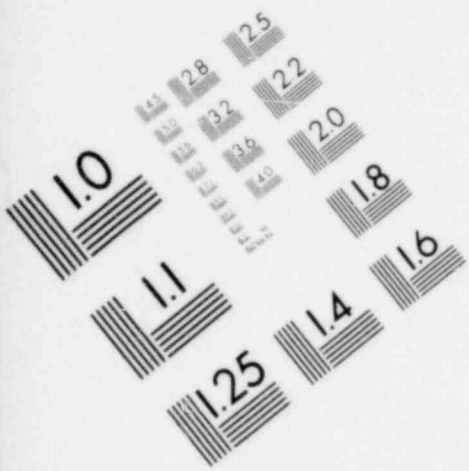

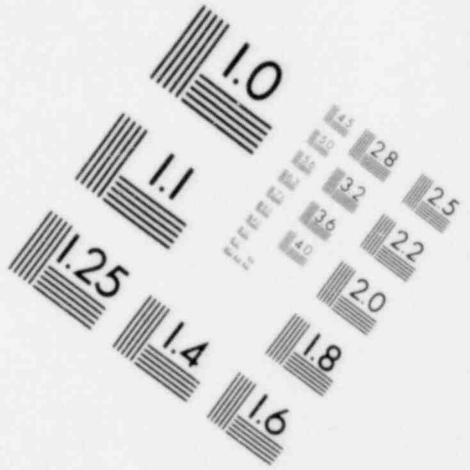

IMAGE EVALUATION TEST TARGET (MT-3)

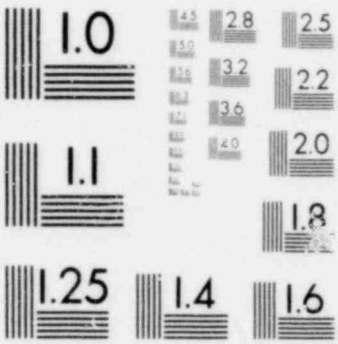

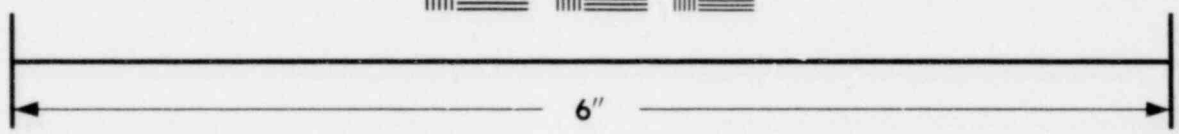

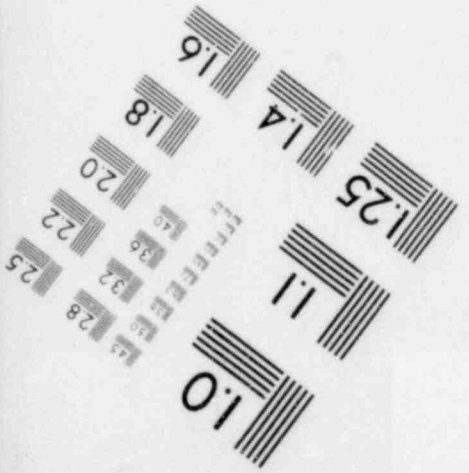

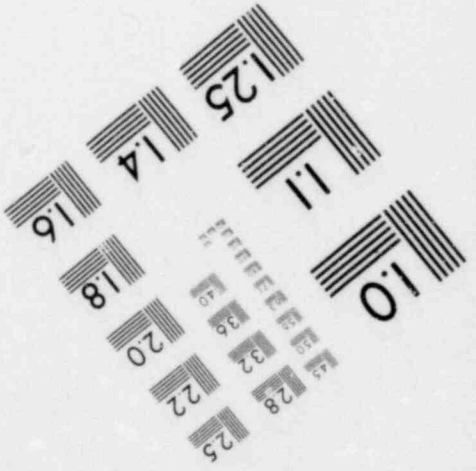

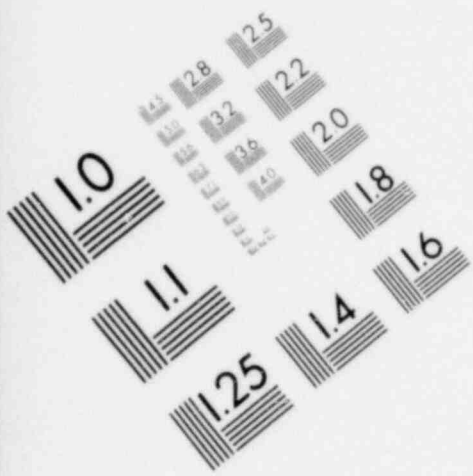

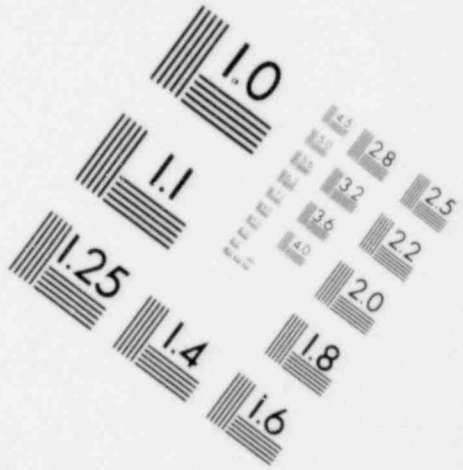

IMAGE EVALUATION TEST TARGET (MT-3)

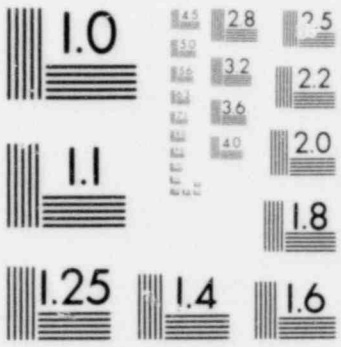

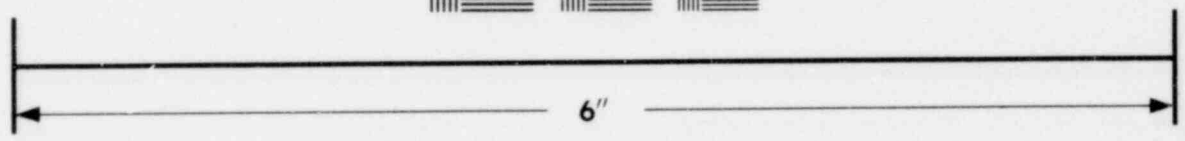

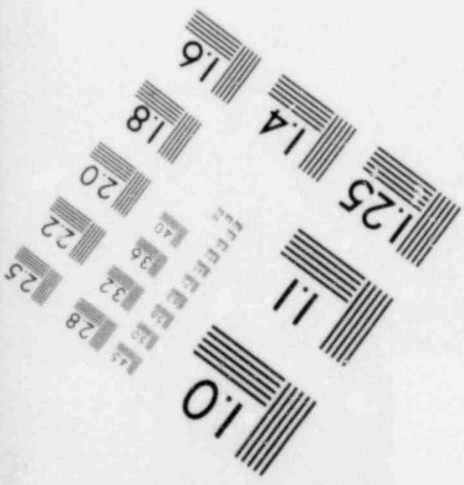

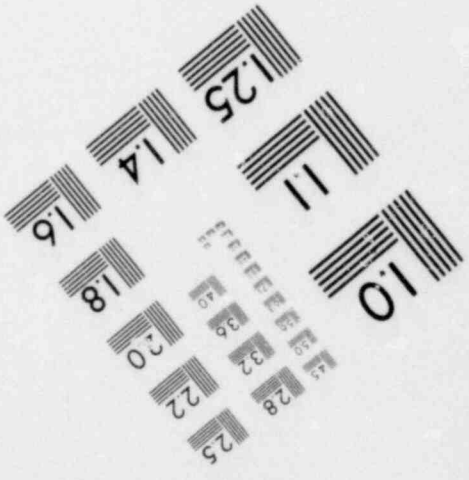

solution of heat conduction depends on fluid temperature and heat transfer coefficient.

Figures 10-63 and 10-64 show the typical [ ] fluid temperature profiles at the counterbore section for the horizontal feedline and elbow feedline, respectively. Steady state temperature data at the counterbore section are tabulated and shown in Appendix 10.2 for reference. | a,c

A dimensionless temperature, θ, can be defined as follows:

$$\theta = \frac{T - T_{cold}}{T_{hot} - T_{cold}} \qquad (10.5)$$

Where

T = [ ] fluid temperature | a,c

T_{cold} = feedwater (cold) inlet temperature

T_{hot} = test tank (hot) water temperature. Steam generator secondary side water temperature.

[ ] a,c

Considering the thermal similitude between the flow model and the steam generator feedline, the equivalent temperature profile for the steam generator feedline can be determined using the model test data. The

temperature profiles derived for the counterbore section can then be used to substantiate or modify the previously established profiles using only the on-site testing data.

a,c

[ ]

10.7.5 HEAT TRANSFER COEFFICIENT OF STEAM GENERATOR FEEDLINE

a,c

According to the flow model tests, heat transfer processes for a stratified pipe can be separated [ ]

a,c

[ ]

[ ] a,c

10.7.5.1 Use of Heat Transfer Correlations

[ ] a,c

a,c [ ]

a,c [ ]

10.7.5.2 Coefficients of Cold and Hot Layers

For the horizontal feedline configuration, Table 10.19 lists the values of heat transfer coefficients for the hot and cold layers. [

a,c

]

10.7.5.3 Combined Heat Transfer Coefficient

According to the values shown in Tables 10.19 and 10.20, the cold layer is of combined forced and free convection regime. [ ] a,c

[ ] a,c

10.7.5.4 Heat Transfer Coefficient [ ] a,c

[ ] a,c

a,c [ ]

10.8 SUMMARY, CONCLUSIONS AND OBSERVATIONS

As part of the total program for the PWR steam generator feedline-nozzle cracking investigation, the flow model tests have been successfully completed.

10.8.1 SUMMARY

a,c The flow model is a [ ] feedline-nozzle assembly and the thermal sleeve, and a portion of the full sized feedring. [ ]

a,c It is a two temperature and [ ] operation. [ ]

[ ] a,c

10.8.2 CONCLUSIONS

Based on the visual and temperature data evaluation, the following conclusions can be drawn:

(1) Thermal and fluid flow stratification will exist in the feedline, [ ] and the interface is subject to flow and thermal oscillations, resulting in temperature fluctuations. The oscillations can occur at any cross section although amplitudes may vary from cross section to cross section. Thus, the feedline is subjected to thermal striping; a direct result of fluid temperature oscillations. a,c

(2) Flow leakage can occur through the annulus formed by the feedwater nozzle and the thermal sleeve, and the leakage flow can be forward into the steam generator and/or backward into the feedline/nozzle. Thus, hot and cold streams can mix inside and/or outside the annulus and thus lead to temperature oscillations.

(3) During fluid flow stratification [ ] a,c

10.8.3 OBSERVATIONS

Certain observations are summarized as follows:

(1) Fluid temperature oscillations have been observed and are believed to be a thermal-hydraulic mechanism for feedline thermal fatigue.

(2) As demonstrated in the vertical elbow feedline tests, the feedline, nozzle and thermal sleeve could be designed to be free from hydraulic stratification (and thus temperature oscillations associated with the interface) [ ]. a,c

(3) The depth of the cold stratified layer [ ] depends on the geometry and discharge flow area of the feedring. [ ]. a,c

(4) [ ] a,c

10.9 REFERENCES

1. C. D. Ungate, D. R. F. Harleman and G. H. Jurka, "Mixing of Submerged Turbulant Jets at Low Reynolds Numbers," Ralph M. Parsons Laboratory, Dept. of Civil Engineering, MIT, Report No. 197, Feb., 1975.

2. E. H. Novendstern and P. S. Marinkovich, "Testing of the CRBRP Direct Heat Removal Service in a 1/21 Scale Model," ASME Paper No. 79-HT-5, 1979.

3. E. R. G. Eckert and R. M. Drake, Jr., "Heat and Mass Transfer," 2nd Ed., p. 332, McGraw-Hill, New York, 1959.

4. S. M. Morcos and A. E. Bergles, "Experimental Investigation of Combined Forced and Free Laminar Convection in Horizontal Tubes," ASME, J. Heat Transfer, pp. 212-219, May, 1975.

5. W. M. Rohsenow and H. Choi, "Heat, Mass, and Momentum Transfer," p. 165, Prentice-Hall, 1961.

6. W. M. Kays, "Convestive Heat and Mass Transfer," pps. 126 a 189, McGraw-Hill, New York, 1966.

7. A. E. Bergles, "Survey ad Evaluation of Techniques to Augment Convective Heat and Mass Transfer," Progress in Heat and Mass Transfer, Vol. 1, Pergamon Press, New York, 1969, pp. 331-424.

TABLE 10.1

CLASSIFICATION OF THE CONFIGURATION OF THE FEEDLINE SYSTEM AND SIZES OF ANNULUS

CASE NO.	TYPE OF FEEDLINE	TYPE OF DISCHARGE
1	Vertical Elbow	Bottom Holes
2	Vertical Elbow	J-Tubes
3	Horizontal Straight Pipe	Bottom Holes
4	Horizontal Straight Pipe	J-Tubes

a,b

SECTION	SIZE OF ANNULUS
Leading Section	[ ]
Rear Section	[ ]

TABLE 10.2

FUNCTIONAL REQUIREMENTS OF THE FLOW MODEL TESTS

ITEM	CONDITION
Feedwater Flow Rate (gpm)	[ ] a,c
Temperature of Feedwater (°F)	[ ] a,c
Temperature of Vessel Hot Water (°F)	[ ] a,c
System Pressure (psia)	[ ] a,c
[ ] Feedwater	a,c
[ ] Hot Water	a,c
[ ]	a,c
Material of Test Section	[ ] a,c

TABLE 10.3

BASIC PARAMETERS FOR STEAM GENERATOR AND TEST MODEL

	STEAM GENERATOR	TEST MODEL
Flow Rate (gpm)	[	]
Feedwater Temperature (°F)		
Vessel Water Temperature (°F)		
[ ] Feedwater		
[ ] Vessel Water		
System Pressure (psia)		
[ ]		
Reynolds Number*		

a,c

*Numbers are based on [ ] feedwater flow and [ ] cold water velocity. [ ]

a,c

TABLE 10.4

REYNOLDS AND VARIOUS GEOMETRIC
SCALES AND SALT CONCENTRATIONS(1)

GEOMETRIC SCALE	STEAM GENERATOR FLOW RATE (GPM)	STEAM GENERATOR FEEDLINE REYNOLDS NUMBER	MODEL FLOW RATE (GPM)	MODEL FEEDLINE REYNOLDS NUMBER
[	[	[	[	[

a,c

NOTE:

[

a,c

TABLE 10.5

THERMOCOUPLE LOCATIONS AND SPECIFICATIONS

Thermocouple Location	Parameter Being Measured	Thermocouple Sheath Diameter	Time Constant	Accuracy	
Inlet Piping					a,c
Drain Piping					
Reservoir Wall					
Reservoir Wall					
Nozzle Section					
Thermal Sleeve/ Feedwater Ring					

TABLE 10.6

THERMOCOUPLE LOCATIONS FOR HORIZONTAL FEEDLINE-NOZZLE TESTS

a,c

Thermocouple Position #	Shown in Figure	Cross Section Number	Cross Section Angle	Method of Attachment
1-0	10-16	1	0°	Comp. Fitting
2-0	10-17 & 10-18	2	0°	Comp. Fitting
2-30			30°	Epoxy Adhesive
2-60			60°	"
2-90			90°	"
2-120			120°	"
2-150			150°	"
2-180			180°	"
3-0	10-17 & 10-19	3	0°	Epoxy Adhesive
3-30A			23°	
3-30			30°	
3-30B			37°	
3-60A			53°	
3-60			60°	
3-60B			67°	
3-90A			83°	
3-90			90°	
3-90B			97°	
3-120A			113°	
3-120			120°	
3-120B			127°	
3-150A			143°	
3-150			150°	
3-150B			157°	
4-0	10-17 & 10-20	4	0°	Epoxy Adhesive
4-30			30°	
4-60			60°	
4-90			90°	
4-120			120°	
4-150			150°	
5-0	10-17 & 10-21	5	0°	Epoxy Adhesive
5-30			30°	
5-90			90°	
5-150			150°	
5-180			180°	
5A-105	10-17 & 10-22	5A	105°	Epoxy Adhesive
5A-120			120°	
5A-135			135°	

TABLE 10.6 (cont.)

THERMOCOUPLE LOCATIONS FOR HORIZONTAL FEEDLINE-NOZZLE TESTS

a,c

Thermocouple Position #	Shown In Figure	Cross Section Number	Cross Section Angle	Method of Attachment
6-180	10-17	6	180°	Epoxy Adhesive
7-0	10-16	7	0°	Comp. Fitting
8-0	10-16	8	0°	Comp. Fitting
W-1 W-2 W-3	10-15	N/A	N/A	Comp. Fitting
I-1	10-14	N/A	N/A	Comp. Fitting
D-1	10-14	N/A	N/A	Comp. Fitting
CAL	10-15	N/A	N/A	Comp. Fitting

TABLE 10.7

THERMOCOUPLE LOCATIONS FOR ELBOW FEEDLINE-NOZZLE TESTS

a,c

Thermocouple Position #	Shown In Figure	Cross Section Number	Cross Section Angle	Method of Attachment
1-0	10-23	1	0°	Comp. Fitting
2-0	10-24 & 10-18	2	0°	Comp. Fitting
2-30			30°	Epoxy Adhesive
2-60			60°	"
2-90			90°	"
2-120			120°	"
2-150			150°	"
2-180			180°	"
3-0	10-24 & 10-19	3	0°	Epoxy Adhesive
3-30A			23°	
3-30			30°	
3-30B			37°	
3-60A			53°	
3-60			60°	
3-60B			67°	
3-90A			83°	
3-90			90°	
3-90B			97°	
3-120A			113°	
3-120			120°	
3-120B			127°	
3-150A			143°	
3-150			150°	
3-150B			157°	
4-0	10-24 & 10-20	4	0°	Epoxy Adhesive
4-30			30°	
4-60			60°	
4-90			90°	
4-120			120°	
4-150			150°	
5-0	10-24 & 10-21	5	0°	Comp. Fitting
5-30			30°	
5-90			90°	
5-150			150°	
5-180			180°	
5A-105	10-24 & 10-22	5A	105°	Epoxy Adhesive
5A-120			120°	
5A-135			135°	

TABLE 10.7 (cont.)

THERMOCOUPLE LOCATIONS FOR ELBOW FEEDLINE-NOZZLE TESTS

a,c

Thermocouple Position #	Shown In Figure	Cross Section Number	Cross Section Angle	Method of Attachment
6-180	10-24	6	180°	Epoxy Adhesive
7-0	10-23	7	0°	Comp. Fitting
8-0	10-23	8	0°	Comp. Fitting
W-1 W-2 W-3	10-15	N/A	N/A	Comp. Fitting
I-1	10-14	N/A	N/A	Comp. Fitting
D-1	10-14	N/A	N/A	Comp. Fitting
CAL	10-15	N/A	N/A	Comp. Fitting

TABLE 10.8

DYE INJECTION LOCATIONS FOR HORIZONTAL FEEDLINE-NOZZLE TESTS

Dye Injection Position #	Color Dye	Shown In Figure	Cross Letter	Section Angle
RA-0 BA-180	Red Blue	10-25	A	0° 180°
RB-0 RB-330 RB-270 BB-210	Red Red Red Blue	10-25 & 10-26	B	0° 330° 270° 210°
BC-180	Blue	10-25&10-26	C	180°
RD-0	Red	10-25&10-26	D	0°
RE-315 BE-225	Red Blue	10-25 & 10-26	E	315° 225°
RF-0 RF-90 RF-270 BF-180	Red Red Red Blue	10-25	F	0° 90° 270° 180°
RG-0 BG-180	Red Blue	10-25	G	0° 180°
RH-0	Red	10-25	H	N/A
RI-0 BI-180	Red Blue	10-25	I	0° 180°

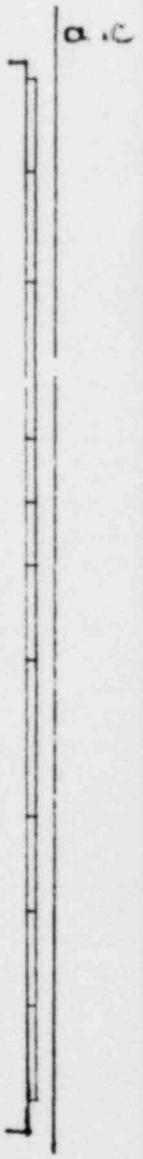

TABLE 10.9

DYE INJECTION LOCATIONS FOR ELBOW FEEDLINE-NOZZLE TESTS

a,c

Dye Injection Position #	Color Dye	Shown In Figure	Cross Lette:	Section Angle
RA-0 BA-180	Red Blue	10-27	A	0° 180°
RB-0 RB-330 RB-270 BB-210	Red Red Red Blue	10-27 & 10-28	B	0° 330° 270° 210°
BC-180	Blue	10-27&10-28	C	180°
RD-0	Red	10-27&10-28	D	0°
RE-315 BE-225	Red Blue	10-27 & 10-28	E	315° 225°
RF-0 RF-90 RF-270 BF-180	Red Red Red Blue	10-27	F	0° 90° 270° 180°
RG-0 BG-180	Red Blue	10-27	G	0° 180°
RH-0	Red	10-27	H	N/A
RI-0 BI-180	Red Blue	10-27	I	0° 180°

TABLE 10

INSTRUMENTATION AND ITS OPERATIONS RANGE AND ACCURACIES

Parameter To Be Measured	Instrumentation	Individual Accuracies	Operational Range	Overall Accuracy	Display Or Output
a,c [ ]	1/2-inch Orifice ΔP Indicator	<± 4%* ± 0.5% F.S.	1-10 GPM	<± 5%	Gage Dial
	1-inch Orifice ΔP Indicator	<± 4% * ± 0.5% F.S.	4-40 GPM	<± 5%	Gage Dial
	2-inch Orifice ΔP Indicator	<± 4%* ± 0.5% F.S.	15-150 GPM	<± 5%	Gage Dial
	4-inch Orifice ΔP Indicator	<± 4% * ± 0.5% F.S.	60-600 GPM	<± 5%	Gage Dial
Reservoir Level	ΔP Cell E to P Converter Controller Chart Recorder	NR NR NR NR	0 to 10 In. Below Tank Top	NR	Chart Recorder With Sight Gage As Check
Hot Water Temperature	Thermocouple Reference Junction DVM	± 2°F ± 1°F < 0.1°F	50-150°F	± 2.3°F	Digital Voltmeter
Cold Water Temperature	Thermocouple Reference Junction Amplifier DVM	± 2°F ± 1°F < 0.1°F < 0.1°F	50-150°F	± 2.3°F	Digital Voltmeter
Test Section Temperatures	Thermocouple Reference Junction Amplifier Tape Recorder	± 2°F ± 1°F < 0.1°F ± 3°F	50-150°F	±3.7°F	Signals May Be Monitored With DVM
a,c [ ]					]

* Conservative Estimate for Accuracy of Theoretical Orifice Calibration Curve

NR -- None Required

TABLE 10.11

TEST RUNS PERFORMED FOR HORIZONTAL AND ELBOW FEEDLINE CONFIGURATION(1, 2, 3, 7)

TEST RUN NUMBER	DATE PERFORMED	FLOW RATES (GPM)	PHOTOS AND MOVIES	J-TUBES	BOTTOM DISCHARGE HOLES		2" HOLES IN FLANGES	
					1" DIA.	2" DIA.	UPPER	LOWER
1	12/10/79	a,c	Yes	Open				
2	12/10/79		Yes	Open				
3	12/11/79		Yes	Open				
4	12/11/79		Yes	Open				
4A	12/12/79		Yes	Open				
5	12/12/79		Yes	Open				
6	12/13/79		Yes	Open				
6A	12/13/79		Yes	Plugged				
7	12/14/79		No	Plugged				
7A	12/14/79		No	Plugged				
7B	12/15/79		No	Open				
7C	12/15/79		No	Open				
8	12/17/79		No	Open				
9	12/18/79		No	Open				
10	12/18/79		No	Plugged				
11	12/19/79		No	Plugged				
12	1/4/80		Yes	Open				
13	1/7/80		Yes	Plugged				
14	1/8/80		No	Plugged				
15	1/8/80		Yes	Plugged				
16	1/8/80		Yes	Plugged				

TABLE 10.11 (CONTINUED)

TEST RUNS PERFORMED FOR HORIZONTAL AND ELBOW FEEDLINE CONFIGURATION(1, 2, 3, 7)

a,c

TEST RUN NUMBER	DATE PERFORMED	FLOW RATES (GPM)	PHOTOS AND MOVIES	J-TUBES	BOTTOM DISCHARGE HOLES	2" HOLES IN FLANGES
17	1/9/80	140	No	Plugged	[	]
18	1/9/80	80/140	Yes	Plugged		
19	1/9/80	60/100/80	Yes	Open		
20	1/10/80	10/20/40	Yes	Open		
21	1/10/80	60/90	Yes	Open		
22(6)	1/10/80	40/60/80	No	Open		

NOTES:

a,c

(1) [ ]

(2) Thermal sleeve is concentric with respect to nozzle except Test Run No. 5 which contacts with nozzle at bottom.

(3) Test Run No. 8-11, 14, 18, and 20-22 are thermocouple tests without dye injection.

(4) Except those holes (8) on straight tubes.

(5) N.E. - Not Existing

(6) Annulus between the nozzle and the sleeve was plugged at flange.

(7) Test Run No. 1-11 are for horizontal feedline configuration and Test Run No. 12-22 are for elbow feedline configuration.

Table 10.12

TEMPERATURE OSCILLATION DATA FOR HORIZONTAL, STRAIGHT FEEDLINE-NOZZLE CONFIGURATION

a,c

NOTE: (1) Average cycles occurring in 100 seconds

(2) During ramp down

(3) Frequency is representative of density

TABLE 10.13

TEMPERATURE OSCILLATION DATA FOR ELBOW FEEDLINE-NOZZLE CONFIGURATION

a,c

a,c

TABLE 10.13 (Continued)

TEMPERATURE ..LLATION DATA FOR ELBOW FEEDLINE-NOZZLE CONFIGURATION

TABLE 10.13 (continued)

TEMPERATURE OSCILLATION DATA FOR ELBOW FEEDLINE-NOZZLE CONFIGURATION

a,c [ ]

NOTE: (1) Average cycles occurring in 100 seconds

(2) During ramp down

(3) Frequency is represnetative of density

Table 10.14

VARIOUS SCALE FACTORS FOR STRAIGHT FEEDLINE

Test Run No.	Test Flow Rate (gpm)	[	]	Hot Water Temperature $(T_H)_M$ (°F)	Cold Water Temperature $(T_C)_M$ (°F)	Velocity Scale Factor S_U*	Oscillation Period Scale Factor S_τ*	Oscillation Amplitude Scale Factor S_A*
a,c	8							
	8							
	8							
	9							
	9							
	10							
	10							
	10							
	11							
	11							

*Evaluate based on

a,c [ ]

Table 10.15

VARIOUS SCALE FACTORS FOR ELBOW FEEDLINE

Test Run No.	Test Flow Rate (gpm)	[redacted]	[redacted]	Hot Water Temperature $(T_H)_M$ (°F)	Cold Water Temperature $(T_C)_M$ (°F)	Velocity Scale Factor S_U*	Oscillation Period Scale Factor S_τ*	Oscillation Amplitude Scale Factor S_A*
14	[redacted]	[redacted]	[redacted]	[redacted]	[redacted]	[redacted]	[redacted]	[redacted]
18								
20								
21								
22								

a,c

*Evaluate based on

a,c [redacted]

Table 10.16

CHARACTERISTICS OF COLD WATER LAYER FOR HORIZONTAL FEEDLINE CONFIGURATION

Test Run No.	Test Flow Rate (gpm)	Cold Layer Angle (°)	Cold Layer Depth (in.)	Flow Area of Cold Layer (ft^2)	S.G. Feedwater Flow Rate (gpm)	S.G. Cold Layer Velocity (ft/sec)	S.G. Cold Layer Reynolds Number*
8	a,c						a,c
9							
10							
11							

Table 10.17

CHARACTERISTICS OF COLD WATER LAYER FOR ELBOW FEEDLINE CONFIGURATION

Test Run No.	Test Flow Rate (gpm)	Cold Layer Angle (°)	Cold Layer Depth (in.)	Flow Area of Cold Layer (ft^2)	S.G. Feedwater Flow Rate (gpm)	S.G. Cold Layer Velocity (ft/sec)	S.G. Cold Layer Reynolds Number*
14	a,c						a,c
14							
14							
18							
18							
20							
20							
20							
21							
21							
22							
22							
22							

Table 10.18

THERMAL AND FLUID PROPERTIES OF WATER

@ 1000 psia

Temperature (°F)	Density ρ (lbm/ft^3)	Viscosity μ (lbm/sec-ft)	Thermal Conductivity k (Btu/hr-ft-°F)	Thermal* Expansion Coefficient, β (1/°F)	Prandtl Number Pr
80	62.42	6.23×10^{-4}	0.3570	1.5×10^{-4}	6.32
200	60.32	2.02×10^{-4}	0.3944	4.0×10^{-4}	1.85
544.6	46.32	6.34×10^{-5}	0.3276	11×10^{-4}	0.9

*This is based on the saturated conditions.

Table 10.19

HEAT TRANSFER COEFFICIENTS FOR THE HORIZONTAL

FEEDLINE OF STEAM GENERATOR AT 1000 psia

a,c [ ]

Table 10.20

HEAT TRANSFER COEFFICIENTS FOR THE ELBOW FEEDLINE OF STEAM GENERATOR

at 1000 psia

a,c [ ]

a,c

a,c

Figure 10-2
Elbow Feedline
Assembly

a,c

a,c

a,c

Figure 10-1 Horizontal Feedline Assembly

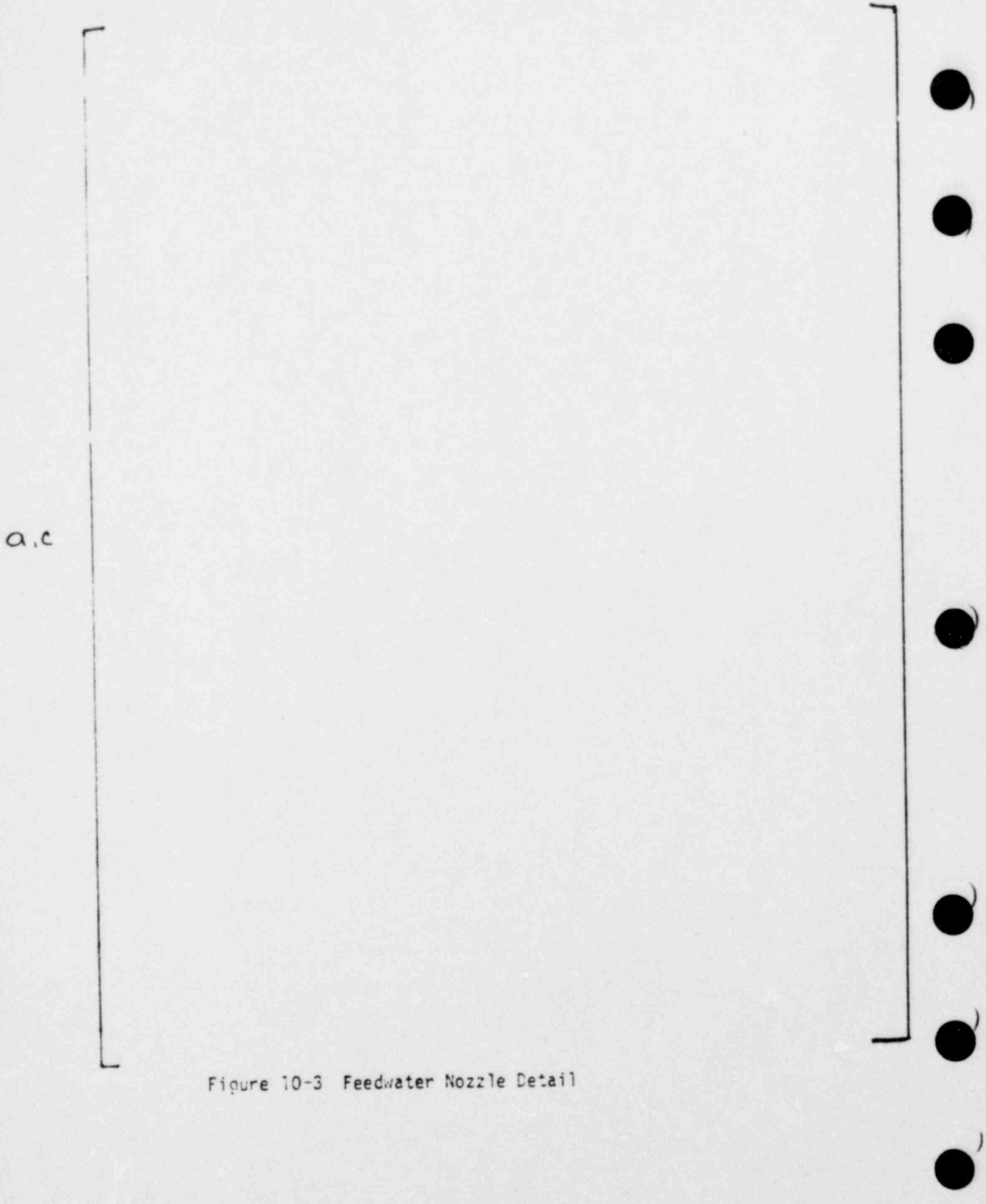

Figure 10-3 Feedwater Nozzle Detail

a,c

Figure 10-4 Thermal Sleeve and Feedwater Bottom Hole Discharge Pipe Assembly

a,c

Figure 10-5 Thermal Sleeve and Feedwater J-Tube Discharge Pipe Assembly

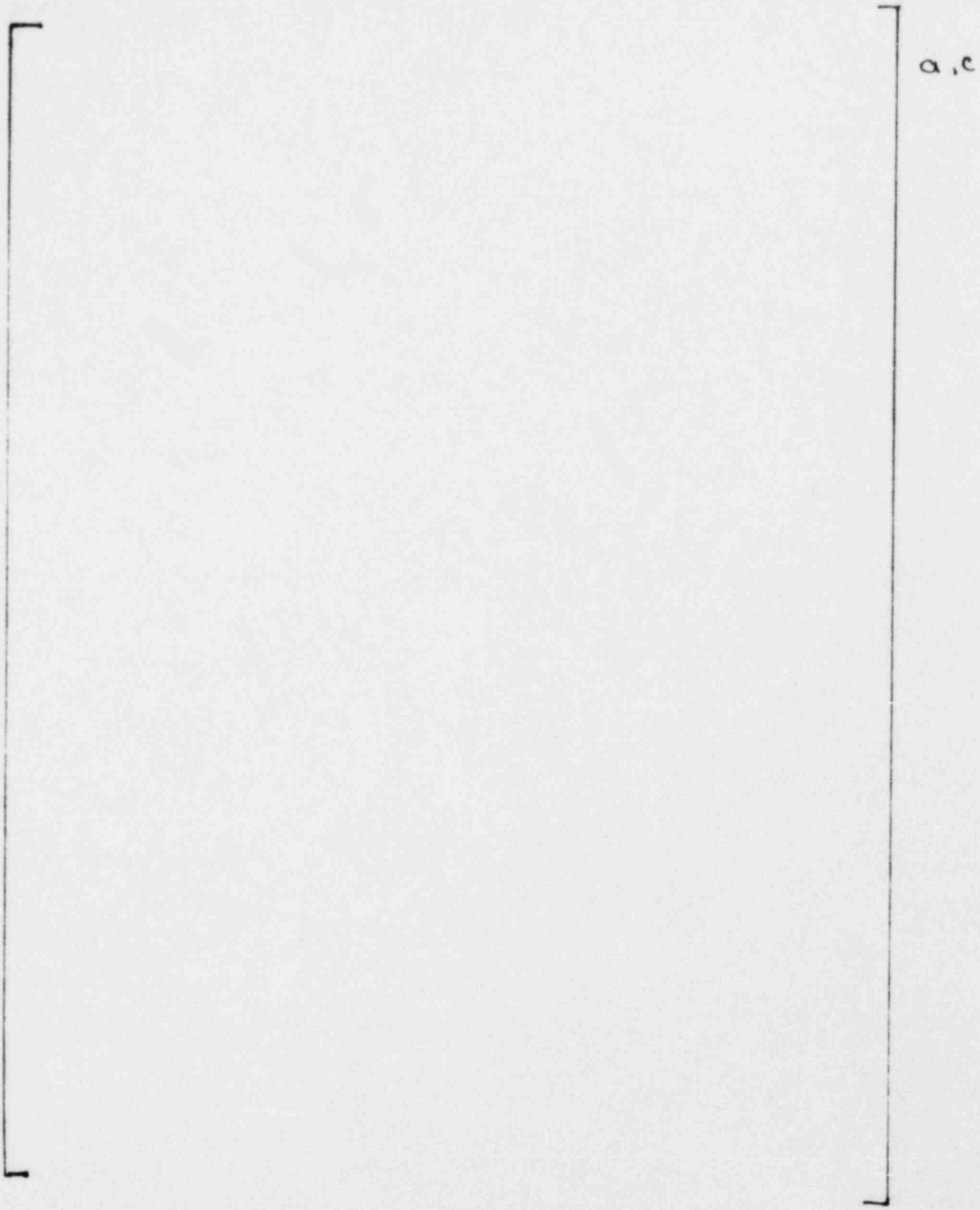

Figure 10-6 J-Tube Detail

a,c

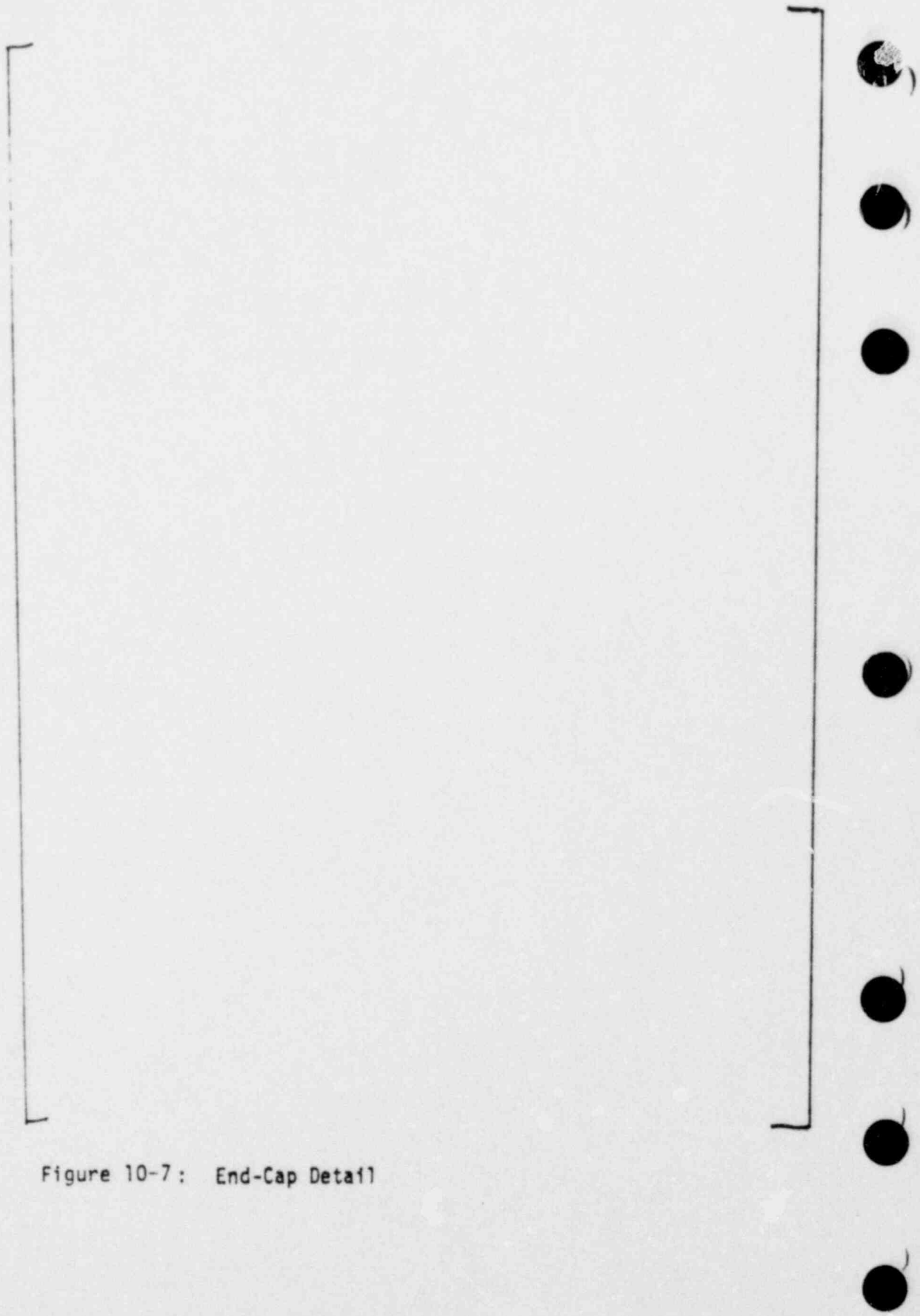

Figure 10-7: End-Cap Detail

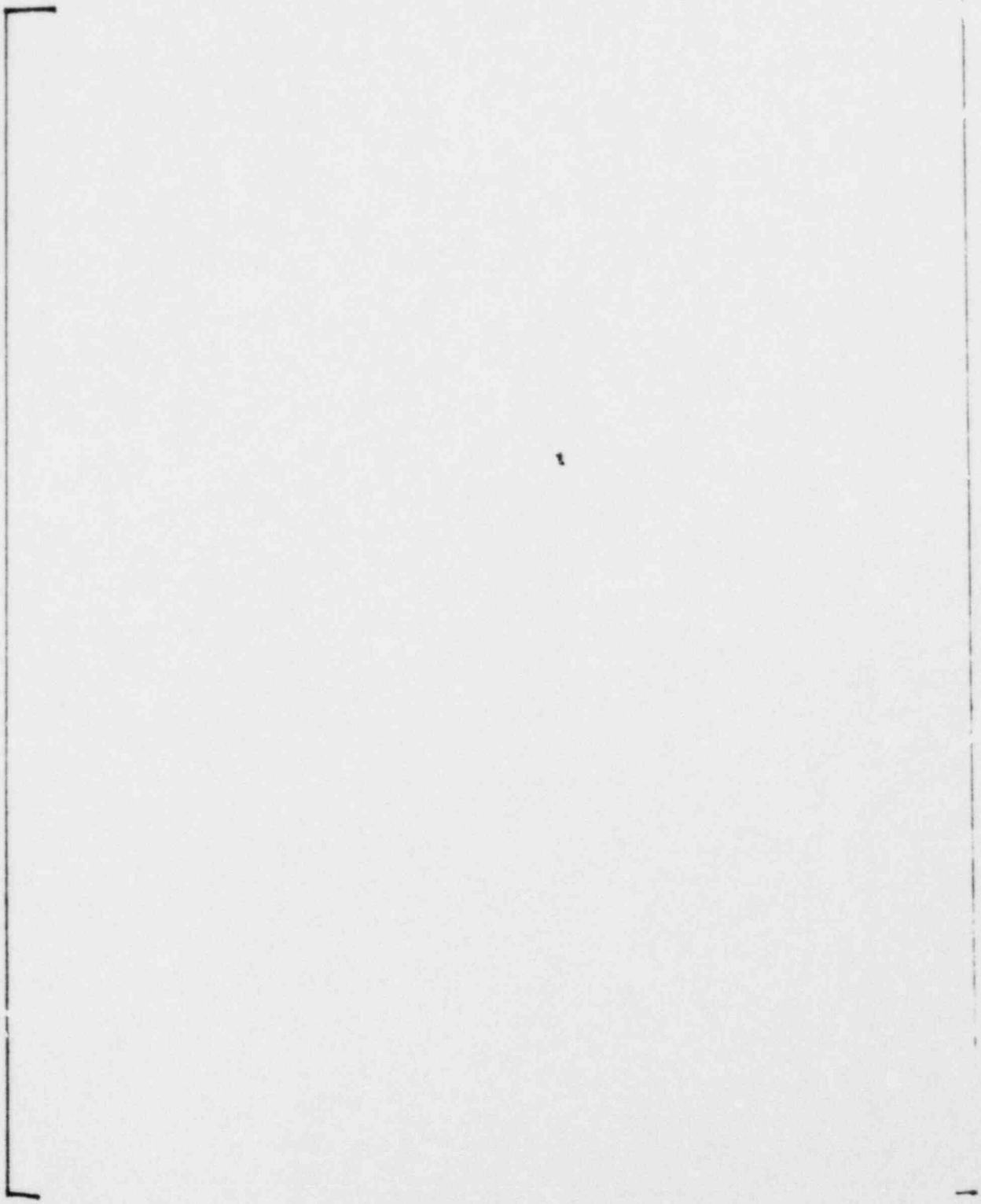

Figure 10-8 Horizontal, Straight Nozzle Test Arrangement with Bottom Discharge Configuration.

a,c

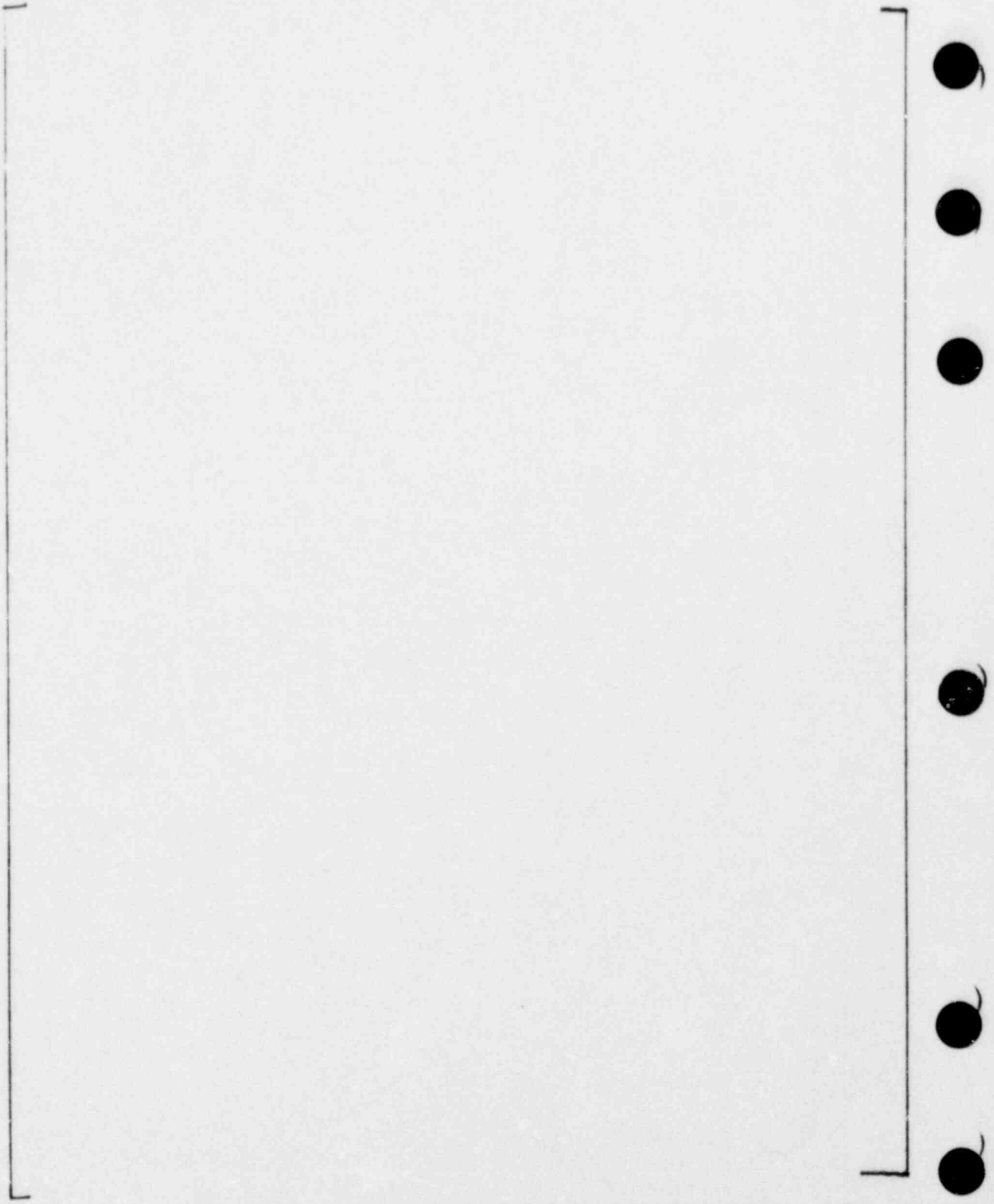

Figure 10-9 Horizontal, Straight Nozzle Test Arrangement with J-Tube Discharge Configuration.

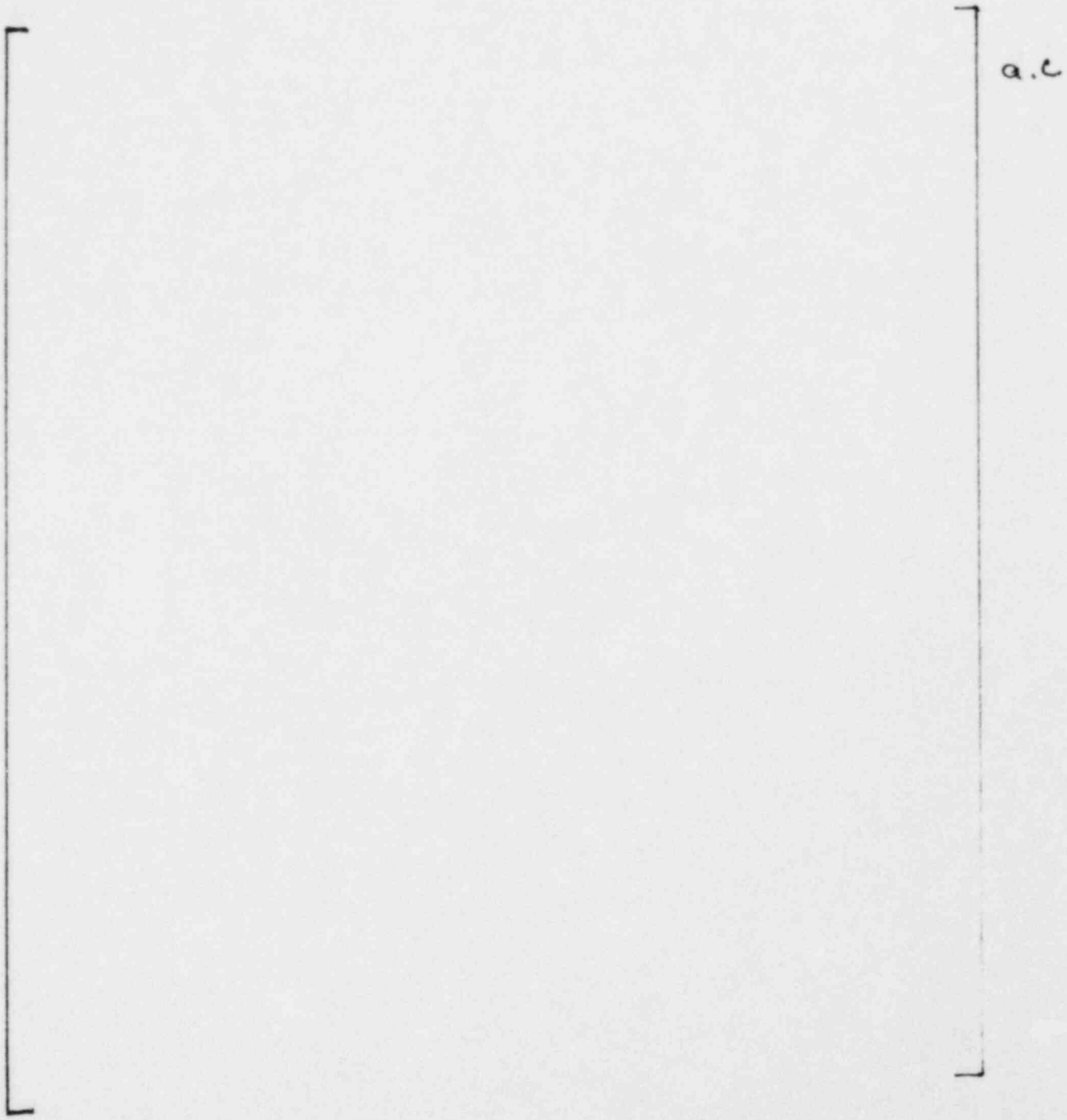

Figure 10-10 Elbow Nozzle Test Arrangement with Bottom Holes.

a,c

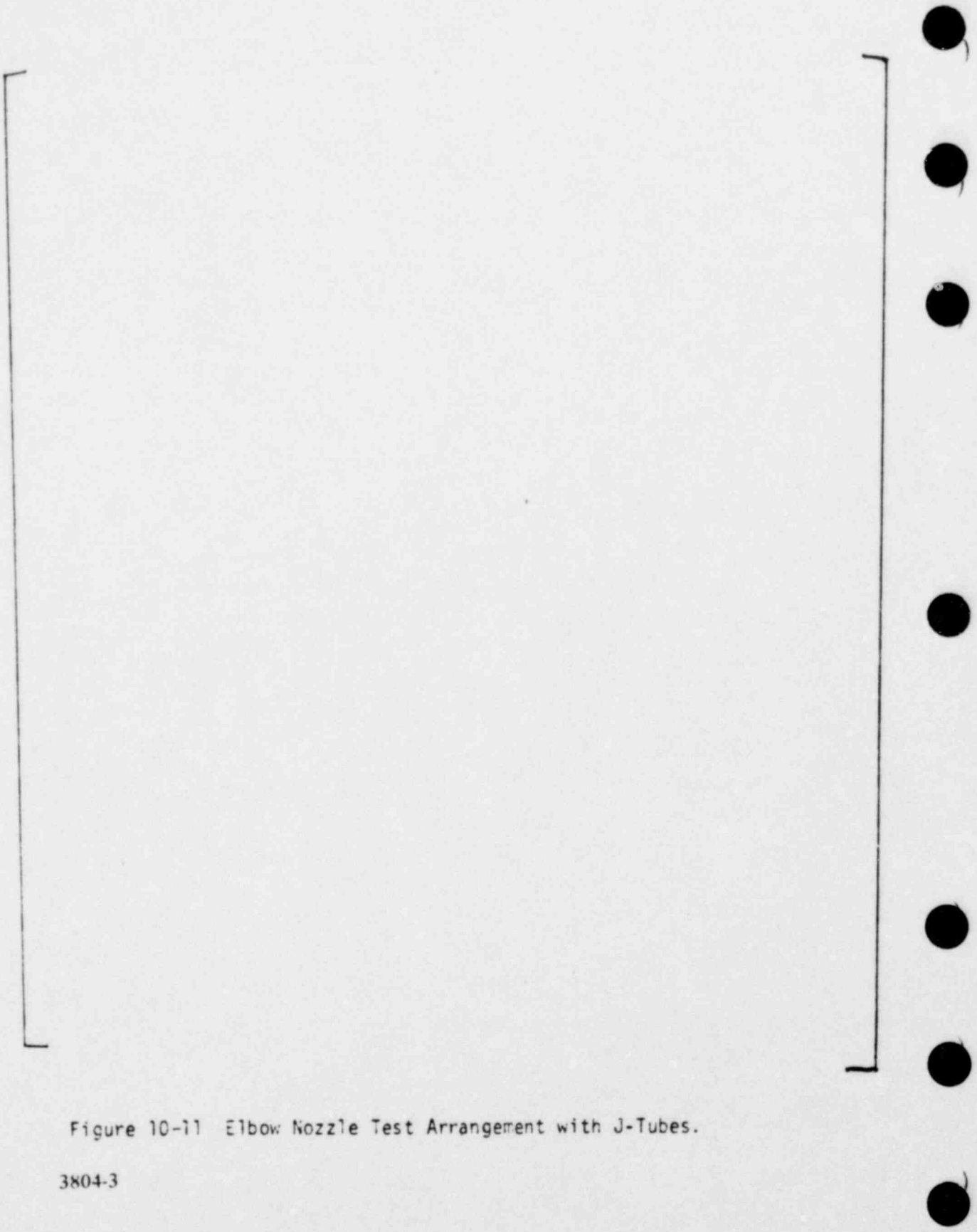

Figure 10-11 Elbow Nozzle Test Arrangement with J-Tubes.

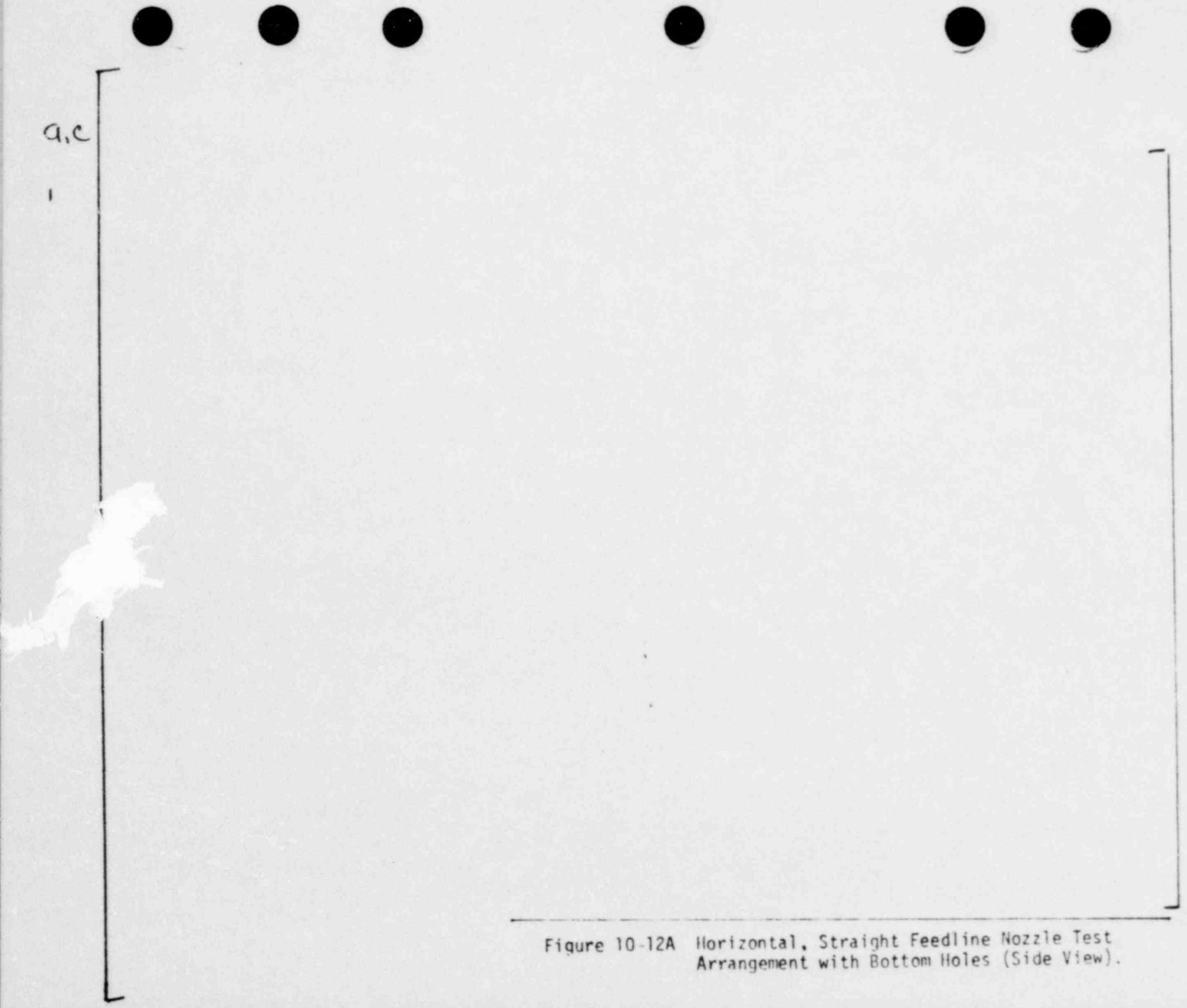

Figure 10-12A Horizontal, Straight Feedline Nozzle Test Arrangement with Bottom Holes (Side View).

a,c

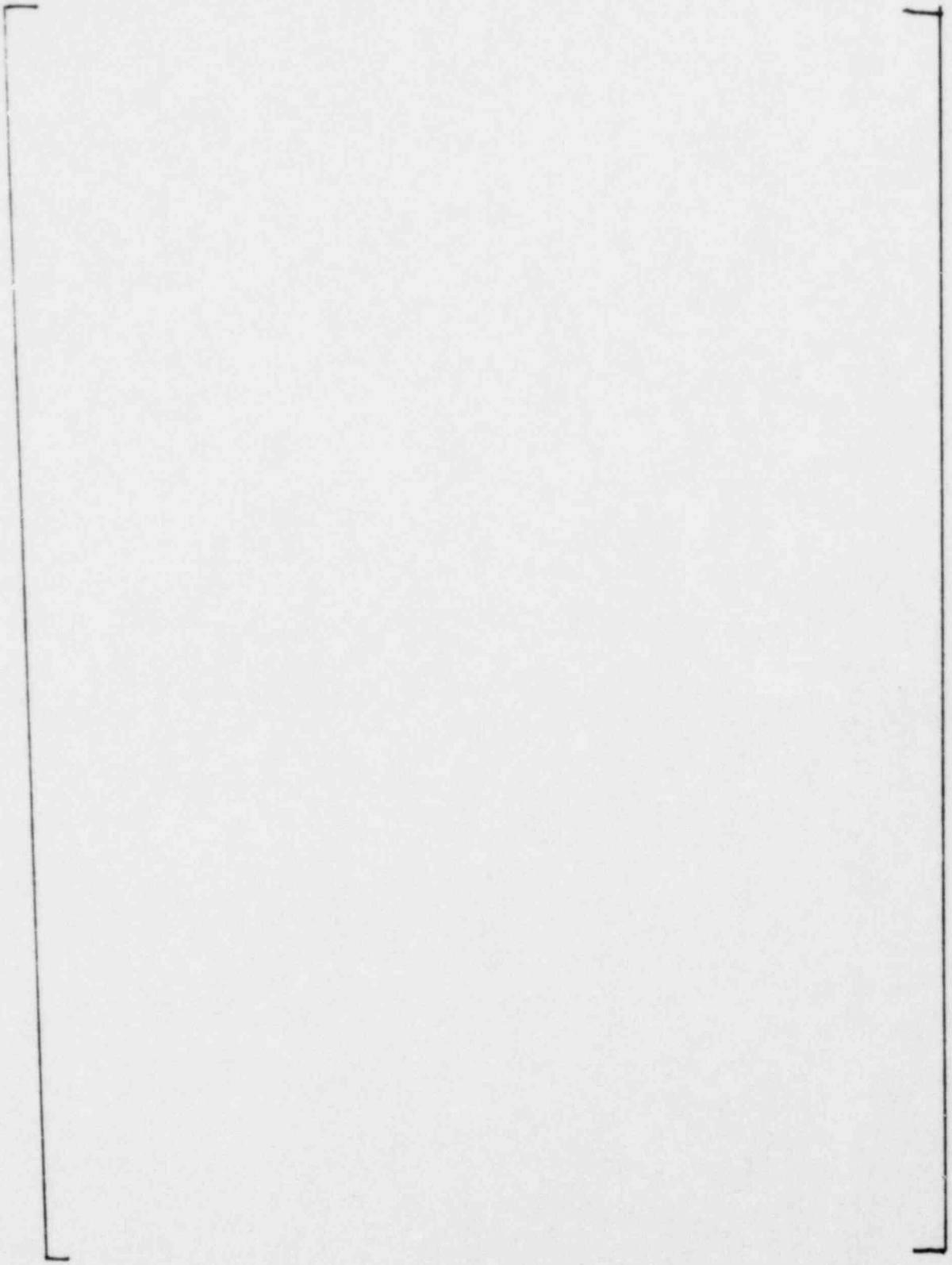

Figure 10-12B Elbow Feedline Nozzle Test Arrangement with Bottom Holes (Side View).

a,c

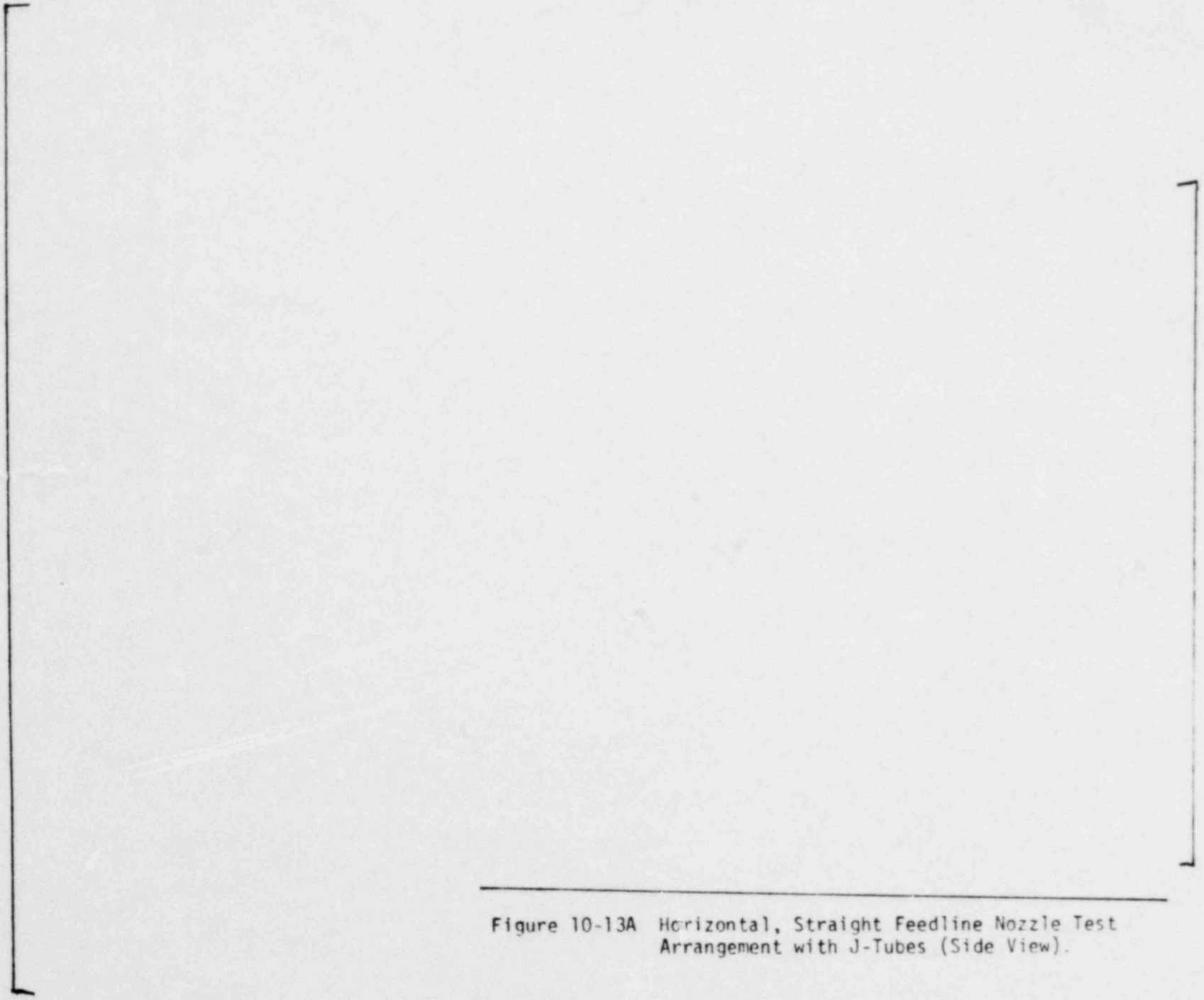

Figure 10-13A Horizontal, Straight Feedline Nozzle Test Arrangement with J-Tubes (Side View).

a,c

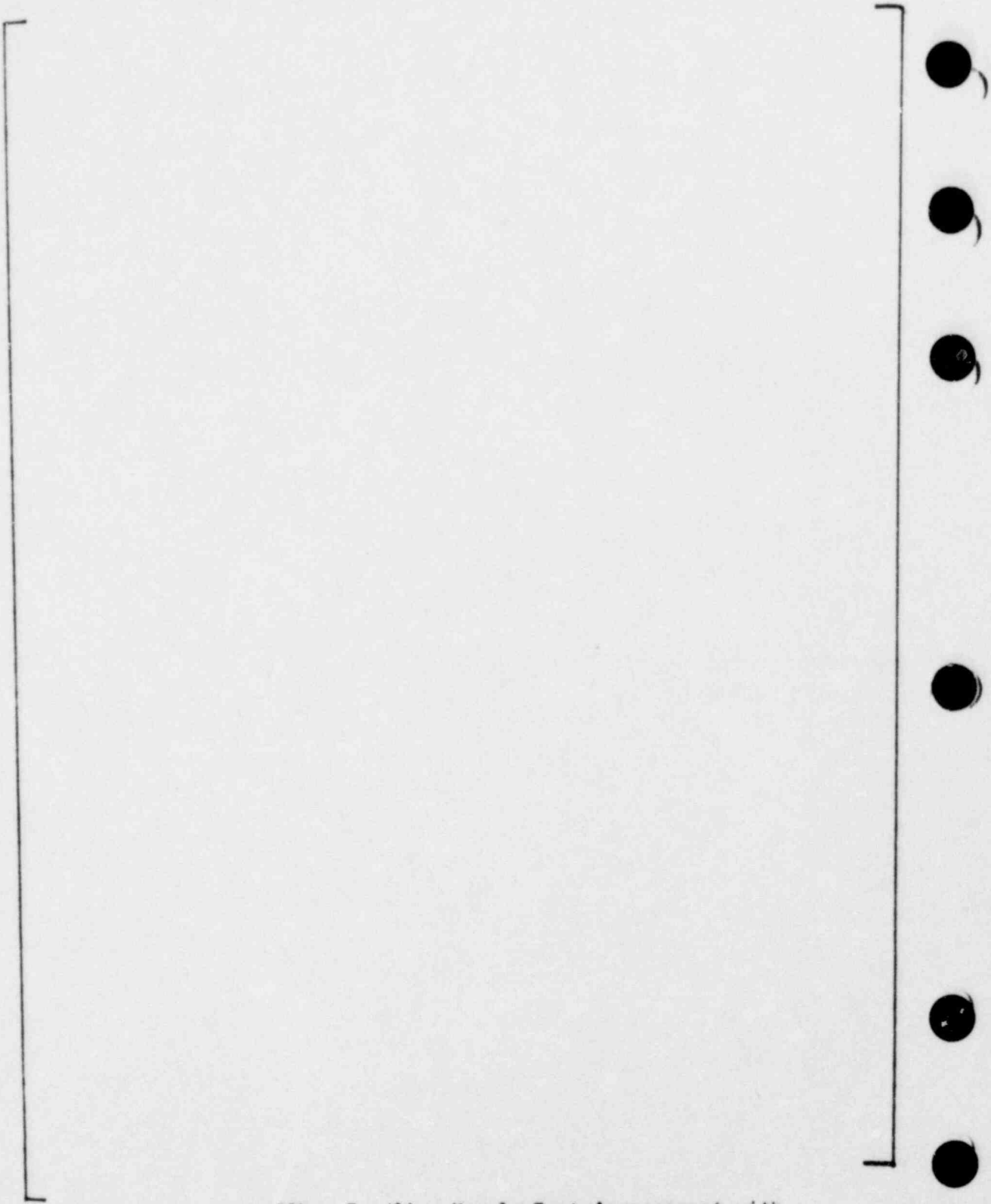

Figure 10-13B Elbow Feedline Nozzle Test Arrangement with J-Tubes (Side View).

3804-2

a.c

Figure 10-14 Feedline Cracking T/H Model Test Facility.

a,c

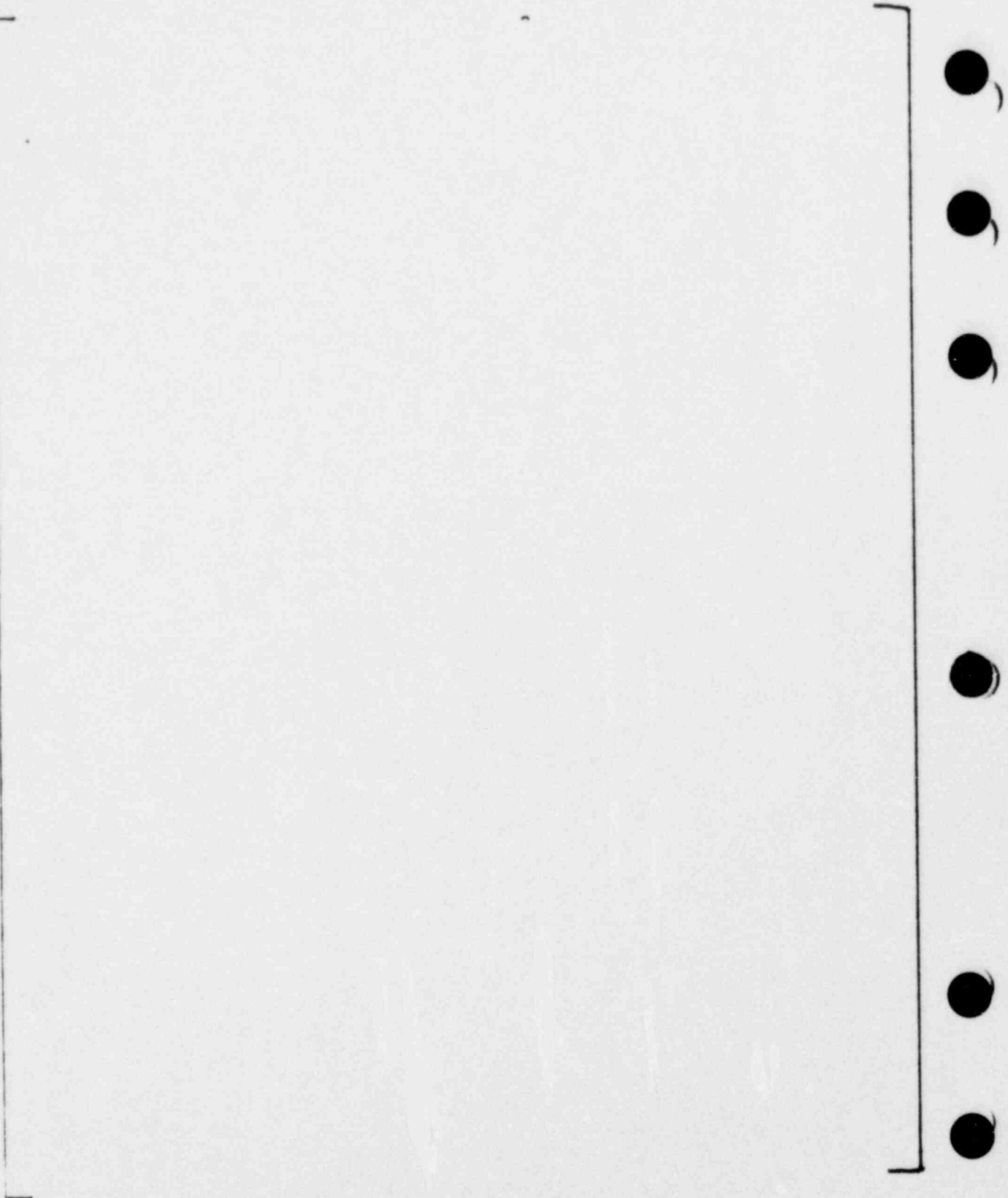

Figure 10-15 Reservoir Thermocouple Locations.

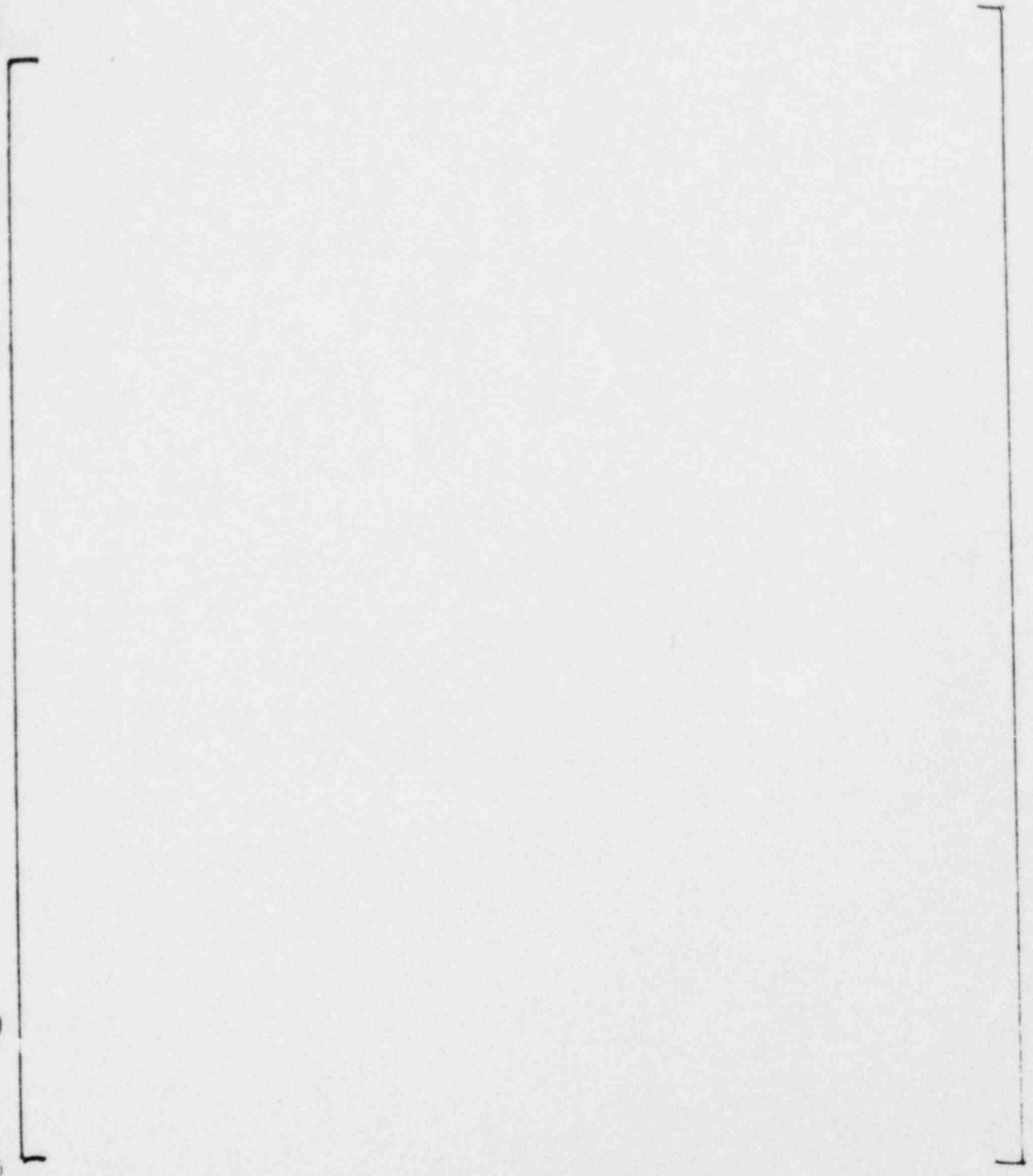

Figure 10-16 Overall Thermocouple Locations for the Feedwater Nozzle/ Horizontal Pipe Test.

a.c

380417

Figure 10-17 Detailed Locations of Thermocouples for the Feedwater Nozzle/Straight Pipe Te[illegible]

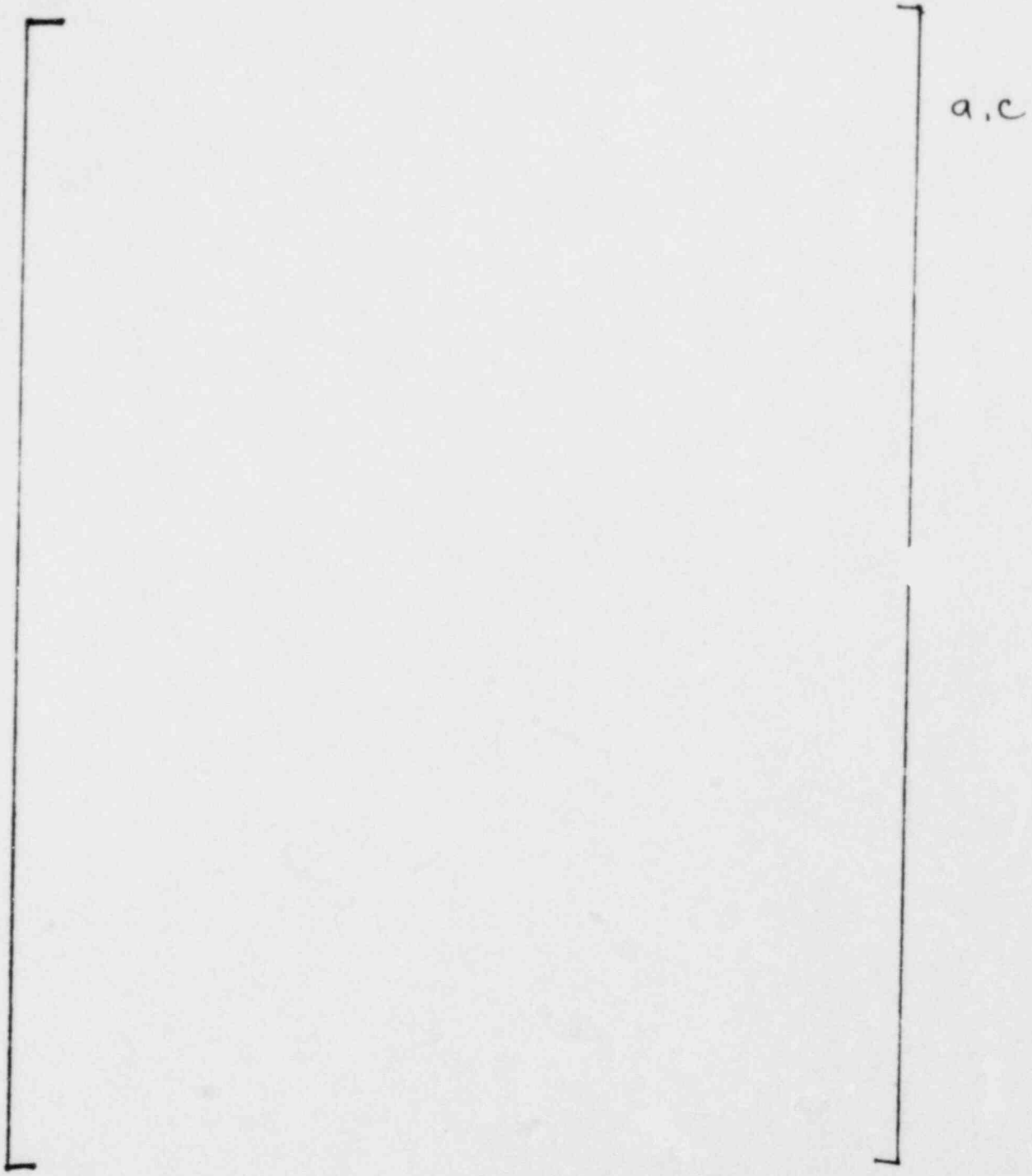

Figure 10-18 Thermocouple Locations for Nozz'e Section 2.

a,c

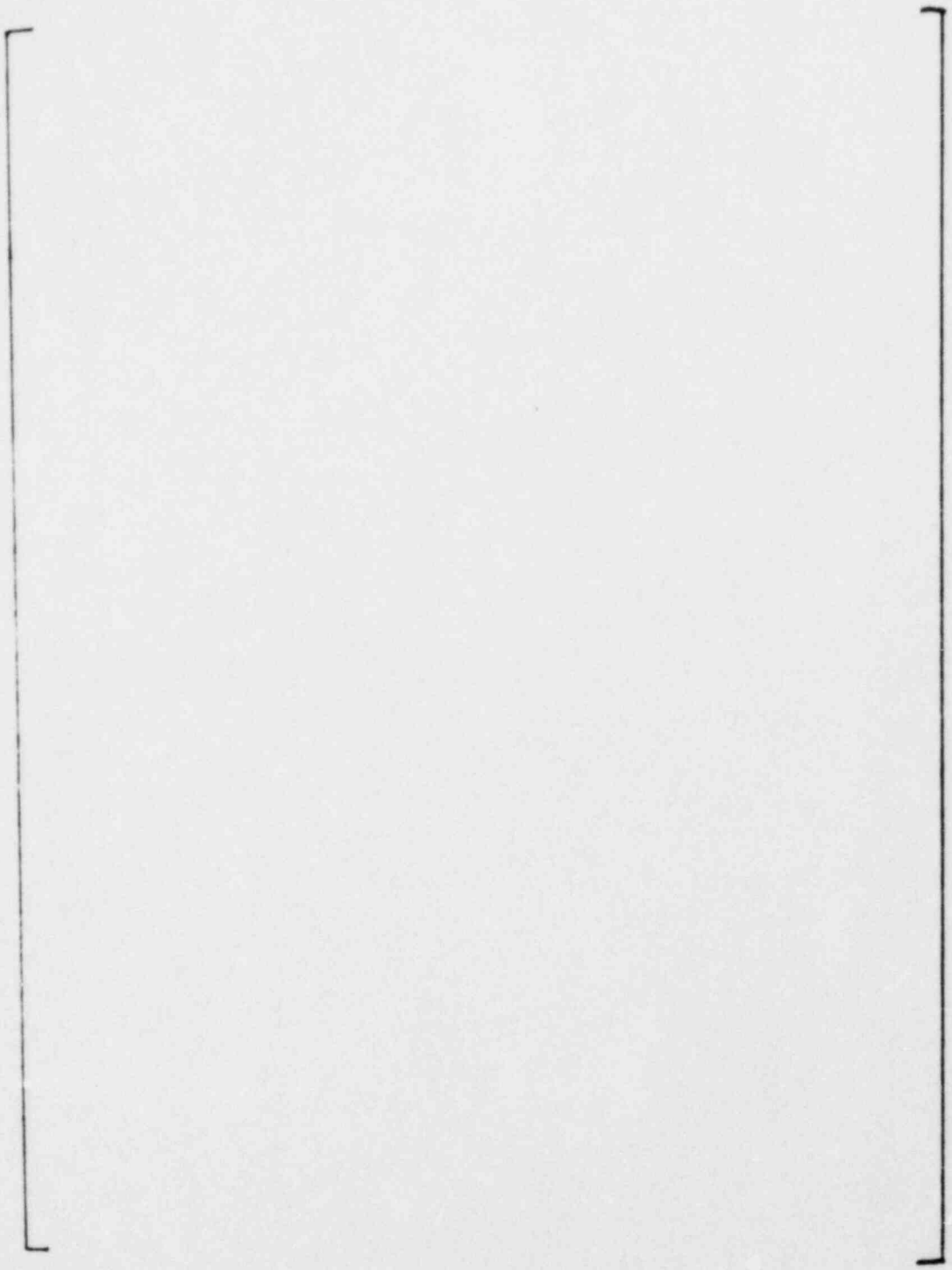

Figure 10-19 Thermocouple Locations for Nozzle Section 3.

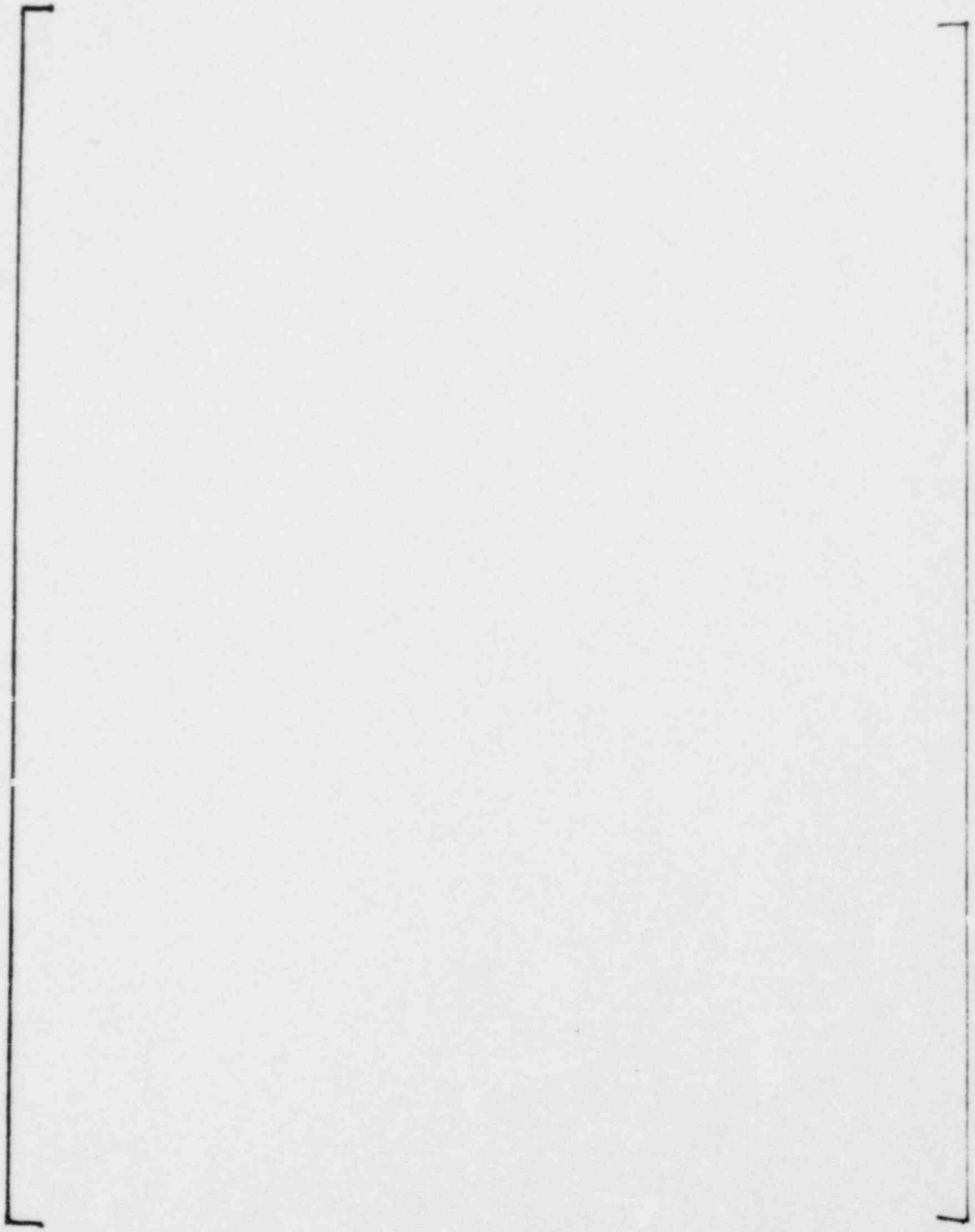

a,c

Figure 10-20 Thermocouple Locations for Nozzle Section 4.

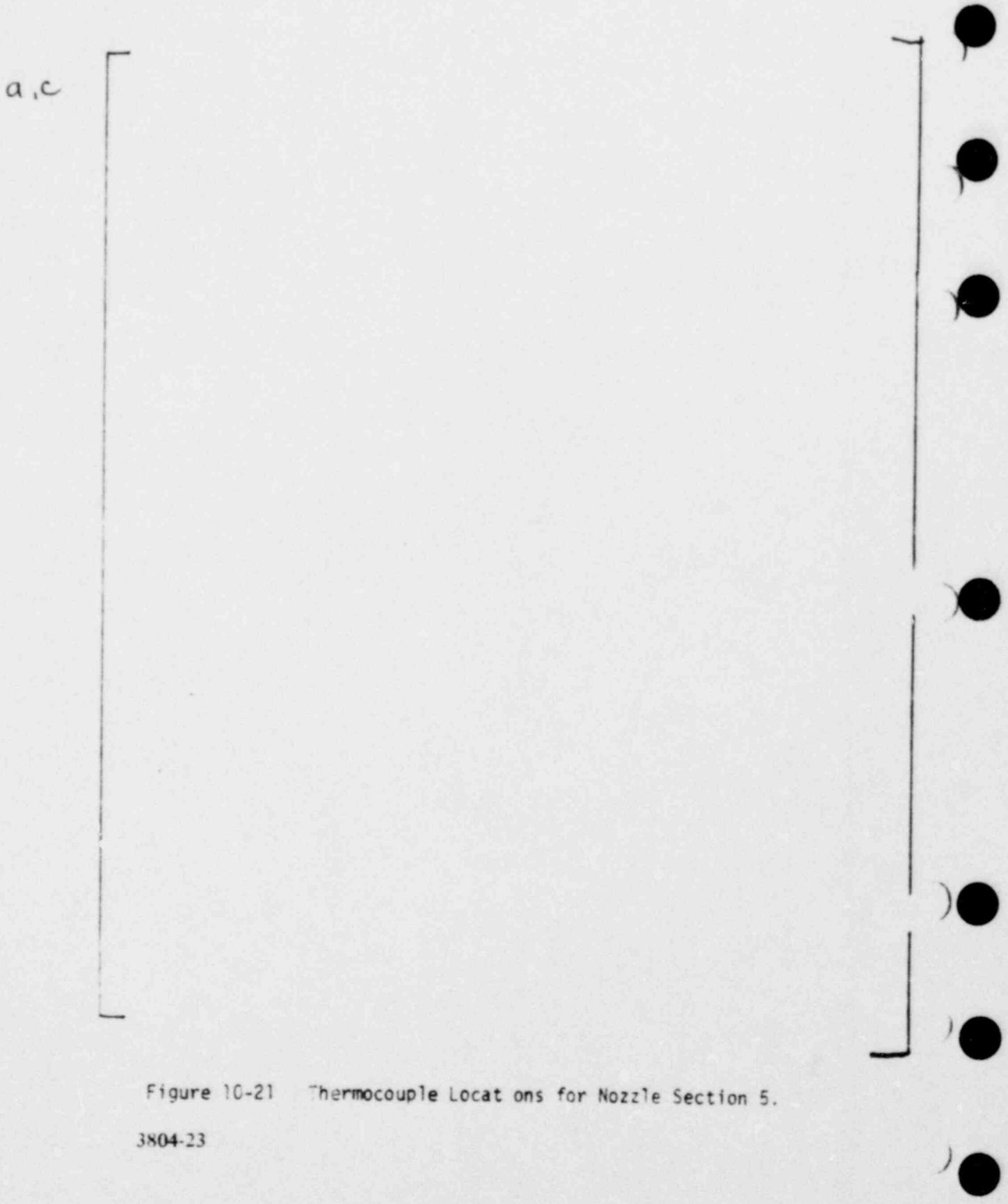

Figure 10-21 Thermocouple Locat ons for Nozzle Section 5.

3804-23

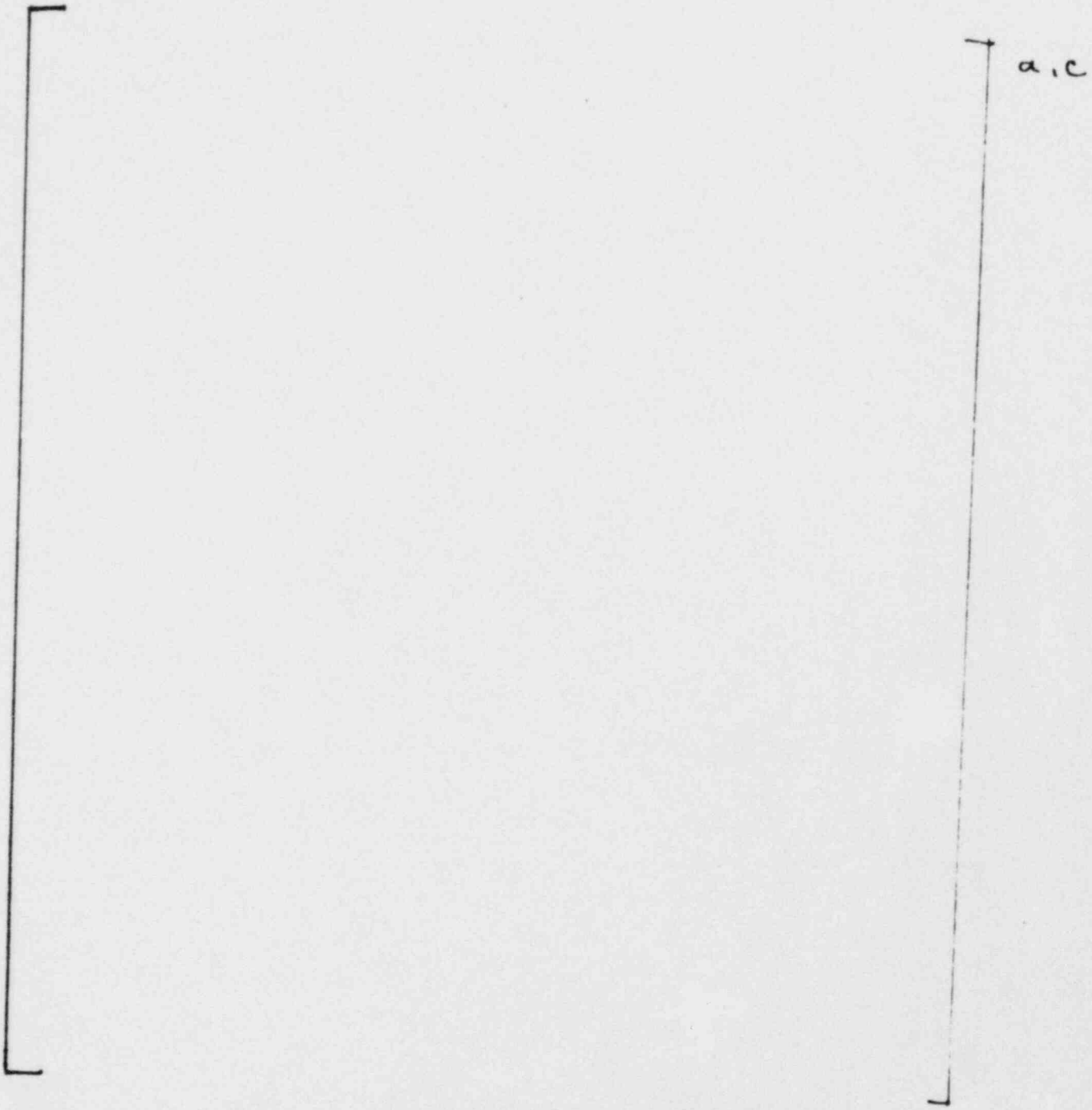

Figure 10-22 Therrocouple Locations for Nozzle Section 5A.

a,c

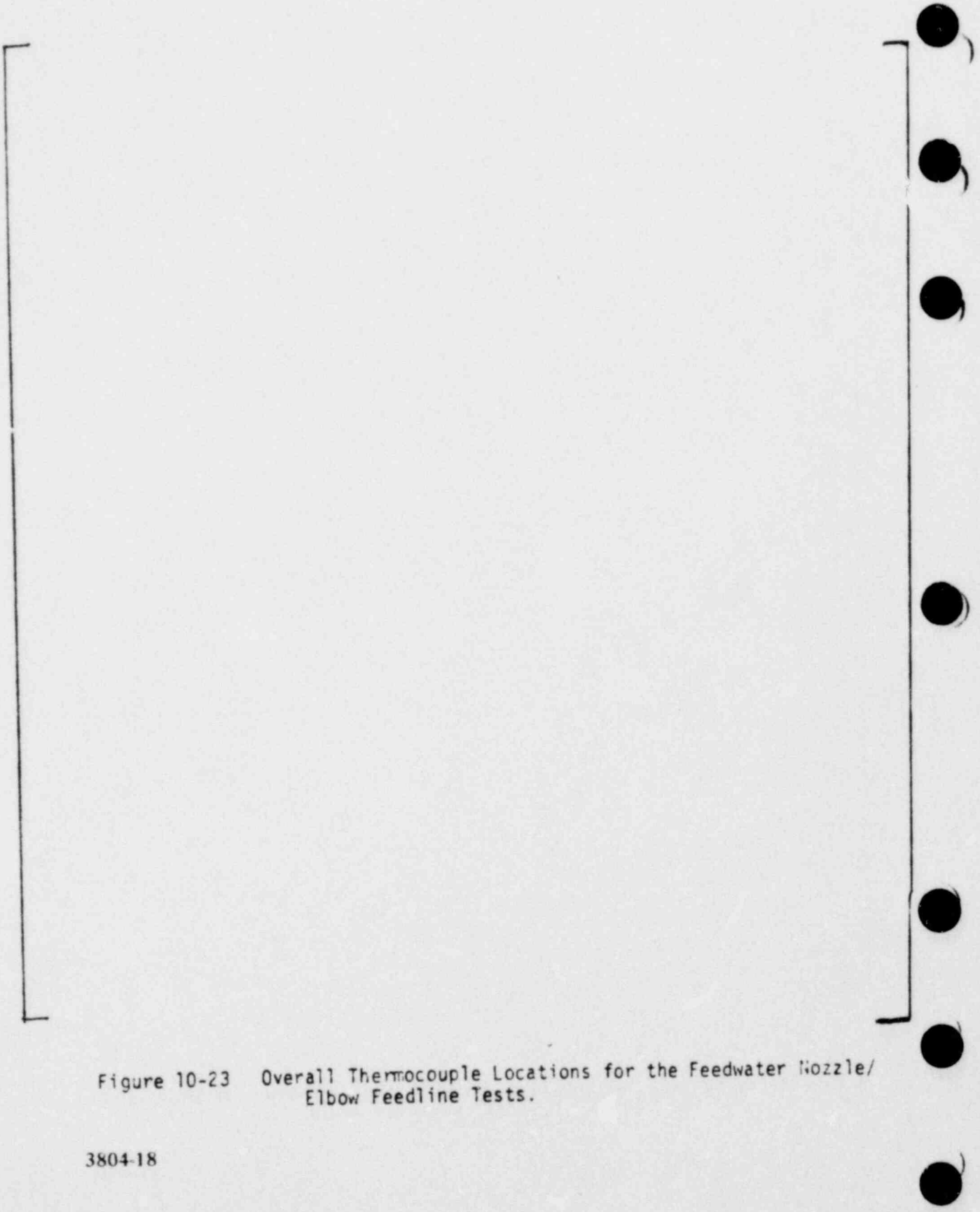

Figure 10-23 Overall Thermocouple Locations for the Feedwater Nozzle/ Elbow Feedline Tests.

a,c 3804-21

Figure 10-24 Detailed Locations of Thermocouples for the Feedwater Nozzle/Elbow Feedline Tests.

a,c

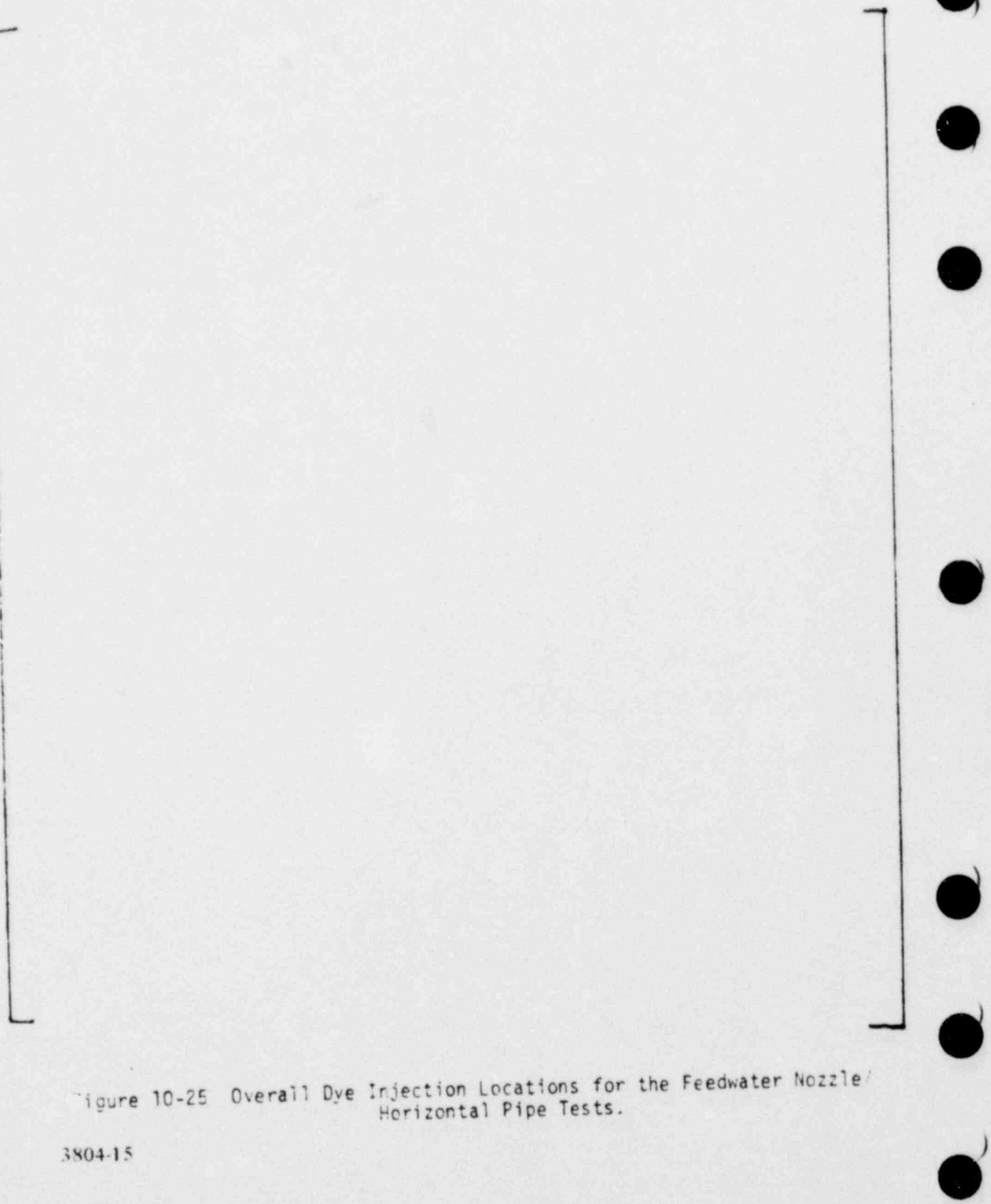

Figure 10-25 Overall Dye Injection Locations for the Feedwater Nozzle/ Horizontal Pipe Tests.

3804-19

a,c

Figure 10-26 Detailed Dye Injection Locations for the Feedwater Nozzle/Horizontal Pipe Tests.

a,c

Figure 10-27 Overall Dye Injection Locations for the Feedwater Nozzle/Elbow Feedline Tests.

a,c

Figure 10-28 Detailed Dye Injection Locations for the Feedwater Nozzle/Elbow Feedline Tests.

Figure 10-29. Stratification in elbow test section at 40 GPM salt solution flow.

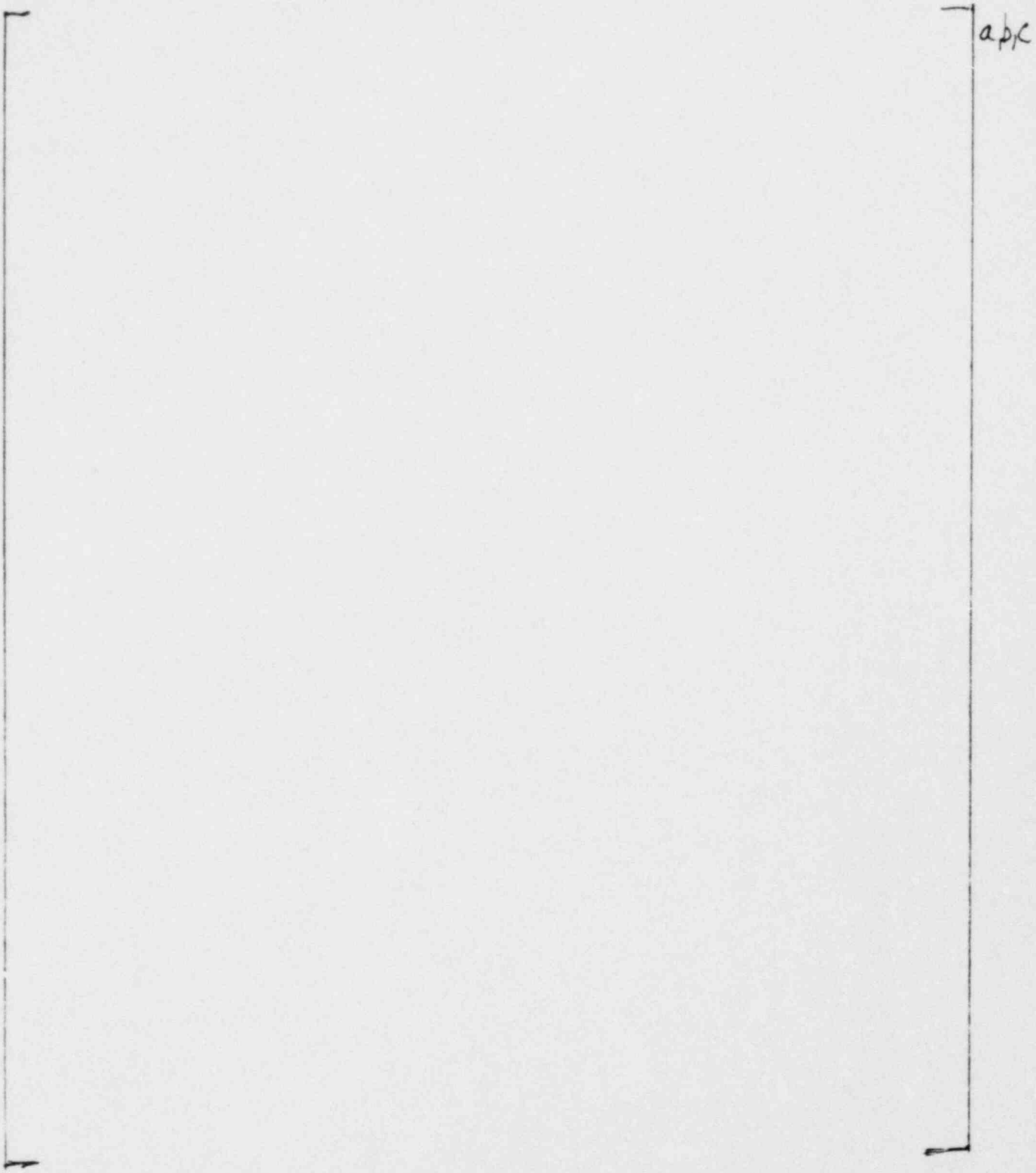

Figure 10-30. Feedline cracking test facility with feedwater nozzle/elbow test section installed.

Figure 10-31. Reservoir with drain line used for feedwater cracking thermal/hydraulic tests.

3804-27

a,c

Figure 10-32 Heater and Level Control Systems.

a,c

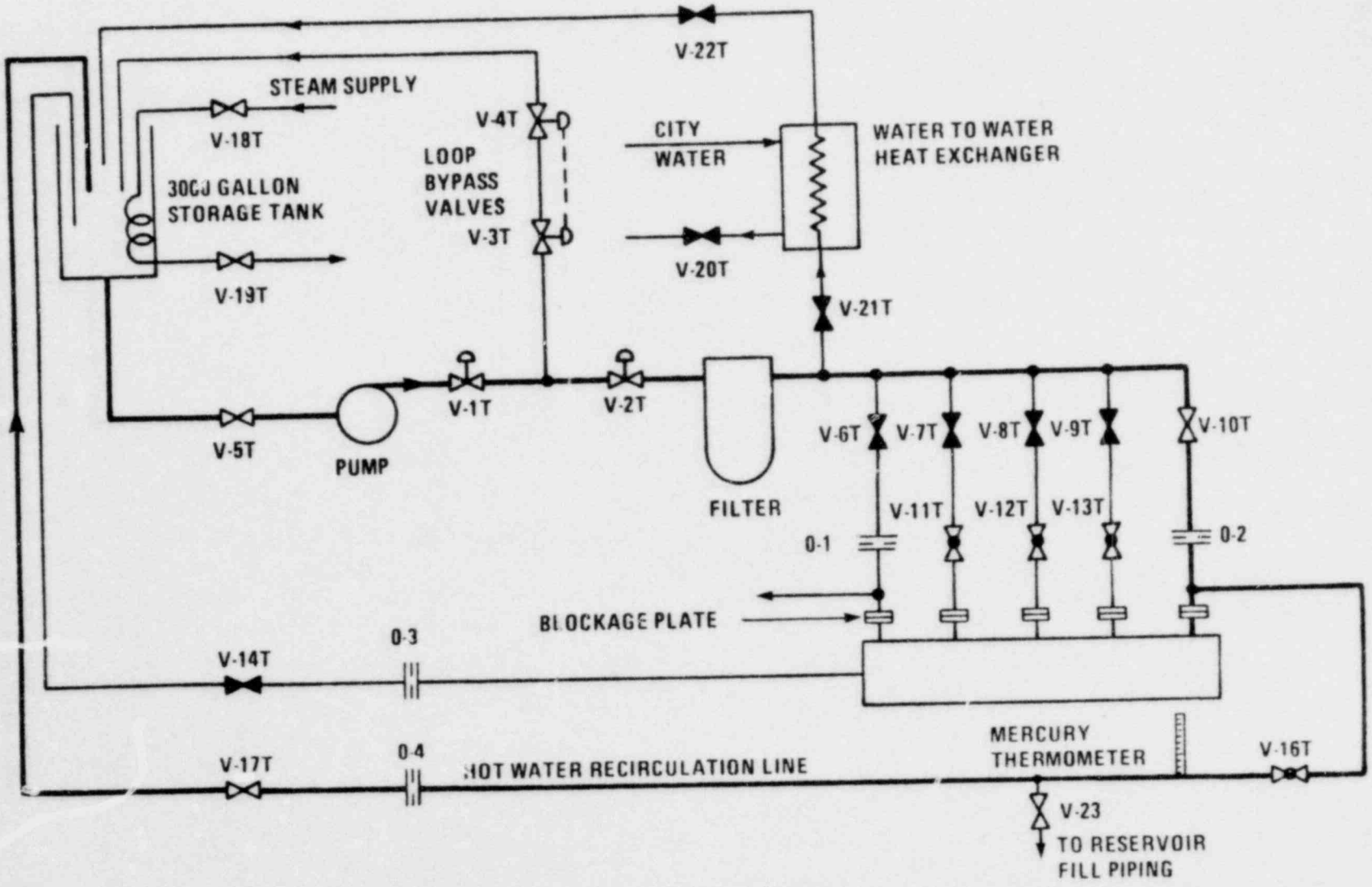

Figure 10-33 Thermal Mixing Hydraulic Loop Schematic

Figure 10-34. Thermal mixing hydraulic loop.

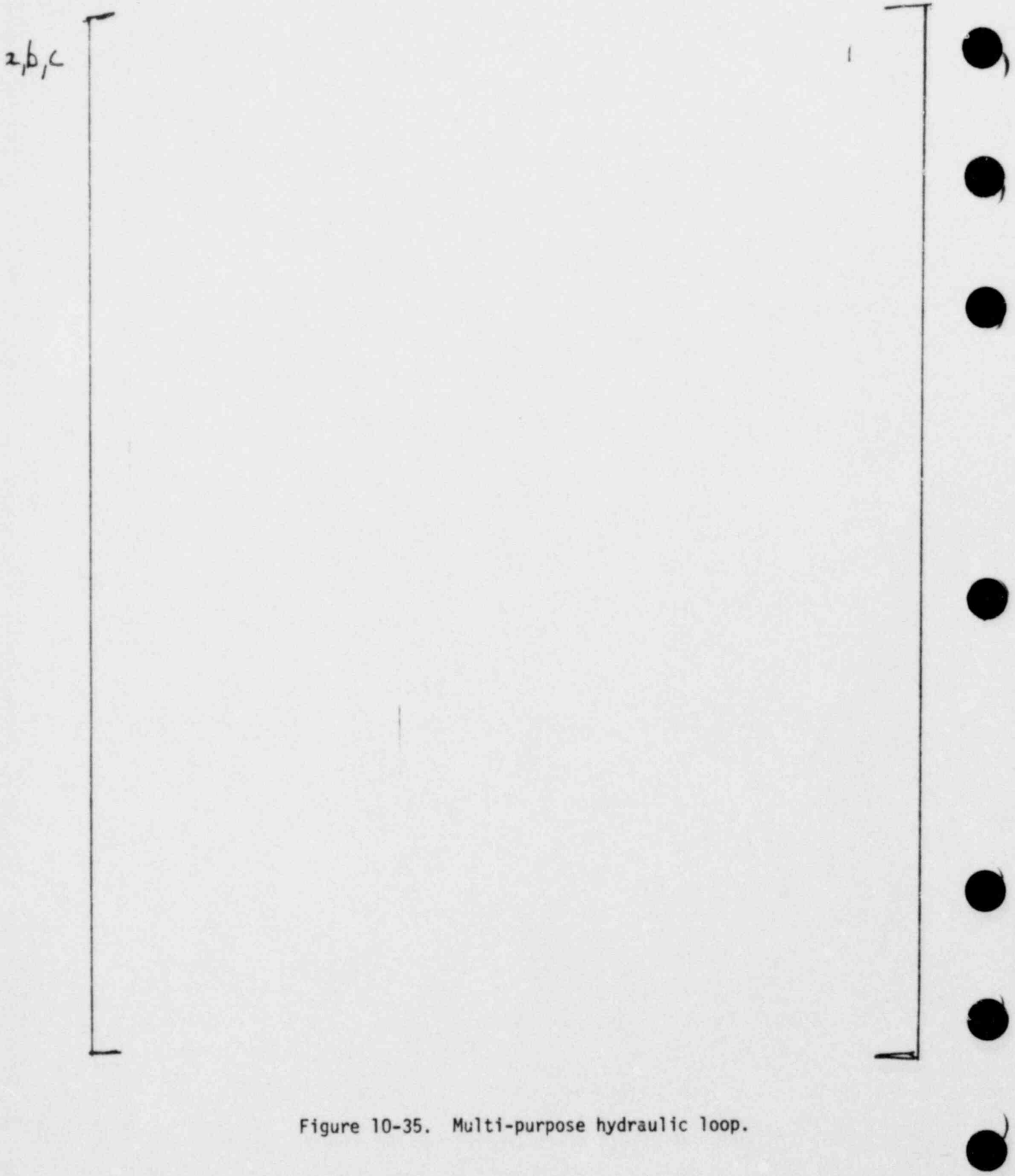

Figure 10-35. Multi-purpose hydraulic loop.

3804-11

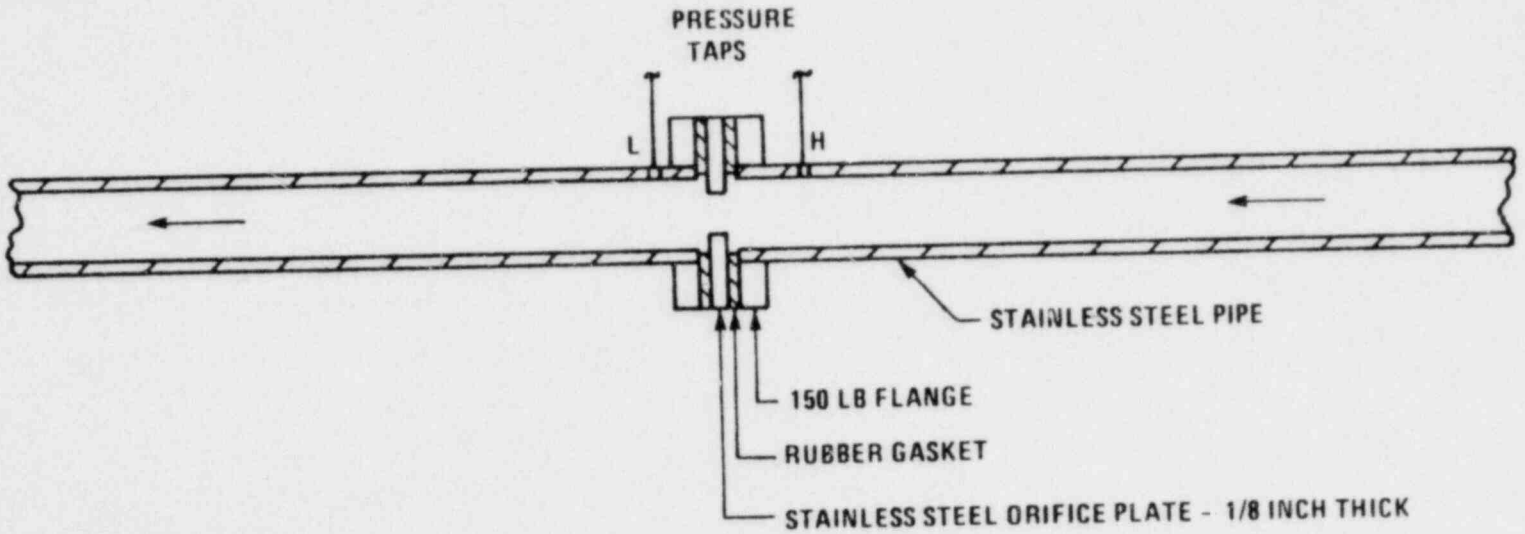

ORIFICE SECTION	PIPE SIZE	ORIFICE DIAMETER	NUMBER OF INSIDE DIAMETERS OF STRAIGHT PIPE		TYPE OF PRESSURE TAPS
			UPSTREAM	DOWNSTREAM	
1/2 - INCH	1/2-SCH 40	0.300 IN.	78	90	FLANGE TAPS
1 - INCH	1-SCH 40	0.592 IN	70	48	FLANGE TAPS
2 - INCH	2-SCH 40	1.145 IN.	34	26	D AND 1/2 D TAPS
4 - INCH	4-SCH 10	2.300 IN.	22	10	D AND 1/2 D TAPS

a,c

Figure 10-36. [ ]

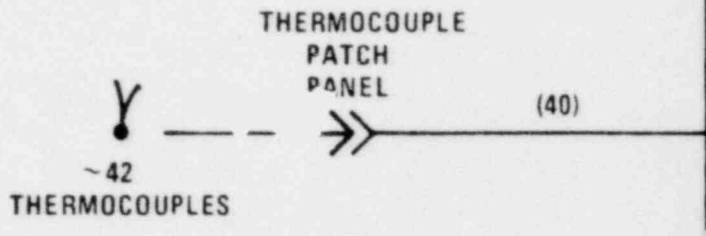

CA
AN
THERMOC
OU

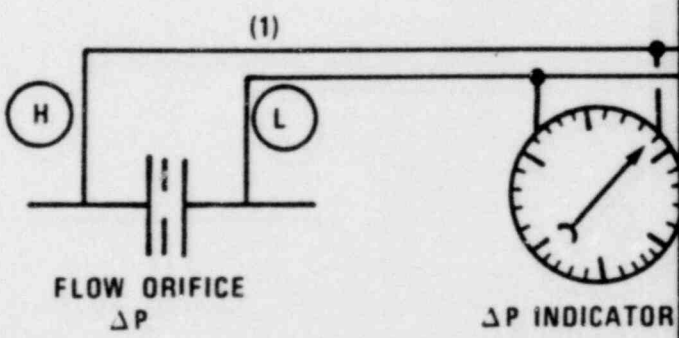

MPHL TEST FACILI

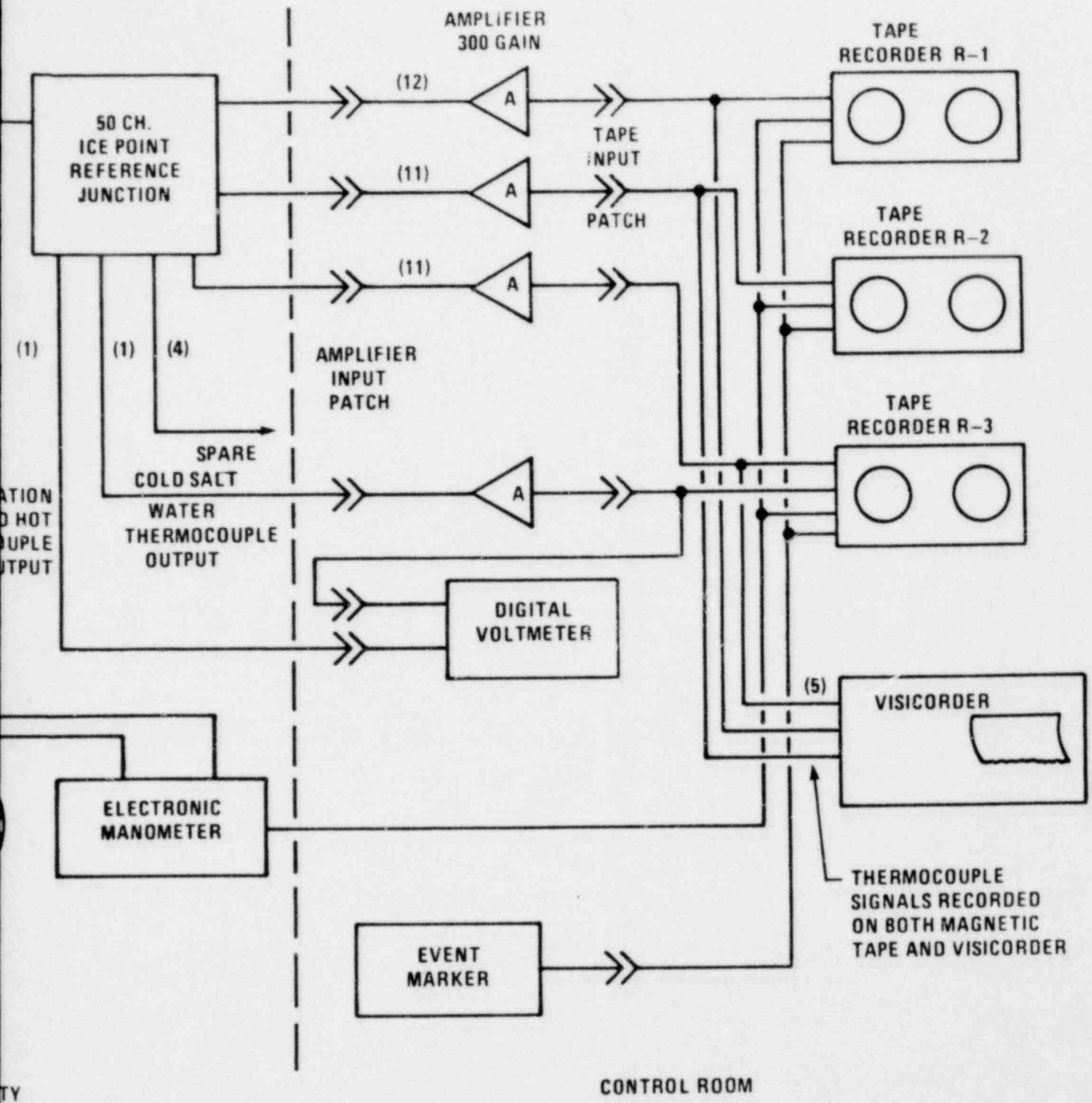

Figure 10-37. Data Acquisition System

3804-13

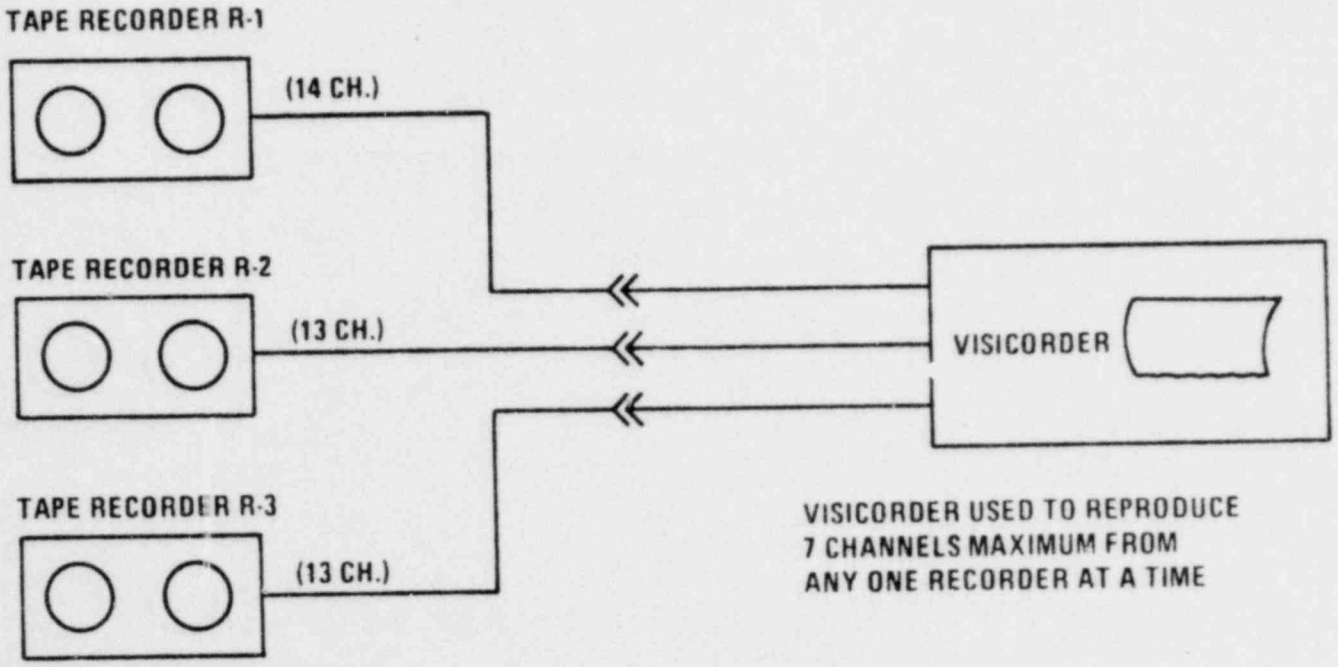

Figure 10-38. Instrumentation Schematic to Obtain Visicorder Plots from Data Recorded on Magnetic Tape

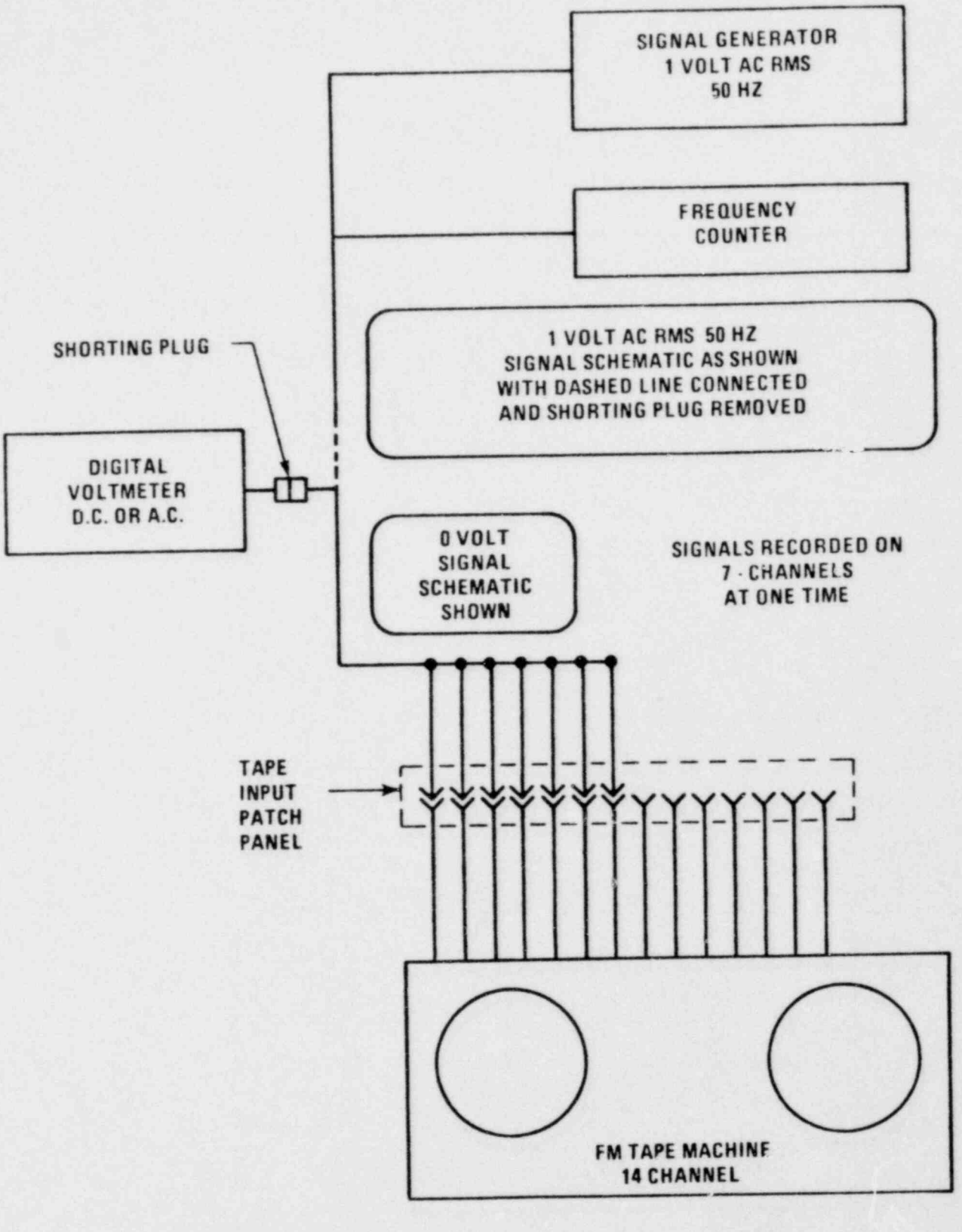

Figure 10-39. Instrumentation Schematic for Recording Calibration Signals on Each Tape

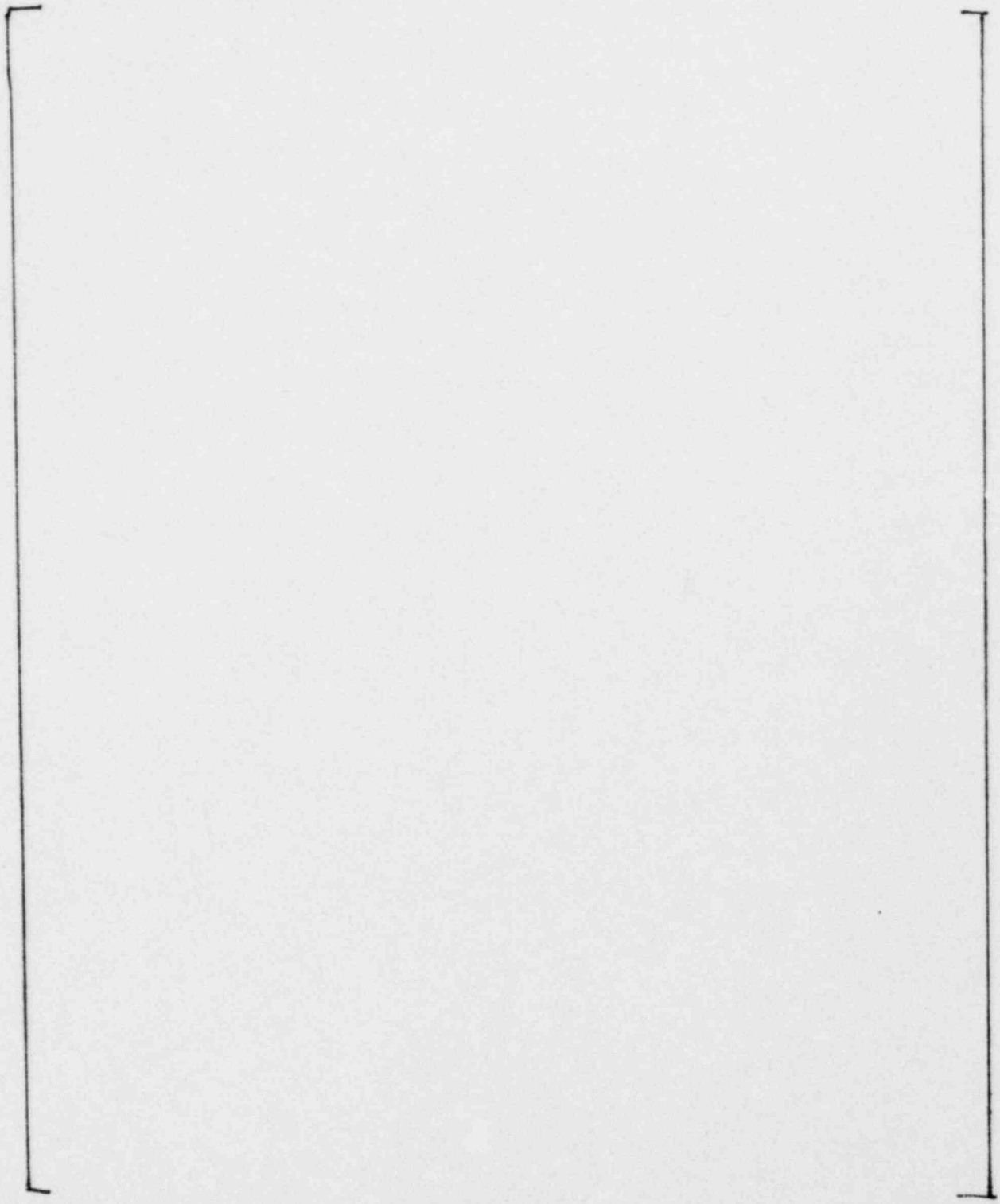

a,c

Figure 10-40. [ ] Measurement System a,c

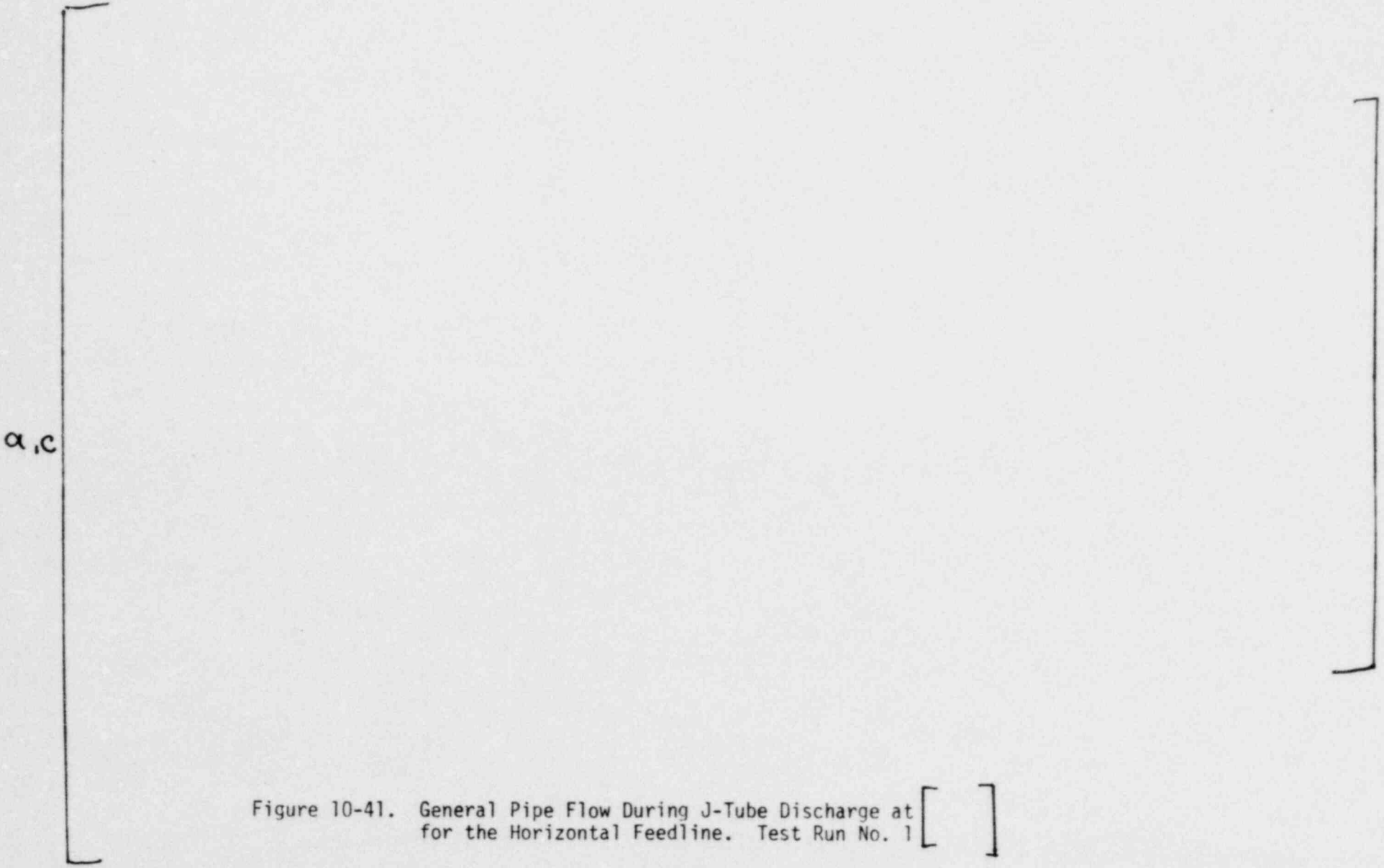

Figure 10-41. General Pipe Flow During J-Tube Discharge at [ ] for the Horizontal Feedline. Test Run No. 1 [ ]

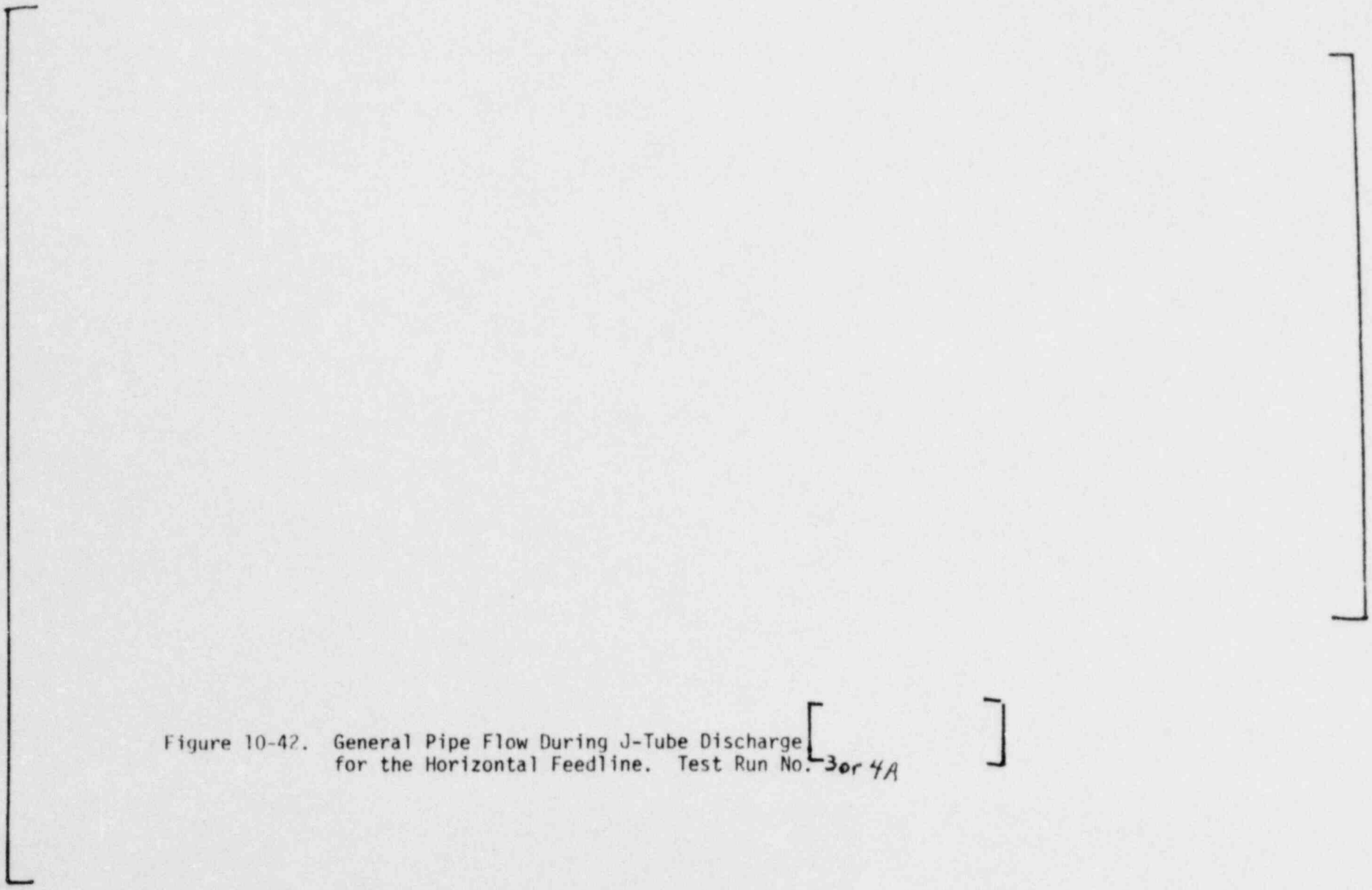

Figure 10-42. General Pipe Flow During J-Tube Discharge [ ] for the Horizontal Feedline. Test Run No. 3 or 4A

[a,c

]

Figure 10-43. General Pipe Flow During J-Tube Discharge [ ] or Higher with 2" Holes Open for the Horizontal Feedline. Test Run No. 7C (See Table 10.11).

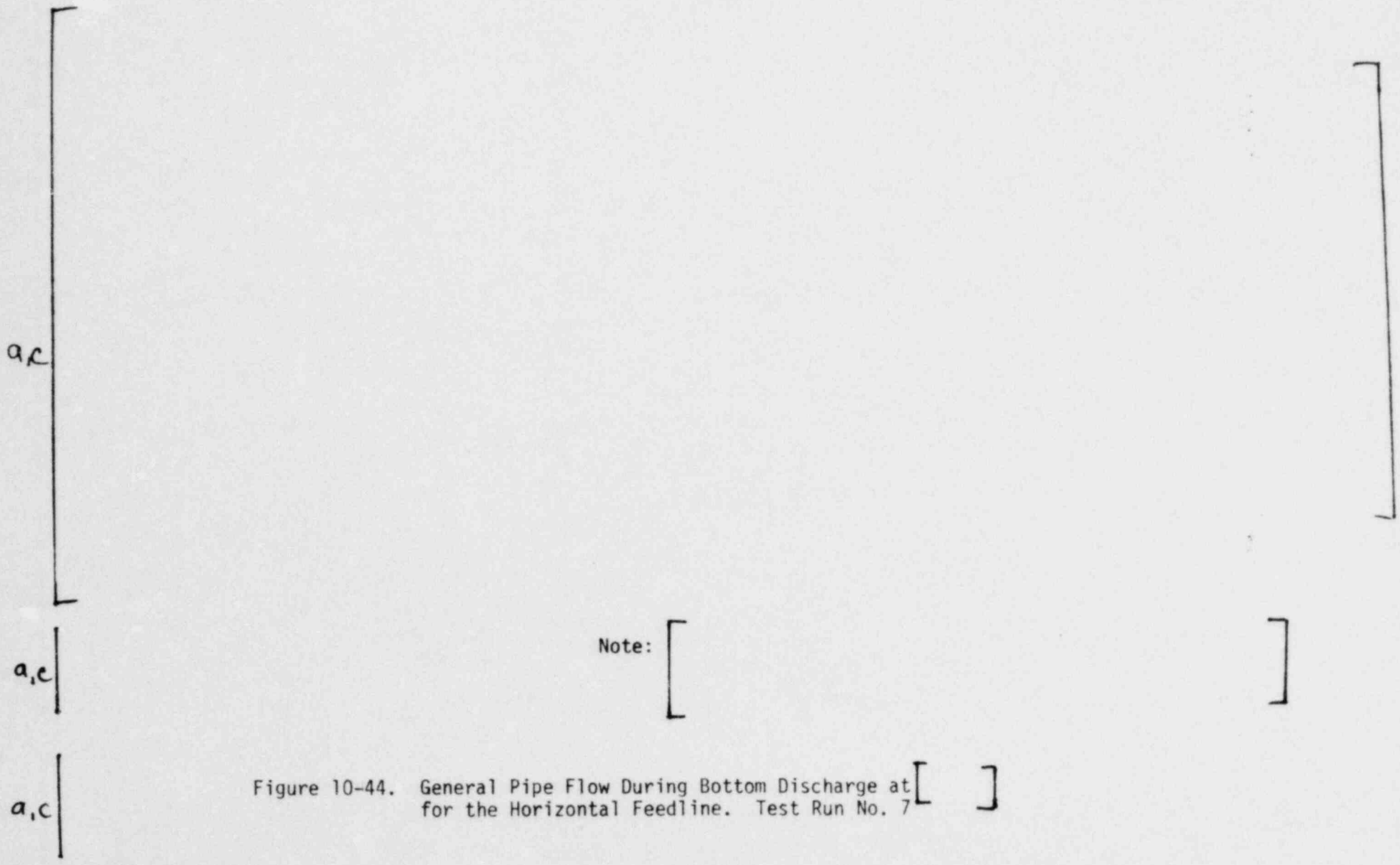

Note: [ ]

Figure 10-44. General Pipe Flow During Bottom Discharge at [ ] for the Horizontal Feedline. Test Run No. 7

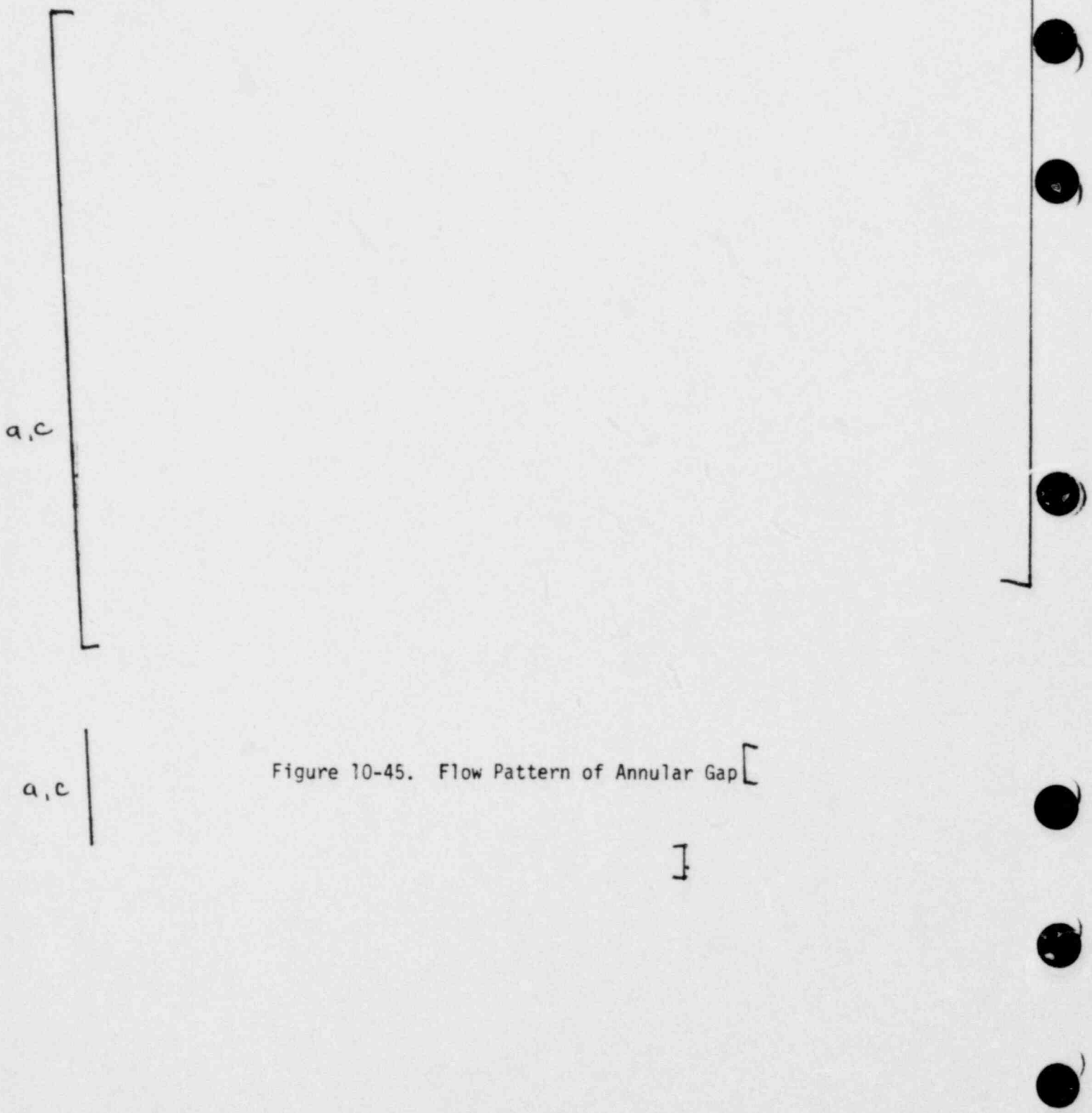

Figure 10-45. Flow Pattern of Annular Gap

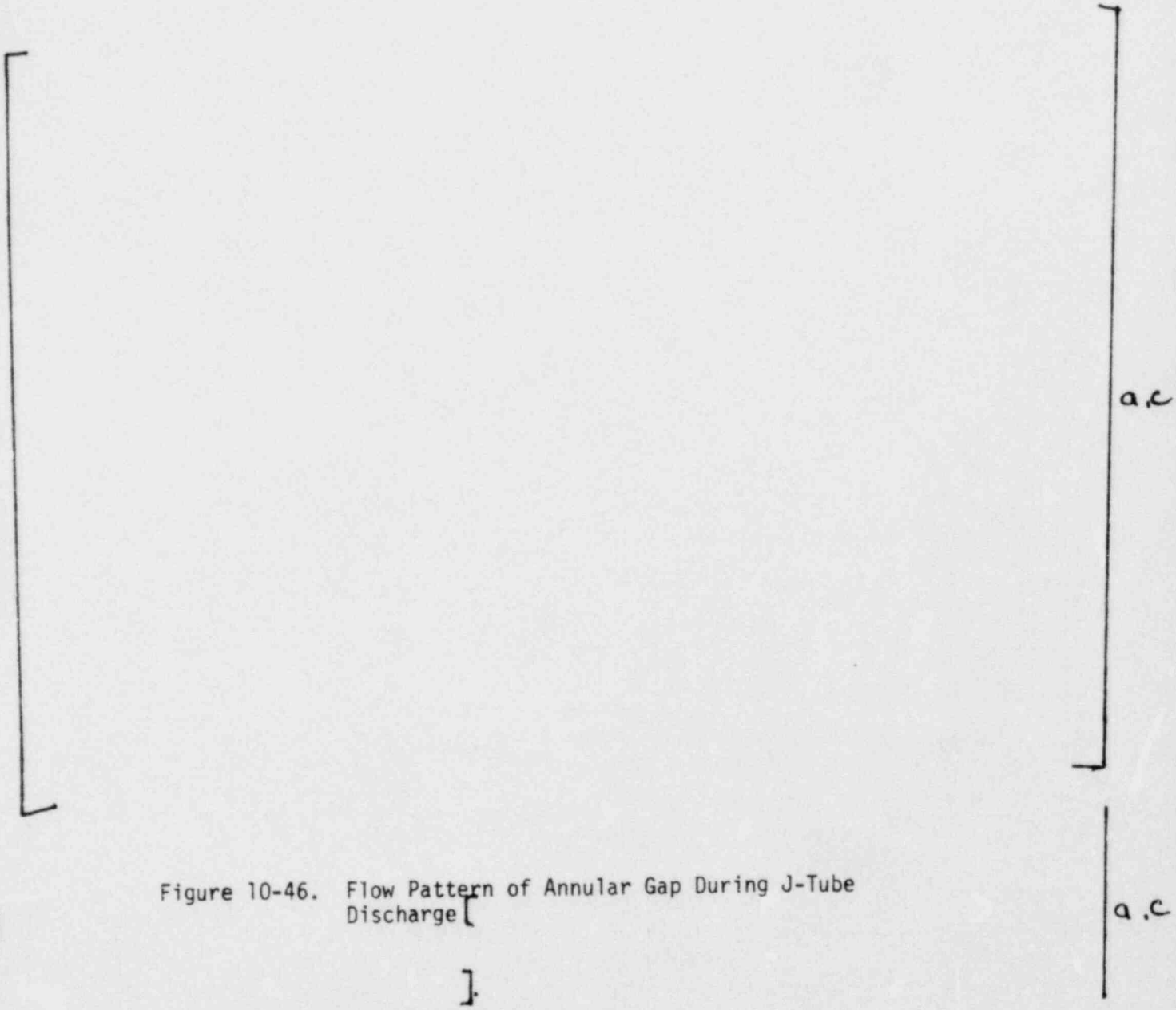

Figure 10-46. Flow Pattern of Annular Gap During J-Tube Discharge[

]

NOTE: [ ]

Figure 10-47. Flow Pattern of Annular Gap During J-Tube Discharge[ ]

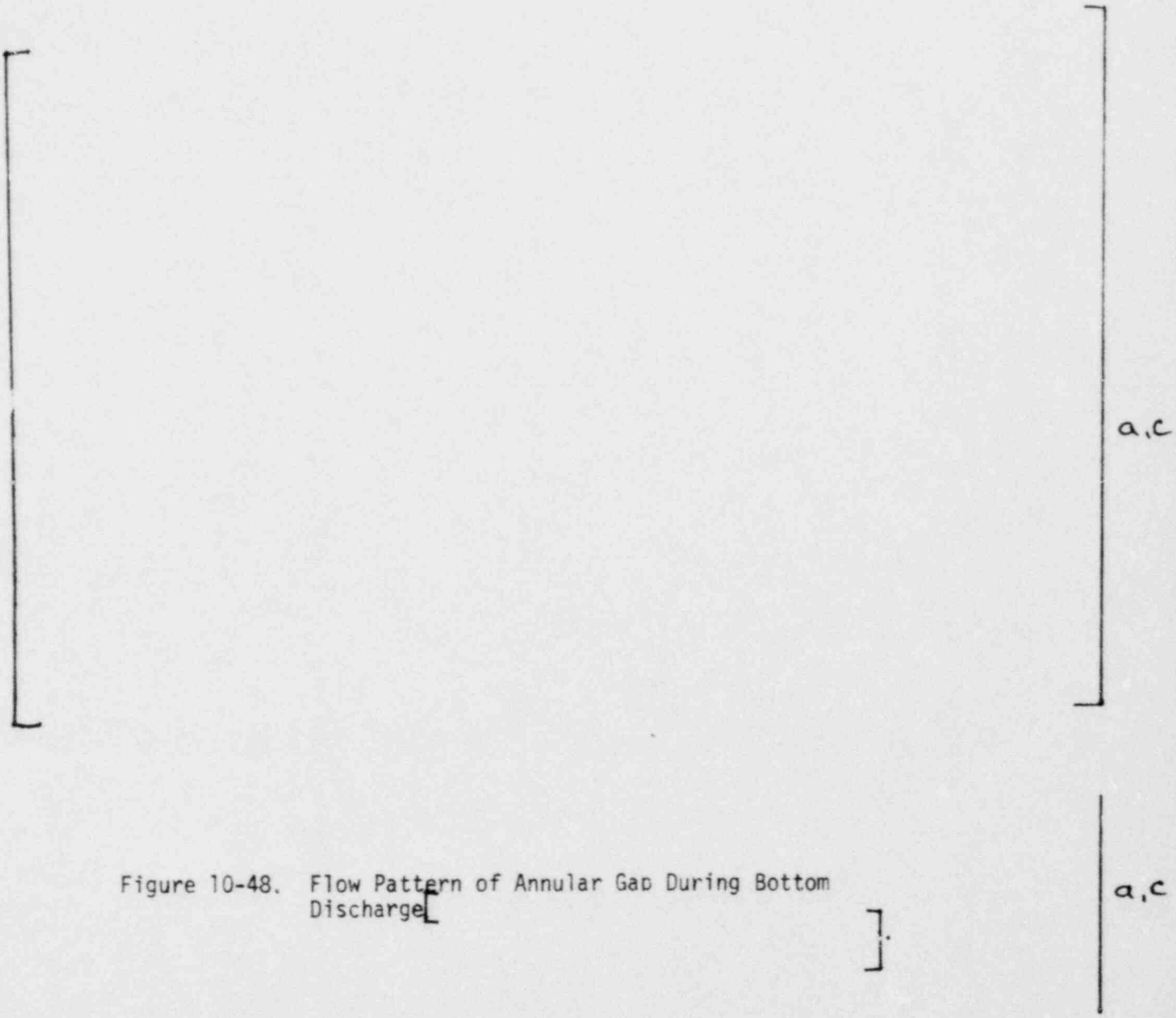

Figure 10-48. Flow Pattern of Annular Gap During Bottom Discharge

a,c

a,c

Figure 10-49. Flow Pattern of Discharge Pipe During Bottom Discharge

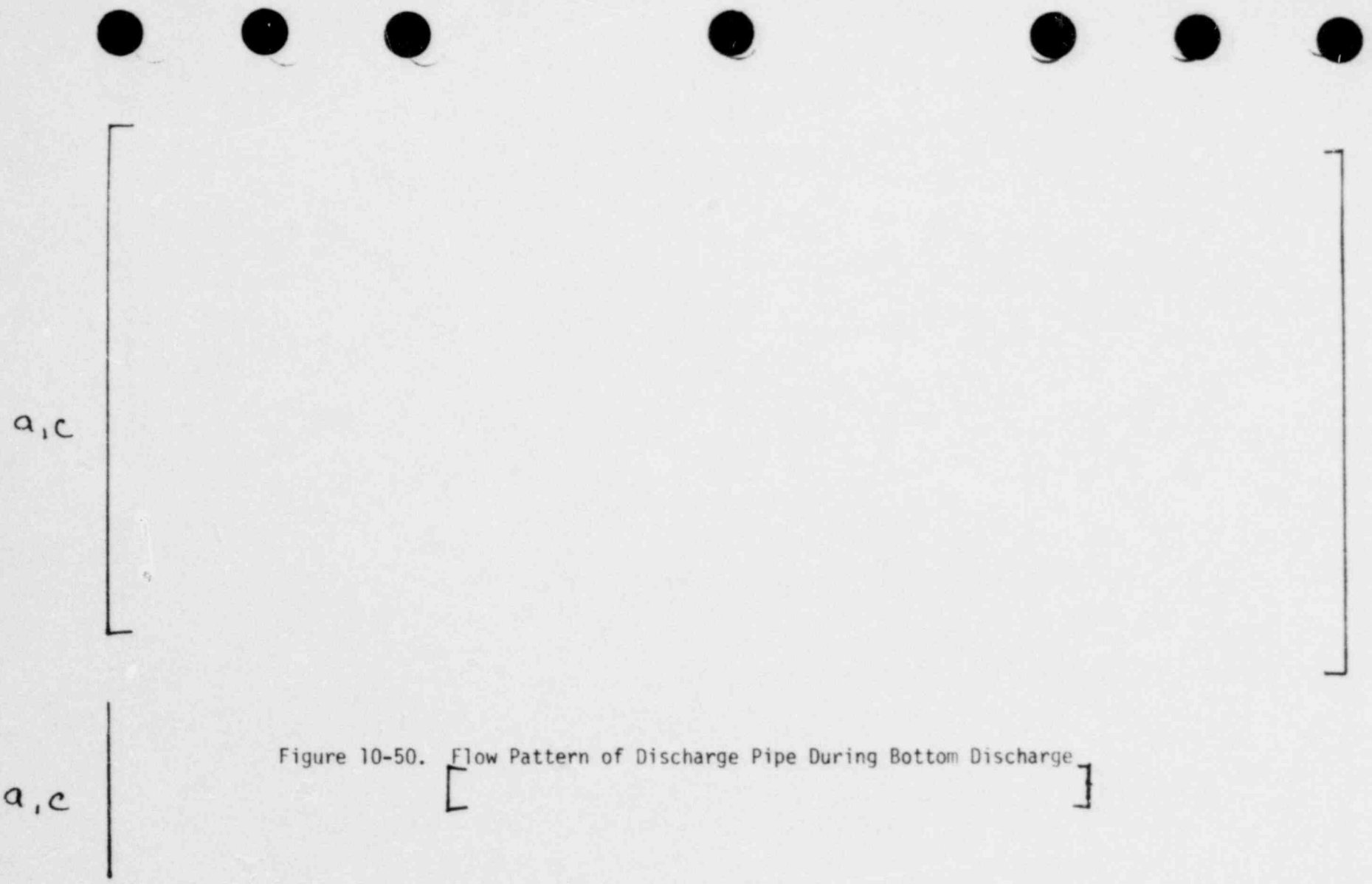

Figure 10-50. Flow Pattern of Discharge Pipe During Bottom Discharge

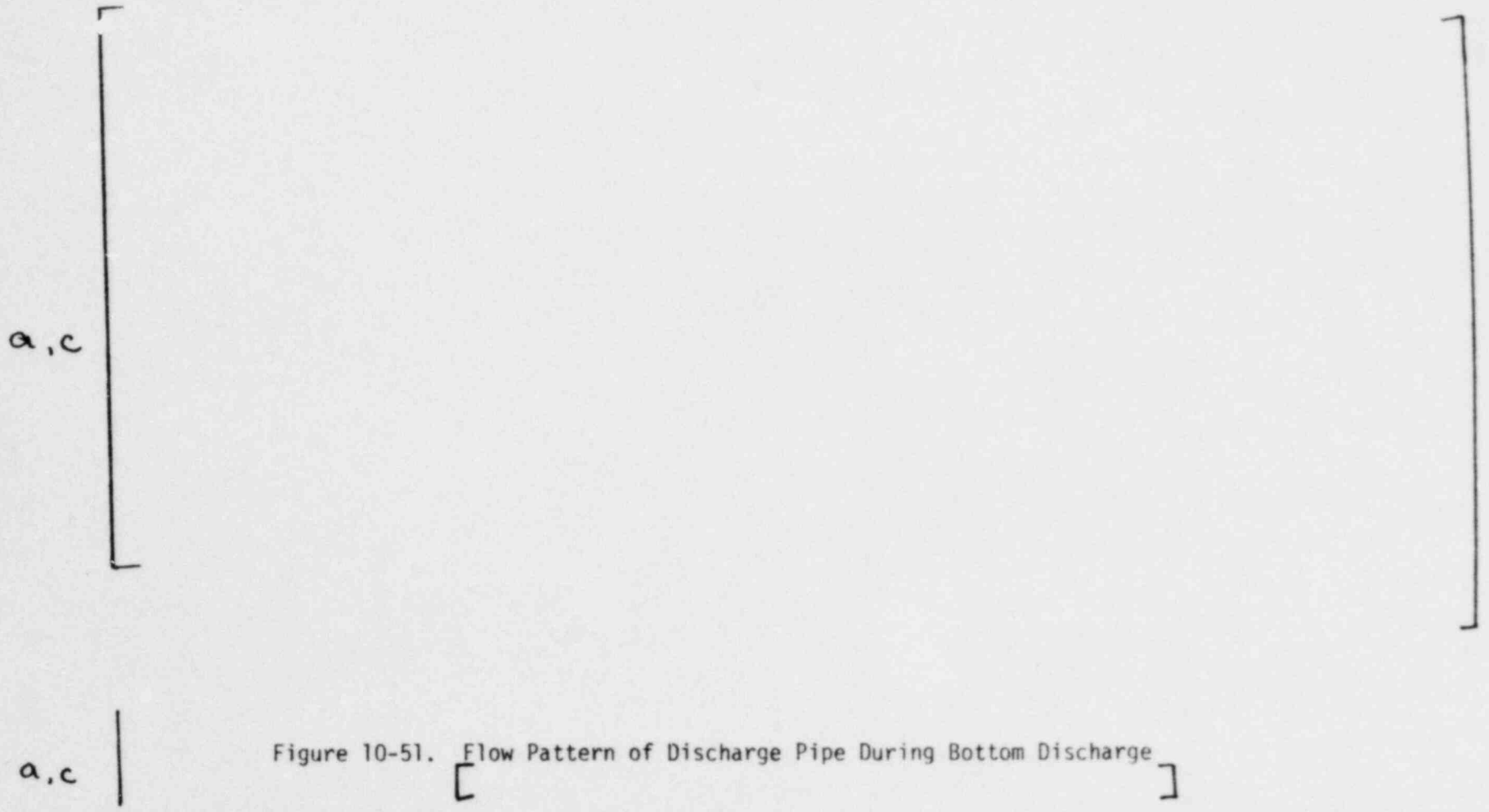

Figure 10-51. Flow Pattern of Discharge Pipe During Bottom Discharge

a,c

a,c

Figure 10-52. Flow Pattern of Discharge Pipe During Bottom Discharge

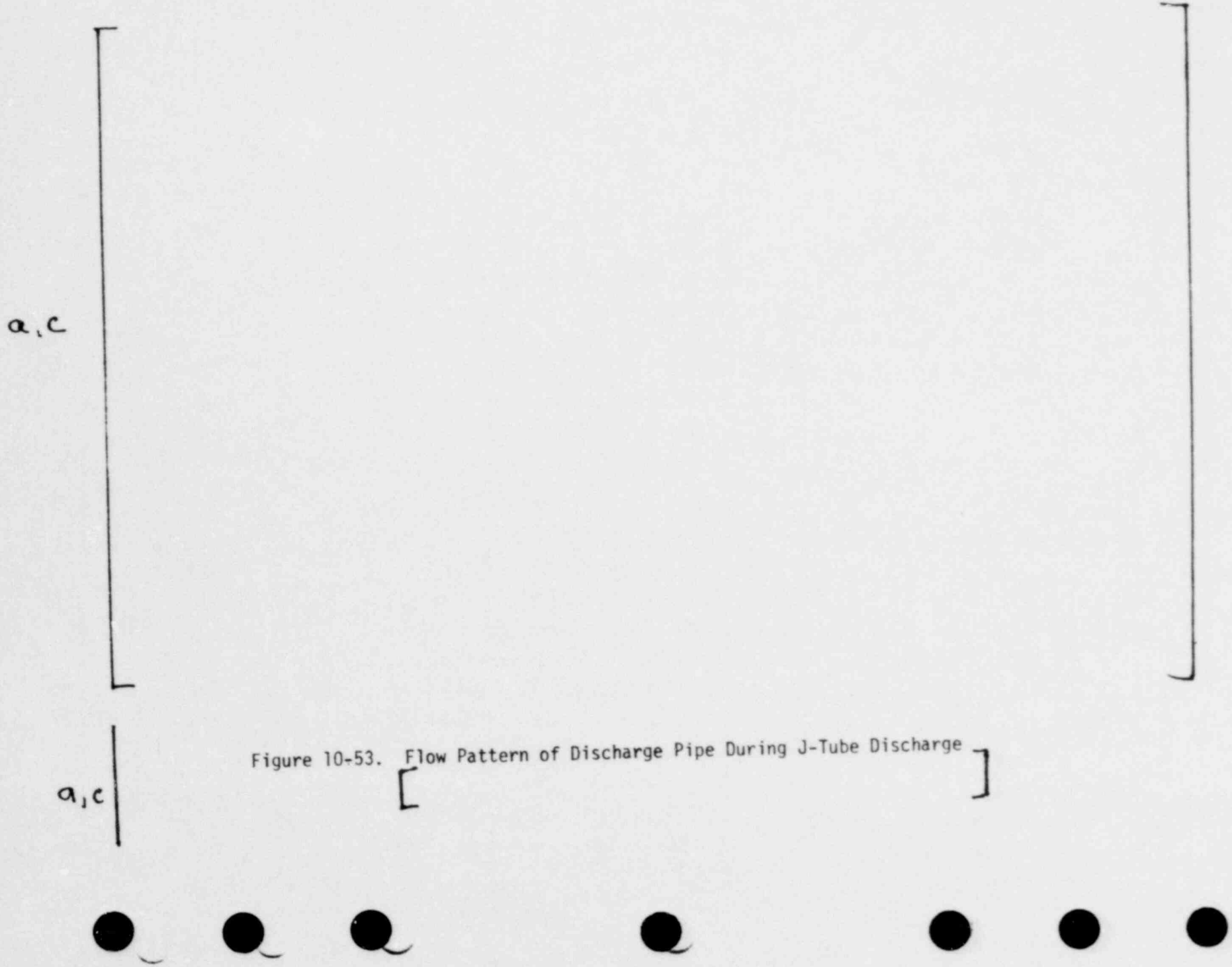

Figure 10-53. Flow Pattern of Discharge Pipe During J-Tube Discharge

a,c

a,c

Figure 10-54. Flow Pattern of Discharge Pipe During J-Tube Discharge[
]

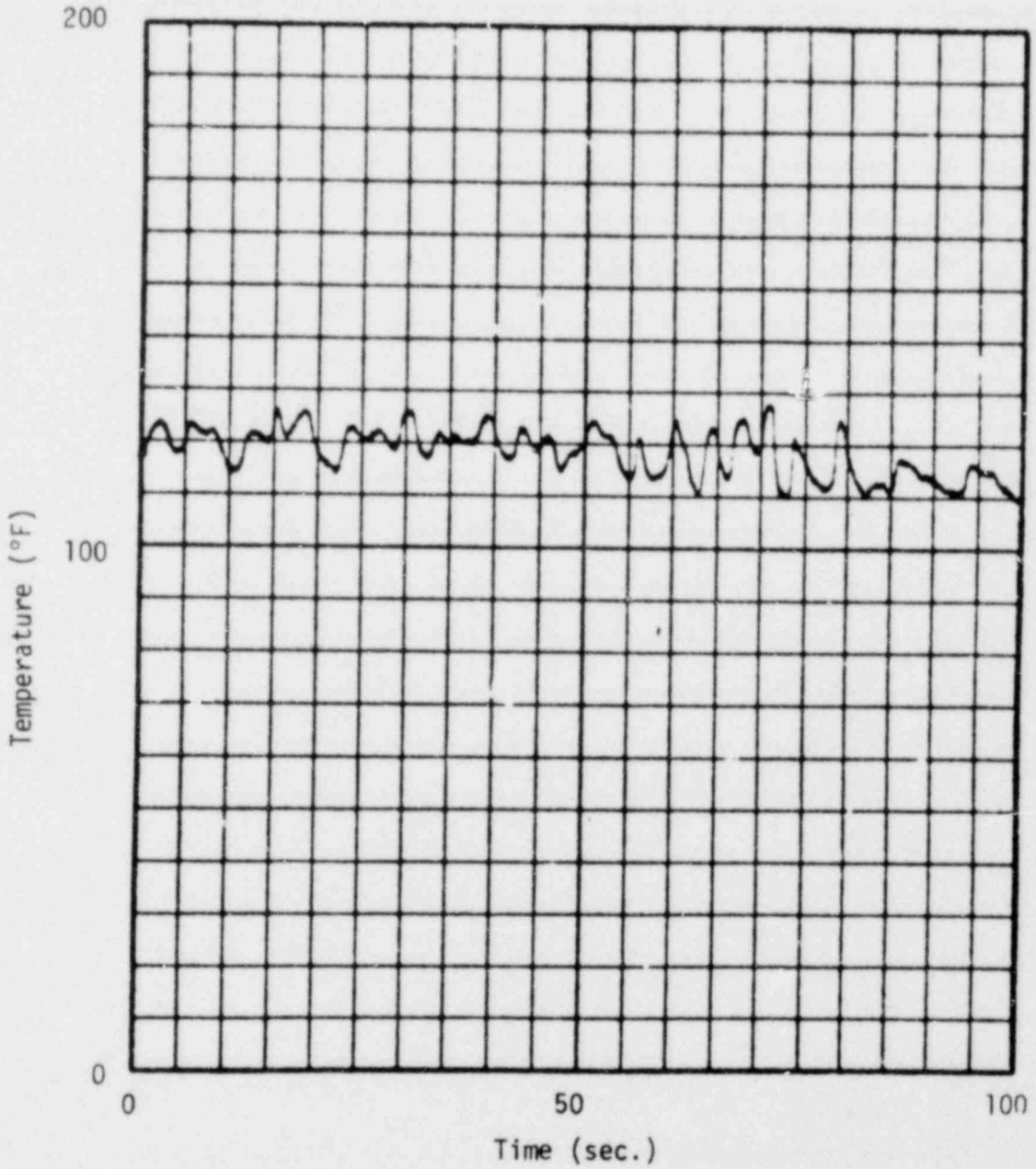

Figure 10-55. Typical Temperature Oscillations for Horizontal Feedline Configuration

a,c

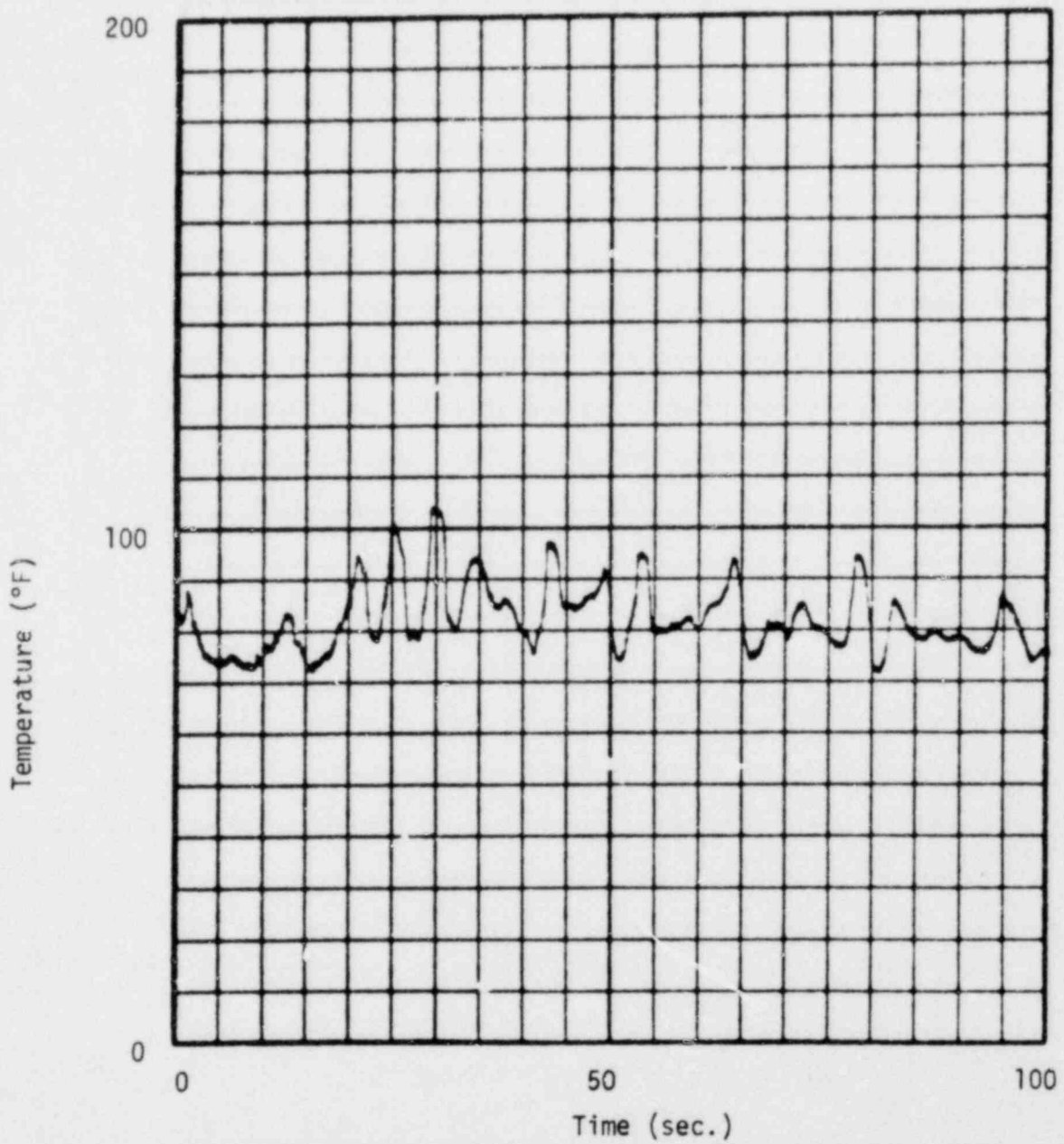

Figure 10-56. Typical Temperature Oscillations for Horizontal Feedline Configuration

[ ]

a,c

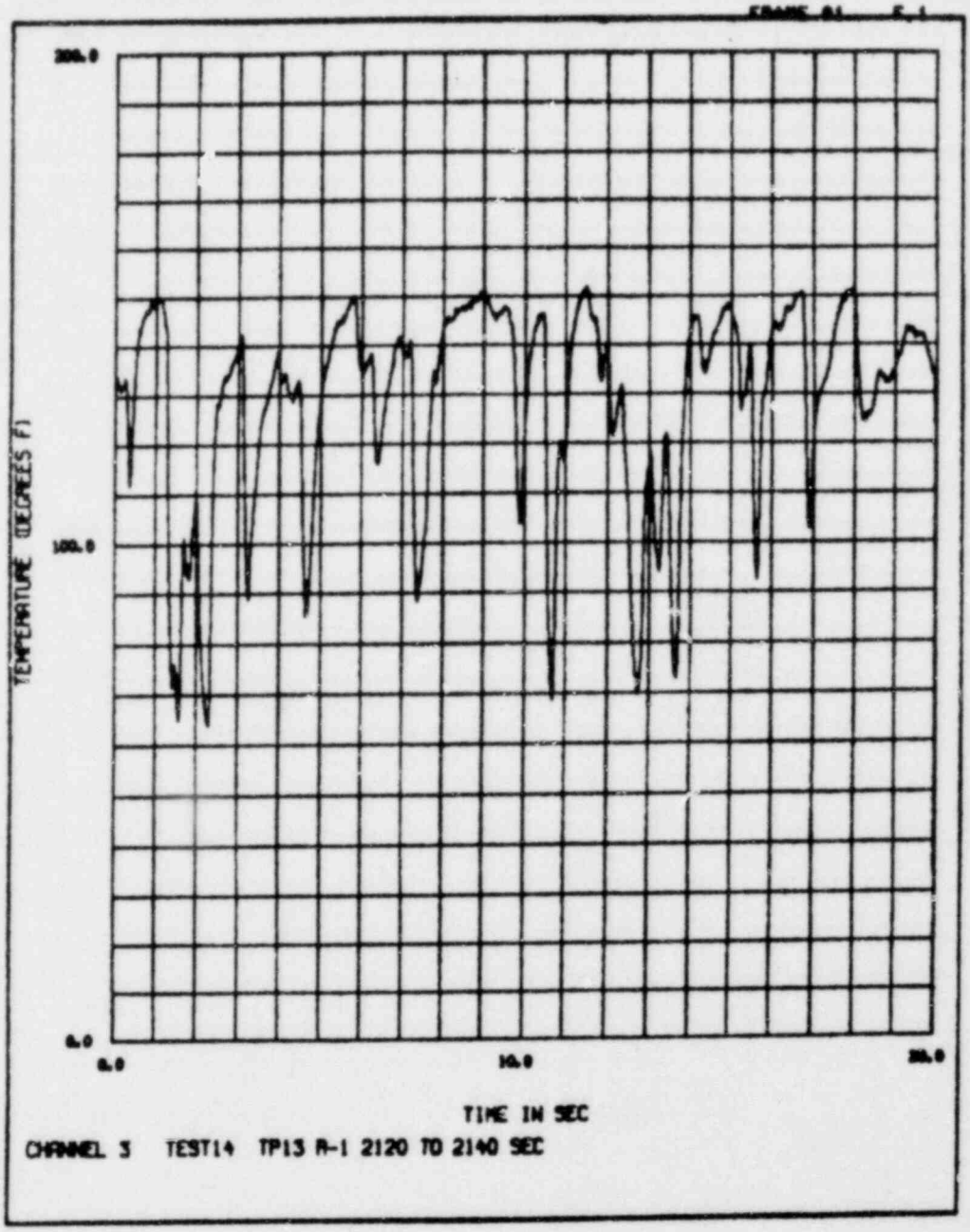

Figure 10-57. Typical Temperature Oscillations for Elbow Feedline Configuration. [

a,c

]

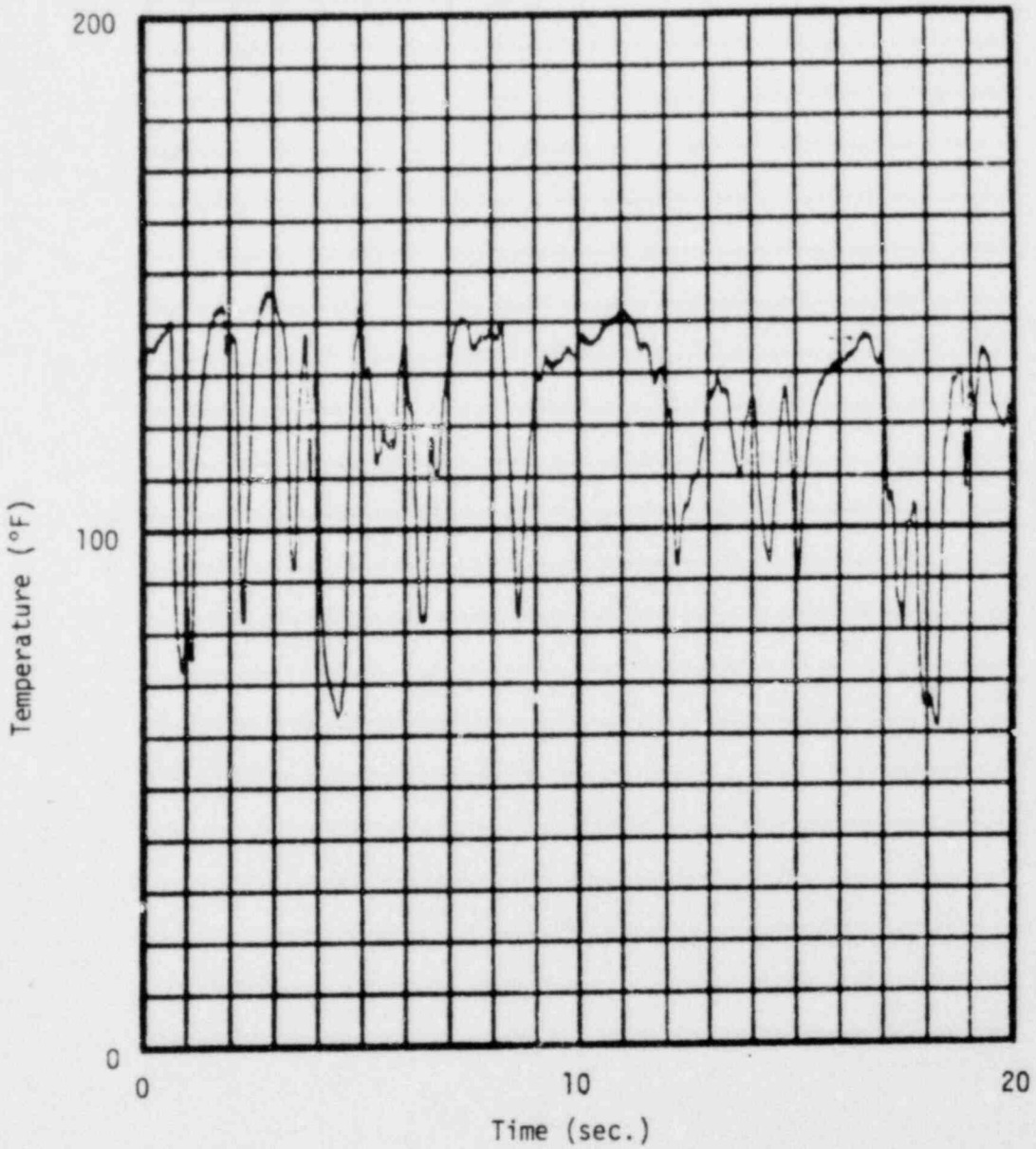

Figure 10-58. Typical Temperature Oscillation for Elbow Feedline Configuration

[ ] a,c

a,c

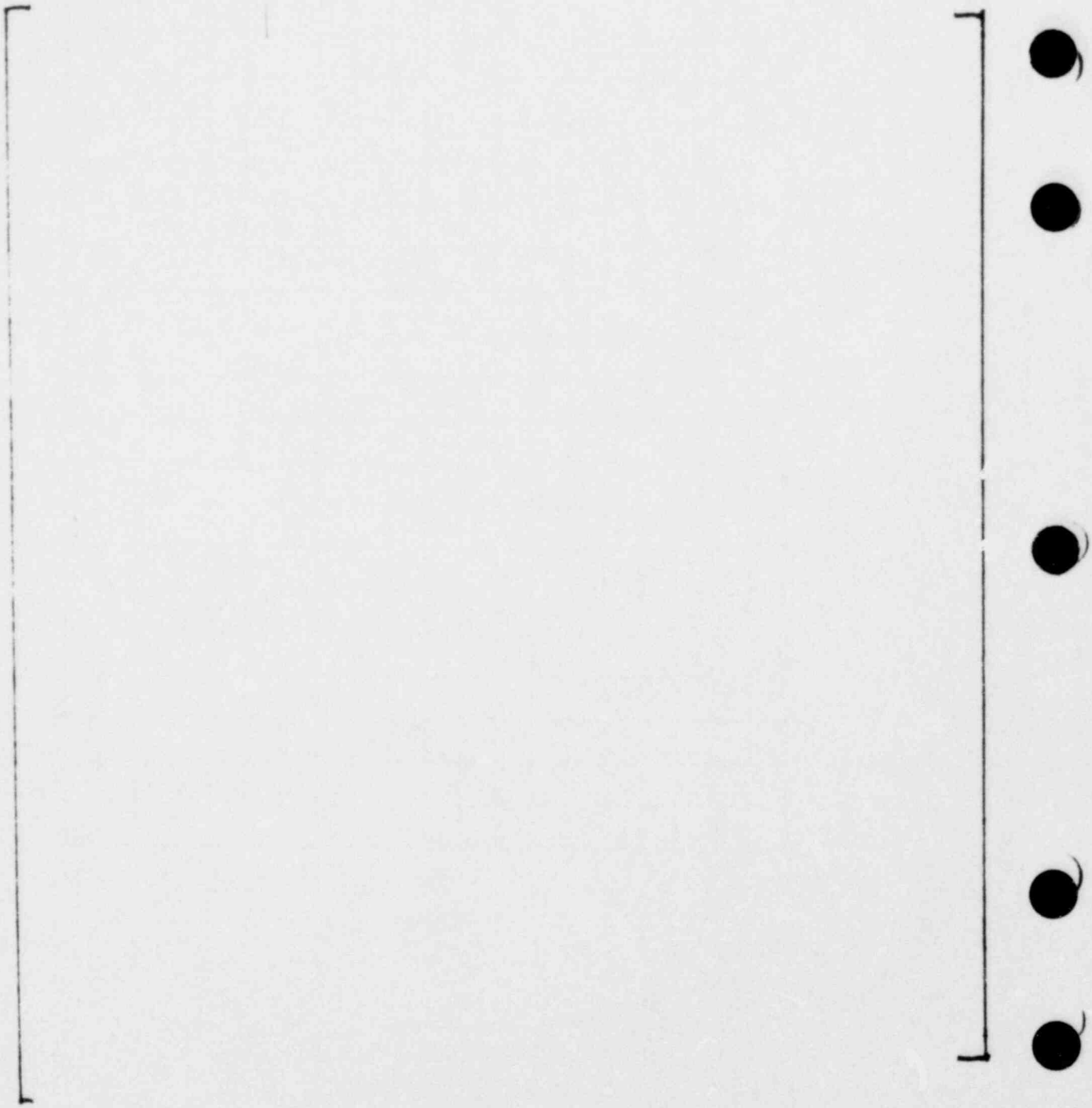

Figure 10-59. Envelope for Peak to Peak Amplitudes of Temperature Oscillations for Horizontal Configuration and Bottom Discharge.

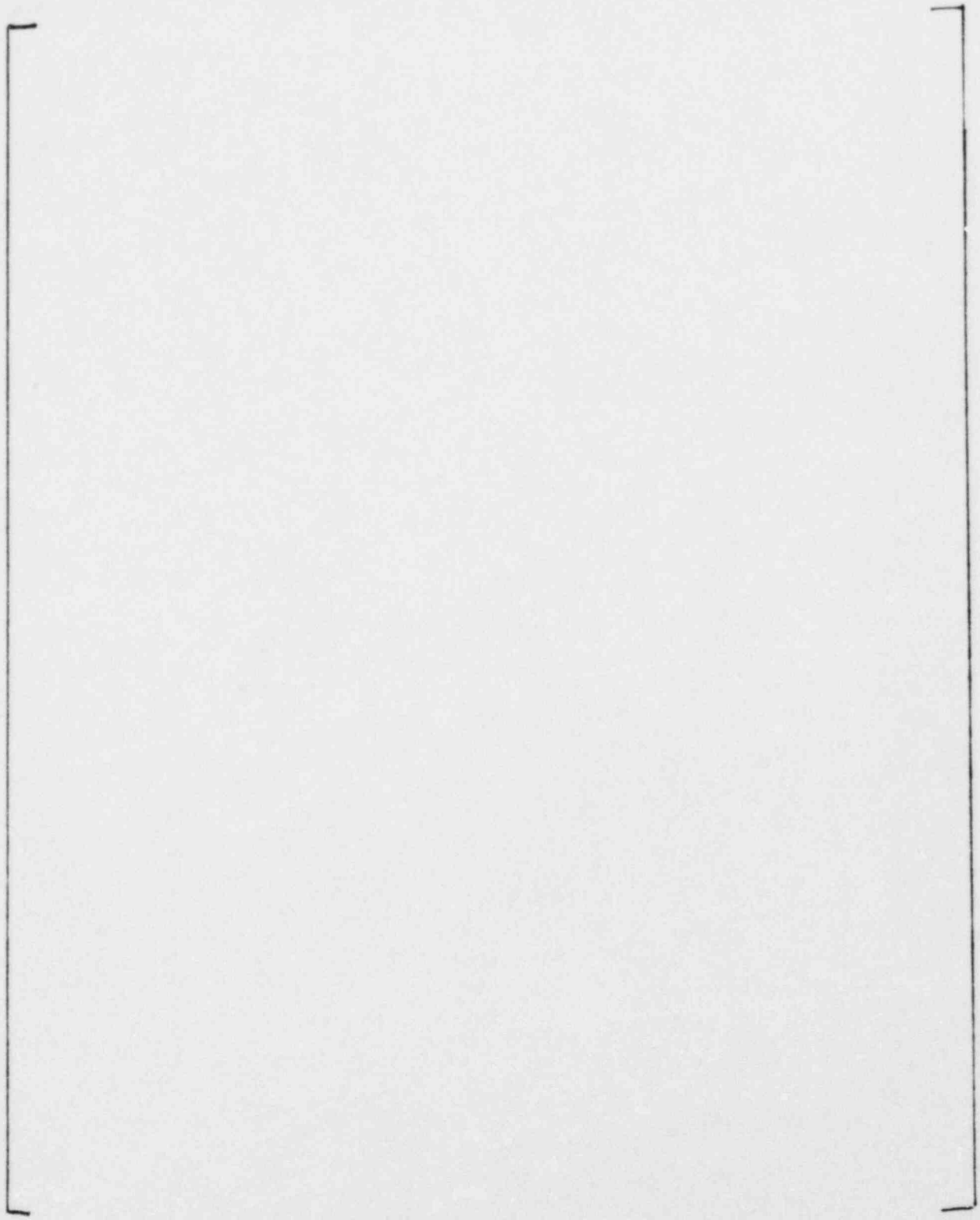

a,c

Figure 10-60. Envelope for Peak to Peak Amplitudes of Temperature Oscillations for Horizontal Configuration and J-Tube Discharge

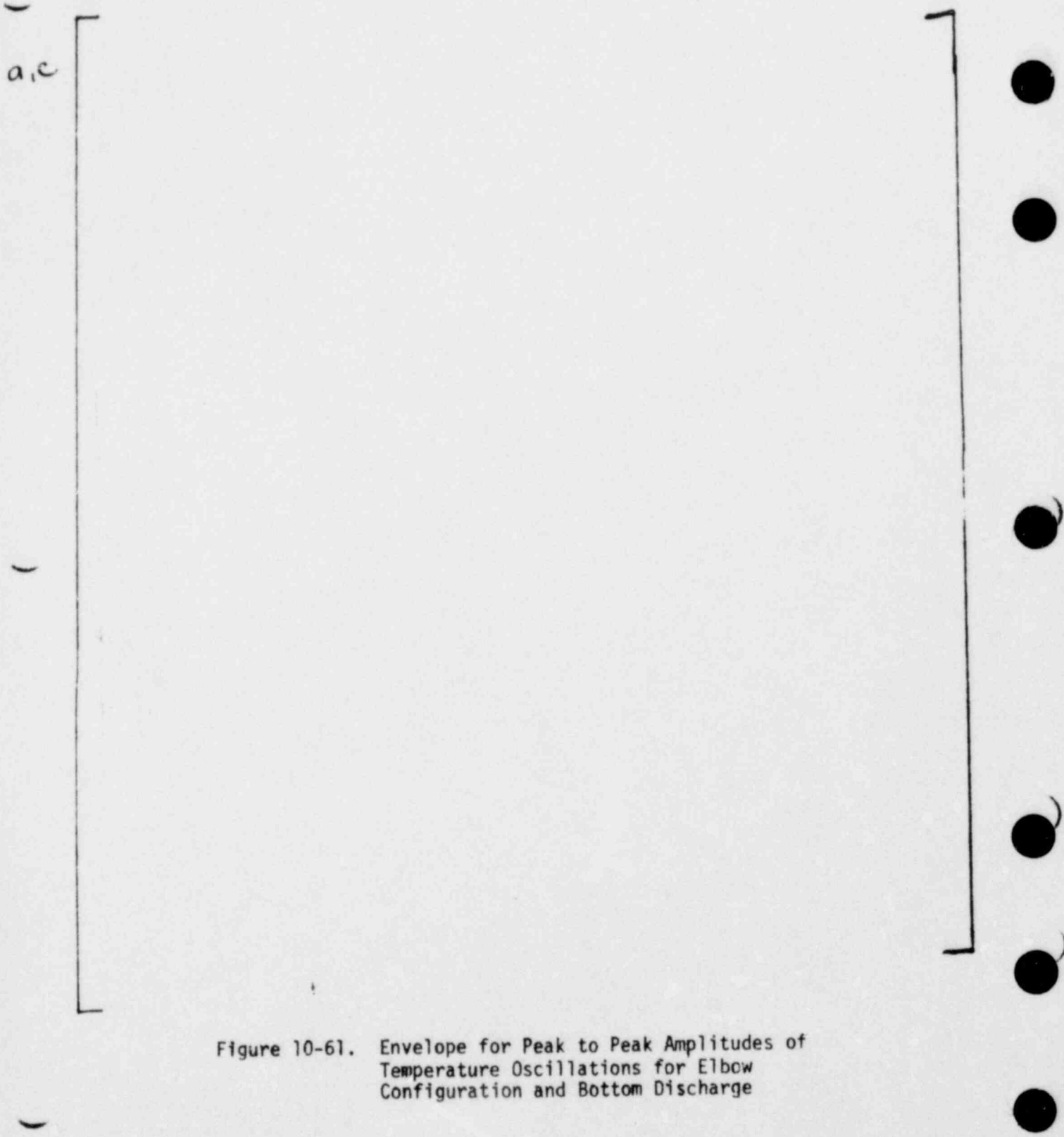

Figure 10-61. Envelope for Peak to Peak Amplitudes of Temperature Oscillations for Elbow Configuration and Bottom Discharge

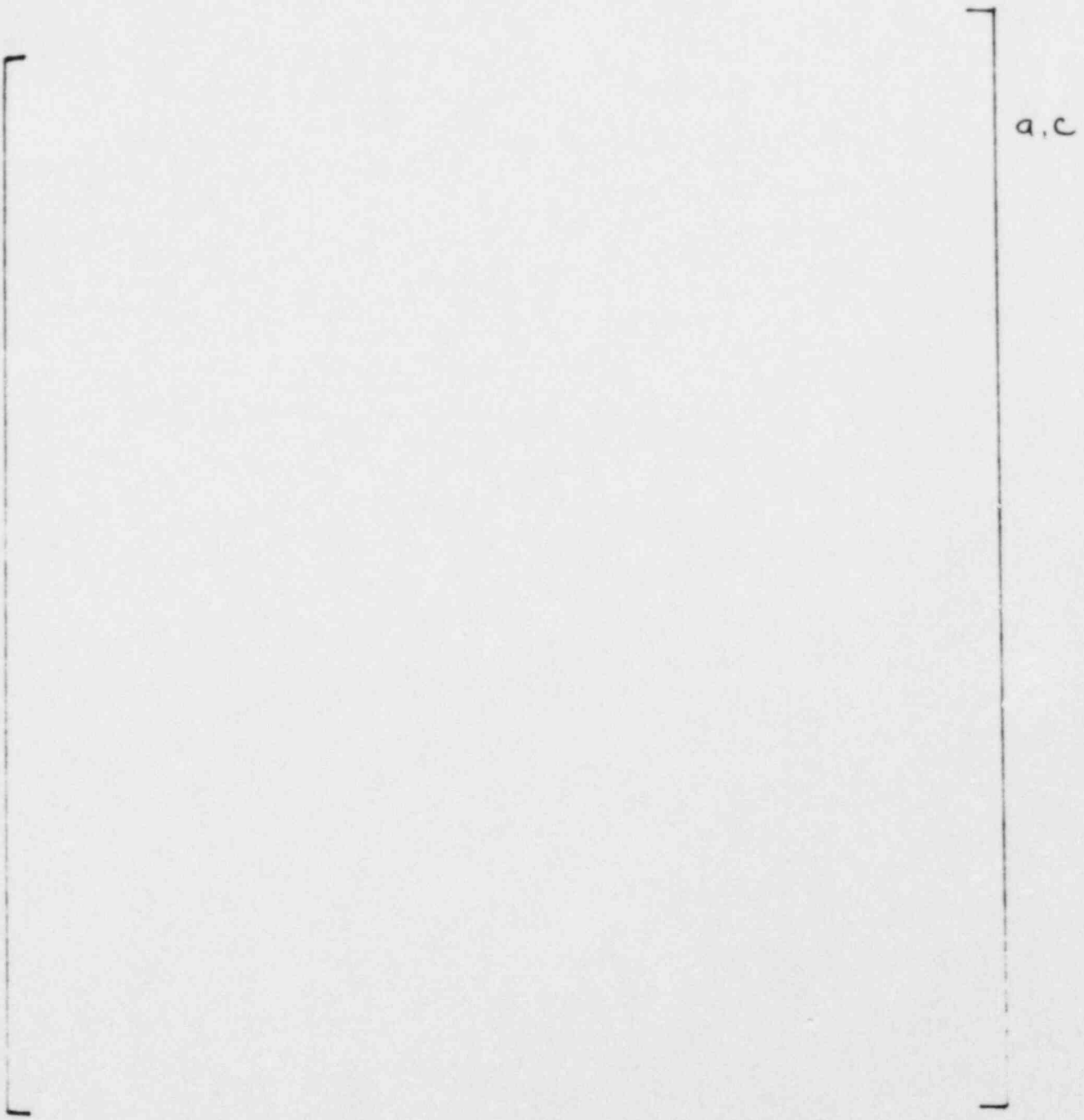

Figure 10-62. Envelope for Peak to Peak Amplitudes of Temperature Oscillations for Elbow Configuration and J-Tube Discharge

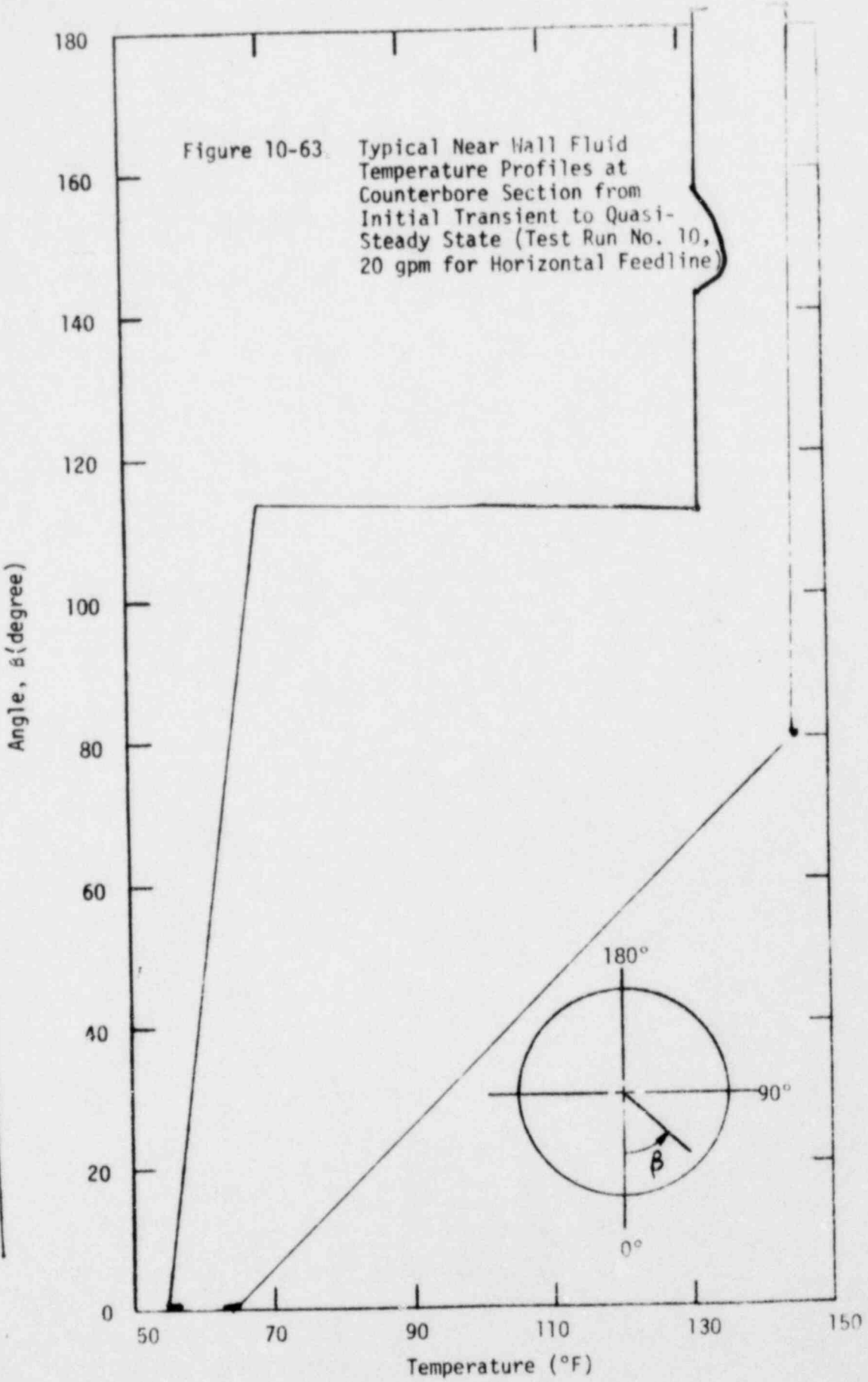

Figure 10-63 Typical Near Wall Fluid Temperature Profiles at Counterbore Section from Initial Transient to Quasi-Steady State (Test Run No. 10, 20 gpm for Horizontal Feedline)

a,c

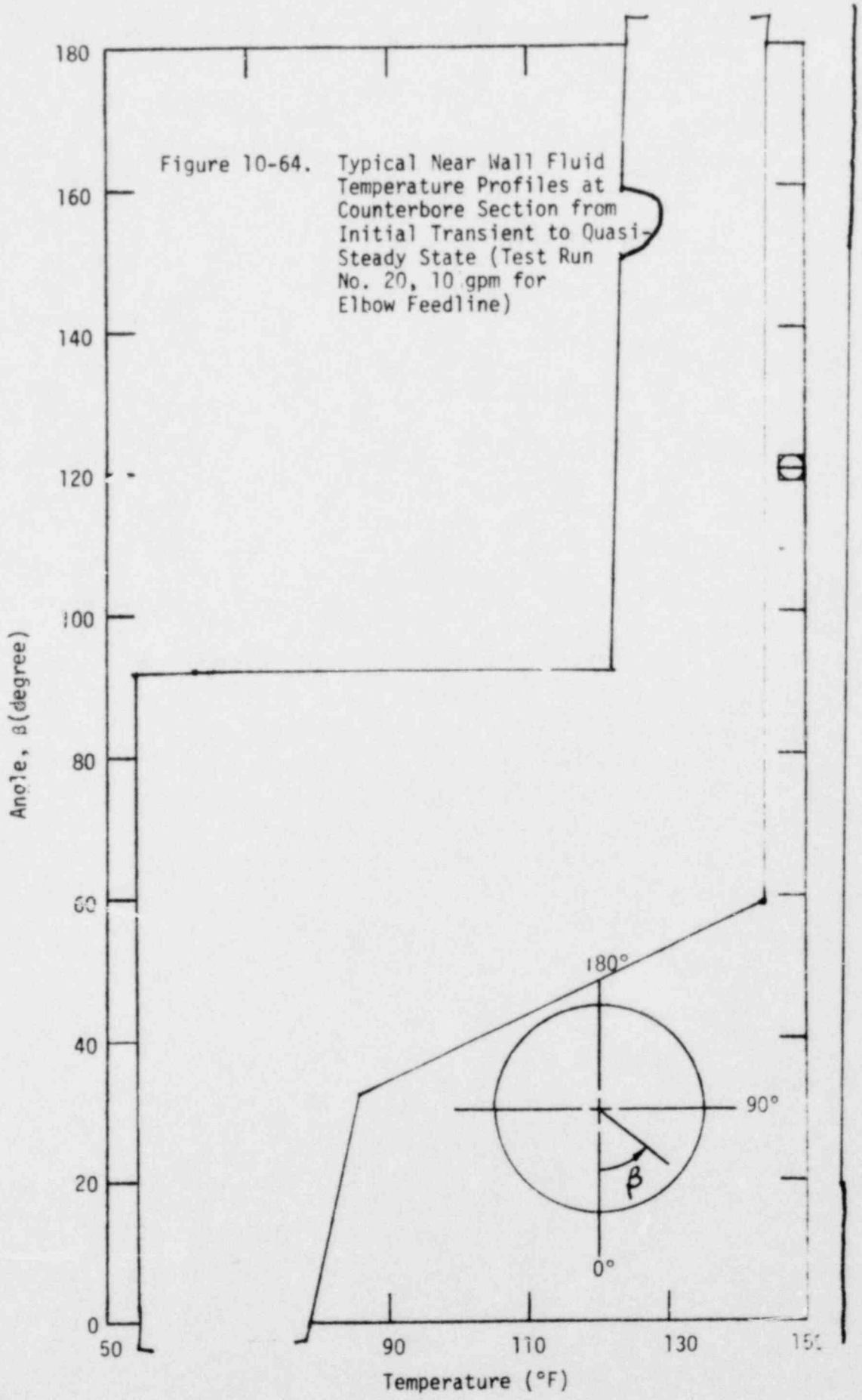

Figure 10-64. Typical Near Wall Fluid Temperature Profiles at Counterbore Section from Initial Transient to Quasi-Steady State (Test Run No. 20, 10 gpm for Elbow Feedline)

a,c

APPENDIX 10A

10A.1 MODEL DESIGN OF DISCHARGE PIPE

10A.1.1 DYNAMIC SIMILITUDE

a,c

[redacted]

10A.1.3 PRESSURE DROP AND DISCHARGE AREA

[ ]

a,c

a,c

[

]

[

] a,c

10A.2 FLUID TEMPERATURES AT COUNTERBORE

Time history of fluid temperature measured for each thermocouple (T/C) had been digitized from FM tapes, stored in CDC 7600 computer and plotted on microfiches. To establish temperature profiles at the counterbore section, quasi-steady state temperatures were read from the time history plottings and were tabulated as Tables 10A.2 - 10A.24. [

]

a,c

Rather than presenting the actual number, temperature profiles were presented using a dimensionless temperature defined as below:

$$\theta = (T - T_{cold})/(T_{hot} - T_{cold})$$

Where

T = fluid mean temperature

T_{cold} = inlet (cold) water temperature

T_{hot} = test tank (hot) water temperature

TABLE 10A.1

PIPE DISCHARGE AREA REQUIRED AT DIFFERENT SALT CONCENTRATION

a,c [ ]

The above are evaluated based on the conditions listed in Section 10A.1.1.

Table 10A.2

CIRCUMFERENTIAL, QUASI-STEADY FLUID TEMPERATURE AT COUNTERBORE SECTION FOR TEST RUN NO. 8

[ ] a,c

T/C Angular Location (degree,°)*	Mean Temp. T(°F)	Dimensionless Temp., θ**
0	[	]
37		
53		
60		
67		
83		
90		
97		
113		
120		
127		
143		
150		
157		
180	]	] a,c

*Measured from bottom

**$\theta = (T - T_{cold})/(T_{hot} - T_{cold})$

[ ] a,c

Table 10A.3

CIRCUMFERENTIAL, QUASI-STEADY FLUID TEMPERATURE

AT COUNTERBORE SECTION FOR TEST RUN NO. 8

a,c [ ]

T/C Angular Location (degree,°)*	Mean Temp. T(°F)	Dimensionless Temp., θ**
0	[	]
37		
53		
60		
67		
83		
90		
97		
113		
120		
127		
143		
150		
157		
180	]	

a,c

*Measured from bottom

**$\theta = (T - T_{cold}) / (T_{hot} - T_{cold})$

a,c [ ]

Table 10A.4

CIRCUMFERENTIAL, QUASI-STEADY FLUID TEMPERATURE

AT COUNTERBORE SECTION FOR TEST RUN NO. 8

[ ] a,c

T/C Angular Location (degree,°)*	Mean Temp. T(°F)	Dimensionless Temp., θ**
0	[	]
37		
53		
60		
67		
83		
90		
97		
113		
120		
127		
143		
150		
157		
180	]	

a,c

*Measured from bottom

**$\theta = [(T - T_{cold})/(T_{hot} - T_{cold})]$ a,c

Table 10A.5

CIRCUMFERENTIAL, QUASI-STEADY FLUID TEMPERATURE

AT COUNTERBORE SECTION FOR TEST RUN NO. 9

a,c [ ]

T/C Angular Location (degree,°)*	Mean Temp. T(°F)	Dimensionless Temp., θ**
0	[	
37		
53		
60		
67		
83		
90		
97		
113		
120		
127		
143		
150		
157		
180	]	]

a,c

*Measured from bottom

**$\theta = (T - T_{cold})/(T_{hot} - T_{cold})$

a,c [ ]

Table 10A.6

CIRCUMFERENTIAL, QUASI-STEADY FLUID TEMPERATURE

AT COUNTERBORE SECTION FOR TEST RUN NO. 9

[ ] a,c

T/C Angular Location (degree,°)*	Mean Temp. T(°F)	Dimensionless Temp., θ**
0	[	]
37		
53		
60		
67		
83		
90		
97		
113		
120		
127		
143		
150		
157		
180	]	

a,c

*Measured from bottom

**$\theta = (T - T_{cold})/(T_{hot} - T_{cold})$

[ ] a,c

Table 10A.7

CIRCUMFERENTIAL, QUASI-STEADY FLUID TEMPERATURE

AT COUNTERBORE SECTION FOR TEST RUN NO. 10

[ ]

a.c

T/C Angular Location (degree,°)*	Mean Temp. T(°F)	Dimensionless Temp., θ**
0	[	]
30		
37		
53		
60		
67		
83		
90		
97		
113		
120		
127		
143		
150		
157		
180		

a.c

a.c

*Measured from bottom

**$\theta = (T - T_{cold})/(T_{hot} - T_{cold})$

[ ]

Table 10A.8

CIRCUMFERENTIAL, QUASI-STEADY FLUID TEMPERATURE AT COUNTERBORE SECTION FOR TEST RUN NO. 10

[ ] a,c

T/C Angular Location (degree,°)*	Mean Temp. T(°F)	Dimensionless Temp., θ**
0	[	[
37		
53		
60		
67		
83		
90		
97		
113		
120		
127		
143		
150		
157		
180	]	]

a,c

*Measured from bottom

**$\theta = [(T - T_{cold})/(T_{hot} - T_{cold})]$ a,c

Table 10A.9

CIRCUMFERENTIAL, QUASI-STEADY FLUID TEMPERATURE

AT COUNTERBORE SECTION FOR TEST RUN NO. 10

a,c [ ]

T/C Angular Location (degree,°)*	Mean Temp. T(°F)	Dimensionless Temp., θ**
0		
37		
53		
60		
67		
83		
90		
97		
113		
120		
127		
143		
150		
157		
180		

a,c

*Measured from bottom

**$\theta = (T - T_{cold})/(T_{hot} - T_{cold})$ [ ]

a,c

Table 10A.10

CIRCUMFERENTIAL, QUASI-STEADY FLUID TEMPERATURE AT COUNTERBORE SECTION FOR TEST RUN NO. 11

[ ] a,c

T/C Angular Location (degree,°)*	Mean Temp. T(°F)	Dimensionless Temp., θ**
0	[	]
37		
53		
60		
67		
83		
90		
97		
113		
120		
127		
143		
150		
157		
180	]	

a,c

*Measured from bottom

**$\theta = (T - T_{cold})/(T_{hot} - T_{cold})$

[ ] a,c

Table 10A.11

CIRCUMFERENTIAL, QUASI-STEADY FLUID TEMPERATURE

AT COUNTERBORE SECTION FOR TEST RUN NO.11

a,c [ ]

T/C Angular Location (degree,°)*	Mean Temp. T(°F)	Dimensionless Temp., θ**
0	[	]
37		
53		
60		
67		
83		
90		
97		
a,c 113		
120		
127		
143		
150		
157		
180		

*Measured from bottom

**$\theta = (T - T_{cold})/(T_{hot} - T_{cold})$

a,c [ ]

Table 10A.12

CIRCUMFERENTIAL, QUASI-STEADY FLUID TEMPERATURE AT COUNTERBORE SECTION FOR TEST RUN NO. 14

[ ] a.c

T/C Angular Location (degree,°)*	Mean Temp. T(°F)	Dimensionless Temp., θ**
0	[	]
23		
30		
37		
53		
60		
67		
83		
90		
97		
113		
120		
127		
143		
150		
157		
180		

a.c

*Measured from bottom

**$\theta = (T - T_{cold})/(T_{hot} - T_{cold})$

[ ] a.c

Table 10A.13

CIRCUMFERENTIAL, QUASI-STEADY FLUID TEMPERATURE

AT COUNTERBORE SECTION FOR TEST RUN NO. 14

[ ]

a,c

T/C Angular Location (degree,°)*	Mean Temp. T(°F)	Dimensionless Temp., θ**
0		
23		
30		
37		
60		
67		
83		
90		
97		
113		
120		
127		
143		
150		
157		
180		

a,c

*Measured from bottom

**$\theta = (T - T_{cold})/(T_{hot} - T_{cold})$

[ ]

a,c

Table 10A.14

CIRCUMFERENTIAL, QUASI-STEADY FLUID TEMPERATURE

AT COUNTERBORE SECTION FOR TEST RUN NO. 14

[ ] a,c

T/C Angular Location (degree, °)*	Mean Temp. T(°F)	Dimensionless Temp., θ**
0	[	
23		
30		
37		
60		
67		
83		
90		
97		
113		
120		
127		
143		
150		
157		
180	]	] a,c

*Measured from bottom

**$\theta = (T - T_{cold})/(T_{hot} - T_{cold})$

[ ] a,c

Table 10A.15

CIRCUMFERENTIAL, QUASI-STEADY FLUID TEMPERATURE

AT COUNTERBORE SECTION FOR TEST RUN NO. 18

[ ]

T/C Angular Location (degree,°)*	Mean Temp. T(°F)	Dimensionless Temp., θ**
0	[	]
23		
30		
37		
60		
67		
83		
90		
113		
120		
127		
143		
150		
157		
180		

*Measured from bottom

**$\theta = (T - T_{cold})/(T_{hot} - T_{cold})$ [ ]

Table 10A.16

CIRCUMFERENTIAL, QUASI-STEADY FLUID TEMPERATURE AT COUNTERBORE SECTION FOR TEST RUN NO. 18 [ ] a,c

T/C Angular Location (degree,°)*	Mean Temp. T(°F)	Dimensionless Temp., θ**
0	[	[
23		
30		
37		
60		
67		
83		
90		
113		
120		
127		
143		
150		
157		
180	]	]

a,c

*Measured from bottom

**$\theta = (T - T_{cold})/(T_{hot} - T_{cold})$ [ ] a,c

Table 10A.17

CIRCUMFERENTIAL, QUASI-STEADY FLUID TEMPERATURE

AT COUNTERBORE SECTION FOR TEST RUN NO. 20

[ ]

a,c

T/C Angular Location (degree,°)*	Mean Temp. T(°F)	Dimensionless Temp., θ**
0	[	[
23		
30		
37		
53		
60		
67		
83		
90		
97		
113		
120		
127		
143		
150		
157		
180	]	]

a,c

*Measured from bottom

**$\theta = [(T - T_{cold})/(T_{hot} - T_{cold})]$

[ ]

a,c

Table 10A.18

CIRCUMFERENTIAL, QUASI-STEADY FLUID TEMPERATURE AT COUNTERBORE SECTION FOR TEST RUN NO. 20

[ ] a.c

T/C Angular Location (degree,°)*	Mean Temp. T(°F)	Dimensionless Temp., θ**
0	[	]
23		
30		
37		
53		
60		
67		
83		
90		
97		
113		
120		
127		
143		
150		
157		
180	]	]

a.c

*Measured from bottom

**$\theta = (T - T_{cold})/(T_{hot} - T_{cold})$

[ ] a.c

Table 10A.19

CIRCUMFERENTIAL, QUASI-STEADY FLUID TEMPERATURE

AT COUNTERBORE SECTION FOR TEST RUN NO. 20

[ ]

a,c

T/C Angular Location (degree,°)*	Mean Temp. T(°F)	Dimensionless Temp., θ**
0	[	[
23		
30		
37		
53		
60		
67		
83		
90		
97		
113		
120		
127		
143		
150		
157		
180	]	]

a,c

*Measured from bottom

**$\theta = (T - T_{cold})/(T_{hot} - T_{cold})$

[ ]

Table 10A.20

CIRCUMFERENTIAL, QUASI-STEADY FLUID TEMPERATURE

AT COUNTERBORE SECTION FOR TEST RUN NO. 21

[ ] a,c

T/C Angular Location (degree,°)*	Mean Temp. T(°F)	Dimensionless Temp., θ**
0	[	]
23		
30		
37		
53		
60		
67		
83		
90		
97		
113		
120		
127		
143		
150		
157		
180		

a,c

*Measured from bottom

**$\theta = (T - T_{cold})/(T_{hot} - T_{cold})$

[ ] a,c

Table 10A.21

CIRCUMFERENTIAL, QUASI-STEADY FLUID TEMPERATURE

AT COUNTERBORE SECTION FOR TEST RUN NO. 21

a,c

T/C Angular Location (degree,°)*	Mean Temp. T(°F)	Dimensionless Temp., θ**
0		
23		
30		
37		
53		
60		
67		
83		
90		
97		
113		
120		
127		
143		
150		
157		
180		

a,c

*Measured from bottom

**$\theta = (T - T_{cold})/(T_{hot} - T_{cold})$

a,c

Table 10A.22

CIRCUMFERENTIAL, QUASI-STEADY FLUID TEMPERATURE AT COUNTERBORE SECTION FOR TEST RUN NO. 22

[ ] a,c

T/C Angular Location (degree,°)*	Mean Temp. T(°F)	Dimensionless Temp., θ**
0	[	]
23		
30		
37		
53		
60		
67		
83		
90		
113		
120		
127		
143		
150		
157		
180		

a,c

*Measured from bottom

**$\theta = (T - T_{cold})/(T_{hot} - T_{cold})$ [ ] a,c

Table 10A.23

CIRCUMFERENTIAL, QUASI-STEADY FLUID TEMPERATURE

AT COUNTERBORE SECTION FOR TEST RUN NO. 22

a,c [ ]

T/C Angular Location (degree,°)*	Mean Temp. T(°F)	Dimensionless Temp., θ**
0	[	]
23		
30		
37		
53		
60		
67		
83		
90		
113		
120		
127		
143		
150		
157		
180		

*Measured from bottom

**$\theta = (T - T_{cold})/(T_{hot} - T_{cold})$

a,c [ ]

Table 10A.24

CIRCUMFERENTIAL, QUASI-STEADY FLUID TEMPERATURE AT COUNTERBORE SECTION FOR TEST RUN NO. 22

[ ] a,c

T/C Angular Location (degree,°)*	Mean Temp. T(°F)	Dimensionless Temp., θ**
0	[	]
23		
30		
37		
53		
60		
67		
83		
90		
97		
113		
120		
127		
143		
150		
157		
180		

a,c

*Measured from bottom

**$\theta = [(T - T_{cold})/(T_{hot} - T_{cold})]$ a,c

Figure 10A-1 Dimensionless Temperature Profile at Counterbore Section (Test Run No. [ ])

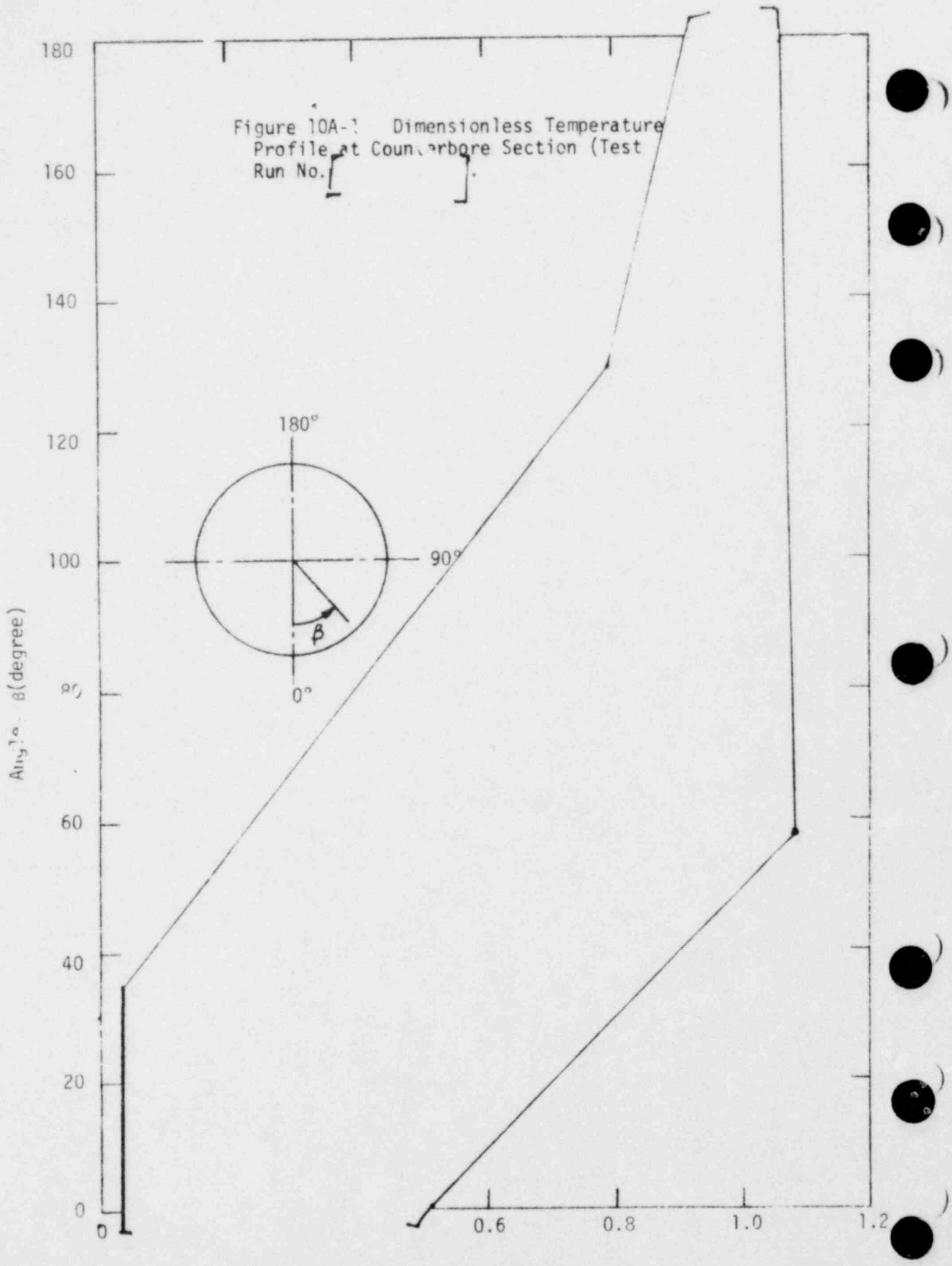

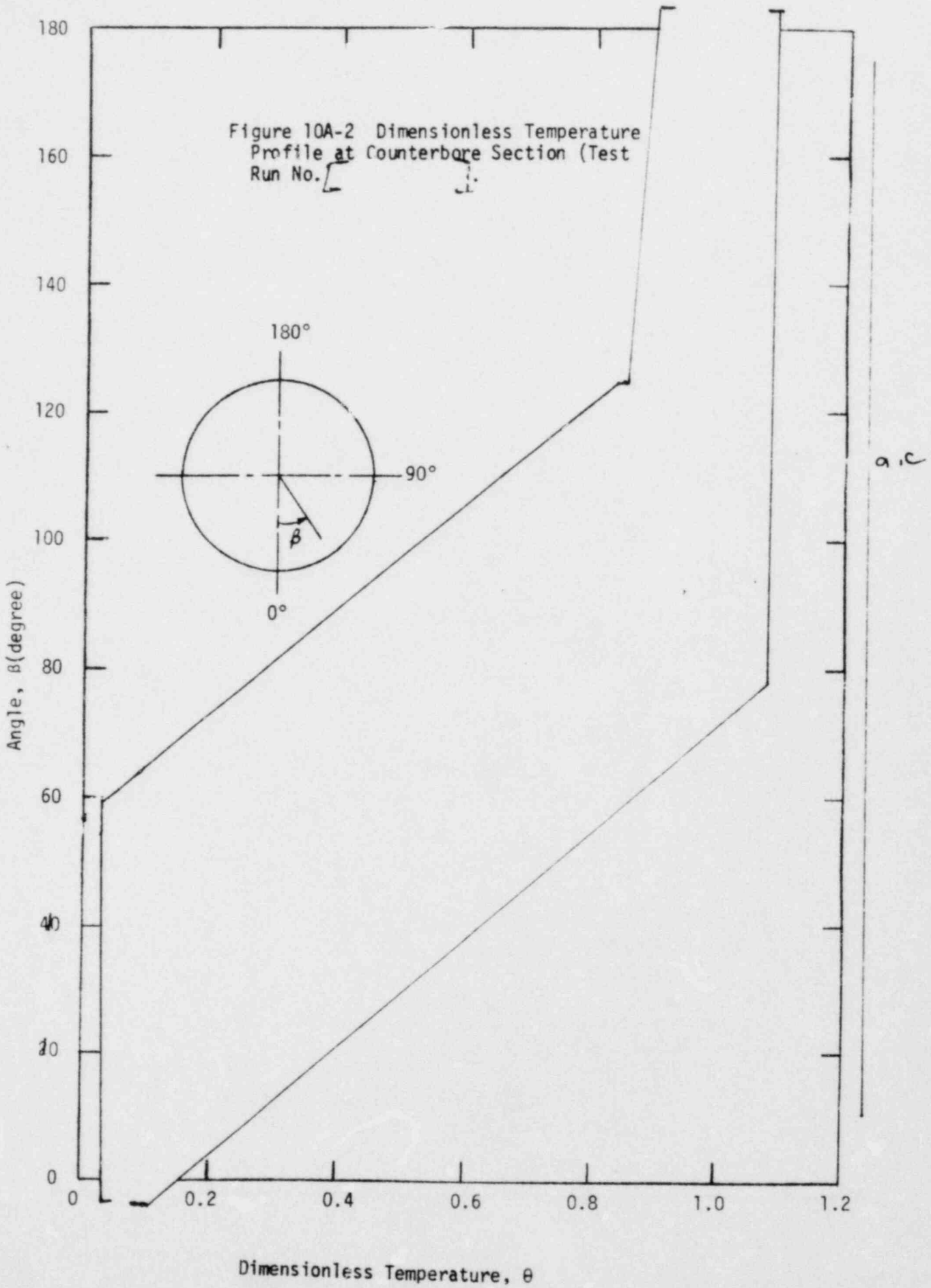

Figure 10A-2 Dimensionless Temperature Profile at Counterbore Section (Test Run No. [redacted])

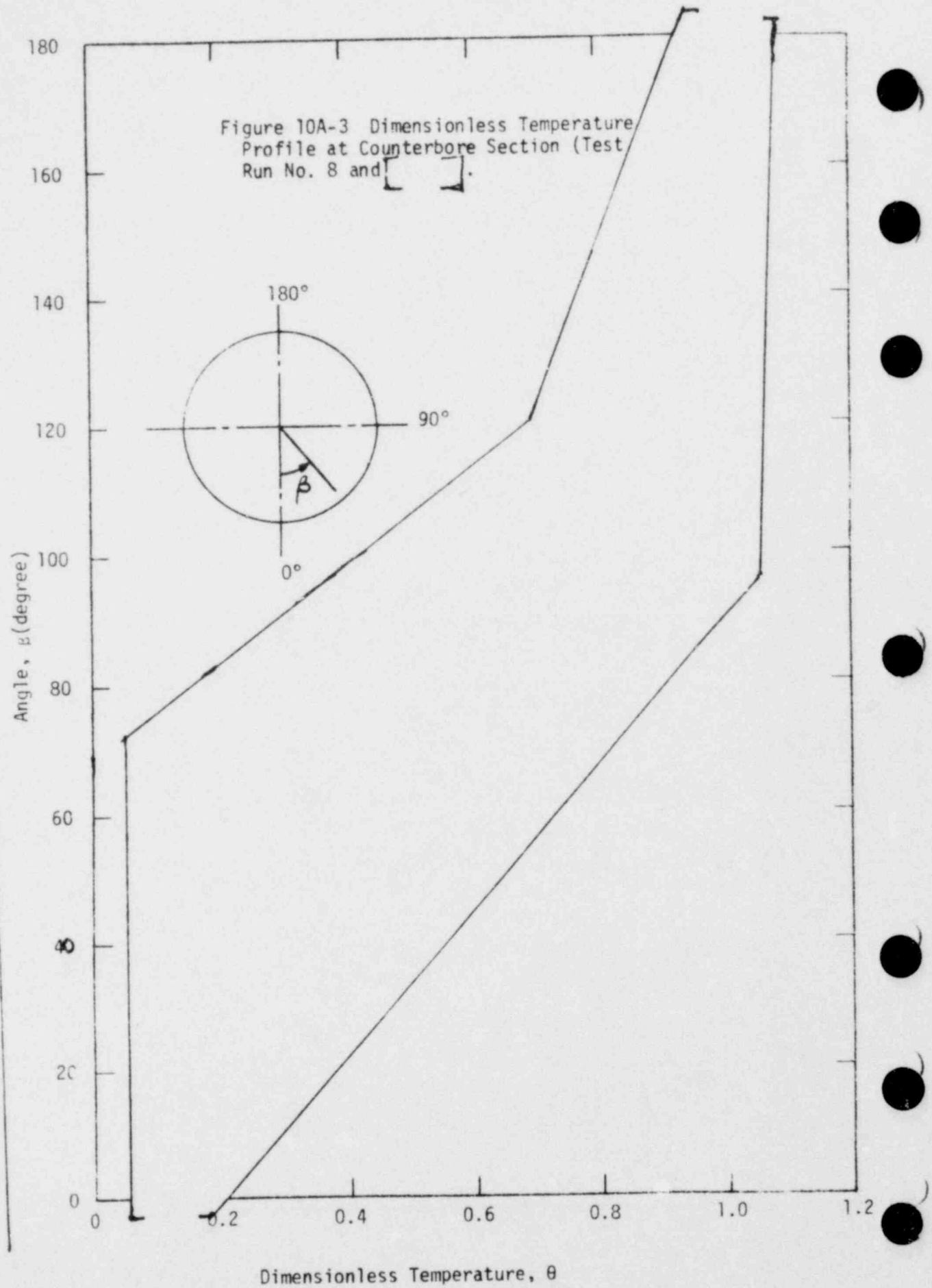

Figure 10A-3 Dimensionless Temperature Profile at Counterbore Section (Test Run No. 8 and [ ].

a,c

Figure 10A-4 Dimensionless Temperature Profile at Counterbore Section (Test Run No. 9 and [ ].

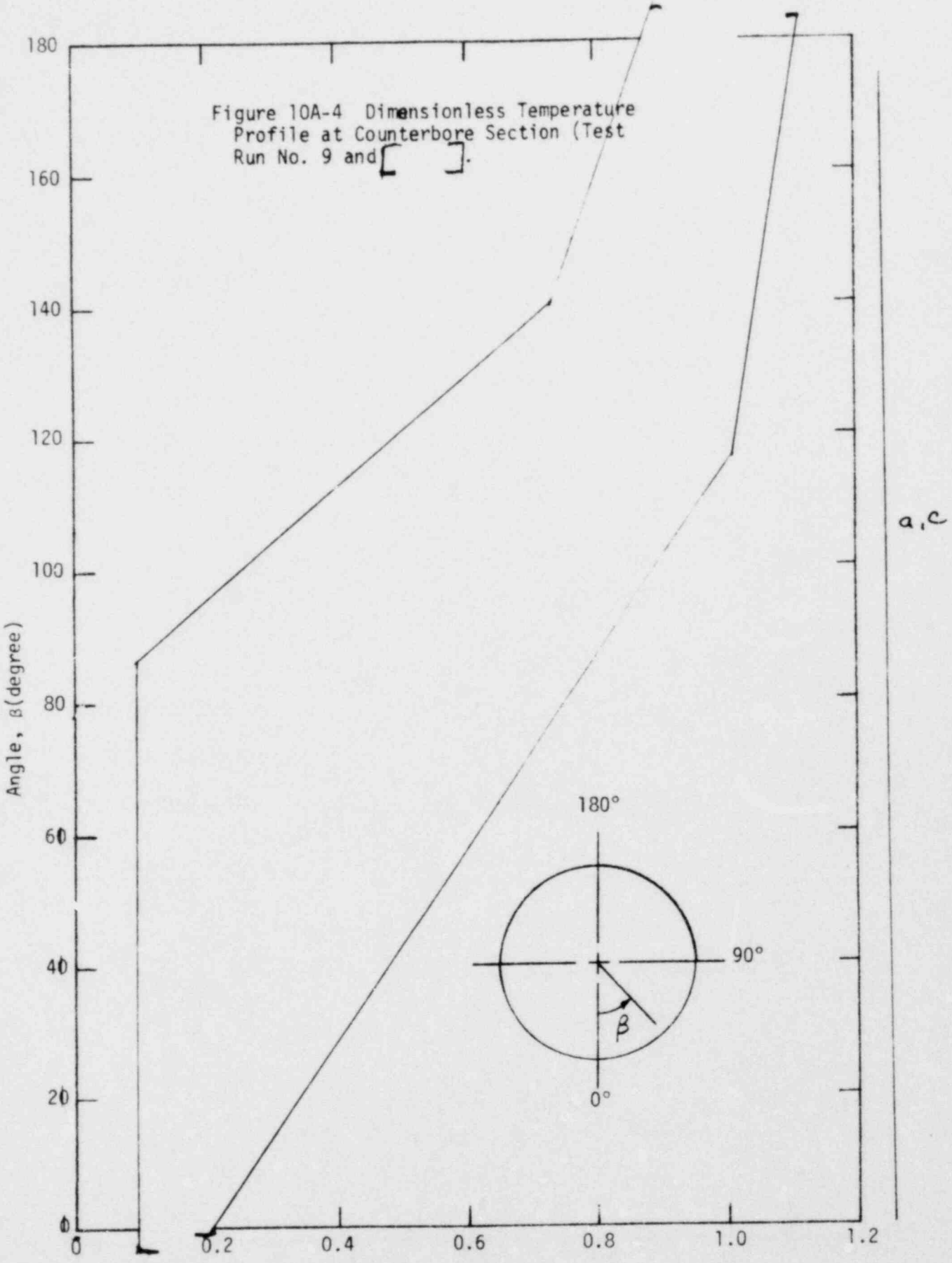

a,c

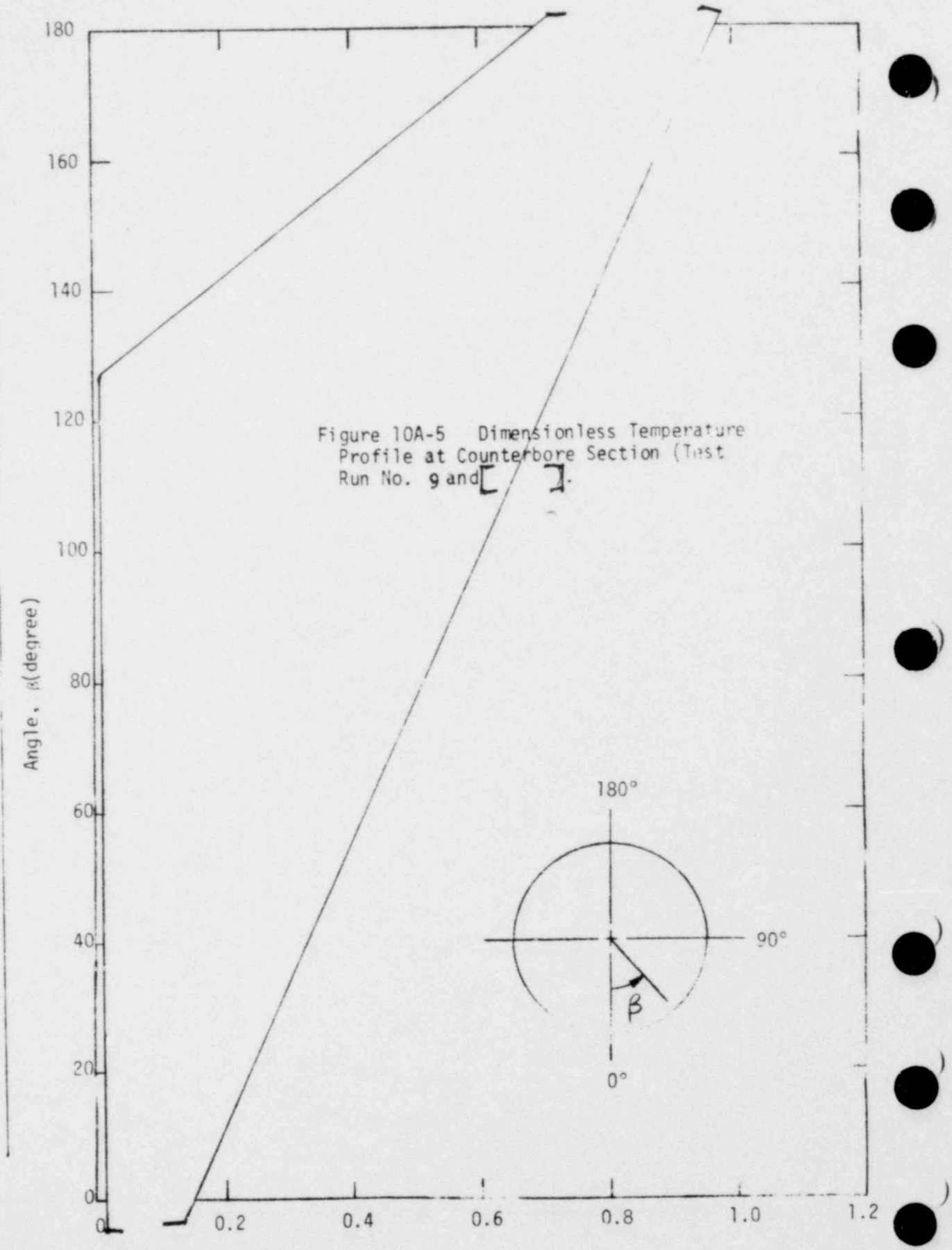

Figure 10A-5 Dimensionless Temperature Profile at Counterbore Section (Test Run No. 9 and [ ].

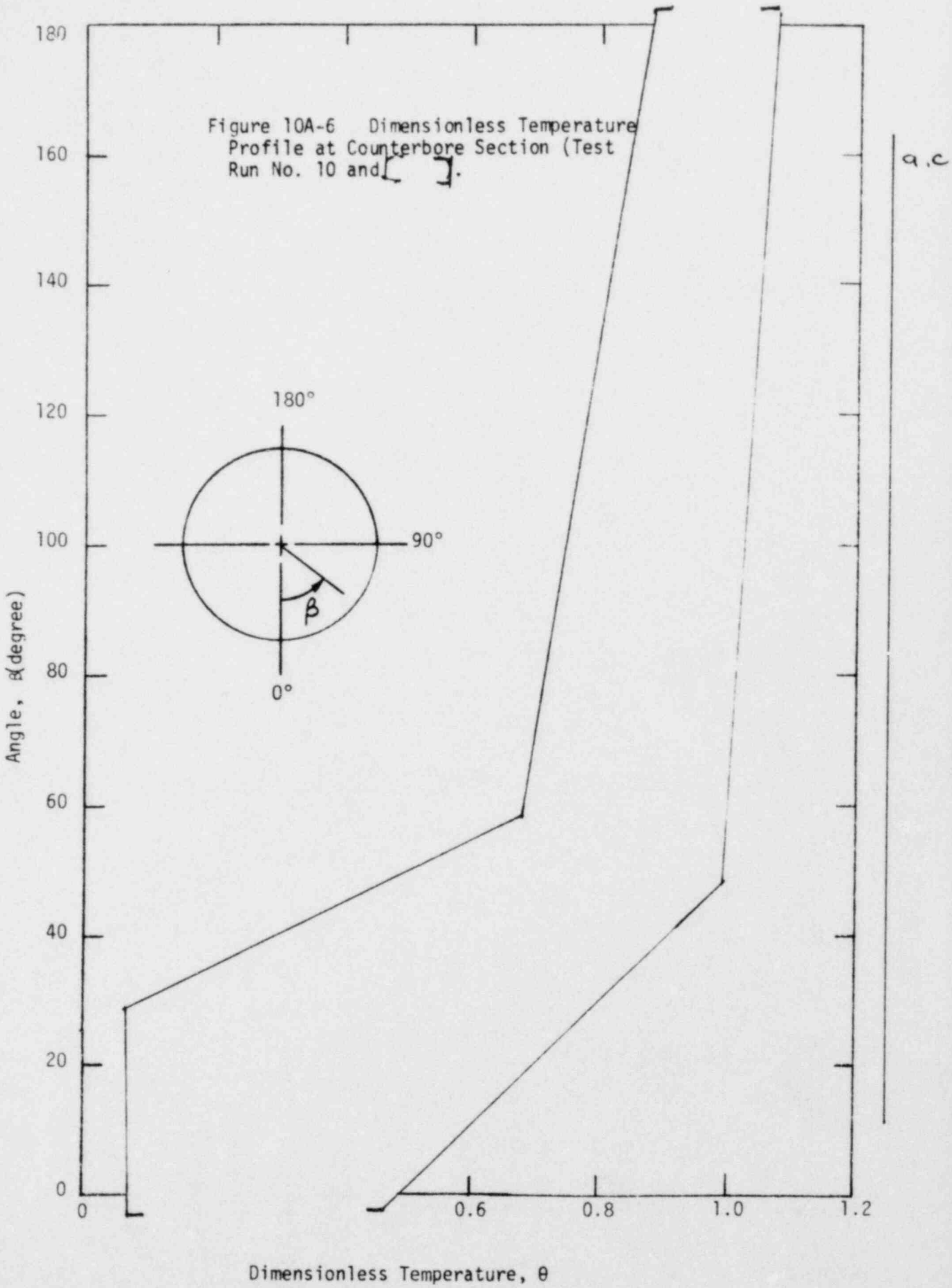

Figure 10A-6 Dimensionless Temperature Profile at Counterbore Section (Test Run No. 10 and [ ].

Figure 10A-7 Dimensionless Temperature Profile at Counterbore Section (Test Run No. 10 and [ ].

a,c

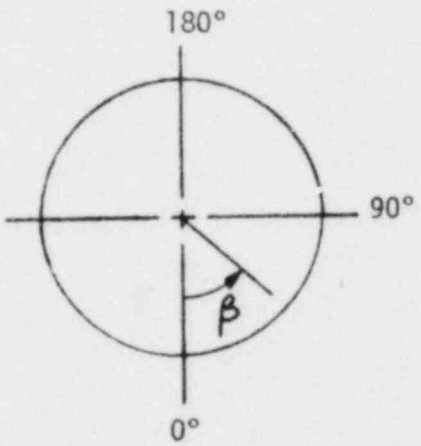

Angle, β(degree)

180
160
140
120
100
80
60
40
20
0

0
0.4
0.6
0.8
1.0
1.2

Dimensionless Temperature, θ

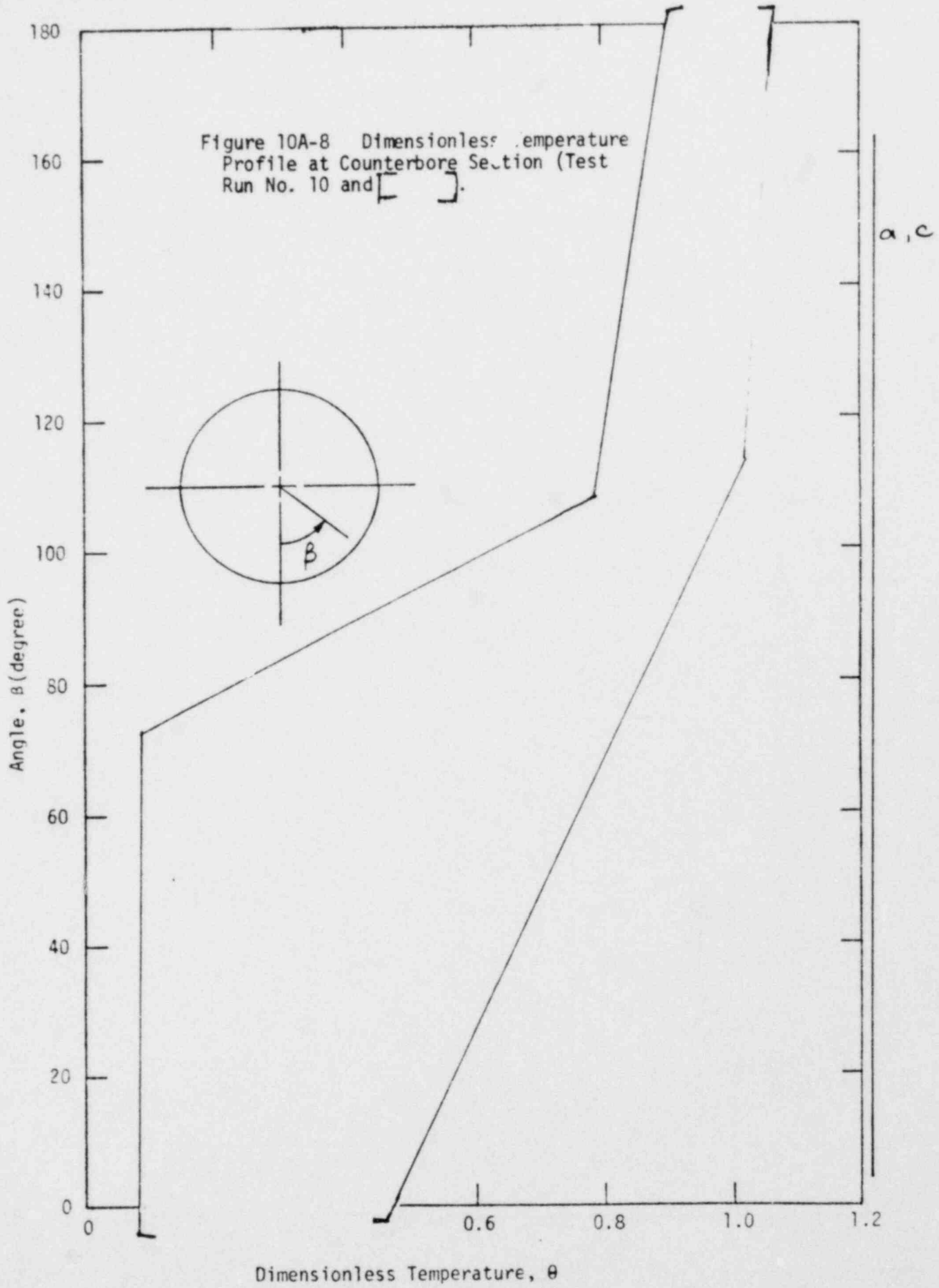

Figure 10A-8 Dimensionless Temperature Profile at Counterbore Section (Test Run No. 10 and [ ].

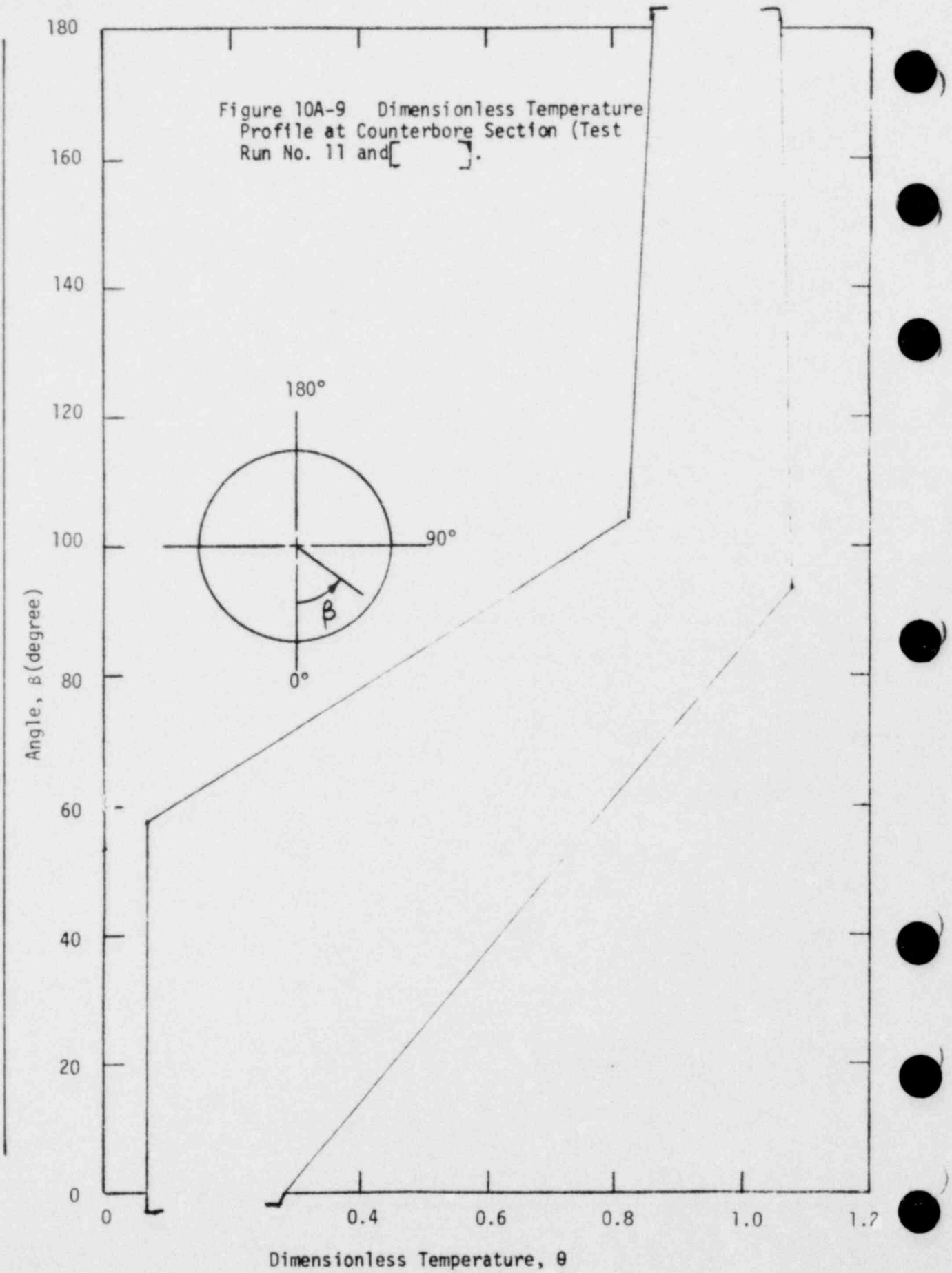

Figure 10A-9 Dimensionless Temperature Profile at Counterbore Section (Test Run No. 11 and [ ].

a, c

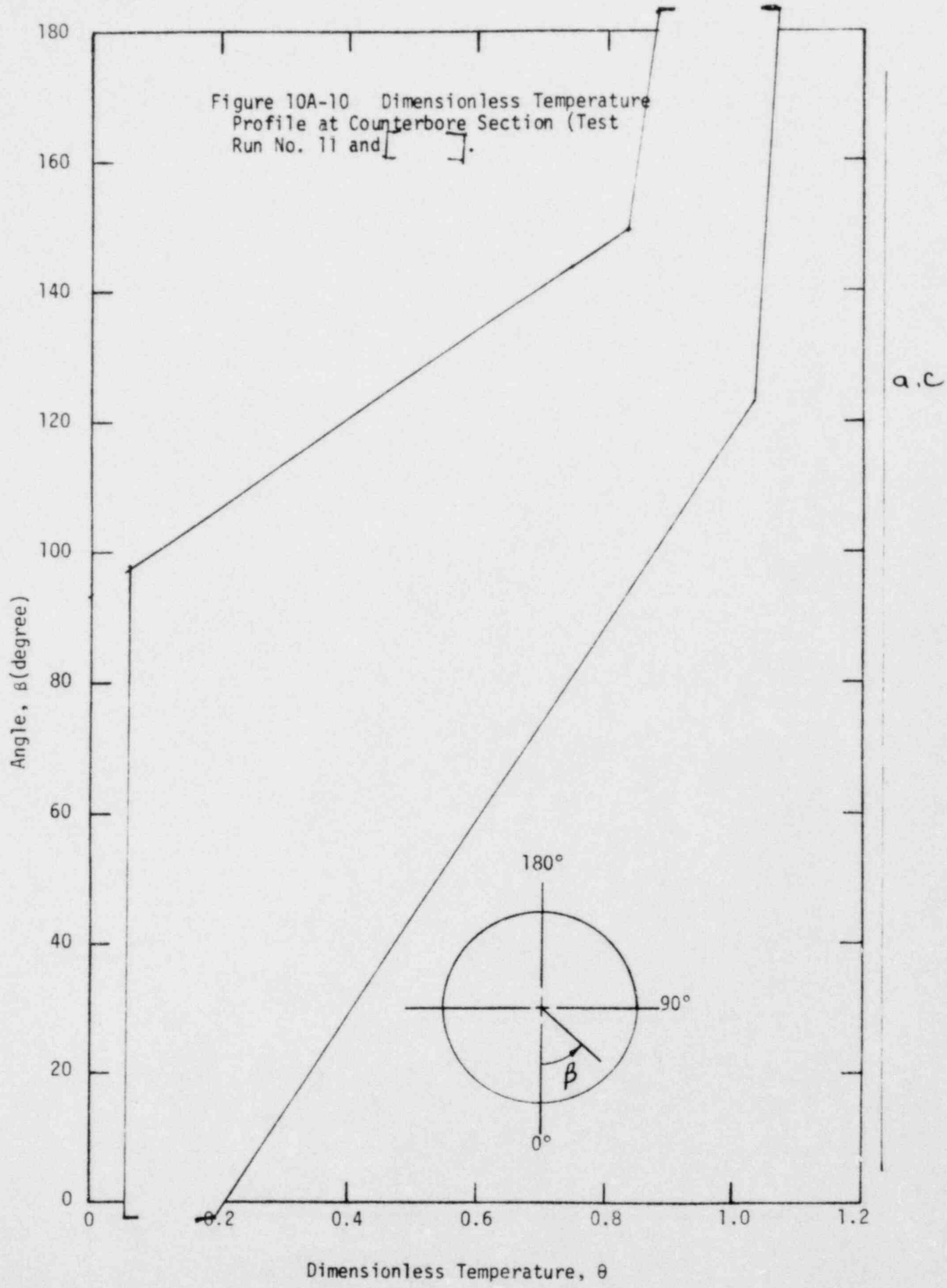

Figure 10A-10 Dimensionless Temperature Profile at Counterbore Section (Test Run No. 11 and [redacted].

a,c

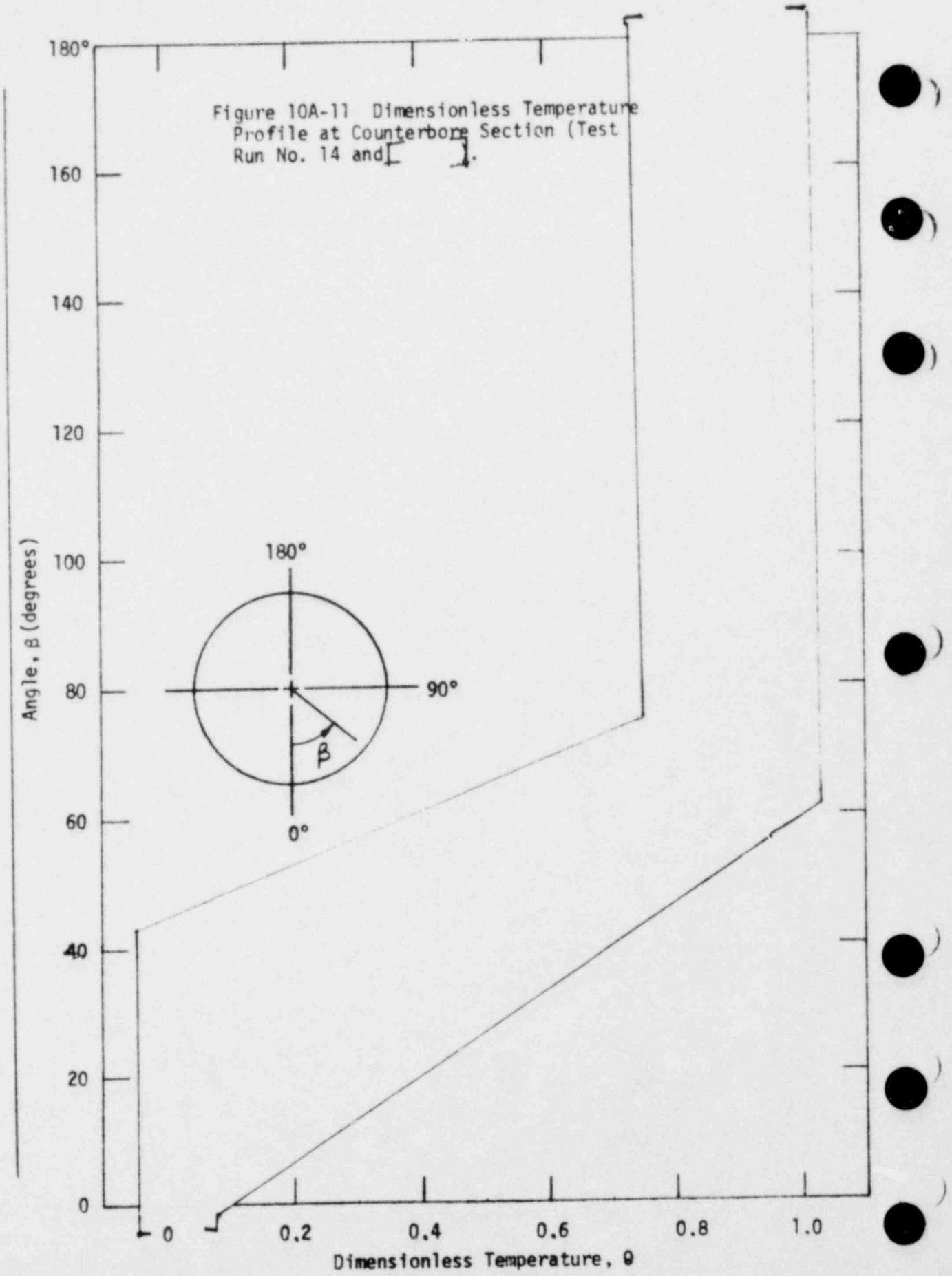

Figure 10A-11 Dimensionless Temperature Profile at Counterbore Section (Test Run No. 14 and [ ].

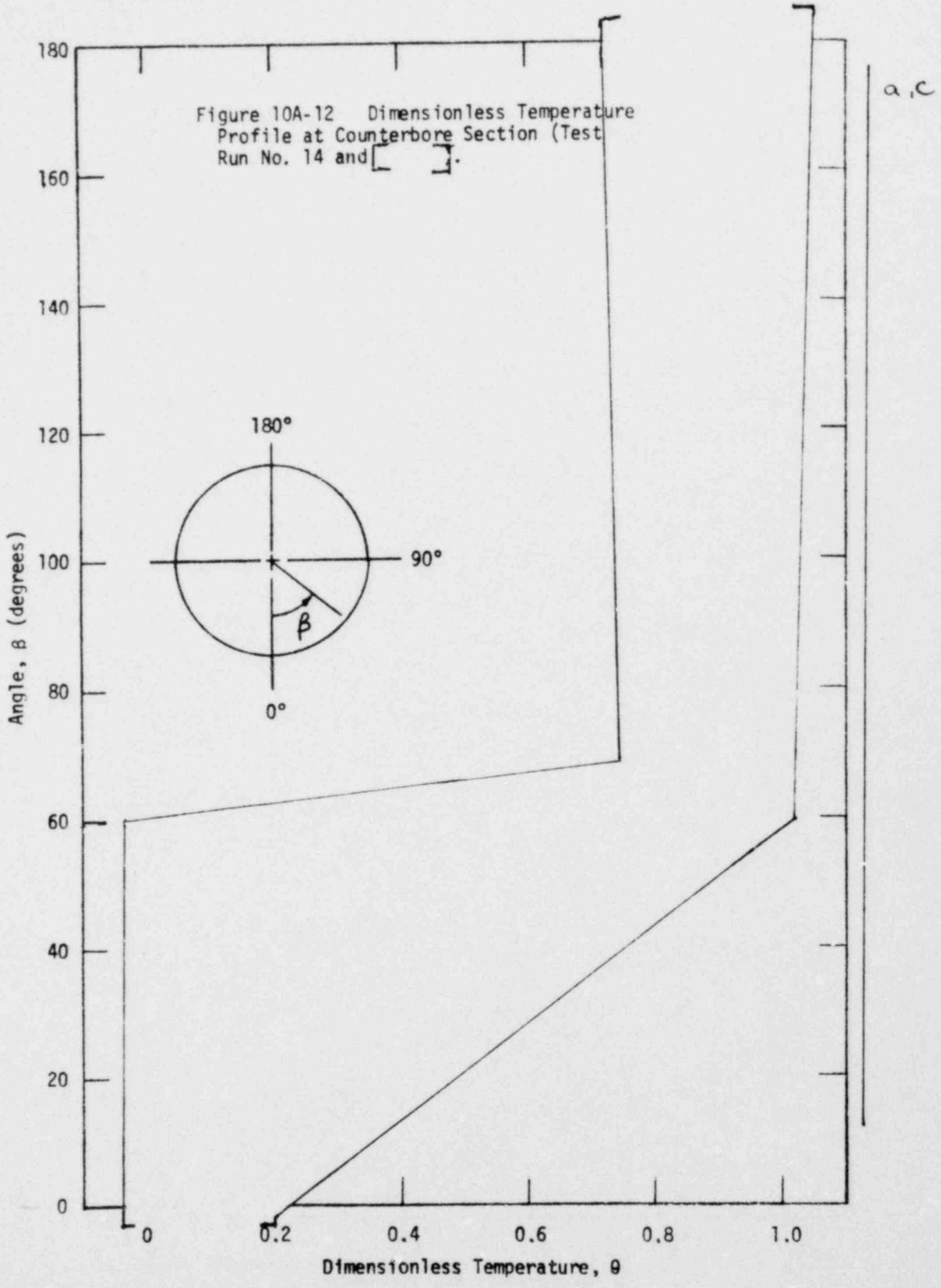

Figure 10A-12 Dimensionless Temperature Profile at Counterbore Section (Test Run No. 14 and [ ].

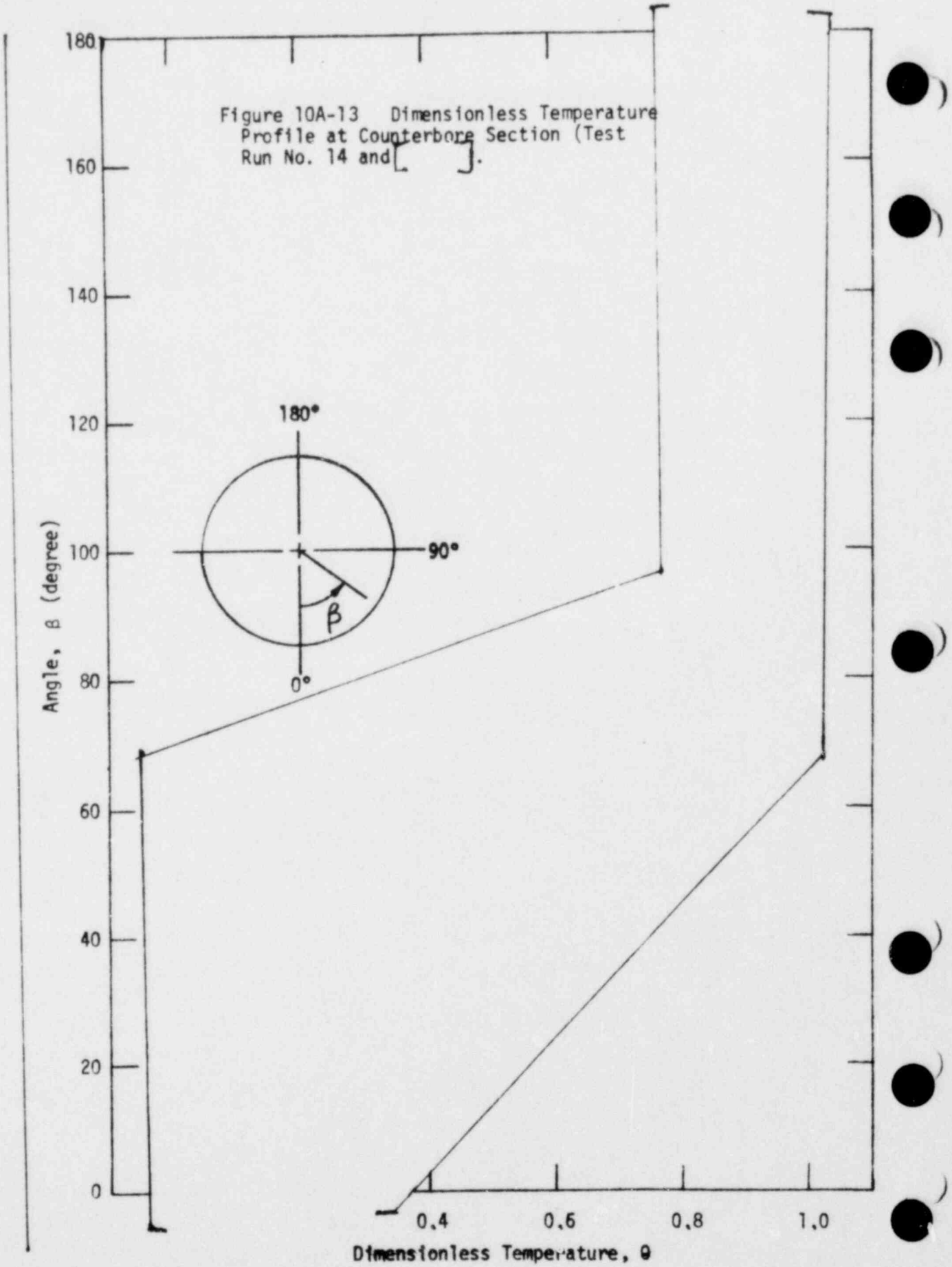

Figure 10A-13 Dimensionless Temperature Profile at Counterbore Section (Test Run No. 14 and [ ].

a,c

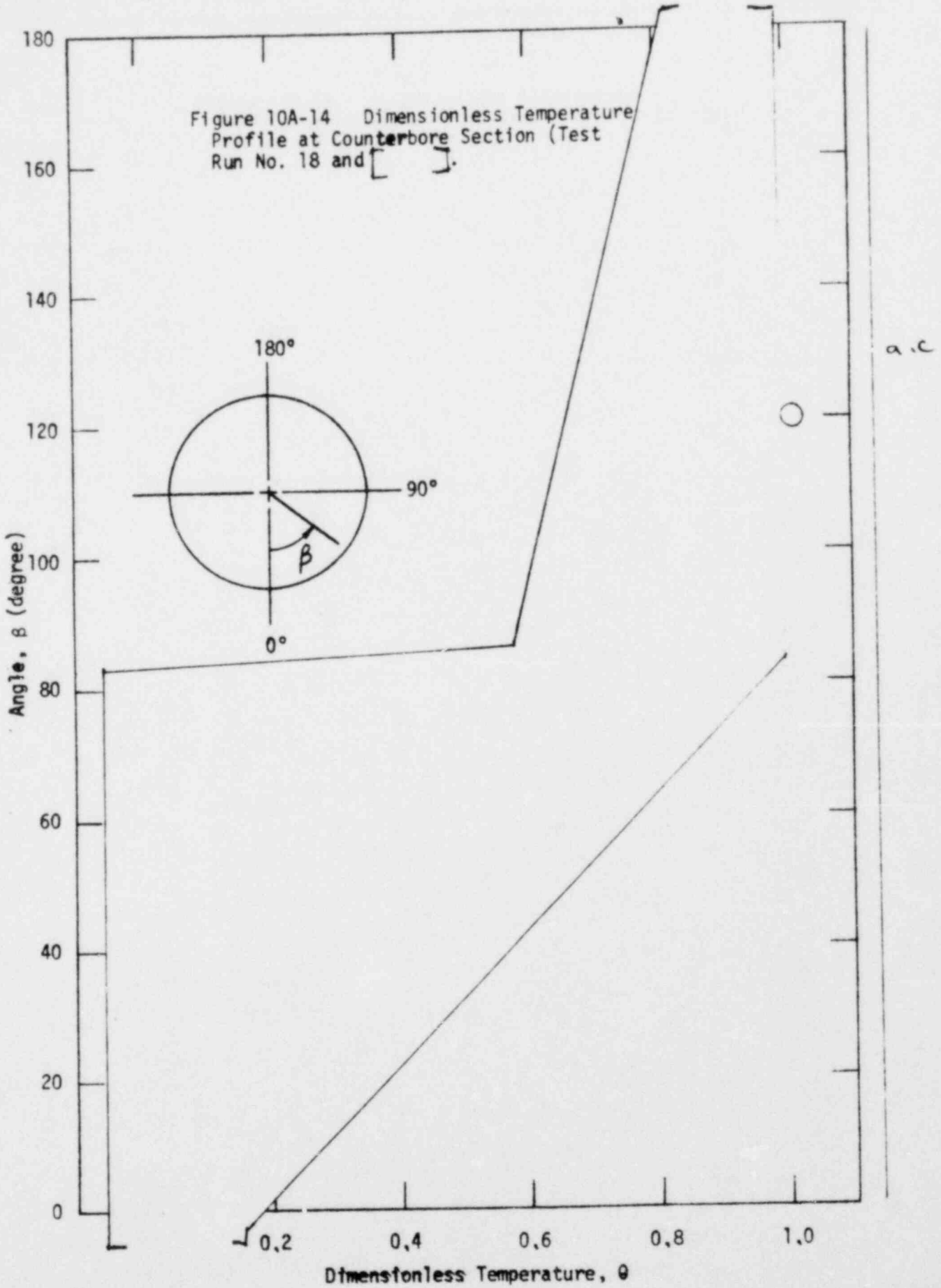

Figure 10A-14 Dimensionless Temperature Profile at Counterbore Section (Test Run No. 18 and [ ].

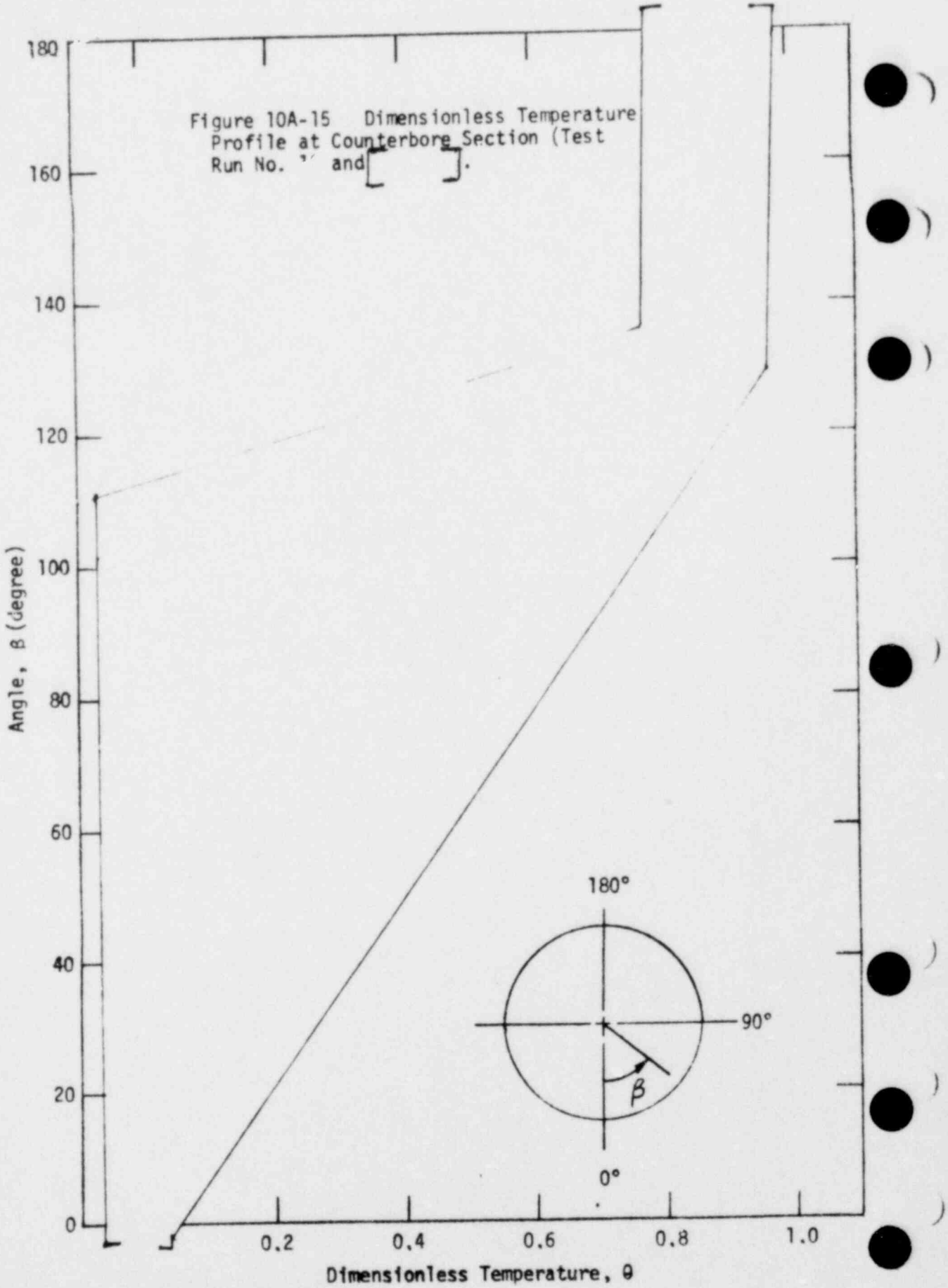

Figure 10A-15 Dimensionless Temperature Profile at Counterbore Section (Test Run No. ' and [ ].

a,c

Figure 10A-16 Dimensionless Temperature Profile at Counterbore Section (Test Run No. 20 and [redacted].

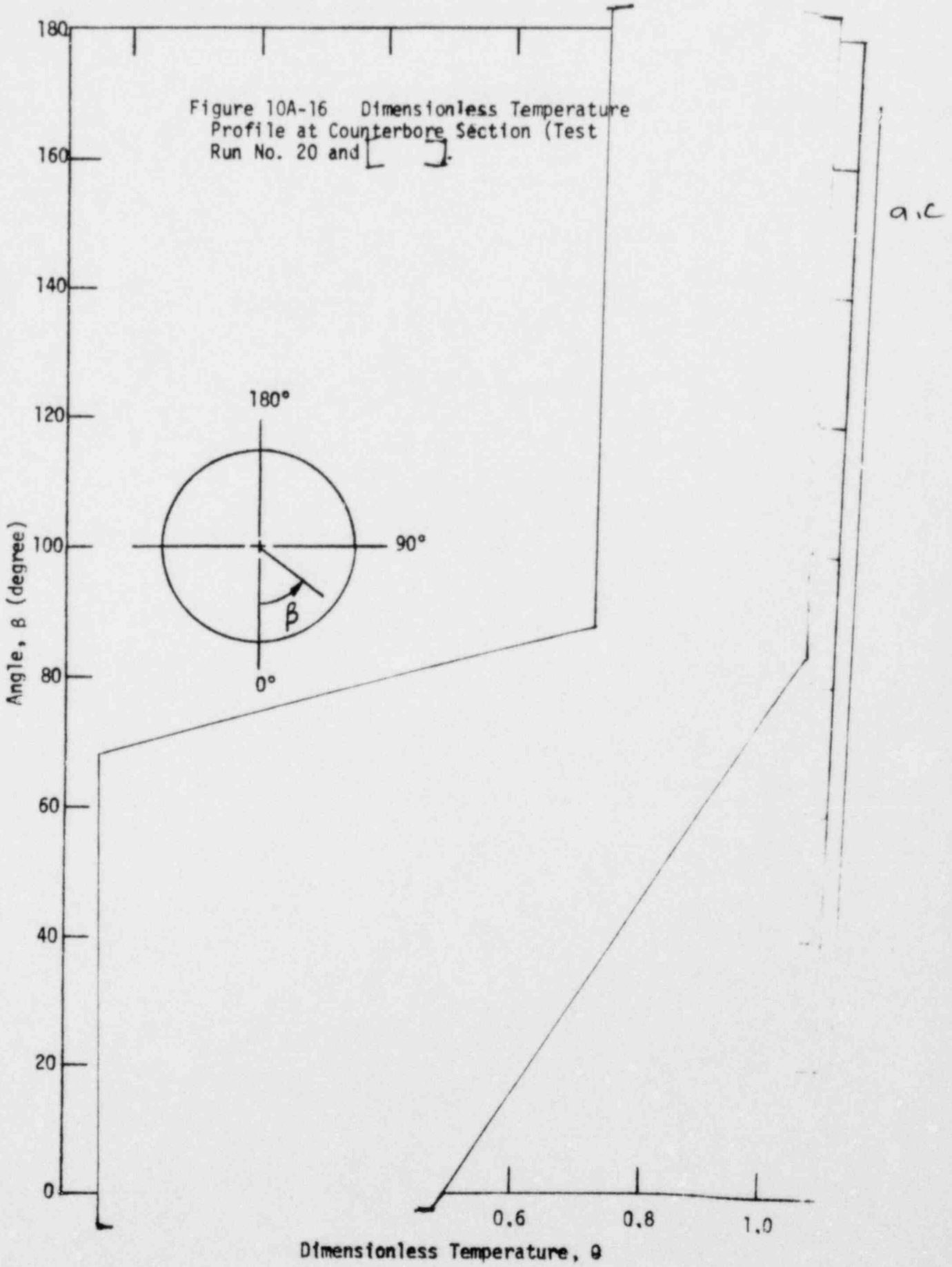

a,c

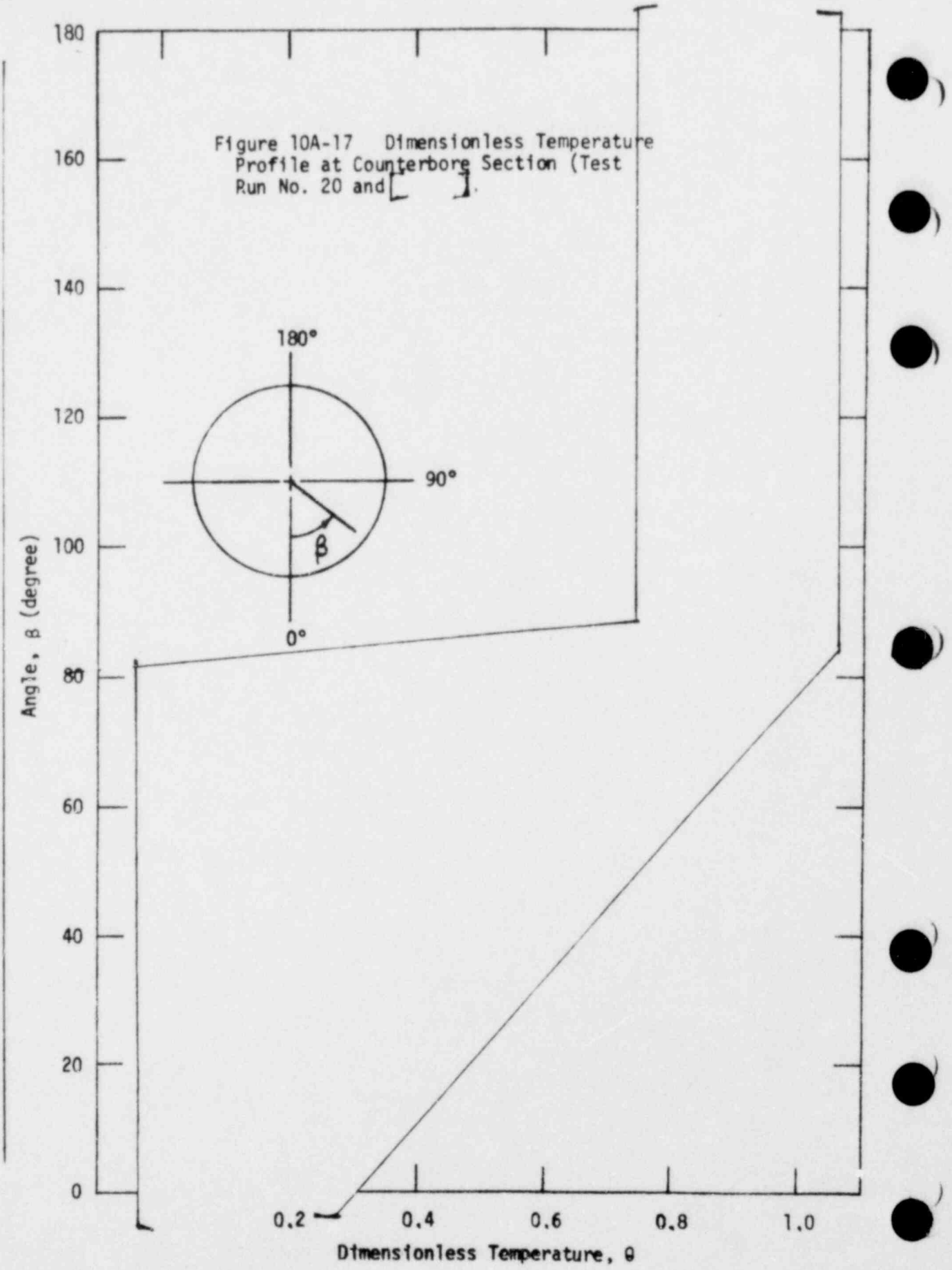

Figure 10A-17 Dimensionless Temperature Profile at Counterbore Section (Test Run No. 20 and [ ].

a,c

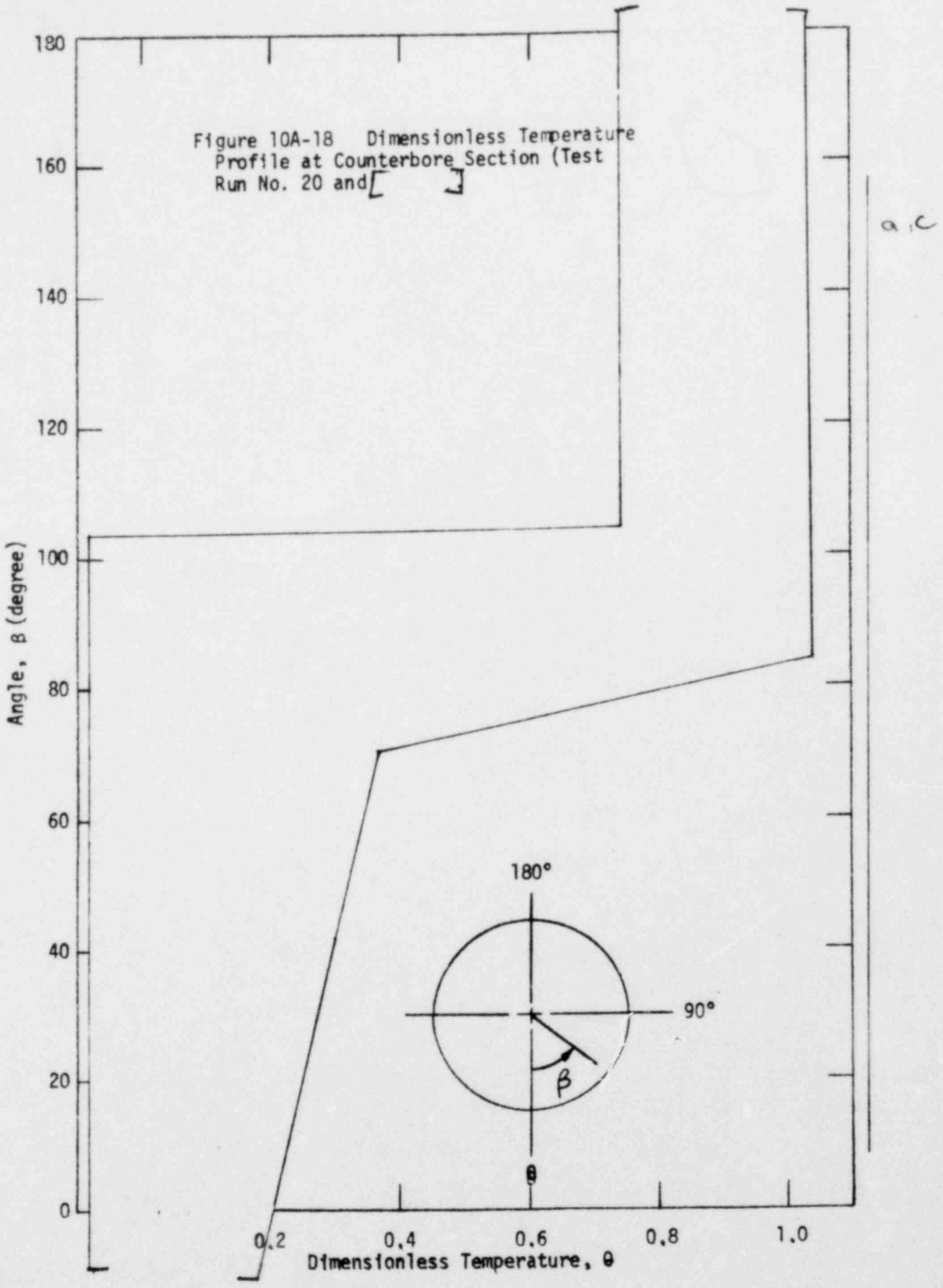

Figure 10A-18 Dimensionless Temperature Profile at Counterbore Section (Test Run No. 20 and [ ]

a,c

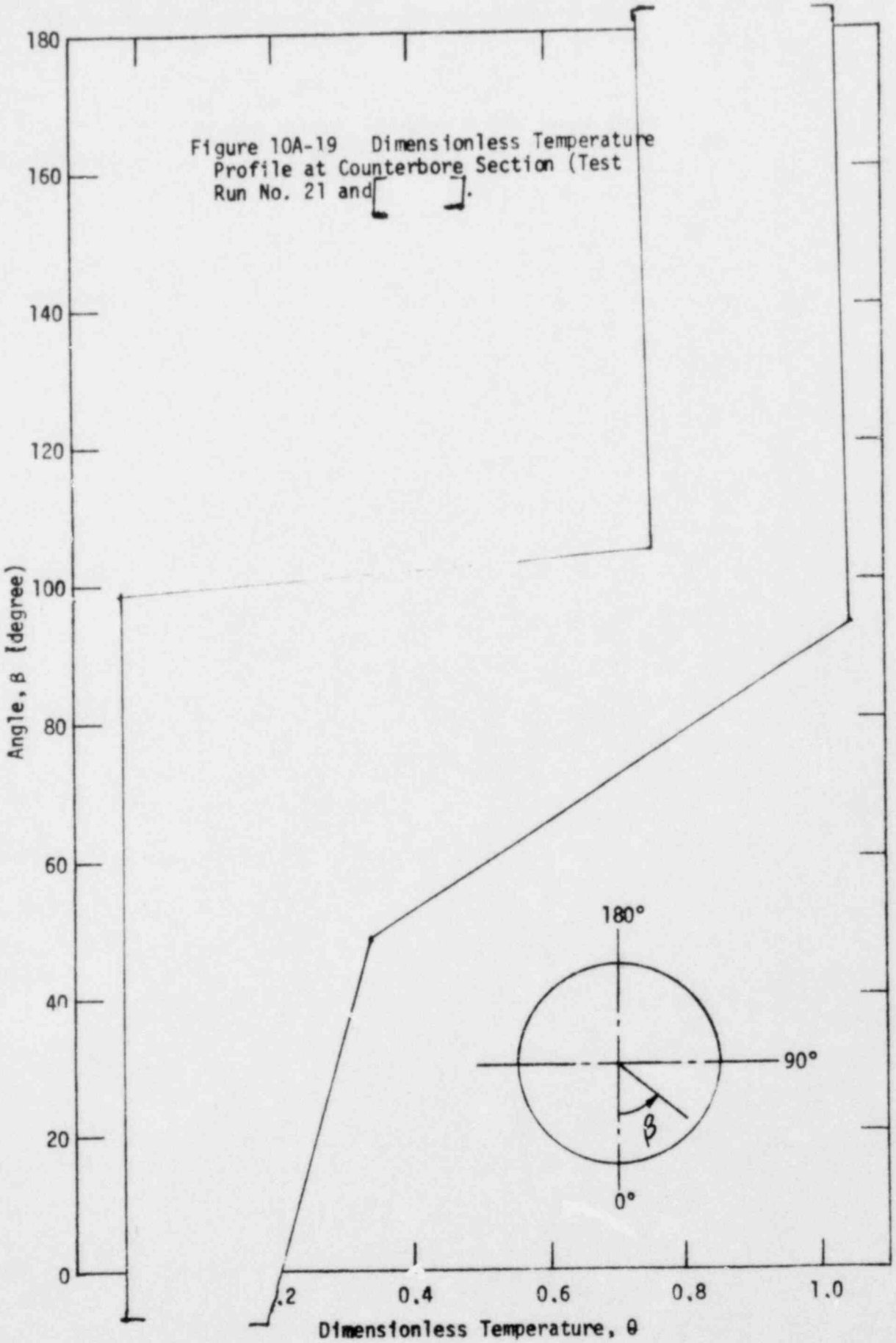

Figure 10A-19 Dimensionless Temperature Profile at Counterbore Section (Test Run No. 21 and [ ].

a,c

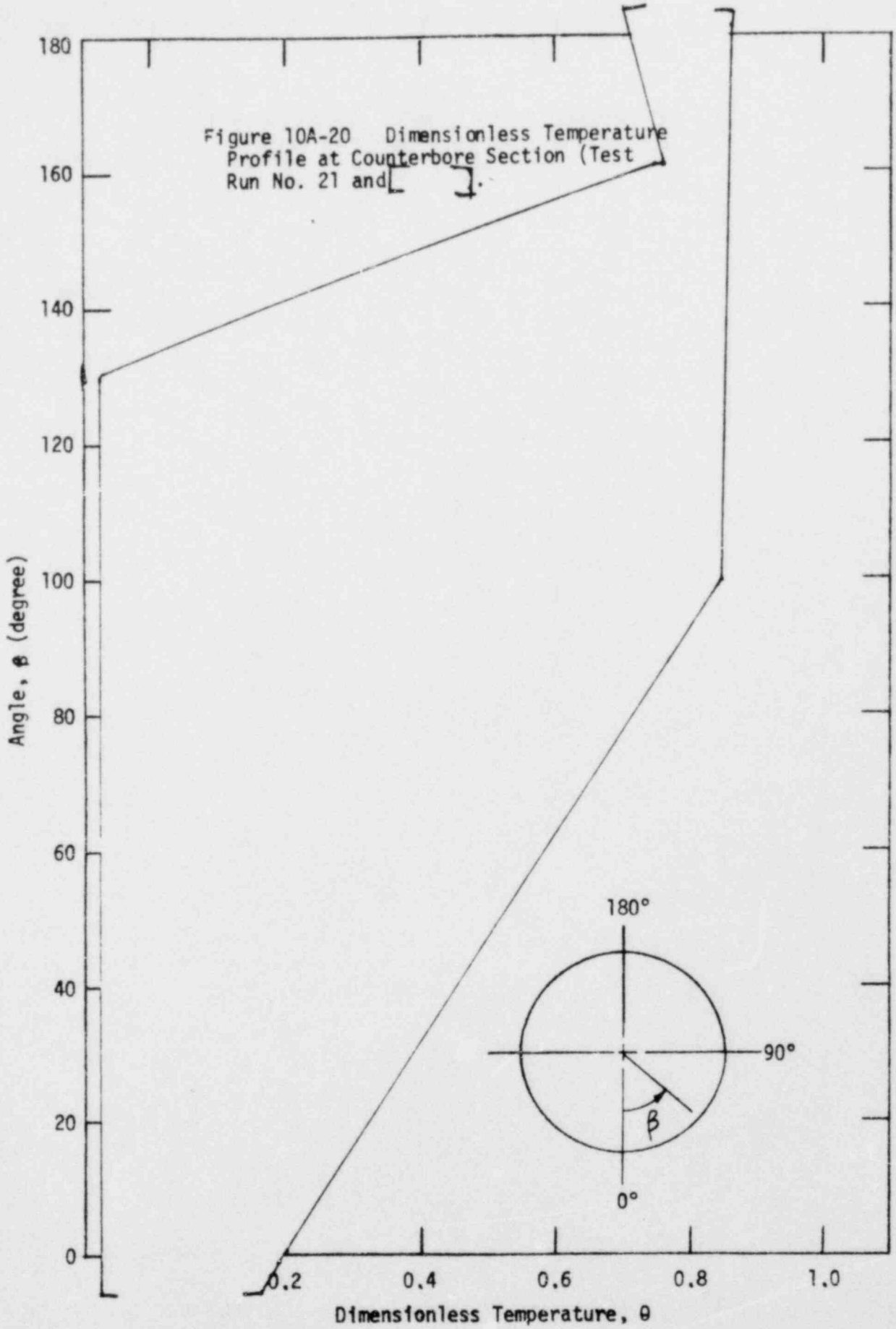

Figure 10A-20 Dimensionless Temperature Profile at Counterbore Section (Test Run No. 21 and [redacted].

9,C

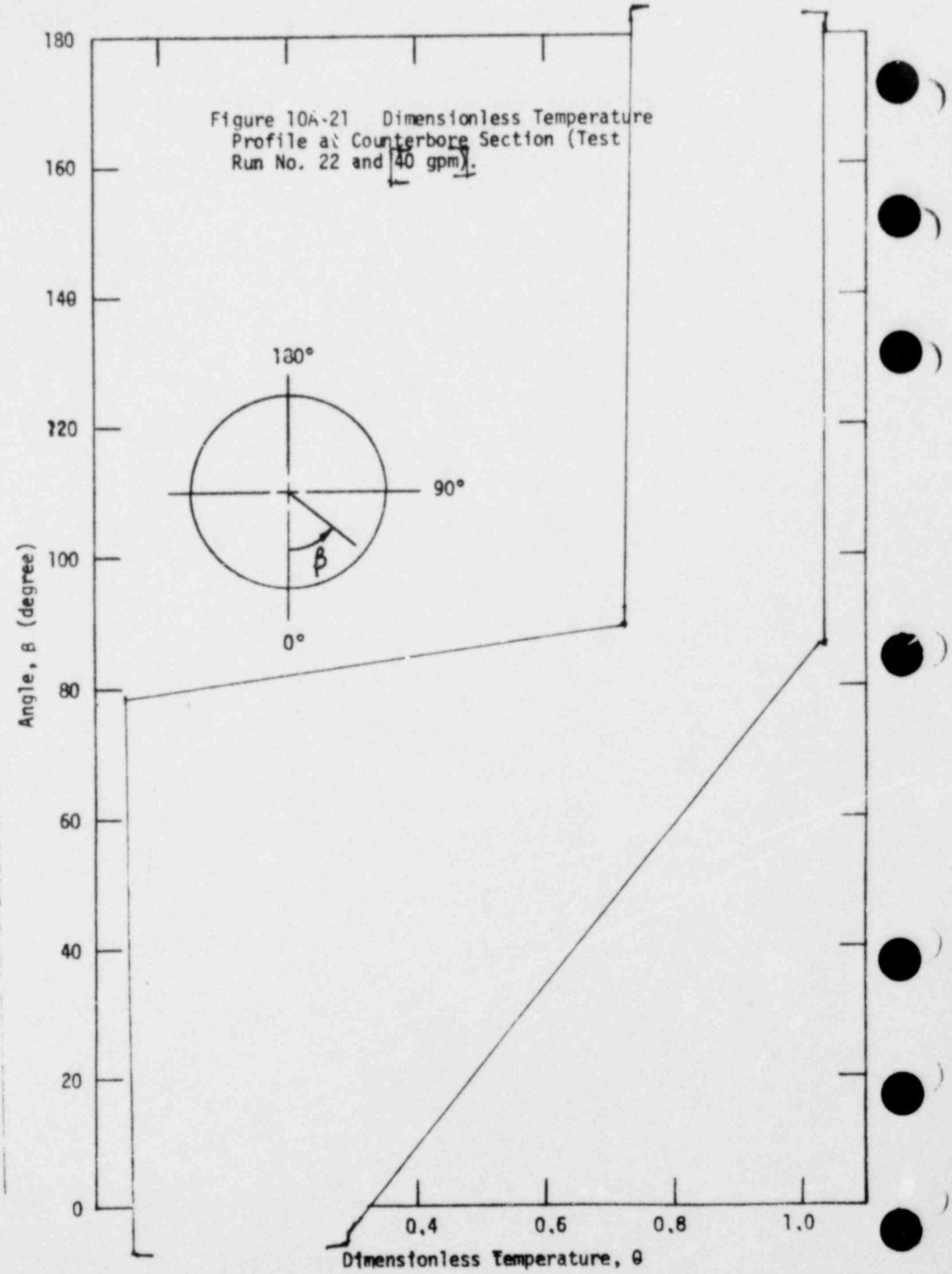

Figure 10A-21 Dimensionless Temperature Profile at Counterbore Section (Test Run No. 22 and 40 gpm).

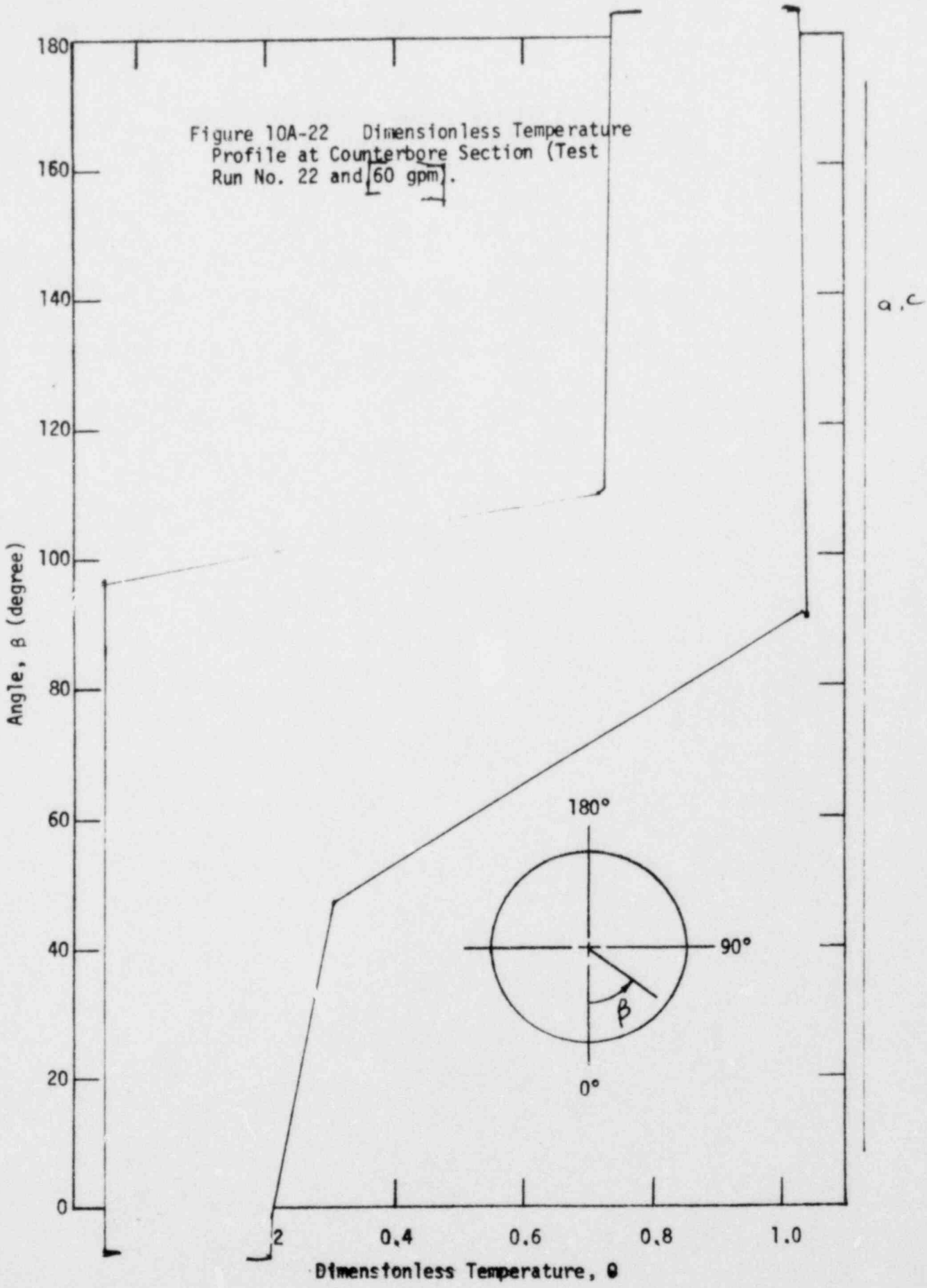

Figure 10A-22 Dimensionless Temperature Profile at Counterbore Section (Test Run No. 22 and 60 gpm).

a,c

Figure 10A-23 Dimensionless Temperature Profile at Counterbore Section (Test Run No. 22 and [redacted]

a,c

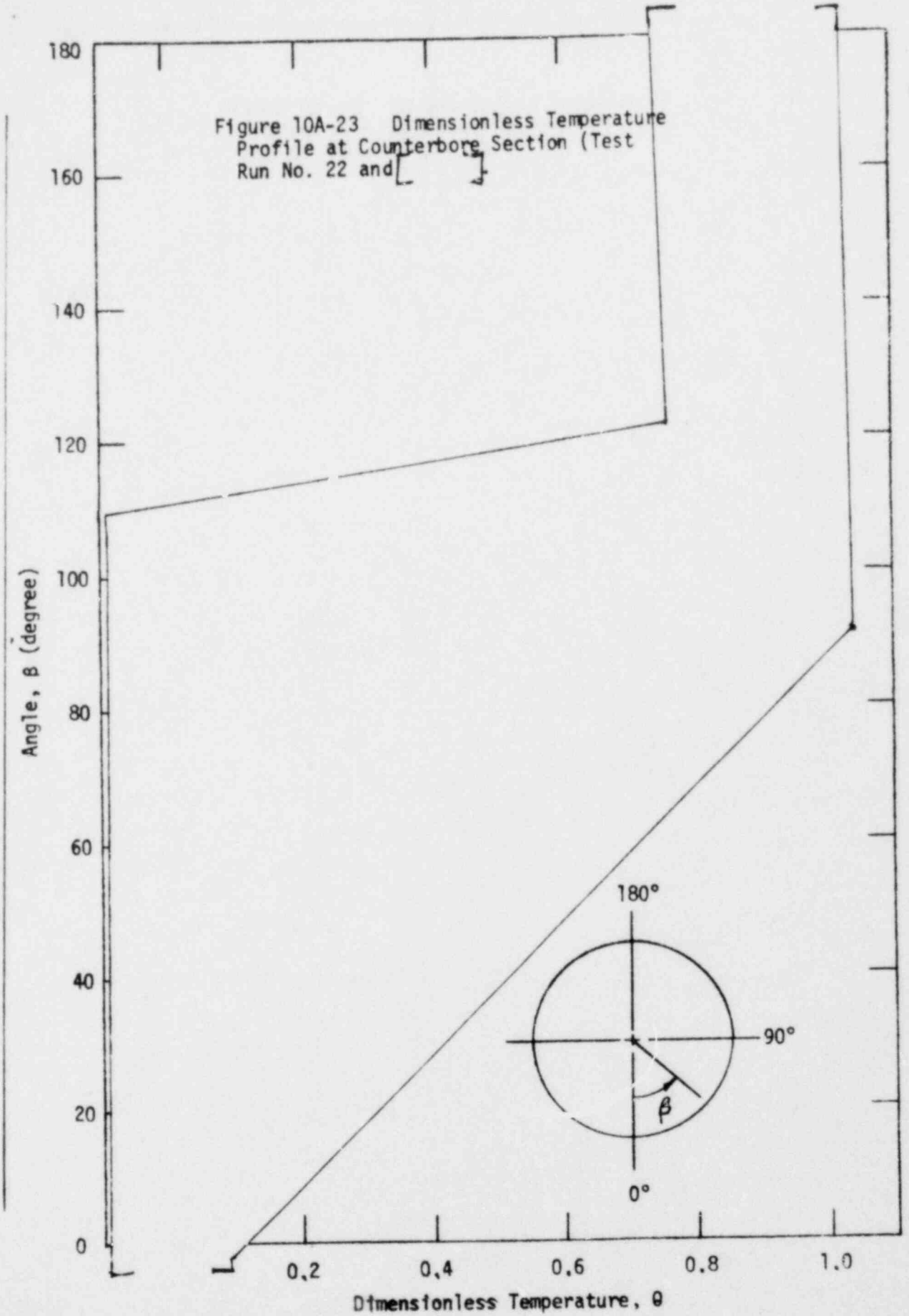

SECTION 11.0

STRESS ANALYSIS AND STRUCTURAL EVALUATION

A. L. Thurman
M. S. Manlab
J. L. Houtman
R. E. Boylstein
T. J. Batt

ACKNOWLEDGEMENT

The authors wish to express our thanks to the following persons who have made valuable contributions to this report:

D. A. Bierman
J. M. Hall
D. T. Entenman
D. L. LaPay
T. A. Vukson

11.0 STRESS ANALYSIS AND STRUCTURAL EVALUATION

This section presents the results of the 3-D stress analysis performed to determine the contribution of thermally stratified flow conditions to the feedwater line cracking.

Two piping configurations are considered in this analysis - a 90 degree elbow welded to the nozzle and a straight pipe connected to the nozzle. Generic stratified temperature profiles are developed for each configuration, based on field data and temperature measurements made during the flow test described in Section 10.

The on-site data described in Section 8 are used to determine the stratified load conditions along with their number of occurrences for the [ ] plants; [ ]. The stress states produced by the generic profiles are scaled to obtain the plant-specific load conditions which are then used in the maximum range of stress intensity and fatigue evaluations for each plant. a,c,e

The striping stresses, produced by local temperature oscillations at the hot-cold fluid interface are determined analytically. The striping is then combined with the steady state stratification to determine the total fatigue usage produced by thermally stratified flow conditions.

Excessive fatigue damages are predicted [ ] at locations which correlate well with the observed cracks. Thus thermal stratification and the associated striping are prime contributors to the feedwater line cracking. a,c,e

11.1 COMPONENT INDENTIFICATION

The design drawings and the materials used for the construction of both the nozzle/elbow and nozzle/pipe configurations are described in this

section. As-built dimensions are used whenever possible. The appropriate temperature dependent material properties and Code allowables are also included.

11.1.1 NOZZLE/ELBOW CONFIGURATION

Figure 11.1-1 is the Westinghouse design drawing for the feedwater nozzle used for this analysis. The nozzle/elbow assembly is shown in Figure 11.1-2. [

a,c

]

11.1.2 NOZZLE/STRAIGHT PIPE CONFIGURATION

a,c [ ]

11.1.3 MATERIAL PROPERTIES

Table 11.1.1 lists the bill of materials for both the nozzle/elbow and nozzle/pipe configurations. Table 11.1.2 thru Table 11.1.5 list the material properties for the components of the feedwater nozzle and the connecting pipe assembly. All properties are from ASME Code Reference (1). The consistent units used in the analysis are as follows:

Density: $\rho = (\frac{Lb}{ft^3}) \cdot \frac{ft^3}{1728\ in^3} \cdot \frac{1}{386} \frac{sec^2}{in}$

Thermal Conductivity: $TC = (BTU/hr.ft.\ ^oF) \frac{hr}{3600\ sec} \cdot \frac{ft}{12\ in}$

Specific Heat: $C_p = (BUT/lb\ ^oF) \cdot 386 \frac{in}{sec^2}$

The Thermal Diffusivity is defined as:

$$\text{Thermal Diffusivity} = \frac{\text{Thermal Conductivity (BUT/hr-ft-}^oF)}{\text{Density (lb/ft}^3) * \text{Specific Heat (BTU/lb-}^oF)}$$

or

$$T_D = \frac{TC}{\rho C_p}$$

and

$$C_p = \frac{TC}{\rho T_D}$$

$$C_p = \frac{TC(BTU/hr\text{-}ft\text{-}^oF)}{\rho(lb/ft^3)\ T_D(ft^2/hr)} \cdot 386 \frac{in}{sec^2} = (\frac{BTU - sec^2}{lb - in^oF})$$

The specific heat values presented in the material tables are calculated using the above relationship.

11.2 LOAD CONDITIONS

The feedwater nozzle/elbow (or straight pipe) assembly is subjected to several types of loads during its service life. Those load conditions considered for this analysis are:

1. Pressure - acting on the inside surfaces of the steam generator shell, the nozzle, and the elbow (or pipe).

2. Nozzle piping loads.

3. Thermal stratification loads - the temperature profiles derived from field data and the flow test were used to obtain the corresponding stratification stresses.

4. Thermal striping loads - Local stress produced by the rapid oscillation of fluid temperature at the interface between the hot and cold stratified layers.

5. Design thermal transients - Heatup and cooldown, load and unload, and loss of power are the transients normally encountered during the operation of each of the plants analyzed.

The individual load cases will be discussed in more detail in the sections to follow.

11.2.1 MECHANICAL LOADS

The nozzle piping loads for several plants were evaluated in Section 7.2, with the stresses caused by these loads given in Table 7.1. These stress magnitudes are small and are essentially steady state. The number of occurences of different stress levels from piping loads is small compared to those of other load conditions. Since this investigation is concerned with load conditions that have the potential to initiate cracks in a relatively short period of time, either through high stresses acting over a small number of cycles or lower stresses occurring for a large number of cycles, the piping loads will not be considered in this analysis.

Stresses produced by internal pressure have been included, however, as they are needed for the crack propagation analysis of Section 12.

11.2.2 THERMAL STRATIFICATION LOADS

[ ] a,c

Thermally stratified flow has been observed during heatup, hot standby, and variation between 0-20% power. As discussed in Section 8, an extensive series of temperature measurements have been taken at five plants during heatup, hot standby and the 0-20Δ power condition. These measurements and the flow test described in Section 10 form the basis for the analysis presented in the following sections.

11.2.3 THERMAL STRIPING LOADS

Thermal striping is a local phenomenon that occurs at the interface between hot and cold flowing fluids. As seen from a point on the pipe wall, the interface level oscillates rapidly with periods ranging from [ ]. This point is thus exposed to a rapidly varying | a,c

fluid temperature, which results in fluctuating surface stresses at that point. The magnitude of these stresses is a function of the difference in temperature between the hot and cold fluids, the film coefficent between the fluid and wall, thermal conductivity, and the wall thickness. [

a,c,e

]

Thermal striping has been observed and measured at the interface between the hot and cold fluids in the flow test discussed in Section 10. The striping analysis in this report is based on those flow test measurements.

11.2.4 DESIGN THERMAL TRANSIENTS

The design thermal transients normally encountered during the operation of each of the plants analyzed are heatup and cooldown, load and unload, and feedwater injection following a trip. All of these transients are included in the Steam Generator E-Spec[2], and analyses[3] have shown acceptable usage factors for the feedwater nozzle for the design life of the plants. Since the thermal stresses from these transients are lower at the nozzle to piping junction than in the nozzle, these transients do not contribute significantly to the feedwater line cracking.

The design transients only need to be considered if their character has been observed to be fundamentally different from that specified in the E-Spec (e.g., hot standby), or if their maximum stresses lie outside the extremes produced by the loads included in the analysis. On this basis, the load-unload transients may be eliminated immediately. [

a,c,e

]

A conservative 2-D analysis for sudden injection of cold feedwater was presented in Section 7. The maximum stresses calculated for this condition are less than those produced by thermal stratification. Since this condition occurs only once each hot standby, it would not contribute to the observed cracking, and is not considered in the analysis to follow.

11.3 TEMPERATURE PROFILES DURING THERMAL STRATIFICATION

During normal plant operation a series of temperature measurements have been taken [ ]. Temperatures have been measured during reactor heatup, hot standby and variation between 0-20 percent power for the [ ] plants [ ]. Those measurements were taken on the inside surface of the [ ] as well as on the outside. a,c

Analysis of the test data for the above series of tests indicates that the stratified temperature distributions may be grouped into basic profiles [ ]. The analysis to follow must start with the temperature distribution within the fluid, and the plant data, by itself, does not provide enough information to determine the fluid temperature variation which produces a given temperature profile in the metal. a,b,c

The flow test described in Section 10 provides detailed fluid temperature profiles for various interface levels for both the elbow and straight pipe configurations. These profiles, modified to account for the heat transfer between the metal and water which the test could not model, were combined with the plant data to determine the basic profiles for both the elbow and straight pipe configurations. These profiles are assumed to be at steady state conditions because of their long duration observed during the tests.

The straight pipe configuration was determined to have five basic profiles, while the elbow configuration had six profiles. The extra profile for the elbow was needed to bracket the wider band of data provided by the greater number of elbow plants instrumented.

11.3.1 ELBOW STRATIFICATION PROFILES

The six profiles for the elbow configuration are shown in Figures 11.3-1 to 11.3-6. On these figures, the solid lines represent the fluid temperature, the x's are the calculated metal temperatures on the outside surface, and the other symbols correspond to measured plant data. Note that the plant data for profiles T_5 and T_6 is identical and that these two profiles bracketed the data.

a,b,c

One characteristic of the flow in the elbow determined during the flow test is that the interface level [ ] as shown in Figure 11.3-7. [ ]. This figure is the basis for [ ] of each of the points defining the fluid temperatures on Figures 11.3-1 to 11.3-6.

11.3.2 STRAIGHT PIPE STRATIFICATION PROFILES

Four profiles for the straight pipe configuration are shown in Figures 11.3-8 to 11.3-11. The fifth profile is identical to profile T_4 for the elbow and is not repeated here. These figures follow the same format as those for the elbow.

11.4 OPERATING HISTORIES

The individual plant data collected as described in Section 8 has been organized to identify every occurrence of each profile along with its duration and the temperature difference from the top to the bottom of the pipe. The operating histories used in this analysis are based on that data. After eliminating profiles that had not reached steady state conditions, the remaining occurrences were ranked by ΔT under the appropriate profile. In order to have a manageable number of load conditions, these occurrences were then divided into groups for which the average ΔT was calculated, typically three groups for each profile for each plant.

Tables 11.4.1 to 11.4.5 summarize the results of this process for the [ ] plants [ ]. On each of these tables, the second column is the temperature difference between the top and bottom of the pipe at the nozzle weld on the outside surface as calculated for the generic profiles. The third column is the same temperature difference obtained from the plant data as described above. The fourth column is the ratio of the evaluation ΔT's to the generic ΔT for the corresponding profile type. Since the stresses are proportional to ΔT for a given profile, the generic profile stresses are multiplied by these scale factors to obtain the stress states corresponding to the evaluation ΔT's.

a,c

[

]

a,c

11.5 ANALYSIS PROCEDURE

This section describes the method used to determine the contribution of thermal stratification to the cracking observed in feedwater lines. The 3-D analysis of the shell, feedwater nozzle, and elbow/pipe was performed with the finite element models described in the next section.

The analysis procedure is described by the flow charts in Figures 11.5-1 and 11.5-2. As discussed in Section 11.3, the field data and flow test results are combined to give the six basic profiles T_1-T_6. These profiles are applied to the appropriate finite element model (elbow or pipe) and the stresses resulting from that profile are stored on a WECAN

Tape 12. This is done for each of the profiles and for internal pressure. The evaluation ΔT's and corresponding scale factors from Section 11.4 define the load conditions for each plant to be used in the maximum range of stress intensity analysis performed by the WECEVAL computer program, which is described in Section 11.9. The same load conditions, along with the number of occurrences of each event taken from the tables in Section 11.4 are used in the fatigue analysis performed by WECEVAL. Whenever the code allowable is exceeded in the maximum range of stress intensity analysis, WECEVAL generates K_e factors to be applied to the surface stresses in the fatigue analysis.

A more detailed description of the procedure followed to obtain the stresses produced by a stratification profile is given in Figure 11.5-2. Starting with one of the profiles of Section 11.3, the program TDIST determines the fluid temperature and film coefficient for every element face on the inside surface of the appropriate finite element model and generates the corresponding WECAN input cards. A WECAN thermal run is made to obtain the resulting temperatures at every node in the finite element model. A small program, TEMPINT, reads the Tape 8 written by the WECAN thermal run and writes the nodal temperatures for the converged iteration on another tape. This tape is read by WECAN during the run to calculate the thermal stresses. The Tape 12 created by this run is then processed as described above.

11.5.1 COMBINATION OF STRIPING AND STRATIFICATION

Part of the output of the striping analysis described in Section 11.8 consists of the maximum and minimum local stresses for each evaluation ΔT and each profile on Tables 11.4.1 to 11.4.5. These stresses are added to the appropriate steady state stratification stresses for the node closest to the corresponding profile's interface location. The fatigue evaluation for this node is repeated to determine the increase in usage factor caused by the addition of striping stresses. The total fatigue damage for that node is the combination of the low cycle usage factor described above with the high cycle striping usage factor calculated in Section 11.8.

11.5.2 COMPUTER PROGRAMS USED IN THE ANALYSIS

As was evident in the flow charts presented in the previous section, this analysis made extensive use of various computer programs to minimize errors and increase the efficiency of the analysis.

All finite element models were generated using a combination of the ANSYS[4] pre-processors PREP5 and PREP7. The resulting element and node tapes were then converted to WECAN[5] format, and WECAN was used for all subsequent thermal and stress analysis.

Several pre- and post-processors had been developed previously for this type of analysis. Each program was used extensively to make the analysis more efficient. Among the more important of these programs are:

[a,b]

11.6 FINITE ELEMENT MODELS

Figure 11.6-1 shows the finite element model of part of the steam generator shell, the feedwater nozzle and the connecting elbow. This model (as are all of the finite element models in this analysis) is formed from the 20-node version of WECAN's isoparametric solid 3-D element, STIF48. There are two elements through the thickness and twelve around the circumference throughout this model. Figure 11.6-2 provides a more detailed view of this model in the region around the weld between the nozzle and elbow.

The node and element number scheme is regular throughout the model and is illustrated in Figure 11.6-3. The nodes and elements shown are on the outside surface of the model. [

]

a,c [

]

The finite element model for the nozzle attached to a straight pipe is shown in Figure 11.6-4. The shell and most of the nozzle are identical

a,c to that for the elbow configuration model. The counterbore and pipe dimensions are those from the [ ] plant scaled down from an eighteen inch to a sixteen inch nozzle as described in Section 11.1. A more detailed view of the counterbore region is given in Figure 11.6-5. The node and element numbering schemes for this model are identical to the elbow model, except that there is one less row of elements in this model.

11.7 STRATIFIED THERMAL STRESS ANALYSIS

The unit load approach has been used for this analysis. This technique consists of applying each load separately to the structure to obtain the stresses produced by that load. The principle of superposition thus permits the scaling and combination of stresses from different unit load cases to obtain the stress states corresponding to the various load cases.

The specific unit loads considered for this analysis are:

- Pressure - applied to the inside surface of the model
- Stratification temperature profiles derived from plant and flow test data - six for the elbow configuration and five for the straight pipe model.

11.7.1 BOUNDARY CONDITIONS

Figure 11.7-1 identifies the planes and surfaces on which either displacements or surface loads must be specified for the pressure and thermal loads applied to the structure. All of these loads are symmetric with respect to the geometric plane of symmetry. Table 11.7.1 summarizes the boundary conditions for the pressure load and all thermal stress runs.

The shell/nozzle/elbow model contains three distinct regions with different heat transfer characteristics between the metal and the adjacent fluid. [

a,c

] The part of the nozzle and elbow (or pipe) exposed to the fluid below the interface was given the film coefficient h_B, the material exposed to the interface was given the value

h_I, and the part above the interface was given the value h_T. The values for these film coefficients for each profile are listed in Table 11.7.2. The remaining thermal boundary conditions are shown in Figure 11.7-2.

11.7.2 THERMAL STRATIFICATION STRESSES - ELBOW CONFIGURATION

Figures 11.7-3 through 11.7-8 show the temperature distribution, axial stresses, and stress intensities at the root of the elbow transition
a,c near the nozzle/elbow weld for all six stratified profiles. [ ]

Figures 11.7-9 through 11.7-14 show the same quantities as above on a longitudinal section at the angles of peak stresses identified in the previous six figures. [ ] The peak axial stresses and their locations for each of the six profiles are summarized in Table 11.7.3.

11.7.3 THERMAL STRATIFICATION STRESSES - STRAIGHT PIPE CONFIGURATION

Figures 11 7-15 through 11.7-19 show the temperature distribution, axial stresses, and stress intensities at the root of the nozzle transition
a,c near the nozzle/pipe weld for all five stratified profiles. [ ].

Figures 11.7-20 through 11.7-24 show the same quantities as above on a longitudinal section at the top of the counterbore region. [
a,c]

The peak axial stresses and their locations are summarized in Table 11.7.4.

11.8 STRIPING ANALYSIS

11.8.1 INTRODUCTION

Thermal striping is a phenomena which consists of steady-state oscillations localized to the interface between hot and cold layers of a flowing fluid. The temperatures were measured [ ] during the simulation of the feedwater line flow test, (See section 10 of this report). The temperatures at the interface layer fluctuate rapidly with frequencies ranging between [.05-10 HZ. In some cases, the amplitude of these fluctuations reached the magnitude of the total temperature difference between the hot and the cold layers]. a,c

The pipe wall is exposed to rapidly varying fluid temperatures which results in fluctuating stress on the metal surface. For a given pipe of a given material, the magnitude of the surface stresses are a function of the amplitude of the temperature fluctuation, the frequencies of the fluctuations, the heat transfer films coefficient between the fluid and the metal, and thermal conductivity.

[ ] a,c,e

The striping analysis in this section is based on temperature measurements obtained from the flow test results and the scaling characteristics of this test to the steam generator conditions. In the following subsections the analysis approach and results of the striping loadings are presented.

11.8.2 ANALYSIS APPROACH

The effect of striping and its contribution to the total fatigue usage factor is evaluated in this analysis. A flow chart of the analytical procedure is given below, which summarizes the major steps in the analysis.

a,b,c

a,c

4692A

11.8.3 FLOW TEST MODEL RECORDS DATA

a,c

The flow test [ ] were digitized and permanent file tapes of each recorder were cataloged on the CDC7600. All records were digitized in steps of [ ]. As discussed in Section 10 of this report, each recorder channel with the appropriate gain, calibration and offset were plotted. [ ]. A selected number of records for each flow test configuration were chosen for this analysis. A total number of [ ] cases were selected. The flow test record informations for straight pipe configuration with J-tube discharge - (Cases 1 through 7) - is given in Table 11.8.1. Table 11.8.2 lists record information for straight pipe configurations with bottom discharge - (Cases 8 through 15).

The selected cases for the elbow configuration with bottom discharge are listed in Table 11.8.3, (Cases 16 through 34), and those for J-Tube discharge are in Table 11.8.4 (Cases 35 through 44). Each of the above Tables lists the case number, the flow test number, the duration of the record, the record calibration data, the interface layer level, and the corresponding generic profile type. Computer program [ ] was used to generate temperature time-history plots for each of the cases considered for striping analysis. Each time-history plot is of [ ]. The time-history plots for each of the [ ] cases considered are shown on Figure 11.8-1 through Figure 11.8-44. [exist between J-Tubes and bottom discharge configuration (see Section 10), only two major groups are considered for this analysis - straight].

c [ ]

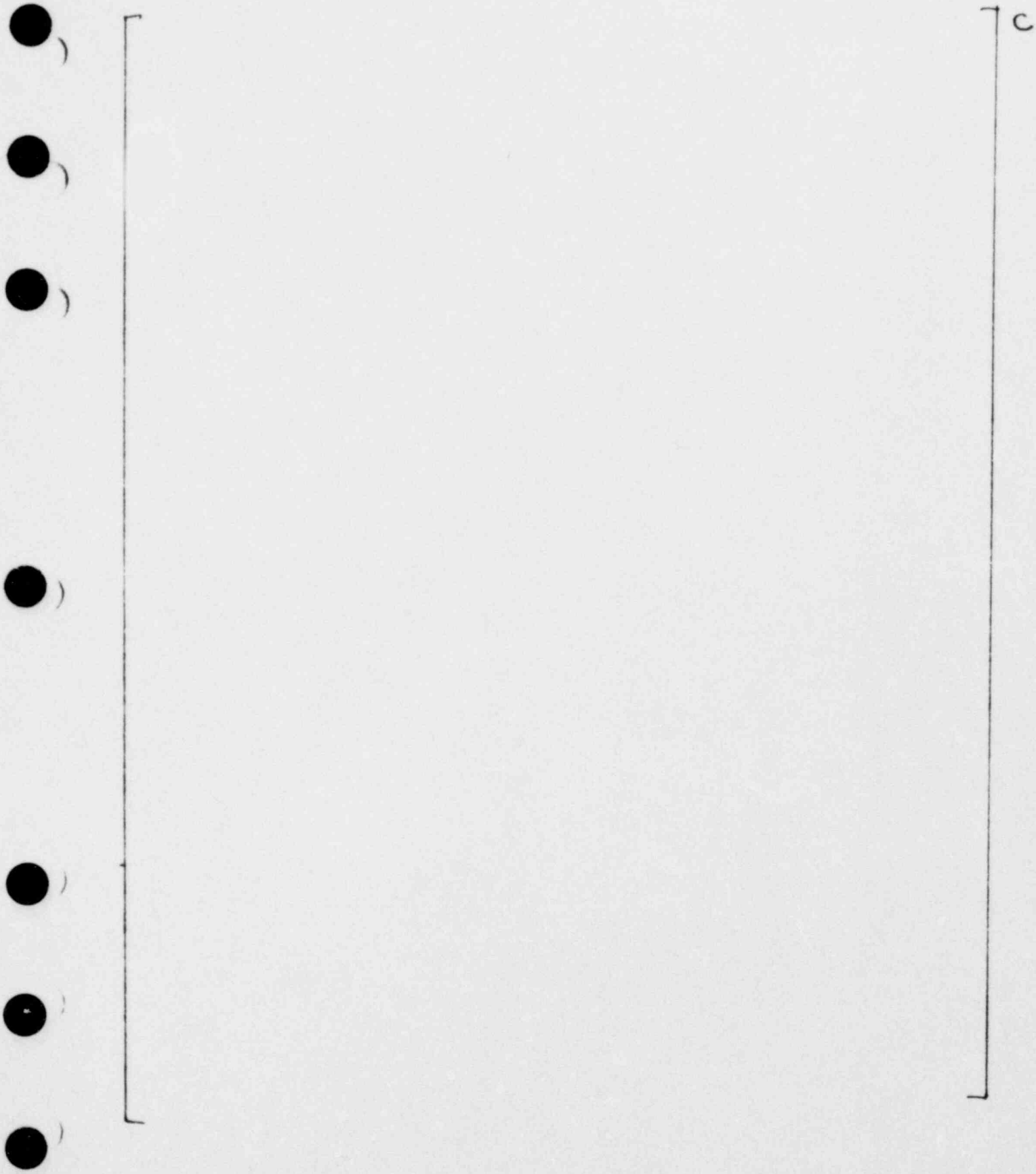
C

C

4692A

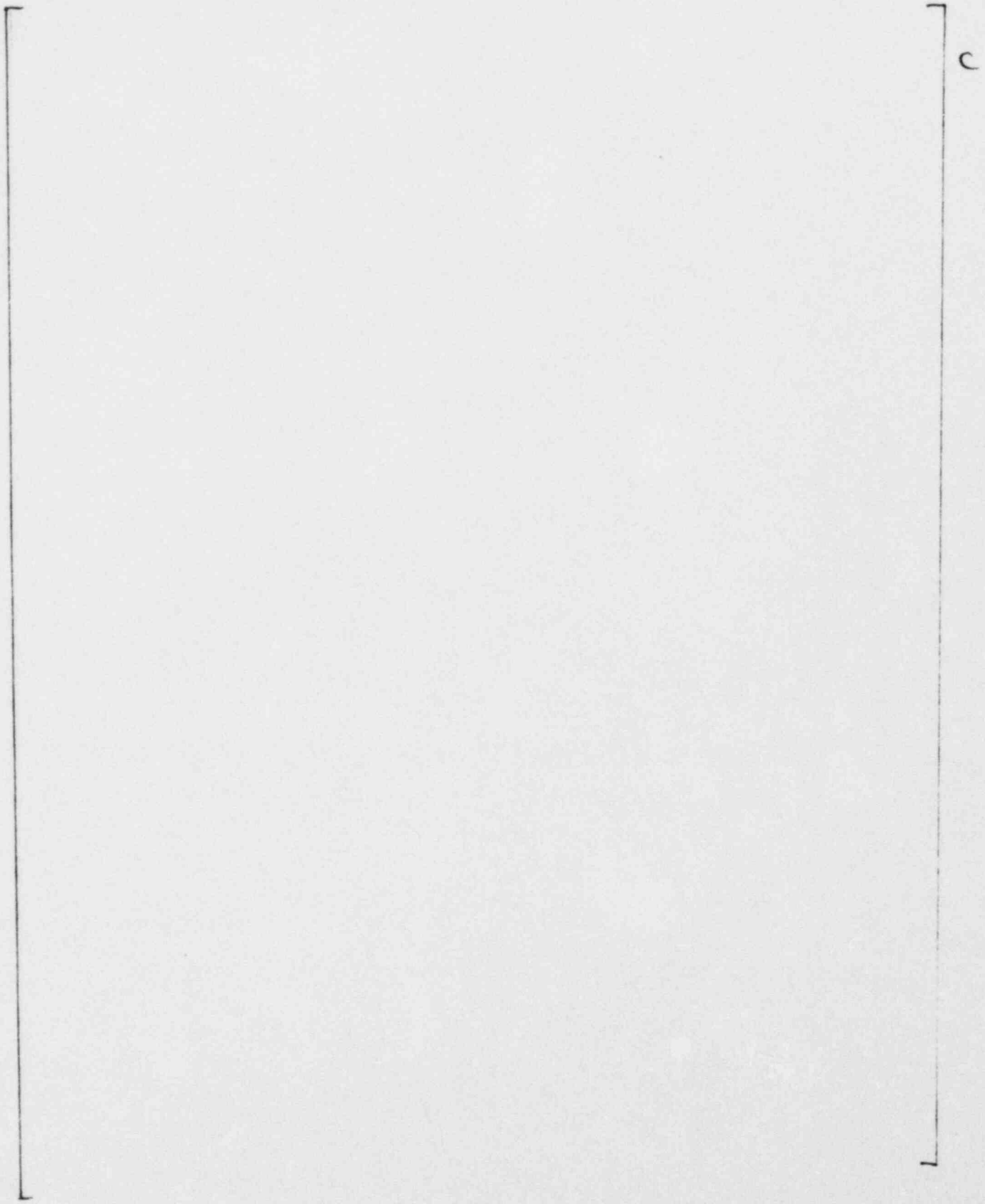

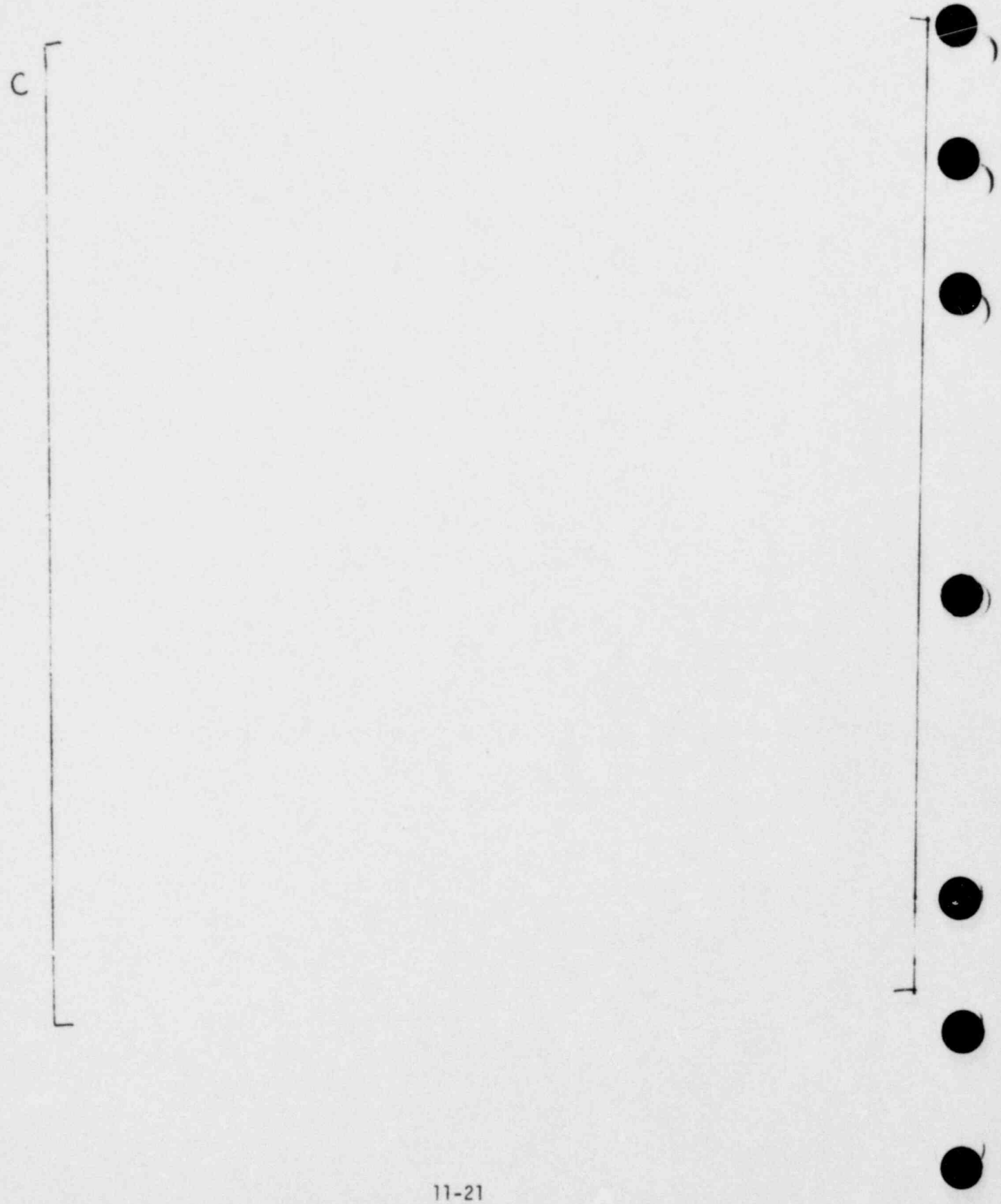
C

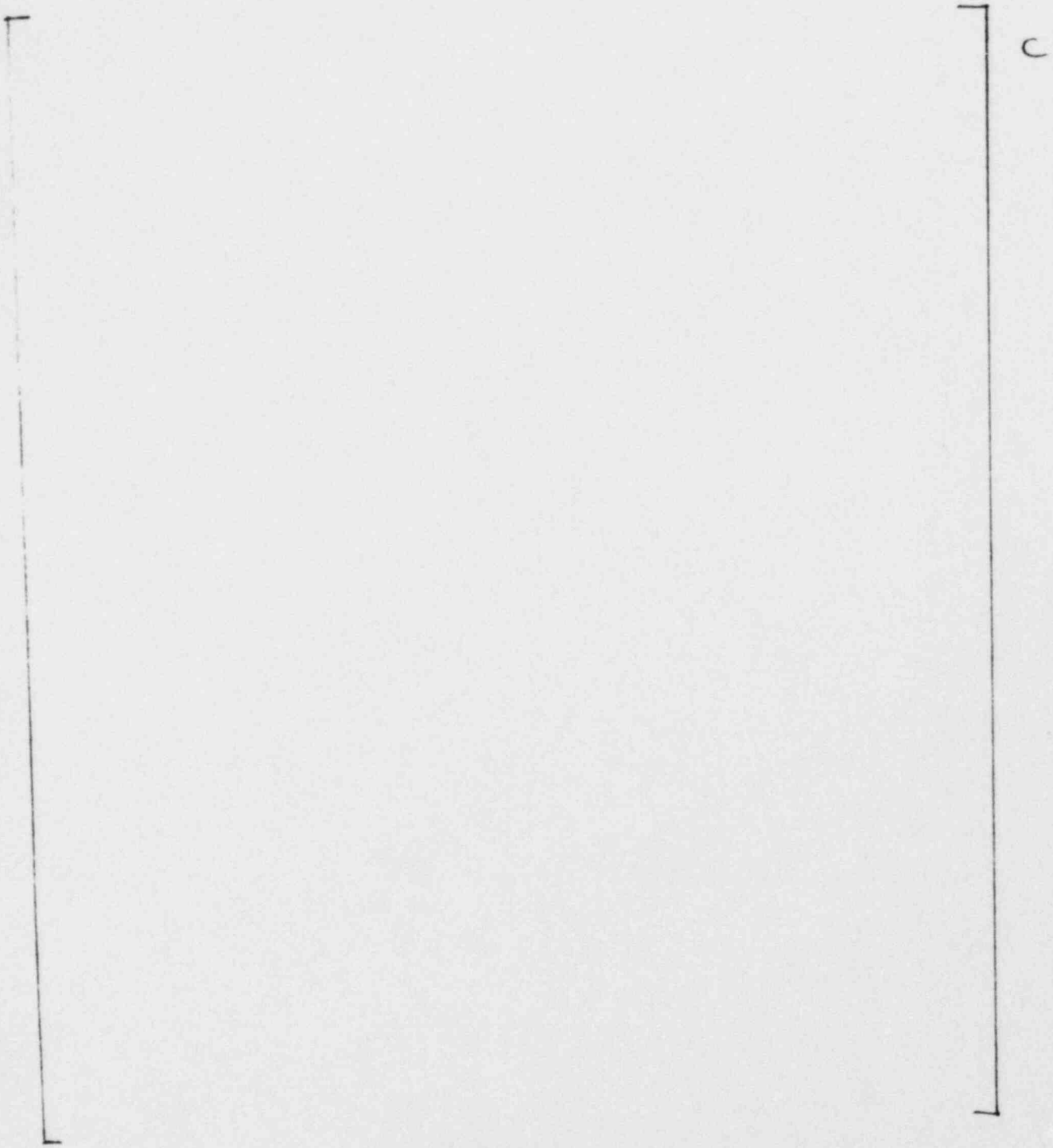

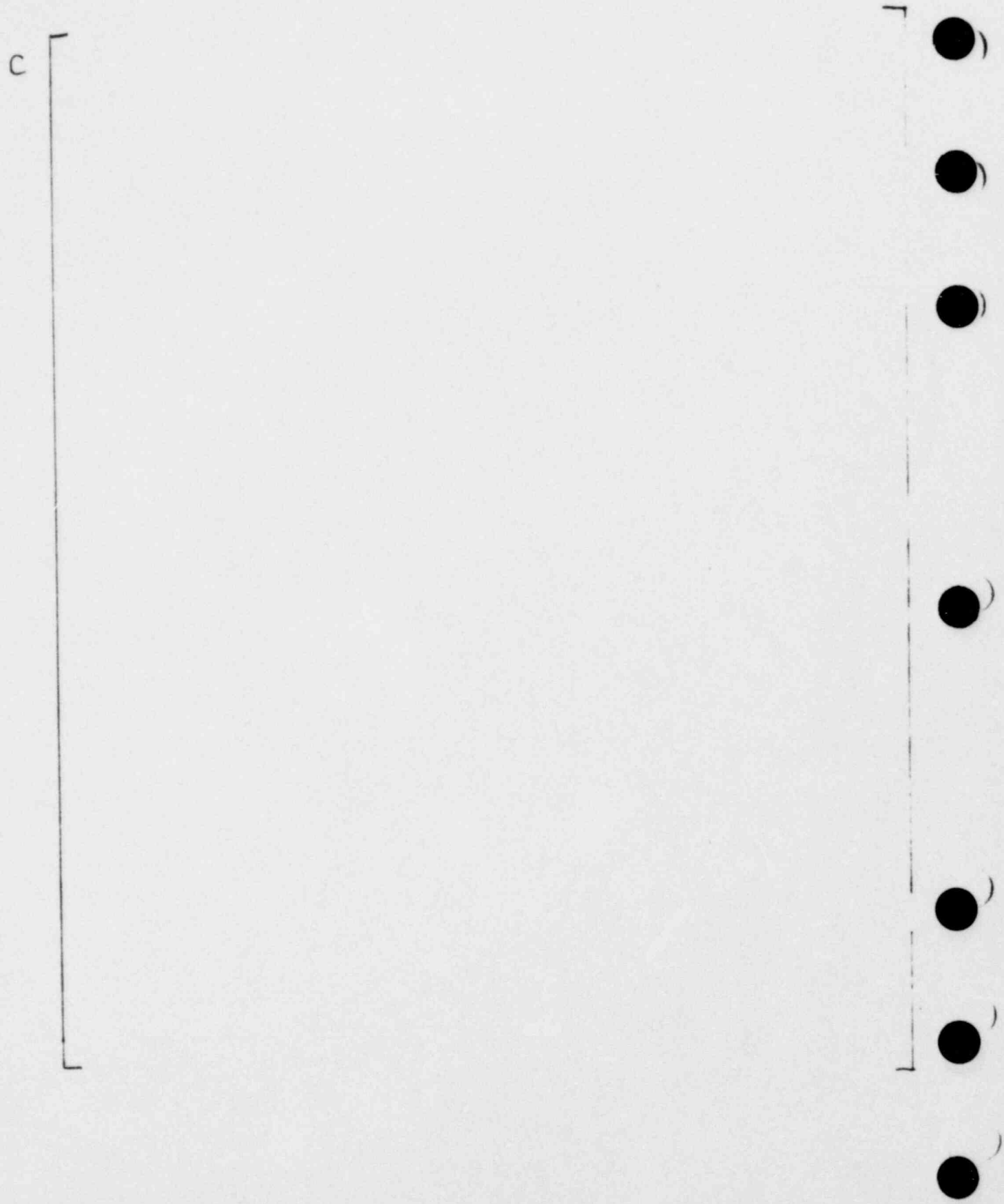

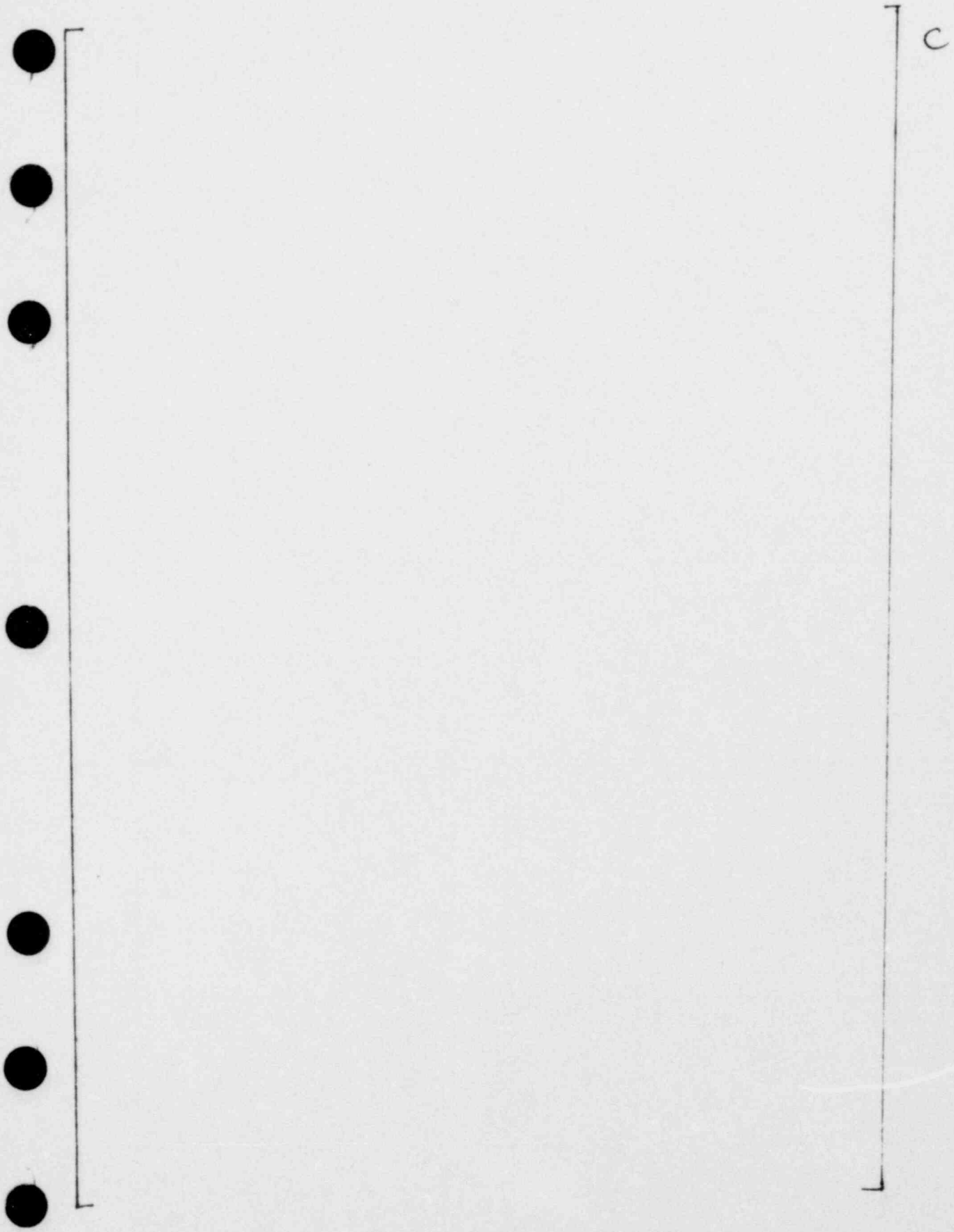
C

C

[redacted]

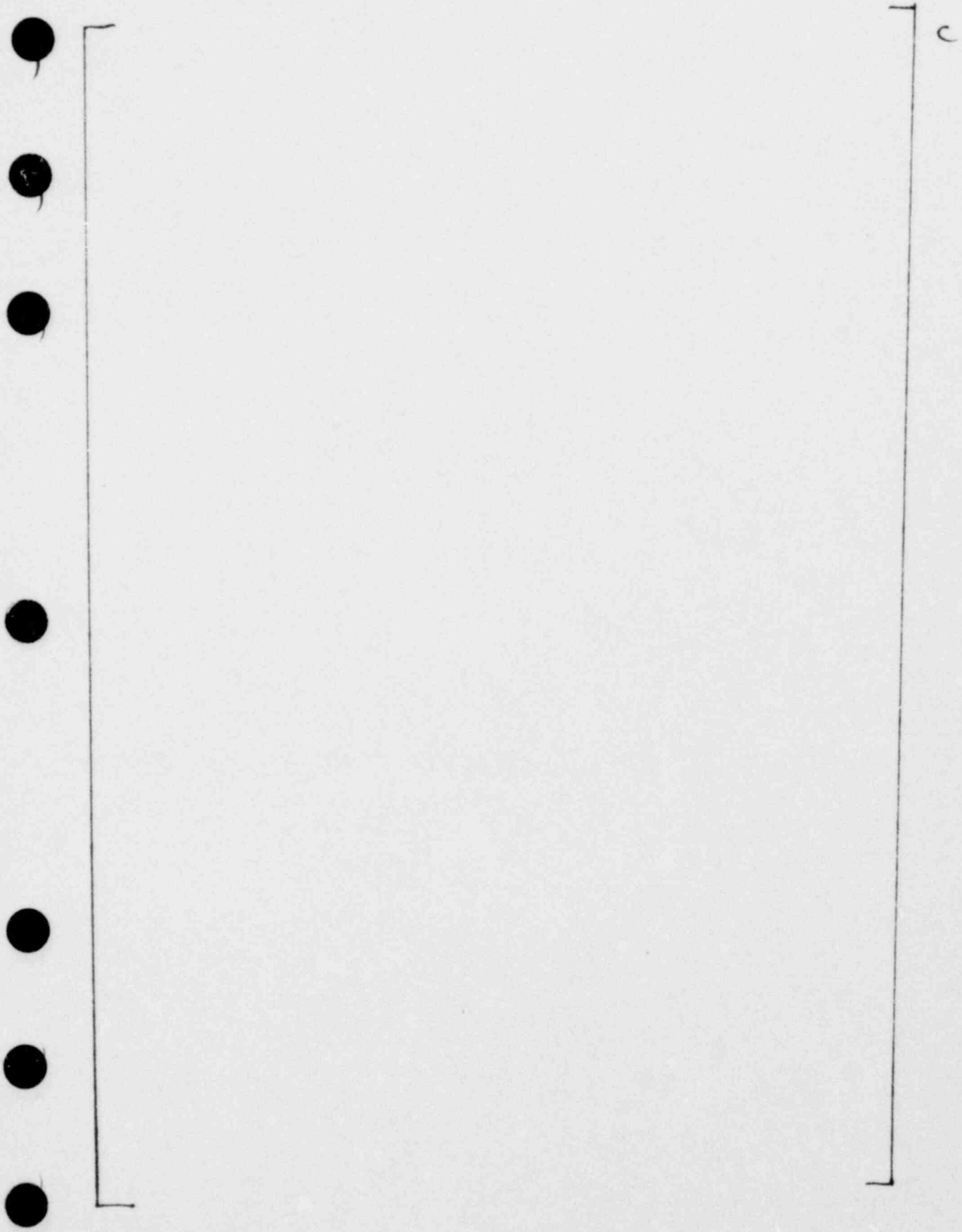

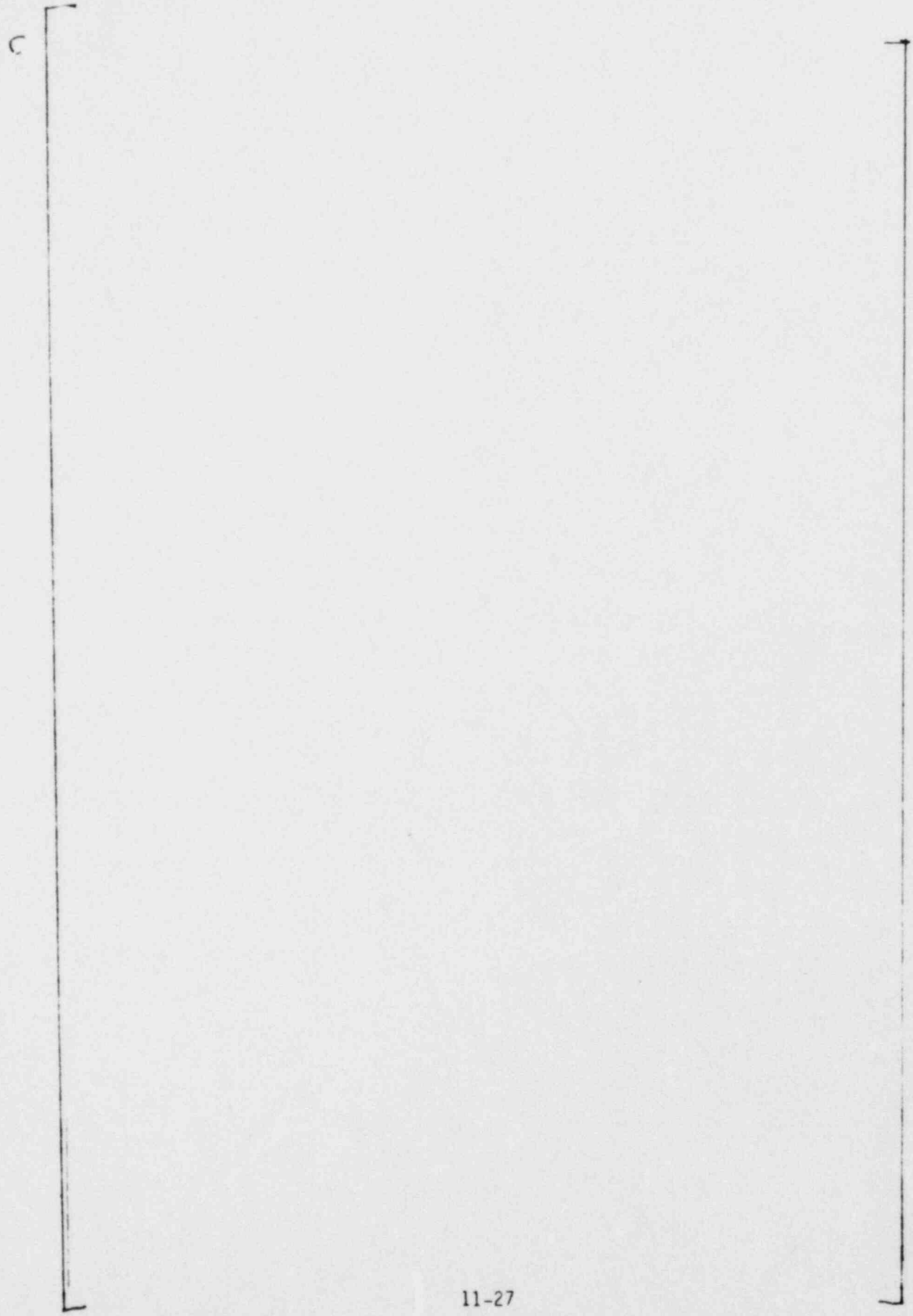

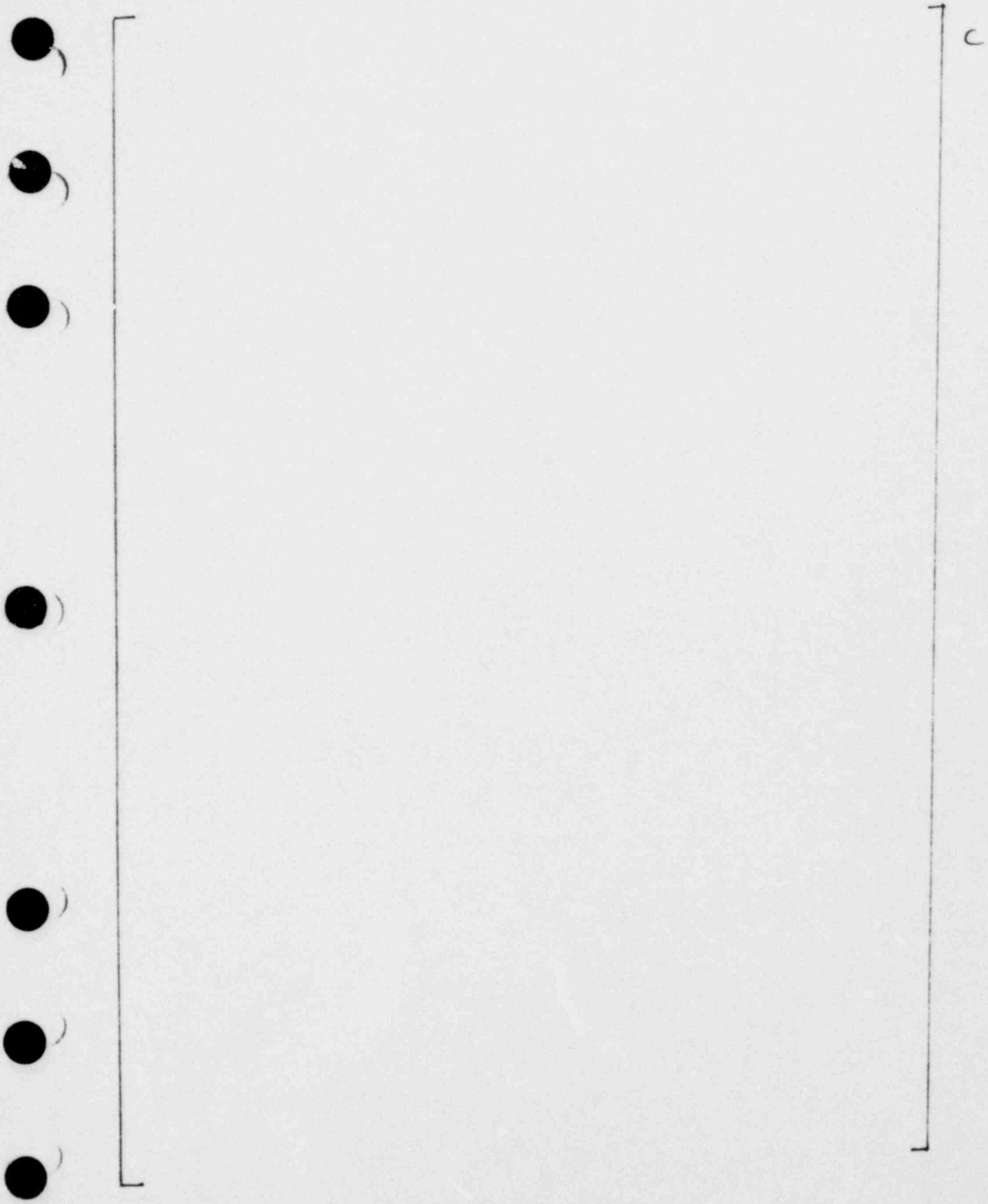
C

c [

]

[ ] C

As seen from Table 11.8.49, the temperature differences for each generic profile are different from the maximum temperature difference used to obtain the alternating stresses of Tables 11.8.5 through 11.8.48. Therefore, the alternating stresses for fatigue evaluation are modified by the ratio of the actual temperature difference to that of [ ] used in the stress analysis. Before entering the fatigue curve (Figure 11.8-177), the alternating stresses are adjusted for the ratio of the modulus of elasticity to 30×10^6 psi. The fatigue calculations for each of the power plants [ ] were based on the flow test data obtained from the elbow configurations. a,c a,c,e

The usage factor calculations results, for all the elbow test configuration data, (Cases 16 through 44), are presented in Table 11.8-50. The maximum usage factor from each group of cases

corresponding to a single generic profile, for each power plant, are given below. These maximum usage values, plotted versus the pipe arc for each power plant, are presented in Figures 11.8-178 through 11.8.182.

a,c,e

Generic Profile	[	]
T_1	[	]
T_2		
T_3		
T_5		
T_6		

As stated previously, the above values of fatigue damage are obtained using the design fatigue curve with mean stresses, to account for the residual stresses in the nozzle/elbow weld region, weld fillet, and machine marks. For other portions of the pipe I.D., the fatigue damage is evaluated considering the design fatigue curve without mean stresses. These maximum values are shown in the following table.

a,c,e

Generic Profile	[	]
T_1	[	]
T_2		
T_3		
T_5		
T_6		

11.8.10 SUMMARY

The analysis described in the previous sections provides the contribution of striping to the initiation of feedwater line cracks.

Many parameters with some degree of uncertainty are used in the course of the analysis. For example, the heat transfer film coefficient, the generic profile, the duration of each profile and the design fatigue curve. Even with the uncertainties contained in this analysis, the fatigue usage factors are good indications of the potential of crack initiation and growth.

As shown in this analysis, the fatigue damage due to striping alone is predicted at the nozzle/elbow counterbore region as well as in the portions of the pipe I.D. [ ]. [ ] c

[ ] c

11.9 STRUCTURAL EVALUATION FOR THERMAL STRATIFICATION

A stress intensity evaluation was performed at numerous potentially high stress locations in accordance with the criteria in the Code, Subsection NB-3200. A post-processor was designed to perform the Code stress intensity evaluations. The post-processor, WECEVAL[7], was written for the WECAN and ANSYS output files, Tape 12, Pfn.

Calculations performed by WECEVAL will be summarized in this section. All calculations were conveniently categorized according to load condition type.

The procedures discussed in this section pertain to a general continuum structure analyzed by a three-dimensional finite-element. Application to an axisymmetric continuum structure analyzed by an axisymmetric finite-element is identical. Particular application to a unique finite-element model will be discussed in the appropriate section.

The criteria for Level A and B load conditions are contained in Code paragraphs NB-3222 and NB-3223, respectively. This section covers stress intensity evaluation of the structure in terms of two Code criteria. The first criterion pertains to the primary-plus-secondary stress intensity; the second, to the fatigue analysis.

11.9.1 PRIMARY-PLUS-SECONDARY STRESS INTENSITY EVALUATION

The criterion for this part of the stress evaluation pertains to the maximum range of principal peak stress difference between two extreme load conditions. The stress intensity criterion is contained in Code paragraph NB-3222.2; it pertains to the highest value of the primary-plus-secondary stress intensity, excluding peak influence, at any point across the thickness. The limit of this criterion is written as follows:

$$P_m + P_b + Q \leq 3\ S_m\ (T_{avg}\ ^\circ F)$$

Load condition stress states were assembled from the unit load case stress states for each load combination identified in Section 11.10. The unit load case stress states were catalogued on WECAN output files, Tape 12, Pfn.

The summation process was performed such that the stress state was maximum for each section analyzed. Maximization was performed according to the following logic:

Non Thermal Conditions - The stress state was due to both surface tractions and body forces. Surface tractions correspond to loads such as external pipe loads and internal pressure; body forces, to inertia loads on the solid. The maximization was performed on the hoop or axial stress component at the inside surface due to internal pressure. The sign of each non-pressure load was selected such that the inside surface hoop or axial stress was maximum; through the thickness, the stress state was consistent with the sign on the non-pressure load.

Thermal Condition - The stress state was due to both surface tractions and body forces. Surface tractions correspond to

loads such as external pipe loads and internal pressure; body forces, to inertia and thermal loads on the solid. The maximization was performed on the hoop or axial stress component at the inside surface due to the thermal load case. The sign on the internal pressure load case was not altered. The sign on each of the additional non-thermal loads was selected such that the inside surface hoop or axial stress was maximum; through the thickness, the stress state was consistent with the sign on the non-thermal load.

The summation process is indicated by the following equation:

$$(\sigma_{ij})^S_k = \rho_\alpha (\sigma_{ij})^S_\alpha + \text{maximum} \quad (\sigma_{ij})^S_T + \sum_{m=1}^{n} \rho_m \phi_m \ (\sigma_{ij})^S_m$$

where

$(\sigma_{ij})^S_T$ = stress state due to a specific thermal transient at node number s.

The stress states for each load condition were linearized via a linear regression analysis through the thickness of each section analyzed. This process resulted in surface stress states which were free of all peak stress effects and were identified by the following notation:

$[\underset{\sim}{\sigma}_{ij}]^S_k$ surface stress at node s for load condition k.

Using the load condition surface stress states, $[\underset{\sim}{\sigma}_{ij}]^S_k$, the stress component ranges for all possible load history combinations were calculated at the stress component level. The calculational procedure is defined by the following equation,

$$[\overline{\underset{\sim}{\sigma}_{ij}}]^S_{rt} = [\underset{\sim}{\sigma}_{ij}]^S_r - [\underset{\sim}{\sigma}_{ij}]^S_t$$

$r = 1, 2, \ldots, i, \ldots n-1$

$t = r+1, \ldots, n$

where each term is defined as follows:

n	number of load conditions
r,t	indices for specific load conditions
rt	specification for the stress range between load conditions r and t
$[\sigma_{ij}]^s_r$	surface stress state for load condition r at node s
$[\sigma_{ij}]^s_t$	surface stress for load condition t at node s
$[\overline{\sigma_{ij}}]^s_{rt}$	surface stress range between load conditions r and t at node s

Principal stress ranges were calculated from the the load history stress ranges, $[\overline{\sigma_{ij}}]^s_{rt}$.

Since the component stress range was three-dimensional, three principal values were calculated from the equation [15].

$$-N^3 + \theta N^2 + AN + B = 0$$

where the coefficients are defined as follows:

$$\theta = \sigma_{xx} + \sigma_{yy} + \sigma_{zz}$$

$$A = \sigma^2_{xy} + \sigma^2_{yz} + \sigma^2_{xz} - (\sigma_{xx}\sigma_{yy} + \sigma_{xx}\sigma_{zz} + \sigma_{yy}\sigma_{zz})$$

$$B = \sigma_{xx}\sigma_{yy}\sigma_{zz} + 2\sigma_{xy}\sigma_{xz}\sigma_{yz} - \sigma_{xx}\sigma^2_{yz} - \sigma_{yy}\sigma^2_{zx} - \sigma_{zz}\sigma^2_{xy}$$

Thus for each stress component range, $[\overline{\sigma_{ij}}]_{rt}$, a principal stress range was calculated with the above equation; the results are indicated as follows:

$$[\sigma_{ij}]^{S}_{rt} \longrightarrow \langle \sigma_1, \sigma_2, \sigma_3 \rangle^{S}_{rt} \quad ;$$

the triplet $\langle \sigma_1, \sigma_2, \sigma_3 \rangle_{rt}$ is defined as the principal stress range between load conditions r and t.

The range of stress intensity (SIJ) was calculated from the principal stress range as follows:

$$(S12)^{rt} = (\sigma_1 - \sigma_2)^{S}_{rt}$$

$$(S23)^{rt} = (\sigma_2 - \sigma_3)^{S}_{rt}$$

$$(S31)^{rt} = (\sigma_3 - \sigma_1)^{S}_{rt}$$

The maximum range of stress intensity was obtained from the results of the range of stress intensity calculations; the process is indicated as follows:

$$(SIJ)^{rt}_{max} \leq 3\ S_m\ (T_{avg}\ ^{\circ}F)$$

11.9.2 FATIGUE EVALUATION

The Code fatigue criterion and evaluation procedure (for cyclic operation) are in paragraph NB-3222.4. The criterion pertains to half of the maximum range of principal peak stress difference between two load conditions and to the number of cycles for that stress intensity.

The peak stress intensities used in the fatigue analysis for this project correspond to surface nodal stress intensities at each location selected for evaluation. Surface stresses used to calculate the surface stress intensities were assembled for each Level A and B load condition. The total load surface stress state at each point analyzed was assembled from the unit load case analyses and the applicable thermal transients.

Each total stress state, $(\sigma_{ij})^S_k$, like that for the maximum Primary-Plus-Secondary Stress Intensity Range, was the result of a maximum summation process. [

C]. The summation rule was determined by the load combination classification (thermal and non-thermal). For both types of load combinations, the stress states were summed for a maximum hoop or axial stress. [

]. This process was performed for each of the points (nodes) considered for the Level A and B load condition evaluation. The process was identical to that for the primary plus secondary summation.

Upon obtaining the optimized load history stress states, $(\sigma_{ij})^S_k$, the stress component ranges for all possible load history combinations were calculated at the stress component level. The calculation procedure is identical to that defined for the maximum range of stress intensity calculation; i.e.,

$$(\overline{\sigma_{ij}})^S_{rt} = (\sigma_{ij})^S_r - (\sigma_{ij})^S_t.$$

The range of peak stress was used to calculate the range of principal stress; the range of peak stress intensity was calculated from the principal stress range. The calculational process was identical to that defined for the maximum range of stress intensity.

The fatigue usage factor (u) was calculated for load cycle (rt) from the fatigue curve in the Code with one half of the maximum range of principal peak stress difference and the number of load applications associated with cycle (rt). The total usage factor for all load cycles was calculated; the calculation process is indicated as follows:

$$u^S_{rt} = \left(\frac{n}{N}\right)^S_{rt}$$

$$u^S = \sum_{i=1}^{a} (u^S_{rt})_i$$

a = number of peak stress intensity ranges, $(SIJ)_{rt}$

N = number of allowable cycles for peak stress intensity range $(SIJ)_{rt}$ obtained from the fatigue curve

n = number of load applications associated with load cycle (rt).

The fatigue curves on Code Figure I-9.1, Design Fatigue Curves for Carbon, Low Alloy, and High Tensile Steels; and Figure I-9.2, Design Fatigue Curve for Austenitic Steels, Nickel-Chromium-Iron Alloy, Nickel-Iron-Chromium Alloy, and Nickel-Copper Alloy, were programmed into the post-processor. The applicable fatigue curve was logarithmicly interpolated for the number of allowable cycles (N) associated with each value of the alternating peak stress intensity range.

11.10 FATIGUE USAGE PRODUCED BY THERMAL STRATIFICATION

This section presents the results of the fatigue evaluations for the five plants for which on-site operating data had been obtained. All of the evaluations have been performed with the program [ ] c described in Section 11.9. The analysis sections selected for the elbow configuration are shown on Figures 11.10-1 and 11.10-2. Figure 11.10-1 shows the analysis sections used to evaluate the elbow transition root, and Figure 11.10-2 shows the analysis sections along the top and side of the weld counterbore region. [ ] a,c,e

The analysis sections selected for the straight pipe configuration are shown on Figures 11.10-3 to 11.10-5. Figure 11.10-3 shows the analysis

sections used to evaluate the pipe counterbore transition root, and Figure 11.10-4 shows the analysis sections around the nozzle counterbore transition root. The analysis sections along the top and side of the weld counterbore region are shown in Figure 11.10-5.

a,c The load conditions and number of occurrences for each plant are those identified on Tables 11.4.1 to 11.4.5 combined with a pressure load of [ ]. Two additional load conditions, pressure and ambient, were also included in the evaluation for each plant.

A maximum range of stress intensity analysis was performed prior to each fatigue evaluation to determine whether the simplified elastic plastic analysis procedure of Section NB-3228.3 would be required, and, if so, to calculate the K_e factor by which the peak alternating stresses are multiplied.

The expression of K_e specified in NB-3228.3 is nonconservative for stress intensity ranges less than twice the yield stress, and quickly becomes overly conservative at higher stress intensities. This evaluation uses a modified expression for K_e which is a much better approximation to the values of K_e derived from plastic analysis[16]. The comparisons of the Code and modified K_e to the results of plastic analysis are shown in Figure 11.10-6.

The sections to follow present the results of the fatigue evaluations for each of the [ ] plants analyzed.

a,c,e 11.10.1 [ ] FATIGUE EVALUATION

Figures 11.10-7 to 11.10-10 present the results of the fatigue evaluation for the nozzle/elbow weld area of [ ] The variation of fatigue usage factor with the angle around the elbow transition root is shown on Figure 11.10-7. The cross-hatched area represents the uncertainty range on the number of cycles. The uncertainty range of number of cycles is based on a [ ] of uncertainty on

actual number of cycles during the test period and a [ ] event similarity factor, i.e. the similarity of the test startup with all previous startup. This results in a total uncertainty range of [ ] for estimation of total number of cycles over the plant operating history. Note that the peak usage factors are well above 1.0 and occur at the [ ], matching the cracking observed at those locations. [ ]. | C

Figure 11.10-8 compares the usage factors calculated by the Code K_e with the modified K_e used in this evaluation. The Code K_e tends to magnify the peak usage factors and to narrow the region over which the higher usage factors occur, relative to the usage factors calculated with the modified K_e.

The variation of usage factors along the top and side of the counterbore region are shown in Figures 11.10-9 and 11.10-10. [ ]. | C

11.10.2 [ ] FATIGUE EVALUATION

The results from [ ], Line C fatigue evaluation are shown on Figures 11.10-11 to 11.10-13. The peak usage factors are greater than 1.0 and occur at the [ ]. Unlike the other plants, the highest fatigue damage [ ] is located on the [ ]. This correlates with the location of the deepest cracks for this plant. [ ]. | a,c,e

11.10.3 [ ] FATIGUE EVALUATION

The results for [ ], Line 1B fatigue evaluation are shown on Figures 11.10-14 to 11.10-17. The peak usage factors are well above 1.0 and occur at the [ ], correlating with observed crack locations.

Figure 11.10-15 is a comparison of the usage factors as calculated with the Code K_e and modified K_e for this plant. This comparison shows the same differences as noted in the comparison of the [ ] results.

a,c,e

Figures 11.10-16 and 11.10-17 show the axial variation of usage factors along the top and side of the counterbore region. Again, the peak usage factors are concentrated at the elbow transition root.

a,c,e

11.10.4 [ ] FATIGUE EVALUATION

The results for [ ], Line 13 fatigue evaluation are shown on Figures 11.10-18 to 11.10-21. The peak usage factors are well above 1.0 and occur at the [ ], correlating with crack locations observed in a limited UT exam.

C

Figure 11.10-19 is a comparison of the usage factors as calculated with the Code K_e and modified K_e for this plant. This comparison shows the same differences as noted in the comparison of the [ ] results.

a,c,e

Figures 11.10-20 and 11.10-21 show the axial variation of usage factors along the top and side of the counterbore region. [ ].

C

a,c,e

11.10.5 [ ] FATIGUE EVALUATION

The results for the [ ] fatigue evaluation are shown in Figures 11.10-22 to 11.10-24. The peak usage factors are located at [ ] which correlates with observed crack locations, [ ]. [

a,c

]. Since the number of occurrences of the stratified profiles used in the

evaluation is directly proportional to the number observed, which is, in turn, proportional to the length of time at low feedwater flow conditions, the extrapolation of the [ ] test data to the operating life of the plant could result in [ ] the number of stratified profiles by a factor of [ ]. [ ] a,c,e

Figures 11.10-23 and 11.10-24 show the axial variation of usage factors along the top and side of the counterbore region. [ ] a,c

11.10.6 SUMMARY

The results of the previous five sections are summarized in Table 11.10.1. Another way of presenting this data is as the percentage of each plant's operating history required to initiate a crack. This information is given as a function of angular location for each of the plants evaluated on Table 11.10.2. [ ] a,c

11.11 FATIGUE USAGE FACTORS FOR SINGLE HOT STANDBY CONDITION

The combined contribution from stratif ion and striping for a single hot standby event are presented in Tab e 11.11.1 This Table is based on linear summations of the maximum usage factors from stratification and striping at each generic profile. Since each generic profile corresponds to a region on the pipe circumference, the combined usage factor

is assigned to this region. Figure 11.11-1 through Figure 11.11-5 present the circumferential fatigue usage factors at the elbow transition root per single hot standby event for [ ] respectively. The shaded area in the figures are the range of the usage value due to uncertainties on the number of cycles during the event. Table 11.11.2 presents the percentage of the total hot standby events to date required to reach usage factor of one, for each generic profile at each power plant considered.

a,c,e

a,c,e [ ]

a.c,e

a,c,e

[redacted]

[ ] a,c,e

11.13 OBSERVATIONS ON THE EFFECT OF THERMAL STRATIFICATION AND ASSOCIATED STRIPING

The analysis described in the previous sections provided a best estimate of the contribution of thermal stratification to the feedwater line cracking. [ ] Only data from one period of low a,c

feedwater flow was available for each of the plants analyzed. This data had to be extrapolated to account for all of the hot standby and other low flow conditions experienced by a plant during its operating history. Practical considerations limited the number of generic temperature profiles and geometries which could be included in the analysis. Uncertainty factors were introduced in an attempt to account for the above sources of uncertainty, [

C

].

However, the fatigue usage factors produced by thermal stratification and the associated thermal striping are a good indication of the contribution of these phenomena to the observed feedwater line cracking. The calculated fatigue damage due to stratification dwarfs that produced by all other load conditions considered in Section 7. [

C

]. In addition, the location of the highest fatigue usage factors correlates well, both axially and circumferentially, with the observed crack locations. These high usage factors conclusively implicate thermal stratification and the associated thermal striping during low flow conditions as prime contributors to the observed feedwater line cracking.

11.14 REFERENCES

1. ASME Boiler and Pressure Vessel Code Section III, 1977 Edition; Nuclear Plant Components - Appendices.

2. Steam Generator Series 51 E-Spec, Volume 1, American Electric Power Service Corp., Donald C. Cook Nuclear Power Station Unit 1 and Unit 2. Shop Order AEP-120 Addendum 677029, Revision 5, February 27, 1976.

3. "51 Series Steam Generator Feedwater Nozzle Analysis", O. Bertsch 10/69, W Tampa Division.

4. ANSYS, Swanson Analysis Systems, Inc., Houston, PA.

5. WECAN, Westinghouse Computer Analysis, A General Finite-Element Program for Structural Analysis, Westinghouse Research Laboratories, 1973.

[ ] a,c,e

10. Rohsenow and Hartnett - "Handbook of Heat Transfer" - McGraw-Hill, Inc., Section 3 by P. J. Schneider.

[ ] a,c,e

14. Criteria of the ASME Boiler and Pressure Vessel Code for Design by Analysis in Sections III and VII, Division 2.

15. N. J. Muskhelishvili as translated by J. R. M. Radock, "Some Basic Problems of the Mathematical Theory of Elasticity", P. Noordhoff Ltd., Gronigen - Holland, 1953. See page 22.

[ ] a,c,e

TABLE 11.1.1

BILL OF MATERIALS

Configuration	Component	Material Designation
[		SA-533 Cl.2
		SA-508 Cl.2
		SA-106 GR.B
		SA-106 GR.B
		SA-533 Cl.2
		SA-508 Cl.2
		SA-508 Cl.1
		SA-106 Gr.B
		SA-106 Gr.B

a,c

TABLE 11.1.2 SA-533 CL 2

Properties \ Temp	70	100	150	200	300	350	400	500	600	650	700
E $\times 10^6$ psi	29.9	-	-	29.5	29.0	-	28.6	28.0	27.4	-	26.6
α 10^{-6} $in/_{in}$ ^oF	7.02	7.13	7.29	7.45	7.74	7.88	8.01	8.25	8.46	8.55	-
ρ 10^{-4} Lb $sec^2/_{in}$	7.345	7.342	-	7.330	7.312	-	7.291	7.268	7.247	7.238	-
ν -	0.3										
TC $BTU/_{hr,ft,^oF}$	23.3	23.6	24.1	24.4	24.7	24.7	24.6	24.2	23.5	23.2	-
TD ft^2/hr	.455	.451	.444	.437	.420	.409	.398	.377	.353	.340	-
Cp $BTU/_{in\ Lb\ ^oF/Sec^2}$	40.35	41.25	-	44.08	46.54	-	49.06	51.11	53.16	54.56	-

E - Moduli of Elasticity (Table I-6.0 of ASME Code)

α - Instantaneous Coefficient of Thermal Expansion (Table I - 5.0 of ASME Code)

ρ - Mass Density - Nuclear Systems Material Handbook

ν - Poison Ratio (Assumed to be constant in the Temperature Range)

TC - Coefficient of Thermal Conductivity (Table I-4.0 of ASME Code)

TD - Coefficient of Thermal Diffusivity (Table I-4.0 of ASME Code)

Cp - Specific Heats; Where $Cp = \frac{Tc}{\rho TD}$ (calculated values)

TABLE 11.1.3 SA-508 CL 2

Properties \ Temp	70	100	150	200	300	350	400	500	600	650	700
E $x10^6$ psi	29.9	-	-	29.5	29.0	-	28.6	28.0	27.4	-	26.6
α 10^{-6} $in/_{in}$ ^oF	6.41	6.53	6.73	6.95	7.30	7.49	7.60	8.03	8.33	8.51	-
ρ 10^{-4} Lb $sec^2/_{in}$	7.345	7.342	-	7.330	7.312	-	7.291	7.258	7.247	7.238	-
ν -	0.3										
TC $BTU/_{hr,ft,^oF}$	23.6	23.7	23.9	24.0	23.9	23.7	23.6	23.1	22.4	22.1	-
TD ft^2/hr	.454	.447	.437	.427	.406	.396	.385	.362	.339	.327	-
Cp $BTU/_{in\ Lb\ ^oF/Sec^2}$	40.96	41.79	-	44.37	46.59	-	48.65	50.81	52.77	54.04	-

E - Moduli of Elasticity (Table I-6.0 of ASME Code)

α - Instantaneous Coefficient of Thermal Expansion (Table I - 5.0 of ASME Code)

ρ - Mass Density - Nuclear Systems Material Handbook

ν - Poison Ratio (Assumed to be constant in the Temperature Range)

TC - Coefficient of Thermal Conductivity (Table I-4.0 of ASME Code)

TD - Coefficient of Thermal Diffusivity (Table I 4.0 of ASME Code)

Cp - Specific Heats; Where $Cp = \frac{Tc}{\rho T_D}$ (calculated values)

TABLE 11.1.4 SA-106 GRB (SA-234 WPB) AND SA-508 Cl. 1

Properties \ Temp	70	100	150	200	300	350	400	500	600	650	700
E $x10^6$ psi	27.9	-	-	27.7	27.4	-	27.0	26.4	25.7	-	24.8
α 10^{-6} in/in ^oF	5.60	5.83	6.20	6.55	7.18	7.47	7.73	8.18	8.55	8.70	-
ρ 10^{-4} Lb sec^2/in	7.345	7.342	-	7.330	7.312	-	7.291	7.268	7.247	7.238	-
ν -	0.3										
TC BTU/hr,ft,^oF	30.0	29.9	29.6	29.2	28.4	28.0	27.6	26.6	25.6	25.1	-
TD ft^2/hr	.582	.567	.544	.521	.481	.464	.447	.414	.385	.370	-
Cp BTU/in Lb $^oF/Sec^2$	40.61	41.57	-	44.25	46.73	-	49.01	51.16	53.10	54.24	

E - Moduli of Elasticity (Table I-6.0 of ASME Code)

α - Instantaneous Coefficient of Thermal Expansion (Table I - 5.0 of ASME Code)

ρ - Mass Density - Nuclear Systems Material Handbook

ν - Poison Ratio (Assumed to be constant in the Temperature Range)

TC - Coefficient of Thermal Conductivity (Table I-4.0 of ASME Code)

TD - Coefficient of Thermal Diffusivity (Table I 4.0 of ASME Code)

Cp - Specific Heats; Where $Cp = \frac{Tc}{\rho^1 D}$ (calculated values)

TABLE 11.1.5

CODE STRESS LIMITS

Mat.		Temp. °F 100°	200°	300°	400°	500°	600°	650°	700°
SA-533 CL 2	Sm	30.0	30.0	30.0	30.0	30.0	30.0	30.0	30.0
	Sy	70.0	66.6	64.5	63.0	62.4	61.9	61.2	60.0
	Su	90.0	90.0	90.0	90.0	90.0	90.0	90.0	90.0
SA-508 CL 2	Sm	26.7	26.7	26.7	26.7	26.7	26.7	26.7	26.7
	Sy	65.0	61.8	60.3	59.0	58.0	57.1	56.6	56.0
	Su	80.0	80.0	80.0	80.0	80.0	80.0	80.0	80.0
SA-106 GrB	Sm	20.0	20.0	20.0	20.0	18.9	17.3	17.0	16.8
	Sy	35.0	31.9	31.0	30.0	28.3	25.9	25.4	25.2
	Su	60.0	60.0	60.0	60.0	60.0	60.0	60.0	60.0
SA-508 Cl. 1	Sm	23.3	21.9	21.3	20.6	19.4	17.8	17.4	17.3
	Sy	36.0	32.8	31.9	30.8	29.1	26.6	26.1	25.9
	Su	70.0	70.0	70.0	70.0	70.0	70.0	70.0	70.0

a,c

TABLE 11.4.1

OPERATING HISTORY FOR [ ] LINE 21 DURING THERMAL STRATIFICATION

PROFILE TYPE	GENERIC ΔT	EVALUATION ΔT	SCALE FACTOR	NUMBER OF OCCURRANCES	TOTAL NUMBER	DURATI (MIN)
a,c						

TABLE 11.4.2

OPERATING HISTORY FOR [ ] LINE C DURING THERMAL STRATIFICATION [a,c,e]

PROFILE TYPE	GENERIC ΔT	EVALUATION ΔT	SCALE FACTOR	NUMBER OF OCCURRANCES	TOTAL NUMBER	DURATION (MIN)
[ ]						[a,c]

a,c,e

TABLE 11.4.3

OPERATING HISTORY FOR [ ], LINE 1B DURING THERMAL STRATIFICATION

PROFILE TYPE	GENERIC ΔT	EVALUATION ΔT	SCALE FACTOR	NUMBER OF OCCURRANCES	TOTAL NUMBER	DURATION (MIN)
a,c						

TABLE 11.4.4

OPERATING HISTORY FOR [ ], LINE 13 DURING THERMAL STRATIFICATION [a,c,e]

PROFILE TYPE	GENERIC ΔT	EVALUATION ΔT	SCALE FACTOR	NUMBER OF OCCURRANCES	TOTAL NUMBER	DURATION (MIN)
[						a,c]

a,c,e

TABLE 11.4.5

OPERATING HISTORY FOR [ ], LINE 2 DURING THERMAL STRATIFICATION

a,c

PROFILE TYPE	GENERIC ΔT	EVALUATION ΔT	SCALE FACTOR	NUMBER OF OCCURRANCES	TOTAL NUMBER	DURATION (MIN)

TABLE 11.7.1

BOUNDARY CONDITIONS FOR STRESS SOLUTIONS

Plane,[1] Surface Or Point	Pressure	All Thermal Stresses
1	UY = 0	UY = 0
2	$UY_{tan} = 0$	$UY_{tan} = 0$
3	UZ = 0	UZ = 0
4	P=-10626	--------
5	P=-10626	--------
6	P=[3]3709.35	L.C.E. (2)
7	P = 1000	--------

NOTES: (1) See Figure 11.7-1 for definition of these locations.

(2) Linear constraint equations were specified for this surface to ensure that the end of the pipe remained plane for the straight pipe model.

(3) For the straight pipe model this load was -5358.25 psi.

TABLE 11.7.2

FILM COEFFICIENTS FOR STRATIFIED THERMAL PROFILES

Model	Profile	Film Coefficients (BTU/hr - sq. ft.-°F) h_B	h_I	h_T
a,c	[redacted]			

TABLE 11.7.3

PEAK AXIAL STRESSES CAUSED BY THERMAL STRATIFICATION - ELBOW

Profile	Peak Stress	Location (Top 0°)
[		] a,c

NOTE: (1) All peak stresses are located on the inside surface except for this one.

TABLE 11.7.4

PEAK AXIAL STRESSES CAUSED BY THERMAL STRATIFICATION - STRAIGHT PIPE

a,c

Profile	Peak Stress	Location (Top 0°)
[redacted]	[redacted]	[redacted]

NOTE: (1) All peak stresses are located on the inside surface except for those produced by T_4.

a,b,c

Case	
1	
2	
3	
4	
5	
6	
7	

TABLE 11.8.1 FLOW TEST DATA FOR STRAIGHT PIPE CONFIGURATION WITH J-TUBE DISCHARGE

a,b,c

Case
8
9
10
11
12
13
14
15

TABLE 11.8.2 FLOW TEST DATA FOR STRAIGHT PIPE CONFIGURATION WITH BOTTOM DISCHARGE

a,b,c

| Case | | |

a,b
c

| Case | | |

a,b,c

Case

35

36

37

38

39

40

41

42

43

44

TABLE 11.8.4 FLOW TEST DATA FOR ELBOW CONFIGURATION WITH BOTTOM DISCHARGE

CASE 1 , TEST 8 TP8 CH5 A2 2380-2400 SEC

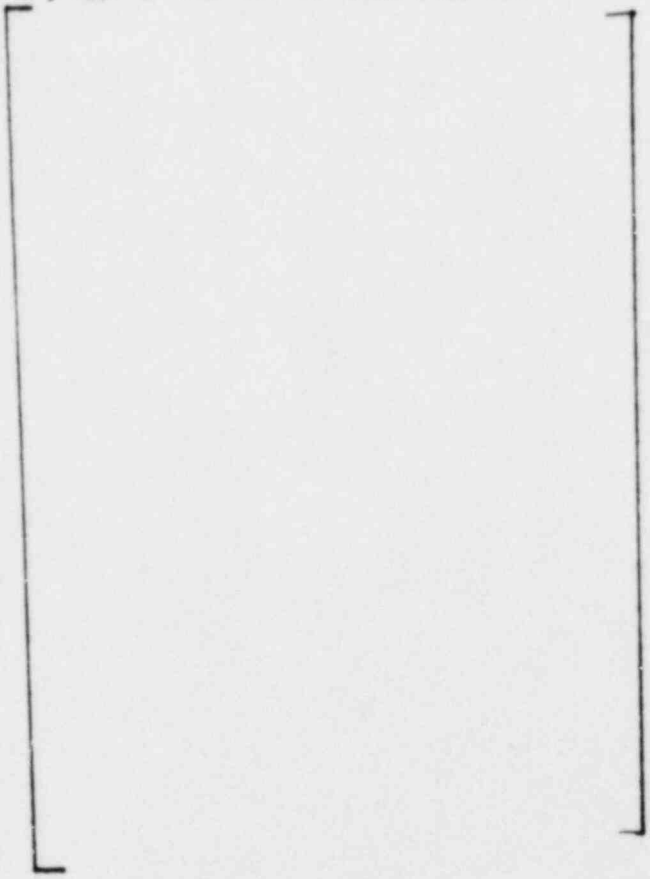

a,b,c,e

Case No. : 1

Generic Profile: T_2

Run No. : [ ]

TABLE 11.8.5 CASE NO. 1, MAXIMUM, MINIMUM AND ALTERNATING THERMAL STRESSES

CASE 2 , TEST 8 TP9 CH4 R3 4050-4070 SEC

TOTAL STRESS RANGES

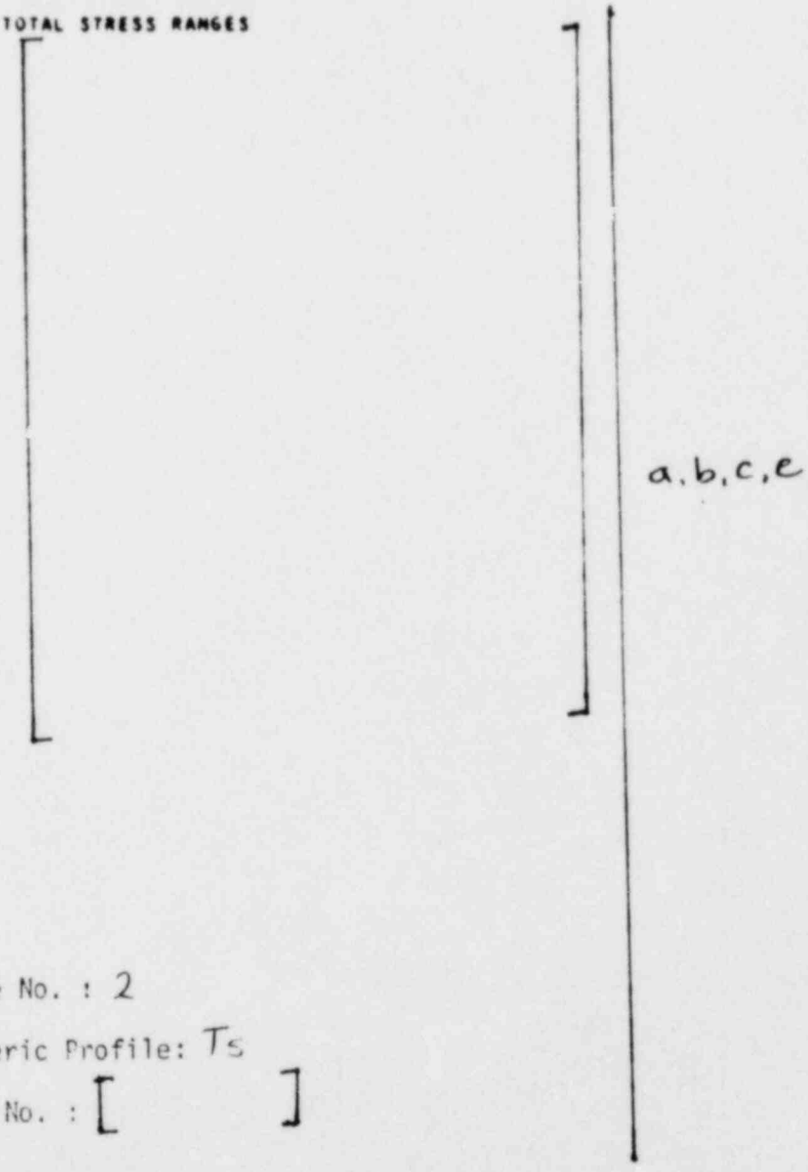

Case No. : 2

Generic Profile: Ts

Run No. : [ ]

TABLE 11.8.6 CASE NO. 2, MAXIMUM, MINIMUM AND ALTERNATING THERMAL STRESSES

CASE 3 , TEST 8 TP7 CH9 R1 6450-6470 SEC

TOTAL STRESS RANGES

[ ]

a,b,c,e

Case No. : 3

Generic Profile: T3

Run No. : [ ]

TABLE 11.3.7 CASE NO. 3, MAXIMUM, MINIMUM AND ALTERNATING THERMAL STRESSES

CASE 4 , TEST 8 TPB CHB R2 5880-5900 SEC

TOTAL STRESS RANGES

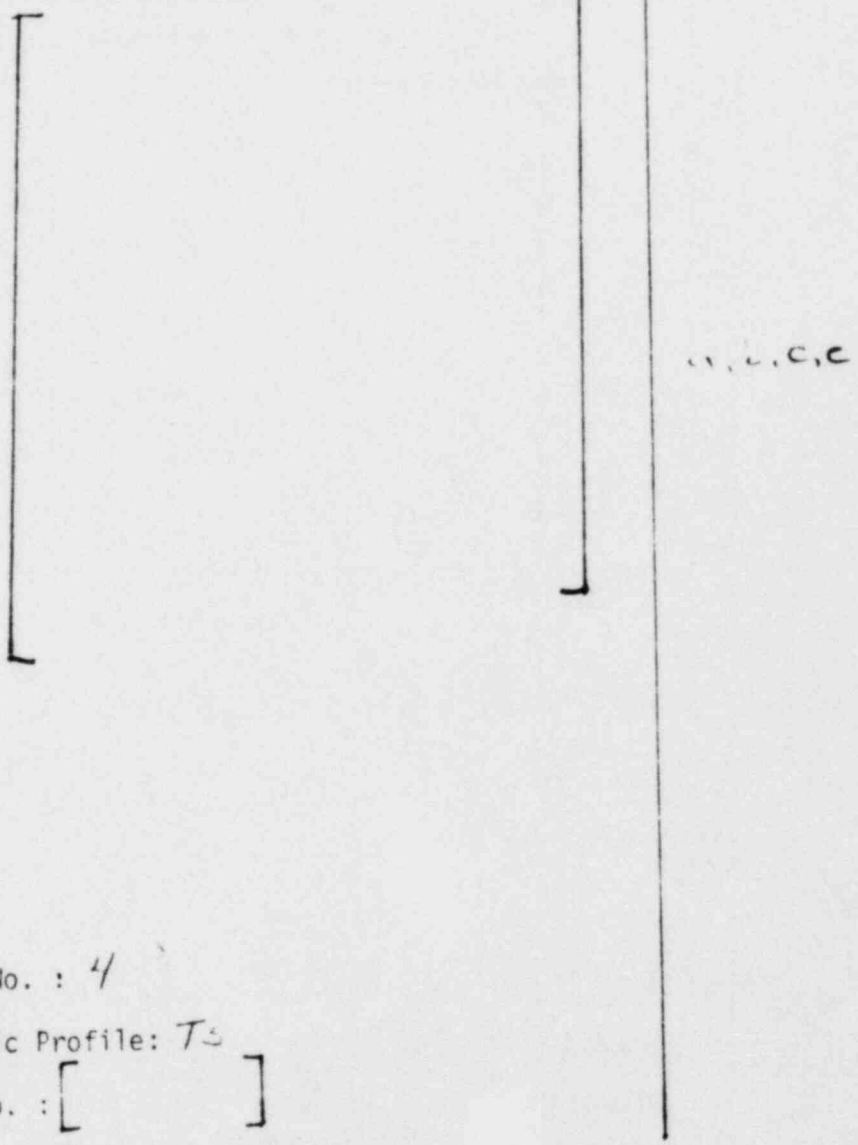

a, c, c, c

Case No. : 4

Generic Profile: T5

Run No. : [ ]

TABLE 11.8.8 CASE NO. 4, MAXIMUM, MINIMUM AND ALTERNATING THERMAL STRESSES

CASE 5 , TEST 9 TP8 CH3 R2 1160-1180 SEC

TOTAL STRESS RANGES

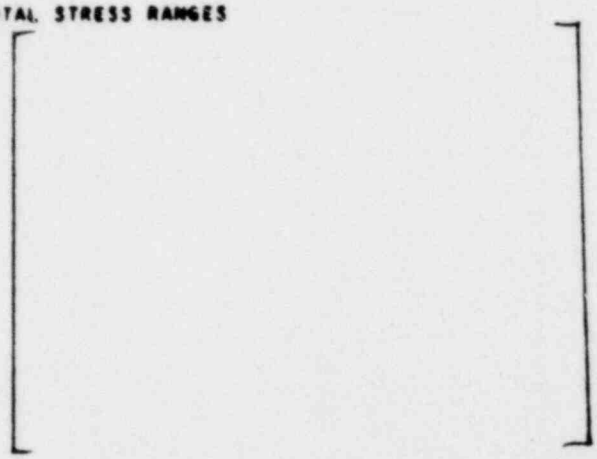

a,b,c,e

Case No. : 5

Generic Profile: T3

Run No. : [ ]

TABLE 11.8.9 CASE NO. 5, MAXIMUM, MINIMUM AND ALTERNATING THERMAL STRESSES

CASE 6 , TEST 9 TP9 CH7 R2 1140-1160 SEC

TOTAL STRESS RANGES

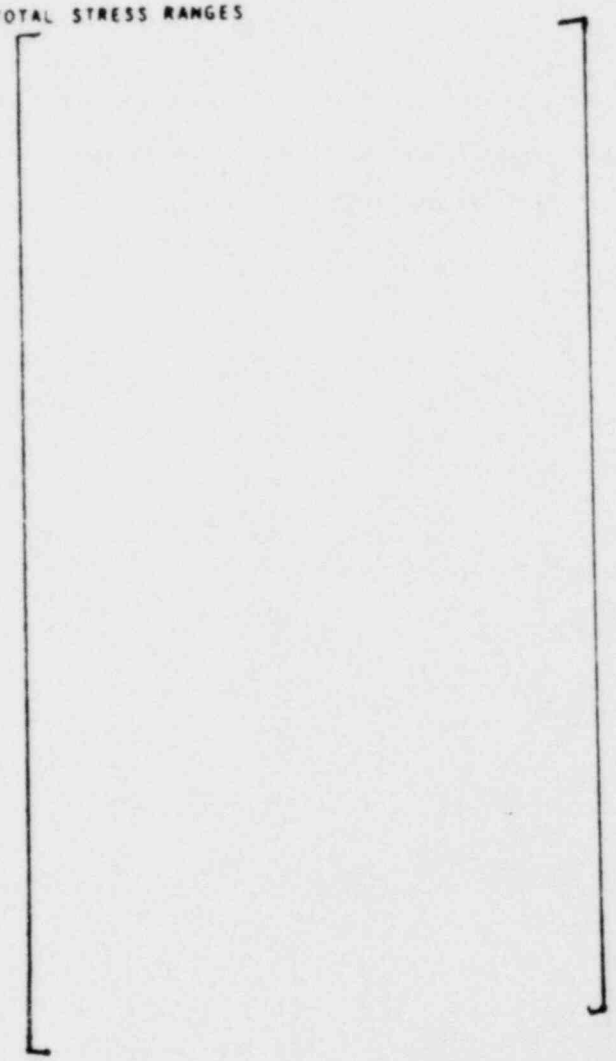

a,b,c,e

Case No. : 6

Generic Profile: T3

Run No. : [ ]

TABLE 11.8.10 CASE NO. 6, MAXIMUM, MINIMUM AND ALTERNATING THERMAL STRESSES

CASE 7 , TEST 9 TP7 CH6 R1 1910-1930 SEC

TOTAL STRESS RANGES

a,b,c,e

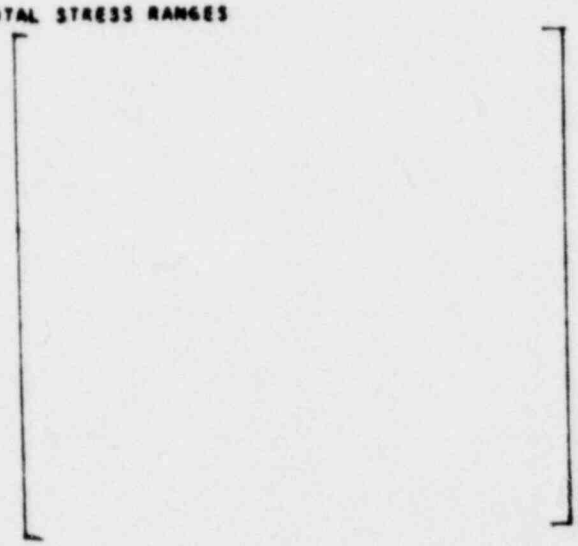

Case No. : 7

Generic Profile: T_1

Run No. : [ ]

TABLE 11.8.11 CASE NO. 7, MAXIMUM, MINIMUM AND ALTERNATING THERMAL STRESSES

CASE 8 , TEST 10 TP12 CH13 R3 2090-2130 SEC

TOTAL STRESS RANGES

[ ]

a,b,c,e

Case No. : 8

Generic Profile: T2

Run No. : [ ]

TABLE 11.8.12 CASE NO. 8, MAXIMUM, MINIMUM AND ALTERNATING THERMAL STRESSES

CASE 9 , TEST 10 TP12 CH13 R3 2150-2190 SEC

TOTAL STRESS RANGES

[ ]

a.b.c.e

Case No. : 9

Generic Profile: T2

Run No. : [ ]

TABLE 11.8.13 CASE NO. 9, MAXIMUM, MINIMUM AND ALTERNATING THERMAL STRESSES

CASE 10 , TEST 10 TP11 CH4 R2 5930-5970 SEC

TOTAL STRESS RANGES

[ ]

a,b,c,e

Case No. : 10

Generic Profile: T5

Run No. : [ ]

TABLE 11.8.14 CASE NO. 10, MAXIMUM, MINIMUM AND ALTERNATING THERMAL STRESSES

CASE 11 , TEST 10 TP11 CHB R2 5920-5960 SEC

TOTAL STRESS RANGES

a,b,c,e

Case No. : 11

Generic Profile: T5

Run No. : [ ]

TABLE 11.8.15 CASE NO. 11, MAXIMUM, MINIMUM AND ALTERNATING THERMAL STRESSES

CASE 12 , TEST 11 TP11 CH4 A2 1280-.300 SEC

TOTAL STRESS RANGES

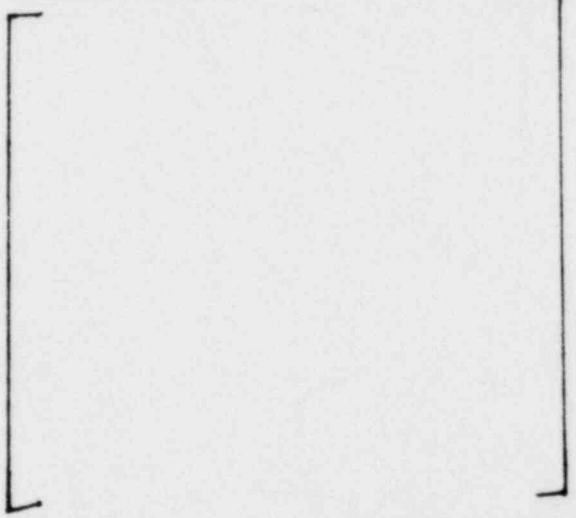

a,b,c,e

Case No. : 12

Generic Profile: T5

Run No. : [ ]

TABLE 11.8.16 CASE NO. 12, MAXIMUM, MINIMUM AND ALTERNATING THERMAL STRESSES

CASE 13 , TEST 11 TP11 CH8 R2 1270-1290 SEC

TOTAL STRESS RANGES

[ ]

a,b,c,e

Case No. : 13

Generic Profile: Ts

Run No. : [ ]

TABLE 11.8.17 CASE NO. 13, MAXIMUM, MINIMUM AND ALTERNATING THERMAL STRESSES

CASE 14 , TEST 11 TP11 CH3 R2 1860-1880 SEC

TOTAL STRESS RANGES

[ ]

a,b,c,e

Case No. : 14

Generic Profile: T_3

Run No. : [ ]

TABLE 11.8.18 CASE NO. 14, MAXIMUM, MINIMUM AND ALTERNATING THERMAL STRESSES

CASE 15 , TEST 11 TP11 CH7 R2 1880-2000 SEC

TOTAL STRESS RANGES

[ ]

a,b,c,e

Case No. : 15

Generic Profile: T3

Run No. : [ ]

TABLE 11.8.19 CASE NO. 15, MAXIMUM, MINIMUM AND ALTERNATING THERMAL STRESSES

CHANNEL 3 TEST 13 TP13 R-1 2476-2496 SEC

TOTAL STRESS RANGES

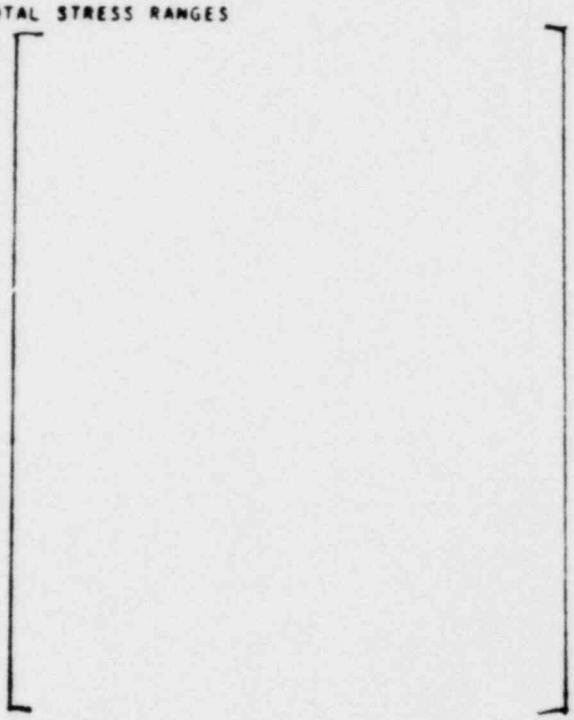

a,b,c,e

Case No. : 16

Generic Profile: T6

Run No. : [ ]

TABLE 11.8.20 CASE NO. 16, MAXIMUM, MINIMUM AND ALTERNATING THERMAL STRESSES

CHANNEL 3 TEST 14 TP13 R-1 940-960 SEC

TOTAL STRESS RANGES

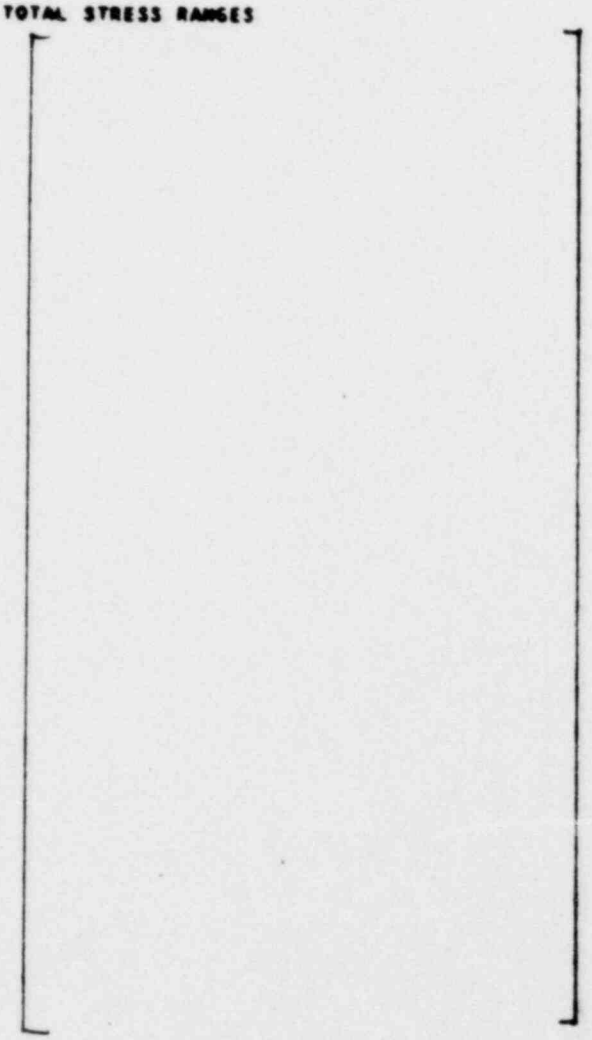

a,b,c,e

Case No. : 17

Generic Profile: T2

Run No. : [ ]

TABLE 11.8.21 CASE NO. 17, MAXIMUM, MINIMUM AND ALTERNATING THERMAL STRESSES

CASE 18, TEST 14 TP14 CH12 R2 1480-1500 SEC

TOTAL STRESS RANGES

[ ]

a,b,c,e

Case No. : 18

Generic Profile: Tz

Run No. : [ ]

TABLE 11.8.22 CASE NO. 18, MAXIMUM, MINIMUM AND ALTERNATING THERMAL STRESSES

CASE 19, TEST 14 TP14 CH 5 R2 1818-1838 SEC

TOTAL STRESS RANGES

a,b,c,e

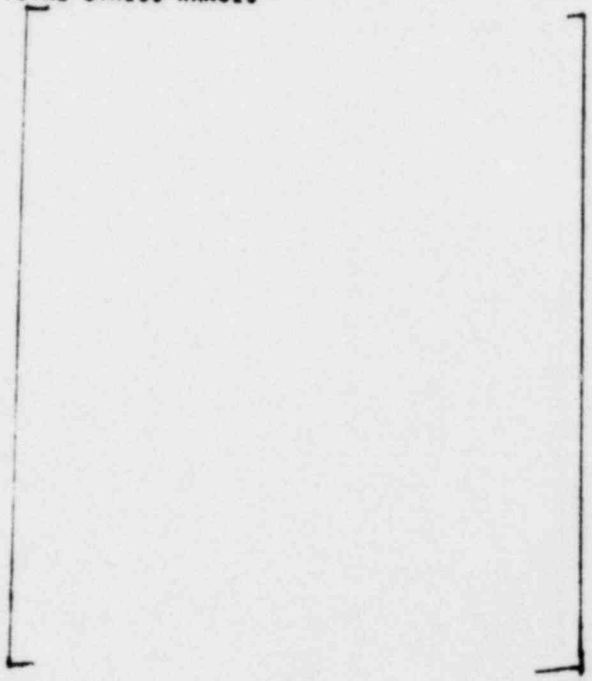

Case No. : 19

Generic Profile: T_2

Run No. : [ ]

TABLE 11.8.23 CASE NO. 19, MAXIMUM, MINIMUM AND ALTERNATING THERMAL STRESSES

CHANNEL 3 TEST 14 TP13 R-1 2120-2140 SEC

TOTAL STRESS RANGES

[ ]

a,b,c,e

Case No. : 20

Generic Profile: T5

Run No. : [ ]

TABLE 11.8.24 CASE NO. 20, MAXIMUM, MINIMUM AND ALTERNATING THERMAL STRESSES

CHANNEL 3 TEST 15 TP13 A-1 535-555 SEC

TOTAL STRESS RANGES

a,b,c,e

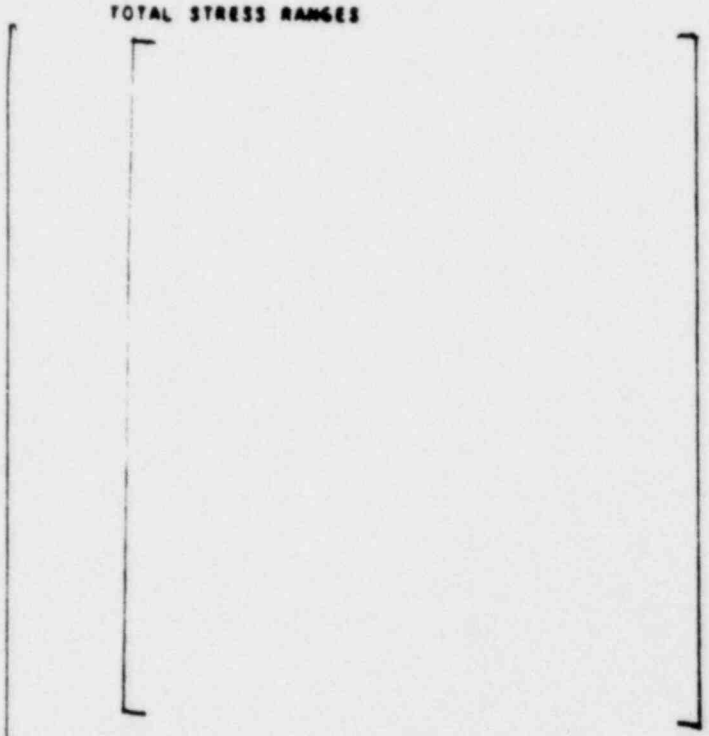

Case No. : 21

Generic Profile: T5

Run No. : [ ]

TABLE 11.8.25 CASE NO. 21, MAXIMUM, MINIMUM AND ALTERNATING THERMAL STRESSES

CHANNEL 3 TEST 15 TP13 R-1 845-865 SEC

TOTAL STRESS RANGES

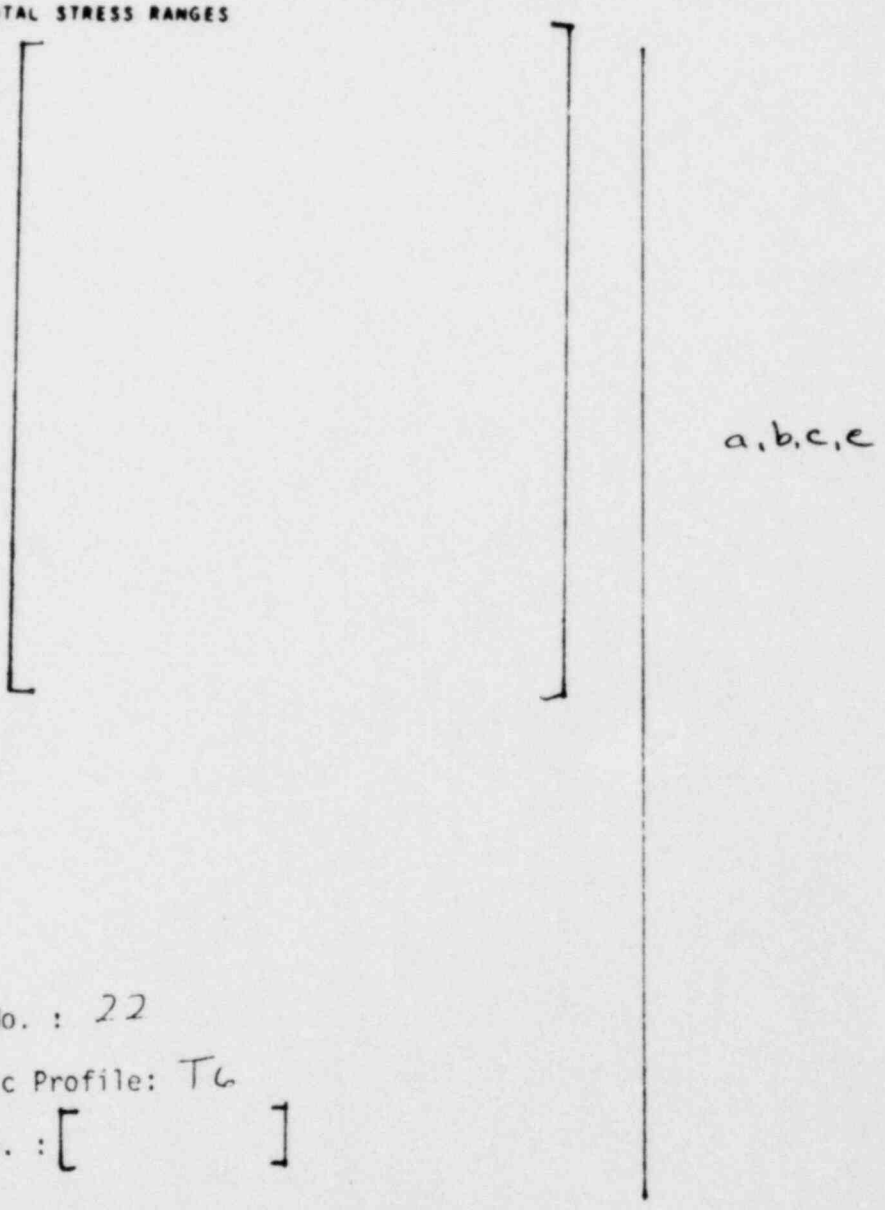

a,b,c,e

Case No. : 22

Generic Profile: T6

Run No. : [ ]

TABLE 11.8.26 CASE NO. 22, MAXIMUM, MINIMUM AND ALTERNATING THERMAL STRESSES

CHANNEL 4 TEST 15 TP13 R-1 840-860 SEC

TOTAL STRESS RANGES

a,b,c,e

[ ]

Case No. : 23

Generic Profile: T6

Run No. : [ ]

TABLE 11.8.27 CASE NO. 23, MAXIMUM, MINIMUM AND ALTERNATING THERMAL STRESSES

CHANNEL 3 TEST 16 TP13 R-1 585-605 SEC

TOTAL STRESS RANGES

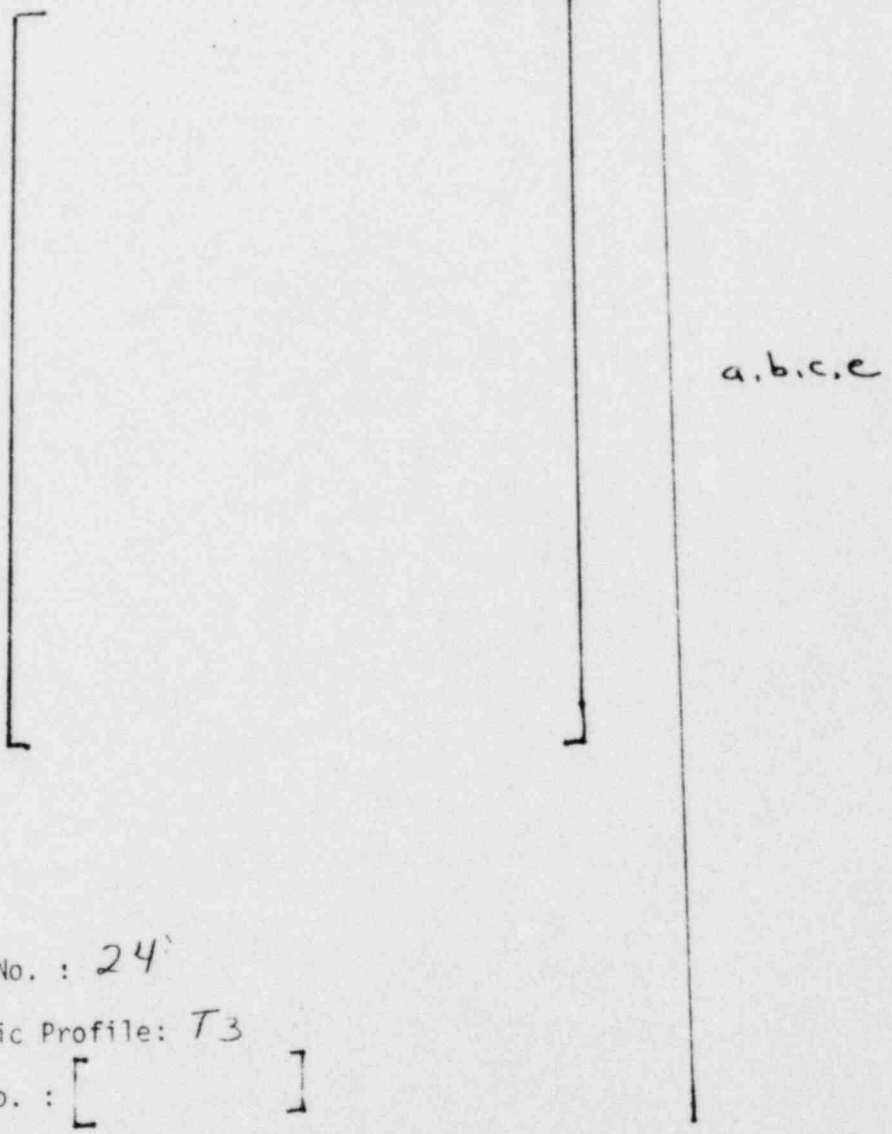

a,b,c,e

Case No. : 24

Generic Profile: T3

Run No. : [ ]

TABLE 11.8.28 CASE NO. 24, MAXIMUM, MINIMUM AND ALTERNATING THERMAL STRESSES

CHANNEL 3 TEST 16 TP13 R-1 540-560 SEC

TOTAL STRESS RANGES

a,b,c,e

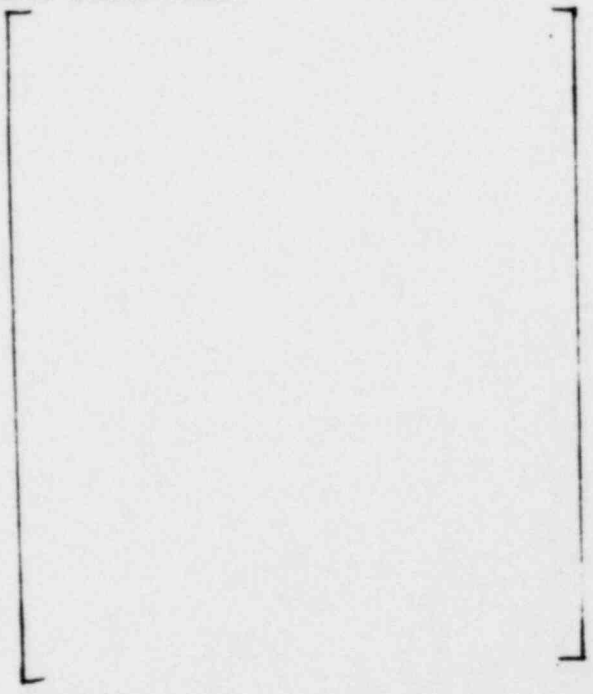

Case No. : 25

Generic Profile: T3

Run No. : [ ]

TABLE 11.8.29 CASE NO. 25, MAXIMUM, MINIMUM AND ALTERNATING THERMAL STRESSES

CHANNEL 3 TEST 17 TP13 R-1 390-410 SEC

TOTAL STRESS RANGES

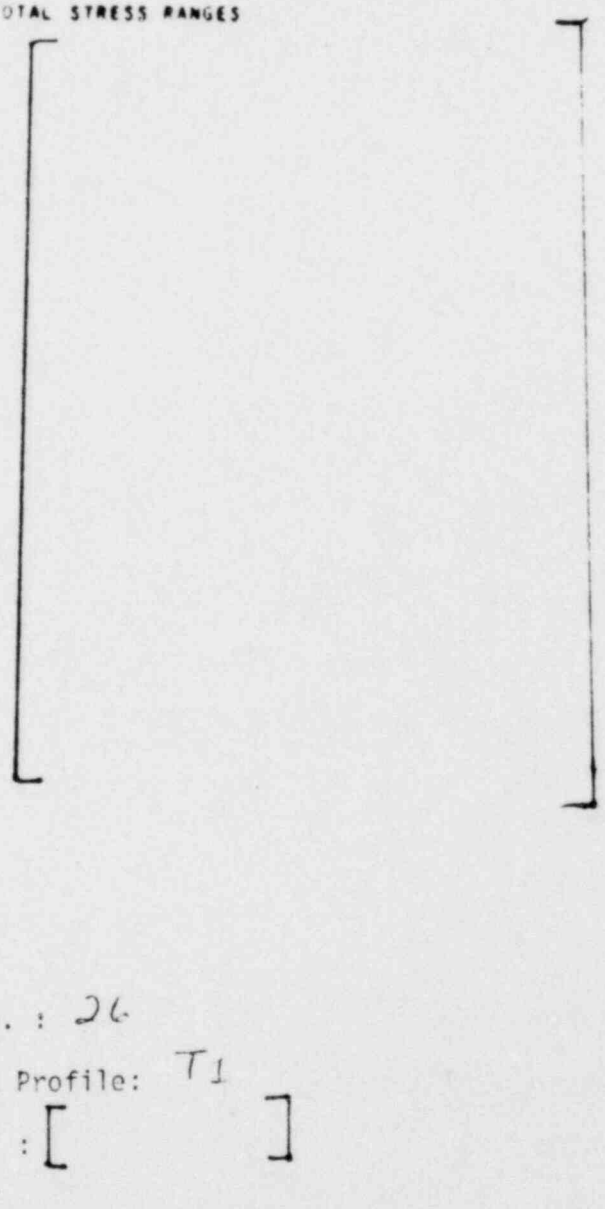

a,b,c,e

Case No. : 26

Generic Profile: T1

Run No. : [ ]

TABLE 11.8.30 CASE NO. 26, MAXIMUM, MINIMUM AND ALTERNATING THERMAL STRESSES

CHANNEL 3 TEST 17 TP13 R-1 470-490 SEC

TOTAL STRESS RANGES

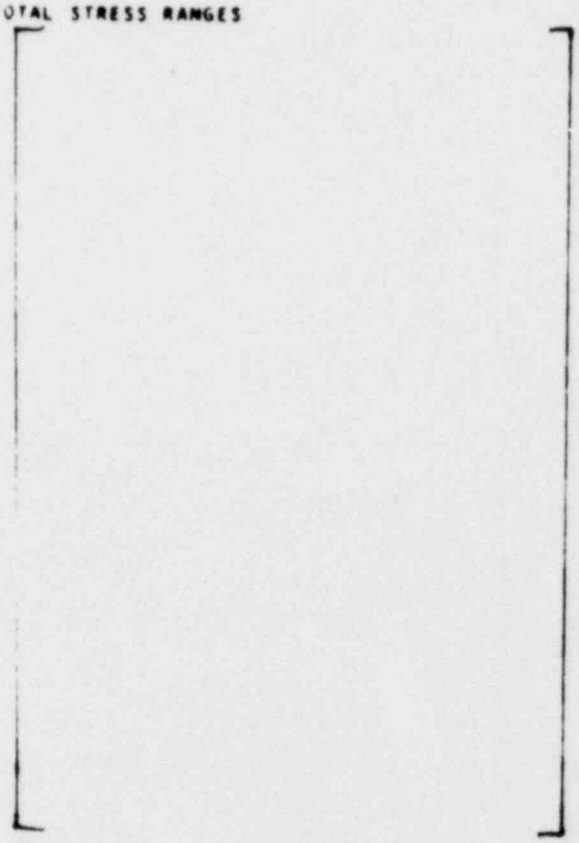

a,b,c,e

Case No. : 27

Generic Profile: T1

Run No. : [ ]

TABLE 11.8.31 CASE NO. 27, MAXIMUM, MINIMUM AND ALTERNATING THERMAL STRESSES

CHANNEL 7 TEST 18 TP15 R-7 310-330 SEC

TOTAL STRESS RANGES

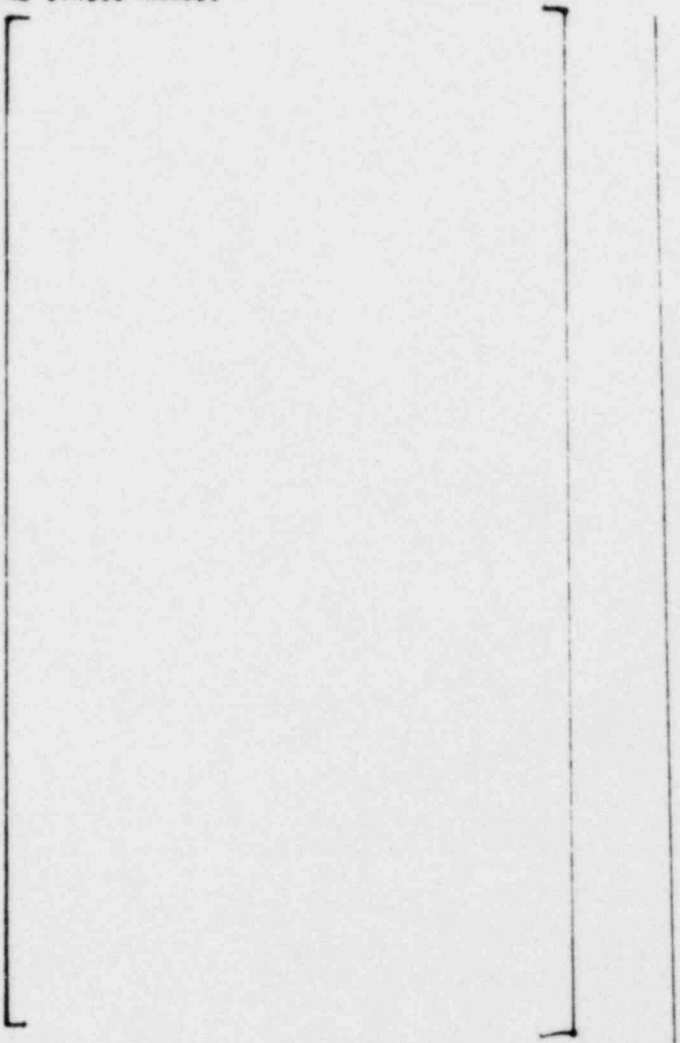

a,b.c,e

Case No. : 28

Generic Profile: T5

Run No. : [ ]

TABLE 11.8.32 CASE NO. 28, MAXIMUM, MINIMUM AND ALTERNATING THERMAL STRESSES

CHANNEL 14 TEST 18 TP15 R-3 360-380 SEC

TOTAL STRESS RANGES

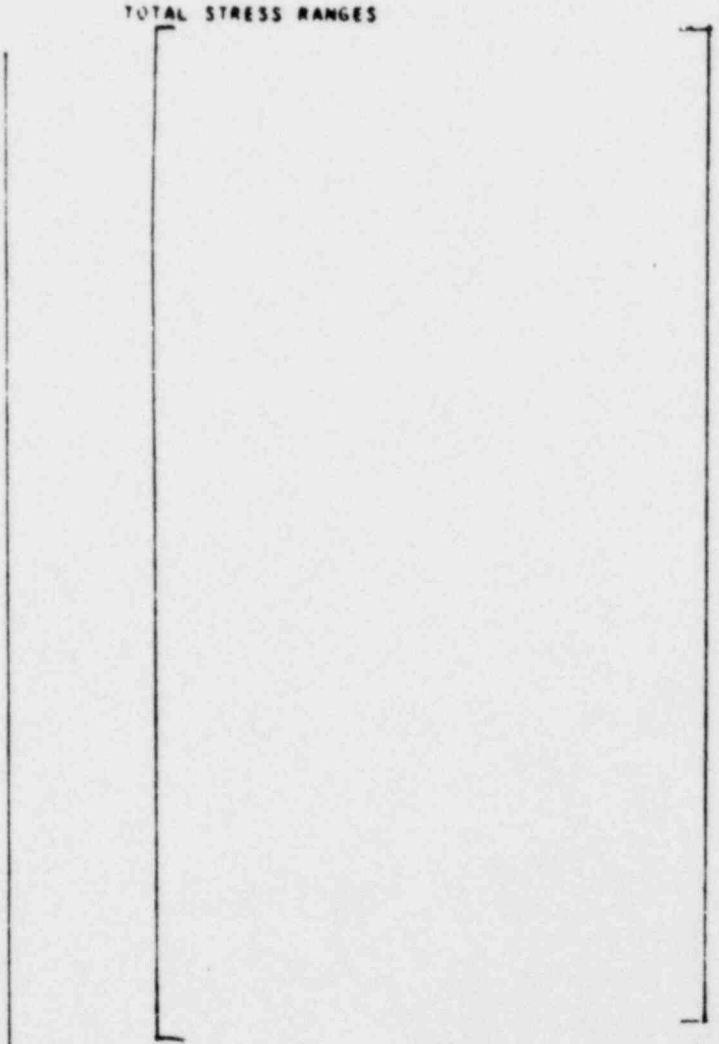

a,b,c,e

Case No. : 29

Generic Profile: T5

Run No. : [ ]

TABLE 11.8.33 CASE NO. 29, MAXIMUM, MINIMUM AND ALTERNATING THERMAL STRESSES

CHANNEL 14 TEST 18 TP15 R-3 510 530 SEC

TOTAL STRESS RANGES

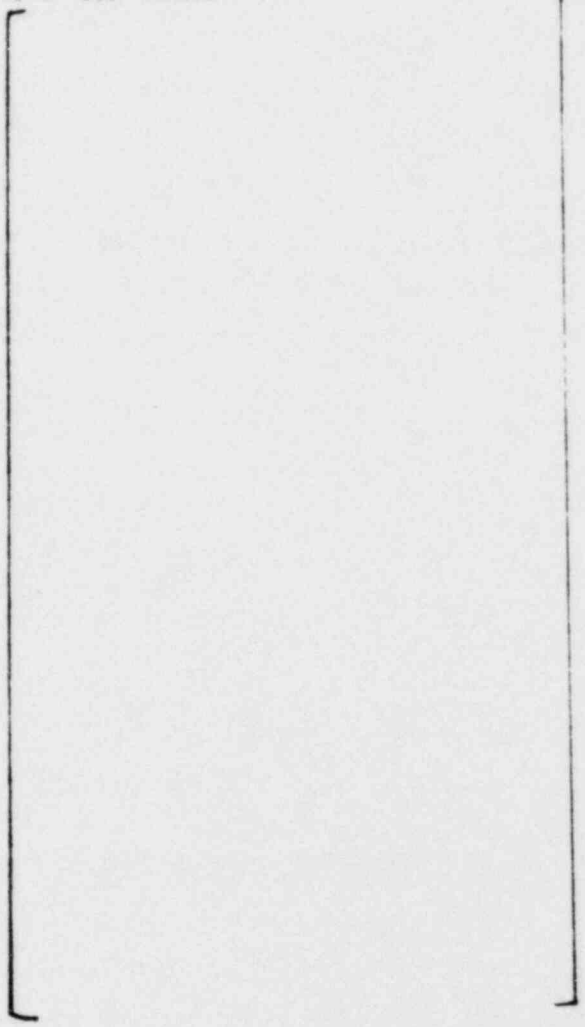

a,b,c,e

Case No. : 30

Generic Profile: T3

Run No. : [ ]

TABLE 11.8.34 CASE NO. 30, MAXIMUM, MINIMUM AND ALTERNATING THERMAL STRESSES

CASE 31, TEST 18 TP14 CH 4 A2 495- 515 SEC

TOTAL STRESS RANGES

[ ]

a,b,c,e

Case No. : 31

Generic Profile: T3

Run No. : [ ]

TABLE 11.8.35 CASE NO. 31, MAXIMUM, MINIMUM AND ALTERNATING THERMAL STRESSES

CHANNEL 4 TEST 18 TP13 R-1 490-510 SEC

TOTAL STRESS RANGES

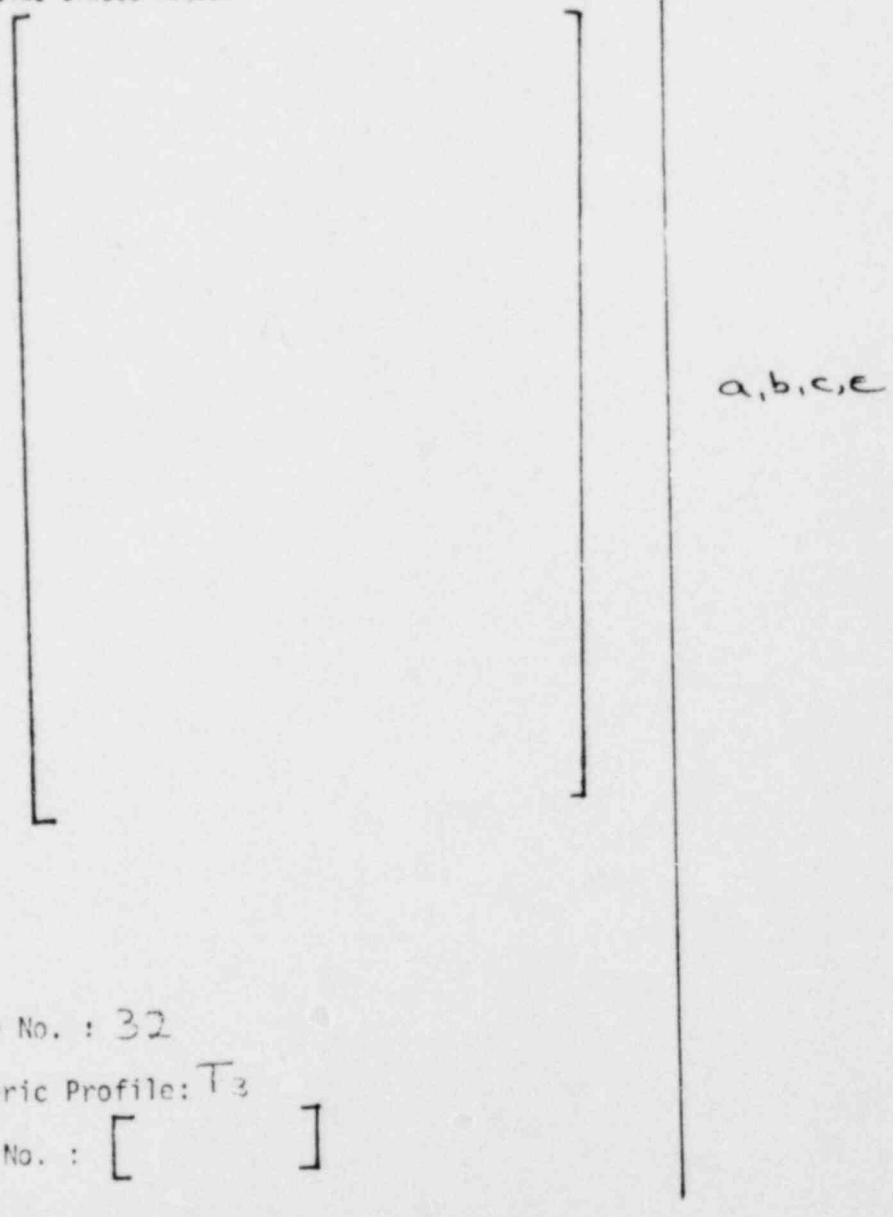

a,b,c,e

Case No. : 32

Generic Profile: T3

Run No. : [ ]

TABLE 11.8.36 CASE NO. 32, MAXIMUM, MINIMUM AND ALTERNATING THERMAL STRESSES

BLANK

Case No. : 33

Generic Profile:

Run No. :

TABLE 11.8.37 CASE NO. 33, MAXIMUM, MINIMUM AND ALTERNATING THERMAL STRESSES

CASE 34, TEST 18 TP14 CH 3 R2 680-700 SEC

TOTAL STRESS RANGES

[ ]

a,b,c,e

Case No. : 34

Generic Profile: T_3

Run No. : [ ]

TABLE 11.8.38 CASE NO. 34, MAXIMUM, MINIMUM AND ALTERNATING THERMAL STRESSES

a,b,c,e

CHANNEL 3 TEST 19 TP16 A-1 194-214 SEC

TOTAL STRESS RANGES

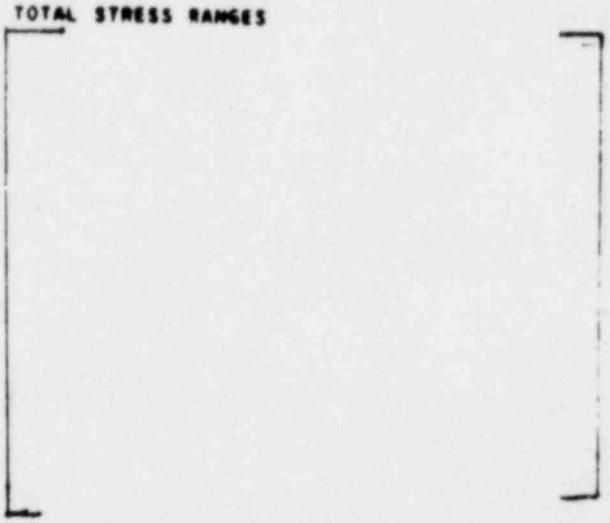

Case No. : 35

Generic Profile: T4

Run No. : [ ]

TABLE 11.8.39 CASE NO. 35, MAXIMUM, MINIMUM AND ALTERNATING THERMAL STRESSES

CASE 36, TEST 19 TP16 CH 8 R1 586-606 SEC

TOTAL STRESS RANGES

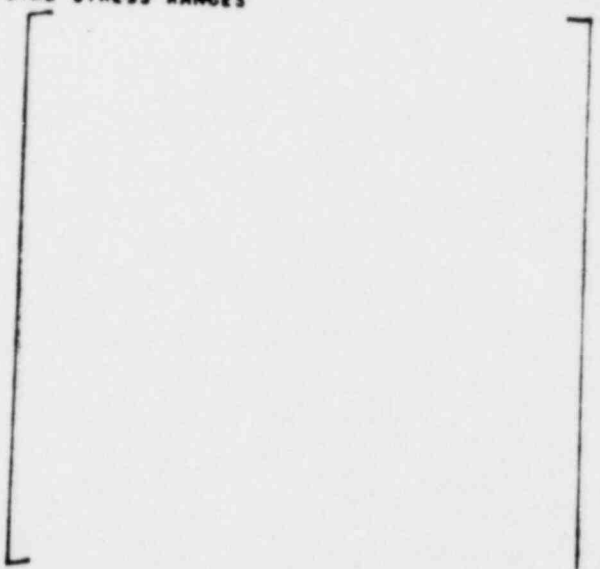

a,b,c,e

Case No. : 36

Generic Profile: T,

Run No. : [ ]

TABLE 11.8.40 CASE NO. 36, MAXIMUM, MINIMUM AND ALTERNATING THERMAL STRESSES

CHANNEL 3 TEST 20 TP16 R-1 920-940 SEC

TOTAL STRESS RANGES

a,b,c,e

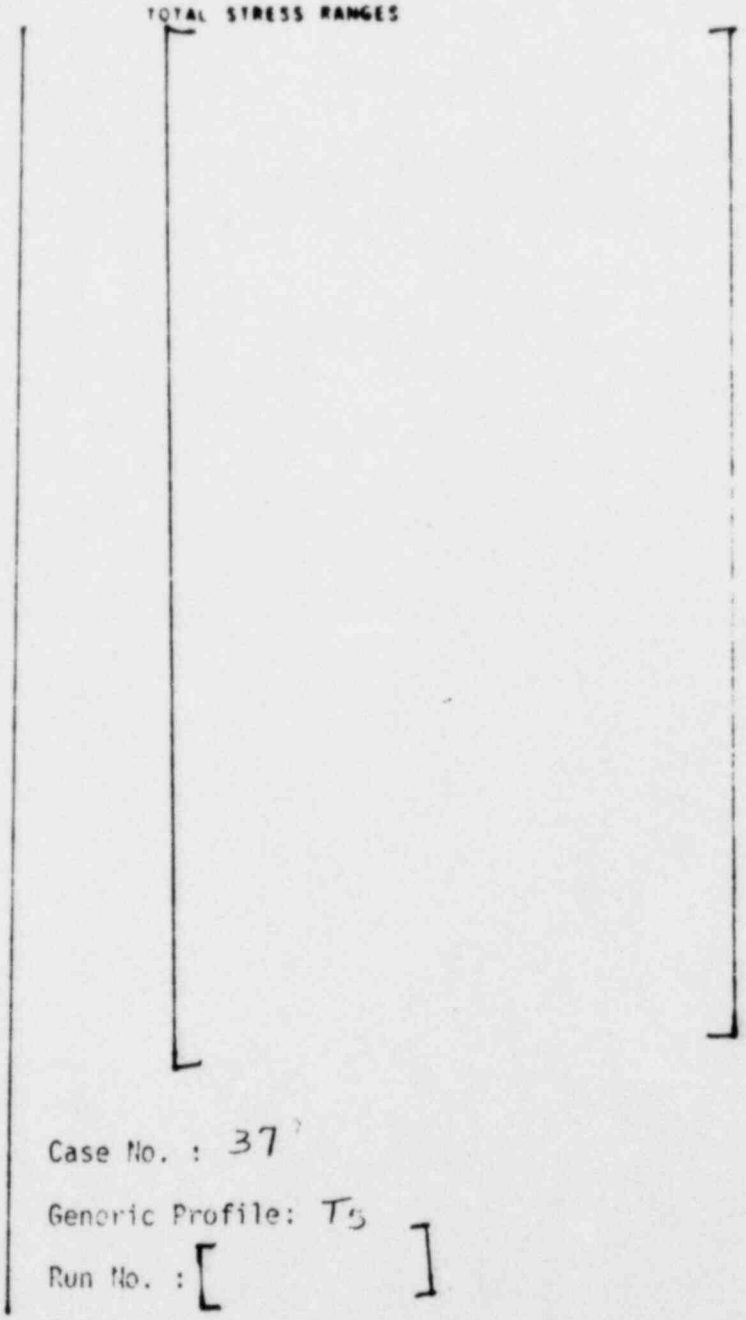

Case No. : 37

Generic Profile: T5

Run No. : [ ]

TABLE 11.8.41 CASE NO. 37, MAXIMUM, MINIMUM AND ALTERNATING THERMAL STRESSES

BLANK

Case No. : 38

Generic Profile:

Run No. :

TABLE 11.8.42 CASE NO. 38, MAXIMUM, MINIMUM AND ALTERNATING THERMAL STRESSES

CHANNEL 3 YEST 20 TP16 R-1 1750-1770 SEC

TOTAL STRESS RANGES

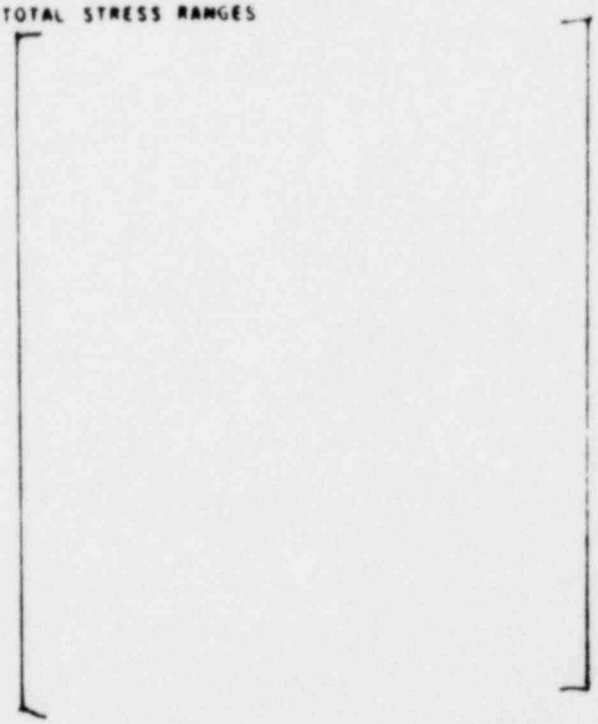

a,b,c,e

Case No. : 39

Generic Profile: T6

Run No. : [ ]

TABLE 11.8.43 CASE NO. 39, MAXIMUM, MINIMUM AND ALTERNATING THERMAL STRESSES

CHANNEL 3 TEST 20 TP16 A-1 1805-1825 SEC

TOTAL STRESS RANGES

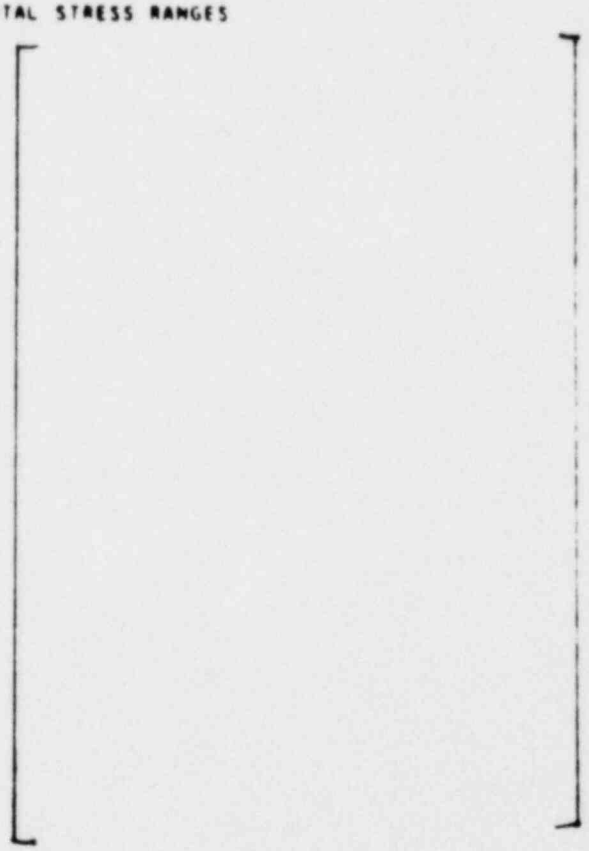

a.b.c.e

Case No. : 40

Generic Profile: T6

Run No. : [ ]

TABLE 11.8.44 CASE NO. 40, MAXIMUM, MINIMUM AND ALTERNATING THERMAL STRESSES

CHANNEL 4 TEST 21 TP16 R-1 320-340 SEC

TOTAL STRESS RANGES

a,b,c,e

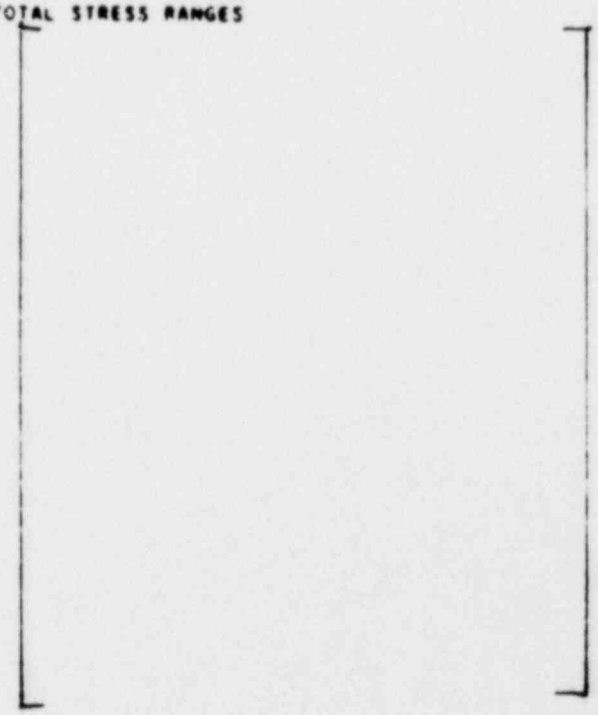

Case No. : 41

Generic Profile: T6

Run No. : [ ]

TABLE 11.8.45 CASE NO. 41, MAXIMUM, MINIMUM AND ALTERNATING THERMAL STRESSES

CASE 42, TEST 21 TP16 CH 8 R1 635-655 SEC

TOTAL STRESS RANGES

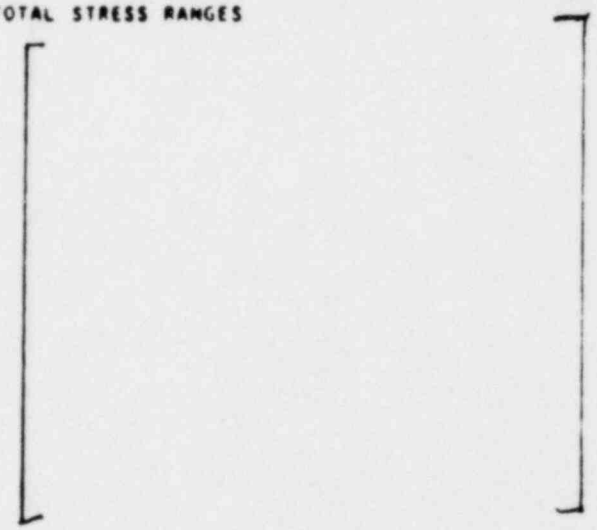

a,b,c,e

Case No. : 42

Generic Profile: T1

Run No. : [ ]

TABLE 11.8.46 CASE NO. 42, MAXIMUM, MINIMUM AND ALTERNATING THERMAL STRESSES

CHANNEL 4 TEST 22 TP16 R-1 775-795 SEC

TOTAL STRESS RANGES

a,b,c,e

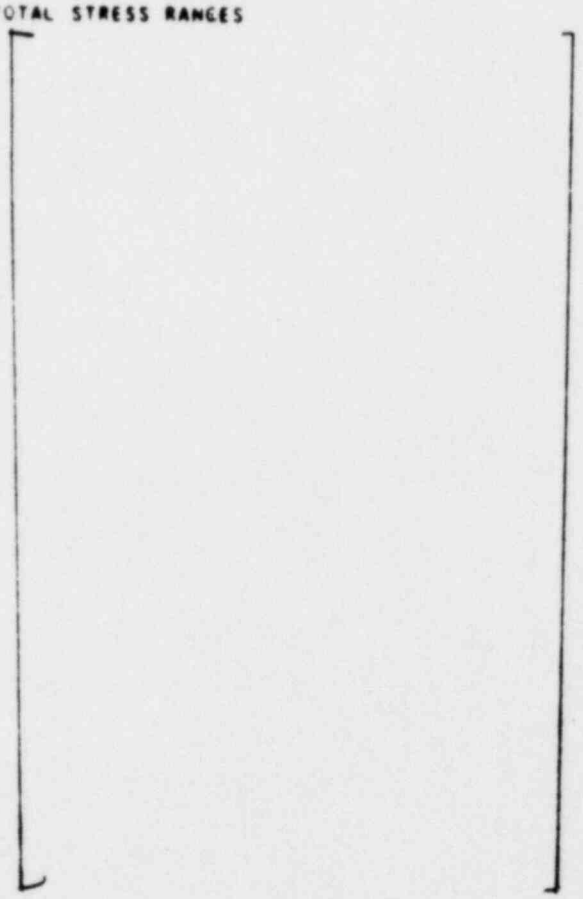

Case No. : 43

Generic Profile: T6

Run No. : [ ]

TABLE 11.8.47 CASE NO. 43, MAXIMUM, MINIMUM AND ALTERNATING THERMAL STRESSES

CASE 44, TEST 22 TP17 CH 4 A2 910-930 SEC

TOTAL STRESS RANGES

[ ] a,b,c,e

Case No. : 44

Generic Profile: T_3

Run No. : [ ]

TABLE 11.8.48 CASE NO. 44, MAXIMUM, MINIMUM AND ALTERNATING THERMAL STRESSES

a,c

ELBOW - CONFIGURATION

TABLE 11.8.49: POTENTIAL TEMPERATURES AND TIME DURATIONS (MINUTES) OF GENERIC PROFILE IN POWER PLANTS

TABLE 11.8.50

FATIGUE USAGE FACTOR - ELBOW CONFIGURATION

a,c,e

Generic Profile	Case #	Interface Level	FATIGUE USAGE FACTOR
T_1	26		
	27		
	36		
	42		
T_2	17		
	18		
	19		
T_3	24		
	25		
	30		
	31		
	32		
	34		
	44		
T_5	20		
	21		
	28		
	29		
	37		
	38		

TABLE 11.8.50

(CONTINUED)

Generic Profile	Case #	Interface Level	FATIGUE USAGE FACTOR
T_6	18.		[redacted]
	22.		
	23		
	38.		
	39.		
	40.		
	41.		
	43.		

TABLE 11.10.1

SUMMARY OF FATIGUE USAGE PRODUCED BY THERMAL STRATIFICATION

a,c,e

Plant	Range of Usage Factors	Location
[		[ ]

TABLE 11.10.2

u.c.e

PERCENTAGE OF HOT STANDBYS REQUIRED TO INITIATE CRACKING
(STRATIFICATION ONLY)

Node	Angle (Top = 0°)	[
3405		
3415		
3425		
3445		
3455		
3465		
3475		

NOTE: [

TABLE 11.11.1

COMBINED USAGE FACTORS FROM STRATIFICATIONS AND STRIPING

PER SINGLE HOT STANDBY EVENT

a,c,e

	Plant
Generic Profile Generic Profile	
T_1	
T_2	
T_3	
T_4	
T_5	
T_6	
Total Hot Standby To Date	

a,c,e

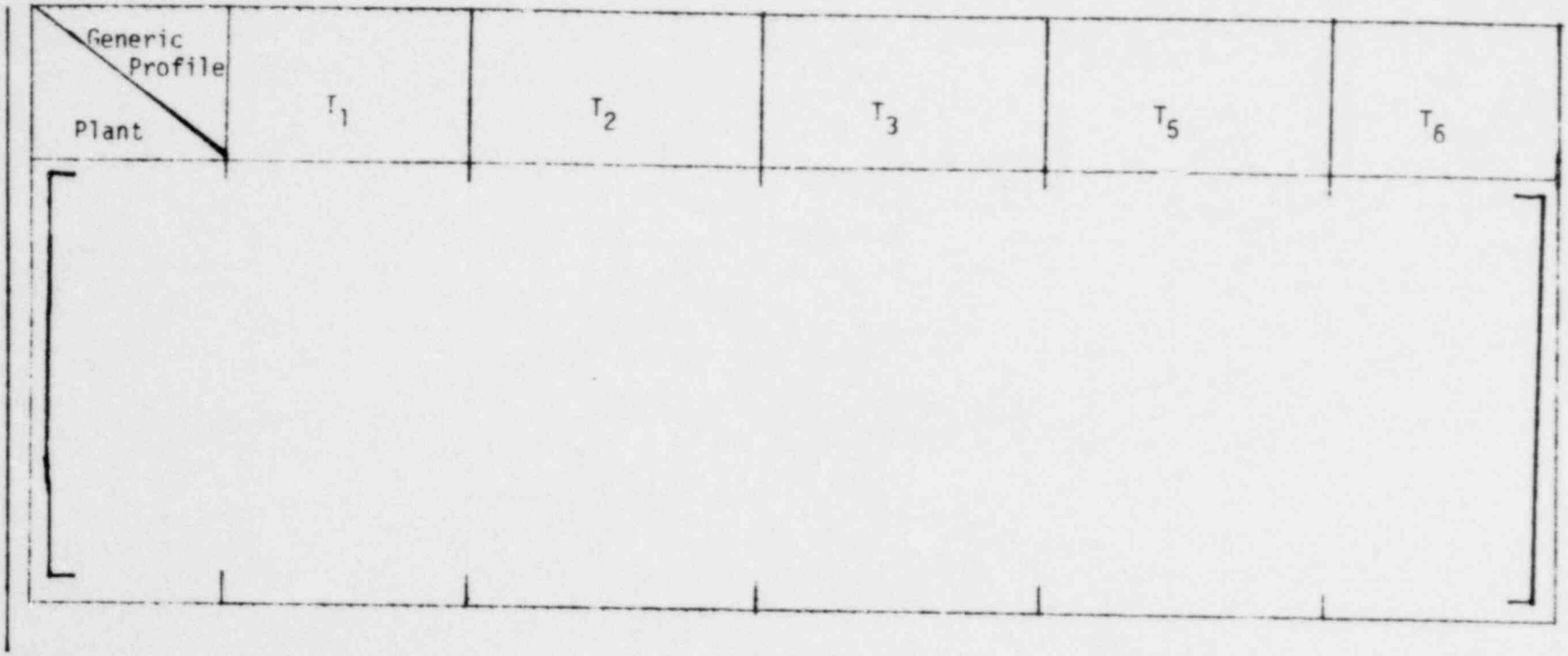

TABLE 11.11.2: PERCENTAGE OF TOTAL HOT STANDBY TO DATE, REQUIRED TO REACH USAGE FACTOR OF ONE - (STRATIFICATION PLUS STRIPING)

a,b

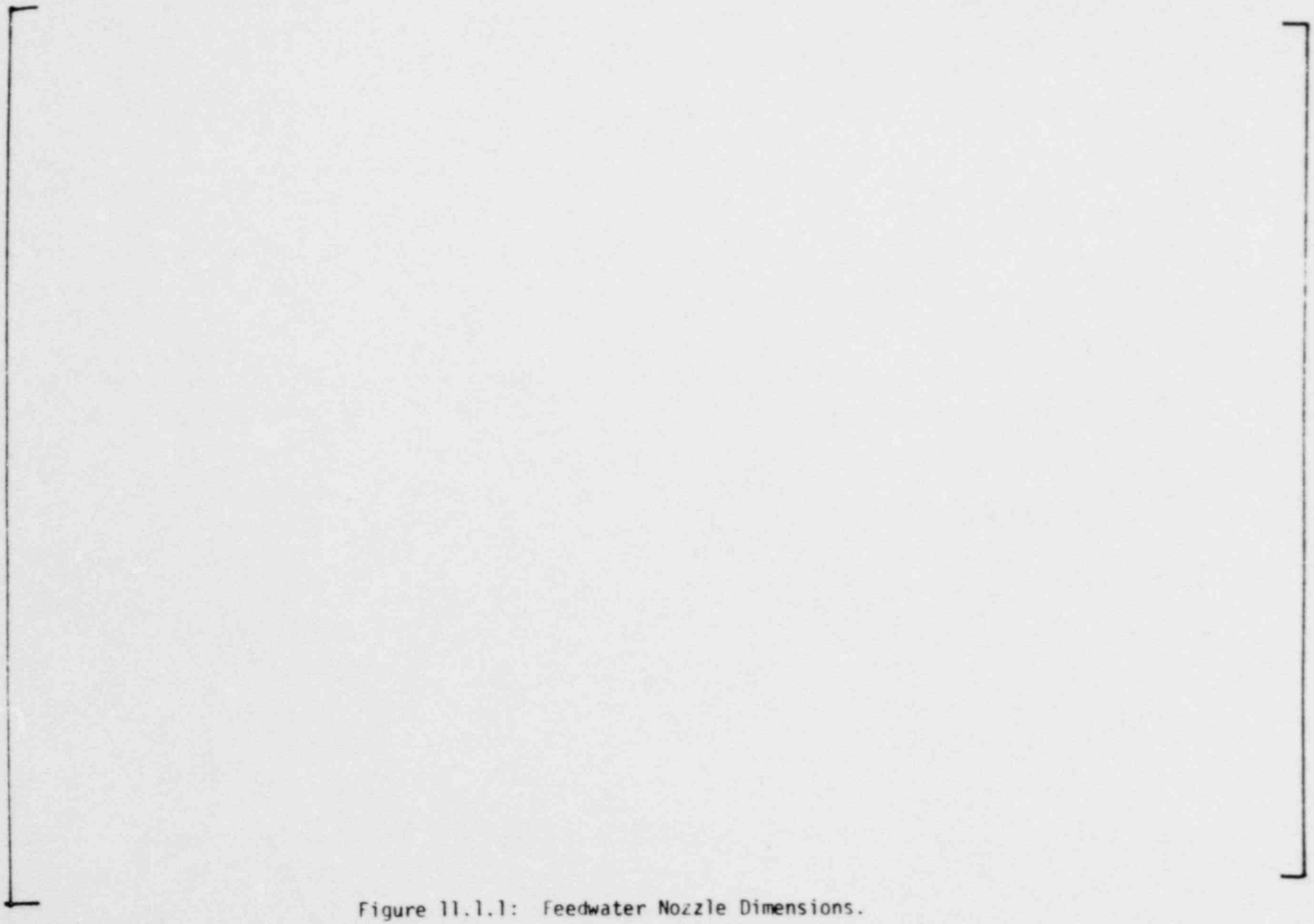

Figure 11.1.1: Feedwater Nozzle Dimensions.

a.c

Figure 11.1-2 Feedwater Nozzle and Connecting Elbow

a,c

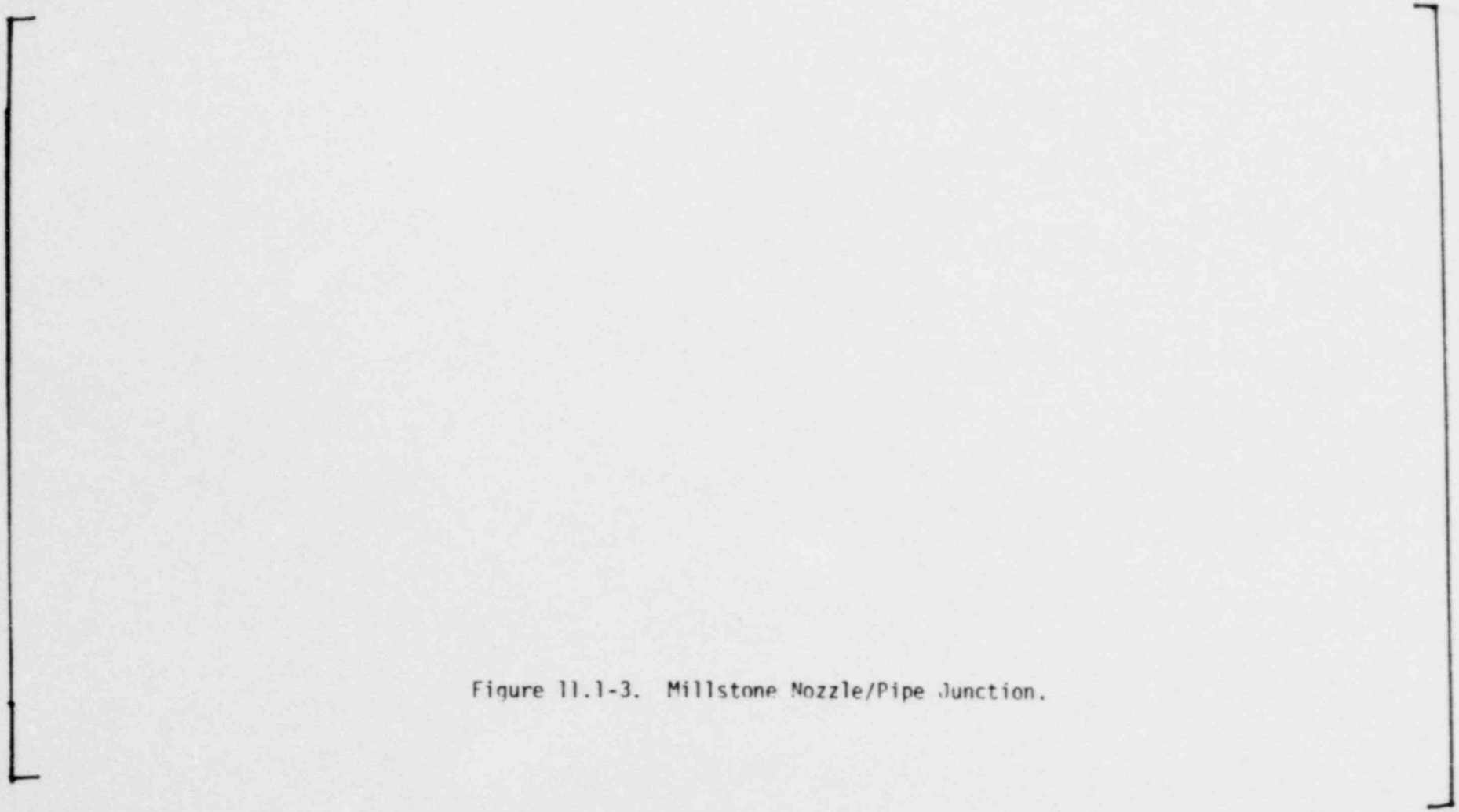

Figure 11.1-3. Millstone Nozzle/Pipe Junction.

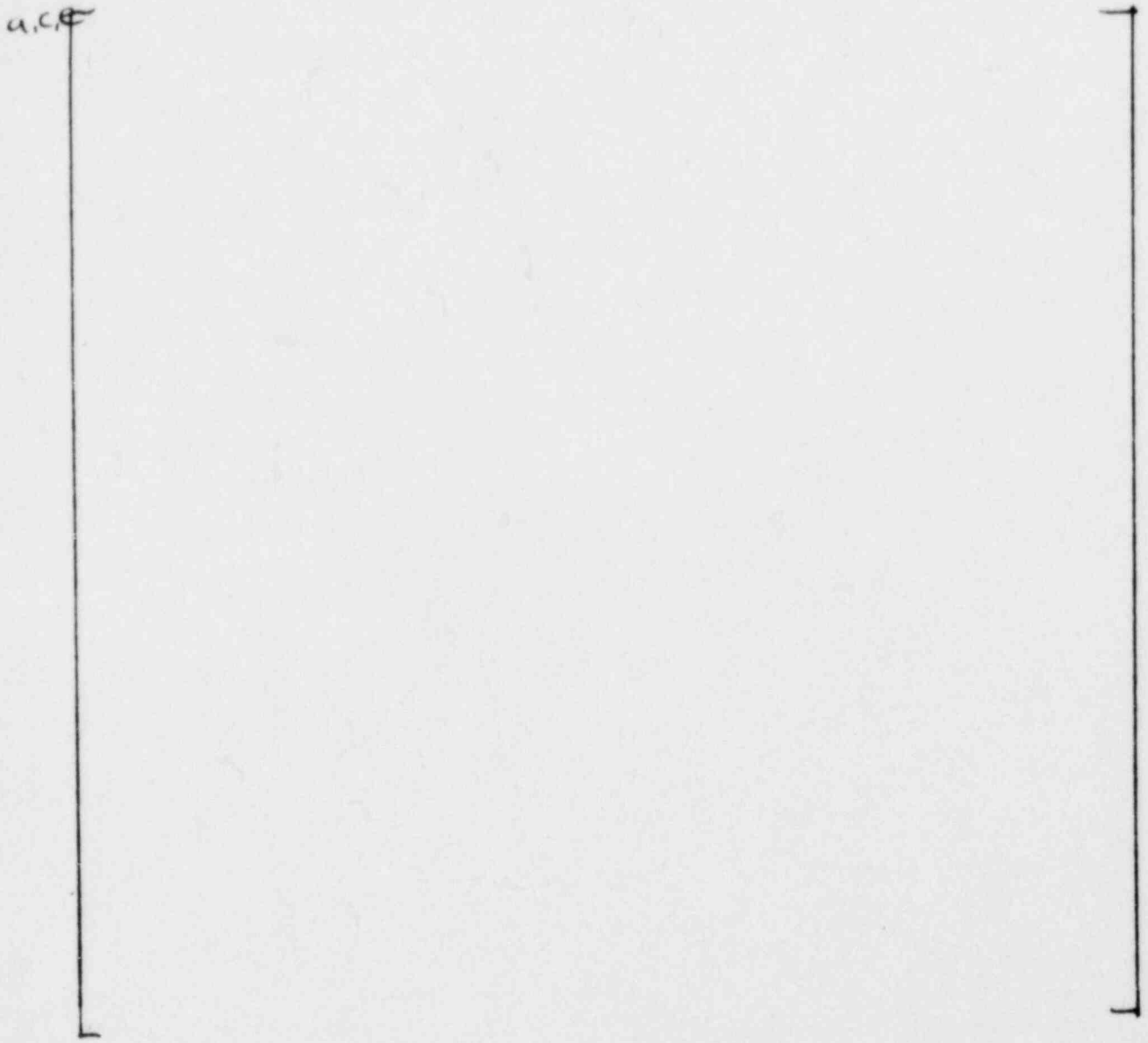

Figure 11.3-1. Stratified Temperature Profile T_1 for Elbow Configuration.

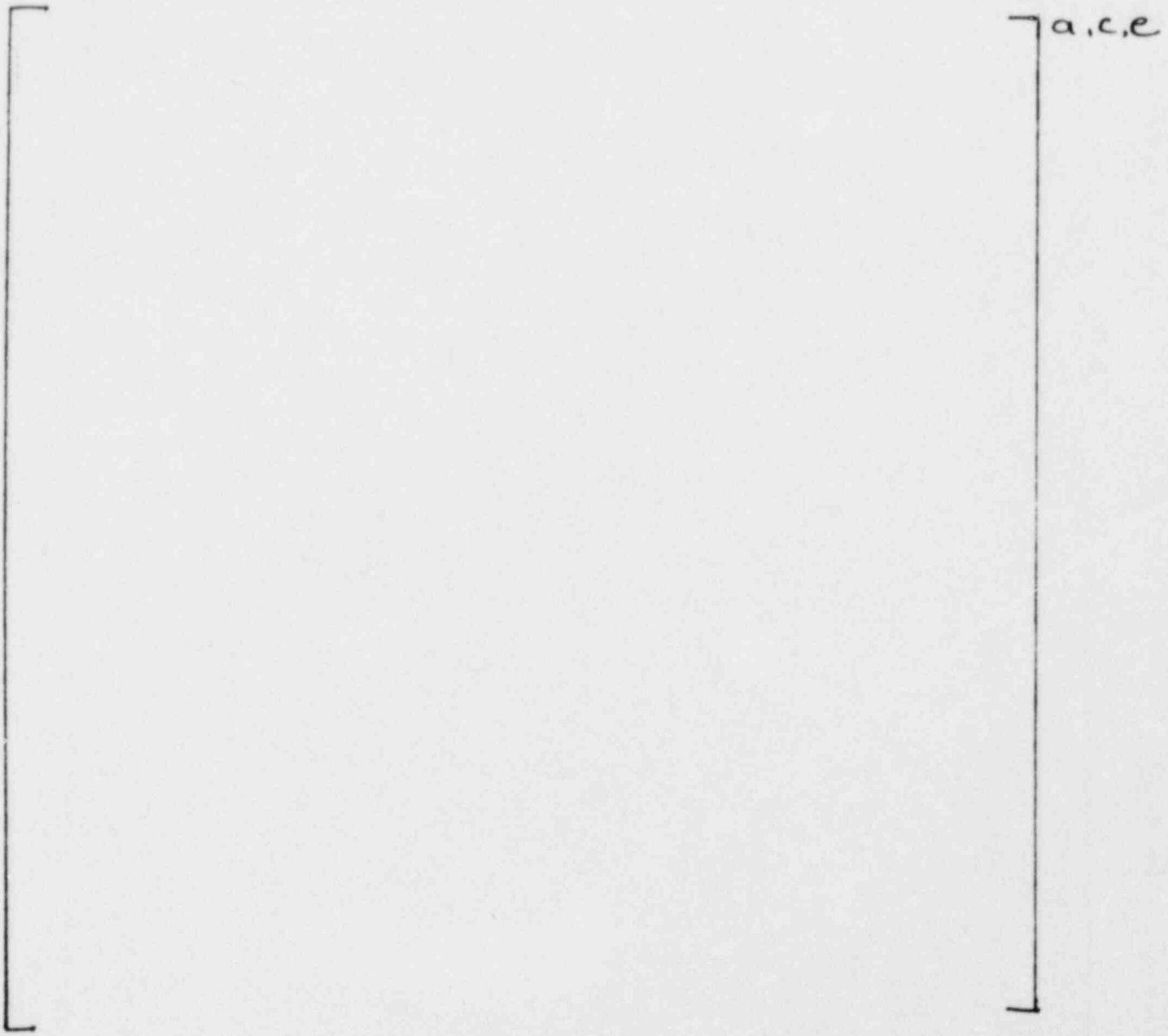

Figure 11.3-2. Stratified Temperature Profile T_2 for Elbow Configuration.

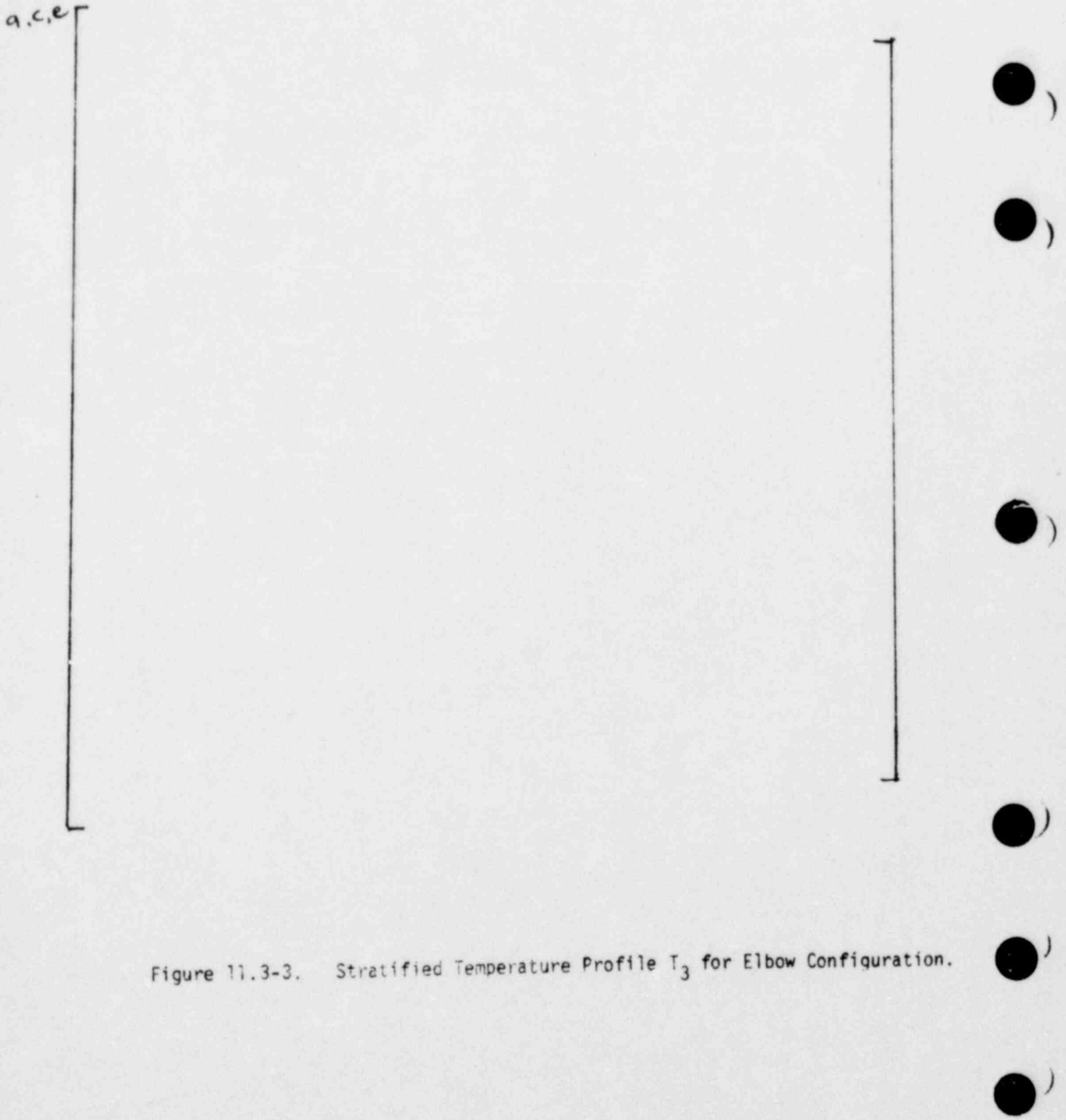

Figure 11.3-3. Stratified Temperature Profile T_3 for Elbow Configuration.

Figure 11.3-4. Stratified Temperature Profile T_4 for Elbow Configuration.

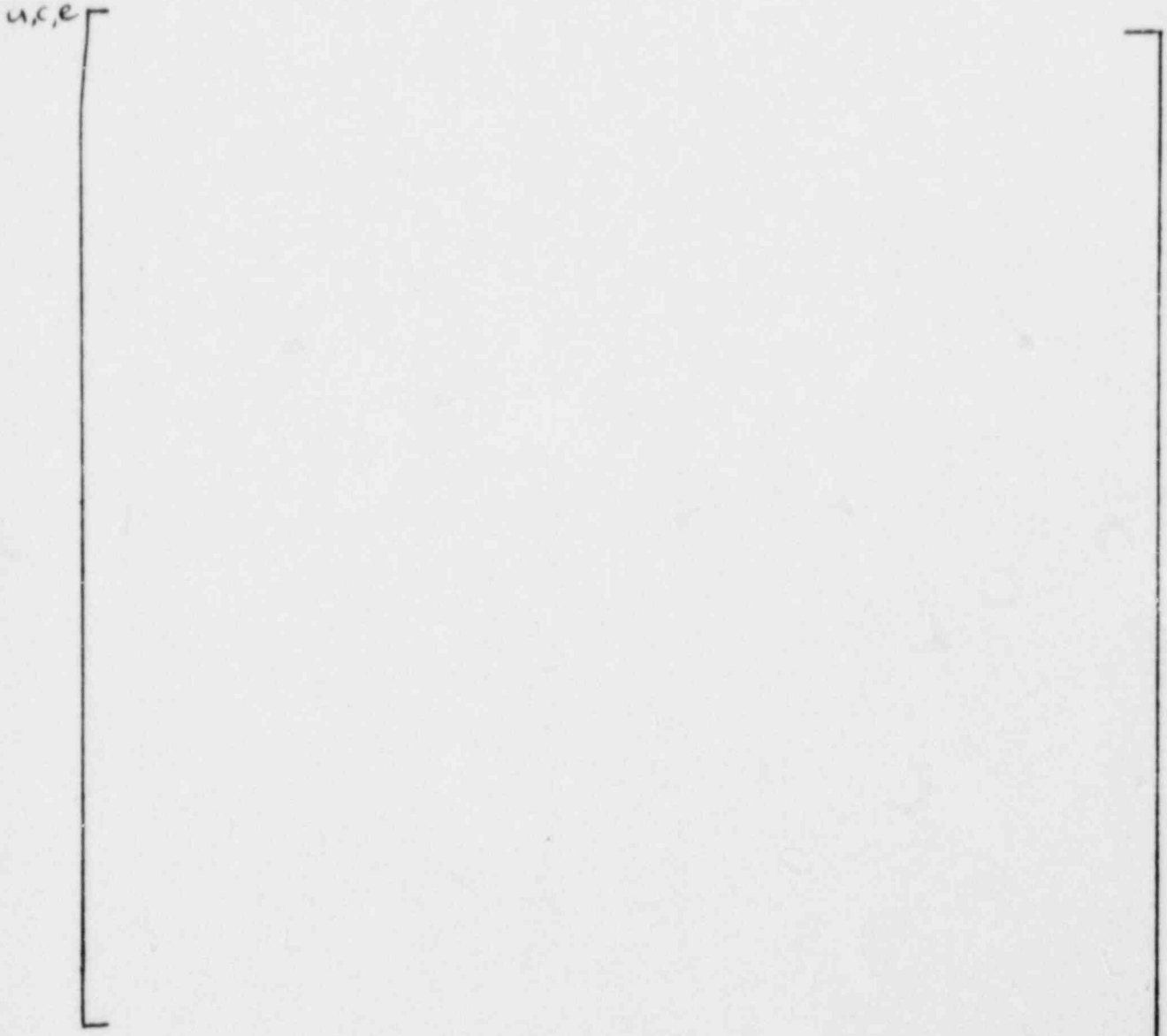

Figure 11.3-5. Stratified Temperature Profile T_5 for Elbow Configuration.

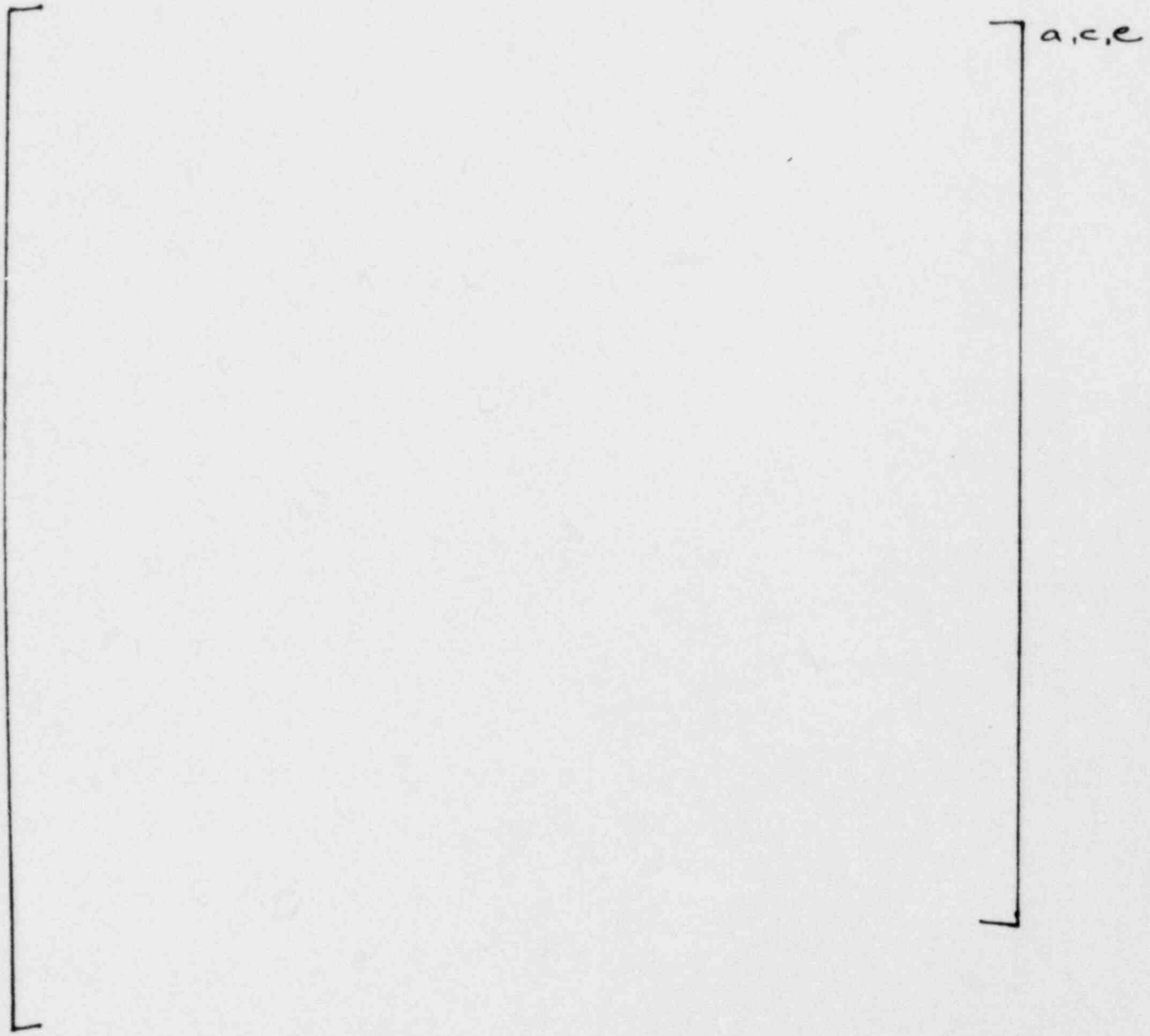

Figure 11.3-6. Stratified Temperature Profile T_6 for Elbow Configuration.

a,c,e

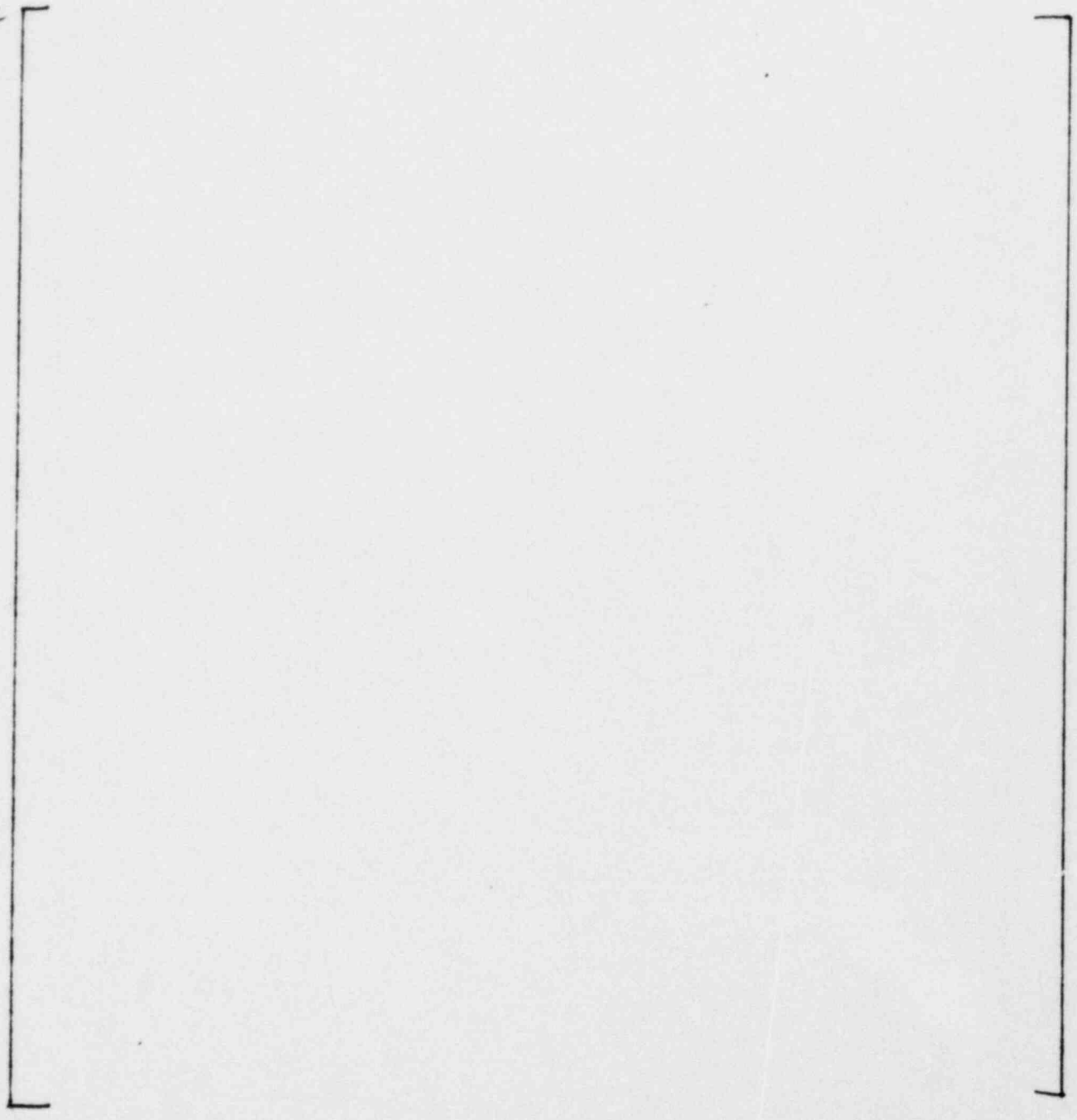

Figure 11.3-7. Axial Variation of Interface Levels Along Elbow.

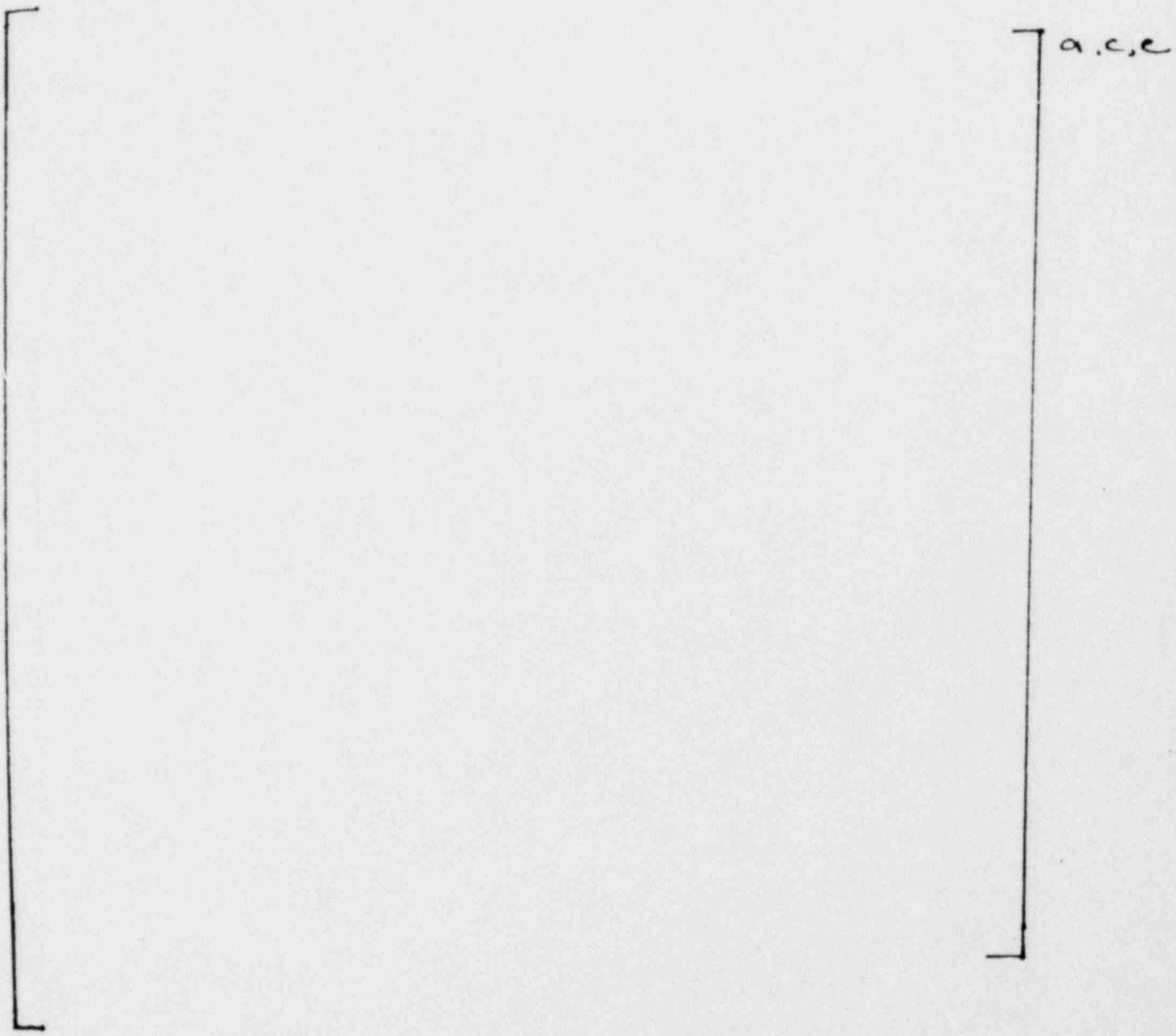

Figure 11.3-8. Stratified Temperature Profile T_1 for Straight Pipe.

a,c,e

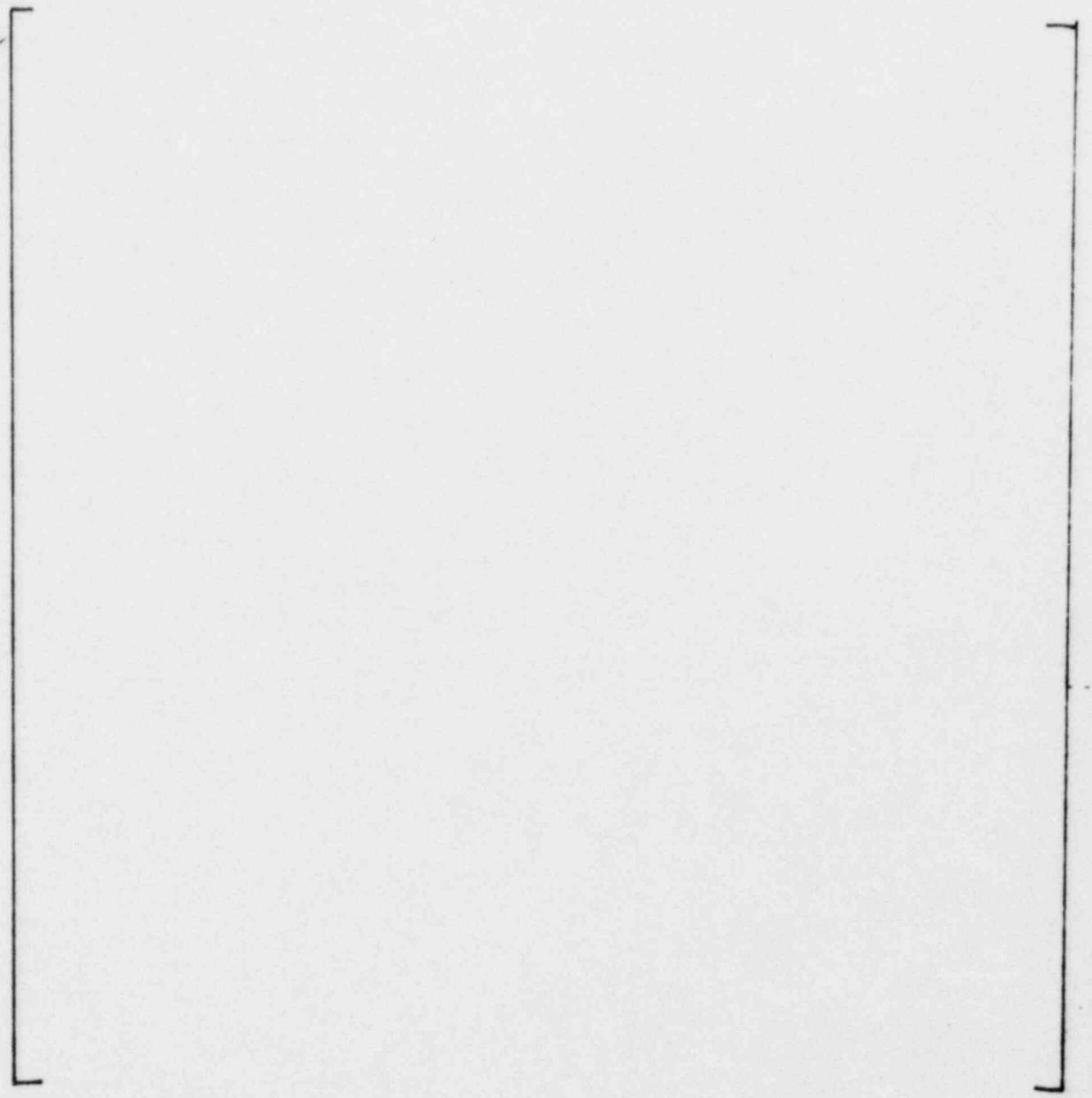

Figure 11.3-9. Stratified Temperature Profile T_2 for Straight Pipe.

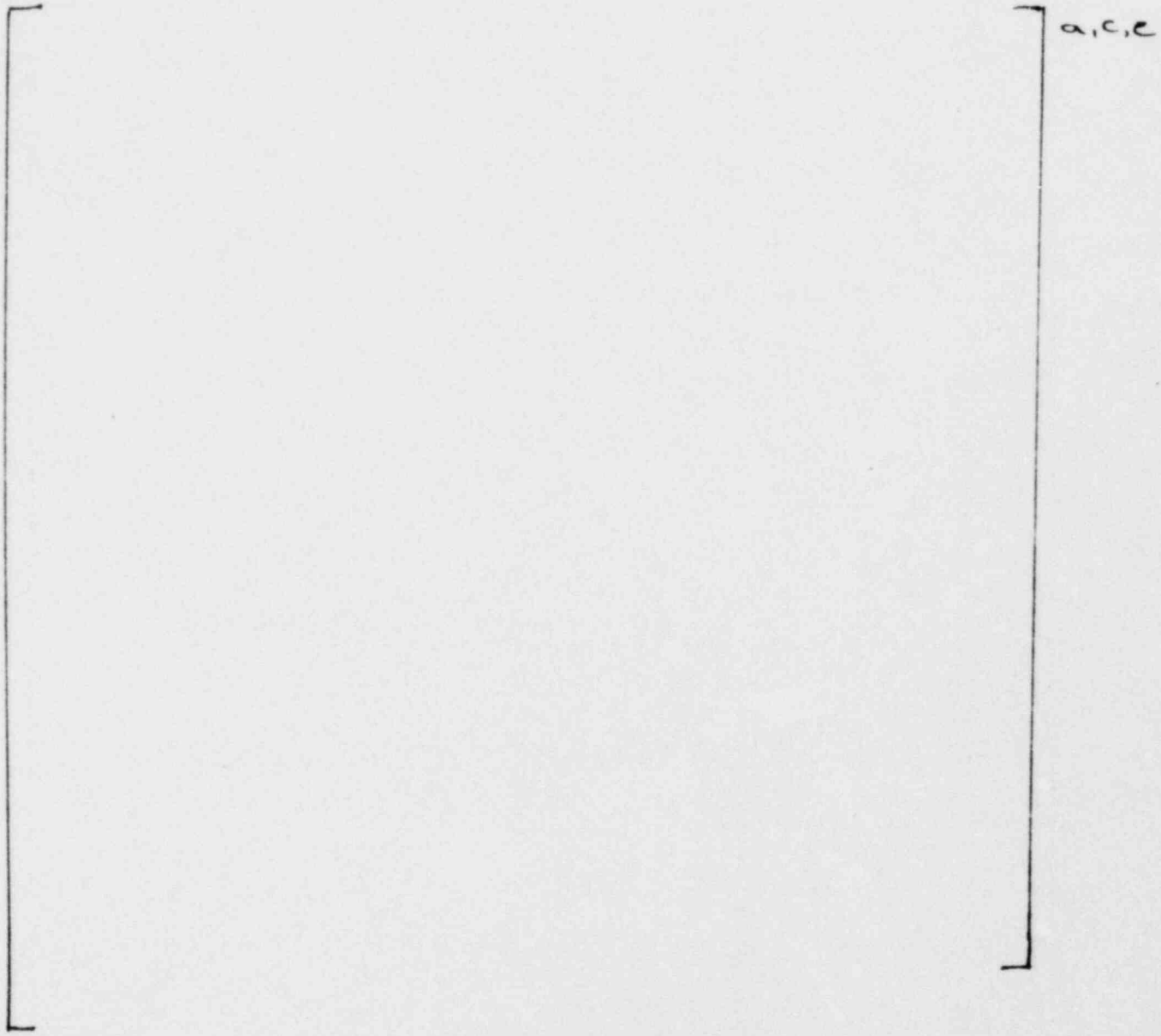

Figure 11.3-10. Stratified Temperature Profile T_3 for Straight Pipe.

a,c

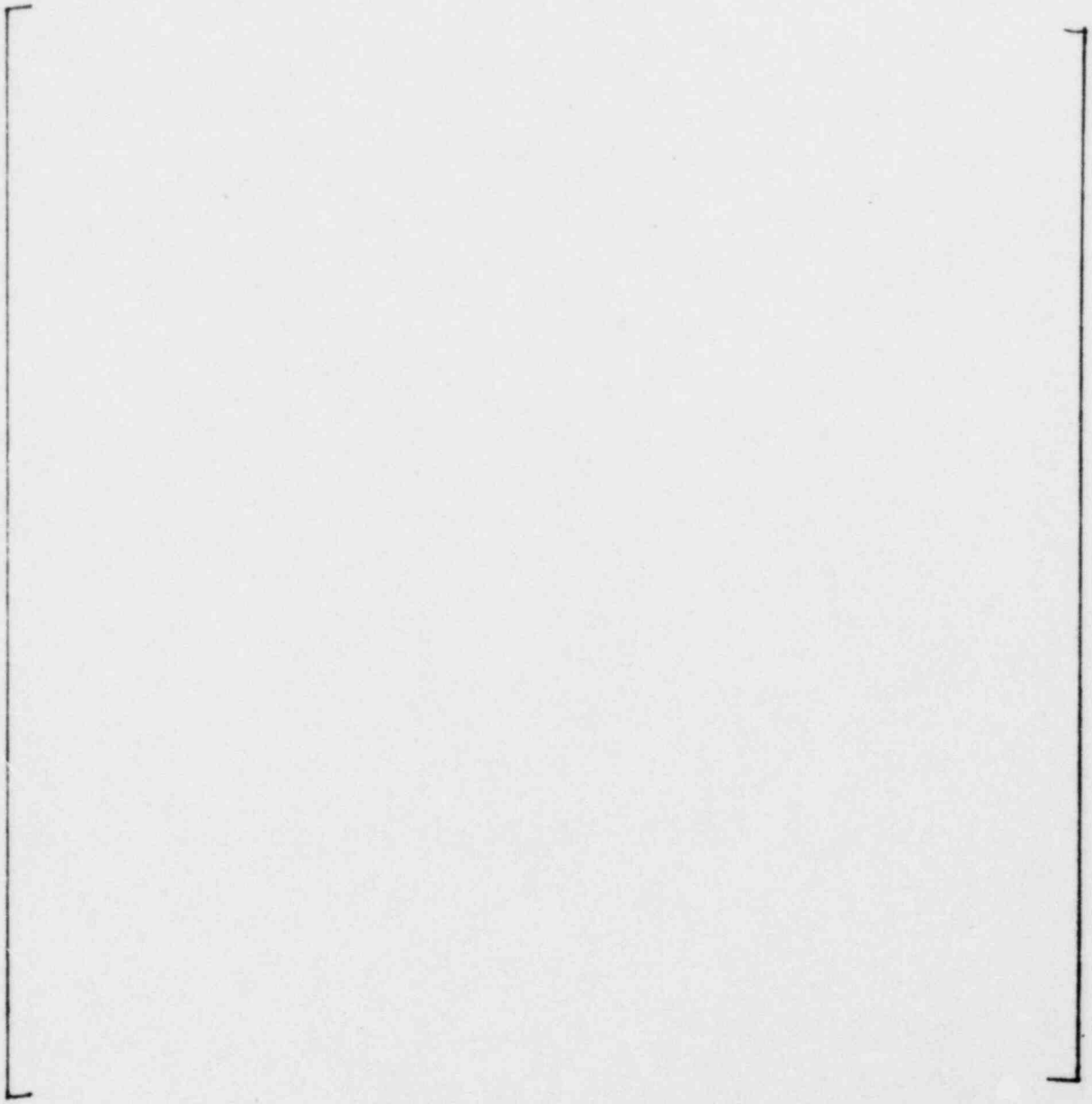

Figure 11.3-11. Stratified Temperature Profile T_5 for Straight Pipe.

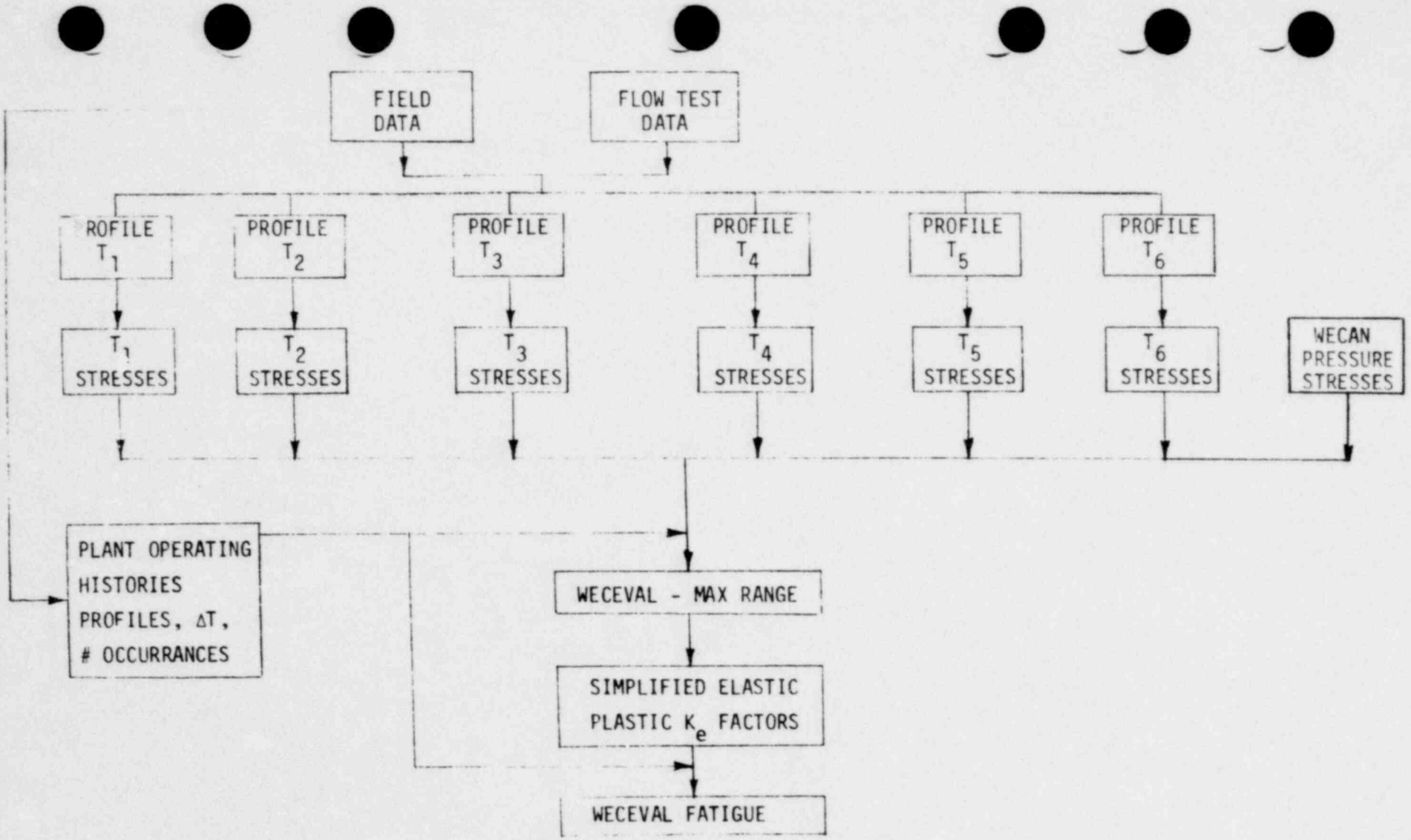

Figure 11.5-1: Flow Chart of Thermal Stratification Analysis Procedure.

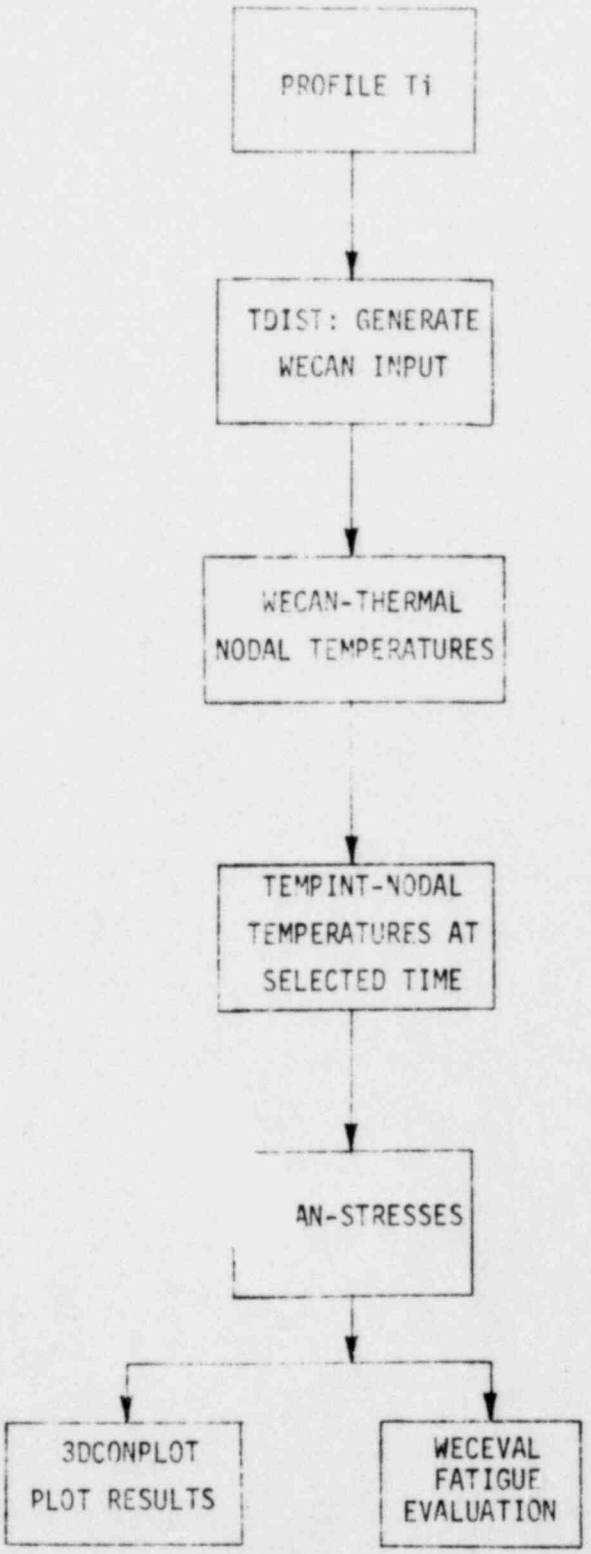

Figure 11.5-2: Flow Chart For Calculating Stratification Thermal Stresses.

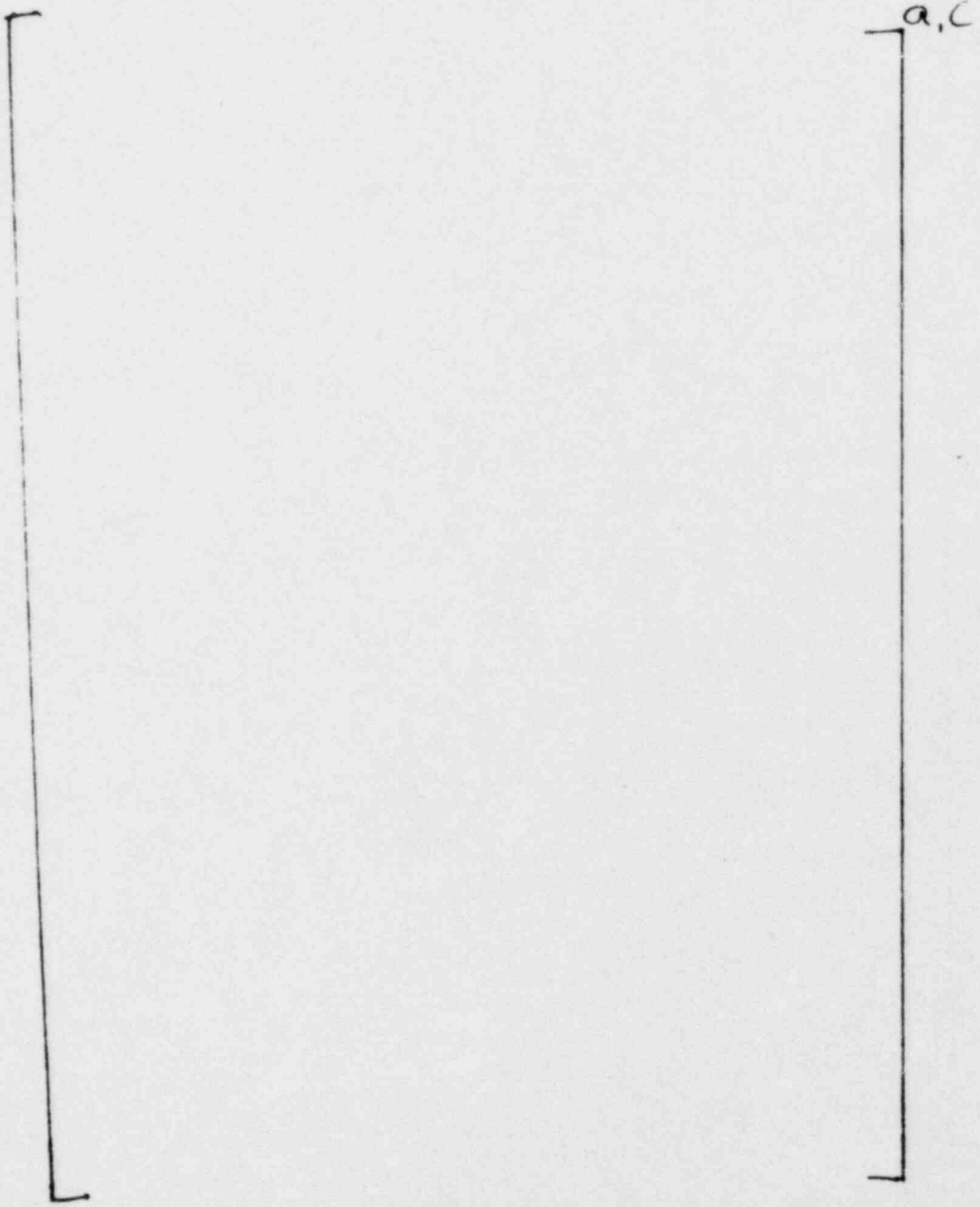

Figure 11.6-1: Finite Element Model of Steam Generator Shell, Feedwater Nozzle, and Elbow.

a,c

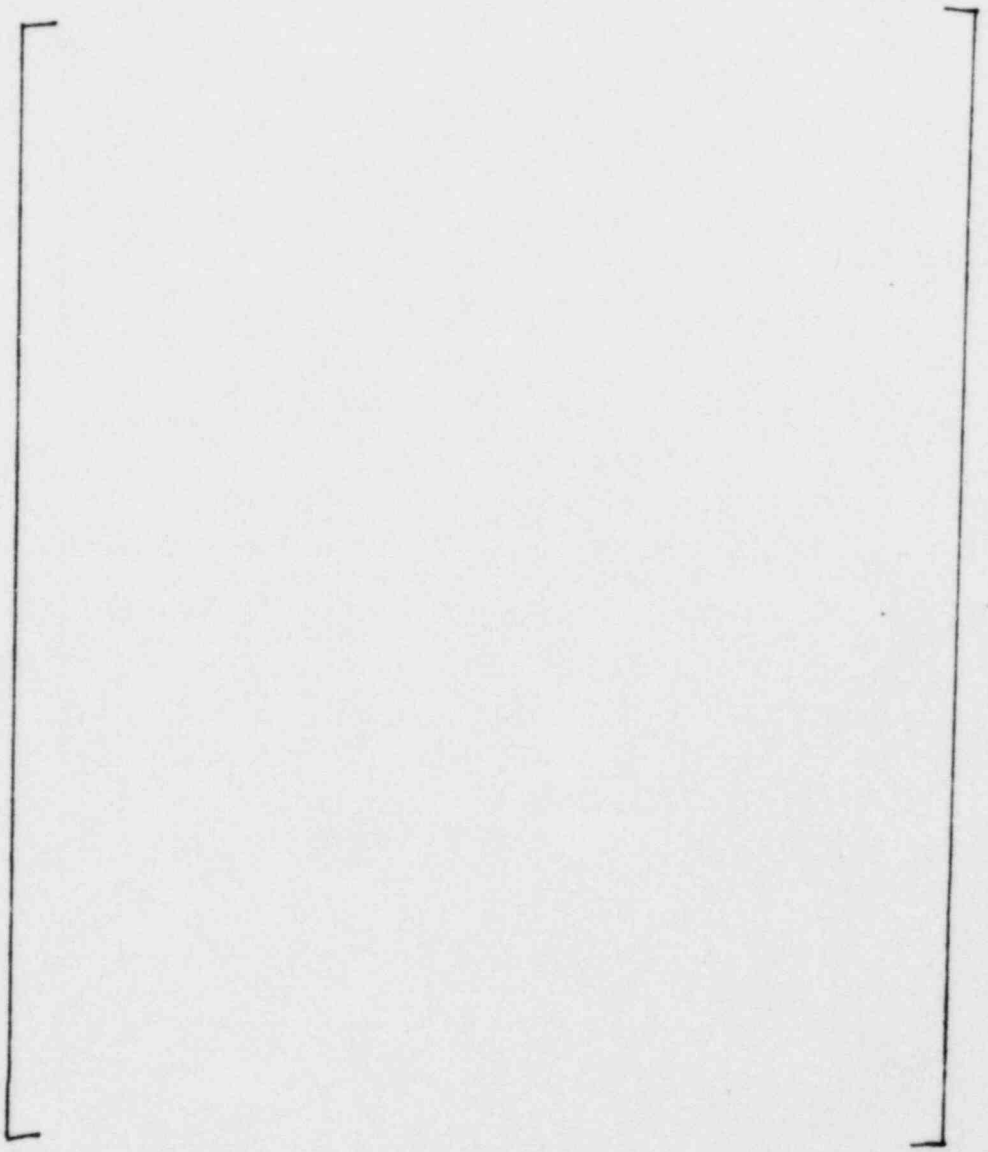

Figure 11.6-2: Nozzle/Elbow Weld Area of Finite Element Model Shown in Figure 11.6-1.

a,c

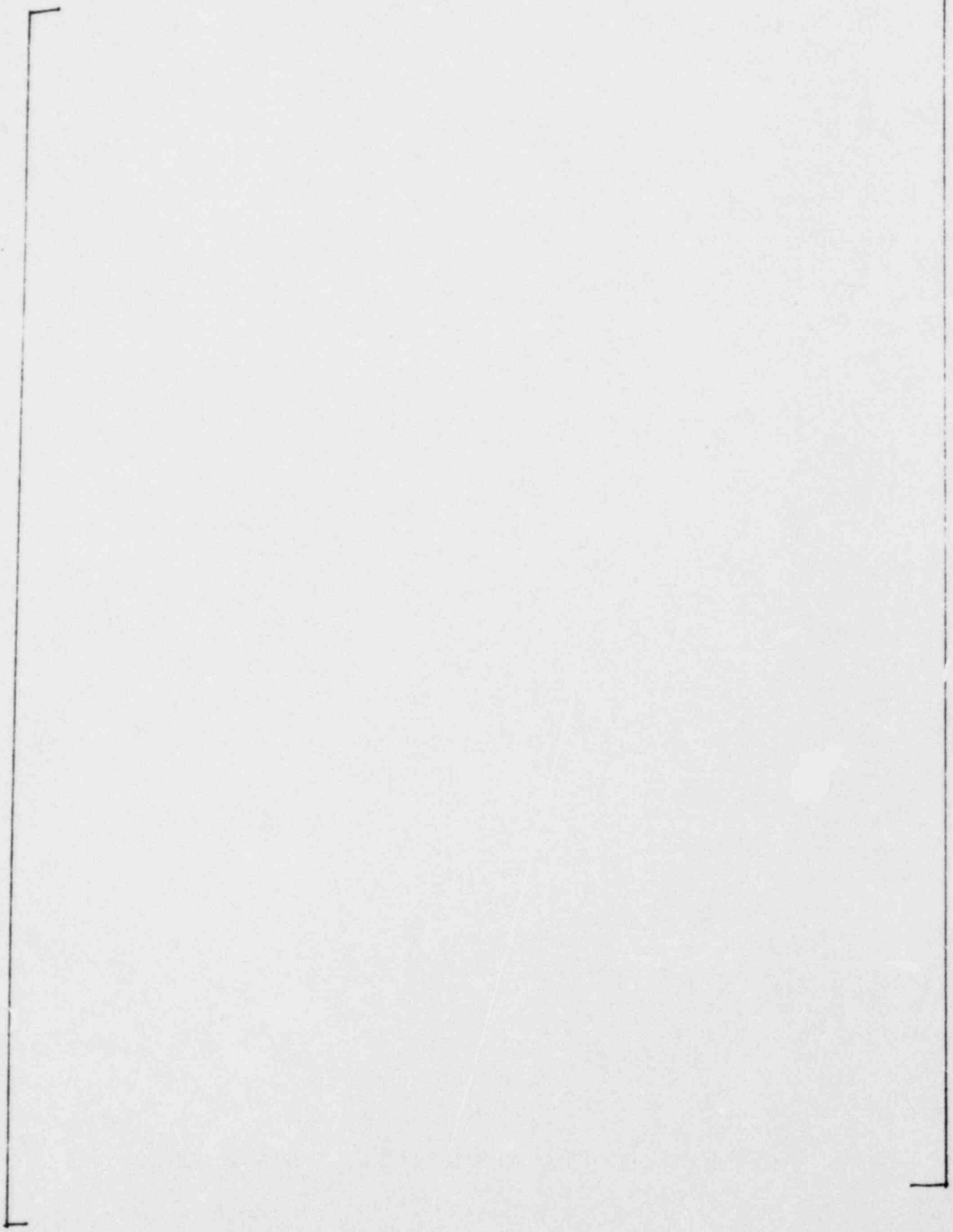

Figure 11.6-3: Schematic of Node and Element Numbering for Finite Element Model Shown in Figure 11.6-1.

a,c

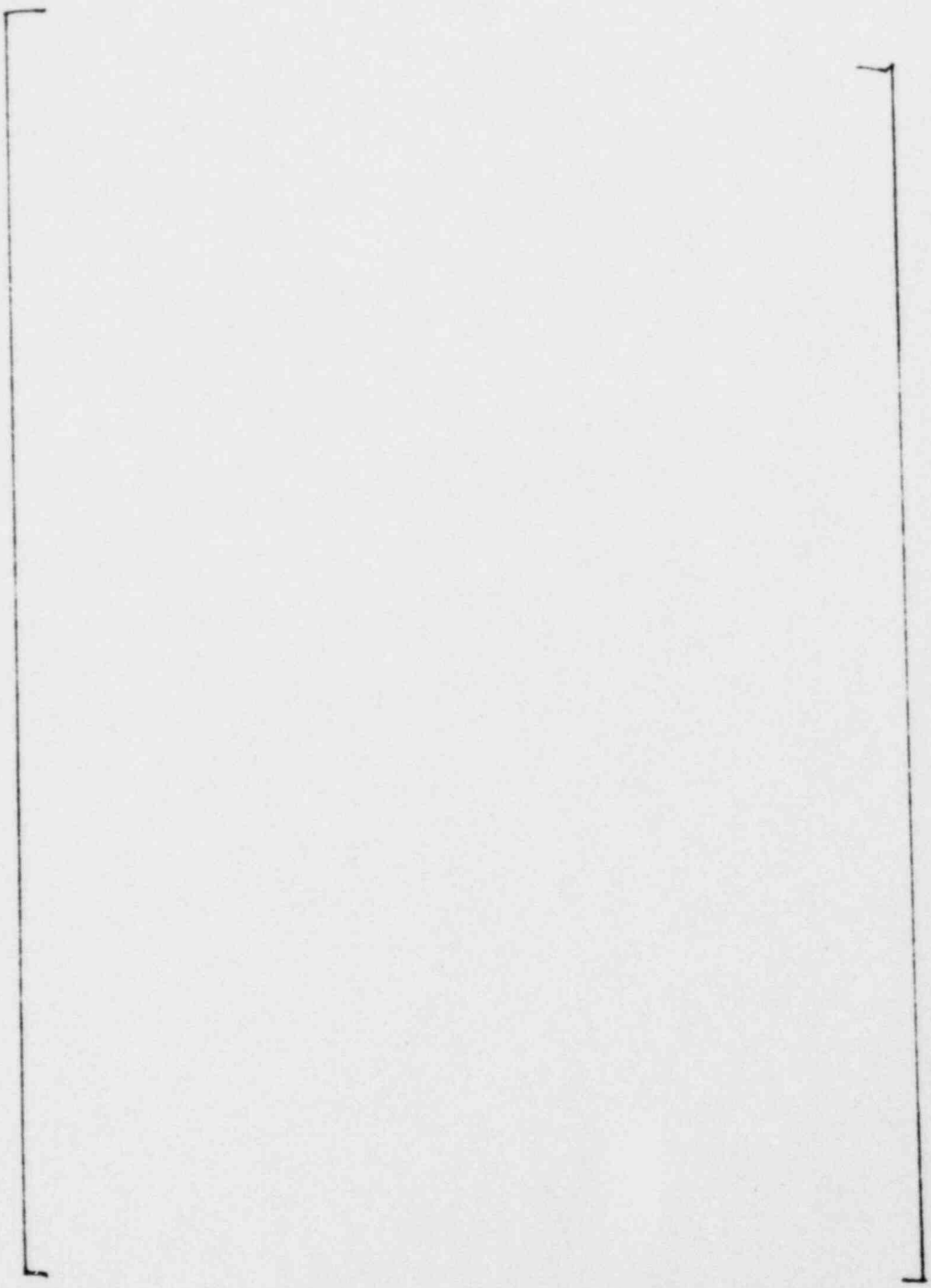

Figure 11.6-4: Finite Element Model of Shell, Nozzle and Straight Pipe.

a,c

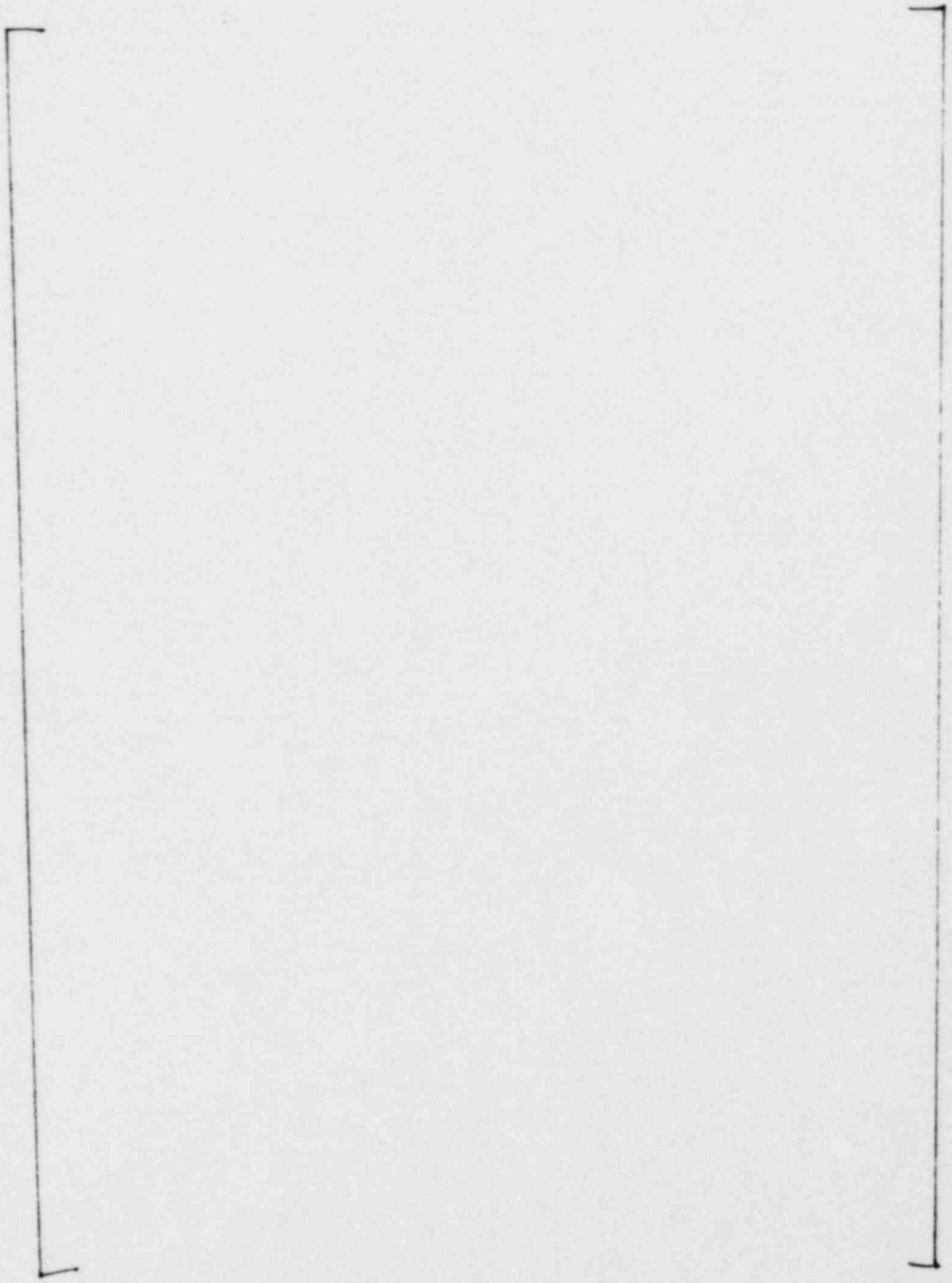

Figure 11.6-5: Nozzle/Pipe Weld Area of Finite Element Model Shown in Figure 11.6-4.

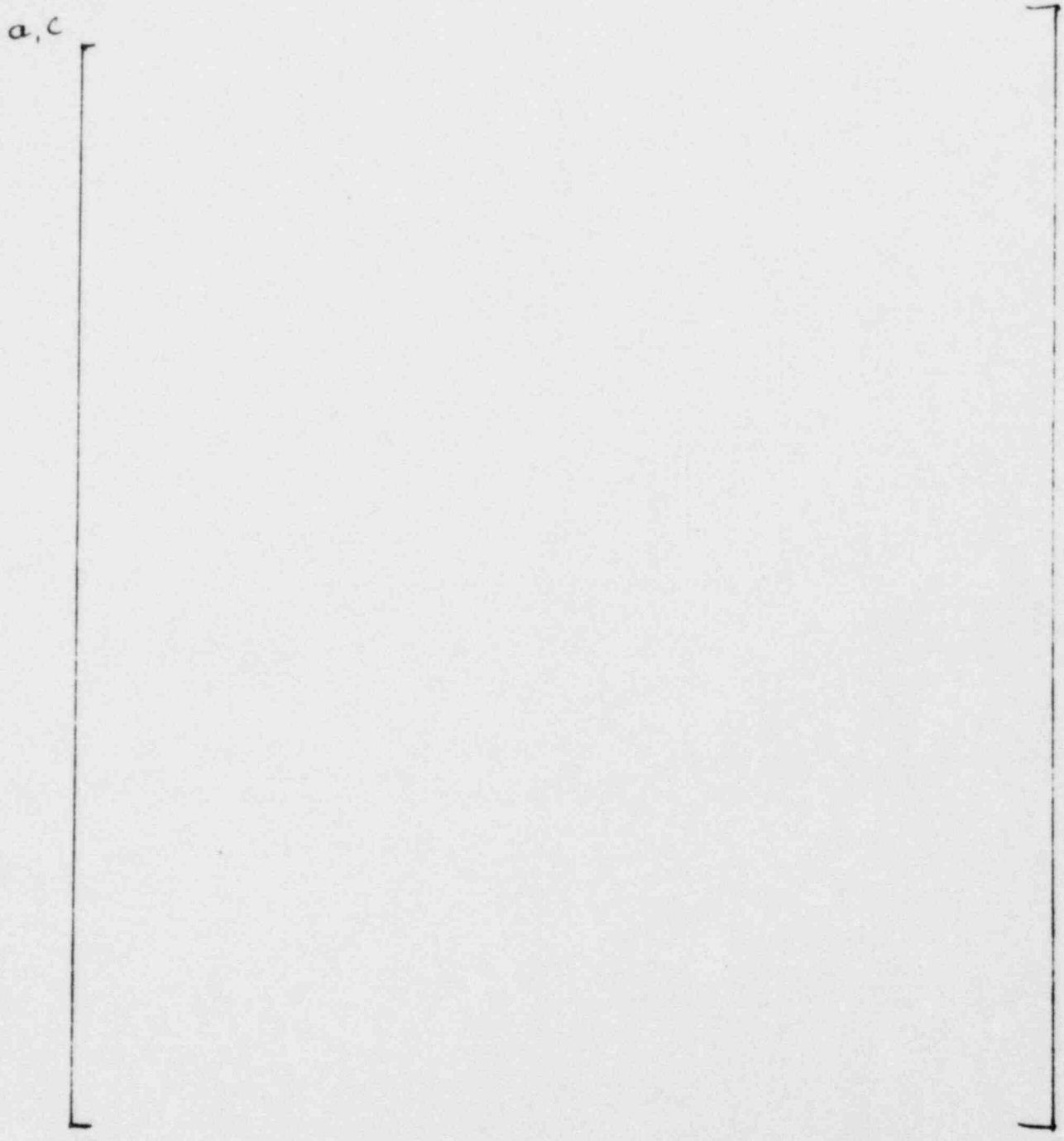

Figure 11.7-1: Planes and Surfaces for Imposition of Boundary Conditions.

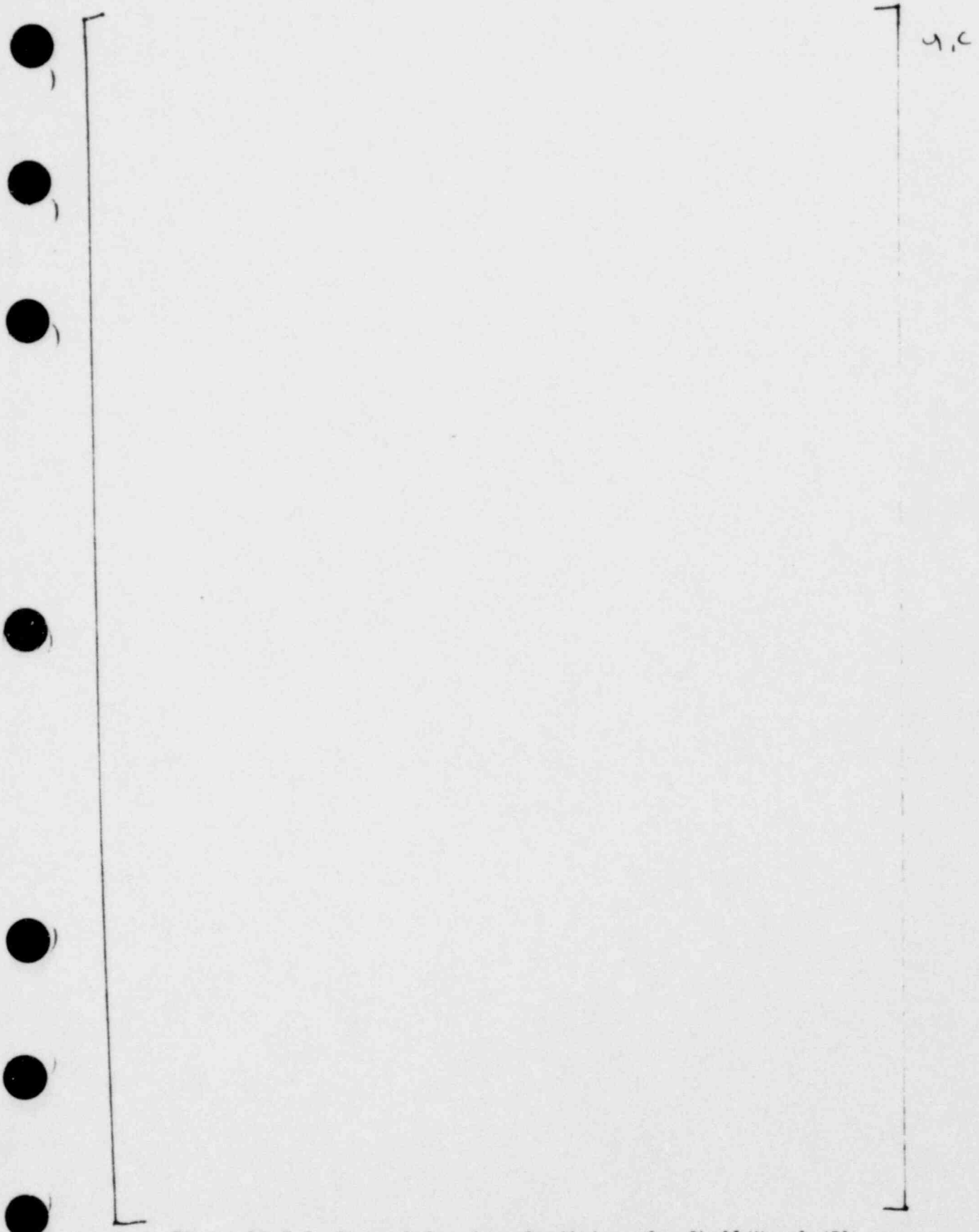

Figure 11.7-2: Thermal Boundary Conditions for Shell/Nozzle/Elbow.

a,c

Figure 11.7-3: Stresses and Temperatures At Elbow Transition Root for Profile T_1.

a,c

Figure 11.7-4: Stresses and Temperatures At Elbow Transition Root for Profile T_2.

a,c

Figure 11.7-5: Stresses and Temperatures At Elbow Transition Root for Profile T_3.

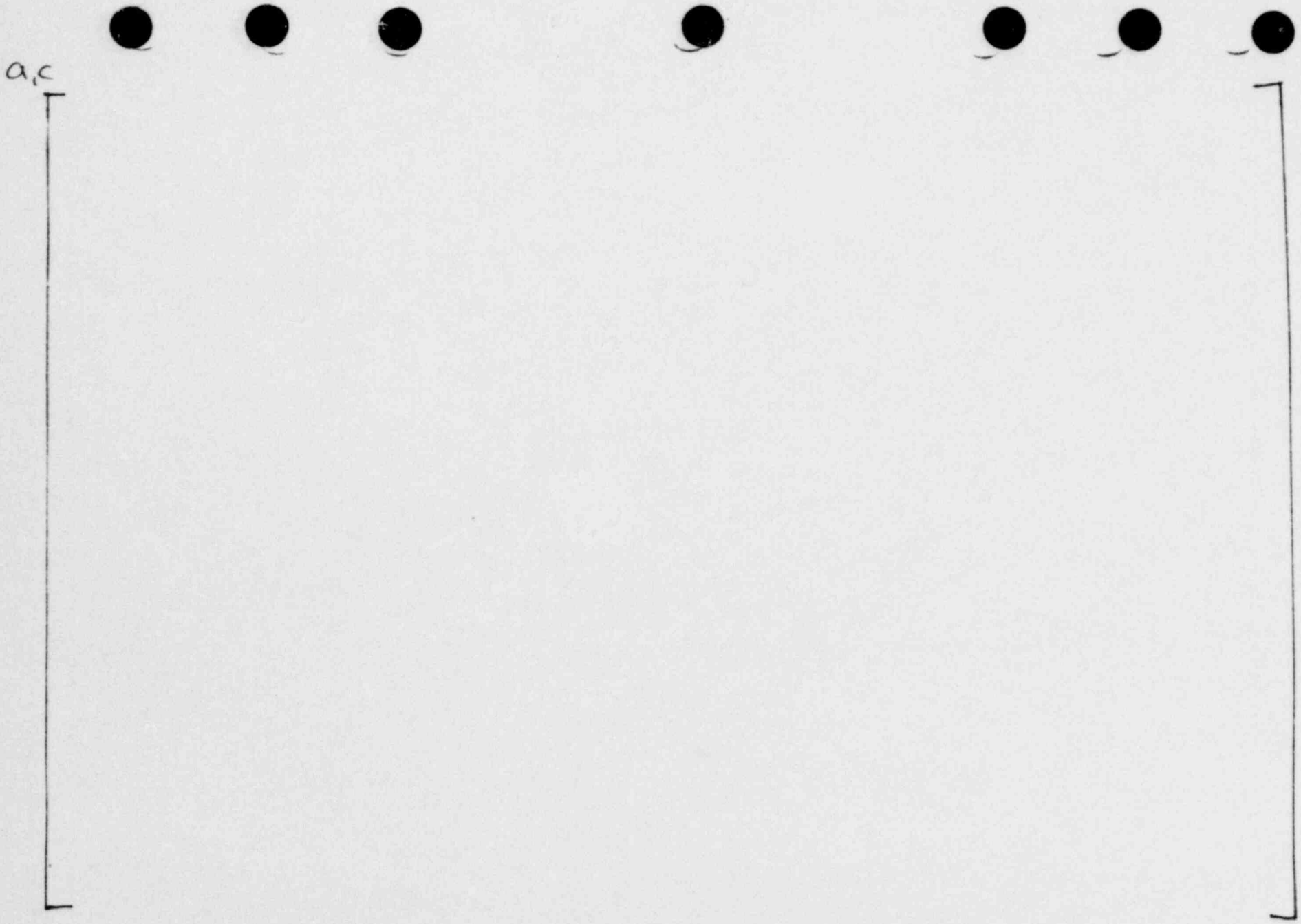

Figure 11.7-6: Stresses and Temperatures At Elbow Transition Root for Profile T_4.

a.c

Figure 11.7-7: Stresses and Temperatures At Elbow Transition Root for Profile T_5.

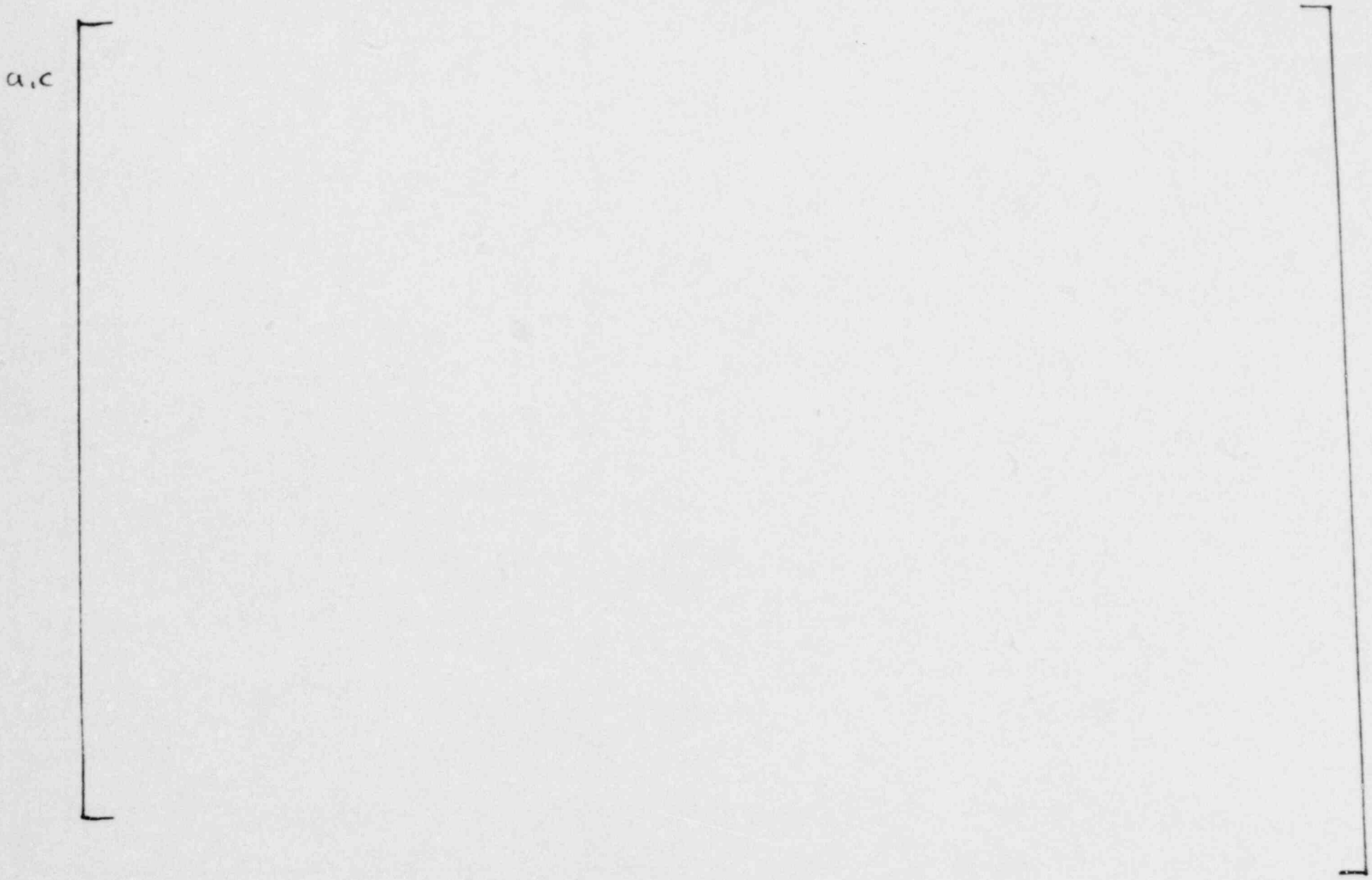

Figure 11.7-8: Stresses and Temperatures At Elbow Transition Root for Profile T_6.

a.c

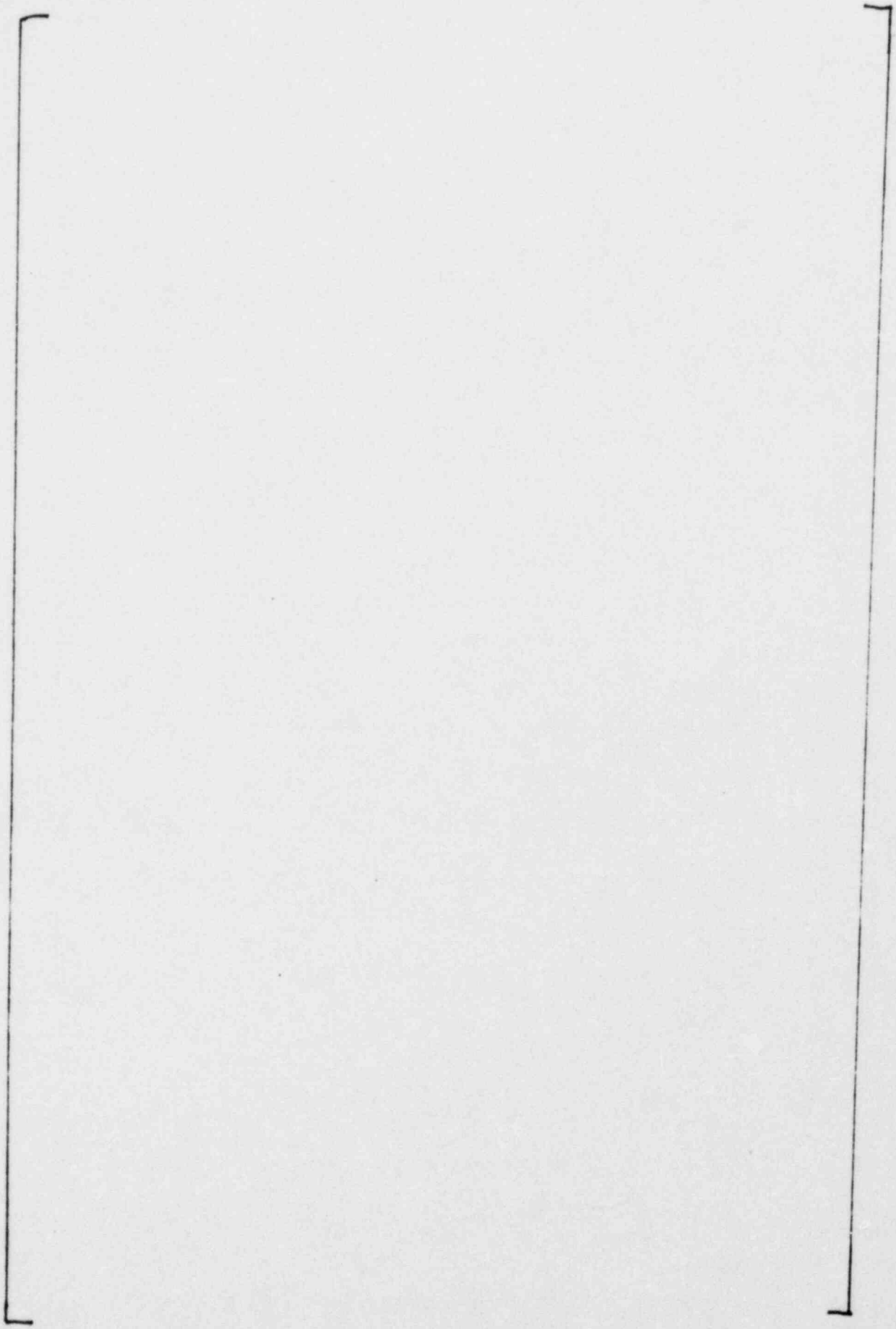

Figure 11.7-9: Stresses and Temperatures At Counterbore, θ=0° For Profile T_1.

a,c

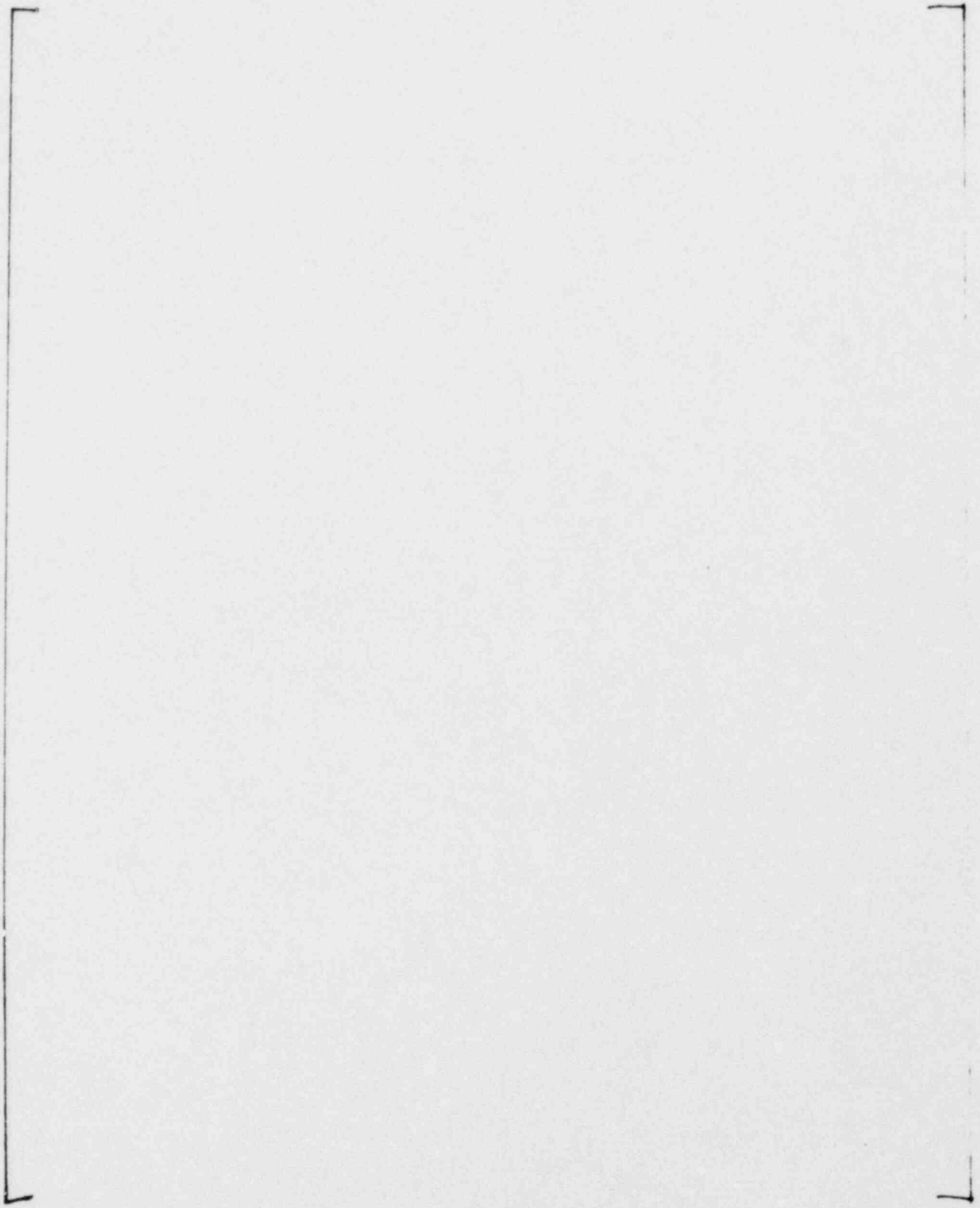

Figure 11.7-10: Stresses and Temperatures At Counterbore, θ=157° For Profile T_2.

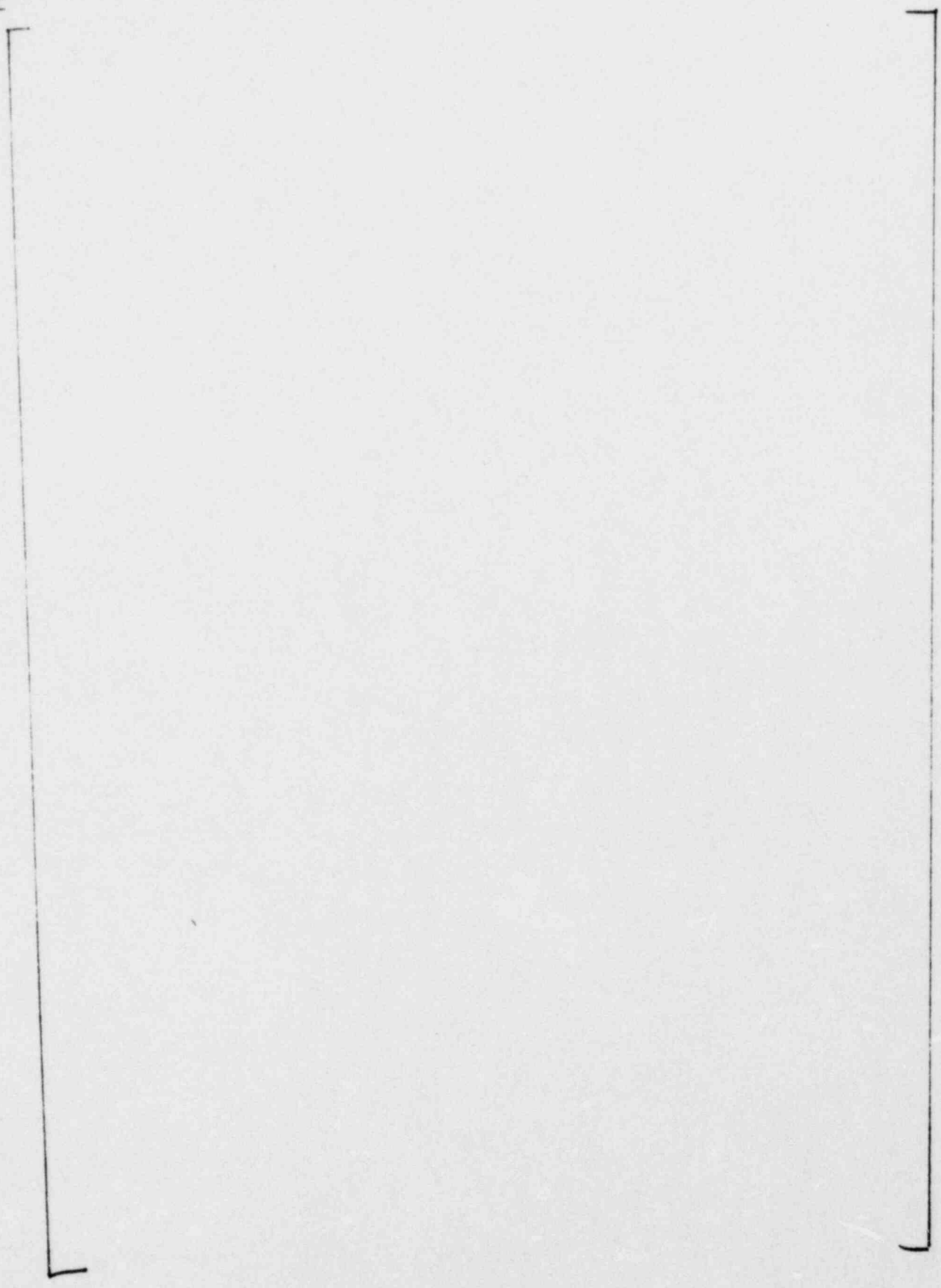

Figure 11.7-11: Stresses and Temperatures At Counterbore, θ=0° For Profile T_3.

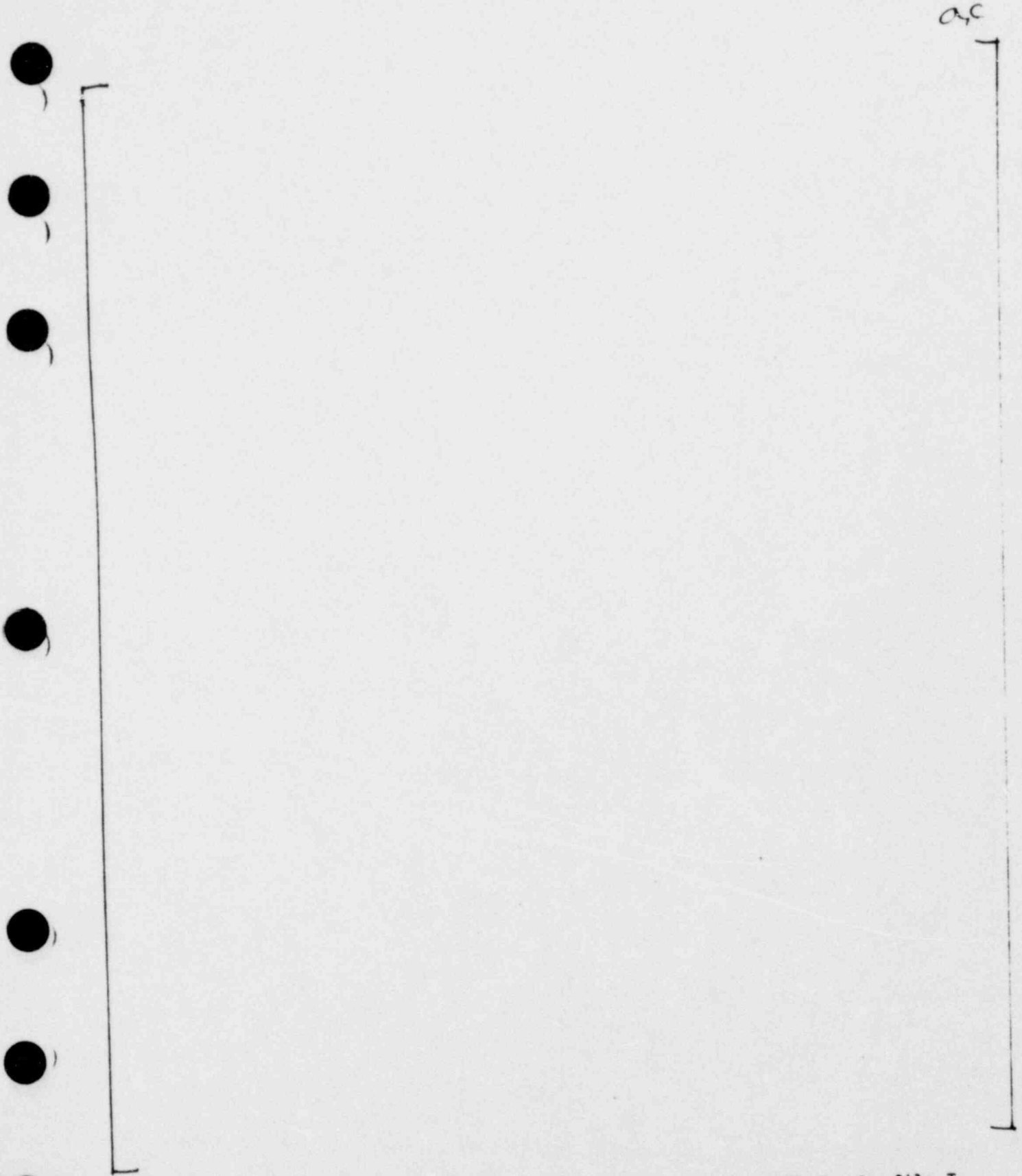

Figure 11.7-12: Stresses and Temperatures At Counterbore, θ=82° For Profile T_4.

a.c

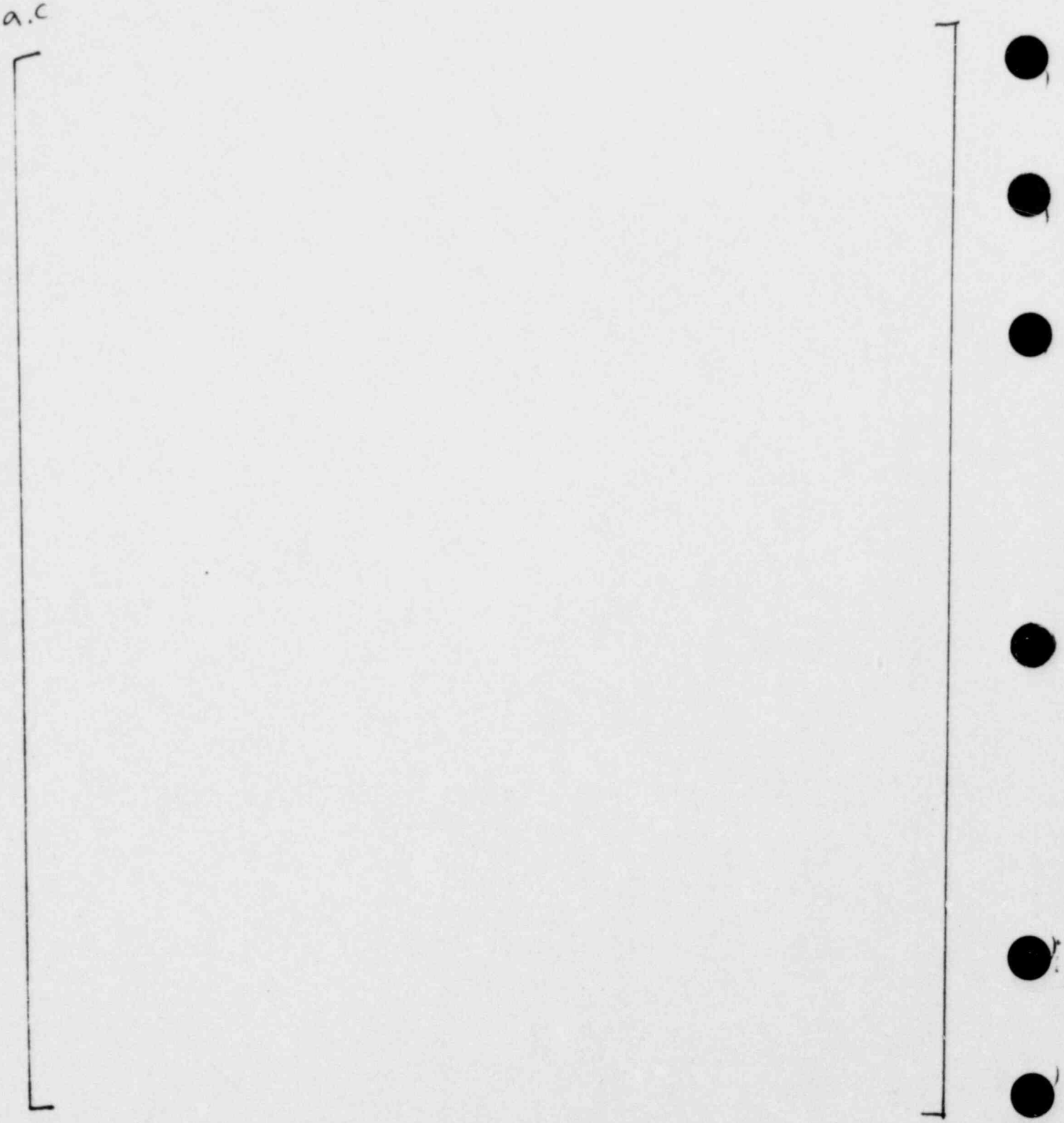

Figure 11.7-13: Stresses and Temperatures At Counterbore, θ=82° For Profile T_5.

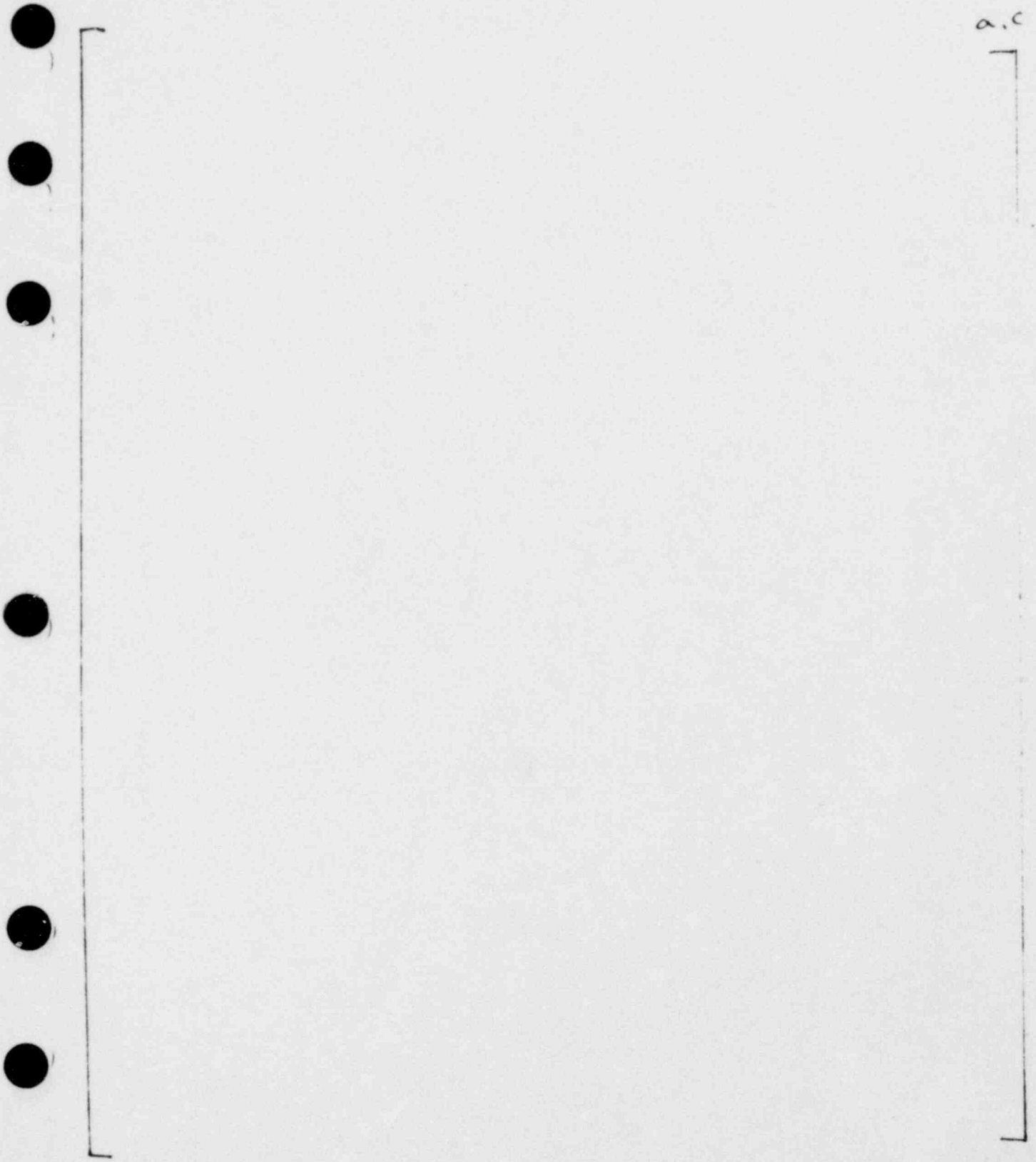

a,c

Figure 11.7-14: Stresses and Temperatures At Counterbore, θ=97° For Profile T_6.

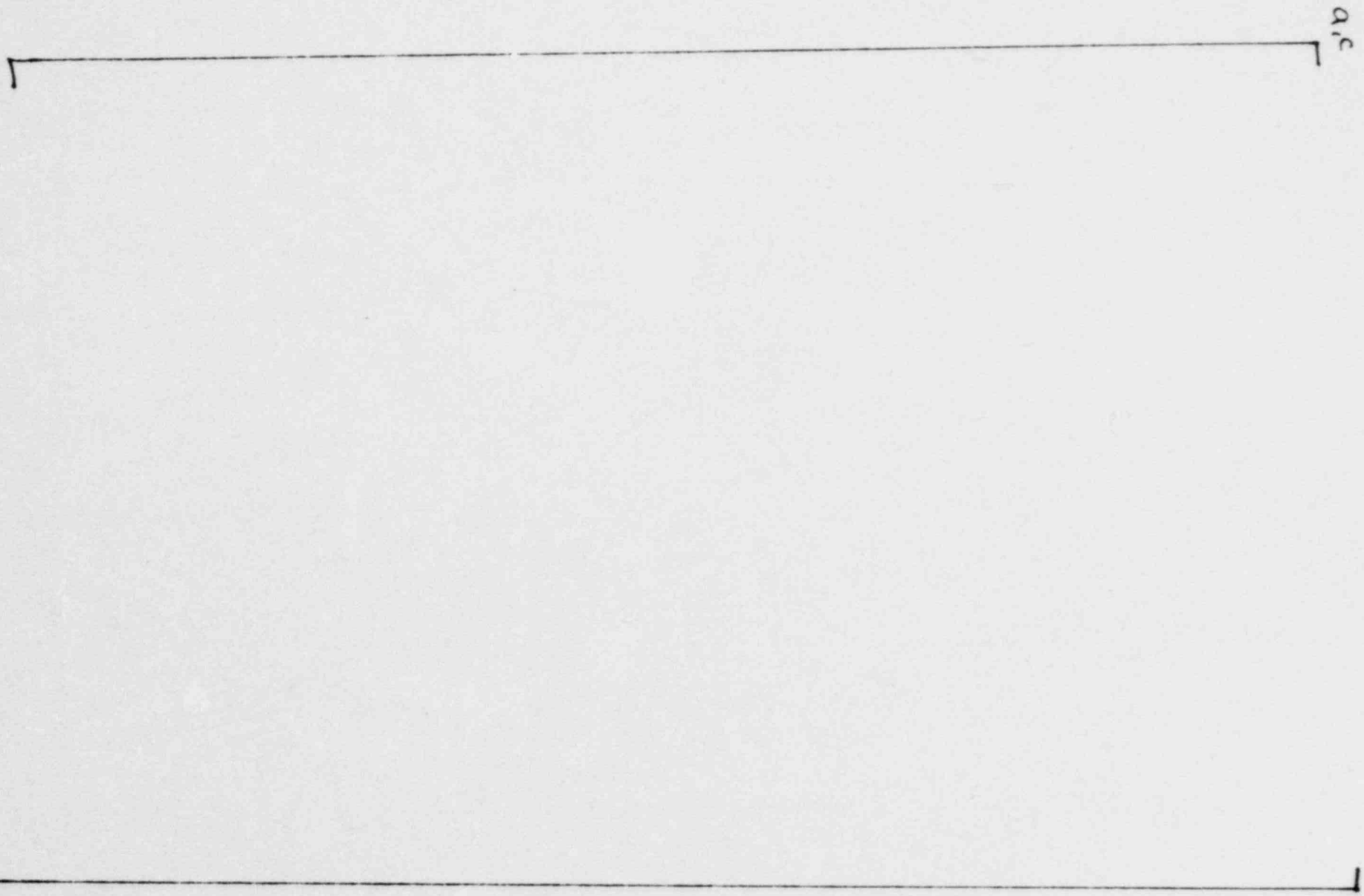

Figure 11.7-15: Stresses and Temperatures At Nozzle Transition Root for Pipe Profile T_1.

Figure 11.7-16: Stresses and Temperatures At Nozzle Transition Root for Pipe Profile T_2.

a,c

Figure 11.7-17: Stresses and Temperatures At Nozzle Transition Root for Pipe Profile T_3.

Figure 11.7-18: Stresses and Temperatures At Nozzle Transition Root for Pipe Profile T_4.

a,c

Figure 11.7-19: Stresses and Temperatures At Nozzle Transition Root for Pipe Profile T_5.

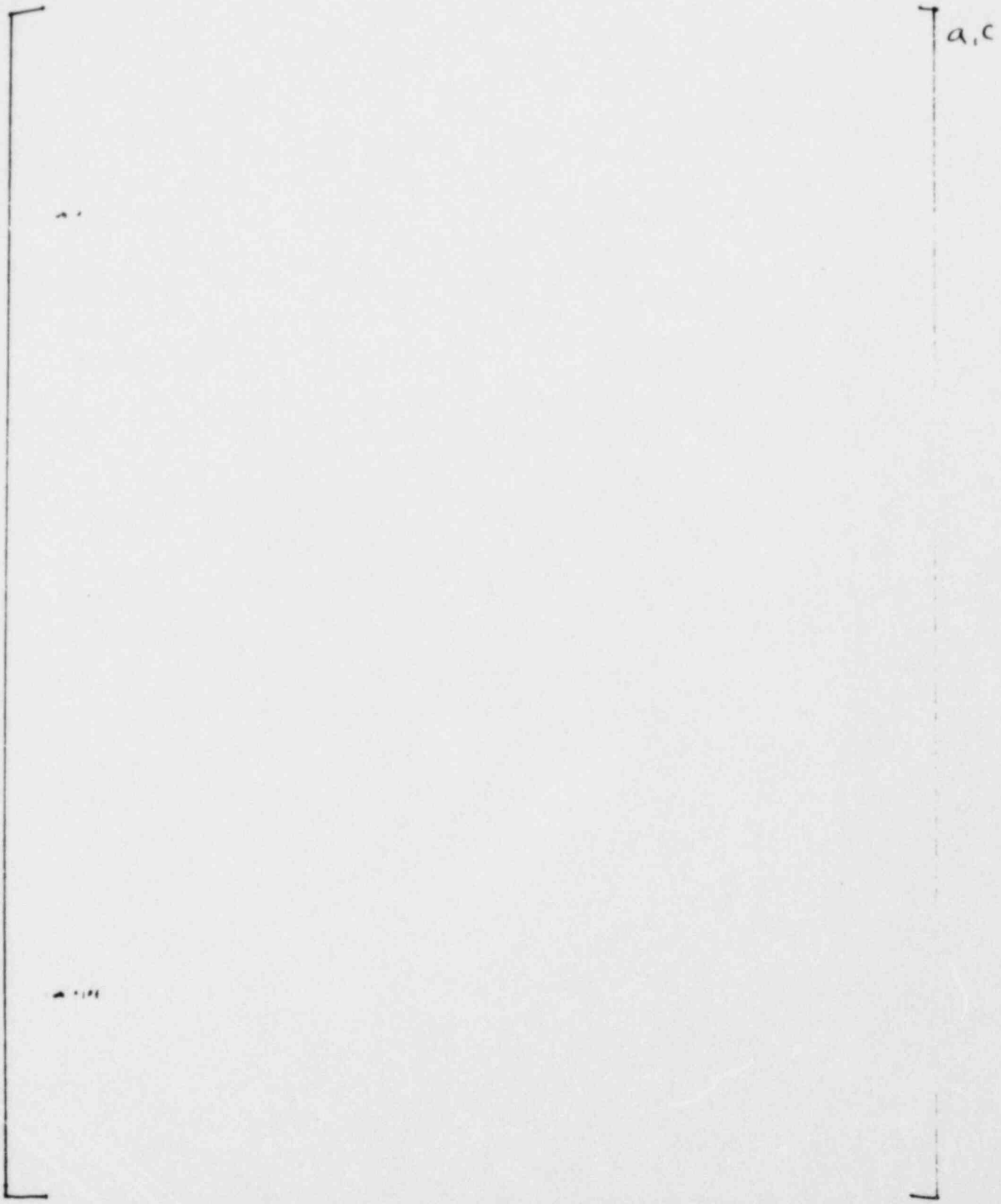

Figure 11.7-20: Stresses and Temperatures At Top of Counterbore For Pipe Profile T_1.

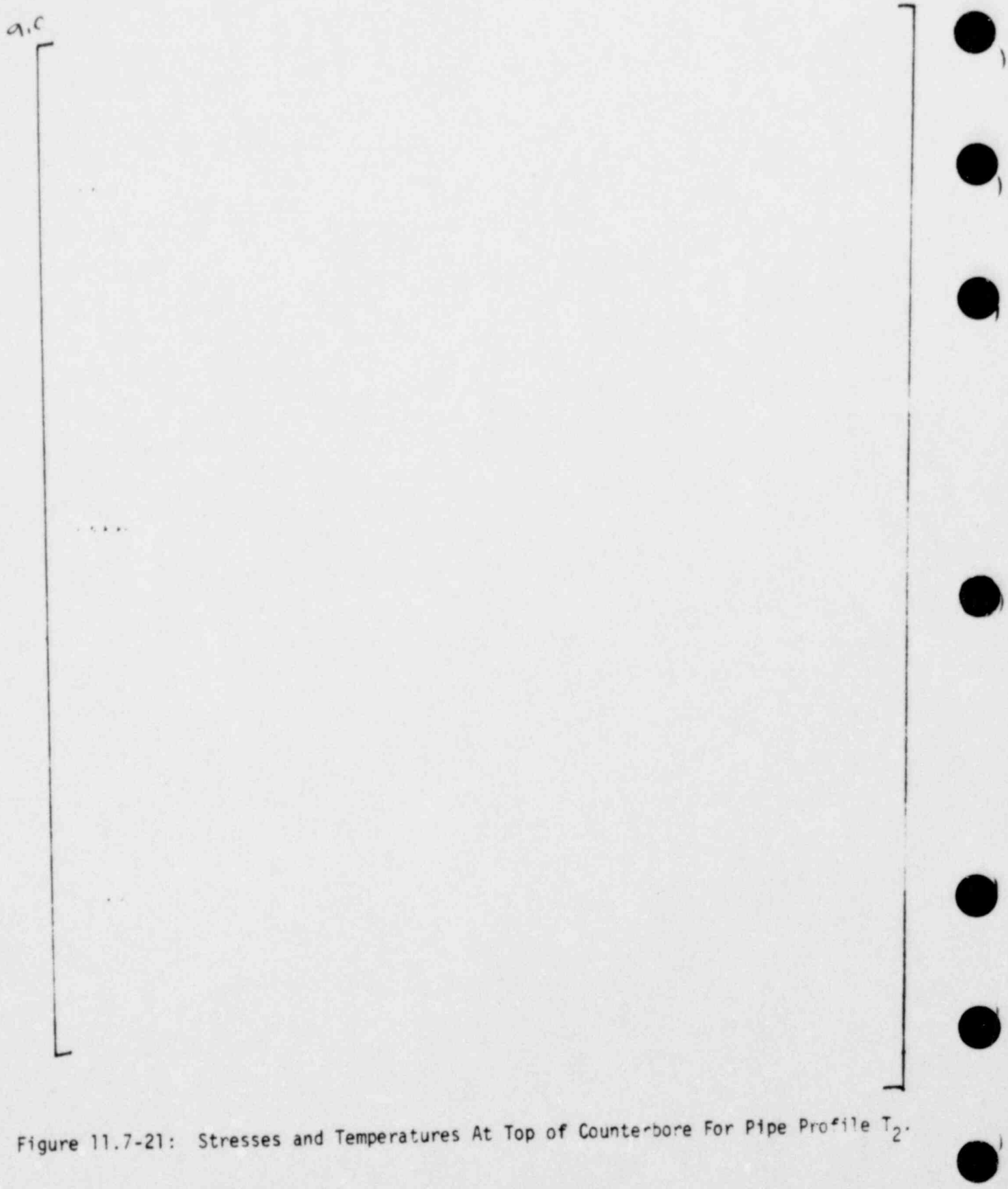

Figure 11.7-21: Stresses and Temperatures At Top of Counterbore For Pipe Profile T_2.

a,c

Figure 11.7-22: Stresses and Temperatures At Top of Counterbore For Pipe Profile T_3.

a,c

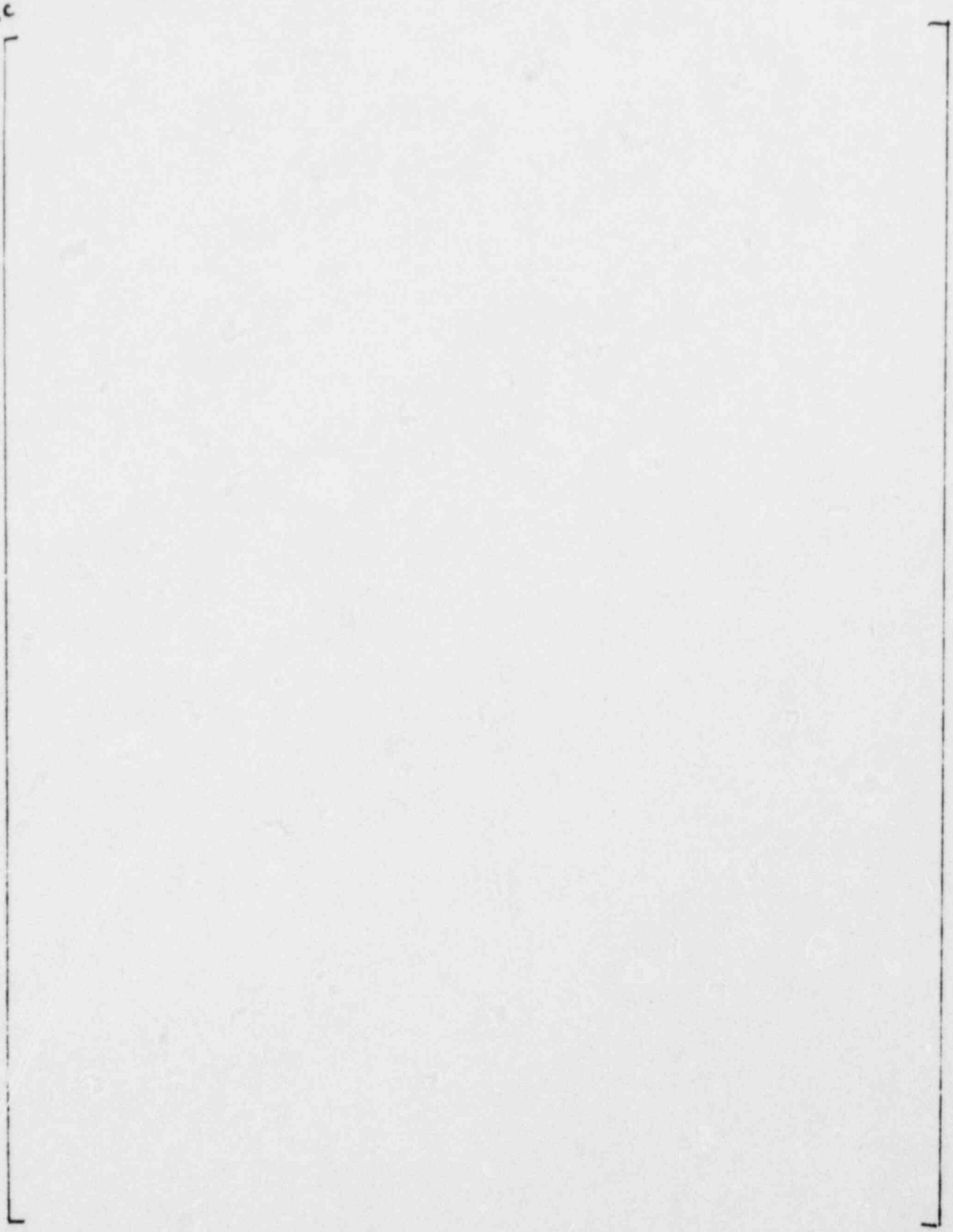

Figure 11.7-23: Stresses and Temperatures At Top of Counterbore For Pipe Profile T_4.

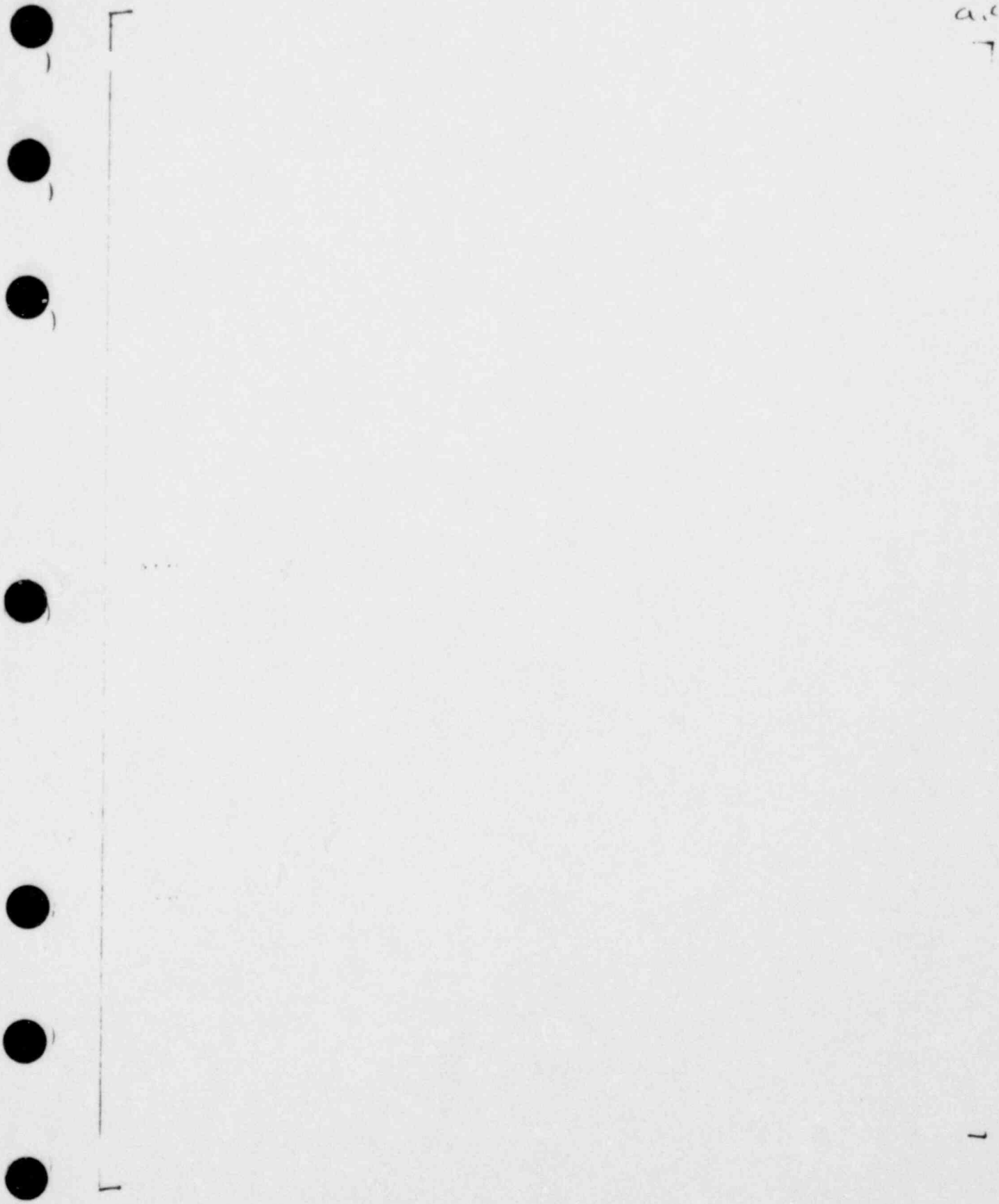

Figure 11.7-24: Stresses and Temperatures At Top of Counterbore For Pipe Profile T_5.

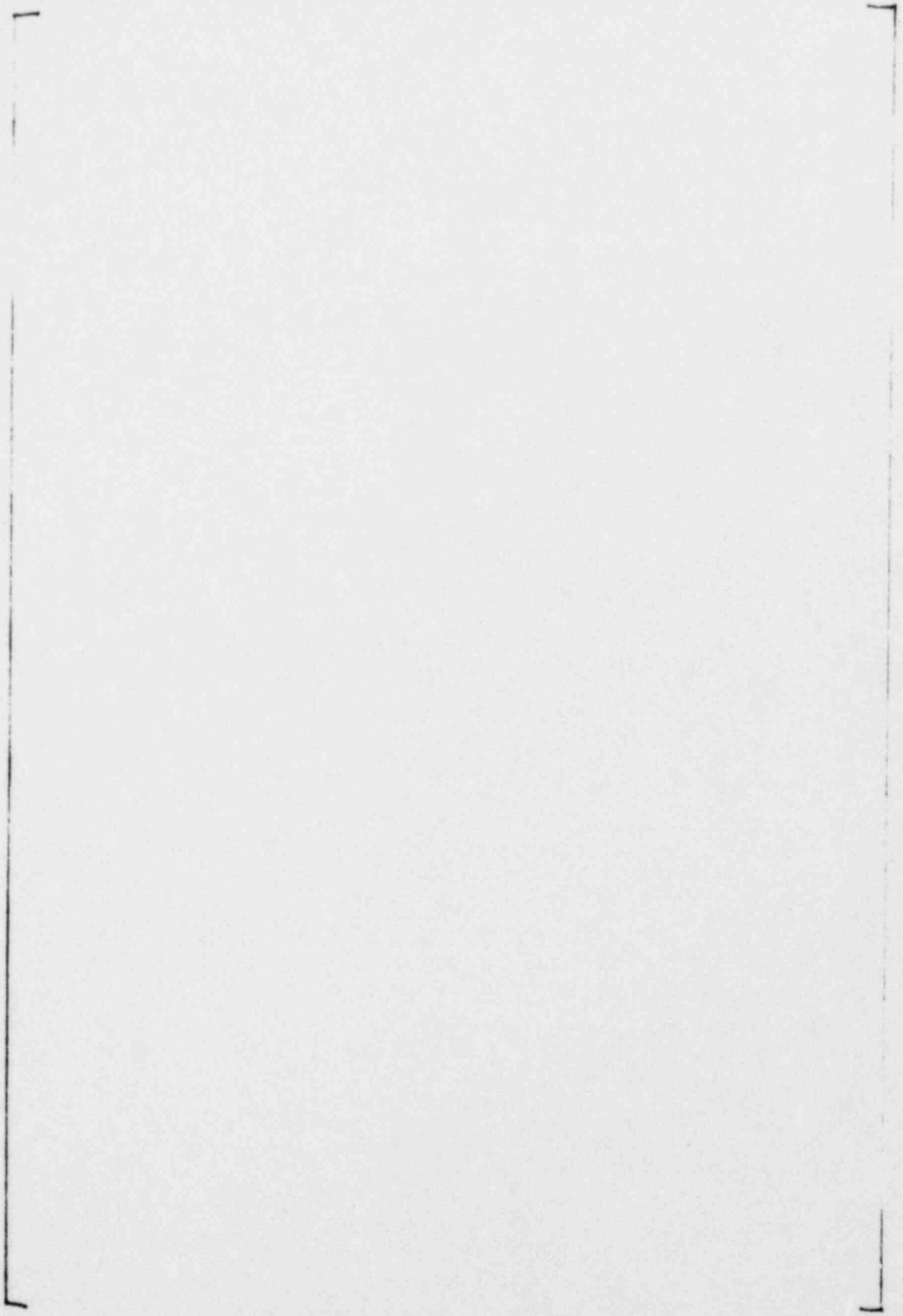

a,b,c,e

FIGURE 11.8-1: CASE NO. 1, FLOW TEST TEMPERATURE RECORD

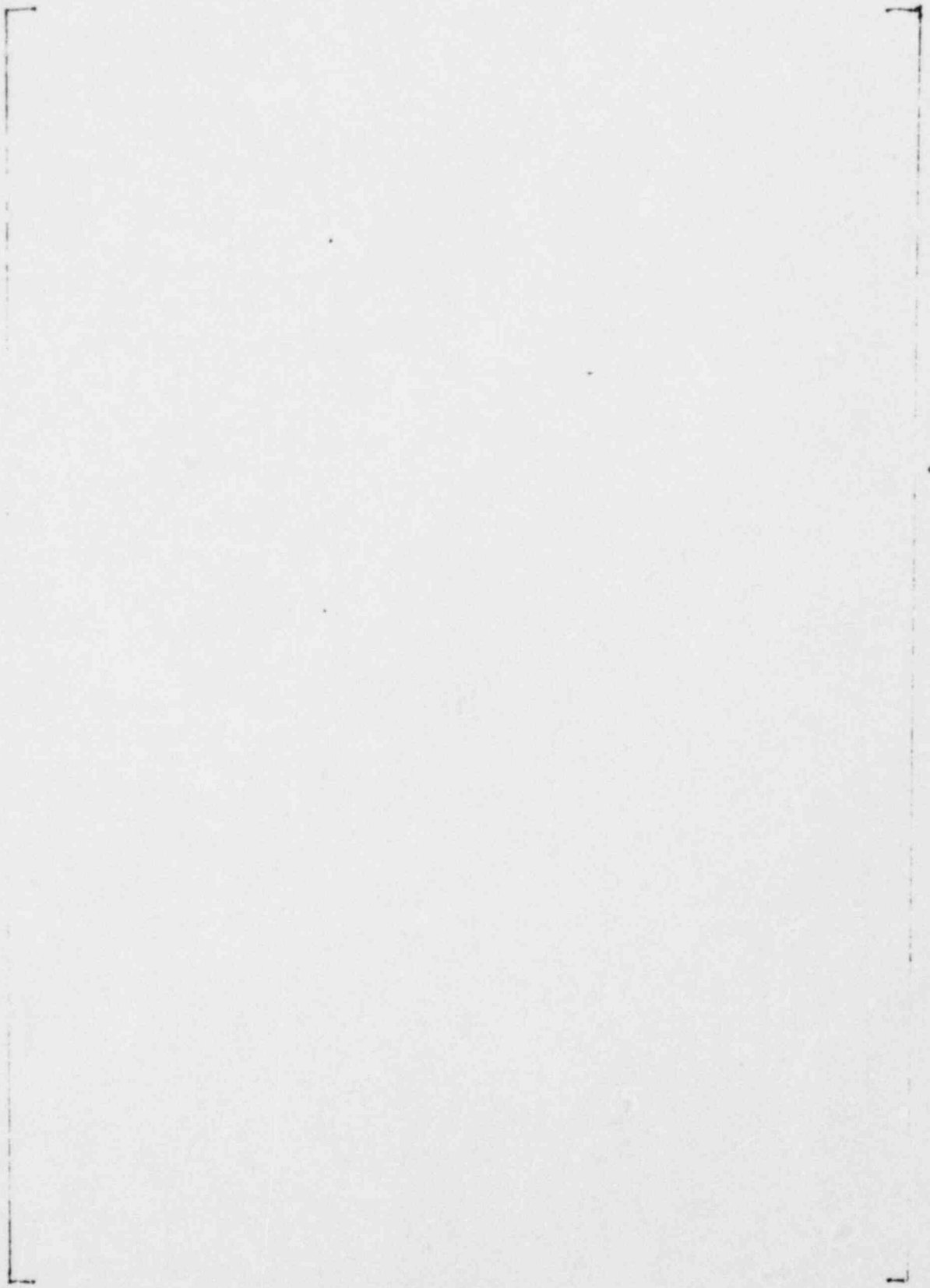

a,b,c,e

FIGURE 11.8-2: CASE NO. 2, FLOW TEST TEMPERATURE RECORD

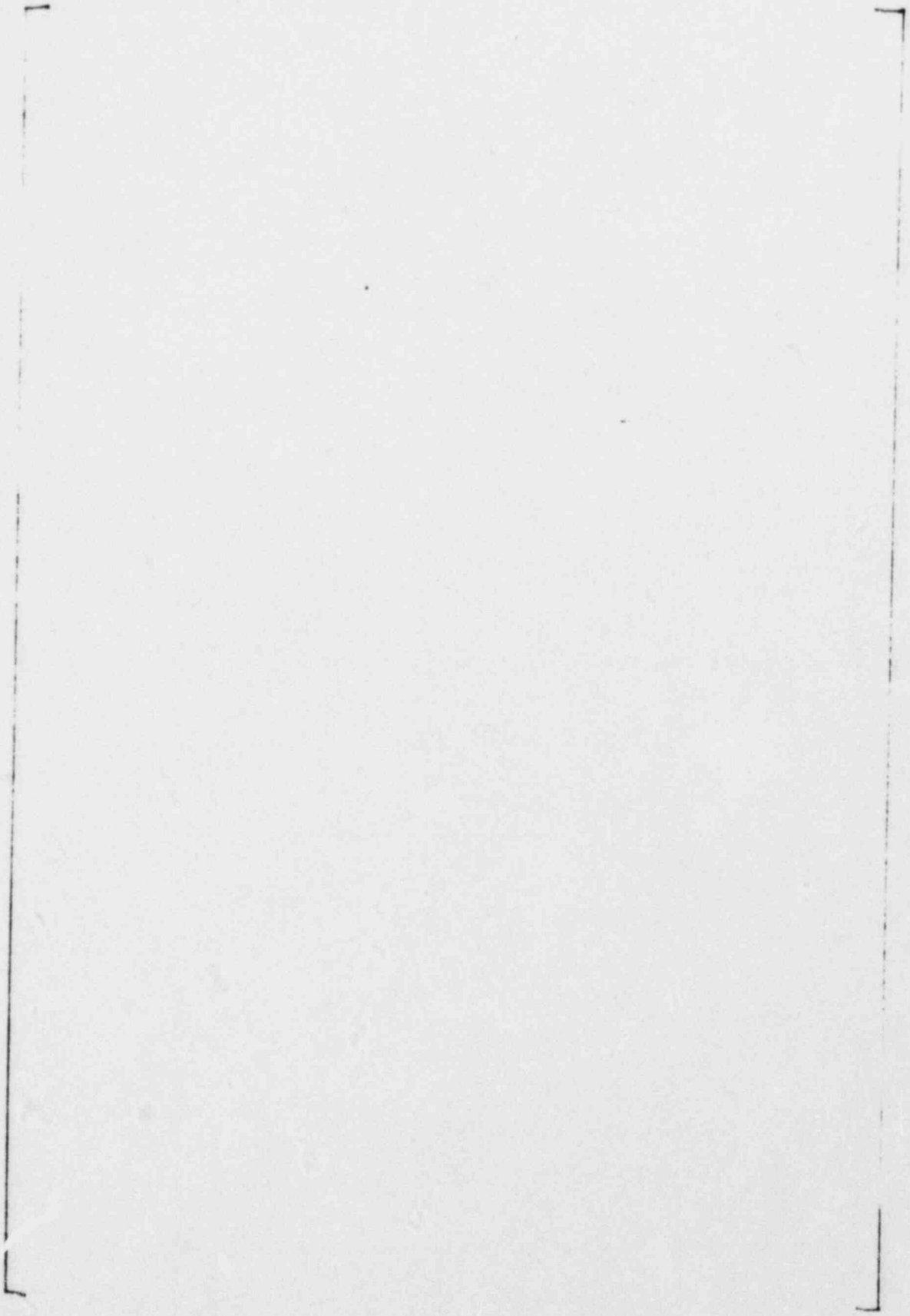

a.b.c.e

FIGURE 11.8-3: CASE NO. 3, FLOW TEST TEMPERATURE RECORD

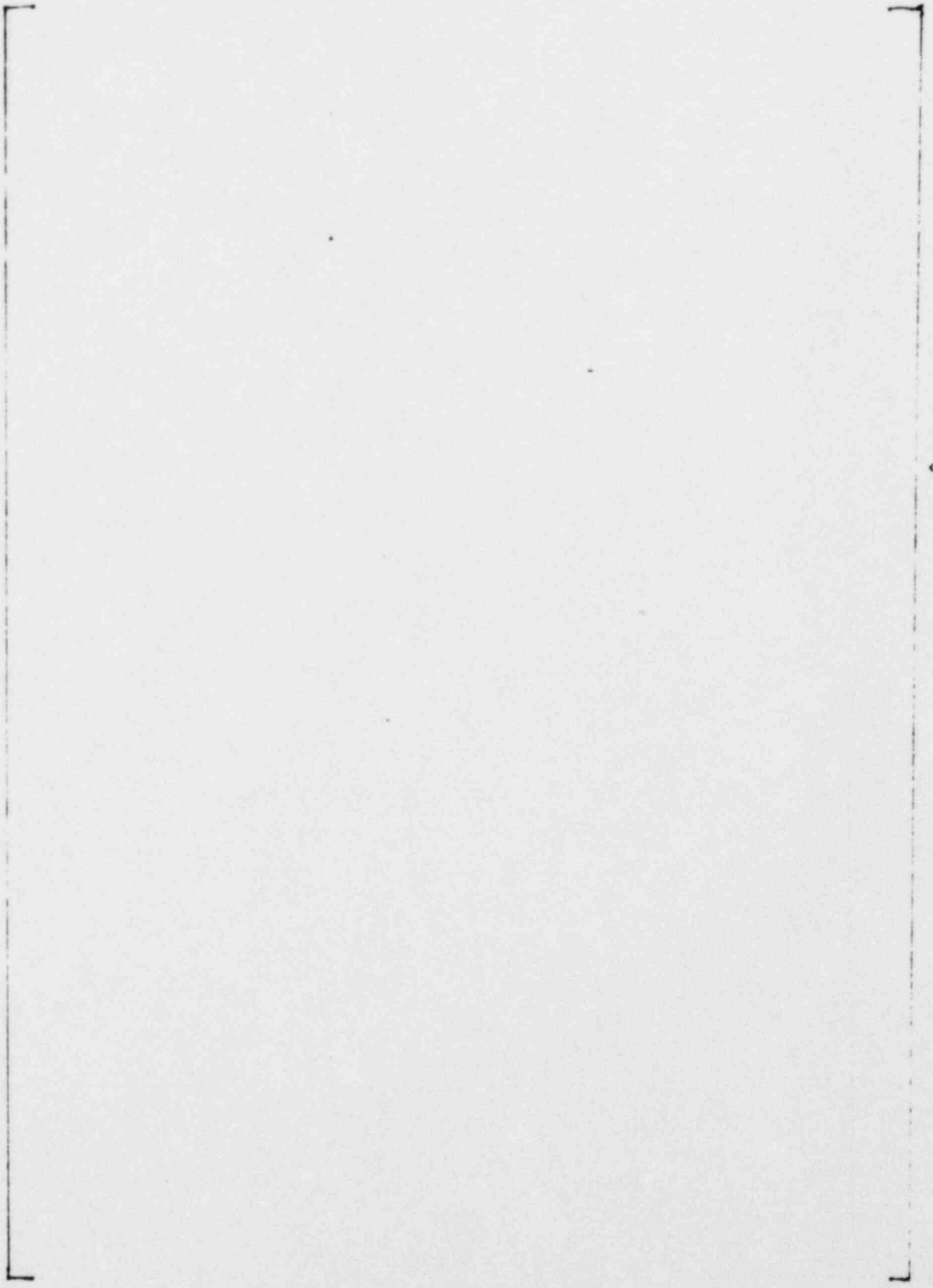

a,b,c,e

FIGURE 11.8-4: CASE No. 4, FLOW TEST TEMPERATURE RECORD

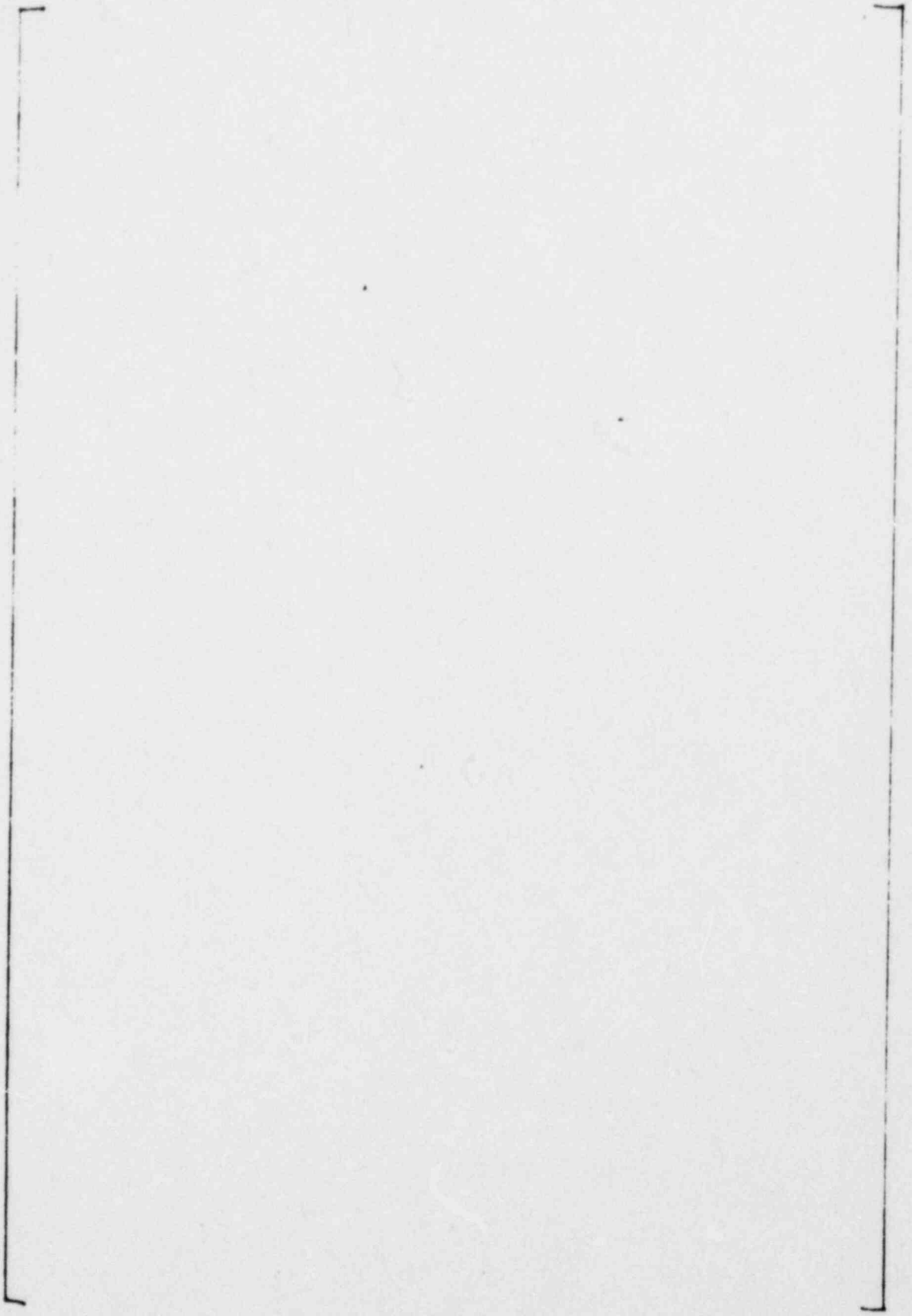

a.b.c.e

FIGURE 11.8-5, CASE NO. 5, FLOW TEST TEMPERATURE RECORD

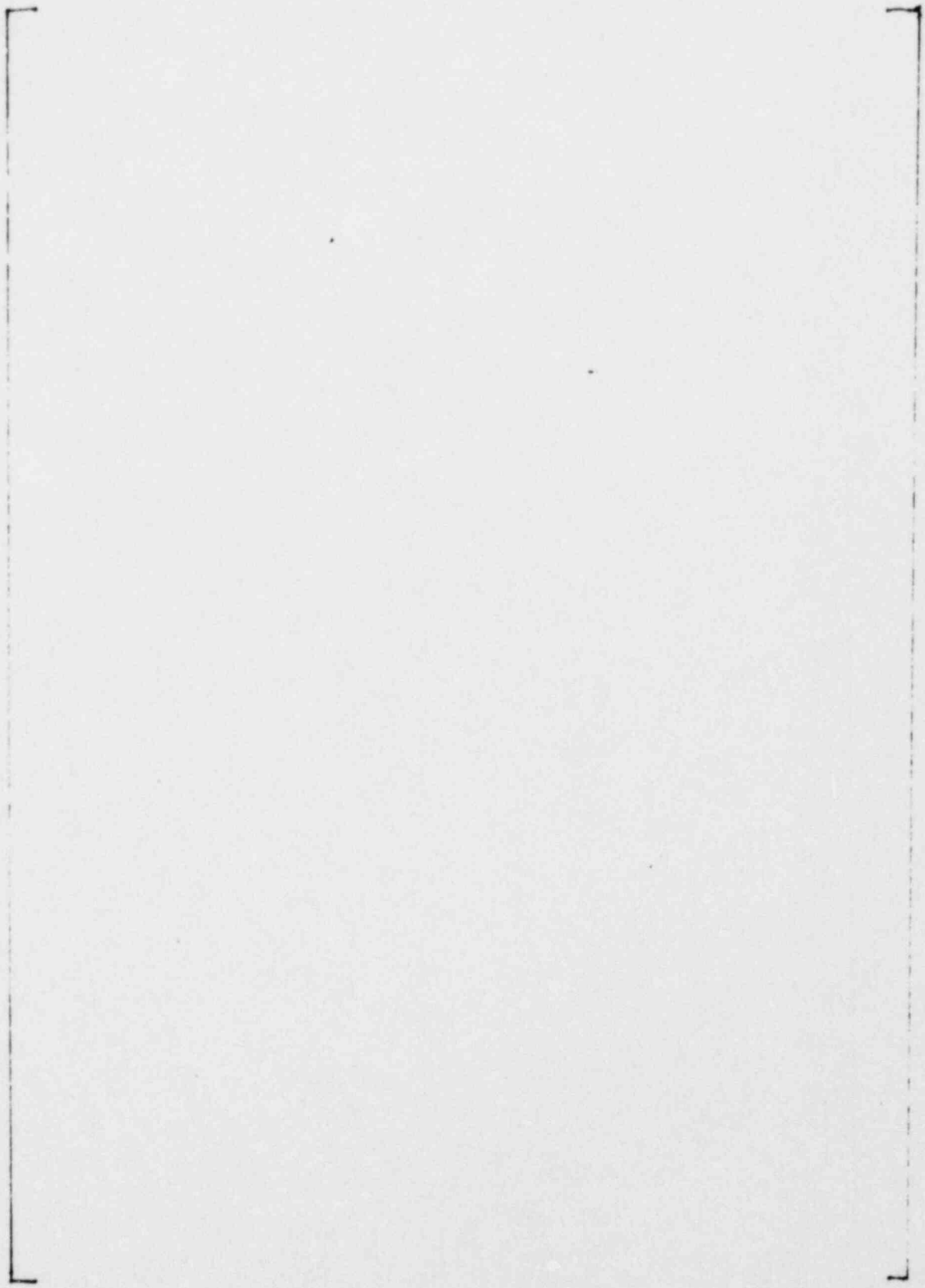

a,b,c,c

FIGURE 11.8-6, CASE NO. 6, FLOW TEST TEMPERATURE RECORD

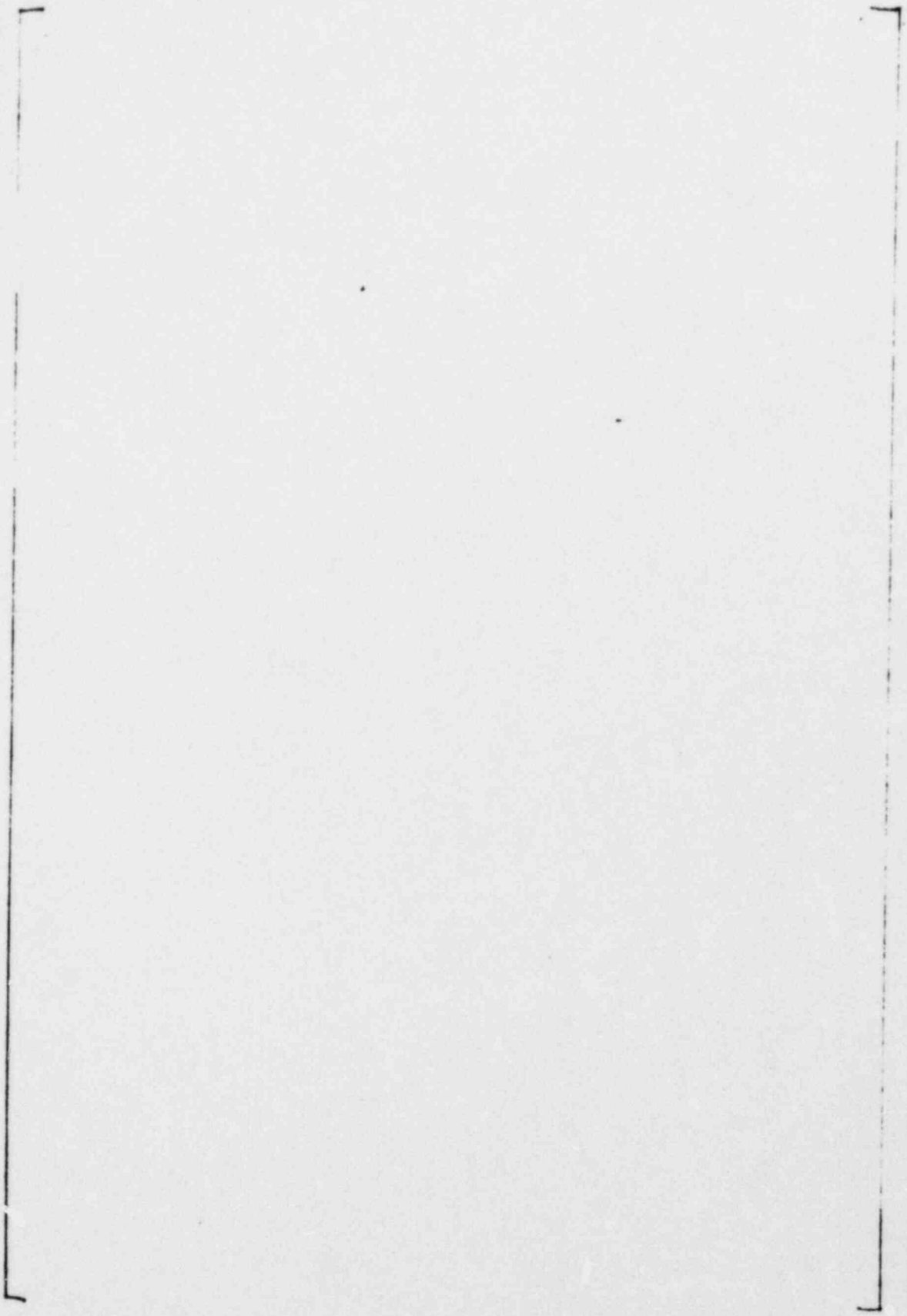

a.b.c.e

FIGURE 11.8-7, CASE NO. 7, FLOW TEST TEMPERATURE RECORD

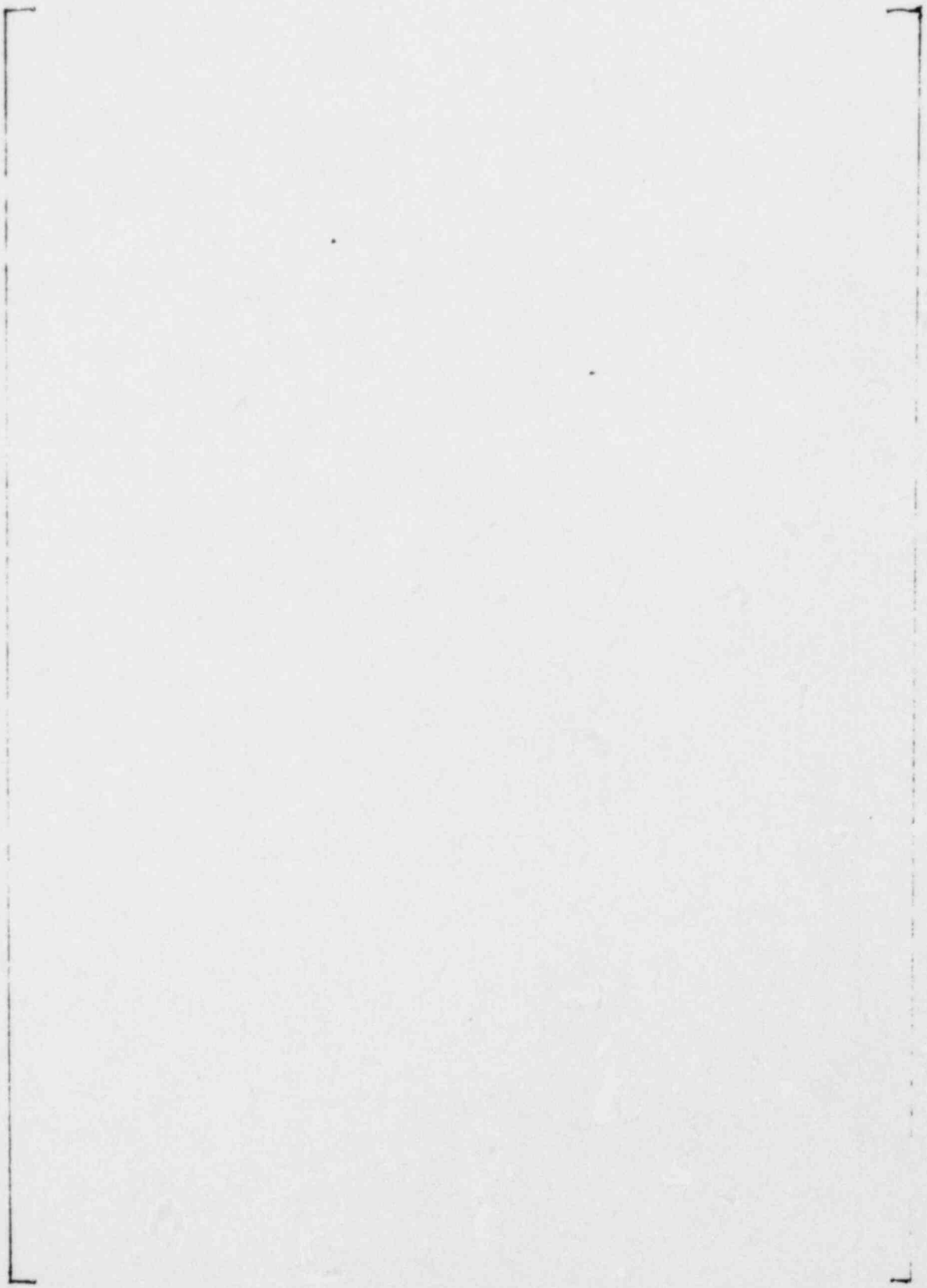

a,b,c,e

FIGURE 11.8-8, CASE NO. 8, FLOW TEST TEMPERATURE RECORD

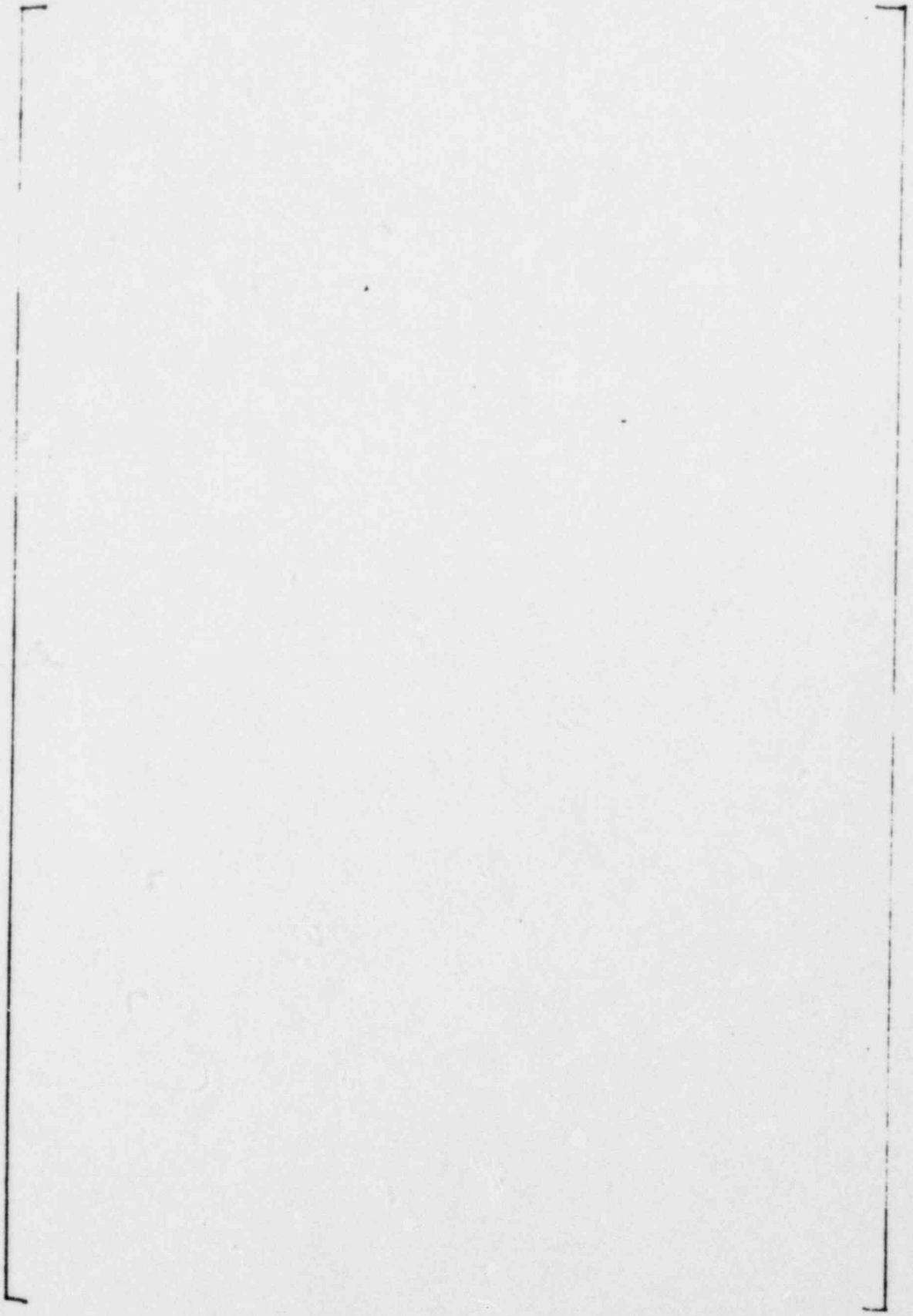

a.b.c.e

FIGURE 11.8-9, CASE NO. 9, FLOW TEST TEMPERATURE RECORD

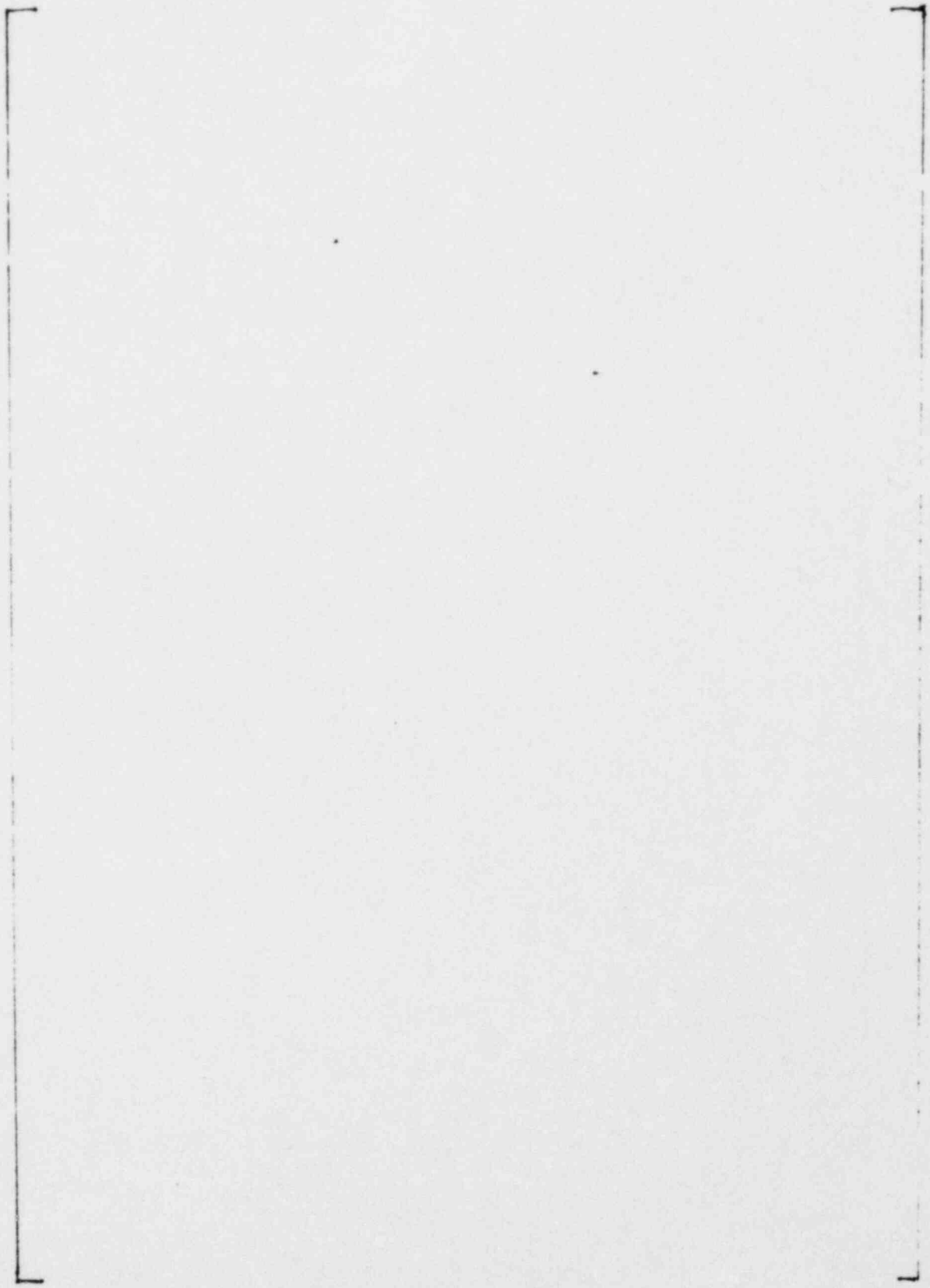

a,b,c,e

FIGURE 11.8-10, CASE NO.10, FLOW TEST TEMPERATURE RECORD

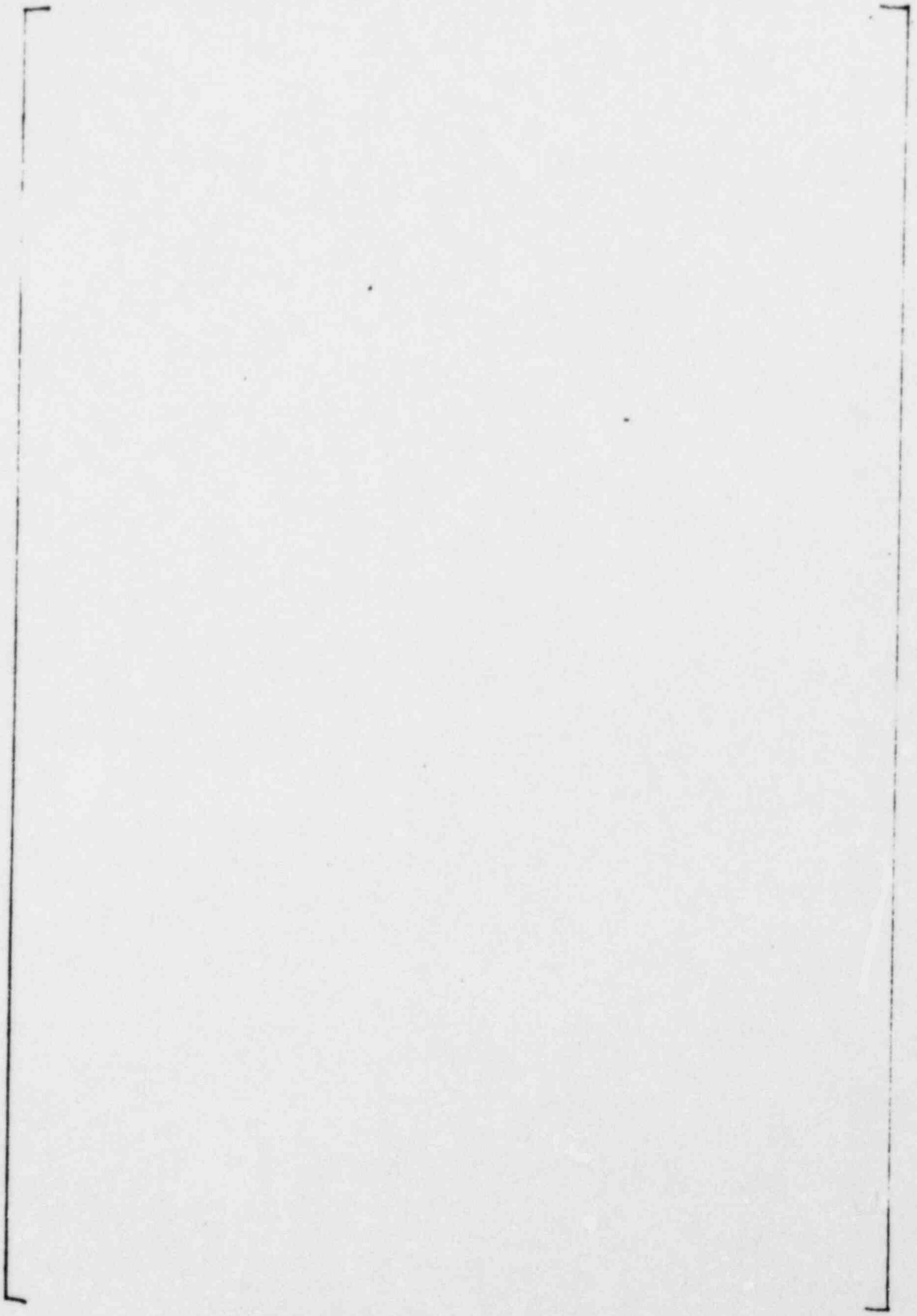

a,b,c,e

FIGURE 11.8-11, CASE NO.11, FLOW TEST TEMPERATURE RECORD

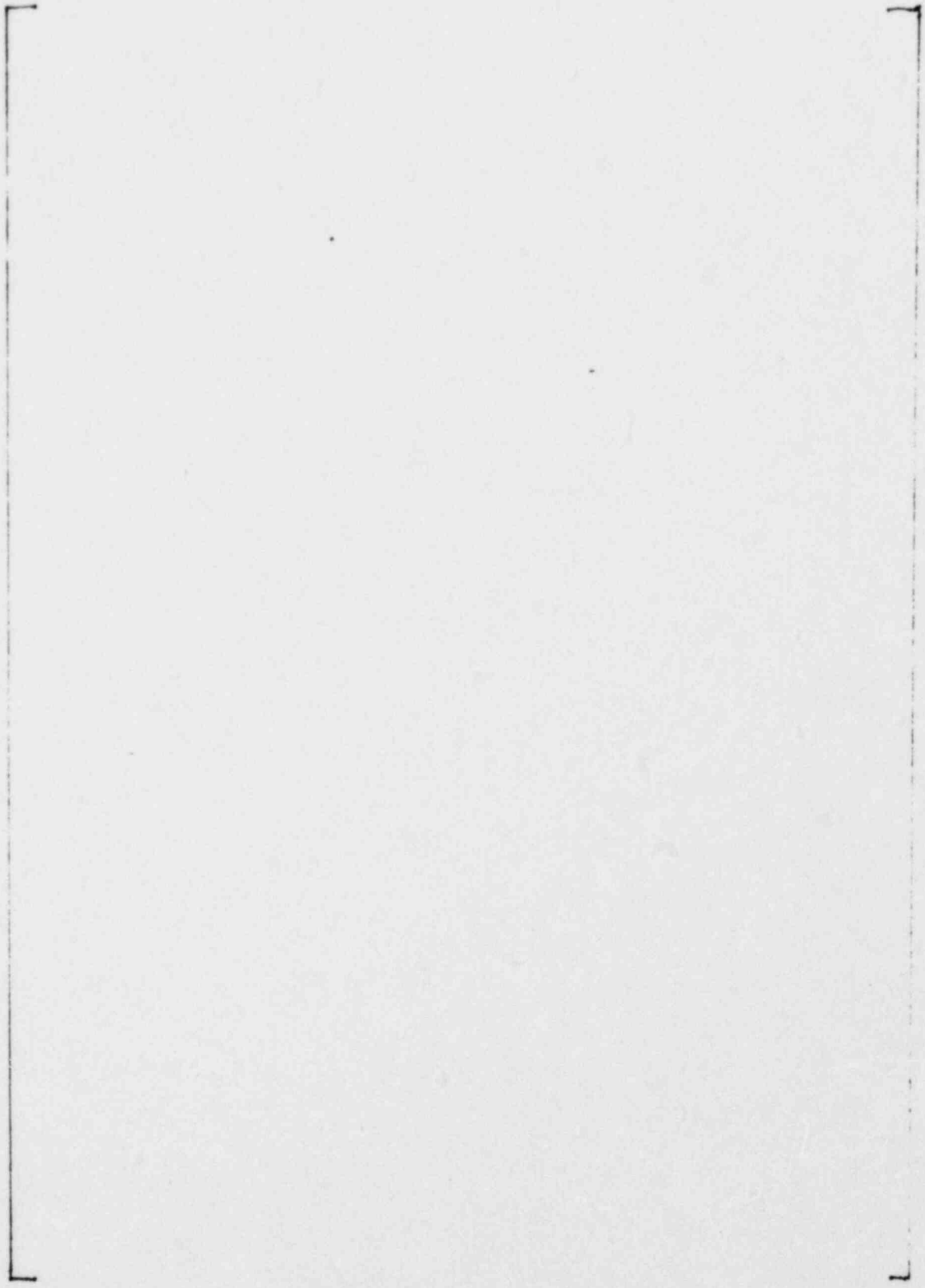

a,b,c,e

FIGURE 11.8-12, CASE NO.12, FLOW TEST TEMPERATURE RECORD

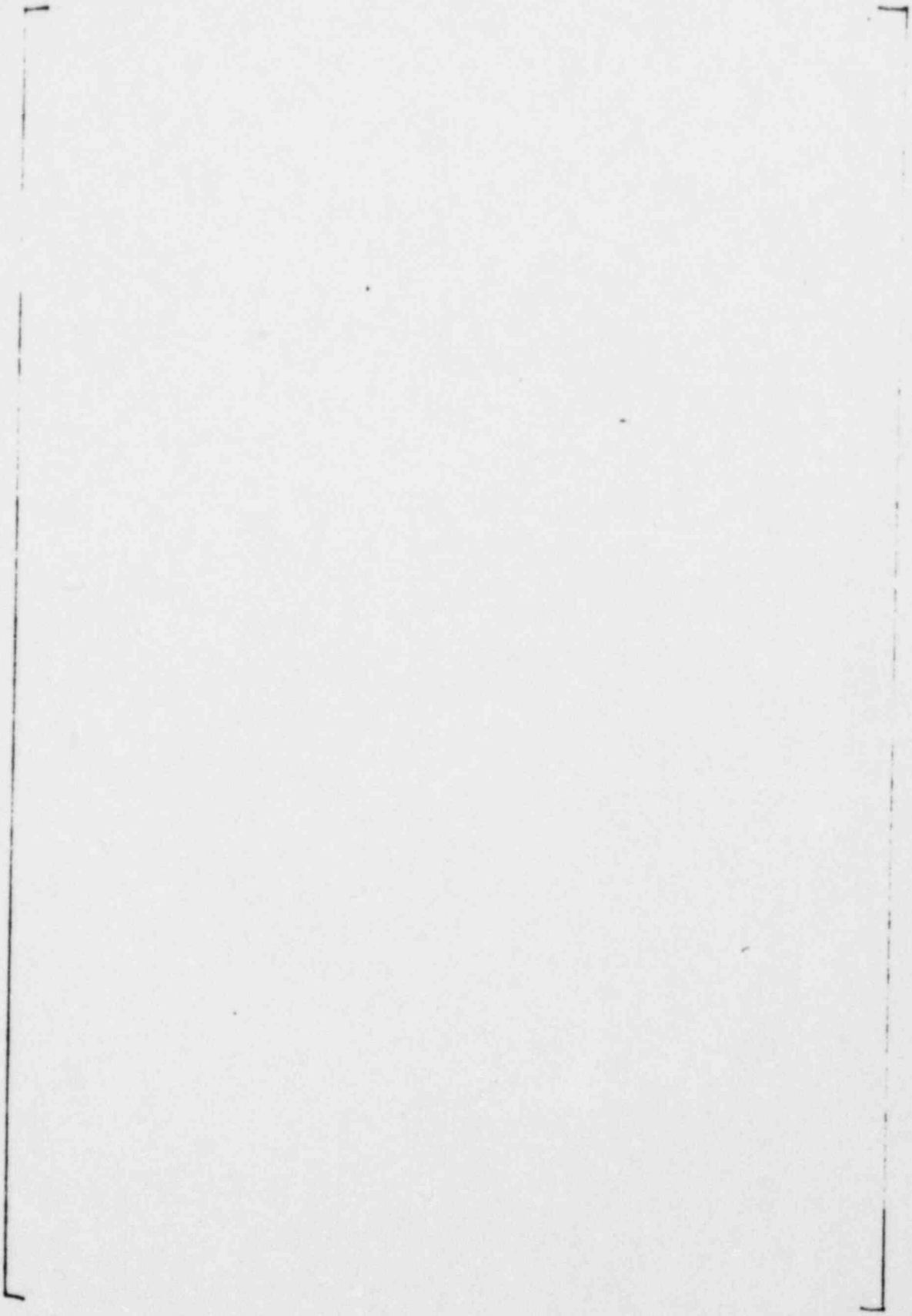

a,b,c,e

FIGURE 11.8-13, CASE NO.13, FLOW TEST TEMPERATURE RECORD

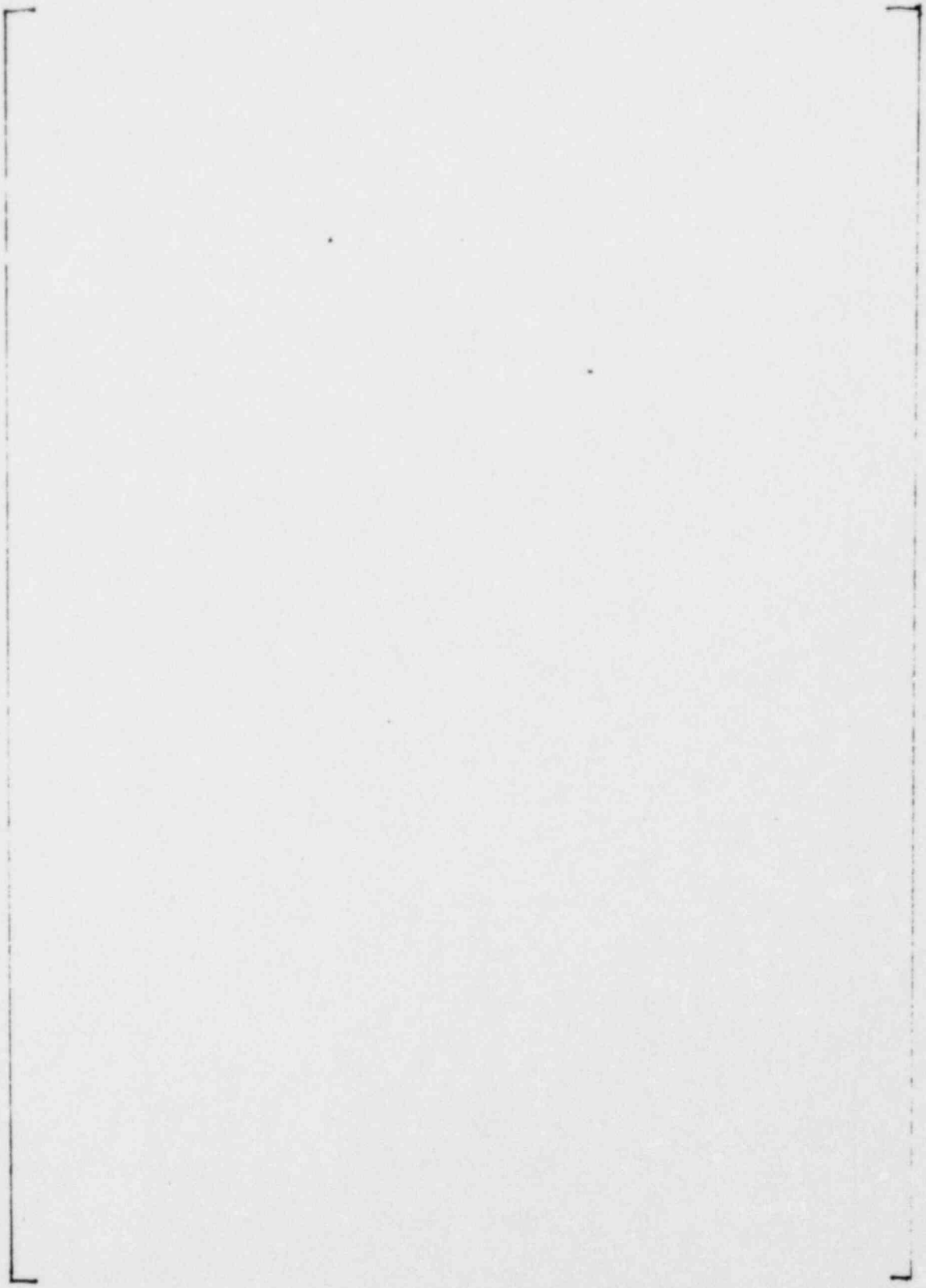

a,b,c,e

FIGURE 11.8-14, CASE NO.14, FLOW TEST TEMPERATURE RECORD

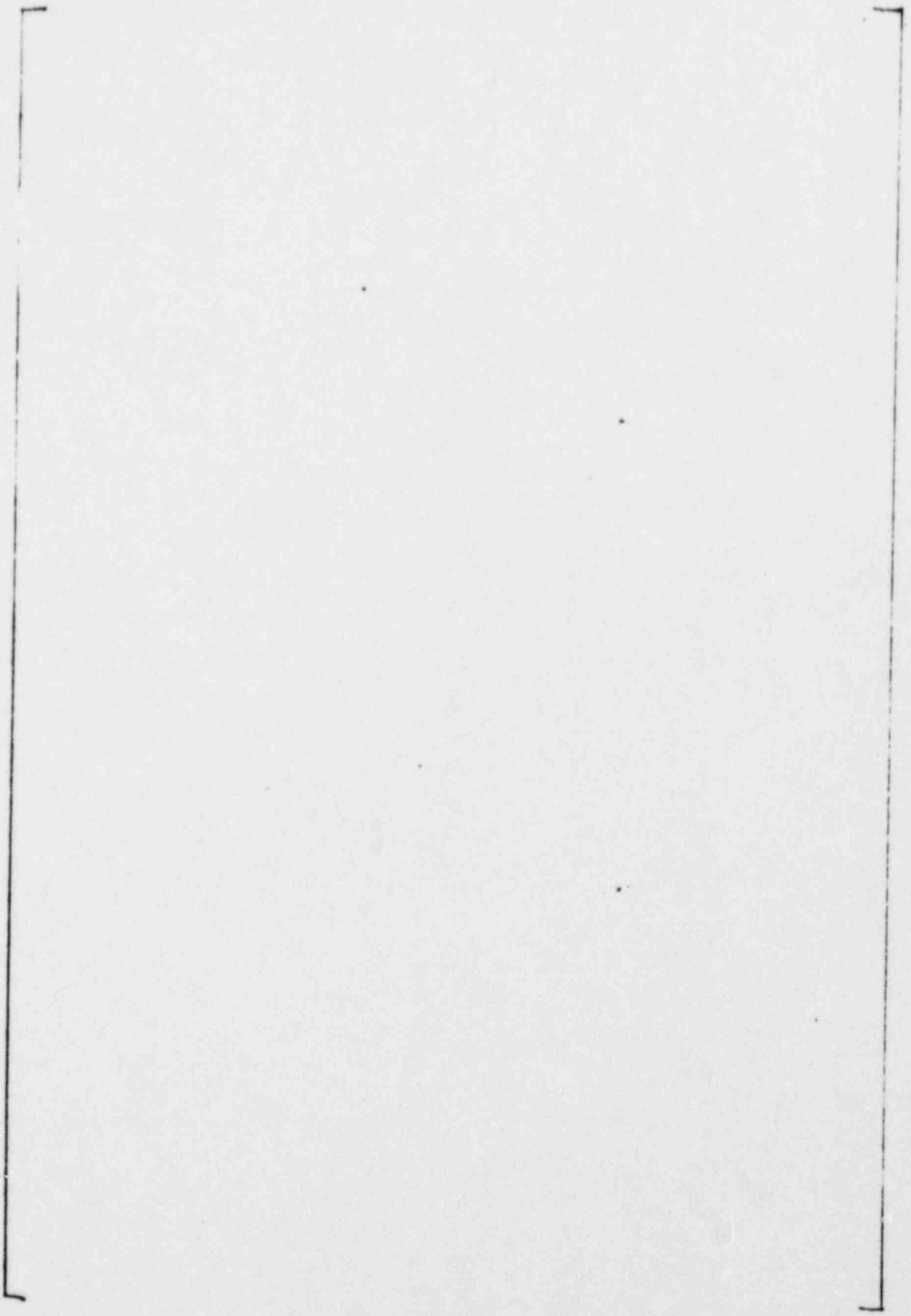

a.b.c.e

FIGURE 11.8-15, CASE NO.15, FLOW TEST TEMPERATURE RECORD

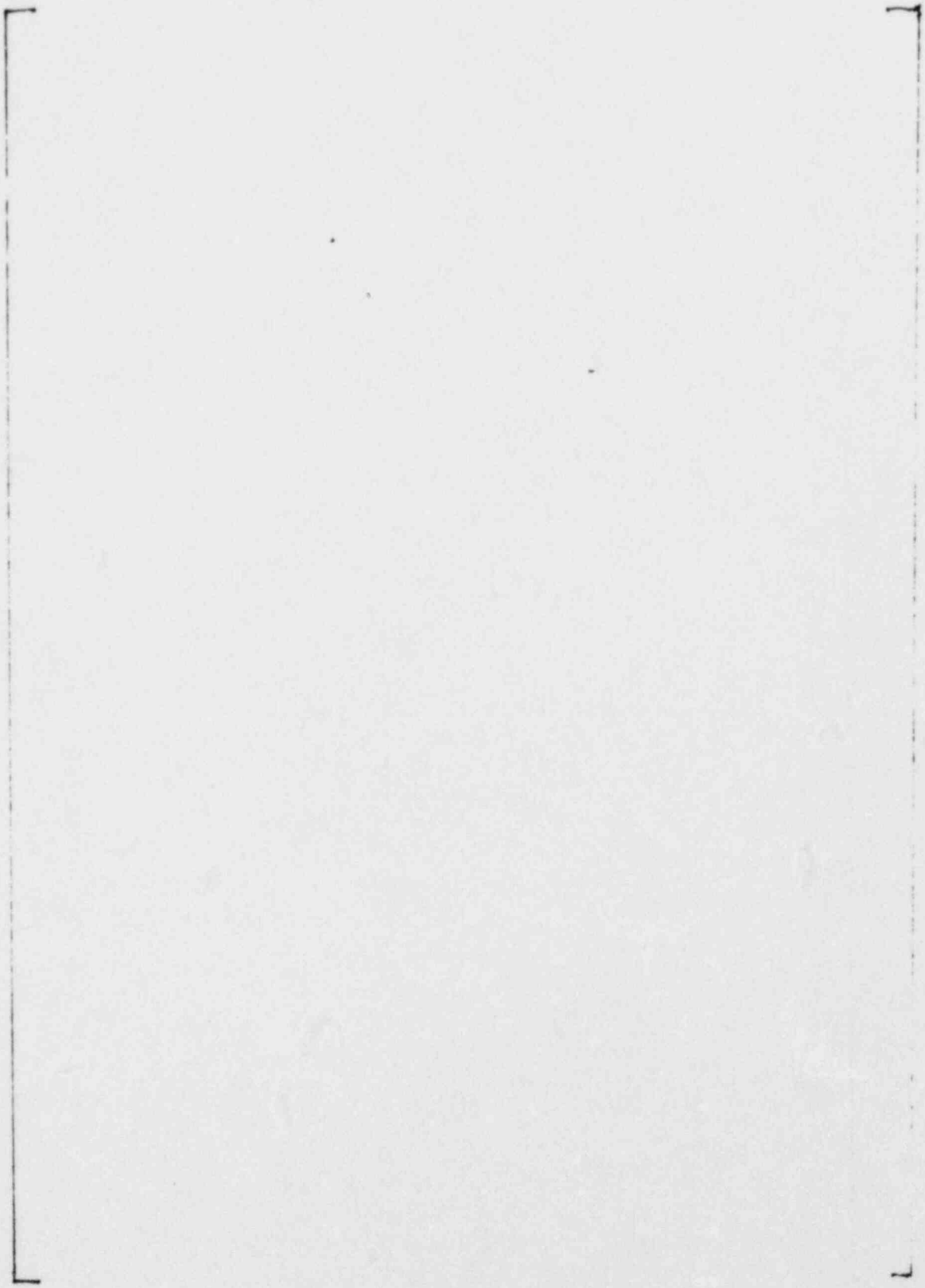

a,b,c,e

FIGURE 11.8-16, CASE NO.16, FLOW TEST TEMPERATURE RECORD

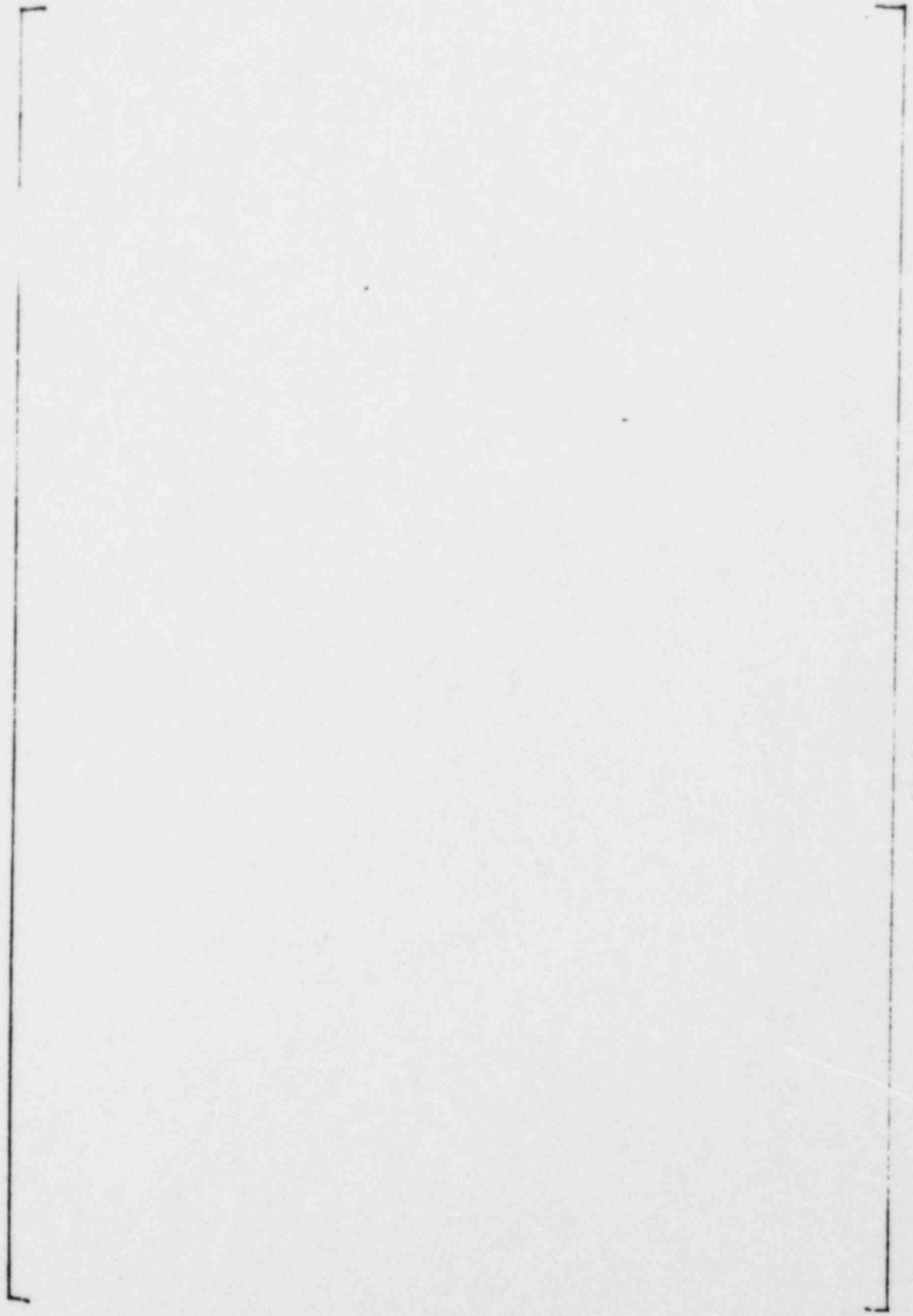

a.b.c.e

FIGURE 11.8-17, CASE NO.17, FLOW TEST TEMPERATURE RECORD

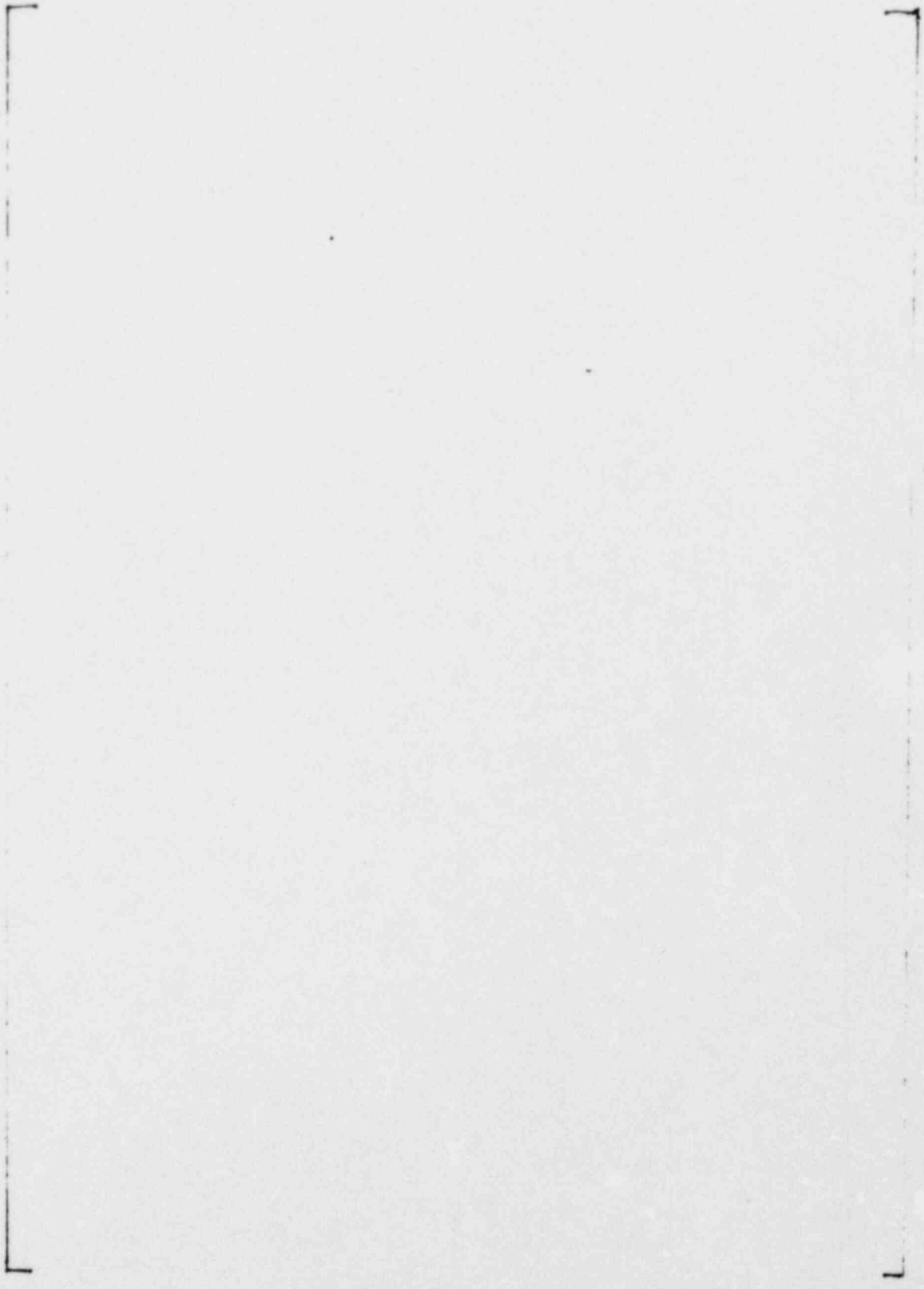

a,b,c,e

FIGURE 11.8-18, CASE No.18, FLOW TEST TEMPERATURE RECORD

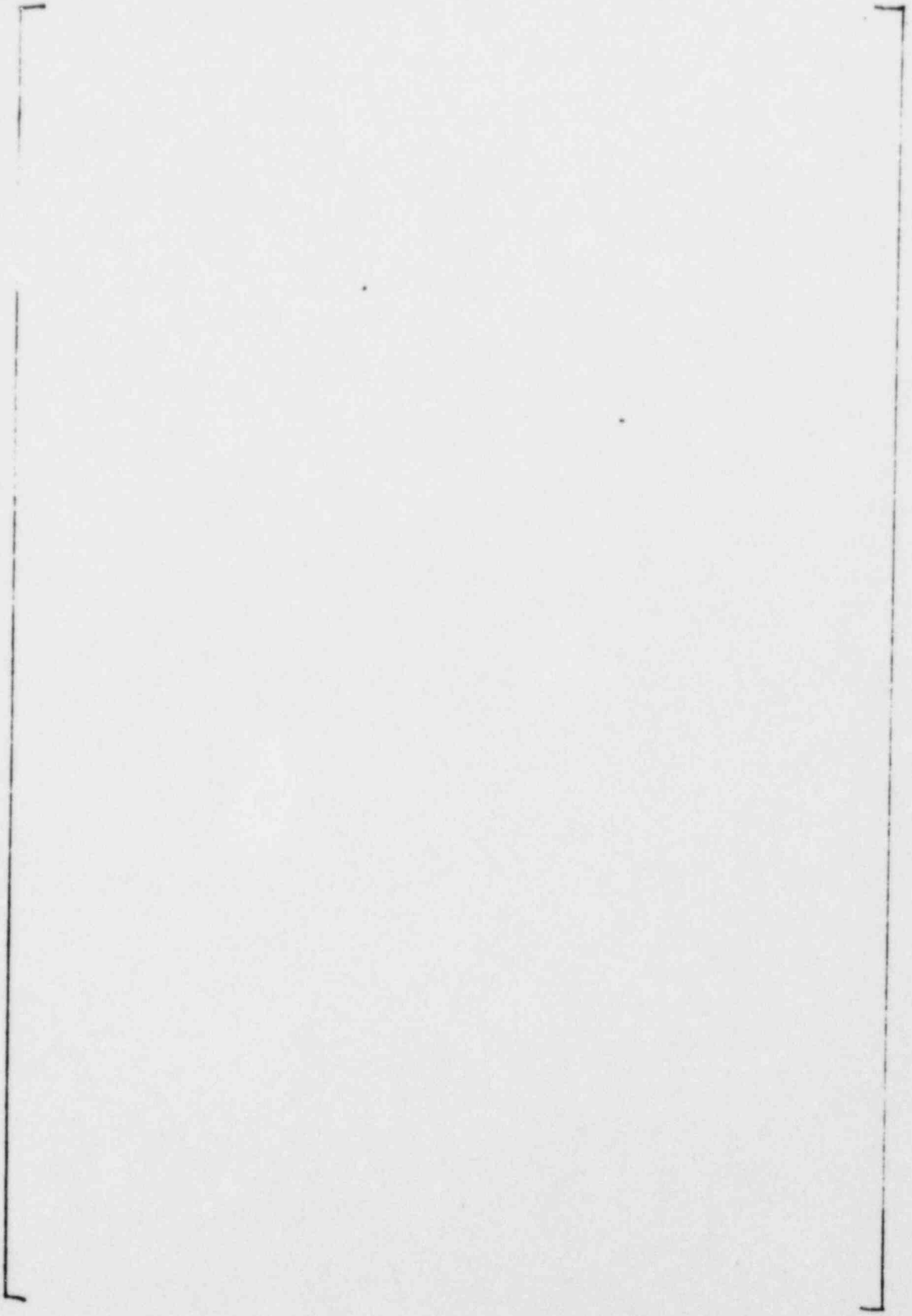

a,b,c,e

FIGURE 11.8-19, CASE NO.19, FLOW TEST TEMPERATURE RECORD

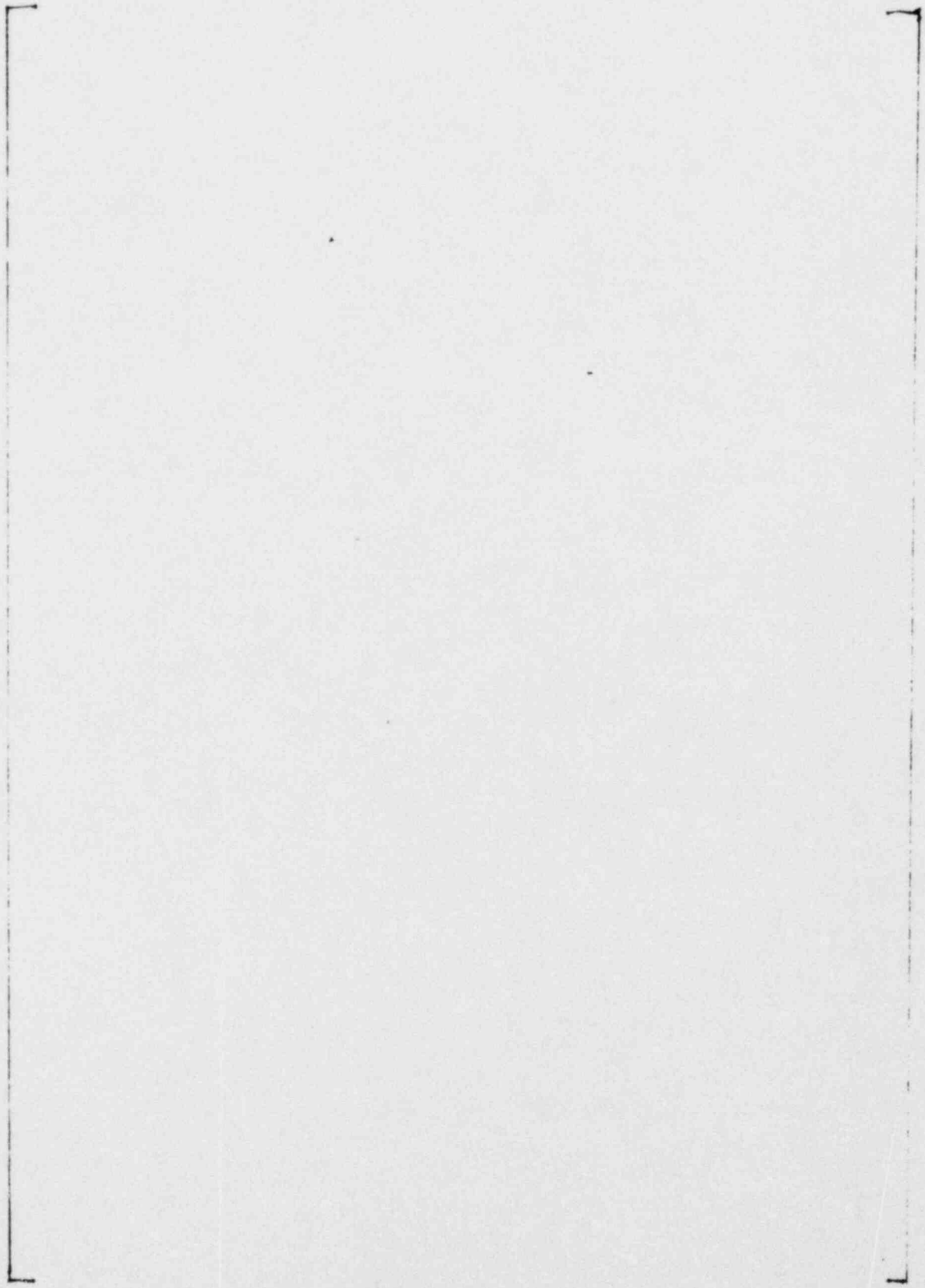

a,b,c,e

FIGURE 11.8-20, CASE NO.20, FLOW TEST TEMPERATURE RECORD

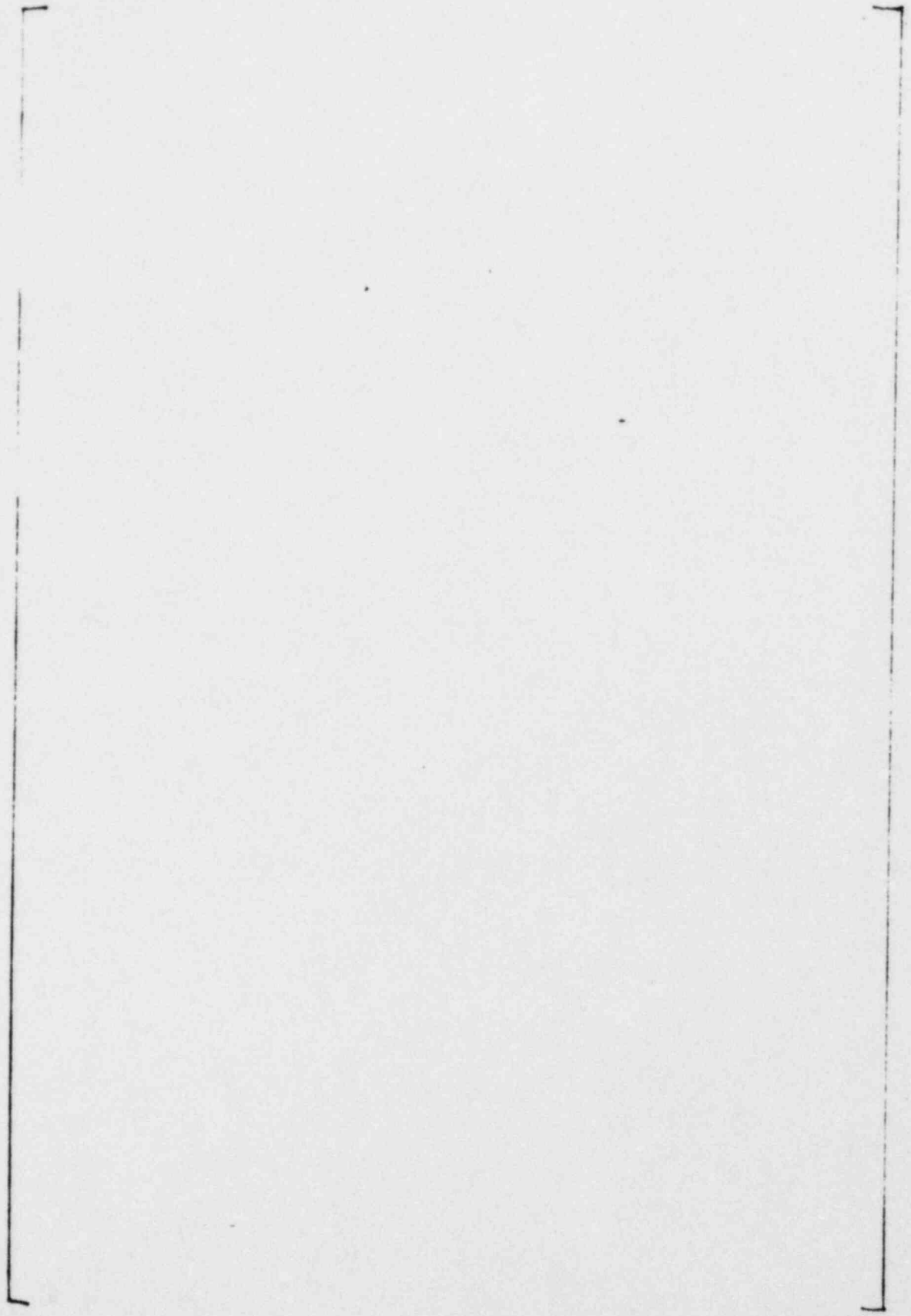

a.b.c.e

FIGURE 11.8-21, CASE NO.21, FLOW TEST TEMPERATURE RECORD

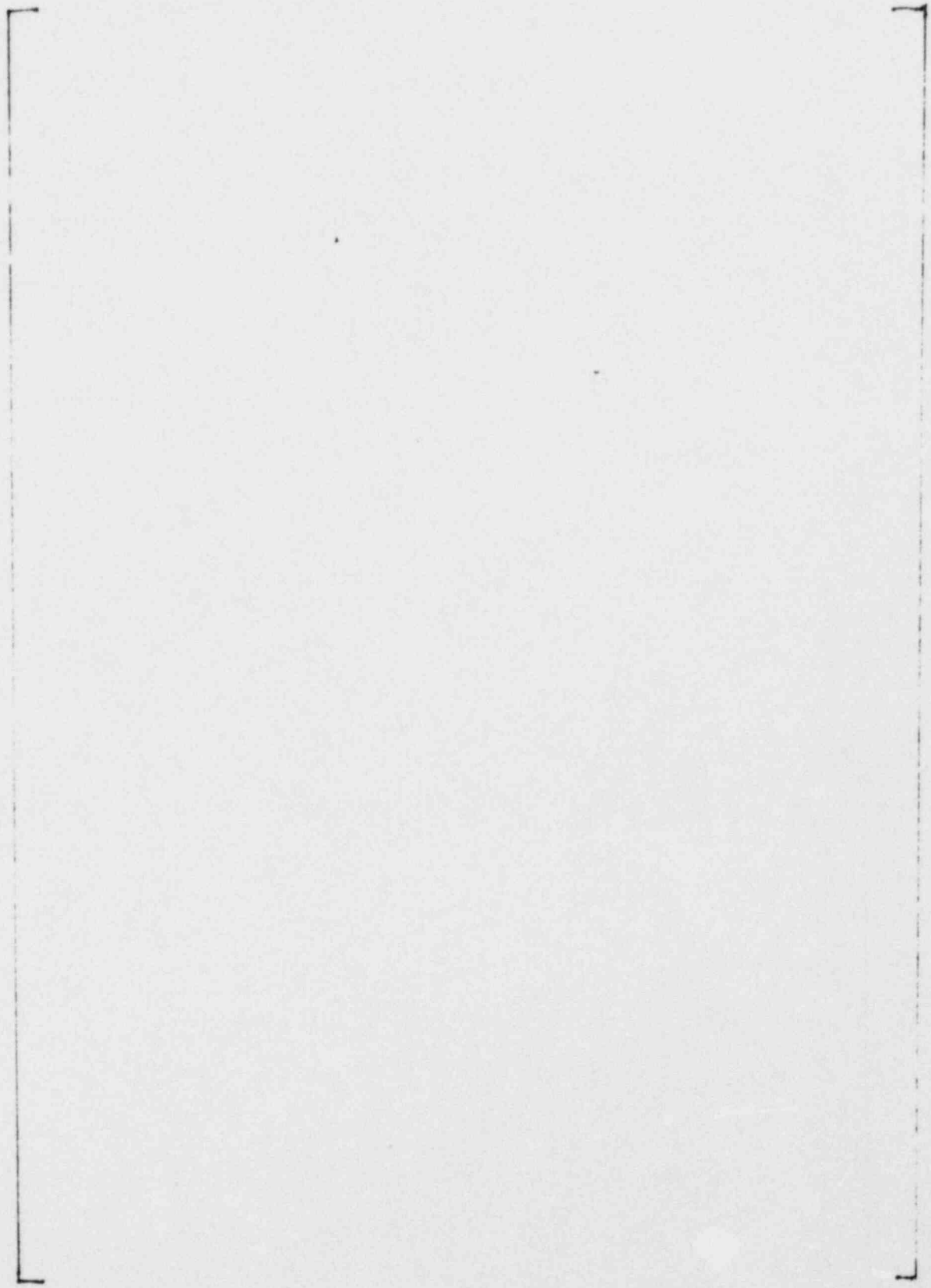

a,b,c,e

FIGURE 11.8-22, CASE NO.22, FLOW TEST TEMPERATURE RECORD

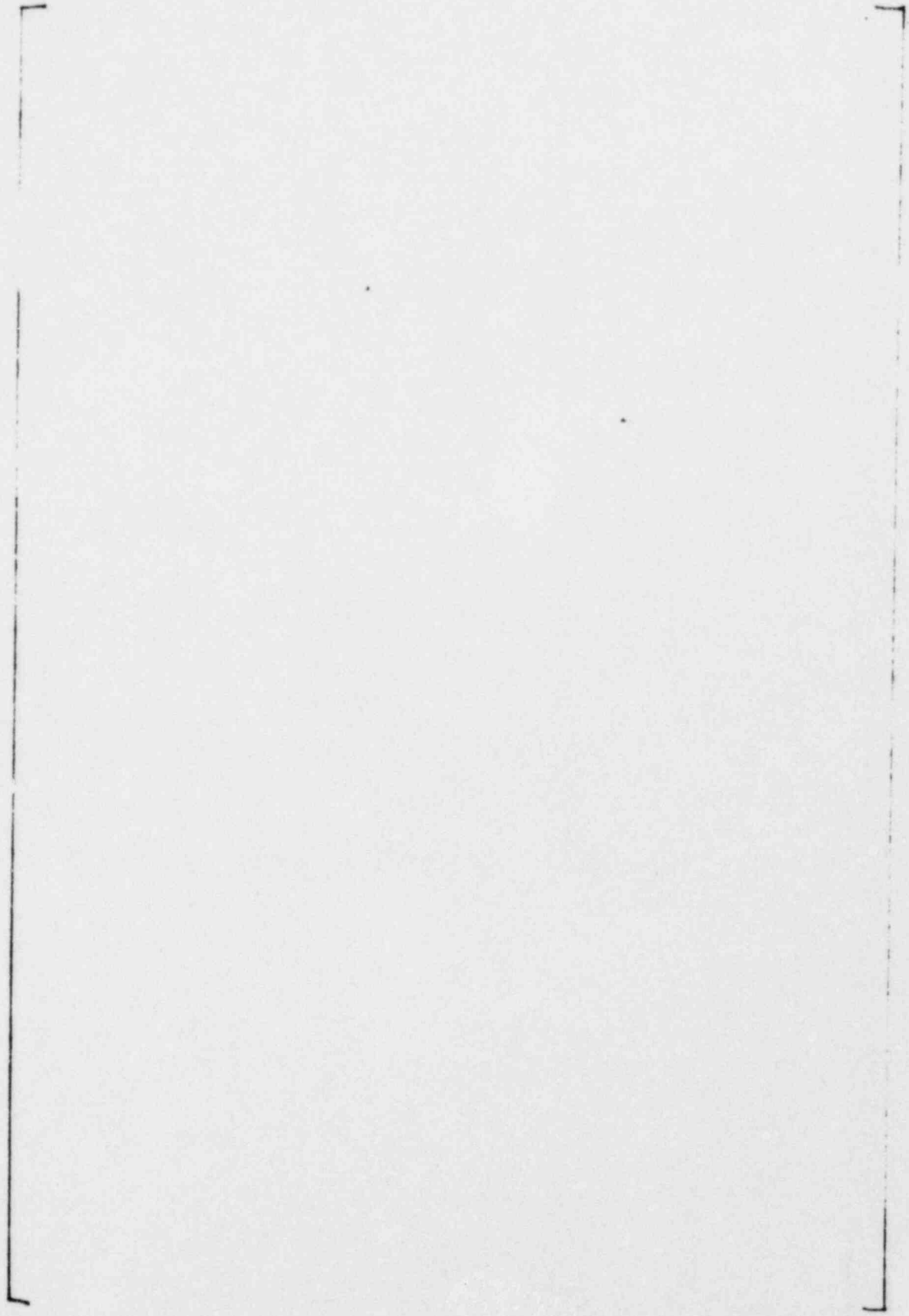

a.b.c.e

FIGURE 11.8-23, CASE NO.23, FLOW TEST TEMPERATURE RECORD

a,b,c,e

FIGURE 11,8-24, CASE NO.24, FLOW TEST TEMPERATURE RECORD

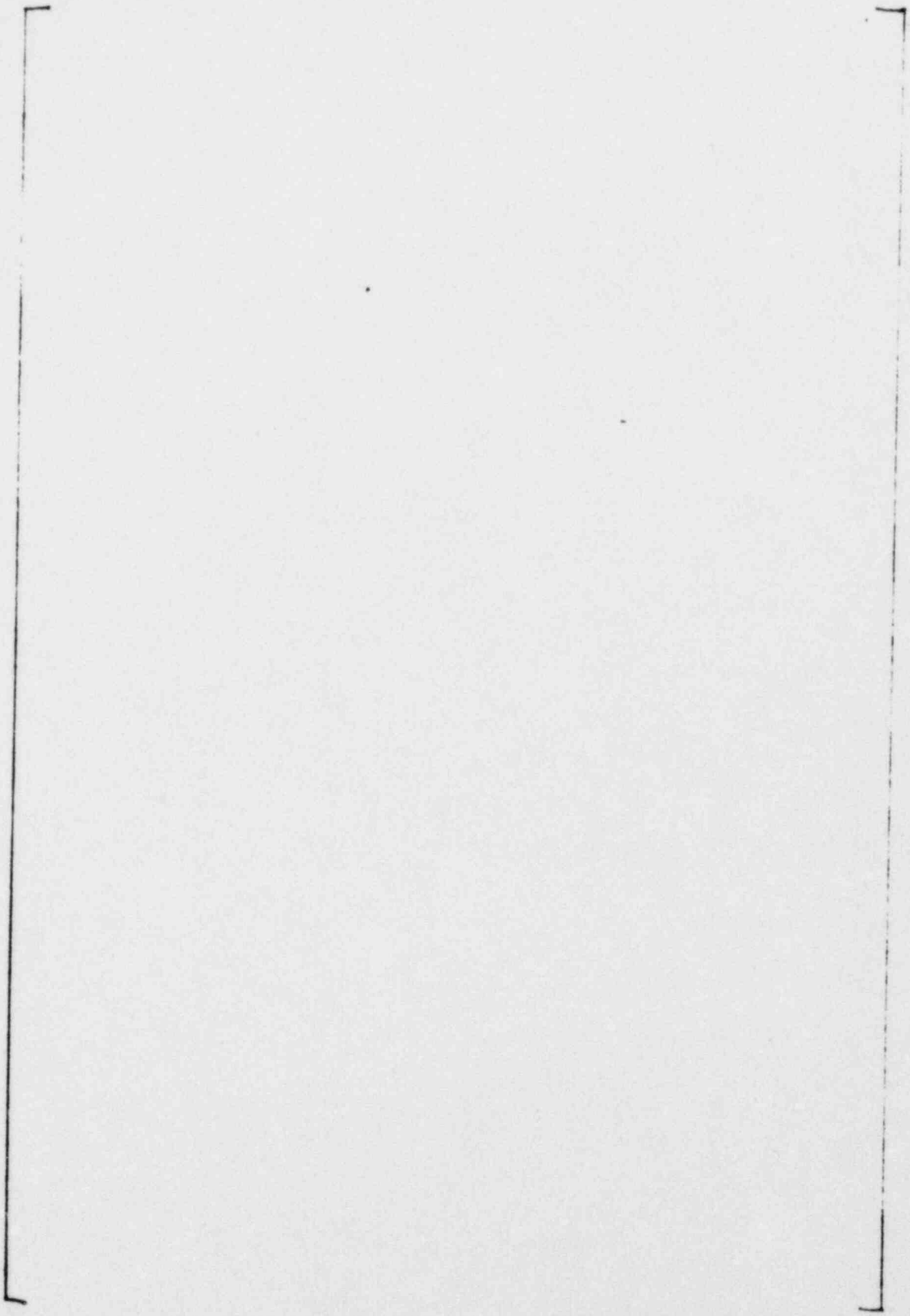

a.b.c.e

FIGURE 11.8-25, CASE NO.25, FLOW TEST TEMPERATURE RECORD

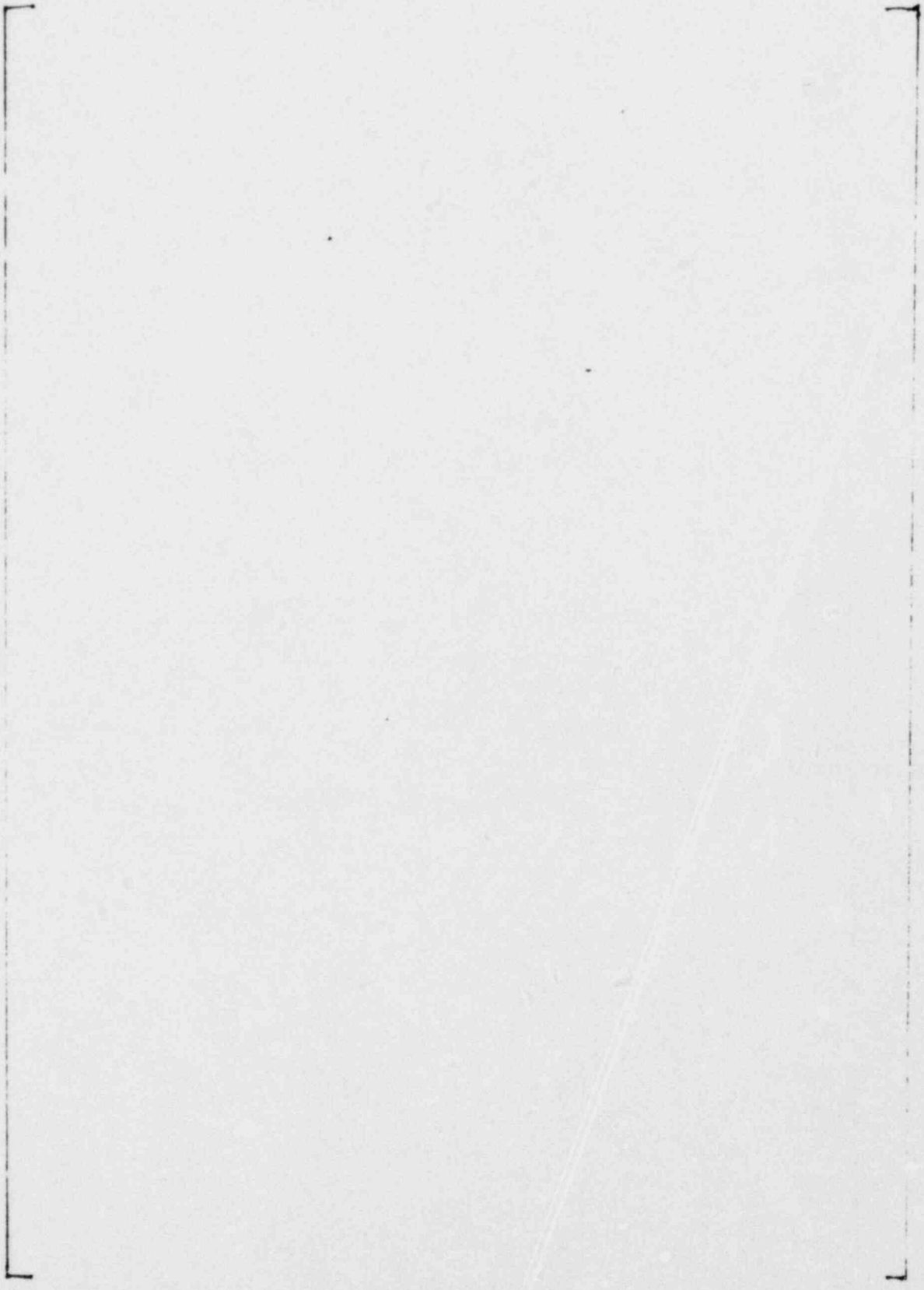

a,b,c,e

FIGURE 11.8-26, CASE NO.26, FLOW TEST TEMPERATURE RECORD

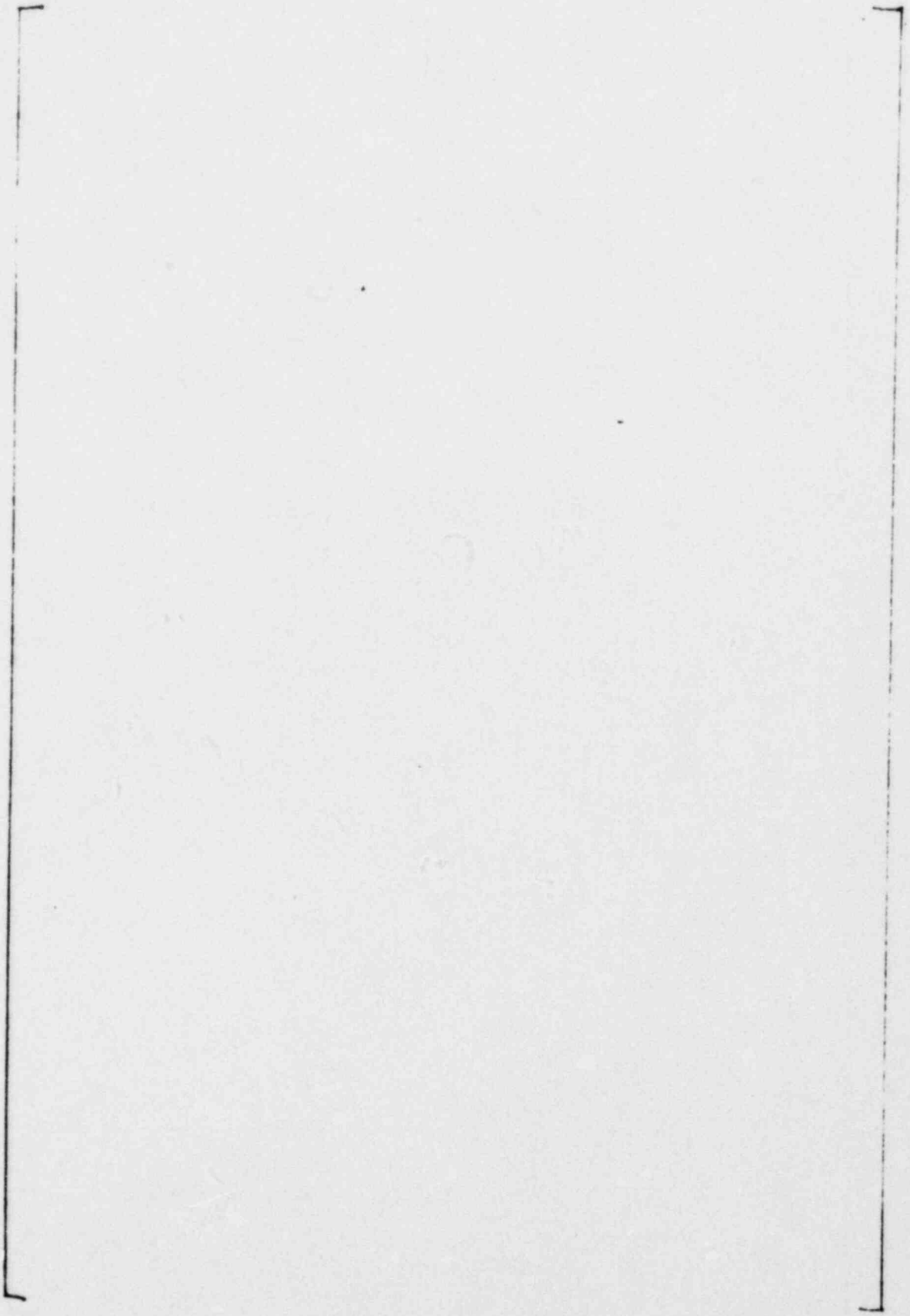

a.b.c.e

FIGURE 11.8-27, CASE NO.27, FLOW TEST TEMPERATURE RECORD

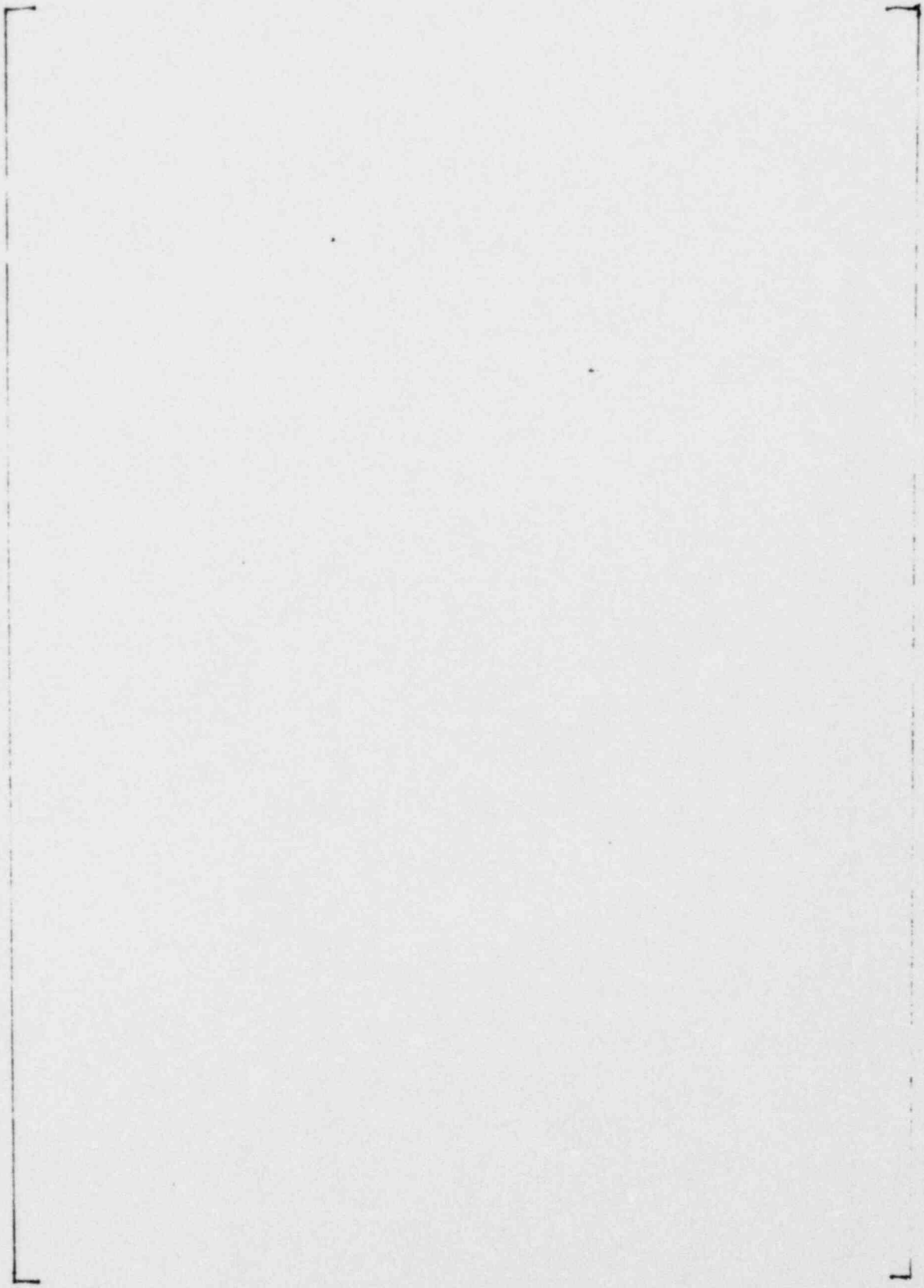

a,b,c,e

FIGURE 11.8-28, CASE NO.28, FLOW TEST TEMPERATURE RECORD

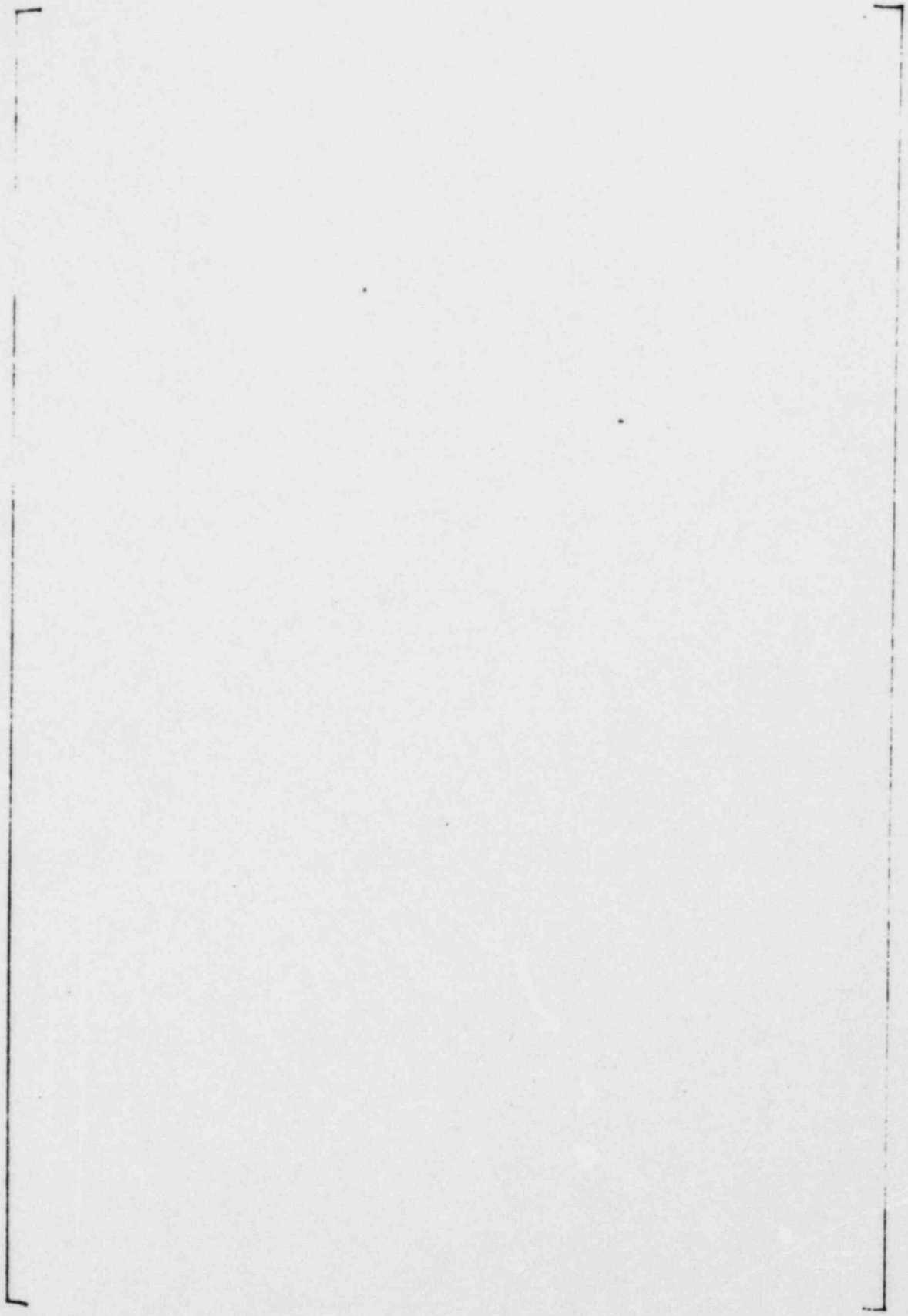

a.b.c.e

FIGURE 11.8-29, CASE NO.29, FLOW TEST TEMPERATURE RECORD

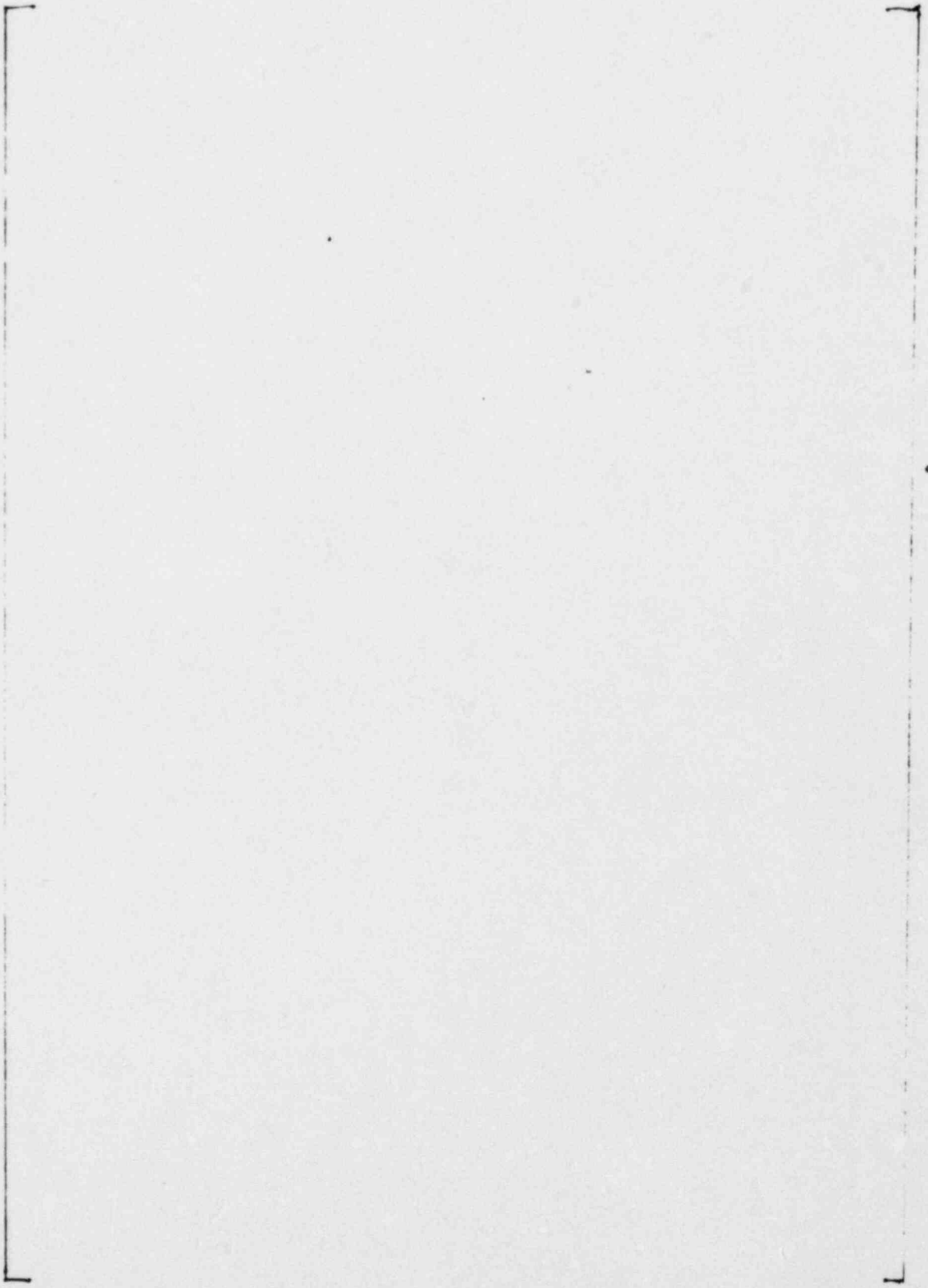

a,b,c,e

FIGURE 11.8-30, CASE NO.30, FLOW TEST TEMPERATURE RECORD

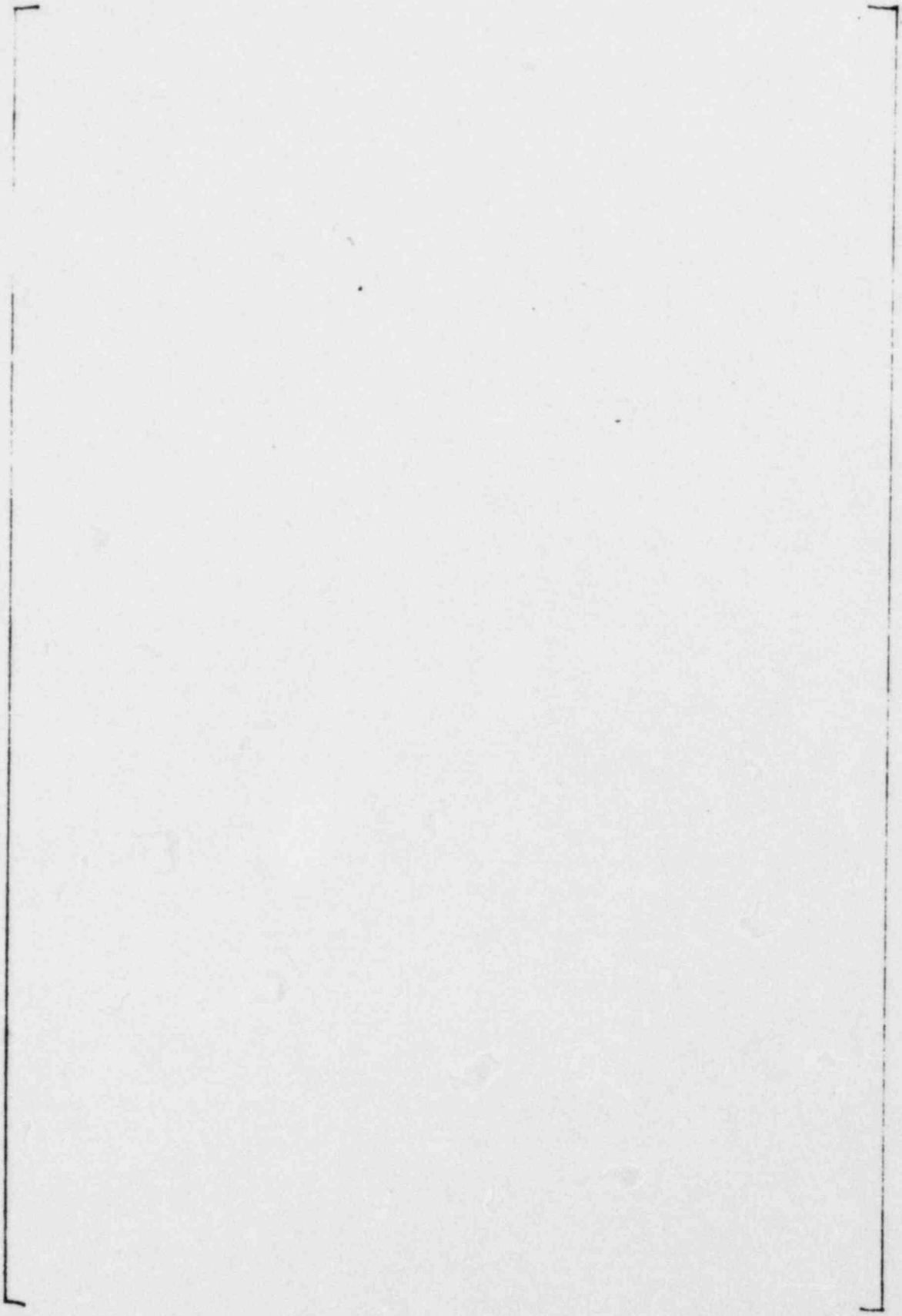

a,b,c,e

FIGURE 11.8-31, CASE NO.31, FLOW TEST TEMPERATURE RECORD

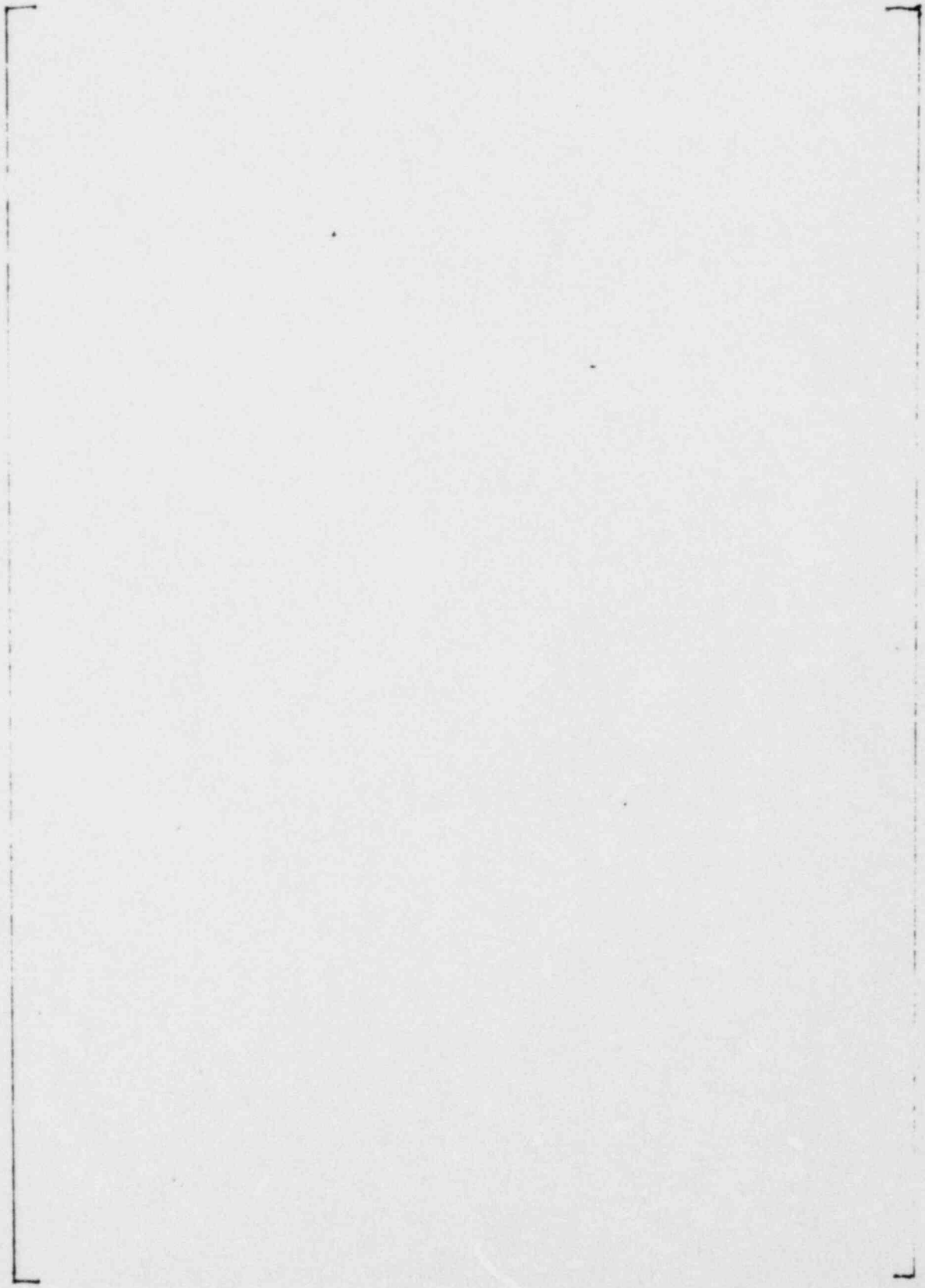

a,b,c,e

FIGURE 11.8-32, CASE NO.32, FLOW TEST TEMPERATURE RECORD

BLANK

Case No.: 33

Generic Profile:

Interface Level:_____ Angle Measured From The Bottom of Pipe

Run No.: Y6 _____

FIGURE 11.8-33, CASE NO.33, FLOW TEST TEMPERATURE RECORD

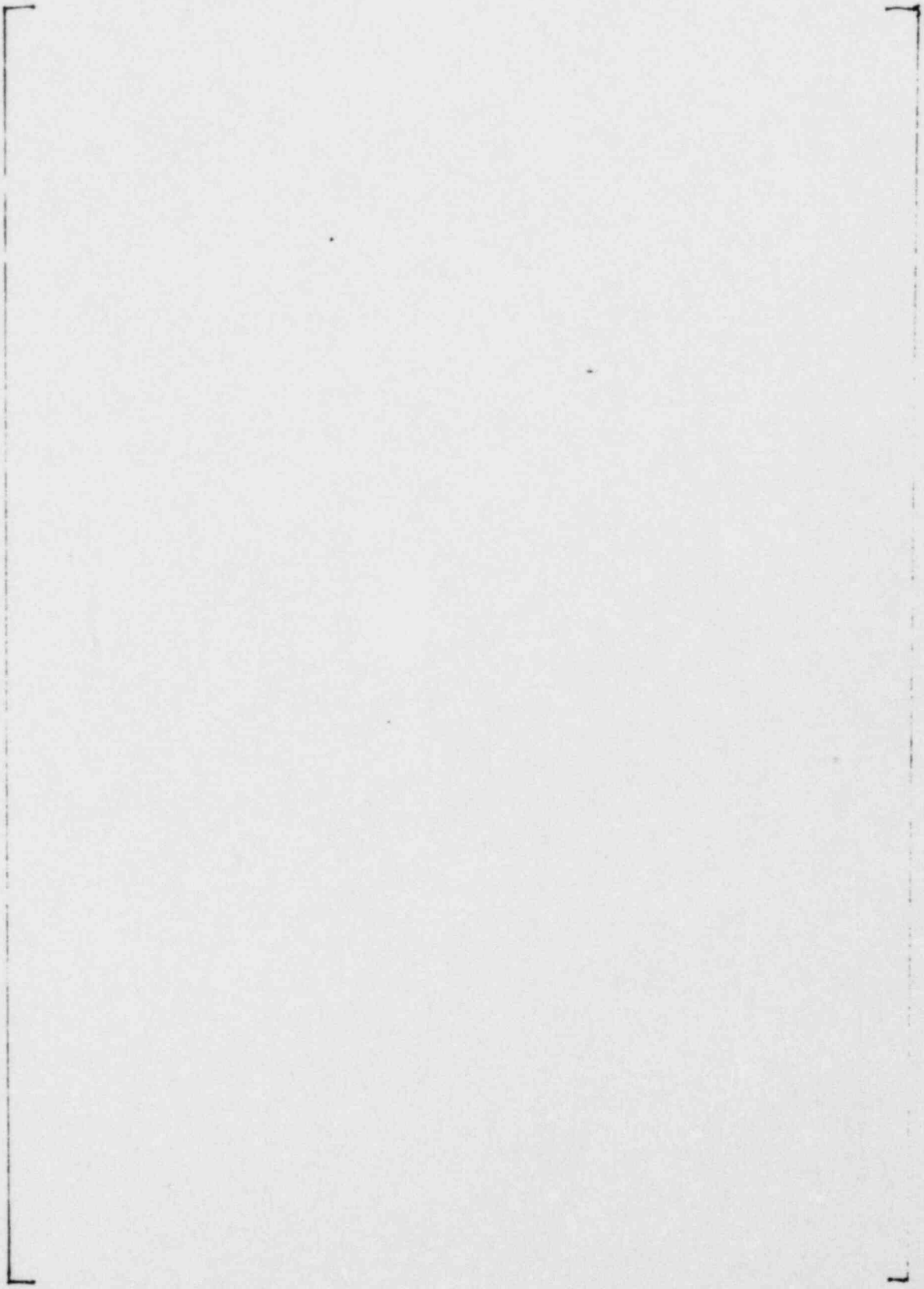

a,b,c,c

FIGURE 11.8-34, CASE NO.34, FLOW TEST TEMPERATURE RECORD

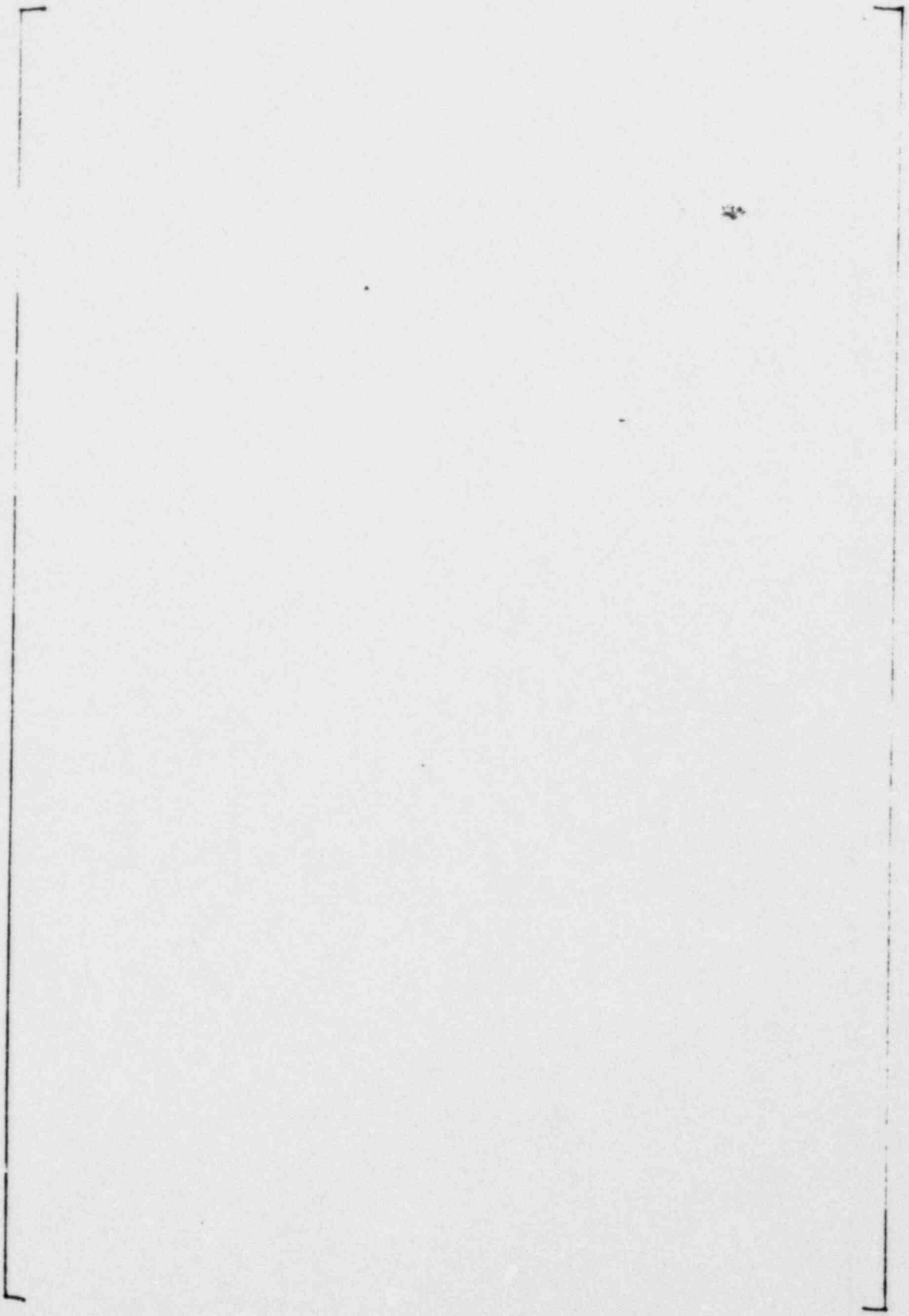

a,b,c,e

FIGURE 11.8-35, CASE NO.35, FLOW TEST TEMPERATURE RECORD

a,b,c,e

FIGURE 11.8-36, CASE NO.36, FLOW TEST TEMPERATURE RECORD

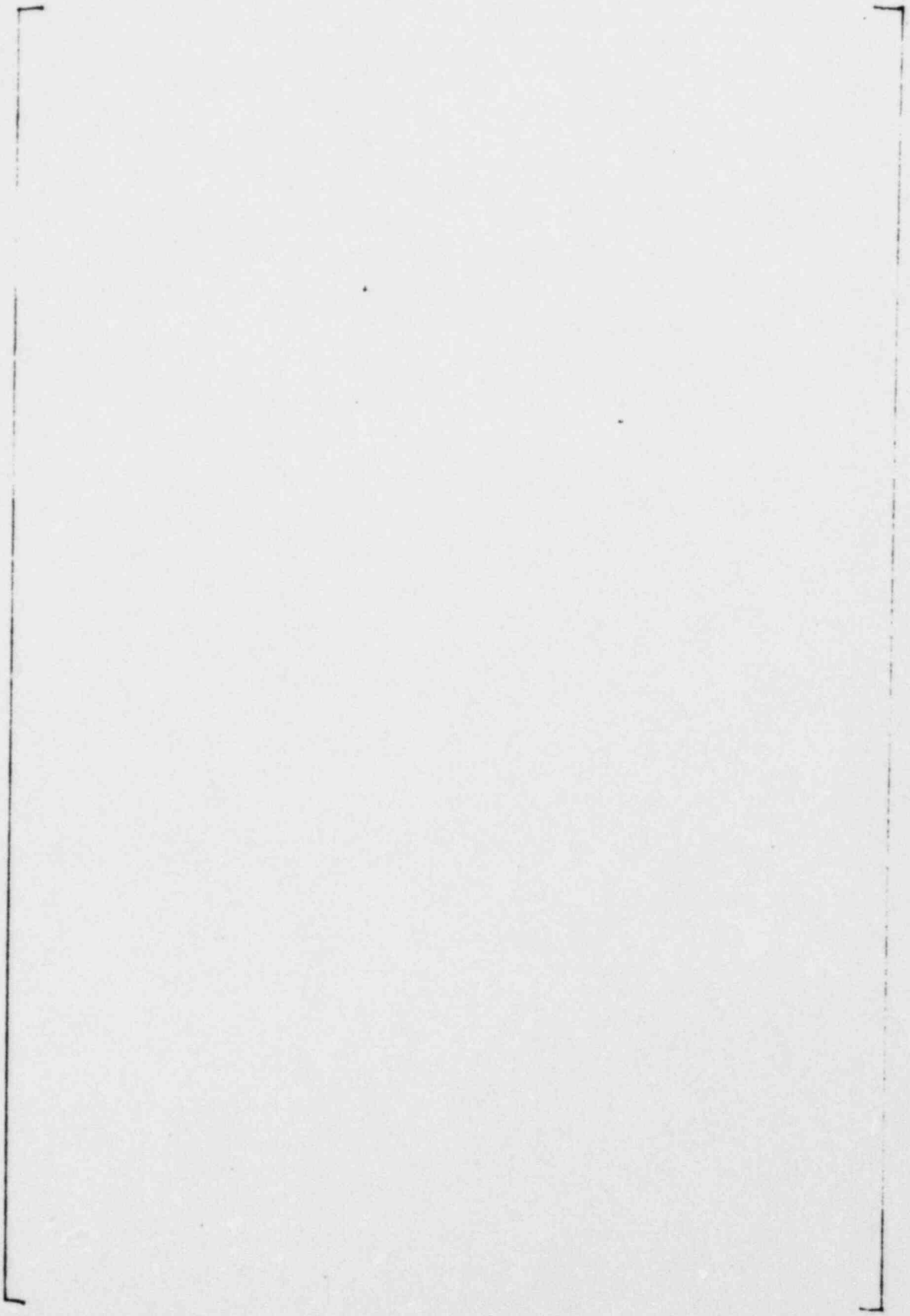

a,b,c,e

FIGURE 11.8-37, CASE NO.37, FLOW TEST TEMPERATURE RECORD

BLANK

Case No.: 38

Generic Profile:

Interface Level:_____ Angle Measured From The Bottom of Pipe

Run No.: Y6 _____

FIGURE 11.8-38, CASE NO.38, FLOW TEST TEMPERATURE RECORD

a,b,c,e

FIGURE 11.8-39, CASE NO.39, FLOW TEST TEMPERATURE RECORD

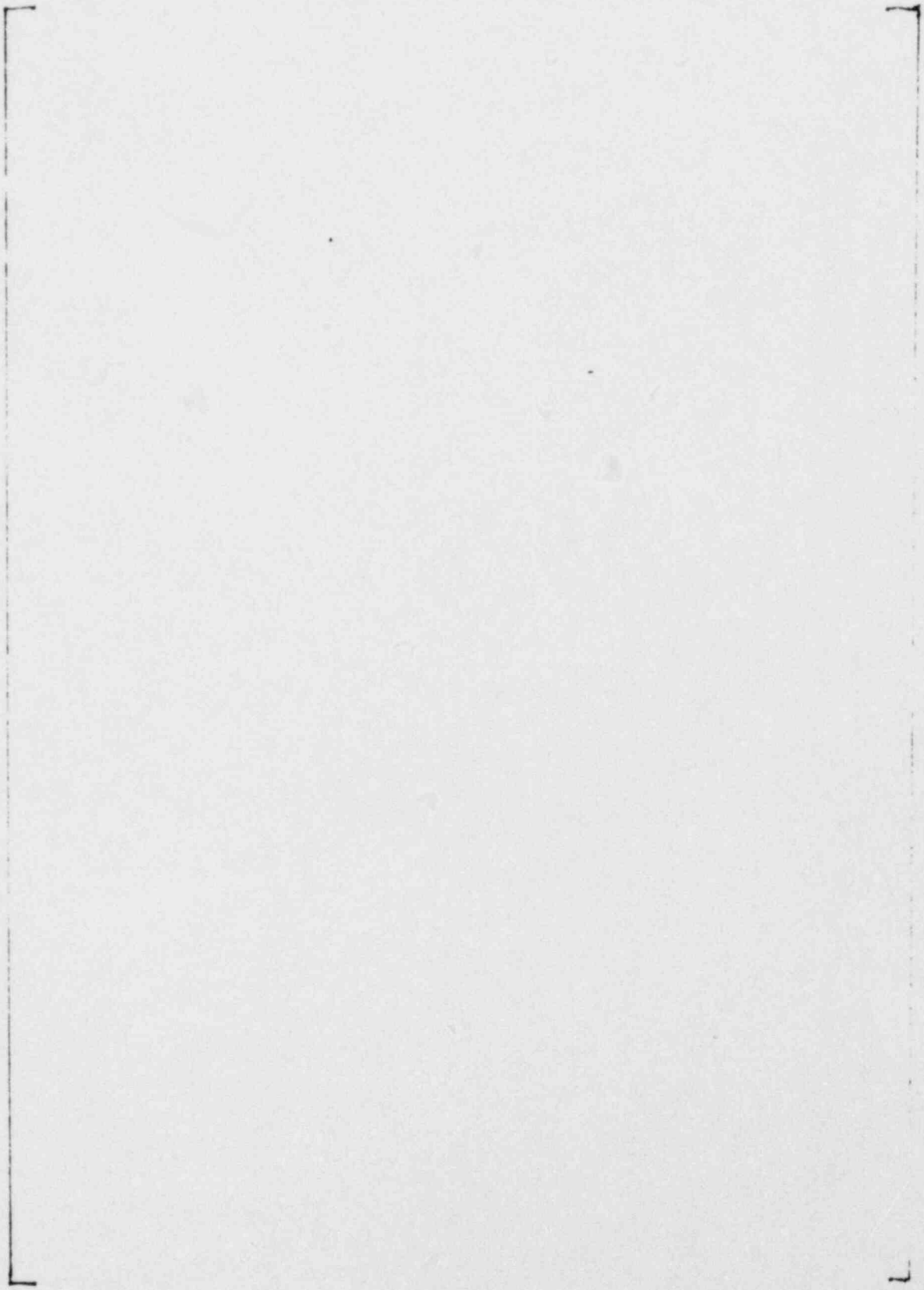

a,b,c,e

FIGURE 11.8-40, CASE NO.40, FLOW TEST TEMPERATURE RECORD

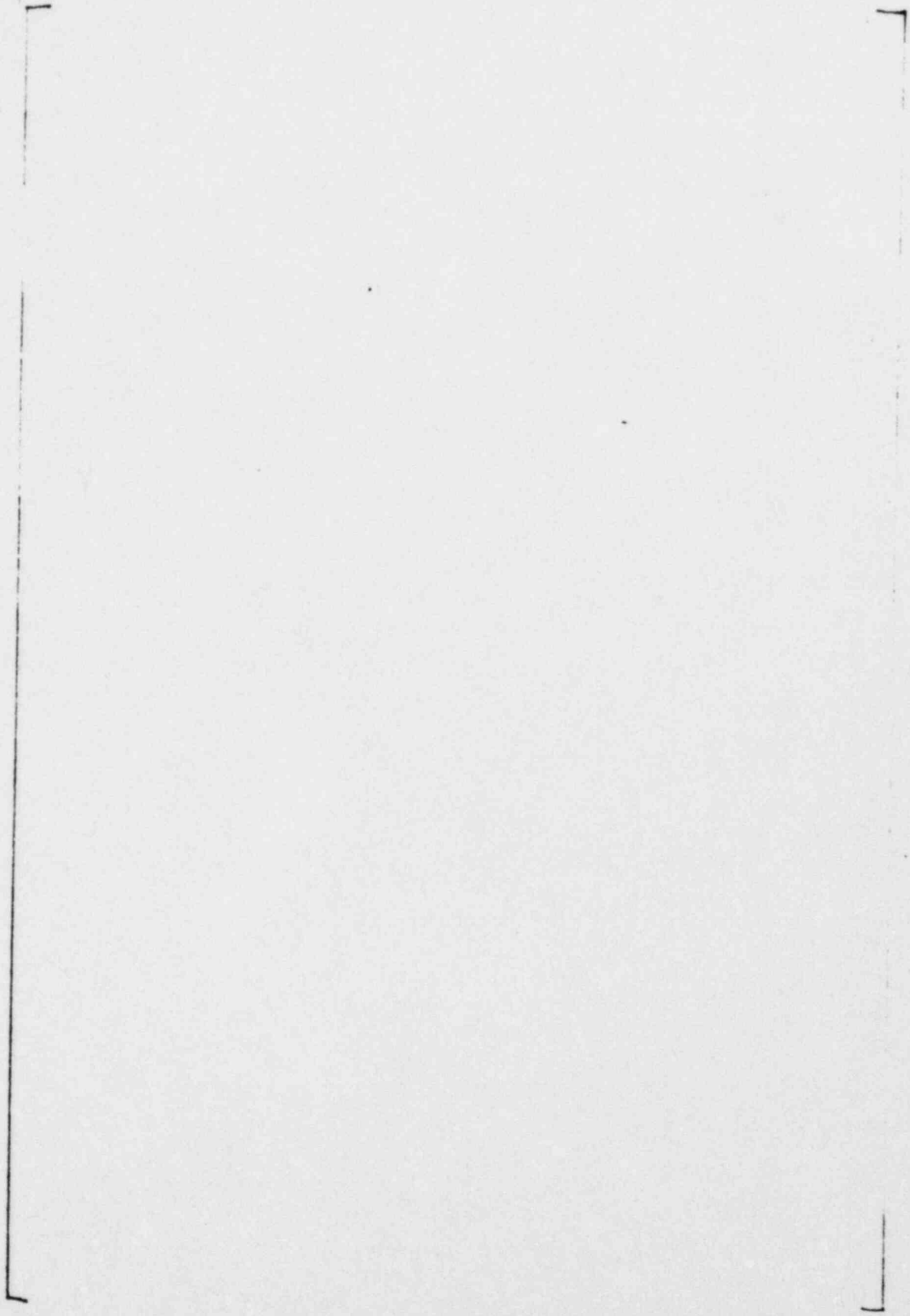

a.b.c.e

FIGURE 11.8-41, CASE NO.41, FLOW TEST TEMPERATURE RECORD

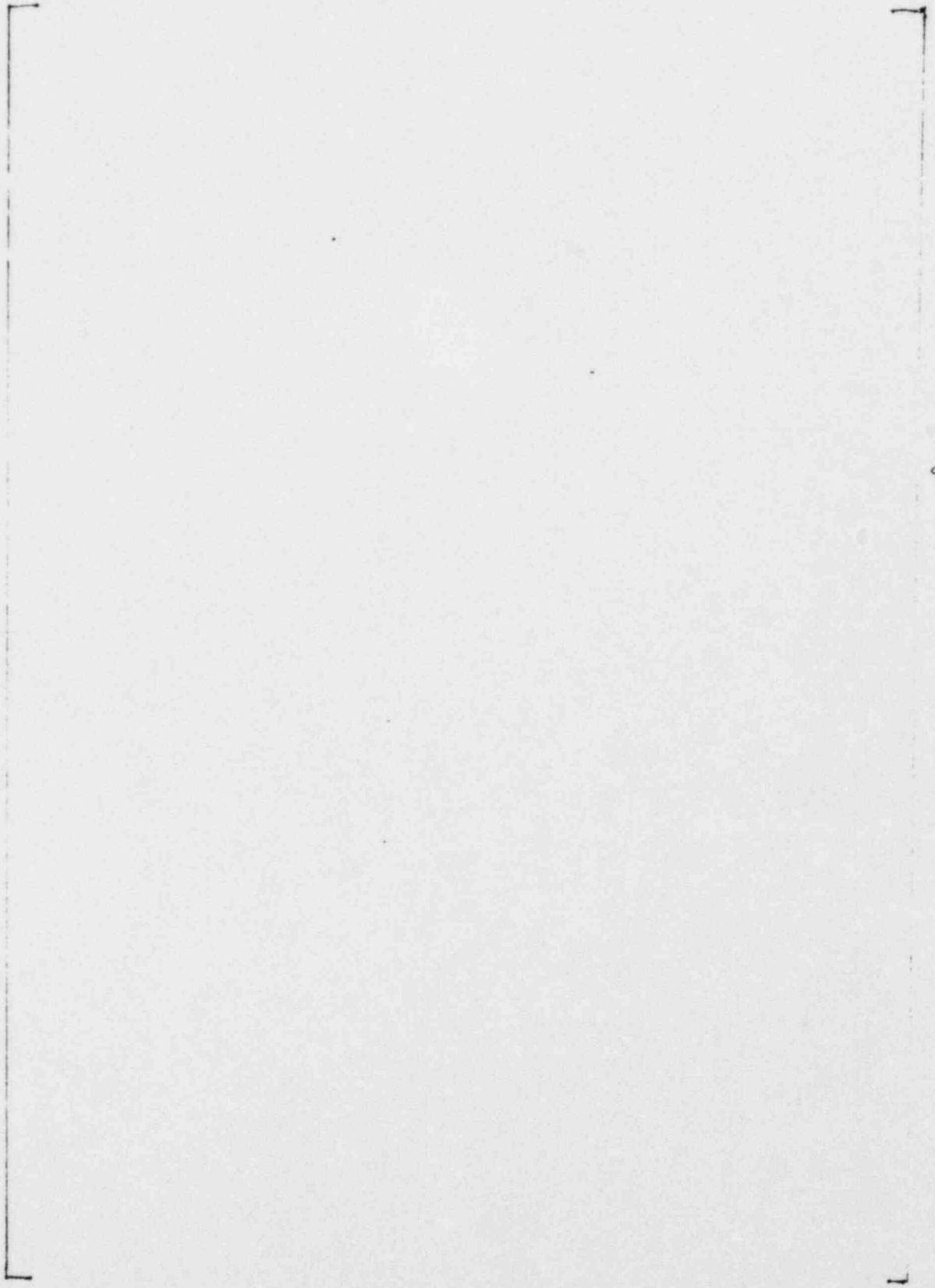

a,b,c,e

FIGURE 11.8-42, CASE NO.42, FLOW TEST TEMPERATURE RECORD

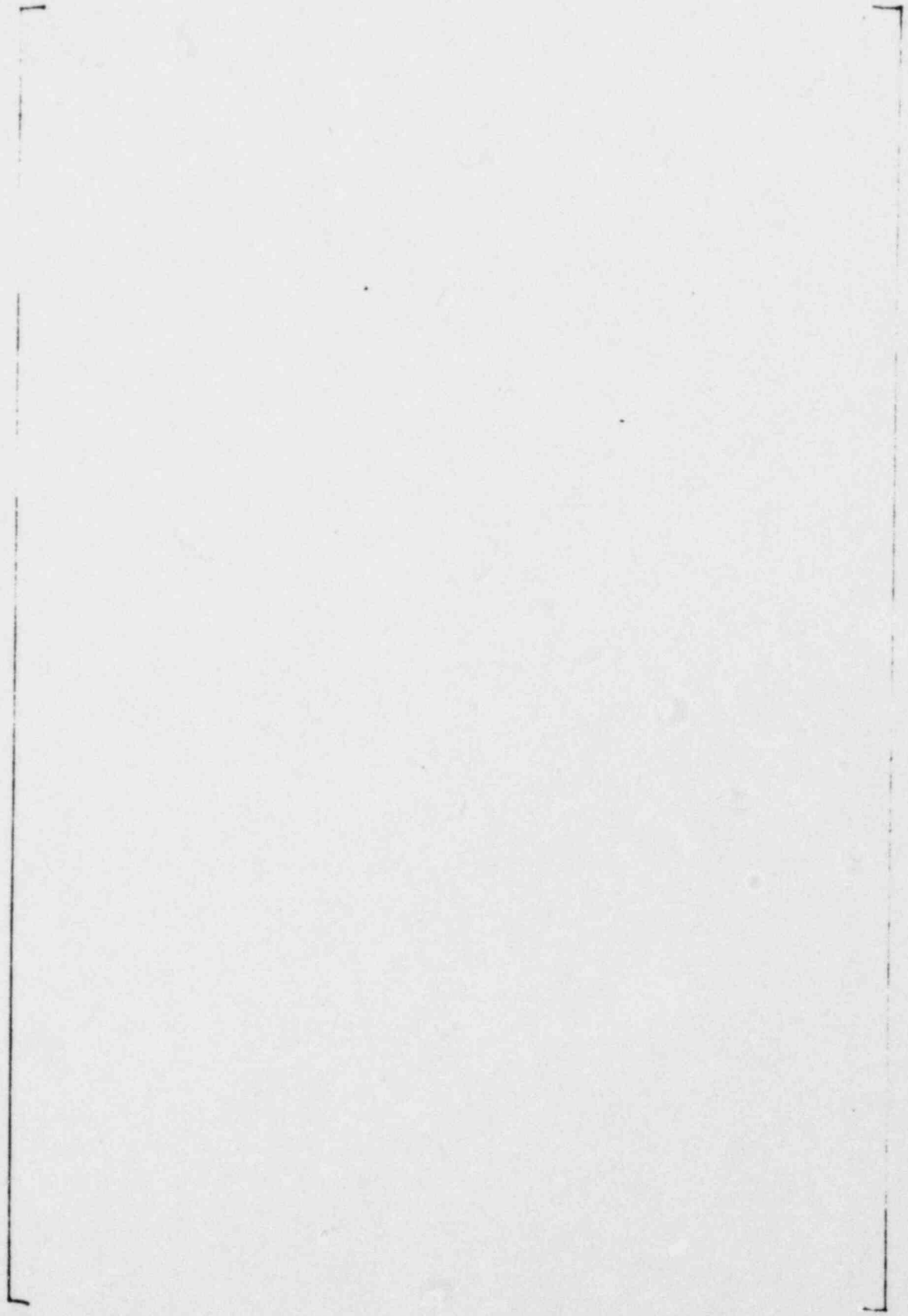

a.b.c.e

FIGURE 11.8-43, CASE NO.43, FLOW TEST TEMPERATURE RECORD

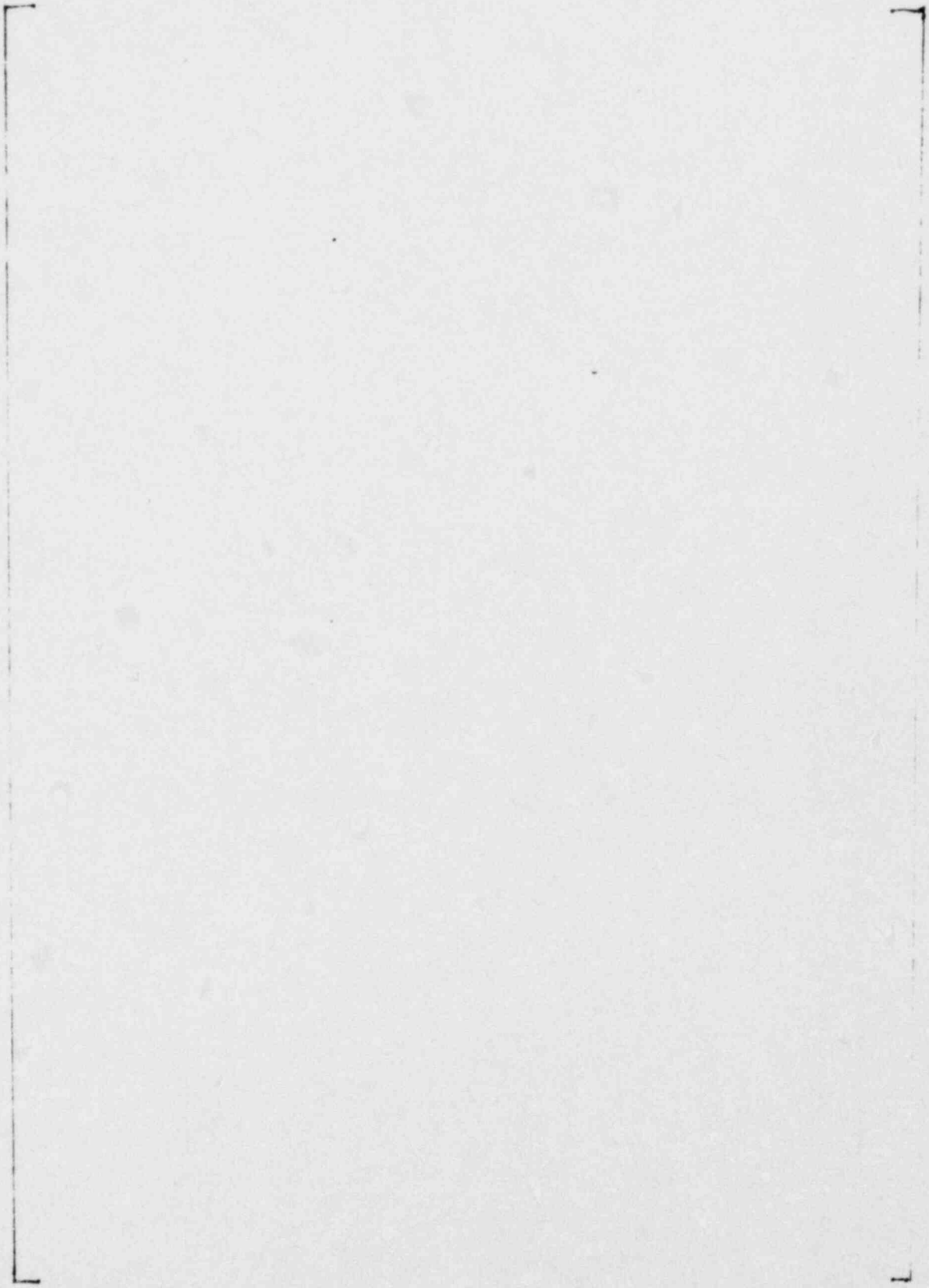

a,b,c,e

FIGURE 11.8-44, CASE NO.44, FLOW TEST TEMPERATURE RECORD

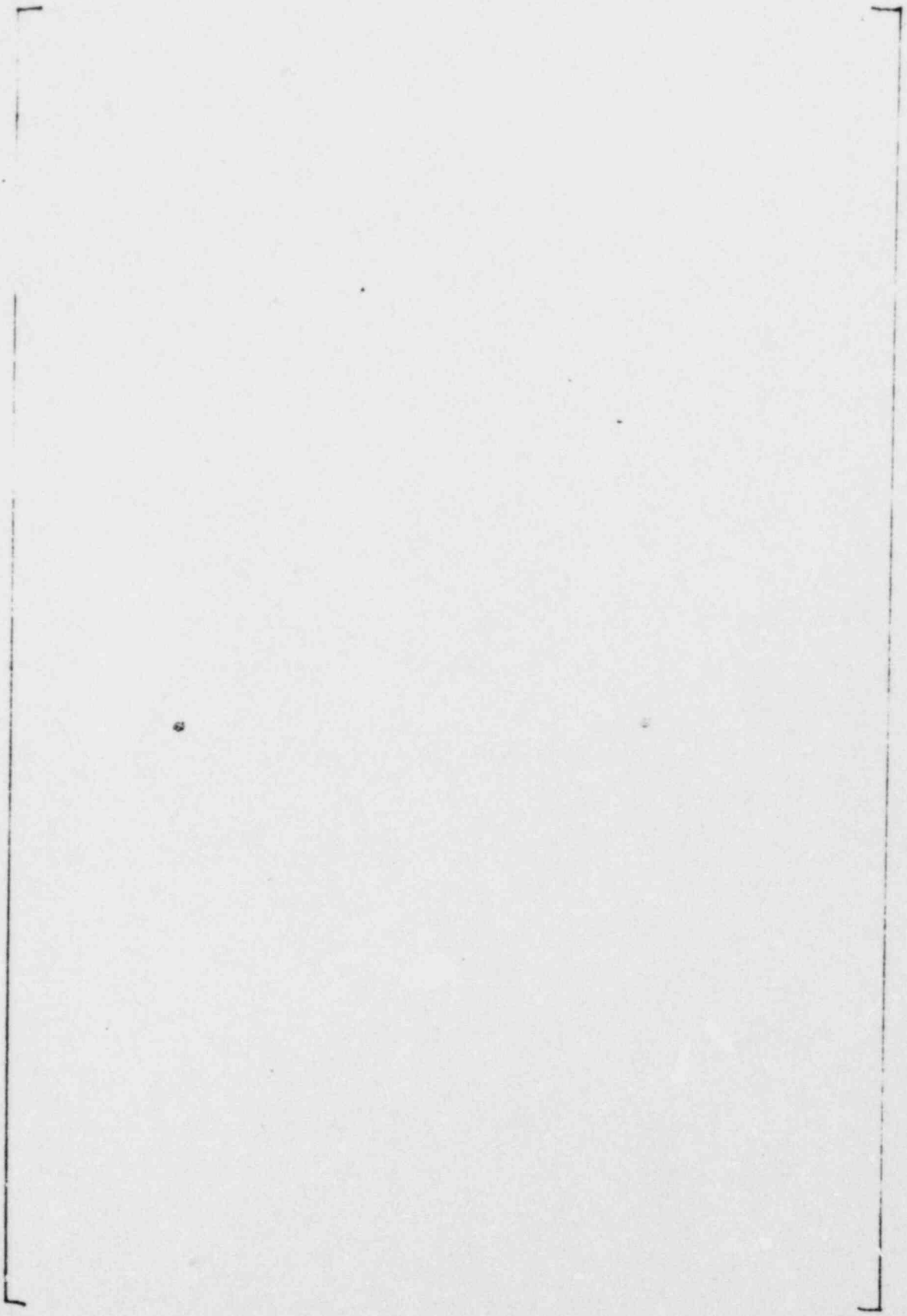

a.b.c.e

FIGURE 11.8-45, CASE NO. 1, FLOW TEST TEMPERATURE RECORD VS. 100 TERMS OF FOURIER SERIES

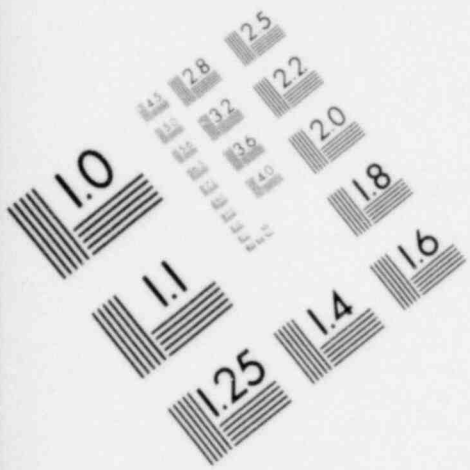

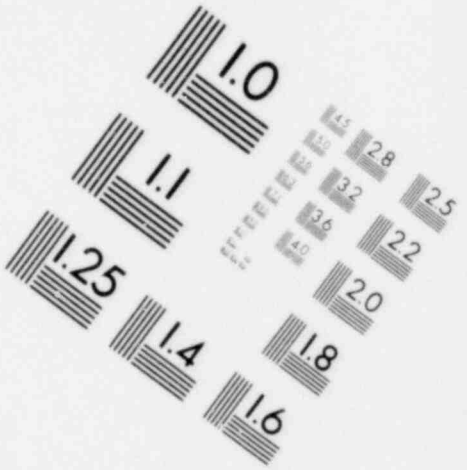

IMAGE EVALUATION TEST TARGET (MT-3)

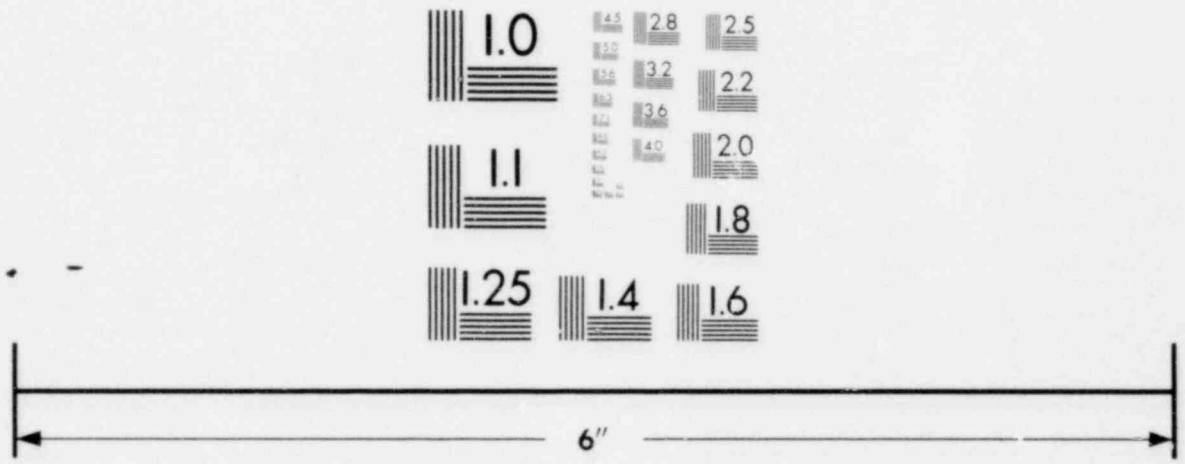

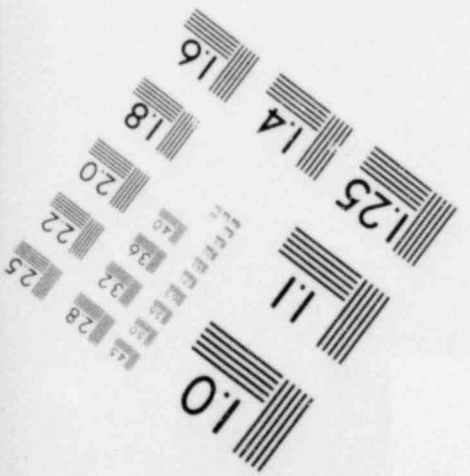

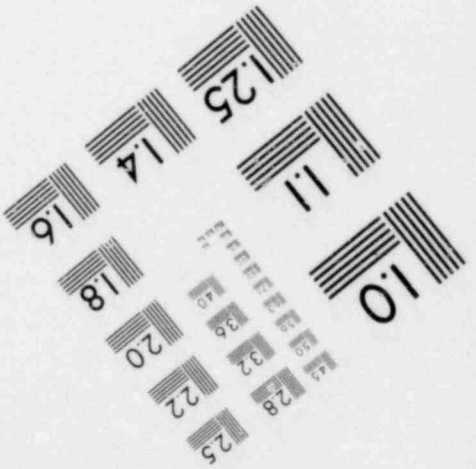

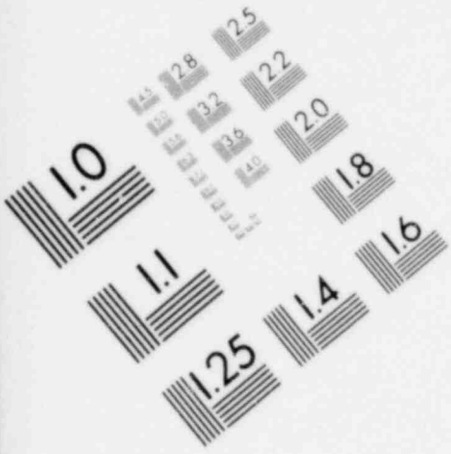

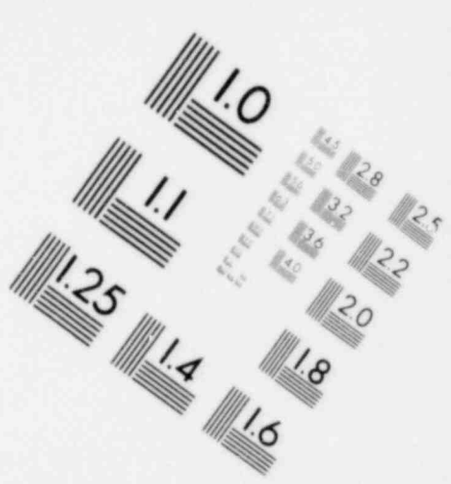

IMAGE EVALUATION TEST TARGET (MT-3)

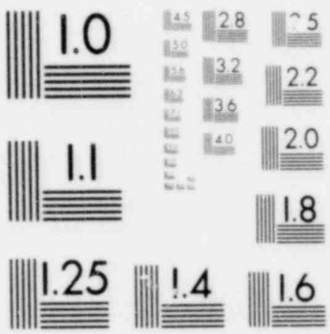

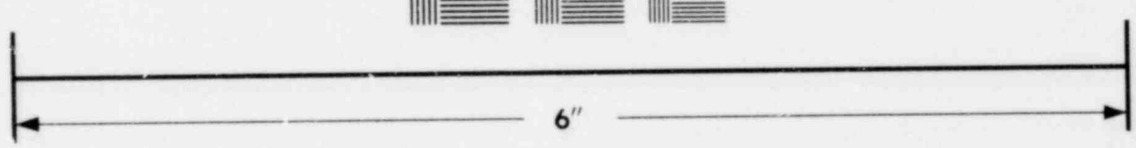

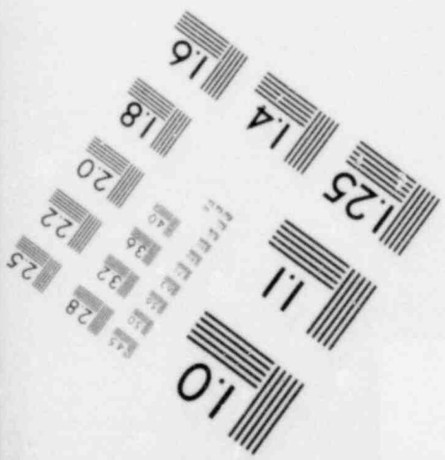

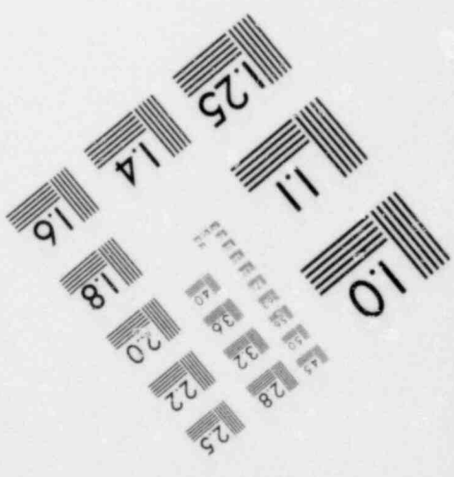

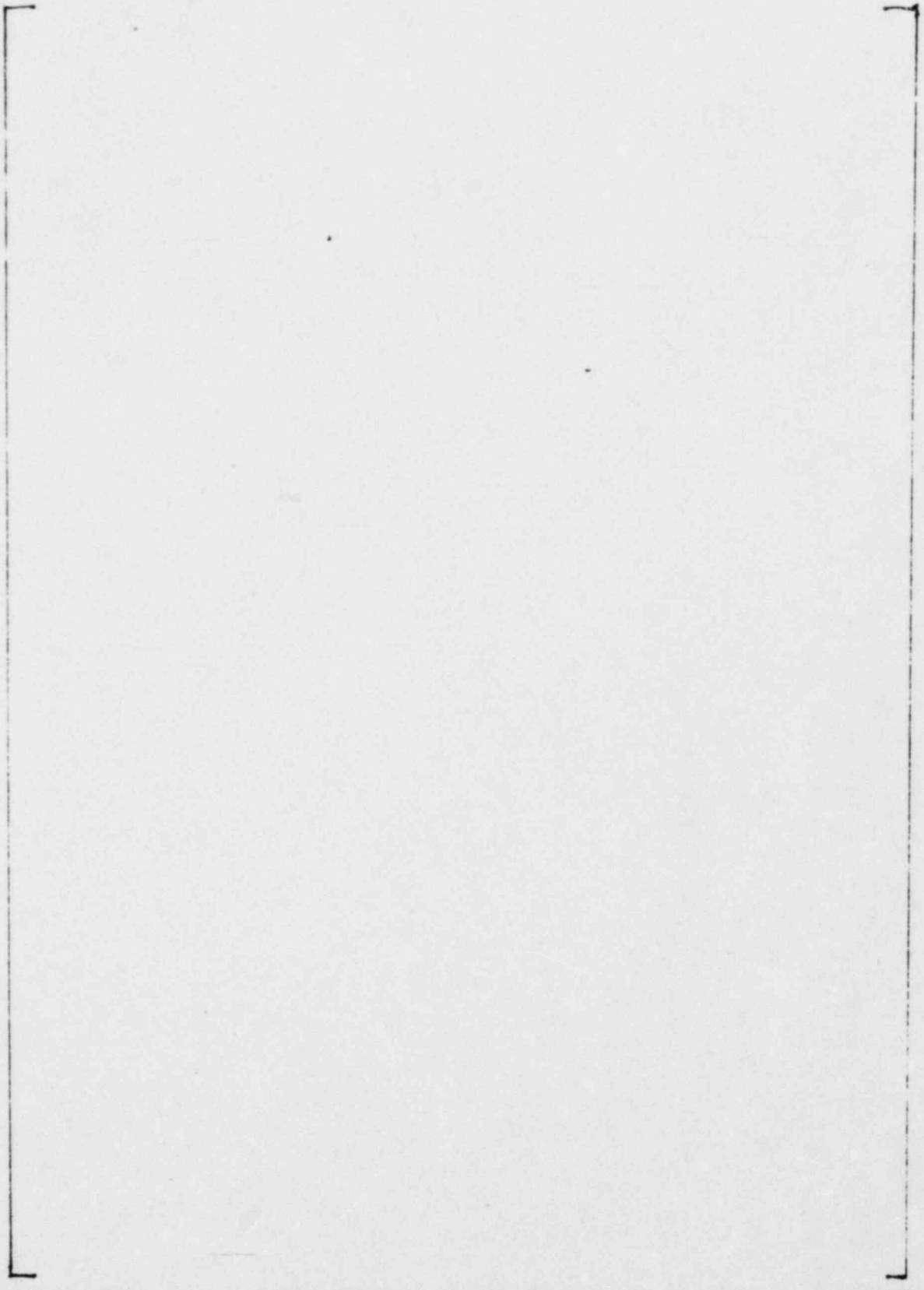

a,b,c,e

FIGURE 11.8-46, CASE NO. 2, FLOW TEST TEMPERATURE RECORD VS. 100 TERMS OF FOURIER SERIES

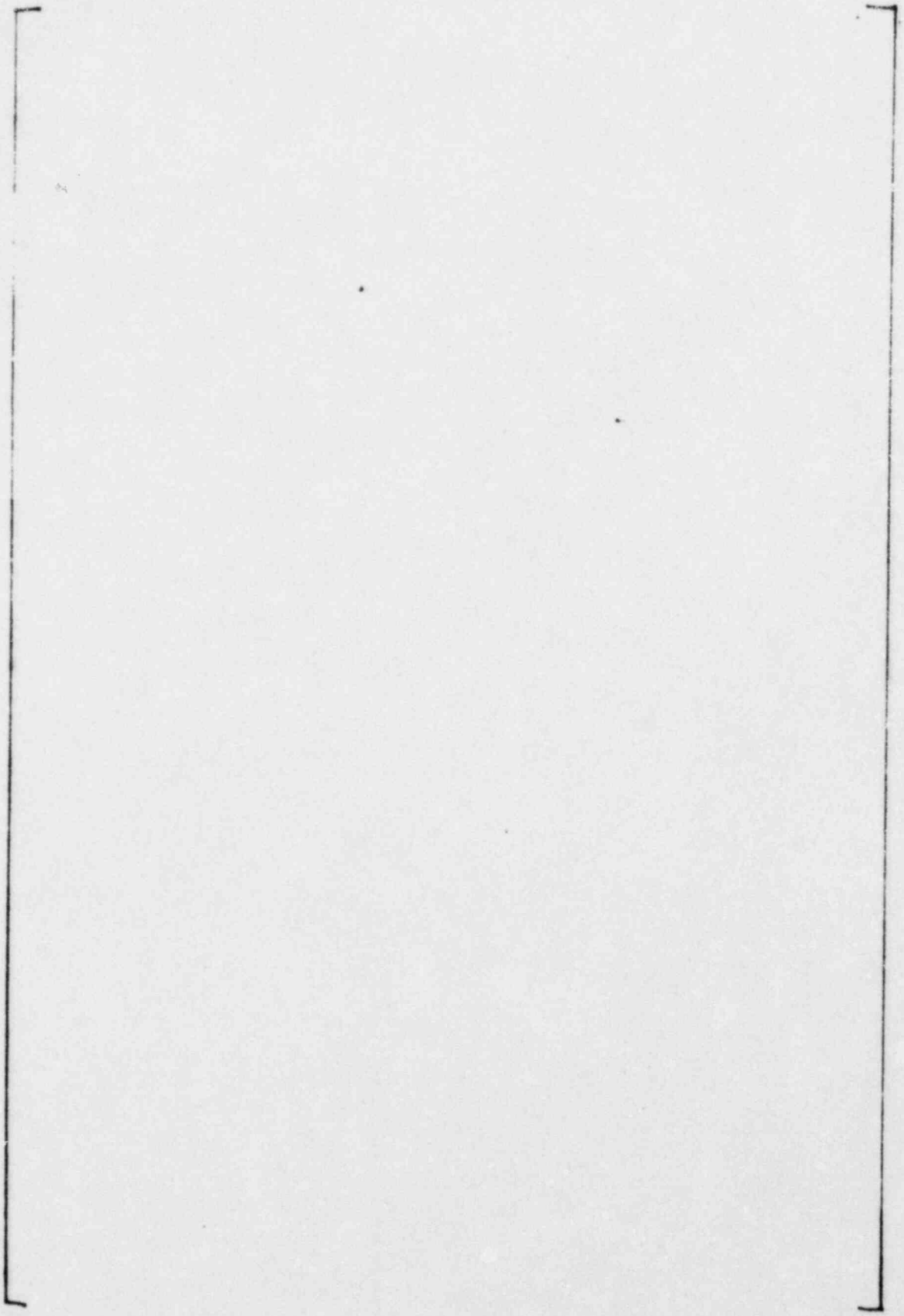

a,b,c,e

FIGURE 11.8-47, CASE NO. 3, FLOW TEST TEMPERATURE RECORD VS. 100 TERMS OF FOURIER SERIES

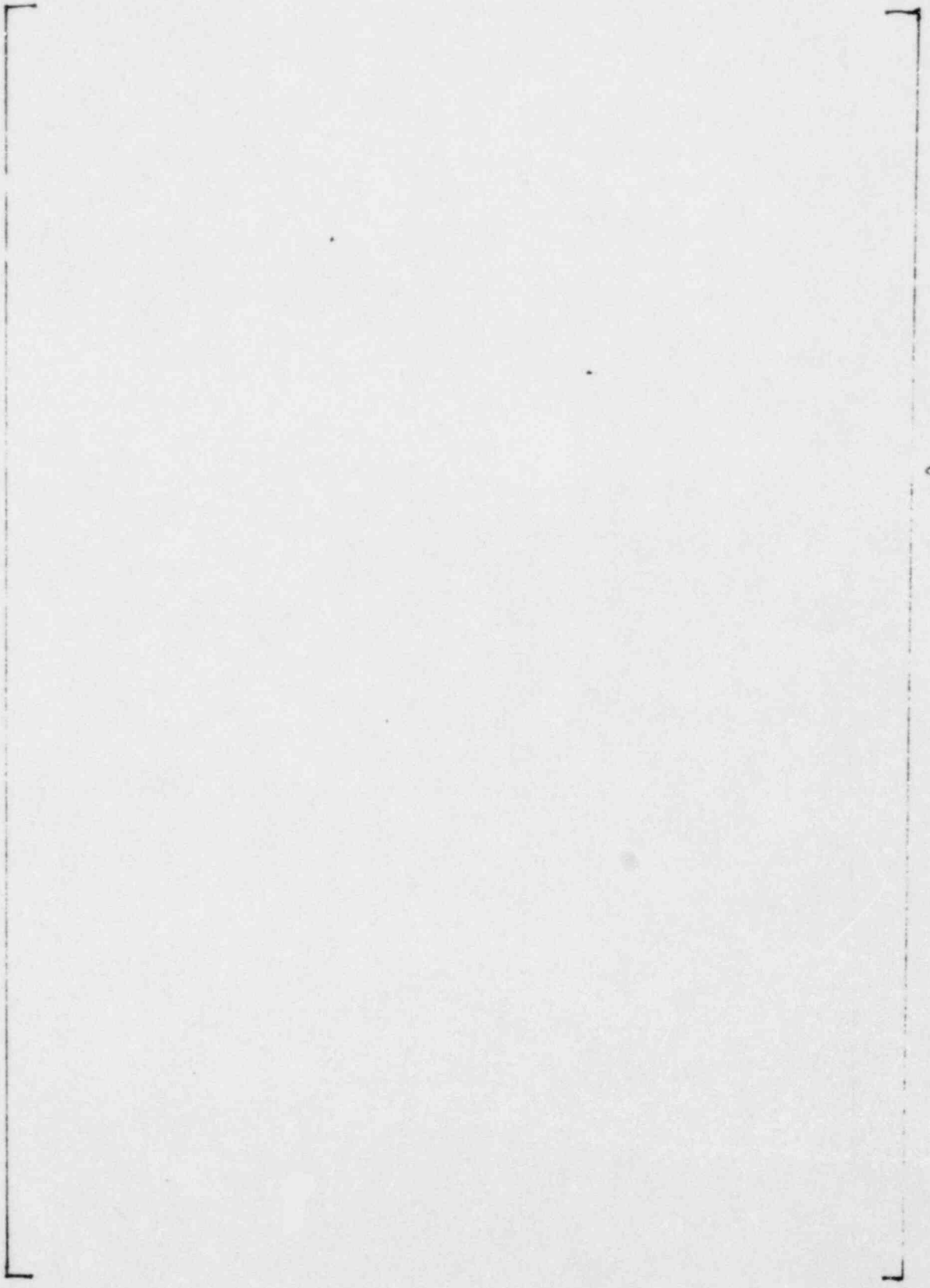

a,b,c,e

FIGURE 11.8-48, CASE NO. 4, FLOW TEST TEMPERATURE RECORD VS. 100 TERMS OF FOURIER SERIES

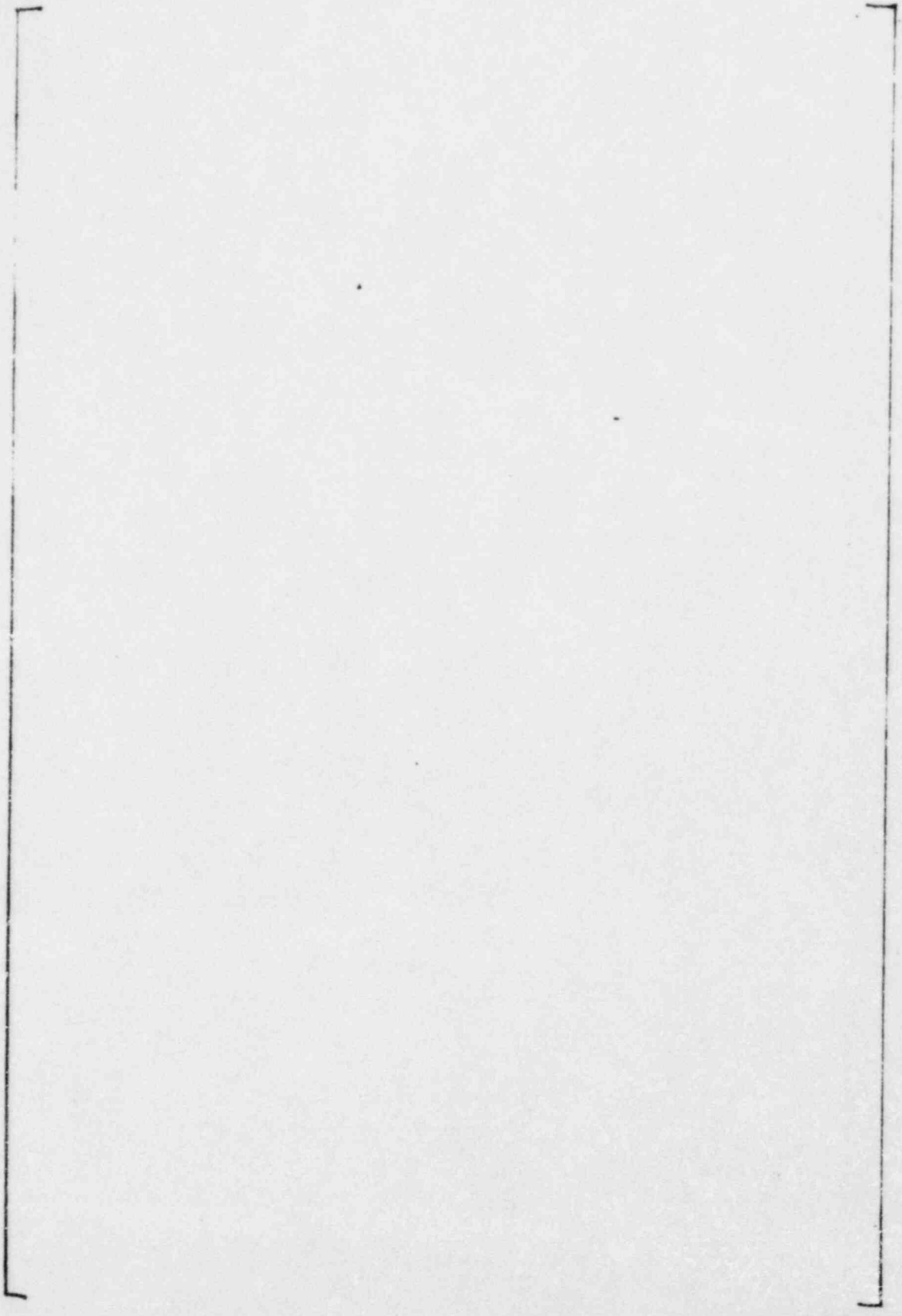

a.b.c.e

FIGURE 11.8-49, CASE NO. 5, FLOW TEST TEMPERATURE RECORD VS. 100 TERMS OF FOURIER SERIES

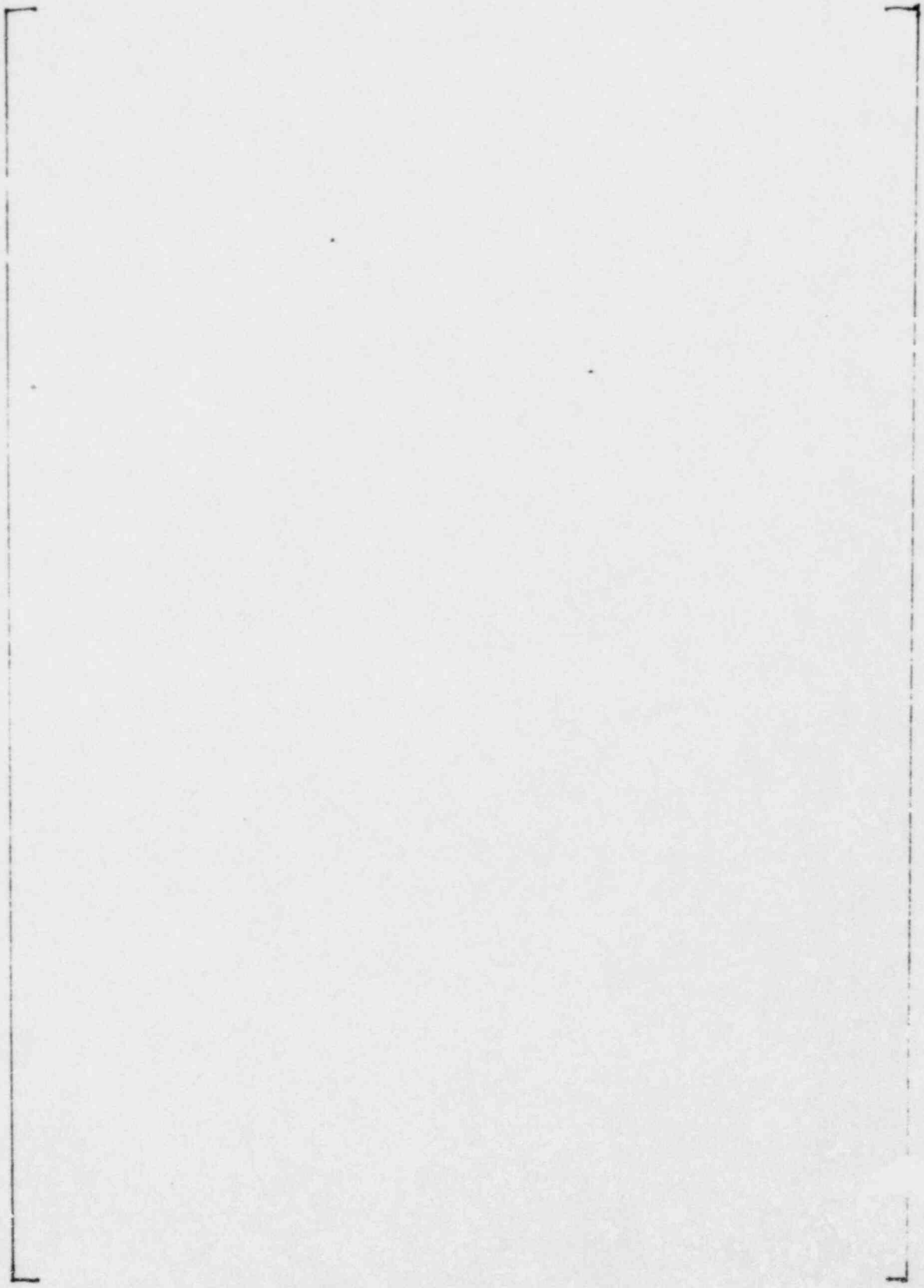

a,b,c,e

FIGURE 11.8-50, CASE NO. 6, FLOW TEST TEMPERATURE RECORD VS. 100 TERMS OF FOURIER SERIES

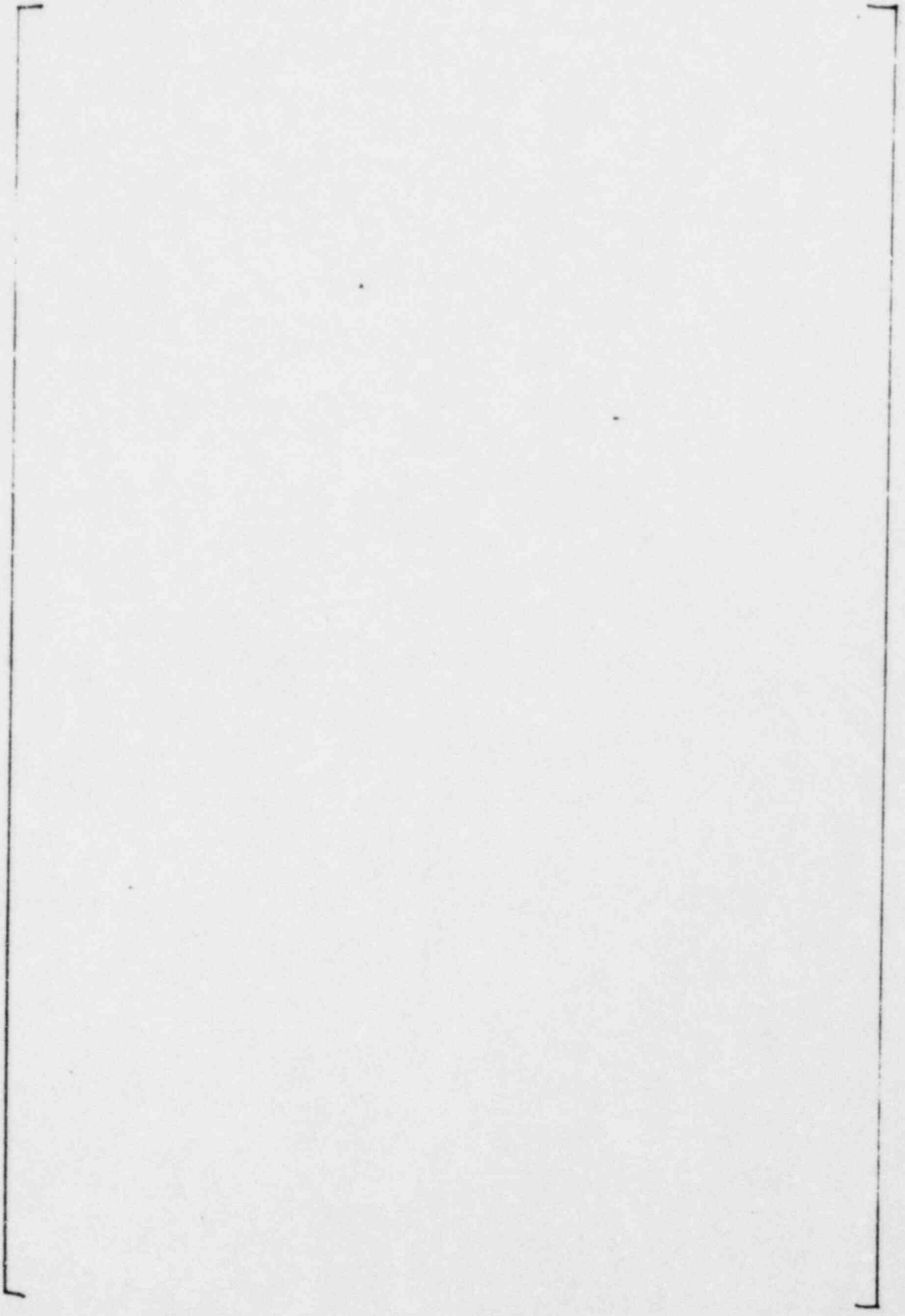

a,b,c,e

FIGURE 11.8-51, CASE NO. 7, FLOW TEST TEMPERATURE RECORD VS. 100 TERMS OF FOURIER SERIES

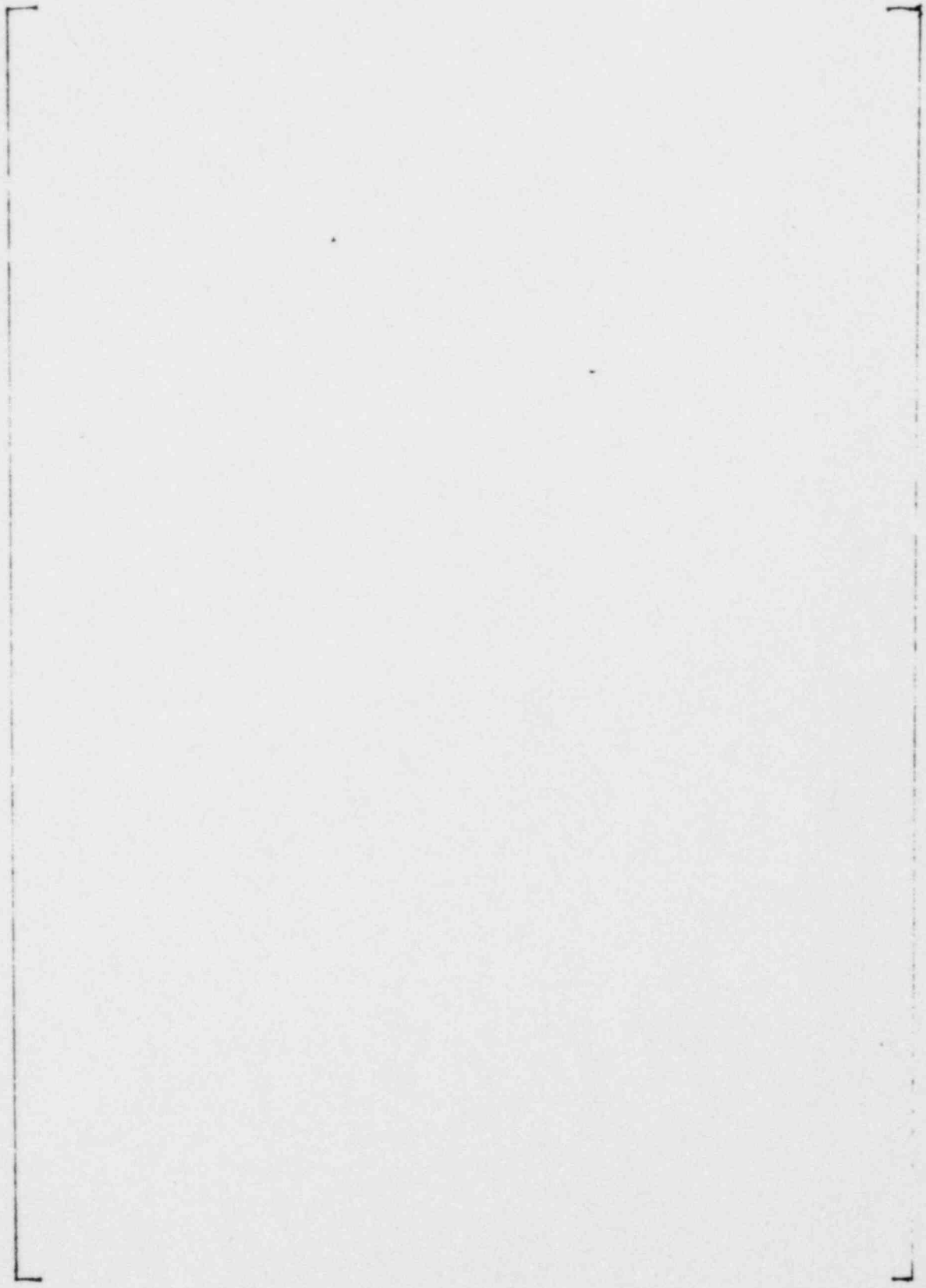

a,b,c,e

FIGURE 1.8-52, CASE NO. 8, FLOW TEST TEMPERATURE RECORD VS. 100 TERMS OF FOURIER SERIES

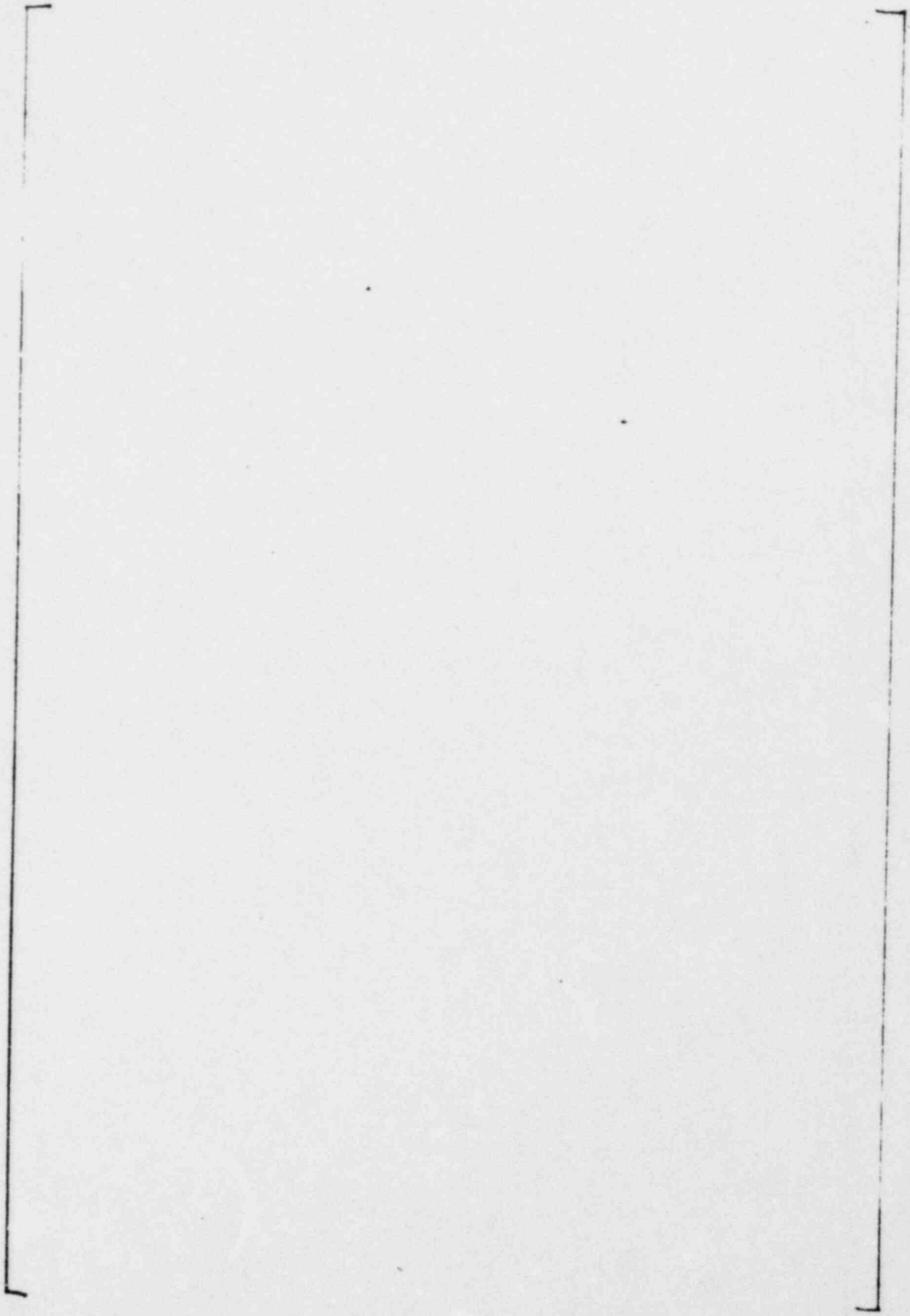

a,b,c,e

FIGURE 11.8-53, CASE NO. 9, FLOW TEST TEMPERATURE RECORD VS. 100 TERMS OF FOURIER SERIES

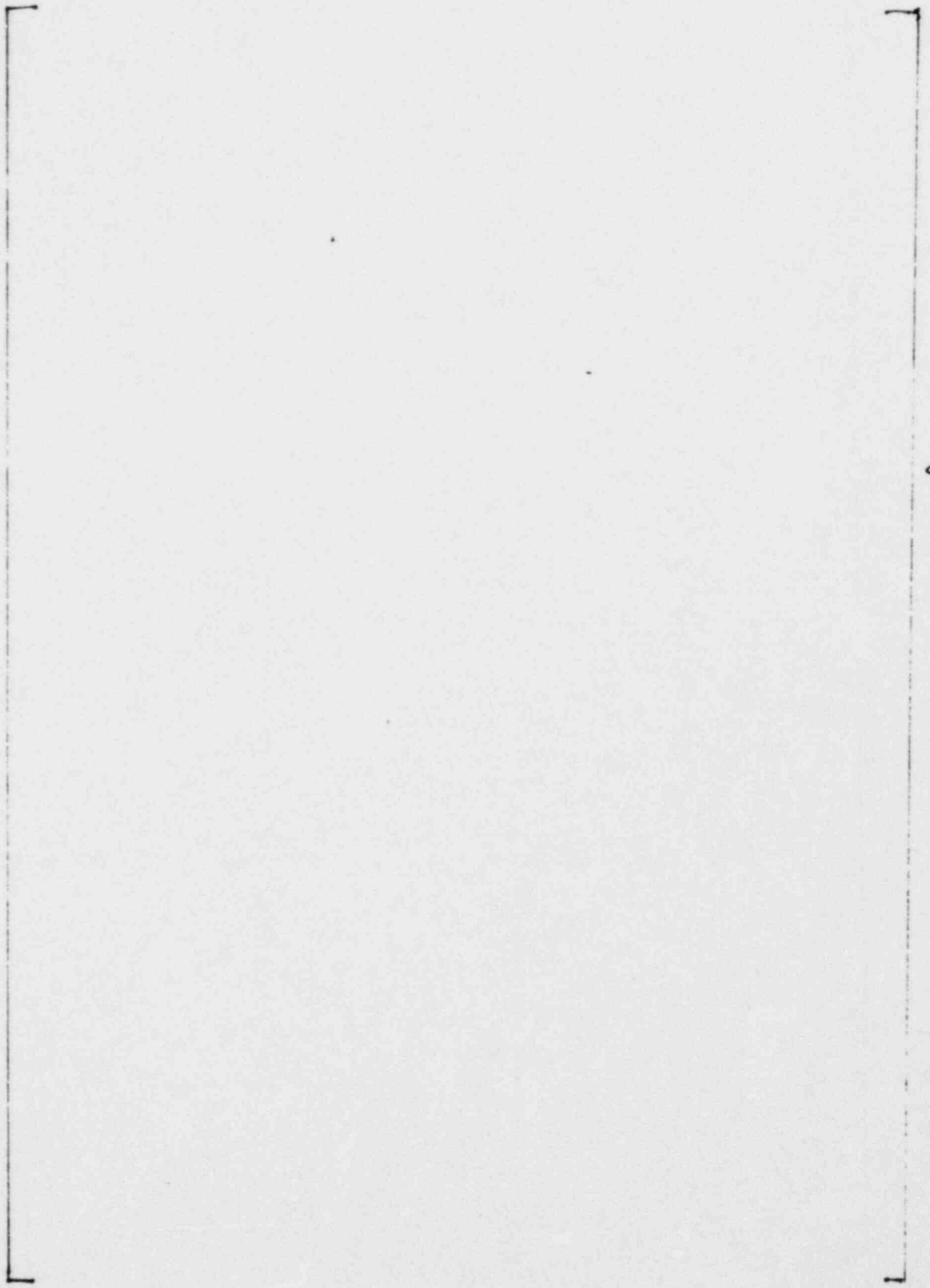

a,b,c,e

FIGURE 11.8-54, CASE NO.10, FLOW TEST TEMPERATURE RECORD VS. 100 TERMS OF FOURIER SERIES

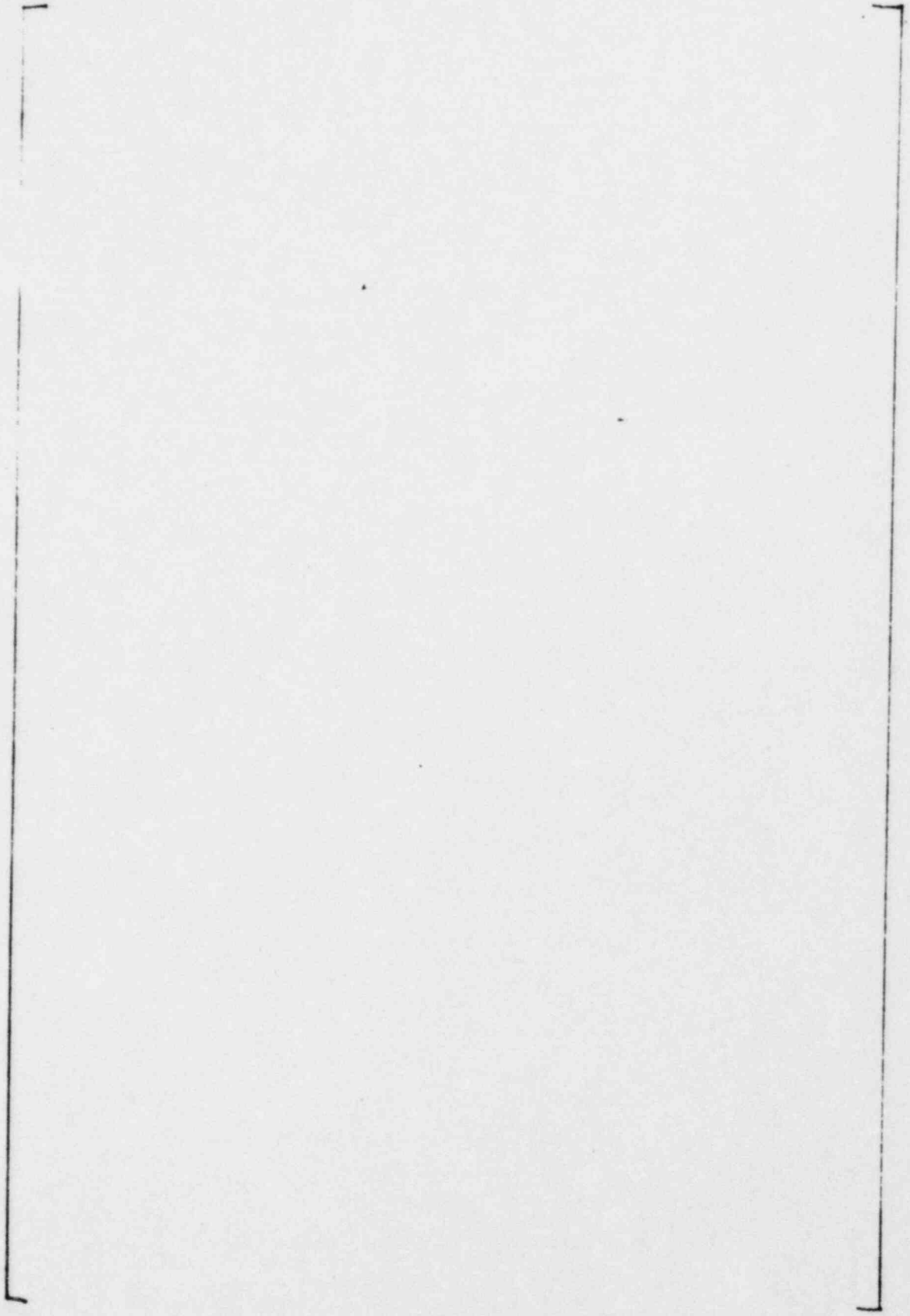

a.b.c.e

FIGURE 11.8-55, CASE NO.11, FLOW TEST TEMPERATURE RECORD VS. 100 TERMS OF FOURIER SERIES

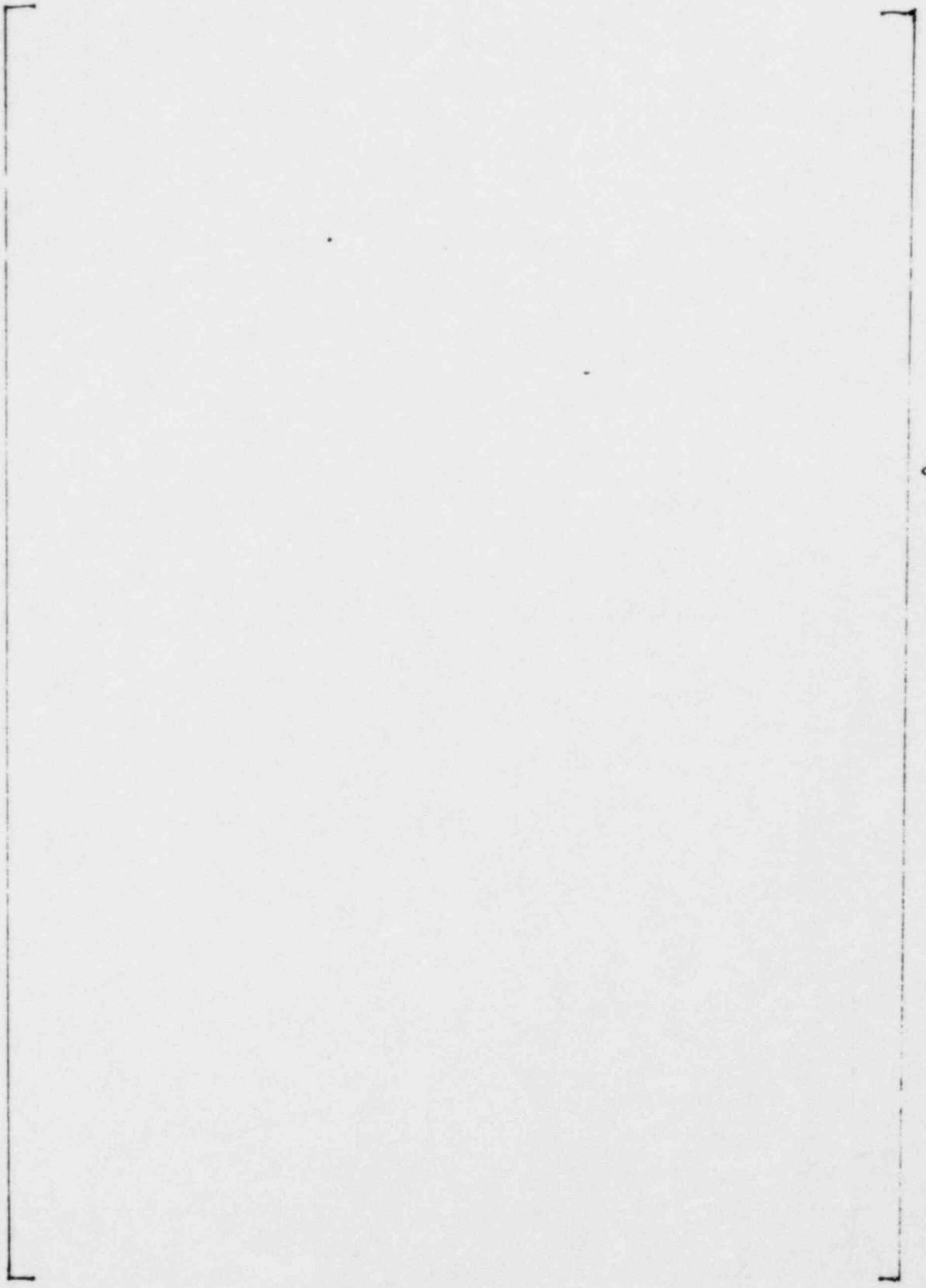

a,b,c,e

FIGURE 11.8-56, CASE NO.12, FLOW TEST TEMPERATURE RECORD VS. 100 TERMS OF FOURIER SERIES

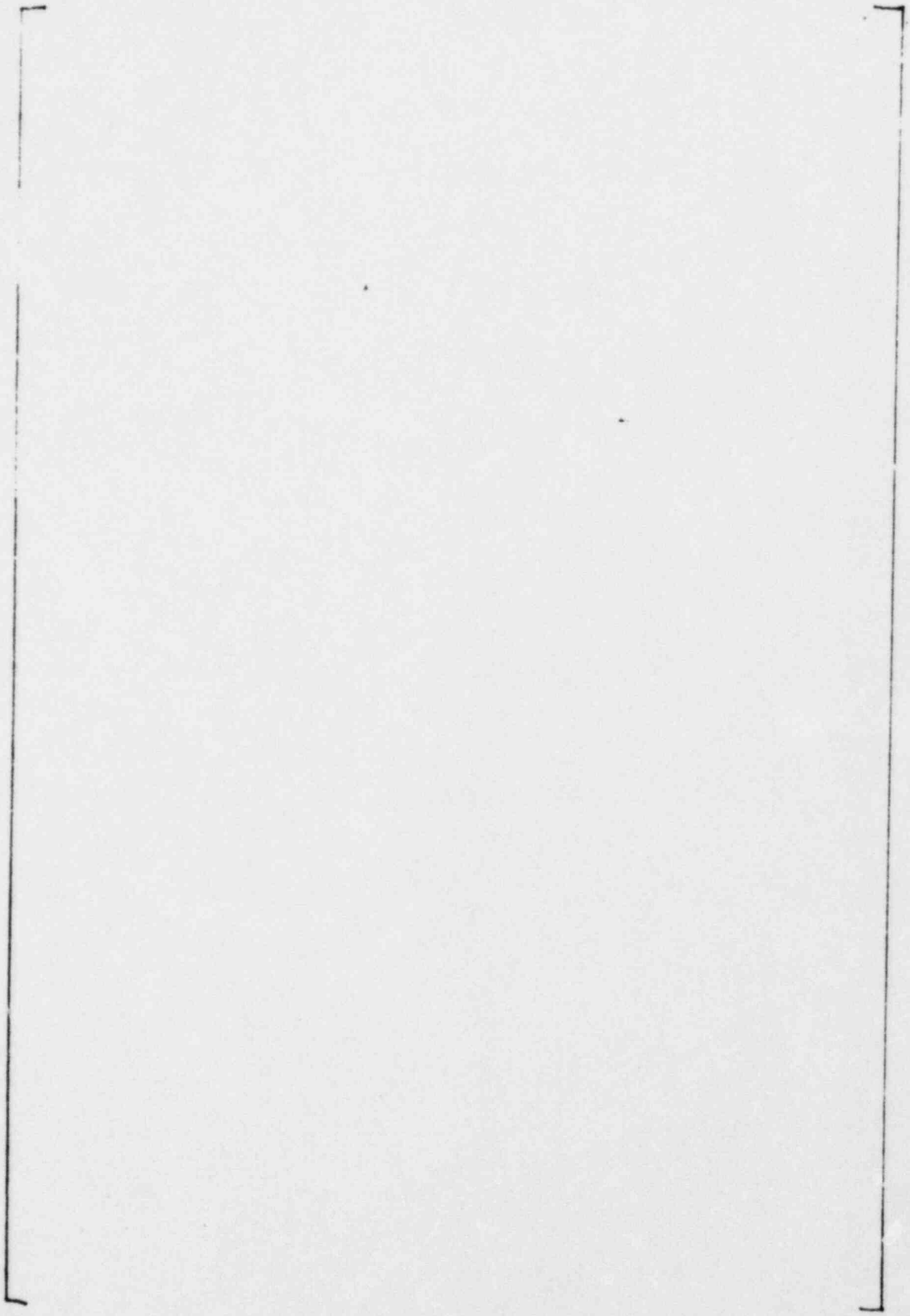

a.b.c.e

FIGURE 11.8-57, CASE NO.13, FLOW TEST TEMPERATURE RECORD VS. 100 TERMS OF FOURIER SERIES

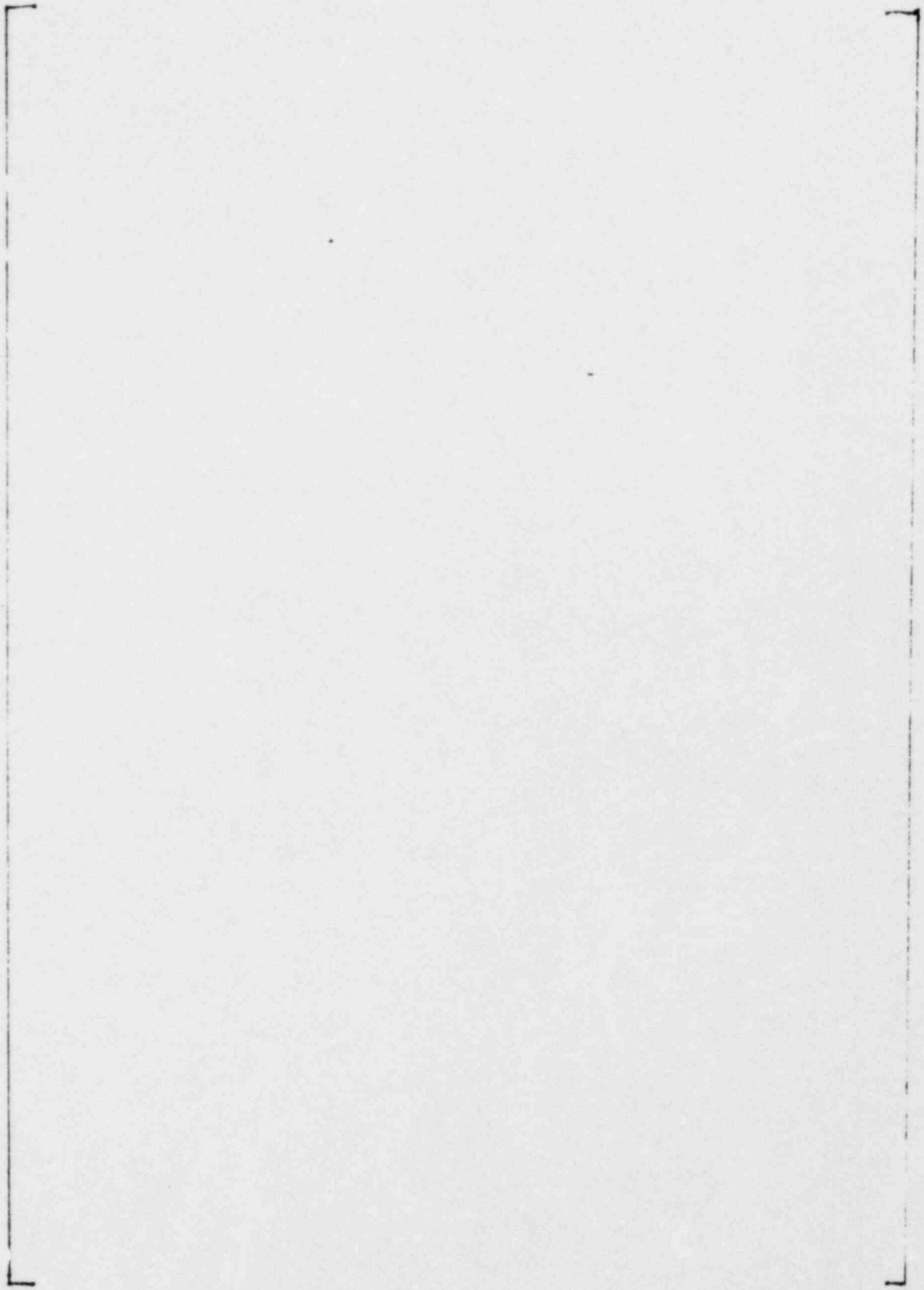

a,b,c,e

FIGURE 11.8-58, CASE NO.14, FLOW TEST TEMPERATURE RECORD VS. 100 TERMS OF FOURIER SERIES

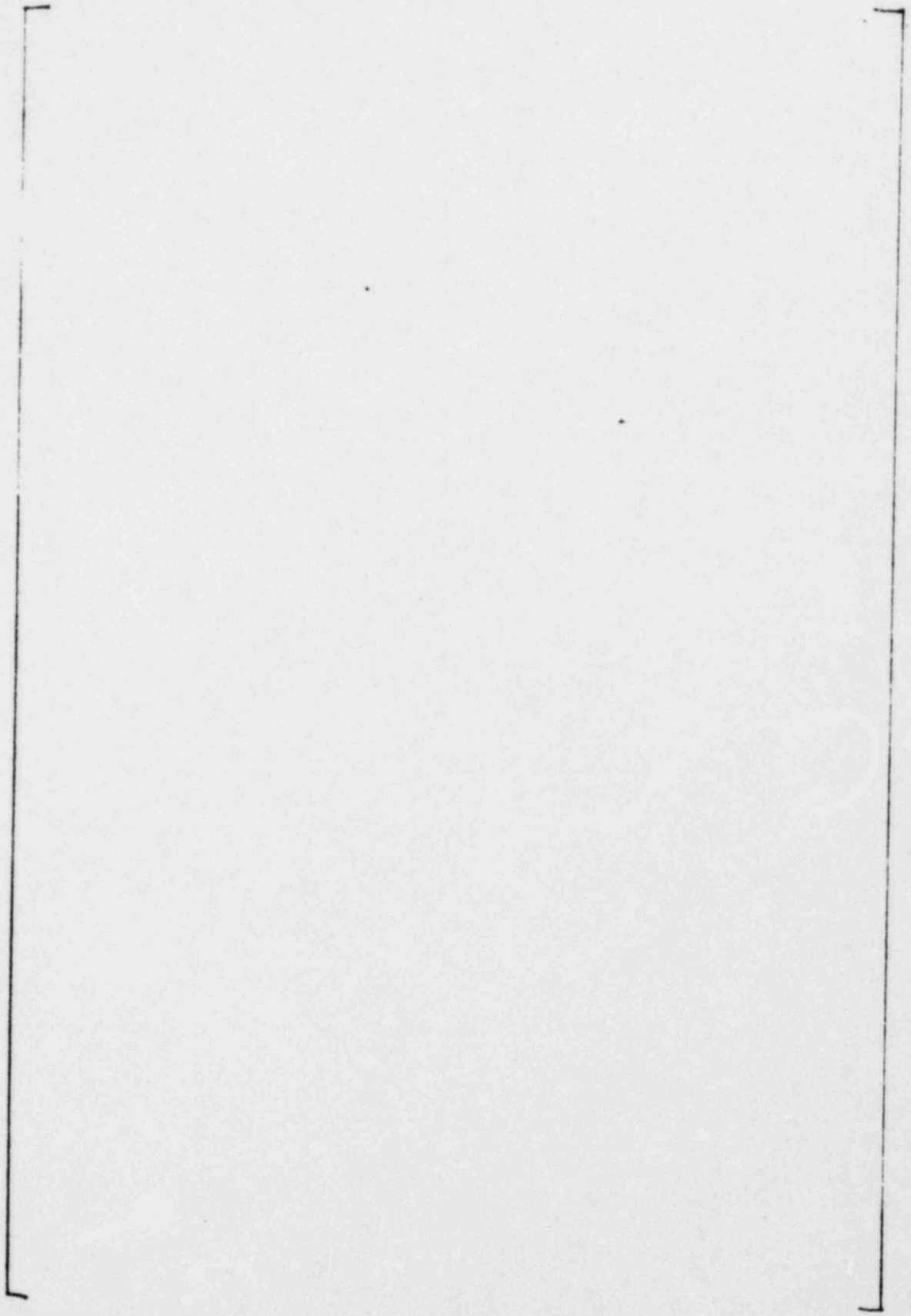

a.b.c.e

FIGURE 11.8-59, CASE NO.15, FLOW TEST TEMPERATURE RECORD VS. 100 TERMS OF FOURIER SERIES

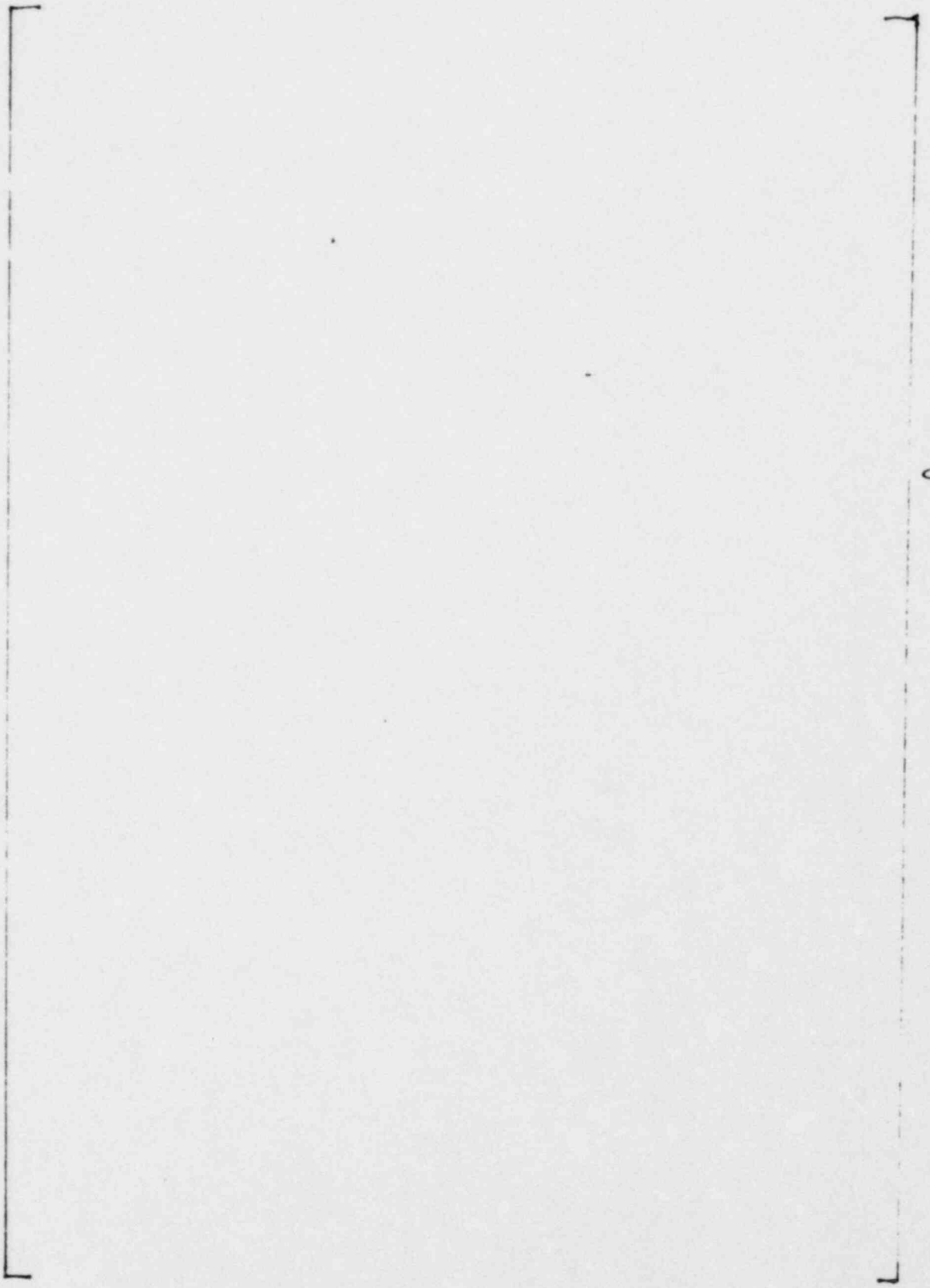

a,b,c,e

FIGURE 11.8-60, CASE NO.16, FLOW TEST TEMPERATURE RECORD VS. 100 TERMS OF FOURIER SERIES

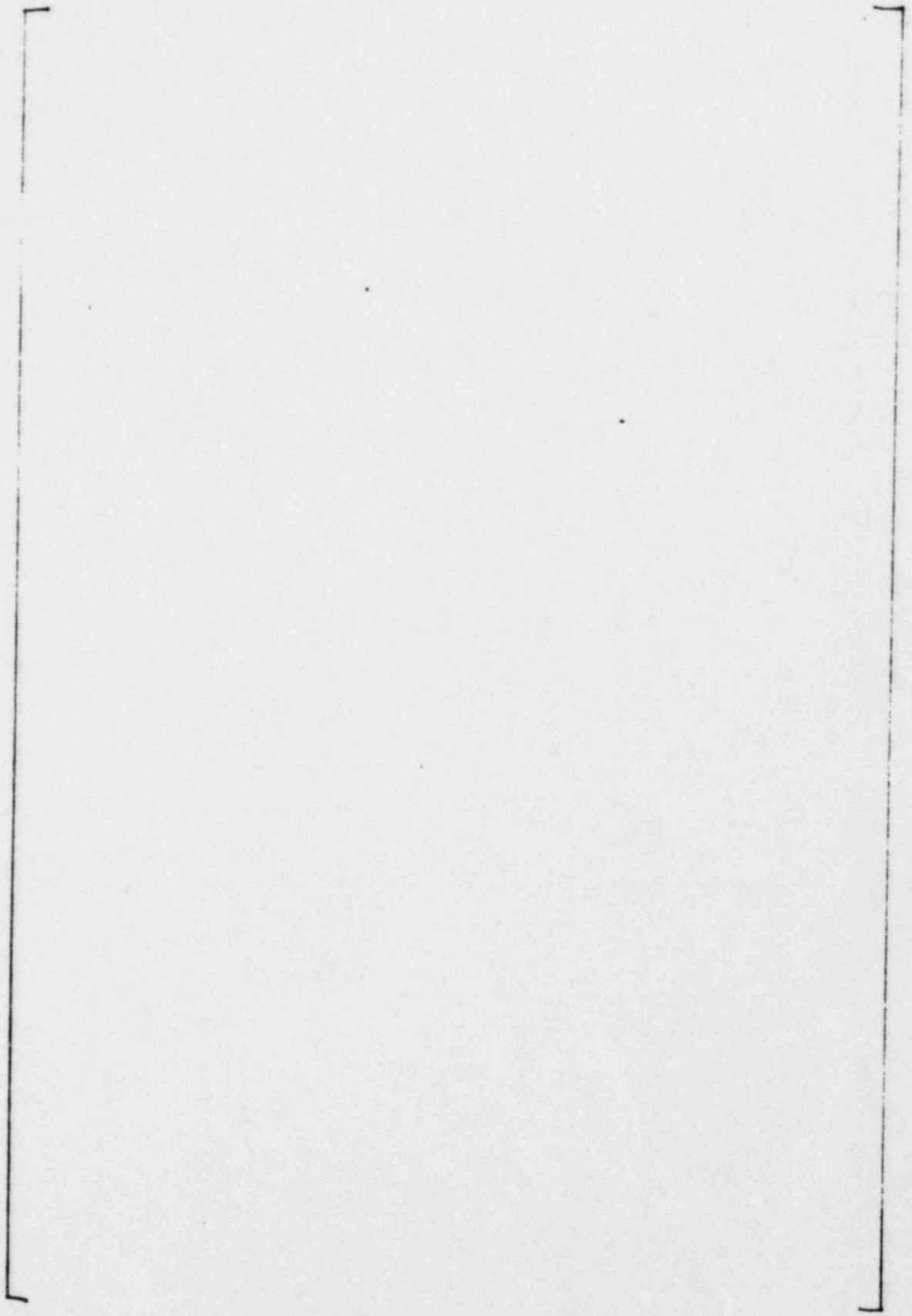

a,b,c,e

FIGURE 11.8-61, CASE NO.17, FLOW TEST TEMPERATURE RECORD VS. 100 TERMS OF FOURIER SERIES

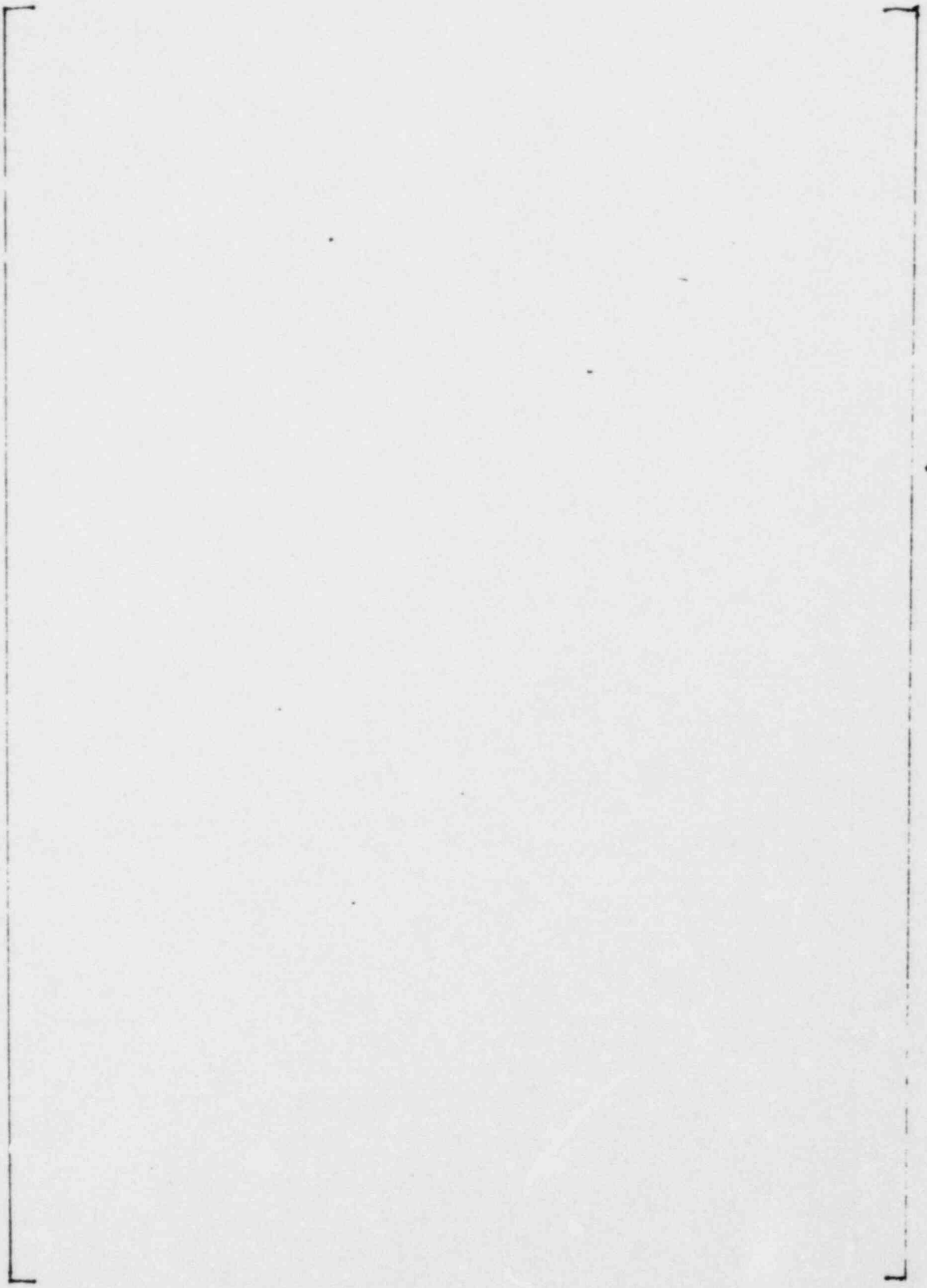

a,b,c,e

FIGURE 11.8-62, CASE NO.18, FLOW TEST TEMPERATURE RECORD VS. 100 TERMS OF FOURIER SERIES

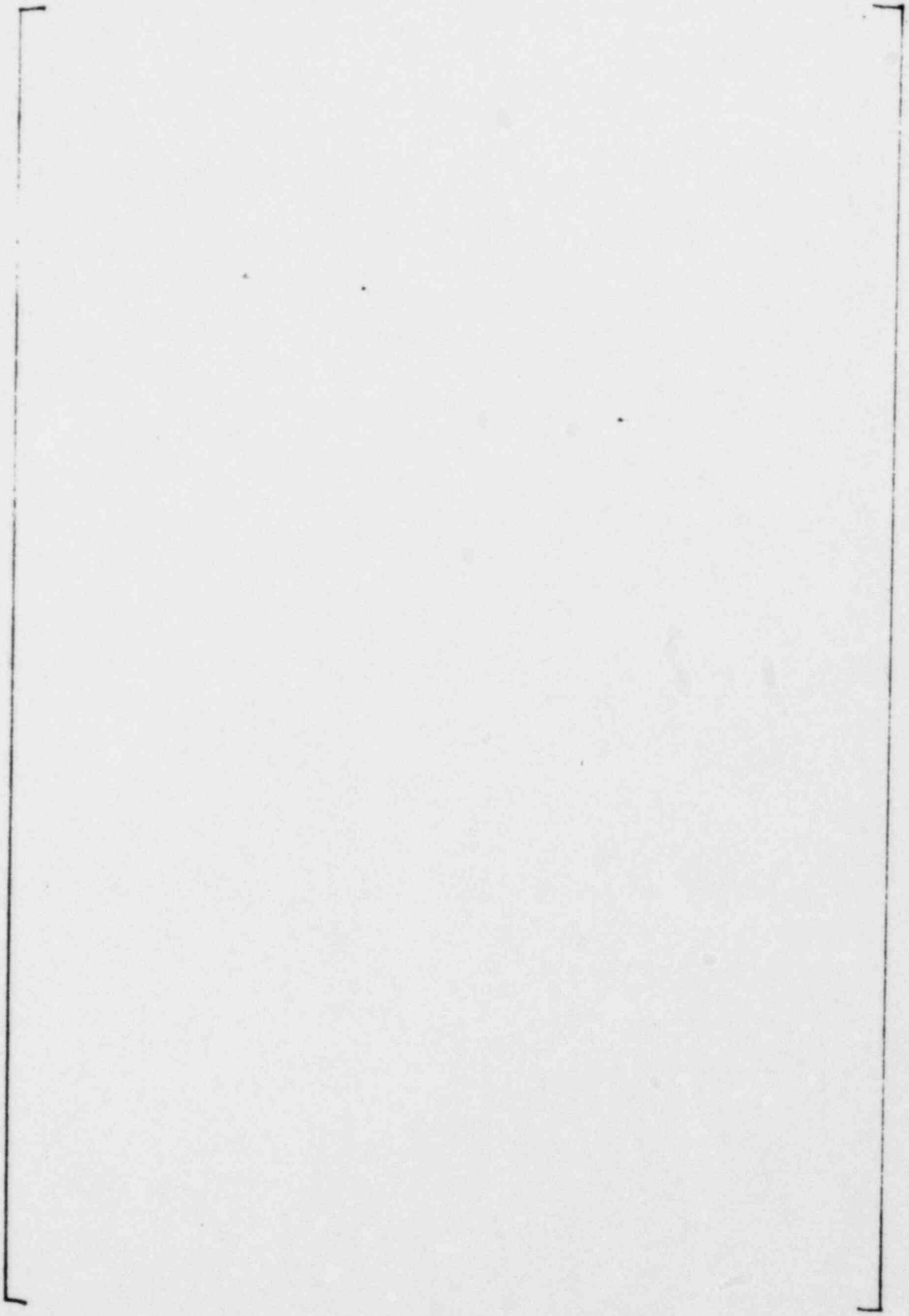

a.b.c.e

FIGURE 11.8-63, CASE NO.19, FLOW TEST TEMPERATURE RECORD VS. 100 TERMS OF FOURIER SERIES

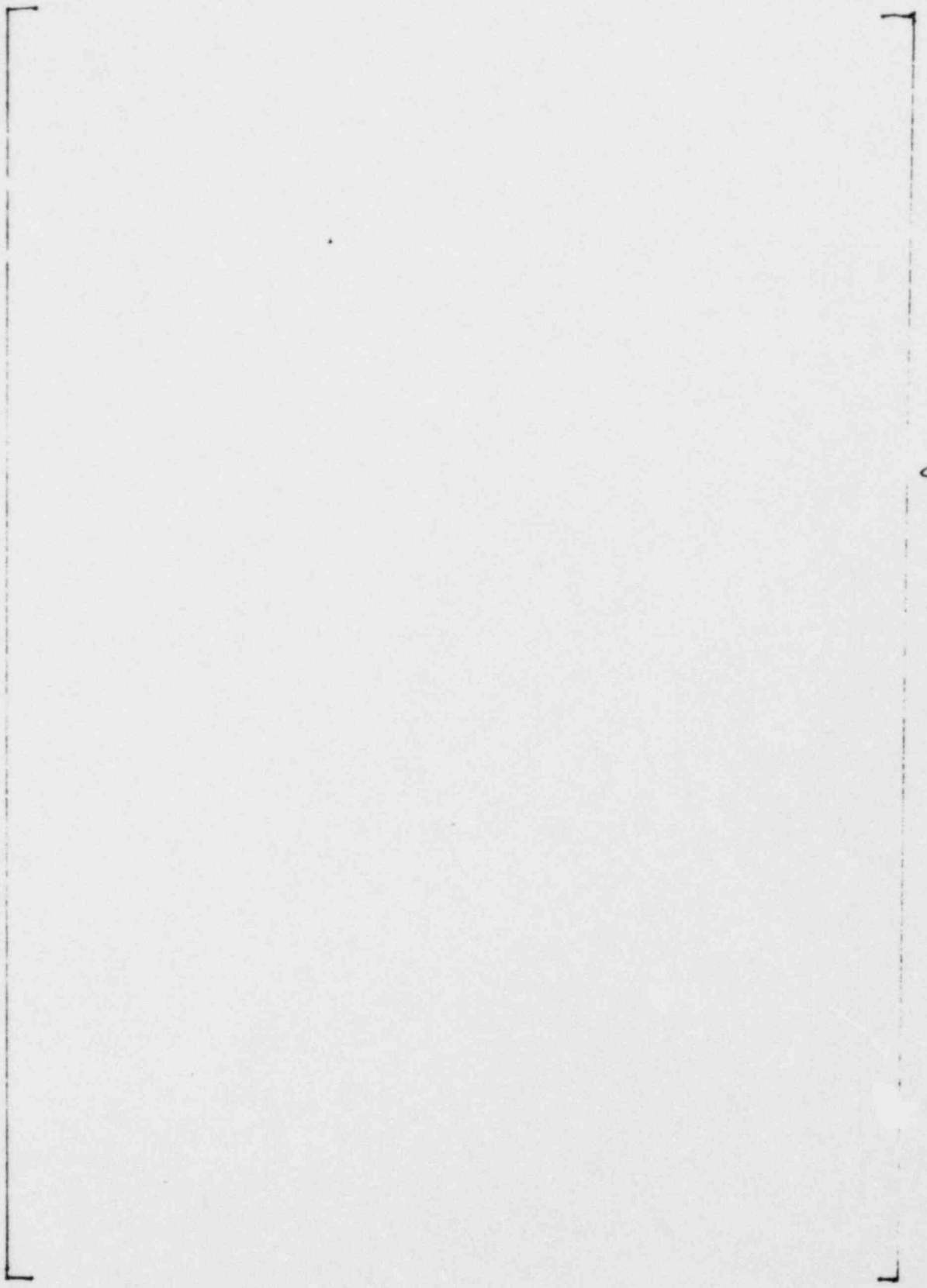

a,b,c,e

FIGURE 11.8-64, CASE NO.20, FLOW TEST TEMPERATURE RECORD VS. 100 TERMS OF FOURIER SERIES

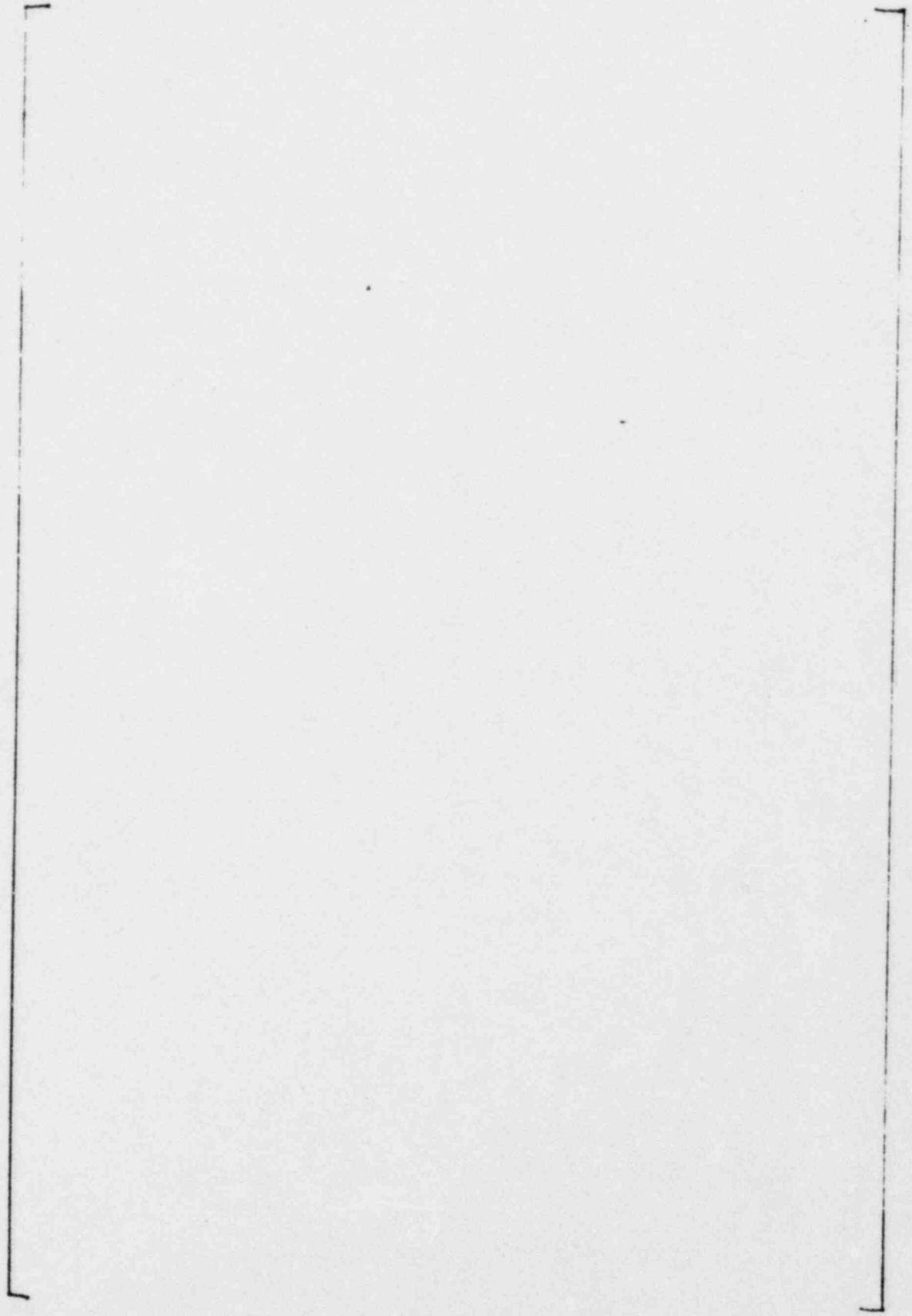

a.b.c.e

FIGURE 11.8-65, CASE NO.21, FLOW TEST TEMPERATURE RECORD VS. 100 TERMS OF FOURIER SERIES

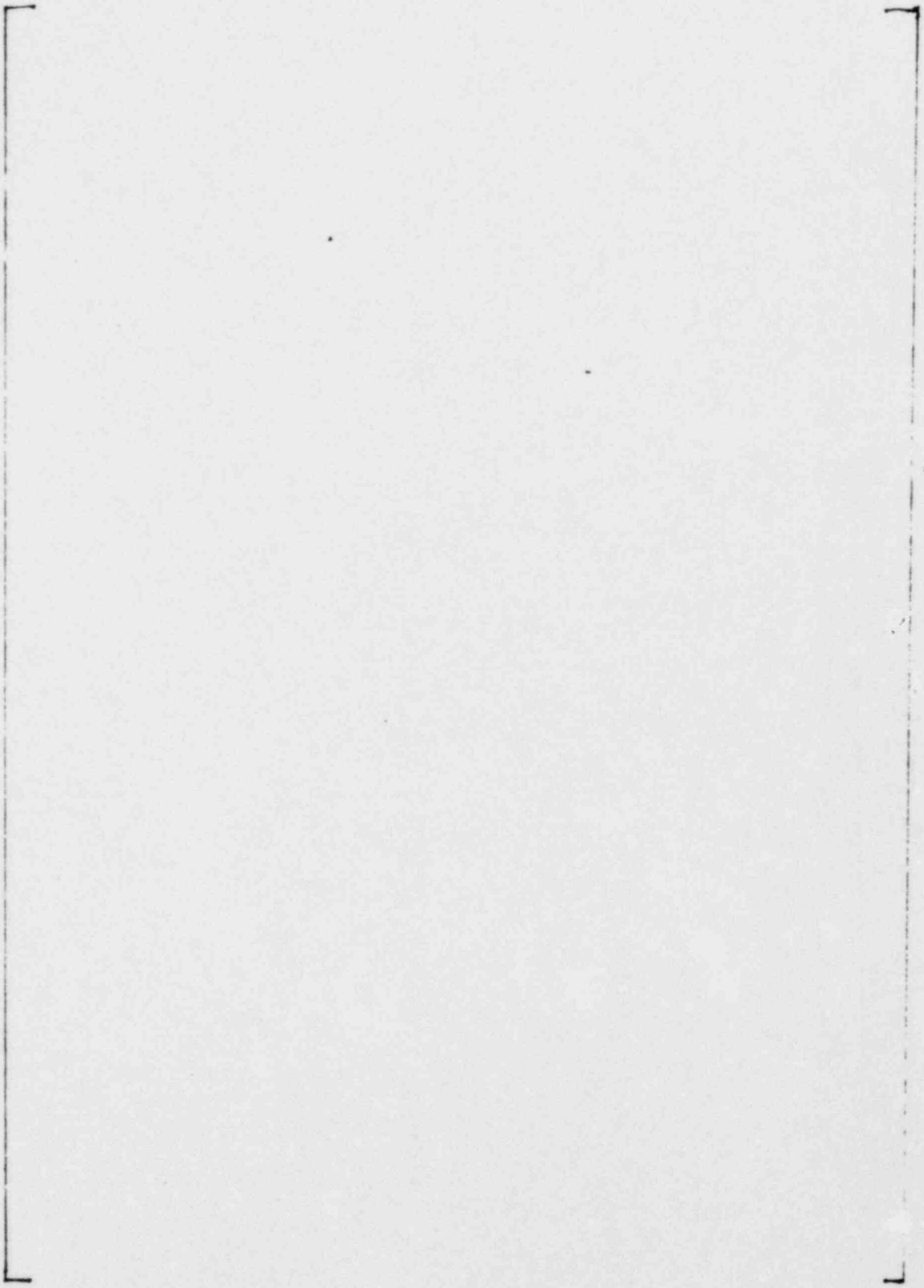

a,b,c,e

FIGURE 11.8-66, CASE NO.22, FLOW TEST TEMPERATURE RECORD VS. 100 TERMS OF FOURIER SERIES

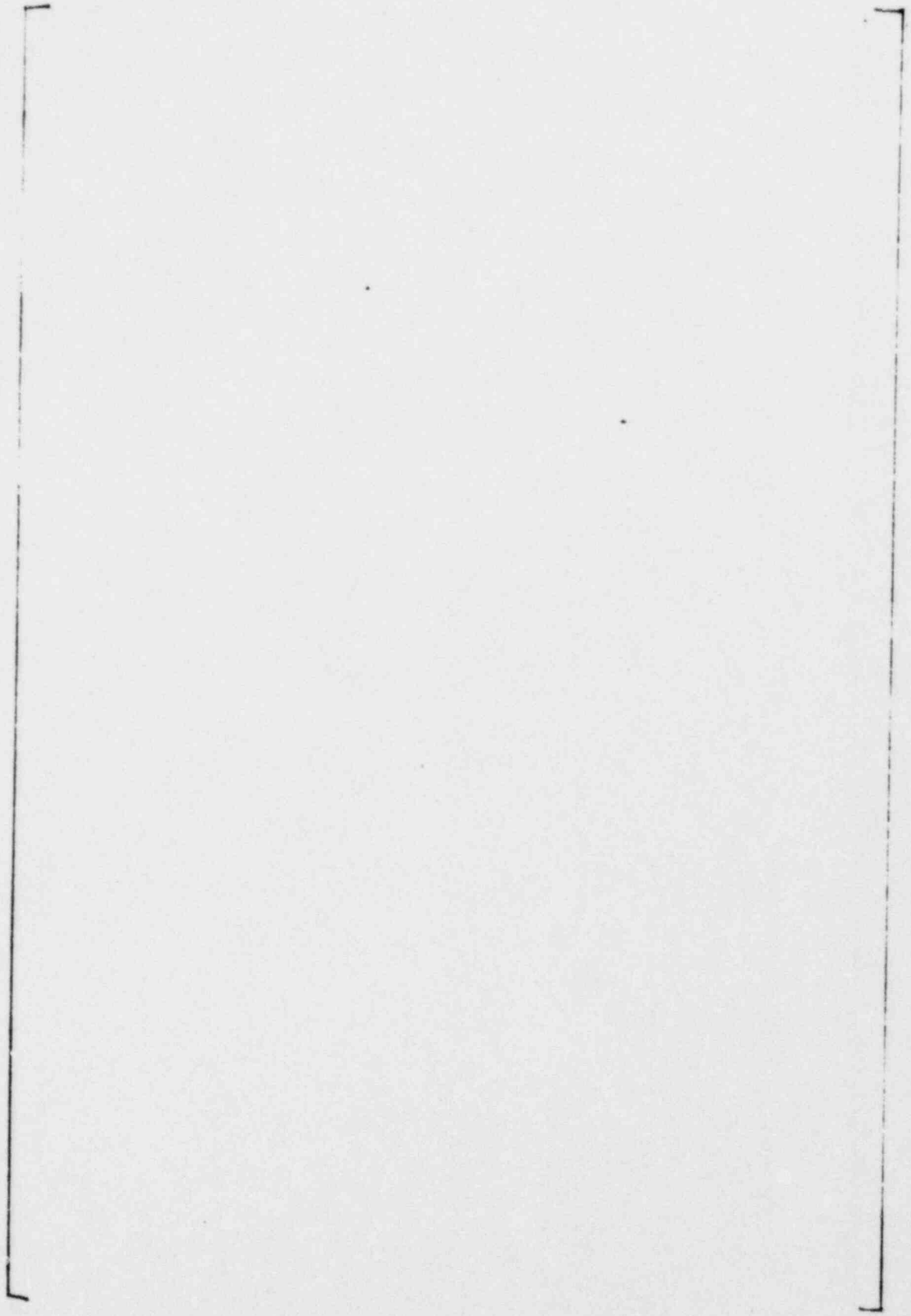

a,b,c,e

FIGURE 11.8-67, CASE NO.23, FLOW TEST TEMPERATURE RECORD VS. 100 TERMS OF FOURIER SERIES

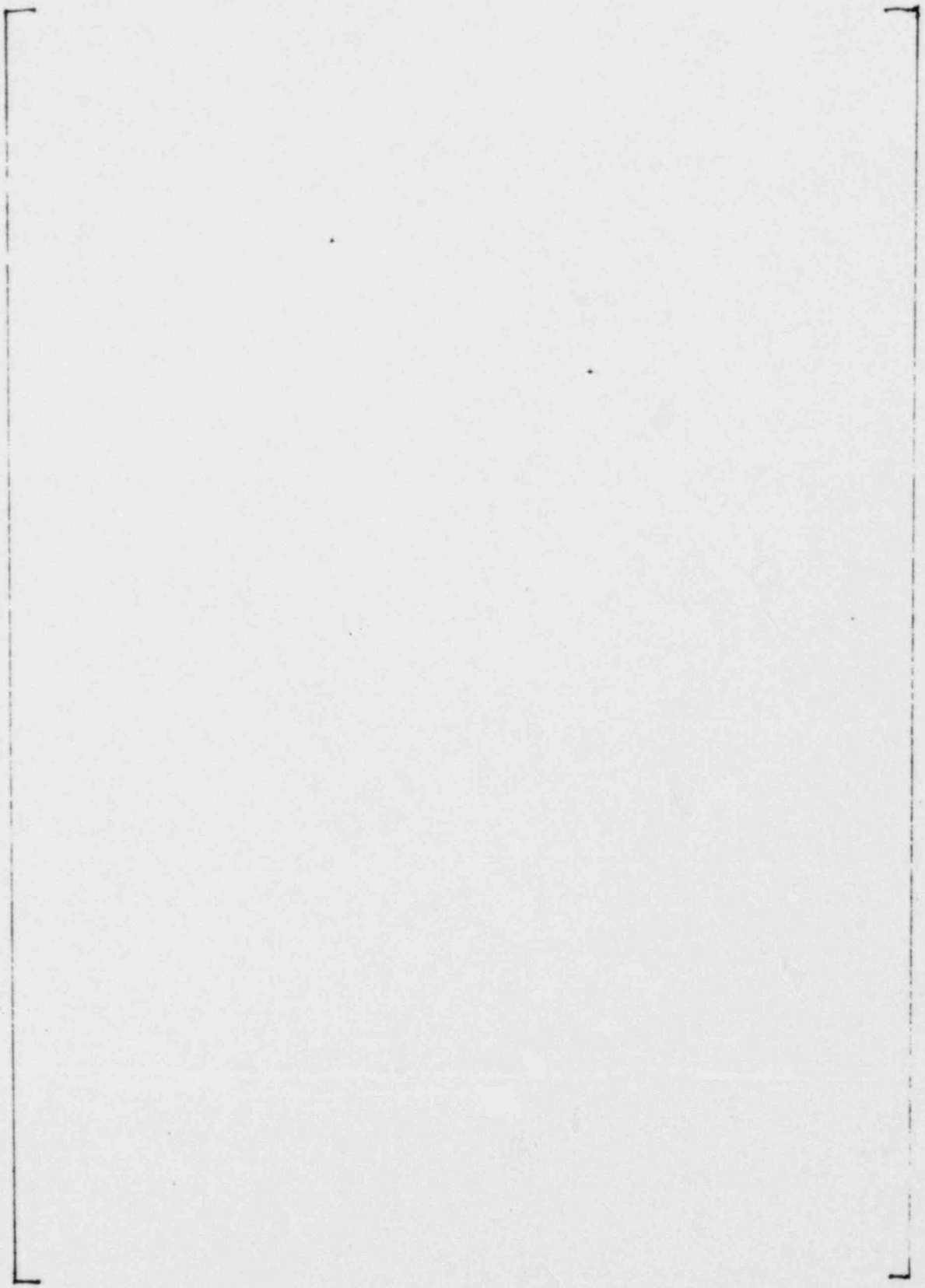

a,b,c,e

FIGURE 11.8-68, CASE NO.24, FLOW TEST TEMPERATURE RECORD VS. 100 TERMS OF FOURIER SERIES

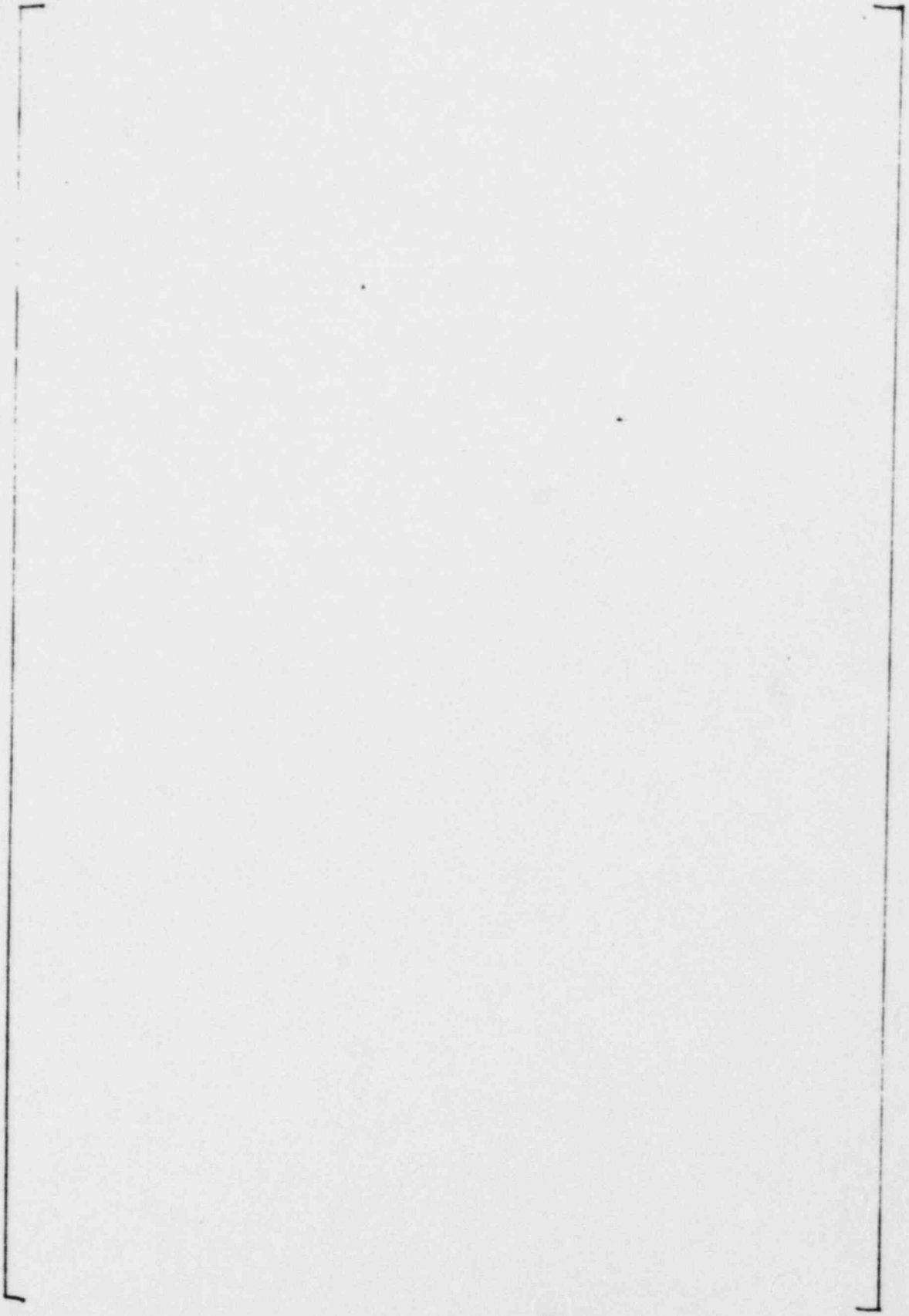

a.b.c.e

FIGURE 11.8-69, CASE NO.25, FLOW TEST TEMPERATURE RECORD VS. 100 TERMS OF FOURIER SERIES

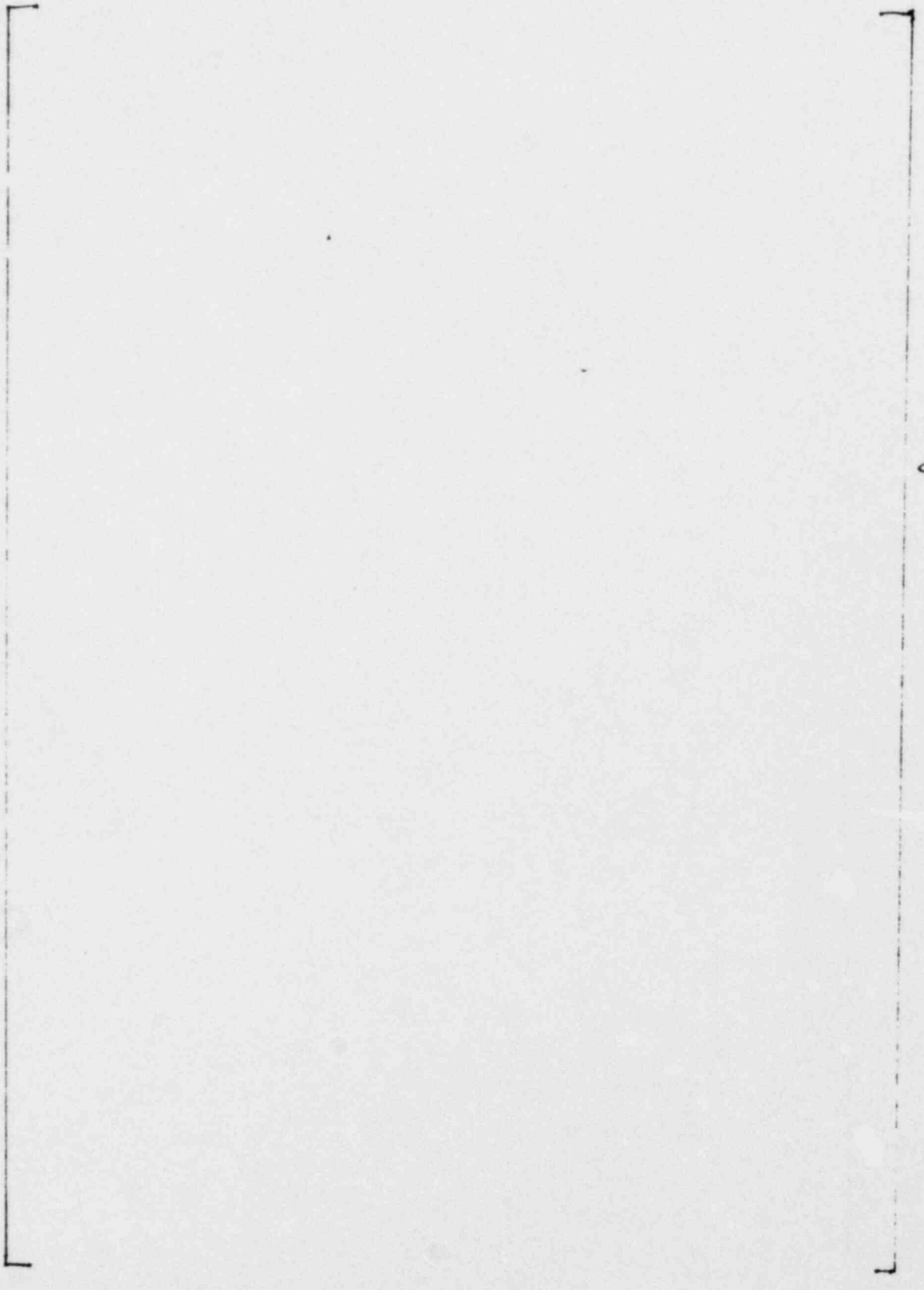

a,b,c,e

FIGURE 11.8-70, CASE NO.26, FLOW TEST TEMPERATURE RECORD VS. 100 TERMS OF FOURIER SERIES

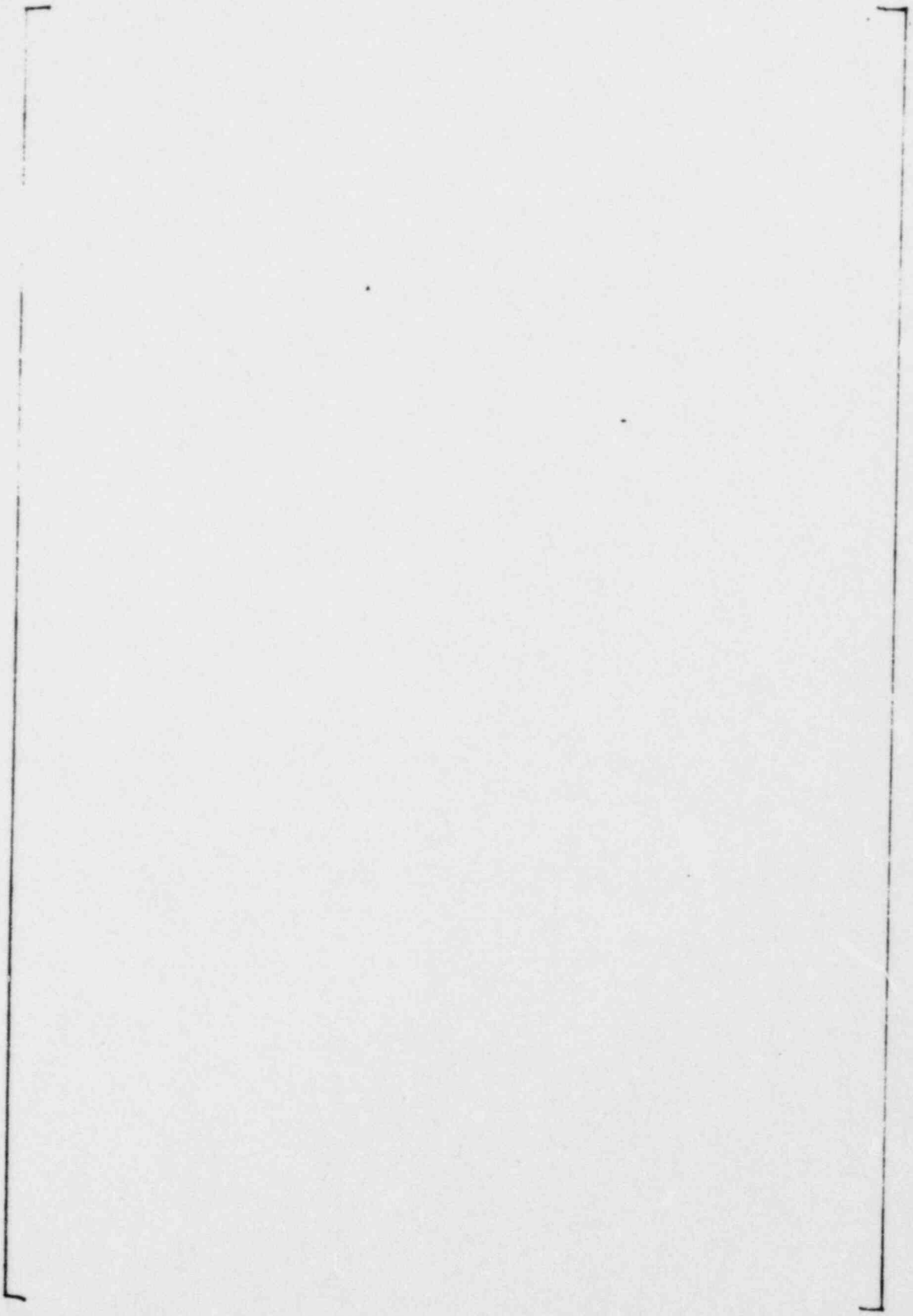

a,b,c,e

FIGURE 11.8-71, CASE NO.27, FLOW TEST TEMPERATURE RECORD VS. 100 TERMS OF FOURIER SERIES

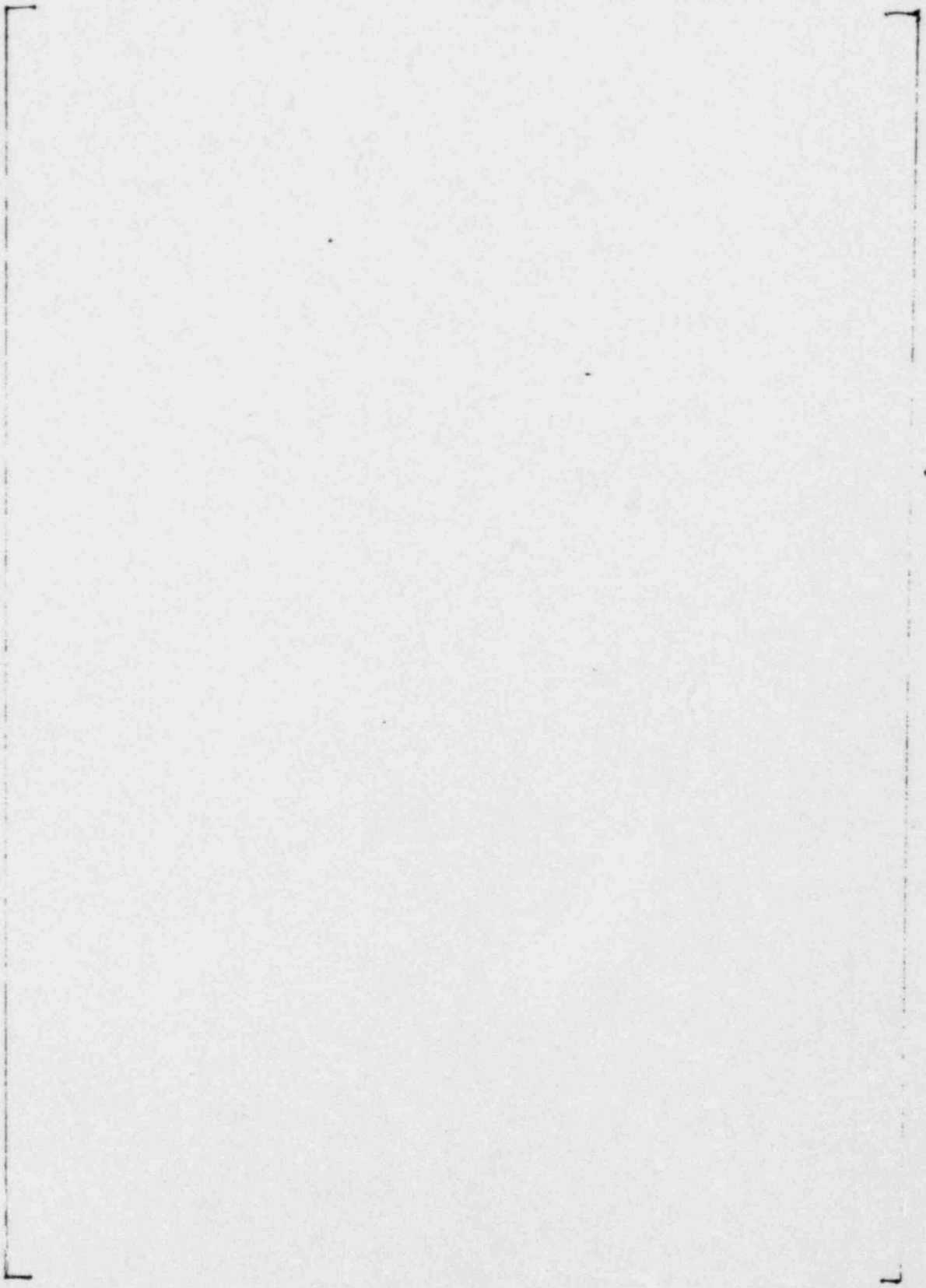

a,b,c,e

FIGURE 11.8-72, CASE NO.28, FLOW TEST TEMPERATURE RECORD VS. 100 TERMS OF FOURIER SERIES

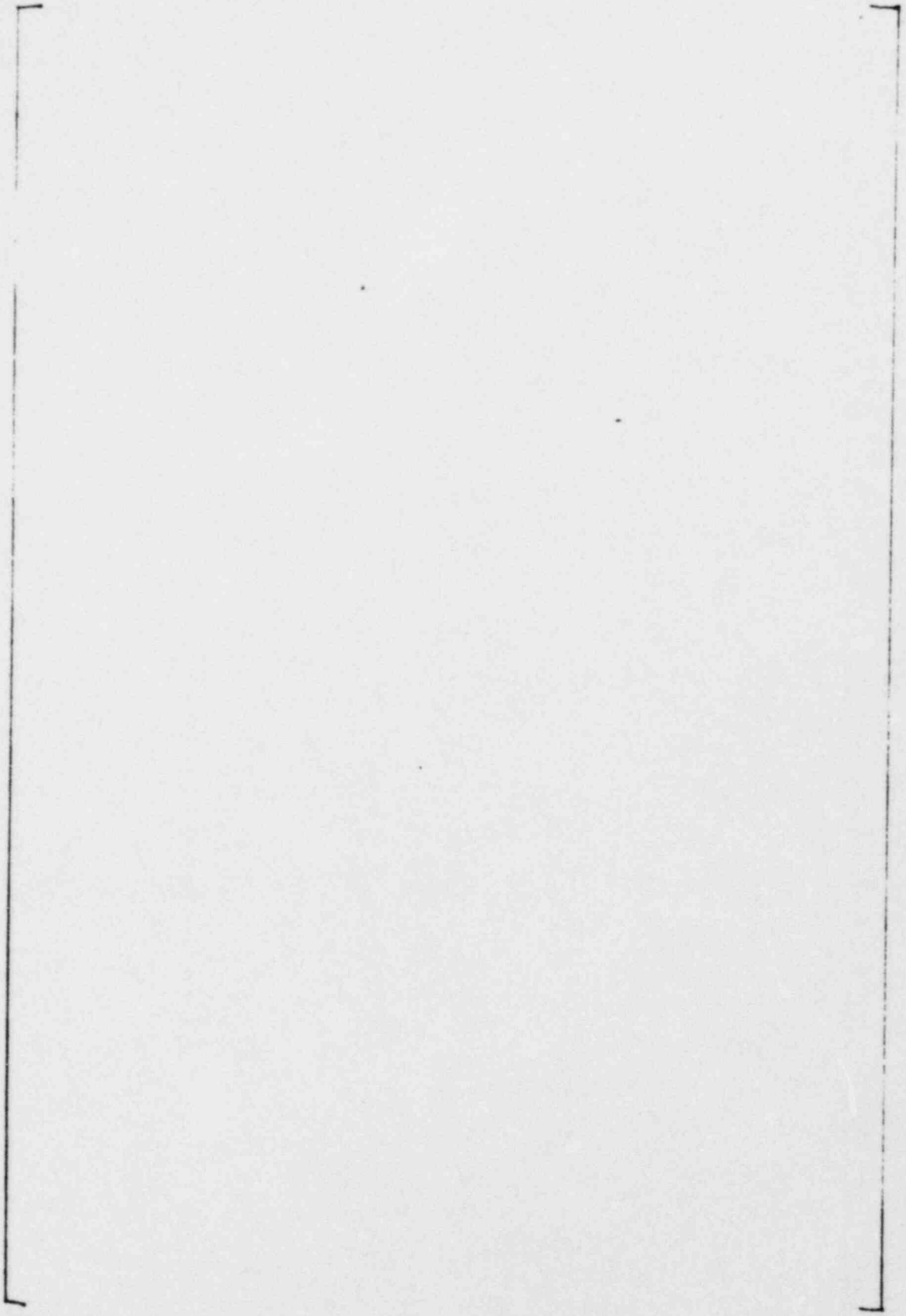

a.b.c.e

FIGURE 11.8-73, CASE NO.29. FLOW TEST TEMPERATURE RECORD VS. 100 TERMS OF FOURIER SERIES

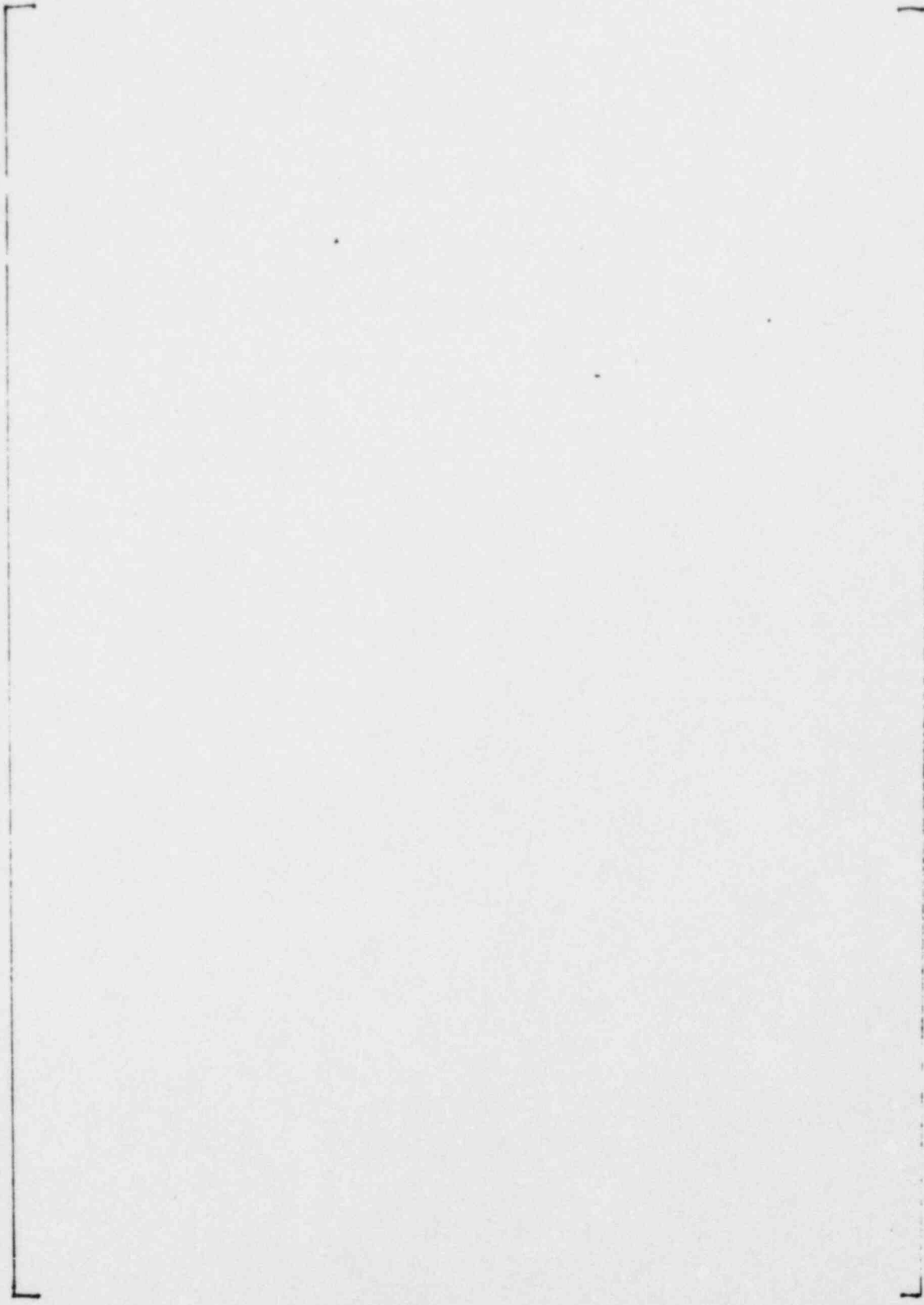

a,b,c,e

FIGURE 11.8-74, CASE NO.30, FLOW TEST TEMPERATURE RECORD VS. 100 TERMS OF FOURIER SERIES

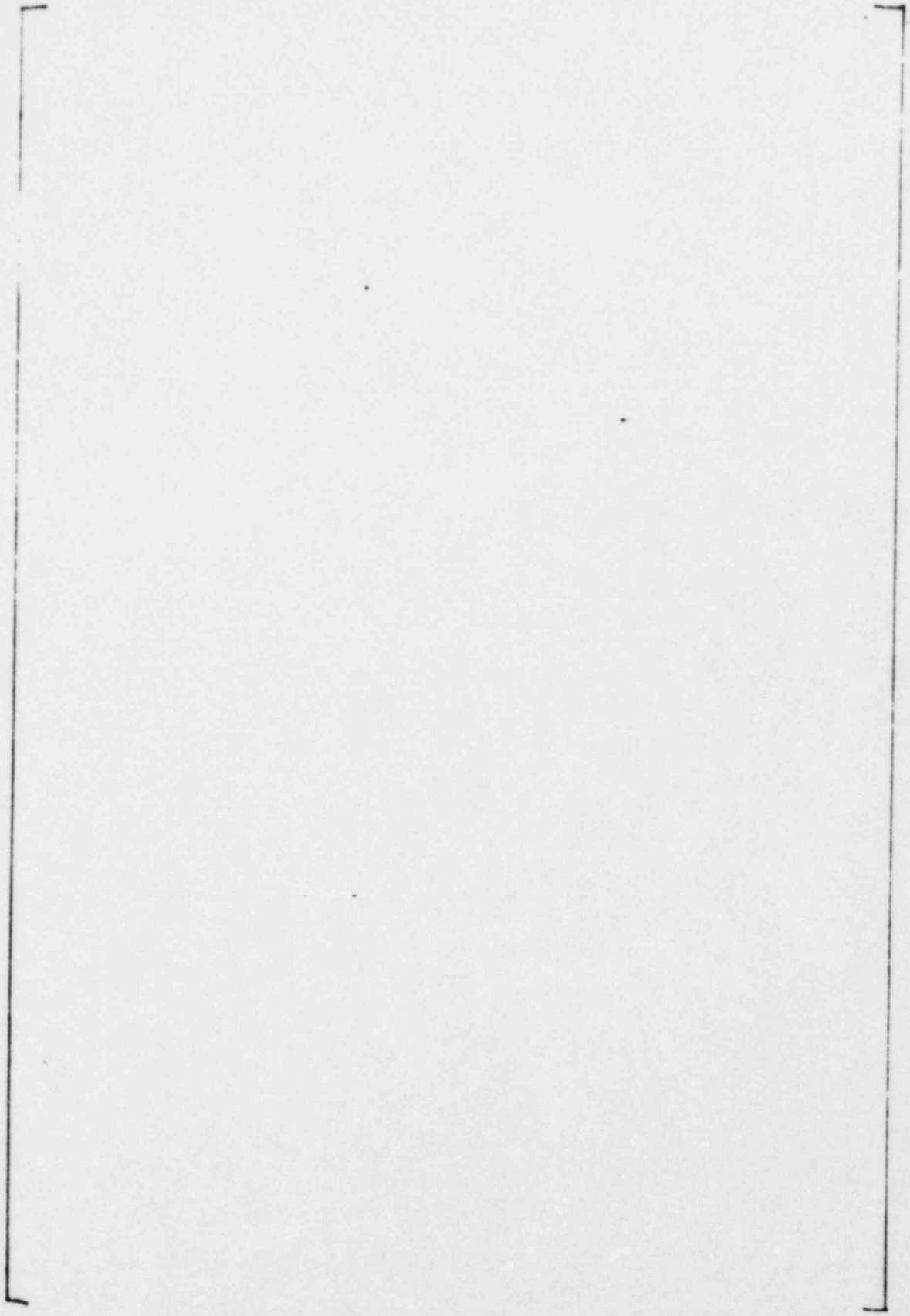

a,b,c,e

FIGURE 11.8-75, CASE NO.31, FLOW TEST TEMPERATURE RECOFD VS. 100 TERMS OF FOURIER SERIES

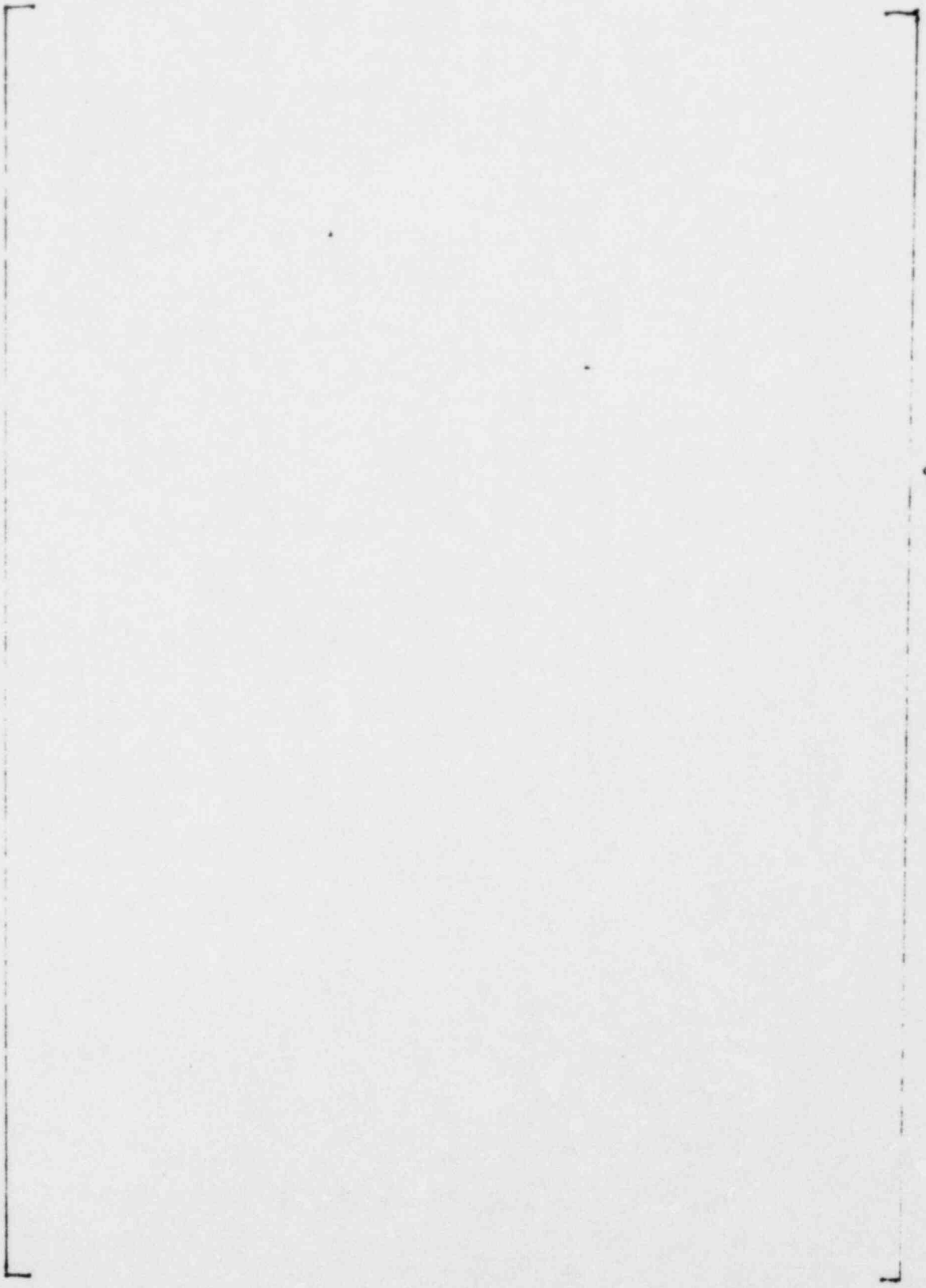

a,b,c,e

FIGURE 11.8-76, CASE NO.32, FLOW TEST TEMPERATURE RECORD VS. 100 TERMS OF FOURIER SERIES

BLANK

Case No.: 33

Generic Profile:

Interface Level:_____ Angle Measured From The Bottom of Pipe

Run No.: Y6 _____

FIGURE 11.8-77, CASE NO.33, FLOW TEST TEMPERATURE RECORD VS. 100 TERMS OF FOURIER SERIES

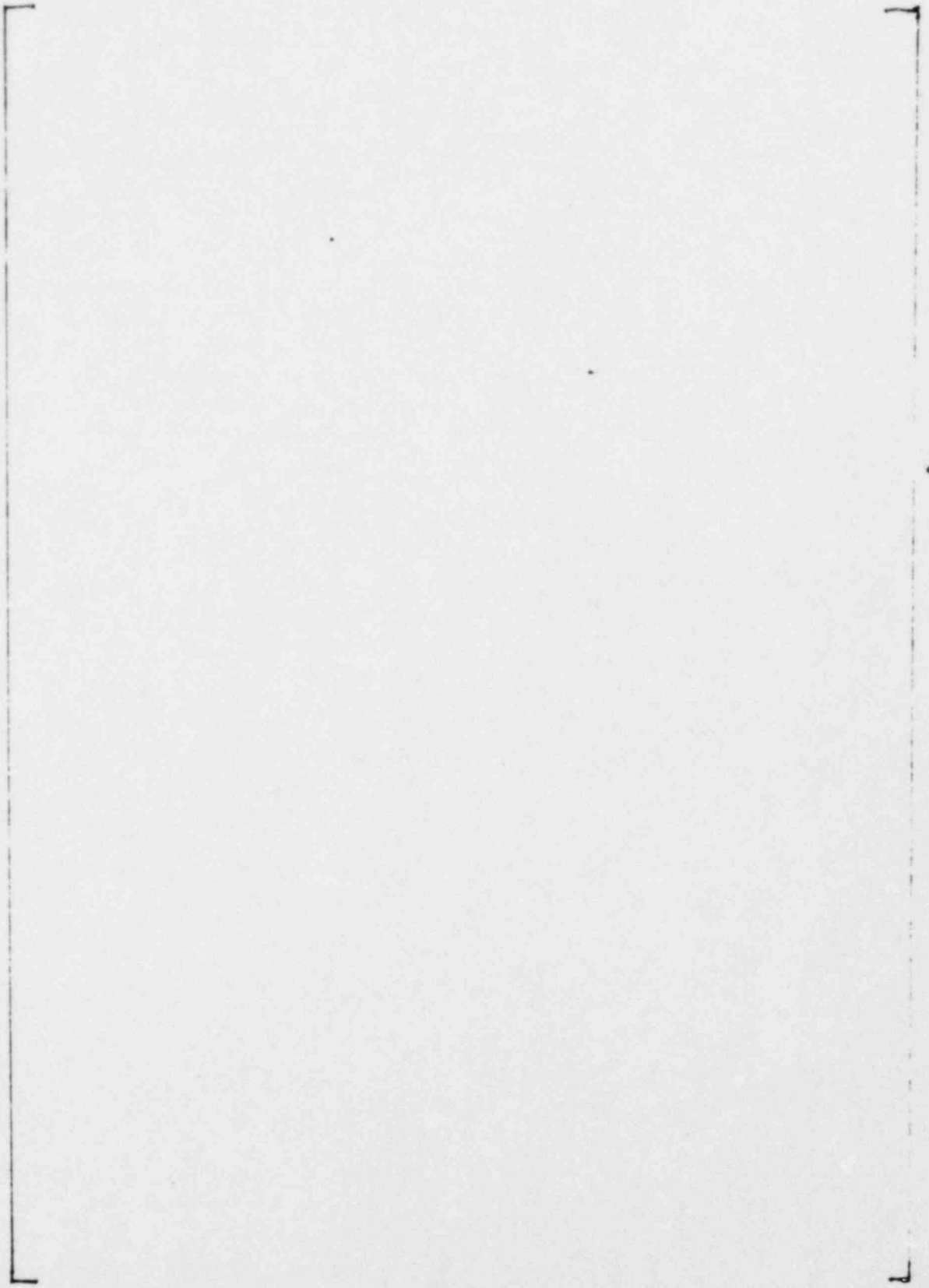

a,b,c,e

FIGURE 11.8-78, CASE NO.34, FLOW TEST TEMPERATURE RECORD VS. 100 TERMS OF FOURIER SERIES

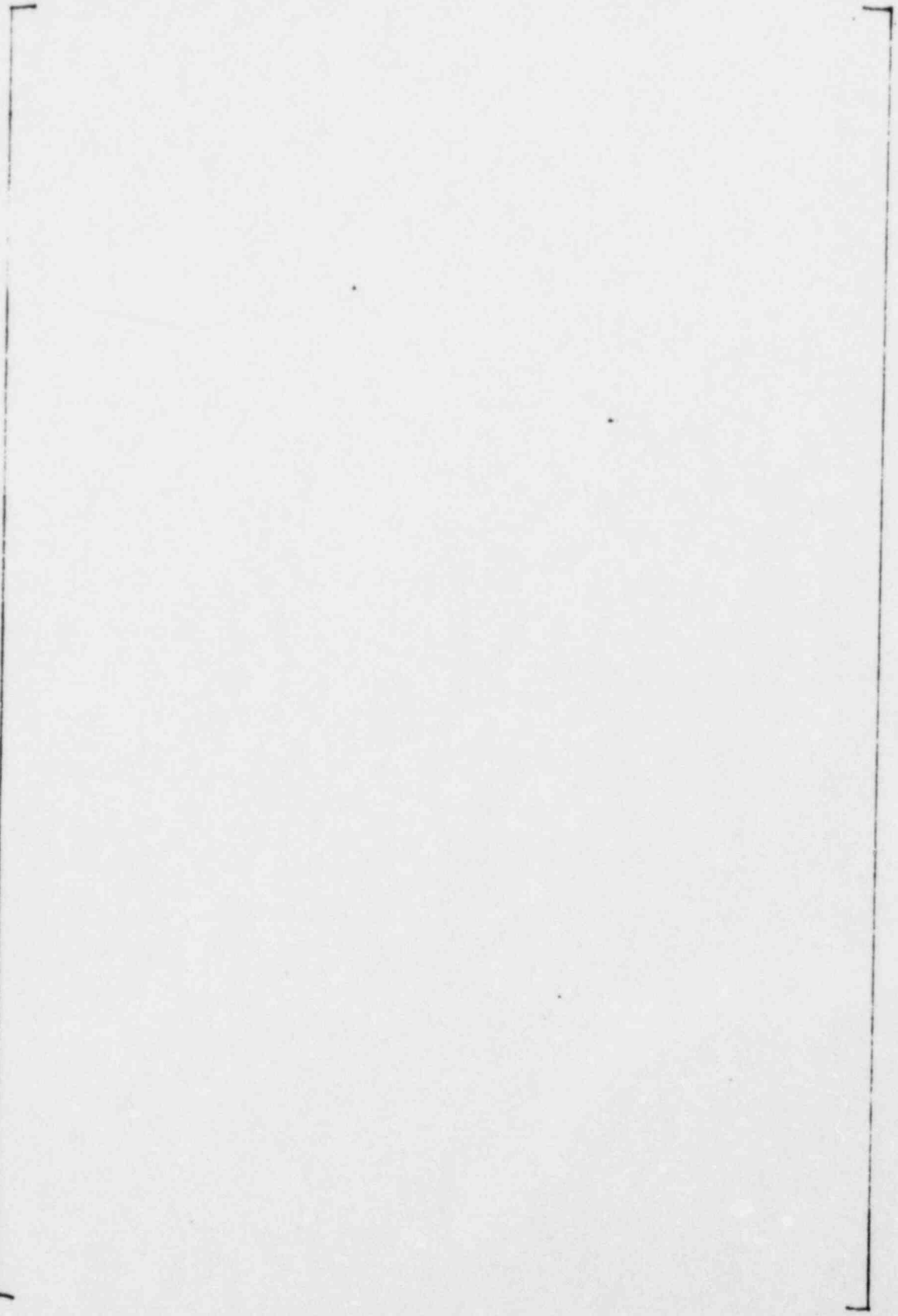

a,b,c,e

FIGURE 11.8-79, CASE NO.35, FLOW TEST TEMPERATURE RECORD VS. 100 TERMS OF FOURIER SERIES

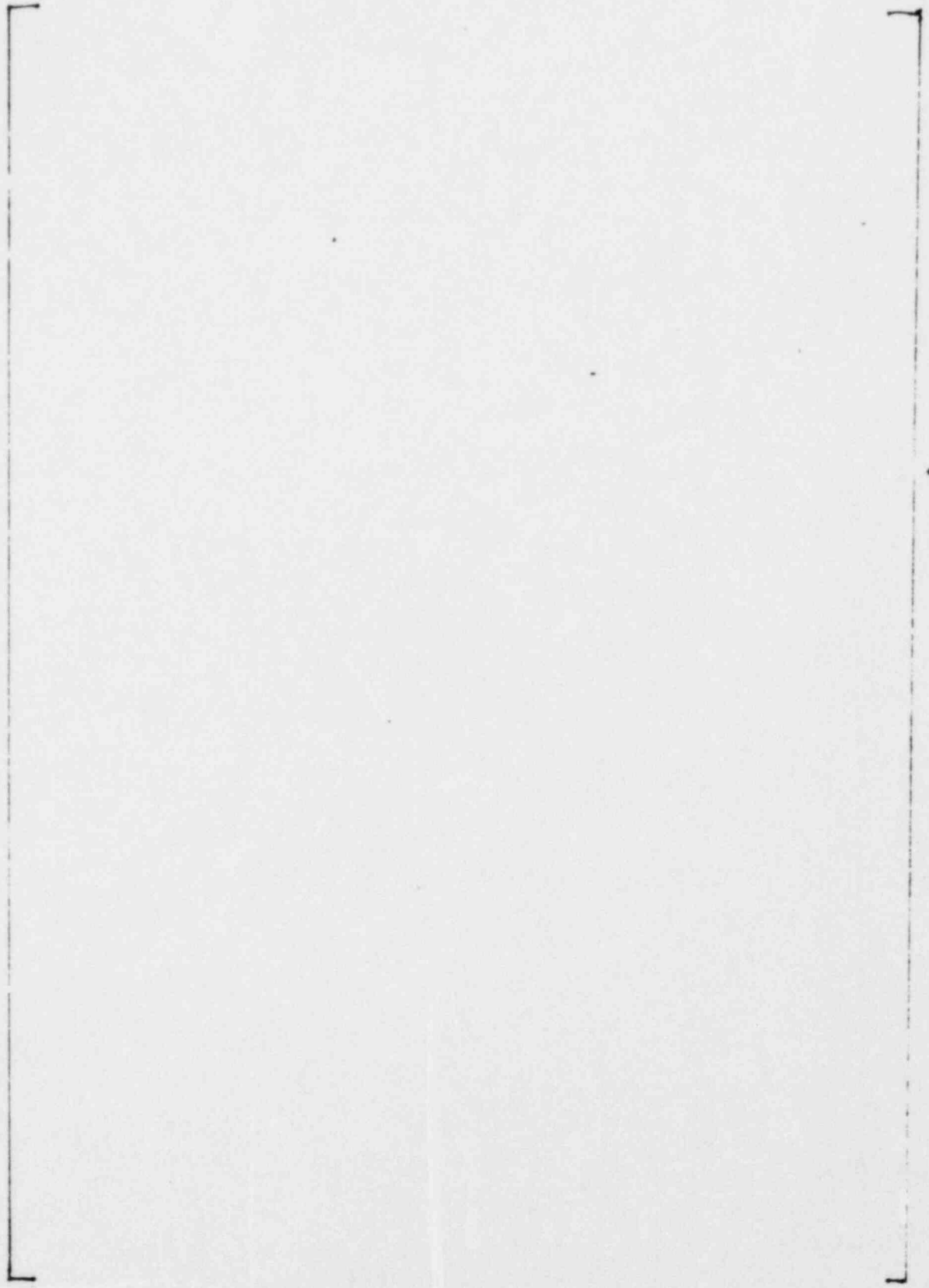

a,b,c,e

FIGURE 11.8-80, CASE NO.36, FLOW TEST TEMPERATURE RECORD VS. 100 TERMS OF FOURIER SERIES

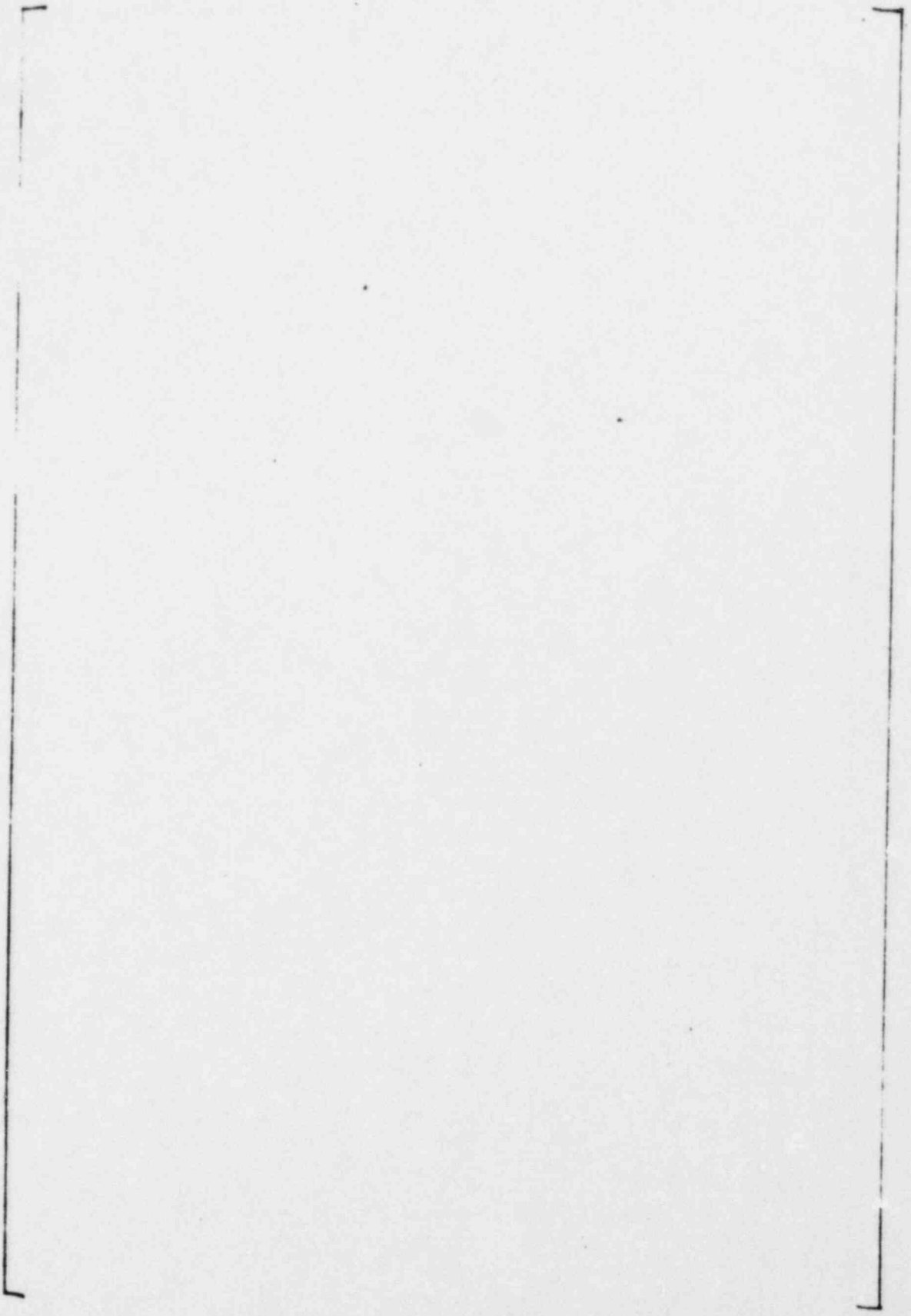

a.b.c.e

FIGURE 11.8-81, CASE NO.37, FLOW TEST TEMPERATURE RECORD VS. 100 TERMS OF FOURIER SERIES

BLANK

Case No.: 38

Generic Profile:

Interface Level:_____ Angle Measured From The Bottom of Pipe

Run No.: Y6 _____

FIGURE 11.8-82, CASE NO.38, FLOW TEST TEMPERATURE RECORD VS. 100 TERMS OF FOURIER SERIES

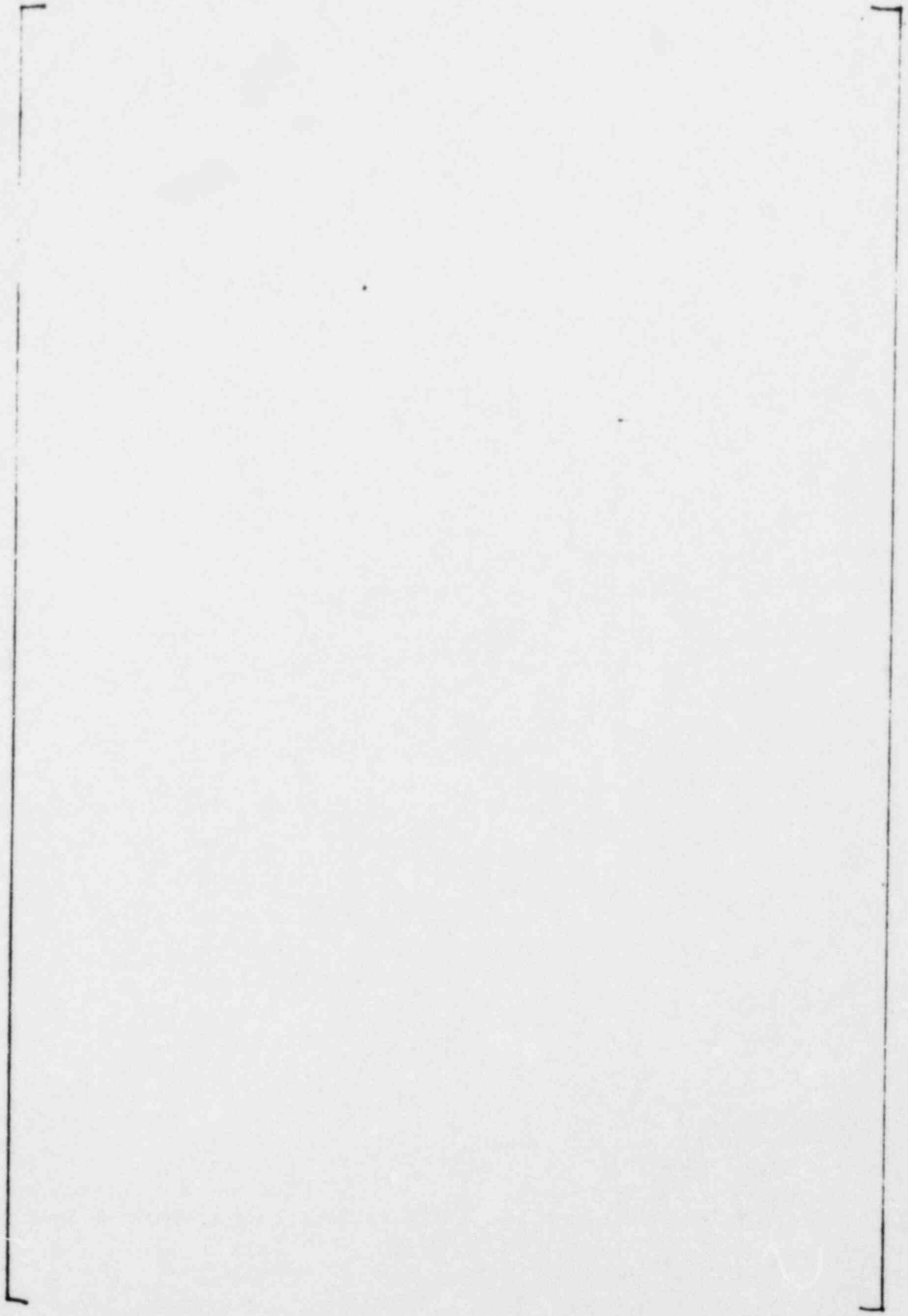

a.b.c.e

FIGURE 11.8-83, CASE NO.39, FLOW TEST TEMPERATURE RECORD VS. 100 TERMS OF FOURIER SERIES

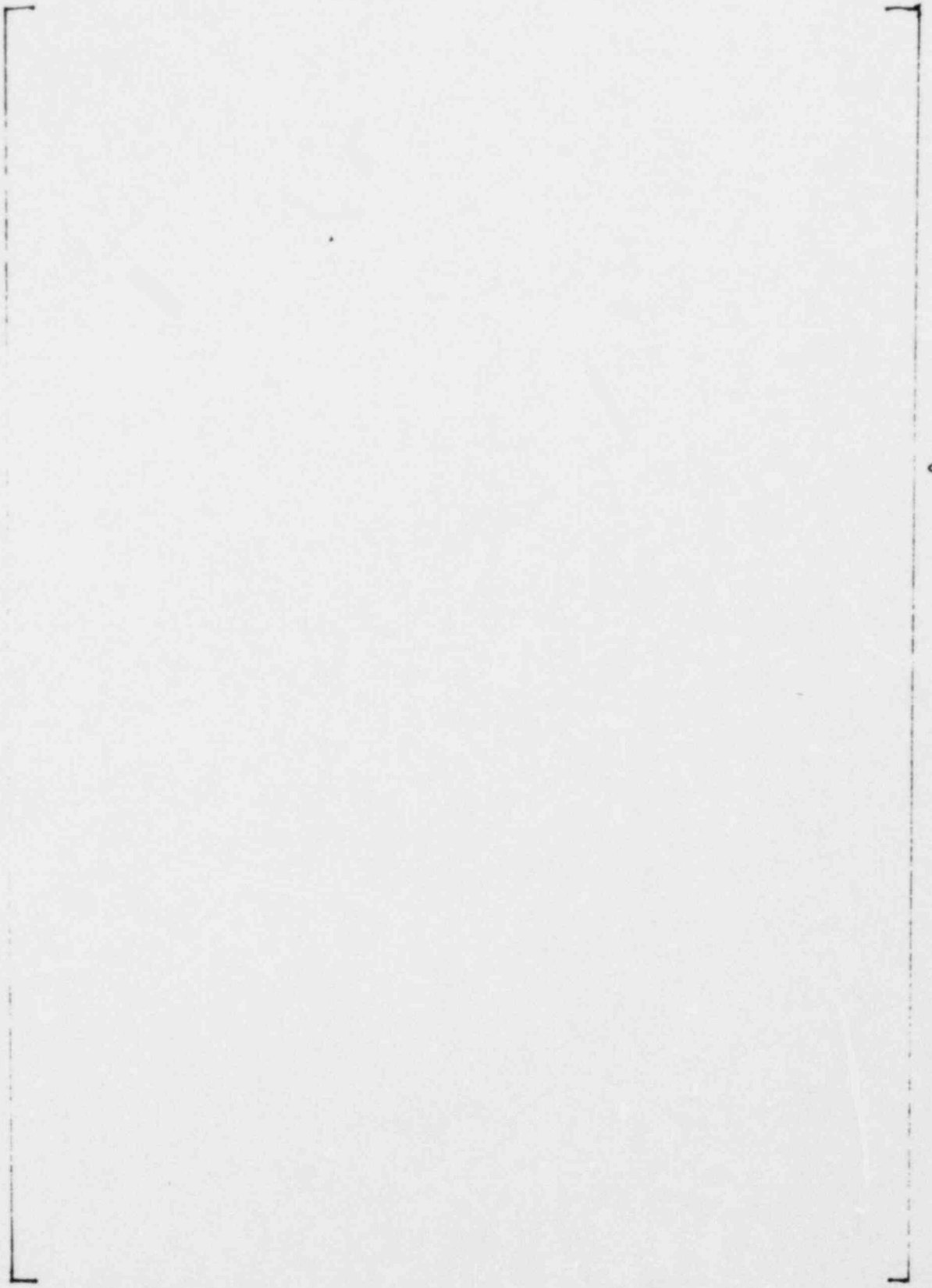

a,b,c,e

FIGURE 11.8-84, CASE NO.40, FLOW TEST TEMPERATURE RECORD VS. 100 TERMS OF FOURIER SERIES

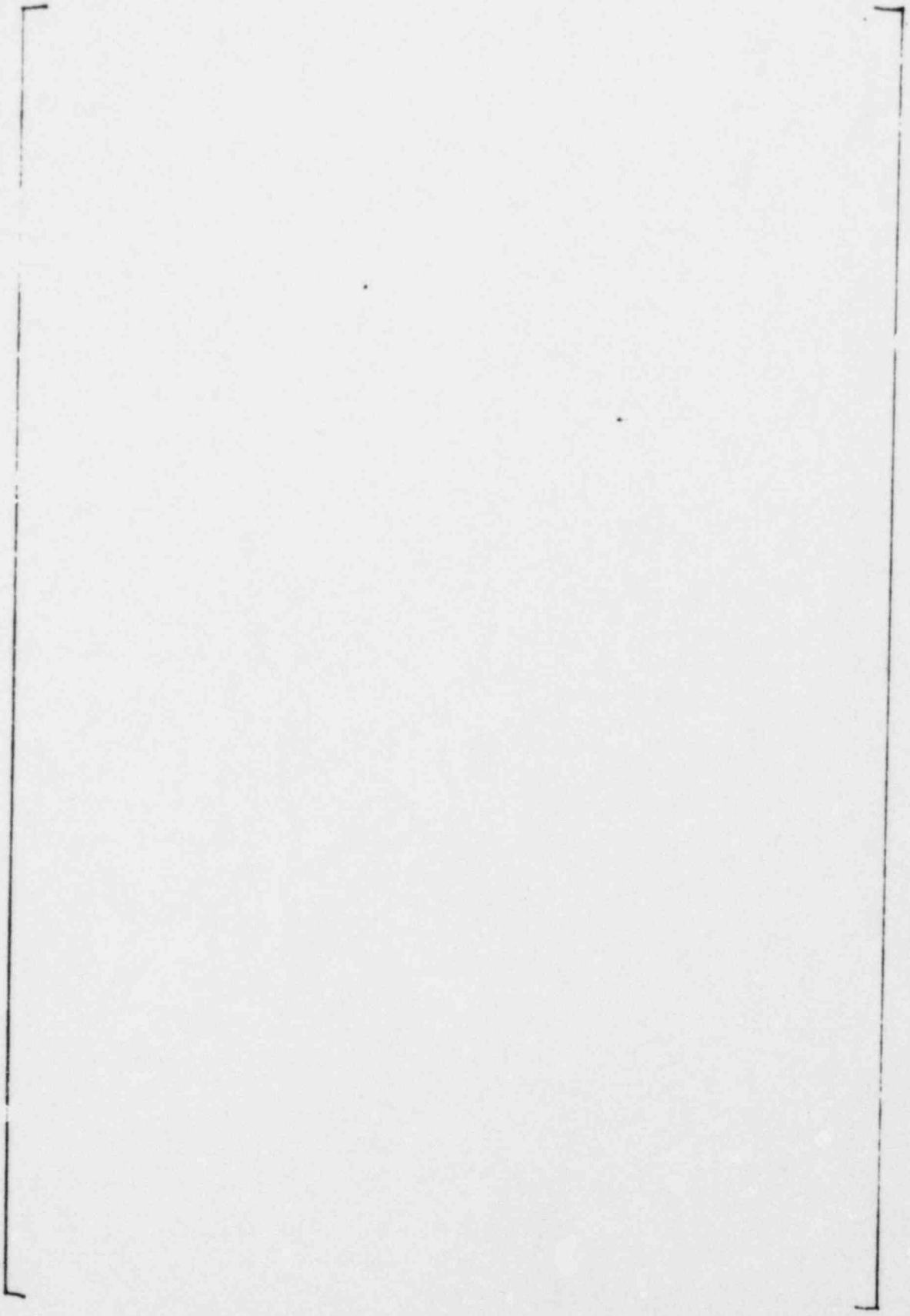

a.b.c.e

FIGURE 11.8-85, CASE NO.41, FLOW TEST TEMPERATURE RECORD VS. 100 TERMS OF FOURIER SERIES

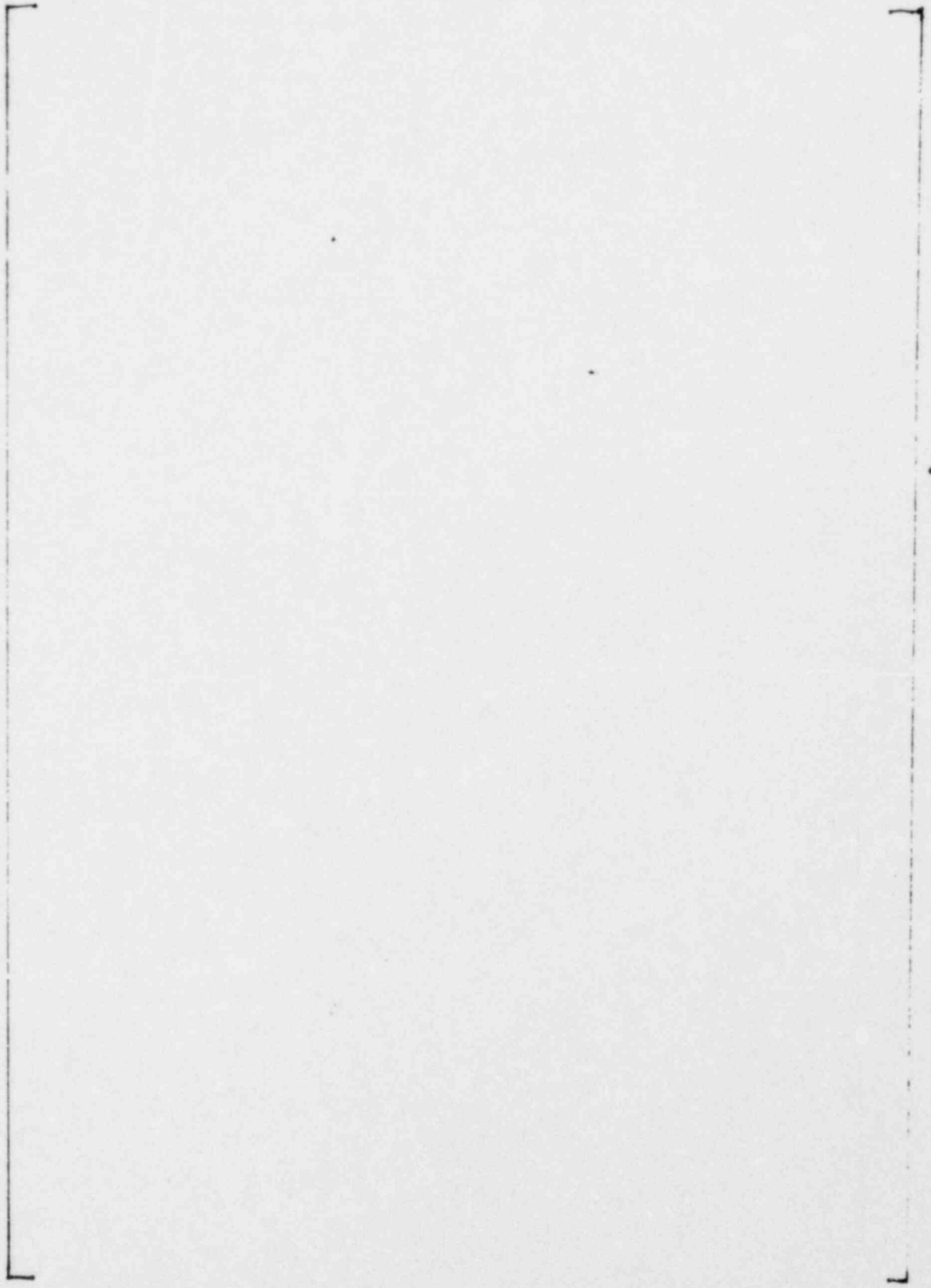

a,b,c,e

FIGURE 11.8-86, CASE NO.42, FLOW TEST TEMPERATURE RECORD VS. 100 TERMS OF FOURIER SERIES

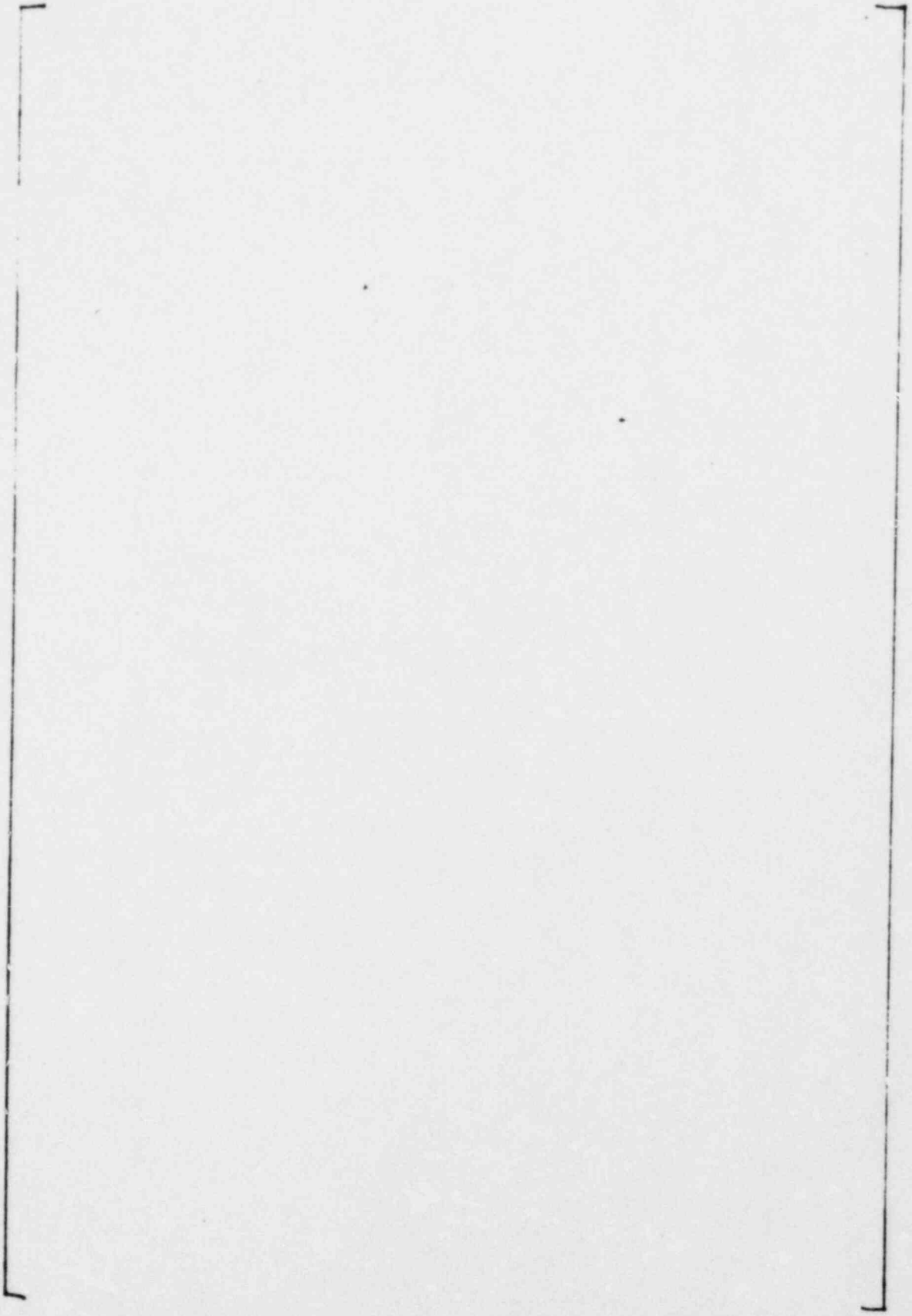

a.b.c.e

FIGURE 11.8-87, CASE NO.43, FLOW TEST TEMPERATURE RECORD VS. 100 TERMS OF FOURIER SERIES

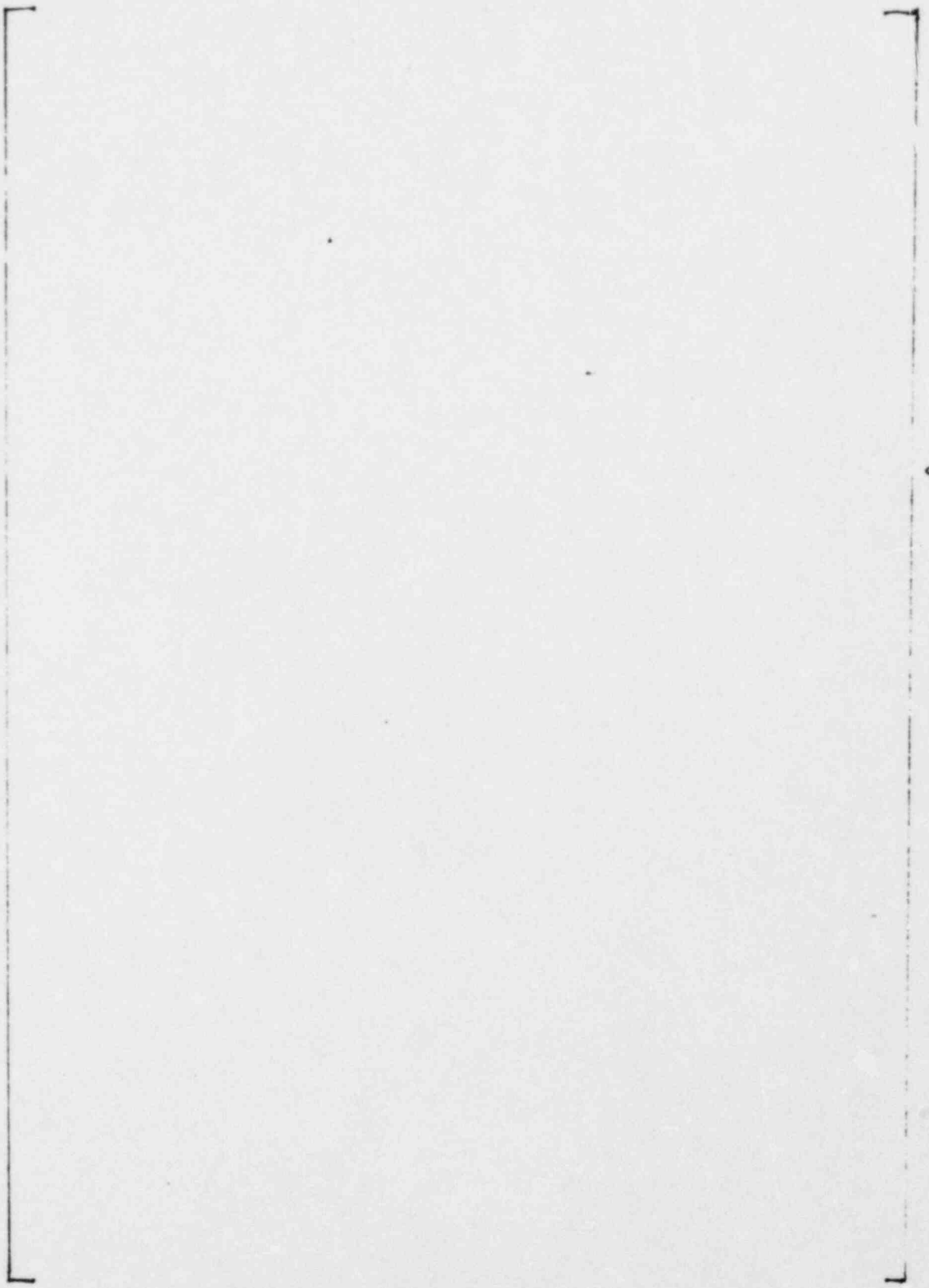

a,b,c,e

FIGURE 11.8-88, CASE NO.44, FLOW TEST TEMPERATURE RECORD VS. 100 TERMS OF FOURIER SERIES

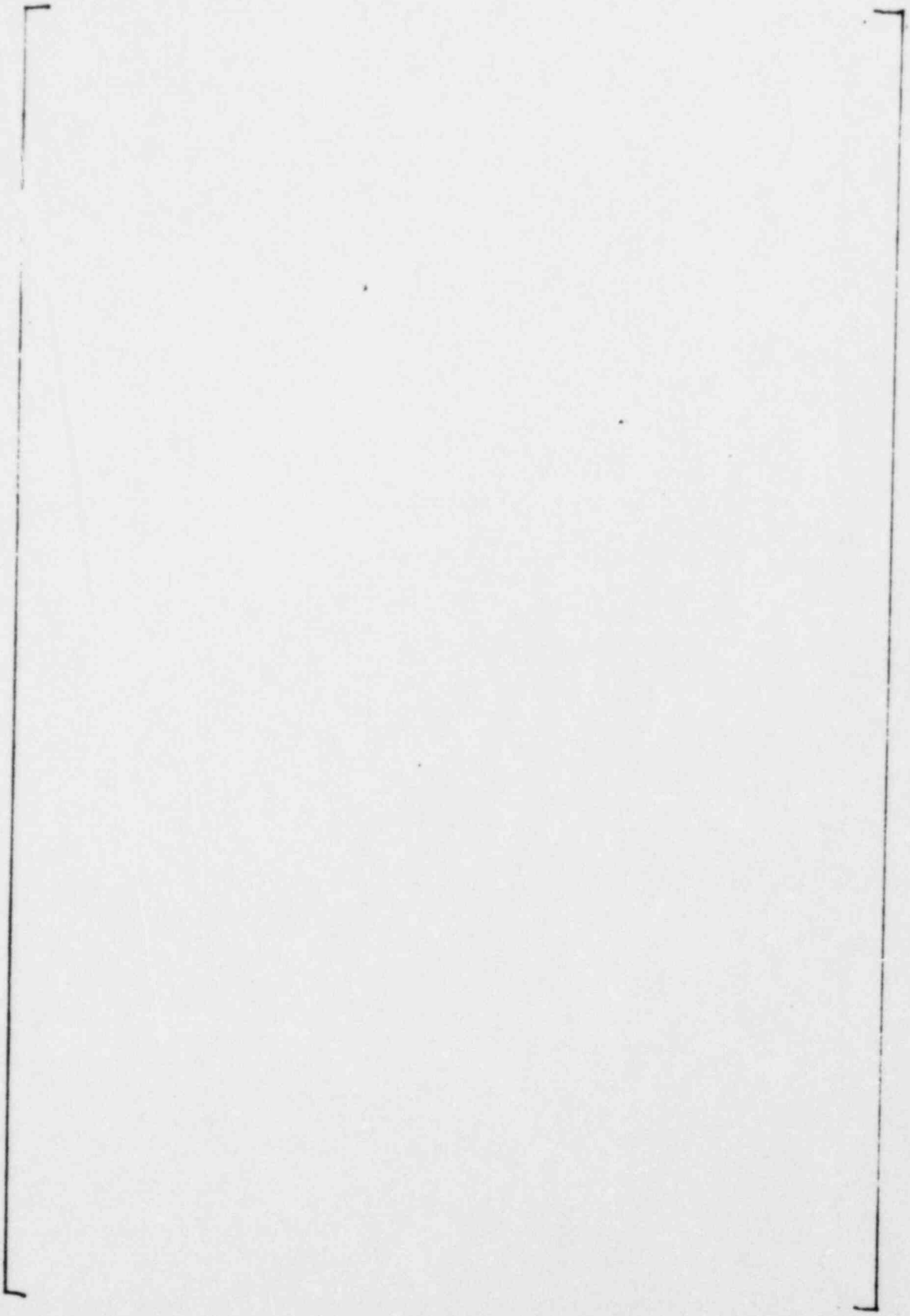

a,b,c,e

FIGURE 11.8-89: CASE NO. 1, THERMAL TEMPERATURE SOLUTION SCALED TO STEAM GENERATOR CONDITIONS

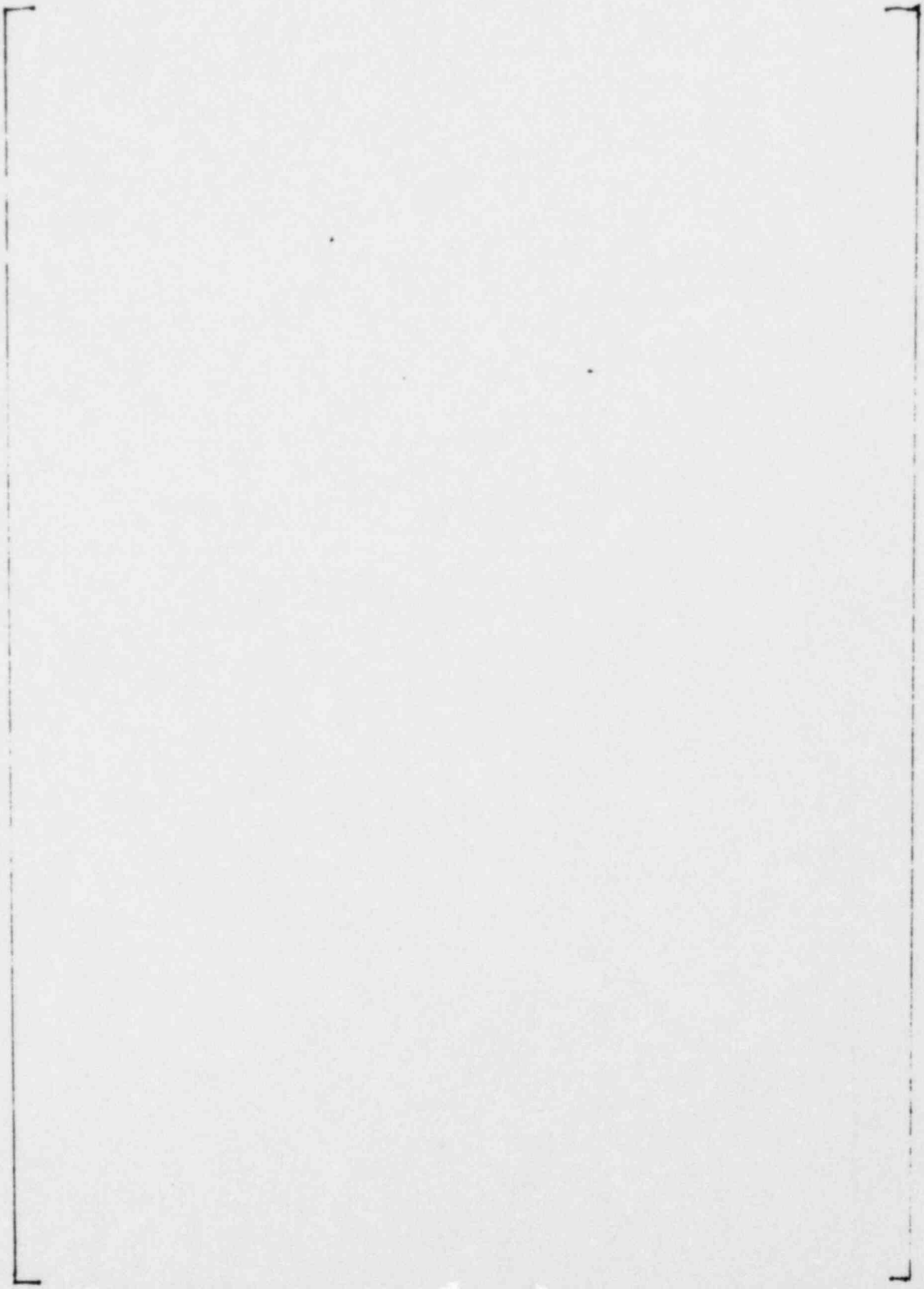

a,b,c,e

FIGURE 11.8-90: CASE NO. 2, TH[illegible]ERATURE SOLUTION SCALED TO STEAM GENERA[illegible]NS

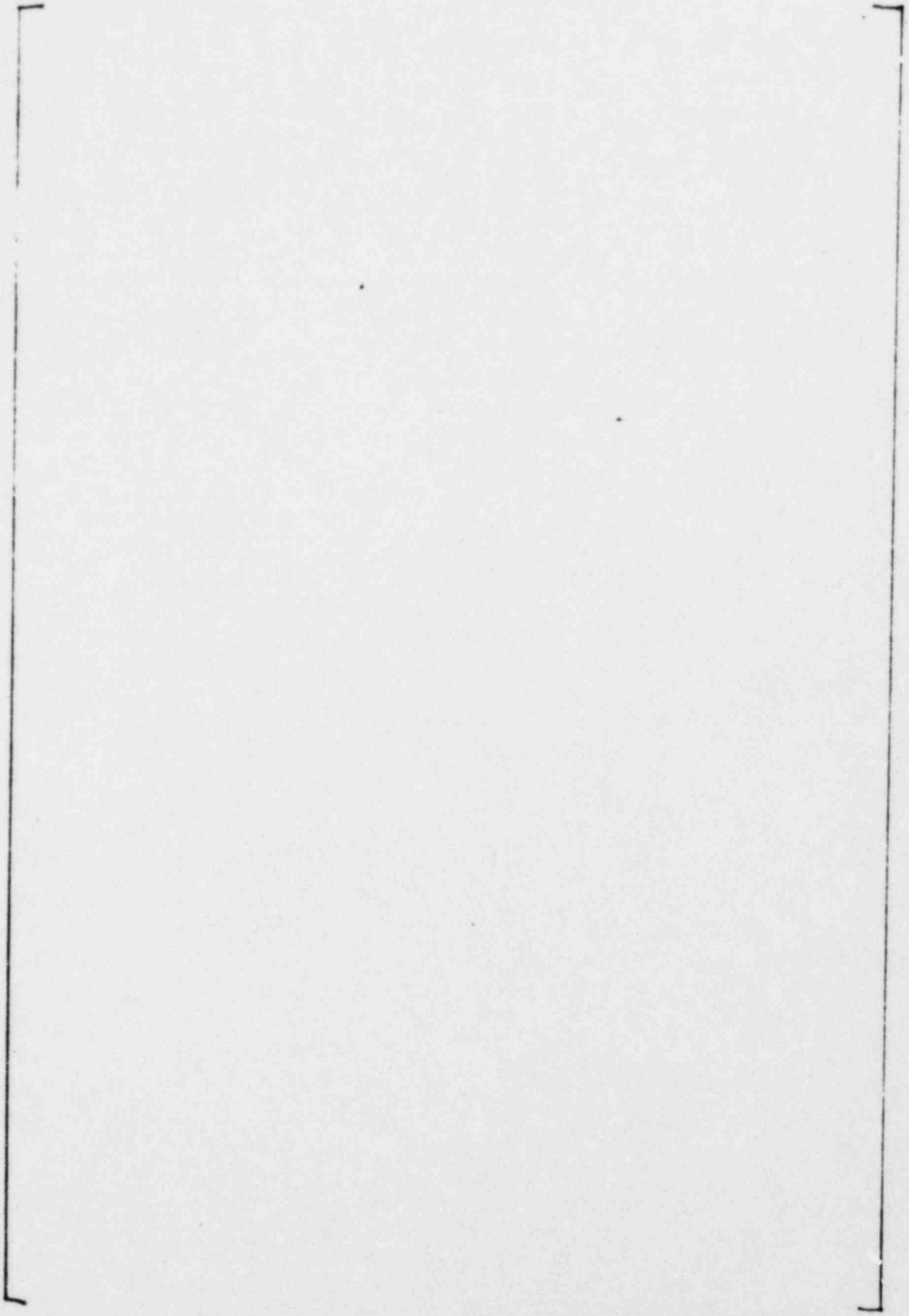

a,b,c,e

FIGURE 11.8-9?: CASE NO. 3, THERMAL TEMPERATURE SOLUTION SCALED TO STEAM GENERATOR CONDITIONS

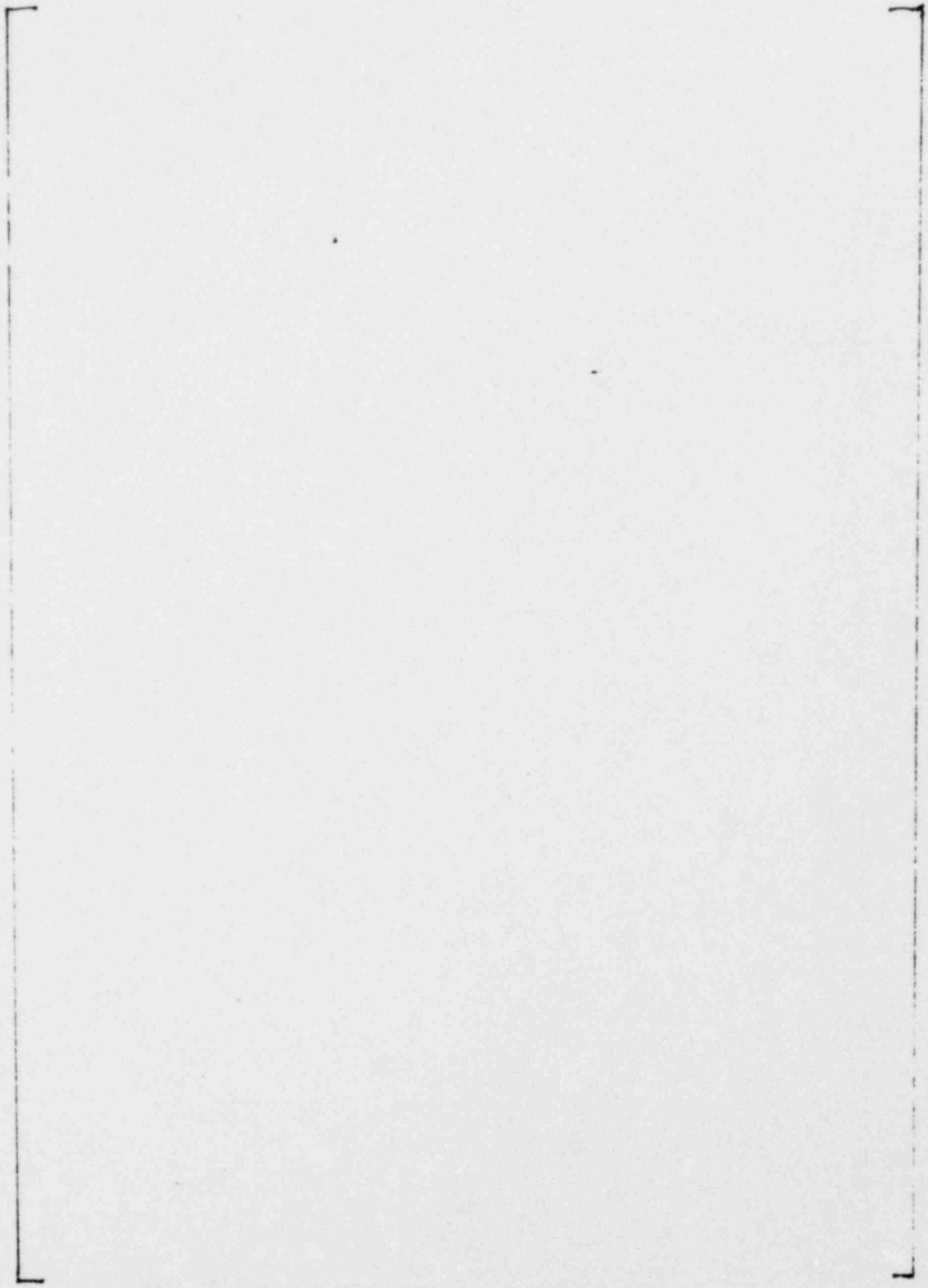

a,b,c,e

FIGURE 11.8-92: CASE NO. 4, THERMAL TEMPERATURE SOLUTION SCALED TO STEAM GENERATOR CONDITIONS

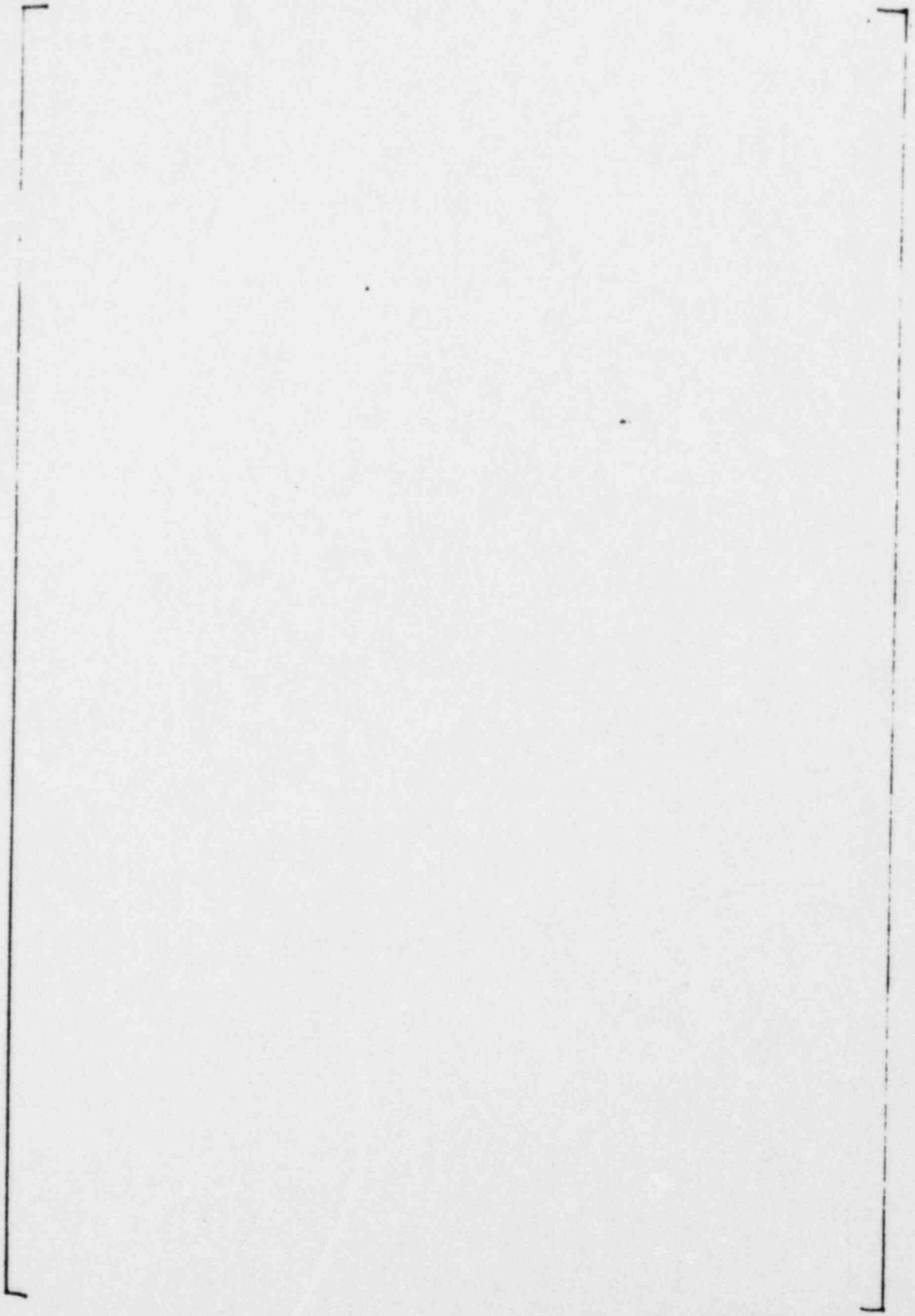

a,b,c,e

FIGURE 11.8-93: CASE NO. 5, THERMAL TEMPERATURE SOLUTION SCALED TO STEAM GENERATOR CONDITIONS

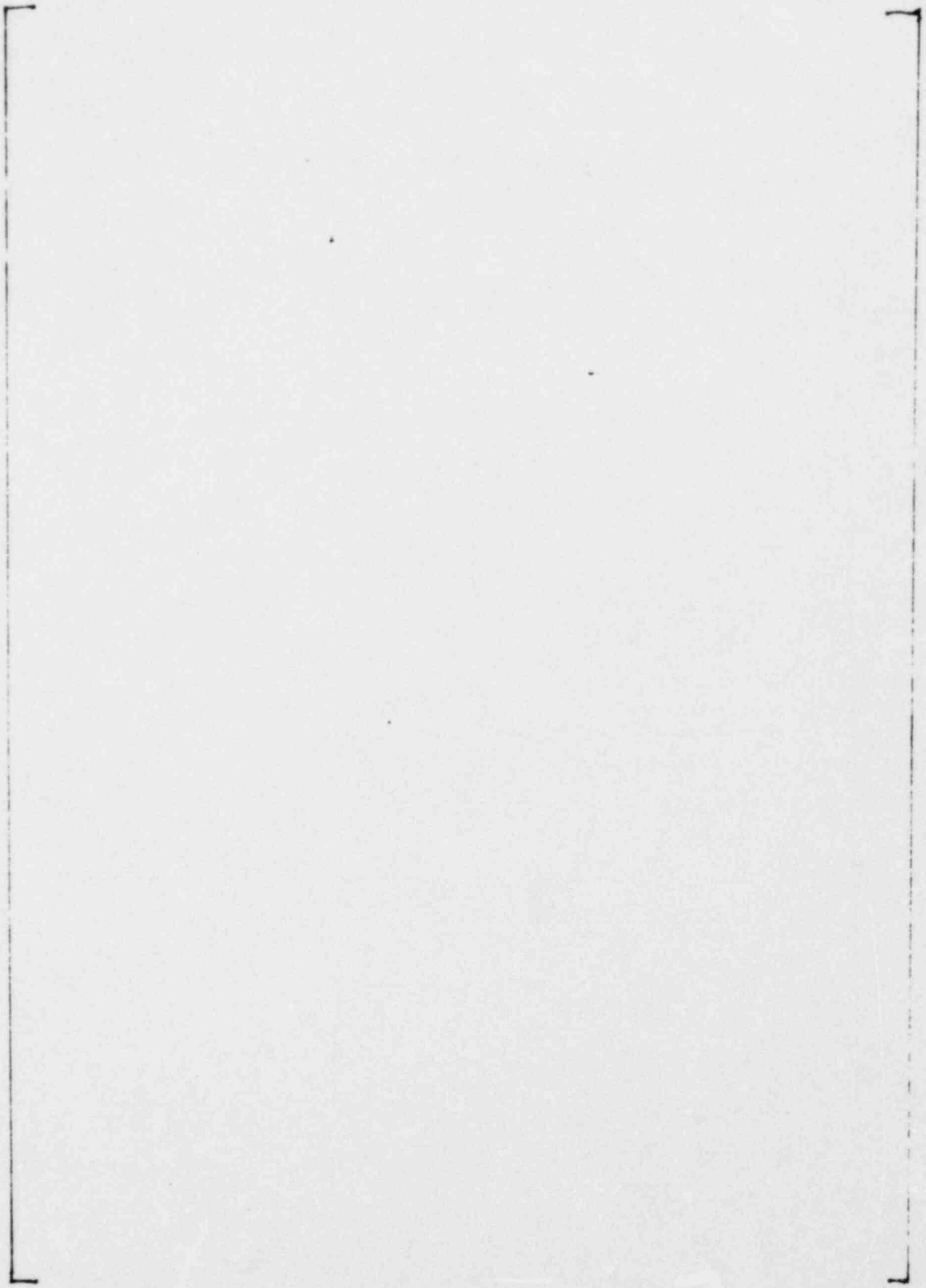

a,b,c,e

FIGURE 11.8-94: CASE NO. 6, THERMAL TEMPERATURE SOLUTION SCALED TO STEAM GENERATOR CONDITIONS

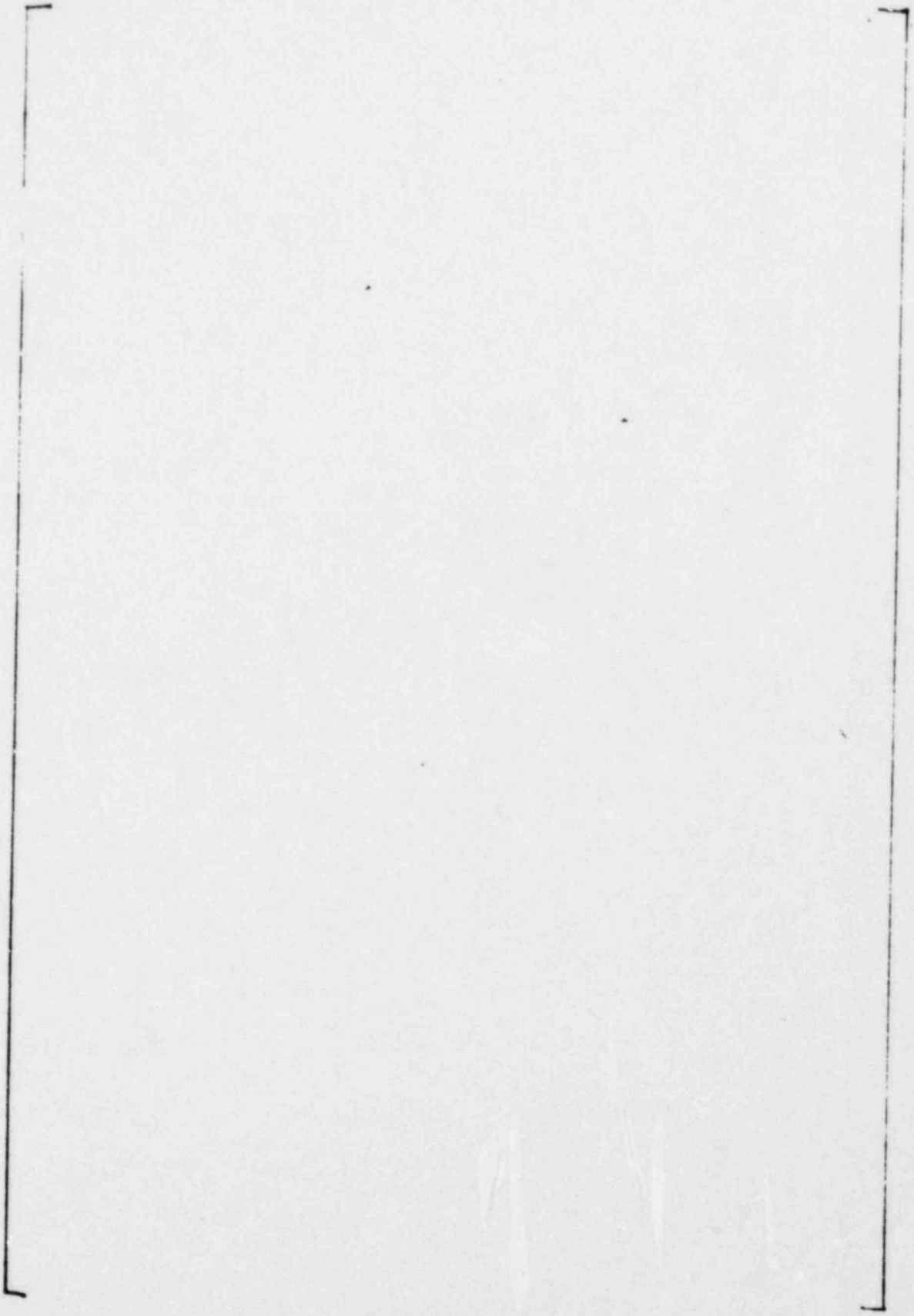

a.b.c.e

FIGURE 11.8-95: CASE NO. 7, THERMAL TEMPERATURE SOLUTION SCALED TO STEAM GENERATOR CONDITIONS

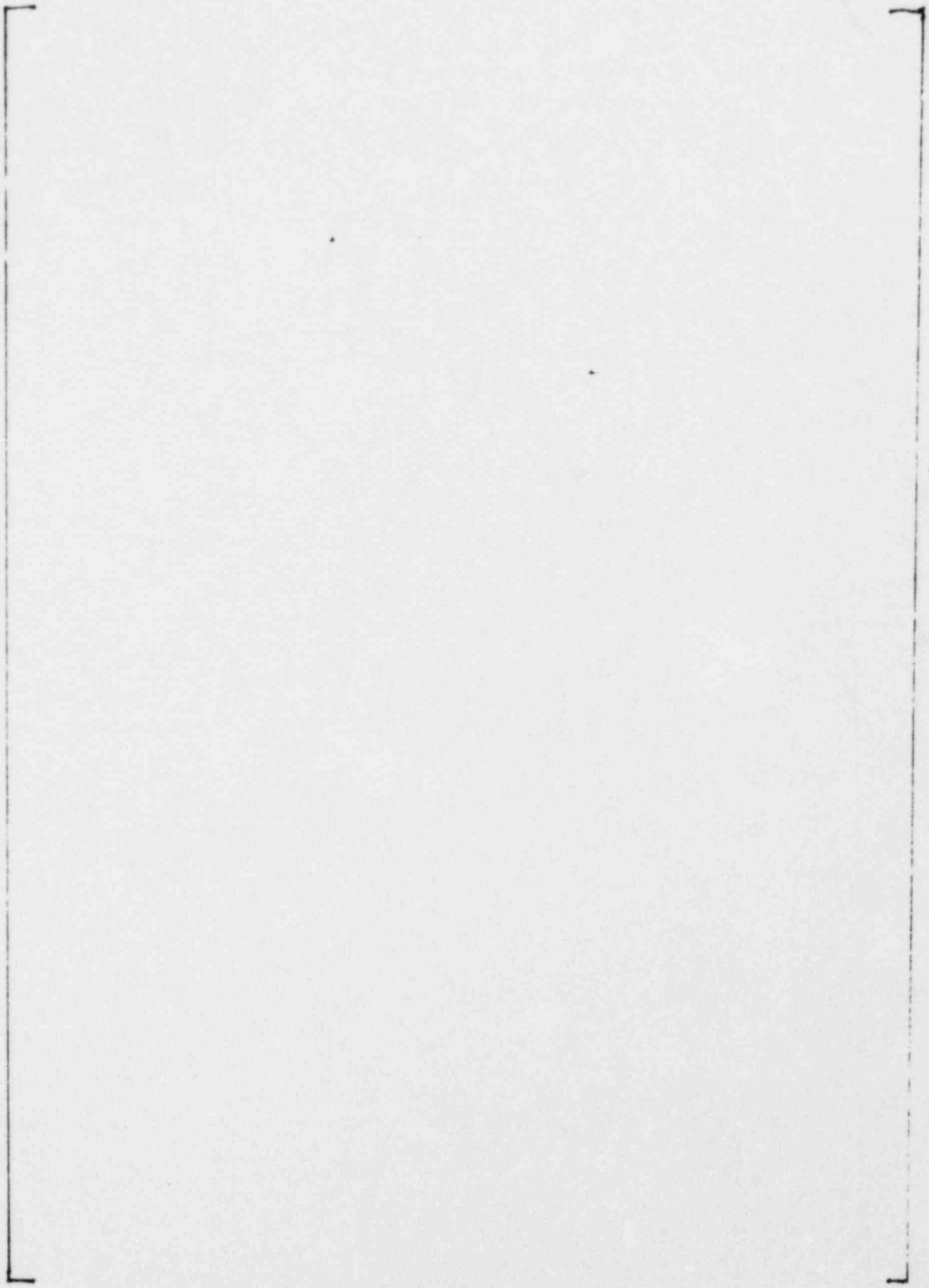

a,b,c,e

FIGURE 11.8-96: CASE NO. 8, THERMAL TEMPERATURE SOLUTION SCALED TO STEAM GENERATOR CONDITIONS

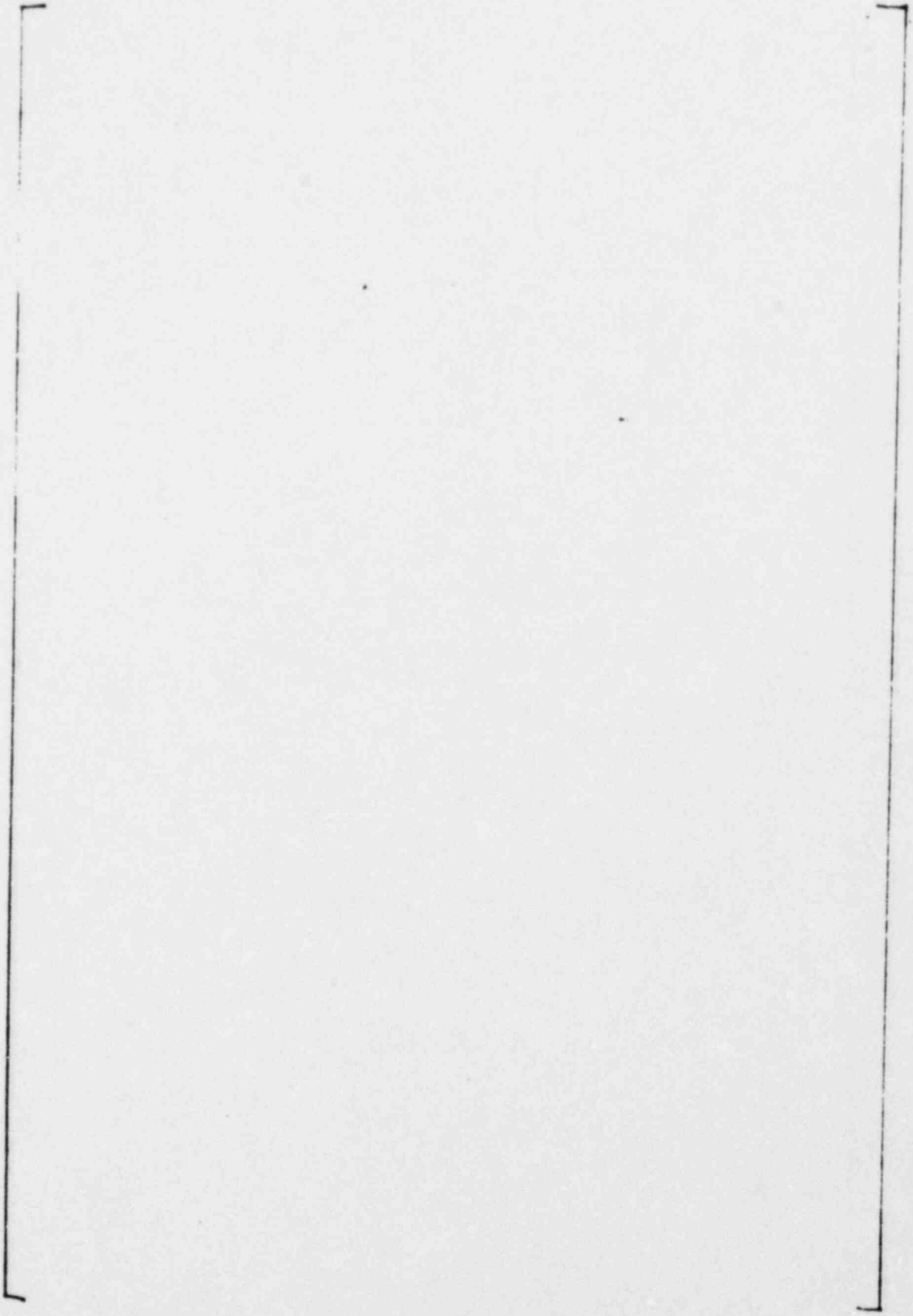

a,b,c,e

FIGURE 11.8-97: CASE NO. 9, THERMAL TEMPERATURE SOLUTION SCALED TO STEAM GENERATOR CONDITIONS

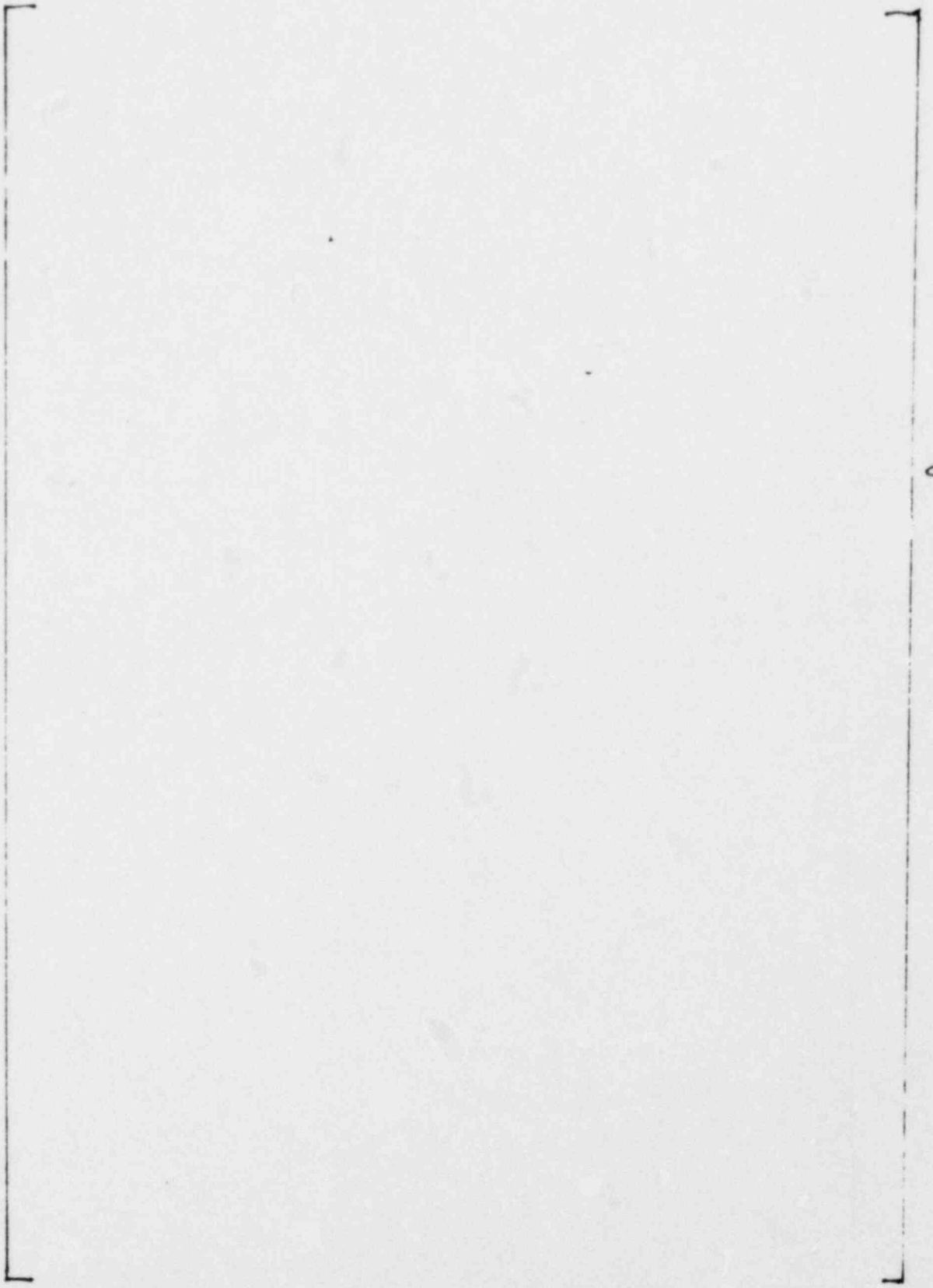

a,b,c,e

FIGURE 11.8-98: CASE NO.10, THERMAL TEMPERATURE SOLUTION SCALED TO STEAM GENERATOR CONDITIONS

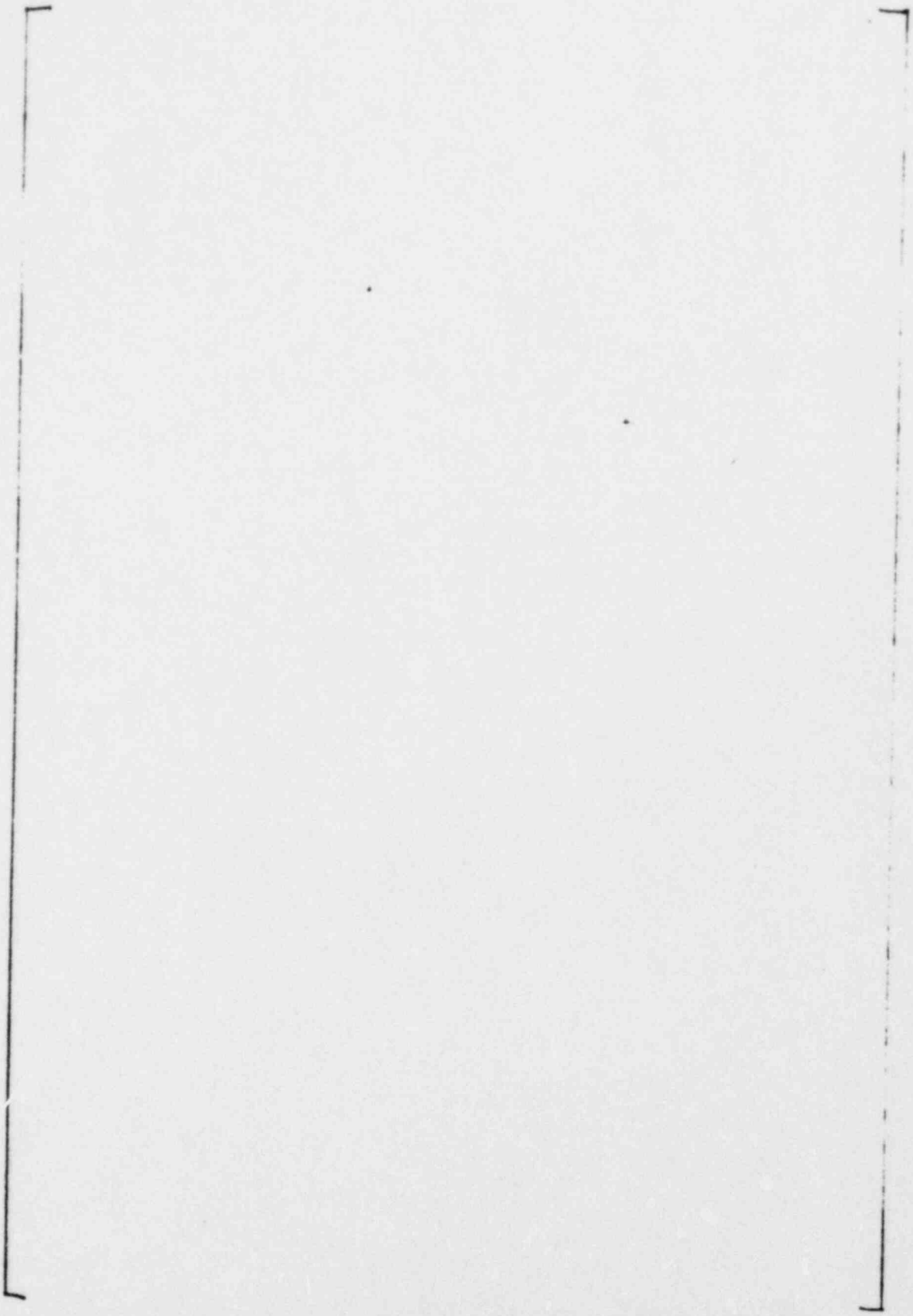

a,b,c,e

FIGURE 11.8-99: CASE NO.11, THERMAL TEMPERATURE SOLUTION SCALED TO STEAM GENERATOR CONDITIONS

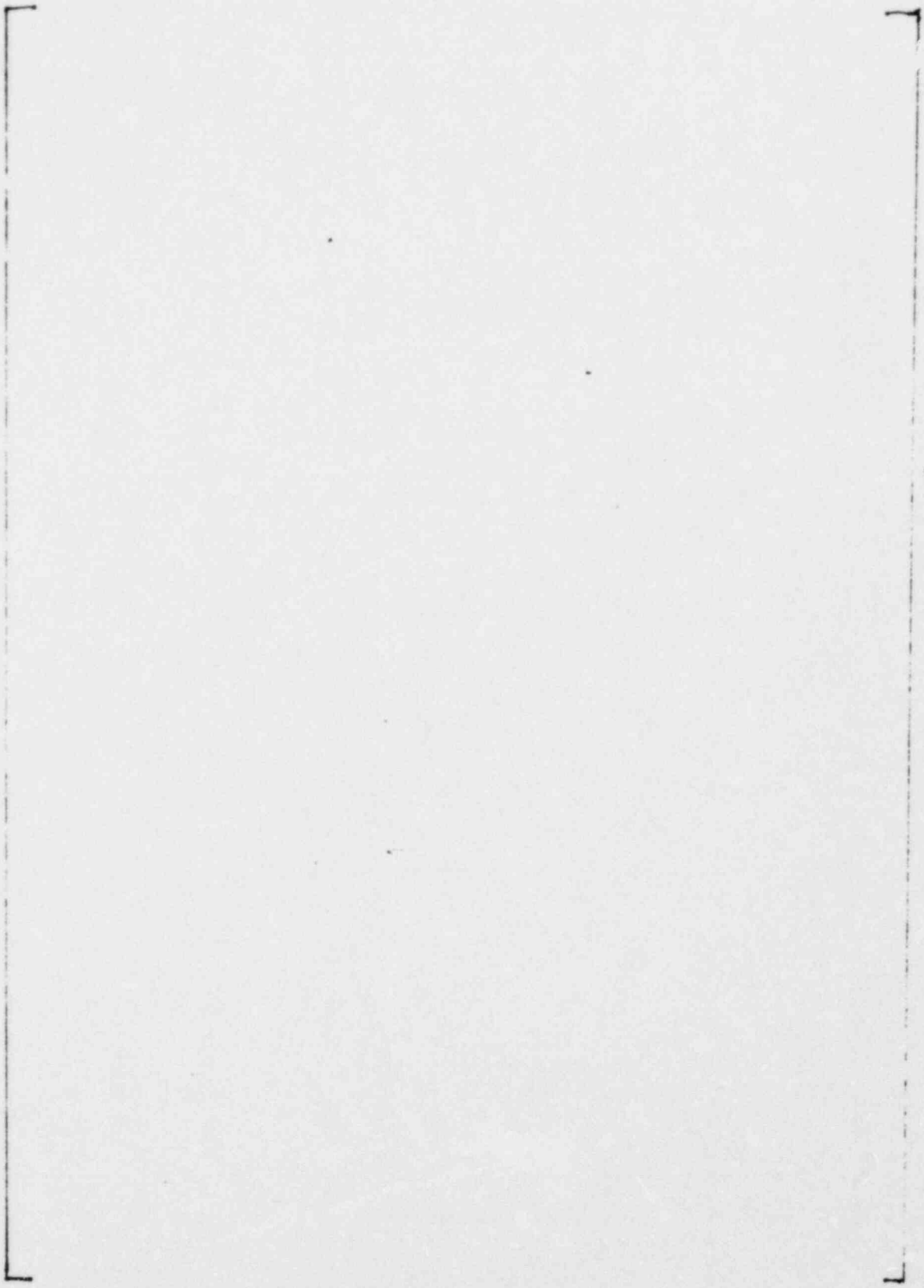

a,b,c,e

FIGURE 11.8-100: CASE NO.12, THERMAL TEMPERATURE SOLUTION SCALED TO STEAM GENERATOR CONDITIONS

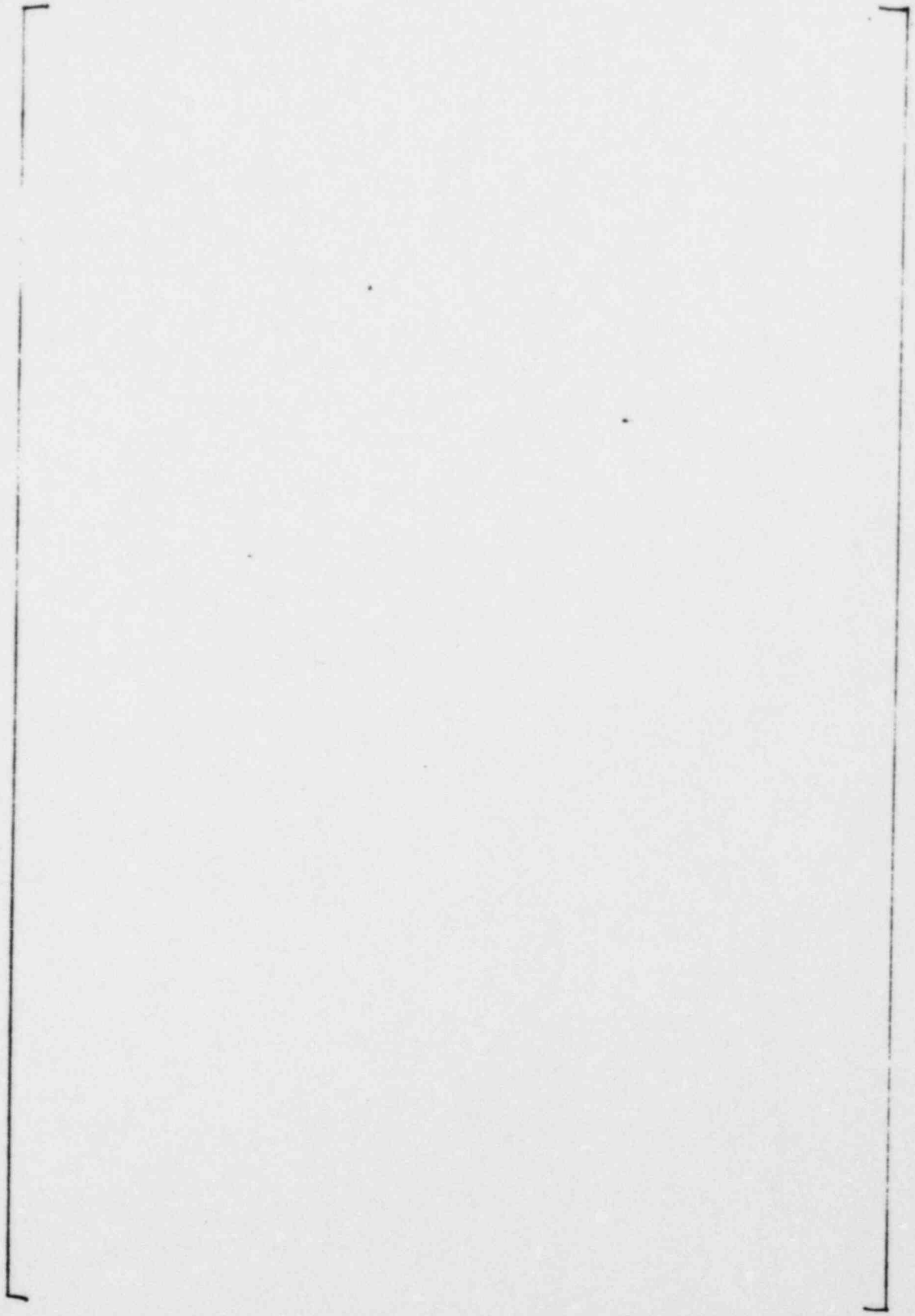

a,b,c,e

FIGURE 11.8-101: CASE NO.13, THERMAL TEMPERATURE SOLUTION SCALED TO STEAM GENERATOR CONDITIONS

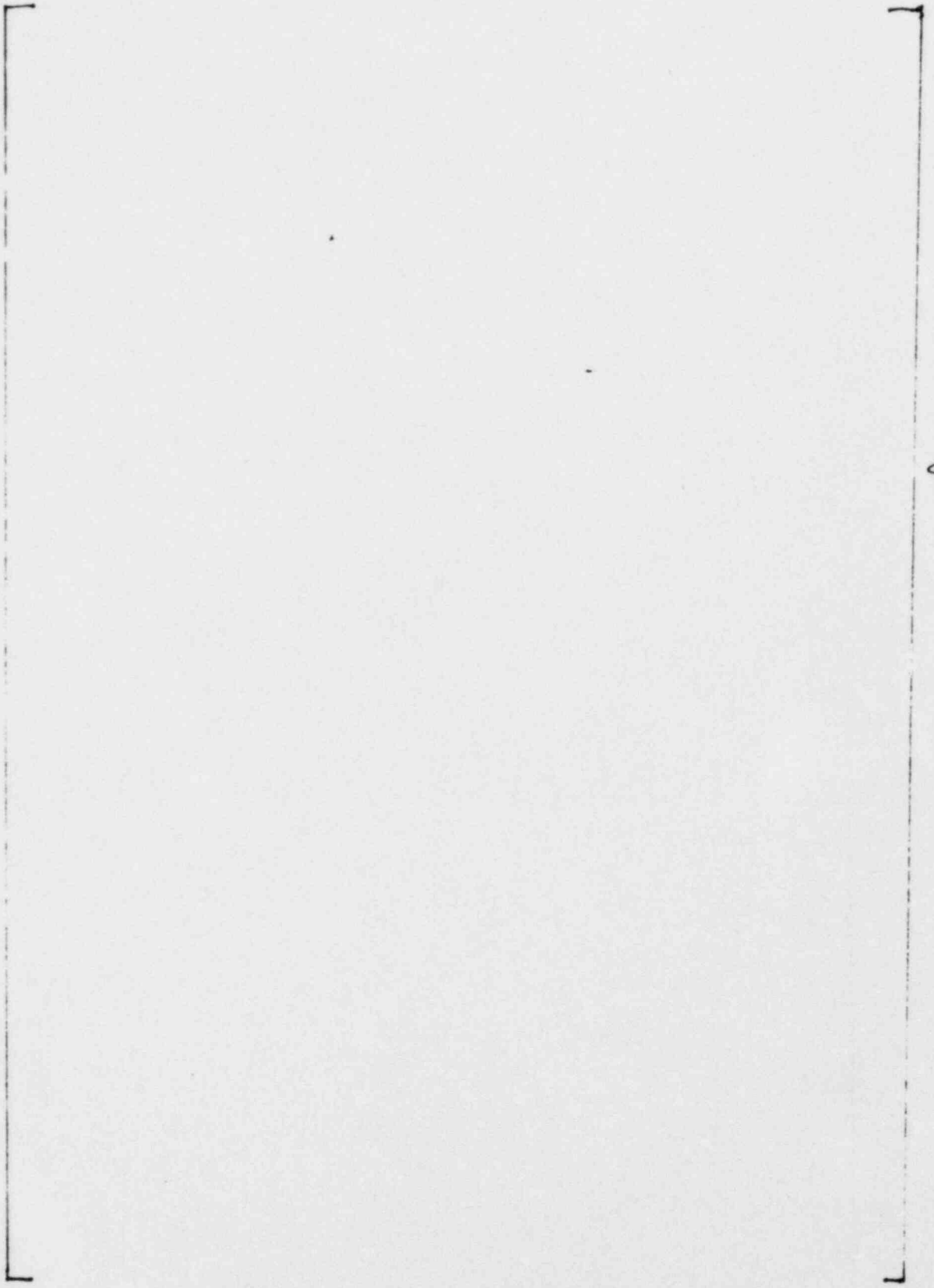

a,b,c,e

FIGURE 11.8-102: CASE NO.14, THERMAL TEMPERATURE SOLUTION SCALED TO STEAM GENERATOR CONDITIONS

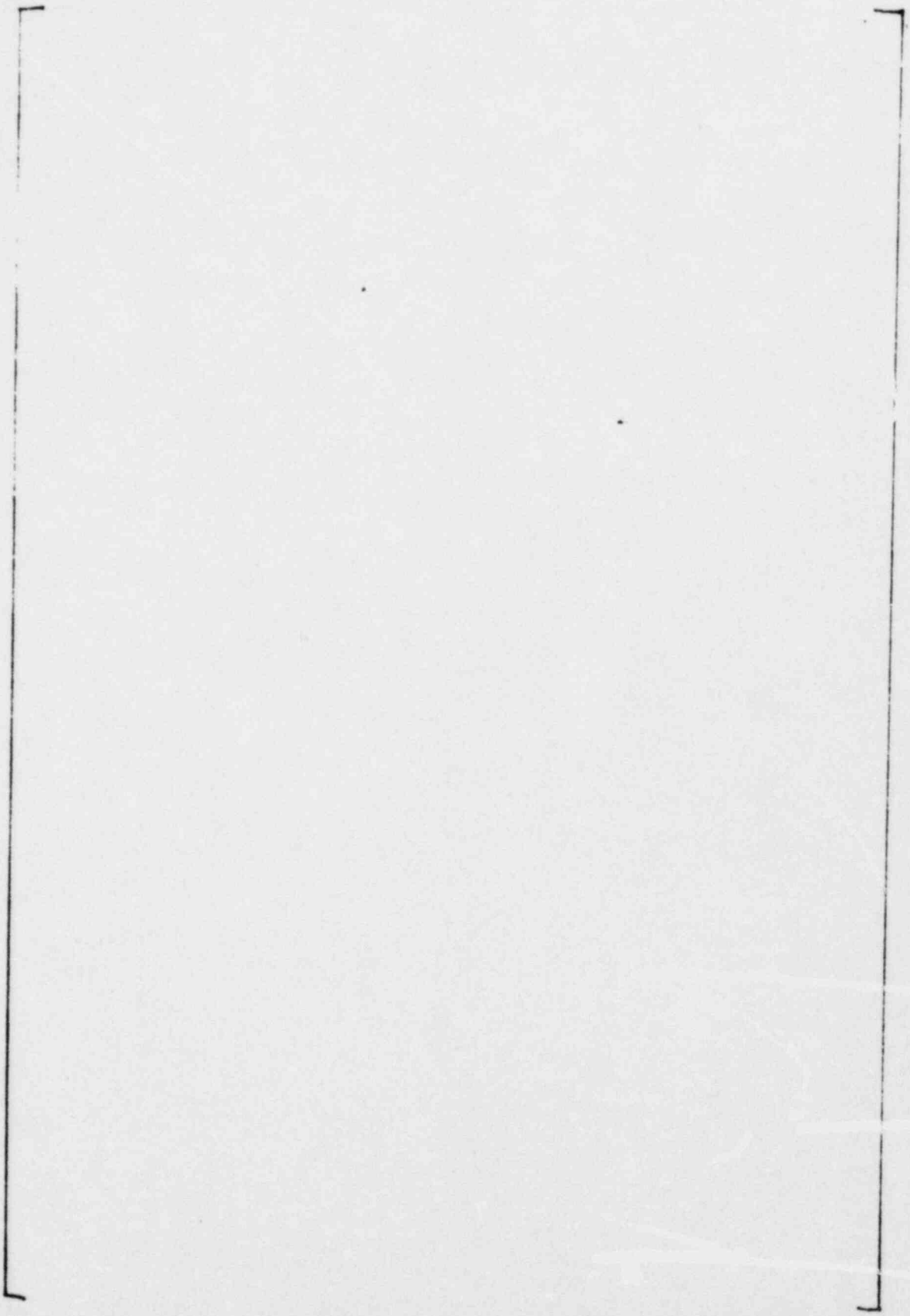

a.b.c.e

FIGURE 11.8-103: CASE NO.15, THERMAL TEMPERATURE SOLUTION SCALED TO STEAM GENERATOR CONDITIONS

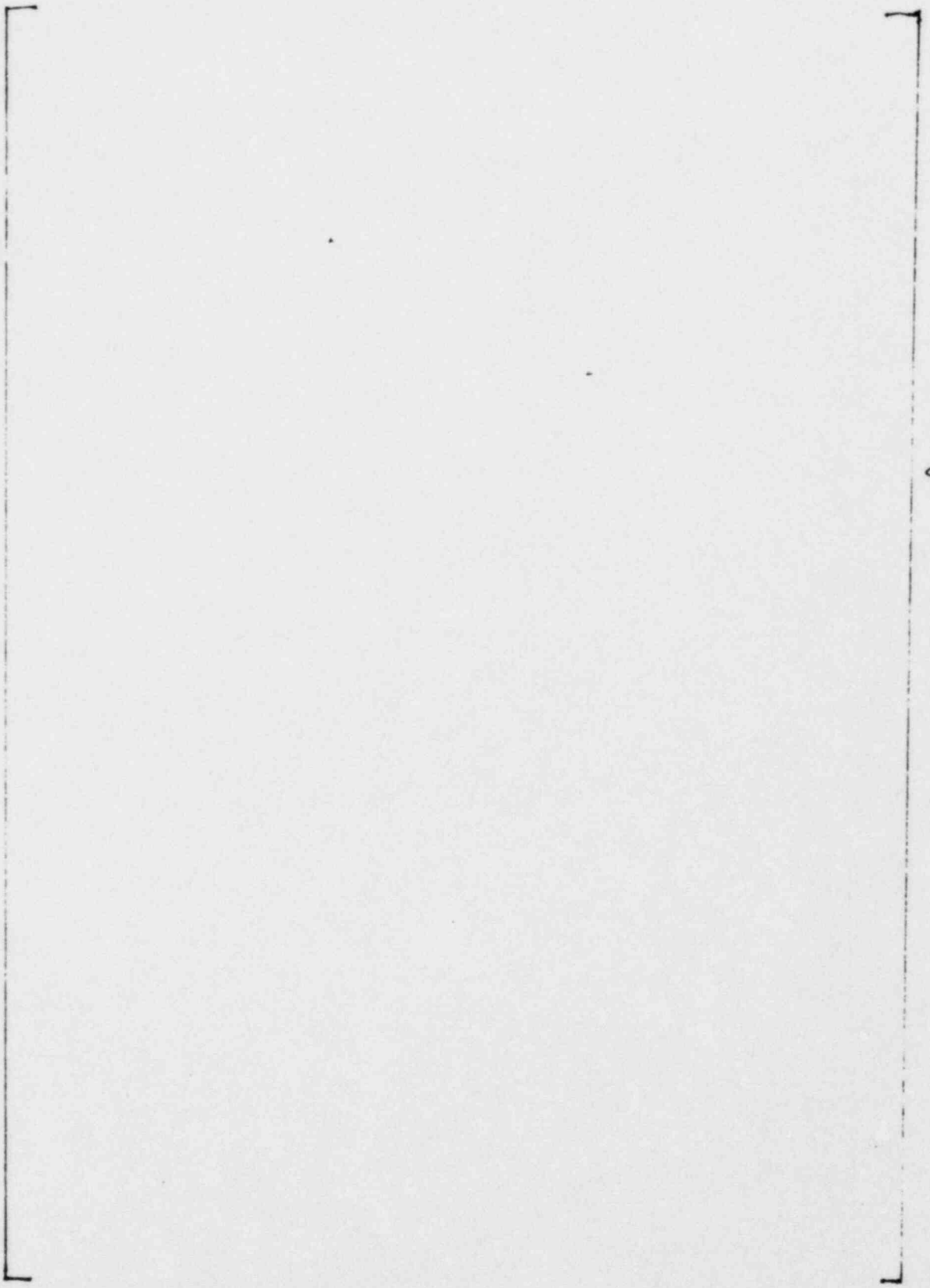

a,b,c,e

FIGURE 11.8-104: CASE No.16, THERMAL TEMPERATURE SOLUTION SCALED TO STEAM GENERATOR CONDITIONS

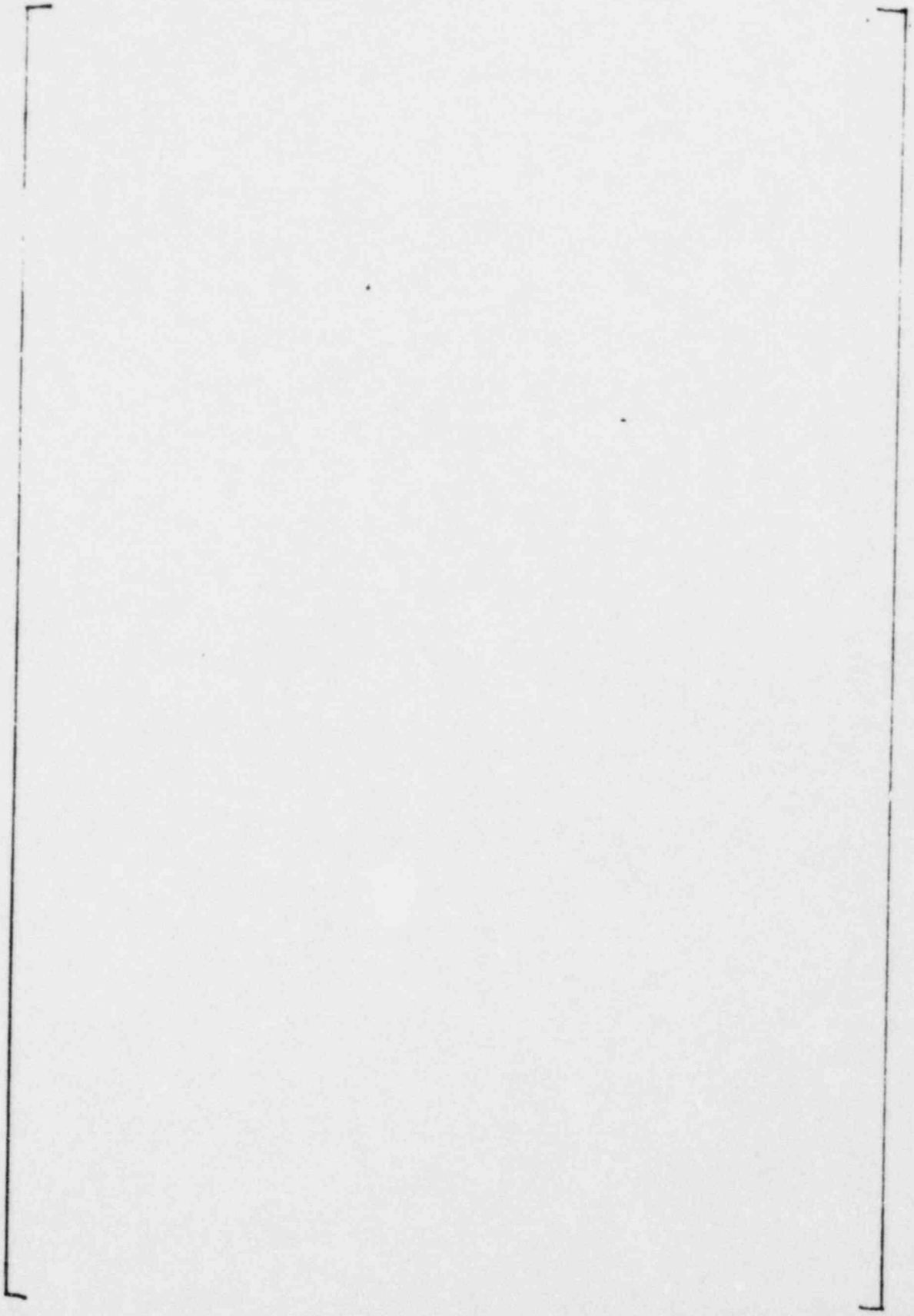

a,b,c,e

FIGURE 11.8-105: CASE NO.17, THERMAL TEMPERATURE SOLUTION SCALED TO STEAM GENERATOR CONDITIONS

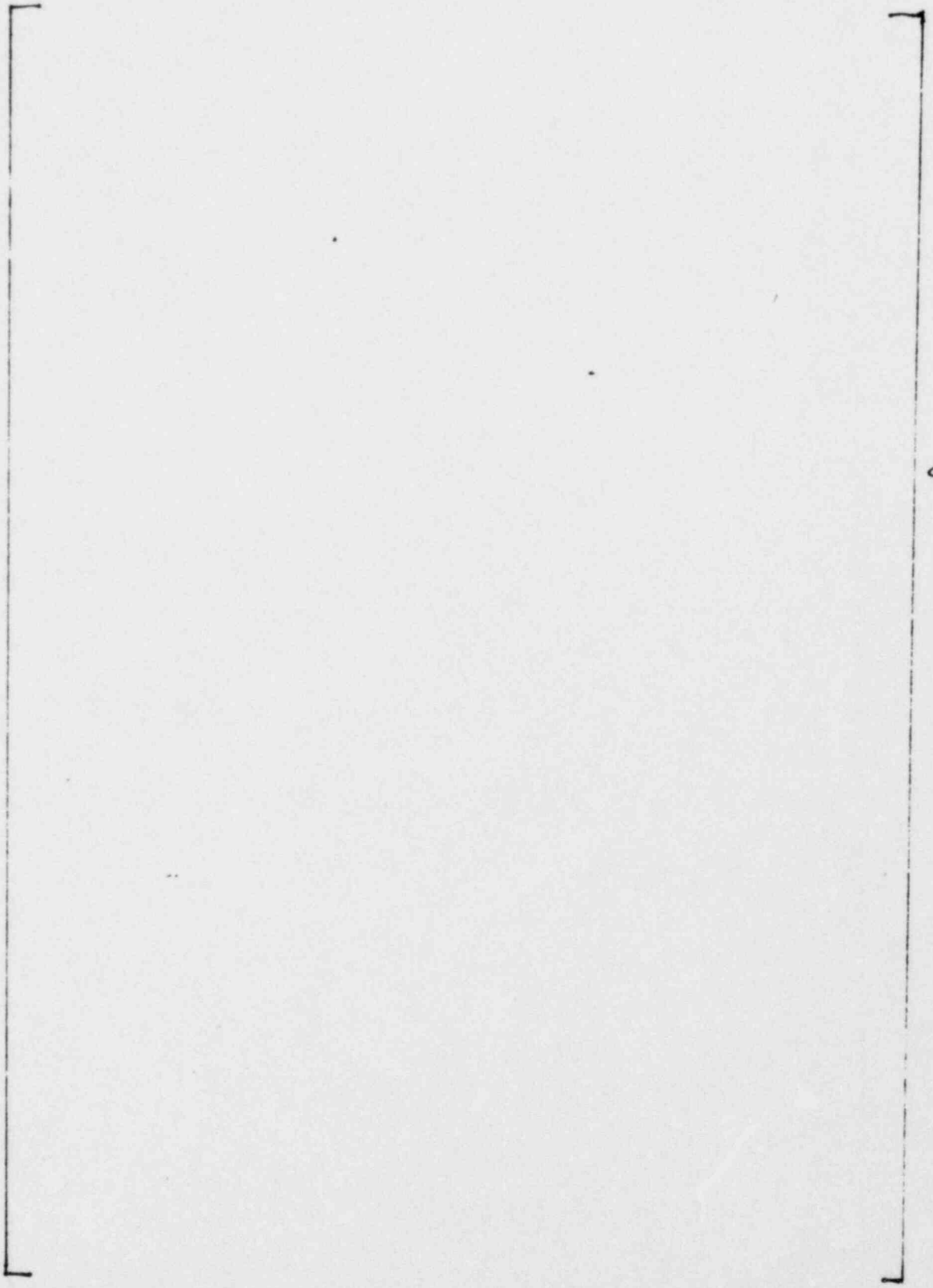

a,b,c,e

FIGURE 11.8-106: CASE NO.18, THERMAL TEMPERATURE SOLUTION SCALED TO STEAM GENERATOR CONDITIONS

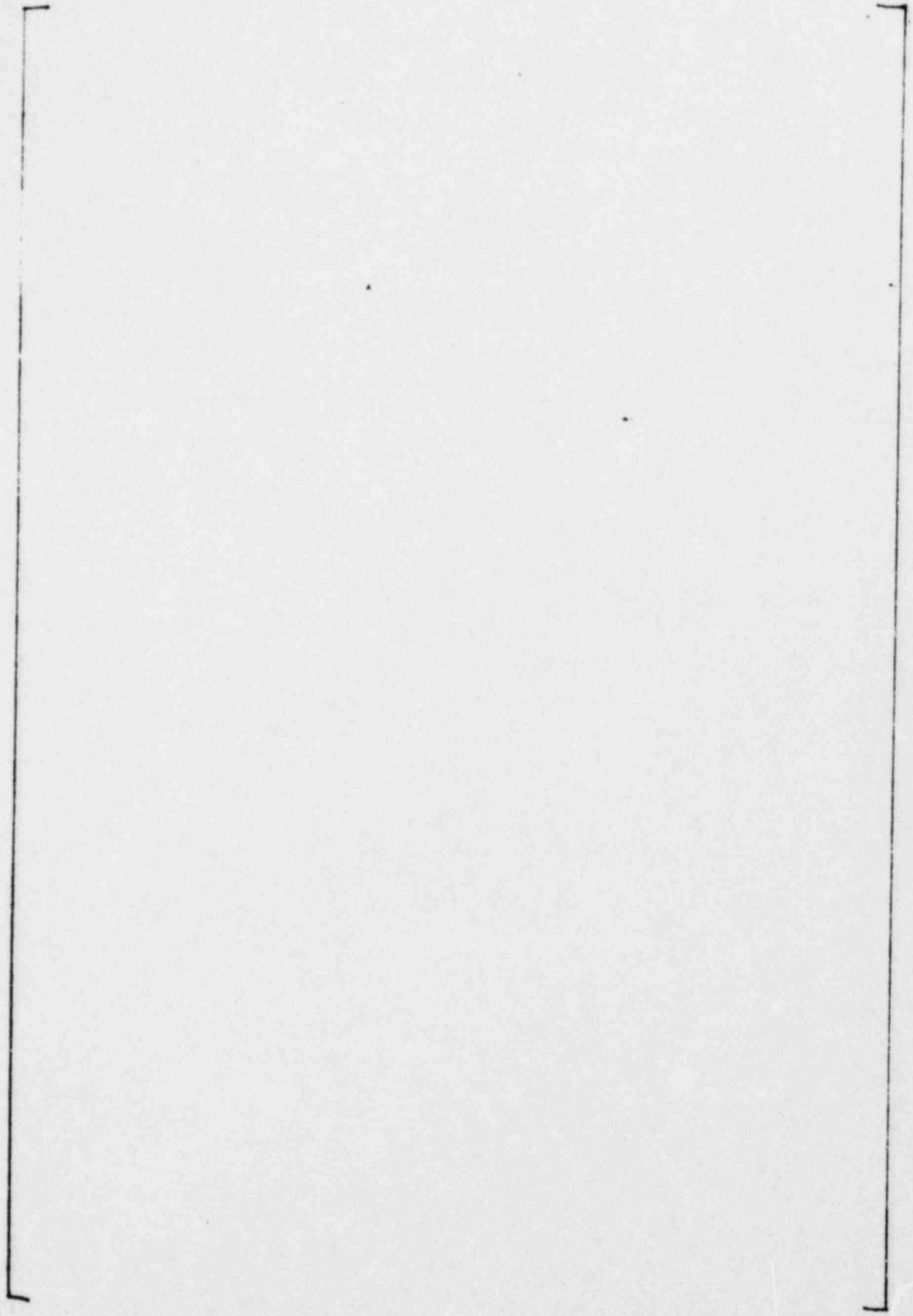

a,b,c,e

FIGURE 11.8-107: CASE NO.19, THERMAL TEMPERATURE SOLUTION SCALED TO STEAM GENERATOR CONDITIONS

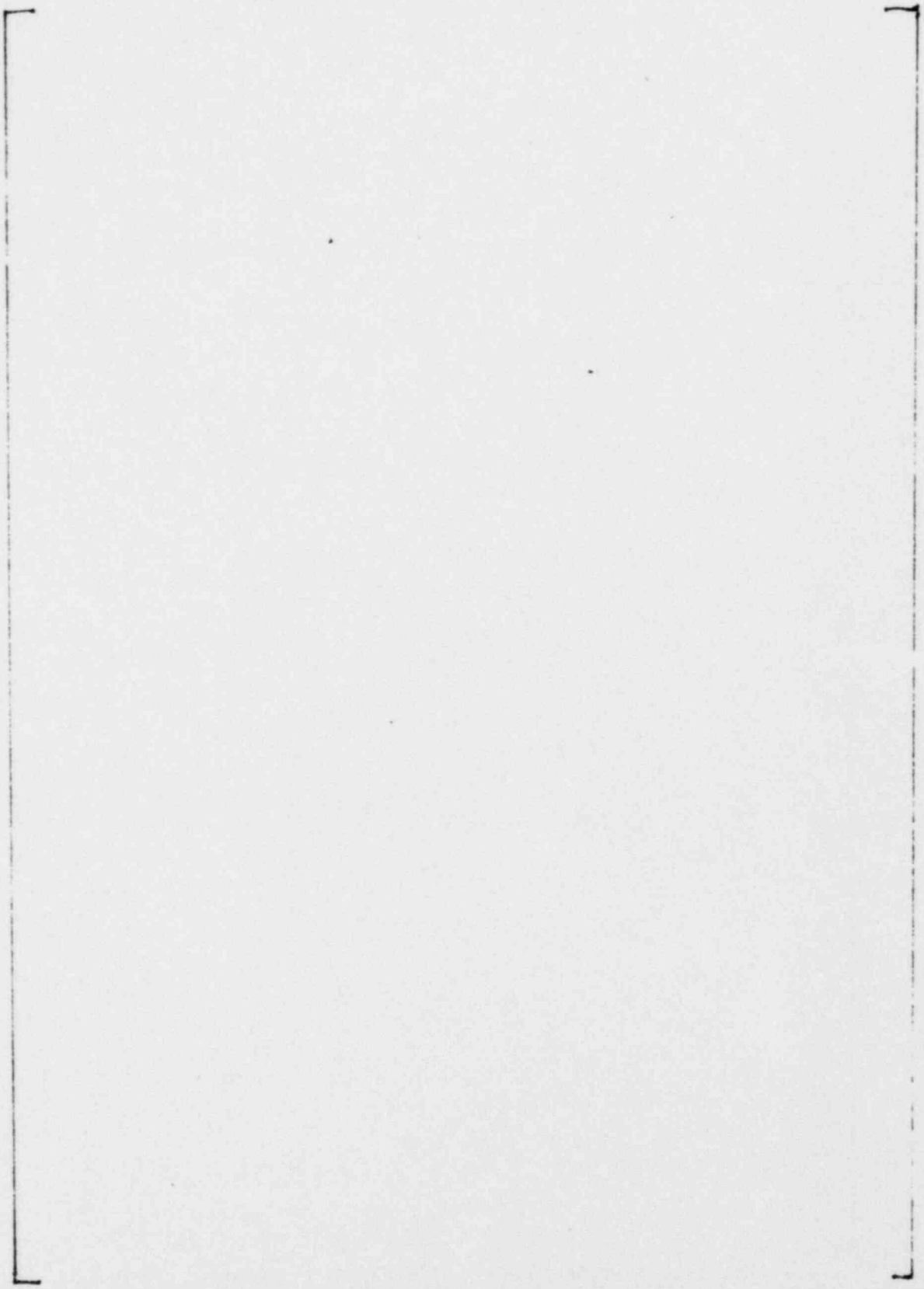

a,b,c,e

FIGURE 11.8-108: CASE NO.20, THERMAL TEMPERATURE SOLUTION SCALED TO STEAM GENERATOR CONDITIONS

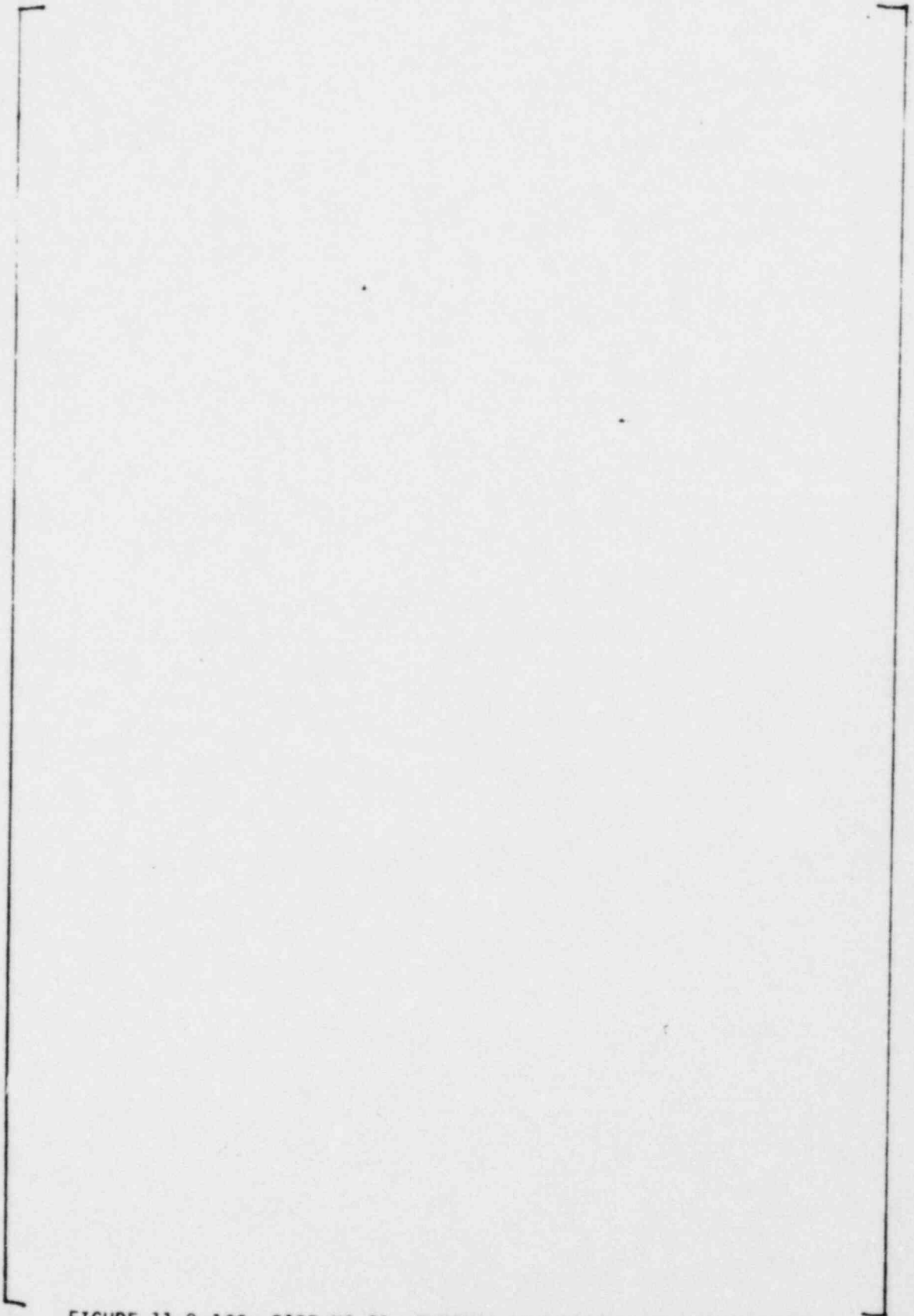

a.b.c.e

FIGURE 11.8-109: CASE NO.21, THERMAL TEMPERATURE SOLUTION SCALED TO STEAM GENERATOR CONDITIONS

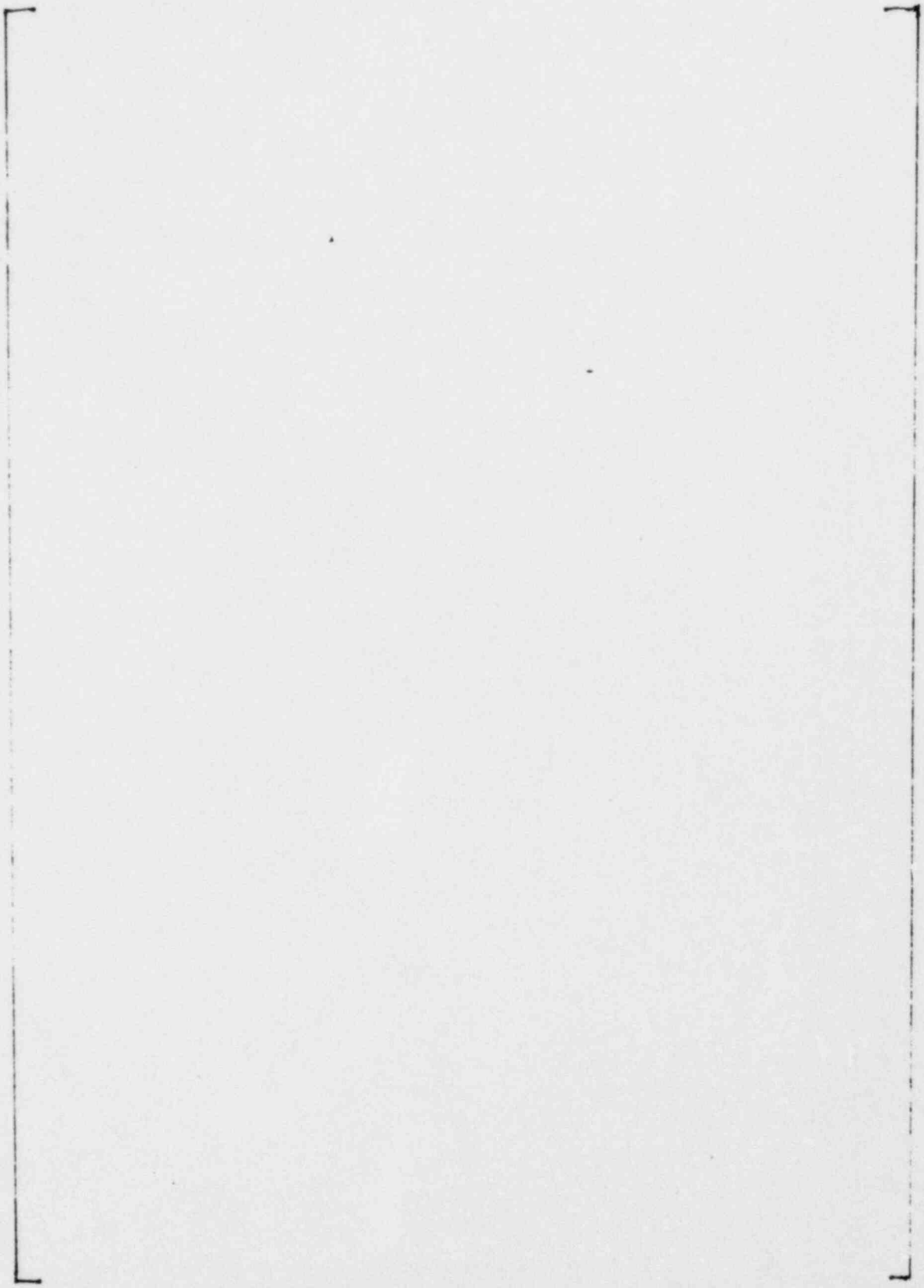

a,b,c,e

FIGURE 11.8-110: CASE NO.22, THERMAL TEMPERATURE SOLUTION SCALED TO STEAM GENERATOR CONDITIONS

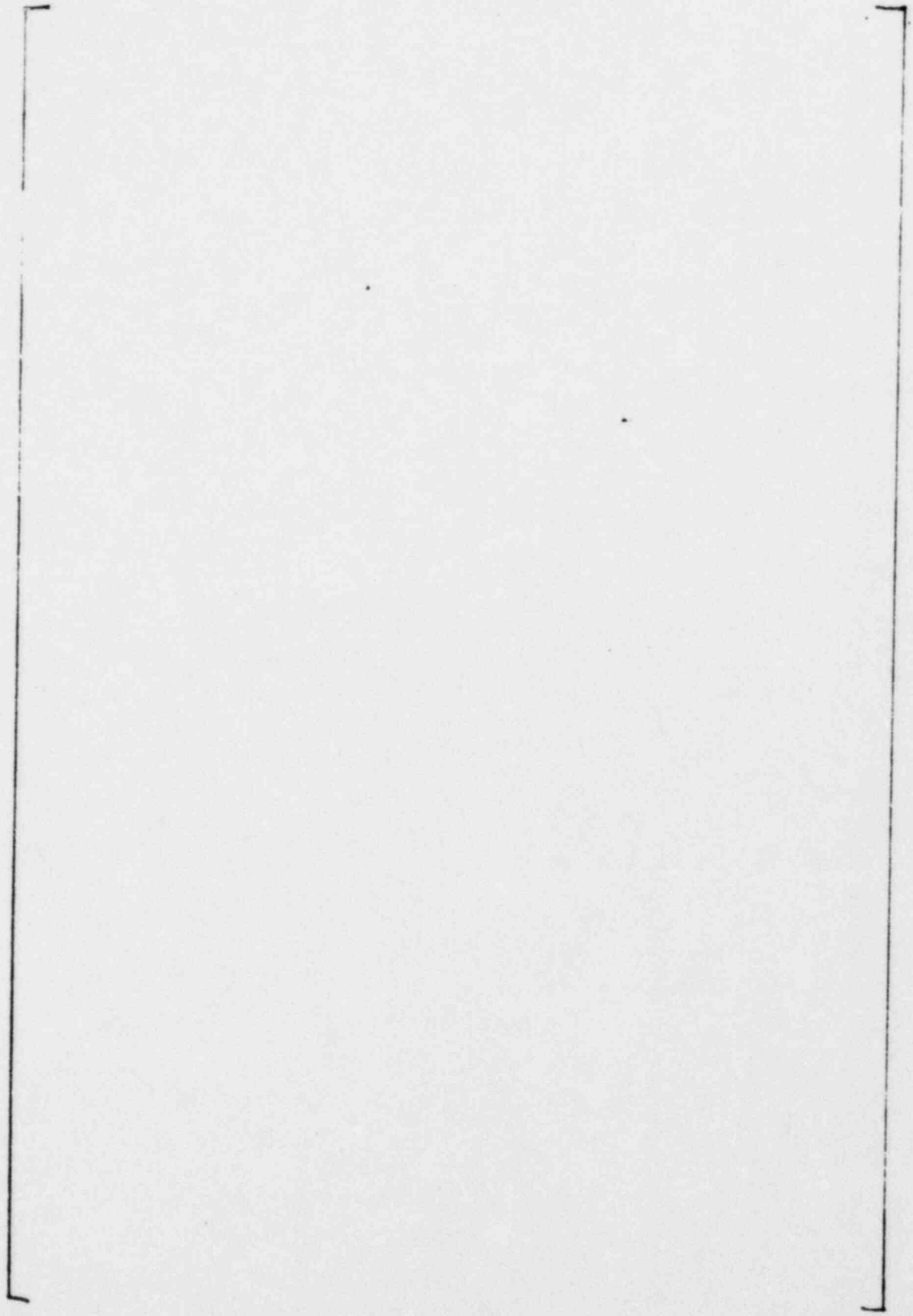

a,b,c,e

FIGURE 11.8-111: CASE NO.23, THERMAL TEMPERATURE SOLUTION SCALED TO STEAM GENERATOR CONDITIONS

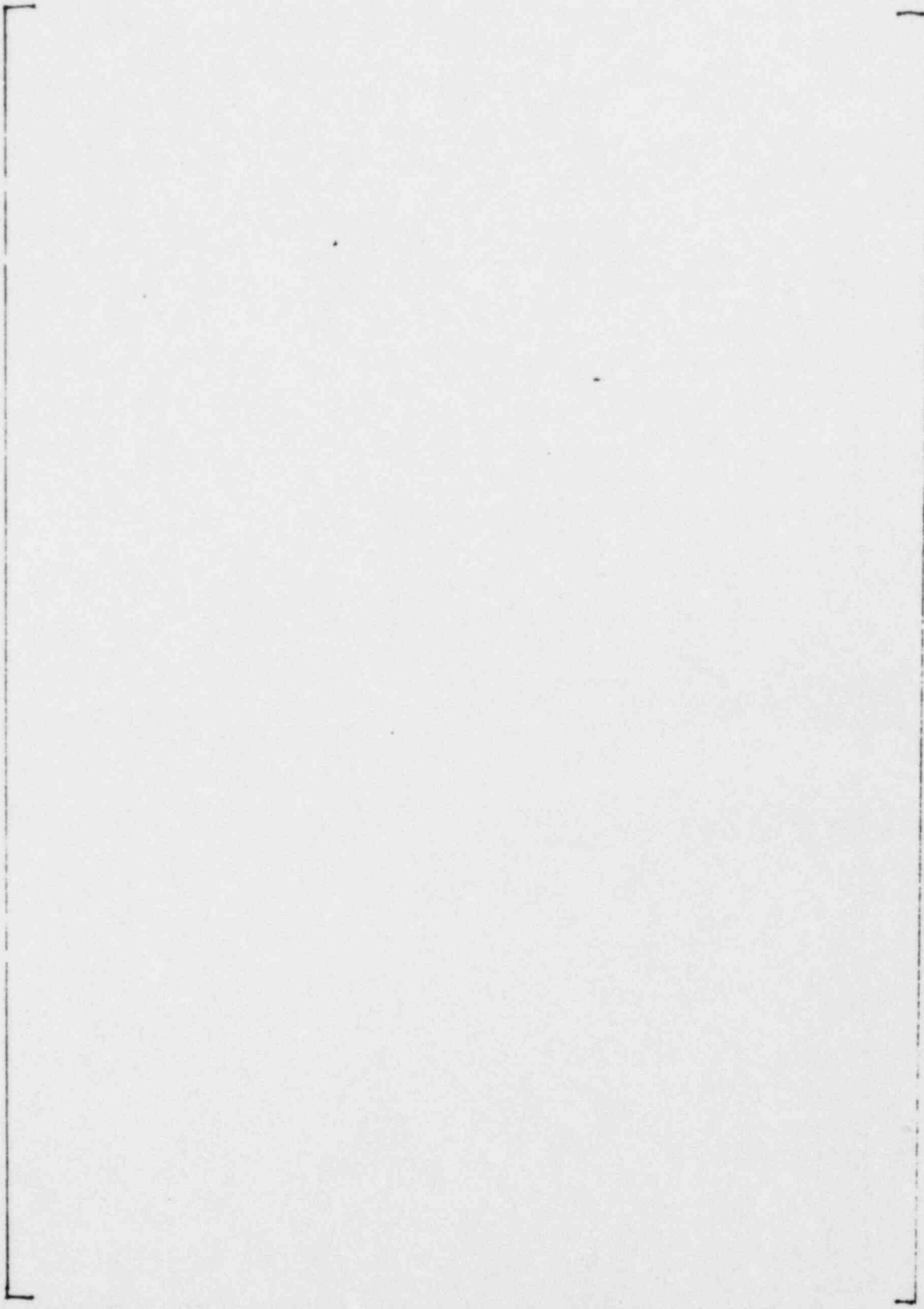

a,b,c,e

FIGURE 11.8-112: CASE NO.24, THERMAL TEMPERATURE SOLUTION SCALED TO STEAM GENERATOR CONDITIONS

a,b,c,e

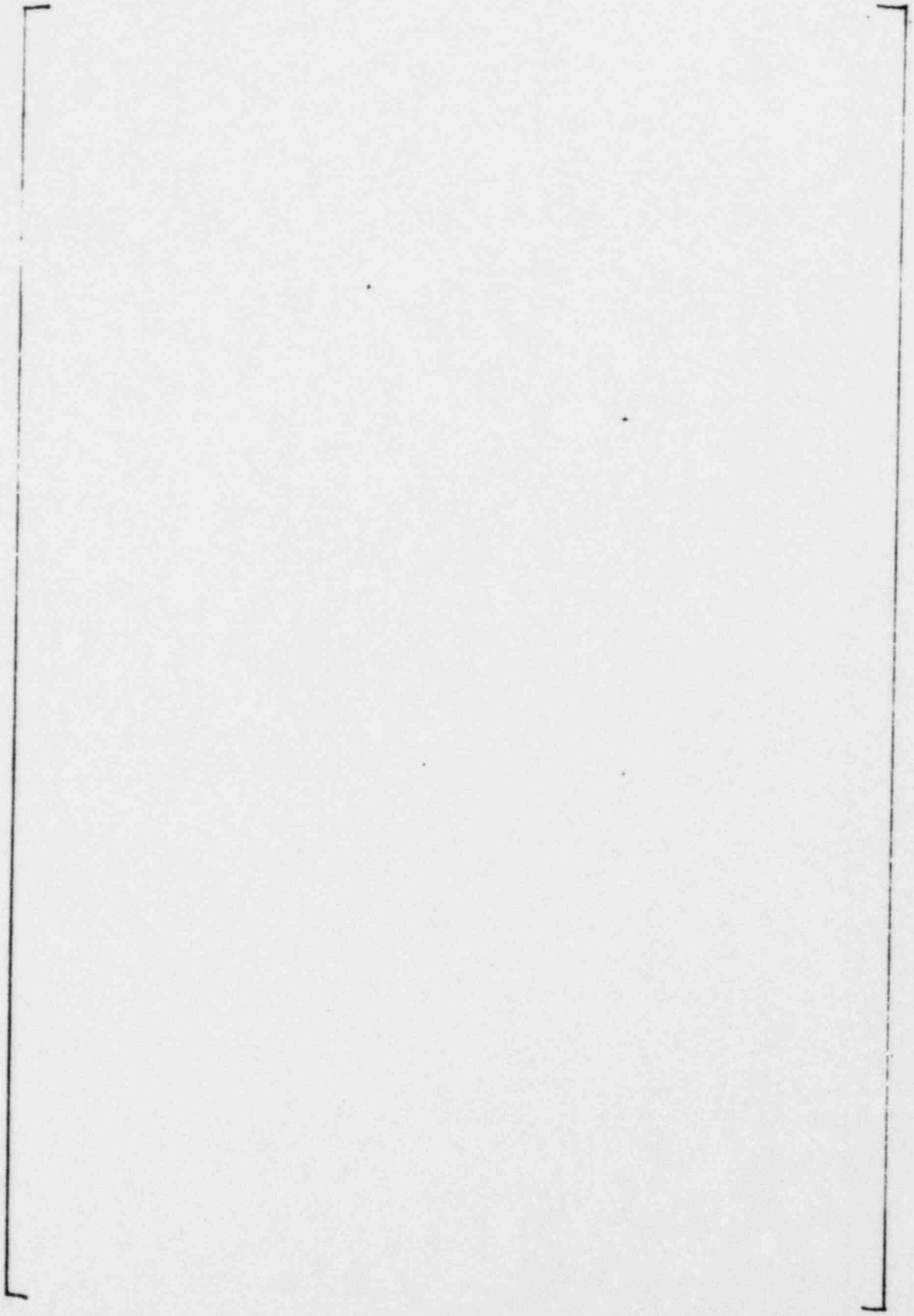

FIGURE 11.8-113: CASE NO.25, THERMAL TEMPERATURE SOLUTION SCALED TO STEAM GENERATOR CONDITIONS

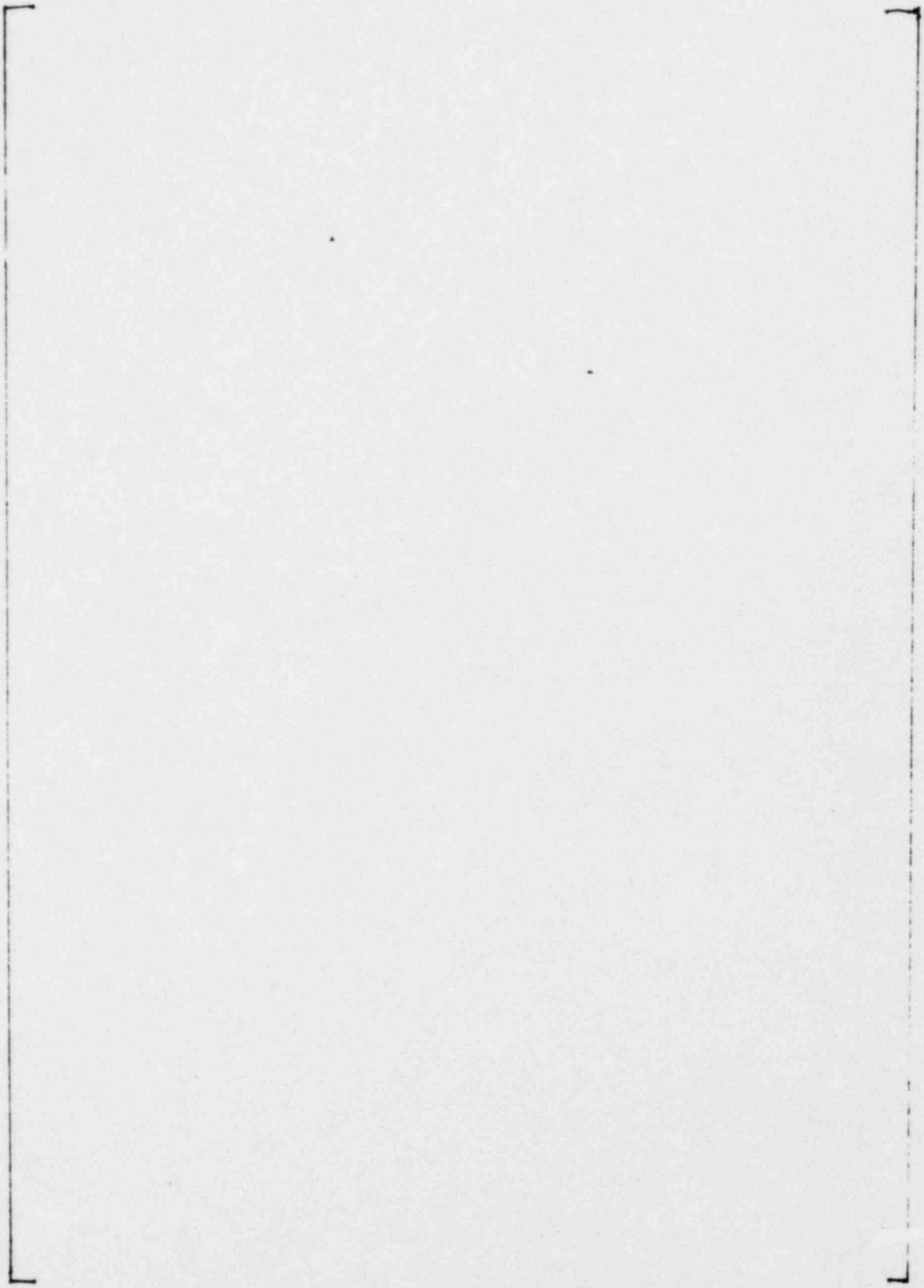

a,b,c,e

FIGURE 11.8-114: CASE NO.26, THERMAL TEMPERATURE SOLUTION SCALED TO STEAM GENERATOR CONDITIONS

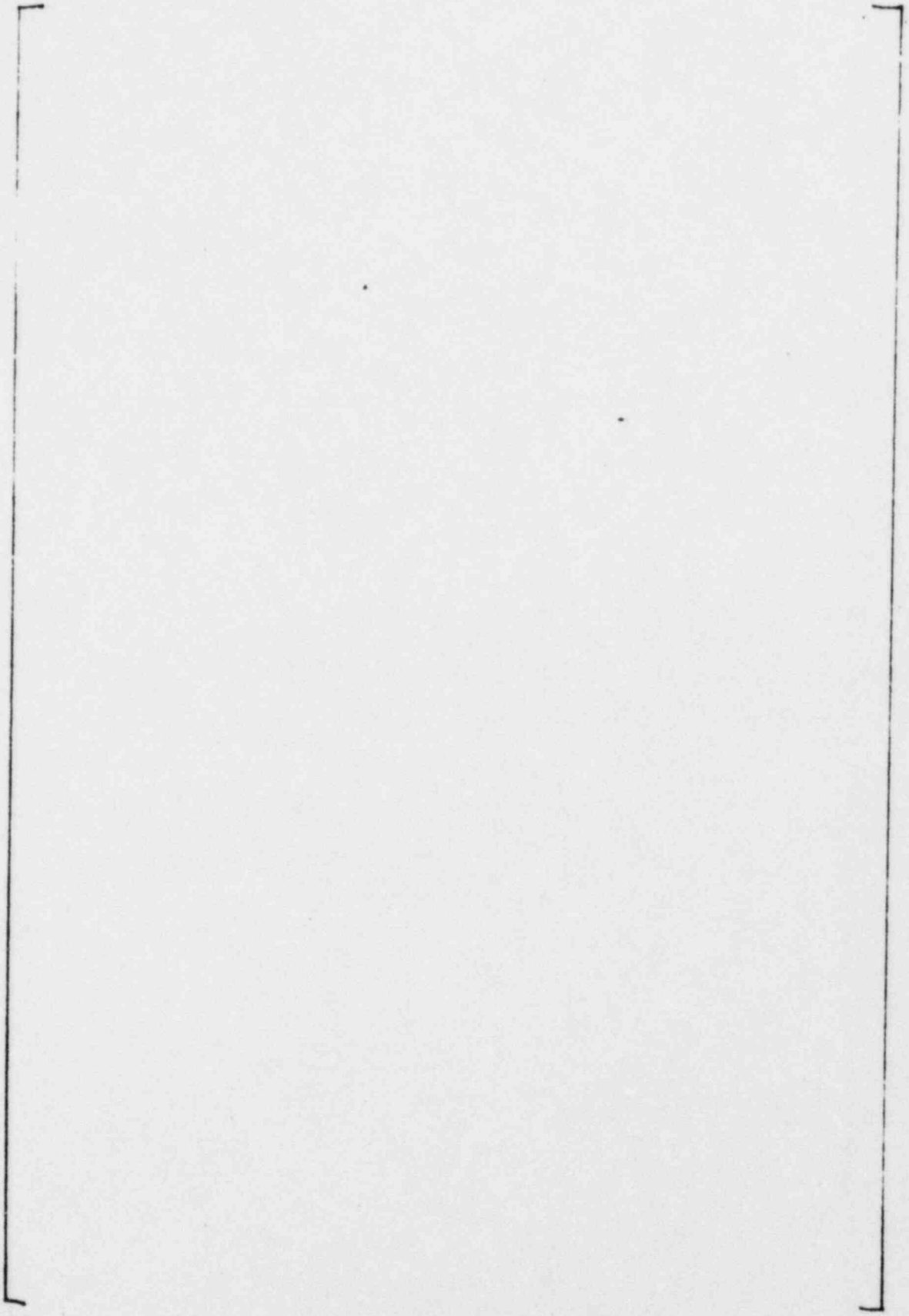

a.b.c.e

FIGURE 11.8-115: CASE NO.27, THERMAL TEMPERATURE SOLUTION SCALED TO STEAM GENERATOR CONDITIONS

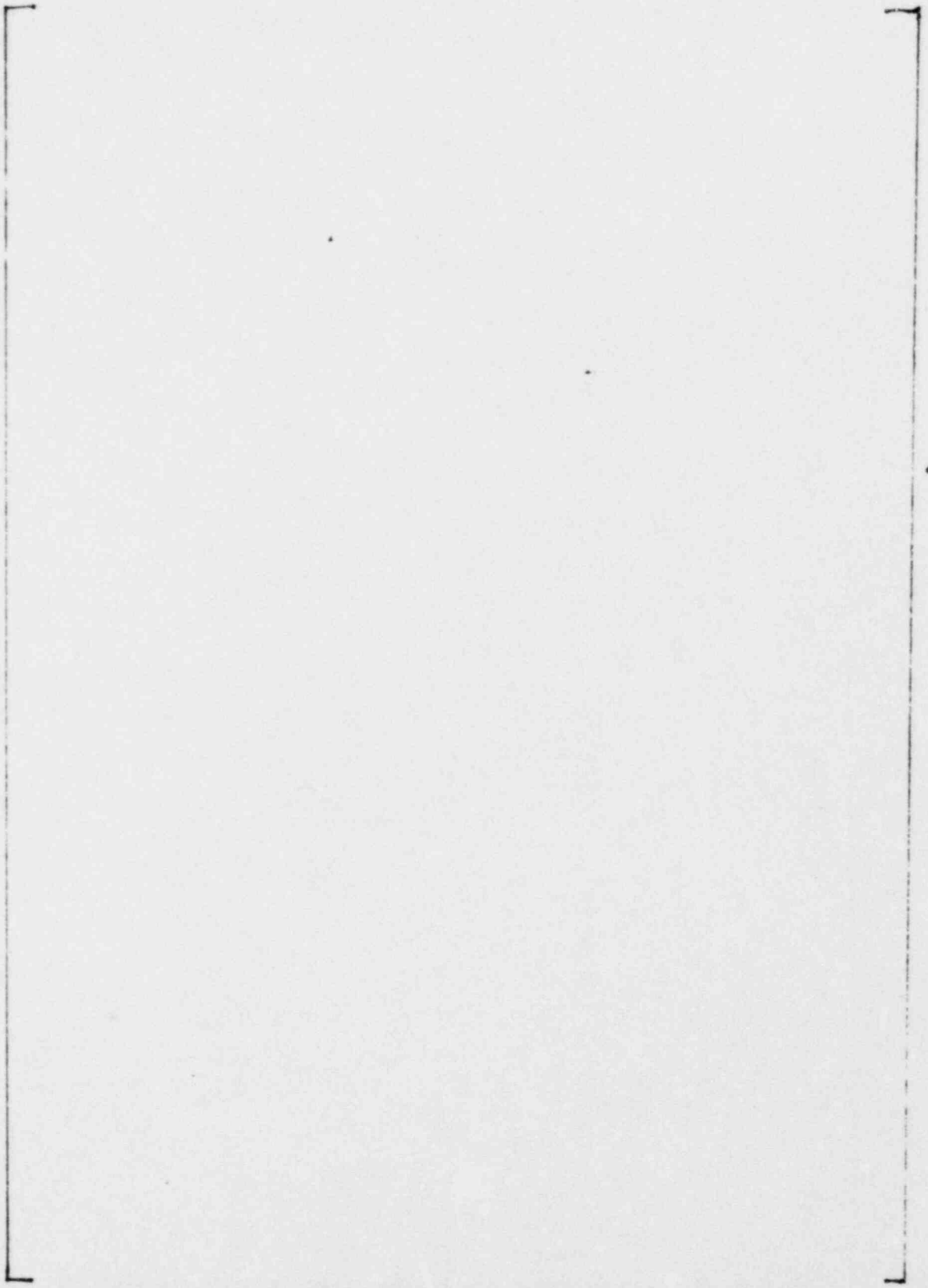

a,b,c,e

FIGURE 11.8-116: CASE NO.28, THERMAL TEMPERATURE SOLUTION SCALED TO STEAM GENERATOR CONDITIONS

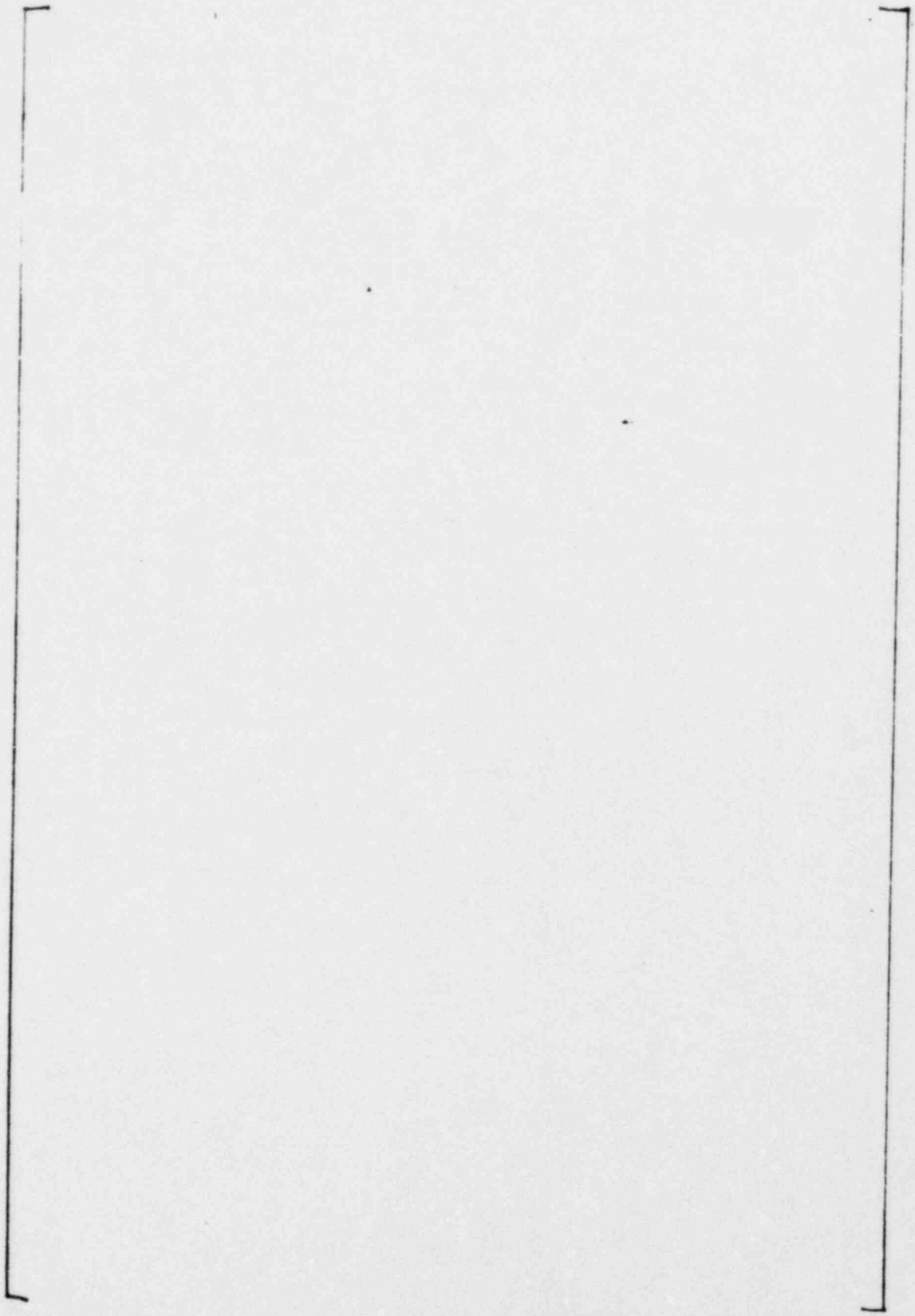

a.b.c.e

FIGURE 11.8-117: CASE NO.29, THERMAL TEMPERATURE SOLUTION SCALED TO STEAM GENERATOR CONDITIONS

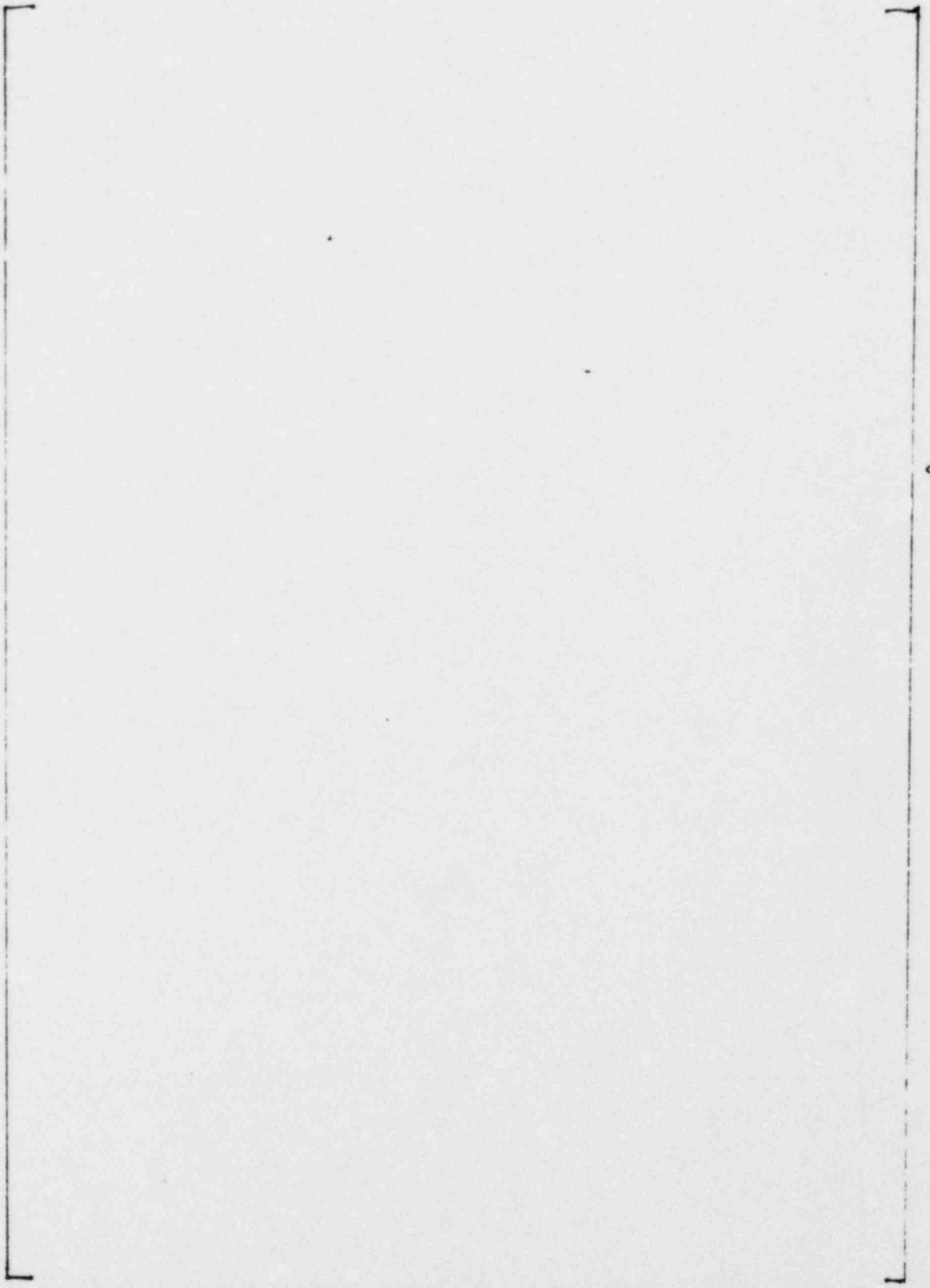

a,b,c,e

FIGURE 11.8-118: CASE NO.30, THERMAL TEMPERATURE SOLUTION SCALED TO STEAM GENERATOR CONDITIONS

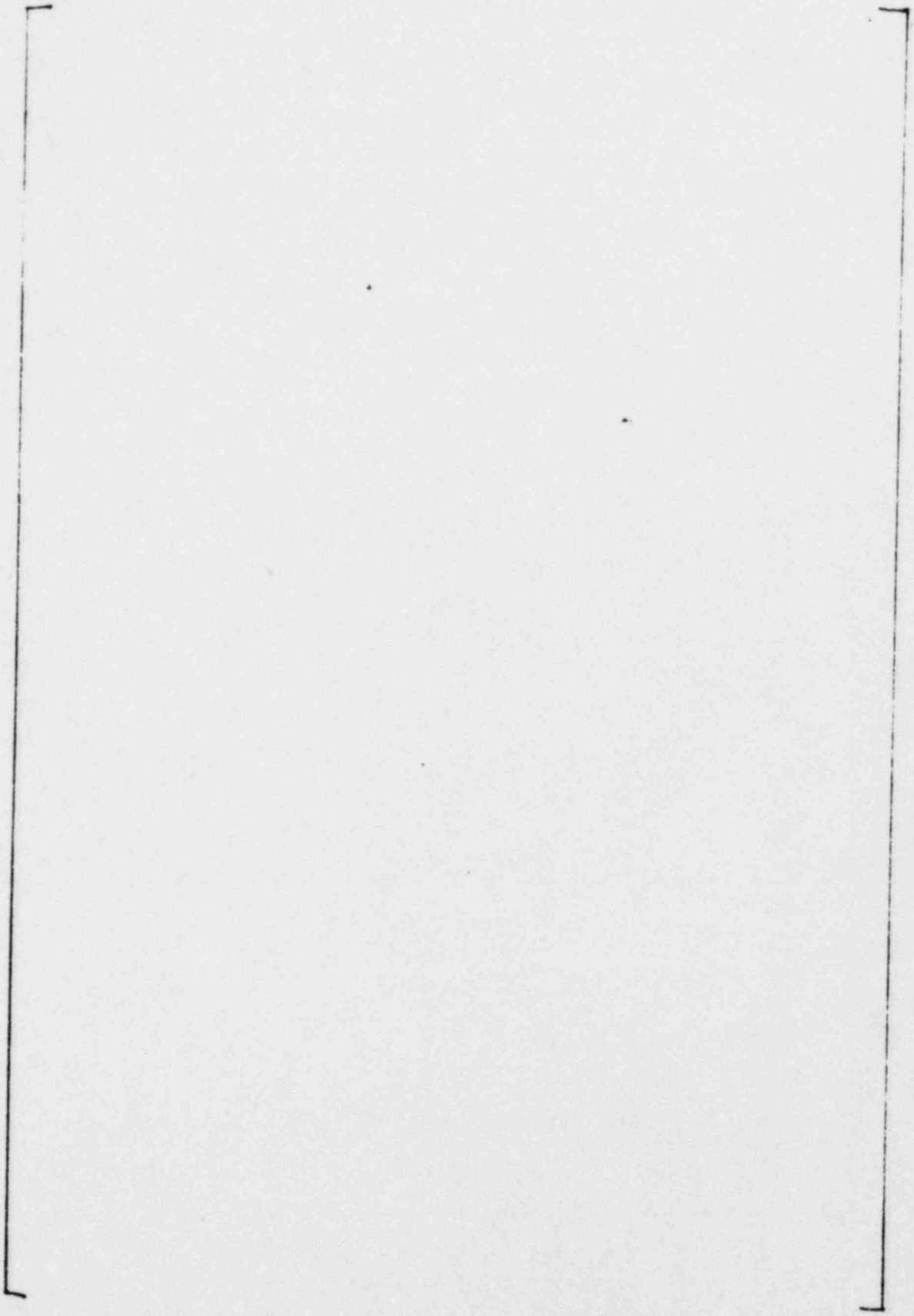

a,b,c,e

FIGURE 11.8-119: CASE NO.31, THERMAL TEMPERATURE SOLUTION SCALED TO STEAM GENERATOR CONDITIONS

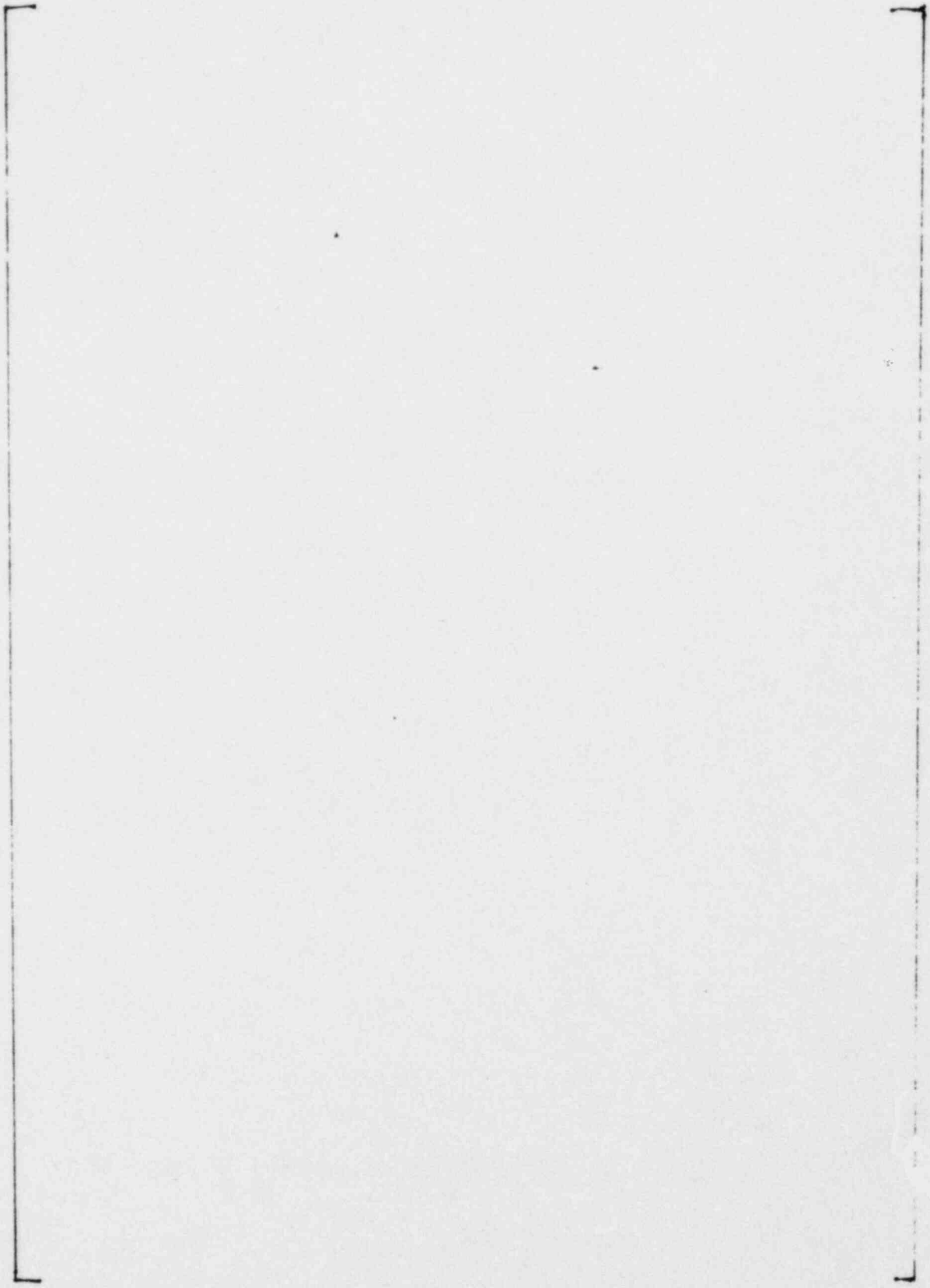

a,b,c,e

FIGURE 11.8-120: CASE NO.32, THERMAL TEMPERATURE SOLUTION SCALED TO STEAM GENERATOR CONDITIONS

BLANK

Case No.: 33

Generic Profile:

Interface Level:_____Angle Measured From The Bottom of Pipe

Run No.: Y6 _____

FIGURE 11.8-121: CASE NO.33, THERMAL TEMPERATURE SOLUTION SCALED TO STEAM GENERATOR CONDITIONS

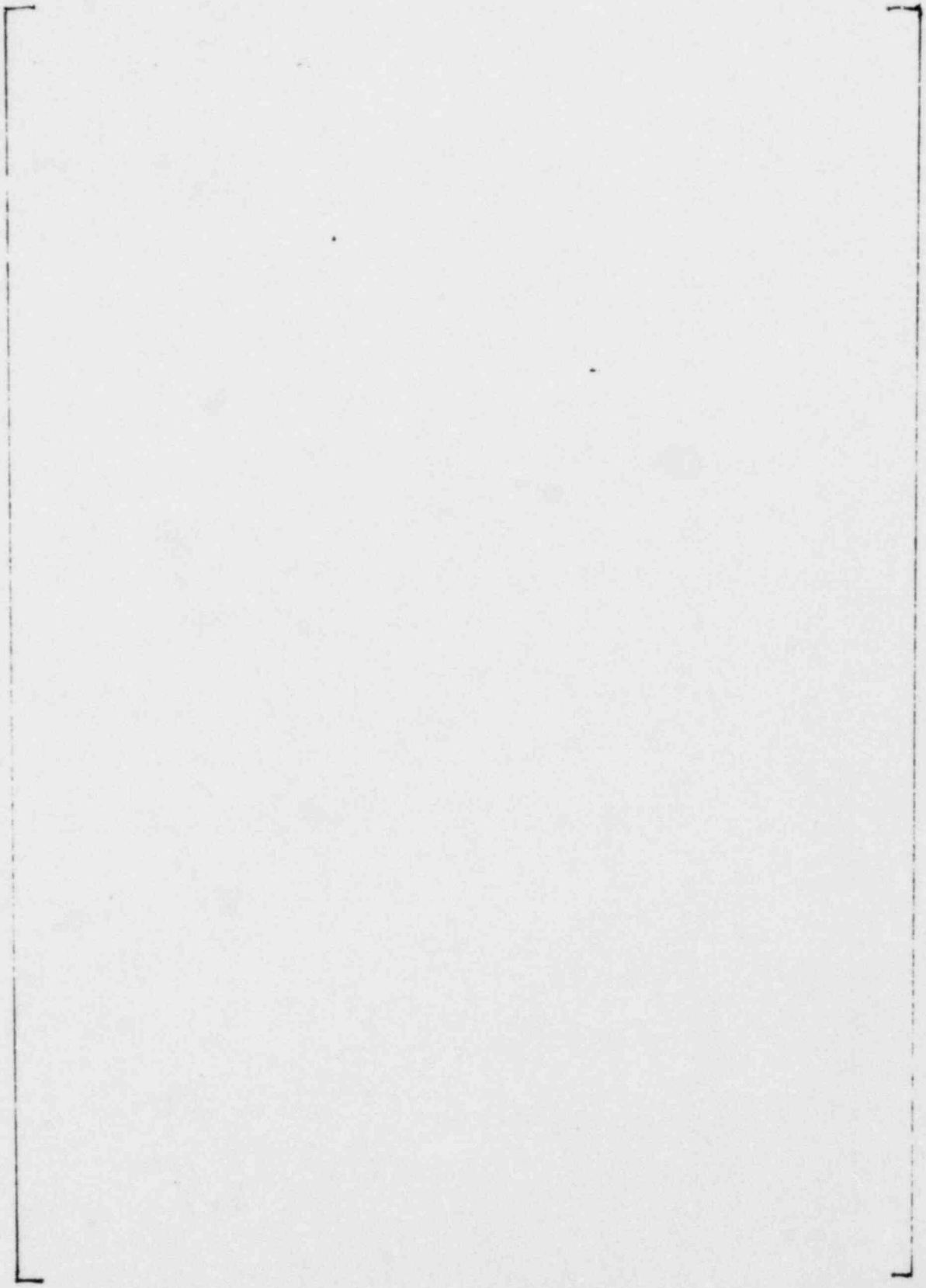

a,b,c,e

FIGURE 11.8-122: CASE NO.34, THERMAL TEMPERATURE SOLUTION SCALED TO STEAM GENERATOR CONDITIONS

a,b,c,e

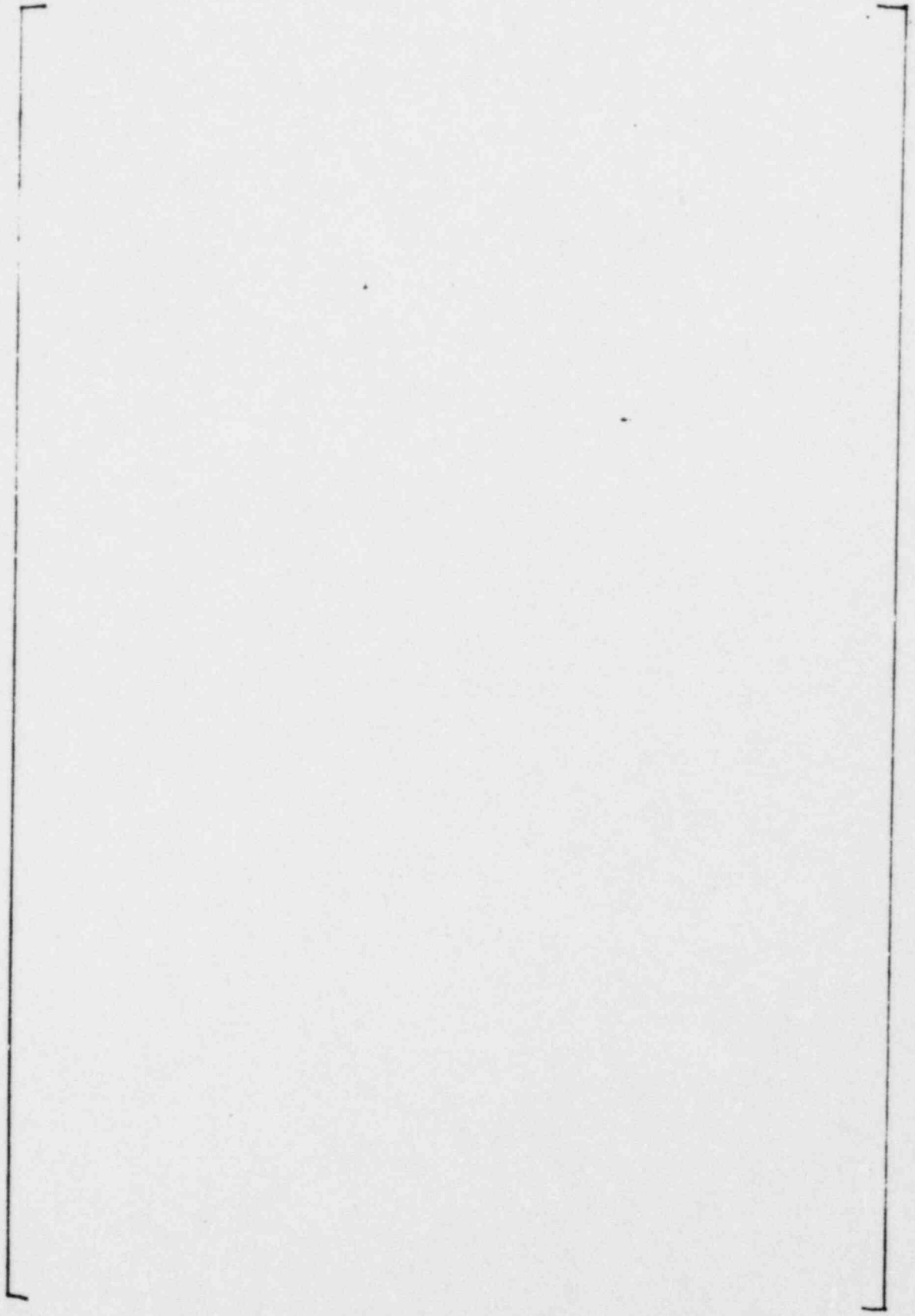

FIGURE 11.8-123: CASE NO.35, THERMAL TEMPERATURE SOLUTION SCALED TO STEAM GENERATOR CONDITIONS

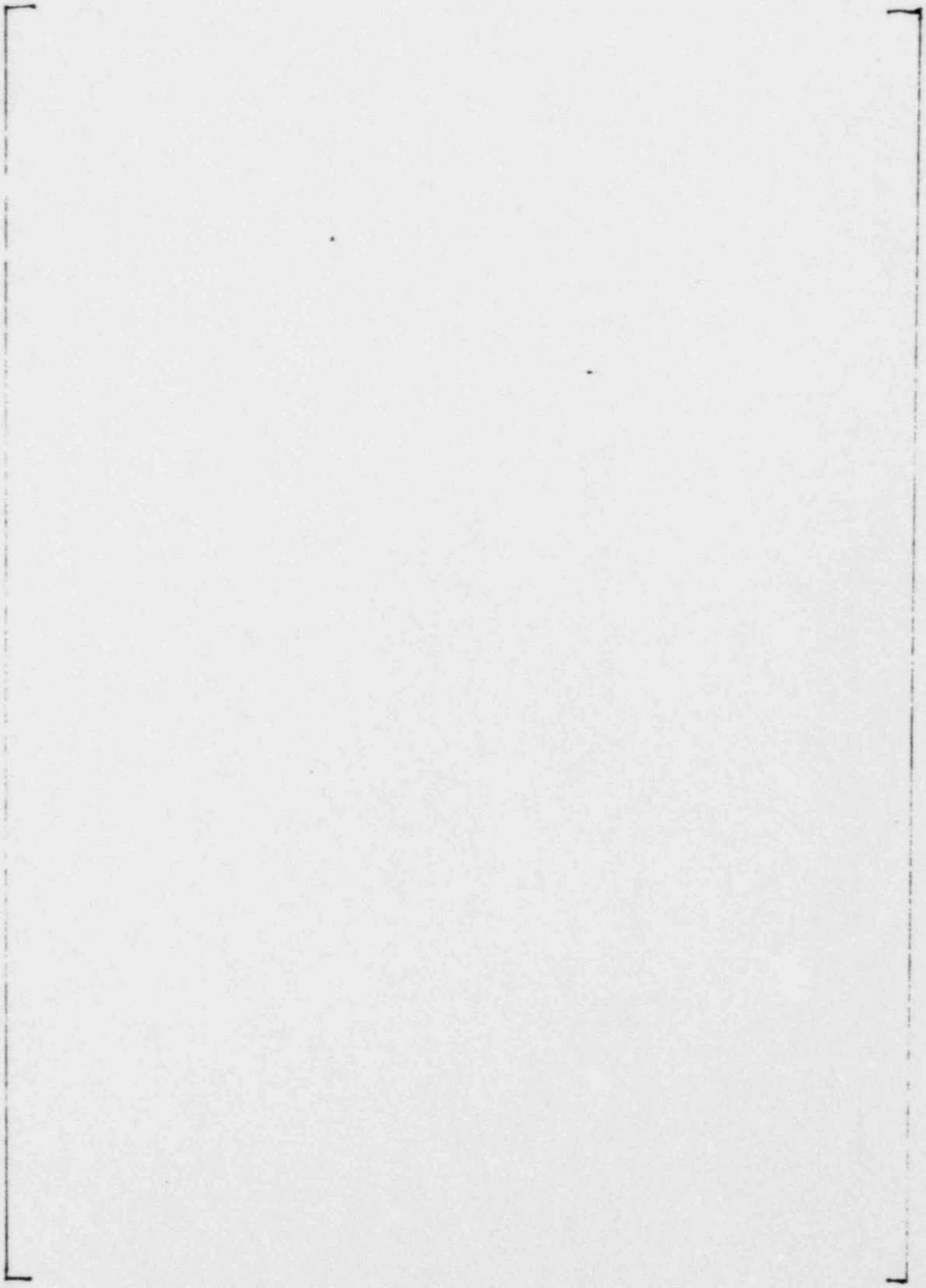

a,b,c,e

FIGURE 11.8-124: CASE NO.36, THERMAL TEMPERATURE SOLUTION SCALED TO STEAM GENERATOR CONDITIONS

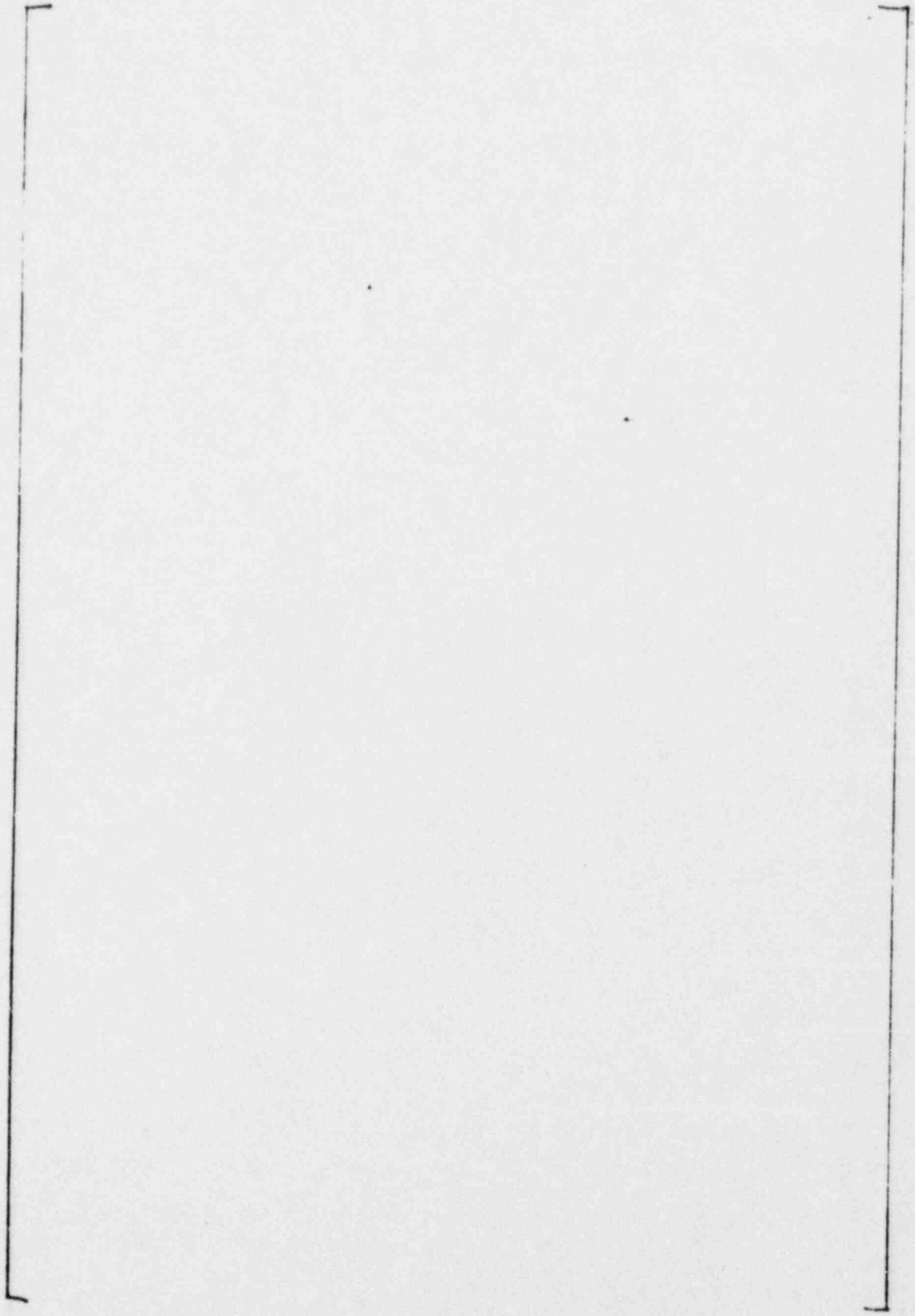

a,b,c,e

FIGURE 11.8-125: CASE NO.37, THERMAL TEMPERATURE SOLUTION SCALED TO STEAM GENERATOR CONDITIONS

BLANK

Case No.: 38

Generic Profile:

Interface Level:_____Angle Measured From The Bottom of Pipe

Run No.: Y6 _____

FIGURE 11.8-126: CASE NO.38, THERMAL TEMPERATURE SOLUTION SCALED TO STEAM GENERATOR CONDITIONS

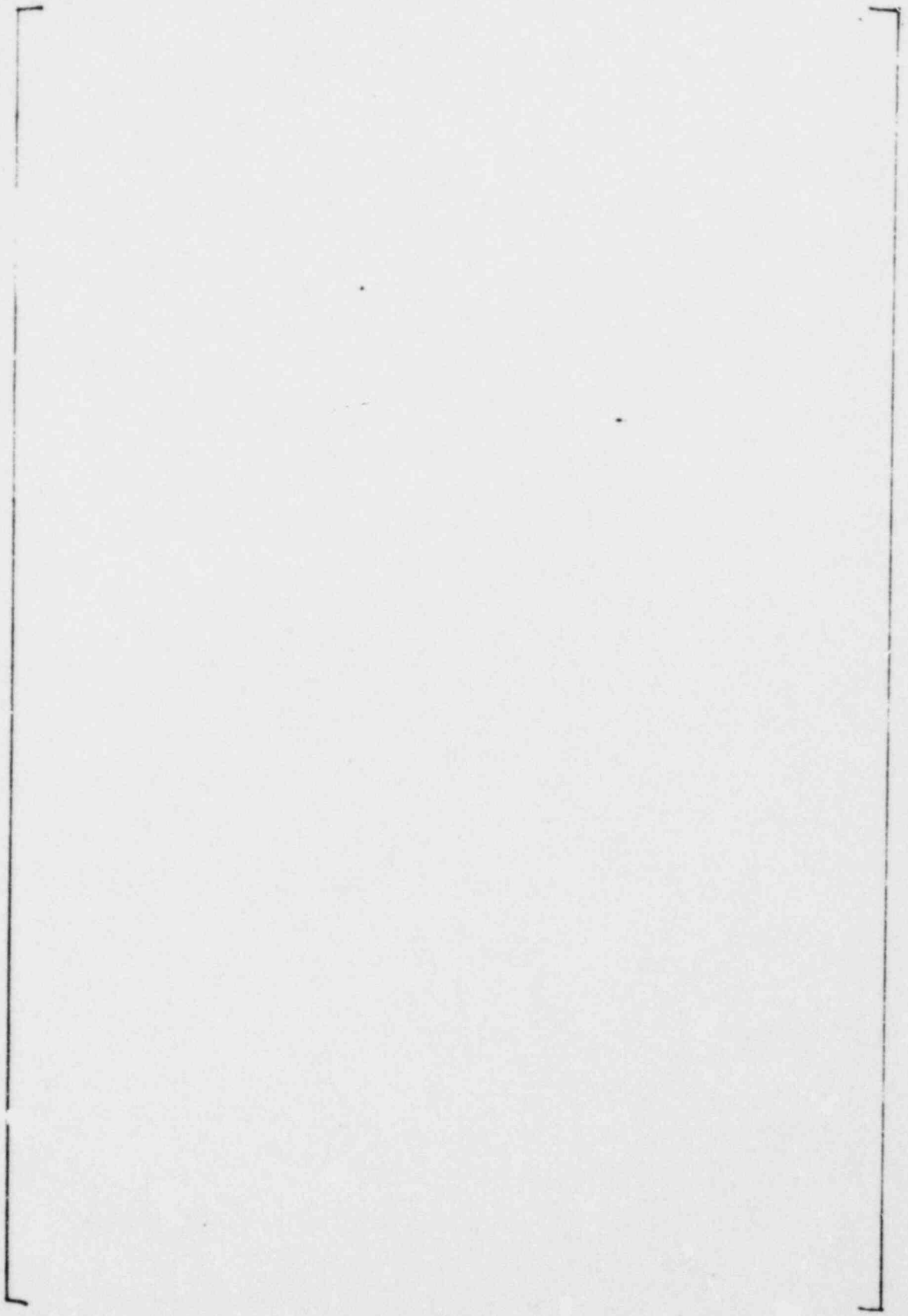

a.b.c.e

FIGURE 11.3-127: CASE NO.39, THERMAL TEMPERATURE SOLUTION SCALED TO STEAM GENERATOR CONDITIONS

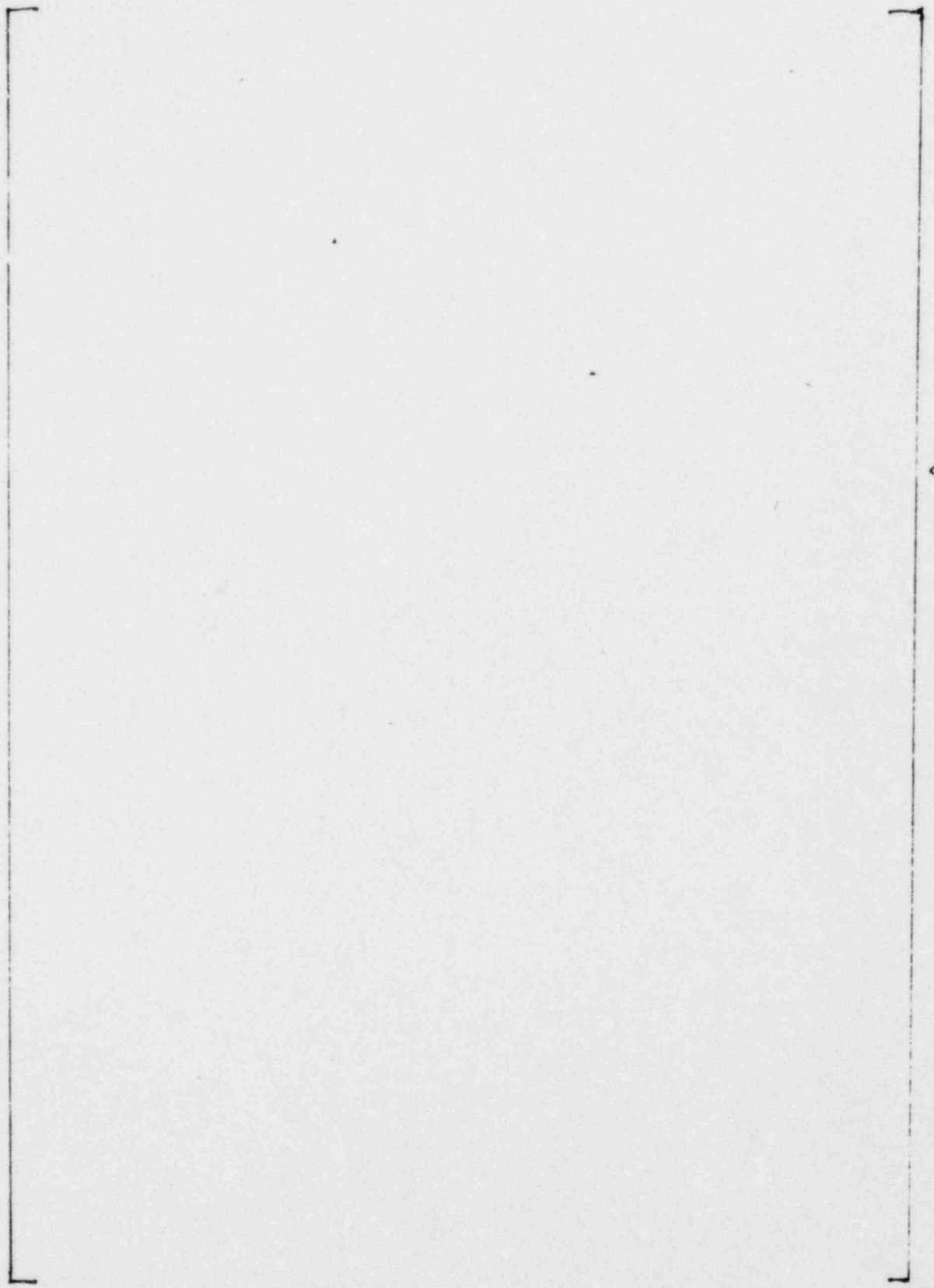

a,b,c,e

FIGURE 11.8-128: CASE NO.40, THERMAL TEMPERATURE SOLUTION SCALED TO STEAM GENERATOR CONDITIONS

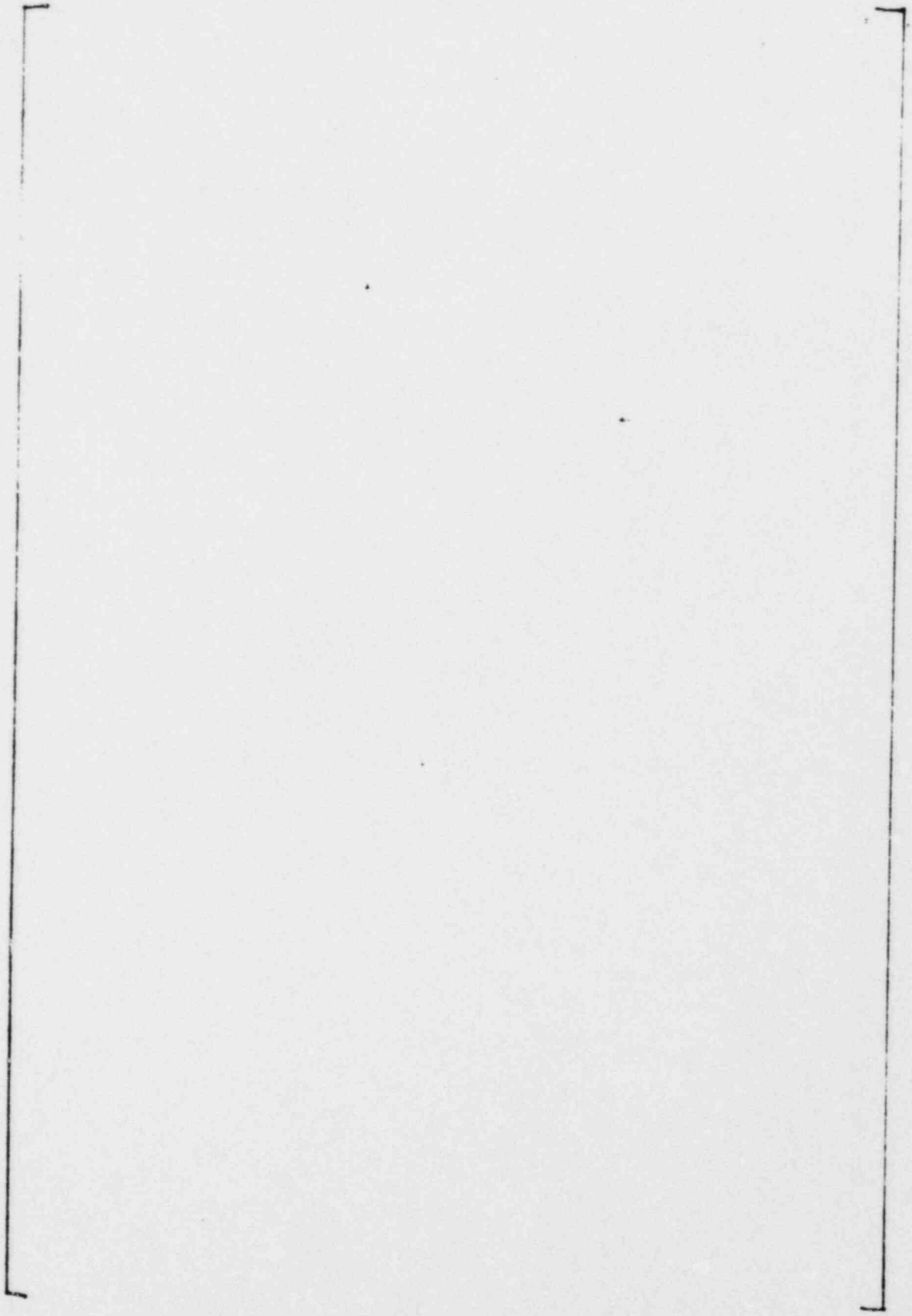

a.b.c.e

FIGURE 11.8-129: CASE NO.41, THERMAL TEMPERATURE SOLUTION SCALED TO STEAM GENERATOR CONDITIONS

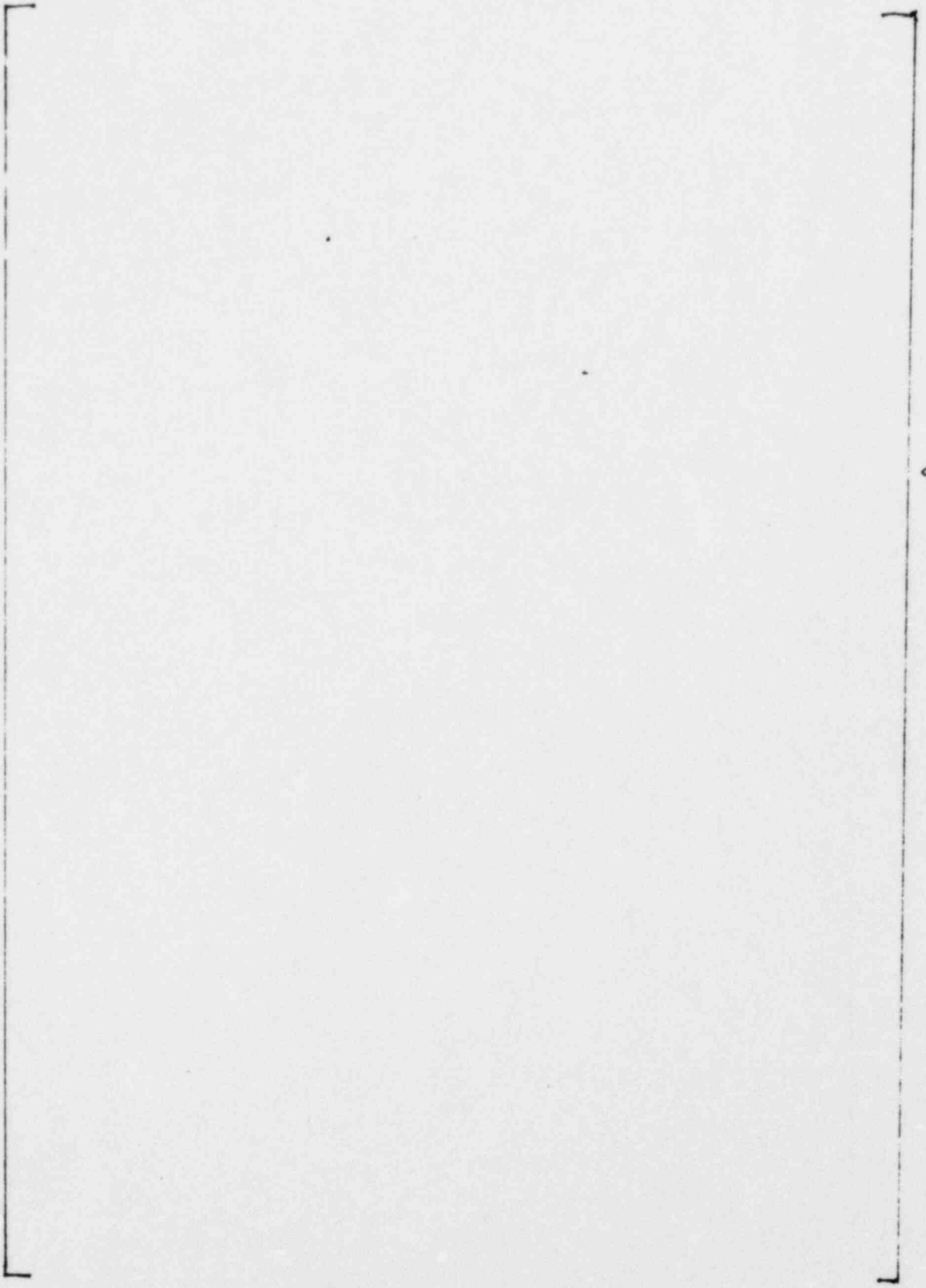

a,b,c,e

FIGURE 11.8-130. CASE NO.42, THERMAL TEMPERATURE SOLUTION SCALED TO STEAM GENERATOR CONDITIONS

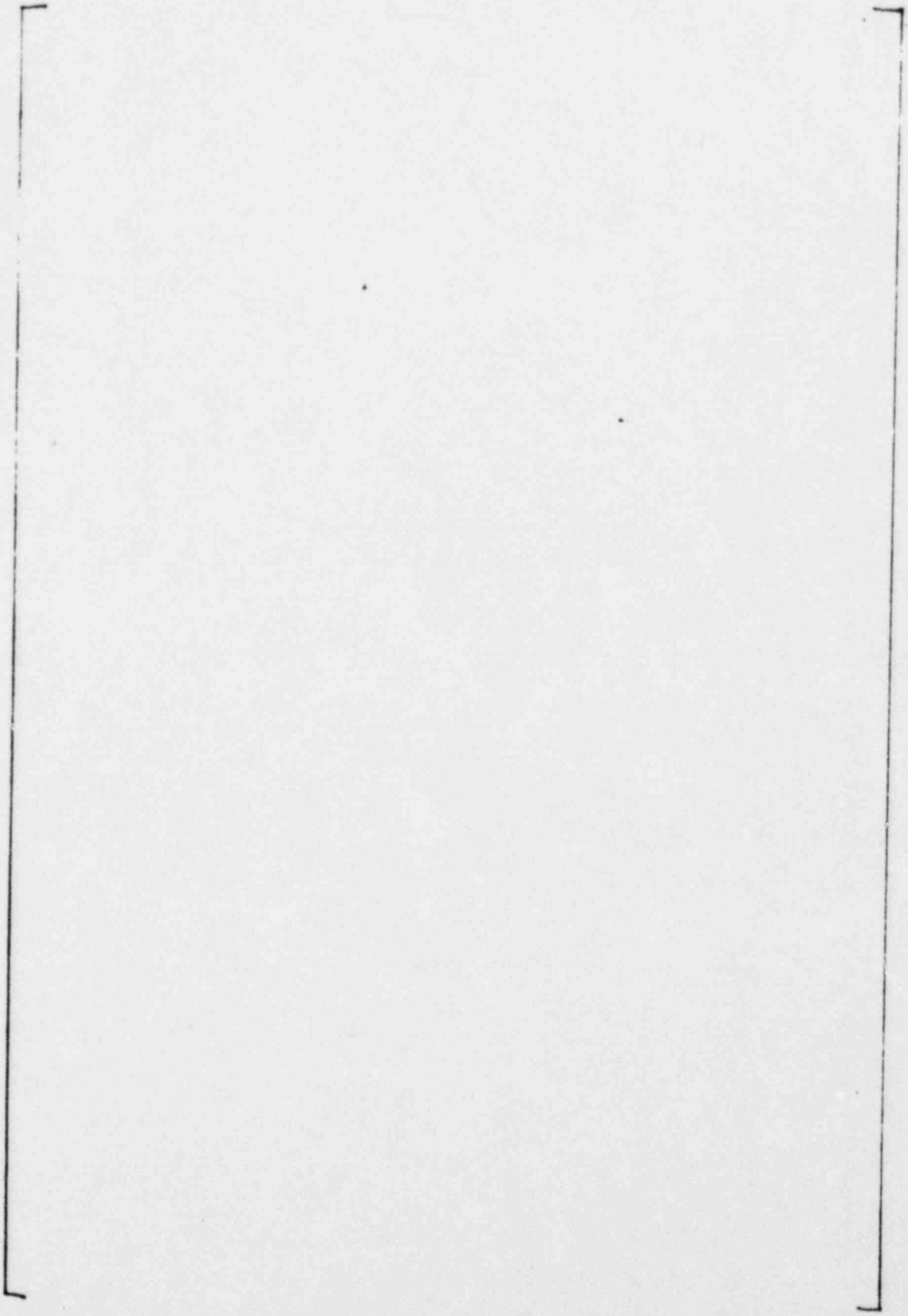

a,b,c,e

FIGURE 11.8-131: CASE NO.43, THERMAL TEMPERATURE SOLUTION SCALED TO STEAM GENERATOR CONDITIONS

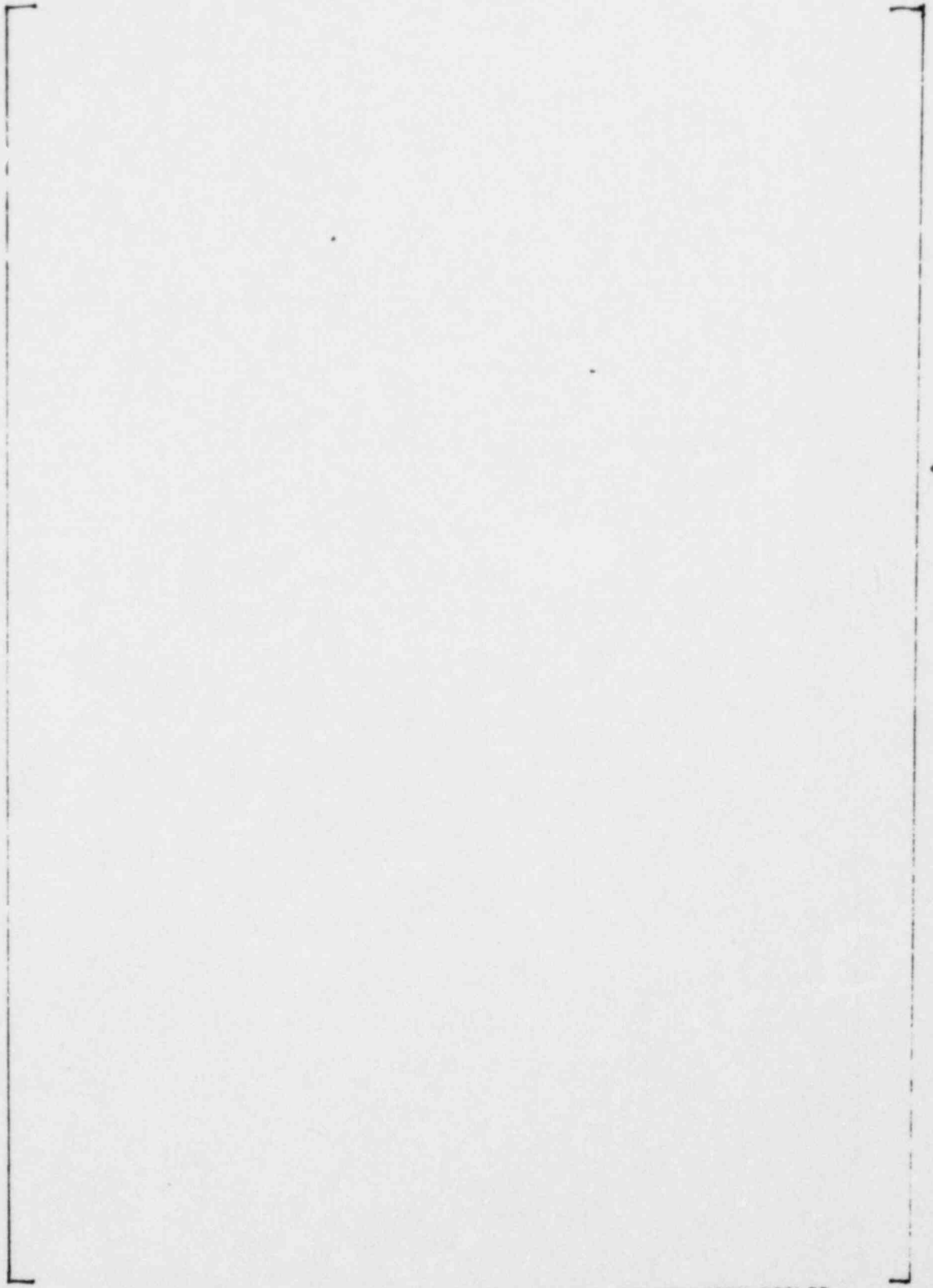

a,b,c,e

FIGURE 11.8-132: CASE NO.44, THERMAL TEMPERATURE SOLUTION SCALED TO STEAM GENERATOR CONDITIONS

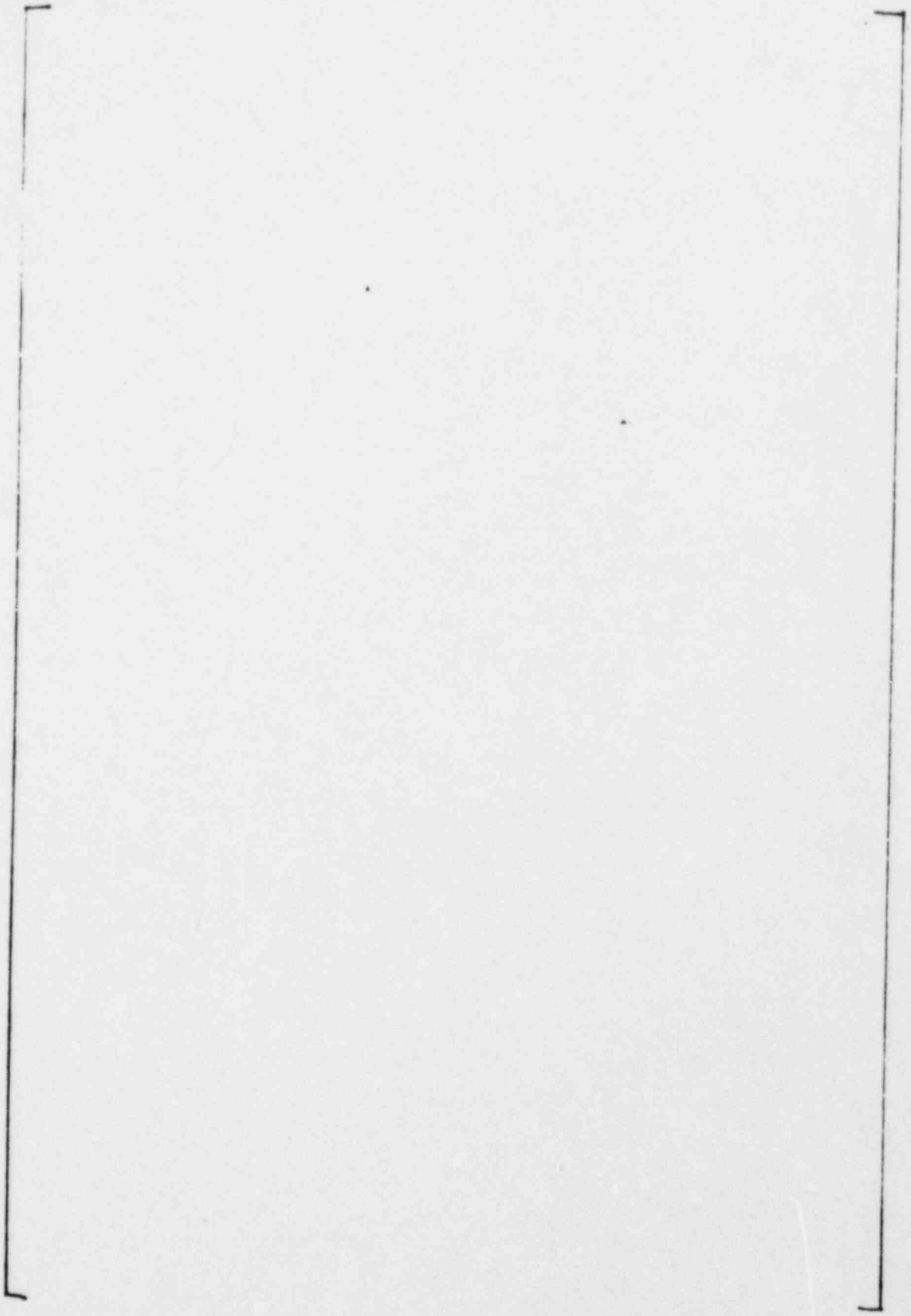

a,b,c,e

FIGURE 11.8-133 CASE NO. 1 SURFACE STRESS TIME HISTORY.

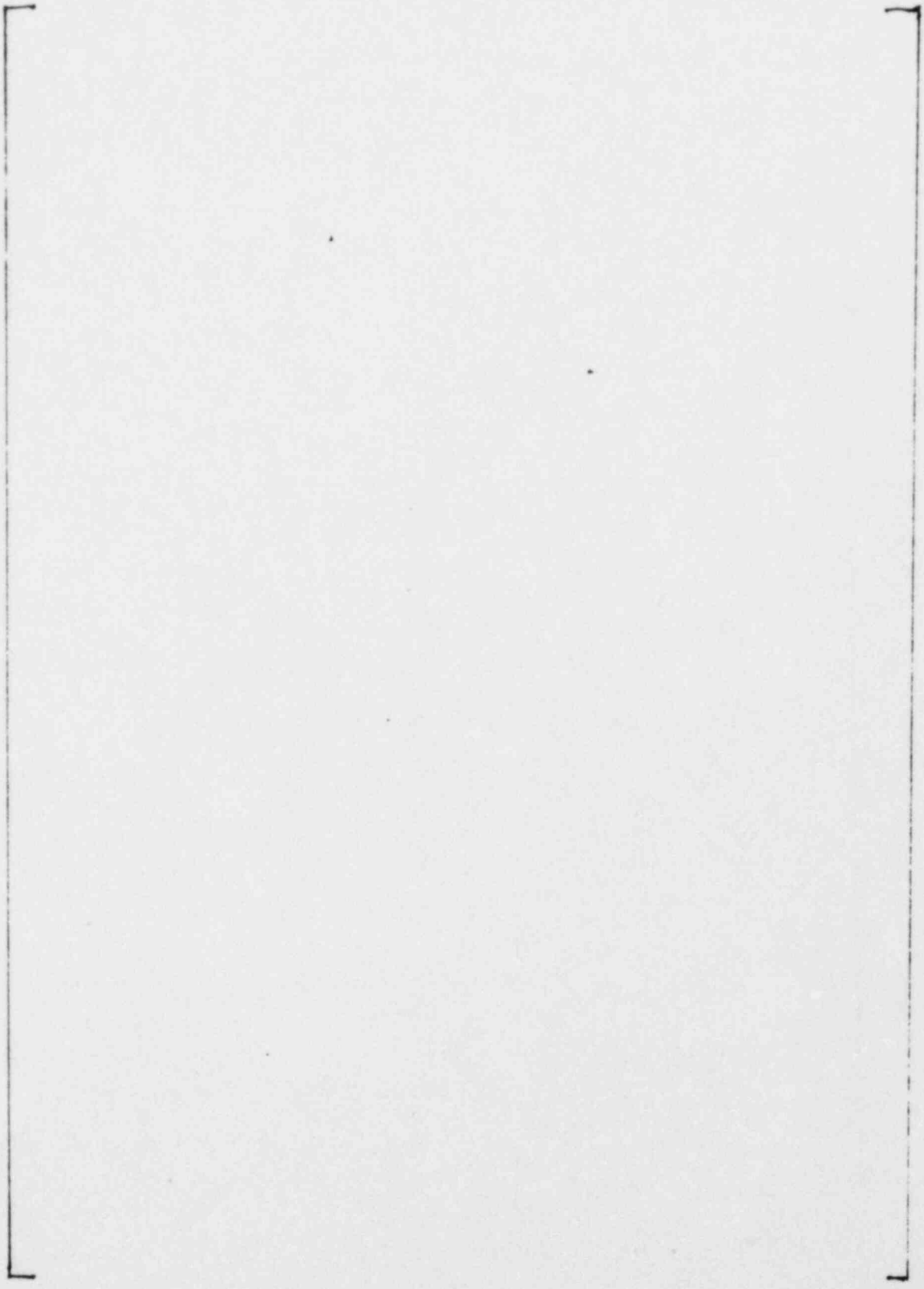

a,b,c,e

FIGURE 11.8-134 CASE NO. 2 SURFACE STRESS TIME HISTORY.

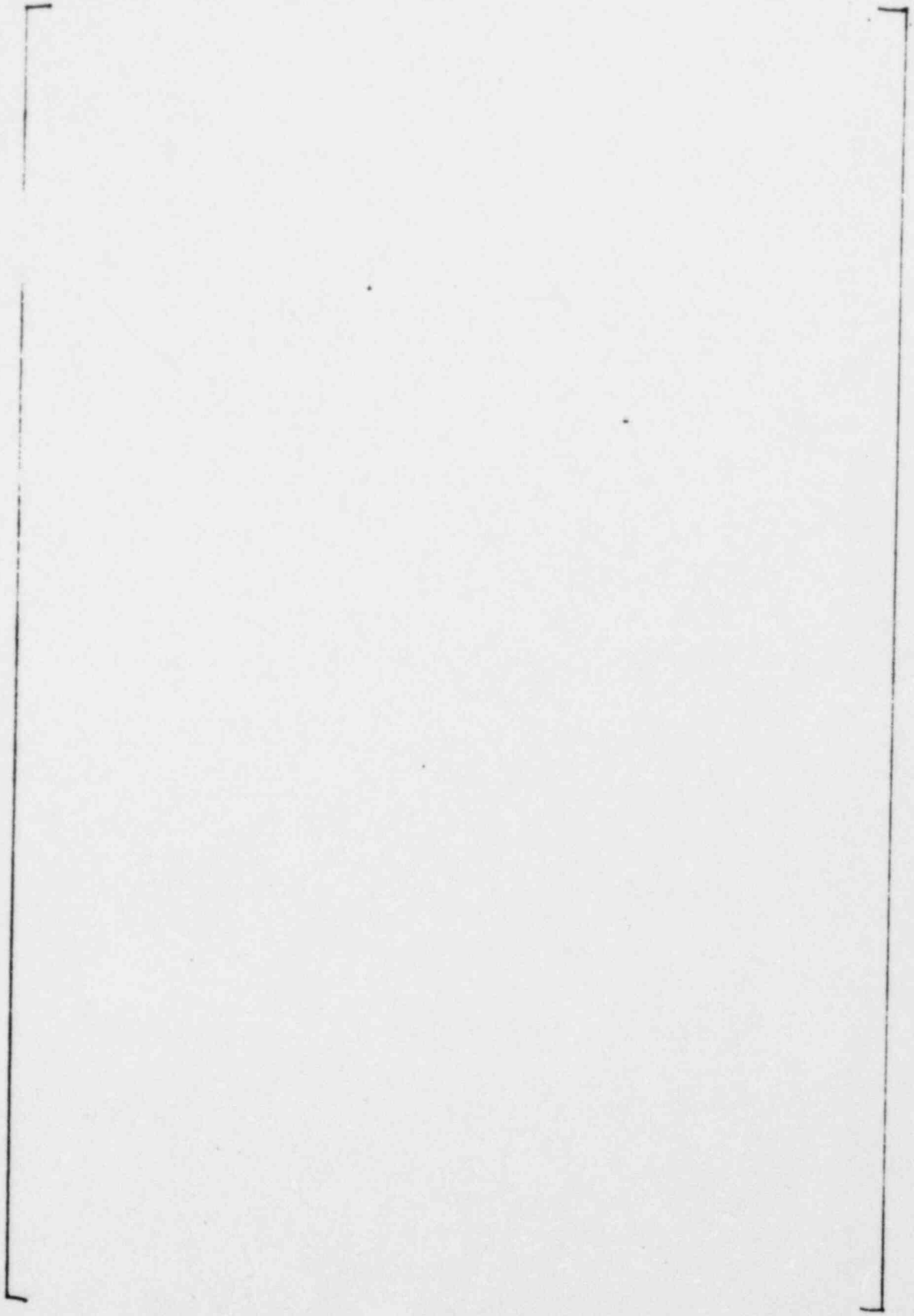

a,b,c,e

FIGURE 11.8-135 CASE NO. 3 SURFACE STRESS TIME HISTORY.

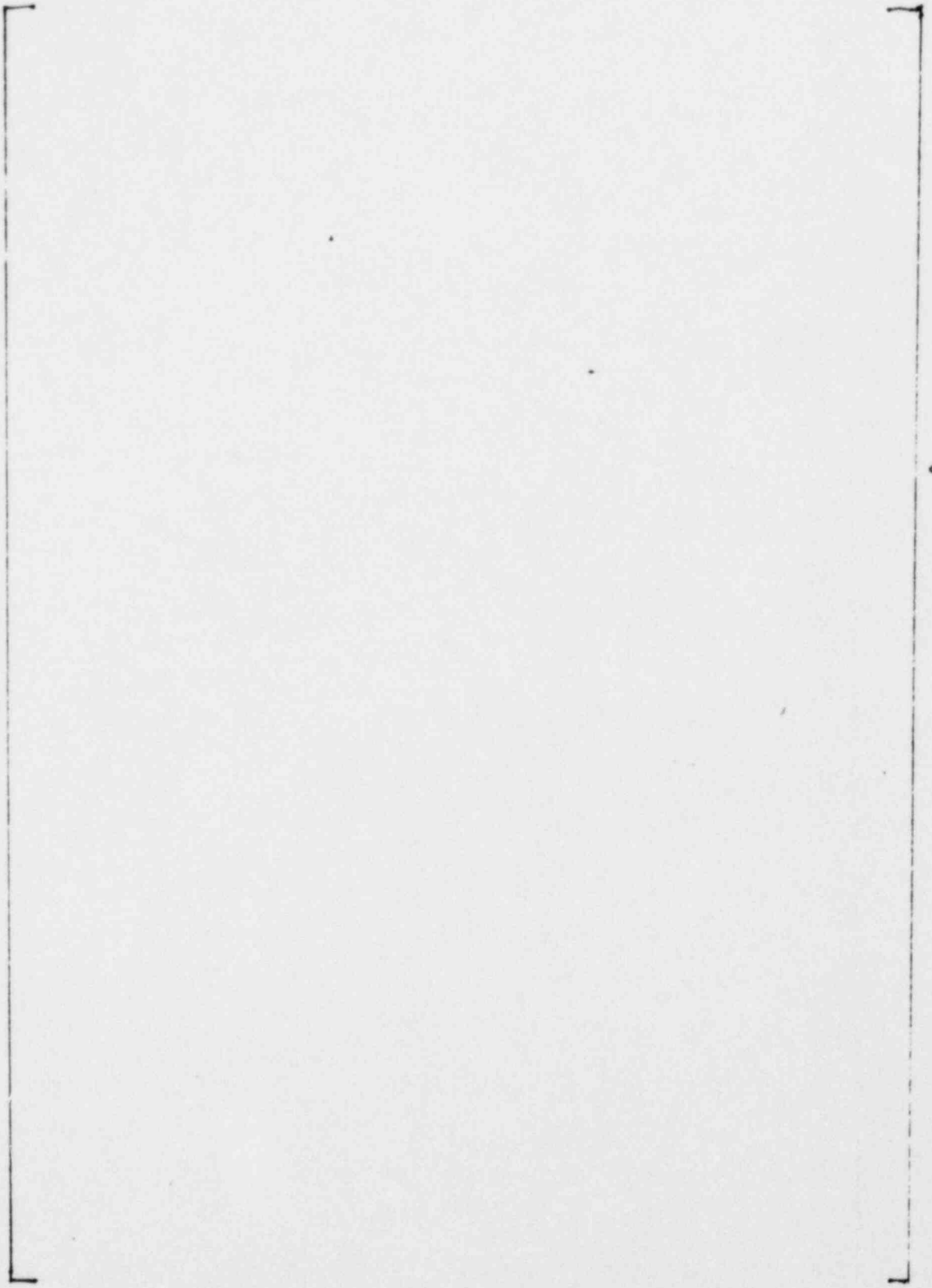

a,b,c,e

FIGURE 11.8-136 CASE NO. 4 SURFACE STRESS TIME HISTORY.

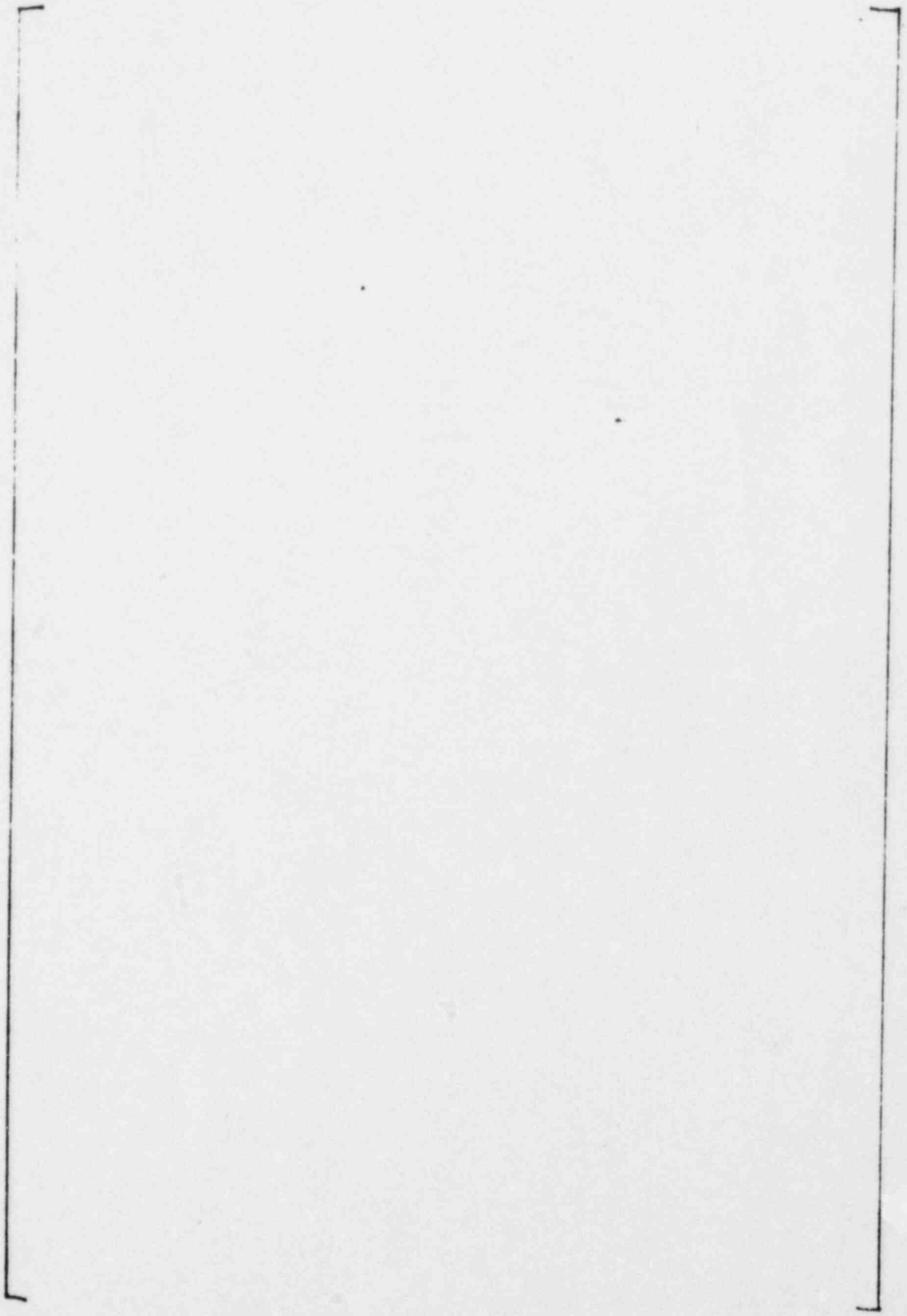

a,b,c,e

FIGURE 11.8-137 CASE NO. 5 SURFACE STRESS TIME HISTORY.

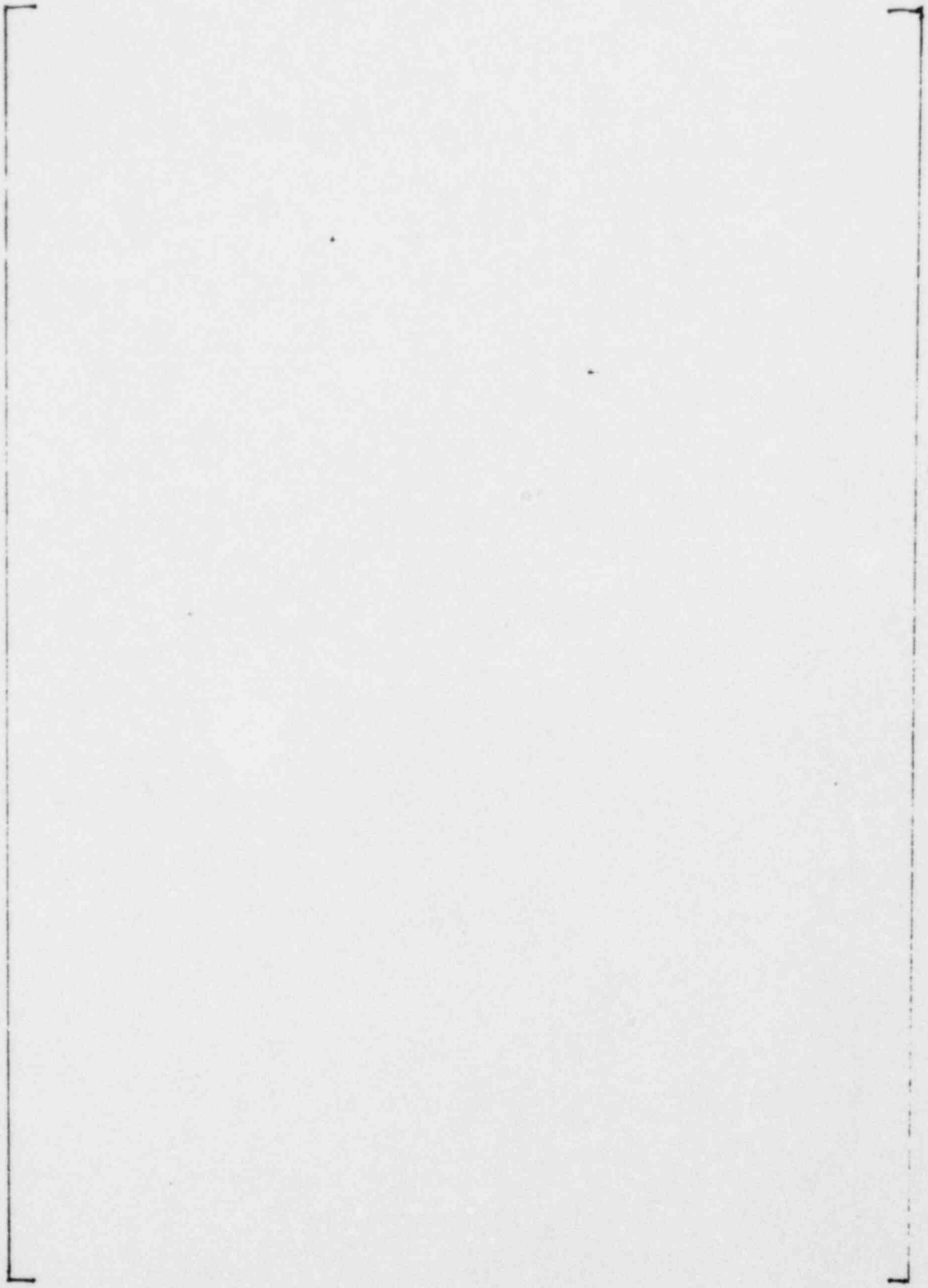

a,b,c,e

FIGURE 11.8-138 CASE NO. 6 SURFACE STRESS TIME HISTORY.

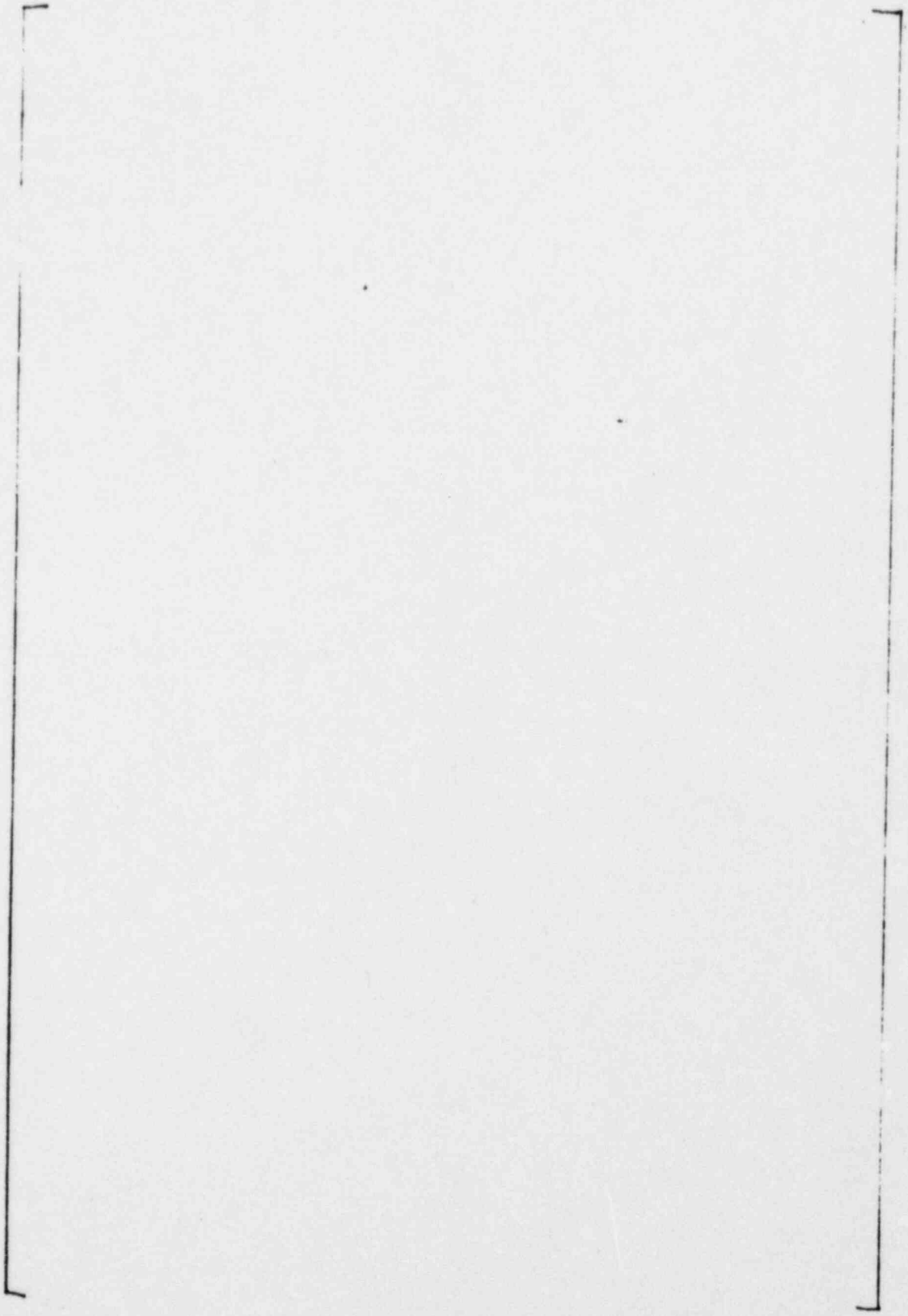

a,b,c,e

FIGURE 11.8-139 CASE NO. 7 SURFACE STRESS TIME HISTORY.

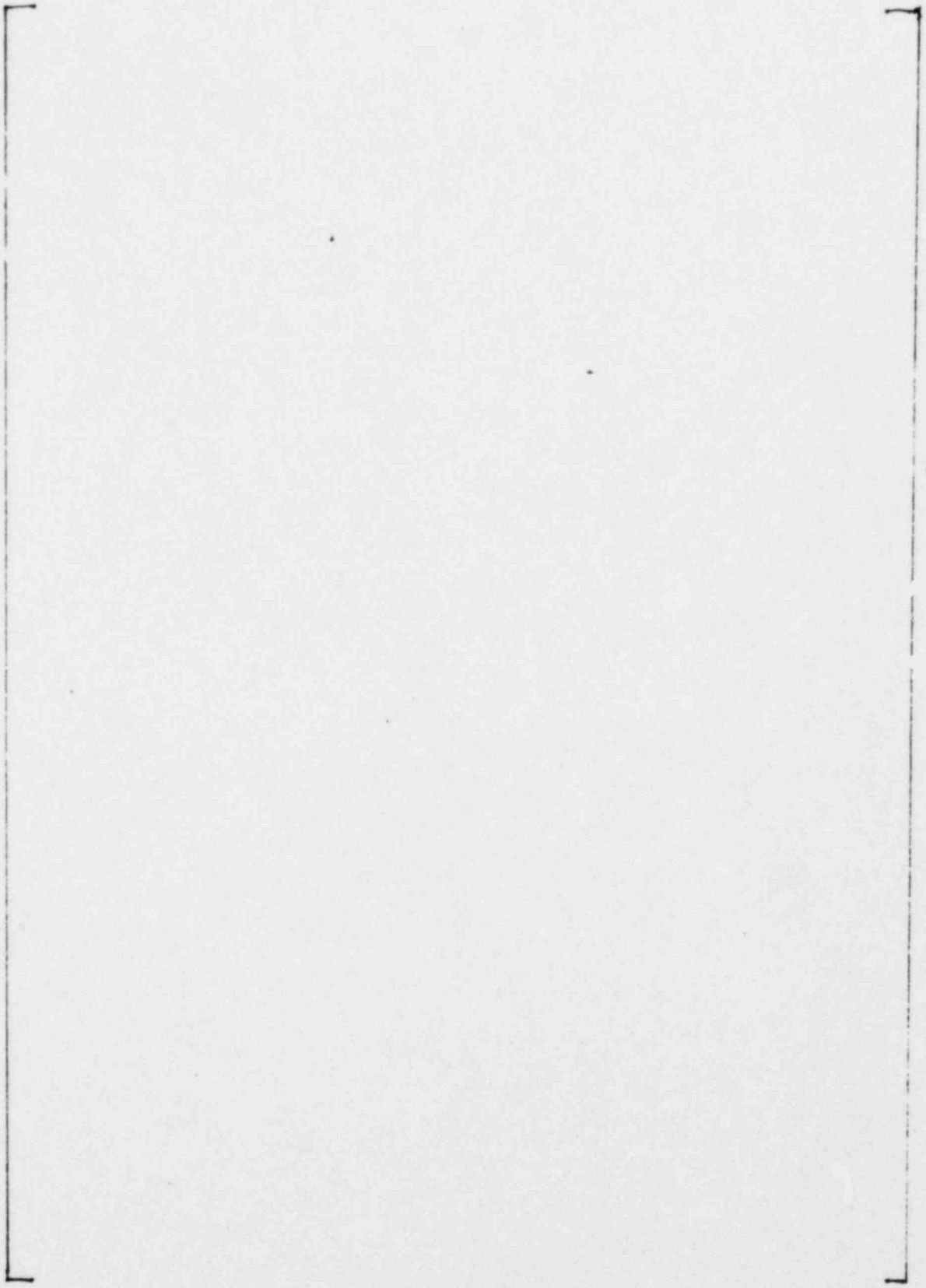

a,b,c,e

FIGURE 11.8-140 CASE NO. 8 SURFACE STRESS TIME HISTORY.

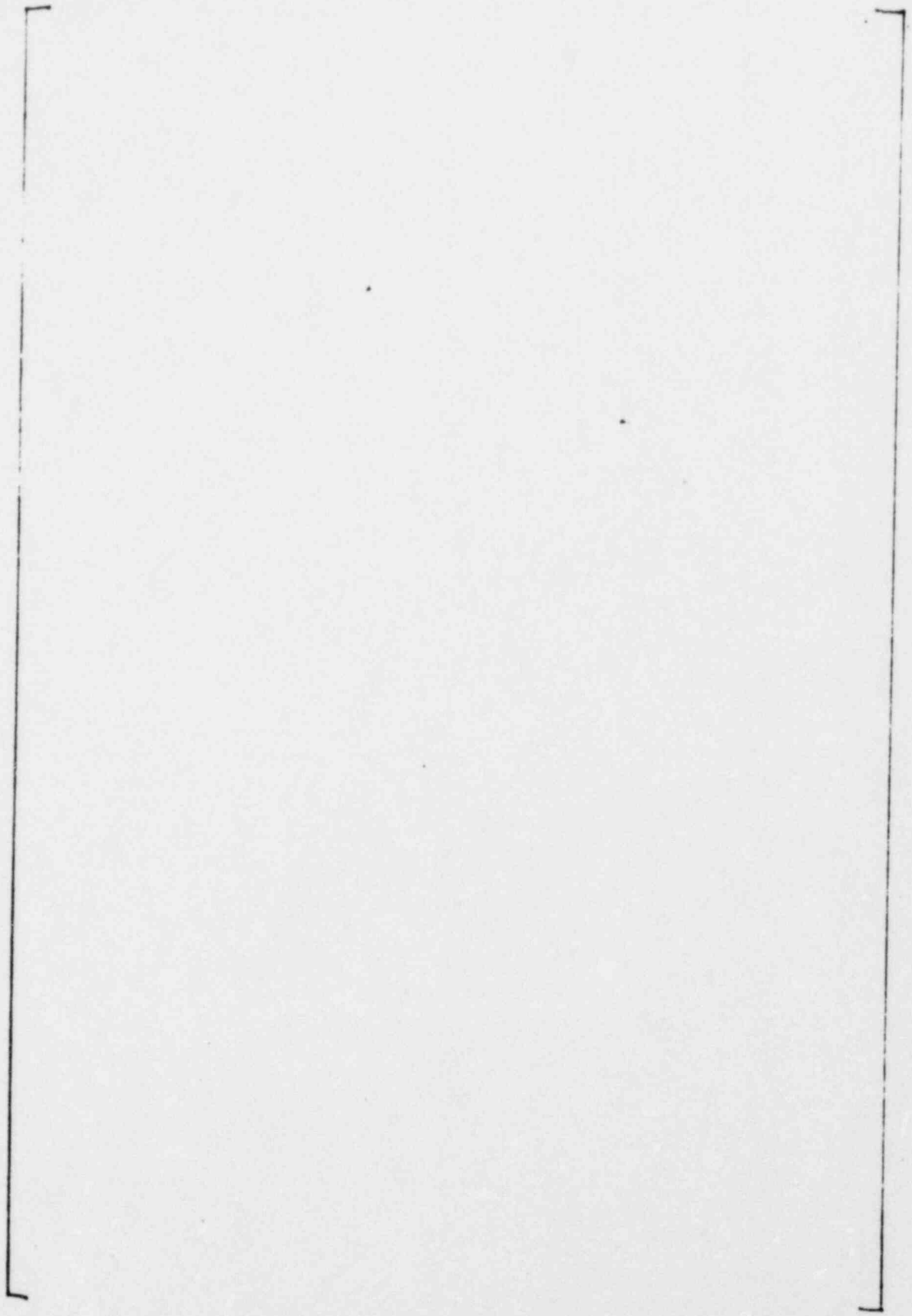

a,b,c,e

FIGURE 11.B-141 CASE NO. 9 SURFACE STRESS TIME HISTORY.

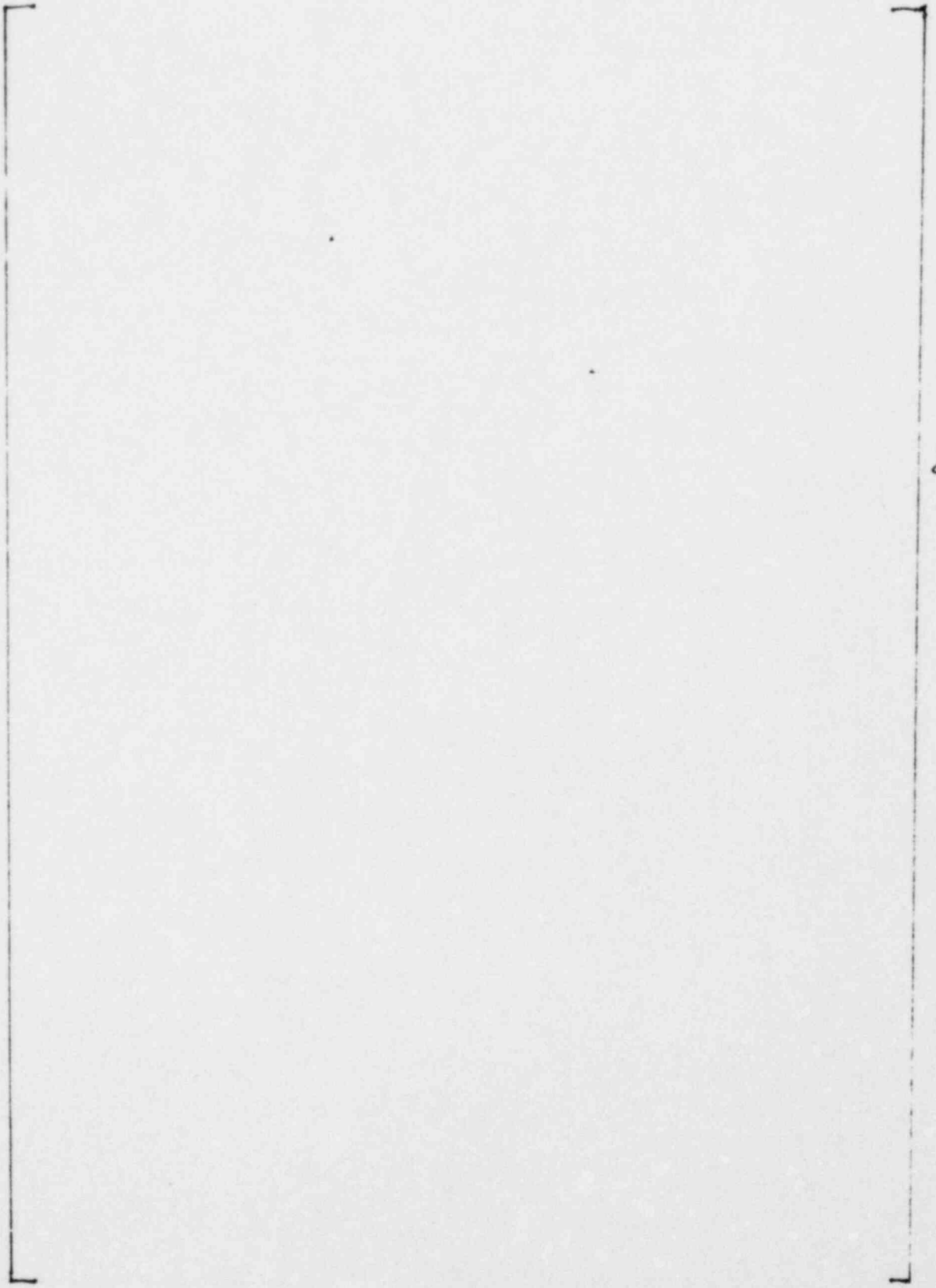

a,b,c,e

FIGURE 11.8-142 CASE NO. 10 SURFACE STRESS TIME HISTORY.

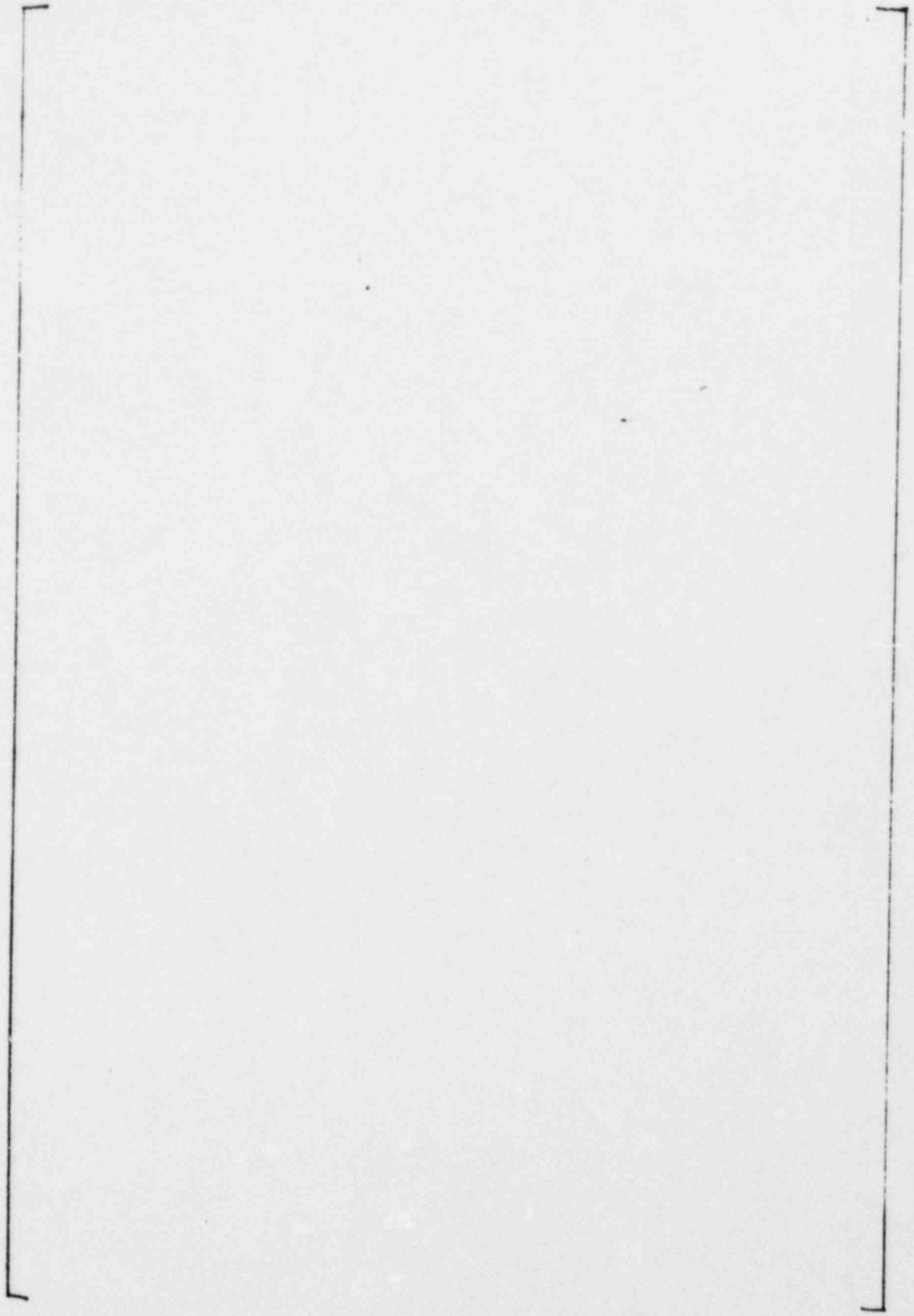

a,b,c,e

FIGURE 11.8-143 CASE NO. 11 SURFACE STRESS TIME HISTORY.

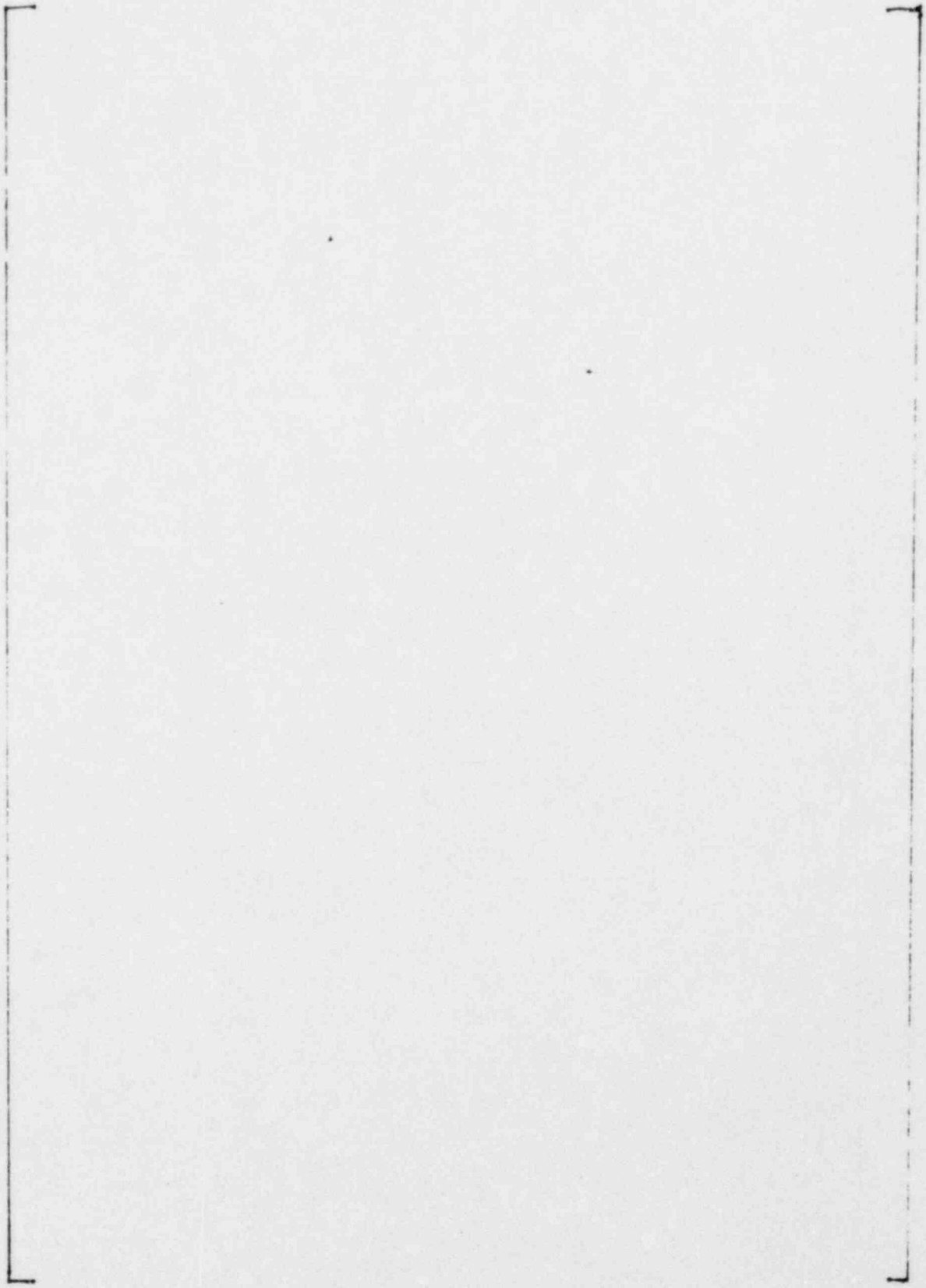

a,b,c,e

FIGURE 11.8-144 CASE NO. 12 SURFACE STRESS TIME HISTORY.

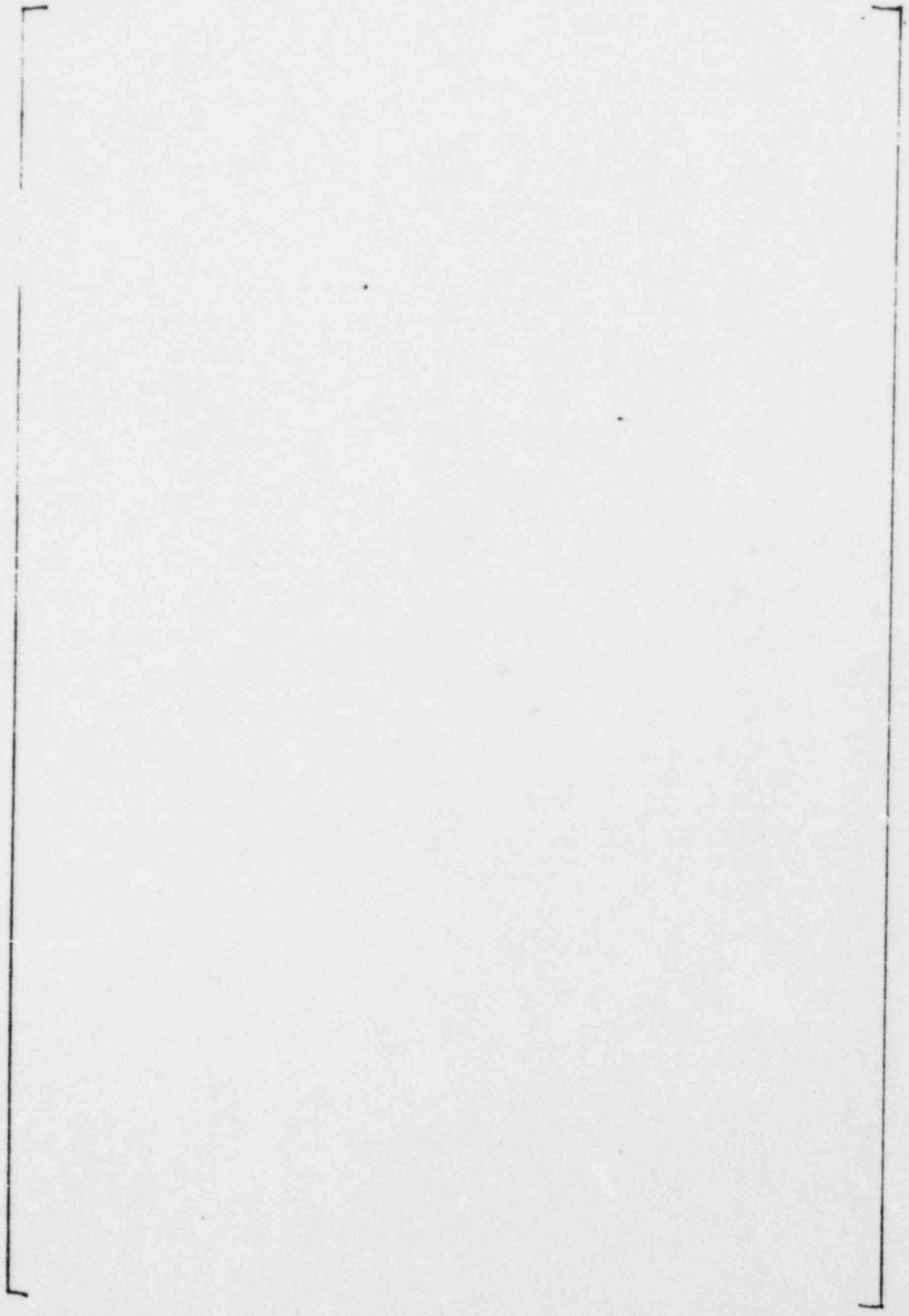

a.b.c.e

FIGURE 11.8-145 CASE NO. 13 SURFACE STRESS TIME HISTORY.

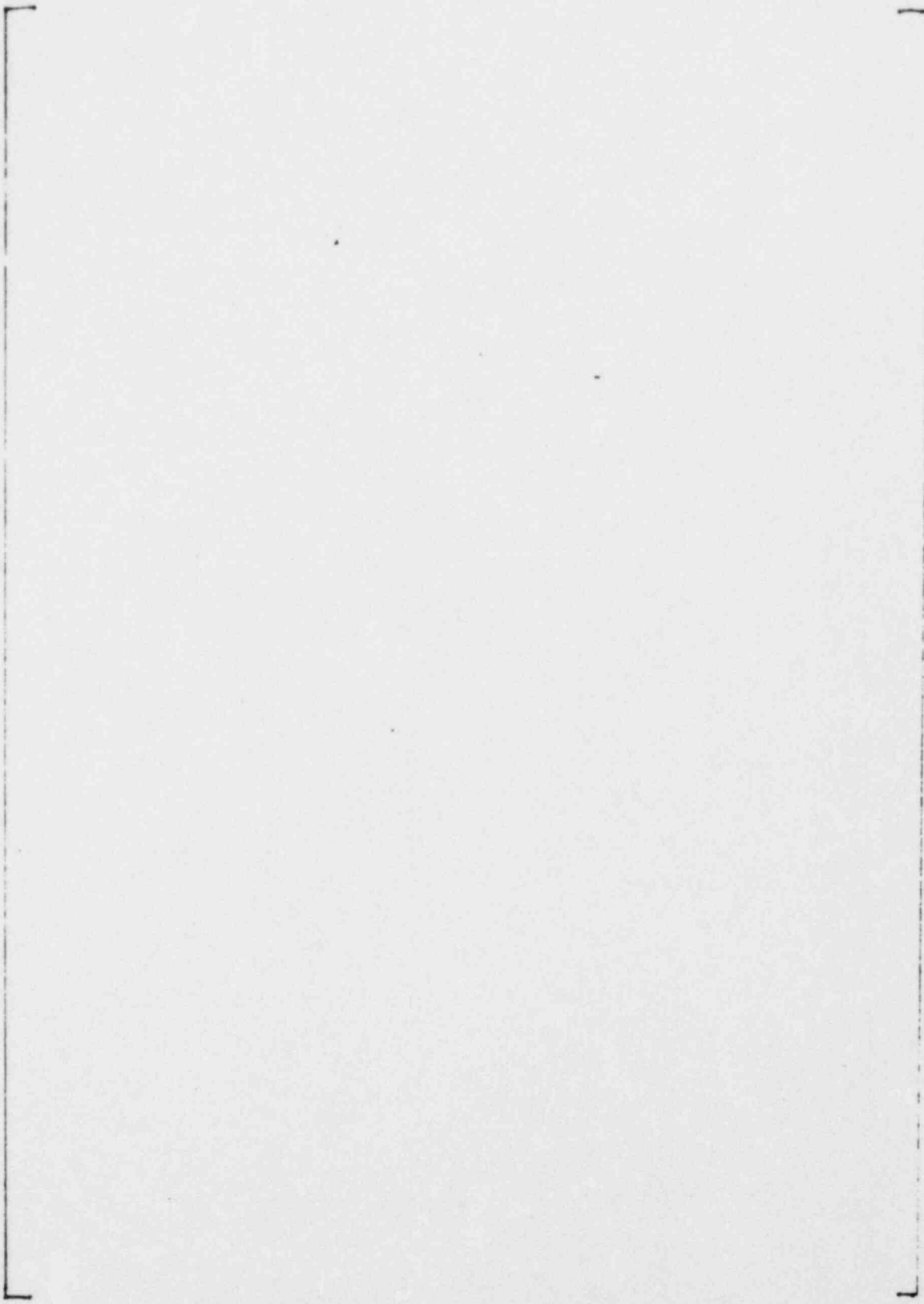

a,b,c,e

FIGURE 11.8-146 CASE NO. 14 SURFACE STRESS TIME HISTORY.

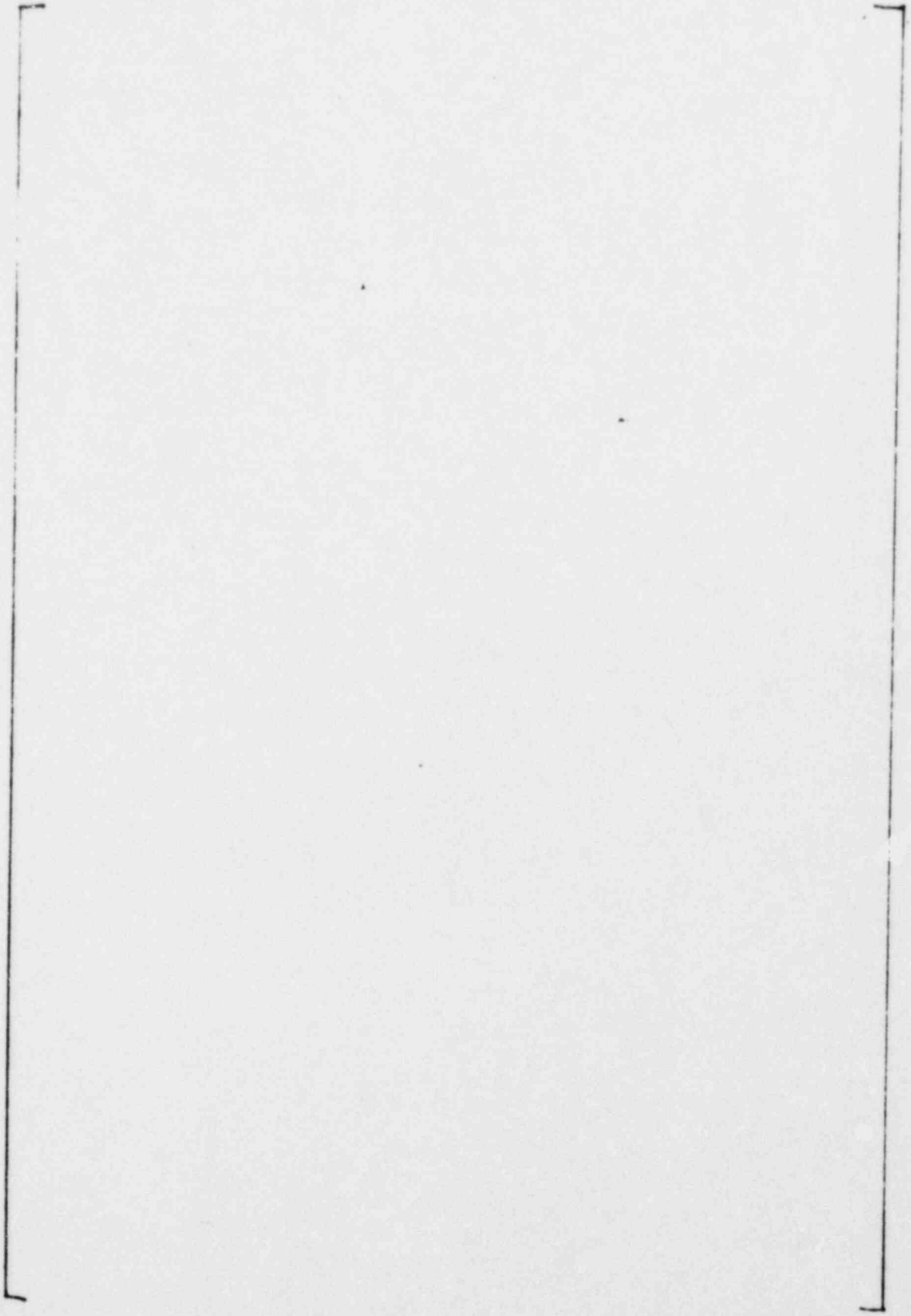

a,b,c,e

FIGURE 11.8-147 CASE NO. 15 SURFACE STRESS TIME HISTORY.

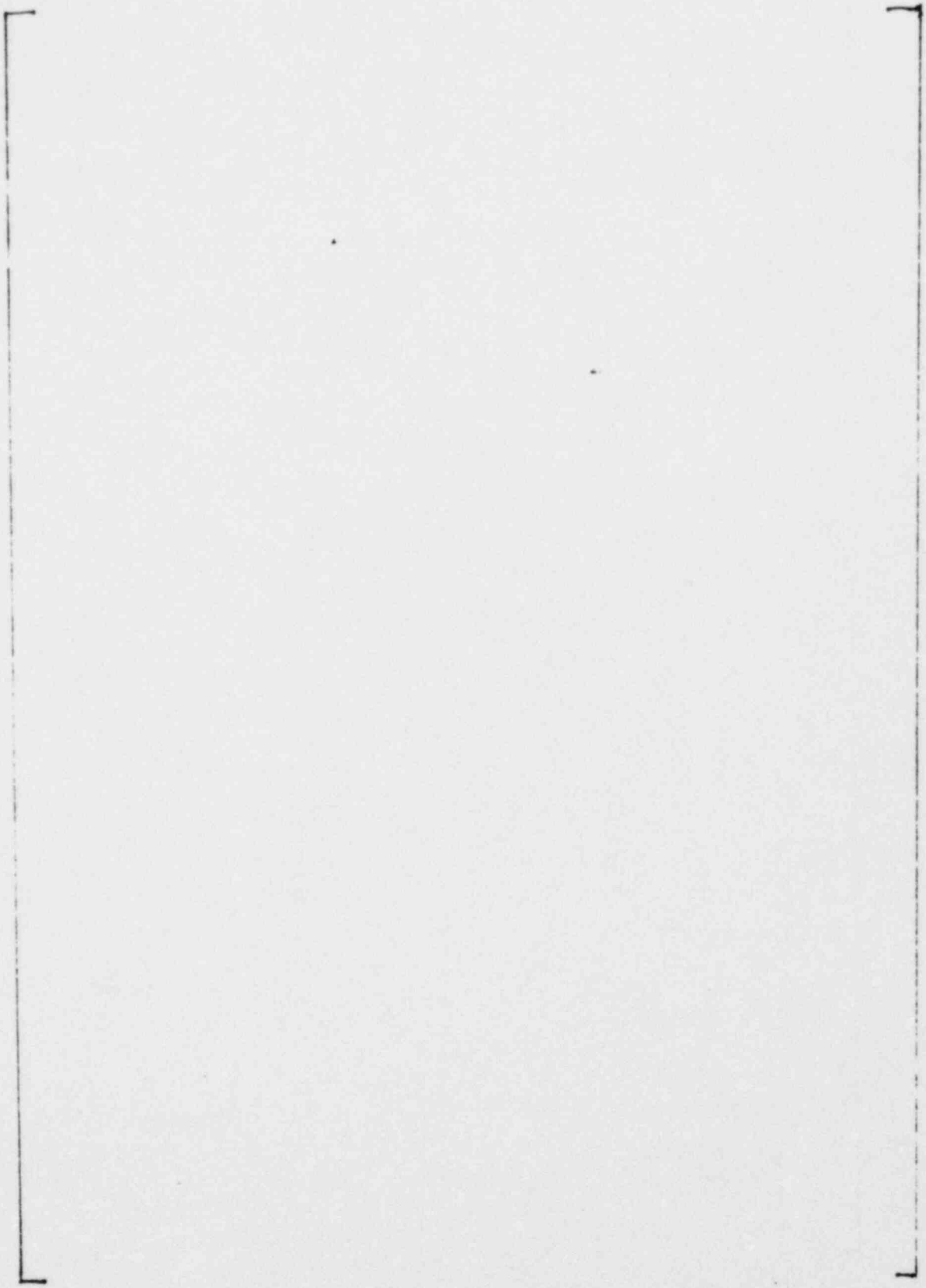

a,b,c,e

FIGURE 11.8-148 CASE NO. 16 SURFACE STRESS TIME HISTORY.

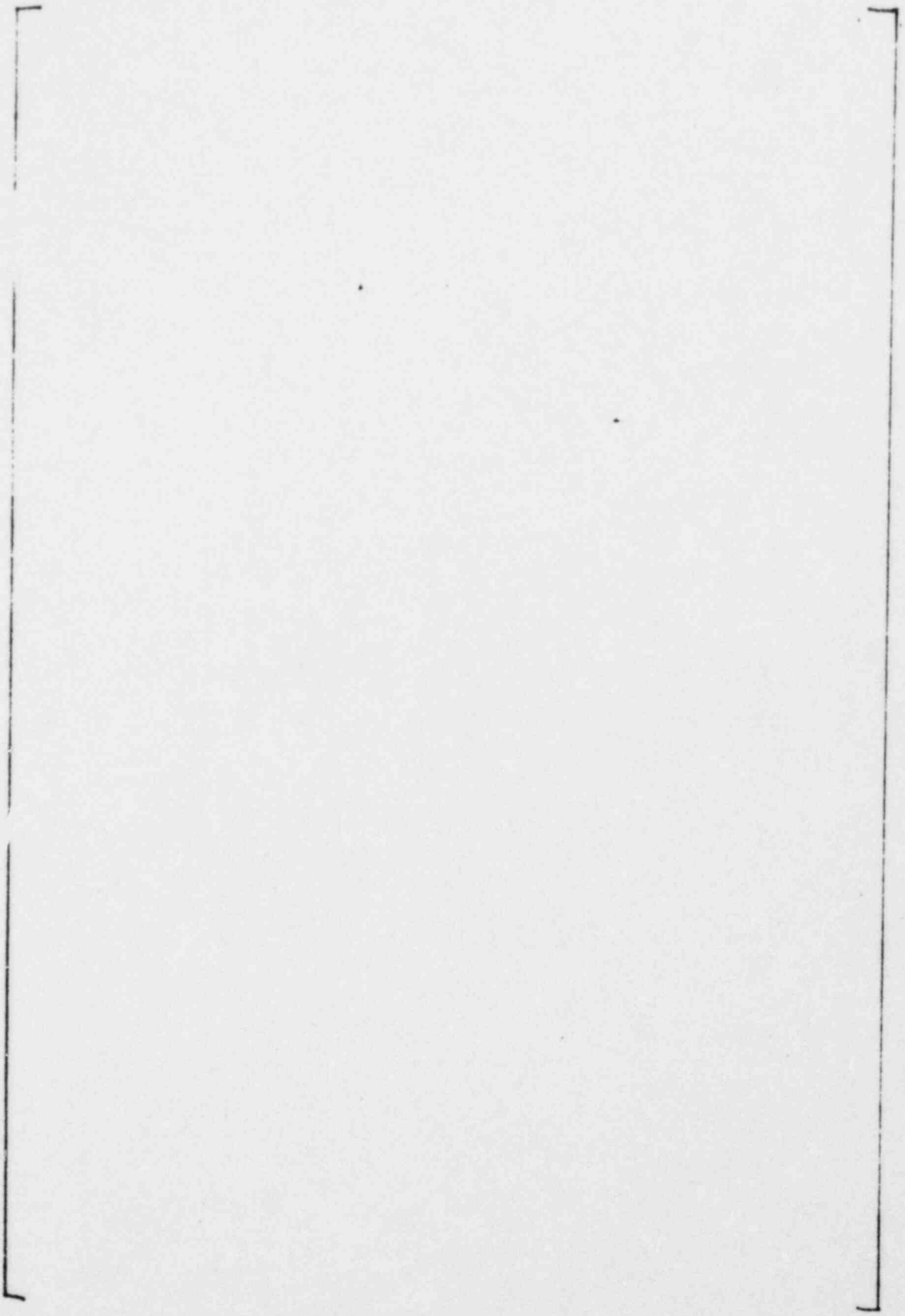

a,b,c,e

FIGURE 11.8-149 CASE NO. 17 SURFACE STRESS TIME HISTORY.

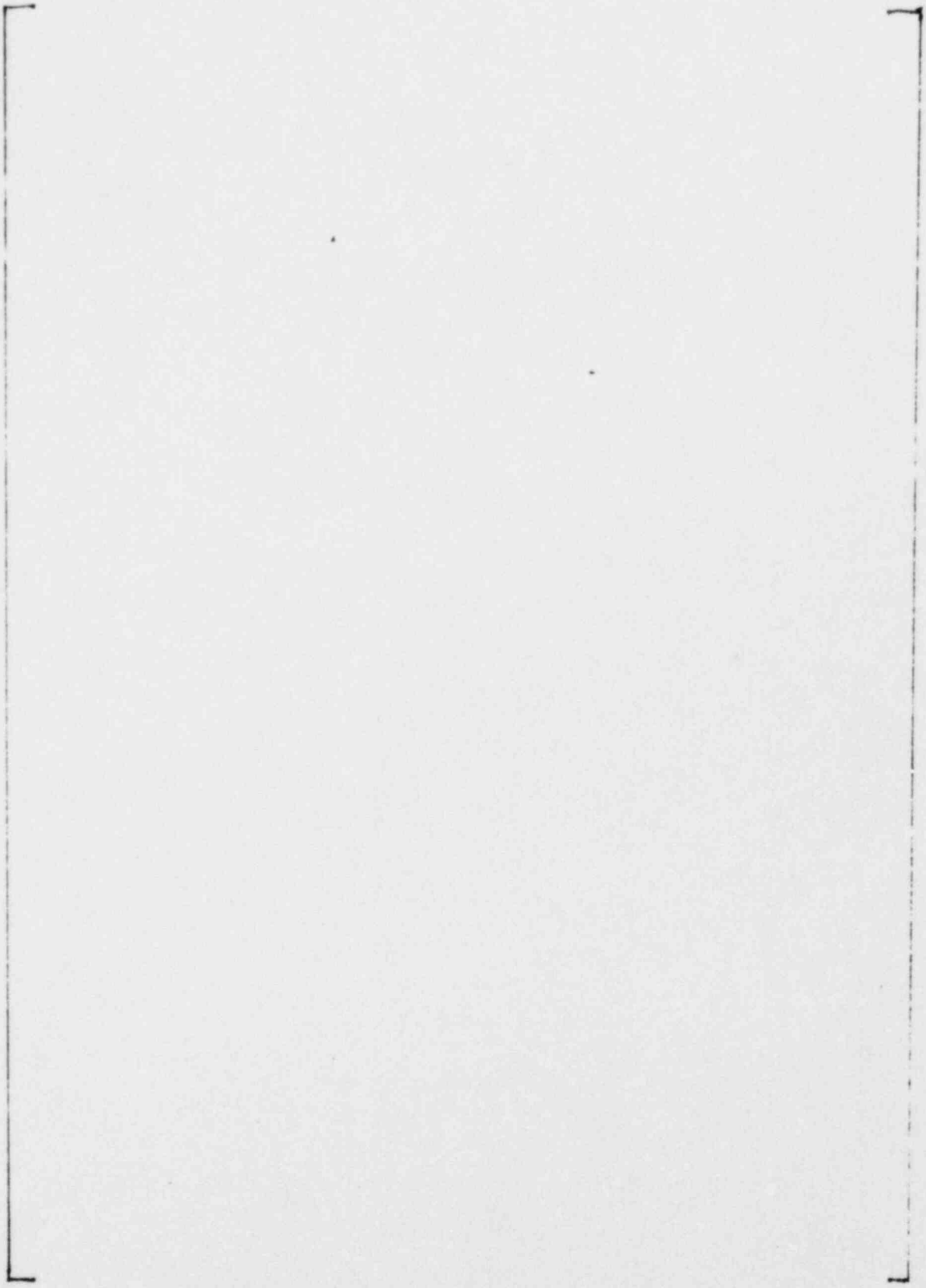

a,b,c,e

FIGURE 11.8-150 CASE NO. 18 SURFACE STRESS TIME HISTORY.

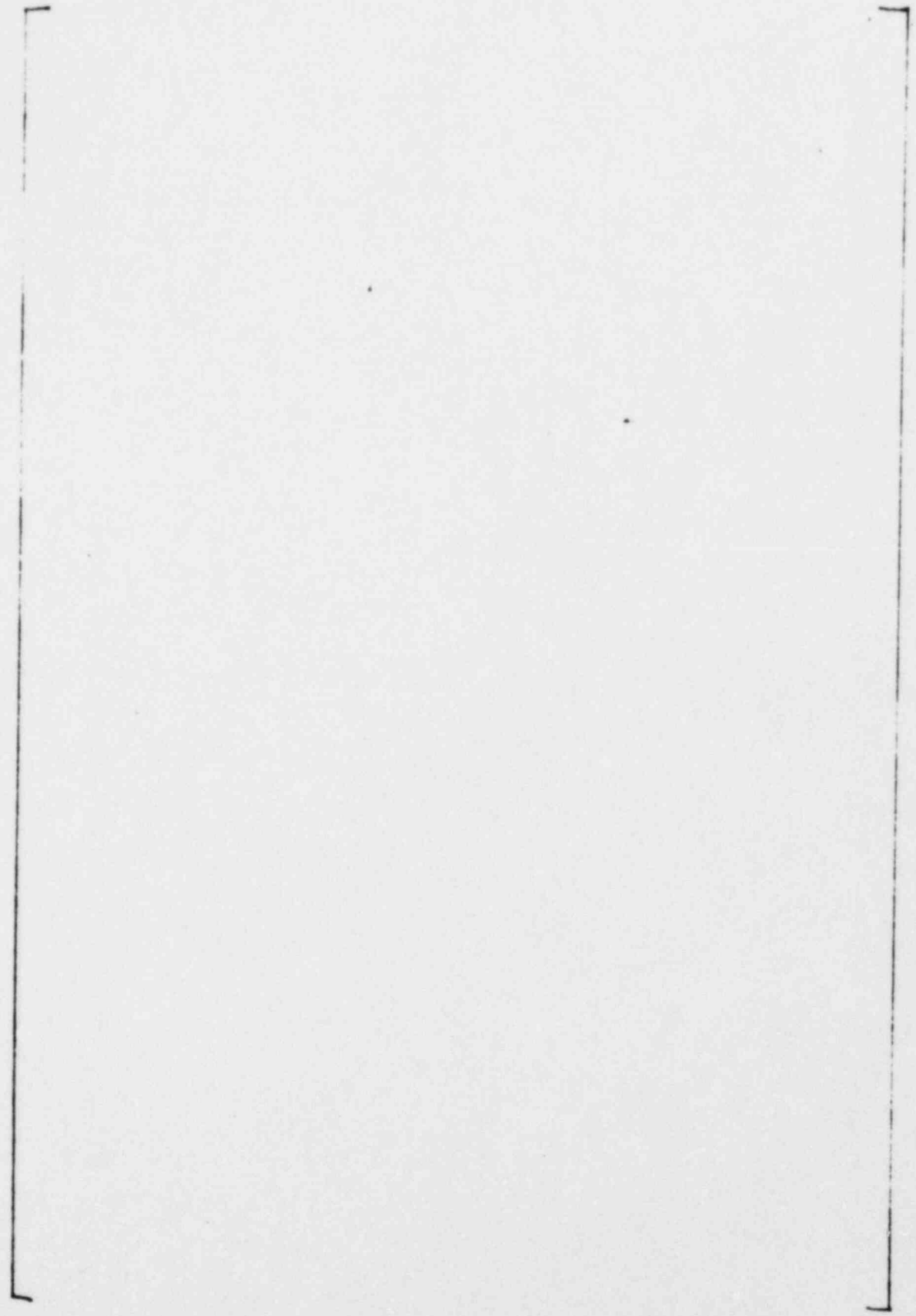

a.b.c.e

FIGURE 11.8-151 CASE NO. 19 SURFACE STRESS TIME HISTORY.

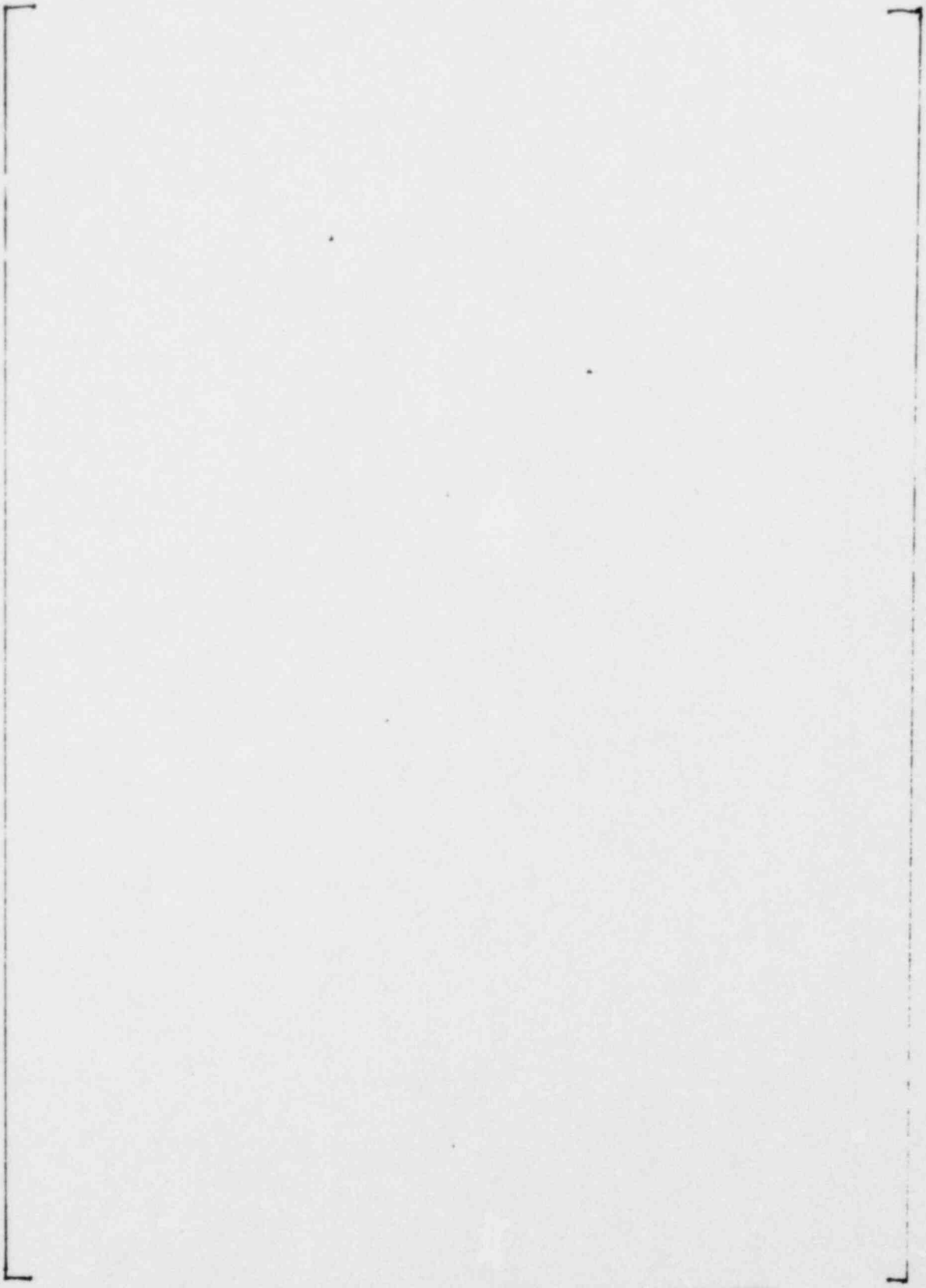

a,b,c,e

FIGURE 11.8-152 CASE NO. 20 SURFACE STRESS TIME HISTORY.

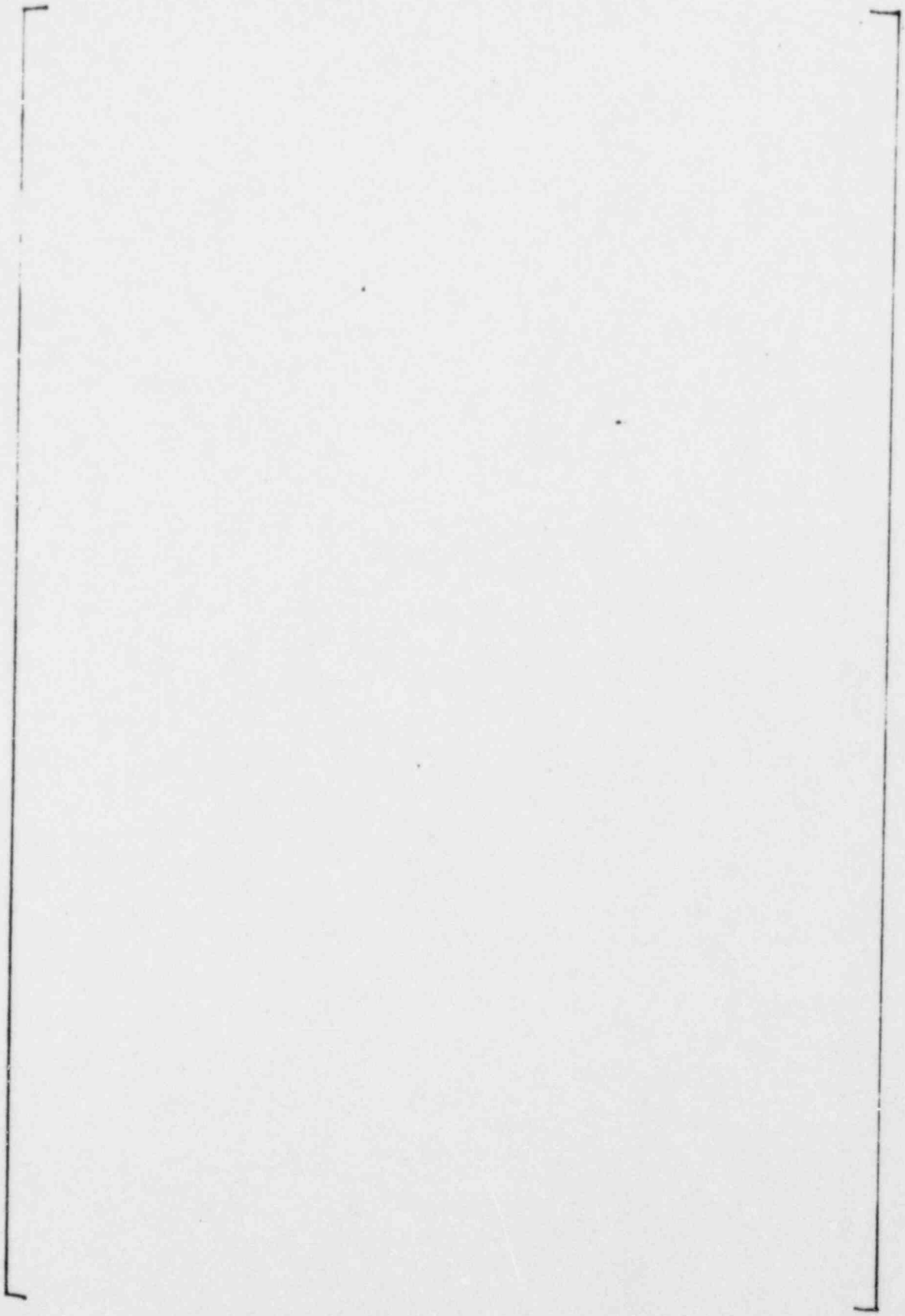

a.b.c.e

FIGURE 11.8-153 CASE NO. 21 SURFACE STRESS TIME HISTORY.

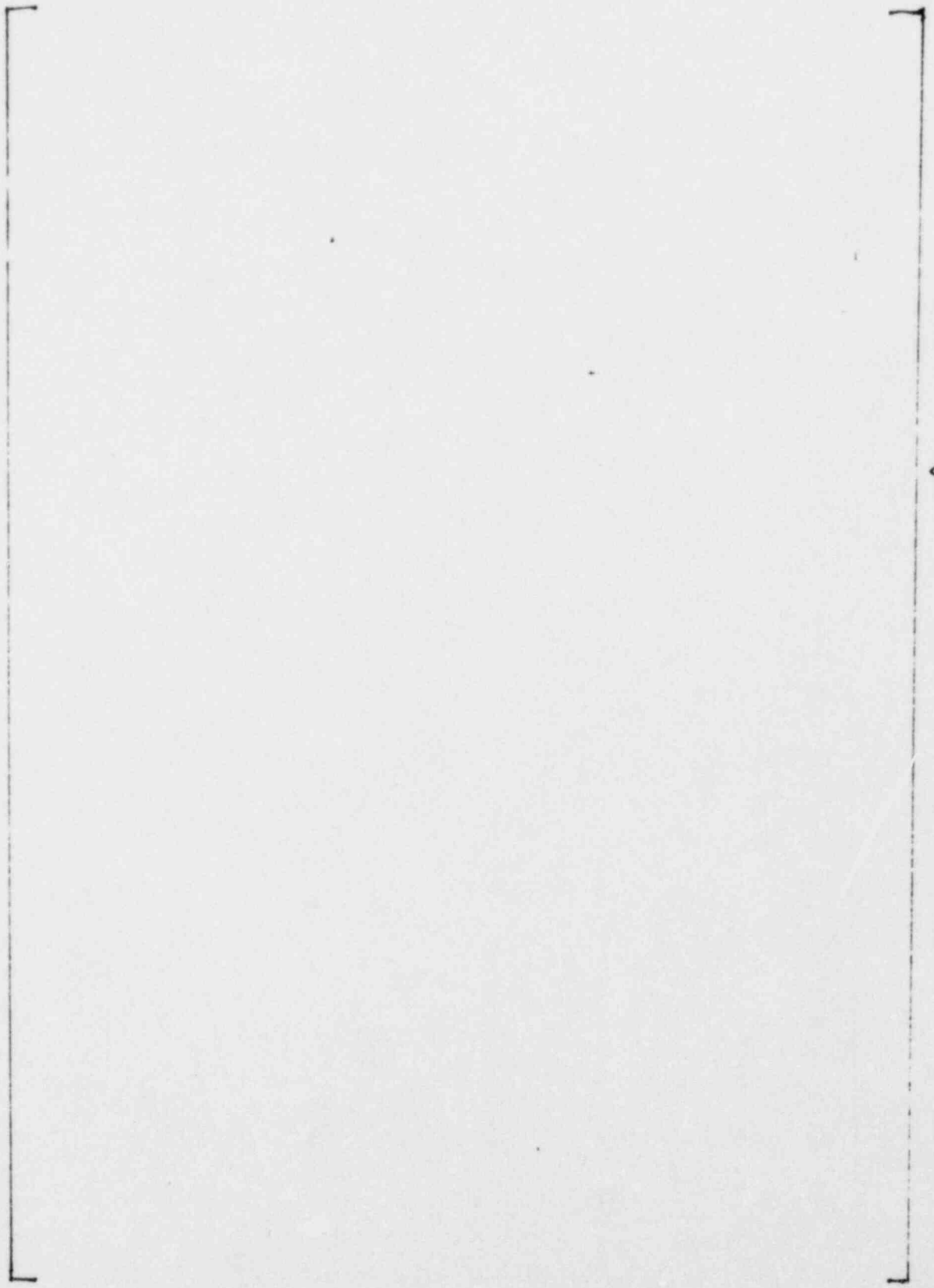

a,b,c,e

FIGURE 11.8-154 CASE NO. 22 SURFACE STRESS TIME HISTORY.

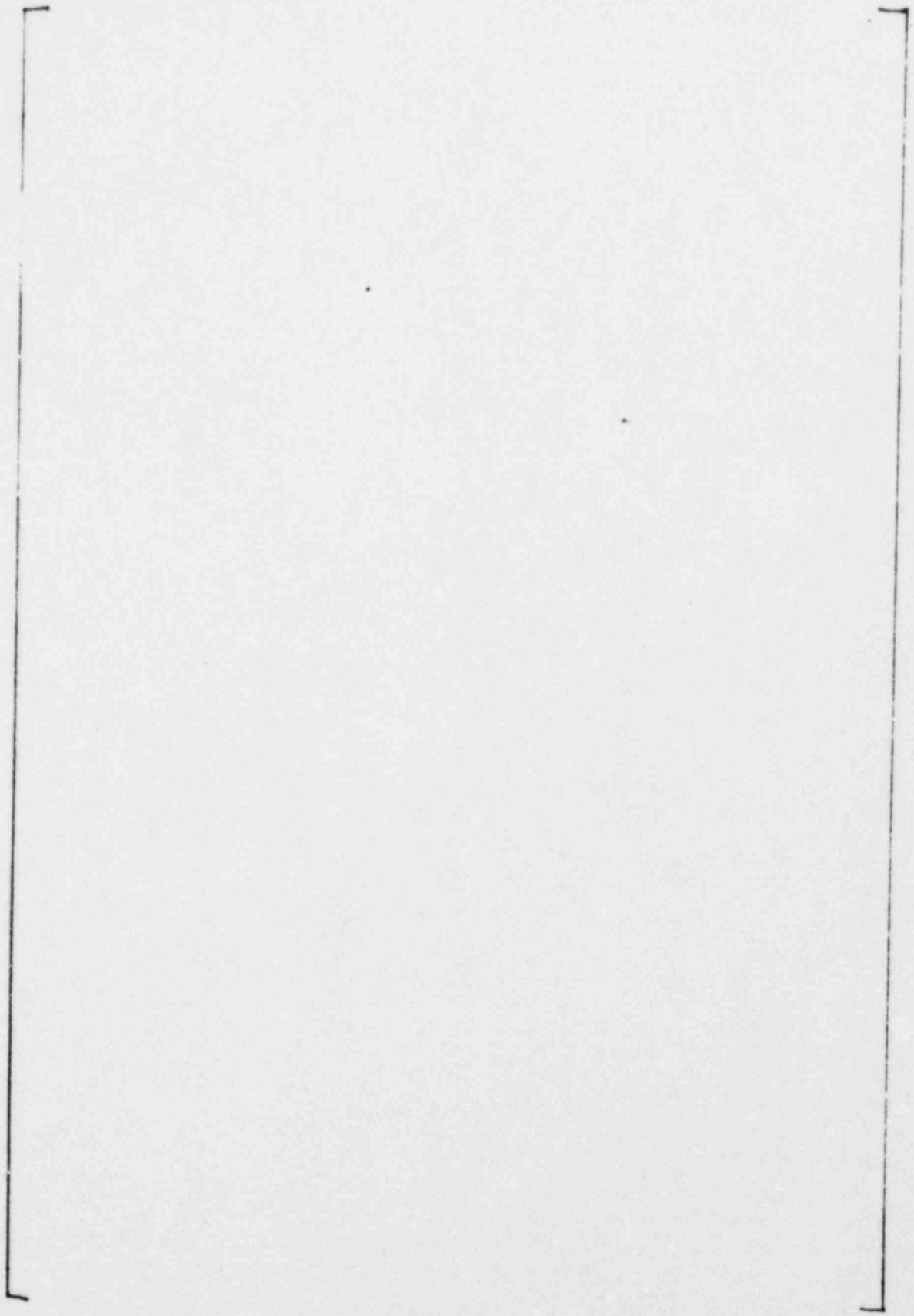

a,b,c,e

FIGURE 11.8-155 CASE NO. 23 SURFACE STRESS TIME HISTORY.

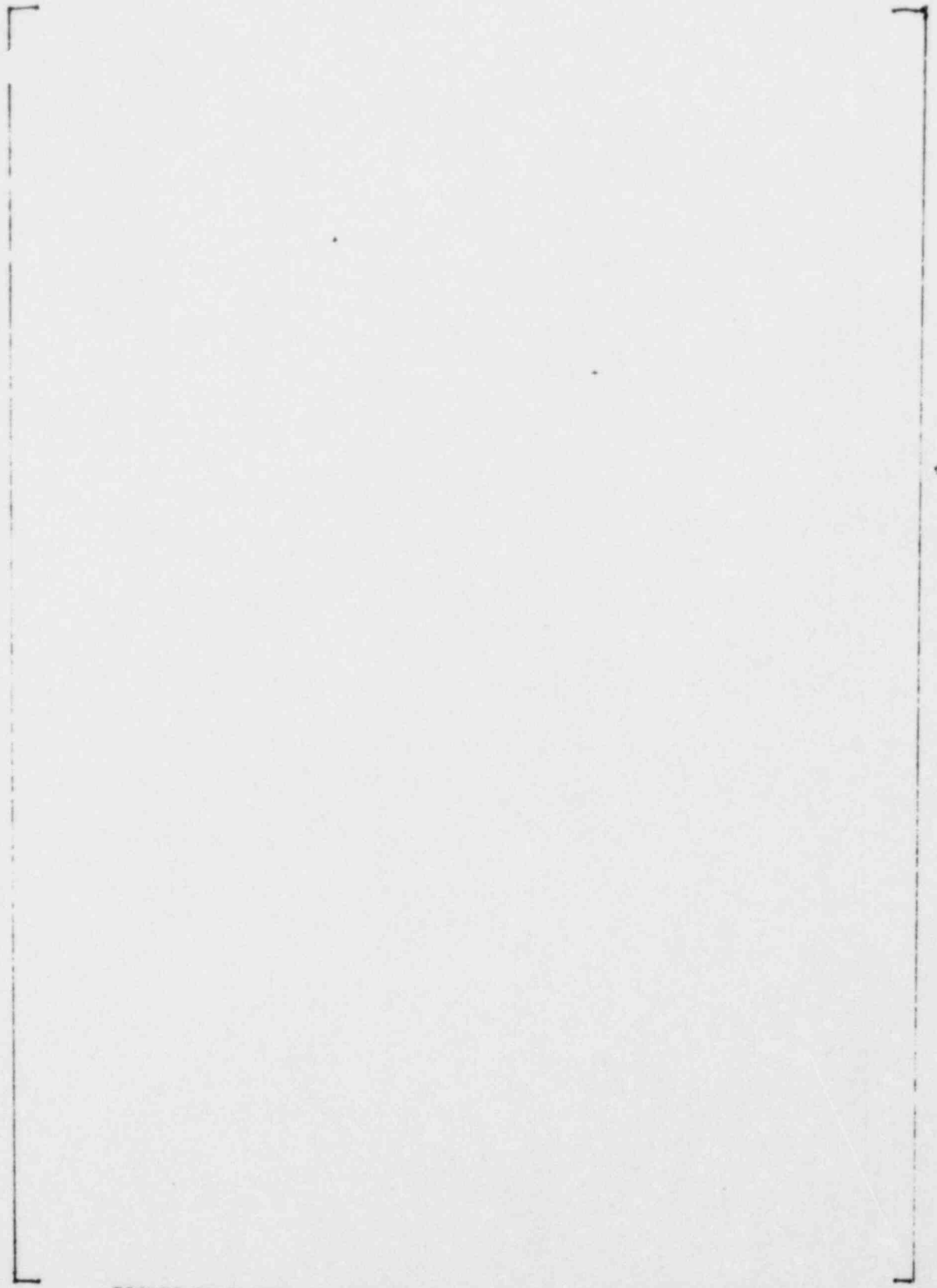

a,b,c,e

FIGURE 11.8-156 CASE NO. 24 SURFACE STRESS TIME HISTORY.

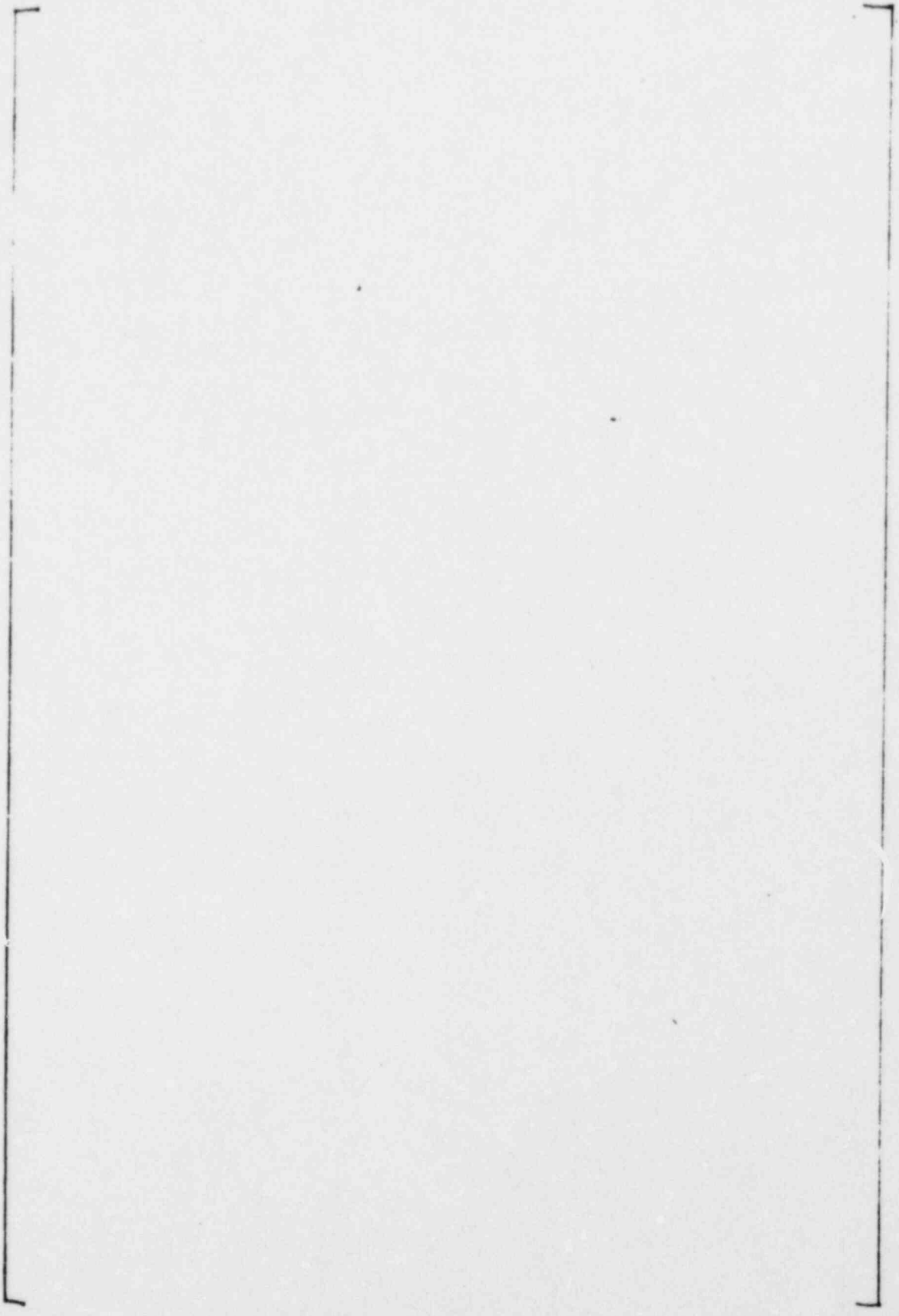

a,b,c,e

FIGURE 11.8-157 CASE NO. 25 SURFACE STRESS TIME HISTORY.

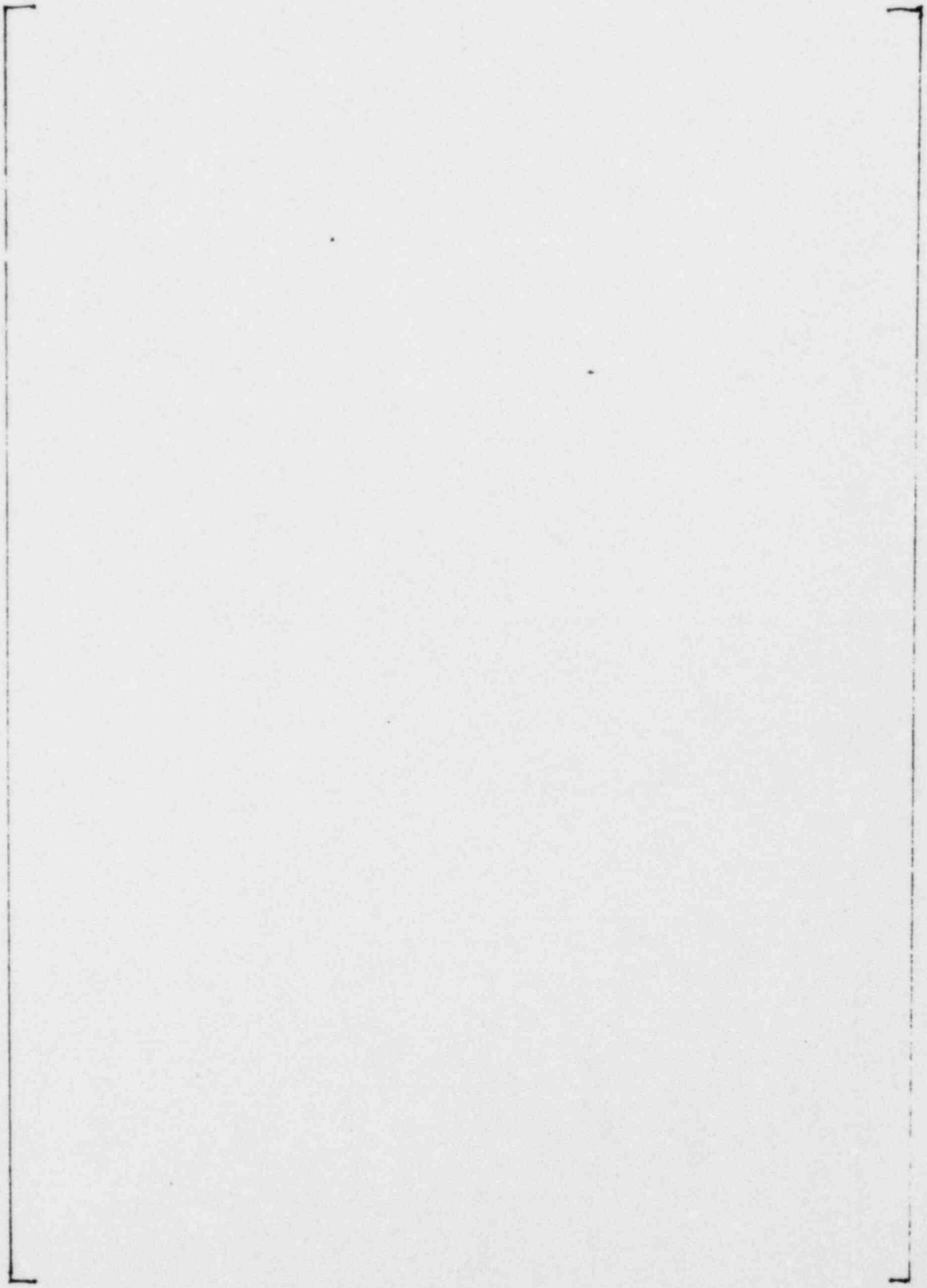

a,b,c,e

FIGURE 11.8-158 CASE NO. 26 SURFACE STRESS TIME HISTORY.

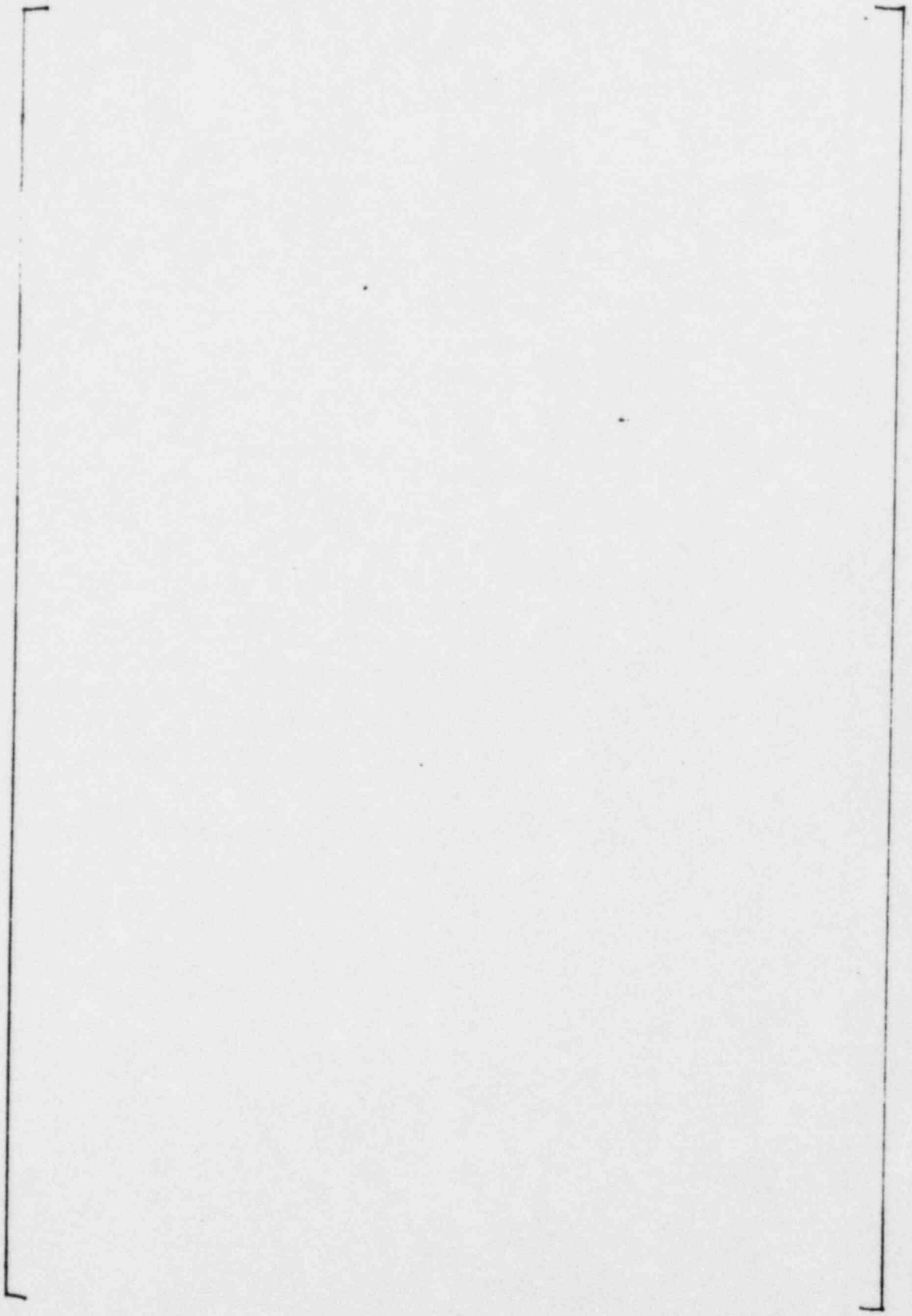

a,b,c,e

FIGURE 11.8-159 CASE NO. 27 SURFACE STRESS TIME HISTORY.

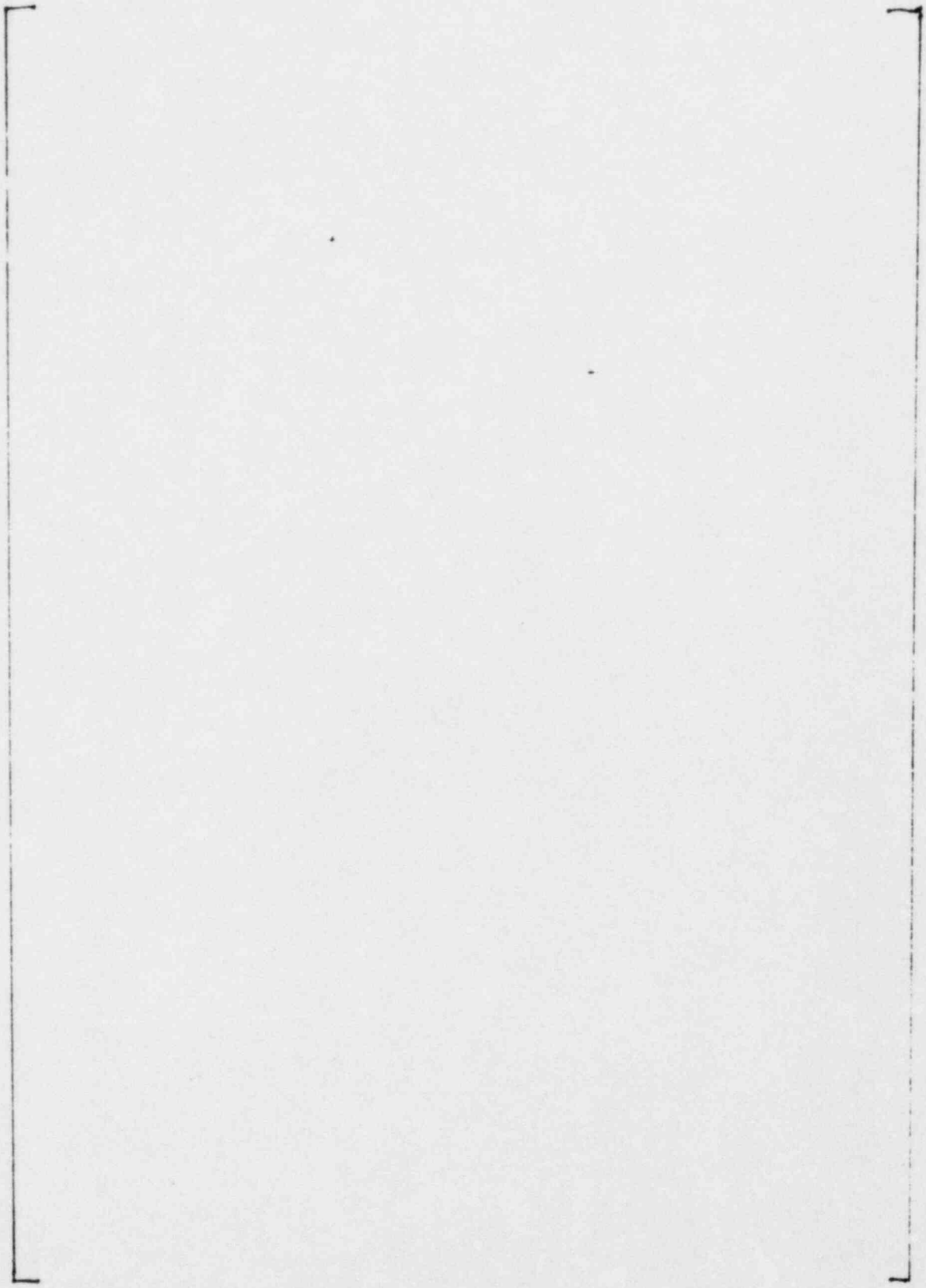

a,b,c,e

FIGURE 11.8-160 CASE NO. 28 SURFACE STRESS TIME HISTORY.

a,b,c,e

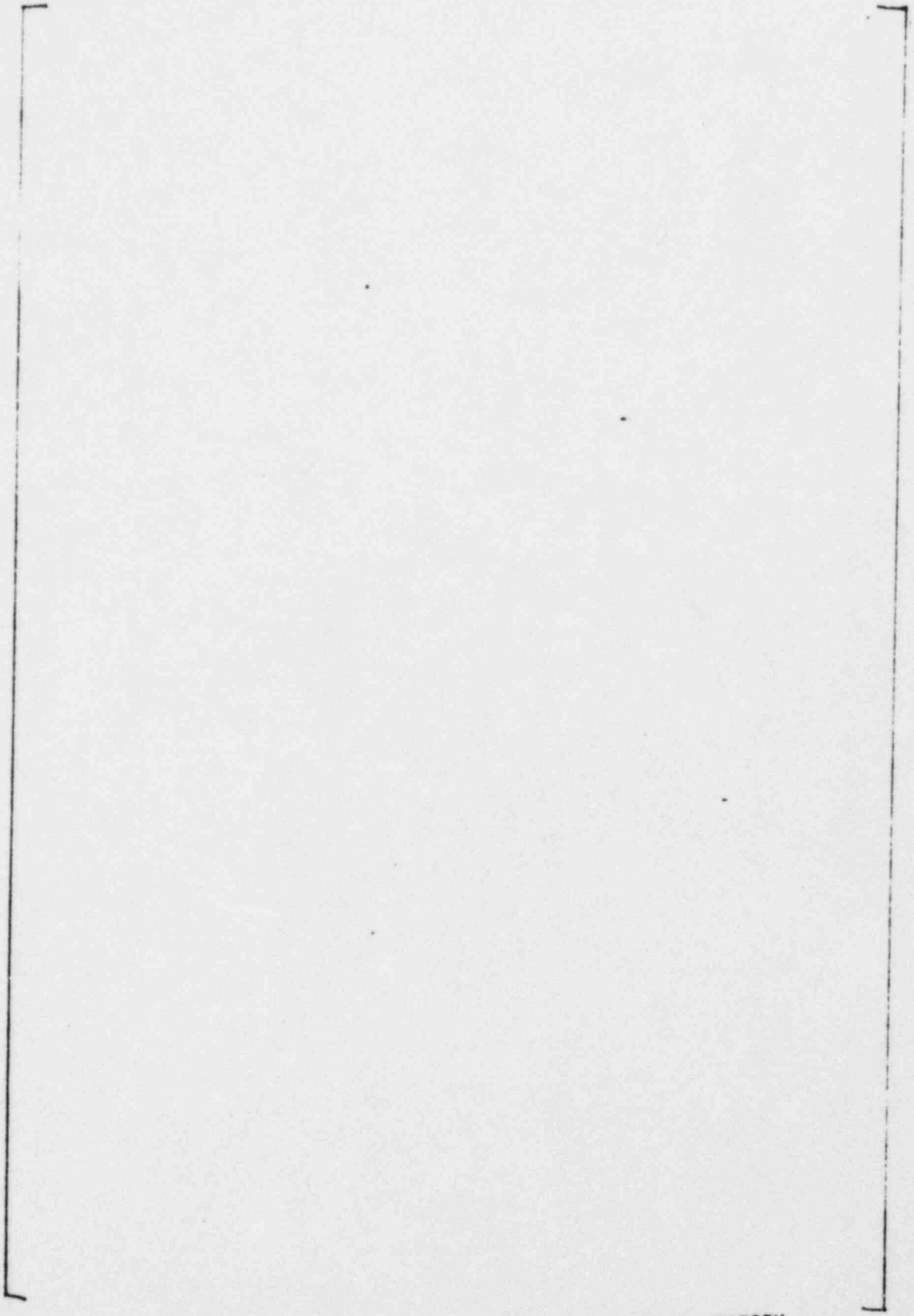

FIGURE 11.8-161 CASE NO. 29 SURFACE STRESS TIME HISTORY.

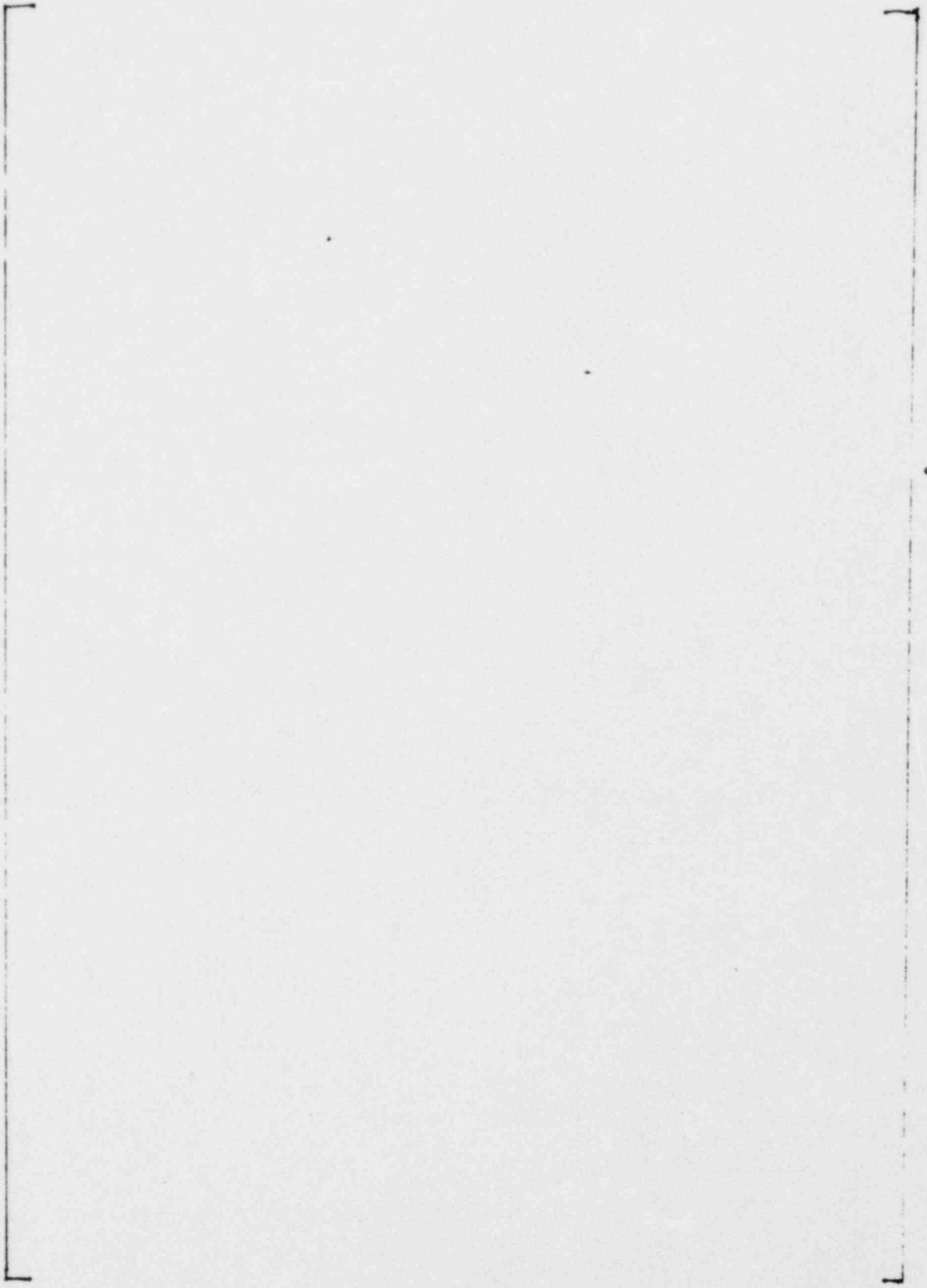

a,b,c,e

FIGURE 11.8-162 CASE NO. 30 SURFACE STRESS TIME HISTORY.

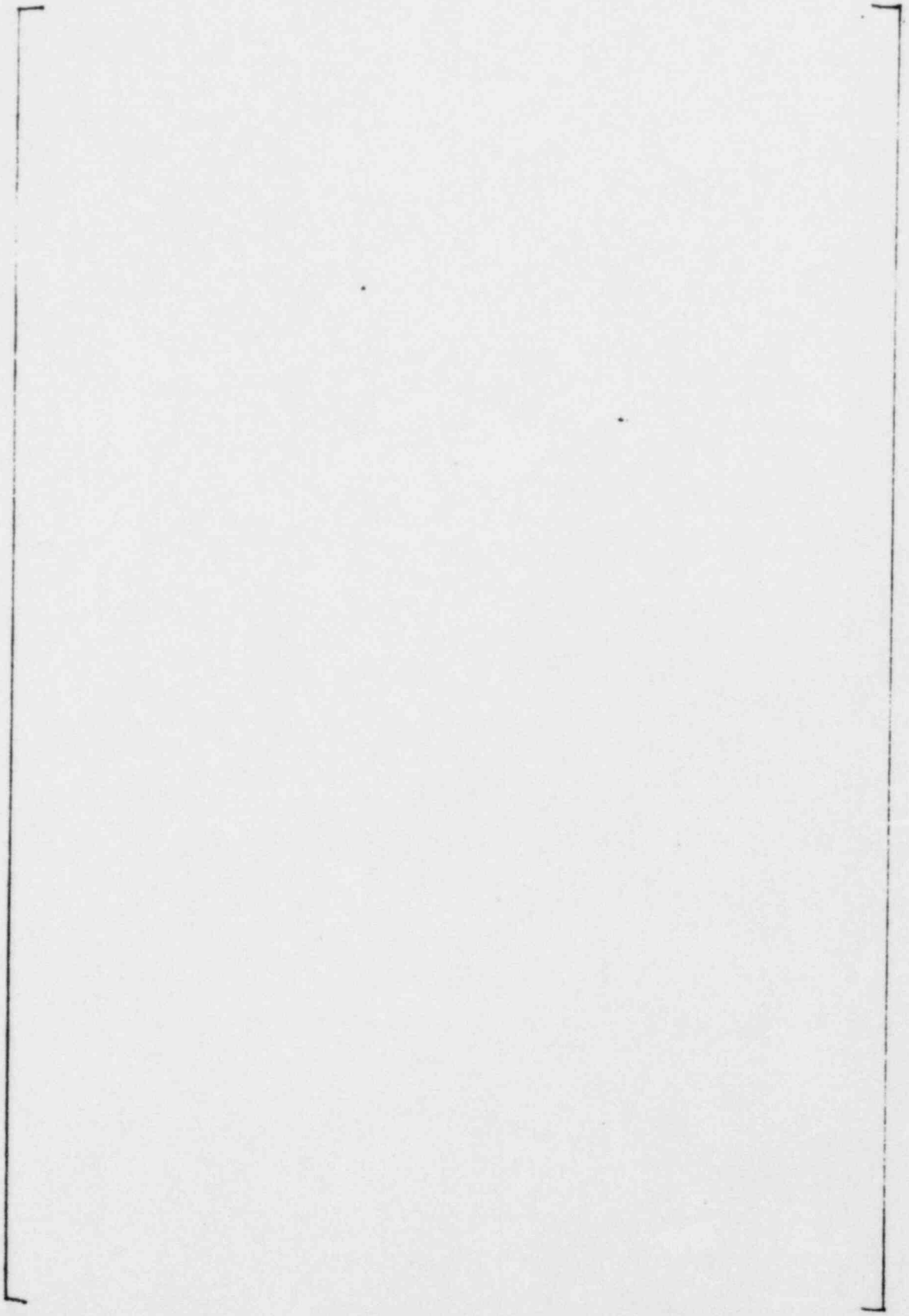

a,b,c,e

FIGURE 11.8-163 CASE NO. 31 SURFACE STRESS TIME HISTORY.

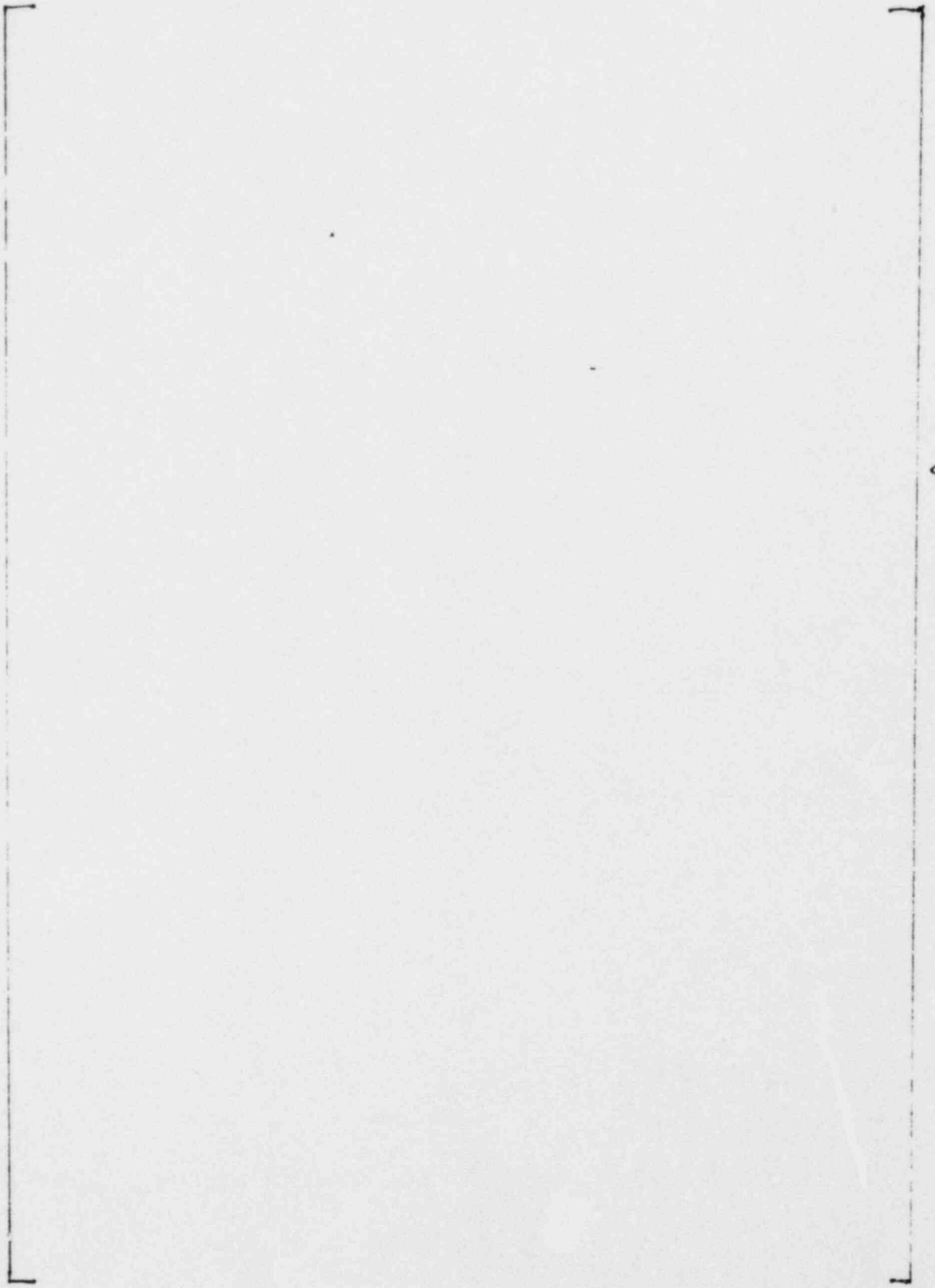

a,b,c,e

FIGURE 11.8-164 CASE NO. 32 SURFACE STRESS TIME HISTORY.

BLANK

Case No.: 33

Generic Profile:

Interface Level:_____ Angle Measured From The Bottom of Pipe

Run No.: Y6 _____

FIGURE 11.8-165 CASE NO. 33 SURFACE STRESS TIME HISTORY.

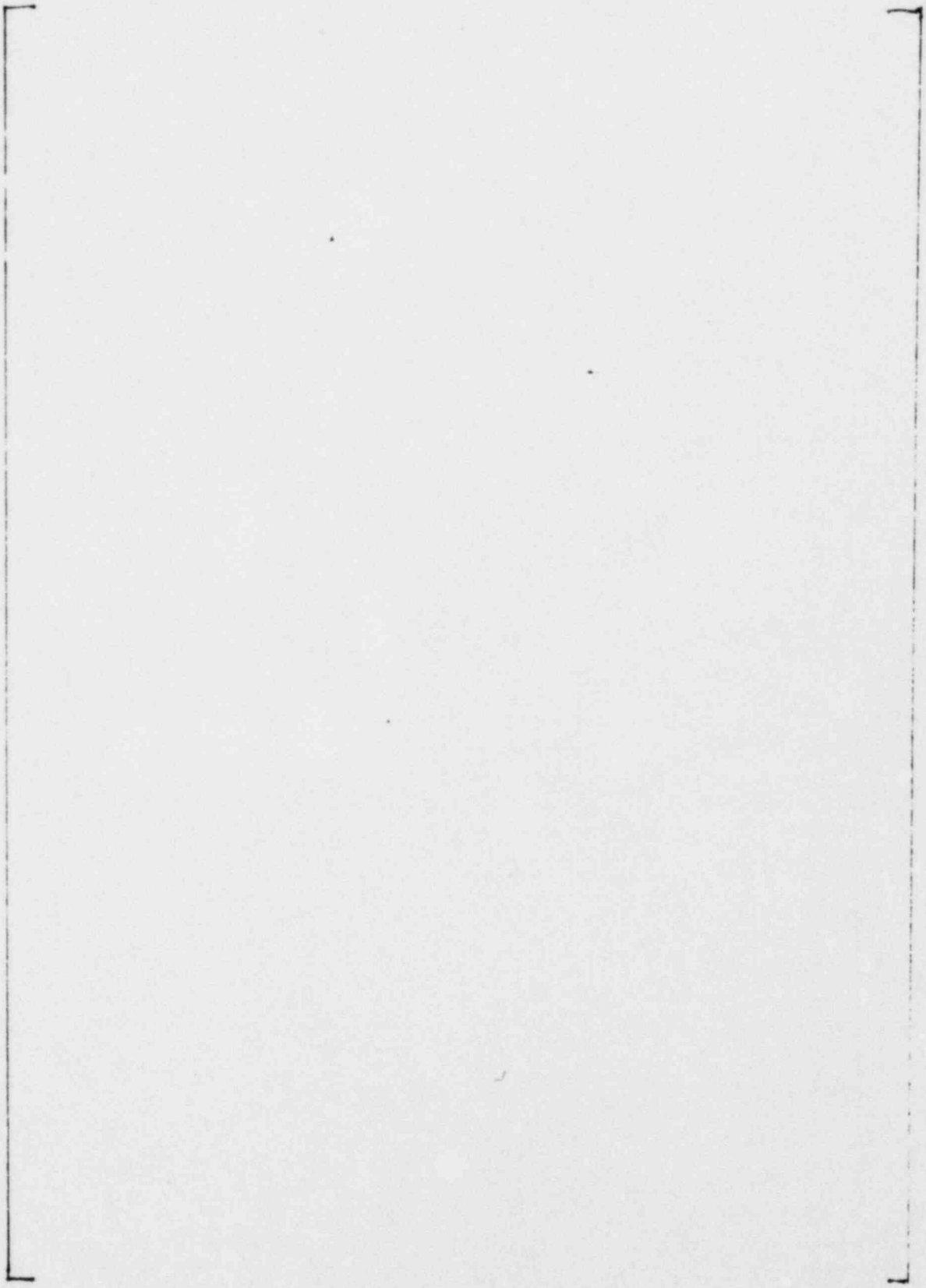

a,b,c,e

FIGURE 11.8-166 CASE NO. 34 SURFACE STRESS TIME HISTORY.

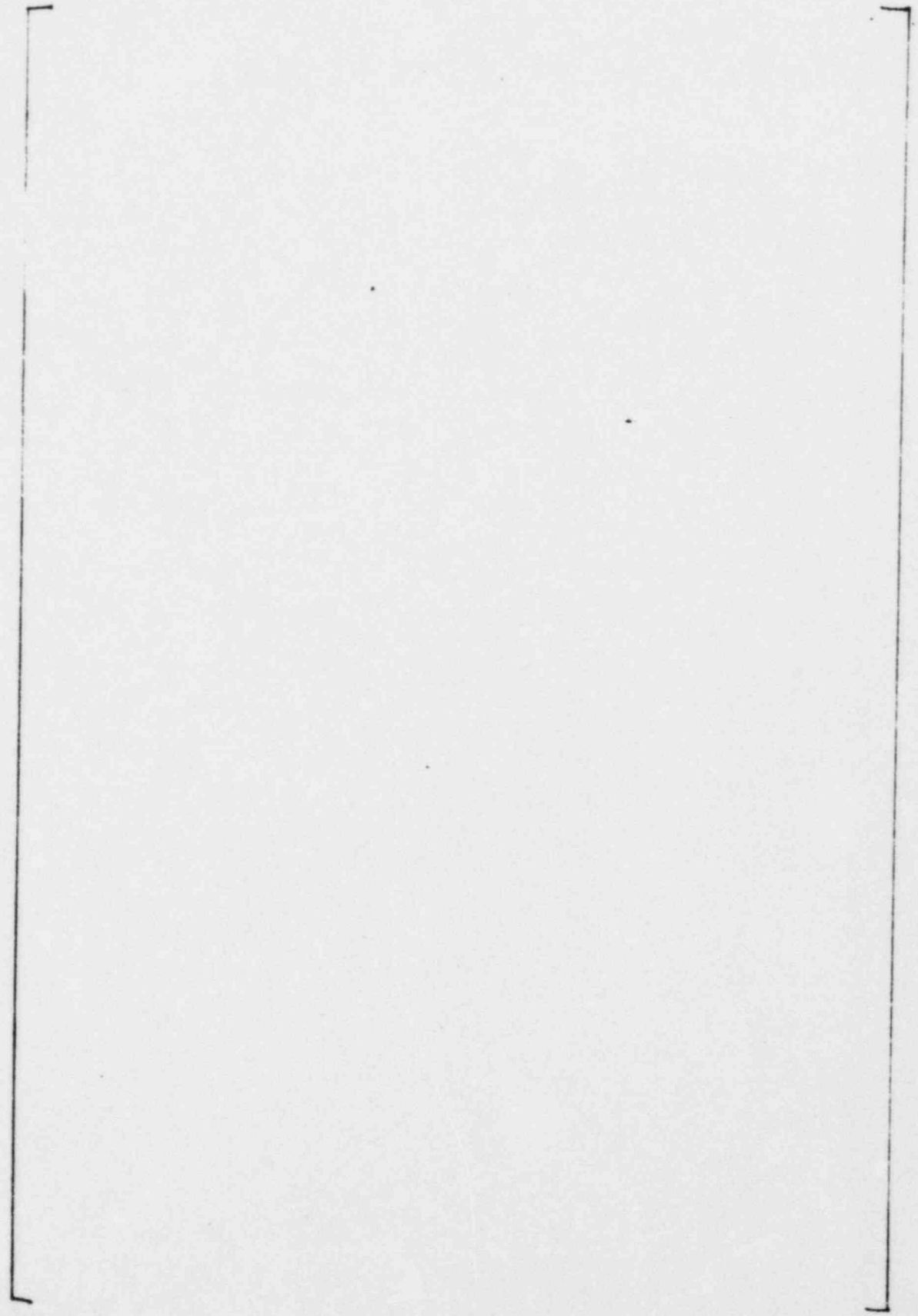

a,b,c,e

FIGURE 11.8-167 CASE NO. 35 SURFACE STRESS TIME HISTORY.

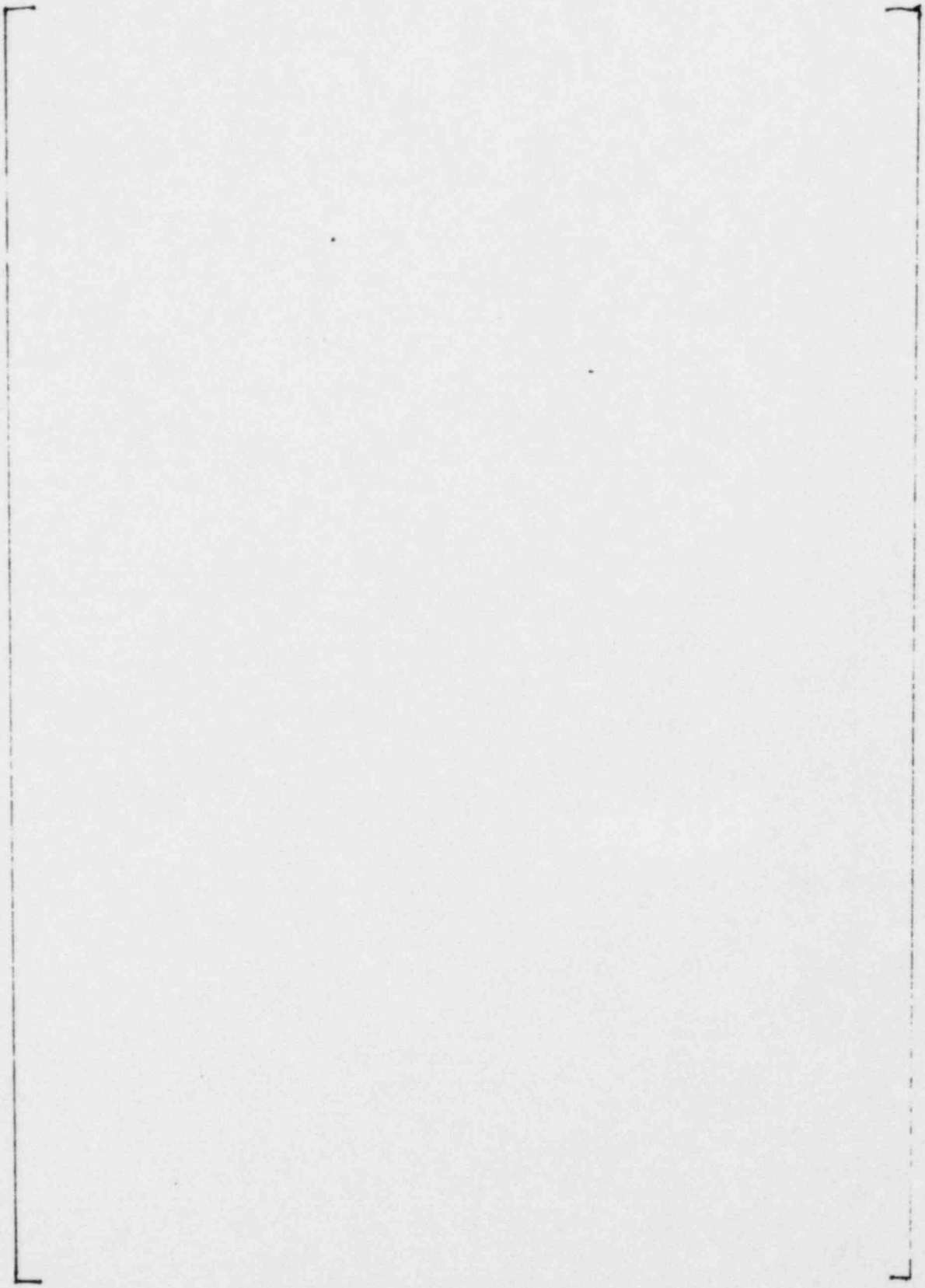

a,b,c,e

FIGURE 1.8-168 CASE NO. 36 SURFACE STRESS TIME HISTORY.

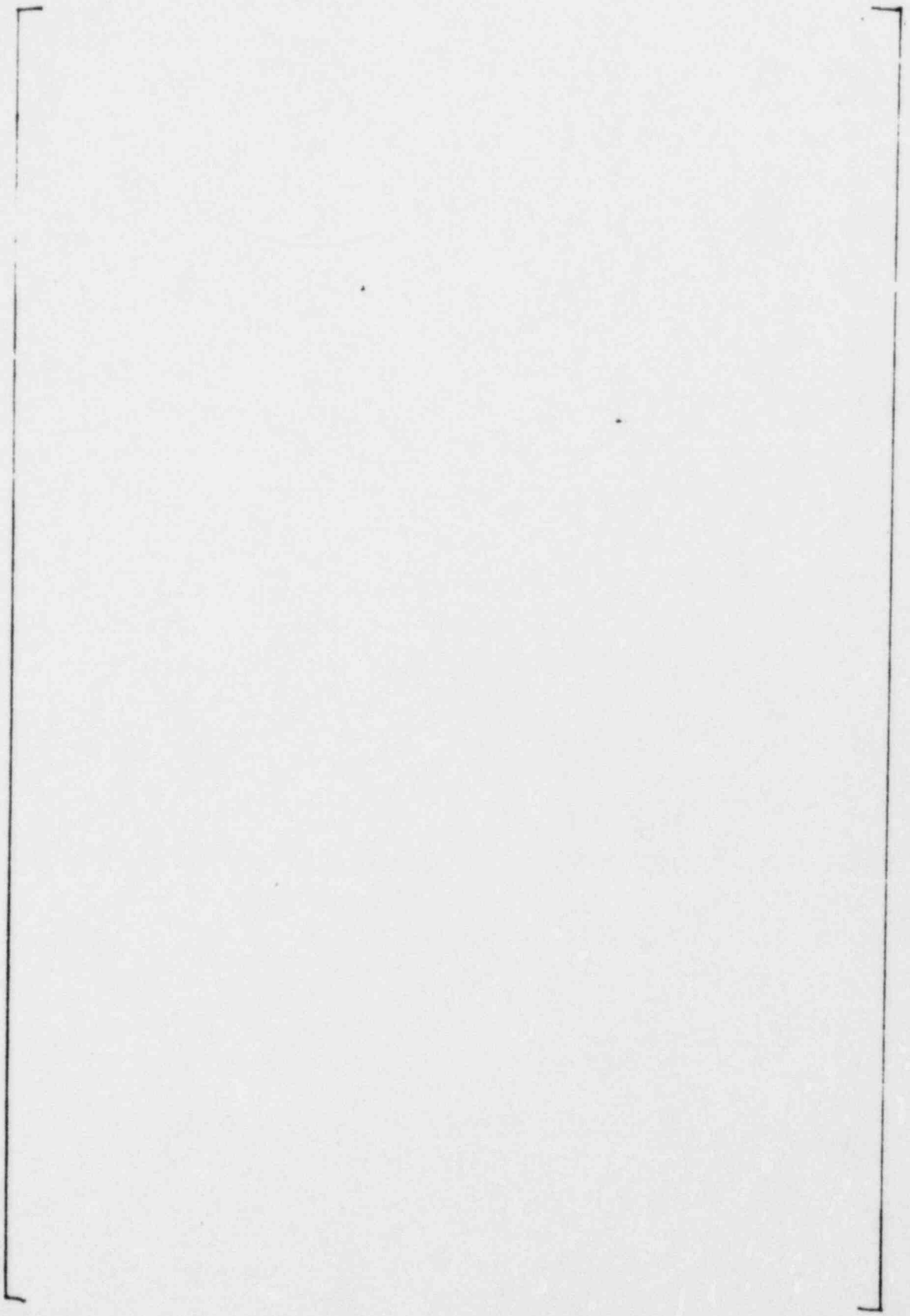

a,b,c,e

FIGURE 11.8-169 CASE NO. 37 SURFACE STRESS TIME HISTORY.

BLANK

Case No.: 38

Generic Profile:

Interface Level:_____ Angle Measured From The Bottom of Pipe

Run No.: Y6 _____

FIGURE 11.8-170 CASE NO. 38 SURFACE STRESS TIME HISTORY.

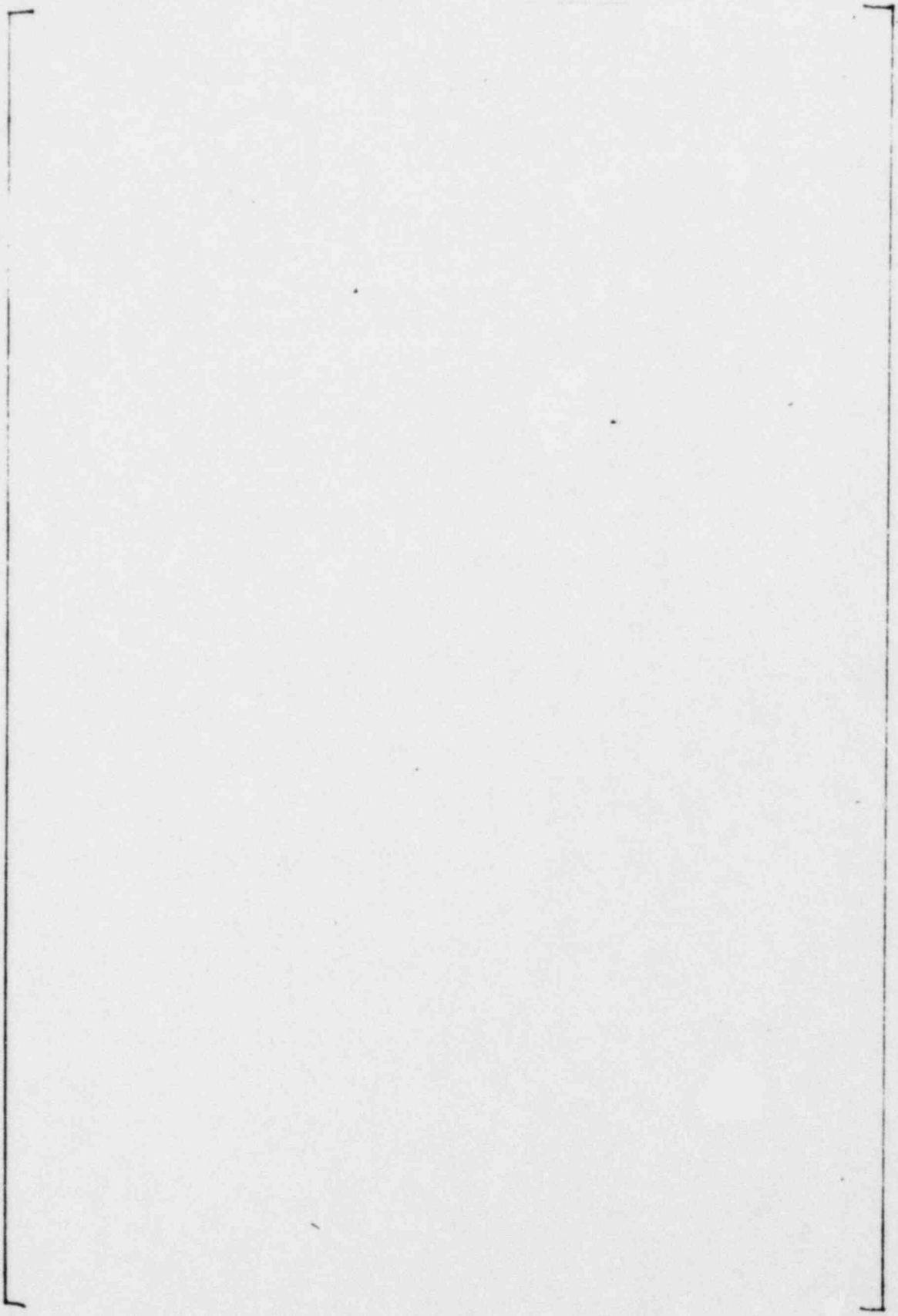

a,b,c,e

FIGURE 11.8-171 CASE NO. 39 SURFACE STRESS TIME HISTORY

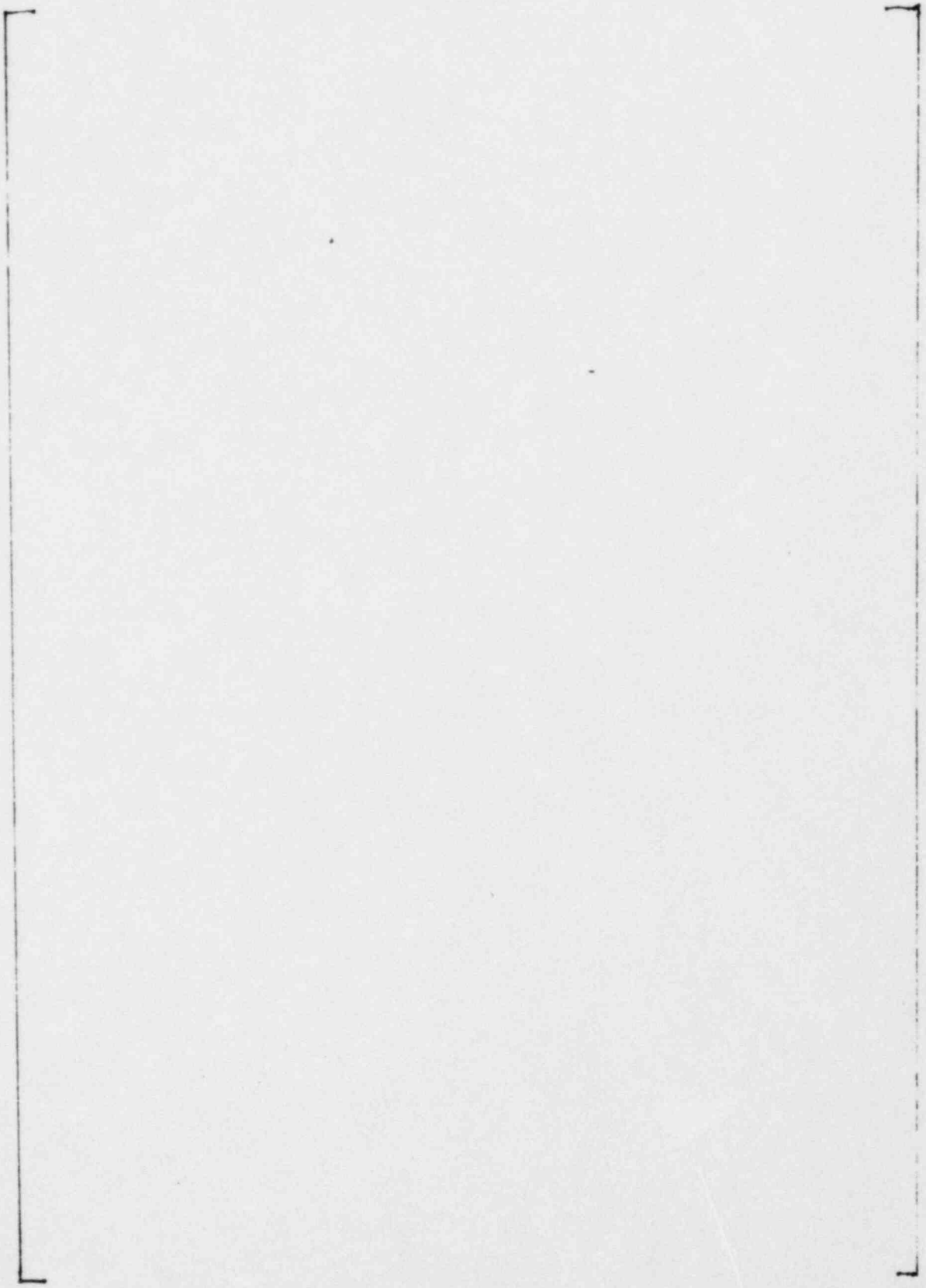

a,b,c,e

FIGURE 11.8-172 CASE NO. 40 SURFACE STRESS TIME HISTORY

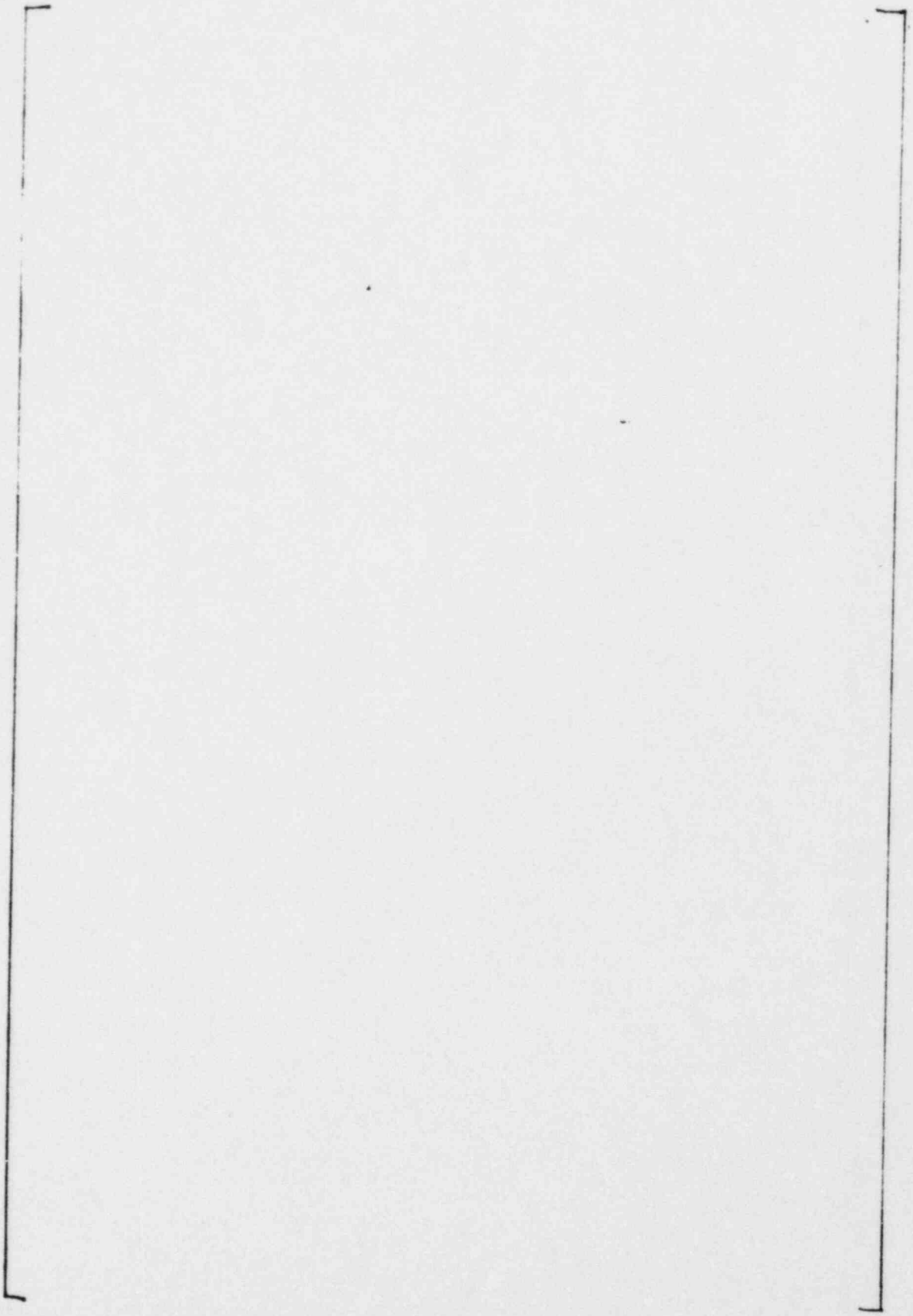

a.b.c.e

FIGURE 11.8-173 CASE NO. 41 SURFACE STRESS TIME HISTORY

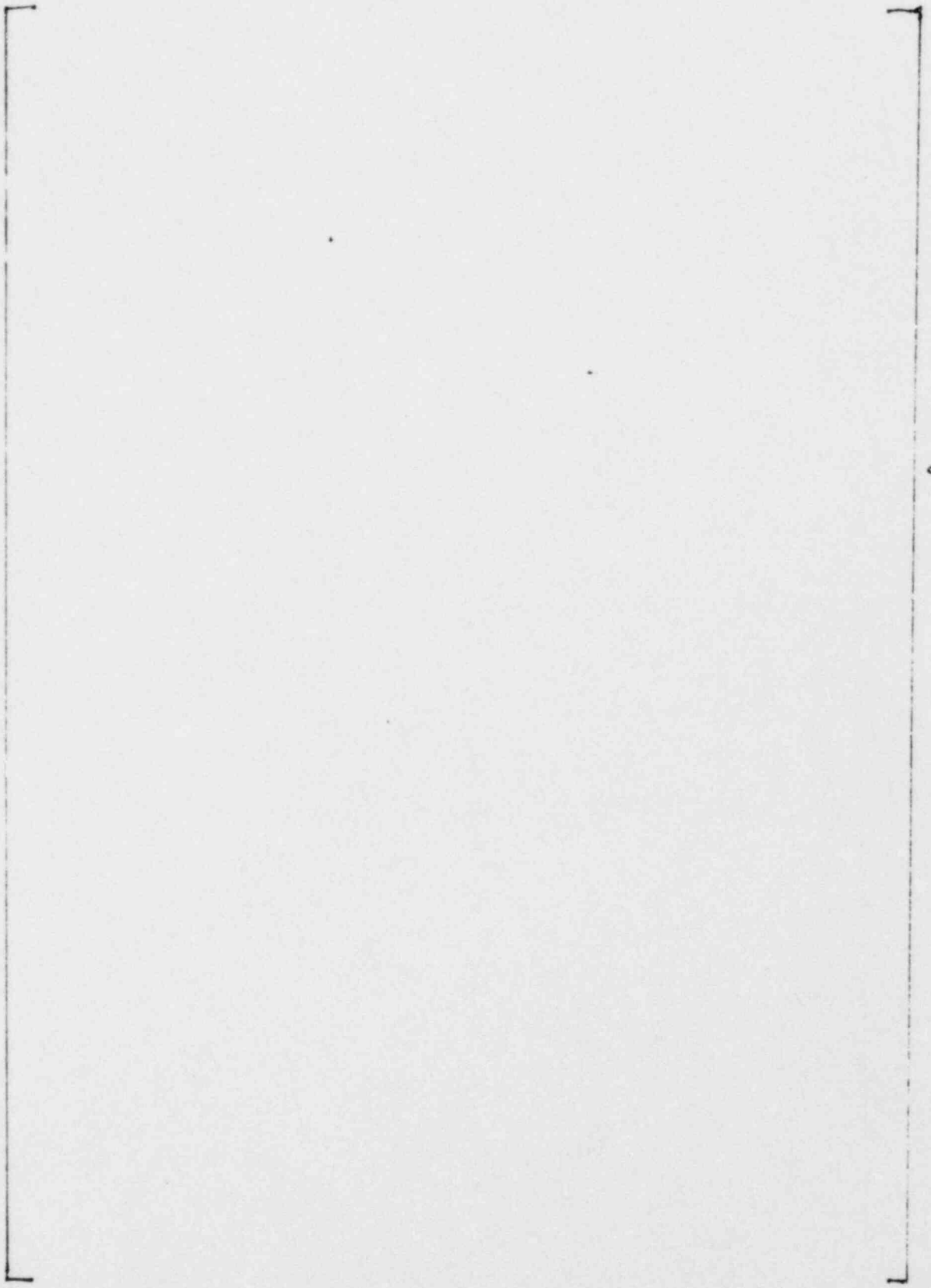

a,b,c,e

FIGURE 11.8-174 CASE NO. 42 SURFACE STRESS TIME HISTORY

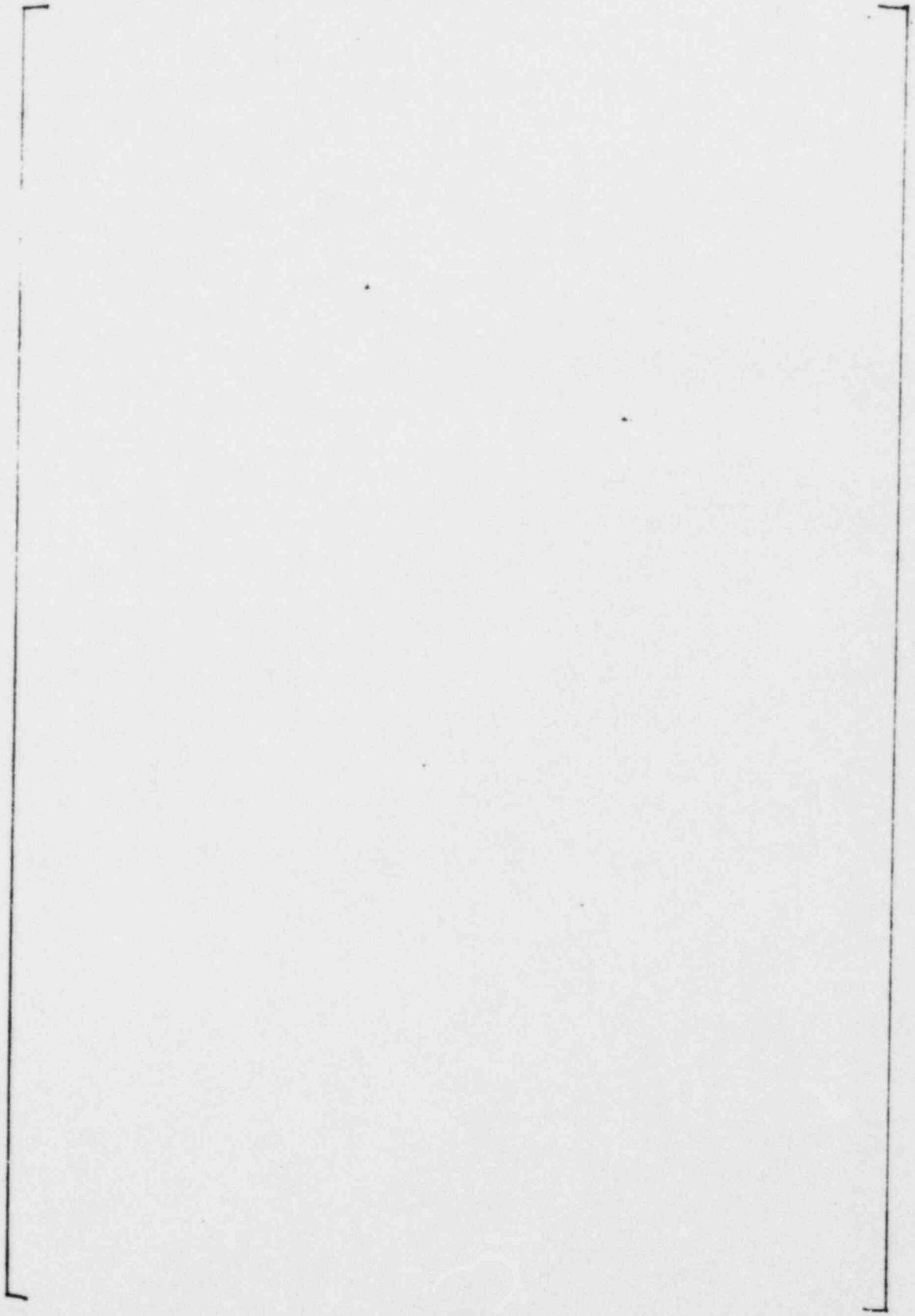

a,b,c,e

FIGURE 11.8-175 CASE NO. 43 SURFACE STRESS TIME HISTORY

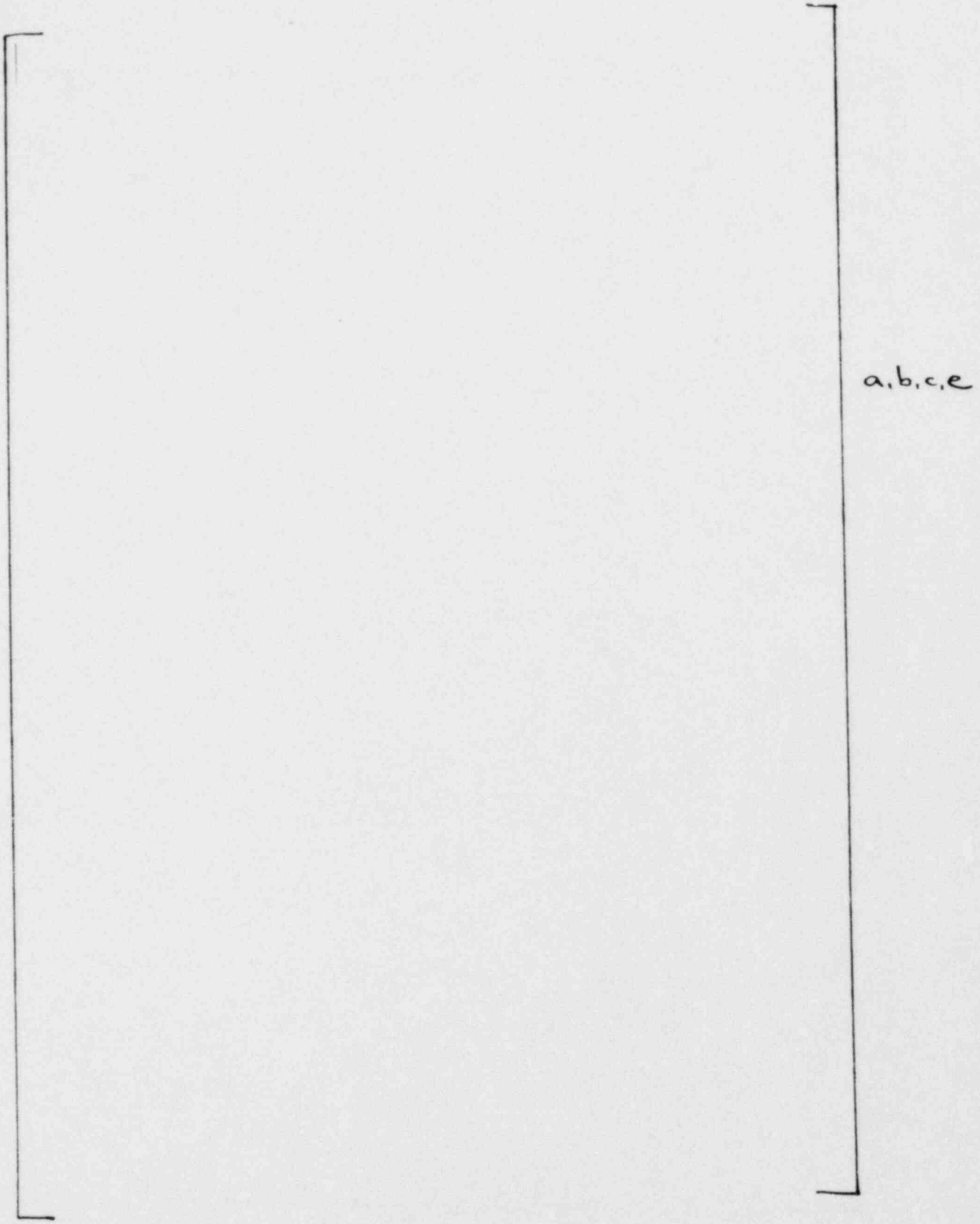

a,b,c,e

FIGURE 11.8-176 CASE NO. 44 SURFACE STRESS TIME HISTORY

FIGURE 11.8-177 HIGH CYCLES ASME FATIGUE DESIGN CURVE.

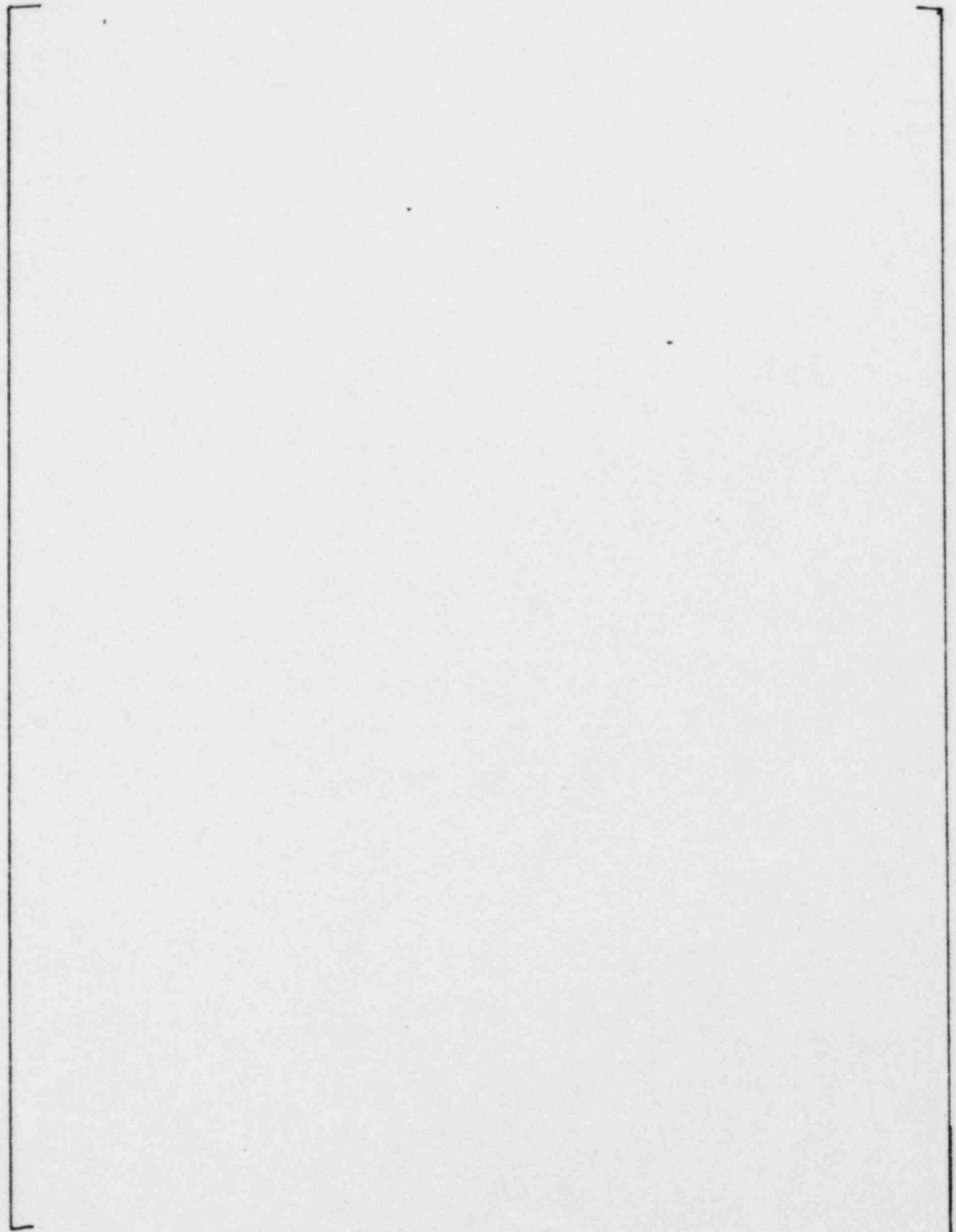

a,c,e

FIGURE 11.8-178 FATIGUE USAGE FACTOR DUE TO STRIPING - [ ]

a.c.e

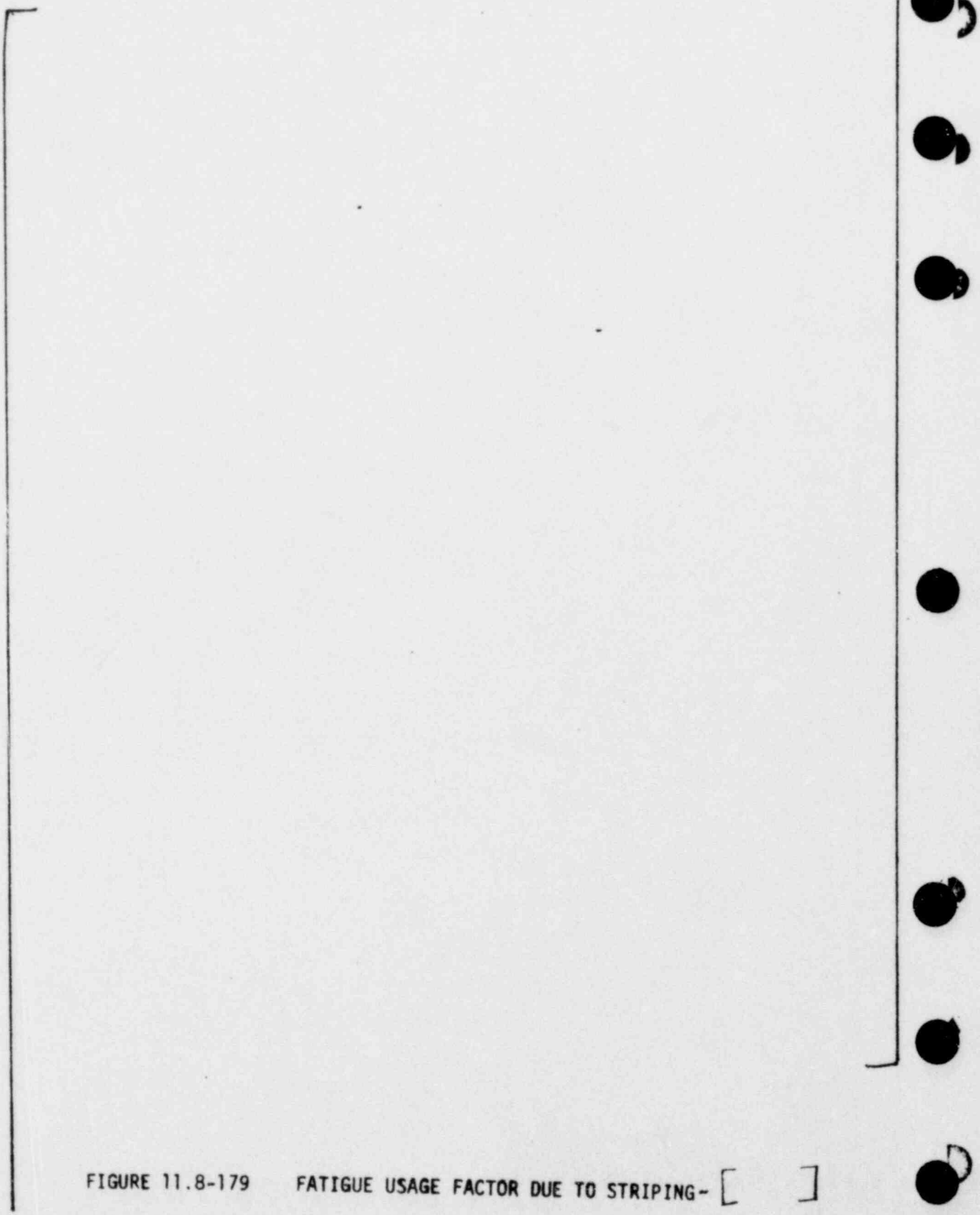

FIGURE 11.8-179 FATIGUE USAGE FACTOR DUE TO STRIPING- [ ]

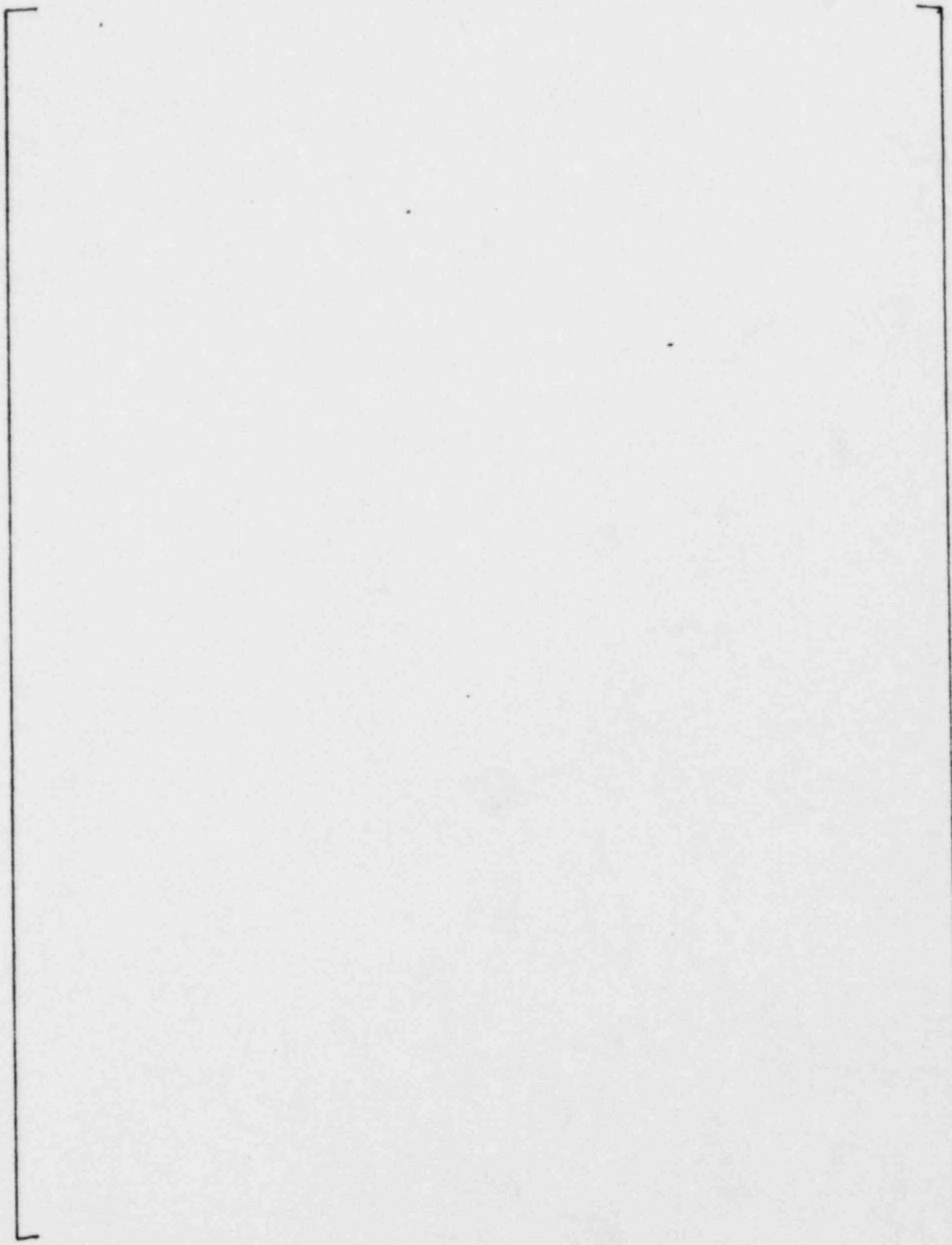

a,c,e

FIGURE 11.8-180 FATIGUE USAGE FACTOR DUE TO STRIPING - [ ]

a.c.e

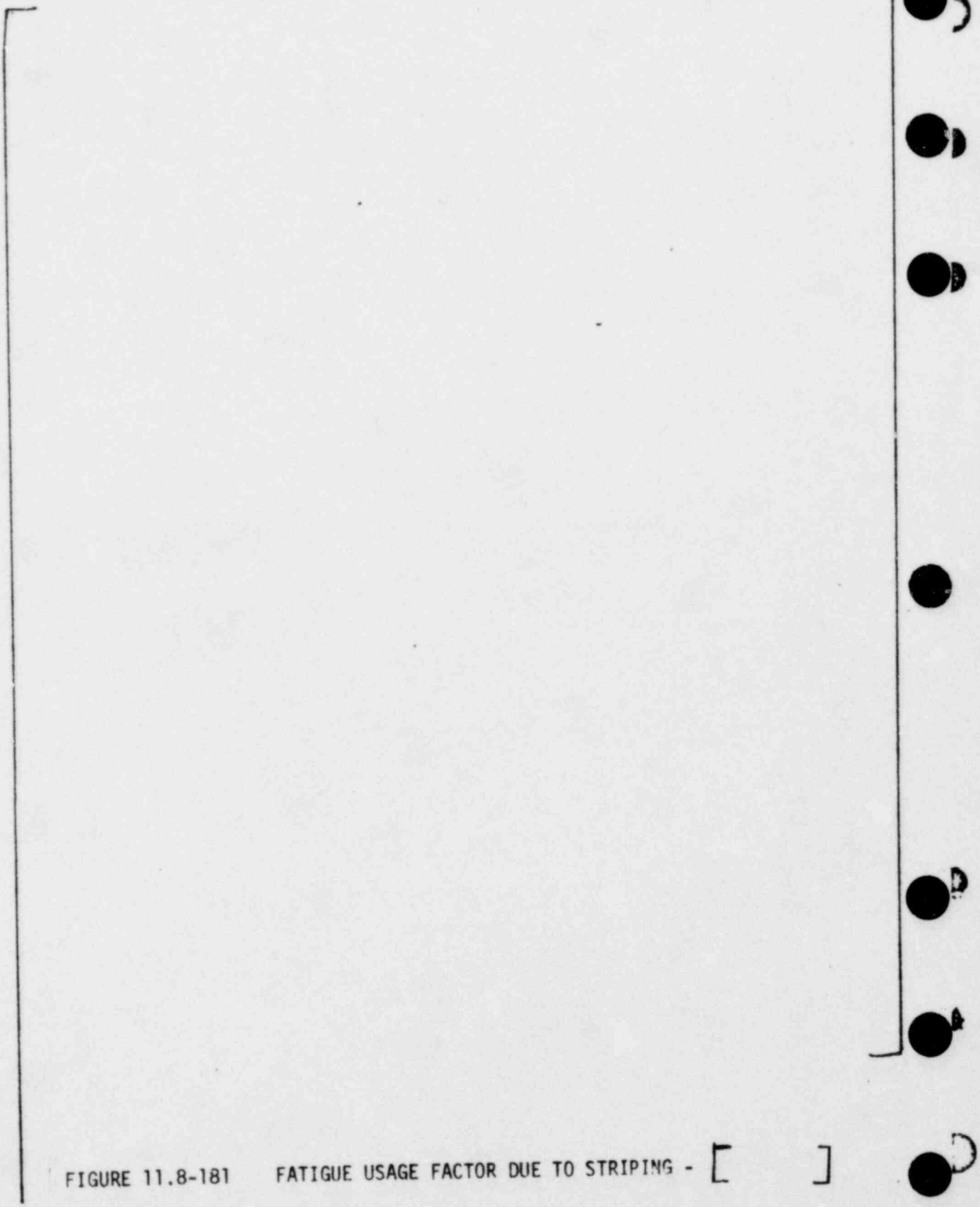

FIGURE 11.8-181 FATIGUE USAGE FACTOR DUE TO STRIPING - [ ]

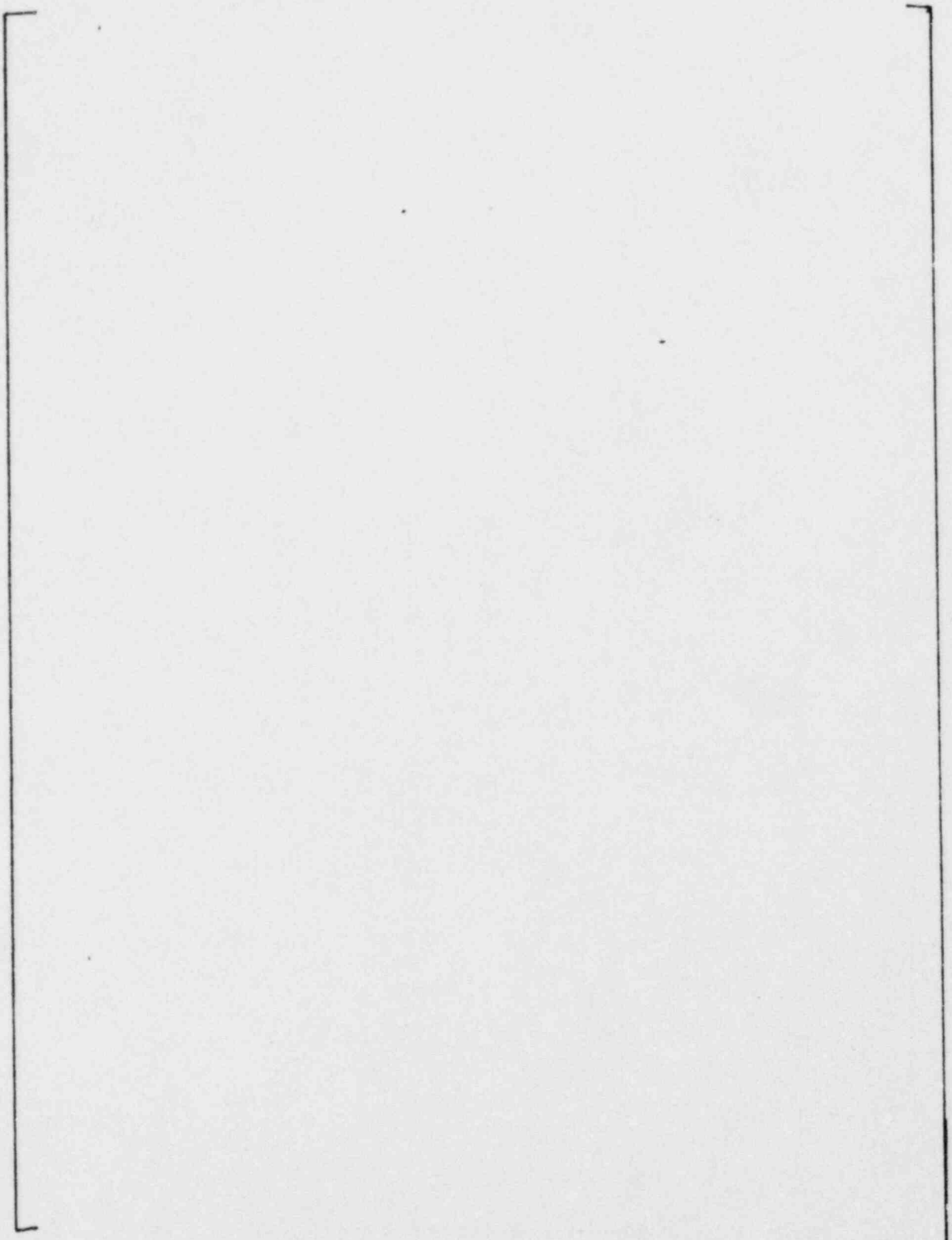

a,c,e

FIGURE 11.8-182 FATIGUE USAGE FACTOR DUE TO STRIPING - [ ]

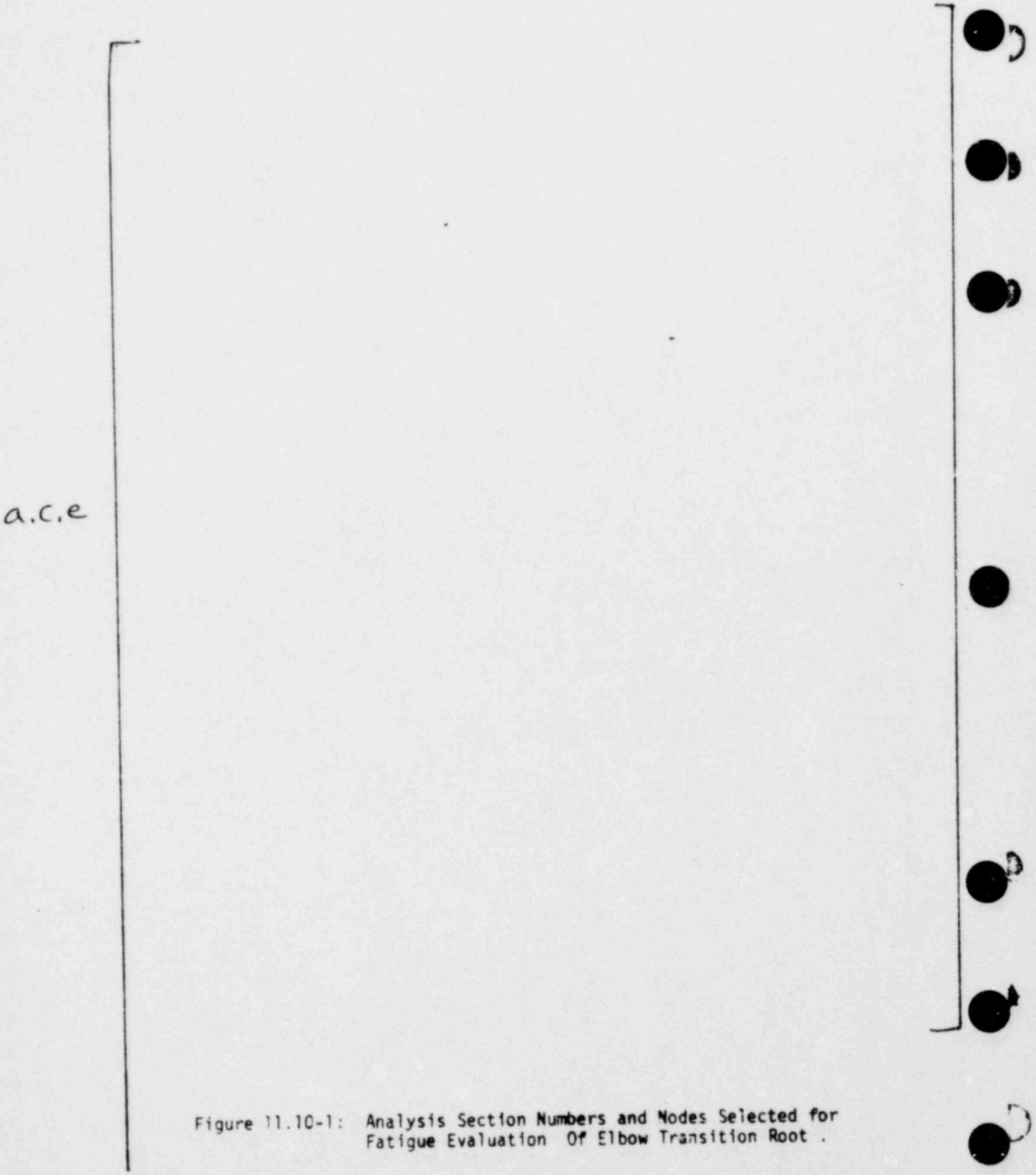

Figure 11.10-1: Analysis Section Numbers and Nodes Selected for Fatigue Evaluation Of Elbow Transition Root .

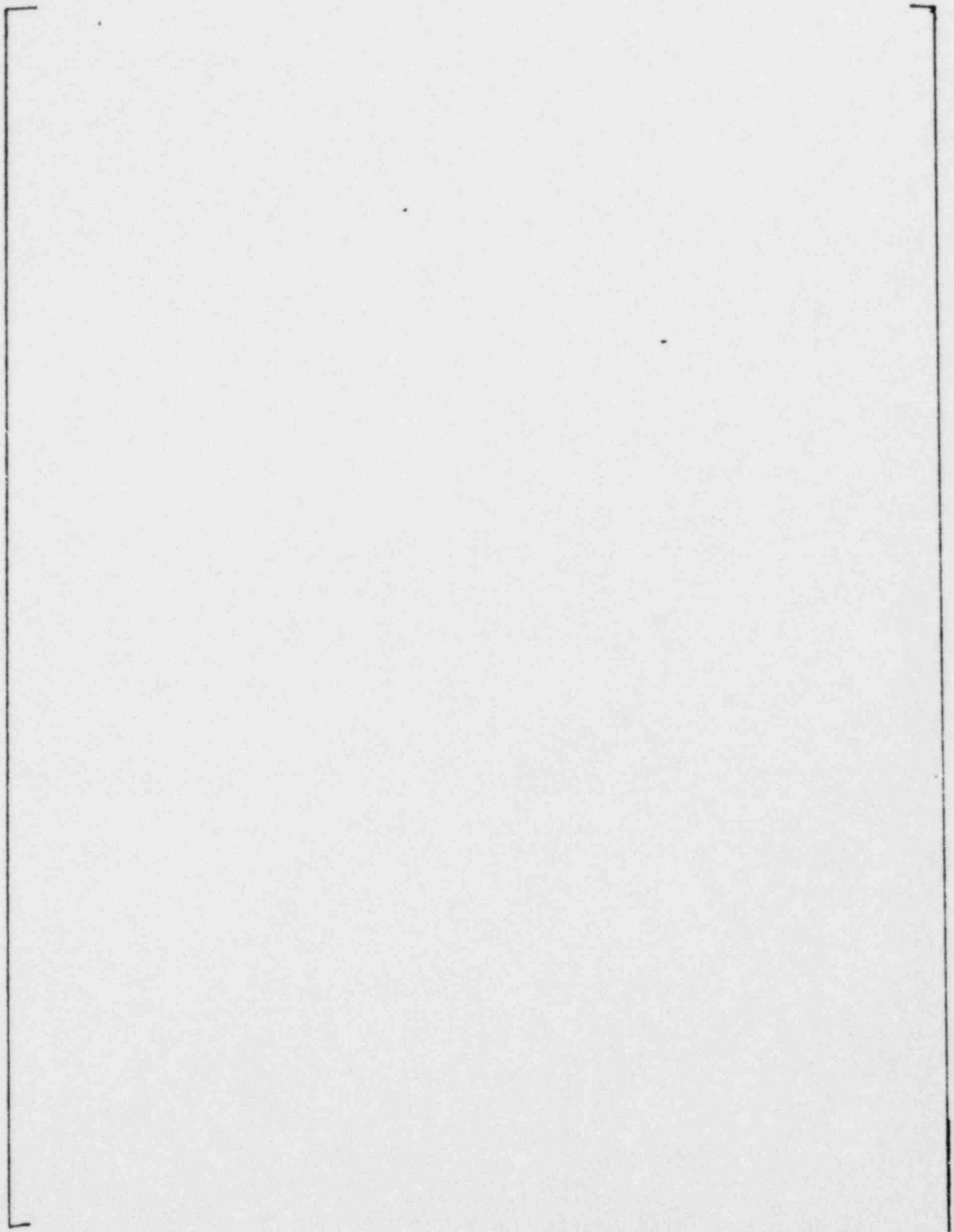

a,c,e

Figure 11.10-2: Analysis Section Numbers and Nodes Selected for Fatigue Evaluation For Top and Side of Weld Counterbore Region .

a.c.e

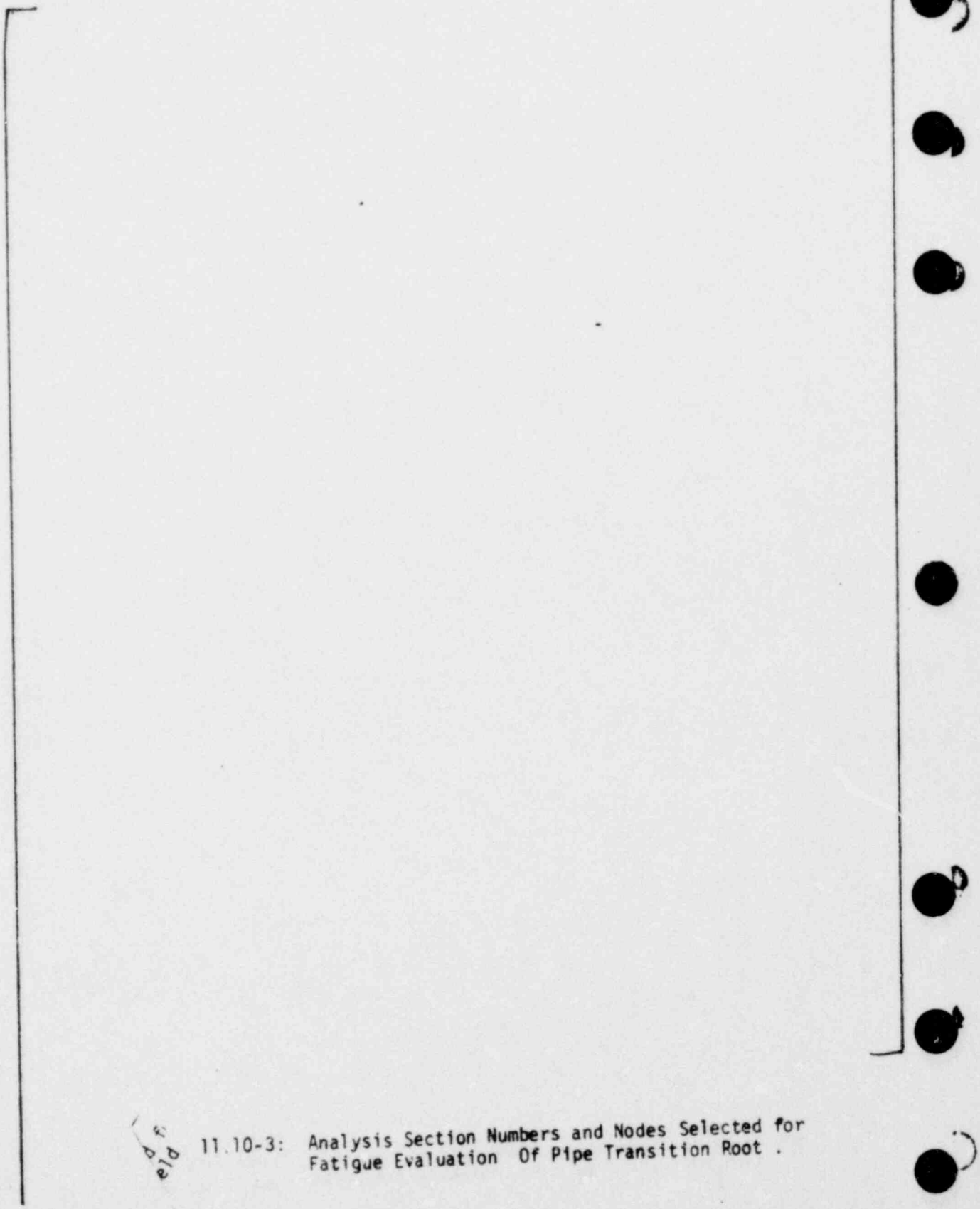

11.10-3: Analysis Section Numbers and Nodes Selected for Fatigue Evaluation Of Pipe Transition Root .

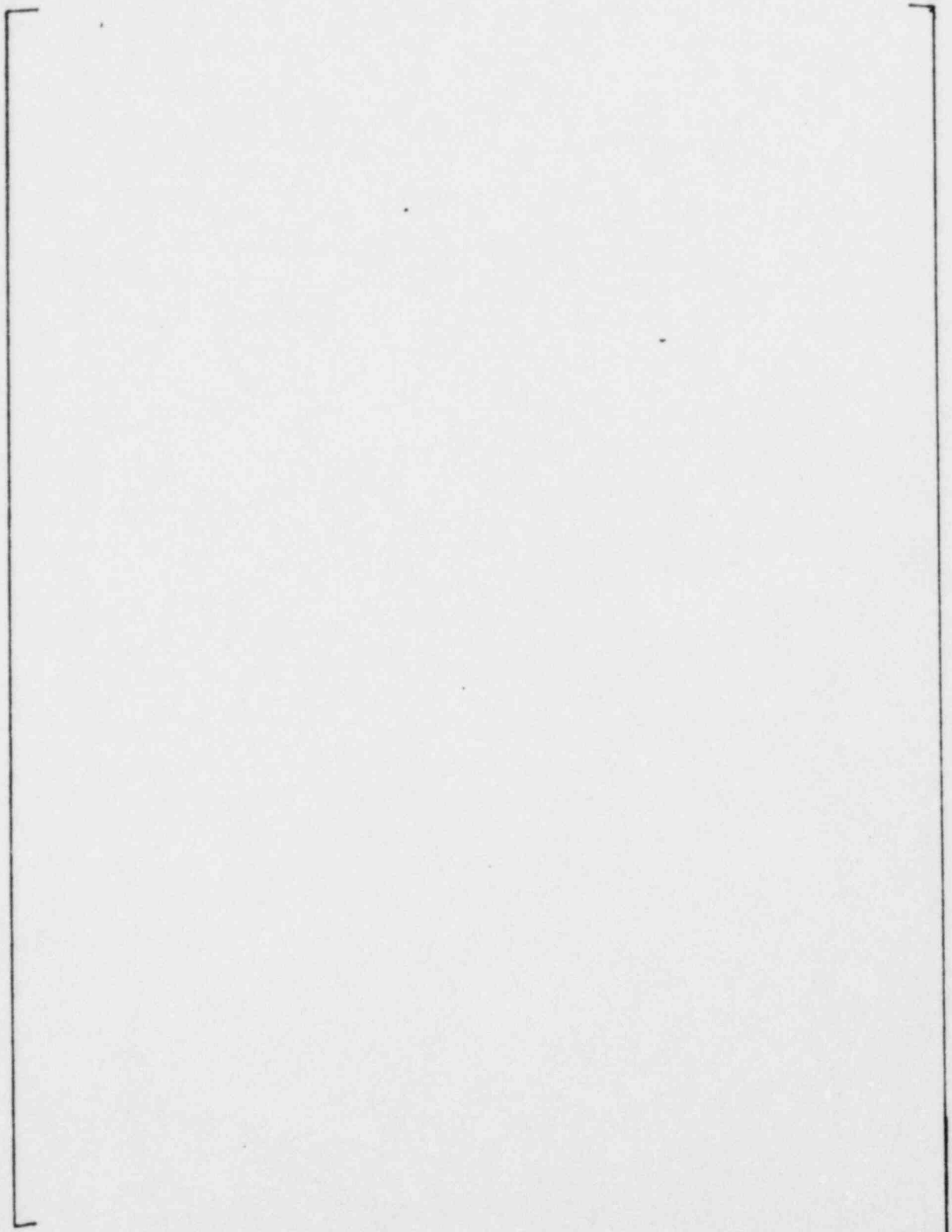

a,c,e

Figure 11.10-4: Analysis Section Numbers and Nodes Selected for Fatigue Evaluation Of Nozzle Transition Root .

a.c.e

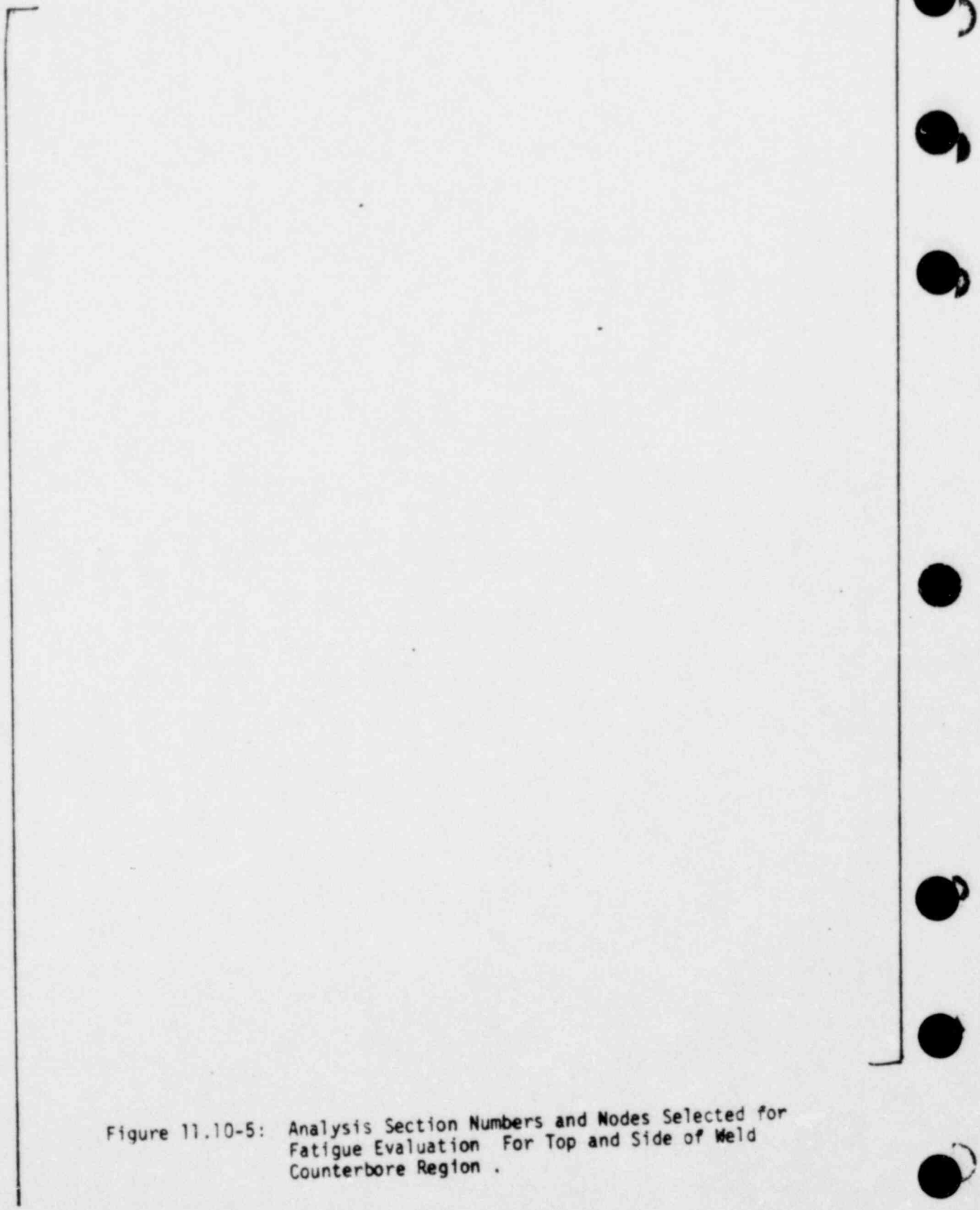

Figure 11.10-5: Analysis Section Numbers and Nodes Selected for Fatigue Evaluation For Top and Side of Weld Counterbore Region .

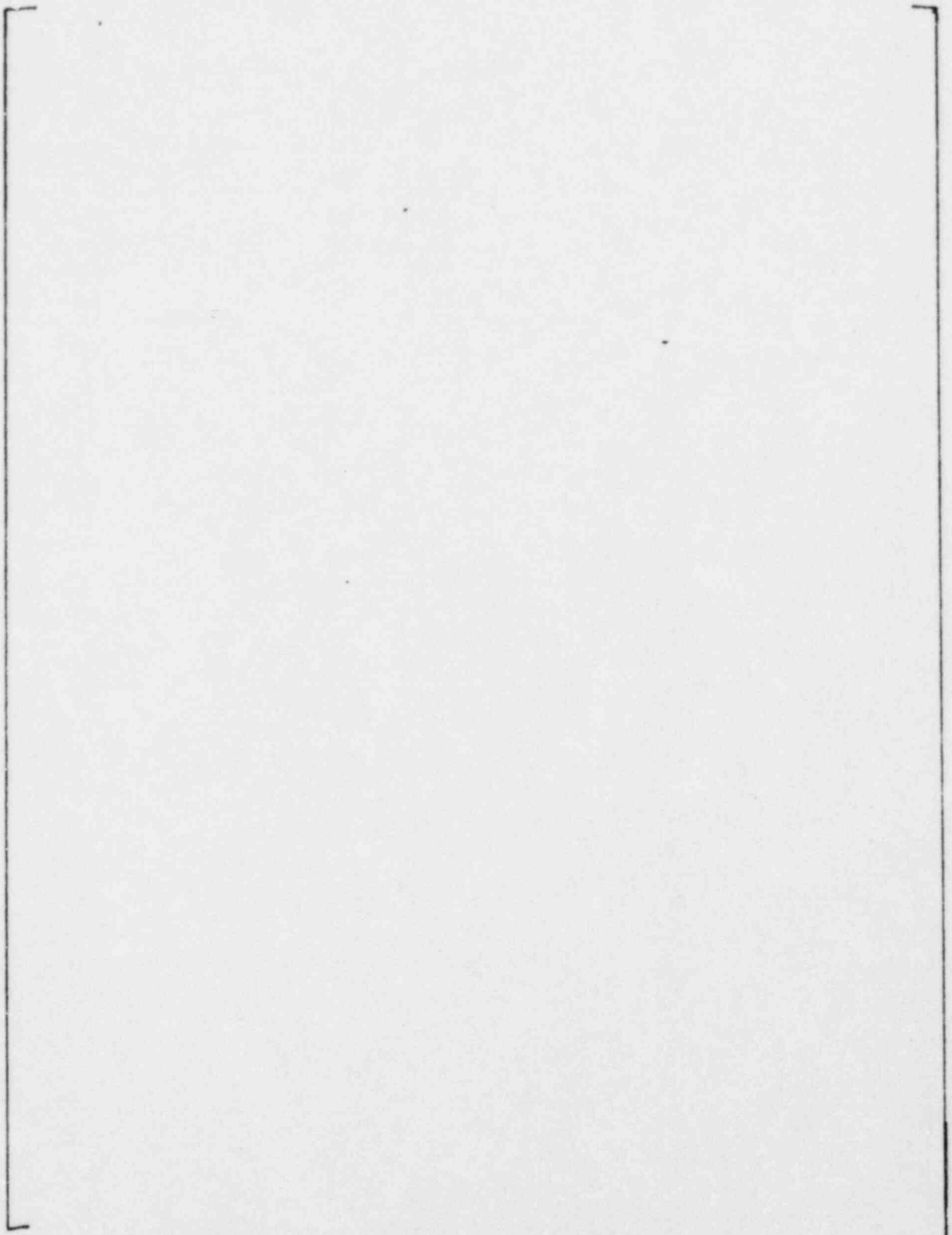

a,c,e

Figure 11.10-6: Comparison of Code and Modified K_e to Results From Plastic Analysis.

a.c.e

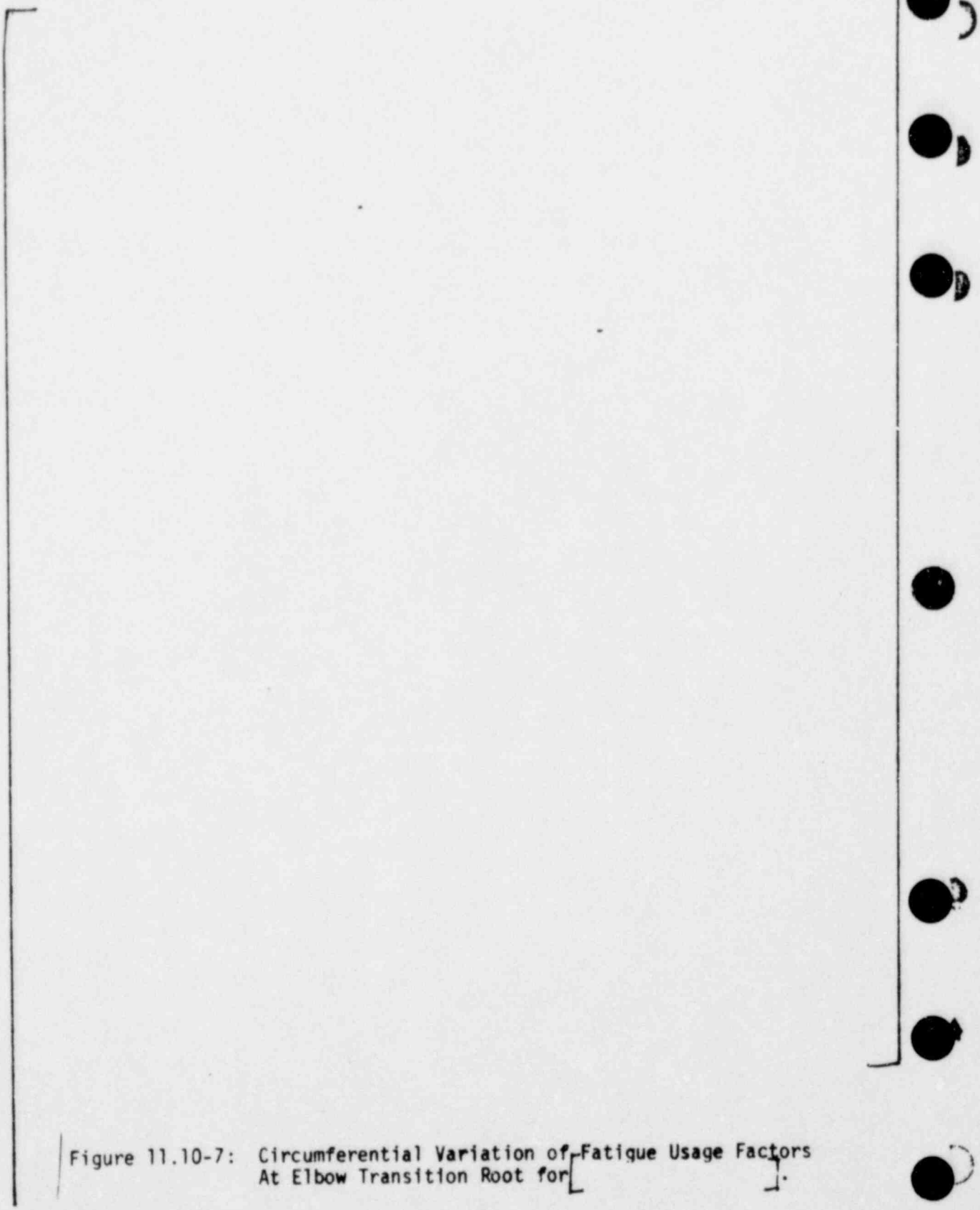

Figure 11.10-7: Circumferential Variation of Fatigue Usage Factors At Elbow Transition Root for [ ].

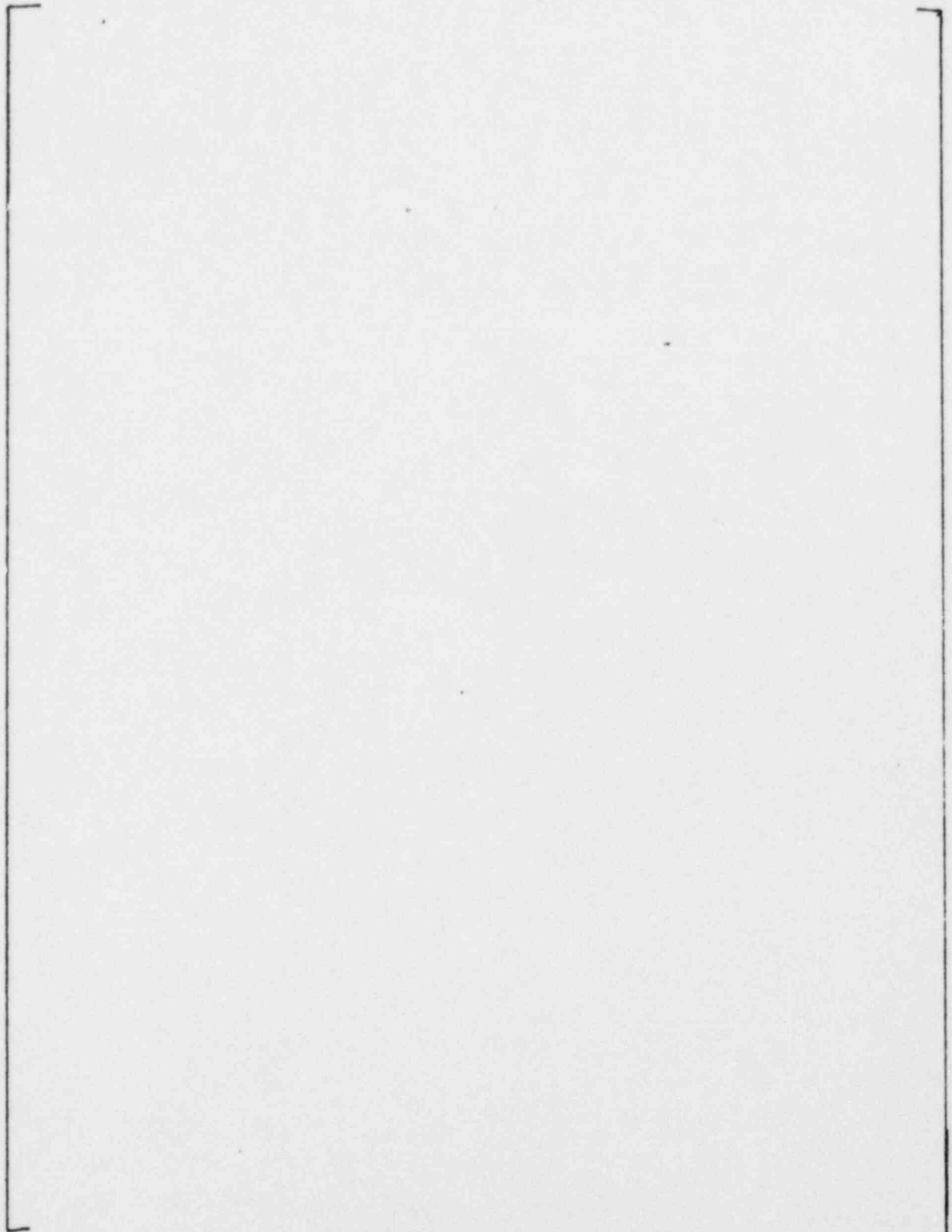

a,c,e

Figure 11.10-8: Comparison of Fatigue Usage Factors Using Code K_e and Modified K_e for [ ]

a.c.e

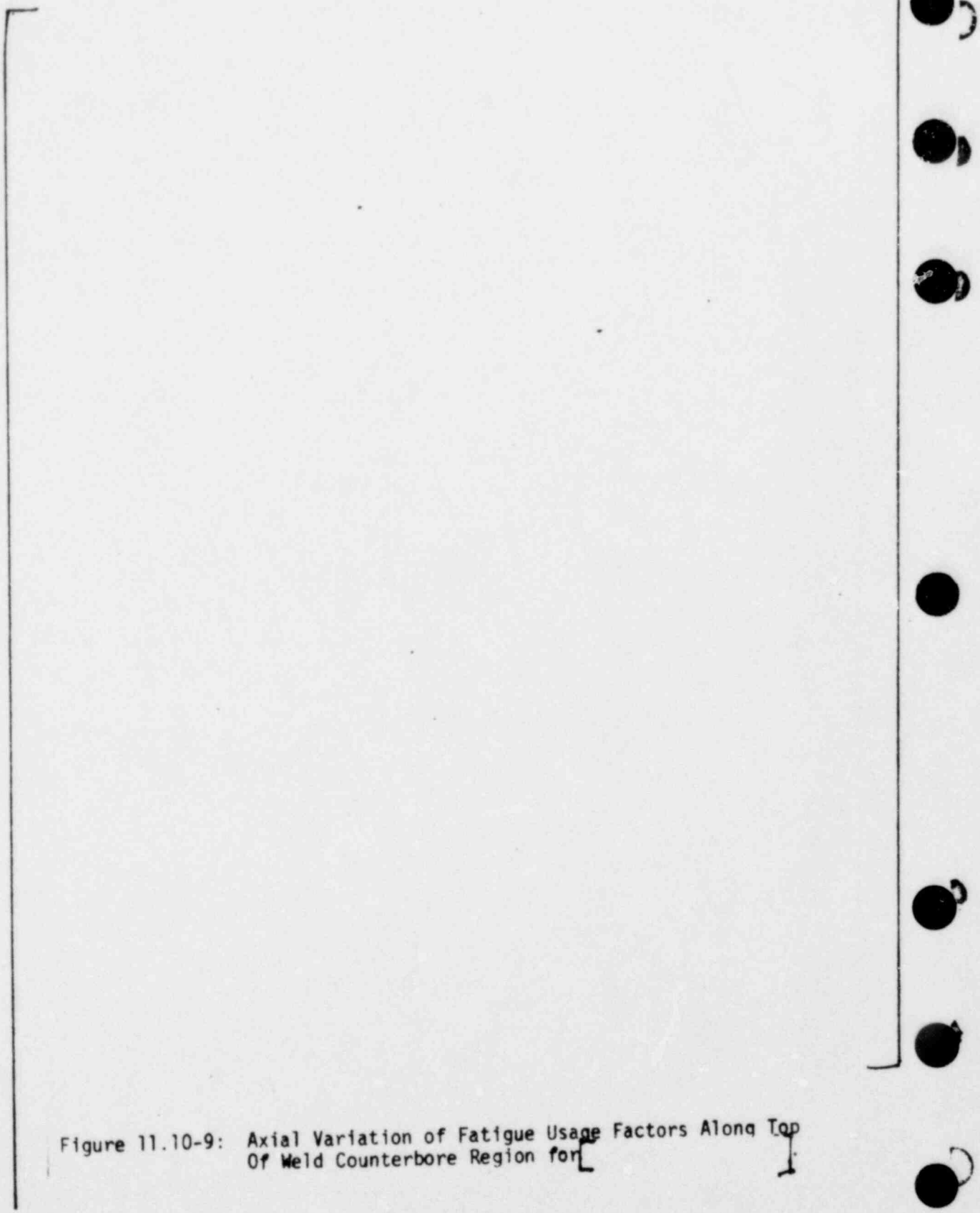

Figure 11.10-9: Axial Variation of Fatigue Usage Factors Along Top Of Weld Counterbore Region for

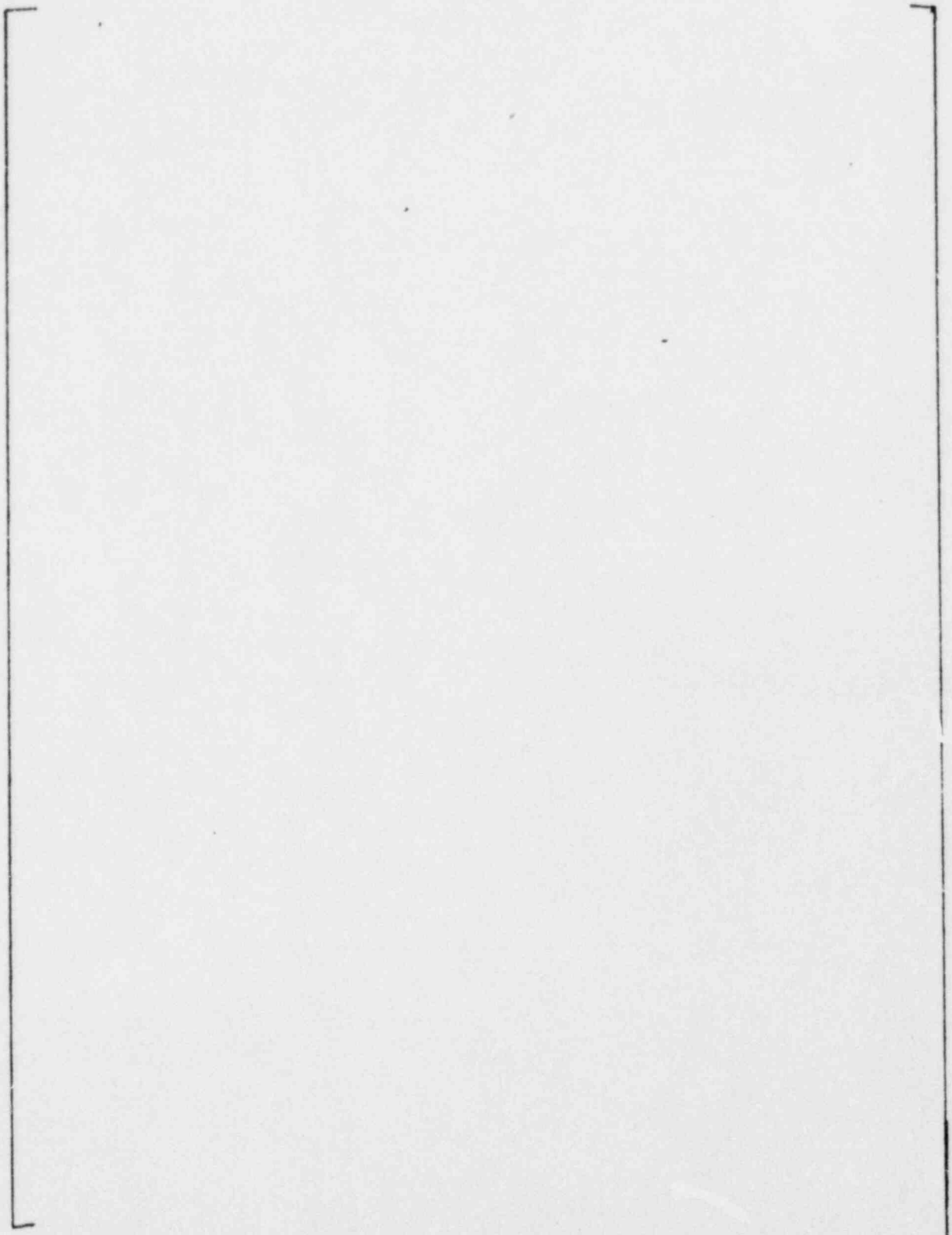

a,c,e

Figure 11.10-10: Axial Variation of Fatigue Usage Factors Along Side of Weld Counterbore Region for [ ], Line 21.

a,c,e

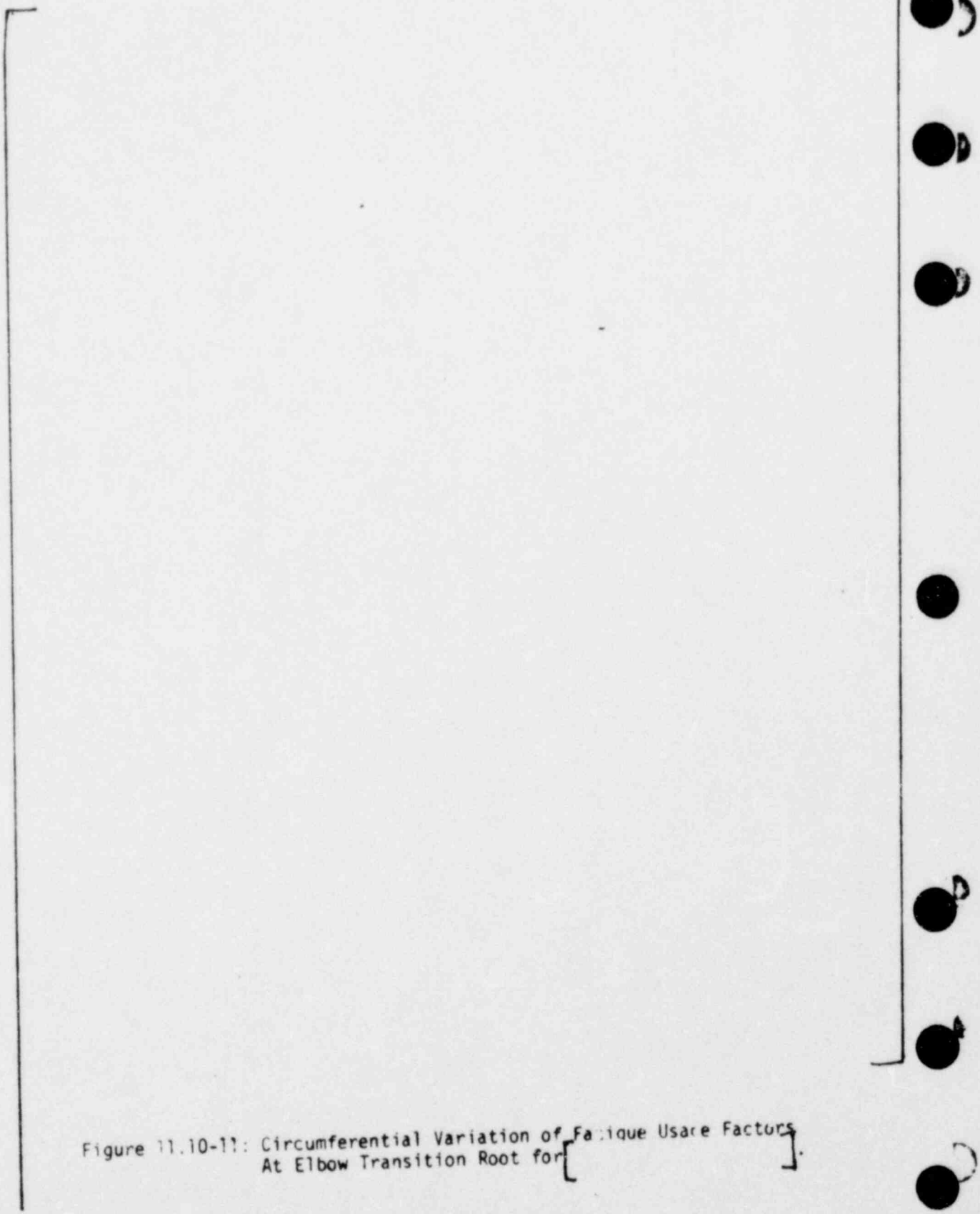

Figure 11.10-11: Circumferential Variation of Fatigue Usage Factors At Elbow Transition Root for [ ].

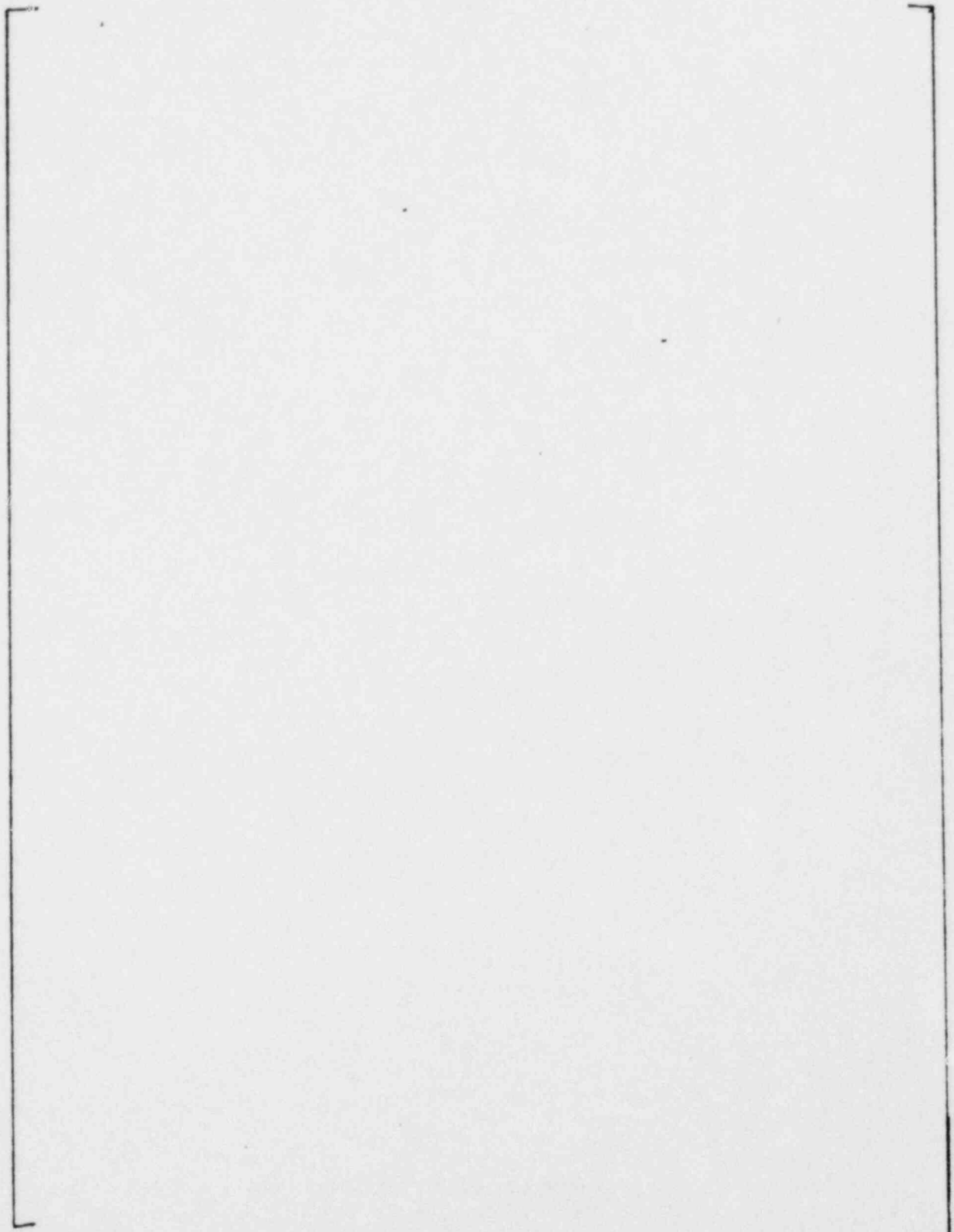

a,c,e

Figure 11.10-12: Axial Variation of Fatigue Usage Factors Along Top Of Weld Counterbore Region for

a.c.e

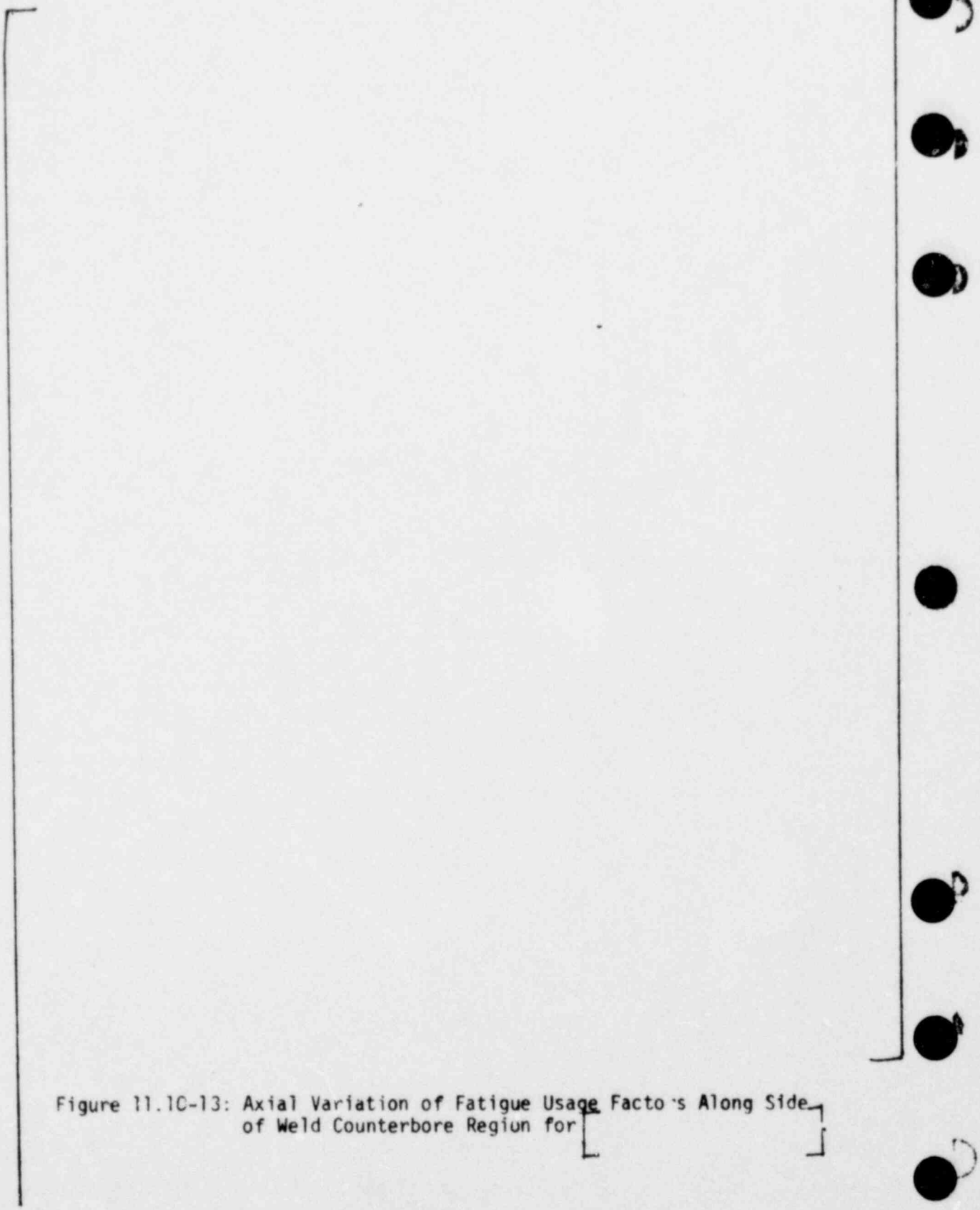

Figure 11.1C-13: Axial Variation of Fatigue Usage Factors Along Side of Weld Counterbore Region for [ ]

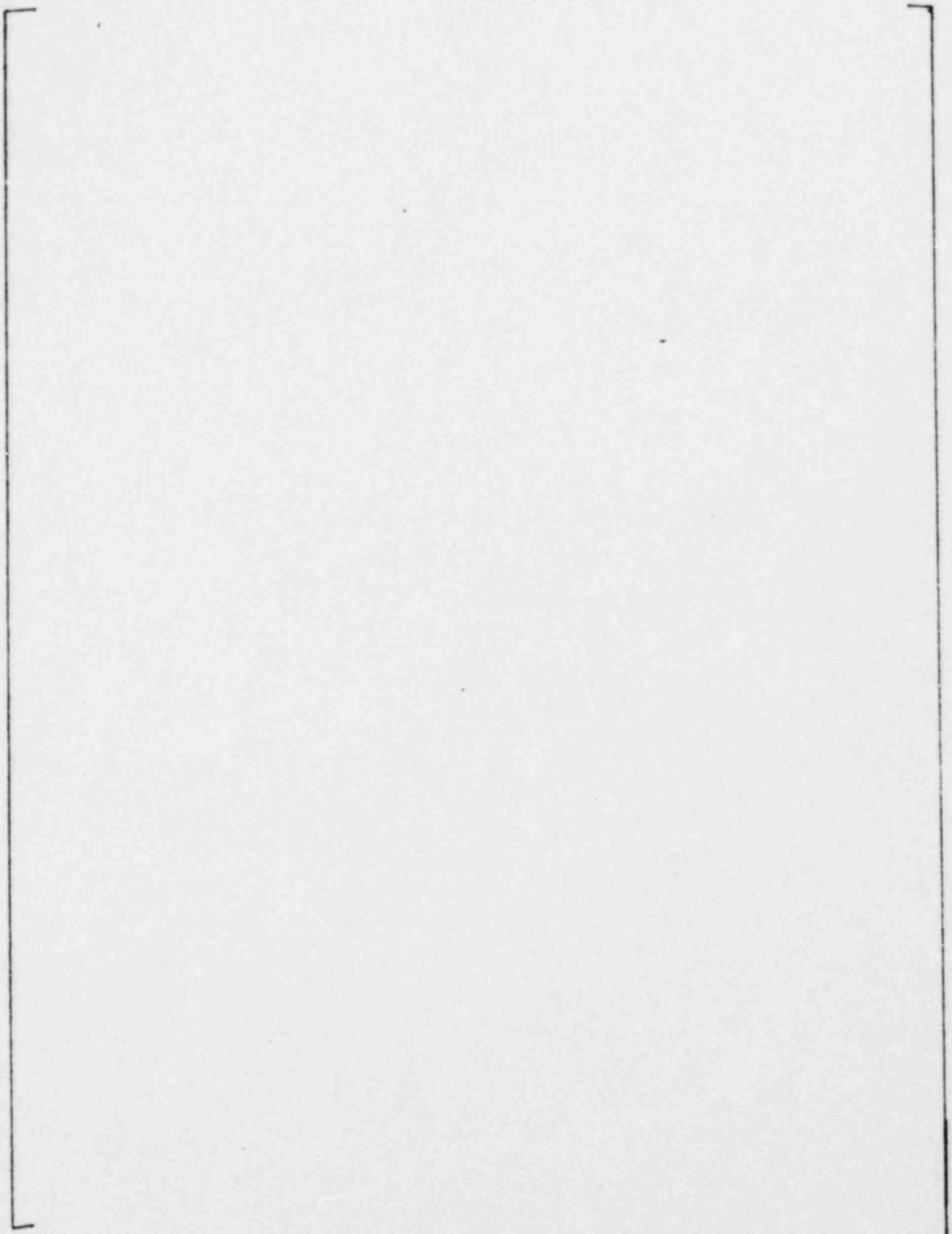

a,c,e

Figure 11.10-14: Circumferential Variation of Fatigue Usage Factors At Elbow Transition Root for [ ].

a.c.e

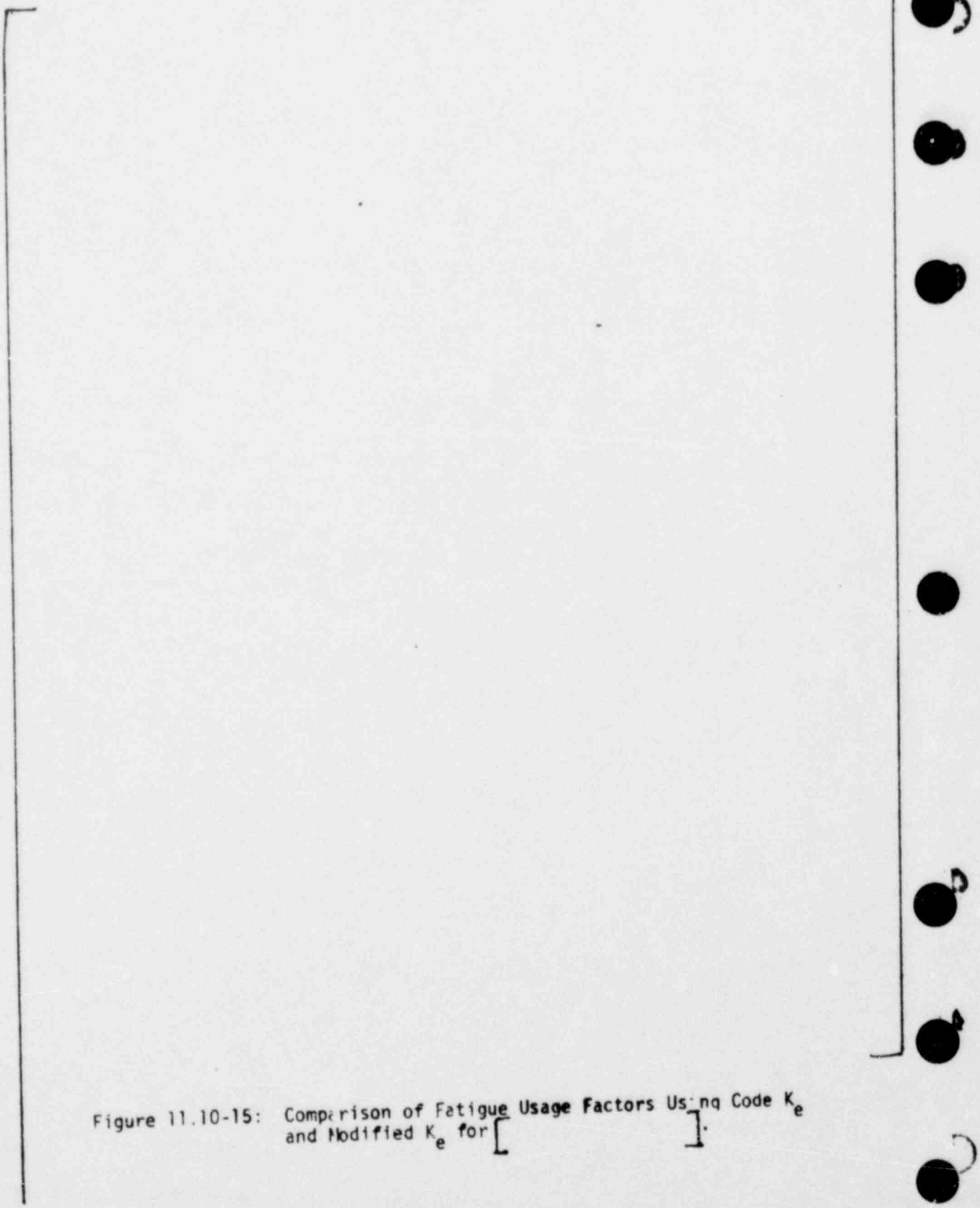

Figure 11.10-15: Comparison of Fatigue Usage Factors Using Code K_e and Modified K_e for [ ].

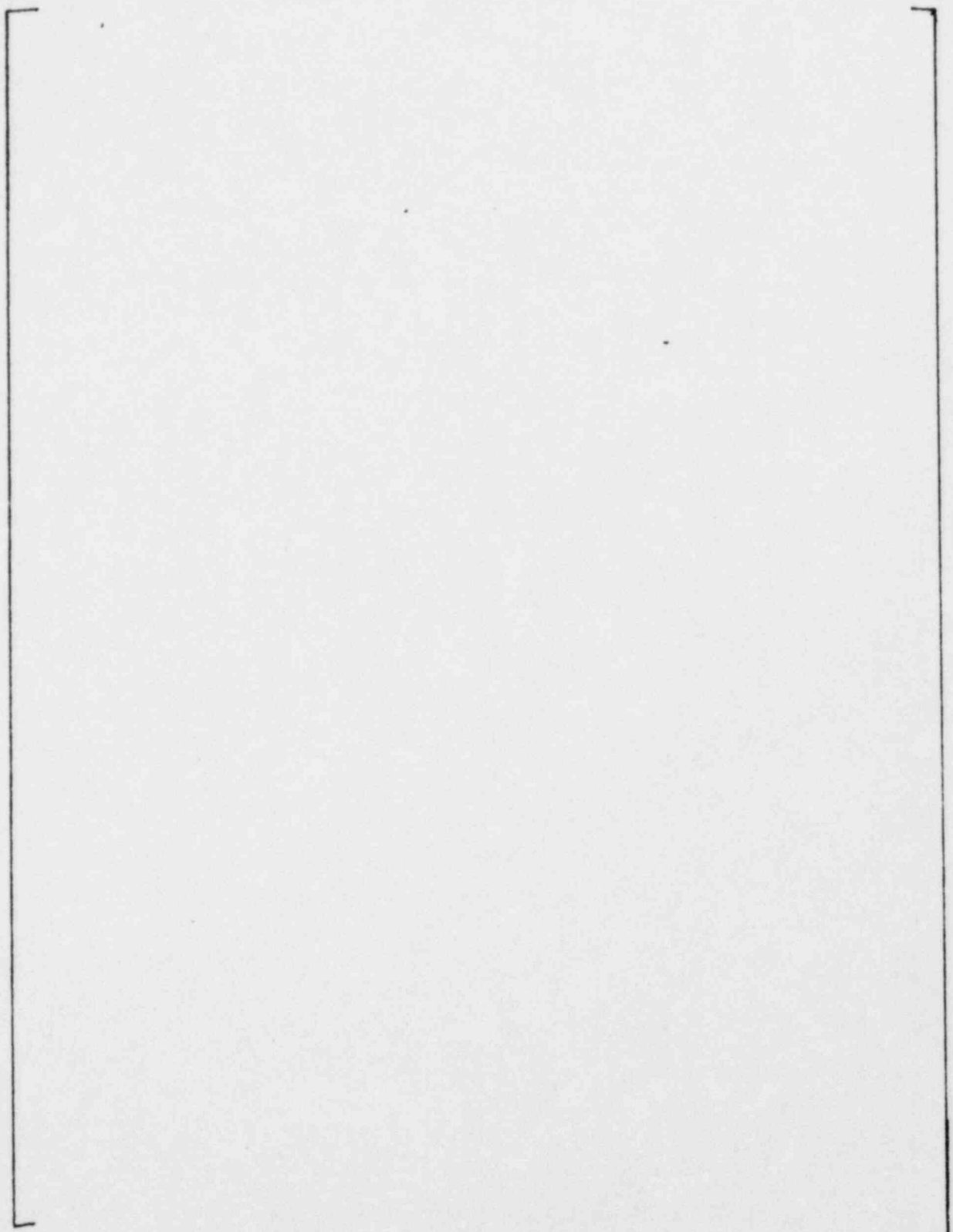

a,c,e

Figure 11.10-16: Axial Variation of Fatigue Usage Factors Along Top Of Weld Counterbore Region for [ ].

a.c.e

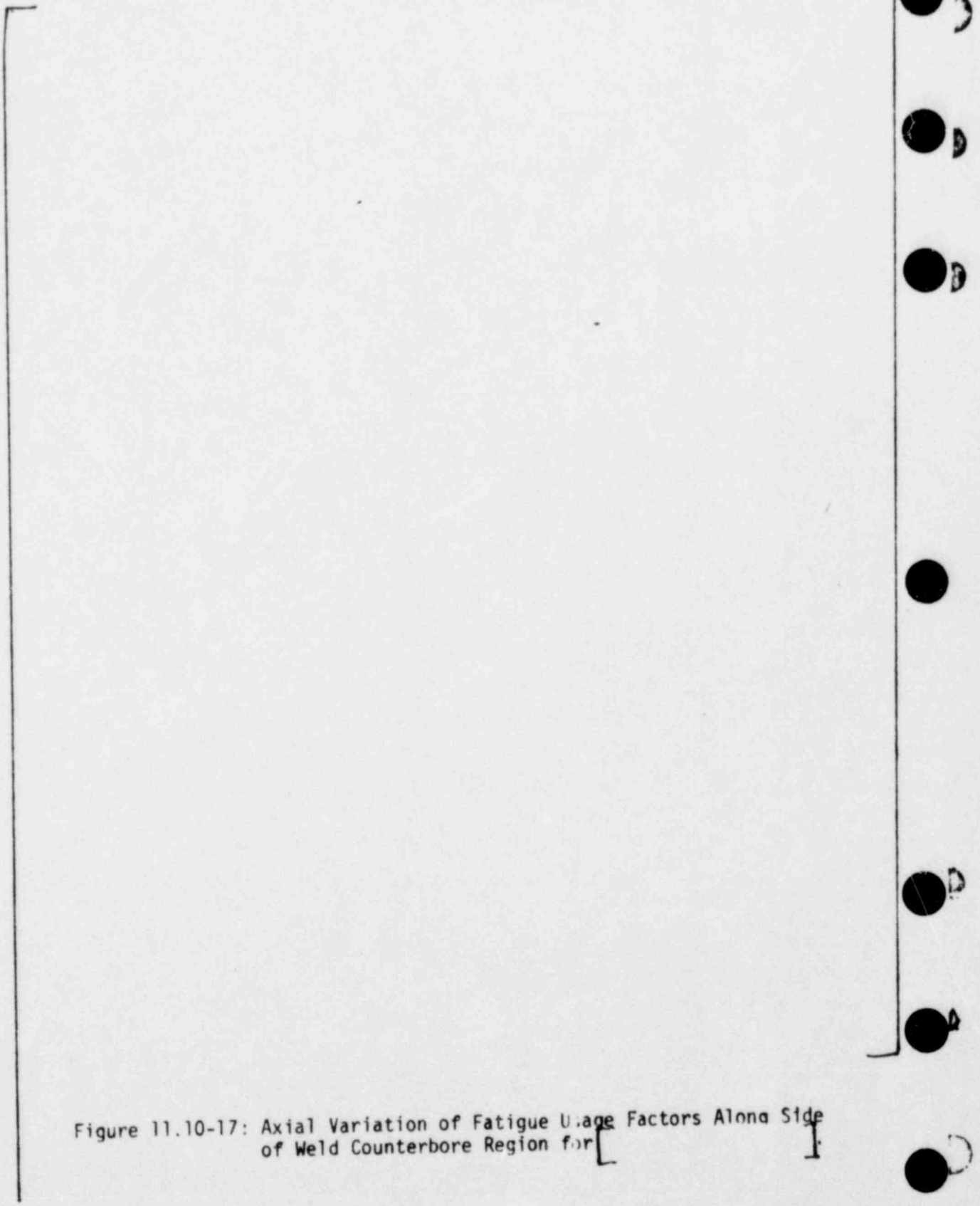

Figure 11.10-17: Axial Variation of Fatigue Usage Factors Along Side of Weld Counterbore Region for [ ]

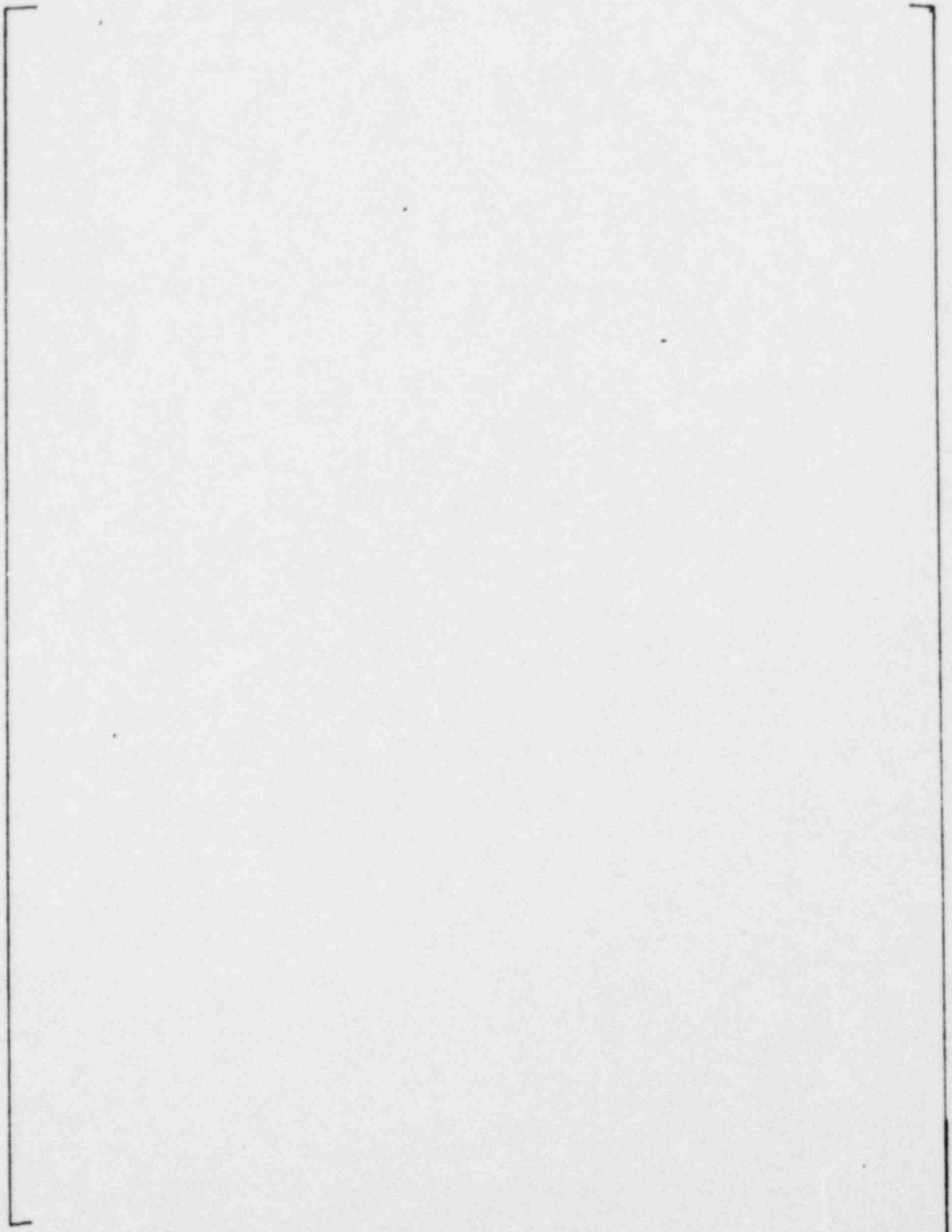

a,c,e

Figure 11.10-18: Circumferential Variation of Fatigue Usage Factors At Elbow Transition Root for [ ] Line 13.

a.c.e

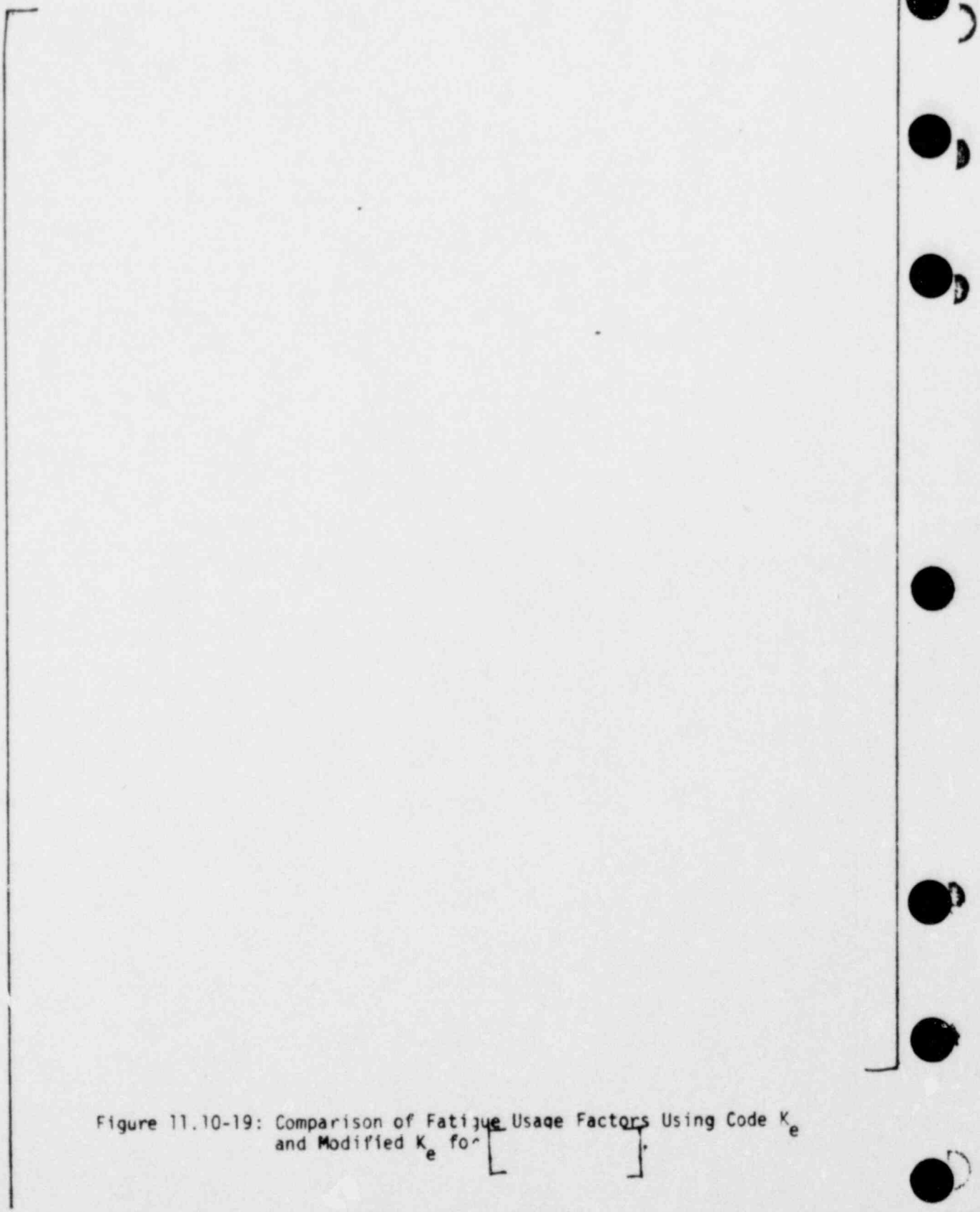

Figure 11.10-19: Comparison of Fatigue Usage Factors Using Code K_e and Modified K_e for [ ].

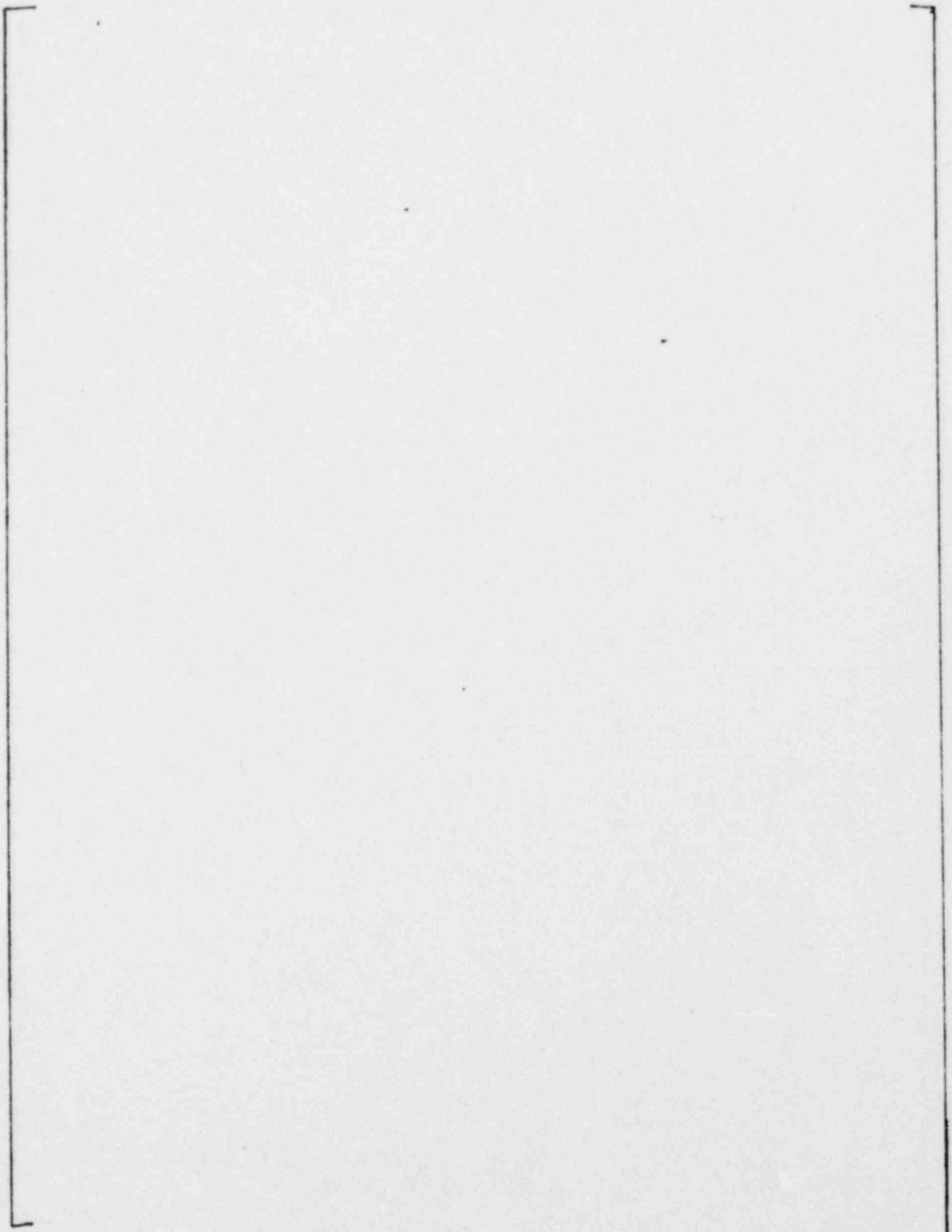

a,c,e

Figure 11.10-20: Axial Variation of Fatigue Usage Factors Along Top of Weld Counterbore Region for [ ]

a.c.e

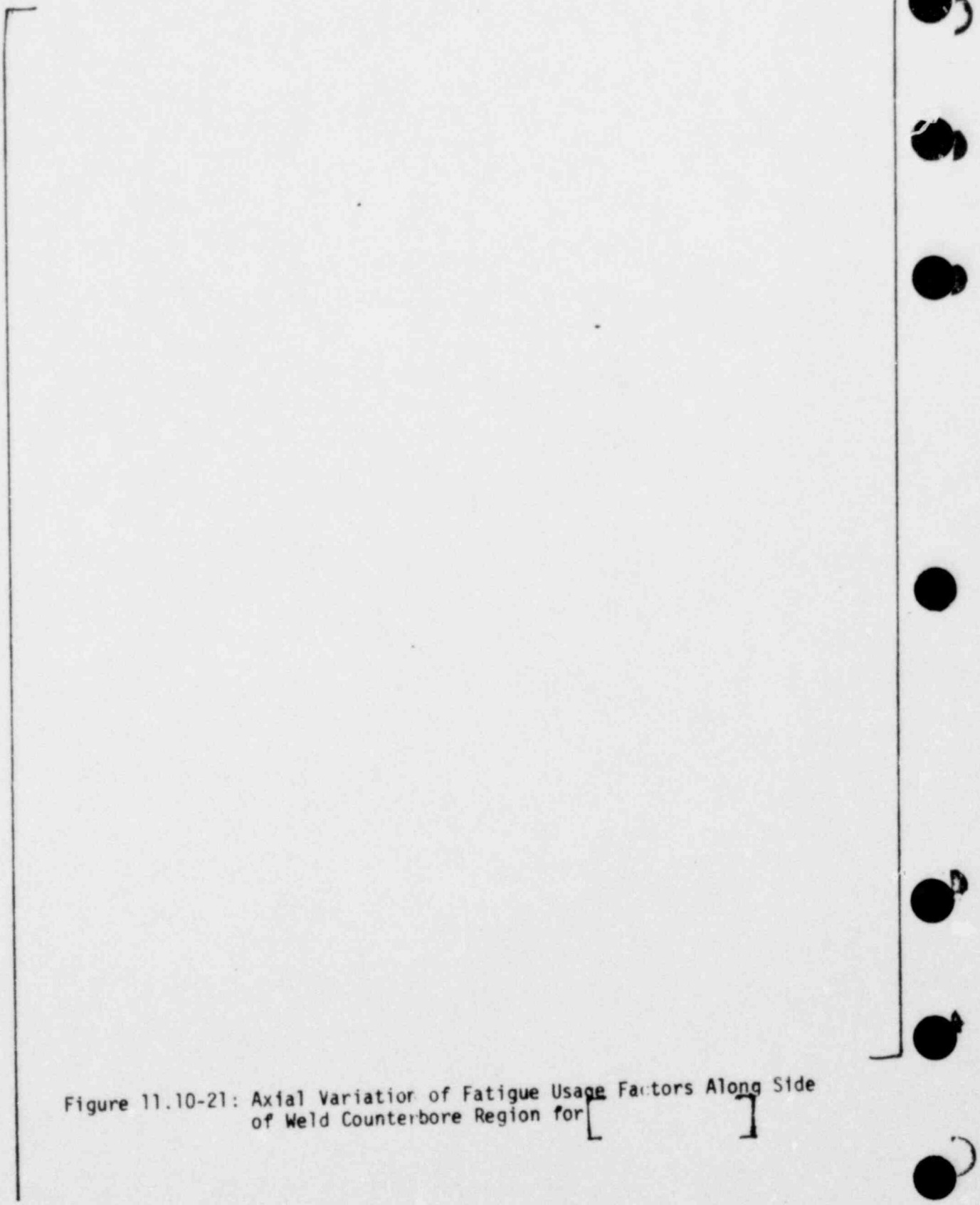

Figure 11.10-21: Axial Variation of Fatigue Usage Factors Along Side of Weld Counterbore Region for [ ]

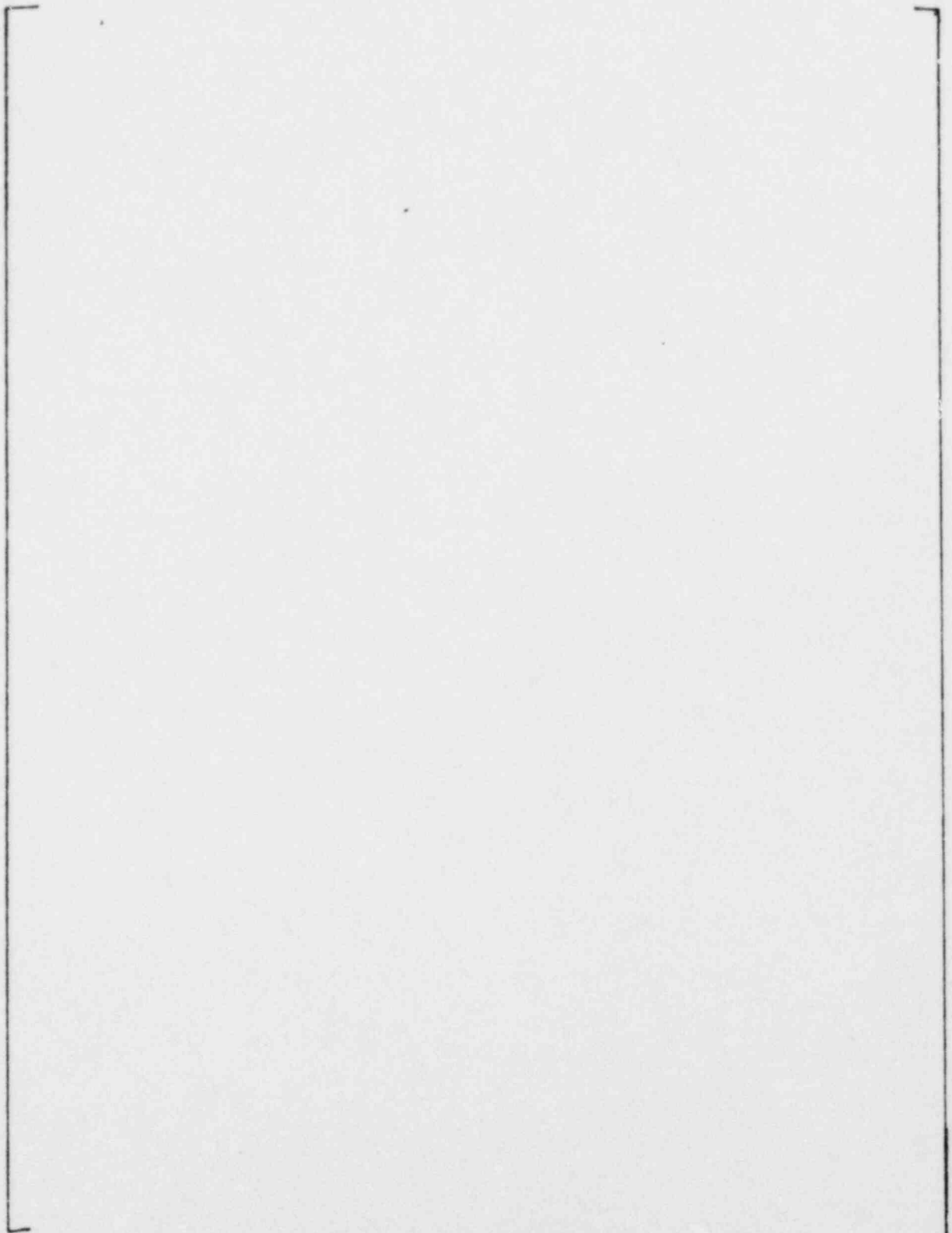

a,c,e

Figure 11.10-22: Circumferential Variation of Fatigue Usage Factors at Nozzle Transition Root for [ ]

a.c.e

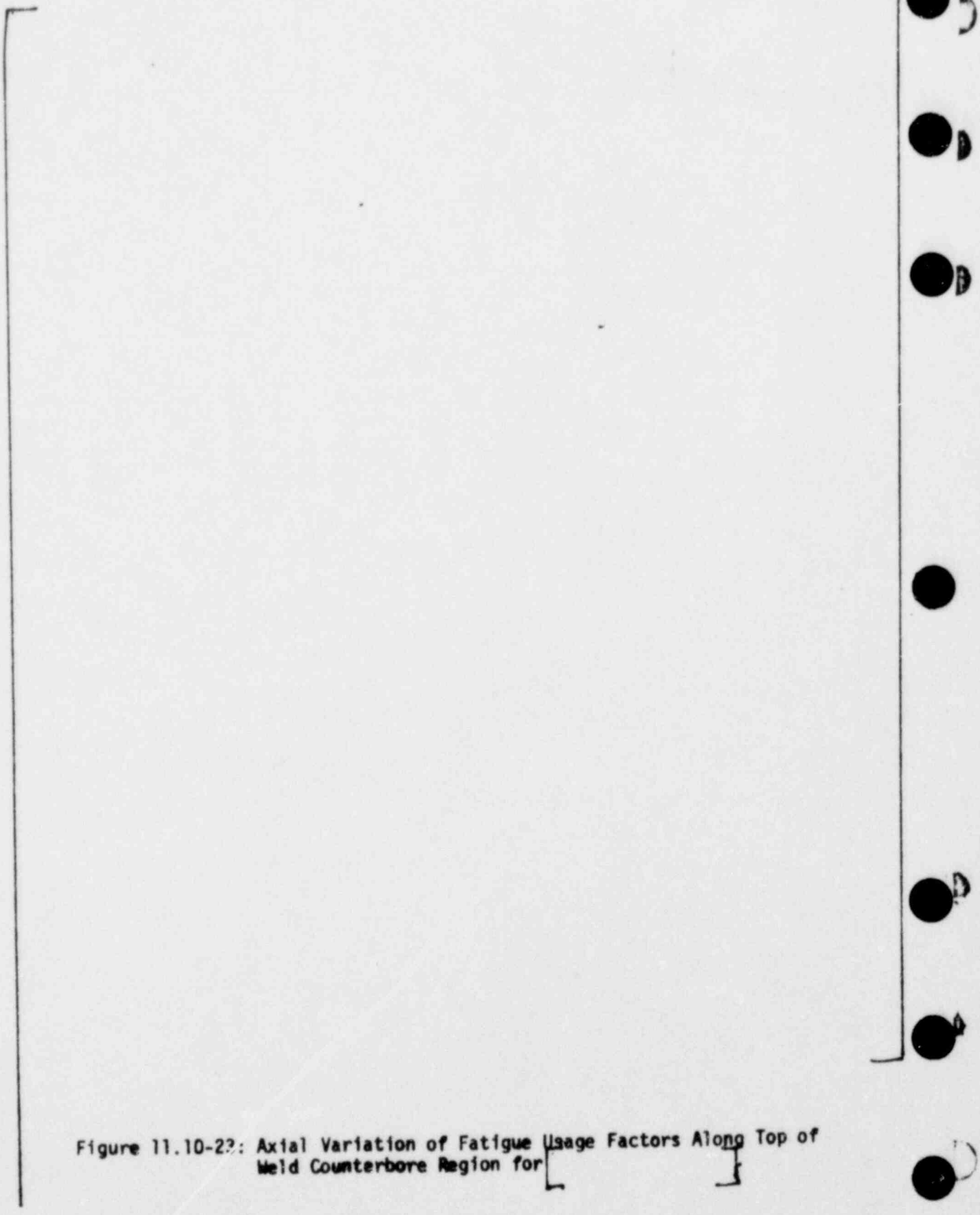

Figure 11.10-23: Axial Variation of Fatigue Usage Factors Along Top of Weld Counterbore Region for [ ]

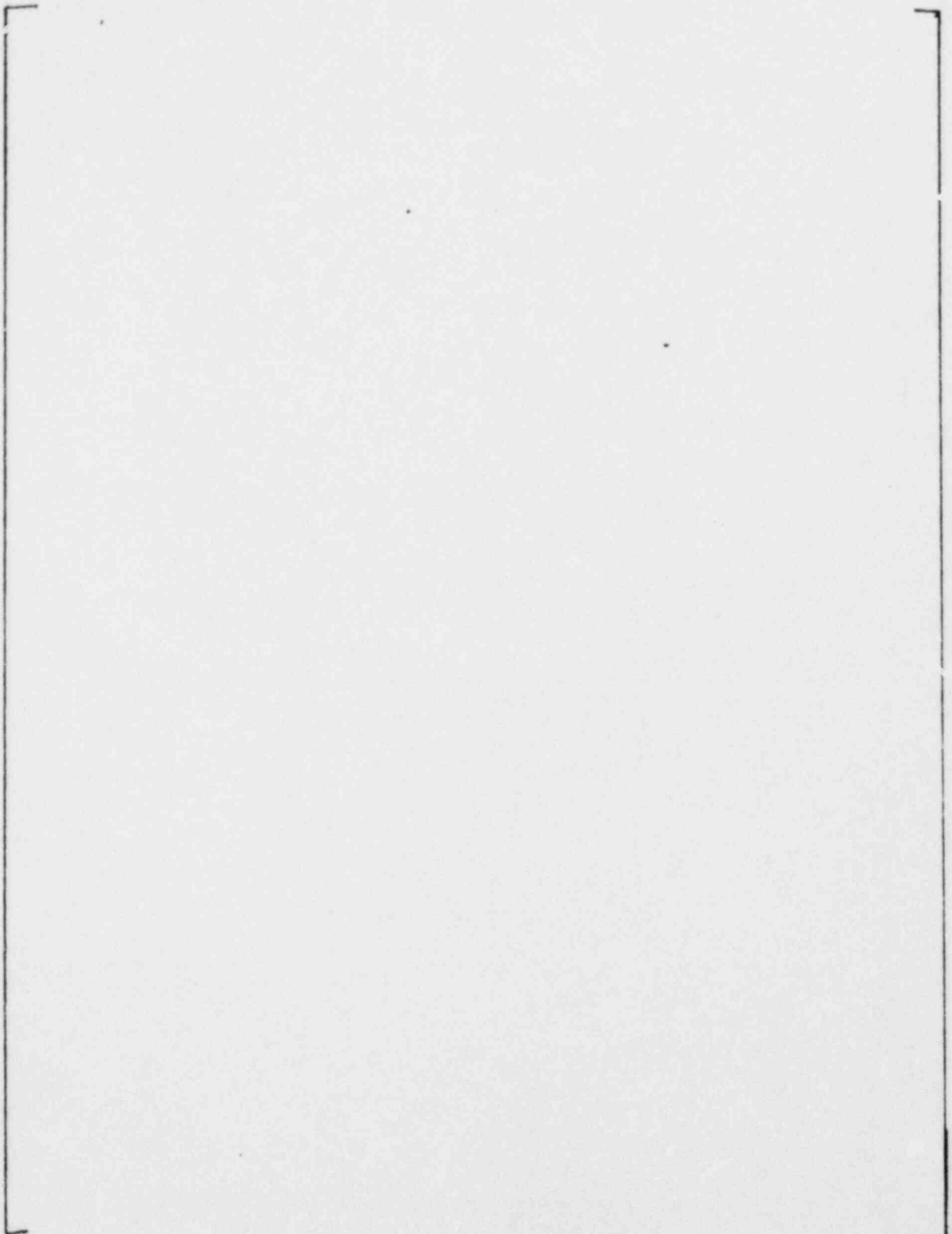

a,c,e

Figure 11.10-24: Axial Variation of Fatigue Usage Factors Along Side of Weld Counterbore Region for [ ]

[

a.c.e

]

FIGURE 11.11-1 CIRCUMFERENTIAL USAGE FACTORS PER SINGLE HOT STANDBY EVENT - [ ]

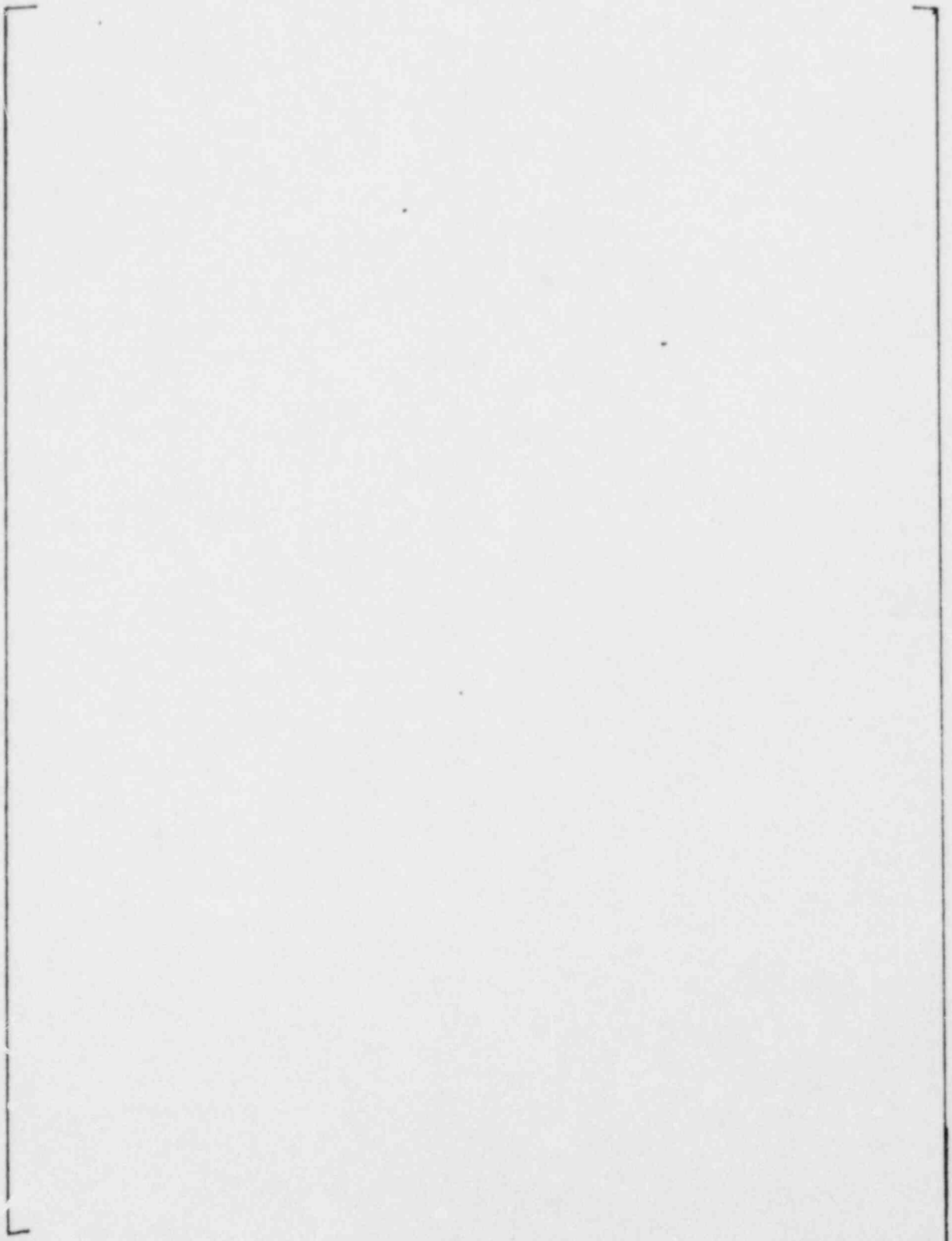

a,c,e

FIGURE 11.11-2 CIRCUMFERENTIAL USAGE FACTORS PER SINGLE HOT STANDBY EVENT -[ ]

a.c.e

FIGURE 11.11-3 CIRCUMFERENTIAL USAGE FACTORS PER SINGLE HOT STANDBY EVENT - [ ]

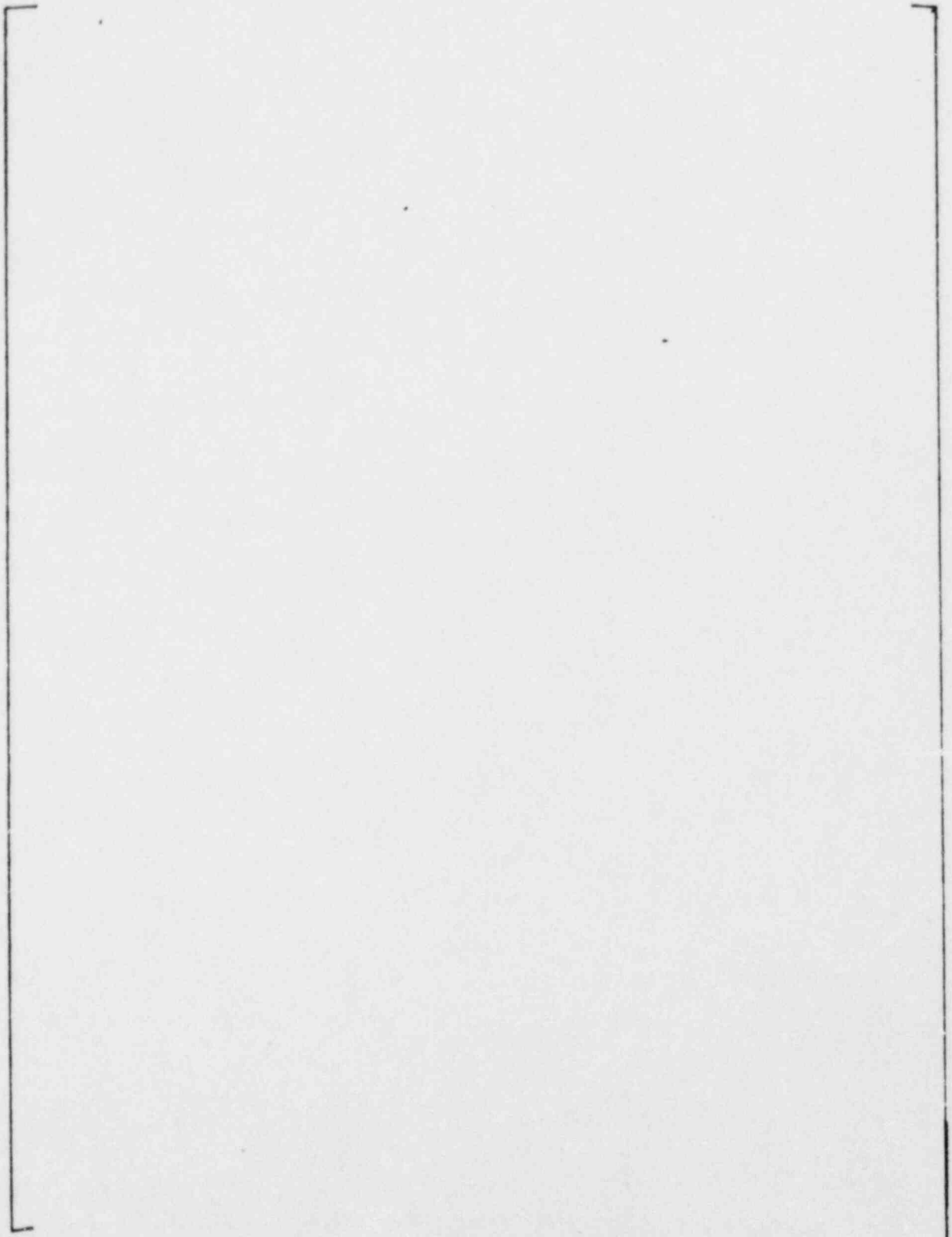

a,c,e

FIGURE 1[illegible].11-4 CIRCUMFERENTIAL USAGE FACTORS PER SINGLE HOT STANDBY EVENT - [ ]

a.c.e

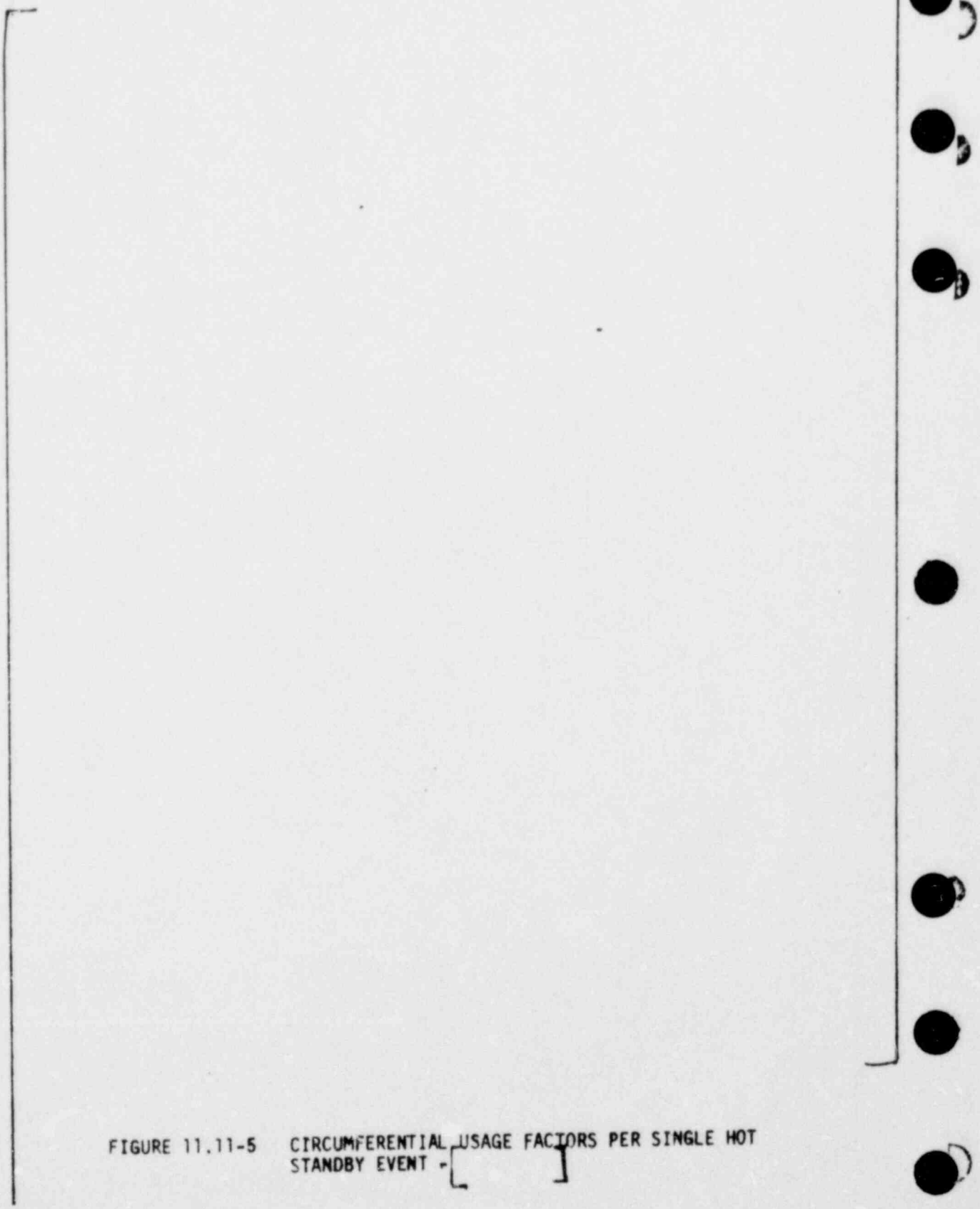

FIGURE 11.11-5 CIRCUMFERENTIAL USAGE FACTORS PER SINGLE HOT STANDBY EVENT - [ ]

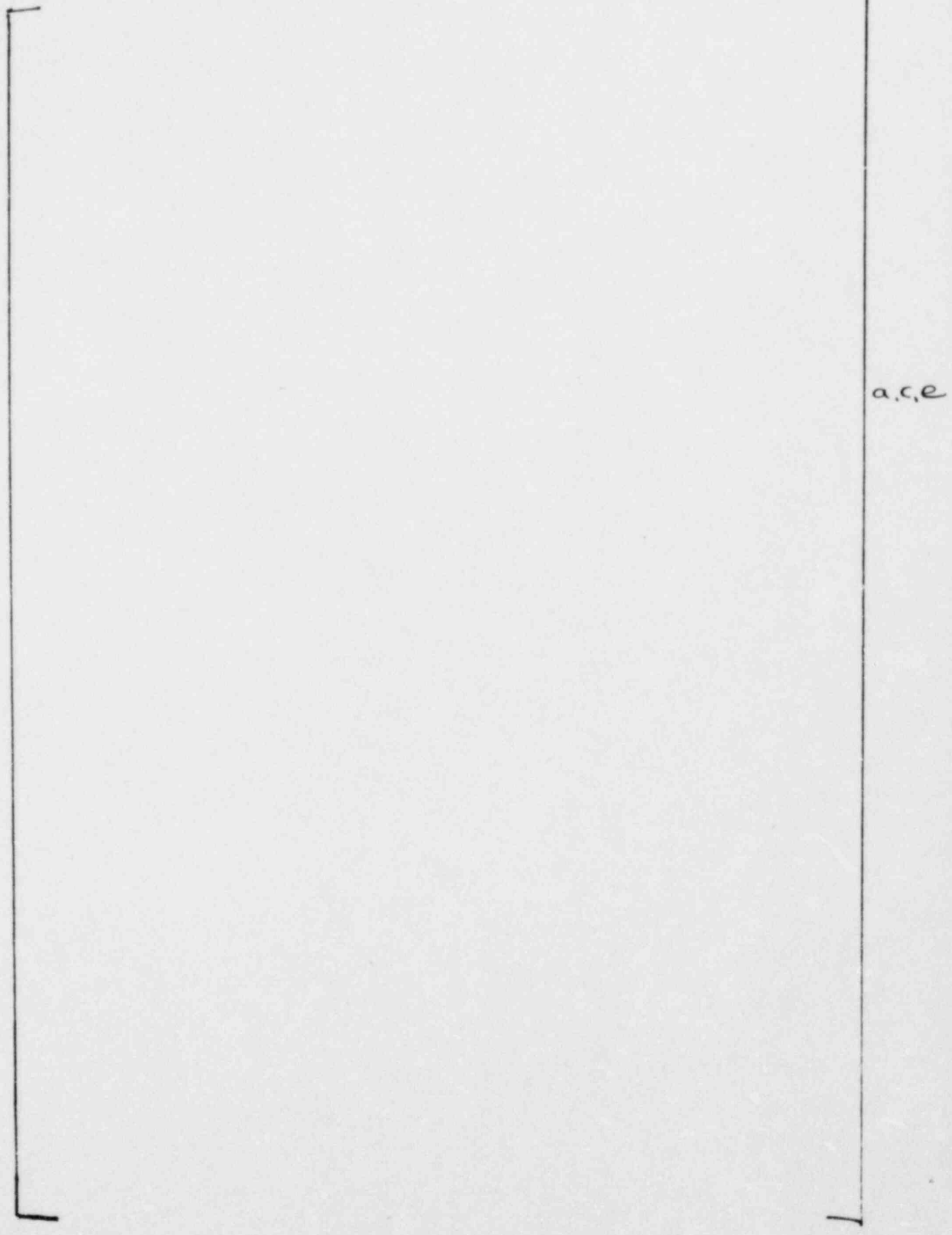

a,c,e

Figure 11.12-1: Effect of Counterbore Geometry on Stress Concentration At Root of Elbow Transition

Figure 11.12-2: Comparison of Measured Temperatures Between Lined and Unlined Pipes for Test Sets 17, 18, and 19.

a.c.e

Figure 11.12-3: Estimate of Axial Stress Ranges for Lined and Unlined Pipes for Test Sets 17, 18, and 19.

Figure 11.12-4: Comparison of Measured Temperatures Between Lined and Unlined Pipes for Test Set 20.

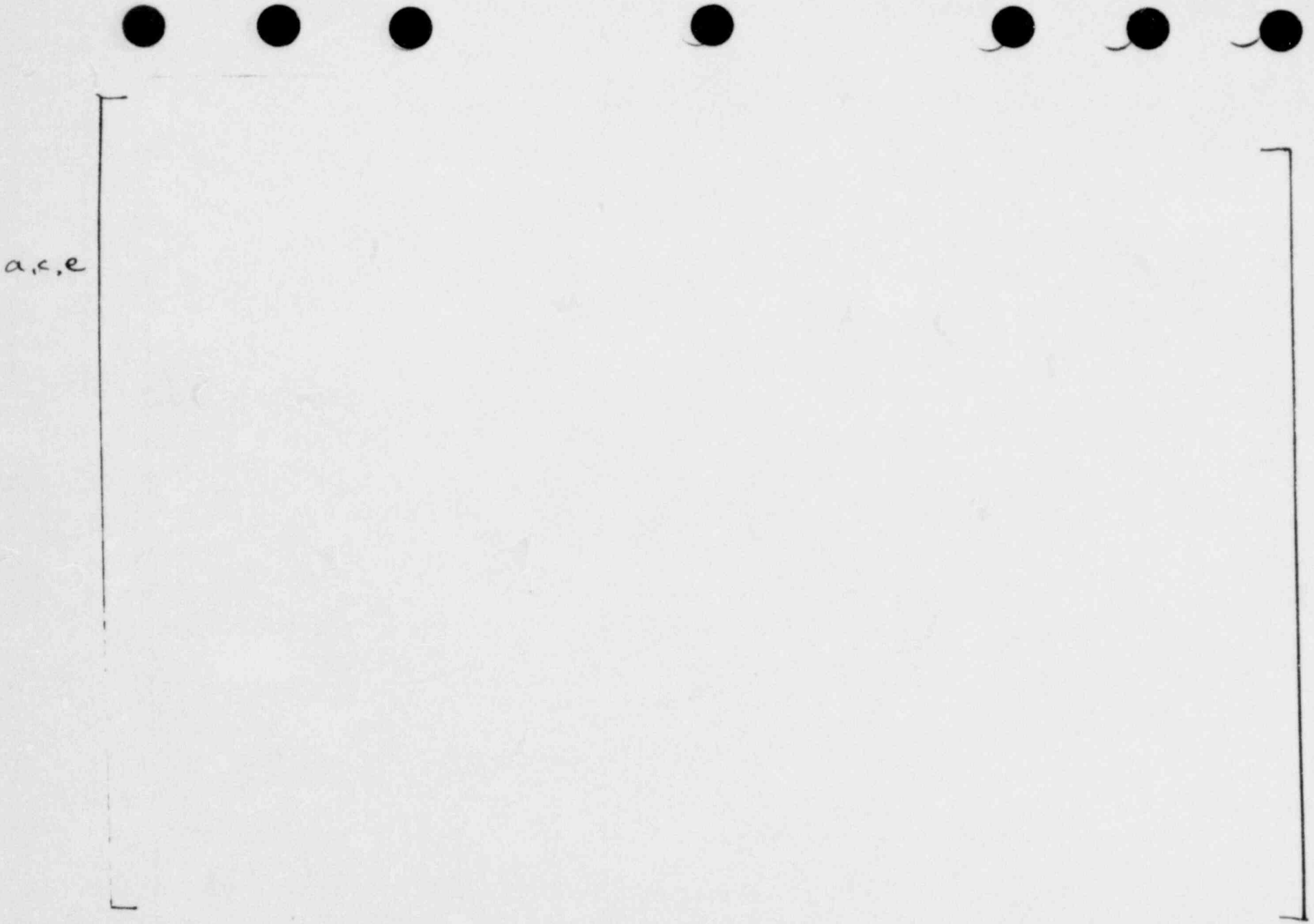

Figure 11.12-5: Estimate of Axial Stress Ranges for Lined and Unlined Pipes for Test Set 20.

Figure 11.12-6: Comparison of Measured Temperatures Between Lined and Unlined Pipes for Initial Power Escalation and Turbine Roll

Figure 11.12-7: Estimate of Axial Stress Ranges for Lined and Unlined Pipes for Initial Power Escalation and Turbine Roll.

C

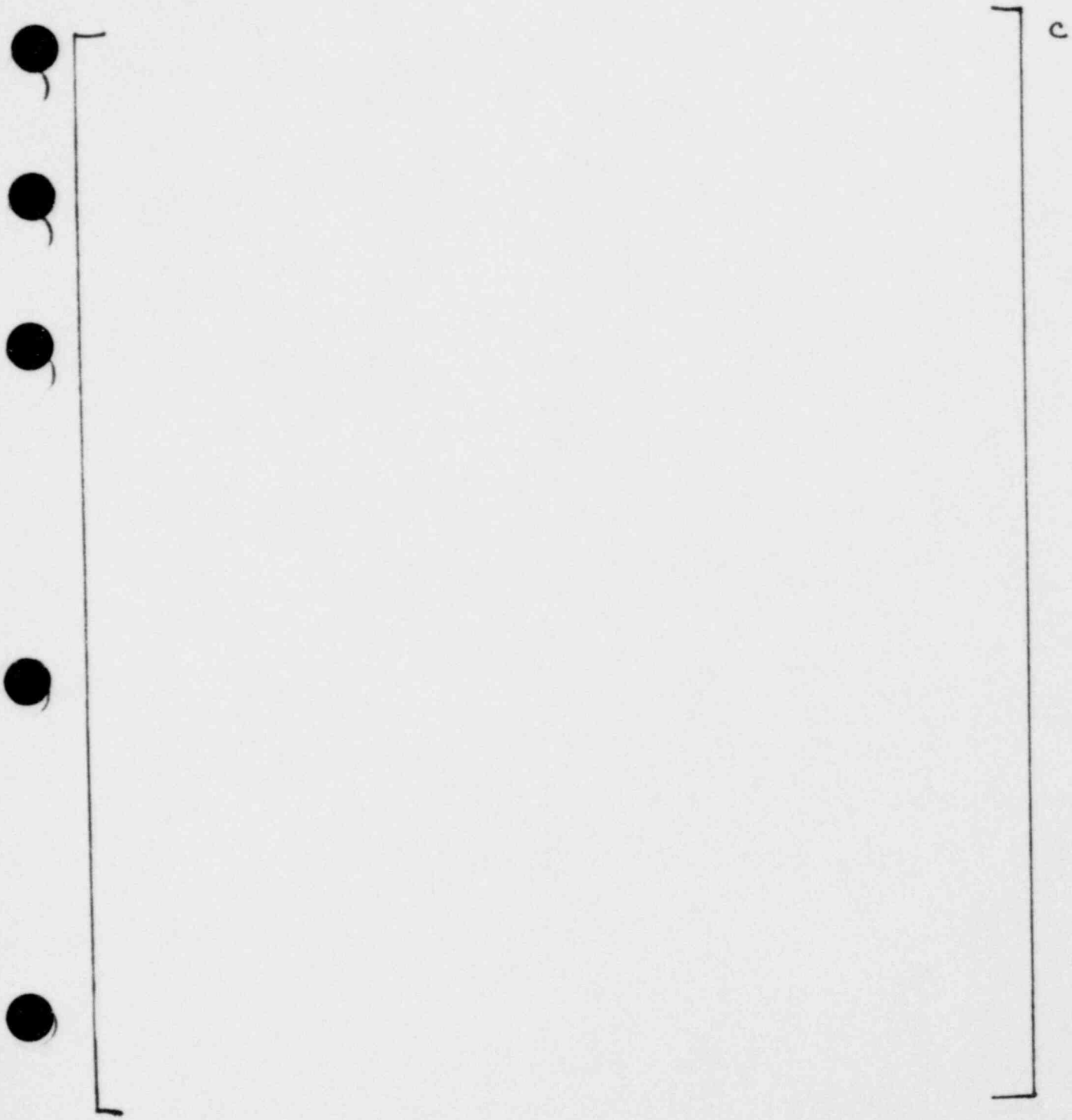
c

Figure 11.A-1: Temperature Distributions Used in 20/30 Comparisons.

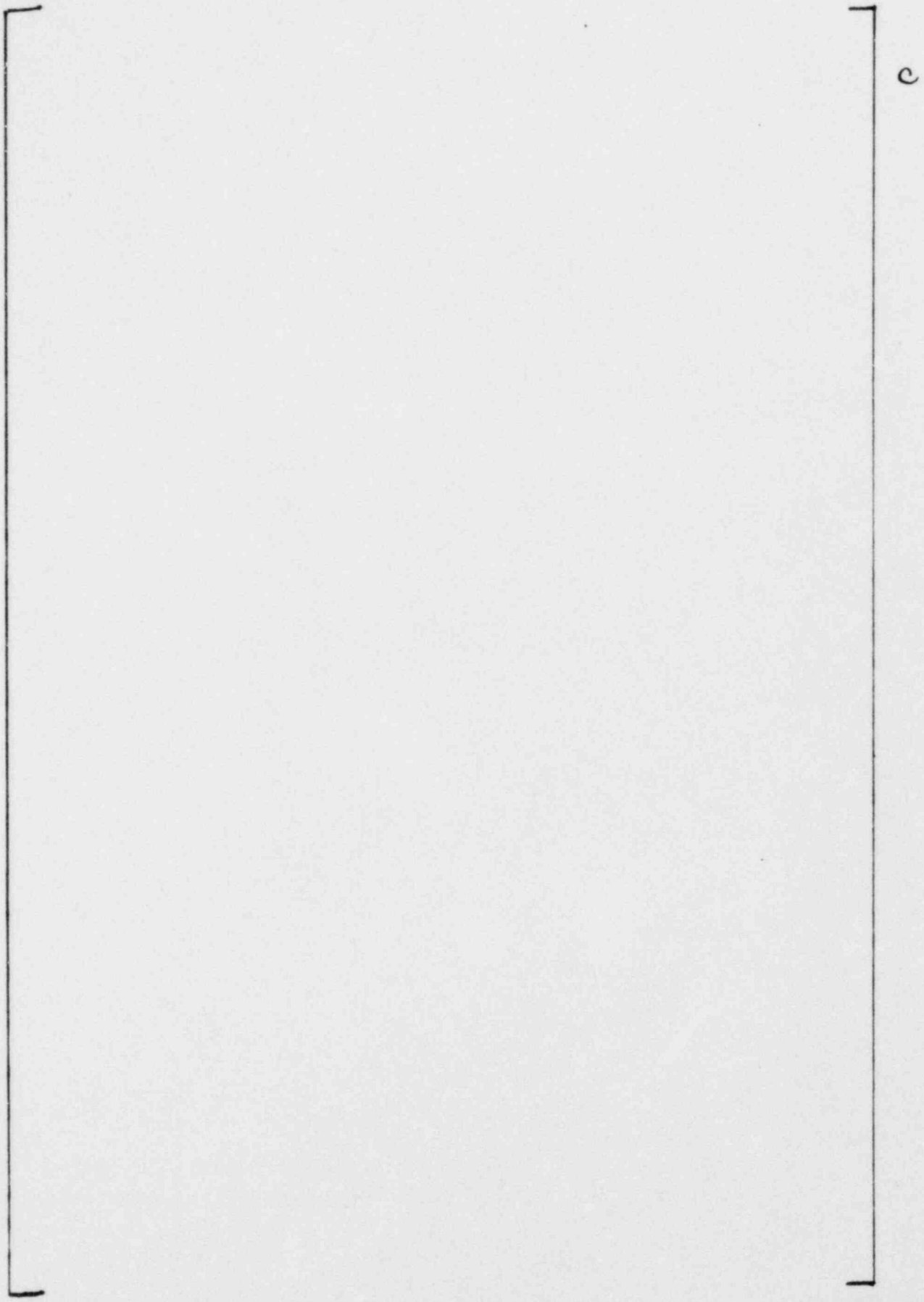

Figure 11.A-2: Verification Finite Element Models.

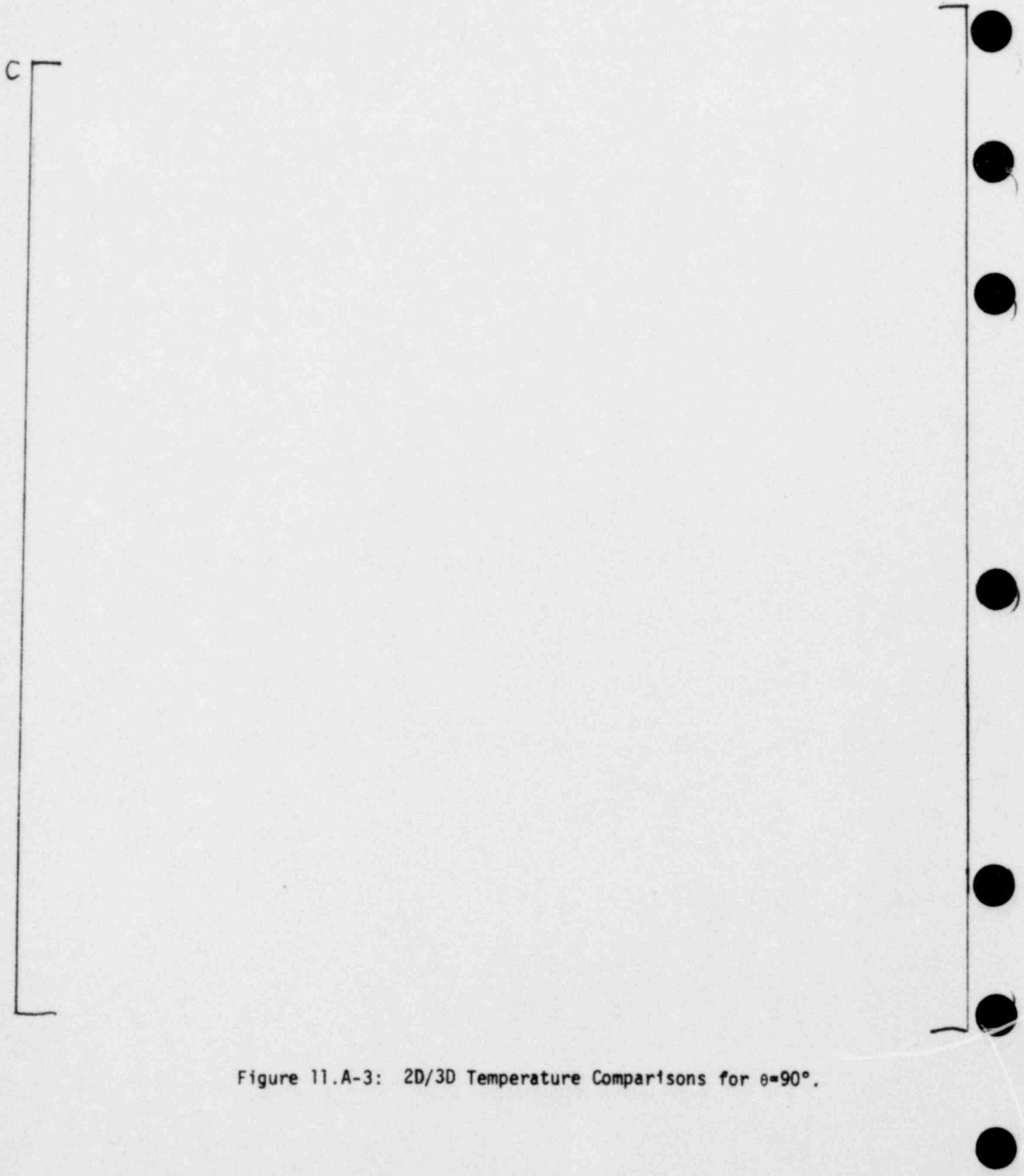

Figure 11.A-3: 2D/3D Temperature Comparisons for θ=90°.

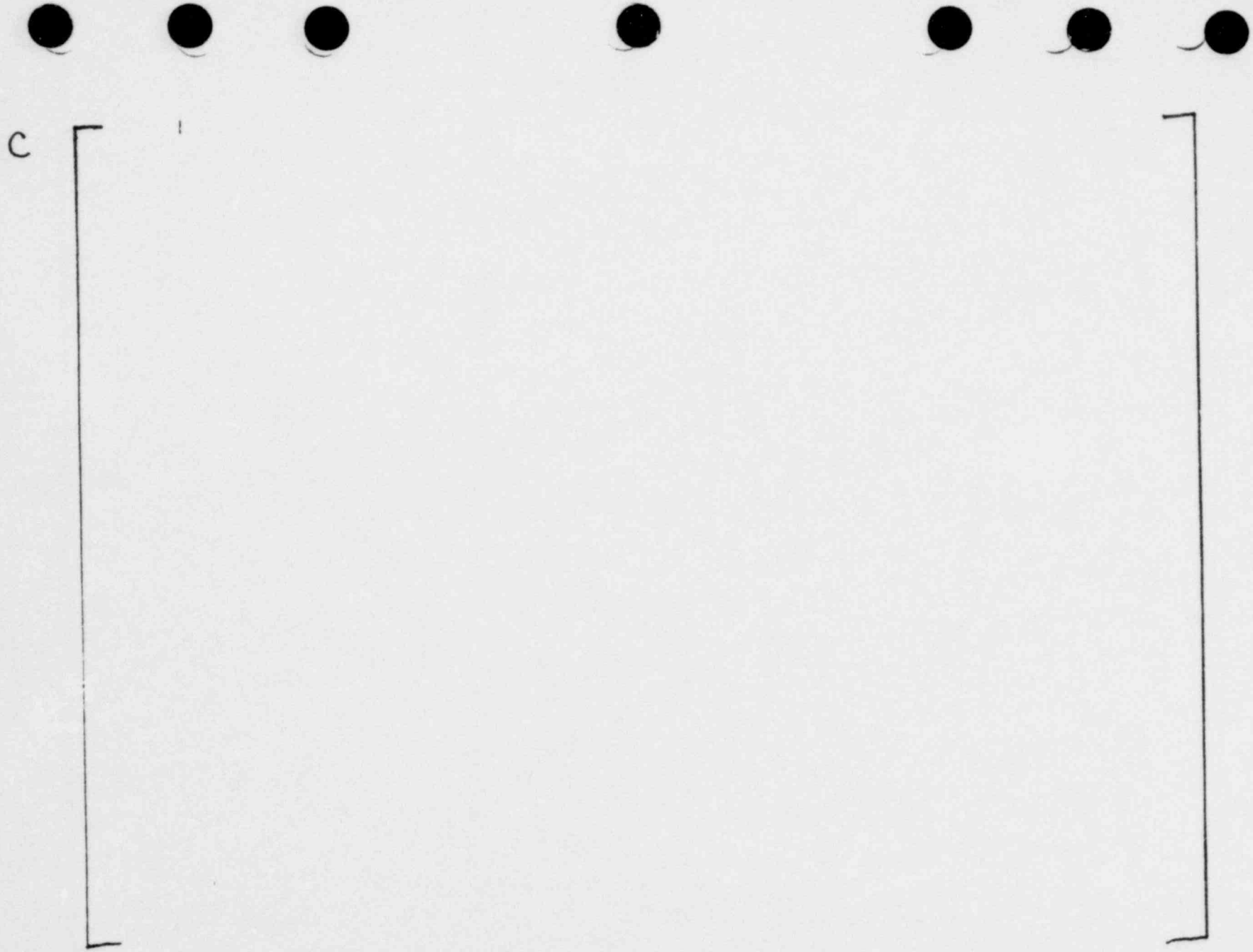

Figure 11.A-4: Comparisons of Axial Stresses for θ=90°.

C

Figure 11.A-5: Comparisons of Stress Intensities for θ=90°.

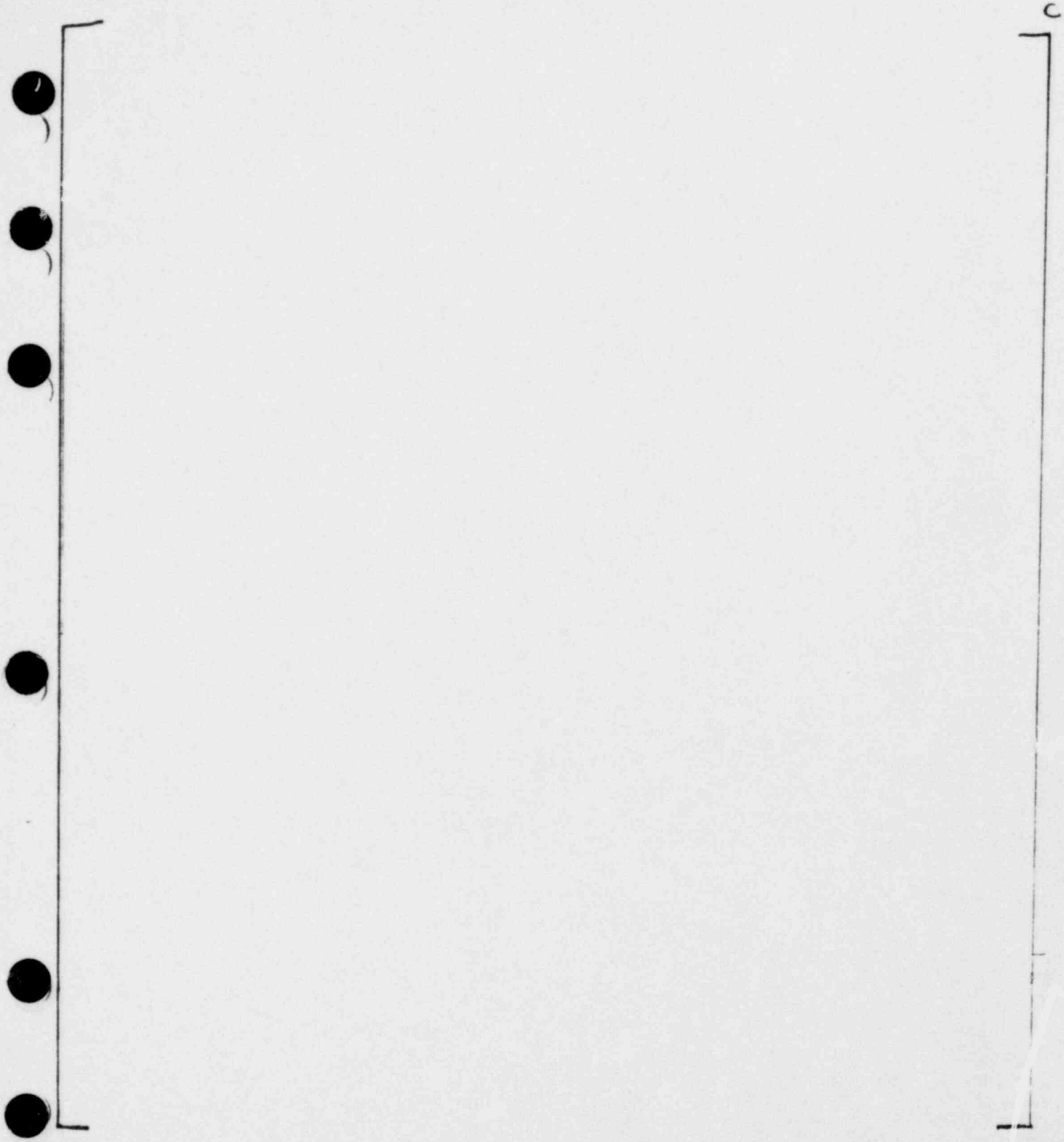

Figure 11.A-6: 2D/3D Temperature Comparisons for θ=45°.

C

Figure 11.A-7: Comparisons of Axial Stresses for θ=45°.

C

Figure 11.A-8: Comparisons of Stress Intensities for θ=45°.

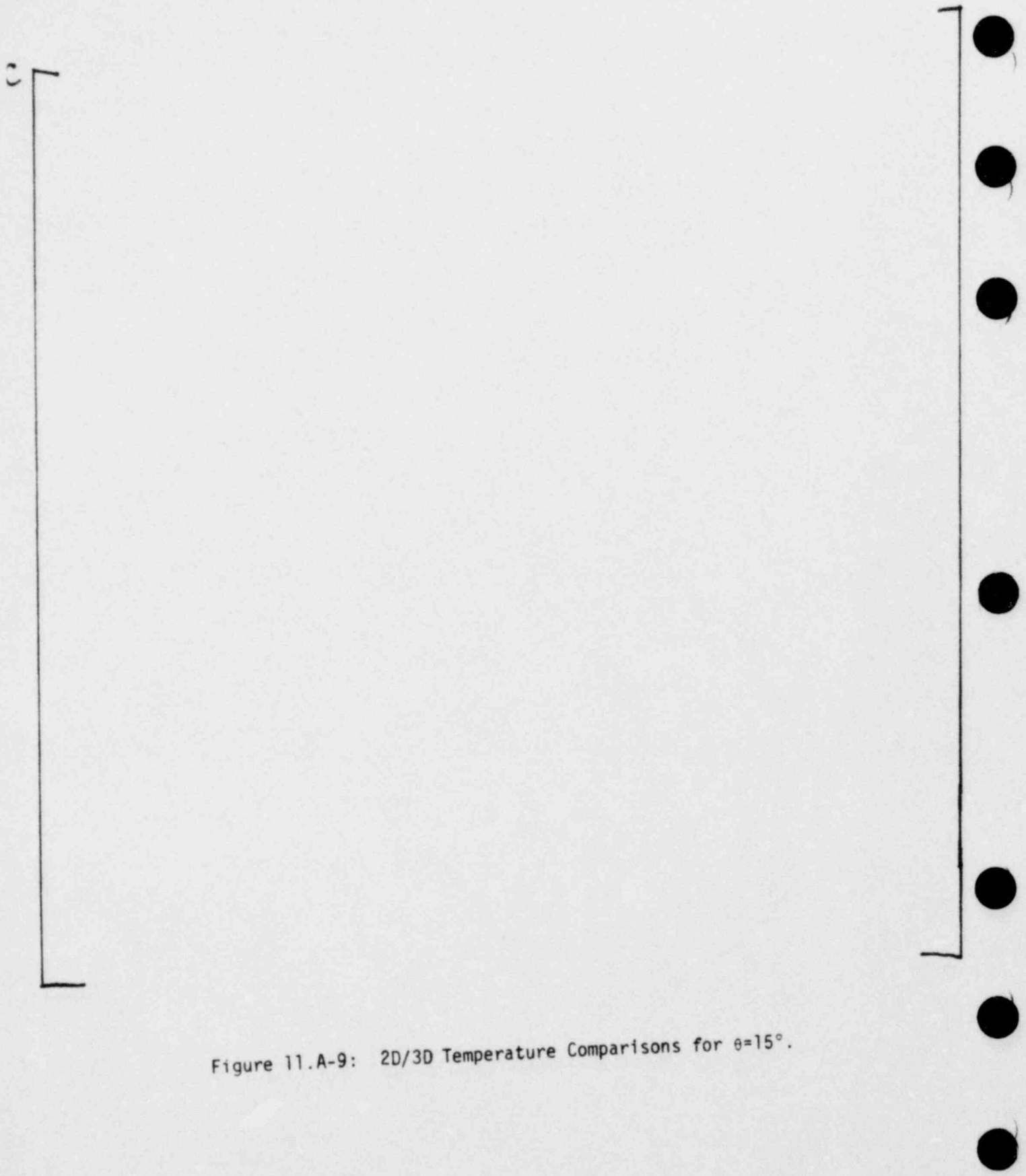

Figure 11.A-9: 2D/3D Temperature Comparisons for θ=15°.

Figure 11.A-10: Comparisons of Axial Stresses for θ=15°.

C

Figure 11.A-11: Comparisons of Stress Intensities for θ=15°.

APPENDIX 11.B

WECEVAL RESULTS FOR MAXIMUM RANGE OF STRESS

INTENSITY AND FATIGUE EVALUATIONS

POOR ORIGINAL

a.c.e

[ ] - MAXIMUM RANGE OF STRESS INTENSITY

SUMMARY - MAXIMUM RANGE OF STRESS INTENSITY ANALYSIS

ANALYSIS SECTION	SURFACE	LOAD CONDITION COMBINATION	SI RANGE (KSI)	ALLOWA (KSI
1	INSIDE	T1-425DEG- T2-450DEG	135.31	56.70
	OUTSIDE	T3-390DEG- AMBIENT	32.31	56.70
2	INSIDE	T1-425DEG- T2-450DEG	137.00	56.70
	OUTSIDE	T3-390DEG- AMBIENT	28.31	56.70
3	INSIDE	T1-425DEG- T2-450DEG	108.16	56.70
	OUTSIDE	T3-390DEG- AMBIENT	30.08	56.70
4	INSIDE	T2-450DEG- T3-390DEG	93.40	56.70
	OUTSIDE	T1-425DEG- T2-450DEG	36.90	56.70
5	INSIDE	T1-425DEG- T2-450DEG	77.40	56.70
	OUTSIDE	T1-425DEG- T2-450DEG	49.89	56.70
6	INSIDE	T1-425DEG- T6-410DEG	60.26	56.70
	OUTSIDE	T1-425DEG- T5-430DEG	42.93	56.70
7	INSIDE	T1-425DEG- T6-410DEG	71.91	56.70
	OUTSIDE	T1-425DEG- T5-430DEG	34.97	56.70
8	INSIDE	T3-390DEG- T5-430DEG	74.08	56.70
	OUTSIDE	T2-450DEG- T3-390DEG	37.23	56.70
9	INSIDE	T3-390DEG- T5-430DEG	85.50	56.70
	OUTSIDE	T2-450DEG- T3-390DEG	32.70	56.70
10	INSIDE	T2-450DEG- T3-390DEG	86.53	56.70
	OUTSIDE	T2-450DEG- T3-390DEG	30.69	56.70
11	INSIDE	T2-450DEG- T3-390DEG	86.91	56.70
	OUTSIDE	T2-450DEG- T6-410DEG	29.20	56.70
12	INSIDE	T2-450DEG- T6-410DEG	87.52	56.70
	OUTSIDE	T2-450DEG- T6-410DEG	31.05	56.70
13	INSIDE	T2-450DEG- T6-410DEG	92.96	56.70
	OUTSIDE	T2-450DEG- T6-410DEG	28.42	56.70
14	INSIDE	T2-450DEG- T6-410DEG	82.30	56.70
	OUTSIDE	T2-450DEG- T6-410DEG	24.33	56.70
15	INSIDE	T2-450DEG- T6-410DEG	67.92	56.70
	OUTSIDE	T2-450DEG- T5-430DEG	23.30	56.70
16	INSIDE	T2-450DEG- T5-430DEG	42.44	56.70
	OUTSIDE	T3-390DEG- T5-430DEG	27.45	56.70
17	INSIDE	T5-430DEG- AMBIENT	27.40	56.70
	OUTSIDE	T2-450DEG- T3-390DEG	32.34	56.70
18	INSIDE	T2-450DEG- T3-390DEG	44.80	56.70
	OUTSIDE	T2-450DEG- T3-390DEG	34.74	56.70
19	INSIDE	T2-450DEG- T6-410DEG	44.17	56.70
	OUTSIDE	T2-450DEG- T6-410DEG	25.80	56.70
20	INSIDE	T2-450DEG- T6-410DEG	42.02	56.70
	OUTSIDE	T6-410DEG- PRESSURE	19.41	56.70

RUN NO. Y6ALTZV

DATE: 2/28/80

REF. FIGS.: 11.10-1, 11.10-7

[ ] - FATIGUE AT ROOT OF ELBOW TRANSITION a,c,e

FATIGUE ANALYSIS LOCATION SUMMARY

LOCATION	STRESS CONCENTRATORS KX	KY	KZ	KXR	KYR	KZR	TOTAL USAGE FACTOR
3405	1.00	1.00	1.00	1.00	1.00	1.00	31.7559
3410	1.00	1.00	1.00	1.00	1.00	1.00	31.0932
3415	1.00	1.00	1.00	1.00	1.00	1.00	16.7247
3420	1.00	1.00	1.00	1.00	1.00	1.00	10.3049
3425	1.00	1.00	1.00	1.00	1.00	1.00	5.0099
3435	1.00	1.00	1.00	1.00	1.00	1.00	1.4058
3440	1.00	1.00	1.00	1.00	1.00	1.00	3.9326
3445	1.00	1.00	1.00	1.00	1.00	1.00	4.5610
3450	1.00	1.00	1.00	1.00	1.00	1.00	6.0558
3455	1.00	1.00	1.00	1.00	1.00	1.00	9.1828
3460	1.00	1.00	1.00	1.00	1.00	1.00	15.8964
3465	1.00	1.00	1.00	1.00	1.00	1.00	16.6592
3470	1.00	1.00	1.00	1.00	1.00	1.00	17.9121
3475	1.00	1.00	1.00	1.00	1.00	1.00	12.2546
3480	1.00	1.00	1.00	1.00	1.00	1.00	6.5280
3485	1.00	1.00	1.00	1.00	1.00	1.00	.1147
3495	1.00	1.00	1.00	1.00	1.00	1.00	.0085
3505	1.00	1.00	1.00	1.00	1.00	1.00	.2102
3515	1.00	1.00	1.00	1.00	1.00	1.00	.2027

RUN NO.: Y6ALTZX

DATE: 2/28/80

REF. FIGS.: 11.10-1, 11.10-7, 11.10-8

POOR ORIGINAL

c.e

[ ] - MAXIMUM RANGE OF STRESS INTENSITY

SUMMARY - MAXIMUM RANGE OF STRESS INTENSITY ANALYSIS

ANALYSIS SECTION	SURFACE	LOAD CONDITION COMBINATION	ST RANGE (KSI)	ALLOWABLE (KSI)
1	INSIDE	11-WEIGHT+PG- 12-45 DEG	155.31	58.7
	OUTSIDE	13-3RD PEAK- 1-DELTA T	52.51	58.7
2	INSIDE	11-WEIGHT+PG- 12-45 DEG	137.[illegible]	58.7
	OUTSIDE	13-3RD PEAK- 1-DELTA T	28.31	58.7
3	INSIDE	11-WEIGHT+PG- 12-45 DEG	108.10	58.7
	OUTSIDE	13-3RD PEAK- 1-DELTA T	[illegible]	58.7
4	INSIDE	12-45 DEG- 13-3RD PEAK	93.[illegible]	58.7
	OUTSIDE	11-WEIGHT+PG- 12-45 DEG	58.[illegible]	58.7
5	INSIDE	11-WEIGHT+PG- 12-45 DEG	77.[illegible]	58.7
	OUTSIDE	11-WEIGHT+PG- 12-45 DEG	46.[illegible]	58.7
6	INSIDE	11-WEIGHT+PG- 12-45 DEG	60.20	58.7
	OUTSIDE	11-WEIGHT+PG- 12-45 DEG	42.43	58.7
7	INSIDE	11-WEIGHT+PG- 12-45 DEG	11.41	58.7
	OUTSIDE	11-WEIGHT+PG- 13-3RD PEAK	34.97	58.7
8	INSIDE	13-3RD PEAK- 13-45 DEG	74.[illegible]	58.7
	OUTSIDE	12-45 DEG- 13-3RD PEAK	37.25	58.7
9	INSIDE	13-3RD PEAK- 13-45 DEG	55.5[illegible]	58.7
	OUTSIDE	12-45 DEG- 13-3RD PEAK	32.7[illegible]	58.7
10	INSIDE	12-45 DEG- 13-3RD PEAK	58.53	58.7
	OUTSIDE	12-45 DEG- 13-3RD PEAK	5[illegible].84	58.7
11	INSIDE	12-45 DEG- 13-3RD PEAK	58.91	58.7
	OUTSIDE	12-45 DEG- 10-WEIGHT+PG	29.2[illegible]	58.7
12	INSIDE	12-45 DEG- 10-WEIGHT+PG	27.5[illegible]	58.7
	OUTSIDE	12-45 DEG- 10-WEIGHT+PG	31.[illegible]3	58.7
13	INSIDE	12-45 DEG- 10-WEIGHT+PG	92.90	58.7
	OUTSIDE	12-45 DEG- 10-WEIGHT+PG	[illegible] 12	58.7
14	INSIDE	12-45 DEG- 10-WEIGHT+PG	82.3[illegible]	58.7
	OUTSIDE	12-45 DEG- 10-WEIGHT+PG	24.53	58.7
15	INSIDE	12-45 DEG- 10-WEIGHT+PG	07.9[illegible]	58.7
	OUTSIDE	12-45 DEG- 13-3RD PEAK	23.3[illegible]	58.7
16	INSIDE	12-45 DEG- 13-3RD PEAK	42.44	58.7
	OUTSIDE	13-3RD PEAK- 13-45 DEG	27.43	58.7
17	INSIDE	13-3RD PEAK- 1-DELTA T	27.4[illegible]	58.7
	OUTSIDE	12-45 DEG- 13-3RD PEAK	56.54	58.7
18	INSIDE	12-45 DEG- 13-3RD PEAK	46.[illegible]	58.7
	OUTSIDE	12-45 DEG- 13-3RD PEAK	54.7[illegible]	58.7
19	INSIDE	12-45 DEG- 10-WEIGHT+PG	44.1[illegible]	58.7
	OUTSIDE	12-45 DEG- 10-WEIGHT+PG	25.[illegible]	58.7
20	INSIDE	12-45 DEG- 10-WEIGHT+PG	42.[illegible]	58.7
	OUTSIDE	10-WEIGHT+PG- PRESSURE	14.41	58.7

RUN NO.: Y6ALTVO

DATE: 2/26/80

REF. FIGS.: 11.10-1, 11.10-8

POOR ORIGINAL

[ ] - FATIGUE AT ROOT OF ELBOW TRANSITION

a,c,e

FATIGUE ANALYSIS LOCATION SUMMARY

LOCATION	STRESS CONCENTRATORS KX	KY	KZ	KXR	KYR	KZR	TOTAL USAGE FACTOR
3405	1.00	1.00	1.00	1.00	1.00	1.00	97.6093
3410	1.00	1.00	1.00	1.00	1.00	1.00	98.7911
3415	1.00	1.00	1.00	1.00	1.00	1.00	26.0387
3420	1.00	1.00	1.00	1.00	1.00	1.00	10.3655
3425	1.00	1.00	1.00	1.00	1.00	1.00	2.2071
3435	1.00	1.00	1.00	1.00	1.00	1.00	.1208
3440	1.00	1.00	1.00	1.00	1.00	1.00	1.0966
3445	1.00	1.00	1.00	1.00	1.00	1.00	1.5218
3450	1.00	1.00	1.00	1.00	1.00	1.00	3.4909
3455	1.00	1.00	1.00	1.00	1.00	1.00	4.3688
3460	1.00	1.00	1.00	1.00	1.00	1.00	11.4639
3465	1.00	1.00	1.00	1.00	1.00	1.00	13.6439
3470	1.00	1.00	1.00	1.00	1.00	1.00	17.7653
3475	1.00	1.00	1.00	1.00	1.00	1.00	7.6595
3480	1.00	1.00	1.00	1.00	1.00	1.00	1.4266
3485	1.00	1.00	1.00	1.00	1.00	1.00	.0379
3495	1.00	1.00	1.00	1.00	1.00	1.00	.0055
3505	1.00	1.00	1.00	1.00	1.00	1.00	.0508
3515	1.00	1.00	1.00	1.00	1.00	1.00	.0566
3525	1.00	1.00	1.00	1.00	1.00	1.00	.0400

RUN NO.: Y6ALTCX

DATE: 2/26/80

REF. FIGS.: 11.10-1, 11.10-8

POOR ORIGINAL

a.c.e

[ ] = FATIGUE AT TOP OF ELBOW

SUMMARY = MAXIMUM RANGE OF STRESS INTENSITY ANALYSIS

ANALYSIS SECTION	SURFACE	LOAD CONDITION COMBINATION	SI RANGE (KSI)	ALLOWABLE (KSI)
21	INSIDE	T1=425DEG- T2=450DEG	19.01	80.10
	OUTSIDE	T1=425DEG- AMBIENT	15.45	80.10
22	INSIDE	T1=425DEG- T2=450DEG	30.48	80.10
	OUTSIDE	T1=425DEG- T2=450DEG	16.85	80.10
23	INSIDE	T1=425DEG- T2=450DEG	62.48	80.10
	OUTSIDE	T1=425DEG- T2=450DEG	19.43	80.10
24	INSIDE	T1=425DEG- AMBIENT	27.27	80.10
	OUTSIDE	T1=425DEG- T2=450DEG	100.80	80.10
25	INSIDE	T1=425DEG- AMBIENT	37.68	80.10
	OUTSIDE	T1=425DEG- T2=450DEG	104.04	80.10
26	INSIDE	T1=425DEG- AMBIENT	43.22	80.10
	OUTSIDE	T1=425DEG- T2=450DEG	74.17	80.10
27	INSIDE	T1=425DEG- T2=450DEG	48.75	80.10
	OUTSIDE	T1=425DEG- T2=450DEG	66.92	80.10
28	INSIDE	T1=425DEG- T2=450DEG	63.87	80.10
	OUTSIDE	T1=425DEG- T2=450DEG	61.14	80.10
29	INSIDE	T1=425DEG- T2=450DEG	88.02	80.10
	OUTSIDE	T2=450DEG- T3=390DEG	38.50	80.10
30	INSIDE	T1=425DEG- T2=450DEG	112.76	56.70
	OUTSIDE	T2=450DEG- T3=390DEG	32.45	56.70
31	INSIDE	T1=425DEG- T2=450DEG	127.36	56.70
	OUTSIDE	T2=450DEG- T3=390DEG	28.91	56.70
32	INSIDE	T1=425DEG- T2=450DEG	135.31	56.70
	OUTSIDE	T3=390DEG- AMBIENT	32.31	56.70
33	INSIDE	T1=425DEG- T2=450DEG	97.62	56.70
	OUTSIDE	T2=450DEG- T3=390DEG	32.08	56.70
34	INSIDE	T2=450DEG- T3=390DEG	60.79	56.70
	OUTSIDE	T1=425DEG- T2=450DEG	47.98	56.70
35	INSIDE	T1=425DEG- T2=450DEG	49.64	56.70
	OUTSIDE	T1=425DEG- T2=450DEG	51.91	56.70
36	INSIDE	T1=425DEG- T2=450DEG	44.34	56.70
	OUTSIDE	T1=425DEG- T2=450DEG	60.66	56.70
37	INSIDE	T1=425DEG- T2=450DEG	44.94	56.70
	OUTSIDE	T1=425DEG- T2=450DEG	56.54	56.70
38	INSIDE	T2=450DEG- T3=390DEG	46.33	56.70
	OUTSIDE	T1=425DEG- T2=450DEG	56.60	56.70
39	INSIDE	T2=450DEG- T3=390DEG	41.68	56.70
	OUTSIDE	T1=425DEG- T2=450DEG	43.65	56.70
40	INSIDE	T2=450DEG- T3=390DEG	34.98	56.70
	OUTSIDE	T2=450DEG- T3=390DEG	51.53	56.70

RUN NO.: Y6ALT26

DATE: 3/11/80

REF. FIGS.: 11.10-2, 11.10-9

a,c,e

[ ] = FATIGUE AT TOP OF ELBOW

FATIGUE ANALYSIS LOCATION SUMMARY

LOCATION	STRESS CONCENTRATORS KX	KY	KZ	KXR	KYR	KZR	TOTAL USAGE FACTOR
1805	1.00	1.00	1.00	1.00	1.00	1.00	0.0000
2005	1.00	1.00	1.00	1.00	1.00	1.00	.0019
2205	1.00	1.00	1.00	1.00	1.00	1.00	.1691
2405	1.00	1.00	1.00	1.00	1.00	1.00	.0000
2605	1.00	1.00	1.00	1.00	1.00	1.00	.0019
2805	1.00	1.00	1.00	1.00	1.00	1.00	.0025
2930	1.00	1.00	1.00	1.00	1.00	1.00	.0101
3005	1.00	1.00	1.00	1.00	1.00	1.00	.1190
3130	1.00	1.00	1.00	1.00	1.00	1.00	2.7473
3205	1.00	1.00	1.00	1.00	1.00	1.00	11.7857
3330	1.00	1.00	1.00	1.00	1.00	1.00	20.3870
3405	1.00	1.00	1.00	1.00	1.00	1.00	31.7554
3530	1.00	1.00	1.00	1.00	1.00	1.00	9.0320
3605	1.00	1.00	1.00	1.00	1.00	1.00	1.2592
3730	1.00	1.00	1.00	1.00	1.00	1.00	.1616
3805	1.00	1.00	1.00	1.00	1.00	1.00	.0433
3930	1.00	1.00	1.00	1.00	1.00	1.00	.0677
4005	1.00	1.00	1.00	1.00	1.00	1.00	.0840
4205	1.00	1.00	1.00	1.00	1.00	1.00	.0216
4405	1.00	1.00	1.00	1.00	1.00	1.00	.0038

RUN NO.: Y6ALT26

DATE: 3/11/80

REF. FIGS.: 11.10-2, 11.10-9

POOR ORIGINAL

I.C.E

[ ] = MAXIMUM RANGE AND FATIGUE AT 90 DEG

SUMMARY = MAXIMUM RANGE OF STRESS INTENSITY ANALYSIS

ANALYSIS SECTION	SURFACE	LOAD CONDITION COMBINATION	SI RANGE (KSI)	ALLOWABLE (KSI)
01	INSIDE	T1=425DEG- T2=450DEG	24.22	80.10
	OUTSIDE	T1=425DEG- AMBIENT	15.42	80.10
02	INSIDE	T1=425DEG- T2=450DEG	34.05	80.10
	OUTSIDE	T1=425DEG- AMBIENT	12.89	80.10
03	INSIDE	T2=450DEG- T3=390DEG	51.74	80.10
	OUTSIDE	T1=425DEG- AMBIENT	11.50	80.10
04	INSIDE	T2=450DEG- T6=410DEG	20.16	80.10
	OUTSIDE	T2=450DEG- T6=410DEG	65.76	80.10
05	INSIDE	T1=425DEG- T2=450DEG	19.43	80.10
	OUTSIDE	T2=450DEG- T6=410DEG	78.32	80.10
06	INSIDE	T2=450DEG- T3=390DEG	34.79	80.10
	OUTSIDE	T2=450DEG- T6=410DEG	65.00	80.10
07	INSIDE	T2=450DEG- T3=390DEG	39.10	80.10
	OUTSIDE	T2=450DEG- T6=410DEG	63.49	80.10
08	INSIDE	T2=450DEG- T3=390DEG	45.13	80.10
	OUTSIDE	T2=450DEG- T6=410DEG	58.26	80.10
09	INSIDE	T2=450DEG- T3=390DEG	54.41	80.10
	OUTSIDE	T2=450DEG- T6=410DEG	41.26	80.10
70	INSIDE	T2=450DEG- T3=390DEG	68.98	56.70
	OUTSIDE	T2=450DEG- T6=410DEG	31.58	56.70
71	INSIDE	T2=450DEG- T6=410DEG	78.55	56.70
	OUTSIDE	T2=450DEG- T6=410DEG	31.53	56.70
72	INSIDE	T2=450DEG- T6=410DEG	87.32	56.70
	OUTSIDE	T2=450DEG- T6=410DEG	31.05	56.70
73	INSIDE	T2=450DEG- T6=410DEG	63.25	56.70
	OUTSIDE	T2=450DEG- T6=410DEG	39.13	56.70
74	INSIDE	T2=450DEG- T3=390DEG	47.12	56.70
	OUTSIDE	T2=450DEG- T6=410DEG	44.64	56.70
75	INSIDE	T2=450DEG- T3=390DEG	59.32	56.70
	OUTSIDE	T2=450DEG- T6=410DEG	46.95	56.70
76	INSIDE	T1=425DEG- T2=450DEG	34.12	56.70
	OUTSIDE	T2=450DEG- T6=410DEG	50.21	56.70
77	INSIDE	T2=450DEG- T3=390DEG	35.79	56.70
	OUTSIDE	T2=450DEG- T6=410DEG	46.29	56.70
78	INSIDE	T2=450DEG- T3=390DEG	36.74	56.70
	OUTSIDE	T2=450DEG- T6=410DEG	43.31	56.70
79	INSIDE	T2=450DEG- T3=390DEG	37.15	56.70
	OUTSIDE	T2=450DEG- T6=410DEG	39.33	56.70
80	INSIDE	T2=450DEG- T3=390DEG	37.30	56.70
	OUTSIDE	T2=450DEG- T6=410DEG	34.31	56.70

RUN NO.: Y6ALTSE

DATE: 3/11/80

REF. FIGS: 11.10-2, 11.10-10

[ ] = MAXIMUM RANGE AND FATIGUE AT 90 DEG

a.c.e

FATIGUE ANALYSIS LOCATION SUMMARY

LOCATION	STRESS CONCENTRATIONS KX	KY	KZ	KXR	KYR	KZR	TOTAL USAGE FACTOR
1805	1.00	1.00	1.00	1.00	1.00	1.00	.0014
2005	1.00	1.00	1.00	1.00	1.00	1.00	.0079
2205	1.00	1.00	1.00	1.00	1.00	1.00	.0937
2405	1.00	1.00	1.00	1.00	1.00	1.00	0.0000
2605	1.00	1.00	1.00	1.00	1.00	1.00	0.0000
2805	1.00	1.00	1.00	1.00	1.00	1.00	.0073
2900	1.00	1.00	1.00	1.00	1.00	1.00	.0084
3005	1.00	1.00	1.00	1.00	1.00	1.00	.0191
3100	1.00	1.00	1.00	1.00	1.00	1.00	.0802
3205	1.00	1.00	1.00	1.00	1.00	1.00	5.6444
3300	1.00	1.00	1.00	1.00	1.00	1.00	10.0783
3405	1.00	1.00	1.00	1.00	1.00	1.00	16.6593
3500	1.00	1.00	1.00	1.00	1.00	1.00	4.4599
3605	1.00	1.00	1.00	1.00	1.00	1.00	.2246
3700	1.00	1.00	1.00	1.00	1.00	1.00	.0131
3805	1.00	1.00	1.00	1.00	1.00	1.00	.0067
3900	1.00	1.00	1.00	1.00	1.00	1.00	.0072
4005	1.00	1.00	1.00	1.00	1.00	1.00	.0072
4205	1.00	1.00	1.00	1.00	1.00	1.00	.0072
4405	1.00	1.00	1.00	1.00	1.00	1.00	.0089

RUN NO.: Y6ALTSE

DATE: 3/11/80

REF. FIGS.: 11.10-2, 11.10-10

a,c,e

[ ] = MAXIMUM RANGE AND FATIGUE STRATIFICATION AND STRIPING

SUMMARY = MAXIMUM RANGE OF STRESS INTENSITY ANALYSIS

ANALYSIS SECTION	SURFACE	LOAD CONDITION COMBINATION	ST RANGE (KSI)	ALLOWABLE (KSI)
5	INSIDE	T1=425=S - T2=45 DEG	77.4	56.70
	OUTSIDE	T1=425=S - T2=45 DEG	49.95	56.70

a,c,e

[ ] = MAXIMUM RANGE AND FATIGUE STRATIFICATION AND STRIPING

FATIGUE ANALYSIS LOCATION SUMMARY

LOCATION	STRESS CONCENTRATORS KX	KY	KZ	KXR	KYR	KZR	TOTAL USAGE FACTOR
3425	1.00	1.00	1.00	1.00	1.00	1.00	7.9233

RUN NO.: Y6ALTJX

DATE: 3/7/80

REF. FIGS.: 11.10-1, 11.10-7

POOR ORIGINAL

a,c,e

[ ] = MAXIMUM RANGE AND FATIGUE STRATIFICATION AND STRIPING

SUMMARY = MAXIMUM RANGE OF STRESS INTENSITY ANALYSIS

ANALYSIS SECTION	SURFACE	LOAD CONDITION COMBINATION	SI RANGE (KSI)	ALLOWABLE (KSI)
7	INSIDE	T3=390+S = 16=410DEG	73.59	56.70
	OUTSIDE	T1=425DEG= 15=430DEG	34.97	56.70

a,c,e

[ ] = MAXIMUM RANGE AND FATIGUE STRATIFICATION AND STRIPING

FATIGUE ANALYSIS LOCATION SUMMARY

LOCATION	STRESS CONCENTRATORS KX	KY	KZ	KXR	KYR	KZR	TOTAL USAGE FACTOR
3440	1.00	1.00	1.00	1.00	1.00	1.00	5.2054

RUN NO.: Y6ALTAD

DATE: 3/7/80

REF. FIGS: 11.10-1, 11.10-7

POOR ORIGINAL

a,c,e

[ ] = MAXIMUM RANGE AND FATIGUE STRATIFICATION AND STRIPING

SUMMARY - MAXIMUM RANGE OF STRESS INTENSITY ANALYSIS

ANALYSIS SECTION	SURFACE	LOAD CONDITION COMBINATION	SI RANGE (KSI)	ALLOWABLE (KSI)
10	INSIDE	T2=45DEG+ T3=390DEG	66.55	58.70
	OUTSIDE	T2=45DEG+ T3=390DEG	50.64	58.70

a,c,e

[ ] = MAXIMUM RANGE AND FATIGUE STRATIFICATION AND STRIPING

FATIGUE ANALYSIS LOCATION SUMMARY

LOCATION	STRESS CONCENTRATIONS KX	KY	KZ	KXY	KYZ	KZX	INITIAL USAGE FACTOR
3455	1.00	1.00	1.00	1.00	1.00	1.00	11.7142

RUN NO.: Y6ALTP0

DATE: 3/7/80

REF. FIGS: 11.10-1, 11.10-7

POOR ORIGINAL

a.c.e

[ ] = MAXIMUM RANGE AND FATIGUE STRATIFICATION AND STRIPING

SUMMARY = MAXIMUM RANGE OF STRESS INTENSITY ANALYSIS

ANALYSIS SECTION	SURFACE	LOAD CONDITION COMBINATION	SI RANGE (KSI)	ALLOWABLE (KSI)
14	INSIDE	T2=450DEG= 16=410DEG	62.30	56.70
	OUTSIDE	T2=450DEG= 16=410DEG	24.35	56.70

a.c.e

[ ] = MAXIMUM RANGE AND FATIGUE STRATIFICATION AND STRIPING

FATIGUE ANALYSIS LOCATION SUMMARY

LOCATION	STRESS CONCENTRATORS KX	KY	KZ	KXR	KYR	KZR	TOTAL USAGE FACTOR
3475	1.00	1.00	1.00	1.00	1.00	1.00	12.2444

RUN NO.: Y6ALTOT

DATE: 3/7/80

REF. FIGS.: 11.10-1, 11.10-7

POOR ORIGINAL

a,c,e

[ ] = MAXIMUM RANGE AND FATIGUE STRATIFICATION AND STRIPING

SUMMARY - MAXIMUM RANGE OF STRESS INTENSITY ANALYSIS

ANALYSIS SECTION	SURFACE	LOAD CONDITION COMBINATION	ΔT RANGE (KSI)	ALLOWABLE (KSI)
16	INSIDE	T2-450-S - T5-450DEG	43.00	56.70
	OUTSIDE	T5-590DEG- T5-450DEG	27.45	56.70

a,c,e

[ ] = MAXIMUM RANGE AND FATIGUE STRATIFICATION AND STRIPING

FATIGUE ANALYSIS LOCATION SUMMARY

LOCATION	STRESS CONCENTRATIONS						TOTAL USAGE FACTOR
	KX	KY	KZ	KXR	KYR	KZR	
5405	1.00	1.00	1.00	1.00	1.00	1.00	.2089

RUN NO.: Y6ALT77

DATE: 3/7/80

REF. FIGS.: 11.10-1, 11.10-7

POOR ORIGINAL

POOR ORIGINAL

a.c.e

[ ] = FATIGUE = ELBOW TRANSITION RUDT

SUMMARY = MAXIMUM RANGE OF STRESS INTENSITY ANALYSIS

ANALYSIS SECTION	SURFACE	LOAD CONDITION COMBINATION	SI RANGE (KSI)	ALLOWABLE (KSI)
1	INSIDE	T2=410DEG= T3=335DEG	93.93	56.70
	OUTSIDE	T3=335DEG= AMBIENT	29.10	56.70
2	INSIDE	T2=410DEG= T3=335DEG	94.00	56.70
	OUTSIDE	T3=335DEG= AMBIENT	25.59	56.70
3	INSIDE	T2=410DEG= T3=335DEG	86.83	56.70
	OUTSIDE	T3=335DEG= AMBIENT	27.16	56.70
4	INSIDE	T2=410DEG= T3=335DEG	81.54	56.70
	OUTSIDE	T3=335DEG= AMBIENT	21.33	56.70
5	INSIDE	T2=410DEG= T3=335DEG	64.20	56.70
	OUTSIDE	T3=335DEG= AMBIENT	22.14	56.70
6	INSIDE	T2=410DEG= T3=335DEG	36.12	56.70
	OUTSIDE	T3=335DEG= T5=385DEG	24.14	56.70
7	INSIDE	T3=335DEG= T6=345DEG	56.88	56.70
	OUTSIDE	T3=335DEG= T5=385DEG	28.75	56.70
8	INSIDE	T3=335DEG= T5=385DEG	64.46	56.70
	OUTSIDE	T2=410DEG= T3=335DEG	32.34	56.70
9	INSIDE	T2=410DEG= T3=335DEG	74.52	56.70
	OUTSIDE	T2=410DEG= T3=335DEG	28.50	56.70
10	INSIDE	T2=410DEG= T3=335DEG	76.19	56.70
	OUTSIDE	T2=410DEG= T3=335DEG	26.91	56.70
11	INSIDE	T2=410DEG= T3=335DEG	78.68	56.70
	OUTSIDE	T2=410DEG= T6=345DEG	25.39	56.70
12	INSIDE	T2=410DEG= T6=345DEG	77.03	56.70
	OUTSIDE	T2=410DEG= T6=345DEG	27.07	56.70
13	INSIDE	T2=410DEG= T6=345DEG	81.95	56.70
	OUTSIDE	T2=410DEG= T6=345DEG	24.92	56.70
14	INSIDE	T2=410DEG= T6=345DEG	72.77	56.70
	OUTSIDE	T2=410DEG= T6=345DEG	21.49	56.70
15	INSIDE	T2=410DEG= T6=345DEG	60.22	56.70
	OUTSIDE	T2=410DEG= T5=385DEG	21.05	56.70
16	INSIDE	T2=410DEG= T5=385DEG	38.32	56.70
	OUTSIDE	T3=335DEG= T5=385DEG	24.10	56.70
17	INSIDE	T5=385DEG= AMBIENT	25.67	56.70
	OUTSIDE	T2=410DEG= T3=335DEG	28.61	56.70
18	INSIDE	T2=410DEG= AMBIENT	40.75	56.70
	OUTSIDE	T2=410DEG= T3=335DEG	30.90	56.70
19	INSIDE	T2=410DEG= T6=345DEG	39.44	56.70
	OUTSIDE	T2=410DEG= T6=345DEG	22.13	56.70
20	INSIDE	T2=410DEG= T6=345DEG	37.49	56.70
	OUTSIDE	T6=345DEG= PRESSURE	16.33	56.70

RUN NO.: Y6ALTJJ

DATE: 3/11/80

REF. FIGS.: 11.10-1, 11.10-11

POOR ORIGINAL

a,c,e

[ ] = FATIGUE - ELBOW TRANSITION RUOT

FATIGUE ANALYSIS LOCATION SUMMARY

LOCATION	STRESS CONCENTRATORS						TOTAL USAGE FACTOR
	KX	KY	KZ	KXR	KYR	KZR	
3405	1.00	1.00	1.00	1.00	1.00	1.00	3.3254
3410	1.00	1.00	1.00	1.00	1.00	1.00	3.1894
3415	1.00	1.00	1.00	1.00	1.00	1.00	2.5358
3420	1.00	1.00	1.00	1.00	1.00	1.00	1.9445
3425	1.00	1.00	1.00	1.00	1.00	1.00	.9112
3435	1.00	1.00	1.00	1.00	1.00	1.00	.0029
3440	1.00	1.00	1.00	1.00	1.00	1.00	.5253
3445	1.00	1.00	1.00	1.00	1.00	1.00	.8580
3450	1.00	1.00	1.00	1.00	1.00	1.00	1.4449
3455	1.00	1.00	1.00	1.00	1.00	1.00	2.0658
3460	1.00	1.00	1.00	1.00	1.00	1.00	4.3409
3465	1.00	1.00	1.00	1.00	1.00	1.00	4.7320
3470	1.00	1.00	1.00	1.00	1.00	1.00	5.0222
3475	1.00	1.00	1.00	1.00	1.00	1.00	3.4591
3480	1.00	1.00	1.00	1.00	1.00	1.00	1.6964
3485	1.00	1.00	1.00	1.00	1.00	1.00	.0061
3495	1.00	1.00	1.00	1.00	1.00	1.00	.0016
3505	1.00	1.00	1.00	1.00	1.00	1.00	.0231
3515	1.00	1.00	1.00	1.00	1.00	1.00	.0172
3525	1.00	1.00	1.00	1.00	1.00	1.00	.0075

RUN NO. Y6ALTJJ

DATE: 3/11/80

REF. FIGS.: 11.10-1, 11.10-11

POOR ORIGINAL

[ ] - FATIGUE - ELBOW TOP

a,c,e

SUMMARY - MAXIMUM RANGE OF STRESS INTENSITY ANALYSIS

ANALYSIS SECTION	SURFACE	LOAD CONDITION COMBINATION	SI RANGE (KSI)	ALLOWABLE (KSI)
21	INSIDE	T4=120DEG- AMBIENT	25.26	80.10
	OUTSIDE	T2=410DEG- T4=120DEG	27.57	80.10
22	INSIDE	T3=335DEG- T4=120DEG	23.93	80.10
	OUTSIDE	T2=410DEG- T4=120DEG	26.05	80.10
23	INSIDE	T3=335DEG- T4=120DEG	38.25	80.10
	OUTSIDE	T2=410DEG- T4=120DEG	26.94	80.10
24	INSIDE	T2=410DEG- T4=120DEG	18.69	80.10
	OUTSIDE	T2=410DEG- T3=335DEG	64.77	80.10
25	INSIDE	T3=335DEG- AMBIENT	16.41	80.10
	OUTSIDE	T2=410DEG- T3=335DEG	72.13	80.10
26	INSIDE	T3=335DEG- AMBIENT	25.06	80.10
	OUTSIDE	T2=410DEG- T3=335DEG	53.46	80.10
27	INSIDE	T3=335DEG- AMBIENT	27.83	80.10
	OUTSIDE	T2=410DEG- T3=335DEG	49.71	80.10
28	INSIDE	T2=410DEG- T3=335DEG	34.45	80.10
	OUTSIDE	T2=410DEG- T3=335DEG	45.90	80.10
29	INSIDE	T2=410DEG- T3=335DEG	49.61	80.10
	OUTSIDE	T2=410DEG- T3=335DEG	33.94	80.10
30	INSIDE	T2=410DEG- T3=335DEG	67.54	56.70
	OUTSIDE	T2=410DEG- T3=335DEG	29.43	56.70
31	INSIDE	T2=410DEG- T3=335DEG	61.10	56.70
	OUTSIDE	T3=335DEG- AMBIENT	26.16	56.70
32	INSIDE	T2=410DEG- T3=335DEG	93.93	56.70
	OUTSIDE	T3=335DEG- AMBIENT	29.10	56.70
33	INSIDE	T2=410DEG- T3=335DEG	73.34	56.70
	OUTSIDE	T2=410DEG- T3=335DEG	28.27	56.70
34	INSIDE	T2=410DEG- T3=335DEG	53.07	56.70
	OUTSIDE	T2=410DEG- T3=335DEG	35.79	56.70
35	INSIDE	T2=410DEG- T3=335DEG	40.92	56.70
	OUTSIDE	T2=410DEG- T3=335DEG	36.03	56.70
36	INSIDE	T2=410DEG- T3=335DEG	33.28	56.70
	OUTSIDE	T2=410DEG- T3=335DEG	38.98	56.70
37	INSIDE	T2=410DEG- T3=335DEG	36.07	56.70
	OUTSIDE	T2=410DEG- T3=335DEG	36.96	56.70
38	INSIDE	T2=410DEG- T3=335DEG	40.28	56.70
	OUTSIDE	T2=410DEG- T3=335DEG	35.95	56.70
39	INSIDE	T2=410DEG- T3=335DEG	36.30	56.70
	OUTSIDE	T2=410DEG- T3=335DEG	35.45	56.70
40	INSIDE	T2=410DEG- T3=335DEG	30.52	56.70
	OUTSIDE	T2=410DEG- T3=335DEG	44.90	56.70

RUN NO.: Y6ALTJN

DATE: 3/11/80

REF. FIGS.: 11.10-2, 11.10-12

POOR ORIGINAL

a.c.e

[ ] • FATIGUE • ELBOW TOP

FATIGUE ANALYSIS LOCATION SUMMARY

LOCATION	STRESS CONCENTRATORS						TOTAL USAGE FACTOR
	KX	KY	KZ	KXR	KYR	KZR	
1805	1.00	1.00	1.00	1.00	1.00	1.00	.0000
2005	1.00	1.00	1.00	1.00	1.00	1.00	.0002
2205	1.00	1.00	1.00	1.00	1.00	1.00	.0011
2405	1.00	1.00	1.00	1.00	1.00	1.00	0.0000
2605	1.00	1.00	1.00	1.00	1.00	1.00	0.0000
2805	1.00	1.00	1.00	1.00	1.00	1.00	.0000
2930	1.00	1.00	1.00	1.00	1.00	1.00	.0009
3005	1.00	1.00	1.00	1.00	1.00	1.00	.0009
3130	1.00	1.00	1.00	1.00	1.00	1.00	.0100
3205	1.00	1.00	1.00	1.00	1.00	1.00	.8356
3330	1.00	1.00	1.00	1.00	1.00	1.00	1.7304
3405	1.00	1.00	1.00	1.00	1.00	1.00	3.3254
3530	1.00	1.00	1.00	1.00	1.00	1.00	1.2086
3605	1.00	1.00	1.00	1.00	1.00	1.00	.2065
3730	1.00	1.00	1.00	1.00	1.00	1.00	.0069
3805	1.00	1.00	1.00	1.00	1.00	1.00	.0009
3930	1.00	1.00	1.00	1.00	1.00	1.00	.0009
4005	1.00	1.00	1.00	1.00	1.00	1.00	.0087
4205	1.00	1.00	1.00	1.00	1.00	1.00	.0013
4405	1.00	1.00	1.00	1.00	1.00	1.00	.0009

RUN NO.: Y6ALTJN
DATE: 3/11/80
REF. FIGS.: 11.10-2, 11.10-12

POOR ORIGINAL

[ ] = MAXIMUM RANGE AND FATIGUE AT 90 DEG

acc

SUMMARY = MAXIMUM RANGE OF STRESS INTENSITY ANALYSIS

ANALYSIS SECTION	SURFACE	LOAD CONDITION COMBINATION	SI RANGE (KSI)	ALLOWABLE (KSI)
01	INSIDE	T2=410DEG- T4=120DEG	37.11	80.10
	OUTSIDE	T4=120DEG- AMBIENT	24.80	80.10
02	INSIDE	T2=410DEG- T4=120DEG	48.81	80.10
	OUTSIDE	T4=120DEG- PRESSURE	19.03	80.10
03	INSIDE	T2=410DEG- T4=120DEG	49.26	80.10
	OUTSIDE	T4=120DEG- AMBIENT	15.46	80.10
04	INSIDE	T2=410DEG- T4=120DEG	20.06	80.10
	OUTSIDE	T2=410DEG- T6=345DEG	57.63	80.10
05	INSIDE	T2=410DEG- AMBIENT	18.54	80.10
	OUTSIDE	T2=410DEG- T6=345DEG	68.56	80.10
06	INSIDE	T2=410DEG- T3=335DEG	30.60	80.10
	OUTSIDE	T2=410DEG- T6=345DEG	56.87	80.10
07	INSIDE	T2=410DEG- T3=335DEG	34.56	80.10
	OUTSIDE	T2=410DEG- T6=345DEG	55.53	80.10
08	INSIDE	T2=410DEG- T3=335DEG	39.84	80.10
	OUTSIDE	T2=410DEG- T6=345DEG	50.92	80.10
09	INSIDE	T2=410DEG- T3=335DEG	48.10	80.10
	OUTSIDE	T2=410DEG- T6=345DEG	36.00	80.10
..	INSIDE	T2=410DEG- T3=335DEG	61.22	56.70
	OUTSIDE	T2=410DEG- T6=345DEG	27.61	56.70
71	INSIDE	T2=410DEG- T6=345DEG	69.10	56.70
	OUTSIDE	T2=410DEG- T6=345DEG	27.52	56.70
72	INSIDE	T2=410DEG- T6=345DEG	77.03	56.70
	OUTSIDE	T2=410DEG- T6=345DEG	27.07	56.70
73	INSIDE	T2=410DEG- T6=345DEG	55.70	56.70
	OUTSIDE	T2=410DEG- T6=345DEG	34.16	56.70
74	INSIDE	T2=410DEG- T3=335DEG	41.72	56.70
	OUTSIDE	T2=410DEG- T6=345DEG	40.80	56.70
75	INSIDE	T2=410DEG- T3=335DEG	34.73	56.70
	OUTSIDE	T2=410DEG- T6=345DEG	41.05	56.70
76	INSIDE	T2=410DEG- T3=335DEG	30.20	56.70
	OUTSIDE	T2=410DEG- T6=345DEG	43.91	56.70
77	INSIDE	T2=410DEG- T3=335DEG	31.53	56.70
	OUTSIDE	T2=410DEG- T6=345DEG	40.40	56.70
78	INSIDE	T2=410DEG- T3=335DEG	32.30	56.70
	OUTSIDE	T2=410DEG- T6=345DEG	37.80	56.70
79	INSIDE	T2=410DEG- T3=335DEG	32.70	56.70
	OUTSIDE	T2=410DEG- T6=345DEG	34.37	56.70
80	INSIDE	T2=410DEG- T3=335DEG	32.90	56.70
	OUTSIDE	T2=410DEG- T6=345DEG	30.01	56.70

RUN NO.: Y6ALTCL

DATE: 3/11/80

REF. FIGS.: 11.10-2, 11.10-13

POOR ORIGINAL

a,c,e [ ] = MAXIMUM RANGE AND FATIGUE AT 90 DEG

FATIGUE ANALYSIS LOCATION SUMMARY

LOCATION	STRESS CONCENTRATORS KX	KY	KZ	KXR	KYR	KZR	TOTAL USAGE FACTOR
1805	1.00	1.00	1.00	1.00	1.00	1.00	.0016
2005	1.00	1.00	1.00	1.00	1.00	1.00	.0056
2205	1.00	1.00	1.00	1.00	1.00	1.00	.0197
2405	1.00	1.00	1.00	1.00	1.00	1.00	0.0000
2605	1.00	1.00	1.00	1.00	1.00	1.00	0.0000
2805	1.00	1.00	1.00	1.00	1.00	1.00	.0029
2900	1.00	1.00	1.00	1.00	1.00	1.00	.0030
3005	1.00	1.00	1.00	1.00	1.00	1.00	.0031
3100	1.00	1.00	1.00	1.00	1.00	1.00	.0150
3205	1.00	1.00	1.00	1.00	1.00	1.00	1.4765
3300	1.00	1.00	1.00	1.00	1.00	1.00	2.8647
3405	1.00	1.00	1.00	1.00	1.00	1.00	4.7320
3500	1.00	1.00	1.00	1.00	1.00	1.00	.9256
3605	1.00	1.00	1.00	1.00	1.00	1.00	.0175
3700	1.00	1.00	1.00	1.00	1.00	1.00	.0030
3805	1.00	1.00	1.00	1.00	1.00	1.00	.0025
3900	1.00	1.00	1.00	1.00	1.00	1.00	.0029
4005	1.00	1.00	1.00	1.00	1.00	1.00	.0030
4205	1.00	1.00	1.00	1.00	1.00	1.00	.0029
4405	1.00	1.00	1.00	1.00	1.00	1.00	.0030

RUN NO.: Y6ALTCL

DATE: 3/11/80

REF. FIGS.: 11.10-2, 11.10-13

a,c,e

[ ] = MAXIMUM RANGE AND FATIGUE STRATIFICATION AND STRIPING

SUMMARY - MAXIMUM RANGE OF STRESS INTENSITY ANALYSIS

ANALYSIS SECTION	SURFACE	LOAD CONDITION COMBINATION	SI RANGE (KSI)	ALLOWABLE (KSI)
10	INSIDE	T2=410DEG- T3=355DEG	76.14	56.70
	OUTSIDE	T2=410DEG- T3=355DEG	26.91	56.70

a,c,e

[ ] = MAXIMUM RANGE AND FATIGUE STRATIFICATION AND STRIPING

FATIGUE ANALYSIS LOCATION SUMMARY

LOCATION	STRESS CONCENTRATORS						TOTAL USAGE FACTOR
	KX	KY	KZ	KXR	KYR	KZR	
3455	1.00	1.00	1.00	1.00	1.00	1.00	2.7735

RUN NO.: Y6ALT7L

DATE: 3/11/80

REF. FIGS: 11.10-1, 11.10-11

POOR ORIGINAL

a,c,e

[ ]- MAXIMUM RANGE AND FATIGUE STRATIFICATION AND STRIPING

SUMMARY - MAXIMUM RANGE OF STRESS INTENSITY ANALYSIS

ANALYSIS SECTION	SURFACE	LOAD CONDITION COMBINATION	SI RANGE (KSI)	ALLOWABLE (KSI)
14	INSIDE	T2-410DEG- T6-345DEG	72.77	56.70
	OUTSIDE	T2-410DEG- T6-345DEG	21.49	56.70

a,c,e

[ ]- MAXIMUM RANGE AND FATIGUE STRATIFICATION AND STRIPING

FATIGUE ANALYSIS LOCATION SUMMARY

LOCATION	STRESS CONCENTRATORS KX	KY	KZ	KXR	KYH	KZR	TOTAL USAGE FACTOR
3475	1.00	1.00	1.00	1.00	1.00	1.00	3.4386

RUN NO.: Y6ALT70

DATE: 3/11/80

REF. FIGS.: 11.10-1, 11.10-11

POOR ORIGINAL

a.c.e

[ ] = MAXIMUM RANGE AND FATIGUE STRATIFICATION AND STRIPING

SUMMARY - MAXIMUM RANGE OF STRESS INTENSITY ANALYSIS

ANALYSIS SECTION	SURFACE	LOAD CONDITION COMBINATION	SI RANGE (KSI)	ALLOWABLE (KSI)
16	INSIDE	T2-410-S - T5-385DEG	38.89	56.70
	OUTSIDE	T3-335DEG- T5-385DEG	24.10	56.70

a.c.e

[ ] = MAXIMUM RANGE AND FATIGUE STRATIFICATION AND STRIPING

FATIGUE ANALYSIS LOCATION SUMMARY

LOCATION	STRESS CONCENTRATIONS						TOTAL USAGE FACTOR
	KX	KY	KZ	KXR	KYR	KZR	
3485	1.00	1.00	1.00	1.00	1.00	1.00	.0118

RUN NO.: Y6ALTFI

DATE: 3/11/80

REF. FIGS.: 11.10-1, 11.10-11

POOR ORIGINAL

POOR ORIGINAL

[ ] ELBOW TRANSITION ROOT
- MAXIMUM RANGE OF STRESS INTENSITY

SUMMARY - MAXIMUM RANGE OF STRESS INTENSITY ANALYSIS

ANALYSIS SECTION	SURFACE	LOAD CONDITION COMBINATION	SI RANGE (KSI)	ALLOWABLE (KSI)
1	INSIDE	T1-430DEG- T5-430DEG	119.62	56.70
	OUTSIDE	T3-400DEG- AMBIENT	32.84	56.70
2	INSIDE	T1-430DEG- T2-205DEG	121.24	56.70
	OUTSIDE	T3-400DEG- AMBIENT	28.80	56.70
3	INSIDE	T1-430DEG- T2-205DEG	93.42	56.70
	OUTSIDE	T3-400DEG- AMBIENT	30.61	56.70
4	INSIDE	T2-205DEG- T3-400DEG	81.45	56.70
	OUTSIDE	T1-430DEG- T5-430DEG	35.59	56.70
5	INSIDE	T1-430DEG- T5-430DEG	63.92	56.70
	OUTSIDE	T1-430DEG- T5-430DEG	49.68	56.70
6	INSIDE	T1-430DEG- T6-415DEG	60.98	56.70
	OUTSIDE	T1-430DEG- T5-430DEG	43.37	56.70
7	INSIDE	T1-430DEG- T6-415DEG	72.76	56.70
	OUTSIDE	T1-430DEG- T5-430DEG	35.31	56.70
8	INSIDE	T3-400DEG- T5-430DEG	75.40	56.70
	OUTSIDE	T3-400DEG- T5-430DEG	37.93	56.70
9	INSIDE	T3-400DEG- T5-430DEG	86.97	56.70
	OUTSIDE	T3-400DEG- T5-430DEG	32.26	56.70
10	INSIDE	T3-400DEG- T5-430DEG	81.44	56.70
	OUTSIDE	T3-400DEG- T5-430DEG	28.54	56.70
11	INSIDE	T3-400DEG- T5-430DEG	75.62	56.70
	OUTSIDE	T2-205DEG- T6-415DEG	23.06	56.70
12	INSIDE	T2-205DEG- T6-415DEG	61.53	56.70
	OUTSIDE	T2-205DEG- T6-415DEG	23.89	56.70
13	INSIDE	T2-205DEG- T6-415DEG	64.39	56.70
	OUTSIDE	T2-205DEG- T6-415DEG	20.77	56.70
14	INSIDE	T2-205DEG- T6-415DEG	55.24	56.70
	OUTSIDE	T1-430DEG- T6-415DEG	17.12	56.70
15	INSIDE	T2-205DEG- T6-415DEG	44.24	56.70
	OUTSIDE	T1-430DEG- T5-430DEG	22.33	56.70
16	INSIDE	T5-430DEG- AMBIENT	33.08	56.70
	OUTSIDE	T3-400DEG- T5-430DEG	27.79	56.70
17	INSIDE	T5-430DEG- AMBIENT	27.40	56.70
	OUTSIDE	T3-400DEG- T5-430DEG	25.84	56.70
18	INSIDE	T2-205DEG- T3-400DEG	27.24	56.70
	OUTSIDE	T2-205DEG- T3-400DEG	24.41	56.70
19	INSIDE	T2-205DEG- T6-415DEG	26.58	56.70
	OUTSIDE	T2-205DEG- T6-415DEG	22.92	56.70
20	INSIDE	T2-205DEG- T6-415DEG	25.52	56.70
	OUTSIDE	T6-415DEG- PRESSURE	19.65	56.70

RUN NO.: Y6ALTZ9

DATE: 2/28/80

REF. FIGS.: 11.10-1, 11.10-14, 11.10-15

[ ] - FATIGUE - ELBOW TRANSITION ROOT a,c,e

FATIGUE ANALYSIS LOCATION SUMMARY

LOCATION	STRESS CONCENTRATORS KX	KY	KZ	KXR	KYR	KZR	TOTAL USAGE FACTOR
3405	1.00	1.00	1.00	1.00	1.00	1.00	32.4720
3410	1.00	1.00	1.00	1.00	1.00	1.00	31.5901
3415	1.00	1.00	1.00	1.00	1.00	1.00	16.6453
3420	1.00	1.00	1.00	1.00	1.00	1.00	9.9011
3425	1.00	1.00	1.00	1.00	1.00	1.00	5.0573
3435	1.00	1.00	1.00	1.00	1.00	1.00	1.5801
3440	1.00	1.00	1.00	1.00	1.00	1.00	6.3667
3445	1.00	1.00	1.00	1.00	1.00	1.00	8.3988
3450	1.00	1.00	1.00	1.00	1.00	1.00	11.0275
3455	1.00	1.00	1.00	1.00	1.00	1.00	9.0596
3460	1.00	1.00	1.00	1.00	1.00	1.00	7.1415
3465	1.00	1.00	1.00	1.00	1.00	1.00	2.9659
3470	1.00	1.00	1.00	1.00	1.00	1.00	1.1965
3475	1.00	1.00	1.00	1.00	1.00	1.00	.3448
3480	1.00	1.00	1.00	1.00	1.00	1.00	.0300
3485	1.00	1.00	1.00	1.00	1.00	1.00	.0065
3495	1.00	1.00	1.00	1.00	1.00	1.00	.0046
3505	1.00	1.00	1.00	1.00	1.00	1.00	.0028
3515	1.00	1.00	1.00	1.00	1.00	1.00	.0006
3525	1.00	1.00	1.00	1.00	1.00	1.00	.0006

RUN NO.: Y6ALTOA

DATE: 2/28/80

REF. FIGS.: 11.10-1, 11.10-14, 11.10-15

,c,e

[ ] ELBOW TRANSITION ROOT
- MAXIMUM RANGE OF STRESS INTENSITY

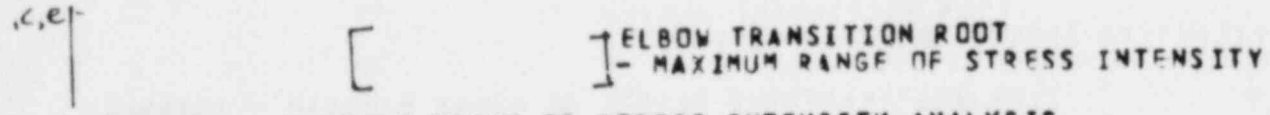

SUMMARY - MAXIMUM RANGE OF STRESS INTENSITY ANALYSIS

ANALYSIS SECTION	SURFACE	LOAD CONDITION COMBINATION	SI RANGE (KSI)	ALLOWABLE (KSI)
1	INSIDE	T1-430DEG- T5-430DEG	119.62	56.70
	OUTSIDE	T3-400DEG- AMBIENT	32.89	56.70
2	INSIDE	T1-430DEG- T2-205DEG	121.24	56.70
	OUTSIDE	T3-400DEG- AMBIENT	28.80	56.70
3	INSIDE	T1-430DEG- T2-205DEG	93.42	56.70
	OUTSIDE	T3-400DEG- AMBIENT	30.61	56.70
4	INSIDE	T2-205DEG- T3-400DEG	81.45	56.70
	OUTSIDE	T1-430DEG- T5-430DEG	35.59	56.70
5	INSIDE	T1-430DEG- T5-430DEG	68.92	56.70
	OUTSIDE	T1-430DEG- T5-430DEG	49.68	56.70
6	INSIDE	T1-430DEG- T6-415DEG	60.98	56.70
	OUTSIDE	T1-430DEG- T5-430DEG	43.37	56.70
7	INSIDE	T1-430DEG- T6-415DEG	72.76	56.70
	OUTSIDE	T1-430DEG- T5-430DEG	35.31	56.70
8	INSIDE	T3-400DEG- T5-430DEG	75.40	56.70
	OUTSIDE	T3-400DEG- T5-430DEG	37.93	56.70
9	INSIDE	T3-400DEG- T5-430DEG	86.97	56.70
	OUTSIDE	T3-400DEG- T5-430DEG	32.26	56.70
10	INSIDE	T3-400DEG- T5-430DEG	81.44	56.70
	OUTSIDE	T3-400DEG- T5-430DEG	28.54	56.70
11	INSIDE	T3-400DEG- T5-430DEG	75.62	56.70
	OUTSIDE	T2-205DEG- T6-415DEG	23.06	56.70
12	INSIDE	T2-205DEG- T6-415DEG	61.53	56.70
	OUTSIDE	T2-205DEG- T6-415DEG	23.89	56.70
13	INSIDE	T2-205DEG- T6-415DEG	64.39	56.70
	OUTSIDE	T2-205DEG- T6-415DEG	20.77	56.70
14	INSIDE	T2-205DEG- T6-415DEG	55.24	56.70
	OUTSIDE	T1-430DEG- T6-415DEG	17.12	56.70
15	INSIDE	T2-205DEG- T6-415DEG	44.24	56.70
	OUTSIDE	T1-430DEG- T5-430DEG	22.33	56.70
16	INSIDE	T5-430DEG- AMBIENT	33.08	56.70
	OUTSIDE	T3-400DEG- T5-430DEG	27.79	56.70
17	INSIDE	T5-430DEG- AMBIENT	27.40	56.70
	OUTSIDE	T3-400DEG- T5-430DEG	25.84	56.70
18	INSIDE	T2-205DEG- T3-400DEG	27.24	56.70
	OUTSIDE	T2-205DEG- T3-400DEG	24.41	56.70
19	INSIDE	T2-205DEG- T6-415DEG	26.58	56.70
	OUTSIDE	T2-205DEG- T6-415DEG	22.92	56.70
20	INSIDE	T2-205DEG- T6-415DEG	25.52	56.70
	OUTSIDE	T6-415DEG- PRESSURE	19.65	56.70

RUN NO.: Y6ALTZP

DATE: 2/28/80

REF. FIGS.: 11.10-1, 11.10-15

a.c,e

[ ]- FATIGUE - ELBOW TRANSITION ROOT

FATIGUE ANALYSIS LOCATION SUMMARY

LOCATION	STRESS CONCENTRATORS						TOTAL USAGE FACTOR
	KX	KY	KZ	KXR	KYR	KZR	
3405	1.00	1.00	1.00	1.00	1.00	1.00	58.9745
3410	1.00	1.00	1.00	1.00	1.00	1.00	59.3832
3415	1.00	1.00	1.00	1.00	1.00	1.00	13.6809
3420	1.00	1.00	1.00	1.00	1.00	1.00	5.4289
3425	1.00	1.00	1.00	1.00	1.00	1.00	.8291
3435	1.00	1.00	1.00	1.00	1.00	1.00	.1457
3440	1.00	1.00	1.00	1.00	1.00	1.00	1.6545
3445	1.00	1.00	1.00	1.00	1.00	1.00	3.4379
3450	1.00	1.00	1.00	1.00	1.00	1.00	8.3032
3455	1.00	1.00	1.00	1.00	1.00	1.00	5.3954
3460	1.00	1.00	1.00	1.00	1.00	1.00	3.0606
3465	1.00	1.00	1.00	1.00	1.00	1.00	.2229
3470	1.00	1.00	1.00	1.00	1.00	1.00	.1910
3475	1.00	1.00	1.00	1.00	1.00	1.00	.0347
3480	1.00	1.00	1.00	1.00	1.00	1.00	.0114
3485	1.00	1.00	1.00	1.00	1.00	1.00	.0065
3495	1.00	1.00	1.00	1.00	1.00	1.00	.0046
3505	1.00	1.00	1.00	1.00	1.00	1.00	.0028
3515	1.00	1.00	1.00	1.00	1.00	1.00	.0006
3525	1.00	1.00	1.00	1.00	1.00	1.00	.0006

RUN NO.: Y6ALTZS

DATE: 2/28/80

REF. FIGS.: 11.10-1, 11.10-15

POOR ORIGINAL

a.c.e

[ ] - FATIGUE - ELBOW TOP

SUMMARY - MAXIMUM RANGE OF STRESS INTENSITY ANALYSIS

ANALYSIS SECTION	SURFACE	LOAD CONDITION COMBINATION	SI RANGE (KSI)	ALLOWABLE (KSI)
21	INSIDE	T1-430DEG- T5-430DEG	17.46	80.10
	OUTSIDE	T1-430DEG- AMBIENT	15.58	80.10
22	INSIDE	T1-430DEG- T5-430DEG	27.88	80.10
	OUTSIDE	T1-430DEG- T5-430DEG	15.07	80.10
23	INSIDE	T1-430DEG- T2-205DEG	57.90	80.10
	OUTSIDE	T1-430DEG- T5-430DEG	17.44	80.10
24	INSIDE	T1-430DEG- AMBIENT	27.51	80.10
	OUTSIDE	T1-430DEG- T5-430DEG	89.77	80.10
25	INSIDE	T1-430DEG- AMBIENT	38.00	80.10
	OUTSIDE	T1-430DEG- T5-430DEG	91.60	80.10
26	INSIDE	T1-430DEG- AMBIENT	43.65	80.10
	OUTSIDE	T1-430DEG- T5-430DEG	64.61	80.10
27	INSIDE	T1-430DEG- AMBIENT	47.15	80.10
	OUTSIDE	T1-430DEG- T5-430DEG	57.97	80.10
28	INSIDE	T1-430DEG- T2-205DEG	59.68	80.10
	OUTSIDE	T1-430DEG- T5-430DEG	52.84	80.10
29	INSIDE	T1-430DEG- T2-205DEG	60.01	80.10
	OUTSIDE	T3-400DEG- T5-430DEG	31.26	80.10
30	INSIDE	T1-430DEG- T2-205DEG	101.13	56.70
	OUTSIDE	T3-400DEG- AMBIENT	28.15	56.70
31	INSIDE	T1-430DEG- T5-430DEG	113.59	56.70
	OUTSIDE	T3-400DEG- AMBIENT	29.25	56.70
32	INSIDE	T1-430DEG- T5-430DEG	119.62	56.70
	OUTSIDE	T3-400DEG- AMBIENT	32.89	56.70
33	INSIDE	T1-430DEG- T5-430DEG	85.65	56.70
	OUTSIDE	T3-400DEG- AMBIENT	30.20	56.70
34	INSIDE	T2-205DEG- T3-400DEG	53.02	56.70
	OUTSIDE	T1-430DEG- T5-430DEG	40.20	56.70
35	INSIDE	T1-430DEG- T5-430DEG	43.82	56.70
	OUTSIDE	T1-430DEG- T5-430DEG	43.85	56.70
36	INSIDE	T1-430DEG- T5-430DEG	40.45	56.70
	OUTSIDE	T1-430DEG- T5-430DEG	53.24	56.70
37	INSIDE	T1-430DEG- T5-430DEG	41.35	56.70
	OUTSIDE	T1-430DEG- T5-430DEG	50.02	56.70
38	INSIDE	T2-205DEG- T3-400DEG	42.22	56.70
	OUTSIDE	T1-430DEG- T5-430DEG	53.09	56.70
39	INSIDE	T2-205DEG- T3-400DEG	37.20	56.70
	OUTSIDE	T1-430DEG- T5-430DEG	41.30	56.70
40	INSIDE	T3-400DEG- T5-430DEG	50.75	56.70
	OUTSIDE	T2-205DEG- T3-400DEG	45.89	56.70

RUN. NO.: Y6ALTOJ

DATE: 3/11/80

REF. FIGS.: 11.10-2, 11.10-16

POOR ORIGINAL

[ ] - FATIGUE - ELBOW TOP

a.c.e

FATIGUE ANALYSIS LOCATION SUMMARY

LOCATION	STRESS CONCENTRATORS KX	KY	KZ	KXR	KYH	KZR	TOTAL USAGE FACTOR
1805	1.00	1.00	1.00	1.00	1.00	1.00	0.0000
2005	1.00	1.00	1.00	1.00	1.00	1.00	.0028
2205	1.00	1.00	1.00	1.00	1.00	1.00	.0976
2405	1.00	1.00	1.00	1.00	1.00	1.00	.0000
2605	1.00	1.00	1.00	1.00	1.00	1.00	.0028
2805	1.00	1.00	1.00	1.00	1.00	1.00	.0028
2930	1.00	1.00	1.00	1.00	1.00	1.00	.0114
3005	1.00	1.00	1.00	1.00	1.00	1.00	.0843
3130	1.00	1.00	1.00	1.00	1.00	1.00	2.3383
3205	1.00	1.00	1.00	1.00	1.00	1.00	12.2573
3330	1.00	1.00	1.00	1.00	1.00	1.00	21.2363
3405	1.00	1.00	1.00	1.00	1.00	1.00	32.4719
3530	1.00	1.00	1.00	1.00	1.00	1.00	9.3478
3605	1.00	1.00	1.00	1.00	1.00	1.00	.8097
3730	1.00	1.00	1.00	1.00	1.00	1.00	.0687
3805	1.00	1.00	1.00	1.00	1.00	1.00	.0186
3930	1.00	1.00	1.00	1.00	1.00	1.00	.0243
4005	1.00	1.00	1.00	1.00	1.00	1.00	.0595
4205	1.00	1.00	1.00	1.00	1.00	1.00	.0082
4405	1.00	1.00	1.00	1.00	1.00	1.00	.0046

RUN NO.: Y6ALTOJ

DATE: 3/11/80

REF. FIGS.: 11.10-2, 11.10-16

POOR ORIGINAL

a,c,e

[ ] = MAXIMUM RANGE AND FATIGUE AT 90 DEG

SUMMARY - MAXIMUM RANGE OF STRESS INTENSITY ANALYSIS

ANALYSIS SECTION	SURFACE	LOAD CONDITION COMBINATION	SI RANGE (KSI)	ALLOWABLE (KSI)
01	INSIDE	T1=430DEG- AMBIENT	24.10	60.10
	OUTSIDE	T1=430DEG- AMBIENT	15.50	60.10
02	INSIDE	T1=430DEG- T2=205DEG	30.70	60.10
	OUTSIDE	T1=430DEG- AMBIENT	13.02	60.10
03	INSIDE	T2=205DEG- T3=400DEG	40.90	60.10
	OUTSIDE	T1=430DEG- AMBIENT	11.81	60.10
04	INSIDE	T2=205DEG- T6=415DEG	17.60	60.10
	OUTSIDE	T2=205DEG- T6=415DEG	48.30	60.10
05	INSIDE	T1=430DEG- T5=430DEG	19.10	60.10
	OUTSIDE	T2=205DEG- T6=415DEG	58.05	60.10
06	INSIDE	T3=400DEG- T5=430DEG	30.80	60.10
	OUTSIDE	T2=205DEG- T6=415DEG	48.45	60.10
07	INSIDE	T3=400DEG- T5=430DEG	33.34	60.10
	OUTSIDE	T2=205DEG- T6=415DEG	47.42	60.10
08	INSIDE	T3=400DEG- T5=430DEG	38.34	60.10
	OUTSIDE	T2=205DEG- T6=415DEG	43.82	60.10
09	INSIDE	T3=400DEG- T5=430DEG	43.15	60.10
	OUTSIDE	T2=205DEG- T6=415DEG	31.61	60.10
70	INSIDE	T3=400DEG- T5=430DEG	50.20	56.70
	OUTSIDE	T2=205DEG- T6=415DEG	23.80	56.70
71	INSIDE	T2=205DEG- T6=415DEG	54.97	56.70
	OUTSIDE	T2=205DEG- T6=415DEG	23.90	56.70
72	INSIDE	T2=205DEG- T6=415DEG	51.55	56.70
	OUTSIDE	T2=205DEG- T6=415DEG	23.84	56.70
73	INSIDE	T2=205DEG- T3=400DEG	44.34	56.70
	OUTSIDE	T2=205DEG- T6=415DEG	29.50	56.70
74	INSIDE	T2=205DEG- T3=400DEG	34.85	56.70
	OUTSIDE	T2=205DEG- T6=415DEG	34.85	56.70
75	INSIDE	T2=205DEG- T3=400DEG	29.90	56.70
	OUTSIDE	T2=205DEG- T6=415DEG	35.15	56.70
76	INSIDE	T1=430DEG- T2=205DEG	27.30	56.70
	OUTSIDE	T2=205DEG- T6=415DEG	37.54	56.70
77	INSIDE	T2=205DEG- T3=400DEG	28.22	56.70
	OUTSIDE	T2=205DEG- T6=415DEG	34.64	56.70
78	INSIDE	T2=205DEG- T3=400DEG	28.81	56.70
	OUTSIDE	T2=205DEG- T6=415DEG	32.50	56.70
79	INSIDE	T2=205DEG- T3=400DEG	28.70	56.70
	OUTSIDE	T2=205DEG- T6=415DEG	29.67	56.70
80	INSIDE	T3=400DEG- T5=430DEG	29.57	56.70
	OUTSIDE	T2=205DEG- T6=415DEG	25.67	56.70

RUN NO.: Y6ALTCC

DATE: 3/11/80

REF. FIGS.: 11.10-2, 11.10-17

POOR ORIGINAL

[ ] = MAXIMUM RANGE AND FATIGUE AT 90 DEG

a.c.e

FATIGUE ANALYSIS LOCATION SUMMARY

LOCATION	STRESS CONCENTRATIONS KX	KY	KZ	KXR	KYM	KZR	TOTAL USAGE FACTOR
1805	1.00	1.00	1.00	1.00	1.00	1.00	.0000
2005	1.00	1.00	1.00	1.00	1.00	1.00	.0071
2205	1.00	1.00	1.00	1.00	1.00	1.00	.0107
2405	1.00	1.00	1.00	1.00	1.00	1.00	0.0000
2605	1.00	1.00	1.00	1.00	1.00	1.00	0.0000
2805	1.00	1.00	1.00	1.00	1.00	1.00	.0046
2900	1.00	1.00	1.00	1.00	1.00	1.00	.0071
3005	1.00	1.00	1.00	1.00	1.00	1.00	.0071
3100	1.00	1.00	1.00	1.00	1.00	1.00	.0155
3205	1.00	1.00	1.00	1.00	1.00	1.00	.3398
3360	1.00	1.00	1.00	1.00	1.00	1.00	1.4234
3405	1.00	1.00	1.00	1.00	1.00	1.00	2.9658
3500	1.00	1.00	1.00	1.00	1.00	1.00	.0944
3605	1.00	1.00	1.00	1.00	1.00	1.00	.0071
3700	1.00	1.00	1.00	1.00	1.00	1.00	.0071
3805	1.00	1.00	1.00	1.00	1.00	1.00	.0059
3900	1.00	1.00	1.00	1.00	1.00	1.00	.0059
4005	1.00	1.00	1.00	1.00	1.00	1.00	.0059
4205	1.00	1.00	1.00	1.00	1.00	1.00	.0071
4405	1.00	1.00	1.00	1.00	1.00	1.00	.0065

RUN NO.: Y6ALTCC

DATE: 3/11/80

REF. FIGS.: 11.10-2, 11.10-17

a,c,e

[ ] - MAXIMUM RANGE AND FATIGUE STRATIFICATION AND STRIPING

SUMMARY - MAXIMUM RANGE OF STRESS INTENSITY ANALYSIS

ANALYSIS SECTION	SURFACE	LOAD CONDITION COMBINATION	SI RANGE (KSI)	ALLOWABLE (KSI)
5	INSIDE	T1-430-S - 15-430DEG	68.92	56.70
	OUTSIDE	T1-430-S - 15-430DEG	49.71	56.70

a,c,e

[ ] - MAXIMUM RANGE AND FATIGUE STRATIFICATION AND STRIPING

FATIGUE ANALYSIS LOCATION SUMMARY

LOCATION	STRESS CONCENTRATORS						TOTAL USAGE FACTOR
	KX	KY	KZ	KXR	KYR	KZR	
3425	1.00	1.00	1.00	1.00	1.00	1.00	7.3397

POOR ORIGINAL

RUN NO.: Y6ALTAX

DATE: 3/7/80

REF. FIGS.: 11.10-1, 11.10-14

a,c,e

[ ]- MAXIMUM RANGE AND FATIGUE STRATIFICATION AND STRIPING

SUMMARY - MAXIMUM RANGE OF STRESS INTENSITY ANALYSIS

ANALYSIS SECTION	SURFACE	LOAD CONDITION COMBINATION	SI RANGE (KSI)	ALLOWABLE (KSI)
7	INSIDE	T3-400+S - T6-415DEG	75.17	56.70
	OUTSIDE	T1-430DEG- T5-430DEG	35.31	56.70

a,c,e

[ ]- MAXIMUM RANGE AND FATIGUE STRATIFICATION AND STRIPING

FATIGUE ANALYSIS LOCATION SUMMARY

LOCATION	STRESS CONCENTRATORS KX	KY	KZ	KXR	KYR	KZR	TOTAL USAGE FACTOR
3440	1.00	1.00	1.00	1.00	1.00	1.00	8.9719

RUN NO.: Y6ALT62

DATE: 3/8/80

REF. FIGS.: 11.10-1, 11.10-14

POOR ORIGINAL

a,c,e

[ ] - MAXIMUM RANGE AND FATIGUE STRATIFICATION AND STRIPING

SUMMARY - [illegible]

ANALYSIS SECTION	[illegible]	LOAD CONDITION COMBINATION	[illegible] RANGE (KSI)	ALLOWABLE (KSI)
1.	[illegible]	T3-[illegible]- T5-43[illegible]	[illegible]	56.7[illegible]
	[illegible]	T3-[illegible]- T5-43[illegible]	[illegible]	56.70

a,c,e

[ ] - MAXIMUM RANGE AND FATIGUE STRATIFICATION AND STRIPING

FATIGUE ANALYSIS LOCATION SUMMARY

LOCATION	STRESS CONCENTRATORS						TOTAL USAGE FACTOR
	[illegible]	[illegible]	[illegible]	[illegible]	[illegible]	[illegible]	
[illegible]	[illegible]	[illegible]	[illegible]	1.[illegible]	[illegible]	[illegible]	0.9507

RUN NO.: Y6ALT60

DATE: 3/8/80

REF. FIGS.: 11.10-1, 11.10-14

POOR ORIGINAL

a,c,e

[ ] - MAXIMUM RANGE AND FATIGUE STRATIFICATION AND STRIPING

SUMMARY - MAXIMUM RANGE OF STRESS INTENSITY ANALYSIS

ANALYSIS SECTION	SURFACE	LOAD CONDITION COMBINATION	SI RANGE (KSI)	ALLOWABLE (KSI)
14	INSIDE	T2-205DEG- T6-415DEG	55.24	56.70
	OUTSIDE	T1-430DEG- T6-415DEG	17.12	56.70

a,c,e

[ ] - MAXIMUM RANGE AND FATIGUE STRATIFICATION AND STRIPING

FATIGUE ANALYSIS LOCATION SUMMARY

LOCATION	STRESS CONCENTRATORS KX	KY	KZ	KXR	KYR	KZR	TOTAL USAGE FACTOR
3475	1.00	1.00	1.00	1.00	1.00	1.00	.3431

RUN NO.: Y6ALT6X

DATE: 3/8/80

REF. FIGS.: 11.10-1, 11.10-14

POOR ORIGINAL

a,c,e

[ ]- MAXIMUM RANGE AND FATIGUE STRATIFICATION AND STRIPING

SUMMARY - MAXIMUM RANGE OF STRESS INTENSITY ANALYSIS

ANALYSIS SECTION	SURFACE	LOAD CONDITION COMBINATION	I RANGE (KSI)	ALLOWABLE (KSI)
16	INSIDE	T2-2[illegible]-S - T5-430DEG	31.6[illegible]	56.70
	OUTSIDE	T3-4[illegible]DEG- T5-43[illegible]DEG	27.7[illegible]	56.70

a,c,e

[ ]- MAXIMUM RANGE AND FATIGUE STRATIFICATION AND STRIPING

FATIGUE ANALYSIS LOCATION SUMMARY

LOCATION	STRESS CONCENTRATORS KX	KY	KZ	KXR	KYR	KZR	TOTAL USAGE FACTOR
34[illegible]	1.00	1.00	1.00	1.00	1.00	1.00	.0071

RUN. NO.: Y6ALT6Z

DATE: 3/8/80

REF. FIGS.: [illegible]10-1, 11.[illegible] -14

POOR ORIGINAL

[ ] ELBOW TRANSITION ROOT - MAXIMUM RANGE OF STRESS INTENSITY

a,c, e

SUMMARY - MAXIMUM RANGE OF STRESS INTENSITY ANALYSIS

ANALYSIS SECTION	SURFACE	LOAD CONDITION COMBINATION	S/T RANGE (KSI)	ALLOWABLE (KSI)
1	INSIDE	T1-390DEG- T2-400DEG	123.26	56.70
	OUTSIDE	T3-290DEG- AMBIENT	26.49	56.70
2	INSIDE	T1-390DEG- T2-400DEG	124.83	56.70
	OUTSIDE	T3-290DEG- AMBIENT	23.37	56.70
3	INSIDE	T1-390DEG- T2-400DEG	98.43	56.70
	OUTSIDE	T1-390DEG- AMBIENT	27.02	56.70
4	INSIDE	T1-390DEG- T2-400DEG	84.13	56.70
	OUTSIDE	T1-390DEG- T2-400DEG	33.70	56.70
5	INSIDE	T1-390DEG- T2-400DEG	70.50	56.70
	OUTSIDE	T1-390DEG- T2-400DEG	45.65	56.70
6	INSIDE	T1-390DEG- T6-390DEG	55.97	56.70
	OUTSIDE	T1-390DEG- T5-390DEG	39.34	56.70
7	INSIDE	T1-390DEG- T6-390DEG	66.78	56.70
	OUTSIDE	T1-390DEG- T5-390DEG	32.03	56.70
8	INSIDE	T1-390DEG- T5-390DEG	63.74	56.70
	OUTSIDE	T3-290DEG- T5-390DEG	28.75	56.70
9	INSIDE	T3-290DEG- T5-390DEG	68.23	56.70
	OUTSIDE	T2-400DEG- T3-290DEG	25.48	56.70
10	INSIDE	T2-400DEG- T3-290DEG	69.52	56.70
	OUTSIDE	T2-400DEG- T3-290DEG	24.37	56.70
11	INSIDE	T2-400DEG- T6-390DEG	76.99	56.70
	OUTSIDE	T2-400DEG- T6-390DEG	27.05	56.70
12	INSIDE	T2-400DEG- T6-390DEG	80.22	56.70
	OUTSIDE	T2-400DEG- T6-390DEG	28.69	56.70
13	INSIDE	T2-400DEG- T6-390DEG	85.10	56.70
	OUTSIDE	T2-400DEG- T6-390DEG	26.13	56.70
14	INSIDE	T2-400DEG- T6-390DEG	75.14	56.70
	OUTSIDE	T2-400DEG- T6-390DEG	22.23	56.70
15	INSIDE	T2-400DEG- T6-390DEG	61.86	56.70
	OUTSIDE	T2-400DEG- T5-390DEG	20.91	56.70
16	INSIDE	T2-400DEG- T5-390DEG	38.12	56.70
	OUTSIDE	T1-390DEG- T5-390DEG	24.93	56.70
17	INSIDE	T5-390DEG- AMBIENT	25.86	56.70
	OUTSIDE	T1-390DEG- T2-400DEG	27.48	56.70
18	INSIDE	T2-400DEG- AMBIENT	40.02	56.70
	OUTSIDE	T2-400DEG- T6-390DEG	29.49	56.70
19	INSIDE	T2-400DEG- T6-390DEG	30.98	56.70
	OUTSIDE	T2-400DEG- T6-390DEG	24.17	56.70
20	INSIDE	T2-400DEG- T6-390DEG	38.06	56.70
	OUTSIDE	T6-390DEG- PRESSURE	18.46	56.70

RUN NO.: Y6ALTOE

DATE: 2/28/80

REF. FIGS.: 11.10-1, 11.10-18, 11.10-19

a,c,e

[ ] - FATIGUE - FLOW TRANSITION ROOT

FATIGUE ANALYSIS LOCATION SUMMARY

LOCATION	STRESS CONCENTRATORS KX	KY	KZ	KXR	KYR	KZR	TOTAL USAGE FACTOR
3405	1.00	1.00	1.00	1.00	1.00	1.00	9.3728
3410	1.00	1.00	1.00	1.00	1.00	1.00	9.2286
3415	1.00	1.00	1.00	1.00	1.00	1.00	4.3810
3420	1.00	1.00	1.00	1.00	1.00	1.00	2.2697
3425	1.00	1.00	1.00	1.00	1.00	1.00	1.0747
3435	1.00	1.00	1.00	1.00	1.00	1.00	.2988
3440	1.00	1.00	1.00	1.00	1.00	1.00	1.0482
3445	1.00	1.00	1.00	1.00	1.00	1.00	.8062
3450	1.00	1.00	1.00	1.00	1.00	1.00	1.0909
3455	1.00	1.00	1.00	1.00	1.00	1.00	1.1571
3460	1.00	1.00	1.00	1.00	1.00	1.00	3.6996
3465	1.00	1.00	1.00	1.00	1.00	1.00	4.1928
3470	1.00	1.00	1.00	1.00	1.00	1.00	4.7161
3475	1.00	1.00	1.00	1.00	1.00	1.00	2.6784
3480	1.00	1.00	1.00	1.00	1.00	1.00	.6299
3485	1.00	1.00	1.00	1.00	1.00	1.00	.0057
3495	1.00	1.00	1.00	1.00	1.00	1.00	.0009
3505	1.00	1.00	1.00	1.00	1.00	1.00	.0072
3515	1.00	1.00	1.00	1.00	1.00	1.00	.0077

RUN NO.: Y6ALTOF

DATE: 2/28/80

REF. FIGS.: 11.10-1, 11.10-18, 11.10-19

ELBOW TRANSITION ROUT
- MAXIMUM RANGE OF STRESS INTENSITY

SUMMARY - MAXIMUM RANGE OF STRESS INTENSITY ANALYSIS

ANALYSIS SECTION	SURFACE	LOAD CONDITION COMBINATION	SI RANGE (KSI)	ALLOWABLE (KSI)
1	INSIDE	T1-390DEG- T2-400DEG	123.26	56.70
	OUTSIDE	T3-290DEG- AMBIENT	26.49	56.70
2	INSIDE	T1-390DEG- T2-400DEG	124.83	56.70
	OUTSIDE	T3-290DEG- AMBIENT	23.37	56.70
3	INSIDE	T1-390DEG- T2-400DEG	98.43	56.70
	OUTSIDE	T1-390DEG- AMBIENT	27.02	56.70
4	INSIDE	T1-390DEG- T2-400DEG	84.13	56.70
	OUTSIDE	T1-390DEG- T2-400DEG	33.70	56.70
5	INSIDE	T1-390DEG- T2-400DEG	70.50	56.70
	OUTSIDE	T1-390DEG- T2-400DEG	45.65	56.70
6	INSIDE	T1-390DEG- T6-390DEG	55.97	56.70
	OUTSIDE	T1-390DEG- T5-390DEG	37.34	56.70
7	INSIDE	T1-390DEG- T6-390DEG	66.78	56.70
	OUTSIDE	T1-390DEG- T5-390DEG	32.03	56.70
8	INSIDE	T1-390DEG- T5-390DEG	63.74	56.70
	OUTSIDE	T3-290DEG- T5-390DEG	28.75	56.70
9	INSIDE	T3-290DEG- T5-390DEG	68.23	56.70
	OUTSIDE	T2-400DEG- T3-290DEG	25.48	56.70
10	INSIDE	T2-400DEG- T3-290DEG	69.52	56.70
	OUTSIDE	T2-400DEG- T3-290DEG	24.37	56.70
11	INSIDE	T2-400DEG- T6-390DEG	76.99	56.70
	OUTSIDE	T2-400DEG- T6-390DEG	27.65	56.70
12	INSIDE	T2-400DEG- T6-390DEG	80.22	56.70
	OUTSIDE	T2-400DEG- T6-390DEG	28.69	56.70
13	INSIDE	T2-400DEG- T6-390DEG	85.10	56.70
	OUTSIDE	T2-400DEG- T6-390DEG	26.13	56.70
14	INSIDE	T2-400DEG- T6-390DEG	75.14	56.70
	OUTSIDE	T2-400DEG- T6-390DEG	22.23	56.70
15	INSIDE	T2-400DEG- T6-390DEG	61.86	56.70
	OUTSIDE	T2-400DEG- T5-390DEG	20.91	56.70
16	INSIDE	T2-400DEG- T5-390DEG	38.12	56.70
	OUTSIDE	T1-390DEG- T5-390DEG	24.93	56.70
17	INSIDE	T5-390DEG- AMBIENT	25.86	56.70
	OUTSIDE	T1-390DEG- T2-400DEG	27.48	56.70
18	INSIDE	T2-400DEG- AMBIENT	40.02	56.70
	OUTSIDE	T2-400DEG- T6-390DEG	29.49	56.70
19	INSIDE	T2-400DEG- T6-390DEG	39.98	56.70
	OUTSIDE	T2-400DEG- T6-390DEG	24.17	56.70
20	INSIDE	T2-400DEG- T6-390DEG	38.86	56.70
	OUTSIDE	T5-390DEG- PRESSURE	18.46	56.70

POOR ORIGINAL

RUN NO.: Y6ALTZO

DATE: 2/28/80

REF. FIGS.: 11.10-1, 11.10-19

a.c.e

[ ] - FATIGUE - ELBOW TRANSITION ROOT

FATIGUE ANALYSIS LOCATION SUMMARY

LOCATION	STRESS CONCENTRATIONS KX	KY	KZ	KXR	KYR	KZR	TOTAL USAGE FACTOR
3405	1.00	1.00	1.00	1.00	1.00	1.00	17.4382
3410	1.00	1.00	1.00	1.00	1.00	1.00	17.9182
3415	1.00	1.00	1.00	1.00	1.00	1.00	3.6234
3420	1.00	1.00	1.00	1.00	1.00	1.00	1.0092
3425	1.00	1.00	1.00	1.00	1.00	1.00	.1785
3435	1.00	1.00	1.00	1.00	1.00	1.00	.0380
3440	1.00	1.00	1.00	1.00	1.00	1.00	.1510
3445	1.00	1.00	1.00	1.00	1.00	1.00	.1024
3450	1.00	1.00	1.00	1.00	1.00	1.00	.1784
3455	1.00	1.00	1.00	1.00	1.00	1.00	.1800
3460	1.00	1.00	1.00	1.00	1.00	1.00	.6594
3465	1.00	1.00	1.00	1.00	1.00	1.00	.9465
3470	1.00	1.00	1.00	1.00	1.00	1.00	1.4033
3475	1.00	1.00	1.00	1.00	1.00	1.00	.4334
3480	1.00	1.00	1.00	1.00	1.00	1.00	.0747
3485	1.00	1.00	1.00	1.00	1.00	1.00	.0055
3495	1.00	1.00	1.00	1.00	1.00	1.00	.0009
3505	1.00	1.00	1.00	1.00	1.00	1.00	.0062
3515	1.00	1.00	1.00	1.00	1.00	1.00	.0063
3525	1.00	1.00	1.00	1.00	1.00	1.00	.0057

RUN NO.: Y6ALTZ2

DATE: 2/28/80

REF. FIGS.: 11.10-1, 11.10-19

POOR ORIGINAL

[ ] - FATIGUE - ELBOW TOP

SUMMARY - MAXIMUM RANGE OF STRESS INTENSITY ANALYSIS

ANALYSIS SECTION	SURFACE	LOAD CONDITION COMBINATION	ST RANGE (KSI)	ALLOWABLE (KSI)
21	INSIDE	T1-390DEG- T2-400DEG	17.14	80.10
	OUTSIDE	T1-390DEG- AMBIENT	14.59	80.10
22	INSIDE	T1-390DEG- T2-400DEG	27.67	80.10
	OUTSIDE	T1-390DEG- T2-400DEG	15.29	80.10
23	INSIDE	T1-390DEG- T2-400DEG	57.00	80.10
	OUTSIDE	T1-390DEG- T2-400DEG	17.52	80.10
24	INSIDE	T1-390DEG- AMBIENT	25.60	80.10
	OUTSIDE	T1-390DEG- T2-400DEG	91.52	80.10
25	INSIDE	T1-390DEG- AMBIENT	35.42	80.10
	OUTSIDE	T1-390DEG- T2-400DEG	94.41	80.10
26	INSIDE	T1-390DEG- AMBIENT	40.20	80.10
	OUTSIDE	T1-390DEG- T2-400DEG	67.29	80.10
27	INSIDE	T1-390DEG- T2-400DEG	44.59	80.10
	OUTSIDE	T1-390DEG- T2-400DEG	60.60	80.10
28	INSIDE	T1-390DEG- T2-400DEG	38.35	80.10
	OUTSIDE	T1-390DEG- T2-400DEG	35.41	80.10
29	INSIDE	T1-390DEG- T2-400DEG	80.30	80.10
	OUTSIDE	T1-390DEG- T2-400DEG	32.50	80.10
30	INSIDE	T1-390DEG- T2-400DEG	102.81	56.70
	OUTSIDE	T2-400DEG- T3-290DEG	26.04	56.70
31	INSIDE	T1-390DEG- T2-400DEG	116.00	56.70
	OUTSIDE	T3-290DEG- AMBIENT	24.03	56.70
32	INSIDE	T1-390DEG- T2-400DEG	123.20	56.70
	OUTSIDE	T3-290DEG- AMBIENT	26.49	56.70
33	INSIDE	T1-390DEG- T2-400DEG	88.91	56.70
	OUTSIDE	T1-390DEG- T2-400DEG	28.04	56.70
34	INSIDE	T1-390DEG- T2-400DEG	33.67	56.70
	OUTSIDE	T1-390DEG- T2-400DEG	43.50	56.70
35	INSIDE	T1-390DEG- T2-400DEG	45.10	56.70
	OUTSIDE	T1-390DEG- T2-400DEG	47.10	56.70
36	INSIDE	T1-390DEG- T2-400DEG	40.40	56.70
	OUTSIDE	T1-390DEG- T2-400DEG	55.19	56.70
37	INSIDE	T1-390DEG- T2-400DEG	40.90	56.70
	OUTSIDE	T1-390DEG- T2-400DEG	51.40	56.70
38	INSIDE	T1-390DEG- T2-400DEG	38.23	56.70
	OUTSIDE	T1-390DEG- T2-400DEG	51.59	56.70
39	INSIDE	T2-400DEG- T3-290DEG	32.39	56.70
	OUTSIDE	T1-390DEG- T2-400DEG	39.70	56.70
40	INSIDE	T2-400DEG- T3-290DEG	27.35	56.70
	OUTSIDE	T2-400DEG- T3-290DEG	40.09	56.70

RUN NO.: Y6ALT08

DATE: 3/10/80

REF. FIGS.: 11.10-2, 11.10-20

POOR ORIGINAL

a,c,e

[ ] - FATIGUE - FENCE TOP

FATIGUE ANALYSIS LOCATION SUMMARY

LOCATION	STRESS CONCENTRATIONS						
	KX	KY	KZ	KXM	KYM	KZM	USAGE FACTOR
1305	1.00	1.00	1.00	1.00	1.00	1.00	.00000
2005	1.00	1.00	1.00	1.00	1.00	1.00	.00004
2205	1.00	1.00	1.00	1.00	1.00	1.00	.00004
2405	1.00	1.00	1.00	1.00	1.00	1.00	.00000
2605	1.00	1.00	1.00	1.00	1.00	1.00	.00015
2805	1.00	1.00	1.00	1.00	1.00	1.00	.00015
2905	1.00	1.00	1.00	1.00	1.00	1.00	.00025
3005	1.00	1.00	1.00	1.00	1.00	1.00	.00014
3105	1.00	1.00	1.00	1.00	1.00	1.00	.00027
3205	1.00	1.00	1.00	1.00	1.00	1.00	3.02E-0
3305	1.00	1.00	1.00	1.00	1.00	1.00	9.50E-5
3405	1.00	1.00	1.00	1.00	1.00	1.00	3.51E-5
3505	1.00	1.00	1.00	1.00	1.00	1.00	2.41E-0
3605	1.00	1.00	1.00	1.00	1.00	1.00	.00000
3705	1.00	1.00	1.00	1.00	1.00	1.00	.00150
3805	1.00	1.00	1.00	1.00	1.00	1.00	.00001
3905	1.00	1.00	1.00	1.00	1.00	1.00	.00050
4005	1.00	1.00	1.00	1.00	1.00	1.00	.00020
4205	1.00	1.00	1.00	1.00	1.00	1.00	.00017
4405	1.00	1.00	1.00	1.00	1.00	1.00	.00015

RUN NO.: Y6ALT08

DATE: 3/11/80

REF. FIGS.: 11.10-2, 11.10-20

POOR ORIGINAL

[ ] = MAXIMUM RANGE AND FATIGUE AT 90 DEG

a.c.c

SUMMARY - MAXIMUM RANGE OF STRESS INTENSITY ANALYSIS

ANALYSIS SECTION	SURFACE	LOAD CONDITION COMBINATION	SI RANGE (KSI)	ALLOWABLE (KSI)
01	INSIDE	T1=390DEG- T2=400DEG	22.00	80.10
	OUTSIDE	T1=390DEG- AMBIENT	14.44	80.10
02	INSIDE	T1=390DEG- T2=400DEG	51.02	80.10
	OUTSIDE	T1=390DEG- AMBIENT	12.00	80.10
03	INSIDE	T2=400DEG- T6=390DEG	46.90	80.10
	OUTSIDE	T1=390DEG- AMBIENT	10.75	80.10
04	INSIDE	T2=400DEG- T6=390DEG	18.81	80.10
	OUTSIDE	T2=400DEG- T6=390DEG	00.51	80.10
05	INSIDE	T2=400DEG- AMBIENT	18.37	80.10
	OUTSIDE	T2=400DEG- T6=390DEG	72.12	80.10
06	INSIDE	T1=390DEG- T2=400DEG	50.60	80.10
	OUTSIDE	T2=400DEG- T6=390DEG	59.80	80.10
07	INSIDE	T1=390DEG- T2=400DEG	54.00	80.10
	OUTSIDE	T2=400DEG- T6=390DEG	58.50	80.10
08	INSIDE	T1=390DEG- T2=400DEG	59.17	80.10
	OUTSIDE	T2=400DEG- T6=390DEG	53.72	80.10
09	INSIDE	T2=400DEG- T6=390DEG	47.30	80.10
	OUTSIDE	T2=400DEG- T6=390DEG	38.11	80.10
10	INSIDE	T2=400DEG- T6=390DEG	62.60	56.70
	OUTSIDE	T2=400DEG- T6=390DEG	29.12	56.70
11	INSIDE	T2=400DEG- T6=390DEG	71.90	56.70
	OUTSIDE	T2=400DEG- T6=390DEG	29.10	56.70
12	INSIDE	T2=400DEG- T6=390DEG	60.22	56.70
	OUTSIDE	T2=400DEG- T6=390DEG	28.69	56.70
13	INSIDE	T2=400DEG- T6=390DEG	57.94	56.70
	OUTSIDE	T2=400DEG- T6=390DEG	36.10	56.70
14	INSIDE	T2=400DEG- T6=390DEG	42.00	56.70
	OUTSIDE	T2=400DEG- T6=390DEG	42.90	56.70
15	INSIDE	T1=390DEG- T2=400DEG	55.05	56.70
	OUTSIDE	T2=400DEG- T6=390DEG	43.25	56.70
16	INSIDE	T1=390DEG- T2=400DEG	51.40	56.70
	OUTSIDE	T2=400DEG- T6=390DEG	46.27	56.70
17	INSIDE	T1=390DEG- T2=400DEG	52.30	56.70
	OUTSIDE	T2=400DEG- T6=390DEG	42.60	56.70
18	INSIDE	T1=390DEG- T2=400DEG	52.60	56.70
	OUTSIDE	T2=400DEG- T6=390DEG	39.92	56.70
19	INSIDE	T1=390DEG- T2=400DEG	52.52	56.70
	OUTSIDE	T2=400DEG- T6=390DEG	36.27	56.70
80	INSIDE	T2=400DEG- T6=390DEG	33.42	56.70
	OUTSIDE	T2=400DEG- T6=390DEG	31.62	56.70

RUN NO.: Y6ALTCI

DATE: 3/11/80

REF. FIGS.: 11.10-2, 11.10-21

POOR ORIGINAL

a.c.e

[ ] = MAXIMUM RANGE AND FATIGUE AT 90 DEG

FATIGUE ANALYSIS LOCATION SUMMARY

LOCATION	STRESS CONCENTRATIONS KX	KY	KZ	KXR	KYR	KZR	TOTAL USAGE FACTOR
1R05	1.00	1.00	1.00	1.00	1.00	1.00	0.0000
2005	1.00	1.00	1.00	1.00	1.00	1.00	.0050
2205	1.00	1.00	1.00	1.00	1.00	1.00	.0101
2405	1.00	1.00	1.00	1.00	1.00	1.00	0.0000
2605	1.00	1.00	1.00	1.00	1.00	1.00	0.0000
2R05	1.00	1.00	1.00	1.00	1.00	1.00	.0015
2900	1.00	1.00	1.00	1.00	1.00	1.00	.0050
3005	1.00	1.00	1.00	1.00	1.00	1.00	.0050
3100	1.00	1.00	1.00	1.00	1.00	1.00	.0083
3205	1.00	1.00	1.00	1.00	1.00	1.00	.5861
3300	1.00	1.00	1.00	1.00	1.00	1.00	1.9124
3405	1.00	1.00	1.00	1.00	1.00	1.00	4.1927
3500	1.00	1.00	1.00	1.00	1.00	1.00	.3082
3605	1.00	1.00	1.00	1.00	1.00	1.00	.0089
3700	1.00	1.00	1.00	1.00	1.00	1.00	.0050
3805	1.00	1.00	1.00	1.00	1.00	1.00	.0016
3900	1.00	1.00	1.00	1.00	1.00	1.00	.0020
4005	1.00	1.00	1.00	1.00	1.00	1.00	.0050
4205	1.00	1.00	1.00	1.00	1.00	1.00	.0050
4405	1.00	1.00	1.00	1.00	1.00	1.00	.0060

RUN NO.: Y6ALTCI

DATE: 3/11/80

REF. FIGS.: 11.10-2, 11.10-21

a,c,e

[ ] - MAXIMUM RANGE AND FATIGUE STRATIFICATION AND STRIPING

SUMMARY - MAXIMUM RANGE OF STRESS INTENSITY ANALYSIS

ANALYSIS SECTION	SURFACE	LOAD CONDITION COMBINATION	SI RANGE (KSI)	ALLOWABLE (KSI)
5	INSIDE	11-390-S - 12-400DEG	70.50	56.70
	OUTSIDE	11-390-S - 12-400DEG	45.69	56.70

a,c,e

[ ] - MAXIMUM RANGE AND FATIGUE STRATIFICATION AND STRIPING

FATIGUE ANALYSIS LOCATION SUMMARY

LOCATION	STRESS CONCENTRATORS KX	KY	KZ	KXR	KYR	KZR	TOTAL USAGE FACTOR
3425	1.00	1.00	1.00	1.00	1.00	1.00	1.7554

RUN NO.: Y6ALTJO

DATE: 3/7/80

REF. FIGS.: 11.10-1, 11.10-18

POOR ORIGINAL

a,c,e

[ ]- MAXIMUM RANGE AND FATIGUE STRATIFICATION AND STRIPING

SUMMARY - MAXIMUM RANGE OF STRESS INTENSITY ANALYSIS

ANALYSIS SECTION	SURFACE	LOAD CONDITION COMBINATION	ΔT RANGE (KSI)	ALLOWABLE (KSI)
7	INSIDE	T1-390DEG- T0-390DEG	56.70	56.70
	OUTSIDE	T1-390DEG- T5-390DEG	52.05	56.70

a,c,e

[ ]- MAXIMUM RANGE AND FATIGUE STRATIFICATION AND STRIPING

FATIGUE ANALYSIS LOCATION SUMMARY

LOCATION	STRESS CONCENTRATIONS						TOTAL USAGE FACTOR
	KX	KY	KZ	KXR	KYR	KZR	
SAME	1.00	1.00	1.00	1.00	1.00	1.00	1.0952

RUN NO.: Y6ALTAG
DATE; 3/7/80
REF. FIGS.: 11.10-1, 11.10-18

POOR ORIGINAL

a,c,e

[ ] = MAXIMUM RANGE AND FATIGUE STRATIFICATION AND STRIPING

SUMMARY - MAXIMUM RANGE OF STRESS INTENSITY ANALYSIS

ANALYSIS SECTION ID	SURFACE	LOAD CONDITION COMBINATION	ΔT RANGE (KSI)	ALLOWABLE (KSI)
	INSIDE	T2-400DEG- T3-290DEG	69.52	56.70
	OUTSIDE	T2-400DEG- T3-290DEG	28.37	56.70

a,c,e

[ ] = MAXIMUM RANGE AND FATIGUE STRATIFICATION AND STRIPING

FATIGUE ANALYSIS LOCATION SUMMARY

LOCATION	STRESS CONCENTRATIONS KX	KY	KZ	KXY	KYZ	KZX	TOTAL USAGE FACTOR
SUSS	1.00	1.00	1.00	1.00	1.00	1.00	1.4000

RUN NO.: Y6ALTP1

DATE: 3/7/80

REF. FIGS.: 11.10-1, 11.10-18

POOR ORIGINAL

a,c,e

[ ] = MAXIMUM RANGE AND FATIGUE STRATIFICATION AND STRIPING

SUMMARY = MAXIMUM RANGE OF STRESS INTENSITY ANALYSIS

ANALYSIS SECTION	SURFACE	LOAD CONDITION COMBINATION	SI RANGE (KSI)	ALLOWABLE (KSI)
14	INSIDE	T2=400DEG= 16=390DEG	75.14	56.70
	OUTSIDE	T2=400DEG= 16=390DEG	22.25	56.70

a,c,e

[ ] = MAXIMUM RANGE AND FATIGUE STRATIFICATION AND STRIPING

FATIGUE ANALYSIS LOCATION SUMMARY

LOCATION	STRESS CONCENTRATORS KX	KY	KZ	KXR	KYR	KZR	TOTAL USAGE FACTOR
3475	1.00	1.00	1.00	1.00	1.00	1.00	2.6614

RUN NO.: Y6ALTOX

DATE: 3/7/80

REF. FIGS.: 11[illegible], 11.10-18

POOR ORIGINAL

a.c.e

[ ]- MAXIMUM RANGE AND FATIGUE STRATIFICATION AND STRIPING

SUMMARY - MAXIMUM RANGE OF STRESS INTENSITY ANALYSIS

ANALYSIS SECTION	SURFACE	LOAD CONDITION COMBINATION	ST RANGE (KSI)	ALLOWABLE (KSI)
16	INSIDE	T2-400-S - 15-390DEG	38.66	56.70
	OUTSIDE	T1-390DEG- 15-390DEG	24.93	56.70

a.c.e

[ ]- MAXIMUM RANGE AND FATIGUE STRATIFICATION AND STRIPING

FATIGUE ANALYSIS LOCATION SUMMARY

LOCATION	STRESS CONCENTRATORS KX	KY	KZ	KXR	KYR	KZR	TOTAL USAGE FACTOR
3465	1.00	1.00	1.00	1.00	1.00	1.00	.0083

RUN NO.: Y6ALT78

DATE: 3/7/80

REF. FIGS.: 11.10-1, 11.10-18

POOR ORIGINAL

POOR ORIGINAL

a,c,e

[redacted]

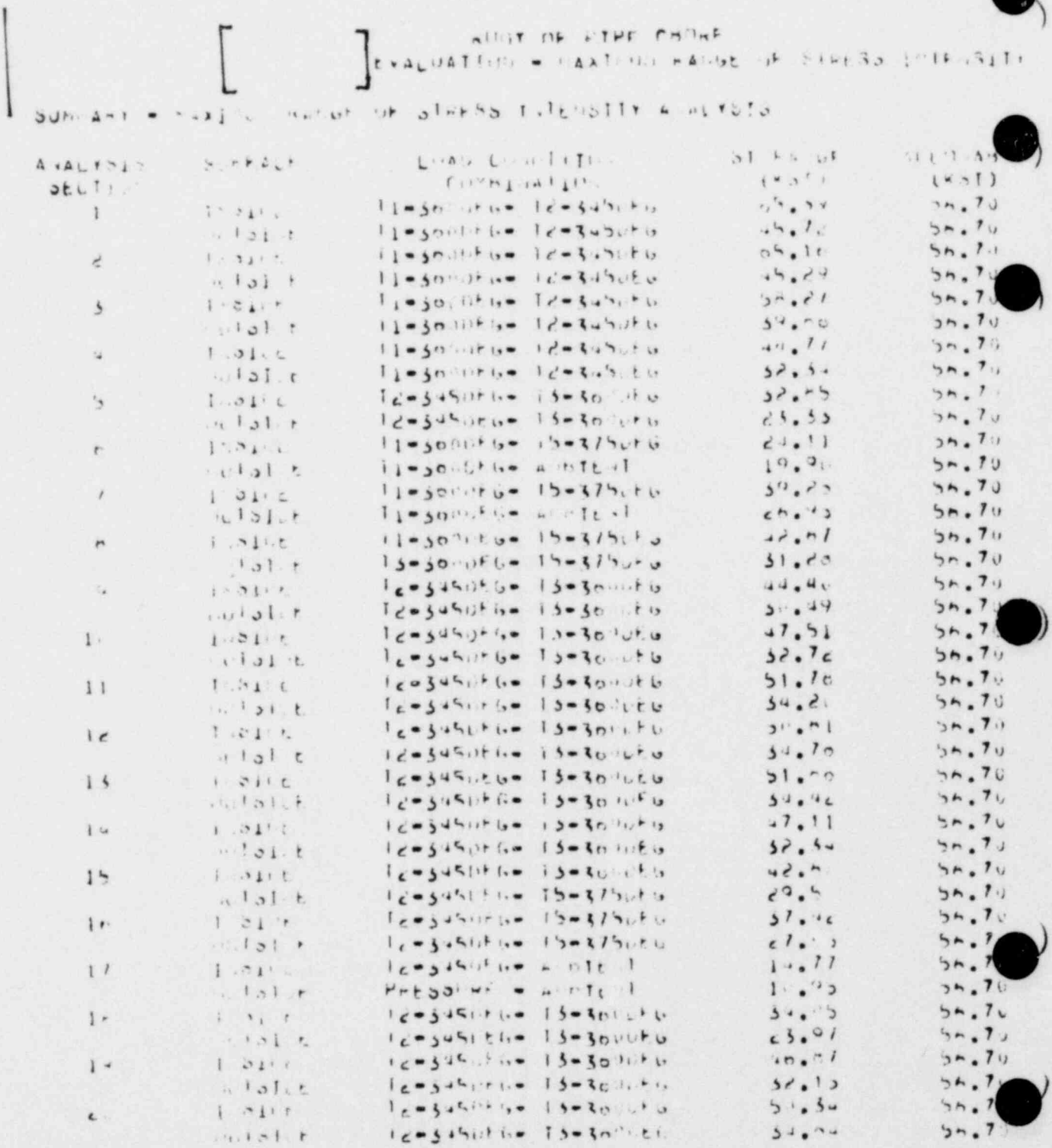

RUN NO.: Y6ALTZ0

DATE: 2/28/80

REF. FIGS.: 11.10-3

POOR ORIGINAL

[ ] EVALUATION - FATIGUE AT MIDT OF PIPE CIRCUMFERENCE | a.c.e

FATIGUE ANALYSIS LOCATION SUMMARY

LOCATION	STRESS CONCENTRATIONS						TOTAL USAGE FACTOR
	KX	KY	KZ	KXY	KYZ	KZX	
4005	1.00	1.00	1.00	1.00	1.00	1.00	.3[illegible]
4010	1.00	1.00	1.00	1.00	1.00	1.00	.3[illegible]
4015	1.00	1.00	1.00	1.00	1.00	1.00	.2[illegible]
4020	1.00	1.00	1.00	1.00	1.00	1.00	.0[illegible]
4025	1.00	1.00	1.00	1.00	1.00	1.00	.0[illegible]
4035	1.00	1.00	1.00	1.00	1.00	1.00	.0[illegible]
4040	1.00	1.00	1.00	1.00	1.00	1.00	.0[illegible]
4045	1.00	1.00	1.00	1.00	1.00	1.00	.0[illegible]
4050	1.00	1.00	1.00	1.00	1.00	1.00	.0[illegible]
4055	1.00	1.00	1.00	1.00	1.00	1.00	.0[illegible]
4060	1.00	1.00	1.00	1.00	1.00	1.00	.1[illegible]
4065	1.00	1.00	1.00	1.00	1.00	1.00	.0[illegible]
4070	1.00	1.00	1.00	1.00	1.00	1.00	.1[illegible]
4075	1.00	1.00	1.00	1.00	1.00	1.00	.0[illegible]
4080	1.00	1.00	1.00	1.00	1.00	1.00	.0[illegible]
4085	1.00	1.00	1.00	1.00	1.00	1.00	.0[illegible]
4095	1.00	1.00	1.00	1.00	1.00	1.00	1.0[illegible]
4105	1.00	1.00	1.00	1.00	1.00	1.00	.0[illegible]
4115	1.00	1.00	1.00	1.00	1.00	1.00	.1[illegible]
4125	1.00	1.00	1.00	1.00	1.00	1.00	.0[illegible]

RUN NO.: Y6ALTZT
DATE: 2/28/30
REF. FIGS.: 11.10-3

POOR ORIGINAL

a,c,e

[ ] RIGHT RF NOZZLE CRORE
EVALUATION - MAXIMUM RANGE OF STRESS INTENSITY

SUMMARY - MAXIMUM RANGE OF STRESS INTENSITY AMPLITUDE

ANALYSIS SECTION	LOCATION	LOAD COMBINATION	SI RANGE (KSI)	ALLOWABLE (KSI)
21	INSIDE	11-3PC+16- 12-3+5C+6	58.00	58.20
	OUTSIDE	11-3PC+16- 12-3+5C+6	51.21	58.20
22	INSIDE	11-3PC+16- 12-3+5C+6	58.00	58.20
	OUTSIDE	11-3PC+16- 12-3+5C+6	51.44	58.20
23	INSIDE	11-3PC+16- 12-3+5C+6	51.94	58.20
	OUTSIDE	11-3PC+16- 2-STEADY	27.27	58.20
24	INSIDE	11-3PC+16- 12-3+5C+6	47.23	58.20
	OUTSIDE	11-3PC+16- 12-3+5C+6	21.44	58.20
25	INSIDE	12-3+5C+6- 13-3PC+6	55.77	58.20
	OUTSIDE	13-3PC+16- 2-STEADY	18.10	58.20
26	INSIDE	11-3PC+16- 15-3+5C+6	28.57	58.20
	OUTSIDE	11-3PC+16- 15-3+5C+6	15.20	58.20
27	INSIDE	11-3PC+16- 15-3+5C+6	41.53	58.20
	OUTSIDE	11-3PC+16- 15-3+5C+6	27.20	58.20
28	INSIDE	11-3PC+16- 15-3+5C+6	45.00	58.20
	OUTSIDE	11-3PC+16- 15-3+5C+6	24.31	58.20
29	INSIDE	12-3+5C+6- 13-3PC+6	47.17	58.20
	OUTSIDE	12-3+5C+6- 2-STEADY	21.7	58.20
30	INSIDE	12-3+5C+6- 13-3PC+6	51.10	58.20
	OUTSIDE	12-3+5C+6- 13-3PC+6	21.5	58.20
31	INSIDE	12-3+5C+6- 13-3PC+6	54.81	58.20
	OUTSIDE	12-3+5C+6- 13-3PC+6	22.24	58.20
32	INSIDE	12-3+5C+6- 13-3PC+6	54.22	58.20
	OUTSIDE	12-3+5C+6- 13-3PC+6	22.01	58.20
33	INSIDE	12-3+5C+6- 13-3PC+6	54.84	58.20
	OUTSIDE	12-3+5C+6- 13-3PC+6	22.44	58.20
34	INSIDE	12-3+5C+6- 13-3PC+6	51.51	58.20
	OUTSIDE	12-3+5C+6- 15-3+5C+6	22.41	58.20
35	INSIDE	12-3+5C+6- 13-3PC+6	45.43	58.20
	OUTSIDE	12-3+5C+6- 15-3+5C+6	21.00	58.20
36	INSIDE	12-3+5C+6- 15-3+5C+6	41.13	58.20
	OUTSIDE	12-3+5C+6- 15-3+5C+6	21.11	58.20
37	INSIDE	12-3+5C+6- 2-STEADY	18.14	58.20
	OUTSIDE	PRESSURE - 2-STEADY	0.13	58.20
38	INSIDE	12-3+5C+6- 13-3PC+6	58.87	58.20
	OUTSIDE	12-3+5C+6- 13-3PC+6	18.54	58.20
39	INSIDE	12-3+5C+6- 13-3PC+6	49.15	58.20
	OUTSIDE	12-3+5C+6- 13-3PC+6	21.11	58.20
40	INSIDE	12-3+5C+6- 13-3PC+6	53.57	58.20
	OUTSIDE	12-3+5C+6- 13-3PC+6	22.44	58.20

RUN NO.: Y6ALTH7

DATE: 2/28/80

REF. FIGS.: 11.10-4, 11.10-22

POOR ORIGINAL

a,c,e

[ ] EVALUATION - FATIGUE AT ROOT OF NOZZLE COUNTERBORE

FATIGUE ANALYSIS LOCATION SUMMARY

LOCATION	STRESS CONCENTRATORS						TOTAL USAGE FACTOR
	KX	KY	KZ	KXR	KYR	KZR	
3805	1.00	1.00	1.00	1.00	1.00	1.00	.4591
3810	1.00	1.00	1.00	1.00	1.00	1.00	.4343
3815	1.00	1.00	1.00	1.00	1.00	1.00	.2978
3820	1.00	1.00	1.00	1.00	1.00	1.00	.0240
3825	1.00	1.00	1.00	1.00	1.00	1.00	.0008
3835	1.00	1.00	1.00	1.00	1.00	1.00	.0008
3840	1.00	1.00	1.00	1.00	1.00	1.00	.0068
3845	1.00	1.00	1.00	1.00	1.00	1.00	.0323
3850	1.00	1.00	1.00	1.00	1.00	1.00	.0362
3855	1.00	1.00	1.00	1.00	1.00	1.00	.0493
3860	1.00	1.00	1.00	1.00	1.00	1.00	.1306
3865	1.00	1.00	1.00	1.00	1.00	1.00	.1268
3870	1.00	1.00	1.00	1.00	1.00	1.00	.1402
3875	1.00	1.00	1.00	1.00	1.00	1.00	.0341
3880	1.00	1.00	1.00	1.00	1.00	1.00	.0157
3885	1.00	1.00	1.00	1.00	1.00	1.00	.0026
3895	1.00	1.00	1.00	1.00	1.00	1.00	0.0000
3905	1.00	1.00	1.00	1.00	1.00	1.00	.0005
3915	1.00	1.00	1.00	1.00	1.00	1.00	.0316
3925	1.00	1.00	1.00	1.00	1.00	1.00	.1131

RUN NO.: Y6ALT5A
DATE: 2/28/80
REF. FIGS.: 11.10-4, 11.10-22

POOR ORIGINAL

[ ] EVALUATION - FATIGUE AT TOP OF COUNTERBORE (INSIDE)

SUMMARY - MAXIMUM RANGE OF STRESS INTENSITY ANALYSIS

ANALYSIS SECTION	SURFACE	LOAD CONDITION COMBINATION	SI RANGE (KSI)	ALLOWABLE (KSI)
101	INSIDE	T4-150DEG- T5-375DEG	22.82	58.20
	OUTSIDE	T1-360DEG- T2-345DEG	68.97	58.20
102	INSIDE	T1-360DEG- AMBIENT	31.06	58.20
	OUTSIDE	T1-360DEG- T2-345DEG	64.62	58.20
103	INSIDE	T1-360DEG- T2-345DEG	45.91	58.20
	OUTSIDE	T1-360DEG- T2-345DEG	44.72	58.20
104	INSIDE	T1-360DEG- T2-345DEG	50.52	58.20
	OUTSIDE	T1-360DEG- T2-345DEG	39.75	58.20
105	INSIDE	T1-360DEG- T2-345DEG	49.33	58.20
	OUTSIDE	T1-360DEG- T2-345DEG	39.79	58.20
106	INSIDE	T1-360DEG- T2-345DEG	48.60	58.20
	OUTSIDE	T1-360DEG- T2-345DEG	40.28	58.20
107	INSIDE	T1-360DEG- T2-345DEG	46.48	58.20
	OUTSIDE	T1-360DEG- T2-345DEG	42.02	58.20
108	INSIDE	T1-360DEG- T2-345DEG	42.92	58.20
	OUTSIDE	T1-360DEG- T2-345DEG	44.08	58.20
109	INSIDE	T1-360DEG- T2-345DEG	40.31	58.20
	OUTSIDE	T1-360DEG- T2-345DEG	47.31	58.20
110	INSIDE	T1-360DEG- T2-345DEG	38.81	58.20
	OUTSIDE	T1-360DEG- T2-345DEG	51.10	58.20
111	INSIDE	T1-360DEG- T2-345DEG	51.63	58.20
	OUTSIDE	T1-360DEG- T2-345DEG	42.45	58.20
112	INSIDE	T1-360DEG- T2-345DEG	69.69	58.20
	OUTSIDE	T1-360DEG- T2-345DEG	31.21	58.20
113	INSIDE	T1-360DEG- T2-345DEG	68.52	56.70
	OUTSIDE	T1-360DEG- T2-345DEG	35.98	56.70
114	INSIDE	T1-360DEG- T2-345DEG	65.39	56.70
	OUTSIDE	T1-360DEG- T2-345DEG	45.72	56.70
115	INSIDE	T1-360DEG- T2-345DEG	55.84	56.70
	OUTSIDE	T1-360DEG- T2-345DEG	52.64	56.70
116	INSIDE	T1-360DEG- T2-345DEG	48.84	56.70
	OUTSIDE	T1-360DEG- T2-345DEG	57.50	56.70
117	INSIDE	T1-360DEG- T2-345DEG	49.01	56.70
	OUTSIDE	T1-360DEG- T2-345DEG	56.30	56.70
118	INSIDE	T1-360DEG- T2-345DEG	49.88	56.70
	OUTSIDE	T1-360DEG- T2-345DEG	55.80	56.70
119	INSIDE	T1-360DEG- T2-345DEG	49.93	56.70
	OUTSIDE	T1-360DEG- T2-345DEG	54.58	56.70
120	INSIDE	T1-360DEG- T2-345DEG	50.48	56.70
	OUTSIDE	T1-360DEG- T2-345DEG	53.13	56.70

RUN NO.: Y6ALTER

DATE: 3/11/80

REF. FIGS.: 11.10-5, 11.10-23

[ ] EVALUATION - FATIGUE AT TOP OF COUNTERBORE (INSIDE) a,c,e

FATIGUE ANALYSIS LOCATION SUMMARY

LOCATION	STRESS CONCENTRATIONS KX	KY	KZ	KXR	KYR	KZR	TOTAL USAGE FACTOR
2405	1.00	1.00	1.00	1.00	1.00	1.00	0.0000
2605	1.00	1.00	1.00	1.00	1.00	1.00	.0007
2805	1.00	1.00	1.00	1.00	1.00	1.00	.0146
3005	1.00	1.00	1.00	1.00	1.00	1.00	.0302
3150	1.00	1.00	1.00	1.00	1.00	1.00	.0261
3205	1.00	1.00	1.00	1.00	1.00	1.00	.0274
3350	1.00	1.00	1.00	1.00	1.00	1.00	.0203
3405	1.00	1.00	1.00	1.00	1.00	1.00	.0095
3510	1.00	1.00	1.00	1.00	1.00	1.00	.0030
3605	1.00	1.00	1.00	1.00	1.00	1.00	.0005
3730	1.00	1.00	1.00	1.00	1.00	1.00	.0624
3805	1.00	1.00	1.00	1.00	1.00	1.00	.4591
3930	1.00	1.00	1.00	1.00	1.00	1.00	.4294
4005	1.00	1.00	1.00	1.00	1.00	1.00	.3966
4150	1.00	1.00	1.00	1.00	1.00	1.00	.1780
4205	1.00	1.00	1.00	1.00	1.00	1.00	.0263
4350	1.00	1.00	1.00	1.00	1.00	1.00	.0301
4405	1.00	1.00	1.00	1.00	1.00	1.00	.0344
4530	1.00	1.00	1.00	1.00	1.00	1.00	.0350
4605	1.00	1.00	1.00	1.00	1.00	1.00	.0553

RUN NO.: Y6ALTER
DATE: 3/11/80
REF. FIGS.: 11.10-5, 11.10-23

POOR ORIGINAL

POOR OPIGINAL

.c,e

[ ]• MAX RANGE AND FATIGUE STRAT • SIDE

SUMMARY • MAXIMUM RANGE OF STRESS INTENSITY ANALYSIS

ANALYSIS SECTION	SURFACE	LOAD CONDITION COMBINATION	SI RANGE (KSI)	ALLOWABLE (KSI)
01	INSIDE	T2-345DEG- T4-150DEG	22.64	60.10
	OUTSIDE	T2-345DEG- T3-300DEG	49.35	60.10
02	INSIDE	T2-345DEG- T3-300DEG	17.12	60.10
	OUTSIDE	T2-345DEG- T3-300DEG	47.22	60.10
03	INSIDE	T2-345DEG- T3-300DEG	32.58	60.10
	OUTSIDE	T2-345DEG- T3-300DEG	33.81	60.10
04	INSIDE	T2-345DEG- T3-300DEG	37.35	60.10
	OUTSIDE	T2-345DEG- T3-300DEG	31.07	60.10
05	INSIDE	T2-345DEG- T3-300DEG	38.37	60.10
	OUTSIDE	T2-345DEG- T3-300DEG	30.67	60.10
06	INSIDE	T2-345DEG- T3-300DEG	34.54	58.20
	OUTSIDE	T2-345DEG- T3-300DEG	28.80	58.20
07	INSIDE	T2-345DEG- T3-300DEG	34.00	58.20
	OUTSIDE	T2-345DEG- T3-300DEG	30.87	58.20
08	INSIDE	T2-345DEG- T3-300DEG	32.93	58.20
	OUTSIDE	T2-345DEG- T3-300DEG	32.21	58.20
09	INSIDE	T2-345DEG- T3-300DEG	31.33	58.20
	OUTSIDE	T2-345DEG- T3-300DEG	35.07	58.20
70	INSIDE	T2-345DEG- T3-300DEG	31.02	58.20
	OUTSIDE	T2-345DEG- T3-300DEG	38.23	58.20
71	INSIDE	T2-345DEG- T3-300DEG	40.21	58.20
	OUTSIDE	T2-345DEG- T3-300DEG	31.54	58.20
72	INSIDE	T2-345DEG- T3-300DEG	54.22	58.20
	OUTSIDE	T2-345DEG- T3-300DEG	22.87	58.20
73	INSIDE	T2-345DEG- T3-300DEG	53.91	56.70
	OUTSIDE	T2-345DEG- T3-300DEG	27.06	56.70
74	INSIDE	T2-345DEG- T3-300DEG	50.81	56.70
	OUTSIDE	T2-345DEG- T3-300DEG	34.70	56.70
75	INSIDE	T2-345DEG- T3-300DEG	43.77	56.70
	OUTSIDE	T2-345DEG- T3-300DEG	39.99	56.70
76	INSIDE	T2-345DEG- T3-300DEG	38.57	56.70
	OUTSIDE	T2-345DEG- T3-300DEG	43.64	56.70
77	INSIDE	T2-345DEG- T3-300DEG	38.45	56.70
	OUTSIDE	T2-345DEG- T3-300DEG	42.74	56.70
78	INSIDE	T2-345DEG- T3-300DEG	38.72	56.70
	OUTSIDE	T2-345DEG- T3-300DEG	42.43	56.70
79	INSIDE	T2-345DEG- T3-300DEG	38.63	56.70
	OUTSIDE	T2-345DEG- T3-300DEG	41.47	56.70
80	INSIDE	T2-345DEG- T3-300DEG	38.85	56.70
	OUTSIDE	T2-345DEG- T3-300DEG	40.31	56.70

RUN NO.: Y6ALTDO

DATE: 3/11/80

REF. FIGS.: 11.10-5, 11.10-24

a,c,e

[ ] - MAX RANGE AND FATIGUE STRAT - SIDE

FATIGUE ANALYSIS LOCATION SUMMARY

LOCATION	STRESS CONCENTRATIONS KX	KY	KZ	KXR	KYR	KZR	TOTAL USAGE FACTOR
2405	1.00	1.00	1.00	1.00	1.00	1.00	0.0000
2605	1.00	1.00	1.00	1.00	1.00	1.00	0.0000
2805	1.00	1.00	1.00	1.00	1.00	1.00	.0004
3005	1.00	1.00	1.00	1.00	1.00	1.00	.0004
3100	1.00	1.00	1.00	1.00	1.00	1.00	.0006
3255	1.00	1.00	1.00	1.00	1.00	1.00	.0012
3300	1.00	1.00	1.00	1.00	1.00	1.00	.0004
3405	1.00	1.00	1.00	1.00	1.00	1.00	.0004
3500	1.00	1.00	1.00	1.00	1.00	1.00	.0004
3605	1.00	1.00	1.00	1.00	1.00	1.00	.0004
3700	1.00	1.00	1.00	1.00	1.00	1.00	.0027
3805	1.00	1.00	1.00	1.00	1.00	1.00	.1268
3900	1.00	1.00	1.00	1.00	1.00	1.00	.1351
4005	1.00	1.00	1.00	1.00	1.00	1.00	.0879
4100	1.00	1.00	1.00	1.00	1.00	1.00	.0122
4205	1.00	1.00	1.00	1.00	1.00	1.00	.0005
4300	1.00	1.00	1.00	1.00	1.00	1.00	.0013
4405	1.00	1.00	1.00	1.00	1.00	1.00	.0019
4500	1.00	1.00	1.00	1.00	1.00	1.00	.0017
4605	1.00	1.00	1.00	1.00	1.00	1.00	.0020

RUN NO.: Y6ALTDO

DATE: 3/11/80

REF. FIGS.: 11.10-5, 11.10-24

POOR ORIGINAL

a,c,e

[ ] = MAX RANGE AND FATIGUE STRAT-STRIFING - ROOT NOZZLE CBORE

SUMMARY - MAXIMUM RANGE OF STRESS INTENSITY ANALYSIS

ANALYSIS SECTION	SURFACE	LOAD CONDITION COMBINATION	SI RANGE (KSI)	ALLOWABLE (KSI)
25	INSIDE	12-345DEG- 13-360DEG	35.77	58.2
	OUTSIDE	13-360DEG- ACCIDENT	18.16	58.20

a,c,e

[ ] = MAX RANGE AND FATIGUE STRAT-STRIFING - ROOT NOZZLE CBORE

FATIGUE ANALYSIS LOCATION SUMMARY

LOCATION	STRESS CONCENTRATORS						TOTAL USAGE FACTOR
	KX	KY	KZ	KXR	KYR	KZR	
2825	1.00	1.00	1.00	1.00	1.00	1.00	.0012

RUN NO.: Y6ALTKW

DATE: 3/7/80

REF. FIGS.: 11.10-4, 11.10-22

POOR ORIGINAL

a,c,e

[ ] - MAX RANGE AND FATIGUE STRAT-STRIPING - ROOT NOZZLE CHORE

SUMMARY - MAXIMUM RANGE OF STRESS INTENSITY ANALYSIS

ANALYSIS SECTION	SURFACE	LOAD CONDITION COMBINATION	SI RANGE (KSI)	ALLOWABLE (KSI)
26	INSIDE	T1-360DEG- 15-375DEG	26.50	58.20
	OUTSIDE	T1-360DEG- 15-375DEG	15.20	58.20

a,c,e

[ ] - MAX RANGE AND FATIGUE STRAT-STRIPING - ROOT NOZZLE CHORE

FATIGUE ANALYSIS LOCATION SUMMARY

LOCATION	STRESS CONCENTRATORS KX	KY	KZ	KXR	KYR	KZR	TOTAL USAGE FACTOR
3835	1.00	1.00	1.00	1.00	1.00	1.00	.0009

RUN NO.: Y6ALTAK

DATE: 3/7/80

REF. FIGS.: 11.10-4, 11.10-22

POOR ORIGINAL

a.c.e

[ ]- MAX RANGE AND FATIGUE STRAI-STRIPING - RUN1 NOZZLE CRACK

SUMMARY - MAXIMUM RANGE OF STRESS INTENSITY ANALYSIS

ANALYSIS SELTION	SURFACE	LOAD CONDITION COMBINATION	SI RANGE (KSI)	ALLOWABLE (KSI)
21	INSIDE	T<-545DEG- 13-300DEG	54.87	58.20
	OUTSIDE	T<-545DEG- 13-300DEG	22.24	58.20

a.c.e

[ ]- MAX RANGE AND FATIGUE STRAI-STRIPING - RUN1 NOZZLE CRACK

FATIGUE ANALYSIS LOCATION SUMMARY

LOCATION	KX	KT	STRESS CONCENTRATIONS KZ	KAR	KYM	KZR	TOTAL USAGE FACTOR
5R00	1.00	1.00	1.00	1.00	1.00	1.00	.1420

RUN NO.. Y6ALT03

DATE: 3/7/80

REF. FIGS.: 11.10-4, 11.10-22

POOR ORIGINAL

a,c,e

[ ] - MAX RANGE AND FATIGUE STRAT-STRIPING - ROOT NOZZLE CBORE

SUMMARY - MAXIMUM RANGE OF STRESS INTENSITY ANALYSIS

ANALYSIS SECTION	SURFACE	LOAD CONDITION COMBINATION	ST RANGE (KSI)	ALLOWABLE (KSI)
37	INSIDE	T2-345+S - AMBIENT	18.20	58.20
	OUTSIDE	PRESSURE - AMBIENT	9.05	58.20

a,c,e

[ ] - MAX RANGE AND FATIGUE STRAT-STRIPING - ROOT NOZZLE CBORE

FATIGUE ANALYSIS LOCATION SUMMARY

LOCATION	STRESS CONCENTRATORS						TOTAL USAGE FACTOR
	KX	KY	KZ	KXR	KYR	KZR	
3895	1.00	1.00	1.00	1.00	1.00	1.00	0.0000

RUN NO.: Y6ALT8L

DATE: 3/7/80

REF. FIGS.: 11.10-4, 11.10-22

POOR ORIGINAL

a,c,e

[ ]- MAX RANGE AND FATIGUE STRAT-STRIPING - ROOT PIPE CHORE

SUMMARY - MAXIMUM RANGE OF STRESS INTENSITY ANALYSIS

ANALYSIS SECTION	SURFACE	LOAD CONDITION COMBINATION	SI RANGE (KSI)	ALLOWABLE (KSI)
5	INSIDE	T2-345DEG- T3-300DEG	32.85	56.70
	OUTSIDE	T2-345DEG- T3-300DEG	23.33	56.70

a,c,e

[ ]- MAX RANGE AND FATIGUE STRAT-STRIPING - ROOT PIPE CHORE

FATIGUE ANALYSIS LOCATION SUMMARY

LOCATION	STRESS CONCENTRATORS						TOTAL USAGE FACTOR
	KX	KY	KZ	KXR	KYR	KZR	
4025	1.00	1.00	1.00	1.00	1.00	1.00	.0012

RUN NO.: Y6ALTKX

DATE: 3/7/80

REF. FIGS.: 11.10-3

POOR ORIGINAL

[ ]- MAX RANGE AND FATIGUE STRAIN-STRIPING - RUN1 PIPE CHORE

a,c,e

SUMMARY - MAXIMUM RANGE OF STRESS INTENSITY ANALYSIS

ANALYSIS SECTION	SURFACE	LOAD CONDITION COMBINATION	SI RANGE (KSI)	ALLOWABLE (KSI)
11	INSIDE	T2-545DEG- 13-300DEG	51.70	56.70
	OUTSIDE	T2-545DEG- 13-300DEG	54.20	56.70

POOR ORIGINAL

[ ]- MAX RANGE AND FATIGUE STRAIN-STRIPING - RUN1 PIPE CHORE

a,c,e

FATIGUE ANALYSIS LOCATION SUMMARY

LOCATION	STRESS CONCENTRATIONS KX	KY	KZ	KXY	KYZ	KZX	INIAL USAGE FACTOR
4000	1.00	1.00	1.00	1.00	1.00	1.00	.1017

RUN NO.: Y6ALT04

DATE: 3/7/80

REF. FIGS.: 11.10-3

POOR ORIGINAL

[ ] - MAX RANGE AND FATIGUE STRAI-STRIPING - ROOT PIPE CHORE | a,c,e

SUMMARY - MAXIMUM RANGE OF STRESS INTENSITY ANALYSIS

ANALYSIS SECTION	SURFACE	LOAD CONDITION COMBINATION	SI RANGE (KSI)	ALLOWABLE (KSI)
6	INSIDE	T1-360DEG- 15-375DEG	24.11	56.70
	OUTSIDE	T1-360DEG- AMBIENT	19.90	56.70

[ ] - MAX RANGE AND FATIGUE STRAI-STRIPING - ROOT PIPE CHORE | a,c,e

FATIGUE ANALYSIS LOCATION SUMMARY

LOCATION	STRESS CONCENTRATIONS KX	KY	KZ	KXR	KYR	KZR	TOTAL USAGE FACTOR
4035	1.00	1.00	1.00	1.00	1.00	1.00	.0004

RUN NO.: Y6ALTAO

DATE: 3/7/80

REF. FIGS.: 11.10-3

a.c.e

[ ] - MAX RANGE AND FATIGUE STRAI-STRIPING - RUDI PIPE CHOKE

SUMMARY - MAXIMUM RANGE OF STRESS INTENSITY ANALYSIS

ANALYSIS SELTION	SURFACE	LOAD CONDITION COMBINATION	SI RANGE (KSI)	ALLOWABLE (KSI)
17	INSIDE	Tc-545+5 - AMBIENT	16.90	56.70
	OUTSIDE	Tc-545-5 - AMBIENT	11.50	56.70

a.c.e

[ ] - MAX RANGE AND FATIGUE STRAI-STRIPING - RUDI PIPE CHOKE

FATIGUE ANALYSIS LOCATION SUMMARY

LOCATION	STRESS CONCENTRATIONS						INITIAL USAGE FACTOR
	KX	KY	KZ	KXR	KYR	KZR	
4045	1.00	1.00	1.00	1.00	1.00	1.00	0.0000

RUN NO.: Y6ALT8G

DATE: 3/7/80

REF. FIGS.: 11.10-3

POOR ORIGINAL

APPENDIX 11C

C [

TEMPERATURE STRIPING ANALYSIS

]

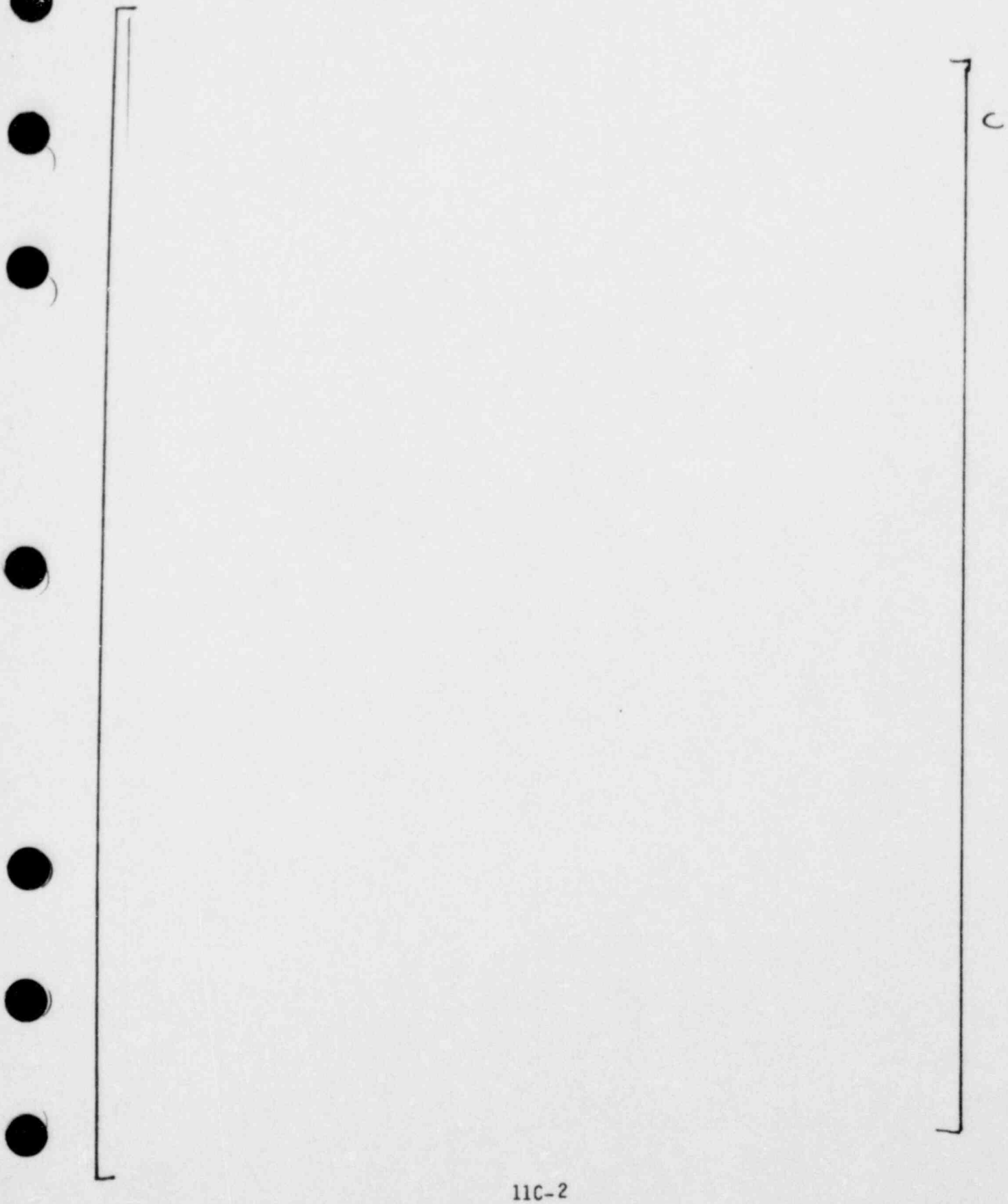

C

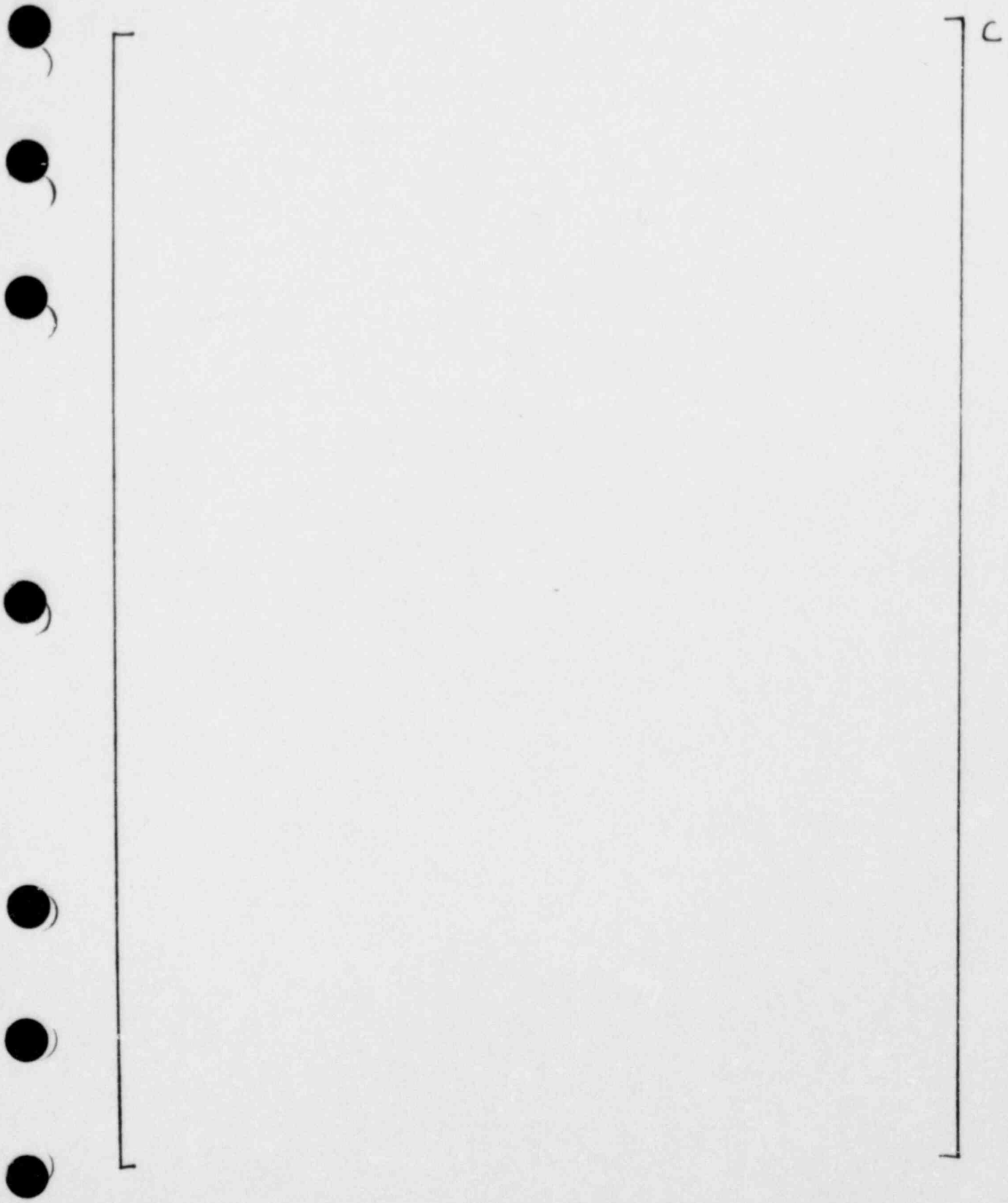
C

C

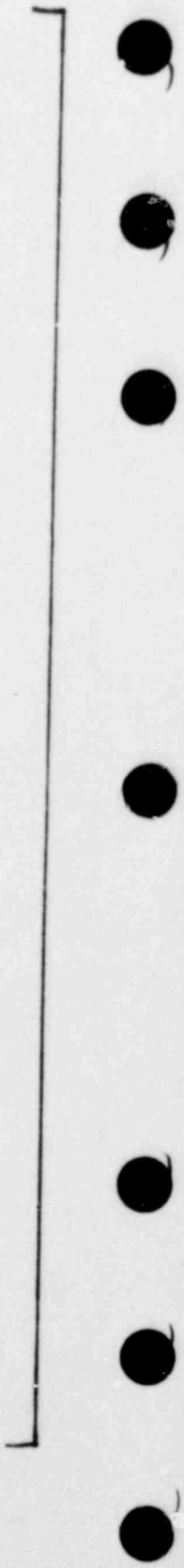

05643

[

]

C

TABLE 11C.1

C

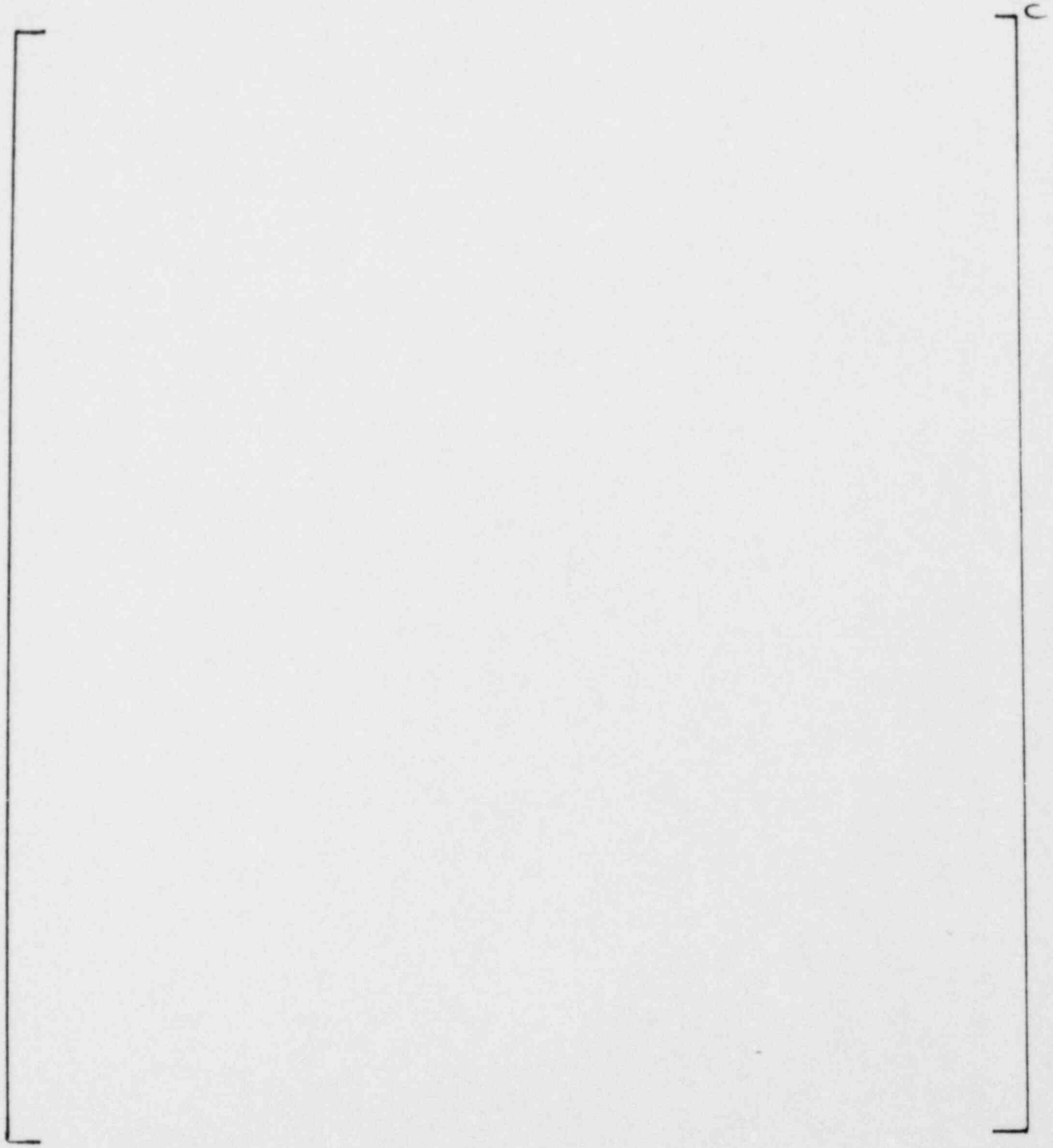

FIGURE 11C-1: THROUGH THE WALL TEMPERATURE DISTRIBUTION AT SEVERAL TIMES, PLUS ENVELOPE, H = 100
PERIOD = .1, THICKNESS = .25

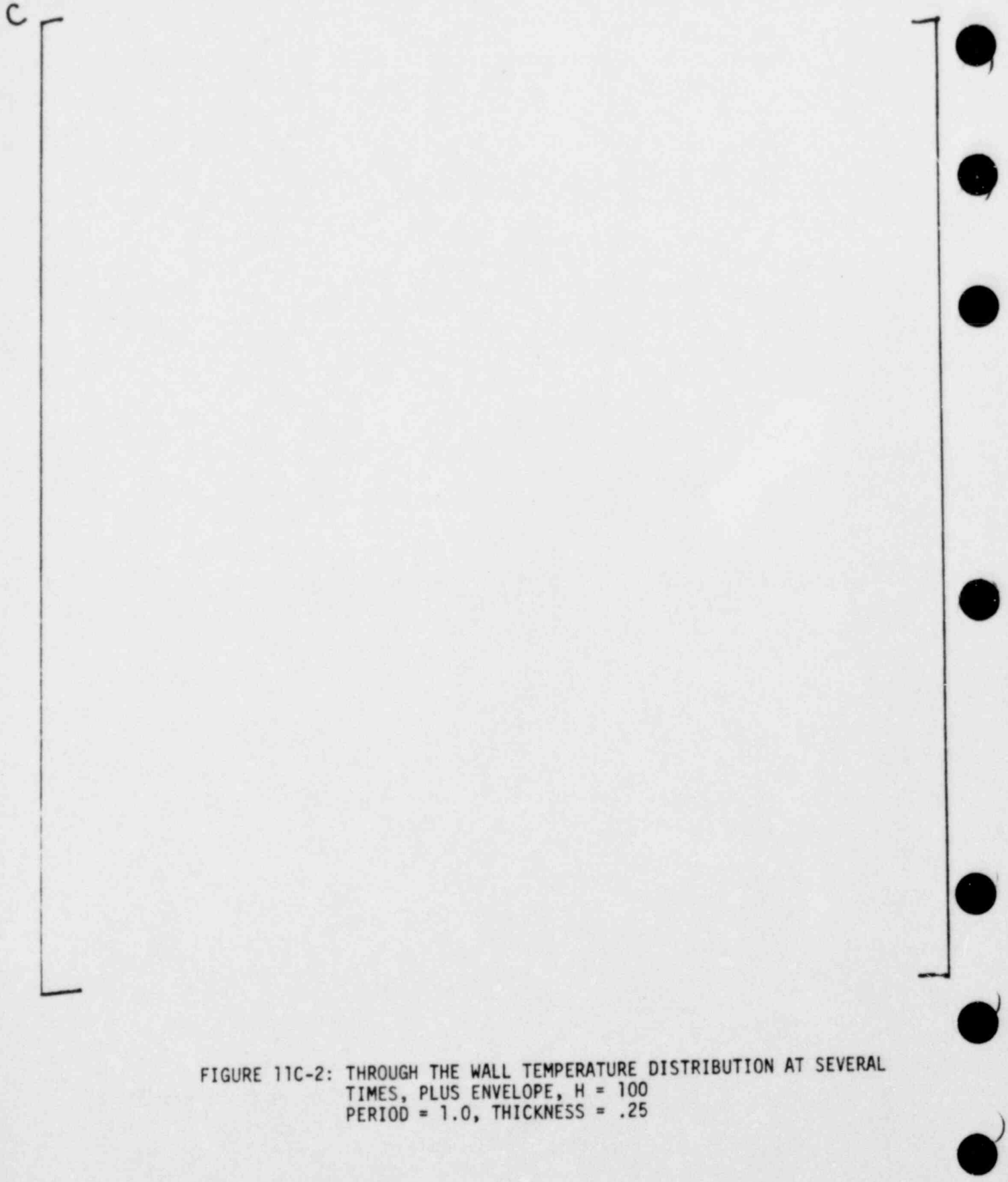

FIGURE 11C-2: THROUGH THE WALL TEMPERATURE DISTRIBUTION AT SEVERAL TIMES, PLUS ENVELOPE, H = 100
PERIOD = 1.0, THICKNESS = .25

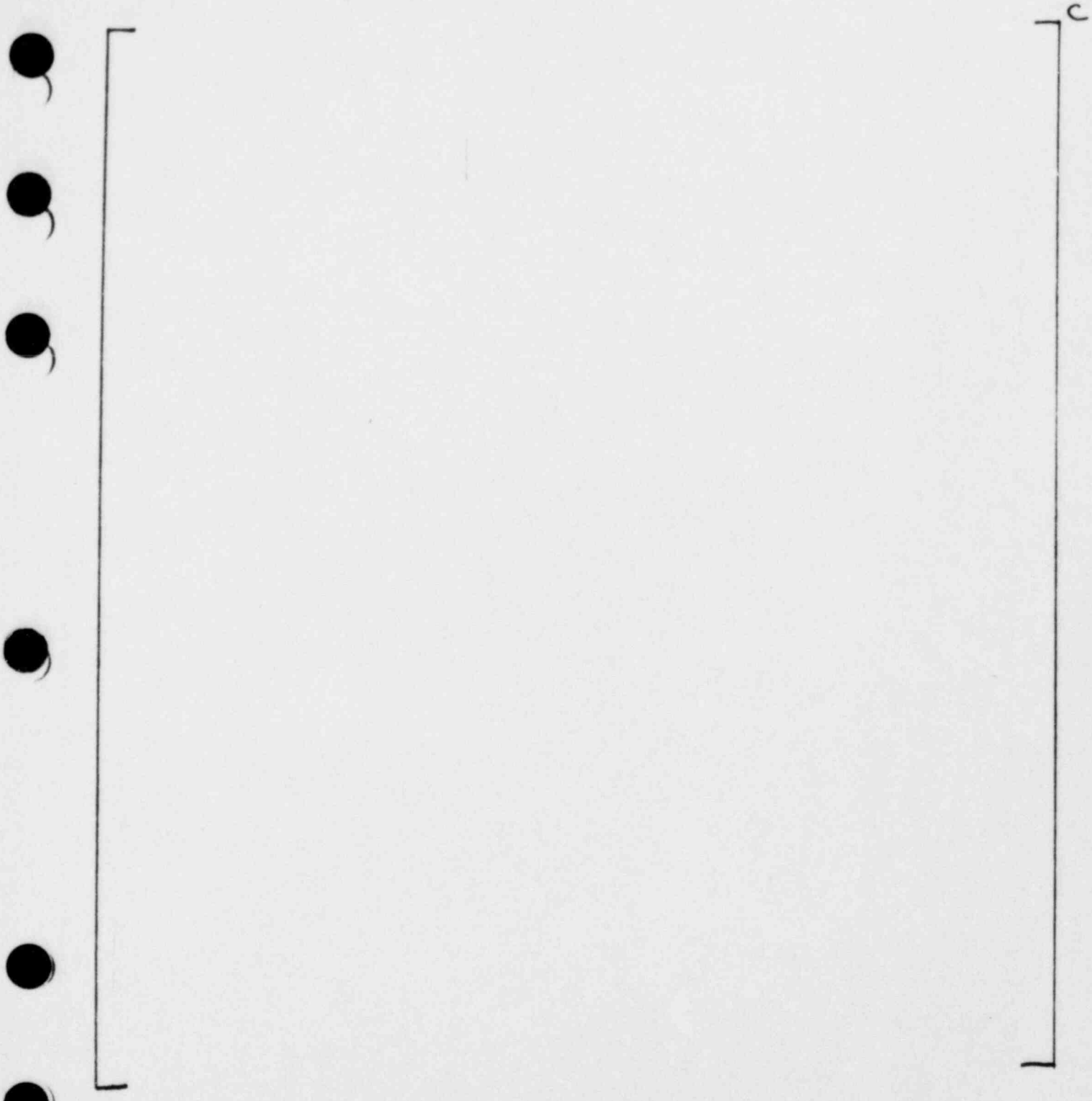

FIGURE 11C-3: THROUGH THE WALL TEMPERATURE DISTRIBUTION AT SEVERAL TIMES, PLUS ENVELOPE, H = 100
PERIOD = 10, THICKNESS = .25

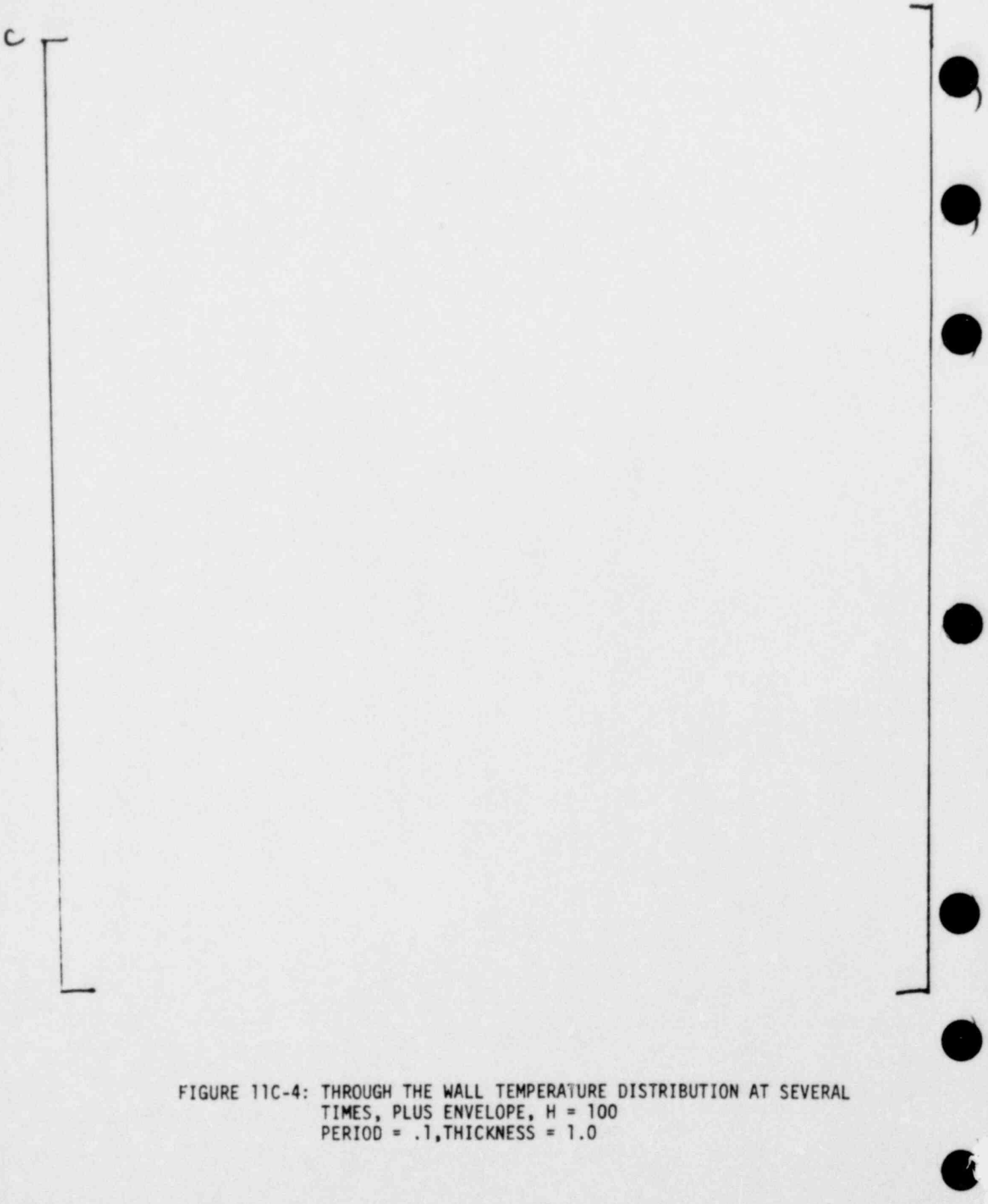

FIGURE 11C-4: THROUGH THE WALL TEMPERATURE DISTRIBUTION AT SEVERAL TIMES, PLUS ENVELOPE, H = 100
PERIOD = .1,THICKNESS = 1.0

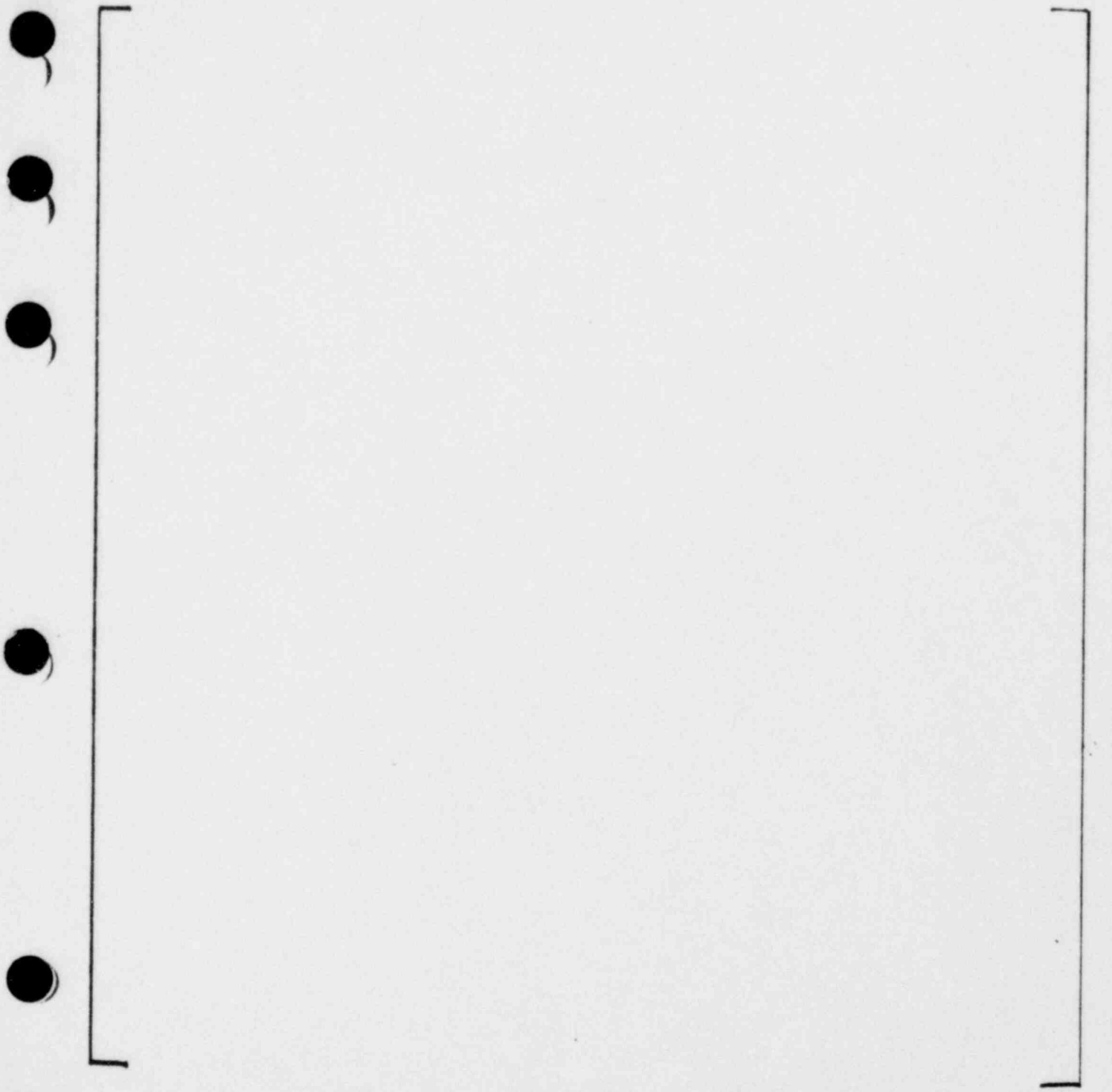

FIGURE 11C-5: THROUGH THE WALL TEMPERATURE DISTRIBUTION AT SEVERAL TIMES, PLUS ENVELOPE, H = 100
PERIOD = 1.0,THICKNESS = 1.0

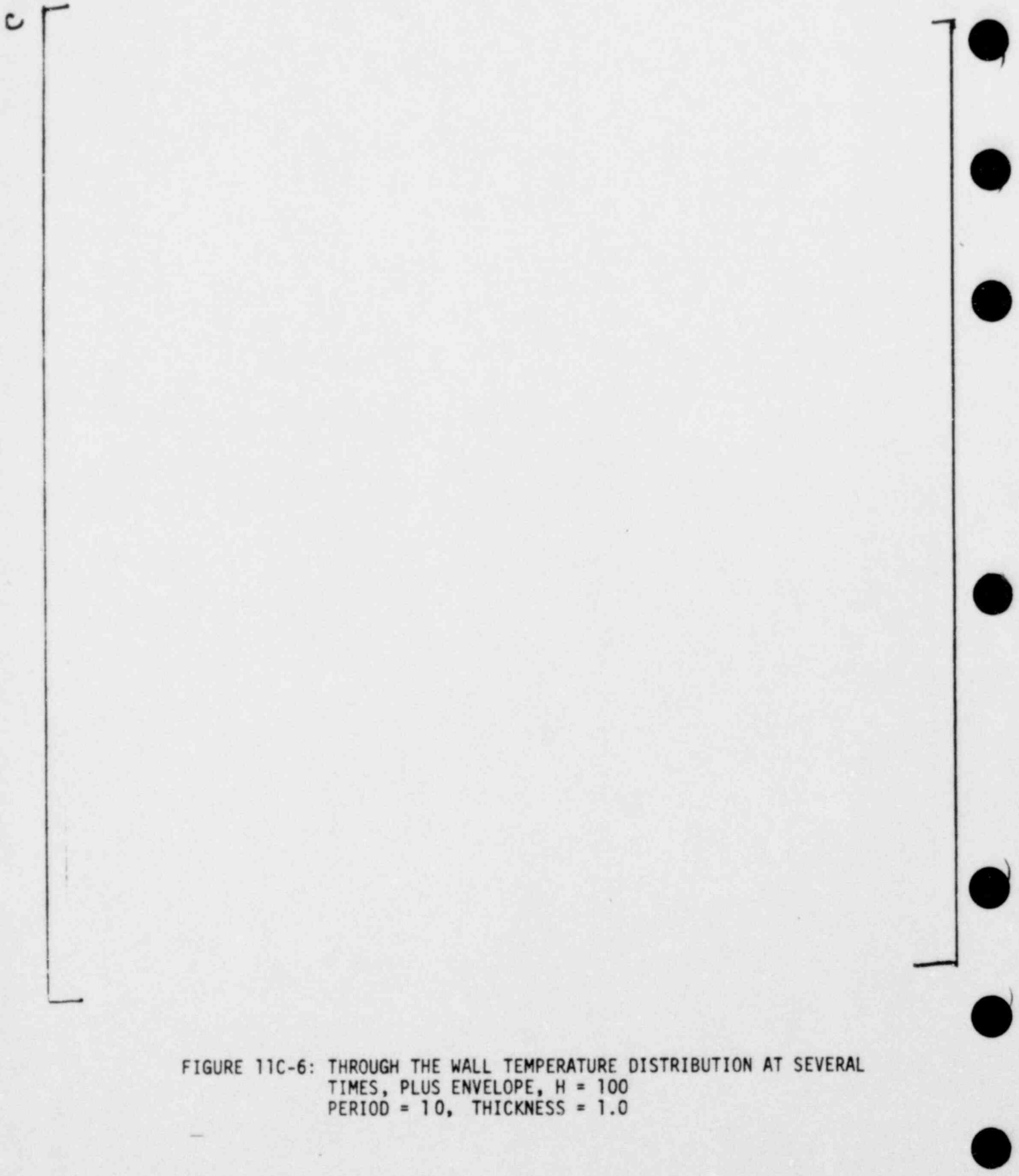

FIGURE 11C-6: THROUGH THE WALL TEMPERATURE DISTRIBUTION AT SEVERAL TIMES, PLUS ENVELOPE, H = 100
PERIOD = 10, THICKNESS = 1.0

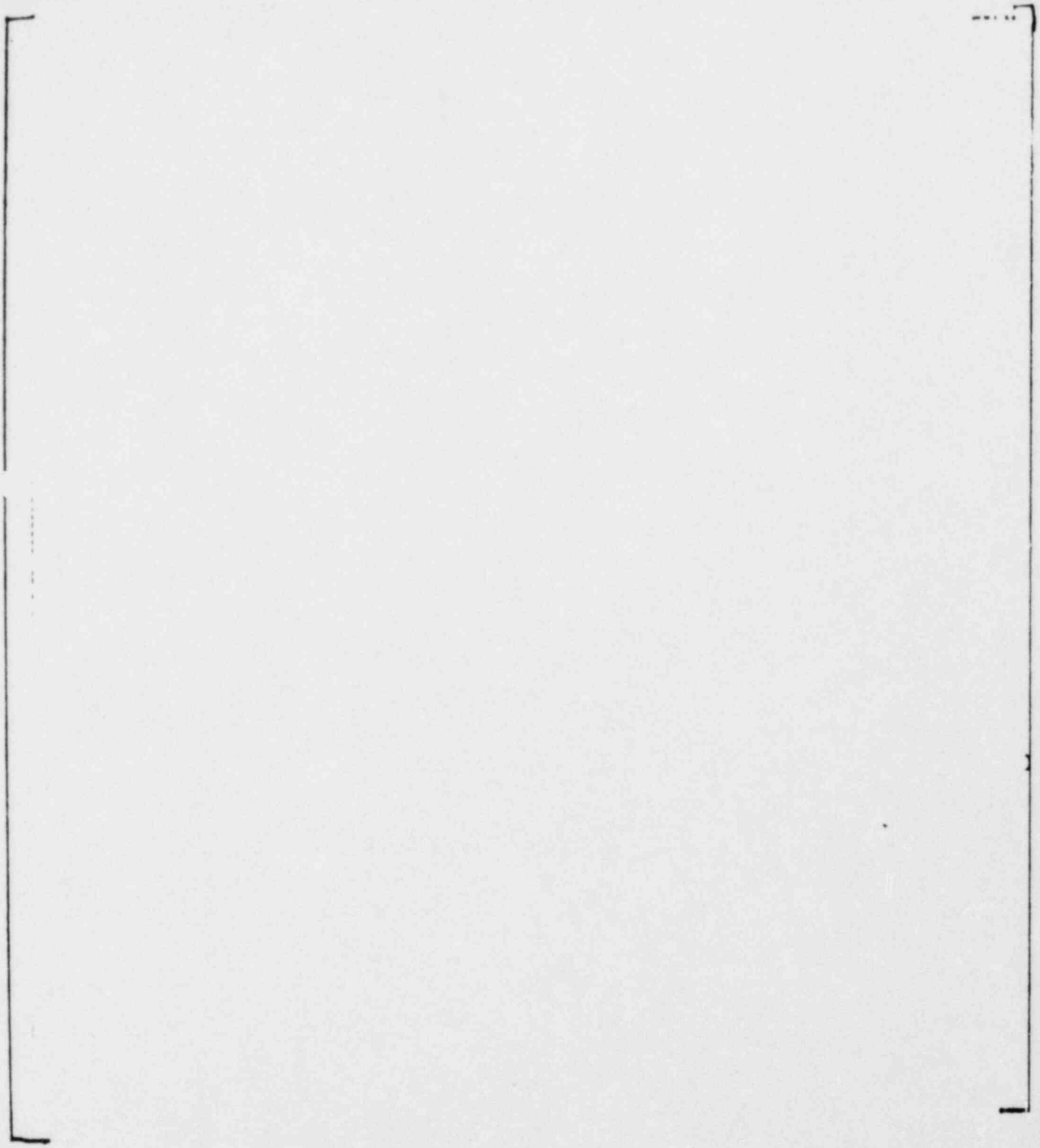

FIGURE 11C-7: MAXIMUM INSIDE SURFACE TEMPERATURES, H = 100-9999

FIGURE 11C-8: MAXIMUM VALUE OF $|T_{MAX} - T_{AVG}|$, H = 100-9999

THICKNESS = .25

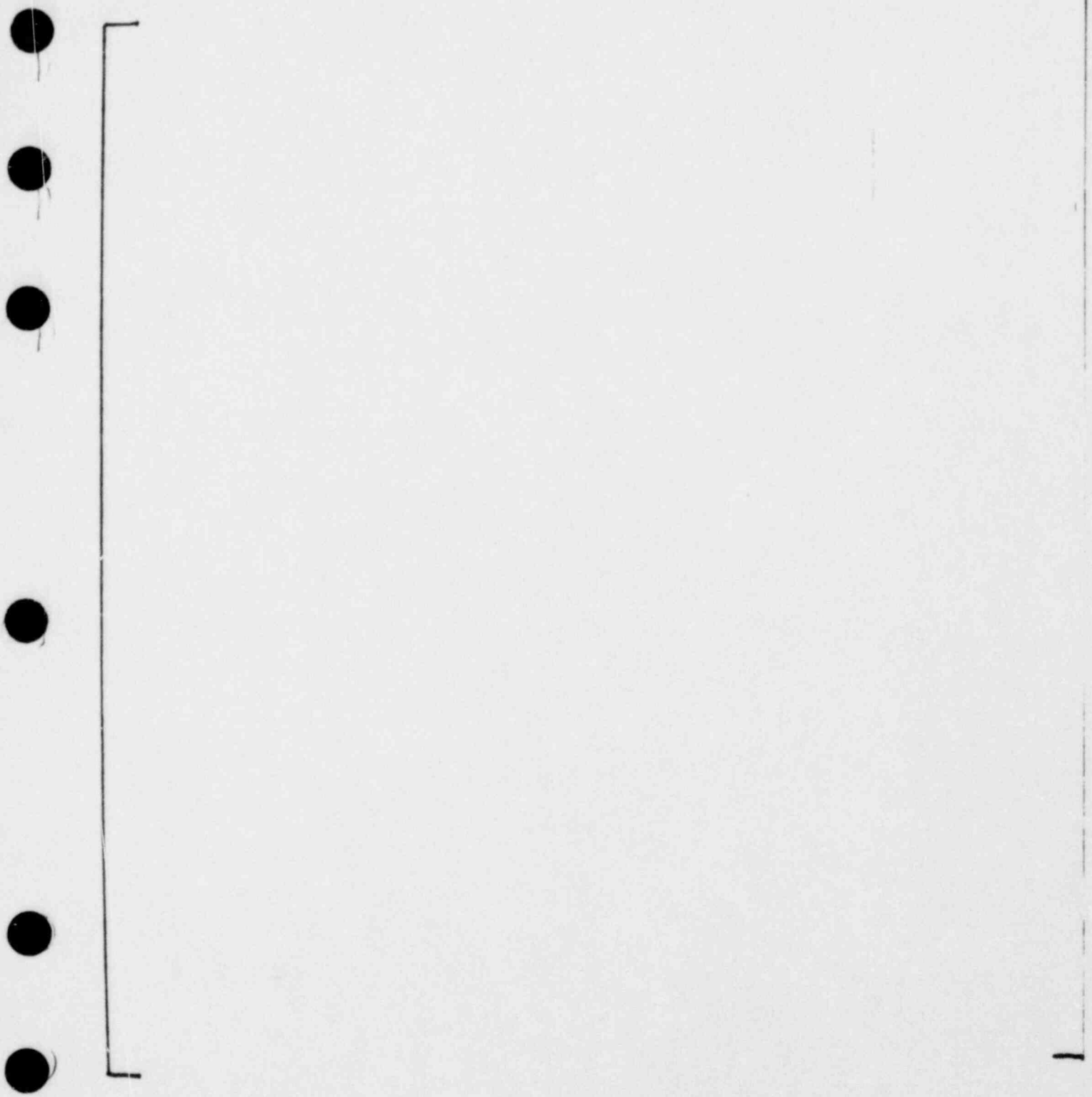

FIGURE 11C-9: MAXIMUM VALUE OF $|T_{MAX} - T_{AVG}|$, H = 100-9999

THICKNESS = .50

FIGURE 11C-10: MAXIMUM VALUE OF $|T_{MAX} - T_{AVG}|$, H = 100-9999

THICKNESS = .75

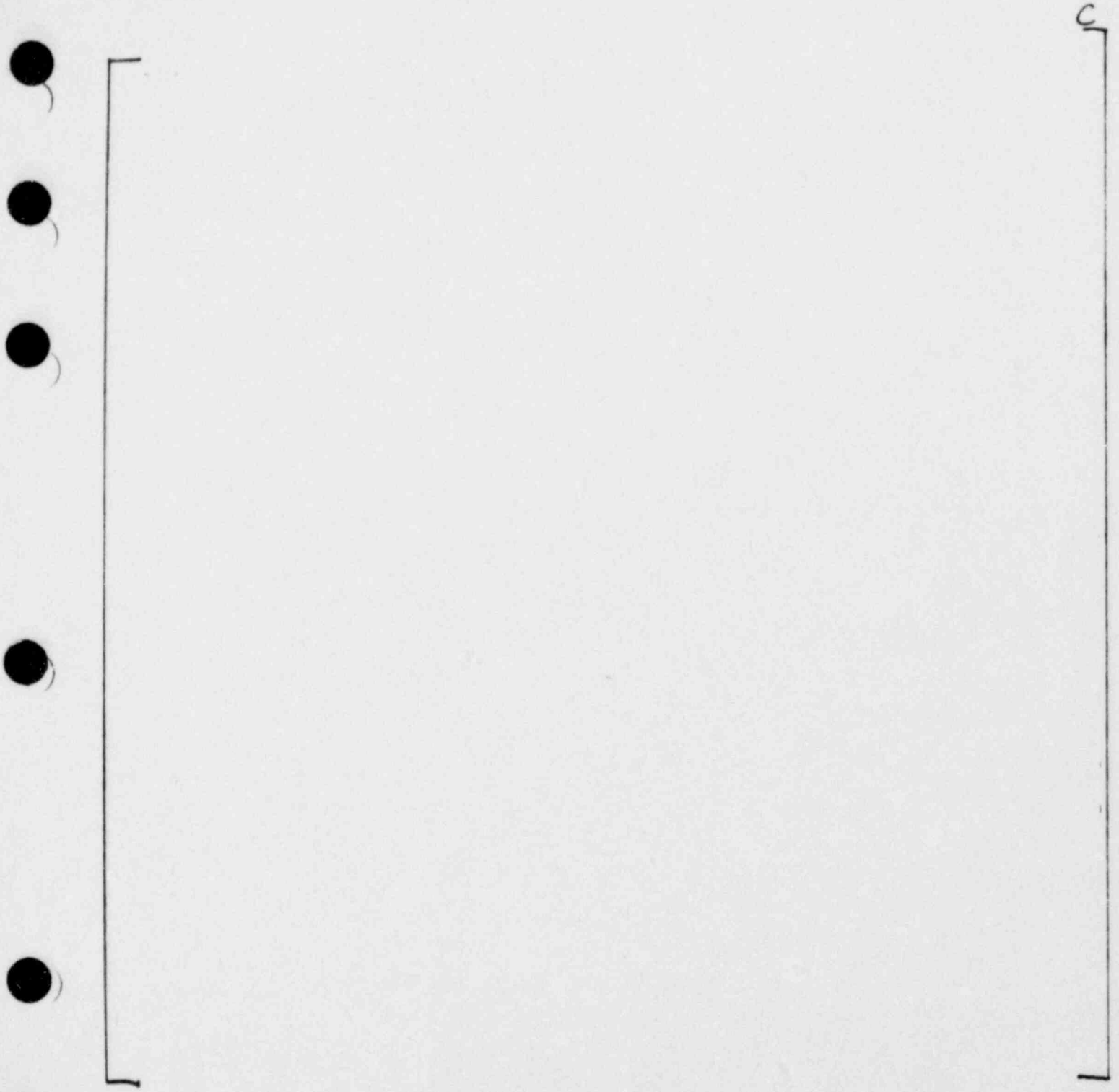

FIGURE 11C-11: MAXIMUM VALUE OF $|T_{MAX} - T_{AVG}|$, H = 100-9999

THICKNESS = 1.0

FIGURE 11C-12: MAXIMUM STRESS, H = 100-9999
THICKNESS = .25

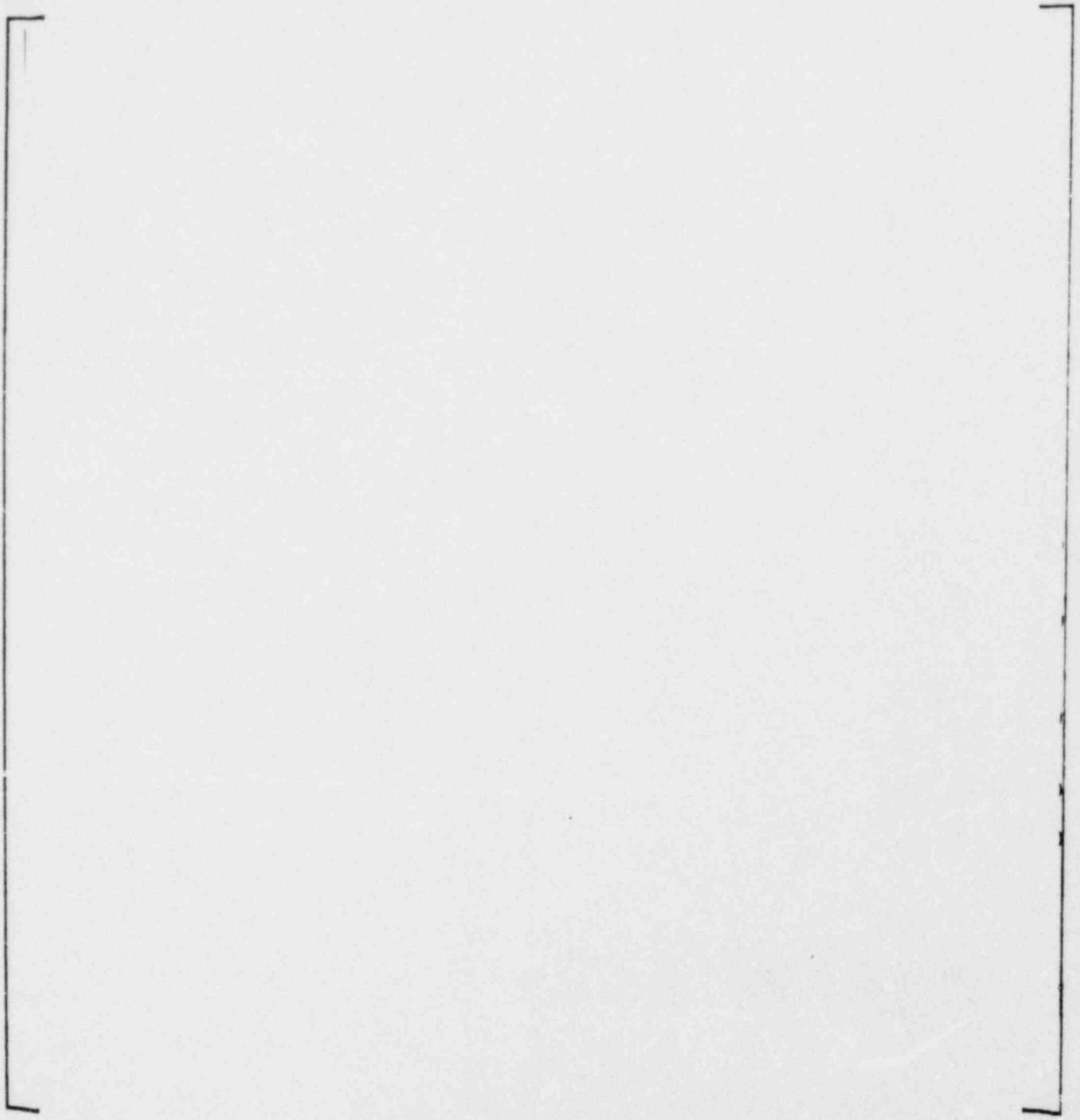

FIGURE 11C-13: MAXIMUM STRESS, H = 100-9999
THICKNESS = .5

FIGURE 11C-14: MAXIMUM STRESS, H = 100-9999
THICKNESS = .75

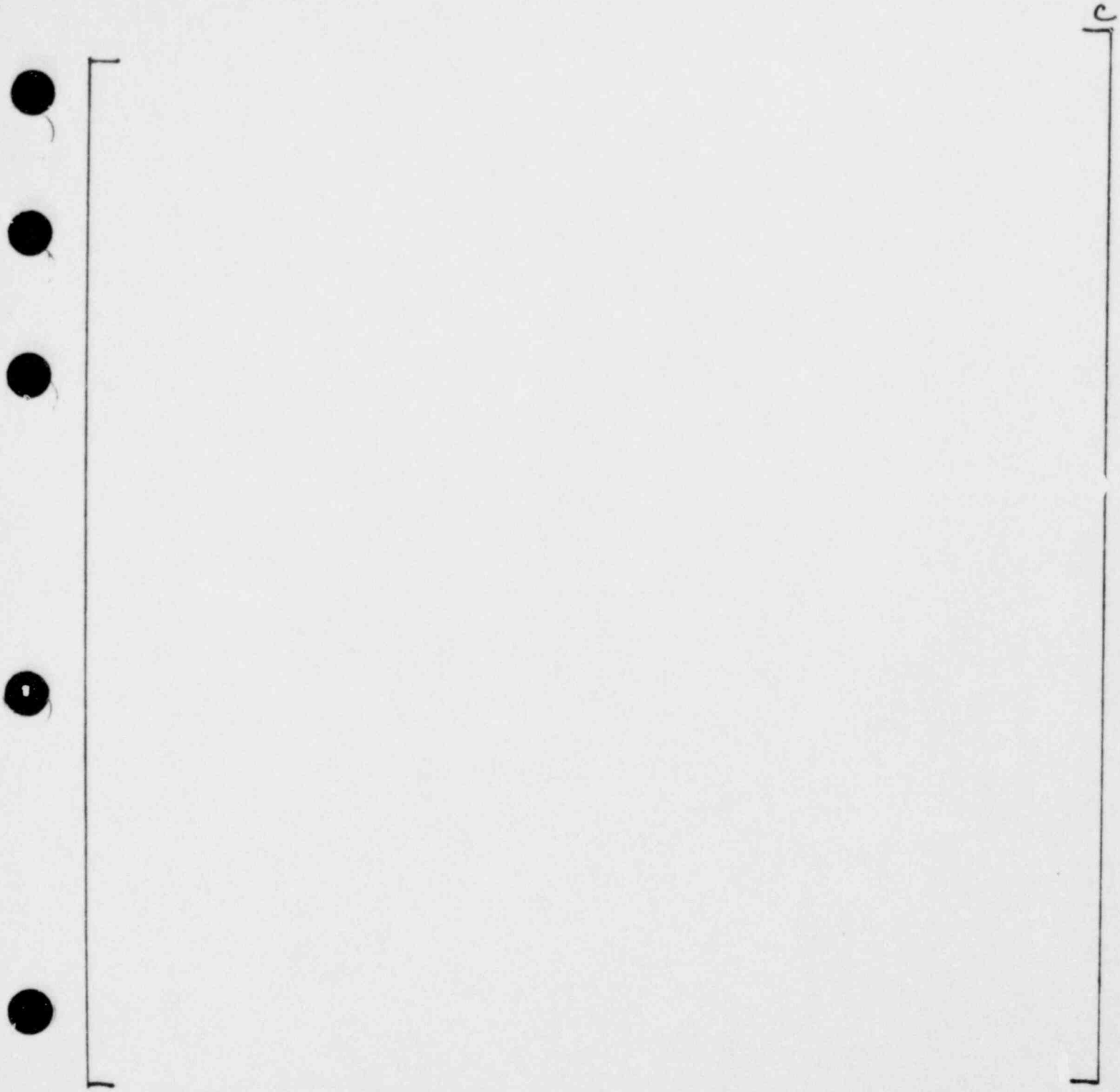

FIGURE 11C-15: MAXIMUM STRESS, H = 100-9999
THICKNESS = 1.0

SECTION 12.0

FATIGUE CRACK GROWTH CONSIDERATIONS

BY

W. H. BAMFORD

ACKNOWLEDGEMENT

This work would not have been possible without the dedicated work of my associates S. Swamy and J. Petsche and excellent cooperation from the other authors.

12.0 FATIGUE CRACK GROWTH CONSIDERATIONS

12.1 INTRODUCTION

The metallurgical analysis detailed in Section 5 indicated that the cracks were the result of fatigue loadings rather than some form of material deterioration. This was also the most likely case from the point of view of service experience with this material and environment. This section will present a discussion of the important material and environmental variables known to influence corrosion fatigue and crack growth, and provide estimates of the loads and cycles necessary to cause the observed cracking incidences. A discussion will be included to consider the effect of water chemistry on the observed cracking, and to relate these observations with the results of the chemistry survey detailed in Section 6.

The emphasis of this section will be the results of fatigue crack growth analyses carried out on five of the operating plants for which field measurements were made of feedwater temperatures, as detailed in Section 8. The results of the crack growth analyses are compared with the measurements made of the actual crack morphologies, to evaluate the predictive capability of the models developed in this project.

12.2 METHODOLOGY FOR FATIGUE CRACK GROWTH ANALYSIS

The fatigue crack growth analyses presented herein were conducted in the same manner as suggested by Section XI, Appendix A of the ASME Boiler and Pressure Vessel Code. The analysis procedure involves assuming an initial flaw exists at some point and predicting the growth of that flaw due to an imposed series of stress transients. The growth of a crack per loading cycle is dependent on the range of applied stress intensity factor ΔK, by the following relation:

$$\frac{da}{dN} = Co\ \Delta K^{n} \qquad (12\text{-}1)$$

where "Co" and the exponent "n" are material properties. For inert environments these material properties are constants, but for water environments they are dependent on the level of mean stress present during the cycle. This can be accounted for by adjusting the values of "Co" and "n" by a function of the ratio of minimum to maximum stress for any given transient as will be discussed later.

The input required for a fatigue crack growth analysis is basically the information necessary to calculate the parameter ΔK, which depends on crack and structure geometry and the range of applied stresses in the area where the crack exists. Once ΔK is calculated, the growth due to that particular cycle can be calculated by equation (12-1). This increment of growth is then added to the original crack size, and the analysis proceeds to the next transient. The procedure is continued in this manner until all the transients known to occur in the period of evaluation have been analyzed.

The flaws analyzed in the feedwater pipes were circumferential in orientation, and were assumed to be precisely radial in their orientation, even though the actual cracks often showed some angular inclination, as can be seen in some of the figures in Section 5. The stresses used as input to the calculation of ΔK were different, depending on the individual analyses carried out, and so these will be detailed separately in the parts which follow.

The crack tip stress intensity factors (K_I) were calculated using an expression for a continuous flaw oriented circumferentially at the inside surface of the pipe. The stresses were linearized through the pipe wall thickness, and then the expression below was used to calculate K_I(1). The range of applied K_I was determined from considering the minimum and maximum values of K_I resulting from the changing stresses during a given transient.

$$K_I = \sqrt{\pi a}\ A_0 F_1 + \frac{2a}{\pi} A_1 F_2 \qquad (12\text{-}2)$$

where

a = crack depth

A_0 = axial stress at inside surface

$A_1 = \frac{\sigma_o - A_o}{t}$

t = wall thickness

$F_1 = 1.126 + 0.234\ a/t + 2.20\ (a/t)^2 - 0.208\ (a/t)^3$

$F_2 = 1.073 + 0.267\ a/t + 0.666\ (a/t)^2 + 0.635\ (a/t)^3$

σ_o = axial stress at outside surface

The stress profile was represented by the linearization,

$$\sigma = A_o + A_1\ x \qquad (12\text{-}3)$$

where x = distance from the inside surface of the pipe.

The number of occurrences of each transient considered were equally spaced over the time period of interest. The cycles used in each of the calculations to follow will be detailed at the appropriate time. The size of the initial crack used in the analyses will also be discussed individually.

Calculation of the fatigue crack growth for each cycle was then carried out using a reference fatigue crack growth rate law determined from consideration of the available data for carbon and low alloy steels exposed to a water environment. The reference law is provided in Figure 12-1, and is actually an improvement over the present ASME Section XI reference crack growth law for water environments. The revised curves have been proposed as a replacement for the present ASME Section XI reference curves. The background and basis for the revised reference curves are provided in reference[2]. The revised reference law allows for the effect of mean stress or R ratio (Kminimum/Kmaximum) on the growth rates, and results in slightly higher growth than the present Section XI reference law in cases of predominantly high mean stress cycles.

The fatigue crack growth rate data on which these reference crack growth

a,c [ ]

12.3 CRACK GROWTH CALCULATIONS FOR DESIGN CONDITIONS, NEGLECTING THERMAL STRATIFICATION CYCLES

The growth of a crack is the result of fluctuations in the crack tip stress field due to coolant pressure and temperature variations during transients. The analysis is executed by finding the crack growth during each individual transient, and adding this growth to the initial crack size before proceeding to the next transient. The transients used as a design basis for the feedwater lines are listed in Table 12-1, along with the number of expected occurrances in the 40 year design lifetime of a typical plant. The transient occurrences were divided up equally for the entire lifetime, and the crack growth was calculated for periods of ten, twenty, thirty, and forty years.

For each transient, the pressure and temperature fluctuations were used to calculate stresses in the following manner. The heat transfer analysis was carried out by an explicit finite difference technique(3). The resulting temperature distribution was then used to calculate thermal stresses, using the equations for thermal stresses in a hollow cylinder from Timoshenko and Goodier(4). The axial stresses were calculated as:

$$\sigma_z = \frac{\alpha E}{1-\nu} \frac{2}{b^2 - a^2} \int_a^b Trdr - T \qquad (12\text{-}4)$$

where

T = temperature
a = inner radius of pipe
b = outer radius of pipe
ν = Poisson's ratio
αE = the product of the coefficient of thermal expansion and the modulus of elasticity, assumed constant, requiring a conservative value to cover the entire temperature range

The mechanical loadings for the pipe which contribute to crack growth result from changes in internal pressure, and the stress for a given value of internal pressure, P, was calculated from:

$$\sigma_z = P \frac{a^2}{(b^2 - a^2)} \qquad (12\text{-}5)$$

The stresses calculated in equations 12-1 and 12-2 are axial stresses, which would tend to propagate a circumferential flaw. The material properties used in the stress analysis are given in Table 12-2, and the input stresses for the analysis are provided in Table 12-3. Note that this analysis procedure differs from that used for the consideration of thermal stratification cycles, where a three dimensional finite element analysis procedure was required because of the unsymmetric nature of the loading.

The remainder of the analysis procedure was just as described in Section 12.2, and the results of the crack growth analysis are presented in Table 12-4. The crack growth which results from these design cycles is very small, even for a rather large assumed initial flaw of .100 inches, and for forty full years of operation. Thus, the extensive crack growth experienced in a few plants could not be explained on the basis of these cycles.

This leads to the conclusion that the cracks were most likely the result of circumstances that were unique to the environmental and operational characteristics of each individual plant.

12.4 CONSIDERATION OF POSSIBLE CAUSES

In studying the observed behavior of the cracks found in feedwater lines it quickly becomes apparent that there must be large differences between the conditions existing at different plants. These differences might take many forms, but the factors most likely to have an impact on the fatigue crack growth behavior fall into two categories:

1. Factors which would increase either the imposed stresses or the number of loading cycles on the feedwater lines.

2. Factors which could cause an increase in the fatigue crack growth rates to be expected for the feedwater line materials.

These factors are discussed in some detail in the parts which follow. As will become apparent later, the investigations of individual plants revealed that both of these factors could have been important in the cracking behavior.

The fatigue crack growth analysis was extended to determine the combinations of loads and cycles necessary to produce large cracks. This will provide insight in defining the environmental/operational characteristics contributing to the problem. To accomplish this, a uniform circumferential flaw was postulated at the inside of the pipe, and fluctuating stresses were applied. Both the magnitude of the stresses and the R ratio were varied, but not independently. The highest magnitudes of stress fluctuations were applied with low R ratio and the lowest fluctuations were combined with the highest R ratio. This combination is consistent with real occurrences, since high fluctuations in load never occur in conjunction with high mean stress (or R ratio).

The results of these estimations of crack growth are shown in Figure 12-2. For each of the curves shown, a continuous circumferential crack was assumed to exist at the inside surface of the pipe, and a single alternating stress was applied to it, with crack growth being calculated using the methodology detailed earlier. The single alternating stress as well as the R ratio assumed in the calculation are shown next to each curve. The results of these calculations are only qualitative, because in the real case many different combinations of cycles will exist, but they reveal a number of interesting effects.

[ ] a,c

It is evident from the above discussion that a satisfactory explanation of the cause of the cracking incidents could involve differences in plant operational cycles, both in the number of loading cycles and the magnitude of those cycles. Another equally important possibility to consider is that the cracking could have resulted from a combination of material and environmental effects. Factors which affect both initiation and growth must be considered. Although these factors are not

completely characterized at the present time, considerable information is available, and a discussion of the known effects will shed considerable light on the problem at hand.

It is well known that both crack initiation and growth are strongly affected by the presence of a water environment. With its presence, the individual effects of oxygen and temperature also become important. The presence of geometrical discontinuities act as preferential sites of crack initiation. Fatigue tests of A106 Gr B and A333 Gr 6 carbon steel pipes in oxygenated water[5] have shown cracks initiate at discontinuites without regard to base metal, weld or heat affected zones.

The cycles required to initiate a crack are strongly affected by mechanical variables such as the strength level of the steel and the reduction in area. Manson's universal slopes equation[6] has been found to give reasonable estimates of low cycle fatigue behavior at temperatures well below the creep range. The total strain range, $\Delta\varepsilon_t$, is written

$$\Delta\varepsilon_t = \frac{3.5\ \sigma_{uts}}{E}\ N_f^{-0.12} + D^{0.6}\ N_f^{-0.6}$$

where

$D = \ln \frac{100}{100-RA}$

σ_{uts} = ultimate tensile strength

E = Young's modulus

N_f = cycles to failure

RA = reduction in area, %

Note that the strain range that corresponds with a given number of cycles to failure gets larger as the ultimate tensile strength increases, and also increases as the reduction in area increases, thus showing improved performance.

Another expression for prediction of high cycle fatigue behavior was proposed by Langer and Harding[7] in 1964. Here the stress amplitude S is given by

$$S = \frac{E}{4N_f^{1/2}} \ln \frac{100}{100-RA} + Se$$

where

Se = endurance limit $\leq 0.5\ \sigma_{uts}$

N_f = cycles to failure

Once again it can be seen that increasing the ultimate tensile strength and reduction in area of the material results in improved fatigue behavior. [a,c

]

[

a,c

]

The level of oxygen in the water environment has a strong influence on the corrosion potential which exists at the steel surface, and thereby impacts both crack initiation and growth. Tests by Indig[5] have shown that the corrosion potential increases dramatically with small increases in oxygen, as shown in Figure 12-4. Knowledge of the impact

of the corrosion potential on fatigue crack initiation and growth is incomplete, but it is thought that low corrosion potentials are beneficial both from the standpoint of fatigue crack initiation and growth and of static stress corrosion cracking. Note that the most important effect on cracking comes from the environmental reaction of the steel and water. The corrosion products in the crack tip area are a secondary concern in this situation.

Vosikovsky's[9] fatigue crack growth experiments on line pipe steel, in water environments demonstrated that increasing the corrosion potential increased the fatigue crack growth rate considerably, so the oxygen level of the feedwater could play an important part in the degree of cracking which occurred in any given plant. It is well known that high oxygen levels decrease the cycles to failure in smooth bar fatigue tests. The recommended oxygen level in the feedwater [ ] would result in operation in the lower range of potential, but it is clear that much higher levels are rather common during some periods of operation, as disccused in Section 6.

a,c

The effects of temperature on the corrosion and corrosion fatigue behavior of these materials are not well known as yet, but there are indications that this variable could be much more important than previously believed. The effect of water and temperature in ductility has been discussed above and it was pointed out that at 400-450°F (204-232°C) a minimum occurs in the reduction in area value. Likewise, the effect of dissolved oxygen on corrosion potential in Figure 12-4 indicates that the highest corrosion potentials regardless of oxygen level occur at 390°F (200°C).

Kondo[10] showed in his studies of fatigue crack growth of A302B low alloy steel in oxygenated water (100 ppb) that the fatigue crack growth rates appeared to reach a maximum at about 392°F (200°C), which is completely consistent with the other observations above.

Recent work by Prater and Coffin[8] have shown that fatigue crack growth rates in highly oxygenated water (800 ppb) can be even higher than those in water environments with controlled oxygen [ ]

a,c

[ ]. The characterization of fatigue crack growth in a highly oxygenated environment is not yet complete, so the degree of this further enhancement is difficult to quantify at present. a,c

Prater and Coffin have also shown that static stress corrosion cracking can occur in these piping carbon steels in a water environment high in Oxygen [ ]. Static load tests of precracked specimens have shown that K_{ISCC} in this environment at 550F is between 30-40 ksi $in.^{1/2}$ This means that once cracks were initiated by the thermal fatigue mechanism or other cause it is possible that they could propagate even without the imposition of cyclic loads. The likelihood of this static load propagation occurring in the feedwater piping is difficult to determine because only limited test results are available, but this mechanism of cracking must be given serious consideration. a,c

Thus, we see that there appears to be a particular range of temperature and oxygen level for this material-environment combination which could lead to high potential for cracking. The synergisms between the variables may be such that the most susceptible conditions seldom occur together, which may also help to explain why serious cracking seldom occurs. Another explanation, which is perhaps more likely, is that serious cracking only occurs when the material-environmental conditions are just right and are combined with the cycles and loading conditions described earlier. This subject will be discussed in further detail in the work which follows, dealing with the results of individual pant investigations.

12.5 INVESTIGATION OF INDIVIDUAL PLANTS

A preliminary investigation of feedwater line operation at the [ ] site indicated that thermal stratification was occurring in the feedwater lines during periods of low flow rate, when cold auxiliary feedwater is introduced to maintain a given level of water in the steam a,c,e

generator. Both the magnitude of the stresses produced by these cycles and the number of cycles which appeared to be occurring were sufficient to produce significant crack growth, according to the estimations shown in Figure 12-2. Therefore, a detailed recording was made of the thermal stratification behavior in the feedwater lines of five different plants which had experienced cracking. The details of this monitoring program have been described in an earlier section.

The fatigue crack growth analysis methodology described in Section 12-2 was applied to the prediction of crack growth in the plants where these thermal measurements were recorded during the hot standby portion of plant operation. These measurements were augmented by flow model tests conducted on plexiglass models, and described in Section 10. Results of these measurements were then used as input to three dimensional stress analyses (Section 11) and these stresses were used as a basis for the fatigue crack growth predictions. The predictions were then compared with crack profiles determined from ultrasonic testing and destructive metallography. The results obtained from study of the water chemistry of individual plants (Section 6) were also factored into the discussion of results for each of the five plants.

As a result of the individual plant temperature measurements, a number of "typical" temperature profiles were developed, as detailed in Section 11.3. These profiles were particularized for different plants by use of the actual measurements, which also allowed the counting of the number of occurrences of each profile type. The stresses produced by these different temperature profiles are by nature three-dimensional, because they result from the differentials in expansion within the piping cross section, and are also dependent on the axial location along the pipe. They are affected by the presence (or absense) of an elbow near the steam generator inlet, and are strongly affected by the counterbore which is present at every pipe-to-steam generator nozzle weld. [

a,c

]

a,c

[ ] Because of the pipe symmetry the stresses at any given cross section are symmetric with respect to the vertical centerline of the pipe.

As a result of the flow model tests it was found that in addition to the changing temperature profiles there exists an oscillating thermal fluctuation at the interface between the hot and cold water, which produces a large number of cycles of small amplitude at various cross sections of the pipe as the hot-cold interface moves up and down from bottom to top of the pipe. [

a,c

] These cycles were considered in separate analyses so their impact could be clearly delineated.

Since the stresses acting on the pipe were three dimensional in nature, a three dimensional fatigue crack growth analysis procedure was required. This was accomplished by a modification of the procedure described in Section 12.2. Stresses were obtained at a number of locations around the pipe, and at each location the crack growth was calculated separately, using the K_I expression of equation 12.2, after linearizing the stress through the wall. Different stresses existed at each location around the pipe, and also different numbers of cycles of each transient type, so the crack growth was often very different at different points around the circumference.

The input stresses are listed for several locations in each plant in Tables 12.5 to 12.13. The transients resulted from changes from one temperature profile to another, and therefore different cross sections would experience different transients, and often certain cross sections would not even experience a given transient type. The crack growth which resulted from these individual calculations was then plotted on a cross section of the pipe at the counterbore region, and a picture of the three dimensional crack growth profile emerged.

A number of different cases were considered for each of the plants analyzed, and these will be described in detail here, after which each plant analyzed will be discussed separately. Four distinct analyses were carried out for these studies, and in all the cases analyzed only the thermal loads resulting from the stratification were considered. The other transients which each plant experienced as listed in Table 12-1, would contribute only a negligible amount to the total crack growth, as discussed earlier, so they were not used.

The possibility of water hammer or check valve slamming producing significant fatigue crack growth does not exist, because large numbers of such incidents would have to exist. No plant is known to have experienced large numbers of these transients, and furthermore such loadings would not cause crack growth in patterns which were observed around the pipe, as shown in Section 5.

The first analysis for each plant considered the thermal stratification cycles for the plant, and resulted in crack growth calculated at 20 locations around the pipe from top to bottom, as seen for example in the top left sketch of Figure 12-5. It was assumed that a uniform circumferential crack existed in the pipe, oriented circumferentially, and the total estimated cycles which the plant had experienced until such time as the crack was repaired were used in the analysis. Initial crack depths of 0.02, 0.05, and 0.100 inches were assumed. The crack which is most realistic to assume is 0.02 inches deep, since this is approximately the depth of crack which would result from initiation due to fatigue. In most cases the results from assuming an initial crack of this depth were reported, but occasionally results for the other assumed initial depths were reported, when this would aid in visualizing the resulting shape of the crack as it grew.

The second analysis completed for each plant was an attempt to add more realism to the crack growth results by considering the number of cycles necessary to initiate a crack at any given location. A crack was assumed to initiate when the usage factor became equal to one. These

determinations were made in Section 11, but the results are repeated here for reference in Table 12-14. Table 12-14 gives the percentage of the total hot standby cycles experienced by a given plant which would be necessary to reach a usage factor of 1.0. Note that a range of percentages are given in most cases. The high end of the range was used for the second analysis, and only the cycles remaining after the crack initiated were applied to the crack growth prediction. An example of the result of this calculation is shown in the upper left figure of Figure 12-5. Again twenty locations around half the pipe were considered, and in general it was assumed that the crack was 0.020 inches deep when it initiated. Thus the results of the first and second analyses provide a set of bounds to bracket the expected growth due to stratification. The first assumes immediate initiation, while the second assumes the latest initiation possible, according to the fatigue calculations of Section 11.

The third analysis carried out was an attempt to account for the effect of the thermal oscillations at the hot-cold water interface, which have been termed "striping". The stresses resulting from this phenomenon were calculated in Section 11 as the result of [ ] analysis of the results of the flow model tests. Because of the complexity involved in the calculation of these stresses, results were obtained at only five discrete locations. As detailed in Section 11, the frequency of these cycles is rather high, and this results in a highly nonlinear stress profile, since the only fluctuating stresses occur near the inside diameter of the pipe. Because of the requirement of the crack growth analysis for linearized stresses, these stress profiles were linearized as shown in Figure 12-14. [

] An example is shown in the top left of Figure 12-6.

a,c

a,c

The fourth and last analysis completed considered the impact of cycles to initiation on the crack growth calculations, including the striping cycles. The analysis was done just as in the third case described

above, but only the cycles after crack initiation were applied to the growth calculations. An example is shown in the top right of Figure 12-6.

In all the cases analyzed the predicted crack growth was compared with the actual crack profile. General agreement was good qualitatively, but exact predictions were not accomplished. [

a,c [

]

This behavior was found in both the analyses and in the actual pipe sections.

a,c,e [ ]

a,c,e [

]

[

a,c,e

]

a.c.e

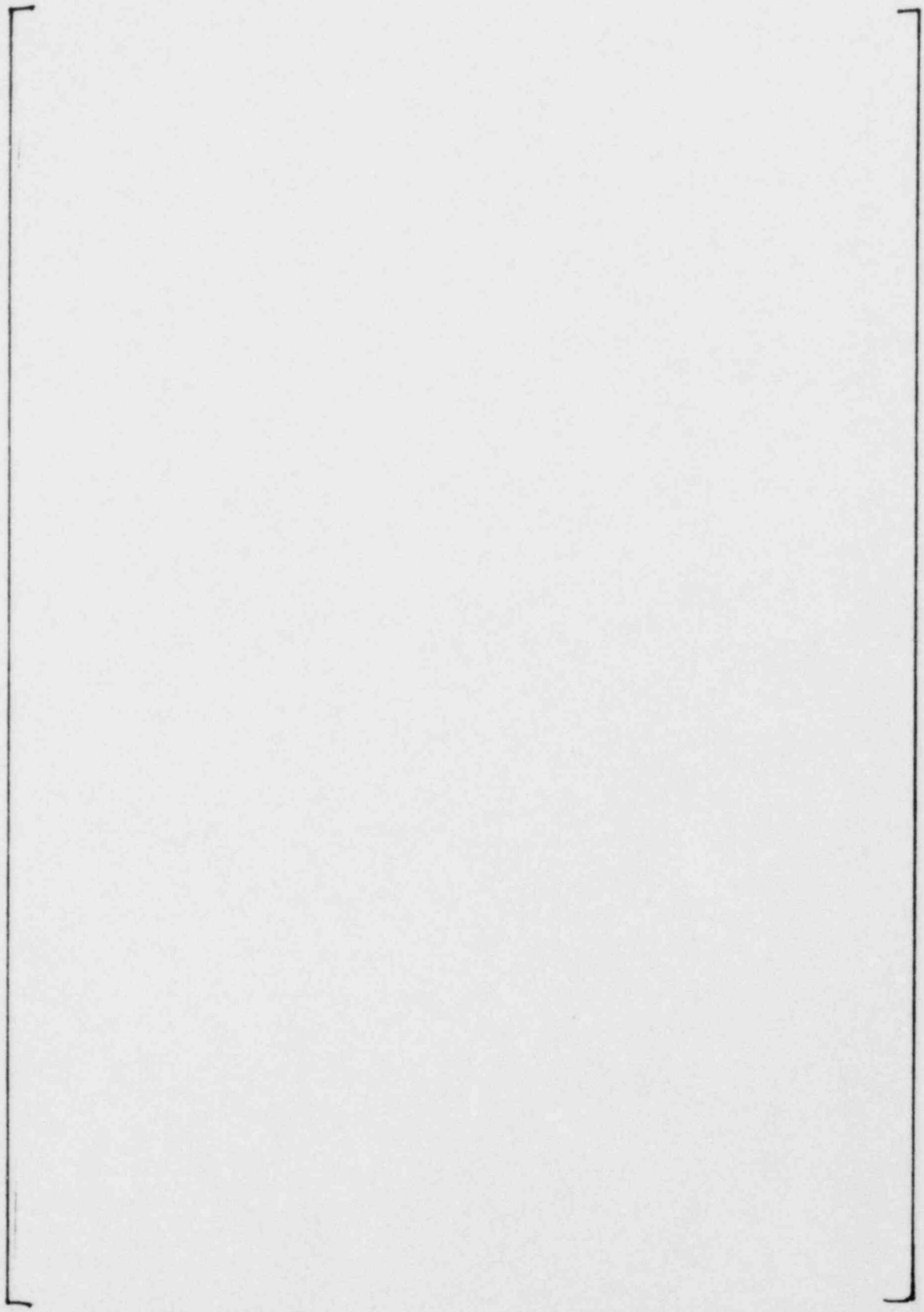

[

a,c,e

]

a,c,e [

]

12.6 CONSIDERATION OF CRACKS AT LOCATIONS OTHER THAN THE COUNTERBORE

a,c,e [

]

[

a,c,e

]

12.7 SUMMARY AND DISCUSSION

The major cause for the growth of the cracks was found to be the thermal stratification cycles, which occur during low flows, primarily at hot

standby. In addition to this phenomenon, it was found that oscillations occur at the interface between hot and cold water, but these oscillations were found to have little influence on the crack growth even though there was some impact on the crack initiation predictions.

The five plants studied could be divided into three categories. In two cases, the cracking was significant and the thermal loads were significant, so the predictions of crack growth were qualitatively good. In two other cases, the cracking was not extensive and the thermal cycles were not severe, so again the crack growth predictions were fairly accurate. [

a,c

]

The general crack growth behavior predicted was in good qualitative agreement with the observed growth. The most extensive cracking was

a,c

predicted to occur either at the [

] The observed cracks were always deepest at these same locations, although in several cases the predicted crack depths were not in perfect agreement.

In looking at the results of the crack growth predictions, one is led to consider changing one input or another to find out if better agreement could be obtained. This process is not likely to be successful, however, because so many inputs are involved, each of which has its own assumptions and uncertainties. A partial list would include:

Thermal measurements
Stress analysis
Cycle counting

a,c

Striping [ ] analysis

Fatigue initiation determinations
Fatigue crack growth law

In addition to this list, the effect of the environmental chemistry on crack initiation and growth is a potentially important factor, which cannot be directly accounted for at present.

The results of the fatigue crack growth studies lead to the conclusion that the largest single factor affecting both the existance and the penetration of the feedwater line cracks is the thermal stratification cycles. The magnitude and number of these cycles varies greatly from plant to plant, which helps to explain why such large differences in cracking were encountered from plant to plant. [a,c] This can have an adverse impact on both crack initiation and growth, but it is felt that improper chemistry control is unlikely to be the major cause in itself of the cracking problem.

12.8 REFERENCES

[a,c,e]

[a,c,e]

3. Holman, J. P., Heat Transfer, McGraw Hill Book Co., New York, 1963.

4. Timoshenko, S. P. and Goodier, J. H., Theory of Elasticity, McGraw Hill Book Co., New York, 1970.

5. "BWR Environmental Cracking Margins for Carbon Steel Piping", First Semiannual Progress Report, July-December 1978. General Electric Report NEDC 24625, January 1978.

6. Manson, S. S., "A Simple Procedure for Estimating High Temperature Low Cycle Fatigue" Experimental Mechanics, August 1968.

7. Langer, B. L. and Harding, W. L., "Material Requirements for Long-Life Pressure Vessels", TransASME Journal of Engineering for Industry, October 1964, pp. 403-410.

TABLE 12-1

DESIGN TRANSIENTS - TYPICAL FEEDWATER LINE

Transient	Number of Occurrences in 40 Years
Secondary Side Hydrotest	[ ] a
Hot Standby	
Unit Load - Unload 5% per minute	
Small Step Load Decrease	
Large Step Load Decrease	
Loss of Power	
Partial Loss of Flow	
Loss of Load	
Reactor Trip	

TABLE 12-2

MATERIAL PROPERTIES USED IN FATIGUE CRACK GROWTH ANALYSES

Property (550°F)	Materials SA533 Grade B Class 1 and SA508 Class 2
Young's Modulus (psi)	27×10^6
Density (lb/in.^{3})	0.280
Conductivity (Btu/hr-in.-°F)	1.948
Heat Capacity (Btu/hr-°F)	0.135
Coefficient of Thermal Expansion (in/in.°F)	7.30×10^{-6}
Poisson's Ratio	0.30

TABLE 12-3

STRESSES USED IN FATIGUE CRACK GROWTH ANALYSIS OF DESIGN CYCLES

	Axial Stress* Inside Surface		Axial Stress* Outside Surface	
	Maximum	Minimum	Maximum	Minimum
Hot Standby	[			] a,c
Unit load-unload 5% per minute				
Small stepload decrease				
Large stepload decrease				
Loss of power				
Partial loss of flow				
Loss of load				
Reactor trip				
Secondary Side Hydrotest				

* All stress values are in ksi

TABLE 12-4

RESULTS OF FATIGUE CRACK GROWTH ANALYSIS FOR DESIGN CYCLES

	Initial Crack Depth (inches)	Crack Depth After Year (Inches) 10	20	30	40
a,c	0.020	[			]
	0.050				
	0.100				

TABLE 12-5

INPUT DATA FOR FATIGUE CRACK GROWTH ANALYSIS-[ ] a,c,e

Maximum Axial Membrane Stress (ksi)	Maximum Axial Bending Stress (ksi)	Total Cycles	Minimum Axial Membrane Stress (ksi)	Minimum Axial Bending Stress (ksi)

a,c

TABLE 12-6

a,c,e

INPUT DATA FOR FATIGUE CRACK GROWTH ANALYSIS- Including Thermal Striping

[ ]

Maximum Axial Membrane Stress (ksi)	Maximum Axial Bending Stress (ksi)	Total Cycles	Minimum Axial Membrane Stress (ksi)	Minimum Axial Bending Stress (ksi)

a,c

TABLE 12-7

INPUT DATA FOR FATIGUE CRACK GROWTH ANALYSIS-[ ] a,c,e

Maximum Axial Membrane Stress (ksi)	Maximum Axial Bending Stress (ksi)	Total Cycles	Minimum Axial Membrane Stress (ksi)	Minimum Axial Bending Stress (ksi)
[				] a,c

TABLE 12-8

INPUT DATA FOR FATIGUE CRACK GROWTH ANALYSIS- Including Thermal Striping

a,c

Maximum Axial Membrane Stress (ksi)	Maximum Axial Bending Stress (ksi)	Total Cycles	Minimum Axial Membrane Stress (ksi)	Minimum Axial Bending Stress (ksi)
a,c				

TABLE 12-9

INPUT DATA FOR FATIGUE CRACK GROWTH ANALYSIS- [ ] a,c,e

Maximum Axial Membrane Stress (ksi)	Maximum Axial Bending Stress (ksi)	Total Cycles	Minimum Axial Membrane Stress (ksi)	Minimum Axial Bending Stress (ksi)
[				] a,c

TABLE 12-10

a,c,e

INPUT DATA FOR FATIGUE CRACK GROWTH ANALYSIS- Including Thermal Striping

[ ]

Maximum Axial Membrane Stress (ksi)	Maximum Axial Bending Stress (ksi)	Total Cycles	Minimum Axial Membrane Stress (ksi)	Minimum Axial Bending Stress (ksi)
a,c				

TABLE 12-11

INPUT DATA FOR FATIGUE CRACK GROWTH ANALYSIS-[ ]

Maximum Axial Membrane Stress (ksi)	Maximum Axial Bending Stress (ksi)	Total Cycles	Minimum Axial Membrane Stress (ksi)	Minimum Axial Bending Stress (ksi)
[				]

TABLE 12-12

a,c,e

INPUT DATA FOR FATIGUE CRACK GROWTH ANALYSIS- Including Thermal Striping

Maximum Axial Membrane Stress (ksi)	Maximum Axial Bending Stress (ksi)	[ ] Total Cycles	Minimum Axial Membrane Stress (ksi)	Minimum Axial Bending Stress (ksi)
a,c				

TABLE 12-13

INPUT DATA FOR FATIGUE CRACK GROWTH ANALYSIS-[ ] a,c,e

Maximum Axial Membrane Stress (ksi)	Maximum Axial Bending Stress (ksi)	Total Cycles	Minimum Axial Membrane Stress (ksi)	Minimum Axial Bending Stress (ksi)
[				] a,c

TABLE 12-14

Percentage of Hot Standby Cycles Required to Initiate Cracks

Node Location	
1	
2-3	
4-5	
6-7-8	
9	
10-11	
12	
13-20	

(Results including striping cycles)

T1	5
T3	7
T6	10
T5	14
T2	16

NOTE:

The ranges presented in this table result from the application of uncertainty factors to the observed thermal statification cycles. These factors result from uncertainties in (1) the actual thermal measurements and (2) the degree to which these measurements can be considered typical of hot standby operation for a given plant. The derivation of these uncertainty factors is discussed in Section 11.

TABLE 12-15

FATIGUE CRACK GROWTH RESULTS - [ ]
-EFFECT OF AXIAL LOCATION -

LOCATION ALONG PIPE	LOCATION AROUND PIPE	
	Top - 0 Degrees	Side - 90 Degrees
1. Counterbore	[	a,c]
2. Center of Tapered Region - Pipe Side		
3. End of Tapered Region at Nominal Pipe I.D.		

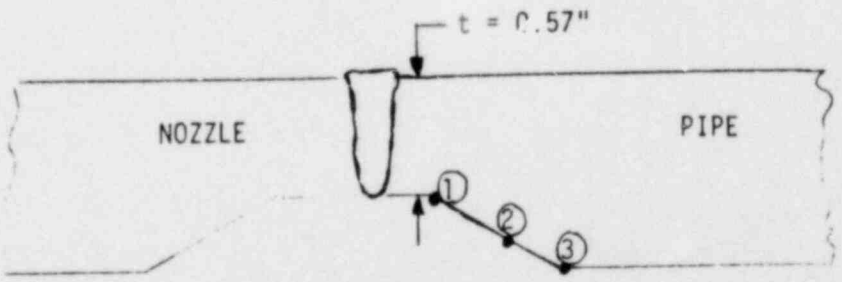

TABLE 12-16

INPUT DATA FOR FATIGUE CRACK GROWTH ANALYSIS - [ ]

(Location 2)

Maximum Axial Membrane Stress (ksi)	Maximum Axial Bending Stress (ksi)	Total Cycles	Minimum Axial Membrane Stress (ksi)	Minimum Axial Bending Stress (ksi)
[				]

TABLE 12-17

INPUT DATA FOR FATIGUE CRACK GROWTH ANALYSIS - [ ] a,c,e

(Location 3)

Maximum Axial Membrane Stress (ksi)	Maximum Axial Bending Stress (ksi)	Total Cycles	Minimum Axial Membrane Stress (ksi)	Minimum Axial Bending Stress (ksi)
[				] a,c

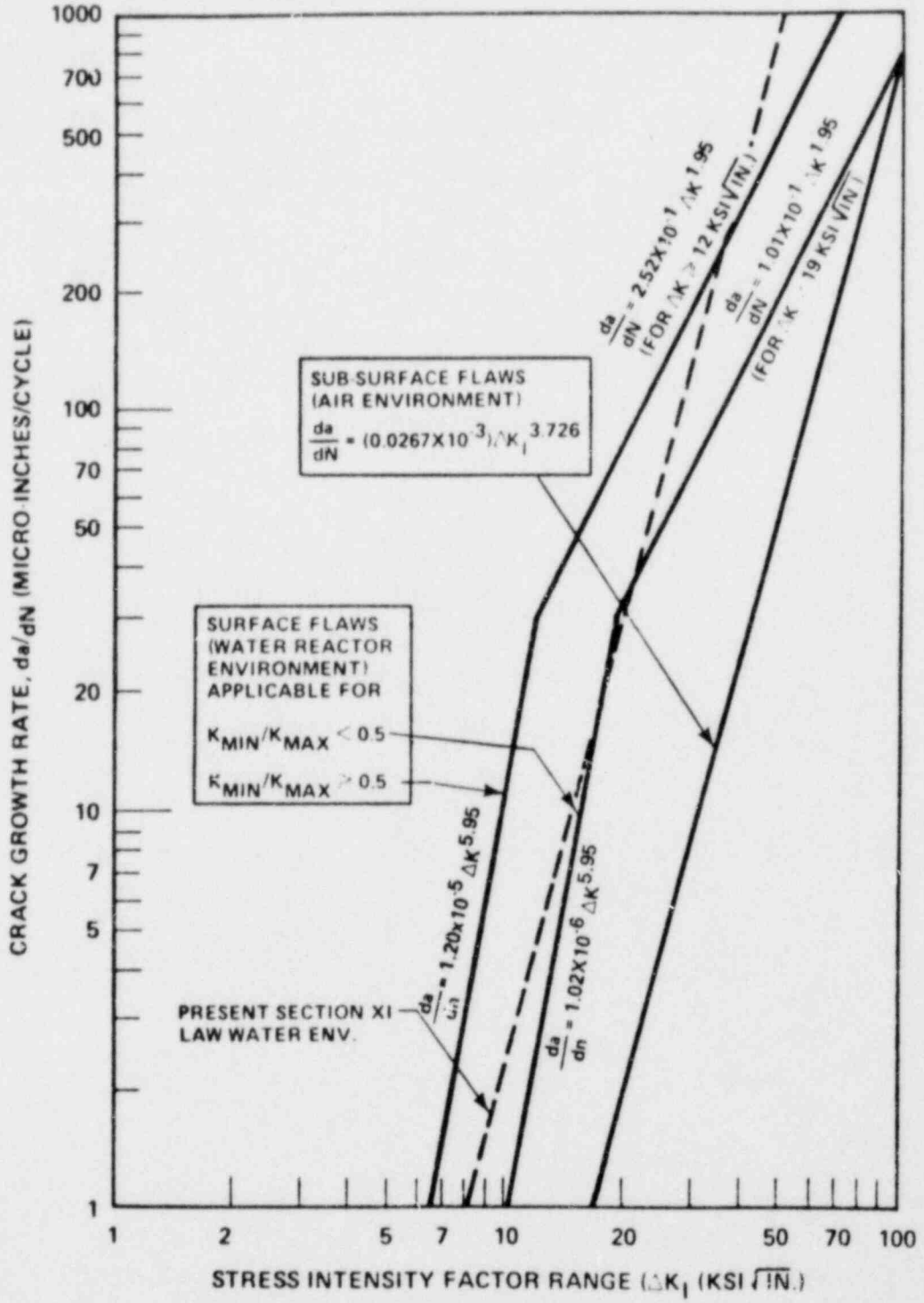

Figure 12-1 **Fatigue Crack Growth Data for Carbon and Low Alloy Ferritic Steels**

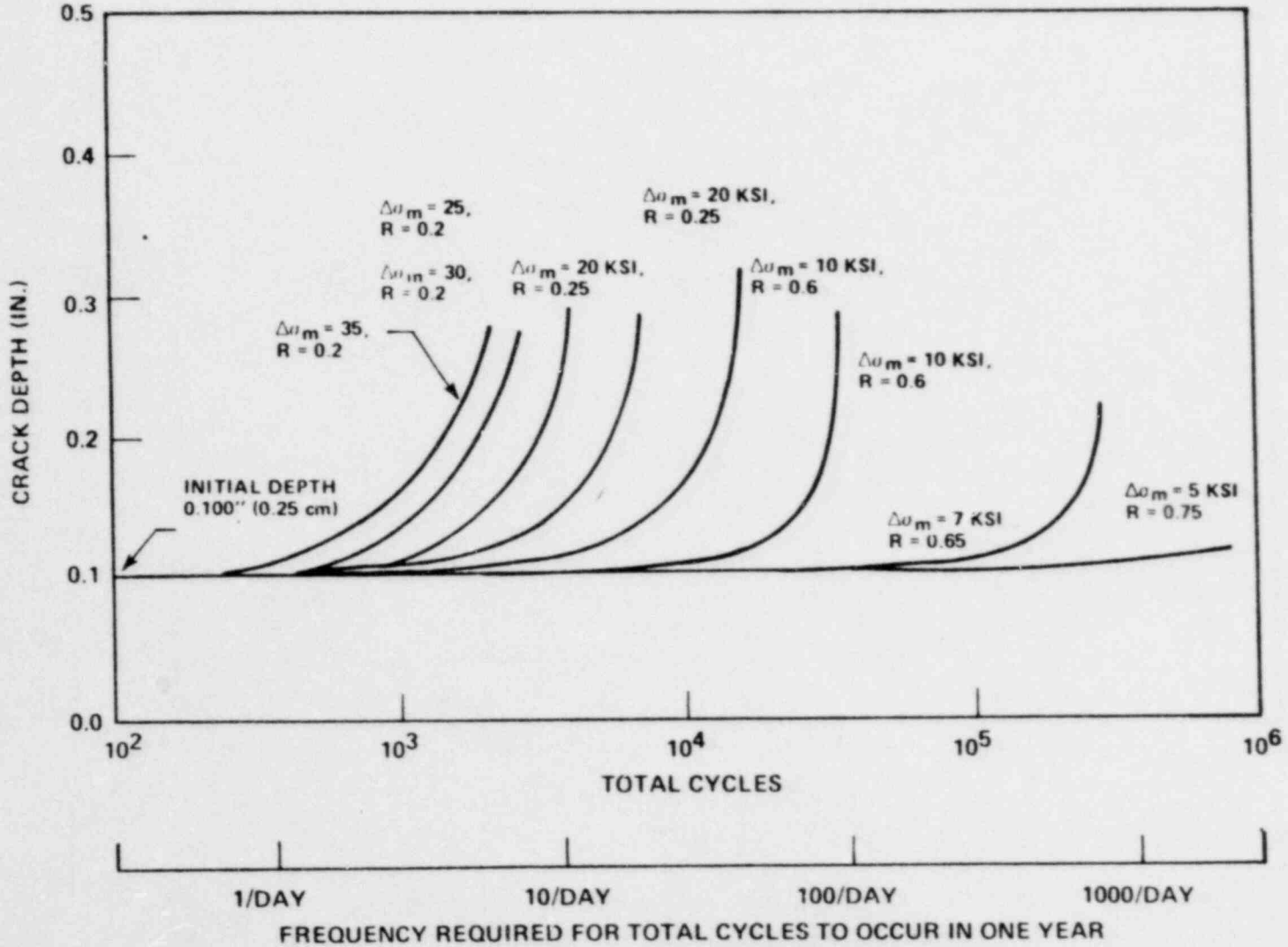

Figure 12-2 Estimation of Fatigue Crack Growth for Various Loads on a Typical Feedwater Line Pipe

160729

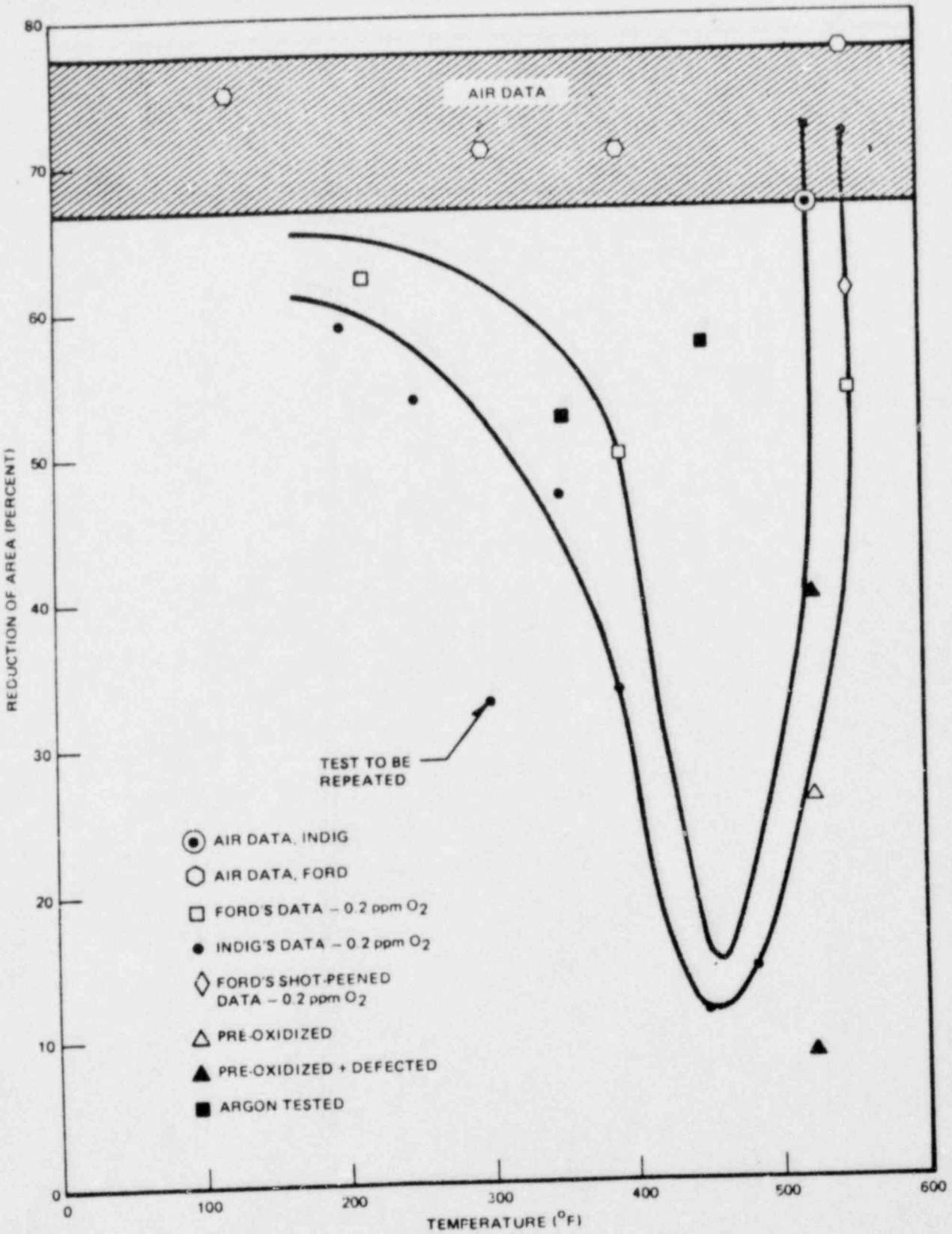

12-3 Effect of Environment on Ductility of SA333 Gr6, Reference 8.

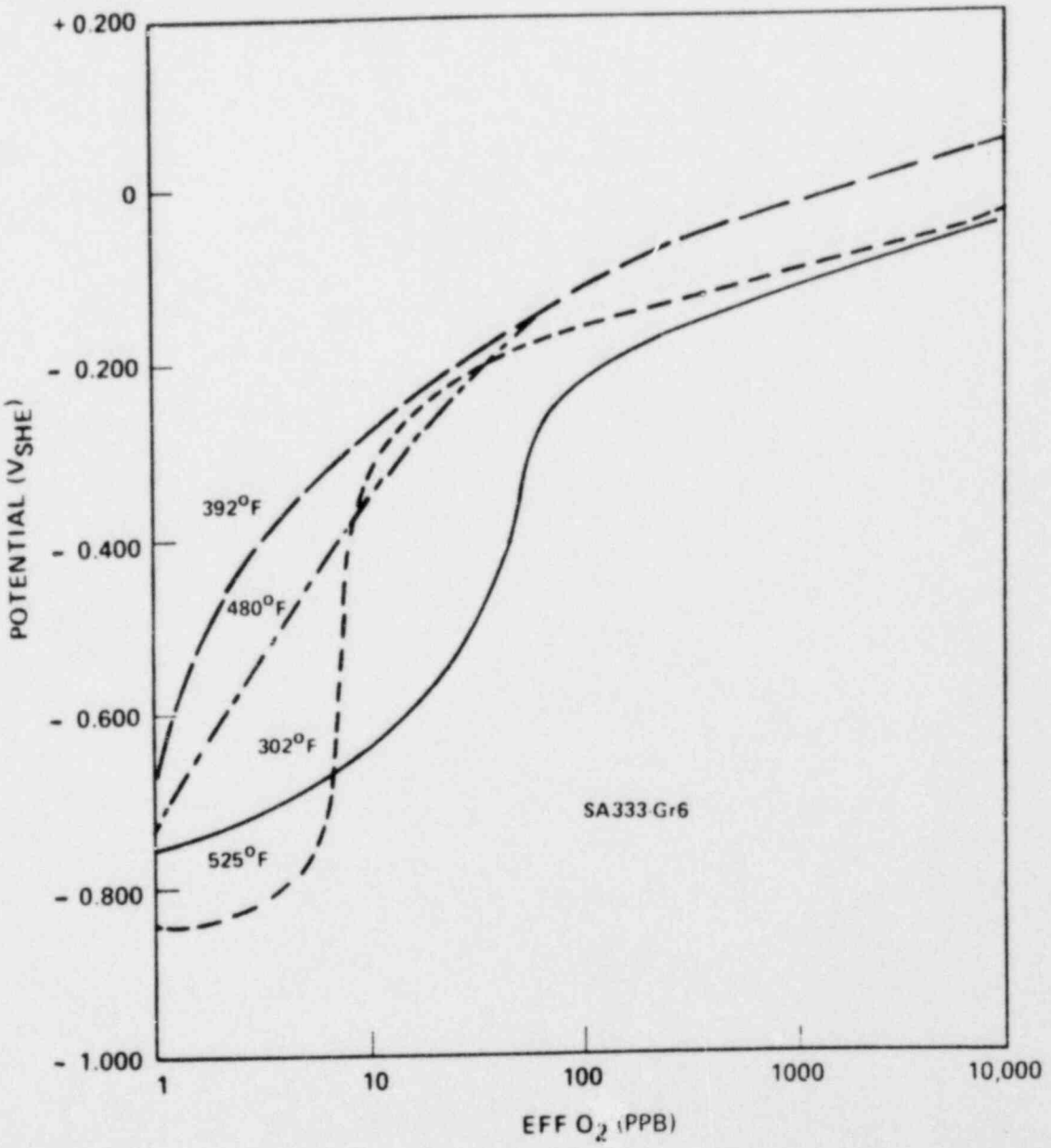

Figure 12-4 **Effect of Oxygen and Temperature on Corrosion Potential, as Determined by Indig, Reference 5**

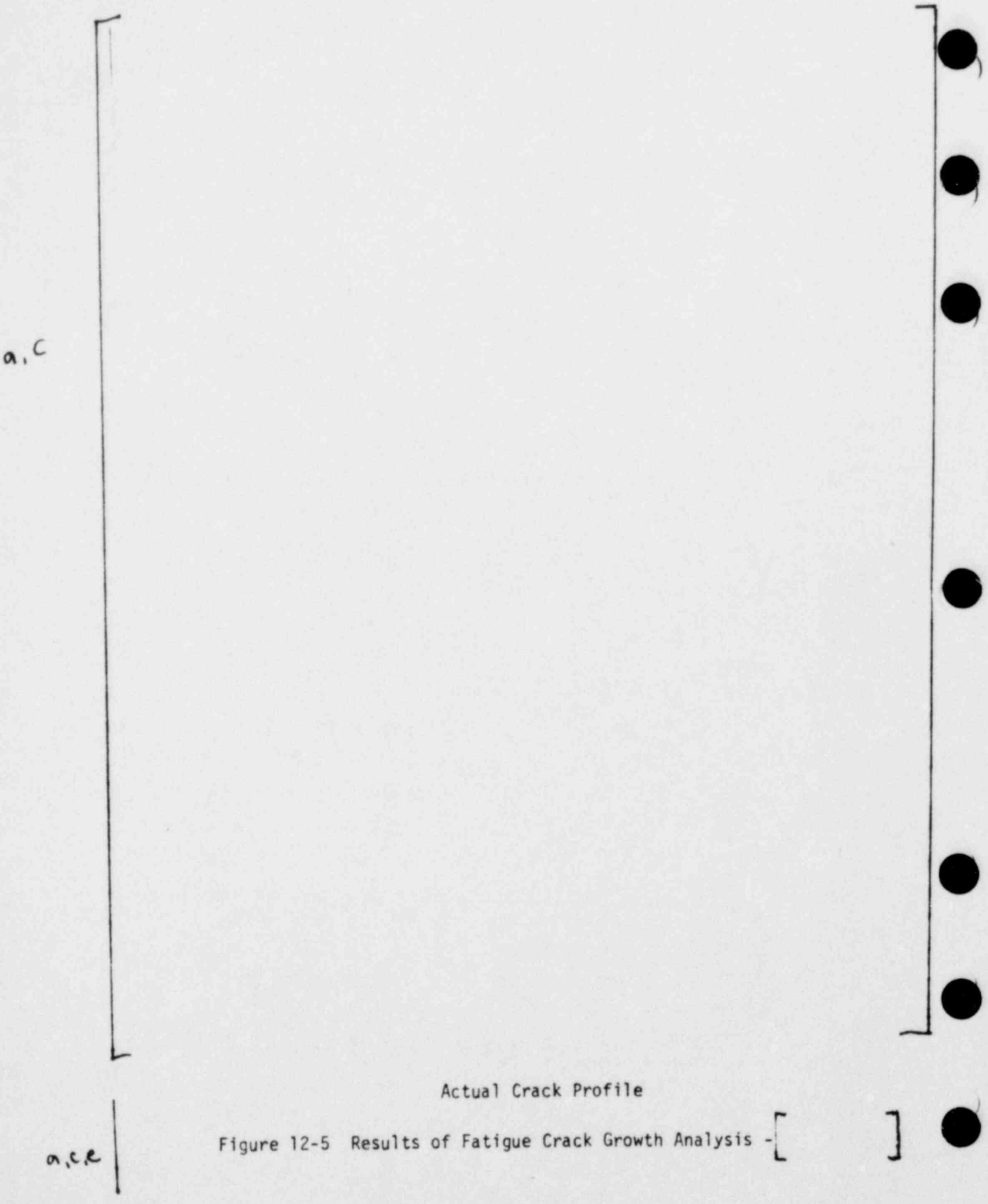

Actual Crack Profile

Figure 12-5 Results of Fatigue Crack Growth Analysis -[ ]

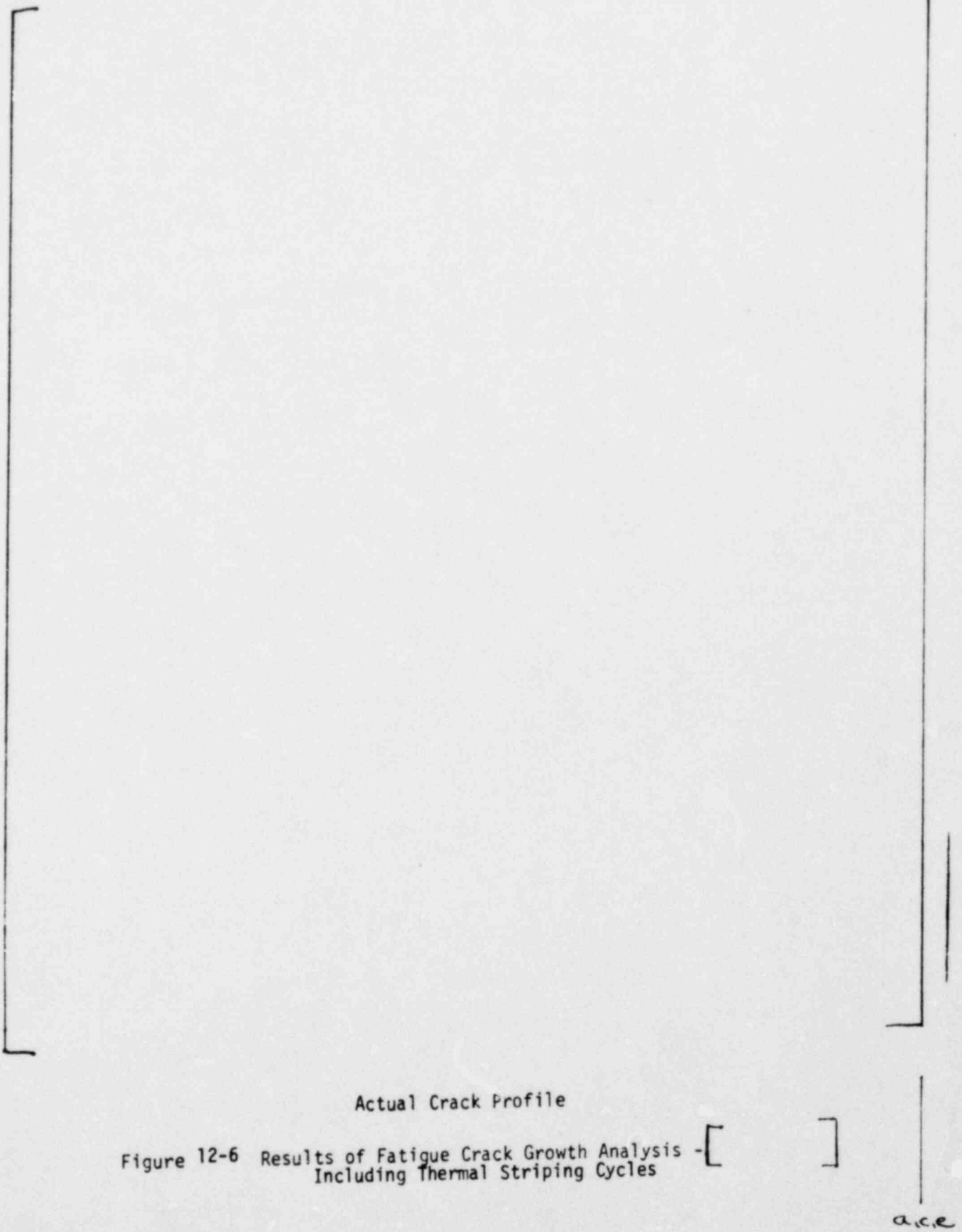

Figure 12-6 Results of Fatigue Crack Growth Analysis - [ ] Including Thermal Striping Cycles

a,c

a,c,e

Figure 12-7 Results of Fatigue Crack Growth Analysis - [ ]

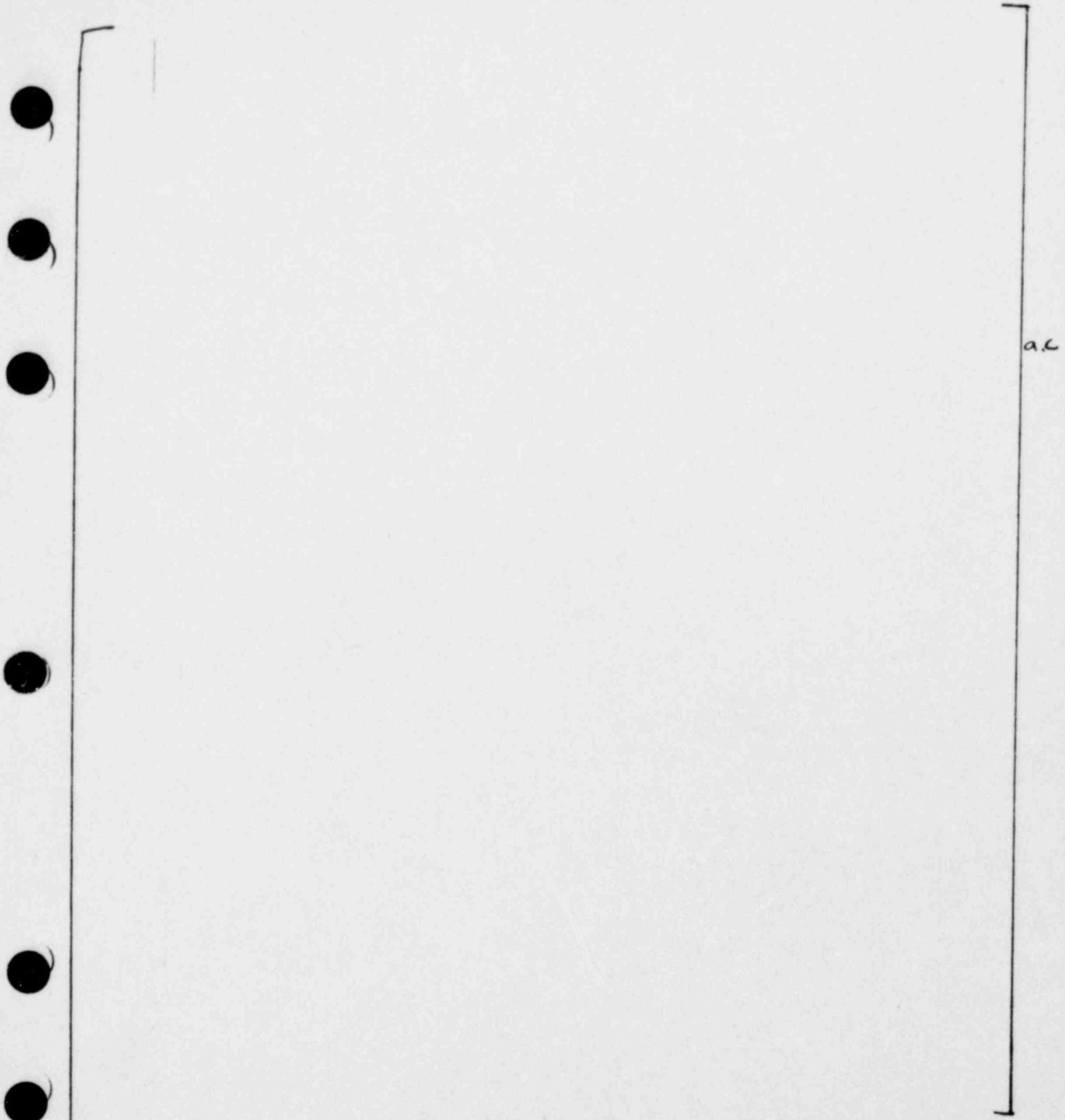

Figure 12-8 Results of Fatigue Crack Growth Analysis - [ ] a,c,e
Including Thermal Striping Cycles

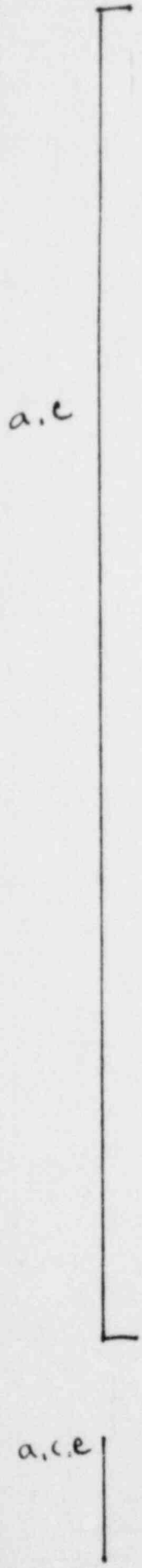

Figure 12-9 Results of Fatigue Crack Growth Analysis - [ ]

[ ] a.c

Figure 12-10 Results of Fatigue Crack Growth Analysis - [ ] a.c.e
Including Thermal Striping Cycles

Figure 12-11 Results of Fatigue Crack Growth Analysis -[ ]

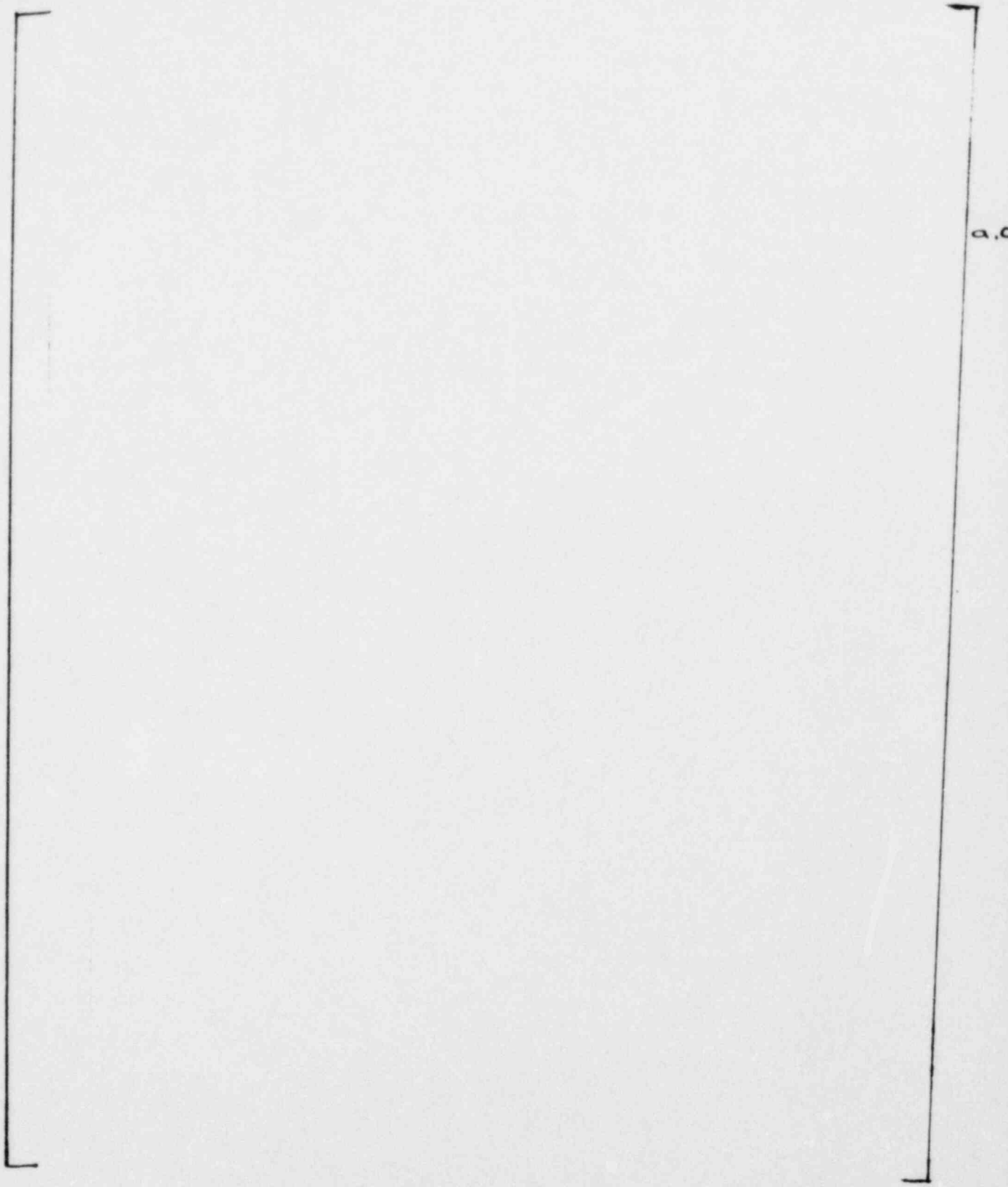

Figure 12-12 Results of Fatigue Crack Growth Analysis - [ ]
Including Thermal Striping Cycles

Figure 12-13 Results of Fatigue Crack Growth Analysis -[ ]

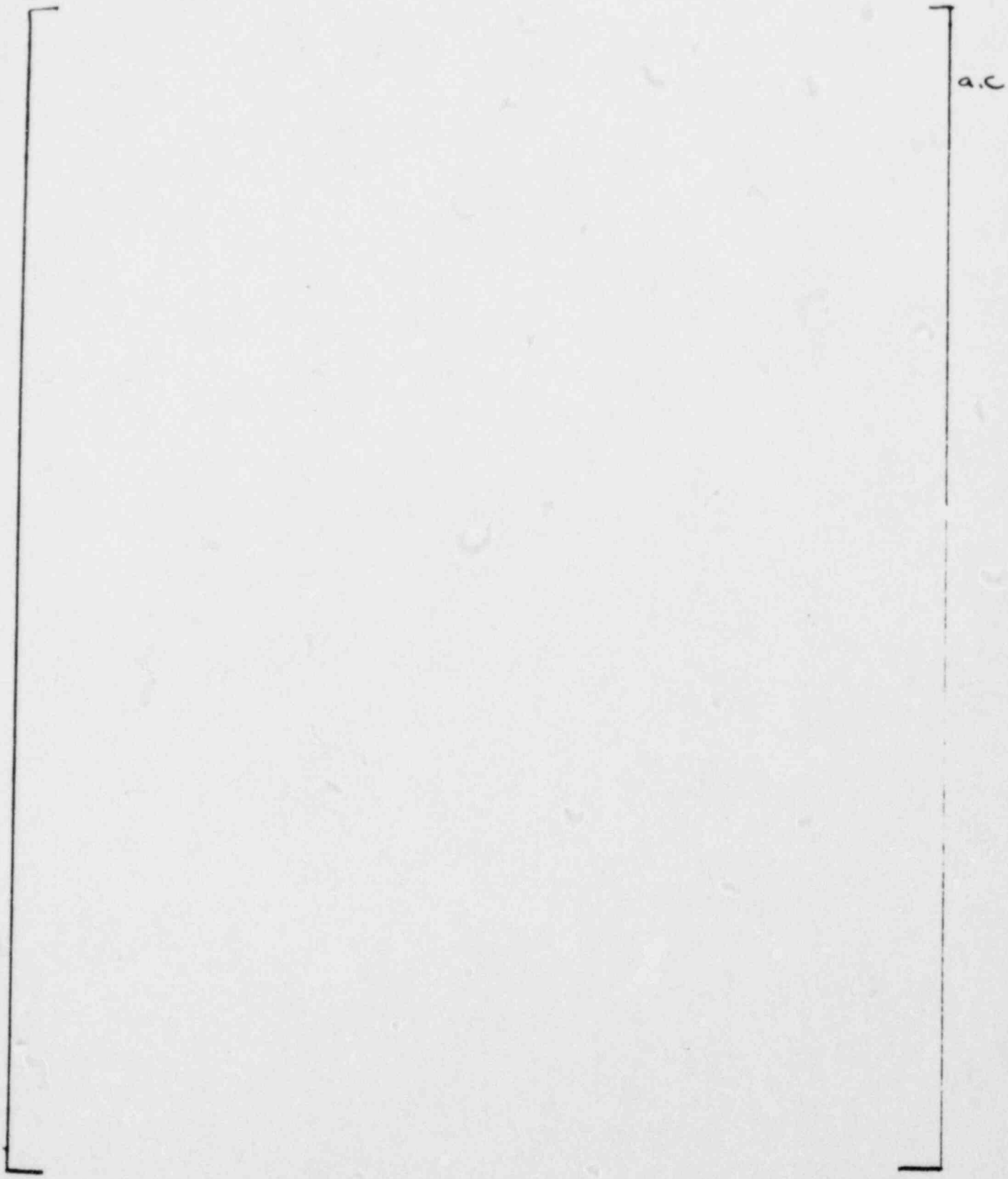

Figure 12-14 Linearization of Stresses for Thermal Striping Analysis

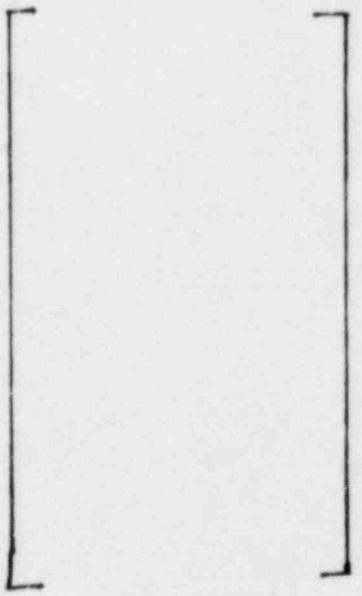

entire section

[redacted]

a,c

a,c

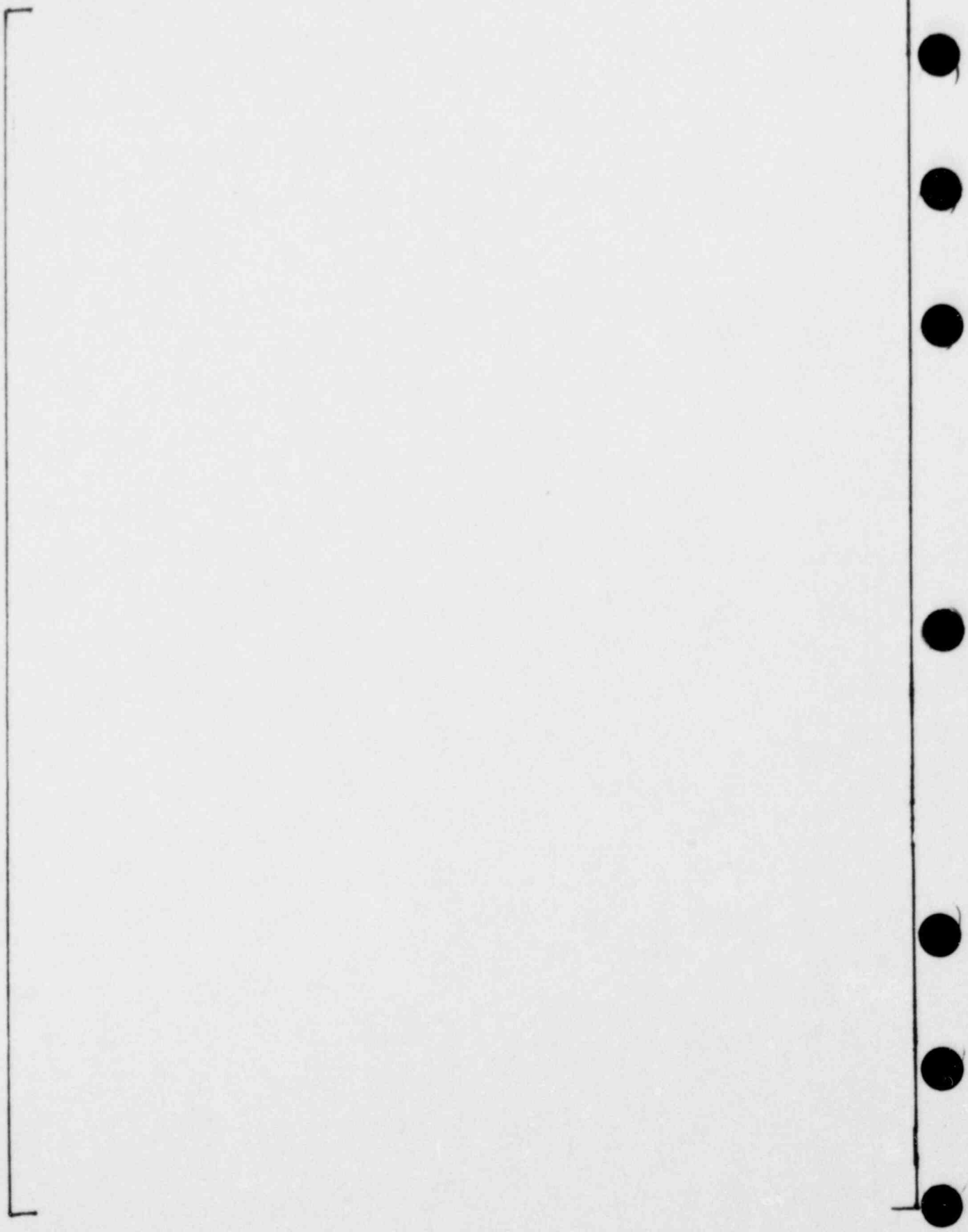

[

a,c

]

[redacted]

a,c

TABLE 13.1

a.c

Table 13.2

TABLE 13.3 FINAL PLANT COMPARISON TABLE - CRACK SEVERITY RANKING

2,c

TABLE 13.4 FINAL PLANT COMPARISON TABLE - OXYGEN EXPOSURE RANKING

a,c

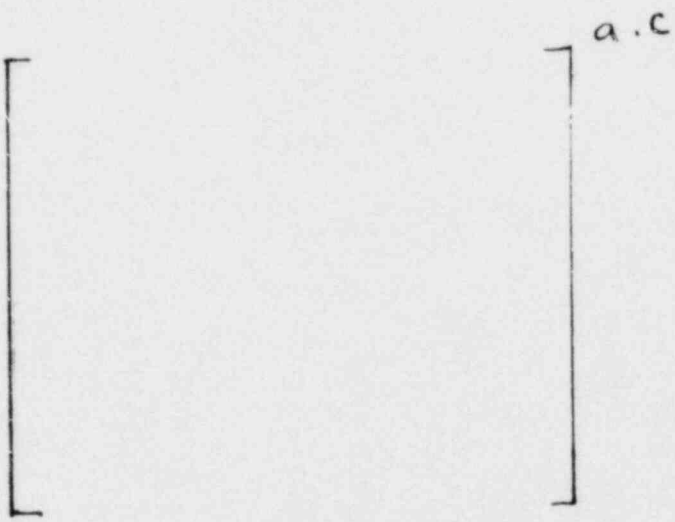

entire section

[

c, e

]

C,e

[

c,e

]

c, e

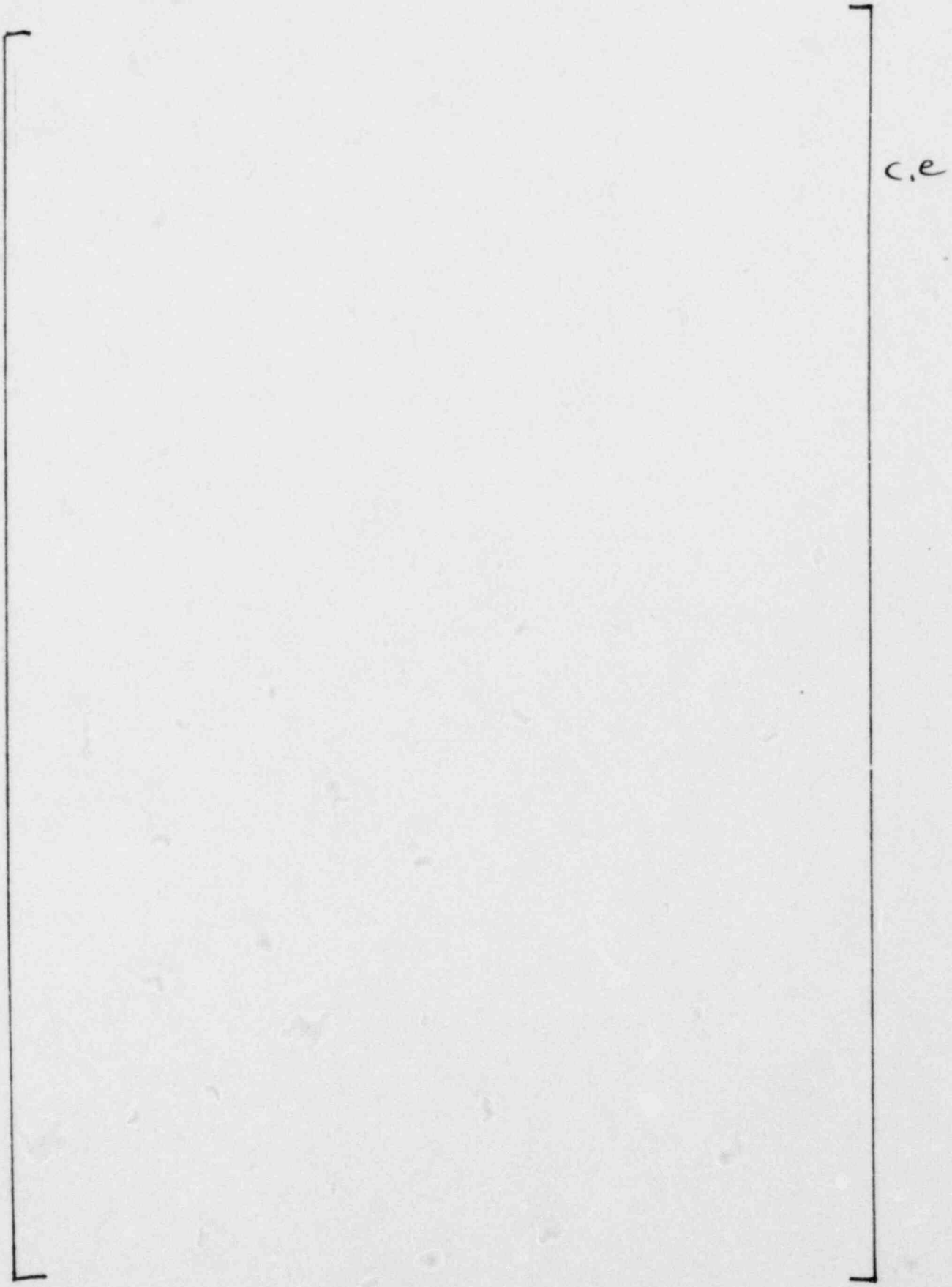

c.e

c,e

[

]

C,e

c,e

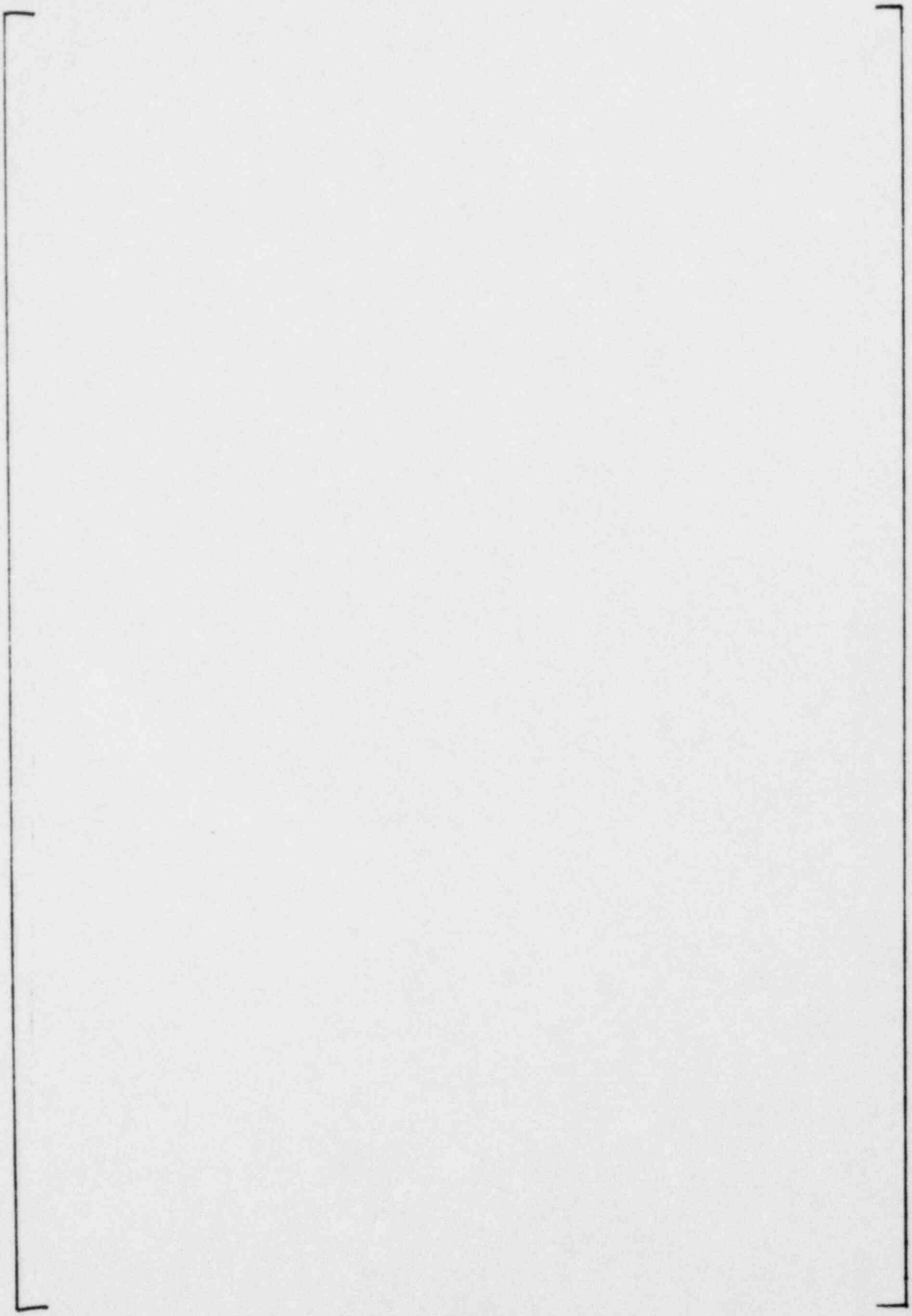

c,e

0535B

c, e

[

c, e

]

C,R

[

c,e

]

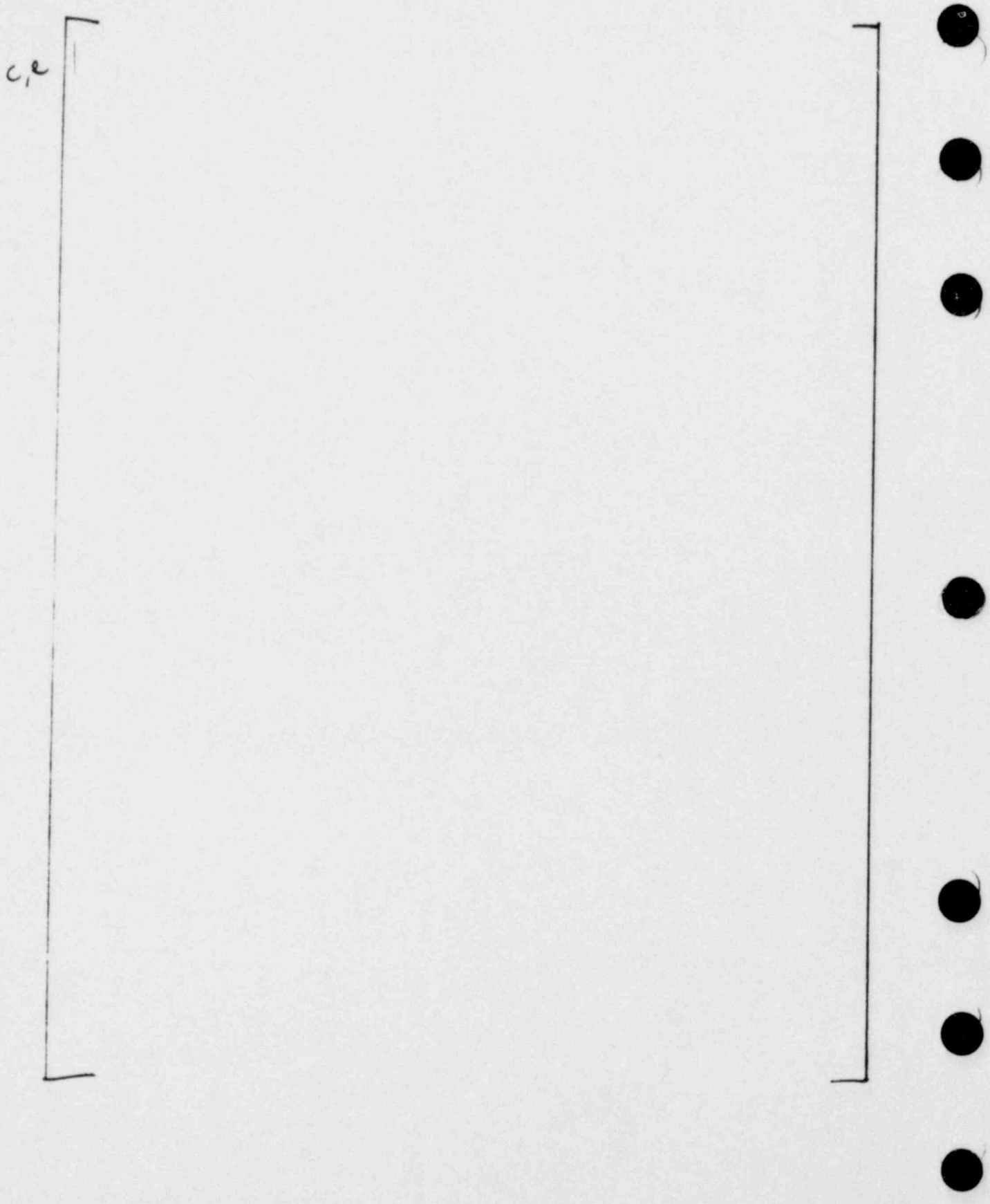

[ ] c,e

c,e [

]

TABLE 14.1

c,e

TABLE 14.2

c,e

TABLE 14.3 (Sheet 1 of 6)

c,e

535B

TABLE 14.3 (Sheet 2 of 6)

c,e

[redacted]

TABLE 14.3 (Sheet 3 of 6)

[redacted]

c,e

[redacted]

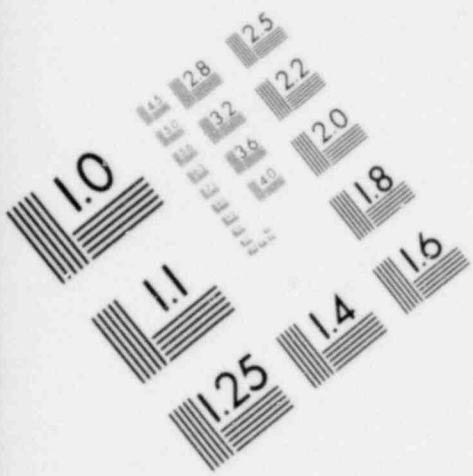

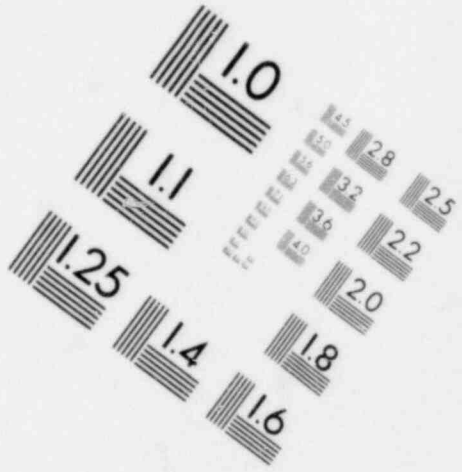

IMAGE EVALUATION TEST TARGET (MT-3)

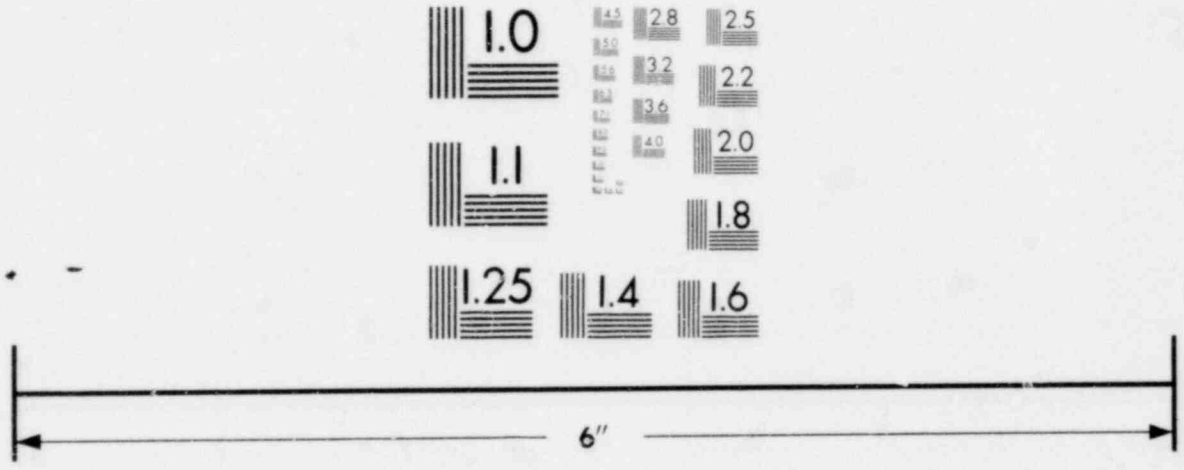

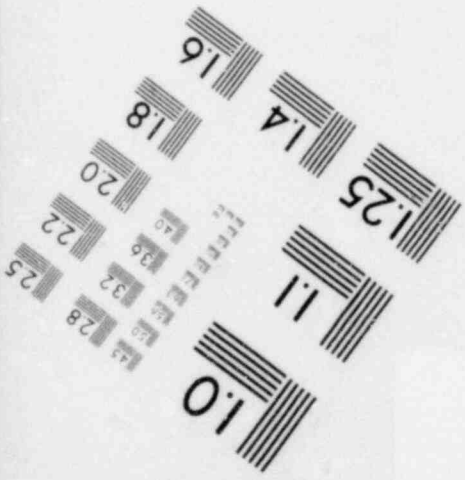

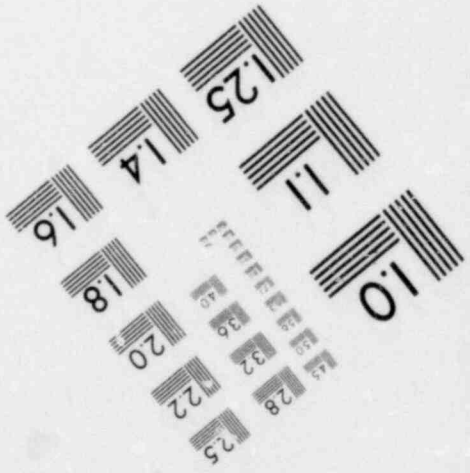

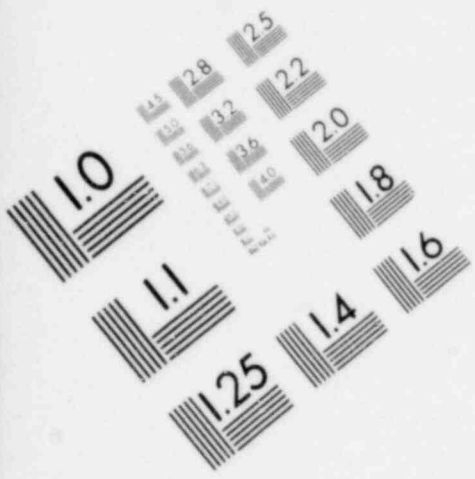

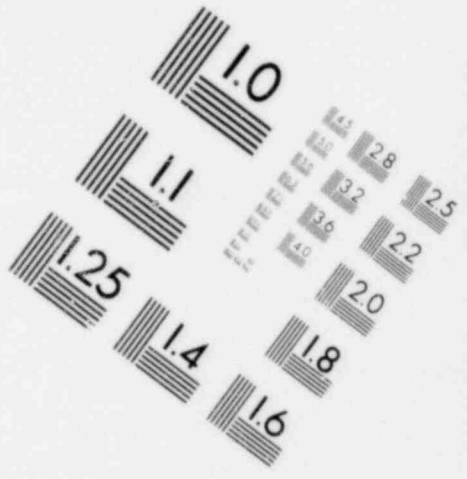

IMAGE EVALUATION TEST TARGET (MT-3)

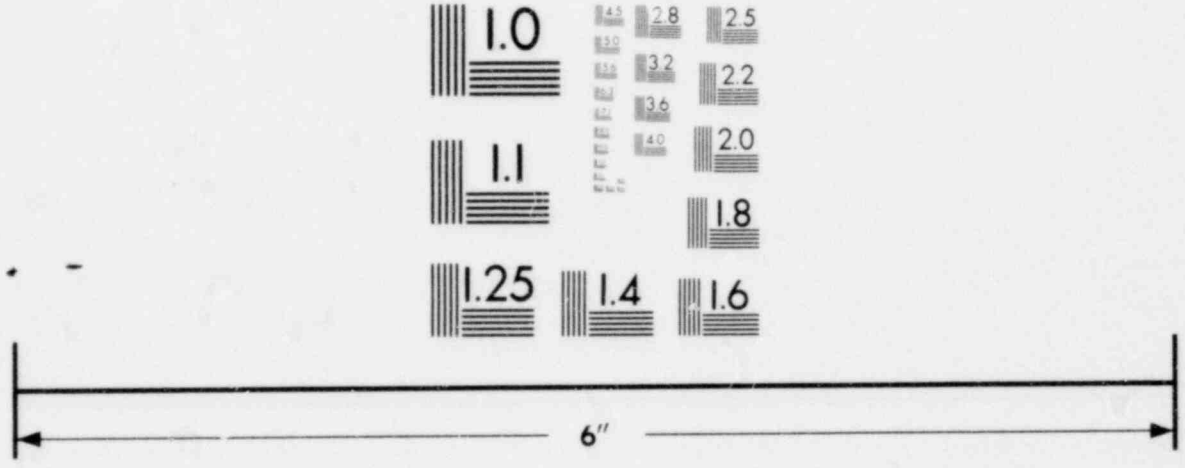

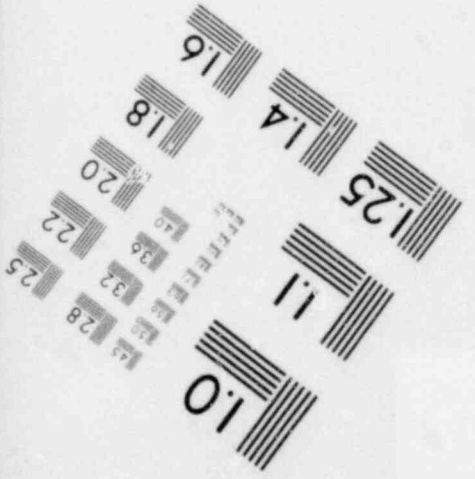

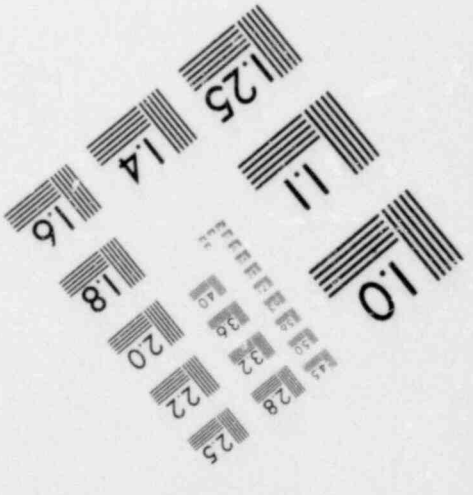

TABLE 14.3 (Sheet 4 of 6)

c,e

[redacted]

TABLE 14.3 (Sheet 5 of 6)

c,e

TABLE 14.3 (Sheet 6 of 6)

c,e

[redacted]

FOOTNOTES FOR TABLE 14.3

C,E

5358

c,e

[ ]

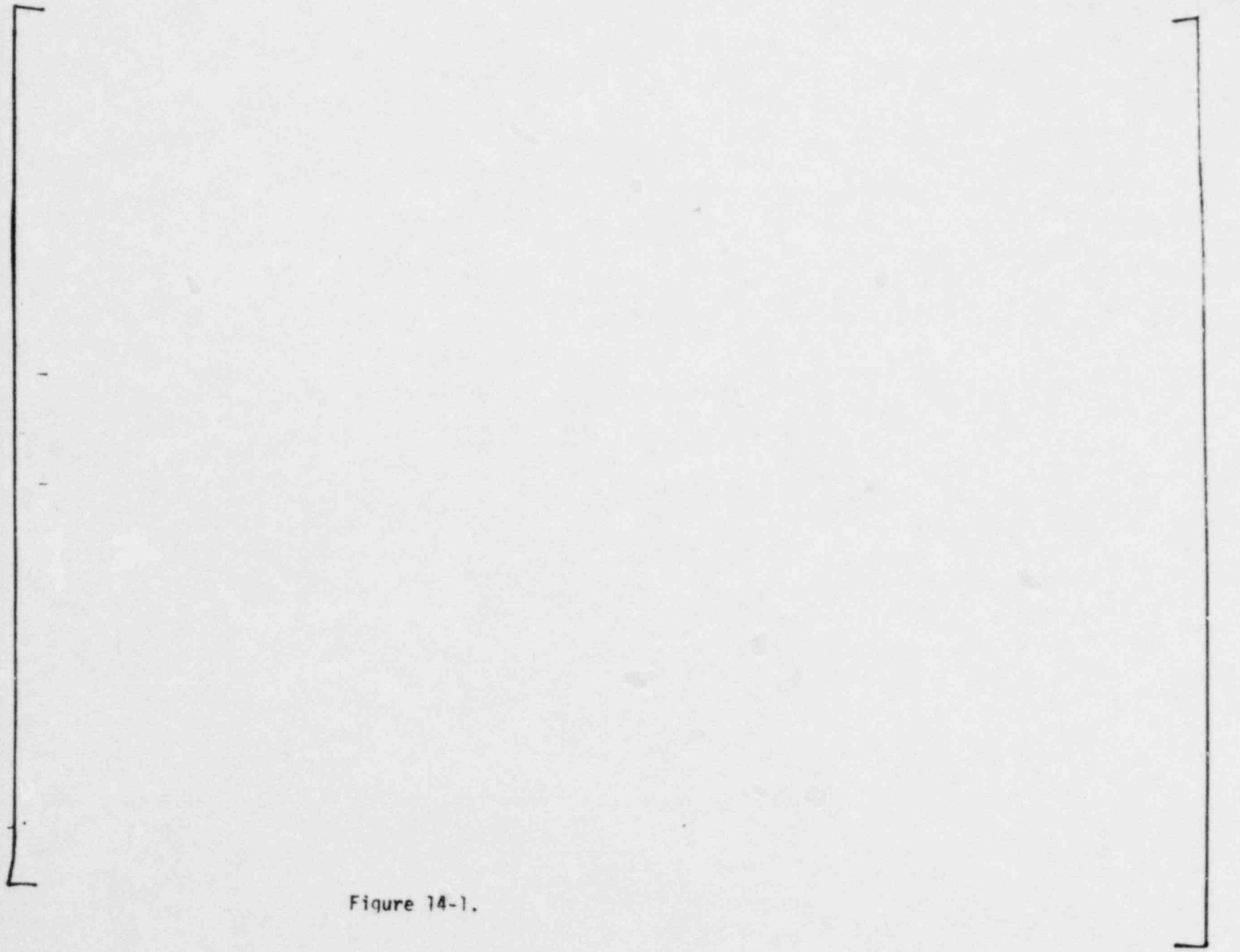

Figure 14-1.

c,e

Figure 14-2.

C,e

Figure 14-3.

c,e

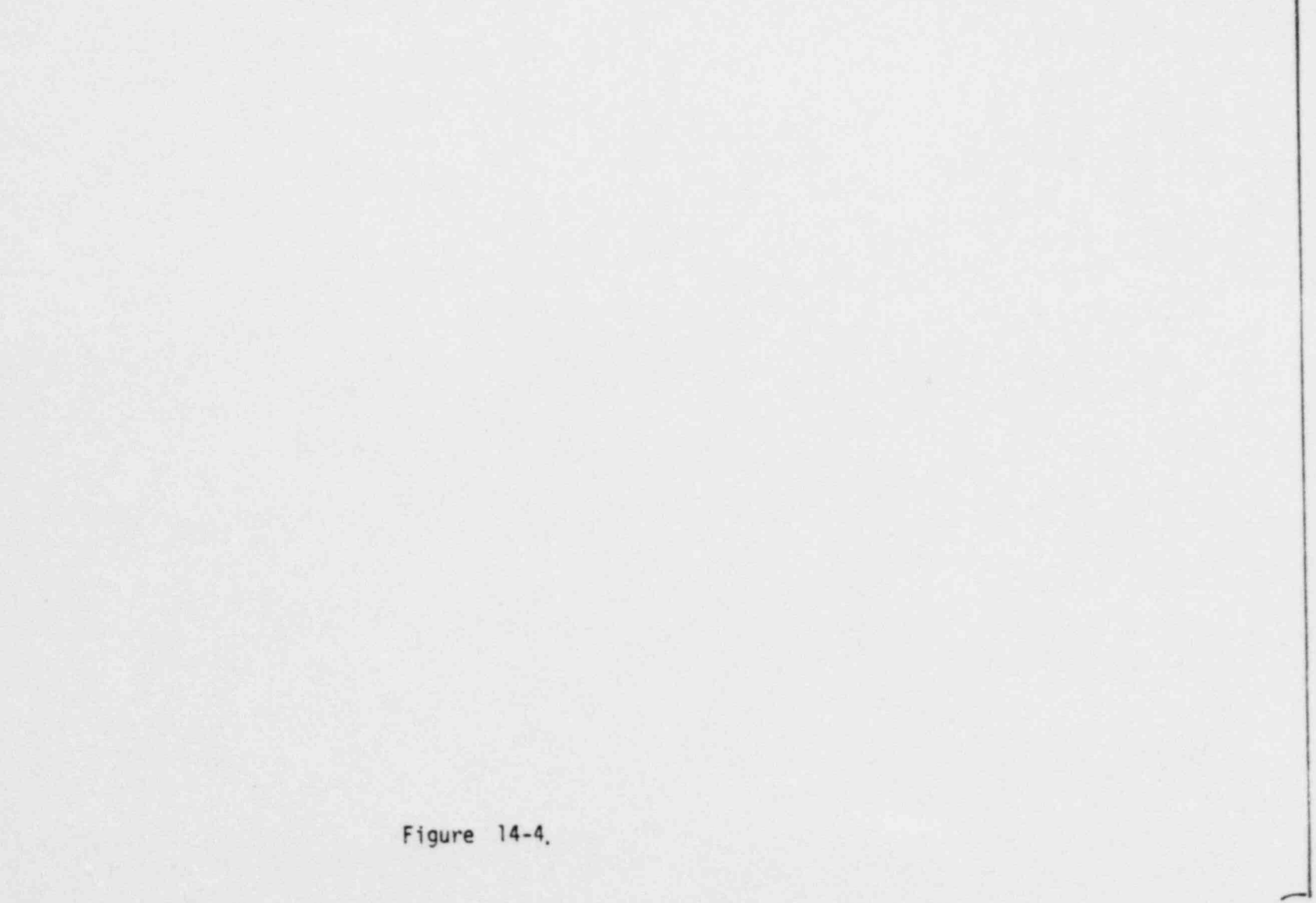

Figure 14-4.

C,e

Figure 14-5.

C,e

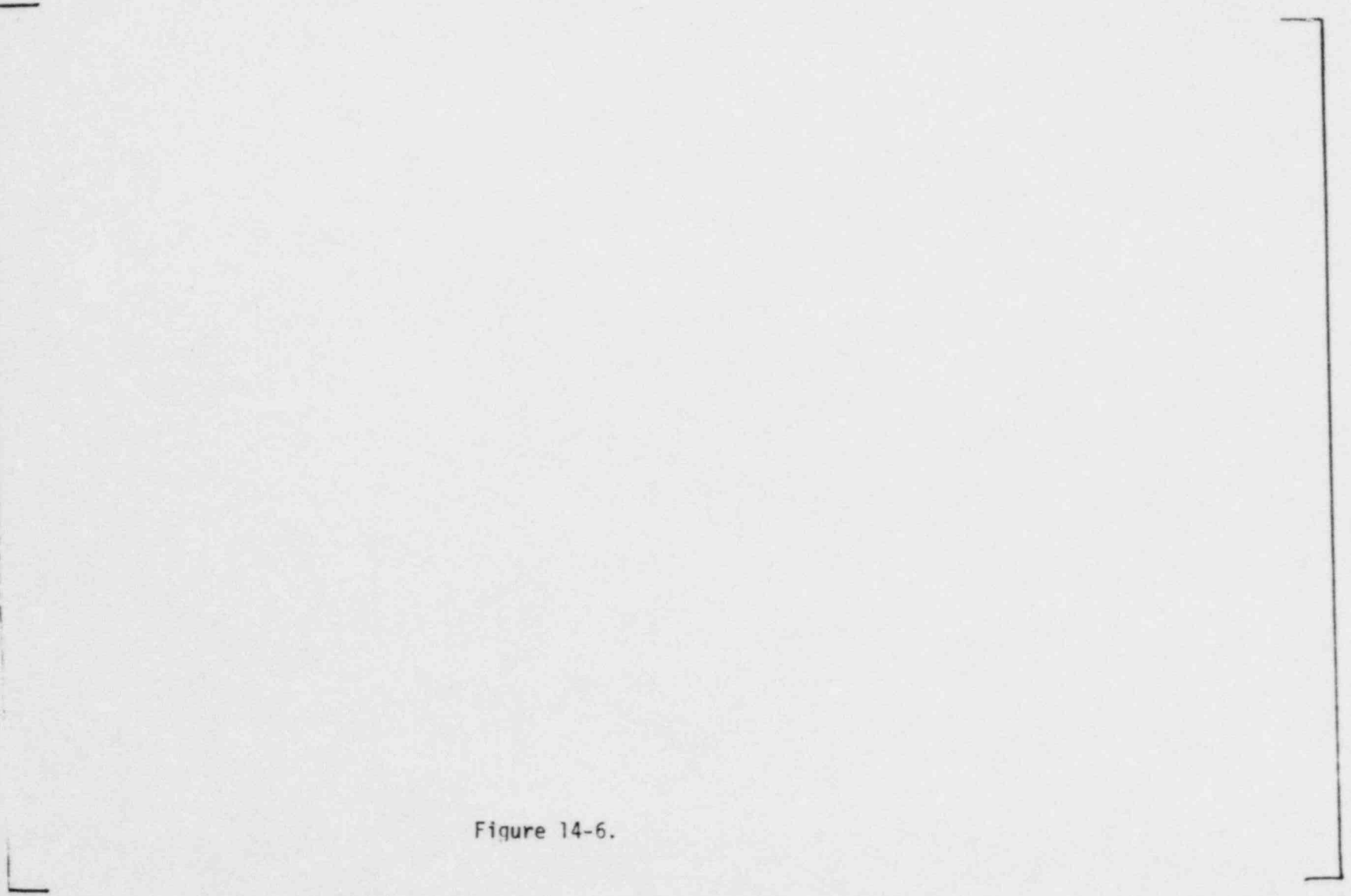

Figure 14-6.

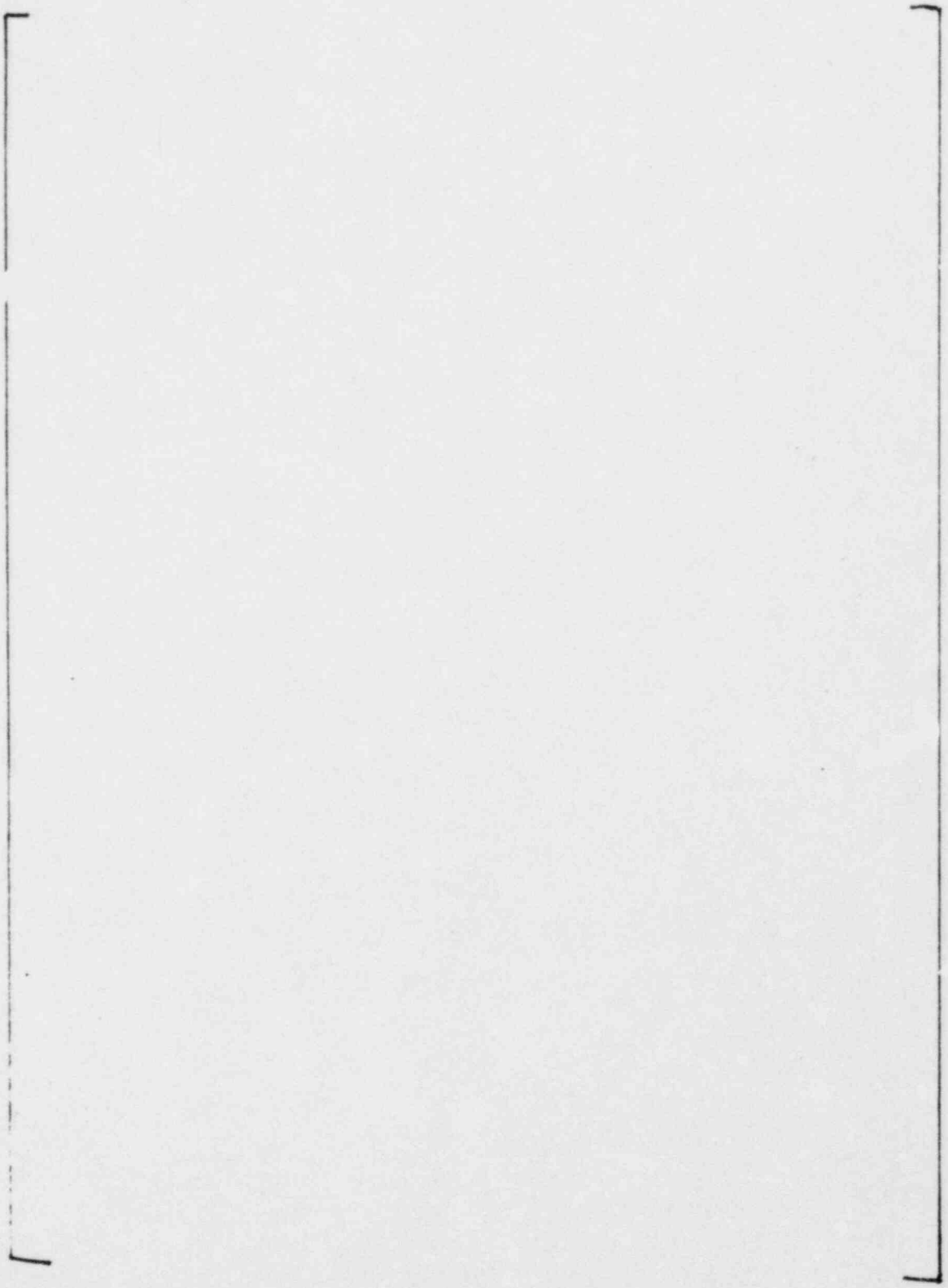

Figure 14-7. Model 51 Auxiliary Nozzle Elevation

c,e

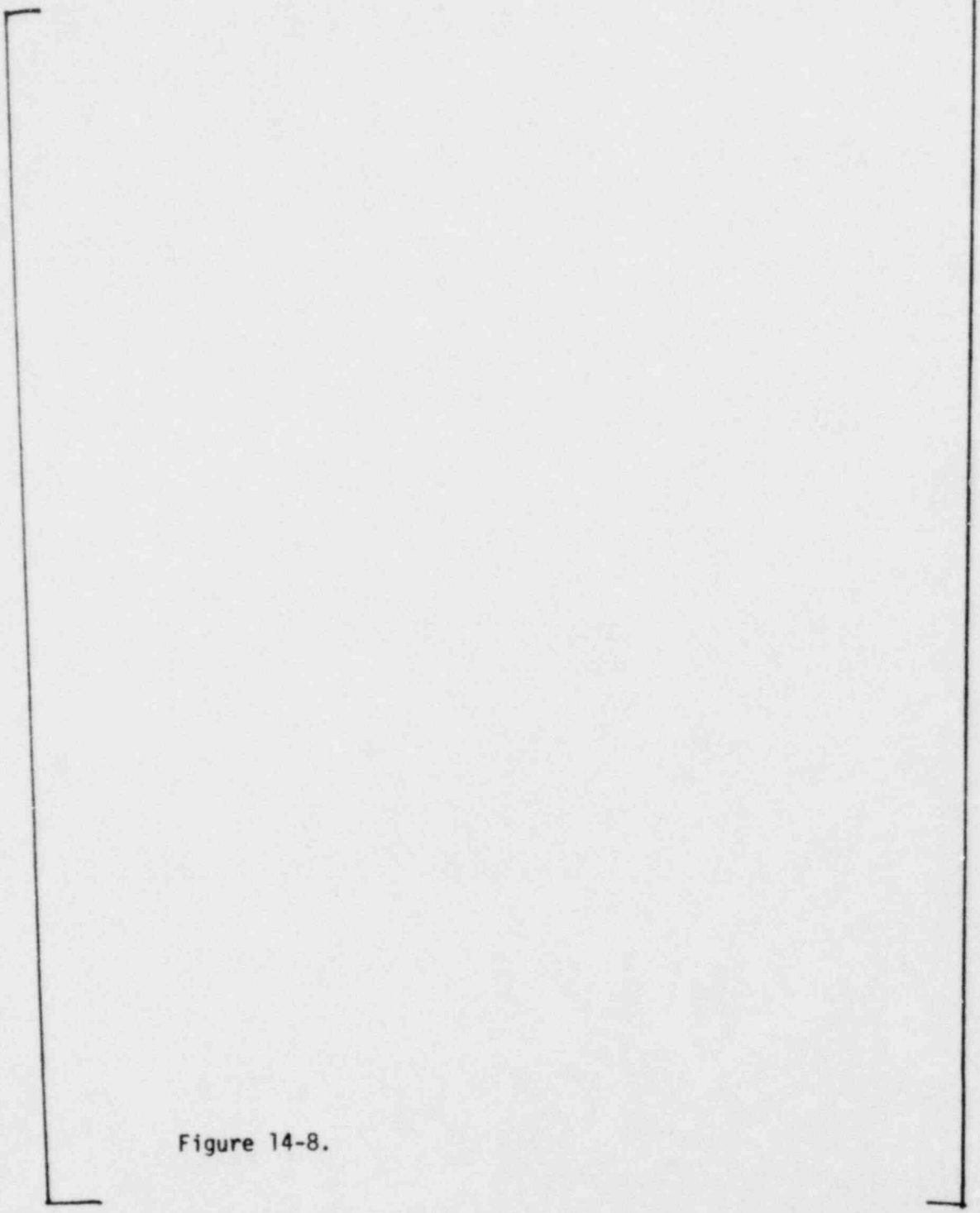

Figure 14-8.

c,e

Figure 14-9:

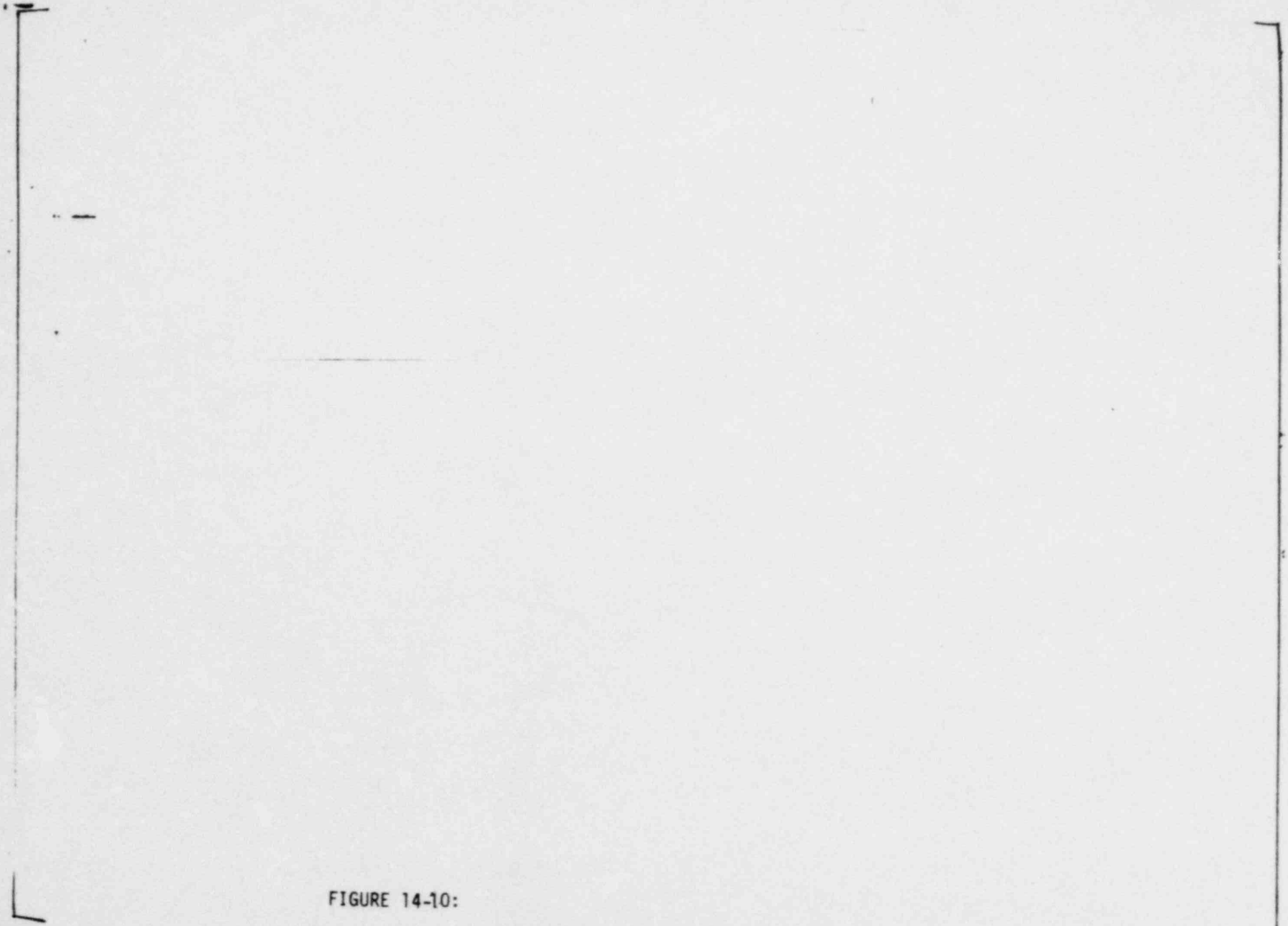

FIGURE 14-10:

c,e

FIGURE 14-11:

c,e

FIGURE 14- 12:

c,e

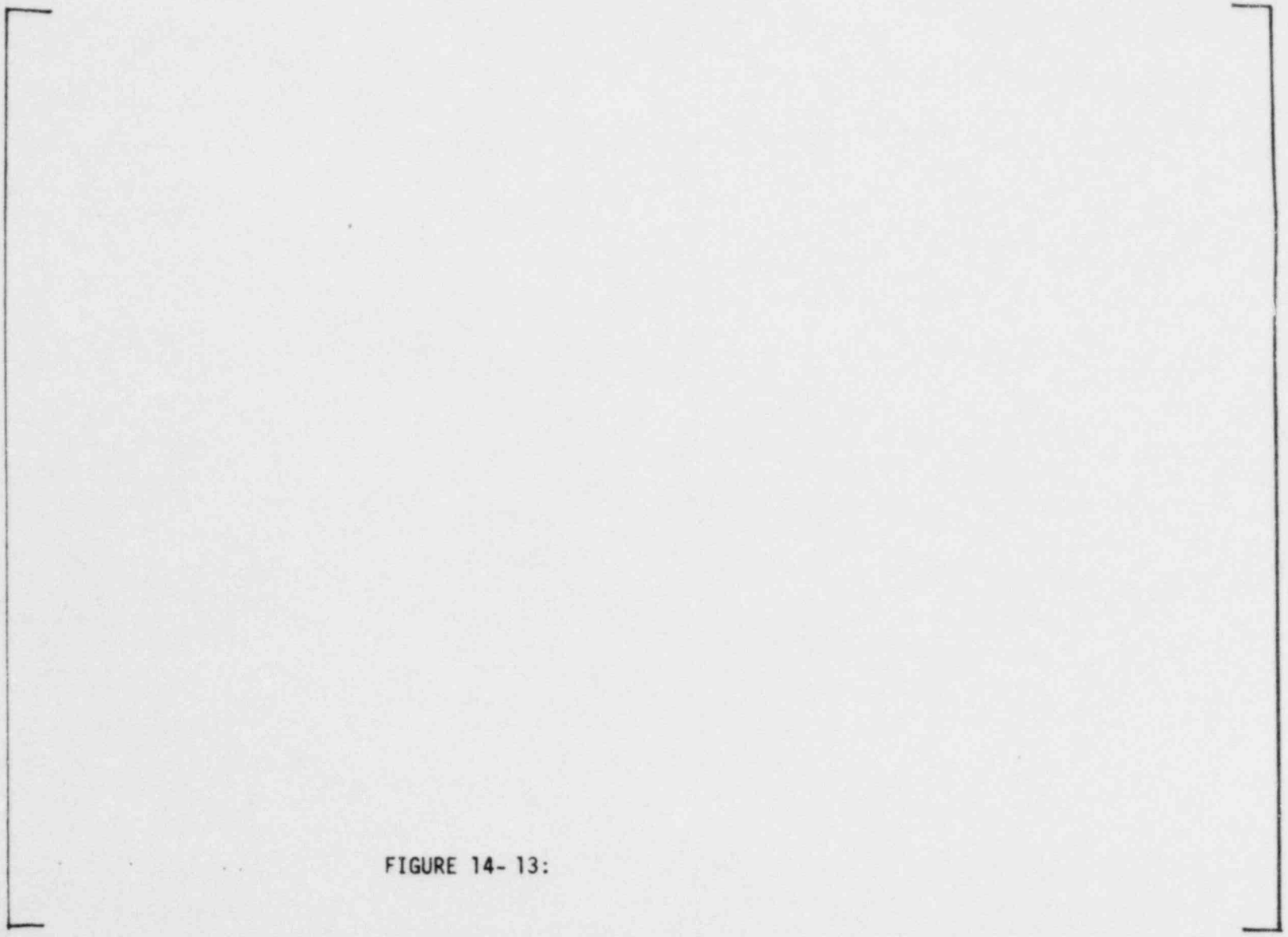

FIGURE 14- 13:

c,e

FIGURE 14-14:

FIGURE 14-15: